The chemistry of
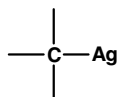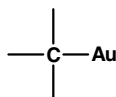# organic derivatives of gold and silver

THE CHEMISTRY OF FUNCTIONAL GROUPS

A series of advanced treatises under the general editorship of
Professors Saul Patai and Zvi Rappoport

The chemistry of alkenes (2 volumes)
The chemistry of the carbonyl group (2 volumes)
The chemistry of the ether linkage
The chemistry of the amino group
The chemistry of the nitro and nitroso groups (2 parts)
The chemistry of carboxylic acids and esters
The chemistry of the carbon–nitrogen double bond
The chemistry of amides
The chemistry of the cyano group
The chemistry of the hydroxyl group (2 parts)
The chemistry of the azido group
The chemistry of acyl halides
The chemistry of the carbon–halogen bond (2 parts)
The chemistry of the quinonoid compounds (2 volumes, 4 parts)
The chemistry of the thiol group (2 parts)
The chemistry of the hydrazo, azo and azoxy groups (2 volumes, 3 parts)
The chemistry of amidines and imidates (2 volumes)
The chemistry of cyanates and their thio derivatives (2 parts)
The chemistry of diazonium and diazo groups (2 parts)
The chemistry of the carbon–carbon triple bond (2 parts)
The chemistry of ketenes, allenes and related compounds (2 parts)
The chemistry of the sulphonium group (2 parts)
Supplement A: The chemistry of double-bonded functional groups (3 volumes, 6 parts)
Supplement B: The chemistry of acid derivatives (2 volumes, 4 parts)
Supplement C: The chemistry of triple-bonded functional groups (2 volumes, 3 parts)
Supplement D: The chemistry of halides, pseudo-halides and azides (2 volumes, 4 parts)
Supplement E: The chemistry of ethers, crown ethers, hydroxyl groups
and their sulphur analogues (2 volumes, 3 parts)
Supplement F: The chemistry of amino, nitroso and nitro compounds and their derivatives
(2 volumes, 4 parts)
The chemistry of the metal–carbon bond (5 volumes)
The chemistry of peroxides
The chemistry of organic selenium and tellurium compounds (2 volumes)
The chemistry of the cyclopropyl group (2 volumes, 3 parts)
The chemistry of sulphones and sulphoxides
The chemistry of organic silicon compounds (2 volumes, 5 parts)
The chemistry of enones (2 parts)
The chemistry of sulphinic acids, esters and their derivatives
The chemistry of sulphenic acids and their derivatives
The chemistry of enols
The chemistry of organophosphorus compounds (4 volumes)
The chemistry of sulphonic acids, esters and their derivatives
The chemistry of alkanes and cycloalkanes
Supplement S: The chemistry of sulphur-containing functional groups
The chemistry of organic arsenic, antimony and bismuth compounds
The chemistry of enamines (2 parts)
The chemistry of organic germanium, tin and lead compounds
The chemistry of dienes and polyenes
The chemistry of organic derivatives of gold and silver

UPDATES

The chemistry of α-haloketones, α-haloaldehydes and α-haloimines
Nitrones, nitronates and nitroxides
Crown ethers and analogs
Cyclopropane derived reactive intermediates
Synthesis of carboxylic acids, esters and their derivatives
The silicon–heteroatom bond
Synthesis of lactones and lactams
Syntheses of sulphones, sulphoxides and cyclic sulphides

Patai's 1992 guide to the chemistry of functional groups — *Saul Patai*

The chemistry of
organic derivatives of gold and silver

Edited by

SAUL PATAI

and

ZVI RAPPOPORT

The Hebrew University, Jerusalem

1999

To

Lisl Patai

How much better is it to get wisdom than gold!
and to get understanding rather to be chosen than silver!

Contributing authors

R. Alan Aitken   School of Chemistry, University of St Andrews, North Haugh, St Andrews, Fife, KY16 9ST, Scotland, UK

Harold Basch   Department of Chemistry, Bar-Ilan University, Ramat-Gan 52900, Israel

Angela Bayler   Lehrstuhl für Anorganische und Analytische Chemie, Technische Universität München, D-85747 Garching, Germany

Alice E. Bruce   Department of Chemistry, University of Maine, 5706 Aubert Hall, Orono, Maine 04469-5706, USA

Mitchell R. M. Bruce   Department of Chemistry, University of Maine, 5706 Aubert Hall, Orono, Maine 04469-5706, USA

Victor Chechik   Department of Chemistry, University of Sheffield, Dainton Building, Sheffield, S3 7HF, UK

John P. Fackler, Jr.   Department of Chemistry, Texas A & M University, College Station, Texas 77843-3012, USA

Simon P. Fricker   AnorMED, Inc., 100 20353-64th Avenue, Langley, British Columbia, V2Y 1N5, Canada

Sarina Grinberg   Institutes for Applied Research, Ben-Gurion University of the Negev, Ernst David Bergman Campus, P. O. B. 653, Beer-Sheeva 84110, Israel

Andreas Grohmann   Lehrstuhl für Anorganische und Analytische Chemie, Technische Universität München, D-85747 Garching, Germany

William M. Horspool   Department of Chemistry, University of Dundee, Dundee, DD1 4HN, Scotland, UK

Tova Hoz   Department of Chemistry, Bar-Ilan University, Ramat-Gan 52900, Israel

Marianna Kańska   Department of Chemistry, University of Warsaw, Warsaw, Poland

Ryszard Kański   Department of Chemistry, University of Warsaw, Warsaw, Poland

Thomas M. Klapötke   Institut für Anorganische Chemie, Universität München (LMU), Butenandtstr. 5–13 (Haus D), D-81377 München, Germany

Joel F. Liebman	Department of Chemistry and Biochemistry, University of Maryland, Baltimore County Campus, 1000 Hilltop Circle, Baltimore, Maryland 21250, USA
Ahmed A. Mohamed	Department of Chemistry, University of Maine, 5706 Aubert Hall, Orono, Maine 04469-5706, USA
Igor Novak	Department of Chemistry, National University of Singapore, Kent Ridge, Singapore 119260
M. Elena Olmos	Lehrstuhl für Anorganische und Analytische Chemie, Technische Universität München, D-85747 Garching, Germany
R. V. Parish	Department of Chemistry, UMIST, P.O. Box 88, Manchester, M60 1QD, UK
Annette Schier	Lehrstuhl für Anorganische und Analytische Chemie, Technische Universität München, D-85747 Garching, Germany
Hubert Schmidbaur	Lehrstuhl für Anorganische und Analytische Chemie, Technische Universität München, D-85747 Garching, Germany
C. Frank Shaw III	Department of Chemistry, University of Wisconsin at Milwaukee, P.O. Box 413, Milwaukee, Wisconsin 53201-0413, USA
José Martinho Simões	Departamento de Química e Bioquímica and CiTecMat, Faculdade de Ciências, Universidade de Lisboa, 1700 Lisboa, Portugal
Suzanne W. Slayden	Department of Chemistry, George Mason University, 4400 University Drive, Fairfax, Virginia 22030-4444, USA
Charles J. M. Stirling	Department of Chemistry, University of Sheffield, Dainton Building, Sheffield, S3 7HF, UK
Suning Wang	Department of Chemistry, Queen's University, Kingston, Ontario K7L 3N6, Canada
Jacob Zabicky	Institutes for Applied Research, Ben-Gurion University of the Negev, Ernst David Bergman Campus, P. O. B. 653, Beer-Sheeva 84110, Israel
Mieczysław Zieliński	Isotope Laboratory, Faculty of Chemistry, Jagiellonian University, ul. Ingardena 3, 30-060 Krakow, Poland

Foreword

In recent years *The Chemistry of Functional Groups* has included several volumes dealing with the chemistry of organometallic derivatives (five volumes edited by F. Hartley in 1982–1989), and *The chemistry of organic germanium, tin and lead compounds* (Ed. S. Patai, 1995). For the reason outlined below, this volume deals with the chemistry of organosilver and organogold compounds.

The volume contains 16 chapters dealing with calculations on organogold compounds, physical and spectroscopic properties (NMR, ESR, PES, Mössbauer spectra), thermochemical and analytical properties, the synthesis and uses of the title compounds and their reactions such as rearrangements, pyrolysis and photochemical reactions. The medicinal use of organogold compounds and the increased use of gold–thiol monolayers are also summarized.

The literature coverage is mostly up to 1998.

I would be grateful to readers who call my attention to mistakes in the present volume.

Jerusalem   Zvi Rappoport
February, 1999

SAUL PATAI
1918–1998

Saul Patai and *The Chemistry of Functional Groups*

In the Foreword to the 96th volume of *The chemistry of the hydrazo, azo and azoxy groups, Vol. 2* in July 1997 Saul Patai wrote in his concise style, 'the series is rapidly approaching the publication of its one-hundredth volume, which most fittingly will deal with the chemistry of organic derivatives of gold and silver. Owing to age and other reasons, in the not too distant future the original series editor will have to terminate his activity'. Saul was 79 years old and for a long time he felt that the publication of the 100th volume would be the appropriate time to retire from the editorship of the series which was begun by him 34 years earlier. Together we decided that an appropriate topic for this 'golden anniversary' would be *The chemistry of organic derivatives of gold and silver* and we then started to plan the volume and look for authors. We also decided that we would include in the foreword to this volume a brief description of the development of the series and Saul was expected to write it. Sadly, Saul died on August 31, 1998, shortly after his eightieth birthday and just after the appearance of the 99th volume, when the present volume was at the earlier stage of editing, and it was left to me to write this foreword. Since Saul and the series were so closely associated it is appropriate on this anniversary of the series to add memorial words about Saul Patai, the creator and main editor of the series.

SAUL PATAI

Saul Patai was born in 1918 in Budapest, Hungary in a Zionist house, where Hebrew was spoken, as preparation for immigration to Palestine. His home served as an intellectual Jewish centre and the whole family was engaged in artistic and literary activities. His mother and sister wrote poetry and painted, and his brother, Raphael, an anthropologist, a folklore researcher and editor, wrote and published more than 40 books during his life, including an autobiography which describes extensively the Patai family. His father, Joseph, who was the chairman of the Hungarian Zionist Organization, was an author, poet, biographer, translator, editor and publisher of the literary Jewish Zionist weekly magazine *Past and Future*, which appeared for 35 years since 1910 in Hungary and had a wide readership in Hungary and its neighbouring countries. The father who travelled extensively, especially to the Holy Land, left young Saul, from the age of 16, as his deputy translator, editor and proofreader without the knowledge of the readers. Consequently, Saul grew up in an editing and printing atmosphere, receiving extensive editorial experience at a young age.

The family immigrated to Palestine in the early 1930s while Saul remained behind to study chemistry and physics at the University in Budapest during 1936–1938. He later followed his family and, in 1938, started his second year of chemistry at the Hebrew

University on Mount Scopus where his brother was the first PhD graduate in 1937. Saul received his MSc degree in physical chemistry in 1941, under the supervision of Professor Ladislaw Farkas, famous for his work on *ortho/para* hydrogen conversion. He continued to work with Farkas on an industrial research topic up to 1942 and in 1943 joined a factory involved in the war effort. In 1943, Saul began his PhD work under Dr Moshe Weizmann (brother of the well-known chemist Chaim Weizmann, the first President of the State of Israel) in the Department of Organic Chemistry at the Hebrew University, finished it in 1947 and was awarded his PhD in the last ceremony on Mt Scopus before the campus was evacuated in the War of Independence. Saul was also a member in 1938–1947 of the 'Haganah', the main Jewish pre-military group during the British rule of Palestine, and he served in the Israeli army and in its 'science unit' during the War of Independence (1947–1949).

All his subsequent academic career was at the Hebrew University of Jerusalem where he served as a teacher, researcher, and academic administrator at times. He was lecturer (1950), senior lecturer (1953), assistant professor (1957) and full professor (1970). He was a committed member of the University and served in many administrative duties such as vice dean of the Faculty of Mathematics and Science, member of the teaching committee, chairman of the graduate student committee, chairman of the Martin Buber Institute for Adult Education and was the first chairman of the Institute of Chemistry (1971–1975) formed by integrating the individual departments. He never sought election but, being an exemplary public servant, he always accepted the call of duty which he then performed in his quiet, efficient and impartial way and was able to advance projects in the face of adverse conditions and without asking anything for himself.

Saul, who started his work as a synthetic organic chemist, spent the years 1954–1956 and 1960 as a research associate in University College London, where he worked with Professor C.K. Ingold, whom he greatly admired. His research with Ingold initiated his interest in organic reaction mechanisms, a subject which he pursued on returning to Jerusalem. He was a visiting professor at several institutes and spent time, among other places, at the University of Auckland in New Zealand, in Monsanto Laboratories in Zürich, Switzerland, and as a Japanese Society for Promotion of Science (JSPS) visitor in Japan.

Saul's research was mainly in the field of organic reaction mechanisms, especially the mechanisms of carbonyl–methylene condensation. He also investigated the pyrolysis of sugars and reactions in the solid state. He supervised more than fifty MSc students and more than twenty PhD candidates and published, with them, over 130 papers. His students, and subsequently their students, occupy central positions in all institutes of higher learning in Israel and he is regarded as one of the founders of physical organic chemistry in Israel. He wrote two textbooks of organic chemistry in Hebrew, a glossary of terms in organic chemistry and participated in the editing of two handbooks of the Chemical Rubber Co., including the organic section of the *Handbook of Chemistry and Physics*.

In addition to his activity within the university Saul found it important to apply his scientific and administrative abilities to public service. After the 'Yom Kippur' war in 1973, he voluntarily dedicated most of his time to form a team of volunteer scientists, mostly from the University, who developed new training equipment and methods for the Israeli army, and he directed their activities in Jerusalem. He initiated and participated in the development of a programme for academic education of air force students/officers in Jerusalem. For these activities he received the 'Volunteer Prize' from the President of Israel.

The main scientific activity of Saul in the last 35 years was the creation, development and editing of the series, *The Chemistry of Functional Groups*, a lifetime achievement which has very few equals. A detailed description is given below. He had great confidence in the ability of the Israeli scientific community and the large number of contributions by

Israeli scientists to his series is evidence of this. For his editorial and other activities in 1995 Saul received the 'Solomon Bublick Prize' of the Hebrew University.

Saul had an impressive personality and commanded the respect of those around him. He was methodical and kept a strict schedule. Tall, upright and soft spoken, still keeping his Hungarian accent he sometimes seemed unsentimental and reserved, especially after the loss of his 17-year-old son, which affected him strongly. However, at the same time he was never remote and indifferent and his door was always open to colleagues and students. He had a soft spot for young students and colleagues and generously devoted his time to helping them, regardless of whether they were ever directly associated with him. Having been asked once for advice in finding a PhD fellowship for a new immigrant from Russia, Saul, who was at that time proposing recipients for fellowships from a memorial fund for his son, thought for a minute and then said, 'OK, I will give him an additional fellowship', and continued immediately with his work. He helped young students and associates in finding doctoral and postdoctoral positions, in their promotions and even in writing papers, using his vast connections, experience and knowledge. When I brought him my own first paper for comments and suggestions, he spent a few days correcting my English and suggested many changes, but did not add his name to the extensively marked manuscript as was the custom at the time. When asked about it he noted that I was independent now and though he would always be willing to give help in the future, he felt it inappropriate to add his name. This very unusual attitude was very characteristic of Saul. He followed the progress of the young colleagues whom he helped and felt deep satisfaction with their progress.

Saul was very talented in many fields, well read and sensitive to human needs around him. Working one day in his office, an enormous noise of breaking glass came from the technician's room. A student told Saul that a big desiccator had broken and that the technician was unharmed but, unlike everybody else who rushed to take a look, Saul remained in his office. When I inquired about it he said that the technician was already sorry and that he did not want to further increase his agony. This was a good lesson for a young student, as I then was.

Saul was gifted with curiosity, vast knowledge and wisdom. It was easy to interest him in many topics, scientific, linguistic, cultural and others and he contributed willingly from his 'life wisdom' and experience to his students, colleagues and friends. He will be missed by all of us.

SAUL PATAI, EDITOR

A natural talent for editing, a lot of accumulated experience, the ability for making quick decisions and personal charm helped Saul in achieving his goal to reduce the time of production of his books from the planning stage to the printed volume while simultaneously maintaining the high quality of the books.

Saul was a superb editor. He had the extraordinary knack of being able to turn around a long-winded sentence and eliminate extraneous matter while retaining the essence. This he did with what seemed to be an effortless, enviable way. He would write quickly, almost without drafts, even a complex paper in an excellent style and an organized manner.

With time, Saul developed an instinct for dealing with late and non-delivering authors, a major problem with multi-author volumes. He had a set of self-imposed rules that tried not to punish the authors who delivered on time and expected prompt publication of their chapter by being strict with authors who caused unnecessary delays, but at the same time he was flexible when an author of a major chapter, or an author with real problems, was late in delivering his manuscript. Consequently, many former authors who never met Saul personally expressed their admiration of the man and his work.

His involvement with the series was a mixture of a 'matter of fact' approach, hard work on current books and pride in the final product. Being a reserved person, he showed some excitement when the first volumes arrived, but with the progress of time the 'matter of fact' approach prevailed. When a new volume arrived from Wiley once or twice a year, I used to watch him open the package, always with the same precise movements, holding out and leafing through the top copy for a minute or two, stamping it, numbering it with his black marker, putting it on the shelf along with the preceding volumes, adding its title to the list of his books and within 10 minutes turning to his next assignment.

The combined prestige of the series and its editor and Saul's charm and personality helped in enrolling the best authors. I was always amazed when accompanying a visitor to the department who asked to pay the 'famous Patai' a courtesy visit, to see the visitor come out of the room a few minutes later with a commission to write a chapter. Warning the unsuspecting guest of this impending outcome would rarely help in the face of Saul's convincing power. Resistance to contribute a chapter, if any, melted immediately. This ability extended also to phone conversations, and when once I asked a newly enrolled author how he was convinced he said, 'How can I resist if a celebrity like Patai calls me personally and asks me to contribute?'

The success of the series, its prestige and the personality of its chief editor reduced to a minimum the expected bureaucratic delays in planning and executing the books. Saul would tell the Wiley office in Chichester on the phone that a new book with a certain title and deadline was planned and the go-ahead was granted immediately. This trust was also extended to the junior editors. A few years ago I planned, together with Professor Peter Stang, a book on 'dicoordinated carbocations', a topic of our expertise which is not part of the series. We had to fill out long forms, present a tentative table of contents, justify the need for the book and visit the Wiley office for discussions. Receiving the publisher's agreement took a few weeks. On one of those days I passed Saul's room when he was on the phone to the Wiley office and I asked him, 'Tell them that I am starting on a book on dienes'; on returning, he called, 'they approve', and that was that.

An undertaking of these dimensions requires hard work and long hours and Saul was a dedicated and industrious editor. Daily he edited the chapters and did not change this habit when he was severely ill and even in hospital. Posted on my door at the department is a picture of Saul editing a chapter while wearing his gas mask during the Gulf War, when we were frequently required to wear our gas masks.

Editing multi-author books by two editors holds a potential for friction between the editors on questions of scientific issues, of general policy and of who will edit what. In seventeen years of on-and-off mutual editorship we had differences and arguments about the former issues, but it is to Saul's credit and nature that we very rarely argued about who will edit what. When one of us was free he took the incoming chapter. Only once after I remarked that he had edited the last chapter to arrive, he immediately returned carrying a freshly arrived 1170-page manuscript saying with a smile, 'so it is your turn'. I have a picture of this event.

Many anecdotes have been collected during the years. On the same week that a critic had written about the 42nd volume, 'How could the organic chemist cope without Saul Patai's Functional Group series', a new secretary at Wiley who dealt with books of past authors sent an internal memo: 'Does anyone know how to find a Saul Patai?', which amused Saul but made him wonder. A young Russian author who visited Saul said that he thought 'the earth trembled, it is like meeting Beilstein', and Saul was amused rather than angry when he learnt about the Japanese pirate 'black edition' of the whole series.

The picture of Saul on a ladder near the series of books with their colored jackets, in a corner of his house, was used by Wiley as an advertisement for the series. There were several collapses of the tower of books during its building and in the last picture few

books were left behind after the tower reached the ceiling, 4 metres above ground. We found a similar picture of Alfred Hitchcock with videos of his films.

Saul dedicated only a very few books. I think that this is due to his use of a dedication on the second volume of the series to the surgeon who treated his son at the time. This was so important to him that I felt, although he never said so, that other dedications would dilute his gratitude. Nevertheless, many years later, he was convinced to dedicate the *'Sulphonic Acids'* volume to the crew of the University post office workers, 'The dependable communicators' as we wrote, for their continuing help in sending and receiving manuscripts and proofs. It was typical of Saul to show such gratitude to them rather than to more highly ranked colleagues.

For many years there was a special connection between Saul and staff members of the publisher, John Wiley & Sons in Chichester, England. These were relations of trust, respect and even admiration of newer generations of Wiley staff to the old veteran. Wiley had organized a birthday dinner on Saul's 70th birthday in Chichester, helped with a celebration for the forthcoming 100th volume organized by the Institute of Chemistry in Jerusalem and a Wiley team visited him in Jerusalem during July 1998 on that occasion. When the first volume was published, Saul thanked the publisher's staff in general but told me that their code of ethics did not allow him to name them, and we continued with this policy along the years. With the 100th volume I feel that the time has come to thank the Wiley staff in Chichester and our helpers in Jerusalem for their work, dedication and support of the series, as well as for their personal support and relations with Saul. I will name only those who were involved with the series in recent years. Mr Paul Greenberg, our copy editor in Jerusalem for the last 12 years, and Ms. Irene Cooper, the senior desk editor in Chichester, who dealt with the daily task of copy-editing and desk-editing of the series, which involve a legion of small and major questions, were always around to help us with great patience. Pat and Keith Raven were the indexers of the series for many years. Mrs Eva Guez in Jerusalem helped Saul with the secretarial work and in other ways during his illness and the last months of his life. Mrs Vanessa Davidson, the assistant editor and Ms. Jenny Cossham, the managing editor in Chichester, made our lives easier by caring for the formal side of contact with authors and management of the publication. Mr Martin Röthlisberger in the Berne office, the senior publishing editor, was always available and helpful in planning, making suggestions and offering advice, and Dr Ernest Kirkwood, the editorial director in Chichester, was very supportive of the series. Our sincere thanks (I talk for Saul too) are due to all of them. Thanks are also due to Professors S. Biali, M. Michman and A. Treinin, friends, colleagues and former students of Saul and contributors to the series who read the present foreword.

Finally, without the help of Lisl, Saul's wife, who supported his work during the years, by sharing his life and taking burdens off his shoulders, especially in the last, not easy years, the series would not be what it is. Saul thanked her on many occasions and also formally in Forewords to various volumes, and I want to join in thanking her. This book is dedicated to Lisl.

SAUL PATAI: THE SERIES

I finished my PhD work on the 'Nucleophilic Cleavage of Carbon–Carbon Double Bonds' under the supervision of Saul Patai in 1962. The cleavage was the reversal of the carbonyl–methylene condensation, a topic which was at the centre of Saul's research at the time. The thesis started with a lengthy review in Hebrew on nucleophilic reactions at carbon–carbon double bonds. There was no literature review of this topic at the time and Saul considered writing one. At the same time, Professor Arnold Weissberger, a scientist in Kodak and an editor for Interscience/Wiley Publishing Company, visited Jerusalem

Saul Patai

and invited Saul to write a book on the topic. Saul thought that a book dealing with all aspects of 'alkene' chemistry would be an appropriate medium for the chapter and agreed to edit such a book. Thus, *The chemistry of alkenes* was born in 1964 and our chapter, which served as a catalyst, became a small part in a voluminous volume.

Saul, who always loved to be engaged in new activities, enjoyed very much his association with the best authors in their fields, and the actual editing with which he was associated from a young age. He decided during his work on the alkenes volume that a series of books, each dealing with all aspects of the chemistry of a single or several functional group(s), would be a new approach to present organic chemistry. The high quality of the contributions to the first volume convinced him that editing such a series would be a valuable service to the chemical community and at the same time an outlet for his editorial talents. With Wiley's blessings the series *The Chemistry of Functional Groups* was then launched.

Until 1969 Saul had edited alone six volumes and laid the general framework of chapters that the series followed, with minor changes, for three decades. In 1969 Saul tried two new approaches, the first two-volume set on 'nitro and nitroso' was edited by an external expert on these groups, Professor Feuer, and two young former students, Drs Zabicky and Rappoport, were invited to edit volumes on their own. This was typical of Saul who always tried to encourage young colleagues, and believed that the editing would benefit their academic career. During the next decade Saul edited alone 27 additional volumes of the series. In the 1980s a new period had begun. Charles Stirling, a friend and a sulfur chemist, edited a 'sulphonium' book, Frank Hartley started his five-volume sub-series on the 'metal–carbon bonds' and I joined Saul in mutual editorship of what resulted, until today, in twenty-seven volumes, including the present one. Whereas seven volumes were published independently in the last decade by myself and four by Hartley (on 'organophosphorus'), Saul still edited eighteen volumes, more than both of his two associates together.

This was the time of the large two-volume sets on many functional groups, and of supplements on new chemistry of 'old' functional groups which were covered earlier. At this time there was also launched, prospered, but eventually closed, a sub-series, called 'Updates' in which a few chapters covered previously in the main series, such as 'Crown Ethers', or 'Synthesis of Lactones and Lactams', were chosen, and were published together with an extensive update in a smaller book. The last of this eight-volume sub-series became as voluminous as those in the original series. During this period the two 'Patai Guides' to the series were published, thus enabling an easy search for the increasing amount of material within the growing series.

To Saul's delight, the immediate topic covered before the present volume was the largest covered at one time, the three-volume set on *The chemistry of organic silicon compounds*, that I edited together with Yitzhak Apeloig, a former student of mine and Saul's scientific 'grandson'. So the series continues with the torch being passed from generation to generation of the same scientific family.

Some statistics: the series, now in its 35th year, has covered so far more than 50 functional groups, both simple and complex (e.g. enols, enamines) in one-hundred main volumes and eight update volumes which contain 83 500 pages. More than 1500 authors from many countries in five continents have contributed 1314 review chapters, which cover an extensive part of organic chemistry.

The choice of topics and authors, the actual editing and even proofreading of a large number of the volumes were done by the editors of the individual volumes. No editorial board and no referees shared the decisions or carried the burden of work and there was only minimal secretarial assistance. Editing even a single multiauthor volume is not a simple job, and remembering that Saul edited alone 54 volumes and shared the editing

of 21 main and eight update volumes, emphasizes Saul's Herculean job in the last three and a half decades.

   Editing has also its benefits and rewards. The 'Functional Groups Series', the so-called 'Patai series', is found on the shelves of all the main libraries, although the rising cost is certainly a major problem. Critics are generally very favorable and phrases like 'This is a highly valuable work', 'Life would be harder without it' or 'These books are classic works' abound in reviews of the books. One can meet authors of the series in almost every university and at every conference and I have frequently observed sessions in meetings where all speakers were former 'Patai series' authors. This is a tribute to Saul Patai who created the series, set its standards and, with continuing dedication and hard work, brought it to its present level.

Jerusalem   ZVI RAPPOPORT
February, 1999

The Chemistry of Functional Groups
Preface to the series

The series 'The Chemistry of Functional Groups' was originally planned to cover in each volume all aspects of the chemistry of one of the important functional groups in organic chemistry. The emphasis is laid on the preparation, properties and reactions of the functional group treated and on the effects which it exerts both in the immediate vicinity of the group in question and in the whole molecule.

A voluntary restriction on the treatment of the various functional groups in these volumes is that material included in easily and generally available secondary or tertiary sources, such as Chemical Reviews, Quarterly Reviews, Organic Reactions, various 'Advances' and 'Progress' series and in textbooks (i.e. in books which are usually found in the chemical libraries of most universities and research institutes), should not, as a rule, be repeated in detail, unless it is necessary for the balanced treatment of the topic. Therefore each of the authors is asked not to give an encyclopaedic coverage of his subject, but to concentrate on the most important recent developments and mainly on material that has not been adequately covered by reviews or other secondary sources by the time of writing of the chapter, and to address himself to a reader who is assumed to be at a fairly advanced postgraduate level.

It is realized that no plan can be devised for a volume that would give a complete coverage of the field with no overlap between chapters, while at the same time preserving the readability of the text. The Editors set themselves the goal of attaining reasonable coverage with moderate overlap, with a minimum of cross-references between the chapters. In this manner, sufficient freedom is given to the authors to produce readable quasi-monographic chapters.

The general plan of each volume includes the following main sections:

(a) An introductory chapter deals with the general and theoretical aspects of the group.

(b) Chapters discuss the characterization and characteristics of the functional groups, i.e. qualitative and quantitative methods of determination including chemical and physical methods, MS, UV, IR, NMR, ESR and PES — as well as activating and directive effects exerted by the group, and its basicity, acidity and complex-forming ability.

(c) One or more chapters deal with the formation of the functional group in question, either from other groups already present in the molecule or by introducing the new group directly or indirectly. This is usually followed by a description of the synthetic uses of the group, including its reactions, transformations and rearrangements.

(d) Additional chapters deal with special topics such as electrochemistry, photochemistry, radiation chemistry, thermochemistry, syntheses and uses of isotopically labelled compounds, as well as with biochemistry, pharmacology and toxicology. Whenever applicable, unique chapters relevant only to single functional groups are also included (e.g. 'Polyethers', 'Tetraaminoethylenes' or 'Siloxanes').

This plan entails that the breadth, depth and thought-provoking nature of each chapter will differ with the views and inclinations of the authors and the presentation will necessarily be somewhat uneven. Moreover, a serious problem is caused by authors who deliver their manuscript late or not at all. In order to overcome this problem at least to some extent, some volumes may be published without giving consideration to the originally planned logical order of the chapters.

Since the beginning of the Series in 1964, two main developments have occurred. The first of these is the publication of supplementary volumes which contain material relating to several kindred functional groups (Supplements A, B, C, D, E, F and S). The second ramification is the publication of a series of 'Updates', which contain in each volume selected and related chapters, reprinted in the original form in which they were published, together with an extensive updating of the subjects, if possible, by the authors of the original chapters. A complete list of all above mentioned volumes published to date will be found on the page opposite the inner title page of this book. Unfortunately, the publication of the 'Updates' has been discontinued for economic reasons.

Advice or criticism regarding the plan and execution of this series will be welcomed by the Editors.

The publication of this series would never have been started, let alone continued, without the support of many persons in Israel and overseas, including colleagues, friends and family. The efficient and patient co-operation of staff-members of the publisher also rendered us invaluable aid. Our sincere thanks are due to all of them.

The Hebrew University   SAUL PATAI
Jerusalem, Israel   ZVI RAPPOPORT

Contents

List of abbreviations used

Ac	acetyl (MeCO)
acac	acetylacetone
Ad	adamantyl
AIBN	azoisobutyronitrile
Alk	alkyl
All	allyl
An	anisyl
Ar	aryl
Bn	benzyl
Bz	benzoyl (C_6H_5CO)
Bu	butyl (also t-Bu or Bu^t)
CD	circular dichroism
CI	chemical ionization
CIDNP	chemically induced dynamic nuclear polarization
CNDO	complete neglect of differential overlap
Cp	η^5-cyclopentadienyl
Cp*	η^5-pentamethylcyclopentadienyl
DABCO	1,4-diazabicyclo[2.2.2]octane
DBN	1,5-diazabicyclo[4.3.0]non-5-ene
DBU	1,8-diazabicyclo[5.4.0]undec-7-ene
DIBAH	diisobutylaluminium hydride
DME	1,2-dimethoxyethane
DMF	N,N-dimethylformamide
DMSO	dimethyl sulphoxide
ee	enantiomeric excess
EI	electron impact
ESCA	electron spectroscopy for chemical analysis
ESR	electron spin resonance
Et	ethyl
eV	electron volt
Fc	ferrocenyl

FD	field desorption
FI	field ionization
FT	Fourier transform
Fu	furyl(OC_4H_3)
GLC	gas liquid chromatography
Hex	hexyl(C_6H_{13})
c-Hex	cyclohexyl(C_6H_{11})
HMPA	hexamethylphosphortriamide
HOMO	highest occupied molecular orbital
HPLC	high performance liquid chromatography
i-	iso
Ip	ionization potential
IR	infrared
ICR	ion cyclotron resonance
LAH	lithium aluminium hydride
LCAO	linear combination of atomic orbitals
LDA	lithium diisopropylamide
LUMO	lowest unoccupied molecular orbital
M	metal
M	parent molecule
MCPBA	*m*-chloroperbenzoic acid
Me	methyl
MNDO	modified neglect of diatomic overlap
MS	mass spectrum
n	normal
Naph	naphthyl
NBS	*N*-bromosuccinimide
NCS	*N*-chlorosuccinimide
NMR	nuclear magnetic resonance
Pc	phthalocyanine
Pen	pentyl(C_5H_{11})
Pip	piperidyl($C_5H_{10}N$)
Ph	phenyl
ppm	parts per million
Pr	propyl (also *i*-Pr or Pr^i)
PTC	phase transfer catalysis or phase transfer conditions
Pyr	pyridyl (C_5H_4N)
R	any radical
RT	room temperature

s-	secondary
SET	single electron transfer
SOMO	singly occupied molecular orbital
t-	tertiary
TCNE	tetracyanoethylene
TFA	trifluoroacetic acid
THF	tetrahydrofuran
Thi	thienyl(SC_4H_3)
TLC	thin layer chromatography
TMEDA	tetramethylethylene diamine
TMS	trimethylsilyl or tetramethylsilane
Tol	tolyl(MeC_6H_4)
Tos or Ts	tosyl(*p*-toluenesulphonyl)
Trityl	triphenylmethyl(Ph_3C)
Xyl	xylyl($Me_2C_6H_3$)

In addition, entries in the 'List of Radical Names' in *IUPAC Nomenclature of Organic Chemistry*, 1979 Edition, Pergamon Press, Oxford, 1979, p. 305–322, will also be used in their unabbreviated forms, both in the text and in formulae instead of explicitly drawn structures.

CHAPTER **1**

General and theoretical aspects of organic gold compounds†

TOVA HOZ and HAROLD BASCH

Department of Chemistry, Bar-Ilan University, Ramat-Gan 52900, Israel

I. INTRODUCTION

Gold chemistry is dominated by the oxidation states (I) and (III) with Au$^+$ and Au^{3+} having the electronic configurations [Xe]5d^{10}6s^{0}6p^0 and [Xe]5d^{8}6s^{0}6p^0, respectively. Gold(I) has received most of the attention since it has been used extensively in different complexes which were shown to have physiologically therapeutic value[1], in contrast to gold(III) whose complexes have been found to be toxic[2]. Accordingly we will concentrate on gold(I) in this chapter.

Numerous experimental studies have been published on Au$^+$–ligand compounds: Wilkins and coworkers[3] reported lower bounds for bond energies for a number of complexes, derived from gas-phase reactions of Au$^+$ with a series of organic compounds. Schröder and coworkers[4] applied a similar technique to determine and characterize the Au−F bond energy. A more detailed work dealing with ligand exchange reactions used ion cyclotron resonance[5] mass spectrometry as an analytical method to provide

---

† This chapter is dedicated to the memory of Prof. Saul Patai, a humane person, educator and outstanding scientist.

1

relative gold(I) cation affinities for various ligands. These were found to follow the order $C_6F_6 < H_2O < CO < C_2H_4 \sim C_6H_6 \sim NH_3 \sim C_3H_6 < C_4H_6$.

While a number of theoretical calculations on neutral gold compounds have been performed using a variety of methods, so far only a few *ab initio* studies have been performed on cationic gold compounds. The smallest positively charged diatomic system, AuH^+ cation, has been studied in great detail, giving a theoretical bond dissociation energy (BDE) prediction for $Au-H^{+}$[6-9] in the order of 44 kcal mol^{-1}. The $AuPH_3^+$ system has been examined at the HF level by Schwerdtfeger and coworkers[8] leading to a relativistic BDE of 47 kcal mol^{-1}. Recently, Veldkamp and Frenking[10] performed MP2 and QCISD(T) calculations on $Au(CO)_n^+$ systems and concluded that the first ($n = 1$) CO molecule was bound by 45 kcal mol^{-1}. Further, Schwarz and coworkers[11] reported CCSD(T) calculations on the AuH_2O^+ complex giving a BDE of 37 kcal mol^{-1}.

Systems containing heavy elements exhibit relativistic effects, which can have a significant influence on physico-chemical properties such as bond lengths, binding energies and, in particular, ionization energies. As pointed out by Pyykko and Desclaux[12], relativistic effects reach a local maximum for group 11 elements within a row of the Periodic Table. A convenient approach to introduce relativistic effects into theoretical calculations is to use spin−orbit averaged relativistic effective core potentials, RECPs[13-15], which offer a simple accounting of relativistic effects such as the mass-velocity and Darwin terms. Schwerdtfeger and coworkers[16] used relativistic effective core potential and basis sets for the gold atom, which permitted the calculation of structures and binding energies for a series of diatomic gold compounds with reasonable accuracy.

In a previous chapter in this series[17] we have discussed the nature of complexes of Au(I), Cu(I) and Ag(I) with ethylene and with various triple-bonded compounds. The geometries of the cation−ligand complexes (including protonated species) were optimized using relativistic compact effective potentials (RCEPs)[18] for Au(I) and non-relativistic analogues (CEP)[13] for the first, second and third row atoms (H, C, N, O, F, S, P and Cl). Geometry optimization was carried out at the RHF and MP2 theory levels. In addition, single point calculations performed at the QCISD(T) theory level using the lower level optimized geometries gave the best agreement with the experimental values.

Schwarz and coworkers[19] have compared relativistic BDEs and geometrical parameters calculated at different levels of theory in order to find the best method for dealing with gold(I) complexes. The main methods used were SCF, MP2, CCSD(T), DFT/BLYP and DFT/BP86[19]. It was found that among those tried, only the latter theory level exactly reproduced the experimental stability order of Au−L$^+$ complexes with L = H_2O, CO, C_2H_4, C_6H_6, NH_3 and C_3H_6. In addition, for the ligand pair ethylene and ammonia, for which an experimental estimate of the difference in the metal−ligand bond strength is available, the computed BDE difference was in good agreement with the experimental value. The conclusion was that gradient-corrected density functional theory (DFT) can be used for studying such complexes.

Trialkylphosphine gold(I) compounds, $(R_3P)AuCl$, have been shown to possess oral anti-arthritic activity[1] resulting from their ability to exchange a ligand with thiols (RSH) in the body to give gold−SR complexes (equation 1). The same activity was observed for $Au(R_3P)_2Cl$ and AuSR compounds. Therefore, the energetics of ligand exchange reactions need to be known for a wide variety of ligands.

$$RSH + ClAuPR_3 \longrightarrow RSAuPR_3 + H^+ + Cl^- \qquad (1)$$
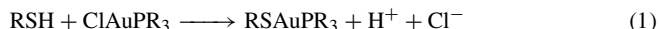
In this chapter we will focus on a systematic *ab initio* study of the complexes of gold(I) with neutral and charged ligands, where the total number of ligands varies from

one to four. One objective is to study the energetics of ligand exchange. The nature of the Au^+–ligand bond is also examined by using the following properties: equilibrium geometry, bond dissociation energy and atomic charge, all as a function of ligand. Besides reviewing the literature, this calculational survey also serves to give the properties of Au^+ complexes within a uniform and consistent theoretical framework for comparison purposes.

All calculations used the DFT/B3LYP theory level[20] using effective core potentials for the chemically inactive core electrons. The basis sets were taken from the respective CEP[18] and RCEP[13] tabulations. For the main group elements the CEP-211G split of the published CEP-31G valence sp atomic orbital basis set was augmented by a double set of polarization d-type basis functions (5 components). The single gaussian exponent values for the sets of d functions were taken from the internally stored values of the GAUSSIAN94[21] program. For the hydrogen atom, the 311G triple-zeta set with a single gaussian p-type polarization function was also taken from GAUSSIAN94.

Au(I) has a $5d^{10}$ (^1S) electronic state configuration. The RCEPs used here were generated from Dirac–Fock (DF) all-electron (AE)[22] relativistic atomic orbitals, and therefore implicitly include the major radial scaling effects of the core electron on the valence electrons[23]. In the closed-shell metal–ion system these indirect relativistic effects are dominant. In the small-core RCEP used here[13] the $5s^2 5p^6$ subshells are included in the valence orbital space together with 5d, 6s and 6p atomic orbitals, and all must be adequately represented by basis functions. The gaussian function basis set on each metal atom consists of the published[13] $[4^{sp}3^d]$ distribution which is double-zeta each for the 5sp and 6sp orbitals, and triple-zeta for the 5d electrons. The standard notation[24] for this basis set is RCEP-4111/311G to show explicitly the gaussian primitive distribution in each basis function.

The atomic charges were determined using the Mulliken population analysis[25]. The Mulliken definition has been shown to suffer from being basis-set dependent and it sometimes gives unreasonable results with diffuse basis functions. This latter defect can manifest itself as a negative electron population. However, for a series of compounds in a common basis set with no especially diffuse basis functions, as is the case here, trends in atomic charges are expected to be reliable.

All geometry optimization was carried out using analytical gradient techniques at the density functional theory (DFT) level using the B3LYP hybrid exchange-correlation functional defined internally in GAUSSIAN94. All energies reported here are simple total energy differences, with no thermodynamics corrections for vibrations, etc.

II. AuL$^+$ COMPLEXES, L = NEUTRAL LIGAND

The calculated optimized geometries of the AuL$^+$ complexes, where L = H_2O, CH_3OH, NH_3, NH_2CH_3, $NH(CH_3)_2$, H_2S, $HSCH_3$, $S(CH_3)_2$, PH_3, PH_2CH_3, PH_2Cl and $PHCl_2$, are given in Table 1. Their binding energies and Mulliken charges are summarized in Table 2. The geometries, energies and charges of the bare ligands (L) are shown in Table 3.

In none of the studied complexes were the Au, the attached atom of the ligand and the two atoms directly bound to the attached atom found to be planar. In two cases, AuH_2O^+ and AuH_2S^+, the energy of the enforced planar conformation was calculated. While for the AuH_2O^+ complex the planar conformation was found to be only 0.9 kcal mol^{-1} higher than the optimal geometry, for the H_2S complex the planar form was found to be 21.7 kcal mol^{-1} higher than the global energy minimum geometry. Using the DFT method, Schwarz and coworkers[11] also found that the energy difference between the

TABLE 1.   Selected bond distances and angles in the geometry optimized AuL$^+$ complexes

AuL$^+$	Bond length (Å)^a			Angle (deg)^a					
	Au−L	L−H	L−C	AuLH	AuLC	HLH	HLC	CLC	AuLHH
AuOH$_2$	2.182	0.974^b	—	115.79	—	107.20	—	—	130.98
AuOH$_2$^{g}	2.171	0.970	—	124.77	—	110.35	—	—	180.00
AuO(H)CH$_3$	2.156	0.971	1.489	110.80	122.34	—	109.53	—	137.90
AuNH$_3$	2.100	1.022^b	—	110.53	—	108.39	—	—	—
AuNH$_2$CH$_3$	2.099	1.022^b	1.512	106.52	116.80	106.48	110.00	—	—
AuNH(CH$_3$)$_2$	2.103	1.021	1.509^b	103.99	112.29	—	107.79	112.16	—
AuSH$_2$	2.352	1.358^b	—	97.77	—	93.14	—	—	98.29
AuSH$_2$^{g}	2.347	1.344	—	127.70	—	105.60	—	—	180.00
AuS(H)CH$_3$	2.337	1.355	1.860	97.65	107.04	—	98.04	—	108.51
AuS(CH$_3$)$_2$	2.330	—	1.843^b	—	105.85	—	—	101.51	110.34
AuPH$_3$	2.282	1.405^b	—	113.50	—	105.16	—	—	—
AuPH$_2$CH$_3$	2.283	1.407^b	1.828	109.92	116.83	103.45	107.94	—	—
AuPH$_2$Cl	2.279	1.407^b	2.011^c	112.80	115.24^d	104.72	105.17	—	—
AuPHCl$_2$	2.281	1.408	2.009^c	113.53	113.31^d	—	103.55^e	108.70^f	—

^{a}L = attached ligand.
^{b}Averaged bond length.
^{c}L−Cl distance.
^{d}AuLCl angle.
^{e}HLCl angle.
^{f}ClLCl angle.
^{g}Planar structure.

TABLE 2.   Total energies (a.u.) of optimized complexes AuL$^+$, charges q on atoms and bond dissociation energy BDE (kcal mol^{-1}) to Au$^+$ + L

AuL$^+$	Charge		Energy	
	q(Au)	q(L)^b	Total (a.u.)	BDE (kcal mol^{-1})
AuOH$_2$	0.76	−0.50	−152.995267	40.0
AuOH$_2$^{a}	0.78	−0.50	−152.993869	39.1
AuO(H)CH$_3$	0.72	−0.30	−159.851933	45.6
AuNH$_3$	0.66	−0.67	−147.570293	66.0
AuNH$_2$CH$_3$	0.60	−0.55	−154.429432	71.6
AuNH(CH$_3$)$_2$	0.54	−0.42	−161.288287	74.0
AuSH$_2$	0.55	−0.01	−147.189993	58.4
AuSH$_2$^{a}	0.65	−0.09	−147.155354	36.7
AuS(H)CH$_3$	0.49	0.12	−162.481223	68.3
AuS(CH$_3$)$_2$	0.42	0.28	−160.940698	76.3
AuPH$_3$	0.48	0.08	−144.186862	75.2
AuPH$_2$CH$_3$	0.43	0.26	−151.073398	87.8
AuPH$_2$Cl	0.46	0.24	−158.525595	70.7
AuPHCl$_2$	0.45	0.35	−172.870231	65.5

^{a}Planar structure.
^{b}L = attached atom.

planar and optimal structures of the H$_2$O complex is rather small (2 kcal mol^{-1}). The surprising difference in the inversion energy for these two complexes originates from the difference in the nature of bonding between the two ligands and Au$^+$. It is generally agreed that H$_2$O binds to Au$^+$ mainly through an ion−dipole electrostatic interaction. In light of the above result, it is therefore highly likely that the covalent component is much

TABLE 3. Bond lengths, angles and charges of the bare ligands in their optimized geometry

Ligand	Bond length (Å)		Angle (deg)			Charge $q(L)^e$	Energy (a.u.)
	$L-H^e$	$L-C^e$	$HLH^{b,e}$	HLC^e	CLC^e		
H_2O	0.966^a	—	104.52	—	—	−0.57	−17.190400
CH_3OH	0.966	1.432	—	108.19	—	−0.30	−24.038136
NH_3	1.019^a	—	106.00	—	—	−0.71	−11.723887
NH_2CH_3	1.018^a	1.477	106.00	109.66^b	—	−0.56	−18.574153
$NH(CH_3)_2$	1.018	1.470	—	108.22^b	112.00	−0.39	−25.429168
H_2S	1.335^a	—	92.84	—	—	−0.25	−11.355729
$S(H)CH_3$	1.348	1.844	—	96.93	—	−0.11	−18.215543
$S(CH_3)_2$	—	1.832^a	—	—	99.53	0.06	−25.078032
PH_3	1.425^a	—	93.28	—	—	−0.14	−8.325862
PH_2Cl	1.426^a	2.117	92.03	96.30^c	—	0.12	−22.671748
$PHCl_2$	1.426	2.103	—	94.17^c	103.33^d	0.30	−37.024699
PH_2CH_3	1.426^a	1.881	93.46	97.64^b	—	0.05	−15.192604
HCN	1.968	—	—	—	—	0.28	−16.137920
HCl	1.287	—	—	—	—	−0.20	−15.534094
HF	0.926	—	—	—	—	−0.38	−24.797507

[a] Averaged bond length.
[b] Averaged angle.
[c] HLCl averaged.
[d] CLCl angle.
[e] L = attached atom.

larger in the AuH_2S^+ complex than in the AuH_2O^+ complex. In making the covalent bond with Au^+ the sulphur may utilize one of its two lone-pairs. In the planar structure H_2S interacts with Au^+ using its σ non-bonding orbital, whereas in the pyramidal structure the sulphur uses a π non-bonding orbital. Because the interacting orbitals, the empty gold 6s orbital and the ligand π orbital are closer in energy, this interaction is stronger and the bond formed is stronger. Although the energy difference between the planar and the non-planar structures in $AuOH_2^+$ complex is small ($1-2$ kcal mol^{-1}) it is still interesting to speculate about its origin. It may also result from a small covalent contribution in the $Au-O$ bond, or, as Schultz and Armentrout[26] have suggested, that in the non-planar structure the repulsion between the electrons in the d orbitals of Au^+ and the non-bonding orbitals on H_2O is minimized.

The bond lengths to the central atom in the free ligands are slightly shorter than in the complexes. This is true for all of the ligands except for phosphine. For example, for the amine series of complexes $AuNH_3^+$, $AuNH_2CH_3^+$ and $AuNH(CH_3)_2^+$ the average $r(N-H)$ values are 1.022, 1.022 and 1.021 Å, while in the free ligand this distance is 1.019 Å. The calculated $r(N-C)$ values for NH_2CH_3 and $NH(CH_3)_2$ are 1.512 and 1.509 Å, while in the free ligand the distances are 1.477 and 1.470 Å, respectively. In contrast, for the phosphine complexes the $r(P-H)$, $r(P-C)$ and $r(P-Cl)$ bond lengths become shorter by complexation. The $r(P-H)$ in PH_3 is 1.425 Å and 1.405 Å in the complex (somewhat longer than the value of 1.401 Å found by Schwerdtfeger and coworkers)[8]. In PH_2CH_3 as a ligand, the P−H distance changes from 1.426 Å in the bare ligand to 1.406 Å in the complex, and the $r(P-C)$ distance decreases from 1.881 Å to 1.831 Å. The changes in the P−Cl distances by complexation are relatively small for the two phosphine ligands containing chlorine.

It is worthwhile to compare the structural changes caused by Au^+ complexation with those brought about by protonation. It is clear that this comparison cannot be taken too far

due to the strong relativistic effects in gold and the presence of the filled d shells. The latter could result in $3d \rightarrow \pi^*$ back bonding and introduce M^+–L closed shell repulsion, which are not possible in a proton. Examination of the optimized geometries of the protonated ligands in Table 4 shows the same pattern described above for AuL^+. This similarity clearly suggests that the calculated trends in the ligand bond lengths to the central atom are due mainly to the nature of the central atom of the ligand.

The fact that the bond lengths to the central atom in the phosphine ligand behave differently than those to the other ligands might originate from the differences in the electronic structures of the free ligands. PH_3 has a smaller calculated HPH angle (93.3°) than <HNH (106.0°) in NH_3. The ammonia molecule has nearly a tetrahedral structure, while the P–H bonds in the PH_3 molecule are almost unhybridized phosphorous p orbitals. Therefore, complexation with either a proton or Au^+, which gives near-tetrahedral structures (Table 1), causes greater ligand orbital changes in PH_3 than in NH_3. Since the non-bonding electrons in free PH_3 consist of mainly s character, and the P–H and P–C bonds consists of mainly p character, hybridization increases the s orbital contribution in the P–H and P–C bonds. Consequently, the ligand bond distances in the complex shorten. For the ligands where the central atom is O, S or N, the bonds of the central atom are already hybridized in the free ligand, as can be deduced from the bond angles: $<$ HOH $= 104.5°$ in water, $<$ HNH $= 106.0°$ in NH_3 and $<$ CSC $= 99.5°$ in $S(CH_3)_2$. Hence, formation of the Au^+/H^+ complex can cause only smaller changes in the hybridization of their bonding orbitals.

The binding energy is defined as the energy of the dissociation process: $AuL^+ \rightarrow Au^+ + L$. All the calculated complexes were found to be stable with respect to the dissociation defined above. This dissociation is preferred relatively to the charge transfer dissociation which produces $Au + L^+$, since the ionization potential (IP) of gold, $IP(Au) = 9.23$ eV[27], is smaller than those of the ligands, which are in the 9.3–12.6 eV range[28].

The covalent contribution to the Au^+–ligand bond is governed by the interaction of the non-bonded electrons in the ligand with the empty orbitals of Au^+. This interaction is described in short as: $L \rightarrow M$. In Au^+ there is a relatively small difference of only 2.25 eV[19] between the filled d_{z^2} orbital and the unfilled valence shell s orbital ($d \rightarrow s$

TABLE 4. Optimized geometries, charges and energies of the protonated ligands LH^+

Ligand–H^+	Bond lengths (Å)		Angles (deg)		Charge $q(L)$	Energy (a.u.)
	$L–H^b$	$L–C^b$	HLH^b	HLC^b		
H_3O^+	0.985	—	112.16	—	−0.29	−17.466026
$OH_2CH_3^+$	0.980	1.543	109.54	113.99	−0.17	−24.339232
NH_4^+	1.028	—	109.45	—	−0.47	−12.062595
$NH_3CH_3^+$	1.026^a	1.528	107.52	111.37	−0.38	−18.931221
$NH_2(CH_3)_2{}^+$	1.025	1.518	106.13	108.86	−0.27	−25.797745
H_3S^+	1.363	—	94.08	—	0.19	−11.635829
$SH_2CH_3^+$	1.358^a	1.864	96.70	99.83	0.25	−18.521258
$SH(CH_3)_2{}^+$	1.355	1.842	—	99.14	0.35	−25.404323
PH_4^+	1.403	—	109.48	—	0.29	−8.633034
$PH_3CH_3^+$	1.404^a	1.813	106.79	112.00	0.42	−15.527376
H_2Cl^+	1.319	—	94.56	—	0.31	−15.753962
H_2F^+	0.973	—	113.21	—	−0.08	−24.992973

^{a} Averaged bond length.
^{b} L = Attached atom.

excitation energy), which permits extensive hybridization of the d_{z^2} and s orbitals. Consequently, the orbital on Au^+ that interacts with the ligand non-bonded electrons is a combination of $5d_{z^2}$ and $6s$.

The bond dissociation energies (BDEs) of $Au-L^+$ complexes follow the order $H_2O < H_2S < NH_3 < PH_3$ with values of 40.0, 58.4, 66.0 and 75.2 kcal mol^{-1}, respectively (Table 2). The calculated trend is also found experimentally[29] in the gas phase and in solution, and is nicely exemplified by the $Ph_2PCH_2NPh_2$, diphenylphosphino-diphenylamino-methane ligand. This bidentate ligand can bond either through the phosphorous or the nitrogen atom to a metal ion. In solution, only the P–monodentate complex is formed in accordance with the calculated binding energy order. The observed order of BDE correlates with the ionization potentials (IPs) of the ligands which are 12.6, 10.4, 10.2 and 9.98 eV[28], respectively. As the IP of the ligand decreases, the bond between the metal ion and the ligand becomes stronger. Therefore, substitution of the ligand by methyl — an electron-donating group — strengthens this interaction, and the binding energy becomes higher. Two methyl groups will have an even greater influence. For example, the BDEs for $Au-NH_3^+$, $Au-NH_2CH_3^+$ and $Au-NH(CH_3)_2^+$ are 66.0, 71.6, and 74.0 kcal mol^{-1}, respectively. The same trend exists for substituted phosphines and sulphides. Substitution by chlorine lowers the donating ability of the ligand and the $L \rightarrow M$ interaction is diminished. The calculated BDEs of $AuPH_3^+$, $AuPH_2Cl^+$ and $AuPHCl_2^+$ are 75.2, 70.7 and 65.5 kcal mol^{-1}, respectively.

Figure 1 shows a plot of the BDE for the protonated complexes vs. BDE for the Au^+ complexes. The data points fall on two lines, one for the second and the other for the third row elements. The slopes of the two lines are 1.55 and 1.16, respectively, indicating a higher sensitivity to ligand in the protonated complexes than in those of Au^+. One can also see that for the same substituents on the central atoms, higher BDEs are obtained for S than for O, and for P than for N ligands in complexation with Au^+. This trend of
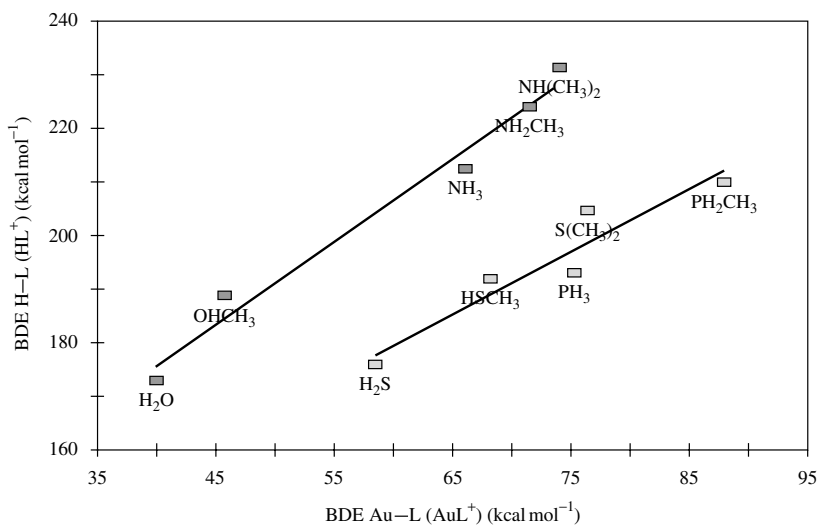
FIGURE 1. BDE of Au–L vs BDE of H–L in kcal mol^{-1}

stronger bonding by the third row element ligands with Au^+ is not found in the bonding to H^+.

A good measure of the L $\rightarrow$ M interaction is the charge on Au, $q(Au)$, calculated by the Mulliken population method. As $q(Au)$ becomes smaller the covalent interaction is presumed to be stronger. The trend found in $q(Au)$ correlates with the BDE in a series as expected. As $q(Au)$ become less positive, the BDE increases. For example, $q(Au)$ values for $AuNH_3^+$, $AuNH_2CH_3^+$ and $AuNH(CH_3)_2^+$ are 0.66, 0.60 and 0.54, respectively, and the BDE values are 66.0, 71.6 and 74.0 kcal mol^{-1}. Substitution of the phosphine ligand by chlorine does not cause a significant change in $q(Au)$, contrary to expectation.

In summary, the charges on Au in the complexes (which correlate with the ionization potential of the ligand) and the difference in planarization energies between sulphur and oxygen ligands strongly suggest that third row element bonding to Au^+ is more covalent than that of the corresponding second row elements.

Another criterion which is usually used to evaluate bond strength is bond distance. Perhaps one of the most universally accepted tenets in chemistry is that a shorter bond of a given type reflects a stronger bond. Examining this 'rule' in our case reveals that it holds nicely in the Au$-$L$^+$ complexes for amines, sulphides and oxides. Here, substitution of a remote atom on the ligand by an electron-donating group strengthens the metal$-$ligand bond and the Au$-$L distance becomes shorter. A different picture is obtained for phosphine ligands. Substitution of hydrogen by methyl gives much higher BDE values, as expected, but the bond distance $r(Au-P)$ remains almost the same. Substitution by chlorine gives lower BDEs but, again, no significant change in the Au$-$P bond length is observed. Similar results for phosphine were obtained by Rosch and coworkers[30], who calculated the structures and energies of the $[Au-PH_3]^+$ and $[Au-P(CH_3)_3]^+$ complexes, and found that the BDEs are 95.8 and 132.2 kcal mol^{-1}, respectively, while the corresponding Au$-$P bond distances are 2.29 Å and 2.25 Å, respectively. This anomalous behaviour exists also in other metal ion complexes with phosphine ligands. It was found experimentally[31] that the Ti$-$P bond lengths in TiL$^+$ complexes increase in the order $PF_3 < P(OEt)_3 < P(CH_3)_3$, while the bond dissociation energies display the opposite trend. A similar effect is found also in the protonation of phosphines. The protonation energy of PH_3 and PH_2CH_3 is 192.8 and 210.1 kcal mol^{-1}, respectively, while the P$-$H bond distances remain nearly constant, 1.403 Å in PH_4^+ and 1.404 Å in $PH_3CH_3^+$. A possible explanation of the different BDEs and Au$-$P bond length trends may be found in the contribution of the s and p atomic orbitals on the phosphorous atom to the Au$-$P bond. Upon binding to Au^+, ligand rehybridization occurs that increases the p character in the interacting lone-pair orbital of the phosporous atom. This mixing raises the energy of the non-bonding orbital of the phosphorous, bringing it closer to the interacting Au^+ valence s orbital[32]. As a result, a stronger bond is obtained as well as a lengthening of the Au$-$P bond due to the larger size of the phosphine p orbital. This mixing depends on the phosphine substituents. The following percentages for phosphorous s-orbital contributions in the Au$-$P molecular orbital are calculated: 15.7, 18.1, 26.5 and 35.2% in $AuPH_2CH_3^+$, $AuPH_3^+$, $AuPH_2Cl^+$ and $AuPHCl_2^+$, respectively. Thus, one should get a shorter and weaker Au$-$P bond when the phosphine is substituted by an electron-donating group.

III. AuX COMPOUNDS, X = NEGATIVELY CHARGED LIGAND

We have carried out similar calculations for AuX complexes where X$^-$ represents the following anions: F$^-$, OH$^-$, Cl$^-$, SH$^-$, PH$_2^-$ and CN$^-$. The optimized geometrical parameters, charges and binding energies are summarized in Table 5. The energies of the anions and their calculated proton affinities are given in Table 6.

TABLE 5. Bond lengths, angles, charges on atoms, dipole moments and BDEs for AuX complexes in the optimized geometry

AuX	Bond length (Å)			Angle (deg)		Charge		Total energy (a.u.)	Dipole moment (D)	BDE[b] (kcal mol^{-1})
	Au–X[e]	H–X[e]	C–X[e]	AuXH	AuXC	q(Au)	q(X)[e]			
AuOH	1.994	0.971	—	103.80	—	0.31	−0.60	−152.655333	2.79	241.1
AuOCH$_3$	2.004	—	1.420	—	116.09	0.31	−0.35	−159.503074	2.07	221.9
AuNH$_2$	2.019	1.026[a]	—	102.91	—	0.22	−0.73	−147.199550	1.69	260.6
AuNHCH$_3$	2.027	1.023	1.477	102.00	113.40	0.16	−0.57	−154.049415	1.16	252.3
AuSH	2.294	1.352	—	94.91	—	0.17	−0.28	−146.873363	2.41	220.0
AuSCH$_3$	2.295	—	1.846	—	104.28	0.11	−0.11	−153.731909	2.01	225.1
AuPH$_2$	2.327	1.430[a]	—	95.56	—	0.01	−0.07	−143.855821	1.11	240.2
AuPHCH$_3$	2.333	1.430	1.883	95.75	103.42	−0.04	0.15	−150.722191	1.11	246.9
AuF	1.974	—	—	—	—	0.45	−0.45	−160.262476	4.34	218.5
AuCl	2.289	—	—	—	—	0.31	−0.31	−151.046052	3.87	197.2
AuCN	1.950	—	1.160[c]	—	179.90[d]	0.33	0.16	−151.644153	6.08	211.2

[a] Averaged bond length.
[b] BDE bond dissociation energy of the Au–L bond.
[c] N–C bond distance.
[d] <AuCN.
[e] X = attached atom.

Tova Hoz and Harold Basch

TABLE 6.   Proton affinity of ligands

X^-	Energy (a.u.)	Proton affinity (kcal mol^{-1})
F^-	-24.173050	391.8
Cl^-	-14.990574	341.1
CN^-	-15.566479	349.6
OH^-	-16.529901	414.5
OCH_3^-	-23.408292	395.2
NH_2^-	-11.043071	427.2
$NHCH_3^-$	-17.906271	419.1
SH^-	-10.781683	360.0
SCH_3^-	-17.632002	366.2
PH_2^-	-7.723349	372.7
$PHCH_3^-$	-14.580722	383.9

   AuF is one of the complexes previously calculated using all-electron relativistic MRCI calculations[16]. The Au−F bond length found was 1.946 Å and a binding energy of 66.2 kcal mol^{-1} was calculated for homolytic cleavage; these values indicate a shorter and stronger bond than what we calculate at 1.974 Å and 60.4 kcal mol^{-1}, respectively. For AuCl[7] a bond distance of 2.278 Å and 58.0 kcal mol^{-1} for homolytic cleavage were calculated, and our results are 2.289 Å and 59.1 kcal mol^{-1}, respectively.

   The binding energies for AuX heterolysis are about 2−3 times larger than for the charged complexes Au$^+$−L. A correlation between the gas-phase protonation energy of X^- to form H−X and the gas-phase binding energies for the corresponding Au−X complexes is shown in Figure 2. Except for X^-=CN$^-$ two lines can be distinguished, one belonging to second row element ligands and the other to third row element ligands. Bonding of X^- to the hydrogen cation in the gas phase is stronger within a column and identical substituents for elements of the second row. In general, with the exception of
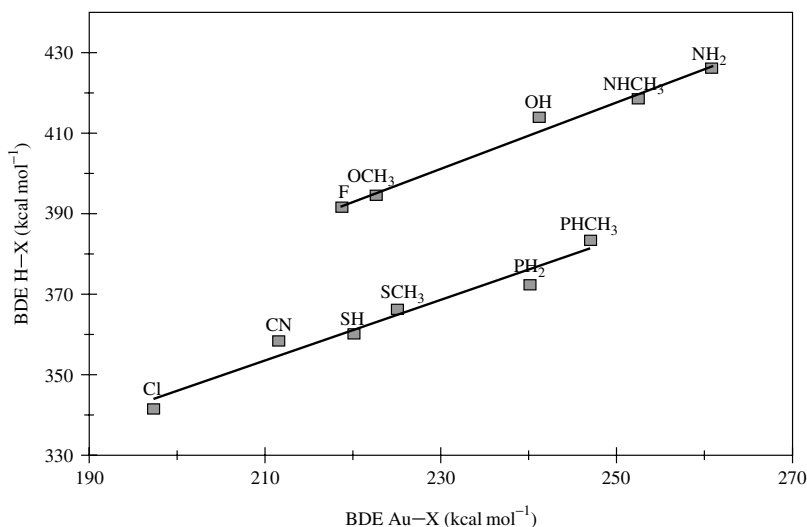
FIGURE 2. BDE of Au−X vs BDE of H−X in kcal mol^{-1}

the OCH_3 and SCH_3 pairs, this holds also for bonding to Au^+. Within each row binding becomes weaker as the group number increases, except for CN^- which forms weaker bonds both to a proton and to the metal ion.

It was shown by Schwerdtfeger and coworkers[7] that the Au$-$X bond is destabilized by electronegative ligands and stabilized by electropositive ligands. Accordingly, one should expect that methyl substitution of the ligand will stabilize the Au$-$X bond. However, Table 5 shows that although methyl substitution strengthens the Au$-$X binding energy in sulphides and phosphines, it lowers the binding energies for oxides and amines. This effect of methyl substitution on BDE is found also for the protonation of X^- (Table 6), and parallels the acidity of those ligands in the gas phase, as shown in Figure 2.

The Mulliken charges on $Au[q(Au)]$ are, as expected, smaller in the (AuX) neutral complexes than in the (AuL^+) charged ones due to a better $L \rightarrow M$ interaction in the latter. Methyl substitution lowers $q(Au)$ in the two systems, as expected.

The Au$-$X bond lengths in the charged AuL^+ are expected to be longer than in the neutral complexes AuX, since the Au$-$X interaction is stronger between two ions, Indeed, this relation exists for all the ligands except for phosphines in which the bond distances are longer in the neutral complex than in the AuL^+ complex. The reason is that in the charged complex the phosphines adopt a tetrahedral geometry, and the phosphorous atom has shorter bonds in the tetrahedral hybridization and longer ones when it is bonded to three atoms without hybridization, as mentioned above.

IV. $LAuL'^+$ COMPLEXES

A computational study was also carried out on gold(I) with two neutral ligands where $L, L' = H_2O, NH_3, NH_2CH_3, H_2S, S(H)CH_3, S(CH_3)_2, PH_3, PH_2CH_3, PH_2Cl$ and $PHCl_2$.

The optimized geometries for the $LAuL'^+$ complexes, atomic charges, and total and binding energies are summarized in Tables 7 and 8. The energetics of exchanging ligands will be discussed.

TABLE 7. Bond lengths and angles in geometrically optimized $LAuL'^+$ complexes

$LAuL'^+$	Bond length (Å)[a]					Angle (deg)			
	Au$-$L[c]	Au$-$L'[c]	H$-$L[c]	H$-$L'[c]	L'$-^c$C	L^{c}AuL'[c]	AuL^{c}H	AuL'H[c]	AuL'C
PH_3AuPH_3	2.366	2.366	1.407	1.407	—	179.88	116.00	116.00	—
PH_3AuH_2S	2.327	2.425	1.407	1.354	—	177.78	115.60	98.46	—
PH_3AuH_2O	2.275	2.180	1.406	0.971	—	179.38	115.37	117.92	—
PH_3AuNH_3	2.302	2.148	1.407	1.021	—	179.72	115.73	111.65	—
$PH_3AuNH_2CH_3$	2.305	2.147	1.407	1.021	1.510	179.74	115.97	108.06	116.60
$PH_3AuS(H)CH_3$	2.330	2.408	1.407	1.352	1.858	176.93	115.68	99.08	107.05
$PH_3AuS(CH_3)_2$	2.334	2.400	1.407	—	1.843	176.45	116.00	—	106.65
H_2SAuH_2S	2.359	2.359	1.342	1.342	—	179.99	99.14	99.14	—
$H_2SAuH_2S^b$	2.365	2.365	1.341	1.341	—	180.00	127.95	127.95	—
NH_3AuH_2S	2.119	2.354	1.021	1.355	—	177.73	111.26	99.44	—
H_2SAuH_2O	2.328	2.160	1.356	0.971	—	178.04	98.96	116.90	—
NH_3AuNH_3	2.091	2.091	1.021	1.021	—	179.85	111.40	111.40	—
NH_3AuH_2O	2.069	2.125	1.021	0.971	—	178.82	111.26	116.05	—
H_2OAuH_2O	2.114	2.114	0.972	0.972	—	179.95	115.17	115.17	—
$H_2OAuH_2O^b$	2.104	2.104	0.968	0.968	—	180.00	124.60	124.60	—

[a] Average bond length.
[b] Planar structure.
[c] L,L' = Attached atom.

Tova Hoz and Harold Basch

TABLE 8. Total energies, charges and bond dissociation energies to $AuL^+ + L'$ or $AuL'^+ + L$ of optimized complexes $LAuL'^+$

$LAuL'^+$	Charge			Energy (a.u)	Binding energy (kcal mol^{-1})	
	$q(Au)$	$q(L)^b$	$q(L')^b$		BDE (Au−L)	BDE (Au−L')
PH_3AuPH_3	0.15	0.06	0.06	−152.596155	52.4	52.4
PH_3AuH_2O	0.35	0.09	−0.52	−161.435979	72.1	36.9
PH_3AuNH_3	0.35	0.05	−0.71	−155.998837	64.5	55.3
$PH_3AuNH_2CH_3$	0.33	0.04	−0.59	−162.853781	61.8	58.3
PH_3AuH_2S	0.25	0.05	−0.07	−155.610774	59.6	42.8
$PH_3AuS(H)CH_3$	0.23	0.04	0.06	−162.481147	56.4	49.5
$PH_3AuS(CH_3)_2$	0.20	0.03	0.22	−169.351931	53.6	54.7
NH_3AuH_2S	0.42	−0.72	−0.07	−159.009157	59.8	52.2
NH_3AuNH_3	0.51	−0.71	−0.71	−159.396728	64.3	64.3
NH_3AuH_2O	0.51	−0.68	−0.52	−164.828546	68.6	42.6
H_2SAuH_2S	0.42	−0.12	−0.12	−158.622195	48.0	48.0
$H_2SAuH_2S^a$	0.40	−0.12	−0.12	−158.564280	11.6	11.6
H_2SAuH_2O	0.42	−0.04	−0.52	−164.442549	57.4	39.0
H_2OAuH_2O	0.55	−0.50	−0.50	−170.256074	44.2	44.2
$H_2OAuH_2O^a$	0.60	−0.50	−0.50	−170.252810	42.1	42.1

[a]Planar structure.
[b]L,L' = attached atom.

The angle between the attached atom of the ligand, the gold atom and the attached atom of the second ligand is around 180° in all these complexes. This geometry is achieved by hybridization of the s, p and d atomic orbitals of gold[33]. The mixing of the $5d_{z^2}$ and 6s orbitals on gold, as described above, gives two orbitals $\Psi_1 = s − d_{z^2}$ and $\Psi_2 = s + d_{z^2}$. The electron pair initially in the d_{z^2} can occupy Ψ_1 whose lobes are concentrated in the xy-plane away from the ligands. Further hybridization of Ψ_2 with $6p_z$ gives two orbitals with lobes concentrated along the $\pm z$-axes, which can then accept electron pairs from the ligands and form the linear complexes. With some ligands π-bonding is also possible between an occupied d orbital on gold and either a π^* or low-lying 3d atomic orbital on the ligand.

The substituents on the attached atoms of the two ligands in the $LAuL'^+$ complexes may adopt an eclipsed or a staggered conformation. In all the cases studied here, there was essentially no energy preference; the barrier for rotation was calculated to be less than 0.01 kcal mol^{-1}. This result is probably due to the long L−L' distances.

The symmetric $LAuL^+$ complexes with H_2O or H_2S as ligands may adopt one of several conformations: a planar one with D_{2h} symmetry, or a non-planar conformation with either C_{2v} symmetry where the two sets of substrates are parallel, or C_{2h} symmetry where the two substituents are antiparallel (cf Figure 3). As mentioned above, the two non-planar conformations, corresponding to eclipsed and staggered, have the same energy. However, there is a significant difference between the planar and non-planar conformations. When the ligands are H_2O or H_2S, the difference between the two conformations is 2.0 and 36.3 kcal mol^{-1}, respectively. These differences are manifested in the charges on Au, $q(Au)$. In the planar complexes $q(Au)$ is larger than in the non-planar complexes, indicating a stronger L → M interaction in the non-planar complex. The explanation for this phenomenon is the same as for AuL^+ given above.

Binding energies were calculated for the two possible heterolytic cleavages shown in equation 2:
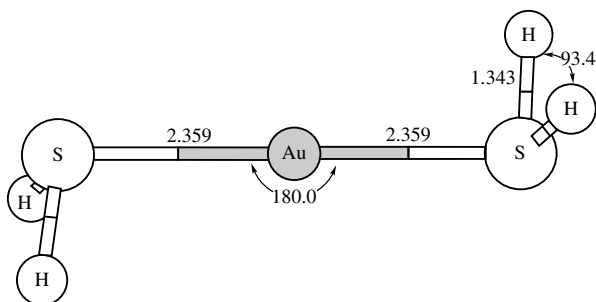
FIGURE 3. The stable structure of $Au(H_2S)_2{}^+$. Bond lengths in ångströms, angles in degress

$$LAuL'^+ \longrightarrow AuL^+ + L' \quad \text{or} \quad AuL'^+ + L \qquad (2)$$
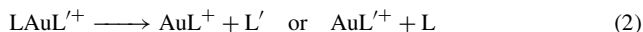
Comparison of the BDE values for complexes with one neutral ligand AuL^+ summarized in Table 2, with the BDE values of $LAuL^+$ complexes in Table 8 shows that, in general, all the $Au-L$ bonds become weaker by the presence of a second ligand, except in the complexes where $L' = L = H_2O$ or $L = NH_3$, and $L' = H_2O$, which will be discussed separately. This influence of one ligand on the strength of the bond to the ligand that is *trans* to it is called the *trans* effect[34]. The smaller binding energy of the second neutral ligand with AuL^+ results from the smaller positive charge on the mono-ligated Au. The *trans* effect is attributable to the fact that the two *trans* ligands both depend on the participation of the same metal orbital, and the more one bonded ligand preempts this orbital, the weaker will be the bond to the other ligand. For $PH_3AuPH_3{}^+$ the BDE of the first cleavage is 52.4 kcal mol^{-1}, and breaking the second $AuPH_3{}^+$, bond requires 75.2 kcal mol^{-1}; the difference of 22.8 kcal mol^{-1} is the lowering in BDE caused by the PH_3 ligand. The calculated sequence of BDE lowering of the second ligand (the *trans* influence) is: $PH_3 > H_2S > NH_3 > H_2O$. The origin of this sequence is probably the different character of the interaction of Au^+ with the bonded ligand when the attached atom is from the third row in the Periodic Table. These $Au-L$ bonds have significant covalent character causing the formation of a weaker second bond to gold(I).

When the attached atom on one ligand is substituted by a methyl group — an electron-donating group — its *trans* influence increases. Since the substituted ligands form stronger bonds, their ability to weaken the bond to the second ligand is greater. For example, substituting methyl on NH_3 changes the BDE of PH_3 from 64.5 to 61.8 kcal mol^{-1}; substitution on H_2S reduces the PH_3 BDE from 59.6 to 56.4 kcal mol^{-1}.

When both ligands have their attached atom from the second row: $L = H_2O$ or NH_3, the BDE of the $LAu-L'$ cleavage is stronger than for Au^+-L'. The higher BDE values in these cases are in agreement with the shorter bond distances of these ligands to Au^+ (Table 7), as compared with the distances found in AuL'^+ (Table 1) complexes. The BDE increases for the binding of the second H_2O ligand to AuH_2O^+ or to $AuNH_3{}^+$ (Table 8) in comparison with the binding of H_2O with Au^+ (Table 2). This trend is also found for the ligation of NH_3 to AuH_2O^+, but not with NH_3 to $AuNH_3{}^+$ in comparison with the binding of NH_3 with Au^+. The enhanced binding energy of the second ligand is experimentally[35–38] well known for the first row transition metal positive ions. It is suggested that the first H_2O-Au^+ interaction is electrostatic in origin, and in order to minimize repulsion the metal ion and H_2O reorient their non-bonding orbitals. But

when two ligand molecules approach from opposite sides they share the cost of s−d hybridization[35] of the forming stronger and shorter bonds. It will be interesting to confirm experimentally our finding for $Au(H_2O)_2{}^+$ and $H_2OAuNH_3{}^+$.

The Au−L bond lengths in $LAuL'^+$ complexes (Table 7) are longer than in the AuL^+ complexes (Table 1), except when $L' = H_2O$. In $LAuL'^+$ complexes the Au is spd-hybridized[32], while in AuL^+ complexes the gold's 6p atomic orbital does not participate in the binding[7], resulting in the above trend in the bond lengths.

The energetics (AE) of exchanging neutral ligands was also examined. There are two possible reactions: reaction with a neutral ligand (equation 3) and reaction with an anion (equation 4).

$$LAuL'^+ + L'' \longrightarrow L''AuL'^+ + L \quad \text{or} \quad LAuL''^+ + L' \qquad (3)$$

$$LAuL'^+ + X^- \longrightarrow XAuL + L' \quad \text{or} \quad XAuL' + L \qquad (4)$$
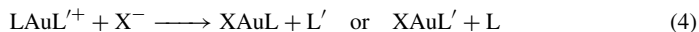
By examining the binding energies in Table 8, the following conclusions are obtained concerning equation 3. The lowest reaction energy is found by exchanging PH_3 by NH_3, or *vice versa*. Both ligands form strong bonds with Au^+, and $\Delta E = 2.9$ to -3.4 kcal mol^{-1}. Exchanging H_2O by PH_3 or NH_3 gives the most exothermic reaction since H_2O binds weakly to gold, and $\Delta E = -20.6$ to -27.9 kcal mol^{-1}. Exchanging H_2S by PH_3 or by NH_3 has $\Delta E = -9.6$ to -14.6 kcal mol^{-1}. The importance of this exchange will be discussed in the following section.

Concerning equation 4, exchanging a neutral ligand by an anion forms a very strong Au−X bond. The next section deals with XAuL-type complexes.

V. XAuL COMPLEXES

A study of the series of neutral complexes of the general type XAuL, where the ligand (L) is PH_3, NH_3, H_2S and H_2O, and X^- stands for the anions, F^-, Cl^-, HO^-, HS^- and CN^-, was performed. The geometry of these complexes was optimized and the parameters obtained are summarized in Table 9. The optimal energies, the charges on atoms and the ligand binding energies are shown in Table 10.

The angle between the central atom in the ligand (L), Au and the atom of X bonded to gold is close to $180°$. Upon complexation a non-planar conformation is obtained, as shown above for the $LAuL'^+$ structures.

The ligand attached to AuX in the complex XAuL has a marked influence on the Au−X bond. The energy of the Au−X bond in the XAuL complex (Table 10) is lower than in AuX (Table 2). The attenuation of the Au−X bond strength decreases in the order: $PH_3 > NH_3 \sim H_2S > H_2O$. The magnitude of the effect is very significant, and the highest value is reached in $HSAuPH_3$ where PH_3 decreases the Au−SH binding energy by 39.1 kcal mol^{-1}. The fact that NH_3 has almost the same effect as H_2S on the Au−X bond binding energies is surprising, since H_2S has a larger (*trans*) effect in reducing energies in $LAuL'^+$ complexes as shown above. Since the NH_3 and H_2S ligands have a similar effect on Au−X bond energies, one would expect similar values for the Mulliken charges on Au, and a similar effect on the Au−X distances, However, for all the (X^-) anions, $q(Au)$ in the NH_3 complexes are higher than for the H_2S complexes, while the bond lengths $r(Au-X)$ are shorter in NH_3 complexes than in the H_2S complexes. These apparently inconsistent results call for further investigation.

Substitution of the ligand (L) by electron-withdrawing groups weakens the Au−L bond, as we have shown above, and strengthens the Au−X bond. The contrary is found when the ligand is substituted with electron-donating groups. Rosch and coworkers[30] calculated

TABLE 9. Bond lengths and angles (deg) of geometrically optimized XAuL complexes

XAuL	Bond length (Å)[a]				Angle (deg)			
	Au−X[c]	Au−L[c]	H−L[c]	C−L[c]	XAuL	HLH[b]	AuLH[b]	AuLC
HOAuPH₃	1.995	2.266	1.412	—	176.50	99.22	118.50	—
HOAuH₂S	1.986	2.334	1.354	—	174.40	92.42	102.51	—
HOAuH₂O	1.970	2.185	0.970	—	175.66	106.32	108.30	—
HOAuNH₃	1.979	2.116	1.019	—	175.95	107.89	111.05	—
ClAuNH₃	2.289	2.127	1.019	—	179.94	107.94	110.94	—
ClAuH₂O	2.274	2.200	0.970	—	179.99	106.25	109.42	—
ClAuH₂S	2.299	2.351	1.354	—	178.89	92.51	100.84	—
ClAuPH₃	2.312	2.277	1.411	—	179.99	99.66	118.05	—
ClAuPH₂Cl	2.306	2.262	1.411	2.070	177.63	99.44	117.62	118.74
ClAuPHCl₂	2.301	2.257	1.409	2.060	177.75	98.51	118.90	116.75
ClAuPH₂CH₃	2.317	2.279	1.412	1.846	179.66	98.95	115.56	118.40
HSAuNH₃	2.304	2.176	1.018	—	178.52	107.84	111.36	—
HSAuH₂O	2.286	2.247	0.969	—	179.22	106.21	109.39	—
HSAuH₂S	2.313	2.400	1.353	—	176.61	92.64	101.14	—
HSAuPH₃	2.332	2.317	1.413	—	178.30	99.09	117.79	—
FAuNH₃	1.959	2.083	1.019	—	179.94	107.84	111.06	—
FAuH₂O	1.951	2.150	0.970	—	179.78	106.41	108.97	—
FAuH₂S	1.968	2.305	1.355	—	178.81	92.39	101.75	—
FAuPH₃	1.974	2.240	1.411	—	179.94	99.76	117.93	—
CNAuNH₃[d]	1.966	2.149	1.019	—	179.89	107.70	111.13	—
CNAuH₂O[d]	1.949	2.198	0.970	—	179.96	106.54	111.52	—
CNAuH₂S[d]	1.984	2.399	1.353	—	178.64	92.79	99.94	—
CNAuPH₃[d]	2.009	2.328	1.411	—	179.93	99.79	118.00	—

[a] Average bond length.
[b] Average angle.
[c] L = attached atom.
[d] A cyanide complex.

the binding energy of Au−PR₃ in PR₃AuCl for R = H and CH₃ and found values of 52.6 and 64.3 kcal mol⁻¹, respectively. His values are higher than ours, but the overall picture is the same.

The ligand (L)−metal ion bond in XAuL complexes is subjected to the influence of X. In general, the XAu−L bond (Table 10) is weaker than in Au−L⁺ (Table 2). The order of weakening of the Au−L bond depends on the electronegativity of X. As the electronegativity of the X anion increases, the weakening effect on the Au−L binding energies decreases. When the ligands are H₂O or NH₃, the Au−L bond weakening order is: HS⁻ > Cl⁻ ∼ OH⁻ > CN⁻ > F⁻, and when the ligands are PH₃ or H₂S, the order is: HS⁻ > CN⁻ > Cl⁻ ∼ OH⁻ > F⁻. The greatest weakening is for HSAu−PH₃, where the BDE for the Au−PH₃ bond in this complex is 36.1 kcal mol⁻¹, while the BDE of the Au−PH₃⁺ bond is 75.2 kcal mol⁻¹. As was mentioned above, the Au−X bond where X belongs to a second row element has a larger ion−dipole interaction than when X belongs to the third row. Therefore, the bonding of a neutral ligand to gold to create XAuL is less affected when X is a second row element than a third row element. The CN⁻ ligand exhibits exceptional behaviour.

A comparison of the *trans* influence of either a neutral ligand (L′) or an anion (X⁻) on the cleavage of the Au−L bond in the XAuL and LAuL′⁺ complexes can be carried out. Comparing the binding energy of Au−L⁺ for a certain ligand (L) with the BDE of the same bond in XAuL complexes for all possible (X⁻) anions, or in LAuL′⁺ complexes

Tova Hoz and Harold Basch

TABLE 10. Total energies (E), charges (q) and bond dissociation energies (BDE)[a] for XAuL complexes.

XAuL	Charges on atoms			Energy		
	q(Au)	q(X)	q(L)	XAu−L BDE neutral (kcal mol^{-1})	LAu−X BDE ionic (kcal mol^{-1})	E (a.u.)
HOAuPH$_3$	0.18	−0.70	0.06	46.4	212.3	−161.055078
HOAuH$_2$S	0.24	−0.70	−0.12	34.6	217.3	−164.066231
HOAuH$_2$O	0.24	−0.67	−0.51	25.9	227.1	−169.887110
HOAuNH$_3$	0.27	−0.70	−0.70	41.6	216.7	−164.445591
ClAuNH$_3$	0.27	−0.43	−0.73	41.6	172.8	−162.836204
ClAuH$_2$O	0.21	−0.37	−0.52	25.4	182.6	−168.276853
ClAuH$_2$S	0.23	−0.43	−0.15	34.4	173.2	−162.456588
ClAuPH$_3$	0.18	−0.41	0.00	46.2	168.2	−159.445421
ClAuPH$_2$Cl	0.18	−0.40	0.20	44.5	171.0	−173.788437
ClAuPHCl$_2$	0.18	−0.39	0.36	41.3	173.0	−188.136141
ClAuPH$_2$CH$_3$	0.17	−0.43	0.20	52.0	161.4	−166.321108
HSAuNH$_3$	0.20	−0.43	0.73	33.6	187.5	−158.650786
HSAuH$_2$O	0.14	−0.38	−0.51	20.3	200.3	−164.096179
HSAuH$_2$S	0.15	−0.16	−0.42	28.6	188.1	−158.271457
HSAuPH$_3$	0.11	−0.42	0.00	36.1	180.9	−155.256630
FAuNH$_3$	0.32	−0.51	−0.71	49.0	201.5	−172.064462
FAuH$_2$O	0.30	−0.47	−0.52	30.8	209.3	−177.501933
FAuH$_2$S	0.29	−0.51	−0.12	41.7	201.8	−171.684585
FAuPH$_3$	0.23	−0.50	0.05	55.2	198.5	−168.676061
CNAuNH$_3$[b]	0.25	0.12	−0.52	43.4	188.6	−163.437255
CNAuH$_2$O[b]	0.23	0.14	0.15	28.2	199.4	−168.879542
CNAuH$_2$S[b]	0.20	0.12	−0.17	33.1	185.9	−163.052693
CNAuPH$_3$[b]	0.15	0.13	−0.03	42.1	178.1	−160.037035

[a]BDE ionic: XAuL → AuL$^+$ + X$^-$+; BDE neutral: XAuL → AuX + L.
[b]A cyanide complex.

for all possible (L′) ligands always gives the relation that the BDE of Au−L is greater in the LAuL′$^+$ systems than in XAuL complexes. This means that anions have a higher *trans* weakening influence.

The Au−L bond lengths also depend on the type of complex. In XAuL complexes (Table 9), when the ligands are NH$_3$ or H$_2$O the Au−L distances are greater than in the Au−L$^+$ complexes (Table 1) for all the anions except F$^-$ (which lengthens the Au−L bond distance). When L = PH$_3$ or H$_2$S the anions of F, Cl, OH shorten the Au−L distance in comparison to their value in Au−L$^+$ complexes, but the SH and CN anions lengthen this bond. The maximum change in the bond length as a result of the presence of X is about 0.07 Å.

In the XAuL complexes the Au−X bond length depends on the ligand and decreases in the order: PH$_3$ > H$_2$S > NH$_3$ > H$_2$O. The maximum change in the Au−X bond lengths is about 0.04 Å. The smaller sensitivity of the Au−X bond lengths to change of the ligand (L) compared to the higher sensitivity of Au−L bond lengths with X substitution originates from the difference in the nature of these bonds. The Au−X bond is much stronger than the Au−L bond; therefore, the presence of L can be viewed as a small perturbation. The opposite is true for Au−L, which is much weaker and presumably has a shallower potential surface, as a result of which a small perturbation can cause more significant structural changes.

The XAuL complex can theoretically react in several ways: (I) exchange ligand (L) by another ligand (L$'$) (equation 5) or by an anion (Y$^-$) (equation 6); (II) exchange the anion (X$^-$) by another anion (Y$^-$) (equation 7) or by a ligand (L$'$) (equation 8).

$$XAuL + L' \longrightarrow XAuL' + L \qquad (5)$$

$$XAuL + Y^- \longrightarrow XAuY^- + L \qquad (6)$$

$$XAuL + Y^- \longrightarrow YAuL + X^- \qquad (7)$$

$$XAuL + L' \longrightarrow LAuL'^+ + X^- \qquad (8)$$
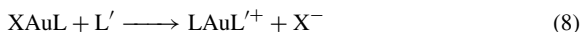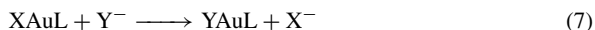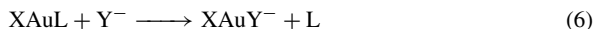
In order to establish which reaction is favoured and how the specific ligands and anions influence the reaction energy, a study of the energetics of each reaction was done comparing the effect of each component.

Exchanging a ligand by another ligand in XAuL complexes (equation 5) follows the same pattern as changing ligands in LAuL$'^+$ complexes. The sequence of BDE lowering is found to be L = PH$_3 \sim$ NH$_3 >$ H$_2$S $>$ H$_2$O, in accordance with the bond strengths of Au$-$L$^+$ compounds as was discussed above. Comparing the ease of changing a neutral ligand in the three types of complexes discussed so far shows that the energy required for exchange descends in the order: AuL$^+ >$ LAuL$'^+ >$ XAuL. In the AuL$^+$ system the maximum energy difference for changing ligands is for replacing H$_2$O by PH$_3$, where the energy difference between the two AuL$^+$ compounds is 35.2 kcal mol^{-1}. For the same ligand exchange in LAuL$'^+$ the energy difference is 27.9 kcal mol^{-1} and for XAuL, 24.4 kcal mol^{-1}.

The anions also influence the energetics of ligand exchange. The most exothermic reaction (equation 5) will be with X$^- =$ F$^-$ and the smallest exchange energy is for X$^- =$ HS$^-$. The overall order is: F$^- >$ OH$^- \sim$ Cl$^- >$ CN$^- >$ HS$^-$.

Changing a neutral ligand by an anion (equation 6) is a very exothermic reaction for all the anions, and the products XAuY$^-$ are known stable compounds, to be discussed in the next section.

Exchanging anions (equation 7) is a very important reaction. It is the basis of the medicinal activity of those compounds[39−42]. For example, the administered anti-arthritic drug (Et$_3$PAuCl) auranofin reacts with thio compounds in the form of albumin, thioglucose etc. to give thiolato(triethylphosphine)gold(I) complexes (Et$_3$PAuSR) by changing the anion. The best nucleophile among the anions examined here is OH$^-$, and the best leaving group is Cl$^-$. The exothermicity order is: Y$^- =$ OH$^- >$ F$^- >$ SH$^- >$ CN$^- >$ Cl$^-$. For the exchange reaction occurring in the bloodstream the reacting anions are in the form of HX and not as free anions, therefore the energetics of exchanging anions according to equation 9 was checked. The order of the reacting acids is: HCN $\sim$ HCl $>$ H$_2$S $>$ H$_2$O which is in accordance with the gas-phase acidity of these compounds. This correlation complements the previously known relationship between the affinities of the thiols RSH for gold(I) and their pK_{RSH}[43,44] values; the more acidic the thiol, the greater its affinity to gold(I).

$$XAuL + HY \longrightarrow YAuL + HX \qquad (9)$$
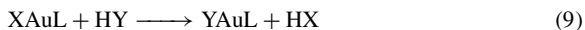
Changing an anion by a neutral ligand (equation 8) is a very endothermic reaction and it seems unreasonable to expect that to happen in these systems.

Summarizing our findings allows us to suggest an overall structure that is ideal for the various reactions. In order to exchange a neutral ligand, the best starting compound should be HSAuH$_2$O, since H$_2$O is the weakest bound ligand, and the SH group has the greatest weakening effect on Au$-$L bonds. In order to exchange an anion, the best

compound is $ClAuPH_3$, since chloride is the best leaving group and PH_3 weakens the Au–X bond most effectively.

VI. YAuX⁻ COMPLEXES

The most common structure observed for gold compounds in the +1 oxidation state is the linear AuX_2^- complex. AuF_2^- has not yet been reported, both $AuCl_2^-$ and $AuBr_2^-$ have been shown to dissolve in water with disproportionation to AuX_4^-, but AuI_2^- is stable in solution[45]. The $Au(CN)_2^-$ ion is probably the most stable Au(I) complex known[46,47] and has been studied in detail[7,45−47]. It has the largest dissociation energy of all calculated Au(I) compounds, which agrees with the experimental findings that it has a very large stability constant in aqueous solution.

There have been only a few theoretical studies of the AuX_2^- complexes. These complexes are linear[48]. Zwanziger and coworkers[49] studied the halide complexes of Au(I) using the semi-empirical SCCC method (self-consistent charge and configuration approximation). Schwerdtfeger and coworkers[8] studied in detail the relativistic effects in linear two-coordinated AuX_2^- complexes (X⁻ = H⁻, F⁻, Cl⁻, Br⁻, I⁻, CN⁻, SCN⁻, CH_3^-) using multi-electron adjusted non-relativistic and relativistic spin–orbit averaged pseudo-potentials within the Hartree–Fock (HF) approach. Configuration interaction (CI) calculations with single and double substitution were also performed for the halide complexes. Mason[50] studied ligand-to-metal charge-transfer transitions (LMCT) in several $Au(CN)_2^-$ complexes.

We have calculated the optimized geometries of XAuY⁻ complexes where X⁻, Y⁻ = F⁻, OH⁻, CN⁻, SH⁻ and Cl⁻, which are given in Table 11. Their XAu–Y⁻ and YAu–X⁻ binding energies and Mulliken charges are summarized in Table 12.

The resultant optimized geometries are in good agreement with experiment. For $Au(CN)_2^-$ the bond distance calculated for $r(Au-CN)$ is 2.021 Å, and the experimental value varies between 1.98 and 2.12 Å[51]. For $AuCl_2^-$ the calculated value for $r(Au-Cl)$ is 2.37 Å, which is slightly overestimated compared to the crystallographic distance of 2.28 Å[52].

All the complexes of the type XAuY⁻ are more stable than any combination of AuX and Y⁻. The binding energy of any anion (X⁻) to the neutral AuY molecule (equation 10)

TABLE 11.   Geometry of optimized complexes XAuY⁻

XAuY⁻	Bond length (Å)				Angle (deg)	
	Au–X	Au–Y	X–H	Y–H	AuXH	AuYH
FAuOH⁻	2.023	2.031	—	0.967	—	103.24
FAuF⁻	2.007	2.007	—	—	—	—
ClAuOH⁻	2.366	2.047	—	0.967	—	103.22
ClAuCl⁻	2.359	2.359	—	—	—	—
ClAuCN⁻	2.366	1.981	—	—	—	—
ClAuSH⁻	2.387	2.345	—	1.351	—	97.11
HOAuOH⁻	2.047	2.046	0.967	0.967	103.30	103.30
HSAuOH⁻	2.347	2.064	1.352	0.967	98.32	103.52
HSAuCN⁻	2.371	2.009	1.351	—	96.96	—
HSAuSH⁻	2.372	2.372	1.351	1.351	97.37	97.31
CNAuOH⁻ ᵃ	1.977	2.045	—	0.967	—	105.58
CNAuCN⁻ ᵃ	2.021	2.021	—	—	—	—

ᵃA cyanide complex.

TABLE 12.   Total energies, charges on atoms and binding energies for XAuY$^-$ complexes

XAuY$^-$	Charges			Energy		
	q(Au)	q(X)	q(Y)	BDE^a (kcal mol^{-1})	BDE$'^b$ (kcal mol^{-1})	Energy (a.u.)
FAuOH$^-$	0.06	−0.56	−0.73	93.0	115.6	−176.976558
FAuF$^-$	0.11	−0.55	−0.55	104.3	104.3	−184.601677
ClAuOH$^-$	0.05	−0.54	−0.74	67.8	111.7	−167.753901
ClAuCl$^-$	0.08	−0.08	−0.08	75.8	75.8	−166.157403
ClAuCN$^-$	0.08	−0.58	−0.08	82.5	96.5	−166.766266
ClAuSH$^-$	0.08	−0.57	−0.56	64.7	87.4	−161.967057
HOAuOH$^-$	0.02	−0.73	−0.73	103.4	103.4	−169.349987
HSAuOH$^-$	0.02	−0.54	−0.74	78.9	100.1	−163.562779
HSAuCN$^-$	0.04	−0.60	0.07	92.4	82.6	−162.571492
HSAuSH$^-$	0.06	−0.57	−0.57	75.0	75.0	−157.774503
CNAuOH^{-c}	0.04	0.09	−0.76	90.1	120.1	−168.365461
CNAuCN^{-c}	−0.03	0.06	0.06	98.4	98.4	−167.367495

^{a}BDE to AuY + X$^-$.
^{b}BDE$'$ to AuX$'$ + Y$^-$.
^{c}A cyanide complex.

is always smaller than the binding energy in the compound AuX (Table 5), and the corresponding bond lengths are longer in these complexes than in AuX compounds. One reason for this bond lengthening may be the additional negative charge on the AuX$_2^-$ compounds, which increase the Au(6s) population. This leads to a more diffuse Au(6s) orbital. The values for the atomic radius of the different ionization stages of Au are: $<r>_{Au^+} = 2.68$, $<r>_{Au} = 3.06$, $<r>_{Au^-} = 3.77^{53}$, therefore a more diffuse Au(6s) orbital should lead to larger gold–ligand bond distances.

$$\text{YAuX}^- \longrightarrow \text{Y}^- + \text{AuX} \qquad (10)$$

The identity of the first anion bonded to Au(I), X$^-$, has an influence on the binding energy of the second anion Y$^-$, bonded to AuX (a *trans* effect). The anions that strengthen the second bond to Au(I) are in the energy order: CN$^-$ > F$^-$ > Cl$^-$ > OH$^-$ > SH$^-$. As the electronegativity of the anion increases, its strengthening effect is larger. The Group VII elements have a bigger influence than the Group VI elements, and the second row elements of the Periodic Table strengthen the second bond more than the third period elements. There is no correlation between either the atomic charges on the Au, q(Au), or the binding energy of Au−X and the binding energy defined in equation 10.

The binding in Au(CN)$_2^-$ is explained as a dual interaction between Au(I) and CN$^-$. The CN$^-$ ligand can interact with the Au$^+$ with its σ orbital and with its π^* orbital. The involvement of the ligand π^* orbitals supports d participation in the gold–ligand bond^8. Thus the preferred sd hybridization gives rise to two interactions: one between the ligand σ orbital and the metal σ-hybrid atomic orbital (L → M) for short, and a second simultaneous back donation (M → L) of the metal and electrons of appropriate symmetry into the ligand π^* molecular orbital. The negative q(Au) value (Table 12) in Au(CN)$_2^-$ supports the L → M interaction, and the very small lengthening of the r(C−N) bond distance in Au(CN)$_2^-$ compared to AuCN (1.164 Å *vs* 1.160 Å) supports the M → L interaction. Since the first factor is larger, one can deduce that L → M is the main interaction in this complex.

VII. AuL₃⁺ AND AuL₂L′⁺ COMPLEXES

The most commonly observed gold(I) compound is a linear two-coordinate complex. Three- and four-coordinate complexes, which will be discussed here and in the following section, are substantially less common. Several examples[54] of three-coordinate complexes are known, some with monodentate phosphine and some with bidentate phosphine ligands. The observation that these complexes have significant antitumor activity has increased interest in these species[29]. The purpose of this work is to calculate the structures of complexes with Au^+ bonded to three neutral ligands in order to compare it to the other types of gold(I) complexes discussed above.

Seven complexes have been geometrically optimized. Their bond lengths and angles are summarized in Table 13. The total energies, charges on the atoms and binding energies are summarized in Table 14.

All the complexes have a planar core geometry; the Au atom and the three bonded central atoms of the ligands are in one plane. Complexes with three identical ligands, either PH_3 or H_2S (Figures 4 and 5), have an almost symmetrical structure with LAuL′ angles close to $120°$. When two of the three ligands are identical, the structure depends on the affinity of the third ligand to the metal ion. As was shown for LAuL′⁺ complexes, the binding energies of a second ligand to AuL^+ follow the order: $PH_3 > NH_3 > H_2S > H_2O$. Accordingly, the ligands that form the strongest bonds will be bound most closely to the gold ion, and the ligands with the smaller Au^+ affinities will have a greater equilibrium bond distance from Au^+. In $Au(H_2S)_2PH_3^+$ (Figure 6) the phosphine forms a strong bond with Au^+ and the two H_2S molecules are almost equally displaced from the gold atom with larger Au−S bond distances than in $Au(H_2S)_3^+$. In $Au(PH_3)_2NH_3^+$ (Figure 7) the affinities of

TABLE 13.   Bond lengths and angles in geometrically optimized complexes AuLL′L″⁺

AuLL′L″⁺	Bond length (Å)						Angle (deg)		
	Au−L	Au−L′	Au−L″	L−H[a]	L′−H[a]	L″−H[a]	LAuL′	LAuL″	L′AuL″
Au(H₂S)₃	2.560	2.537	2.578	1.352	1.352	1.352	123.18	116.64	120.18
Au(H₂S)₂PH₃	2.681	2.627	2.341	1.350	1.351	1.409	96.65	131.90	131.46
Au(H₂S)₂NH₃	4.653	2.357	2.112	1.349	1.355	1.025	137.50	44.43	178.08
Au(H₂S)₂H₂O	2.374	2.386	4.233	1.357	1.354	0.969	176.89	120.21	118.71
Au(PH₃)₃	2.453	2.456	2.455	1.411	1.411	1.411	121.08	120.21	118.71
Au(PH₃)₂H₂S	2.364	2.366	3.944	1.408	1.405	1.348	179.23	112.71	68.06
Au(PH₃)₂NH₃	2.384	2.384	2.547	1.410	1.410	1.019	147.47	106.62	105.92

[a] Averaged bond length.

TABLE 14.   Charges, binding energies and total energies for AuLL′L″⁺ complexes

AuLL′L″⁺	Charge				Energy[a]		
	q(Au)	q(L)	q(L′)	q(L″)	BDE (kcal mol⁻¹)	BDE″ (kcal mol⁻¹)	Energy (e.u.)
Au(H₂S)₃	0.29	−0.14	−0.14	−0.15	3.0	3.0	−169.982631
Au(H₂S)₂PH₃	0.24	−0.17	−0.15	0.01	2.9	14.6	−166.971111
Au(H₂S)₂NH₃	0.41	−0.29	−0.08	−0.73	7.2	19.0	−170.376396
Au(H₂S)₂H₂O	0.30	−0.11	−0.09	−0.52	22.0	13.0	−175.833294
Au(PH₃)₃	0.12	−0.02	−0.02	−0.02	8.2	8.2	−160.935066
Au(PH₃)₂H₂S	0.15	0.05	0.08	−0.29	13.6	4.1	−163.958357
Au(PH₃)₂NH₃	0.21	0.00	0.00	−0.70	6.9	9.8	−164.335620

[a] BDE: AuLL′L″⁺ → AuL′L″⁺ + L; BDE″: AuLL′L″⁺ → AuLL′⁺ + L″.
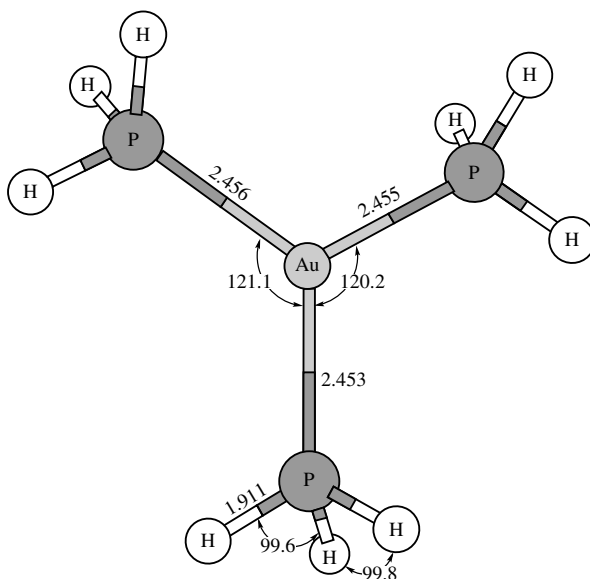
FIGURE 4. The calculated structure of Au(PH$_3$)$_3$$^+$. Bond lengths in ångströms, angles in degrees

FIGURE 5. The calculated structure of Au(H$_2$S)$_3$$^+$. Bond lengths in ångströms, angles in degrees
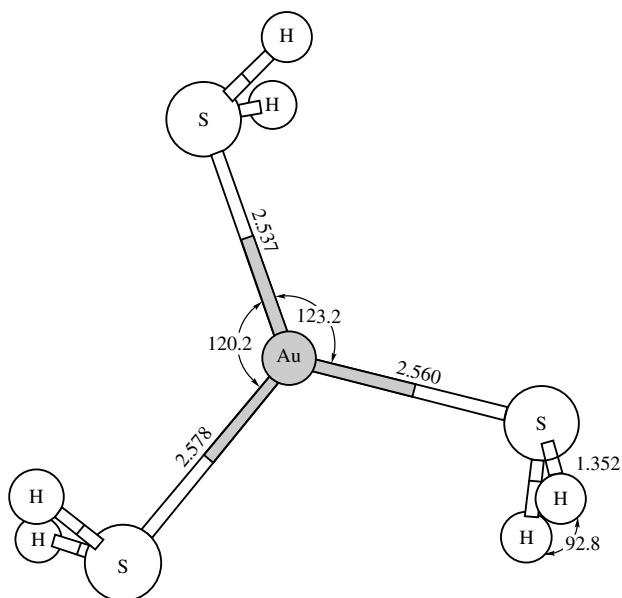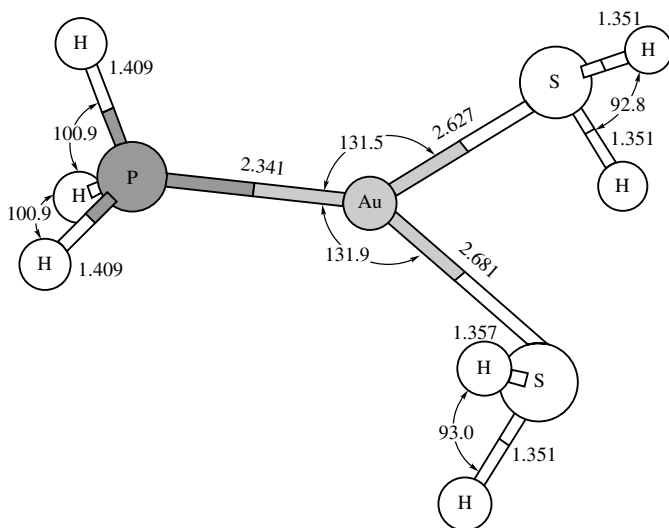
FIGURE 6. The calculated structure of $Au(H_2S)_2PH_3^+$. Bond lengths in ångströms, angles in degrees
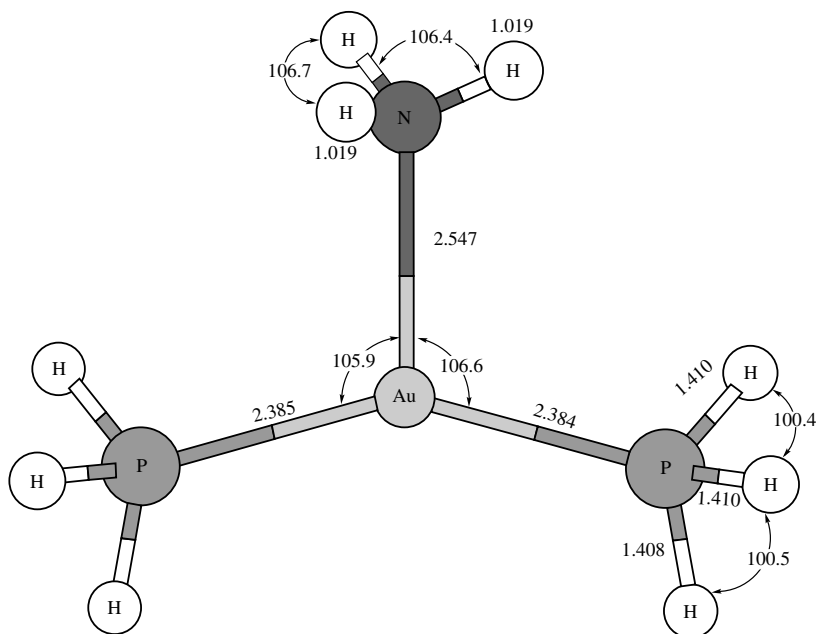
FIGURE 7. The calculated structure of $Au(PH_3)_2NH_3^+$. Bond lengths in ångströms, angles in degrees

the ligands are close, and a 'Y'-shaped complex is formed with the widest angle opposite to the weaker bound ligand. In $Au(H_2S)_2H_2O^+$ (Figure 8) the two H_2S molecules form a linear complex, and the H_2O molecule is weakly bonded to Au^+ with $r(Au-O) = 3.21$ Å and forms with one of the H_2S molecules a hydrogen bond with a $O\cdots H-(S)$ bond length of 2.01 Å. In $Au(H_2S)_2NH_3^+$ (Figure 9) a linear complex is formed by NH_3 and one H_2S molecule, while the second H_2S molecule forms a hydrogen bond with the NH_3 molecule with a $S\cdots H-(N)$ distance of 2.44 Å. In $Au(PH_3)_2H_2S^+$ (Figure 10) a linear complex is formed by the two phosphine ligands, and the H_2S molecule is asymmetrically located close to one of the phosphine molecules and too far from the gold to give any significant stabilization.

The Au−L bond distances in all those complexes are longer than in all the other types of complexes discussed above. For example, in the series $AuPH_3^+$, $Au(PH_3)_2^+$ and $Au(PH_3)_3^+$ the Au−P bond lengths are 2.282, 2.366 and 2.453 Å, respectively. This trend was also found experimentally[55] in X-ray-determined bond distances. The experimental values for $AuPh^+$, $AuPh_2^+$ and $AuPh_3^+$ show $r(Au-P)$ values of 2.235, 2.286 and 2.382 Å, respectively. The same trend exists for all the other ligands. We have previously explained why the Au−L bond is longer in AuL_2^+ than in AuL^+. The accepted explanation for the difference in Au−L bond length between linear complexes and trigonal planar complexes is L−L' repulsion. However, another contribution can come from the three-coordinate gold(I) being sp^2 hybridized. This decrease in the s character in the Au−L bond compared to AuL_2^+ leads to the formation of a longer and weaker σ bond.

The binding energy of the ligands to gold(I) in the three-coordinate complexes is smaller than in all the other types of complexes discussed above. For example, the BDEs
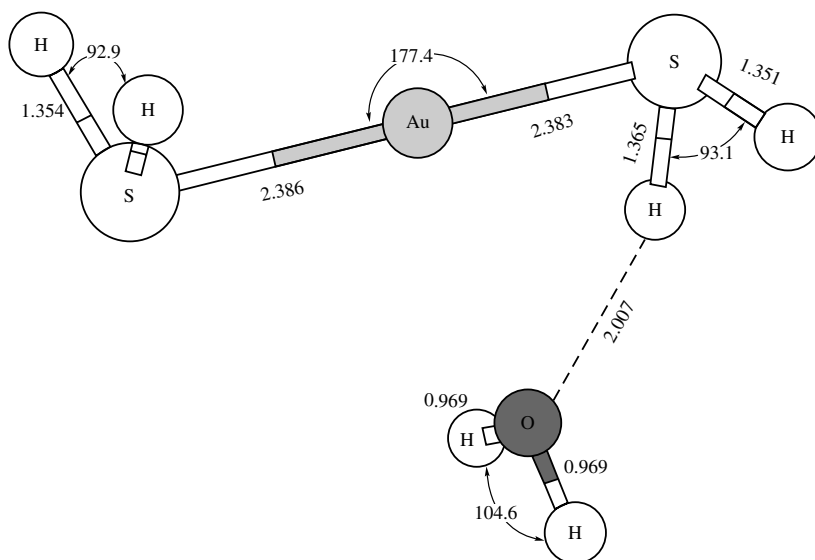
FIGURE 8. The calculated structure of $Au(H_2S)_2H_2O^+$, $r(Au-O) = 3.212$ Å. Bond lengths in ångströms, angles in degrees
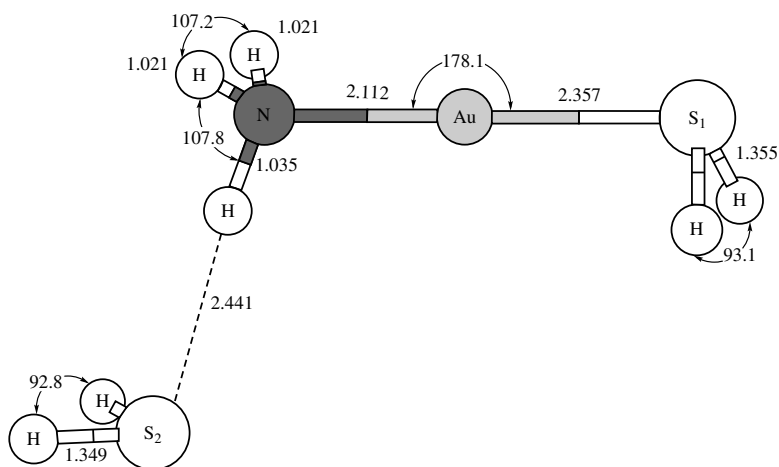
FIGURE 9. The calculated structure of $Au(H_2S)_2NH_3^+$, $r(Au-S_2) = 4.653$ Å. Bond lengths in ångströms, angles in degrees
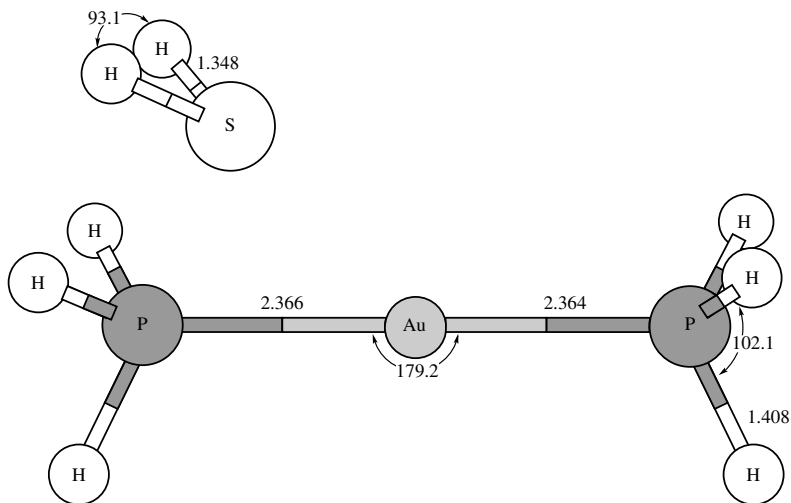
FIGURE 10. The calculated structure of $Au(PH_3)_2H_2S^+$, $r(Au-S) = 3.944$ Å. Bond lengths in ångströms, angles in degrees

$(AuL_n^+ \rightarrow AuL_{n-1}^+ + L)$ for AuH_2S^+, $Au(H_2S)_2^+$ and $Au(H_2S)_3^+$ are 58.4, 48.0 and 3.0 kcal mol^{-1}, respectively.

For all combinations, $AuLL'L''^+$ is more stable than its precursors $AuLL' + L''$. This was found also[55] for complexes in solution $[Au(PEt_3)_3^+]$ and in the solid state $[Au(PPh_3)^+]$[54].

TABLE 15. Bond lengths, angles, charges on atoms, total energies and binding energies of the optimized geometry of AuL_4^+ complexes

AuL_4^+	Bond length (Å)			Angle (deg)			Charge			Energy	
	Au–L[a]	Au–L	L–H	LAuL[a]	LAuL	AuLH	q(Au)	q(L)	q(L)[a]	Total energy (e.u.)	BDE[b] (kcal mol^{-1})
$Au(PH_3)_4^+$	2.517	2.517	1.413	119.17	119.00	97.33	−0.01	−0.04	−0.04	−169.270985	6.4
$Au(H_2S)_4^+$	2.565	3.022	1.350	95.52	119.08	101.45	0.32	−0.23	−0.17	−181.346114	4.9

[a]Averaged for three almost identical Au–L distances.
[b]For $AuL_4^+ \rightarrow AuL_3^+ + L$.

VIII. AuL$_4^+$ COMPLEXES

Gold(I) complexes with four ligands have been prepared and their X-ray structure determined[55,56].

Two complexes with the general formula AuL$_4^+$, with the ligands PH$_3$ and H$_2$S, were studied here. The geometries, partial charges, energies and binding energies of the optimized structures are given in Table 15. The structures of Au(H$_2$S)$_4^+$ and Au(PH$_3$)$_4^+$ are shown in Figures 11 and 12, respectively.

Au(PH$_3$)$_4^+$ is tetrahedral with four almost identical Au−P bond distances and with PAuP angle of about 109.5°.

In Au(H$_2$S)$_4^+$ the gold atom is surrounded by three molecules of H$_2$S with all heavy atoms in one plane at an angle of about 120.0° for the SAuS bonds, and almost identical Au−S bond distances. The fourth molecule lies above the plane at a larger Au−S distance. This sulphur atom lies exactly above the Au atom and its two hydrogens are eclipsed with the two Au−S bonds in the plane.

In Au(H$_2$S)$_4^+$ the three ligands which are in one plane have shorter bonds to the gold than the fourth molecule, 2.565 Å and 3.022 Å, respectively. The three ligands in the plane have almost identical Au−S bond distances to those in Au(H$_2$S)$_3^+$, probably due to sp^2 hybridization in both complexes.

The 2.517 Å bond distances in Au(PH$_3$)$_4^+$ are longer than for the Au−P bonds in all other systems discussed above. Experimental values for Au−P bond distances of 2.449 Å, 2.380 Å and 2.325 Å are available for Au(PPh$_3$)$_4^+$[57], Au(PPh$_3$)$_3^+$ and Au(PPh$_3$)$_2^+$, respectively. The reason for these changes in bond lengths is the additional ligand−ligand
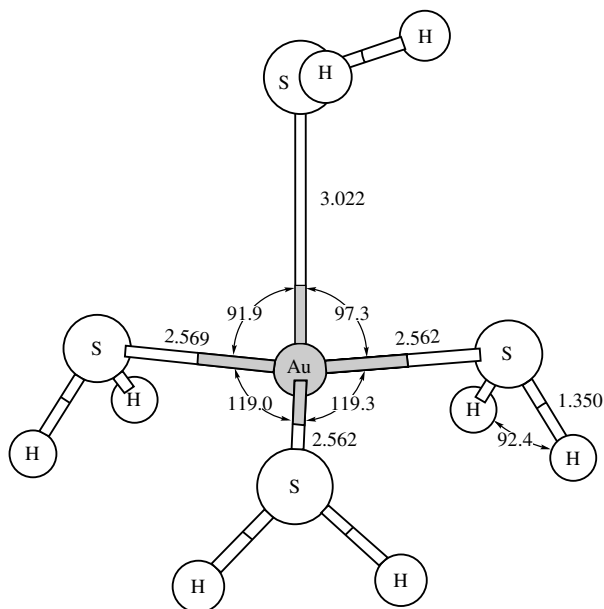
FIGURE 11. The calculated structure of Au(H$_2$S)$_4^+$. Bond lengths in ångströms, angles in degrees
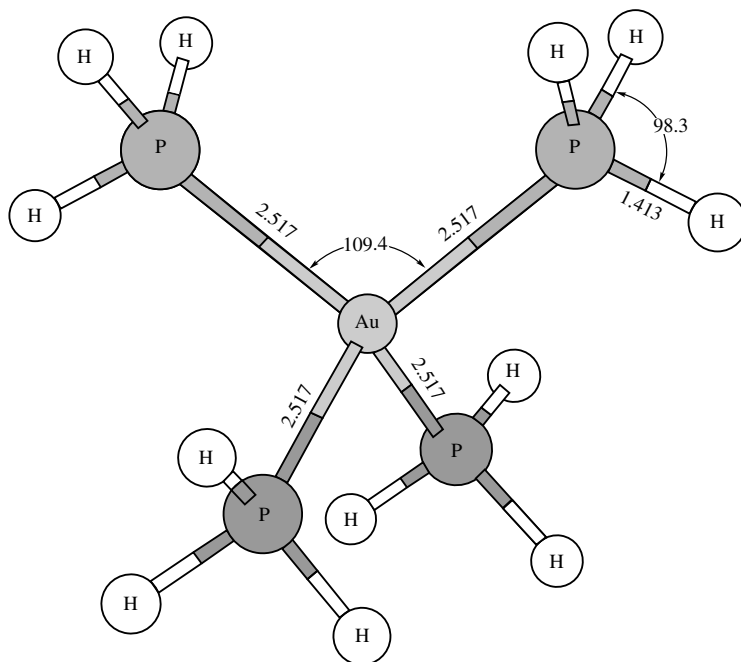
FIGURE 12. The calculated structure of $Au(PH_3)_4{}^+$. Bond lengths in ångströms, angles in degrees

repulsion. Perhaps another explanation is the different hybridization of Au which changes from sp in the linear complex $LAuL'^+$ to sp^2 in the trigonal planar complex $AuL_3{}^+$ and sp^3 in the tetrahedral complex.

These structures are more stable than any combination of complex and free ligands: $AuL^+ + 3L$ or $AuL_2{}^+ + 2L$ or $AuL_3{}^+ + L$ discussed above. The binding energy for the fourth ligand is small: 6.4 and 4.9 kcal mol^{-1} for $Au(PH_3)_4{}^+$ and $Au(H_2S)_4{}^+$, respectively. The BDE for the first ligation of Au^+ has the greatest value, and it decreases as more ligands are bonded to the gold. For example, when $L = PH_3$, the BDE values for the successive ligations are 75.2, 52.4, 8.2 and 6.3 kcal mol^{-1}.

IX. REFERENCES

1. A. J. Lewis and D. T. Walz, in *Progress in Medicinal Chemistry* (Eds. G. P. Ellis and G. B. West), Vol. 19, Elsevier Biomedical Press, Amsterdam, 1982, p. 1.
2. R. J. Puddephatt and S. P. Fricker, *Transition Met. Chem.*, **21**, 377 (1996).
3. (a) D. A. Weil and C. L. Wilkins, *J. Am. Chem. Soc.*, **107**, 7316 (1985).
   (b) A. K. Chowdhury and C. L. Wilkins, *J. Am. Chem. Soc.*, **109**, 5336 (1987).
4. D. Schröder, J. Hrusak, I. C. Tornieporth-Oetting, T. M. Klapotke and H. Schwarz, *Angew. Chem.*, **106**, 223 (1994); *Angew. Chem., Int. Ed. Engl.*, **33**, 212 (1994).
5. (a) J. Hrušák, R. H. Hertwig, D. Schröder, P. Schwerdtfeger, W. Koch and H. Schwarz, (a) *Organometallics*, **14**, 1284 (1995); (b) *Organometallics*, **14**, 312 (1995).
6. (a) G. Ohanessian, M. J. Brusich and W. A. Goddard III, *J. Am. Chem. Soc.*, **112**, 7179 (1990).

(b) G. Ohanessian and W. A. Goddard III, *Acc. Chem. Res.*, **23**, 386 (1990).

(c) Y. Ishikawa, G. L. Malli and N. C. Pyper, *Chem. Phys. Lett.*, **194**, 481 (1992).

7. (a) P. Schwerdtfeger, M. Dolg, W. H. E. Schwarz, G. A. Bowmaker and P. D. W. Boyd, *J. Chem. Phys.*, **91**, 1762 (1989).
   (b) P. Schwerdtfeger, *J. Am. Chem. Soc.*, **111**, 7261 (1989).

8. P. Schwerdtfeger, P. D. W. Boyd, K. Burrell, W. T. Robinson and M. J. Taylor, *Inorg. Chem.*, **29**, 3593 (1990).

9. O. D. Haberlen and N. Rosch, *J. Phys. Chem.*, **97**, 4970 (1993).

10. A. Veldkamp and G. Frenking, *Organometallics*, **12**, 4613 (1993).

11. J. Hrušák, D. Schröder and H. Schwarz, *Chem. Phys. Lett.*, **225**, 416 (1994).

12. P. Pyykko and J. P. Desclaux, *Acc. Chem. Res.*, **12**, 276 (1979).

13. W. J. Stevens, M. Krauss, H. Basch and P. G. Jasien, *Can. J. Chem.*, **70**, 612 (1992).

14. T. R. Cundari and W. J. Stevens, *J. Chem. Phys.*, **98**, 5555 (1993).

15. (a) P. Durand and J. C. Barthelat, *Theor. Chim. Acta*, **38**, 283 (1975).
    (b) W. C. Elmer, R. B. Ross and P. A. Christiansen, *Int. J. Quantum Chem.*, **40**, 829 (1991).
    (c) W. Kuchle, M. Dolg, H. Stoll, H. Preuss and P. Schwerdtfeger, *Mol. Phys.*, **74**, 1245 (1991).

16. P. Schwerdtfeger, J. S. McFeaters, R. L. Stephens, M. J. Liddell, M. Dolg and B. A. Hess, *Chem. Phys. Lett.*, **218**, 362 (1994).

17. H. Basch and T. Hoz, in *Supplement C2: The Chemistry of Triple-bonded Functional Groups* (Ed. S. Patai), Wiley, Chichester, 1992, p. 1.

18. W. J. Stevens, H. Basch and M. Krauss, *J. Chem. Phys.*, **81**, 6026 (1984).

19. R. H. Hertwig, J. Hrušák, D. Schröder, W. Koch and H. Schwarz, *Chem. Phys. Lett.*, **236**, 194 (1995).

20. A. D. Becke, *J. Chem. Phys.*, **98**, 5648 (1993).

21. (a) M. J. Frisch, G. W. Trucks, H. B. Schlegel, P. M. W. Gill, B. G. Johnson, M. A. Robb, J. R. Cheeseman, T. A. Keith, G. A. Peterson, J. A. Montgomery, K. Raghavachari, M. A. Al-Loham, V. G. Zakrzewski, J. V. Ortiz, J. B. Foresman, J. Cioslowski, B. B. Stefanov, A. Nanayakkava, M. Challacombe, C. Y. Peng, P. Y. Ayala, W. Chen, M. W. Wong, J. L. Andres, E. S. Replogle, R. Gomperts, R. L. Martin, D. L. Fox, J. L. Binkley, D. J. Defrees, J. Baker, J. P. Stewart, M. Head-Gordon, C. Gonzalez and J. A. Pople, *Gaussian 94, Revision B. 2*, Gaussian, Inc., Pittsburgh, PA, 1995.
    (b) M. J. Frisch, J. A. Pople and J. S. Binkley, *J. Chem. Phys.*, **80**, 3265 (1984).

22. J. P. Desclaux, *Comput. Phys. Commun.*, **9**, 31 (1975).

23. K. G. Dyall, *J. Chem. Phys.*, **98**, 2191 (1993).

24. W. J. Hehre, L. Radom. P. v. R. Schleyer and J. A. Pople, *Ab Initio Molecular Orbital Theory*, Wiley-Interscience, New York, 1986.

25. R. S. Mulliken, *J. Chem. Phys.*, **55**, 3428 (1962).

26. R. H. Schultz and P. B. Armentrout, *J. Chem. Phys.*, **97**, 596 (1993).

27. C. E. Moore, *Atomic Energy Levels*, Natl. Bur. Stand. Circ. (U.S.) No. 467, 1958.

28. D. R. Lide (Ed.), *CRC Handbook of Chemistry and Physics*, 78th Edn., Chemical Rubber Co, New York, 1997.

29. A-M. Larsonner, R. Turpin, P. Castan and G. Bernardinelli, *Inorg. Chem. Acta*, **227**, 85 (1994).

30. G. A. Bowmaker, H. Schmidbaur, S. Kruger and N. Rosch, *Inorg. Chem.*, **36**, 1754 (1997).

31. R. D. Ernst, J. W. Freeman, L. Stahl, D. R. Wilson, A. M. Arif, B. Nuber and M. L. Ziegler, *J. Am. Chem. Soc.*, **117**, 5075 (1995).

32. O. D. Haberlen and N. Rosch, *J. Phys. Chem.*, **97**, 4970 (1993).

33. G. M. Bancroft, T. Chan, R. J. Puddephatt and J. S. Tse, *Inorg. Chem.*, **21**, 2946 (1982).

34. F. A. Cotton and G. Wilkinson, *Advanced Inorganic Chemistry*, Wiley, New York, 1988, p. 1299.

35. A. Ricca and C. W. Bauschlicher, Jr., *J. Phys. Chem.*, **99**, 9003 (1995).

36. S. R. Langhoff, C. W. Bauschlicher Jr., H. Patridge and M. Sodupe, *J. Phys. Chem.*, **95**, 10677 (1991).

37. M. Rosi and C. W. Bauschlicher, Jr., *J. Chem. Phys.*, **92**, 1876 (1990).

38. R. D. Davy and M. B. Hall, *Inorg. Chem.*, **27**, 1417 (1988).

39. (a) T. Okada, B. K. Patterson, S-Q. Ye and M. E. Gurney, *Virology*, **192**, 631 (1993).
    (b) C. F. Shaw III, M. T. Coffer, J. Klingbeil and C. K. Mirabelli, *J. Am. Chem. Soc.*, **110**, 729 (1988).

40. A. A. Isab, A. L. Hormann, M. T. Coffer and C. F. Shaw III, *J. Am. Chem. Soc.*, **110**, 3278 (1988).

41. A. A. Isab, A. L. Hormann, D. T. Hill, D. E. Griswold, M. J. DiMartino and C. F. Shaw III, *Inorg. Chem.*, **28**, 1321 (1989).
42. C. F. Shaw III, N. A. Schaeffer, R. C. Elder, M. K. Eidsness, J. M. Trooster and G. H. M. Calis, *J. Am. Chem. Soc.*, **106**, 3511 (1984).
43. A. I. Anvarhusein and P. J. Sadler, *J. Chem. Soc., Dalton Trans.*, 135 (1982).
44. A. I. Anvarhusein and P. J. Sadler, *J. Chem. Soc., Dalton Trans.*, 1657 (1981).
45. G. A. Bowmaker, P. D. W. Boyd and R. J. Sorrenson, *J. Chem. Soc., Faraday Trans. 2*, 1627 (1985).
46. (a) R. J. Puddephat, *The Chemistry of Gold*, Elsevier, Amsterdam, 1978.
    (b) R. J. Puddephat, *Comprehensive Organometallic Chemistry* (Eds. G. Wilkinson, F. G. A. Stone and E. W. Abel), Pergamon, Oxford, Vol. 2, Chapter 15, 1982, p. 765; Vol. 5, 1987, p. 861.
    (c) R. Uson and A. Laguna, *Coord. Chem. Rev.*, **70**, 1 (1986).
    (d) M. Melnik and R. V. Parish, *Coord. Chem. Rev.*, **70**, 157 (1986).
47. G. A. Bowmaker, in *Spectroscopy of Inorganic-based Materials* (Eds. R. J. H. Clark and R. E. Hester), Wiley, New York, 1987, p. 1.
48. (a) P. Schwerdtfeger, P. D. W. Boyd, K. Burrell, W. T. Robinson and M. J. Taylor, *Inorg. Chem.*, **29**, 3593 (1990).
    (b) M. Sano, H. Adachi and H. Yamatera, *Bull. Chem. Soc. Jpn.*, **55**, 1022 (1982).
49. H. Zwanziger, J. Reinhold and E. Z. Hoyer, *Z. Chem.*, **14**, 489 (1974).
50. (a) W. R. Mason, *J. Am. Chem. Soc.*, **95**, 3573 (1973).
    (b) W. R. Mason, *J. Am. Chem. Soc.*, **98**, 5182 (1976).
51. (a) A. Rosenzweig and D. T. Croner, *Acta Crystallogr.*, **12**, 709 (1959).
    (b) P. G. Jones, W. Clegg and G. M. Sheldrick, *Acta Crystallogr., Sect. B*, **33**, 137 (1977).
52. H. J. Berthold and W. Z. Ludwig, *Z. Naturforsch., B*, **35**, 970 (1980).
53. I. P. Grant, B. J. Mckenzie, P. H. Norrington, D. F. Mayers and N. C. Pyper, *Comput. Phys. Commun.*, **21**, 207 (1980).
54. O. Crespo, M. C. Gimeno, A. Laguna and P. G. Jones, *J. Chem. Soc., Dalton Trans.*, 1601 (1992).
55. (a) L. J. Guggenberger, *J. Organometal. Chem.*, **81**, 271 (1974).
    (b) P. G. Jones, *Acta Crystallogr., Sect. B*, **36**, 3105 (1980).
56. (a) M. J. Mays and P. A. Vergano, *J. Chem. Soc., Dalton Trans.*, 1112 (1979).
    (b) O. Crespo, M. C. Gimeno, P. G. Jones and A. Laguna, *Inorg. Chem.*, **33**, 6128 (1994).
57. R. S. Elder, E. H. K. Zeiher, M. Onady and R. R. Whittle, *J. Chem. Soc., Chem. Commun.*, 900 (1981).

CHAPTER **2**

Mössbauer spectroscopy with gold compounds

R. V. PARISH

Department of Chemistry, UMIST, PO Box 88, Manchester M60 1QD, UK
Fax: 44-161-200-4521;   e-mail: R.V.PARISH@UMIST.AC. UK

I. INTRODUCTION

Mössbauer spectroscopy is a valuable technique for the characterization of compounds of gold. From a single spectrum, it is possible to determine the oxidation state of the gold and to make very good estimates as to the nature and number of groups bound to it. However, Finagle's Law of Natural Perversity[1] applies, for the technique is inconvenient: it requires relatively large samples, liquid helium temperatures, and a short-lived and expensive radio-isotope. As a result, there are very few practising laboratories.

II. MÖSSBAUER SPECTROSCOPY

A Mössbauer spectrum is, like all other spectra, a plot of intensity or absorption against energy. Each technique has its own energy scale, e.g. cm^{-1} for infrared, ppm for NMR, etc.

In this case, the energy scale is given in units of velocity: $mm\,s^{-1}$. This idiosyncrasy arises as follows. Mössbauer spectroscopy involves the absorption of electromagnetic radiation by nuclei, the reverse of gamma emission. The sample is exposed to gamma radiation and appropriate nuclei can absorb and scatter it. However, this poses a problem in obtaining an absorption spectrum, since the radiation source has a fixed, single environment for the nuclei; hence, a fixed, well-defined gamma energy is emitted. Generally, this will not coincide with the energy required to excite the sample, and a means of modulation of the source gamma energy is needed. Fortunately, the range of energies required is very small, and the necessary modulation can be provided by the Doppler effect: the source is mounted on a controllable transducer (vibrator) and given a velocity. Motion towards the sample gives an increase in the energy perceived by the sample, away a reduction. Velocities of a few $mm\,s^{-1}$ are sufficient for most isotopes. A Mössbauer spectrometer therefore consists essentially of a vibrator bearing the gamma source, the experimental sample through which the radiation passes and a gamma counter. The count rate is recorded as a function of the velocity applied to the source, and velocity becomes the unit in which the parameters are recorded.

In order to ensure that there is an exact match of energies within a reasonable velocity range, Mössbauer spectroscopy is restricted to nuclei for which the energetically excited, gamma-active state can be readily obtained, and the source must contain the same isotope as the sample. In the case of gold-197 the radioactive form is obtained by irradiation of platinum-196 in a nuclear reactor or a cyclotron. It is preferable to use isotopically enriched platinum (natural platinum can be used, but it gives a very rich gamma spectrum, which may overload detection systems). Once irradiated, the source has a half-life of only 18 hours, and so must be transported rapidly to the laboratory and immediately put to work; it can be used for about four days before needing reactivation.

It is usual to scan a suitable range of velocities with a frequency of a few Hz, and to accumulate the counts of successive passes until an adequate signal-to-noise ratio is obtained. This may take from minutes to hours, depending on the concentration of appropriate nuclei in the sample and the brightness of the source. Fortunately, natural gold is mono-isotopic, so that all atoms contain the ^{197}Au nucleus needed. Unfortunately, the intensity of the spectrum depends on the energy of the gamma radiation; higher energies result in lower intensities, of both absorption and emission. Naturally, the energy is dictated by the isotope under investigation, and for gold-197 it is rather large, 77 keV. It is therefore necessary to use samples containing between 50 and 100 mg of gold. (Large, thick samples give problems of self-absorption of the radiation, and the relationship between sample thickness and absorption intensity goes through a maximum; the use of thicker samples does not improve the spectrum.) The intensity of absorption also depends on the temperature of the sample, increasing as the temperature is lowered. The low intensity resulting from the high gamma energy must also be compensated by strongly cooling both source and sample; immersion in liquid helium (4.2 K) is the simplest method. Satisfactory spectra for molecular materials cannot normally be obtained at higher, more convenient temperatures. All samples must be solid, and solutions must be frozen; at 4.2 K this is not a problem.

Since the energy levels of a given nucleus depend on the electronic environment of the atom containing the nucleus, chemical information can be obtained by monitoring the precise energies absorbed. Spectra are usually doublets, so that two main parameters can be found: the position of the centre of the doublet (the *isomer shift*, IS) and the separation of the two peaks (the *quadrupole splitting*, QS). These parameters are shown for a typical spectrum in Figure 1. The zero of velocity is normally defined by running the spectrum of a standard material, in this case metallic gold[2]. When the sample contains gold atoms in different chemical sites, each will give its own spectrum, and some deconvolution of the
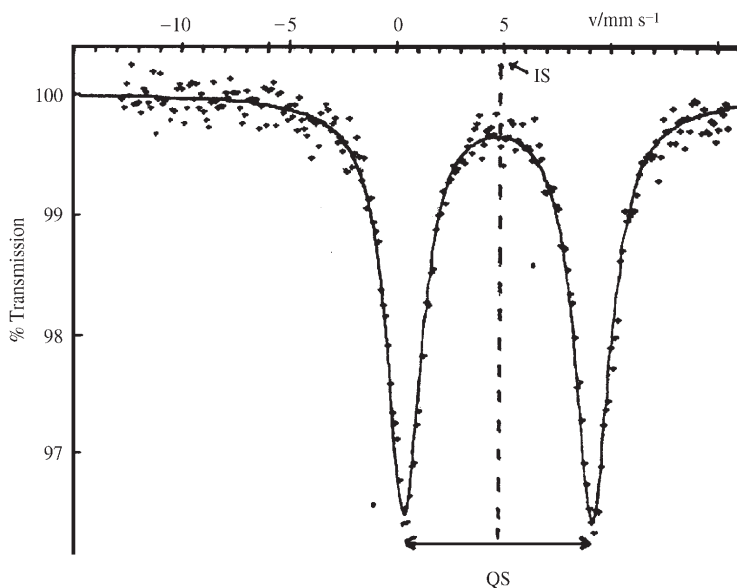
FIGURE 1. Typical ^{197}Au Mössbauer spectrum for a gold(I) compound (the anti-arthritic drug Aura-nofin), having IS 4.79 mm s^{-1} and QS 8.77 mm s^{-1}

spectrum is usually required. The *intensities* of the sub-spectra are a rough guide to the relative populations of the sites, but problems may arise when the sites are very different (see below).

III. THE ORIGIN AND INTERPRETATION OF THE PARAMETERS

The two principal parameters of a Mössbauer spectrum depend on the interaction of the nucleus with its electronic environment. They can therefore be interpreted in terms of chemical factors.

A. Quadrupole Splitting

The quadrupole splitting reflects the interaction of the nucleus with the electric field due to the surrounding electrons. It therefore indicates the nature and arrangement of the gold–ligand bonds.

The electric properties of a nucleus depend on its spin. If the spin is greater than 1/2 the nucleus has a quadrupole moment; effectively, this indicates an unsymmetrical distribution of charge. If such a nucleus is situated in a non-uniform electric field, its energy will depend on its orientation with respect to the direction of the field. Quantization demands that only certain orientations (energies) are allowed. For ^{197}Au, the ground state has spin of 3/2, which gives two possible energies (the energy depends on the square of the quantum number m_I; for ^{197}Au, m_I can be $\pm 1/2$ or $\pm 3/2$). However, the greatest observed energy difference between these two levels is about 100 times less than kT (even

for $T = 4.2$ K), so that the two states have equal populations; nuclei in either state may absorb the gamma photons from the source.

The gamma-excited state has spin of 1/2, and is unaffected by asymmetry in a surrounding electric field. Thus, two transitions are possible (Figure 2) and the Mössbauer spectra are doublets. It sometimes happens that the field has high symmetry [as in gold metal or tetrahedral gold(I) complexes]; the ground-state splitting is then vanishingly small, and single-line spectra are seen.

The doublet separation is the quadrupole splitting (QS), and it reflects the electrical asymmetry at the nucleus. Such asymmetry comes principally from the surrounding valence-shell electrons, bonding or non-bonding. Electrons or ionic charges further away have very much smaller effects. The number and arrangement of valence-shell electrons depend on the oxidation state and co-ordination number of the gold atom. For the two principal oxidation states, +1 and +3, the gold atom has a $5d^{10}$ or $5d^8$ configuration respectively, and the co-ordination numbers vary from two to four.

For gold(I), the non-bonding electrons are all in spherical closed shells, and make no contribution to the QS. The majority of compounds, including all organic derivatives, contain only two ligands, giving linear co-ordination and sp-hybridization of the gold. The electron density donated by the ligands populates the $6p_z$ orbital while $6p_x$ and $6p_y$ remain empty (the 6s orbital is spherical). There is therefore electrical asymmetry about the gold nucleus which increases as the ligands become better donors. Thus, the QS indicates the type of ligand involved, and increases with increasing softness; a rough order is: halide < nitrogen group < tertiary phosphine < organic group.

In a small number of gold(I) complexes, the co-ordination number is three or four. The latter, with tetrahedral geometry and sp^3-hybridization, gives a zero QS (the three p orbitals are populated equally if the ligands are identical). For three-co-ordination and trigonal-planar stereochemistry, it can be shown that the degree of electrical asymmetry is the same as for two-co-ordination with the same ligands (actually, opposite in sign, but this does not affect the spectrum); the QS cannot therefore be used to distinguish these two co-ordination numbers.

In gold(III), the valence shell has only eight d-electrons, with a 'hole' in the $5d_{x^2-y^2}$ orbital. There is thus an intrinsic electrical asymmetry. The normal co-ordination number is four, with a square-planar configuration (the ligand-plane is defined as xy). Bonding involves $d_{x^2-y^2}sp^2$ hybrids, placing electron density in the $d_{x^2-y^2}$, p_x and p_y orbitals,
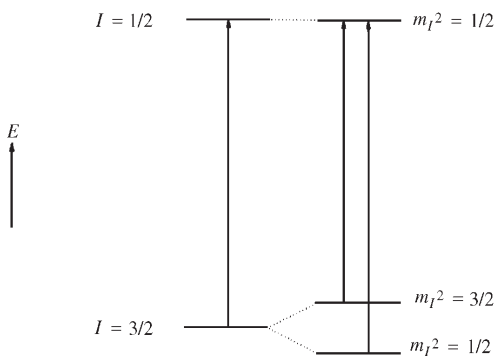
FIGURE 2. Nuclear energy levels and possible Mössbauer transitions for ^{197}Au

which again increases as the ligands become softer. When the ligands are halide ions, the total donated charge in the xy-plane just about reduces the electrical asymmetry to zero, and salts of $[AuX_4]^-$ ions show very small QS. With other ligands, the QS increases in the same order as for gold(I) compounds. From the few measurements available, it appears that *cis* and *trans* isomers of gold(III) complexes give the same parameters (in principle, a slightly greater value might be expected for the *cis* isomer).

In both oxidation states, the QS reflects the combined effects of all the ligands present. To a good approximation, each ligand makes its own contribution, and scales of partial-quadrupole splitting values have been established, from which the QS of a particular complex may be estimated by simple arithmetic[3,4]. These work reasonably well for gold(I), but there are not enough data available for a sufficiently wide range of gold(III) compounds.

B. Isomer Shift

There is an energy-raising interaction between the nucleus and the electron density which penetrates it. Since the nucleus has different radii in its ground state and its gamma-excited state, the energies of the two states are differently affected by the electron density (which is the same for both states). The position of the centroid of the Mössbauer spectrum, the IS, thus reflects the electron density at the nucleus.

Only s and $p_{1/2}$ electrons have finite probability of occurring at the nucleus, and contributing to this effect (other electrons have vanishingly small density within the nuclear volume). The only significant changes in the density at the nucleus come from variation in the valence-shell (6s) population, which depends on the chemical situation. As the donation by the ligands increases, so the s-population and the IS increase. Thus, the IS is expected to increase as the ligands become better, 'softer' donors and the bonds more covalent. The order is again: halide < nitrogen group < tertiary phosphine < organic group.

The rate of change depends on the oxidation state. Bonds to gold(III) are more covalent, and more charge is donated per ligand. This would have the effect of boosting the rate of increase of IS relative to the series for gold(I) with the same ligands. However, in gold(III) more of the donated charge goes into orbitals other than the 6s. Electron density in p and d orbitals has a shielding effect, reducing the electron density at the nucleus. Overall, the IS for gold(III) increases at only a slightly greater rate than for gold(I).

The reduction in number of d-electrons from gold(I) to gold(III) affects the shielding in all compounds so that, for the same ligands, gold(III) shows the greater IS. *cis* and *trans* isomers of gold(III) complexes give the same parameters.

Finally, there is a dependence of the IS on co-ordination number. For gold(I) there are some complexes with three or four ligands and sp^2 or sp^3 hybridization, respectively. The bonds are slightly longer, so that there is less donation per ligand, and the electron density donated into the p-orbital again has a shielding effect. The result is a decrease in IS with increasing co-ordination number.

C. Correlation Diagrams

As seen above, both the IS and the QS change systematically with the nature of the ligands, the co-ordination number and the oxidation state. If the available data are entered on a plot of QS *vs* IS, the various systems occupy distinct regions (Figure 3). Within each band of data, compounds containing the hardest ligands lie at the bottom and those with the softest ligands at the top. Such a correlation diagram is very useful in characterizing new compounds.

Key: ||| P,C   S   N

AuX$_2^-$, AuX$_4^-$

(AuX)$_n$, Au$_2$X$_6$

QS/(mm s^{-1})

12

Au^{I}L$_2$

Au^{I}L$_3$

8

Au^{III}L$_4$

4

0   Au^{I}L$_4$

IS/(mm s^{-1})

0   2   4   6   8
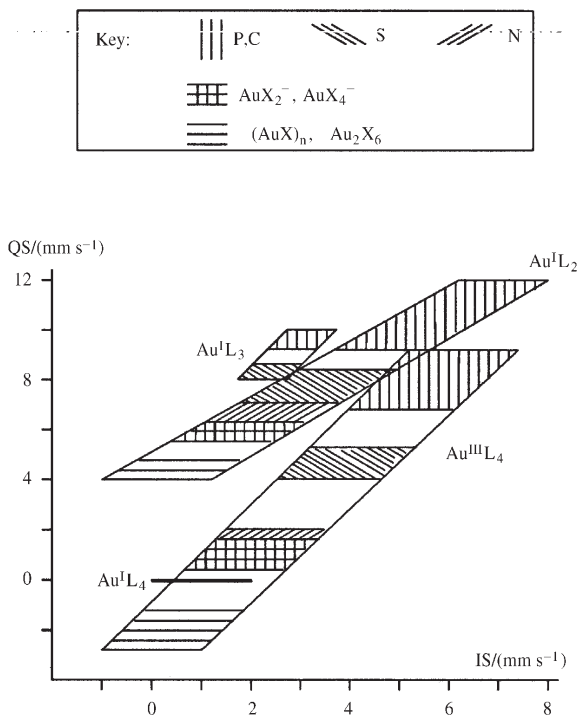
FIGURE 3. IS/QS correlation diagram. The various hatchings refer to the different ligand donor sets shown

D. Intensities

The total area of a doublet spectrum is proportional to the amount of sample in the gamma beam. Each compound has its own 'extinction coefficient' for absorption, which depends on the molecular mass and the tightness of binding of the gold atom to the rest of the molecule or lattice (this effect has its origin in the recoil which the nucleus suffers on collision with a gamma photon). If all the gold atoms are equivalent, this is not a problem; it is only necessary to adjust the amount of sample used to get a good spectrum. However, if the sample contains gold atoms in different sites, the relative intensities of the sub-spectra do not necessarily give a good estimate of the distribution between the sites. The biggest discrepancy is when there is a difference of oxidation state and, other factors being similar, the intensity of the gold(III) sub-spectrum may be 50% or even 100% greater (atom for atom) than the gold(I) sub-spectrum. Examples of this may be found elsewhere[4,5].

IV. DISCUSSION OF DATA

Given the general area of this text, the discussion will be restricted to data for organometallic derivatives of gold. Nevertheless, this gives plenty of material with which to illustrate the factors outlined above and to show the utility of the technique.

A. σ-Bonded Derivatives

Gold forms a variety of 'conventional' organometallics, in which organic groups are σ-bonded to gold(I) or gold(III). Since the co-ordination numbers are two and four, respectively, at least one other ligand must be involved over and above the organic groups required to satisfy the valency. The additional ligand may be another organic group, giving an anionic derivative $[AuR_2]^-$ or $[AuR_4]^-$, or (more often) a neutral ligand such as a tertiary phosphine.

The data (Tables 1 and 2, listed in order of decreasing IS) lie within the regions shown in Figure 1 for gold(I) and gold(III). In each case, the points lie at the top of the band

TABLE 1. Data for σ-bonded gold(I) compounds

Structure number	Compound	IS_{Au} (mm s^{-1})	QS (mm s^{-1})	Reference
1	$(2\text{-}Me_2NC_6H_4)_4Au_2Li_2$	6.86	12.01	6
2	$(2\text{-}Me_2NCH_2C_6H_4)_4Au_2Li_2$	6.48	11.29	7
3	$C_6H_5AuPPh_3$	6.21	10.25	8
4	CH_3AuPPh_3	6.14	10.35	9
5	$4\text{-}CH_3C_6H_4AuPPh_3$	6.13	10.25	8
6	CH_3AuPMe_3	6.11[a]	10.21	10
7	$CpFeC_5H_4AuPPh_3$	6.05	10.18	8
8	$2\text{-}Me_2NC_6H_4AuPPh_3$	6.05[a]	10.11	7
9	$2\text{-}[Et_2PC_6H_4Au]_2$	5.88[a]	10.12	11
10	$2\text{-}Me_2NC_6H_4AuCNC_5H_4$	5.83[a]	10.35	7
11	$2\text{-}[Ph_2PC_6H_4Au]_2$	5.74[a]	9.58	11
12	$[2\text{-}Me_2NCH_2C_6H_4Au]_n$	5.65[a]	7.32	7
13	$CH_3(CF_3)C{=}C(CF_3)AuPPh_2Me$	5.63[a]	9.49	10
14	$(2\text{-}Me_2NC_6H_4)_4Au_2Cu_2$	5.63	9.86	7
15	$Me_3P\textbf{Au}(CF_3)C{=}C(CF_3)Au(CH_3)_2$ $(PMe_3)\text{-}trans^b$	5.58[a]	9.18	10
16	$[(C_6F_3H_2)_2Au]NBu_4$	5.47	10.92	12
17	$[(C_6F_5)_2Au]NBu_4$	5.37	10.70	12
18	$Me_3P\textbf{Au}(CF_3)C{=}C(CF_3)Au(CH_3)_2$ $(PMe_3)\text{-}cis^b$	5.35[a]	9.17	10
19	$1\text{-}HOC_6H_{10}\text{-}C{\equiv}CAuPPh_3$	5.35[a]	10.30	13
20	$PhMe_2P\textbf{Au}C(CF_3)C{=}C(CF_3)Au(CH_3)_2$ $(PMe_2Ph)\text{-}trans^b$	5.34[a]	9.44	10
21	$PhC{\equiv}CAuPPh_3$	5.33[a]	10.21	13
22	$2\text{-}[Ph_2AsC_6H_4Au]_2$	5.29[a]	8.80	11
23	$(C_6F_5AuPPh_2C_5H_4)_2Fe$	5.25	9.65	14
24	$(C_6F_5AuPPh_2)_2CH_2$	5.20	9.91	15
25	$Me_2P(CH_2AuCH_2)_2PMe_2$	4.98[a]	7.19	16
26	$Et_2P(CH_2AuCH_2)_2PEt_2$	4.97[a]	9.60	17
27	$[2\text{-}Me_2NC_6H_4Au]_n$	4.90[a]	6.73	7
28	$[(C_6F_5)_2Au][AgSC_4H_8]$	4.57	9.41	12
29	$2,4,6\text{-}[(C_6F_3H_2)_2Au]\,[AgSC_4H_8]$	4.57	9.41	12
30	$2,4,6\text{-}[(C_6F_3H_2)_2Au]Ag$	3.98	8.63	12

[a]Original data reported relative to Au/Pt.
[b]cis/trans refers to the configuration at gold; stereochemistry at the double bond is cis in all cases.

R. V. Parish

TABLE 2.   Data for σ-bonded gold(III) compounds

Structure number	Compound	IS_{Au} (mm s^{-1})	QS (mm s^{-1})	Reference
31	Me$_3$PAu(CF$_3$)C=C(CF$_3$)**Au**(CH$_3$)$_2$ (PMe$_3$)-*cis*[a]	6.99[b]	9.07	10
32	Me$_3$PAu(CF$_3$)C=C(CF$_3$)**Au**(CH$_3$)$_2$ (PMe$_3$)-*trans*[a]	6.97[b]	9.27	10
33	PhMe$_2$PAu(CF$_3$)C=C(CF$_3$)**Au**(CH$_3$)$_2$ (PMe$_2$Ph)-*trans*[a]	6.32	9.13	10
34	(CH$_3$)$_3$AuPMe$_3$	6.05[b]	9.04	10
35	(CH$_3$)$_2$AuCl(PPh$_3$)	5.28	6.32	18
36	[C$_6$F$_5$AuCl(pdma)]Cl[c]	4.09	4.94	19
37	{CH$_2$P(Et$_2$)CH$_2$AuBr$_2$}$_2$	3.22[b]	5.52	17
38	[C$_6$F$_5$AuCl(phen)]Cl[d]	2.92	2.33	19
39	[C$_6$F$_5$AuBr(phen)]Br[d]	2.78	2.13	19

[a]*cis/trans* refers to the configuration at gold; stereochemistry at the double bond is *cis* in all cases.
[b]Original data reported relative to Au/Pt.
[c]Pdma = 1,2-(Me$_2$As)C$_6$H$_4$.
[d]phen = 1,10-phenanthroline.

shown, that is they have large values for IS and QS, but the IS for gold(III) is the greater. This indicates, as expected, that the Au−C bond is highly covalent; the organic groups act as soft ligands and transfer high electron density to the gold atom. The highest values (with the exception of **1** and **2** of Table 1, discussed below) are for compounds with CAu^{I}P or C$_3$Au^{III}P co-ordination, since tertiary phosphines are also very good donors to gold. The parameters decrease in the order aryl $\simeq$ alkyl > alkynyl > fluoroaryl as expected from the electronegativity of the organic groups. However, discrimination is much more evident in the IS values than the QS, showing that s-character is concentrated more in the Au−C bond than Au−P.

Compounds **1** and **2** of Table 1 are thought to involve two-electron three-centre bonding of the aryl groups with both gold(I) and lithium cations, since there is ^{13}C NMR evidence for some interaction between the bridgehead carbon atom and the lithium ion[7]. However, the very high values of IS and QS show that the electron density concentrates in the Au−C region, so that these compounds approximate to Li$_2$[(YC$_6$H$_4$)$_2$Au] (Y = 2-NMe$_2$, 2-CH$_2$NMe$_2$)[12]. On the other hand, the copper(I) derivative **(14)** has lower Mössbauer
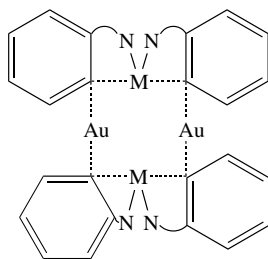
(1,2)   M = Li
(14)   M = Cu

parameters, and probably is electron deficient. Further discussion of electron-deficient compounds is given in Section IV.D below.

Simple salts of bis(perfluorophenyl)aurate(I) anions are found in the middle of Table 1 (**16, 17**) with values lower than those for **1** and **2**, consistent with the greater electronegativity of the fluoroaryl groups. Their parameters are rather higher than for $[Au(PR_2)_2]^+$ (IS 5.0–5.3, QS 9.5–10.2 mm s^{-1})[3,20], and for $R_3PAuC_6F_5$ (**23, 24**), showing that fluoroaryl groups are excellent donors to gold. The silver(I) salts (**28, 29**) show relatively low parameters, even though the compounds involve conventional Au−C bonds[21]; in these cases there is interaction between the gold atom and the cations which reduces the electron density at gold[12].

Mössbauer data were useful in confirming the oxidation state of the products of reaction between CH_3AuL (L = a tertiary phosphine) and $F_3CC{\equiv}CCF_3$[10]. In the presence of excess of the alkyne, simple addition of $H_3C−Au$ across the double bond occurs (structure **13**). When equimolar amounts are used, products containing two gold atoms are obtained, and the Mössbauer spectra show that both gold(I) and gold(III) are present (Table 1, **18, 20**; Table 2, **31–33**). The spectra contain two doublets with similar QS but different IS, the smaller IS showing the higher oxidation state. Together with NMR data, these indicate structures of the type shown for **18, 31** [the geometry at gold(III) varies with L]. Presumably, **13** reacts with CH_3AuL to give oxidative insertion into the viny1−CH_3 bond; interestingly, this reaction appears to be reversible (note that this interpretation differs from that originally proposed)[10]. Reductive elimination of ethane from **18, 31** also occurs to give a bis-gold(I) complex.
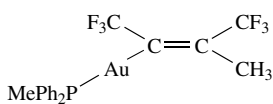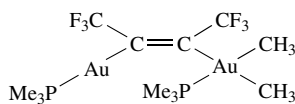
(13)   (18, 31)

Data are available for a small number of organogold(II) compounds (Table 3). They are readily distinguishable from mixed-oxidation-state gold(I/III) systems by the fact that they have simple spectra with distinct parameters[15]. They are recognizable as gold(II) because the IS is lower than for similar gold(III) compounds; in terms of the correlation diagram (Figure 3), they lie between the gold(I) and gold(III) regions. Like the vast majority of gold(II) derivatives, they are binuclear with gold–gold bonds (structures **40–45, 46–48**).
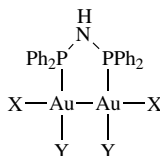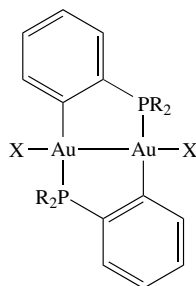
(40 – 45)   (46 – 48)

TABLE 3.   Data for σ-bonded gold(II) compounds

Structure number	Compound	IS_{Au} (mm s^{-1})	QS (mm s^{-1})	Reference
40	{C$_6$Cl$_5$Au(I)PPh$_2$}$_2$NH	4.20	6.56	15
41	{C$_6$F$_5$Au(I)PPh$_2$}$_2$NH	4.30	6.59	15
42	{C$_6$l$_5$Au(Br)PPh$_2$}$_2$NH	4.22	6.26	15
43	{C$_6$F$_5$Au(Br)PPh$_2$}$_2$NH	4.11	6.52	15
44	{C$_6$Cl$_5$Au(Cl)PPh$_2$}$_2$NH	4.20	6.20	15
45	{C$_6$F$_5$Au(Cl)PPh$_2$}$_2$NH	4.19	6.47	15
46	[2-Ph$_2$PC$_6$H$_4$AuBr]$_2$	3.47[a]	6.44	11
47	[2-Ph$_2$PC$_6$H$_4$AuI]$_2$	4.47[a]	6.54	11
48	[2-Et$_2$PC$_6$H$_4$AuI]$_2$	4.81[a]	6.96	11

*Corrected from data reported relative to Au/Pt.

Thus they resemble square-planar gold(III) systems, but one ligand is replaced by the Au−Au bond. The high electron density in this bond gives Mössbauer parameters rather similar to those for gold(III) complexes with one fewer soft ligand[15].

B. π-Bonded Derivatives

Complexes involving organic ligands π-bonded to gold are rather rare, and most contain alkynes[22]. Mössbauer data are available only for cyclo-octatetraene (COT) derivatives[23]. The tetraene reacts with AuCl to give (COT)AuCl, which is presumably a molecular complex with a C=C double bond and a chloride ligand co-ordinated to gold(I). The Mössbauer parameters (IS, QS = 2.87, 6.10 mm s^{-1}) imply that the alkene acts as a rather poor donor to gold(I), comparable to a halide ion. This is reinforced by a second derivative, (COT)Au$_2$Cl$_4$, obtained either by reaction of (COT)AuCl with AuCl$_3$ or of AuCl$_3$ with COT. The spectrum for this material contains two doublets: IS$_1$, QS$_1$ = 1.64, 5.18 mm s^{-1}; IS$_2$, QS$_2$ = 3.11, 0.94 mm s^{-1}. The first is undoubtedly due to two-co-ordinate gold(I) and the second is comparable to many other salts of [AuCl$_4$]$^-$. It is likely that there is a polymeric cation in which the tetraene acts as a bridging ligand co-ordinated to two gold(I) cations: $[\cdots Au-COT-Au-COT\cdots]_n{}^{n+}$.

C. Carbene, Methanide and Ylide Complexes

Large numbers of gold complexes of carbene, ylide and methanide ligands have been synthesized. The majority contain Au−C bonds but, otherwise, the distinction between them is not always clear. A methanide, as the name implies, involves gold bonded to a single aliphatic-type carbon atom with three other groups covalently bonded to it; technically, it is a conventional σ-bonded organometallic but, since they are usually derived from carbene or ylide systems, they are normally discussed together with them. A carbene complex contains a ligand which is, formally at least, a neutral, divalent carbon group :CR$_2$, whose lone pair forms a co-ordinate bond with gold. Ylides are somewhat similar except that there is a third group bonded to the carbon atom; in gold chemistry they are often derived from a phosphonium salt by deprotonation: (CH$_3$)R$_3$P$^+$ → (:CH$_2$)R$_3$P; this species might be envisaged as carbene containing a phosphine ligand: :CH$_2$ ← PR$_3$.

As far as their effect on the gold atom is concerned, a carbene would presumably be the least effective donor of electron density. The donor ability of the methanide and ylide ligands will depend on the substituents at the carbon donor atom.

Two major series of carbene complexes have been investigated: (a) those derived from co-ordinated *p*-tolyl isocyanide[24] (Scheme 1) and (b) those derived from a trimeric complex of a σ-bonded imidazole[4] (Scheme 2). Mössbauer data for these materials are given in Table 4.
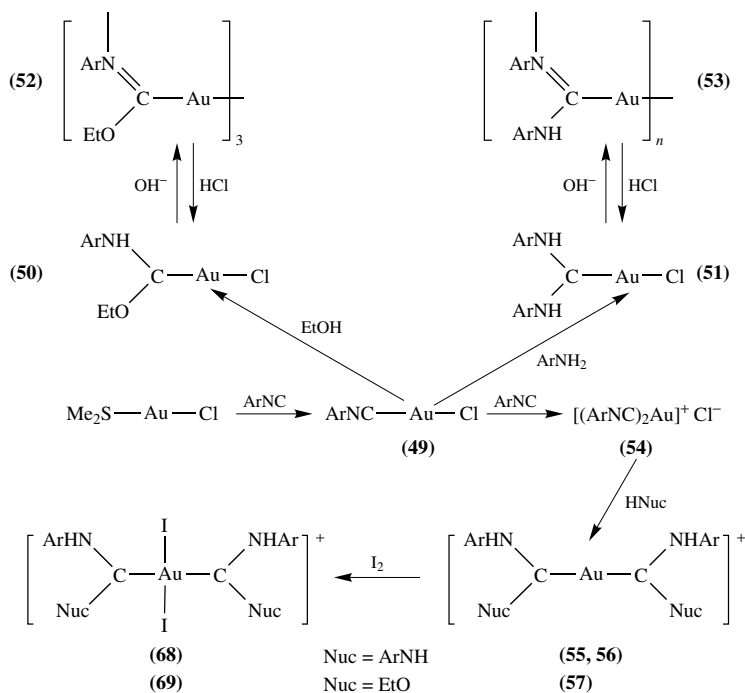
SCHEME 1

Comparison of the data for (carbene)AuCl (50, 51) and [(carbene)$_2$Au]$^+$ (55–57) with those for the starting materials ArNCAuCl and [(Ar(NC)$_2$Au]$^+$ (49, 54) shows that the addition of nucleophiles to the isocyanide gives a substantial increase in parameters, consistent with the carbene acting as a strong σ-donor to gold(I). Compounds containing different stereochemical isomers of the same carbene give indistinguishable Mössbauer spectra. The deprotonated derivatives (52, 53) are, not surprisingly, the strongest donors; these are actually polymeric methanides with covalent C−Au bonds with the nitrogen atoms acting as the second ligand to gold.

It is more difficult to make a similar comparison for the imidazole derivatives, since the starting material (58) has (σ-C)AuN co-ordination similar to 52 and 53; its Mössbauer parameters are also comparable to those of these methanides. The carbene form is obtained by reaction with an organic halide, which puts a carbocation on the second nitrogen atom and a halide ligand on the gold (59–61, Scheme 2). The iodo derivative, 61, obtained
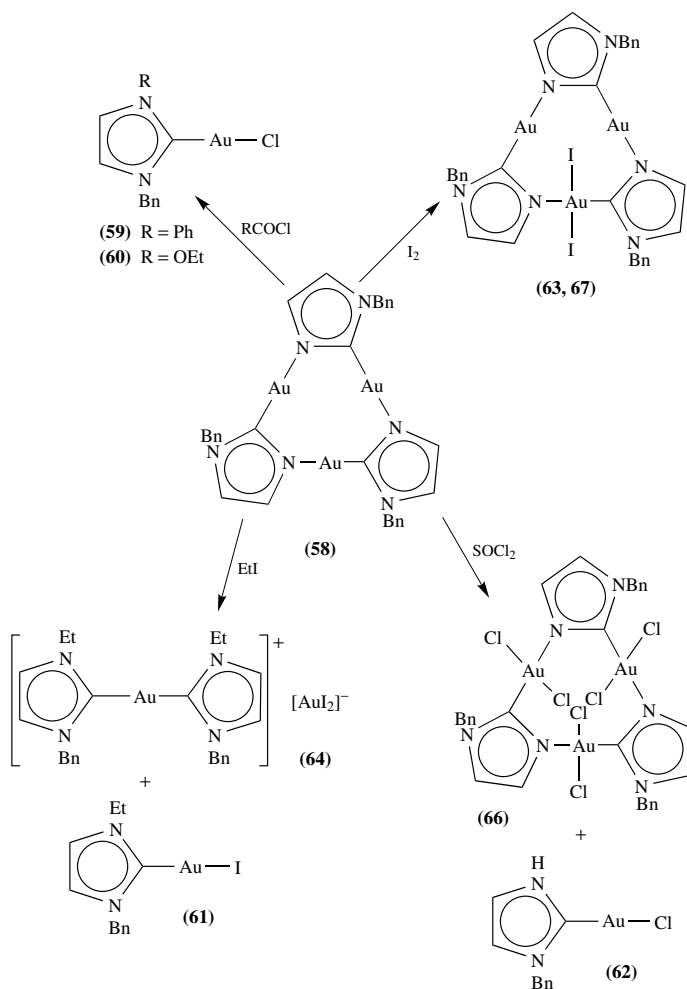
SCHEME 2

by reaction with iodoethane is unstable to disproportionation and gives the cationic bis-carbene complex (64); the other product is the anion $[AuI_2]^-$, identified by its very low parameters (IS, QS = 1.41, 5.23 mm s^{-1}). In these complexes, the carbene is a rather less good donor than the directly σ-bonded imidazole, but very comparable to the other carbene complexes listed.

The bis-carbene complexes 55–57 readily undergo oxidation to gold(III) complexes (68, 69, Scheme 1). In 68 and presumably in 69, the gold(III) has a *trans* configuration, but the stereochemistry cannot be deduced from the spectrum. The trimeric imidazole complex 58 gives an incompletely oxidized form, readily recognized from its composite Mössbauer

TABLE 4. Data for carbene complexes

Structure number	Compound	IS$_{Au}$ (mm s^{-1})	QS (mm s^{-1})	Reference
	Gold(I)			
49	p-TolNCAuCl	3.21[a]	7.61	24
50	{(p-TolNH) (EtO) C}AuCl	4.11[a]	7.36	24
51	{(p-TolNH)$_2$C}AuCl	4.21[a]	7.62	24
52	[{(p-Tol=N)(EtO)C}Au]$_3$	5.11[a]	8.28	24
53	[{(p-Tol=N)(p-TolNH)C}Au]$_n$	5.26[a]	8.88	24
54	[(p-TolNC)$_2$Au]BF$_4$	3.98[a]	9.33	24
55	[{(p-TolNH)$_2$C}$_2$Au]ClO$_4$	3.86[a]	9.51	24
56	[{(p-TolNH)$_2$C}$_2$Au]BF$_4$	5.66	10.73	24
57	[{(p-TolNH)(EtO)C}$_2$Au]ClO$_4$	5.76[a]	10.61	24
58	[C$_2$H$_2$N(Bz)NAu]$_3$	5.08[a]	9.05	4
59	{C$_2$H$_2$N(Bz)N(COPh)C}AuCl	3.81[a]	7.58	4
60	{C$_2$H$_2$N(Bz)N(COOEt)C}AuCl	4.08[a]	8.09	4
61	{C$_2$H$_2$N(Bz)N(Et)C}AuI	4.23[a]	7.80	4
62	{C$_2$H$_2$N(Bz)N(H)C}AuCl	4.26[a]	7.86	4
63	{C$_2$H$_2$N(Bz)CAu}$_2${C$_2$H$_2$N(Bz)CAuI$_2$}	5.17[a]	9.26	4
64	[{C$_2$H$_2$N(Bz)N(Et)C}$_2$**Au**] [AuI$_2$]	5.52[a]	11.12	4
65	[{C$_2$H$_2$N(Bz)N(H)C}$_2$**Au**] [AuI$_2$]	5.61[a]	11.02	4
	Gold (III)			
66	[{C$_2$H$_2$N(Bz)NC}AuCl$_2$]$_3$	3.31[a]	2.79	4
67	{C$_2$H$_2$N(Bz)CAu}$_2${C$_2$H$_2$N(Bz)C**Au**I$_2$}	3.88[a]	3.70	4
68	trans-[{(p-TolNH)$_2$C}$_2$AuI$_2$]BF$_4$• 0.75Et$_2$O	4.17[a]	6.44	24
69	[{(p-TolNH)(EtO)C}$_2$Au$_2$]ClO$_4$• 0.5Et$_2$O	4.43[a]	6.61	24

[a]Corrected from reported IS$_{Au/Pt}$.

(52)
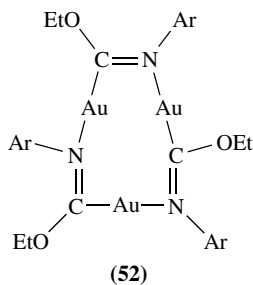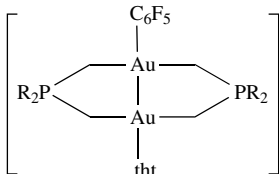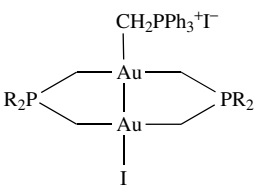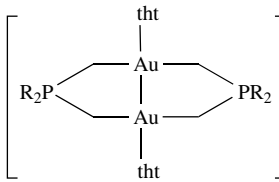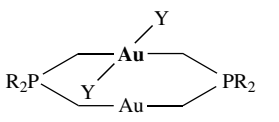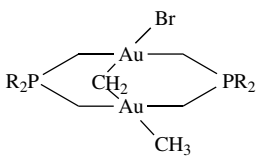
spectrum (**63, 67**), confirming the X-ray determination[25]. The fully oxidized form, **66**, is reported as the product of reaction of **58** with thionyl chloride. However, since it is accompanied by the gold(I) carbene complex **62**, it seems more likely that the reactant is HCl.

Several families of ylide complexes have been examined, of which the most relevant are shown in Table 5. These are all derivatives of the methanide/ylide Ph$_2$P(CH$_2$)$_2$$^-$, which

TABLE 5.   Data for ylide compounds

Structure number	Compound[a]	IS_{Au} (mm s^{-1})	QS (mm s^{-1})	Reference
Gold (I)				
70	R$_2$P—Au—Au—PR$_2$ **(70)**	4.98	7.19	16
71	PR$_2$—Au—Y—Au(Y)—PR$_2$ **(71)**	4.90[b]	9.40	5
	Y = CH$_2$PMe$_3^+$I$^-$			
72	Paddle wheel, Au^I	5.00[b]	9.67	5
Gold (II)				
73	R$_2$P / S$_2$CNEt$_2$—Au—Au—S$_2$CNEt$_2$ / PR$_2$ **(73)**	4.11[b]	6.50	26
74	[R$_2$P / PPh$_3$—Au—Au—PPh$_3$ / PR$_2$] (ClO$_4$)$_2$ **(74)**	4.97	7.41	27
75	[R$_2$P / C$_6$F$_5$—Au—Au—PPh$_3$ / PR$_2$] ClO$_4$ **(75)**	4.85 / 4.85	6.90 / 7.90	27
76	[R$_2$P / PPh$_3$—Au—Au—tht / PR$_2$] (ClO$_4$)$_2$ **(76)**	4.75 / 4.60	7.80 / 6.64	27

TABLE 5. (*continued*)

Structure number	Compound[a]	IS_{Au} (mm s^{-1})	QS (mm s^{-1})	Reference
77	(77)	4.55 4.65	7.60 6.50	27
78	(78)	4.47[b] 4.13[b]	6.94 6.26	5
79	(79)	4.17	6.72	27
Gold (III)				
80	(80) Y = CH$_2$PMe$_3$$^+I^-$	4.80[b]	6.49	5
81	(81)	4.68[b] 5.45[b]	6.52 8.06	28
82	Paddle wheel, Au^{III}	4.64[b]	5.61	5
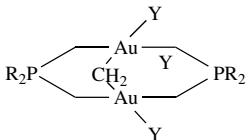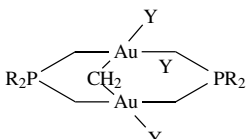
(*continued overleaf*)

TABLE 5.   (*continued*)

Structure number	Compound[a]	IS_{Au} (mm s^{-1})	QS (mm s^{-1})	Reference
83a	(83a) Y = CH$_2$PPh$_3^+$I$^-$	5.25[b]	7.72	29
83b	(83b) Y = CH$_2$PPh$_3^+$Br	5.25[b]	7.72	29

[a]tht = tetrahydrothiophen.
[b]Corrected from reported $IS_{Au/Pt}$.

acts as a bridging ligand, forming dimeric, cyclic complexes involving C−Au−C units. The principal point of interest is to follow the oxidation of the di-gold(I) form **70** where, in addition to the conventional di-gold(III) derivatives **80−83b**, half-oxidized species can be found (Scheme 3). These may be mixed-valence gold(I,III) compounds **(71, 80; 72, 82)**; more usually, they contain di-gold(II) units, with a gold−gold bond **(73−79)**. For a given set of ligands, the parameters for the three oxidation states are distinct; in particular, the QS decreases with increasing oxidation state. Note that, since measurements are made on solid samples, there are no complications of time averaging which sometimes occur in solution.
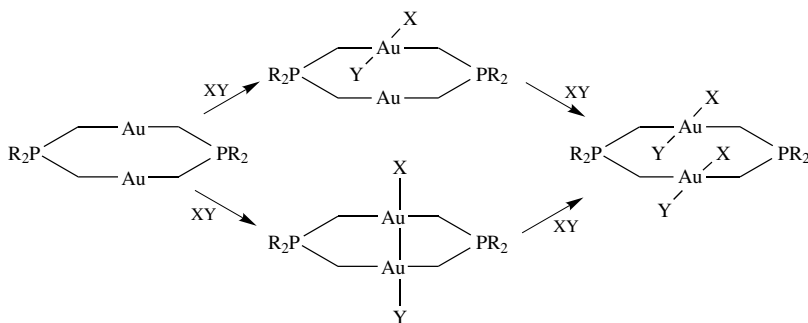
SCHEME 3
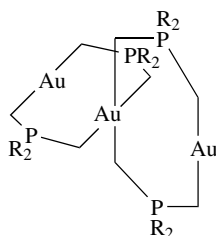
(72, 82)

D. Hypervalent Compounds

There is an ever-growing number of compounds in which a main-group element is bonded to more gold atoms than would be expected from the number of bonding electrons available. As with other electron-deficient systems, sensible molecular-orbital schemes can usually be set up to describe the bonding, but the stability is believed to be aided by the ability of gold atoms to bond to each other[30]. Mössbauer data are available for many of these species (Table 6); unfortunately, the data for most of the carbon–gold derivatives have not been reported. Table 6 includes data for a range of other relevant complexes.

The first compound listed (**84**, $[Me_3PC(AuPPh_3)_3]^+$) is included as a reference material; it is not hypervalent, but contains conventional C–Au σ-bonds. It is noticeable that it

TABLE 6. Data for hypervalent compounds

Structure number	Compound	IS_{Au} (mm s^{-1})	QS (mm s^{-1})	Reference
84	$[Me_3PC(AuPPh_3)_3]Cl$	5.14	8.70	31
85	$[C_6H_5(AuPPh_3)_2]BF_4$	4.26[a]	8.48	32
86	$[C_6H_5(AuPPh_3)_2BF_4$	4.28	8.48	8
87	$[2\text{-}CH_3C_6H_4(AuPPh_3)_2]BF_4$	4.08	8.18	8
88	$[4\text{-}MeC_6H_4(AuPPh_3)_2]BF_4$	4.06[a]	8.18	32
89	$[CpFeC_5H_4(AuPPh_3)_2]BF_4$	3.93	8.07	8
90	$[CpFeC_5H_4(AuPPh_3)_2]BF_4$	3.91[a]	8.07	32
91	$cyclo\text{-}C(O)N(Ph)N{=}C(Me)C(AuPPh_3)_2$	4.73[a]	8.96	32
92	$[BuN(AuPPh_3)_3]BF_4$	4.92	8.33	33
93	$[N(AuPPh_3)_5]BF_4 \cdot 2C_4H_8O$ (Ph$_3$P: 2 = ax, 3 = equ)	$IS_2 > IS_3$	$QS_2 > QS_3$	34
94	$[N_3(AuPPh_3)_2]ClO_4$	3.75	6.74	35
95	$[2\text{-}MeC_6H_4As(AuPPh_3)_3]BF_4$	4.32[a]	7.73	36
96	$[O(AuPPh_3)_3]BF_4$	4.32	7.03	35
97	$[O(AuPPh_3)_2]MnO_4$	4.34	6.94	35
98	$[NCS(AuPPh_3)_2]ClO_4$	3.70	6.54	35
99	$[Cl(AuPPh_3)_2]BF_4$	3.64	6.54	35
100	$[Cl(AuPPh_3)_2]ClO_4$	3.57	6.54	35
101	$[I(AuPPh_3)_2]ClO_4$	3.23	6.21	35

[a]Corrected from reported $IS_{Au/Pt}$.

(85)
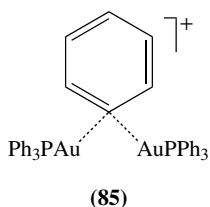
has higher parameters than **85–97** ($[Ar(AuPPh_3)_2]^+$), which involve an aromatic group in which one carbon atom bridges between two gold atoms. The data all lie in the gold(I) band of the correlation diagram, but at the lower end; this suggests that the electron density available to the gold atom is comparable to that provided by a halide in conventional complexes. It also confirms that the gold atom is still sp-hybridized and contributes only one orbital to the bond system. The bonding is comparable to other three-centre two-electron systems, so that one pair of electrons is shared between the two gold atoms and the carbon atom. These data reinforce the suggestion that in **1** and **2** (Table 1) the Au–C bonds are very strong and are not electron-deficient.

In the same way, **92** ($[BuN(AuPPh_3)_3]^+$, conventional) has higher parameters than **94** ($[N_3(AuPPh_3)_2]^+$, hypervalent). The spectrum for **93**, $[N(AuPPh_3)_5]^+$, has been published, but its detailed parameters have not. Nevertheless, two distinct doublets are seen, in 2 : 3 intensity ratio, consistent with the known trigonal-bipyramidal structure[34]. The axial groups give the smaller parameters, and have the longer N–Au bonds. The oxygen and halogen derivatives **96–101** have the lowest parameters of all, consistent with their greater electronegativity. In these cases also, the Mössbauer parameters confirm that the gold atom contributes a single sp-hybrid orbital to the bonding.

V. CONCLUSION

The data discussed above show that Mössbauer spectroscopy is a valuable adjunct to the list of 'sporting' methods. By specifically probing the gold atom, it supplies information not available by other techniques, and aids the characterization of compounds which are not susceptible to X-ray analysis.

VI. REFERENCES

1. After L. Niven *ca* 1950: one version of his Finagle's Law is that 'the perversity of the universe tends towards a maximum'. http://www-sc.ucssc.indiana.edu/jargon.
2. Note that some spectra in the literature use the source as the standard. To convert these data to the gold standard, 1.21 mm s^{-1} should be added to the IS. The QS value is, of course, unaffected.
3. R. V. Parish, in *Mössbauer Spectroscopy Applied to Inorganic Chemistry* (Ed G. J. Long), Vol. 1, Plenum Press, New York, 1984, p. 577.
4. B. Bovio, S. Calogero, F. E. Wagner, A. Burini and B. R. Pietroni, *J. Organomet. Chem.*, **470**, 275 (1994).
5. H. Schmidbaur, C. Hartmann and F. E. Wagner, *Angew. Chem., Int. Ed. Engl.*, **26**, 1148 (1987); **40**, 335 (1988).
6. G. van Koten and J. G. Noltes, *J. Organometal. Chem.*, **174**, 367 (1979).
7. G. van Koten, C. A. Schaap, J. T. B. H. Jastrzebski and J. G. Noltes, *J. Organometal. Chem.*, **186**, 427 (1980).
8. M. Katada, Y. Uchida, H. Sano, H. H. Wei, H. Sakai and Y. Maeda, *Radiochem. Radioanal. Lett.*, **54**, 55 (1982).
9. J. S. Charlton and D. I. Nicholls, *J. Chem. Soc., A*, 1484 (1970).

10. A. Johnson and R. J. Puddephatt, *J. Chem. Soc., Dalton Trans.*, 980 (1978).
11. M. Takeda, M. Takahashi, Y. Ito, T. Takano, M. A. Bennett and S. K. Bhargava, *Chem. Lett.*, 543 (1990).
12. K. Moss, R. V. Parish, A. Laguna, M. Laguna and R. Usón, *J. Chem. Soc., Dalton Trans.*, 2071 (1983).
13. F. Bonati, A. Burini, B. R. Pietroni, E. Torregiani, S. Calogero and F. E. Wagner, *J. Organometal. Chem.*, **408**, 125 (1991).
14. M. Viotte, B. Gautheron, M. M. Kubicki, Y. Munier and R. V. Parish, *Inorg. Chem.*, **34**, 3465 (1995).
15. L. S. Moore, R. V. Parish, R. Usón, A. Laguna, M. Laguna and M. N. Fraile, *J. Chem. Soc., Dalton Trans.*, 23 (1988).
16. H. Schmidbaur, C. Hartmann and F. E. Wagner, *Hyperfine Interact.*, **40**, 335 (1988).
17. H. Schmidbaur, J. R. Mandl, F. E. Wagner, D. F. van der Vondel and G. P. van der Kelen, *J. Chem. Soc., Chem. Commun.*, 170 (1976).
18. R. V. Parish, *Gold Bull.*, **15**, 51 (1982).
19. R. Usón, A. Laguna, M. de la Orden, R. V. Parish and L. S. Moore, *J. Organometal. Chem.*, **282**, 145 (1985).
20. R. V. Parish, O. Parry and C. A. McAuliffe, *J. Chem. Soc., Dalton Trans.*, 2098 (1981).
21. R. Usón, A. Laguna, M. Laguna, P. G. Jones and G. M. Sheldrick, *J. Chem. Soc., Chem. Commun.*, 1097 (1981).
22. R. V. Parish, *Gold Bull.*, **30**, 3 (1997).
23. P. Tauchner and R. Hüttel, *Chem. Ber.*, **107**, 3761 (1974).
24. G. Banditelli, F. Bonati, S. Calogero, G. Valle, F. E. Wagner and R. Wordel, *Organometallics*, **5**, 1346 (1986).
25. L. Manojlovic-Muir, *J. Organometal. Chem.*, **73**, C45 (1974).
26. H. Schmidbaur and J. R. Mandl, *Naturwissenschaften*, **63**, 585 (1976).
27. M. C. Gimeno, J. Jimenez, A. Laguna, M. Laguna, P. G. Jones and R. V. Parish, *J. Organometal. Chem.*, **481**, 37 (1994).
28. H. Schmidbaur, C. Hartmann, J. Riede, B. Huber and G. Muller, *Organometallics*, **5**, 1652 (1986).
29. H. Schmidbaur and C. Hartmann, *Angew. Chem., Int. Ed. Engl.*, **98**, 573 (1986).
30. H. Schmidbaur, *Gold Bull.*, **23**, 11 (1990) and references cited therein.
31. H. Schmidbaur, F. Scherbaum, B. Huber and G. Muller, *Angew. Chem., Int. Ed. Engl.*, **27**, 419 (1988).
32. F. Bonati, A. Burini, B. R. Pietroni, S. Calogero and F. E. Wagner, *J. Organometal. Chem.*, **309**, 363 (1986).
33. A. Grohmann, J. Riede and H. Schmidbaur, *J. Chem. Soc., Dalton Trans.*, 783 (1991).
34. A. Grohman, J. Riede and H. Schmidbaur, *Nature*, **345**, 140 (1990).
35. Y. Uchida, M. Katada, H. Sano, H. Sakai and Y. Maeda, *J. Radioanal. Nucl. Chem.*, **94**, 215 (1985).
36. H. Schmidbaur, E. Zeller, G. Weidenhiller, O. Steigelmann and H. Bruda, *Inorg. Chem.*, **31**, 2370 (1992).

CHAPTER **3**

Thermochemistry of the organometallic compounds of silver and gold

JOEL F. LIEBMAN

Department of Chemistry and Biochemistry, University of Maryland, Baltimore County, 1000 Hilltop Circle, Baltimore, MD 21250, USA
Fax: (+1)-410-455-2608;   e-mail: jliebman@umbc.edu

JOSÉ MARTINHO SIMÕES

Departamento de Química e Bioquímica and CiTecMat, Faculdade de Ciências, Universidade de Lisboa, 1700 Lisboa, Portugal
Fax: (+351)-1-7500088;   e-mail: jams@fc.ul.pt

and

SUZANNE W. SLAYDEN

Department of Chemistry, George Mason University, 4400 University Drive, Fairfax, VA 22030-4444 USA
Fax: (+1)-703-993-1055;   e-mail: sslayden@gmu.edu

I. INTRODUCTION

A perusal of any organometallic chemistry textbook, monograph or encyclopedia will show that the information on silver and gold-containing compounds is conspicuously poor when compared with that for most of the remaining transition elements[1,2]. In counterpoint, it is interesting to note that the 1938 study by Winstein and Lucas on the π-bonded Ag(I)−olefin metal complexes[3] is considered one of the earliest landmarks in organotransition metal chemistry[1]. The relative paucity of silver and gold compounds containing at least one metal−carbon bond is immediately reflected by the rather small thermochemical database for these substances[4] and necessarily limits the scope of a review. Besides stressing exactly this point and giving salient literature references, the present brief survey may lead to a better understanding of the thermodynamic stabilities of silver−and gold−carbon bonds as well as that of more 'popular' organometallic compounds.

As transition metals, both silver and gold have multiple valence states. However, their organometallic chemistry is almost exclusively that of the '+1' state and so for simplicity we will merely say silver and gold, or Ag and Au, without the appended (I). Furthermore, while it has been our prejudice to consider solely enthalpies of formation and occasionally enthalpies of reaction in previous reviews, in the current study we also consider Gibbs energies and equilibrium constants.

II. SILVER ACETYLIDES

A. Disilver Acetylide

It has long been known that silver ions react with acetylene in solution to yield the acetylide compound, $AgC{\equiv}CAg$, where the metal atoms are σ-bonded to carbon. Indeed, the enthalpy of reaction 1, $-65.1 \text{ kJ mol}^{-1}$, was measured at the beginning of this century by Berthelot and Delépine[5] to derive the standard enthalpy of formation of Ag_2C_2:

$$2Ag(NH_3)_2NO_3(aq) + C_2H_2(aq) \longrightarrow Ag_2C_2(cr) + 2NH_4NO_3(aq) + 2NH_3(aq) \quad (1)$$
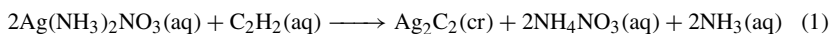
Using the auxiliary data in Table 1[6−8], one obtains $\Delta_f H_m^\circ(Ag_2C_2, cr) = 350.5 \text{ kJ mol}^{-1}$. This value differs by less than 10 kJ mol^{-1} from the reaction−solution calorimetry results published 91 years later by Finch and his coworkers[9]. These latter authors determined the enthalpies of reactions 2a, 2b and 2c as -63.6 ± 0.3, -77.8 ± 0.6 and $-98.4 \pm 0.4 \text{ kJ mol}^{-1}$ which, together with the auxiliary data in Table 1, lead, respectively, to enthalpies of formation of 356.1 ± 1.8, 361.1 ± 1.6

TABLE 1.   Auxiliary data

Compound	$\Delta_f H_m{}^\circ$ (kJ mol^{-1})	Reference
C_2H_2, g	228.2 ± 0.7	8
C_2H_2, aq	$212.9 \pm (1.0)$	6, 8
CO_2, g	-393.51 ± 0.13	7
H_2O, l	-285.830 ± 0.040	7
NH_3, g	-45.94 ± 0.35	7
NH_3, 300 H_2O, sln	$-80.04 \pm (0.5)$	6, 7
NH_3, aq	$-80.12 \pm (0.5)$	6, 7
NH_4NO_3, 10000 H_2O, sln	$-339.75 \pm (0.1)$	6
NH_4NO_3, aq	$-339.87 \pm (0.1)$	6
HCl, 12.3 H_2O, sln	$-162.27 \pm (0.1)$	6
KOH, 20000 H_2O, sln	$-482.28 \pm (0.5)$	6
KCN, 200 H_2O, sln	$-101.3 \pm (0.5)$	6
$KAg(CN)_2$, aq	$18.0 \pm (0.5)$	6
$AgNO_3$, cr	$-124.39 \pm (0.5)$	6
$Ag(NH_3)_2NO_3$, aq	$-318.65 \pm (0.5)$	6
AgCl, cr	$-127.07 \pm (0.5)$	6

and 359.6 ± 3.2 kJ mol^{-1} for the crystalline compound. The average of these values, 359.0 ± 5.0 kJ mol^{-1}, is the currently recommended value for $\Delta_f H_m{}^\circ(Ag_2C_2, cr)$[10].

$$AgNO_3(cr) + 0.5C_2H_2(aq) + (NH_3, 300H_2O) \text{ (sln)} \longrightarrow 0.5Ag_2C_2(cr)$$
$$+ (NH_4NO_3, 10000H_2O) \text{ (sln)} \quad (2a)$$

$$Ag_2C_2(cr) + 2(HCl, 12.3H_2O) \text{ (sln)} \longrightarrow 2AgCl(cr) + C_2H_2(aq) \quad (2b)$$

$$Ag_2C_2(cr) + 4(KCN, 200H_2O) \text{ (sln)} + 2H_2O \longrightarrow 2KAg(CN)_2(aq)$$
$$+ 2(KOH, 20000H_2O) \text{ (sln)} + C_2H_2(aq) \quad (2c)$$
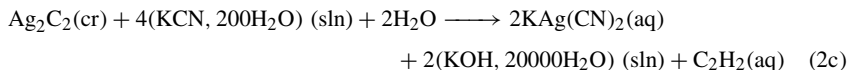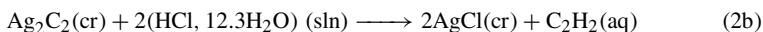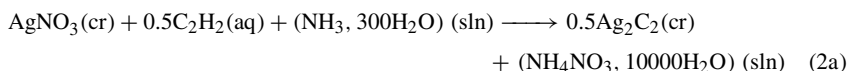
B. Silver Phenylacetylide

To the best of our knowledge, PhC≡CAg is the only other silver acetylide for which there is a measured enthalpy of formation. Indeed, it is the only other 'classical' silver organometallic compound for which the standard enthalpy of formation has become available in this century! Using static-bomb combustion calorimetry, Bykova and her coworkers[11] determined this value to be 346.3 ± 2.0 kJ mol^{-1}.

It is not obvious how to ascertain the 'reasonableness' of the previous two silver acetylide values because there seems to be insufficient data to make meaningful comparisons. Yet, using organic thermochemical data from Reference 12 for diphenylacetylene, the formal, organometallic, solid phase disproportionation reaction 3

$$PhC≡CPh(s) + Ag_2C_2(s) \longrightarrow 2PhC≡CAg(s) \quad (3)$$
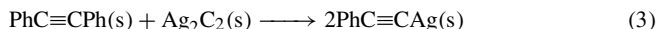
is found to be endothermic by *ca* 21 kJ mol^{-1}. By bond additivity reasoning, this reaction might have been expected to be thermoneutral. After all, the corresponding but simpler

TABLE 2. Enthalpies of formation ($\Delta_f H_m^\circ$) and enthalpies of synthesis [$\Delta_r H_m^\circ$, equation 5] of disilver acetylide silver salt complexes (kJ mol^{-1})

X	m	n	$\Delta_f H_m^\circ$(cr)	$\Delta_r H_m^\circ$(5)
Cl	1	1	209.6	13.8
Cl	2	1	544.3	29.6
I	1	1	283.3	5.4
I	1	2	216.3	0.5
SO$_4$[a]	1	1	−35.6	29.0
SO$_4$[b]	1	2	−191.2	8.5
NO$_3$	1	1	200.4	25.7

[a]Reference 6 referred to this species as a 2:1 complex of Ag_2C_2 and Ag_2SO_4, but here the stoichiometry and the enthalpy of formation are halved in order to describe the compound by the general formula $(Ag_2C_2)_m\bullet(AgX)_n$.
[b]Reference 6 referred to this species as a 1:1 complex of Ag_2C_2 and Ag_2SO_4, but here the stoichiometry and the enthalpy of formation are halved in order to describe the compound by the general formula $(Ag_2C_2)_m\bullet(AgX)_n$.

(gas phase, wholly organic) disproportionation reaction 4

$$PhC\equiv CPh(g) + R_2C_2(g) \longrightarrow 2PhC\equiv CR(g) \tag{4}$$
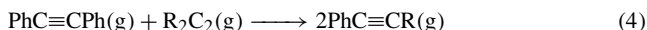
deviates from thermoneutrality by *ca* only 1, 6 and 6 kJ mol^{-1} for R = H, Me and Et, respectively[12]. However, given the complications of the nature of carbon–silver bonding[13] and the unavoidable use of solid state data in equation 3, the thermoneutrality assumption may not be particularly valid.

C. Disilver Acetylide Complexes of Silver Salts

Reference 6 chronicles the thermochemistry of some unusual complexes with the general formula $(Ag_2C_2)_m\bullet (AgX)_n$. Table 2 presents the enthalpies of formation[14] as well as enthalpies of their formal synthesis or complexation reaction 5

$$mAg_2C_2 + nAgX \longrightarrow (Ag_2C_2)_m\bullet(AgX)_n \tag{5}$$
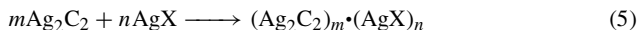
All of the complexation reaction enthalpies are endothermic for all X investigated. This seems unlikely in that this complexation reaction most probably has $\Delta S < 0$. Accordingly, the reaction would have a net $\Delta G > 0$ and so it is not obvious how these complexes would be formed.

III. SILVER CYANO DERIVATIVES

Hydrogen cyanide has the same isoelectronic relationship to acetylene as methylamine has to ethane and pyridine has to benzene. Accordingly, having just considered silver acetylides suggests we consider silver cyanides even though these latter compounds are at least as plausibly inorganic as they are organometallic.

A. Silver Cyanide Itself

We start with AgCN as the archetype of the species of interest and merely accept its crystalline phase enthalpy of formation[6] of 146.0 kJ mol^{-1}. Similar to reaction 3, we

consider the condensed phase reaction 6 which is endothermic[15] by *ca* 45 kJ mol^{-1}.

$$AgCN(cr) + PhC\equiv CH(l) \longrightarrow PhC\equiv CAg(cr) + HCN(l) \qquad (6)$$
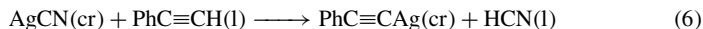
The corresponding reaction for copper-containing organometallics[16] has a comparable endothermicity, and so reaction 7 is thermoneutral.

$$CuCN(cr) + PhC\equiv CAg(cr) \longrightarrow AgCN(cr) + PhC\equiv CCu(cr) \qquad (7)$$

B. Isocyanide Complexes of Silver Cyanide

In 1908, Guillemard reported static bomb combustion measurements on several silver isocyanide species, generically RNCAgCN, and derived the respective enthalpies of formation in the crystalline phase[17]. The data, collected in Table 3, have been recalculated by using the modern values for the enthalpies of formation of $CO_2(g)$ and $H_2O(l)$ (Table 1) and by assuming that metallic silver and $N_2(g)$ are the remaining combustion products. Although the reliability of Guillemard's results (or even of our assumptions) are difficult to assess, it is likely that the trend shown in Table 3 is accurate to *ca* 10 kJ mol^{-1}. In fact, Guillemard also reported the enthalpies of formation of some of the precursor isocyanides[17] from which one may readily calculate the related enthalpies of formation. As shown in Figure 1, when the various $\Delta_f H_m^\circ$ (RNCAgCN, cr) are plotted against $\Delta_f H_m^\circ$(RNC, l) a good linear correlation (equation 8, $r^2 = 0.9994$) is obtained[18]. This suggests that Guillemard's results are, at least, internally consistent.

$$\Delta_f H_m^\circ(\text{RNCAgCN, cr}) = (0.877 \pm 0.013)\Delta_f H_m^\circ(\text{RNC, l}) + (124.06 \pm 1.21) \text{ kJ mol}^{-1} \qquad (8)$$

Further confidence in these early experiments is gained by noting that the recalculated enthalpies of formation for liquid RNC with R = Me and Et are (123.5 ± 4.2) and (113.6 ± 9.2) kJ mol^{-1}, while the currently suggested values[8] are numerically rather close — (130.8 ± 7.3) and (108.6 ± 4.7) kJ mol^{-1}, respectively — indeed, the two sets of values are the same within error bars[19].

C. Other Complexes of Silver Cyanide

With the species in this section, we trespass ever more into the traditional province of inorganic compounds even though they also qualify as organometallics by our simple definition[4] of this class of species. The first of such species is $Ag(CN)_2^-$ which has long

TABLE 3.   Standard enthalpies of formation of silver isocyanide compounds^a (kJ mol^{-1})

Compound	$\Delta_f H_m^\circ$(cr)
MeNCAgCN	233.3 ± 3.3
EtNCAgCN	223.9 ± 11.3
PrNCAgCN	209.7 ± 9.2
i-BuNCAgCN	187.1 ± 0.9
i-PeNCAgCN	154.5 ± 5.1

^{a}See text for a detailed explanation of the tabulated enthalpies of formation.
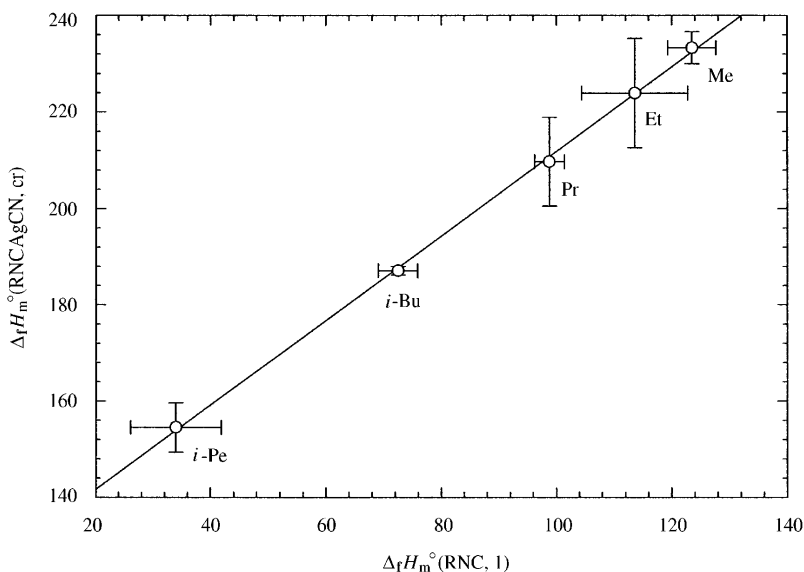
FIGURE 1. Enthalpies of formation of crystalline RNCAgCN compounds versus the enthalpies of formation of the respective liquid isocyanide ligands, RNC

been known as a stable complex ion in aqueous solution and as a constituent of solid metal salts. Let us discuss its energetics in terms of isodesmic reactions and bond additivity reasoning. We accordingly note that the formal solid state reaction 9 is exothermic by nearly 40 kJ mol^{-1}.

$$KAg(CN)_2(s) + Ag(NH_3)_2NO_3(s) \longrightarrow KNO_3(s) + 2AgCN \cdot NH_3(s) \qquad (9)$$
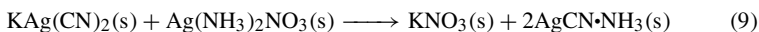
Likewise, reaction 10 for which regrettably the thermochemistry is limited to Gibbs energies in aqueous solution[20] is exoergic[21] by 30 kJ mol^{-1}.

$$Ag(CN)_2{}^- + Ag(OH)_2{}^- \longrightarrow 2Ag(CN)(OH)^- \qquad (10)$$

Finally, one can write the formal reaction[22] relating this ion to AgCN

$$2AgCN(s) + AgCl_2{}^-(*) \longrightarrow 2AgCl(s) + Ag(CN)_2{}^-(*) \qquad (11)$$

From the data in Reference 6 we find that in aqueous solution (* = aq) this reaction is exothermic by *ca* 31 kJ mol^{-1}. By contrast, it is essentially thermoneutral for the solid potassium salts (* = K$^+$, cr).

The next species we consider is AgCN·NH$_3$. Silver ion—ammonia complexes have long been known, in particular Ag(NH$_3$)$_2{}^+$. The Ag–N interaction is strong: from the values in Reference 6, we deduce that reaction 12 is exothermic by almost 100 kJ mol^{-1}.

$$AgCN(s) + NH_3(g) \longrightarrow AgCN \cdot NH_3(s) \qquad (12)$$

The final species we will consider in this section is solid silver fulminate, AgCNO. As the name of the anionic component suggests, the species is highly unstable[23]. By comparison, its enthalpy of formation[6] of 180 kJ mol^{-1} is *ca* 275 kJ mol^{-1} higher than that of its isomer silver cyanate, AgOCN[24]. Another interesting comparison is with AgCN via the formal oxygen transfer between two compounds, each of which has a triply bonded nitrogen (reaction 13).

$$AgCNO(s) + N_2(g) \longrightarrow AgCN(s) + N_2O(g) \tag{13}$$
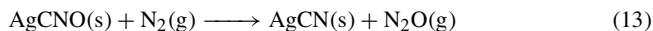
Quite surprisingly[25], this last reaction is 48 kJ mol^{-1} endothermic.

IV. SILVER(I) OLEFIN COMPLEXES IN THE CONDENSED PHASE

As mentioned in the introduction, π-bonded Ag$-$olefin complexes are paradigms in the thermochemistry of organometallic species. Nonetheless, there are comparatively few relevant quantitative data.

A. Direct Measurements of Enthalpies

Experimental information on the energetics of silver$-$olefin bonds comes from a 1973 study by Partenheimer and Johnson[26]. Using titration calorimetry with the 'inert' dichloromethane as solvent, these authors measured the enthalpies of reaction 14 for several olefin complexes (hfacac = 1, 1, 1, 5, 5, 5-hexafluoro-2,4-pentanedionate) whose structure (1) is illustrated below for olefin = cyclohexene.

$$Ag(hfacac)(olefin)(sln) + PPh_3(sln) \longrightarrow Ag(hfacac)(PPh_3)(sln) + olefin(sln) \tag{14}$$
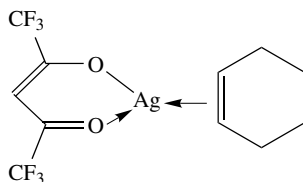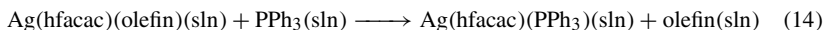
(1)

The data, collected in Table 4, show the trend in Ag$-$olefin bond dissociation enthalpies in solution, the weakest bond being between Ag$^+$ and cyclopentene and the strongest between Ag$^+$ and cyclooctene.

The original authors argued that the solvation effects are similar on both sides of reaction 14 and so the results simulate gas phase data. While this may be so, it is not simple to rationalize the observed trend. The 36 kJ mol^{-1} spread of values is surprisingly large and the origin of the differences is not apparent. As shown in Table 4, gas phase ionization[27], epoxidation[28] and cyclopropanation energies[29] fail to simulate either the observed trends or the range. Thus, the formal reactions 15a, 15b and 15c inadequately mimic the olefin·Ag$^+$ reaction from a thermochemical vantage point.

$$\tag{15a}$$
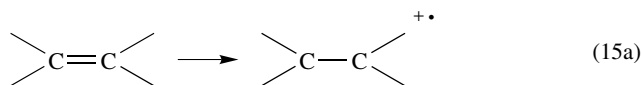
TABLE 4.   Enthalpies of reaction 14 $[-\Delta_r H(14)]$, ionization energies of the parent olefin $[\Delta_r H(15a)]$ and gas phase enthalpies of the 'epoxidation' $[-\Delta_r H(15b)]$ and 'cyclopropanation' $[-\Delta_r H(15c)]$ reactions (kJ mol^{-1})

Olefin	$-\Delta_r H(14)^a$	$\Delta_r H(15a)^b$	$-\Delta_r H(15b)^c$	$-\Delta_r H(15c)^d$
Cyclopentene	77.0 ± 2.1	869	131	5
Cycloheptene	59.8 ± 1.3	862	143	8
Cyclohexene	55.6 ± 1.3	863	121	17
1,5-Cyclooctadiene	49.0 ± 0.8	859		
1,3,5,7-Cyclooctatetraene	44.8 ± 0.8^e	773		
Cyclooctene	41.1 ± 2.1	851	138	6

^{a}Data from Reference 26.
^{b}Ionization energy of the parent olefin.
^{c}Gas phase enthalpy of the 'epoxidation' reactions.
^{d}Gas phase enthalpy of the 'cyclopropanation' reactions.
^{e}See text.

$$ \diagdown C=C \diagup \longrightarrow \text{(epoxide)} \qquad (15b) $$

$$ \diagdown C=C \diagup \longrightarrow \text{(cyclopropane)} \qquad (15c) $$
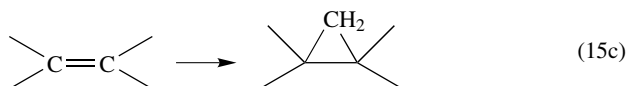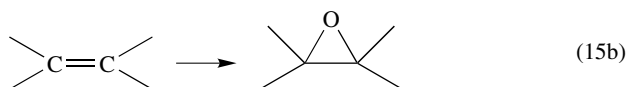
It is also not clear why the diolefin 1,5-cyclooctadiene forms a weaker bond to silver than cyclooctene. The effects of strain differences within the olefins and/or within the complexes is not apparent[30], but in any case suggests, as noted by the original authors, a negligible interaction between the metal and the second double bond. However, the cyclooctatetraene complex is asserted to be polymeric in solution and so currently precludes obtaining useful information derived from these complexation studies of this species.

B. From Equilibrium Constants to Reaction Enthalpies

A considerable number of solution phase equilibrium constants involving silver compounds and olefins have been reported in the literature (e.g. see References 3 and 31–33) but most of these results were determined at a single temperature, usually 298 K. Although some values at two or three different temperatures are available, we do not feel these are enough to derive reliable enthalpies and entropies separately. A possible exception is the work of Quinn and Van Gilder[33], who probed the equilibrium dissociation pressures of several silver–olefin complexes over an adequate temperature range. In particular, they studied AgBF$_4 \cdot$2C$_2$H$_3$X with X = Cl (233.9–260.7 K), F (233.5–254.5 K) and Me (275.4–289.8 K). Van't Hoff plots for these systems afforded the enthalpies of reaction 16 as (39.9 ± 0.1), (35.5 ± 0.4) and (43.5 ± 0.3) kJ mol^{-1} for X = Cl, F and Me, respectively.

$$ AgBF_4 \cdot 2C_2H_3X(cr) \longrightarrow AgBF_4(cr) + 2C_2H_3X(g) \qquad (16) $$
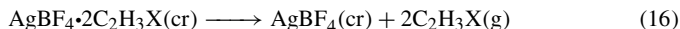
In this case, the earlier authors found a correlation between these values and the basicity (i.e. ionization energy) of the olefins. Assuming the trends in $\Delta_r H_m^{\circ}(16)$ hold for the gas

phase, then the fact that the reaction enthalpy increases with the basicity indicates that the σ ligand-to-metal donation is more important than back donation from the metal to the π^* orbital of the olefin[34].

One might have thought that complications from solvent effects would be ameliorated by considering solid state reactions of the type shown in equation 17. Such a study has been reported[35]. However, it is complicated by unusual stoichiometries, polymorphism and counterion effects.

$$AgX(cr) + olefin(g) \longrightarrow AgX \cdot olefin(cr) \tag{17}$$
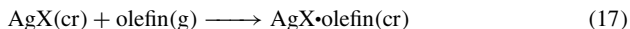
An extensive comparison of the binding enthalpies of alkyl-substituted styrene–silver complexes was reported in Reference 36. The binding enthalpies range from *ca* 12–25 kJ mol^{-1} within each of the $\alpha-$, (Z)-β- and (E)-β-alkyl styrene categories. The effect of the substituents (e.g. R = Me, Et, *n*-Pr, *n*-Bu) on the binding enthalpy is not systematic, however, either within a styrene category or among substituted styrene isomers. A somewhat systematic effect was seen for alkyl-substituted vinyl ethers[37]. For either ethyl or isobutyl ethers, replacing a hydrogen with an alkyl group decreases the binding enthalpy. For substituents in either the (E)-β- or (Z)-β-positions, the binding increases in the order Me < Et < *i*-Pr, the range being larger for the latter category. From the binding enthalpies of styrene and its *p*-methyl derivatives with silver from Reference 38 we again find a small substituent effect but a quite discordant value for the parent hydrocarbon compared to the value cited above. The latter authors presented a variety of ring-substituted derivatives and showed that electron donating power as evidenced by Hammett parameters parallels the observed basicity trends. This Hammett correlation is likewise generally seen for monosubstituted alkenes[3,39] and general monosubstituted arenes[40]. As above, alkyl substitution results in small equilibrium and enthalpy effects[41].

V. SILVER COMPLEXES WITH ACETYLENES

In this section we consider π complexes of silver with acetylenes. There are comparatively few data and so we abandon our earlier disdain for results in aqueous solution. The first study[42] parallels that of Reference 3 in which binding enthalpies of -18.9 and -20.9 kJ mol^{-1} were reported for 3-hexyne and its tetramethylated derivative, di-*t*-butylacetylene, respectively. That these values are numerically so close is suggestive of little geometry change upon complexation. A similar small effect of steric hindrance was shown in Reference 3 where complexation enthalpies of -25.1 and -24.3 kJ mol^{-1} were reported for trimethylethylene and cyclohexene, respectively. That the acetylenes are bonded more weakly than olefins corresponds to the 'folkwisdom' of the lessened basicity of acetylenes *vs* olefins, although we must acknowledge that the most direct comparisons involving 3-hexene and its tetramethylated derivative are seemingly not available. It is nonetheless tempting to say that acetylenes bond to silver *ca* 5 kJ mol^{-1} weaker than olefins.

Consider now the results of Reference 43 in which a series of formally related mono-substituted alkynes and alkenes were directly compared. For five pairs of species under identical solvent conditions a nearly constant ratio of their equilibrium constants of *ca* 2.2 was found.

VI. ORGANOGOLD DERIVATIVES IN THE CONDENSED PHASE

Data on these species are even rarer than for the corresponding, valence isoelectronic, silver species. Indeed, the sole relevant enthalpy of formation we can find is that of aqueous

$Au(CN)_2{}^-$ with the value of 285.8 kJ mol^{-1} from Reference 6. We cannot even find the enthalpy of formation data for AuCN or of $AuCl_2{}^-$ with which to make comparisons analogous to reaction 9. However reaction 18 is exothermic by 65 kJ mol^{-1}.

$$AuCl_2{}^-(aq) + Ag(CN)_2{}^-(aq) \longrightarrow AgCl_2{}^-(aq) + Au(CN)_2{}^-(aq) \qquad (18)$$
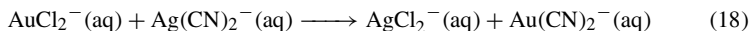
VII. ORGANOSILVER SPECIES IN THE GAS PHASE

One of the general difficulties often found in gas phase studies of metal compounds, especially for those that are coordinately unsaturated, is related to assigning structure. Although the aforementioned Ag^+-olefin complexes in the condensed phase are what the name connotes — silver interacting with a carbon–carbon double bond — there is no such certainty associated with gas phase ions. For example, is a gas phase species with the empirical formula $(C_2H_4Ag)^+$ the silver cation complex with the olefin ethylene or is it $(MeCHAg)^+$? Both ions are precedented by more commonly discussed carbocations of formula $(C_2H_4X)^+$ with X = H, Me and Br. The former structure for the organosilver ion mimics the bridged nonclassical ethyl cation, corner-protonated cyclopropane and bromiranium (ethylenebromonium) ion, respectively, while the latter organosilver ion mimics the classical ethyl, isopropyl and β-protonated vinyl bromide cations, respectively. In addition, returning to the previously mentioned epoxidation and cyclopropanation processes, the two isomeric $(C_2H_4Ag)^+$ ions parallel ethylene oxide and cyclopropane on the one hand, and acetaldehyde and propene on the other.

A. Silver(I) Olefin Cationic Complexes

High pressure mass spectrometry studies by Guo and Castleman[44] led to values of the equilibrium constant of reaction 19 over the temperature range of *ca* 650–740 K. A van't Hoff plot afforded $\Delta_r H°(19) = (135.6 \pm 6.3)$ kJ mol^{-1} and $\Delta_r S°(19) = 126.4$ kJ mol^{-1} K^{-1}). Based on a single value of the equilibrium constant of reaction 19 at 750 K (together with an estimated entropy change of 92.5 kJ mol^{-1} K), the value $\Delta_r H°(20) = (141.0 \pm 12.6)$ kJ mol^{-1} was derived.

$$Ag(C_2H_4)_2{}^+(g) \longrightarrow Ag(C_2H_4)^+(g) + C_2H_4(g) \qquad (19)$$

$$Ag(C_2H_4)^+(g) \longrightarrow Ag^+(g) + C_2H_4(g) \qquad (20)$$
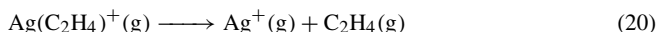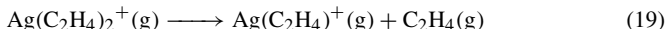
The enthalpies of reactions 19 and 20 may be identified with the *first* and *second* $Ag^+-C_2H_4$ bond dissociation enthalpies in $Ag(C_2H_4)_2{}^+(g)$, respectively. It is a long extrapolation from *ca* 700 K to 298 K.

Chen and Armentrout[45] used guided ion beam mass spectrometry on the ion $(C_2H_4Ag)^+$ and, while they could show it is the aforementioned $Ag\cdot(C_2H_4)^+(g)$, they could only derive a lower limit of (22.2 ± 6.8) kJ mol^{-1} for equation 20 at 0 K. How can the two numerical values of $\Delta_r H°(20)$ be reconciled: the Guo/Castleman one is seemingly *too* high and/or the Chen/Armentrout one is *too* low.

Guo and Castleman's value for the bond enthalpy is consistent with their value for equation 19. Chen and Armentrout's value is consistent with other values in their paper (see Table 5 for a collection of these and other values). From analysis of radiative association kinetics of their Fourier transform ion cyclotron resonance results, Klippenstein, Dunbar and their coworkers[46] derived *first* Ag^+ 2-pentene and isoprene binding energies of (154 ± 29) and (174 ± 29) kJ mol^{-1}, and *second* energies of (164 ± 29) and

TABLE 5.   Gas phase data (in kJ mol^{-1}) for silver and gold organometallic species

M or M$^+$	L	$D(M^+-L)^a$	$D(M-L)^a$	Method/Reference^b
Copper				
Cu	H		243.9 ± 8.4	KC-MS/56
Cu	H		253.8 ± 5.8	GIBMS/59
Cu$^+$	H	87.8 ± 12.5		GIBMS/59
Cu$^+$	CH$_2$	256.7 ± 4.8		GIBMS/59
Cu	Me		242.7 ± 8.4^c	GIBMS/57
Cu$^+$	Me	111.0 ± 6.8		GIBMS/59
Cu$^+$	C$_2$H$_2$	>21.2 ± 9.6^c		GIBMS/58
Cu$^+$	C$_2$H$_4$	>109.0 ± 10.6^c		GIBMS/58
Cu(CO)$_3$$^+$	CO	53 ± 3		GIBMS/49
Cu(CO)$_2$$^+$	CO	75 ± 4		GIBMS/49
Cu(CO)$^+$	CO	172 ± 3		GIBMS/49
Cu$^+$	CO	149 ± 7		GIBMS/49
Cu(C$_6$H$_6$)$^+$	C$_6$H$_6$	155.3 ± 11.6		GIBMS/60
Cu$^+$	C$_6$H$_6$	218.1 ± 9.6		GIBMS/60
Silver				
Ag	H		211.3 ± 8.4	KC-MS/56
Ag	H		198.8 ± 9.6	GIBMS/45
Ag$^+$	H	39.6 ± 5.8		GIBMS/61
Ag$^+$	CH$_2$	⩾107.1 ± 3.9		GIBMS/45
Ag	Me		134.1 ± 6.8	GIBMS/45
Ag$^+$	Me	⩾66.6 ± 4.8		GIBMS/45
Ag$^+$	Et	65.6 ± 7.7		GIBMS/45
Ag(C$_2$H$_4$)$^+$	C$_2$H$_4$	135.6 ± 6.3^d		HPMS/44
Ag$^+$	C$_2$H$_4$	141.0 ± 12.6^d		HPMS/44
Ag$^+$	C$_2$H$_4$	⩾22.2 ± 6.8		GIBMS/45
Ag(CO)$_3$$^+$	CO	45+18 to 45−4		GIBMS/49
Ag(CO)$_2$$^+$	CO	55 ± 8		GIBMS/49
Ag(CO)$^+$	CO	109 ± 4		GIBMS/49
Ag$^+$	CO	89 ± 5		GIBMS/49
Gold				
Au	H		288.3 ± 8.4	KC-MS/56
Au	H		>280^e	ICR/54
Au$^+$	CH$_2$	⩾397^e		ICR/54
Au	Me		192−222^e	ICR/54
Au$^+$	Me	>234^e		ICR/54
Au$^+$	C$_2$H$_4$	>137^e		ICR/54

^{a}Data at 0 K, except when noted otherwise.
^{b}GIBMS = guided ion beam mass spectrometry; HPMS = high pressure mass spectrometry; ICR = ion cyclotron resonance mass spectrometry; KC-MS = Knudsen cell-mass spectrometry.
^{c}Data at 298 K.
^{d}Data at *ca* 700 K. See text.
^{e}Data at *ca* 300 K. See text.

(174 ± 29) kJ mol^{-1}, respectively. We expect these relatively basic olefins[47] to have a somewhat higher silver binding energy than ethylene (recall the above *ca* 40 kJ mol^{-1} spread between cyclopentene and cyclooctene) and so the Guo/Castleman value seems more appropriate. However, recall reaction 16 and assume that its solid state reaction enthalpy is comparable to the formally related gas phase reaction 21.

$$Ag^+(olefin)_2(g) \longrightarrow Ag^+(g) + 2olefin(g) \qquad (21)$$
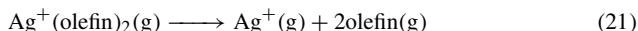
Recalling the enthalpies[33] of *ca* 40 kJ mol^{-1} for reaction 16, whether the olefin be vinyl chloride, vinyl fluoride or propene suggests a value of *ca* 40 kJ mol^{-1} for ethylene is plausible. Since this is the sum of both the first and second bond energies to ethylene, a value of *ca* 20 kJ mol^{-1} for reaction 20 is consistent with this while a value exceeding 100 kJ mol^{-1} is not.

B. Silver(I) Arene Cationic Complexes

Silver arene cationic complexes are well-established. There are nonetheless some interesting thermochemical aspects to this observation. The first is simply asked: 'what are the numerical values for the binding energies?' For benzene there is a range of observed values. Among others are (155 ± 7) kJ mol^{-1} (from Reference 45), (174 ± 29) kJ mol^{-1} (from Reference 46, and interestingly, in essential agreement with that of Reference 45) and, by use of photodissociation[48], an upper bound of (230 ± 21) kJ mol^{-1}. The second aspect is substitution effects. One might expect that methylation would result in increasing the binding energy of toluene over that of benzene. Assuming self-consistency within a given set of experiments corroborates this: i.e. while only upper bounds are found in Reference 48, the upper bound for toluene is *ca* 20 kJ mol^{-1} higher than that for benzene. The third aspect is the effect of multiple arene ligation for a given Ag$^+$ ion. We have already seen that the first and second Ag$^+$–ethylene bond dissociation enthalpies are very similar[44], as are the corresponding energies for 2-pentene and isoprene[46]. Reference 46 shows that the first and second enthalpies are also comparable for benzene — indeed, the values are the same within experimental error.

C. Silver Carbonyl Cations

In Table 5 are also shown the 0 K stepwise Ag$^+$–CO bond dissociation enthalpies of Ag(CO)$_4{}^+$ from Armentrout and his coworkers[49]. From their collision-induced dissociation experiments in a guided ion beam mass spectrometer, one finds a non-monotonic change in $D_0[Ag(CO)_n{}^+$–CO] as a function of n. That the dissociation energy increases from $n = 0$ to $n = 1$ has been explained in terms of 4s–3dσ hybridization: $D_0[Ag^+$–CO] is small because it is reduced by the energy needed to hybridize the metal ion, but $D_0[Ag(CO)^+$–CO] assumes a more conventional value because the Ag(CO)$^+$ fragment already has the metal in the required hybridization. In turn, $D_0[Ag(CO)^+$–CO] $> D_0[Ag(CO)_2{}^+$–CO] because the third carbonyl ligand implies loss of the 4s–3dσ hybridization. Finally, $D_0[Ag(CO)_2{}^+$–CO] $> D_0[Ag(CO)_3{}^+$–CO] is explained by an increase of ligand repulsion.

D. Neutral Species

Ion chemistry experiments can also provide information about the thermochemistry of neutral molecules[50]. Guided ion-beam mass spectrometry experiments[45] allow us to

derive for the formal reaction 22 a 0 K bond enthalpy of (134 ± 7) kJ mol^{-1}.

$$MeAg(g) \longrightarrow Me^{\bullet}(g) + Ag(g) \tag{22}$$
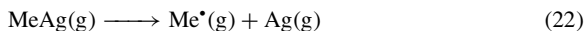
Given the sublimation enthalpy[6] of Ag as 284.6 kJ mol^{-1}, we conclude that reaction 23

$$MeAg(g) \longrightarrow Me^{\bullet}(g) + Ag(s) \tag{23}$$
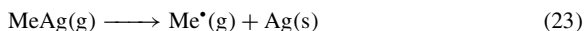
is exothermic by ca $285 - 135 \approx 150$ kJ mol^{-1}. The 298 K value is probably only 'a few' kJ mol^{-1} different from the 0 K value[51]. Upon generalization to other hydrocarbyl groups, we conclude that alkyl silver species are but weakly bound, unstable and difficult to isolate. From References 1, 2 and many other chapters in the current volume we already knew this to be the case, but it is good to see our empirical knowledge thermochemically substantiated.

VIII. ORGANOGOLD SPECIES IN THE GAS PHASE

From ligand exchange reactions using a Fourier transform ion cyclotron resonance mass spectrometer, Schröder and his coworkers[52] showed the following qualitative order of $Au^{+} \bullet L$ bonding: $L = C_6F_6 < H_2O < CO < C_2H_4 < C_6H_6 < NH_3 < MeCH=CH_2 < H_2C=CHCH=CH_2$. In addition, they showed that the $(Au \bullet C_2H_4)^{+}$ bond enthalpy is (276 ± 30) kJ mol^{-1} and that the binding energy of propene and 1,3-butadiene to Au^{+} exceeds 310 kJ mol^{-1}. By an analysis of their radiative association rates from related experiments, Ho and Dunbar[53] showed that the $Au^{+} \bullet C_6HF_5$ complex is bound by 131 kJ mol^{-1}. These latter authors also investigated the chemistry of Au^{-} and found that this ion binds C_6F_6 with an enthalpy of 104 kJ mol^{-1}. Because both condensed phase Au^{-} and Au^{+} salts are known, we look to a rich gas phase chemistry of both auride and aurous ions.

As noted previously, ion chemistry experiments can also give information about the thermochemistry of neutral molecules. Through judicious use of ion cyclotron resonance experiments[54], a 0 K bond energy for $Me-Au$ equal to 207 ± 15 kJ mol^{-1} has been found. From the sublimation enthalpy of gold[6] (-366 kJ mol^{-1}), we find reaction 24 is exothermic by ca 159 kJ mol^{-1}, essentially identical to that for the corresponding reaction for silver.

$$MeAu(g) \longrightarrow Me^{\bullet}(g) + Au(s) \tag{24}$$
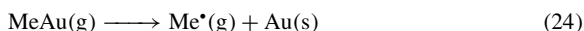
IX. SUMMARY

In contrast to many other metals, a reliable assessment of thermochemical data for silver and gold organometallic compounds is presently almost impossible. Admittedly, quantum chemical calculations have been of increasing utility[52] and so, in a supplemental volume on organometallics in the current series, there is expected to be much more information. As of now, empirical analysis of bond dissociation enthalpy trends involving other metals and ligands are probably still the only alternative for estimating new values[55]. Having that in mind, we decided to include in Table 5 some selected values for the valence isoelectronic copper compounds[56–60] and also thermochemical values for the silver and gold hydride species (MH) and the related cations formed on ionization (MH^{+})[45,54,56,61]. Figure 2 shows some trends: we find similar $D(M^{+}-L) - D(M^{+}-L')$ differences for the three metals. Furthermore, there is the general inequality $D(Au^{+}-L) > D(Cu^{+}-L) >$
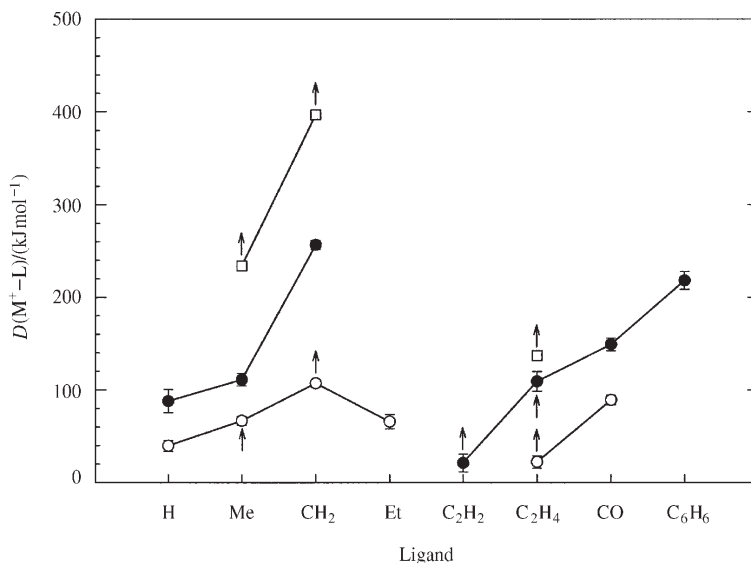
FIGURE 2. M^+-L bond dissociation enthalpies for the Cu (black circles), Ag (white circles) and Au (squares) gas phase ions ML^+. An arrow close to a point indicates that the assigned value is considered a lower limit

$D(Ag^+-L)$. This Au, Cu, Ag order parallels the decrease in $D(M^+-L)$ from 3d to 4d metals from the same group as noted for other middle and late transition elements[18].

X. ACKNOWLEDGMENTS

XI. REFERENCES AND NOTES

1. J. P. Collman, L. S. Hegedus, J. R. Norton and R. G. Finke, *Principles and Applications of Organotransition Metal Chemistry*, University Science Books, Mill Valley, 1987.
2. (a) G. Wilkinson, F. G. A. Stone and E. W. Abel, *Comprehensive Organometallic Chemistry*, Pergamon, Oxford, 1982.
   (b) G. Wilkinson, F. G. A. Stone and E. W. Abel, *Comprehensive Organometallic Chemistry II*, Pergamon, Oxford, 1995.
3. S. Winstein and H. J. Lucas, *J. Am. Chem. Soc.*, **60**, 836 (1938).
4. For the purpose of the present review, organometallic compounds are defined as any species with at least one metal–carbon bond. As such, some of the compounds presented that are often considered as 'inorganic' are adopted by us as being 'organometallic' and so allow us to tell a more coherent and cogent story.
5. M. Berthelot and M. Delépine, *Ann. Chim. Phys.*, **19**, 5 (1900).
6. D. D. Wagman, W. H. Evans, V. B. Parker, R. H. Schumm, I. Halow, S. M. Bailey, K. L. Churney and R. L. Nuttall, 'The NBS Tables of Chemical Thermodynamic Properties: Selected

Values for Inorganic and C_1 and C_2 Organic Substances in SI Units', *J. Phys. Chem. Ref. Data*, **11** (1982), Supplement 2.

7. J. D. Cox, D. D. Wagman and V. A. Medvedev, *Codata Key Values for Thermodynamics*, Hemisphere, New York, 1989.

8. J. B. Pedley, *Thermodynamic Data and Structures of Organic Compounds*, Thermodynamics Research Center Data Series, Vol. 1, Thermodynamics Research Center, College Station, 1994.

9. A. Finch, P. J. Gardner, A. J. Head and H. S. Majdi, *Thermochim. Acta*, **180**, 325 (1991).

10. The uncertainty interval was assigned in Reference 9.

11. T. A. Bykova, E. G. Kiparisova, B. V. Lebedev, N. N. Mukhina, I. R. Gol'ding and A. M. Sladkov, *Izv. Akad. Nauk SSSR, Ser. Khim.*, 468 (1980); *Chem. Abstr.*, **93**, 45709z (1980).

12. The enthalpies of formation of the parent and substituted phenylacetylenes, PhC≡CH and PhC≡CR, are taken from H. E. Davis, N. L. Allinger and D. W. Rogers, *J. Org. Chem.*, **50**, 3601 (1985), while those for the dialkylacetylenes, R_2C_2, are from D. W. Rogers, O. A. Dagdagan and N. L. Allinger, *J. Am. Chem. Soc.*, **101**, 671 (1979).

13. That is, in both silver acetylides we expect both intramolecular σ- and intermolecular π-bonding between the organic and Ag components.

14. For thermochemical consistency we accept in this case the value of $\Delta_f H_m^\circ$ (Ag_2C_2, cr) from Reference 6 of 350.5 kJ mol^{-1}.

15. The enthalpies of formation of AgCN and HCN were taken from Reference 6 and that of silver phenylacetylide from Reference 10. The requisite value for liquid phenylacetylene was found by either
(a) assuming the enthalpy of hydrogenation data from Reference 11 can be directly used for pure liquids (and taking the enthalpy of formation of ethylbenzene from Reference 8) as opposed to dilute hydrocarbon solutions, or
(b) accepting the enthalpy of formation of gaseous phenylacetylene from Reference 11 and adding an estimated enthalpy of vaporization using the hydrocarbon phase change approximation technique in J. S. Chickos, A. S. Hyman, L. H. Ladon and J. F. Liebman, *J. Org. Chem.*, **46**, 4294 (1981).

16. The requisite enthalpy of formation of CuCN(cr) is from Reference 6 and that of copper phenylacetylide(cr) is from Reference 11.

17. H. Guillemard, *Ann. Chim. Phys.*, **14**, 311 (1908).

18. The method illustrated by equation 8 has been applied to thermochemical data of many families of compounds. See, for example, J. A. Martinho Simões and M. E. Minas da Piedade, in *Energetics of Organic Free Radicals* (Eds. J. A. Martinho Simões, A. Greenberg and J. F. Liebman), Chapman & Hall, London, 1996 and references cited therein.

19. There is a lesson here. Many early thermochemical experiments lack a thorough description of the compound of interest, and many also lack error bars for the measurement recorded. It is very tempting to disregard these data. However, in that they are often the only data available for a given species, it would seem that they should not be ignored although care must be taken in their contemporary use.

20. The thermochemistry of many inorganic compounds has been determined by electrochemical measurements in aqueous media and relating the Gibbs energy to the observed electrochemical potential by the Nernst equation.

21. There is a symmetry number correction that equals $2R\ln 2$. This corresponds to a difference of ΔG and ΔH of *ca* 3 kJ mol^{-1}, a quantity easily neglected when compared to expected solvent effects on the individual ion energies.

22. Strictly speaking, this reaction does not qualify as either isodesmic or obeying bond additivity because solid AgCN contains both Ag−CN and Ag−NC bonds. However, in that we have already considered isocyano derivatives of silver cyanide, we would nonetheless like to consider this reaction and admit we do not know how to derive the cyanide/isocyanide enthalpy difference.

23. Care must be taken with the formula as well as the compound. That is, it is not uncommon to see inorganic isocyanates and their sulfur analogs written as containing the anionic substructure CNO and CNS, respectively. While this avoids the question of whether the ambidentate species are chalcogen- and/or nitrogen-bonded, the formulas of fulminates are ambiguous (there being no isolated species with the −CNS or nitrile N-sulfide structure known to the authors) and would seem to invite carelessness with the identity and handling of samples of the compounds.

24. Y.-S. Cheung and W.-K. Li, *Aust. J. Chem.*, **50**, 169 (1997).

25. Our surprise arises because we tend to consider N_2O a highly stable oxide of nitrogen, when in fact, from Reference 6, we find that its enthalpy of formation is positive and is nearly 50 kJ mol^{-1} higher than the much more reactive, but still unstable, NO_2.
26. W. Partenheimer and E. H. Johnson, *Inorg. Chem.*, **12**, 1274 (1973).
27. All ionization energies were taken from S. G. Lias, J. E. Bartmess, J. F. Liebman, J. L. Holmes, R. D. Levin and W. G. Mallard, 'Gas-Phase Ion and Neutral Thermochemistry', *J. Phys. Chem. Ref. Data*, **17** (1988), Supplement 1.
28. The epoxidation energy was defined as the difference between the enthalpies of formation of the epoxide and the olefin: all values for the former were taken from the three-membered ring thermochemical review, J. F. Liebman and A. Greenberg, *Chem. Rev.*, **89**, 1225 (1989).
29. The cyclopropanation energy was defined as the difference between the enthalpies of formation of the cyclopropane and the olefin: all values for the former were taken from the three-membered ring thermochemical review, J. F. Liebman and A. Greenberg, *Chem. Rev.*, **89**, 1225 (1989).
30. For two different (but numerically and conceptually comparable) sets of strain energies of the simple cycloalkenes, see A. Greenberg and J. F. Liebman, *Strained Organic Molecules*, Academic Press, New York, 1978, p. 94.
31. C. D. M. Beverwijk, G. J. M. van der Kerk, A. J. Leusink and J. G. Noltes, *Organometal. Chem. Rev.*, **5**, 215 (1970).
32. Y. Inaki, S. Nozakura and S. Murahashi, *Bull. Chem. Soc. Jpn.*, **42**, 2605 (1969).
33. H. W. Quinn and R. L. Van Gilder, *Can. J. Chem.*, **49**, 1323 (1971).
34. J. A. Martinho Simões and J. L. Beauchamp, *Chem. Rev.*, **90**, 629 (1990).
35. H. W. Quinn and D. N. Glen, *Can. J. Chem.*, **40**, 1103 (1962).
36. Y. Inaki, S. Nozakura and S. Murahashi, *Bull. Chem. Soc. Jpn.*, **42**, 2605 (1969).
37. T. Fueno, O. Kajimoto, T. Okuyama and J. Furukama, *Bull. Chem. Soc. Jpn.*, **41**, 7851 (1968).
38. T. Fueno, T. Okuyama, T. Deguchi and J. Furukama, *J. Am. Chem. Soc.*, **87**, 170 (1965).
39. T. Fueno, O. Kajimoto and J. Furukama, *Bull. Chem. Soc. Jpn.*, **41**, 7821 (1968).
40. L. T. Andrews and R. M. Keefer, *J. Am. Chem. Soc.*, **72**, 3113 (1950).
41. V. N. Rodionov, R. V. Chernyaev, N. S. Verpouskii, L. Vodicka, J. Kriz, A. G. Yurchenko, A. I. Kuzmenko and J. Hlavaty, *Russ. J. Anal. Chem.*, **45**, 1287 (1994).
42. G. K. Helmkamp, F. L. Carter and H. J. Lucas, *J. Am. Chem. Soc.*, **75**, 1306 (1957).
43. T. G. Sukhova, O. N. Temkin, L. I. Kuleshova and R. M. Flid, *Russ. J. Inorg. Chem.*, **18**, 172 (1973) and references cited therein.
44. B. C. Guo and A. W. Castleman, Jr., *Chem. Phys. Lett.*, **181**, 16 (1991).
45. Y.-M. Chen and P. B. Armentrout, *J. Phys. Chem.*, **99**, 11424 (1995).
46. Y.-P. Ho, Y.-C. Yang, S. J. Klippenstein and R. C. Dunbar, *J. Phys. Chem. A*, **101**, 3338 (1997).
47. E. P. L. Hunter and S. G. Lias, *J. Phys. Chem. Ref. Data*, in press.
48. S. Afzaal and B. S. Freiser, *Chem. Phys. Lett.*, **218**, 254 (1994).
49. F. Meyer, Y.-M. Chen and P. B. Armentrout, *J. Am. Chem. Soc.*, **117**, 4071 (1995) and references cited therein.
50. See, for example, J. Berkowitz, G. B. Ellison and D. Gutman, *J. Phys. Chem.*, **98**, 2744 (1994); J. C. Traeger and B. M. Kompe, in *Energetics of Organic Free Radicals* (Eds. J. A. Martinho Simões, A. Greenberg and J. F. Liebman), Chapman & Hall, London, 1996 and references cited therein.
51. A general rule asserts that if a molecule has more than 4 atoms, then the enthalpy of formation at 298 K is *ca* 8 kJ mol^{-1} higher than at 0 K; A. A. Zavitsas, personal communication.
52. D. Schröder, J. Hrušák, R. H. Hertwig, W. Koch, P. Schwedtfeger and H. Schwarz, *Organometallics*, **14**, 312 (1995).
53. Y.-P. Ho and R. C. Dunbar, ASMS 44th Proceedings, Portland, OR (May 1996), 1231, and personal communication from these authors.
54. A. K. Chowdury and C. L. Wilkins, *J. Am. Chem. Soc.*, **109**, 5336 (1987).
55. See Reference 34 and the chapter cited in Reference 18.
56. A. Kant and K. A. Moon, *High Temp. Sci.*, **11**, 52 (1979).
57. P. Georgiadis, E. R. Fisher and P. B. Armentrout, *J. Am. Chem. Soc.*, **111**, 4251 (1989).
58. E. R. Fisher and P. B. Armentrout, *J. Phys. Chem.*, **94**, 1674 (1990); **98**, 8269 (1994).
59. B. L. Kickel and P. B. Armentrout, *J. Phys. Chem.*, **99**, 2024 (1995).
60. F. Meyer, F. A. Khan and P. B. Armentrout, *J. Am. Chem. Soc.*, **117**, 9740 (1995).
61. Y.-M. Chen, J. L. Elkind and P. B. Armentrout, *J. Phys. Chem.*, **99**, 10438 (1995).

CHAPTER **4**

NMR and ESR spectroscopy applied to gold and silver compounds

C. FRANK SHAW III

Department of Chemistry, University of Wisconsin-Milwaukee, P O Box 413, Milwaukee, WI 53201-0413
Fax: 414-229-5530   email: cfsiii@uwm.edu

I. INTRODUCTION

Silver and gold occur in Group 11 (formerly I-B) of the periodic table. With their lighter congener, copper, they comprise a triad known unambiguously as the coinage metals.

TABLE 1. Properties of gold and silver isotopes (compared to the proton)

Isotope	Frequency (Hz)	Abundance (%)	Sensitivity[a]	μ (eh/4πMc)	I (h/2π)	Q (e $\times 10^{-24}$cm^2)
^{1}H	500.00	99.98	1.00	2.79278	$\frac{1}{2}$	—
^{107}Ag	20.234	51.35	6.62×10^{-5}	-0.1135	$\frac{1}{2}$	—
^{109}Ag	23.264	48.65	1.01×10^{-4}	-0.1305	$\frac{1}{2}$	—
^{197}Au	8.585	100.0	2.35×10^{-5}	0.1449	$\frac{3}{2}$	0.56

[a]Sensitivity of detection relative to the proton, ^{1}H = 1.00.

Due to their lustrous appearance, malleability and noble characters, gold and silver have fascinated man since the earliest days of technological innovation. Both form an interesting array of complexes with varying oxidation states and coordination environments.

The properties of the naturally occurring isotopes of gold and silver are compared to those of the proton in Table 1. Gold has a single isotope, ^{197}Au, which is 100 percent abundant. It is, however, a quadrupolar nucleus ($I = \frac{3}{2}$) and, as a result of rapid relaxation, the signals are extremely weak and broad. The consequence is that ^{197}Au NMR detection is not an effective spectroscopic tool. As a practical matter, NMR studies of gold complexes, whether inorganic, organometallic or biological in nature, are based on other isotopes such as ^{31}P, ^{13}C or ^{1}H, which are present in the ligands.

Silver is more interesting, because it has two NMR-active isotopes, ^{107}Ag and ^{109}Ag, which each exhibit $I = \frac{1}{2}$ spin quantum numbers. Their abundances are similar, but, due to its greater sensitivity, the ^{109}Ag isotope has a slight advantage as a probe. When natural abundance silver is coupled to other NMR-active nuclei, there is a diagnostic pattern of two flanking doublets centered at the same frequency. In addition to its utility for studying silver coordination complexes, silver NMR has proven useful in studies of copper proteins, where the ^{109}Ag serves as a probe of the copper coordination environment. Sensitivities are low for both isotopes, but modern Fourier-transform instruments using sophisticated pulse sequences can overcome this disadvantage.

II. SILVER COMPLEXES

Silver has three accessible oxidation states in addition to the elemental state. Silver(I) is a d^{10} ion and, like Cu(I), Au(I) and Hg(II), can form complexes with a variety of coordination geometries. These include linear, two-coordinate complexes, trigonal-planar three-coordinate complexes and tetrahedral four-coordinate complexes. These are all diamagnetic, since the 4d subshell is completely filled. Silver(II) complexes have a d^9 configuration and are paramagnetic, since there is one unpaired electron regardless of the coordination geometry. Most complexes are square planar in geometry and the unpaired electron resides in the d$_{x^2-y^2}$ orbital. Silver(III) complexes are also square planar, but the d$_{x^2-y^2}$ orbital is empty for the d^8 electronic configuration. Thus, the compounds are diamagnetic. The interplay of coordination geometries and electronic configurations of these three oxidation states makes silver (I) and silver(III) readily accessible to study by NMR methods, while Ag(II) can best be examined by ESR spectroscopy.

A. NMR Applied to Silver(I) and Silver(III) Complexes

1. Direct and indirect detection of ^{109}Ag and ^{107}Ag

Measuring chemical shifts by direct detection of the ^{109}Ag resonance is difficult due to the low sensitivity of silver (Table 1) and long relaxation times. The efficient dipolar relaxation mechanisms that operate for ^{13}C are not effective for silver. Rather, the dominant contributions to relaxation of heavy nuclei such as ^{109}Ag are chemical shift anisotropy, T_1^{csa}, for nuclei in asymmetric environments, and spin rotation, T_1^{sr}, for nuclei in symmetric (e.g. octahedral or tetrahedral) environments[1,2]. Scalar coupling to adjacent nuclei with quadrupole moments, T_1^{sc}, can cause additional signal broadening[1,2]. Nonetheless, direct detection can be achieved by using long accumulation times, large samples and high concentrations (as much as 1 M). The presence of a free radical relaxation agent such as TEMPO or TANOL accelerates the relaxation rate and decreases the required accumulation time. Even so, for the series [Ag{o-C$_6$H$_4$(YMe)$_2$}$_2$] BF$_4$ and [Ag{RY(CH$_2$)$_2$YR$_2$}] BF$_4$, Y = S, Se and Te; R = Me and Ph, measured in CH$_2$Cl$_2$ at room temperature, 20 000 scans with a 2-s delay in the presence of TEMPO were required[3,4]. Triplets arising from direct coupling of the phosphorous atoms to silver in complexes of the tetradentate ligands, Ph$_2$P(CH$_2$)$_2$S(CH$_2$)$_2$S(CH$_2$)$_2$PPh$_2$ and Ph$_2$P(CH$_2$)$_2$S(o-C$_6$H$_4$)$_2$S(CH$_2$)$_2$PPh$_2$, were also observed directly[5]. In contrast, the spectra observed for mixed ligand complexes with triphenylphosphine and triazole ligands are averaged signals arising from labile ligand exchange reactions in solution[6].

Indirect 2D NMR methods are generally more facile routes to obtaining chemical shifts for species in solution. The spectra are measured under the conditions (concentration, spectral parameters and accumulation times) characteristic of the nucleus through which the silver is being indirectly observed. DEFT, INEPT, HMQC and HSQC are the techniques most commonly employed. ^{1}H, ^{13}C, ^{19}F and ^{31}P are most frequently used as the observing nuclei in the current literature. Several examples of indirect observation are given here.

Berners-Price and coworkers[7] demonstrated that the retro-INEPT (insensitive nuclei enhancement by polarization transfer) technique provides a rapid method to observe both the ^{109}Ag and ^{31}P NMR spectra in a single experiment. Their examination of [Ag(dppey)$_2$]NO$_3$, where dppey = cis-Ph$_2$PCH=CHPPh$_2$, required only 1024 accumulations to obtain the spectra shown in Figure 1. In spectrum a, which used a ^{31}P 180° decoupling pulse in the acquisition phase, the coupled phosphorous spectrum is recorded in the F$_1$ dimension and the decoupled silver spectrum in the F$_2$ dimension. Omission of the 180° pulse allows observation of a distorted ^{31}P-coupled silver resonance in spectrum b. The ^{31}P spectrum shows the expected doublet for coupling to ^{109}Ag in both cases. The intensity pattern of the coupled silver spectrum, however, exhibits only the four outer signals of the 1 : 4 : 6 : 4 : 1 pentuplet expected for coupling to four equivalent phosphorous atoms, as a consequence of the pulse sequence employed[7].

Heteronuclear single quantum correlation (HSQC) spectra also allow facile observation of the silver resonance by probing through a coupled nucleus. Again, the silver spectrum can be decoupled from or coupled to phosphorous, for example, by including or not a decoupling pulse in the evolution period. The spectra of [Ag$_3$Fe$_2$L$_2$L$_2'$]$^{3+}$ which contains two ferrocenyl complexes, each with one Ph$_2$P−C$_5$H$_4$$^-$ ligand (L) and one 1-Ph$_2$P(2-(R)-CH(Me)NMe(CH$_2$)$_2$NMe$_2$)C$_5$H$_3$$^-$ ligand(L$'$) bound to an iron, reveal that one silver ion exists in an AgP$_2$$^+$ environment and two in an AgPN$_2$ environment (Figure 2)[8]. The

FIGURE 1. Retro-INEPT spectrum of [Ag(dppey)$_2$] NO$_3$ (190 mM in acetone-d$_6$–water at 309 K) measured at 121.50 MHz. ^{31}P decoupling pulse (180°) applied in spectrum (a) and omited in spectrum (b). $\delta_{Ag} = 1413$ ppm; $\delta_P = +1.5$ ppm; $^1J_{PAg} = 271$ Hz. Reproduced with permission from Reference 7

FIGURE 2. HSQC spectrum of $[Ag_3(LFeL')_2](CF_3SO_3)_3$, $L = Ph_2P-C_5H_4^-$ and $L' = 1-Ph_2P(2-(R)-CH(Me)NMe(CH_2)_2NMe_2)C_5H_3^-$ measured at 202 MHz in CD_2Cl_2 at 253 K. Spectral parameters for AgPN$_2$ coordination: $\delta_{Ag} = 540$ ppm; $\delta_P = -4.5$ ppm; $^1J_{PAg} = 749$ Hz. Parameters for AgP$_2$ coordination: $\delta_{Ag} = 690$ ppm; $\delta_P = +2.5$ ppm; $^1J_{PAg} = 560$ Hz. Reprinted with permission from Reference 22. Copyright (1994) American Chemical Society

unique silver is bound terminally to both L ligands, while the other two are each chelated by one L' ligand[8].

The DEPT pulse sequence, applied to the square-planar silver(III) $[Ag(CF_2H)_4^-]$ ion, reveals a beautifully symmetric ^{109}Ag resonance pattern resulting from seven of the nine signals expected for coupling to eight equivalent fluorines (Figure 3)[9]. Each component is

further split into quintets by coupling to four equivalent hydrogens, as shown above the spectrum. In this case, the couplings with fluorine and hydrogen are two-bond interactions[9].

Solid state spectral measurements using magic angle spinning techniques provide an additional method to determine ^{109}Ag chemical shifts. Solids are, of course, intrinsically more concentrated than solutions. A further advantage results because ligand exchange processes and dissociation are generally precluded in the solid state. ^{109}Ag spectra include anisotropic and isotropic contributions to the chemical shifts, which appear as separate resonances and must be interpreted. Fijolek, González-Duarte and coworkers have recently examined a large number of silver thiolates by CP-MAS (cross polarization–magic angle spinning). The advantages of solid state NMR are clearly exemplified by these systems, which are difficult to handle in solution due to solubility and ligand exchange problems.[10−12] Figure 4 shows the CP-MAS spectrum and structure of $[Ag_5\{\mu\text{-}S(CH_2)_3N(CH_2)_3\}_3 \ \{\mu\text{-}S(CH_2)_3NH(CH_2)_3\}_3]$ (ClO$_4$)$_2$. Even if this substance

FIGURE 3. ^{109}Ag spectrum of [Ag(CF$_2$H)$_4$$^-$], obtained by DEPT polarization transfer from ^{19}F. $\delta_{Ag} = 2041.9$ ppm; $^2J_{AgF} = 24.4$ Hz; $^2J_{AgH} = 1.8$ Hz; measured as the PPh$_4$$^+$ salt in CDCl$_3$ at 298 K (14 400 scans, relaxation delay 2s; no decoupling). Reprinted with permission from Reference 9. Copyright (1997) American Chemical Society

FIGURE 4. Solid state ^{109}Ag CP-MAS spectrum[10] (left) and crystal structure[13] (right) of $[Ag_5\{\mu\text{-}S(CH_2)_3N(CH_2)_3\}_3\text{-}\{\mu\text{-}S(CH_2)_3NH(CH_2)_3\}_3]$ $(ClO_4)_2$ [13.852 MHz; 3.5-s pulse delay]. The isotropic resonances for the two silver environments at 826 and 1228 ppm are designated. The upper and lower traces were accumulated at spinning rates of 4.1 and 3.7 kHz and the side bands are marked A or B according to their association with the main resonances. Reprinted with permission from Reference 10. Copyright (1996) American Chemical Society, and from Reference 13 by permission of the Royal Society of Chemistry

were soluble, ligand exchange would probably scramble the distinct AgS_2 and AgS_3 coordination sites revealed by crystallography[13]. The solid state spectrum reveals two isotropic resonances at 826 and 1228 ppm, which have been assigned to the two- and three-coordinate sites[10], in agreement with the earlier assignments for thiolate-bound Ag(I) ions in yeast metallothionein[14,15] (Table 2).

2. ^{109}Ag and ^{107}Ag chemical shifts

The chemical shift range for silver is extensive, with the result that chemical shifts are very sensitive to oxidation state, coordination number and the nature of the ligands bound to a silver center. A 1991 review of transition metal ion NMR chemical shifts[2] quoted a range from -100 ppm for $AgF_{(s)}$ to $+841$ ppm for $[Ag(S_2O_3)_2]^{5-}$. The data recently reported for silver(III) organometallic complexes extend the range beyond $+2500$ ppm[9,16]. The preferred reference standard is $AgNO_3$ at infinite dilution in aqueous solution, but to increase sensitivity, more concentrated solutions, up to 9 M ($\delta_{Ag} = +47$ ppm), are used experimentally. Chemical shift values are typically temperature dependent. For the series $[Ag\{RYCH_2CH_2YR\}_2]^+$, $Y = S$, Se and $R = Me$, Ph, the dependence is ca -0.7 K^{-1}. Since measurements are frequently made at low temperature to minimize labile ligand exchange processes, the temperature of measurement should always be reported and taken into account when chemical shifts are compared and interpreted. The temperature-dependent change, $\Delta\delta = 86$ ppm, from 944 ppm at 300 K to 1030 ppm at 180 K for $[Ag\{PhSCH_2CH_2SPh\}_2]^+$ is greater than the chemical shift difference when the ligand is replaced by $MeSCH_2CH_2SMe$, $\Delta\delta = 60$ ppm[4].

Table 2 collects representative chemical shift values, primarily from the more recent literature. It can be seen, for example, that the tabulated values for linear silver(I) coordinated to two carbon atoms (AgC_2^-) span a range of ca 100 ppm, from roughly 550 to 650 ppm. In stark contrast, the chemical shifts of the recently reported square-planar silver(III) ions with four carbon-donor-atom ligands span a range from 2000 to >2500 ppm[9,16]. These new values expand the previously known range of ca 1500 ppm, primarily for Ag(I), by an additional 1000 ppm! The dominant contribution to the chemical shifts of ^{109}Ag is the paramagnetic term in the treatment of Ramsey[1,2,17].

Ag(I) is a d^{10} ion and, like Au(I), can be two-, three- or four-coordinate with appropriate ligands. The idealized geometries are linear, trigonal planar and tetrahedral, but distortions from the ideal are observed in the solid state and in non-homoleptic complexes where greater silver s character is conferred on the bonds to selected elements. The chemical shift values generally increase with coordination number, other things being equal,

$$AgX_2 < AgX_3 < AgX_4$$

In $[Ag_5\{\mu\text{-}S(CH_2)_3N(CH_3)_2\}_3\{\mu\text{-}S(CH_2)_3NH(CH_3)_2\}_3](ClO_4)_2$[10], for example, the crystallographically defined AgS_2 and AgS_3 sites can be confidently assigned to resonances at 826 and 1228 ppm, respectively. But even for the same donor atoms, the ranges overlap and some care must be exercised in making assignments. Thus, the AgS_4 site in $[Ag(PhSCH_2CH_2SPh)_2]BF_4$ gives rise to a shift of 944 ppm[4], which is lower than the range reported for most AgS_3 sites. This results in part from the different nature of the two ligands. The sulfur in $(CH_3)_2N(CH_2)_3S^-$ is a charged, bridging thiolato anion, whereas those in $PhSCH_2CH_2SPh$ are neutral, terminally-coordinated thioether donor atoms.

All three coordination geometries of silver(I) tend to be labile to ligand exchange reactions, and this requires caution in measuring and interpreting chemical shift values. A classic example is the averaging of signals for $[Ag(CN)_2]^-$, $[Ag(CN)_3]^{2-}$ and

TABLE 2.   Representative silver 109 chemical shifts

Compound or ion	Coordination	δ ^{109}Ag(ppm)		Reference
$[Ag(CF_2H)_2]^-$	$AgC_2{}^-$	634.3	(213 K)	9
$[Ag(CF_2H)(CN)]^-$	$AgC_2{}^-$	579.1	(273 K)	9
$[Ag(CF_3)_2]^-$	$AgC_2{}^-$	565.5	(223 K)	16
$[Ag(CF_3)(CN)]^-$	$AgC_2{}^-$	566	(223 K)	16
$[Ag(CN)_2]^-$	$AgC_2{}^-$	584.3	(223 K)	16
$[Ag(NH_3)_2]^+$	$AgN_2{}^+$	505	(303 K)	17
$[Ag\{NH_2(CH_2CH_2OH)\}_2]^+$	$AgN_2{}^+$	363	(303 K)	17
$[Ag\{NH(CH_2CH_2OH)_2\}_2]^+$	$AgN_2{}^+$	306	(303 K)	17
$[Ag\{N(CH_2CH_2OH)_3\}_2]^+$	$AgN_2{}^+$	232	(303 K)	17
$[Ag^{III}(CF_2H)_4]^-$	$Ag^{III}C_4{}^-$	2041.9	(298 K)	9
cis-$[Ag^{III}(CF_2H)_2(CF_3)_2]^-$	$Ag^{III}C_4{}^-$	2089.7	(298 K)	9
trans-$[Ag^{III}(CF_2H)_2(CF_3)_2]^-$	$Ag^{III}C_4{}^-$	2098.0	(298 K)	9
$[Ag^{III}(CF_2H)_3(CF_3)]^-$	$Ag^{III}C_4{}^-$	2136.5	(298 K)	9
$[Ag^{III}(CF_3)_4]^-$	$Ag^{III}C_4{}^-$	2233.1	(298 K)	9
trans-$[Ag^{III}(CF_2H)_2(CN)_2]^-$	$Ag^{III}C_4{}^-$	2110.8	(298 K)	9
$[Ag^{III}(CF_3)_3(CN)]^-$	$Ag^{III}C_4{}^-$	2250.4	(298 K)	16
cis-$[Ag^{III}(CF_3)_2(CN)_2]^-$	$Ag^{III}C_4{}^-$	2301.6	(298 K)	16
trans-$[Ag^{III}(CF_3)_2(CN)_2]^-$	$Ag^{III}C_4{}^-$	2292.5	(298 K)	16
trans-$[Ag^{III}(CF_3)_2(DMF)_2]^+$	$AgC_2N_2{}^+$	2519.4	(253 K)	16
$[Ag^{III}(CF_3)(CN)_3]^-$	$Ag^{III}C_4{}^-$	2343.7	(298 K)	16
$[Ag^{III}(CF_3)_3Cl]^-$	$Ag^{III}C_3Cl^-$	2187.8	(288 K)	16
$[Ag^{III}(CF_3)_3Br]^-$	$Ag^{III}C_3Br^-$	2135.2	(288 K)	16
$[Ag^{III}(CF_3)_3I]^-$	$Ag^{III}C_3I^-$	2003.0	(288 K)	16
$[PPh_3Me]_2[AgI_3]$	$AgI_3{}^{2-}$	675	(ss)^a	12
$[AgI_4]^{3-}$	$AgI_4{}^{3-}$	744^b		18
$[Ag\{Ph_2P(CH_2)_2S(CH_2)_2$ $S(CH_2)_2PPh_2\}]BF_4$	$AgP_2S_2{}^+$	1017(t)	(220 K)	19
$[Ag\{Ph_2P(CH_2)_2S(o\text{-}C_6H_4)_2$ $S(CH_2)_2PPh_2\}]^+$	$AgP_2S_2{}^+$	1124(t)	(220 K)	5
$[Ag_5\{\mu\text{-}S(CH_2)_3N(CH_2)_3\}_3\text{-}$ $\{\mu\text{-}S(CH_2)_3NH(CH_2)_3\}_3]$ $(ClO_4)_2$	$Ag(\mu\text{-}S)_2$ $Ag(\mu\text{-}S)_3$	826 1228	(ss)^a (ss)^a	10
$[Ag(\mu_3\text{-}S(CH_2)_2CH_3)]$	$Ag(\mu_3 S)_3$	1083 1048	(ss)^a (ss)^a	11
Ag$_7$MT (S. cerevisiae) native metallothionein	AgS$_2$ AgS$_3$	790, 890 1000, 1037, 1183, 1220, 1250		15
Ag$_7$T84 (S. cerevisiae) metallothionein residues 1-84	AgS$_2$ AgS$_3$	788, 888 994, 1033, 1184, 1220, 1249		14
$[Ag(MeSCH_2CH_2SMe)_2]BF_4$	$AgS_4{}^+$	1004	(300 K)	4
$[Ag(PhSCH_2CH_2SPh)_2]BF_4$	$AgS_4{}^+$	944	(300 K)	4
$[Ag(MeSeCH_2CH_2SeMe)_2]BF_4$	$AgSe_4{}^+$	1046	(300 K)	4
$[Ag(PhSeCH_2CH_2SePh)_2]BF_4$	$AgSe_4{}^+$	991	(300 K)	4

TABLE 2. (*continued*)

Compound or ion	Coordination	δ [109]Ag(ppm)		Reference
[Ag{Ph$_2$P(CH$_2$)$_2$PPh$_2$}$_2$]NO$_3$	AgP$_4$$^+$	1378	(300 K)	20
[Ag(*cis*-Ph$_2$PCH=CHPPh$_2$)$_2$]NO$_3$	AgP$_4$$^+$	1413	(300 K)	7,20
[Ag{Ph$_2$P(CH$_2$)$_3$PPh$_2$}$_2$]NO$_3$	AgP$_4$$^+$	1468	(300 K)	20
[Ag(PPh$_3$)$_4$]BF$_4$	AgP$_4$$^+$	1124	(300 K)	21
[Ag(AsPh$_3$)$_4$]BF$_4$	AgAs$_4$$^+$	1056	(300 K)	21
[Ag(SbPh$_3$)$_4$]BF$_4$	AgSb$_4$$^+$	1166	(300 K)	21
[Ag$_3${LFeL'}$_2$] (see Figure 2 for structure)	AgP$_2$O$_x$$^+$	690	(298 K)	22
	AgPN$_2$$^+$	540	(298 K)	
[Ag$_2$Ru$_4$(μ_3-H)$_2${μ-Ph$_2$P(H$_2$PPh$_2$}(CO)$_{12}$]^c	AgPAgRu$_2$	−153^d		23
	AgPAgRu$_{3-}$(μ_3-H)$_2$			
[AgRu$_4$(μ_3-H)$_3$(PPh$_3$)(CO)$_{12}$]	AgPRu$_3$-(μ_3-H)$_3$	−250.4^d		23

^{a}ss = solid state.
^{b}Calculated from the average δ_{Ag}[18] for AgI$_n$$^{-n+1}$, $n = 3, 4$ and the solid state (ss) δ_{Ag}[12] for AgI$_3$$^{2-}$.
^{c}The two silver environments equilibrate in solution.
^{d}Values relative to [Ag{P(OEt)$_3$}$_4$]$^+$.

[Ag(CN)$_4$]$^{3-}$, which causes a single resonance to be observed for all three species[17]. Chemical shift changes may result from dissociative processes,

$$AgL_x \rightleftharpoons AgL_{x-1} + L$$

and from rapid ligand-scrambling equilibria when several ligands are present,

$$AgL_xL'_y \rightleftharpoons \tfrac{1}{2}AgL_{x+1}L'_{y-1} + \tfrac{1}{2}AgL_{x-1}L'_{y+1}$$

For homoleptic complexes, the former effect can be detected or ruled out by adding an excess of ligand to shift the equilibrium toward formation of the coordinatively saturated species. For example, the chemical shift of [Ag{o-C$_6$H$_4$(SMe)$_2$}$_2$] changes from +788 to +803 ppm at 300 K, but only from +846 to +848 ppm at 180 K when excess ligand is added, thus suggesting that dissociation is greater at the higher temperature[3]. On the other hand, spectra of [Ag{RSCH$_2$CH$_2$SR}$_2$]BF$_4$ showed no shift for R = Me at 1004 ppm and R = Ph at 944 ppm upon adding excess ligand, leading to the conclusion that the signals arise from stable AgS$_4$$^+$ centers[4]. Lowering the temperature can sometimes resolve the signals for the components of an equilibrium, but the low sensitivity of silver and/or solubility problems often render this remedy ineffective. In other cases, the equilibrating species are more easily detected by observing another nucleus. For example, Nomiya and coworkers[6] observed only single resonances for [Ag(1,2,3-C$_2$N$_3$H$_2$)(PPh$_3$)$_2$]$_n$ (δ_{Ag} = 994 ppm) and [Ag(1,2,4-C$_2$N$_3$H$_2$)(PPh$_3$)$_2$]$_n$ (δ_{Ag} = 925 ppm), but each compound generated two distinct ^{31}P NMR signals, each with well resolved doublets from coupling to [109]Ag and [107]Ag at 183 K.
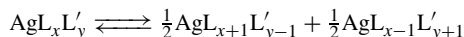
3. [109]Ag and [107]Ag coupling constants

One-bond coupling constants for the donor atoms ^{31}P and ^{13}C are more widely available than [109]Ag chemical shifts, because they can be observed directly in 1D spectra of

the coupled nucleus without resort to more elaborate 2D methods. Two-bond coupling constants are less common but are now reported with increasing frequency. The ^{109}Ag and ^{107}Ag nuclei, which are present at nearly equal abundance, generate a symmetrical pair of doublets, as shown for *trans*-[Ag(CF$_3$)$_2$(CN)Cl] in Figure 5a. This characteristic 4-line pattern uniquely identifies a nucleus coupled to silver, but can be observed only in
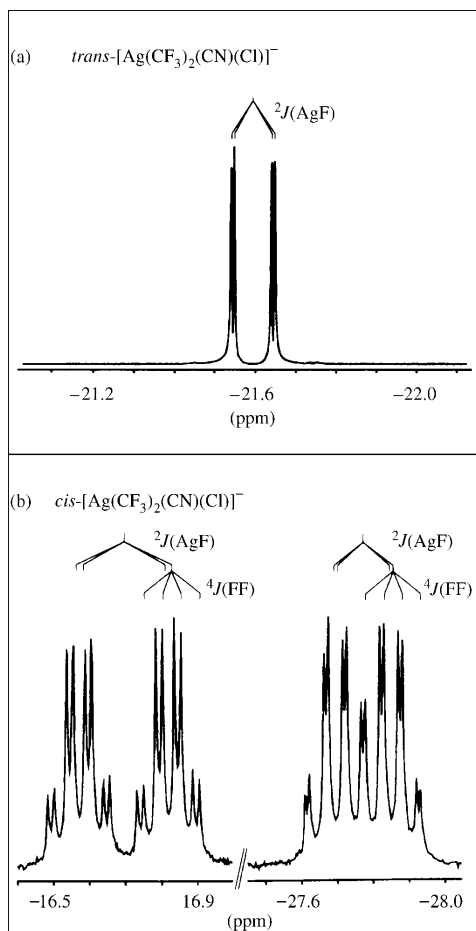
FIGURE 5. ^{19}F spectra of (a) *trans*- and (b) *cis*-[Ag(CF$_3$)$_2$(CN)Cl] exhibiting coupling to the silver ion. The spectrum of the *trans* isomer in (a) reveals the ^{107}Ag (inner) and ^{109}Ag (outer) couplings as a pair of doublets ($^2J_{AgF} = 21.4$ Hz; 24.6 Hz), since the six fluorines are equivalent. The spectrum for the *cis* isomer (b) exhibits additional $^4J_{FF}$ coupling (12.2 Hz) between the trifluoromethyl groups which are opposite to Cl$^-$ and CN$^-$ and therefore inequivalent ($\delta_F = -16.7$ ppm, $^2J_{AgF} = 62.5$, 54.3 Hz; and $\delta_F = -27.8$ ppm, $^2J_{AgF} = 39.5$, 34.3 Hz). Reprinted with permission from Reference 16. Copyright (1997) American Chemical Society

solution spectra where linewidths are narrow and in the absence of rapid ligand exchange. If additional coupling to the observed nucleus is present, as in *cis*-[Ag(CF$_3$)$_2$(CN)Cl] in Figure 5b, the pattern is less obvious but present. The intrinsic line broadening in solid state MAS spectra ($\Delta \nu \approx 40$ Hz) usually results in observation of a simple doublet which is the average of the two coupling constants, although both couplings are observed in rare cases[24]. The pulse sequences used in two-dimensional NMR methods such as INEPT, DEPT, HSQC and HMQC select one isotope, typically ^{109}Ag, for which the coupling constant becomes available. No information is lost, since the ratio of the coupling constants is fixed by the gyromagnetic ratios $\gamma^{109}/\gamma^{107} = 1.15$. Although other spin-$\frac{1}{2}$ donor nuclei such as ^{77}Se or ^{125}Te should give rise to observable $^1J_{SeAg}$ and $^1J_{TeAg}$ coupling constants, rapid dissociation and reassociation frequently obscures the coupling, even for chelate complexes[4].

For a series of homoleptic complexes with a given ligand, increasing the coordination number decreases the value of the coupling constants. Thus, $^1J_{AgC}$ values for three [AgCO]$^+$ compounds fall in the range 245–265 Hz, while the values for two [Ag(CO)$_2$]$^+$ salts are 177 and 189 Hz[25]. The $^1J_{AgP}$ coupling constants of the mono-, bis- and tris-complexes, [^{107}AgL$_x$]$^+$, where L = P(NMe$_2$)$_3$, also decrease systematically: 910, 610 and 393 Hz[26] (Table 3). The same trend was observed for the homologous complexes where L = P(NMeCH$_2$)$_3$CMe (a bicyclic phosphine) and P(NCH$_2$CH$_2$)$_3$[26]. For the ligands PEt$_3$ and P(OEt)$_3$, complete series with X = 1, 2, 3 and 4 have been measured with similar results[28] (Table 3).

When homoleptic complexes with a fixed coordination number are compared, the coupling constants tend to increase with the Allred–Rochow electronegativity of the substituents on phosphorous[28]. Thus, for the series [AgL$_3$]$^+$ the $^1J_{PAg}$ coupling constants for ^{107}Ag are 304 Hz for L = PEt$_3$ ($\chi_C = 2.5$); 393 Hz for L = P(NMe$_2$)$_3$ ($\chi_N = 3.0$); and 472 Hz for L = P(OEt)$_3$ ($\chi_O = 3.5$).

The decrease in coupling constants with increasing coordination number also holds true for recently reported examples of [Ag^{I}R$_2$]$^-$ and [Ag^{III}R$_4$]$^-$ anions, for which the silver ion with higher coordination number also has a higher oxidation state[9,16]. Thus, the $^1J_{CAg}$ values decrease from 277 to 120 Hz for the ^{109}Ag^I and ^{109}Ag^{III} complexes with R = CF$_3$, and from 194 to 88.5 Hz when R = CF$_2$H (Table 3).

4. Applications of silver NMR to chemical problems

This section on NMR studies of silver has focused on the role of $^{107/109}$Ag NMR parameters, because of their unique importance. A great deal of additional information can be obtained by monitoring other nuclei, such as ^{1}H, ^{13}C, ^{19}F, ^{31}P and ^{77}Se, present in the ligands bound to silver. We will not present such studies in detail, because the strategies are similar to those described in the section on NMR studies of gold compounds, for which ^{197}Au NMR is not a practical tool. This section will close with three recent examples of silver NMR studies of interesting systems.

Schmidbaur and coworkers[29] examined the behavior of the bis(trimesitylphosphine) gold(I), -silver(I) and -copper(I) cations in solution. The methyl residues at the 2 and 6 positions of the bulky mesityl (2,4,6-trimethylphenyl) group hinder rotation about the P–C bonds. Thus, the orientation of the three mesityl groups about their gold–carbon bonds generates a propeller-like configuration when viewed along the Au–P bond axis and they are locked into either a left-handed or a right-handed configuration. For a linear

TABLE 3.   One-bond coupling constants for silver complexes

Compound or ion	Coordination	Coupling constants(Hz)			Reference
		$^1J_{EAg}$	^{109}Ag	^{107}Ag	
[Ag(CO)]$_2$[Zn(OTeF$_5$)$_4$]		AgC$^+$	$^1J_{CAg}$	264^a	25
[Ag(CO)OTeF$_5$]		AgC$^+$	$^1J_{CAg}$	247	25
[Ag(CO)$_2$]$_2$[Zn(OTeF$_5$)$_6$]		AgC$_2^+$	$^1J_{CAg}$	189	25
[Ag(CO)$_2$]$_2$[Ti(OTeF$_5$)$_6$]		AgC$_2^+$	$^1J_{CAg}$	177	25
[Ag(CN)$_2^-$]		AgC$_2^+$	$^1J_{CAg}$ 143.0		16
[Ag(CF$_3$)$_2^-$]		AgC$_2^-$	$^1J_{CAg}$ 277.2		16
[Ag(CF$_2$H)$_2$]$^-$		AgC$_2^-$	$^1J_{CAg}$ 194.4		9
[Ag(CF$_3$)(CN)]$^-$	−CF$_3$ −CN	AgC$_2^-$	$^1J_{CAg}$ 325.5 143.9		16
[Ag(C$_6$H$_5$)$_2$]$^-$		AgC$_2^-$	$^1J_{CAg}$ 132		18
[Ag(CH$_2$PPh$_3$)$_2$]$^+$		AgC$_2^+$	$^1J_{CAg}$ 103		27
[Ag^{III}(CF$_2$H)$_4$]$^-$		Ag^{III}C$_4^-$	$^1J_{CAg}$ 88.5		9
cis-[Ag^{III}(CF$_2$H)$_2$(CF$_3$)$_2$]$^-$		Ag^{III}C$_4^-$	$^1J_{CAg}$ 91.5 112.6		9
trans-[Ag^{III}(CF$_2$H)$_2$(CF$_3$)$_2$]$^-$		Ag^{III}C$_4^-$	$^1J_{CAg}$ 70.8 144.7		9
[Ag^{III}(CF$_2$H)(CF$_3$)$_3$]$^-$	−CF$_2$H −CF$_3$ cis −CF$_3$ trans	Ag^{III}C$_4^-$	$^1J_{CAg}$ 76.6 133.9 104.2		9
[Ag^{III}(CF$_3$)$_4$]$^-$		Ag^{III}C$_4^-$	$^1J_{CAg}$ 120.0		9
trans-[Ag^{III}(CF$_2$H)$_2$(CN)$_2$]$^-$	−CF$_2$H −CN	Ag^{III}C$_4^-$	$^1J_{CAg}$ 42 149		9
[AgPEt$_3$]BF$_4$		AgP$^+$	$^1J_{PAg}$		712	28
[AgP(NMe$_2$)$_3$]BF$_4$		AgP$^+$	$^1J_{PAg}$		910	26
[AgP(OEt)$_3$]BF$_4$		AgP$^+$	$^1J_{PAg}$		1038	28
[Ag(PMes$_3$)$_2$]$^+$		AgP$_2^+$	$^1J_{PAg}$ 586		508	29
[Ag(PEt$_3$)$_2$]BF$_4$		AgP$_2^+$	$^1J_{PAg}$		482	28
[Ag{P(NMe$_2$)$_3$}$_2$]BPh$_4$		AgP$_2^+$	$^1J_{PAg}$		610	26
[Ag{P(OEt)$_3$}$_2$]ClO$_4$		AgP$_2^+$	$^1J_{PAg}$		756	28
[Ag(PEt$_3$)$_3$]BF$_4$		AgP$_3^+$	$^1J_{PAg}$		304	28
[Ag{P(NMe$_2$)$_3$}$_3$]BPh$_4$		AgP$_3^+$	$^1J_{PAg}$		393	26
[Ag{P(OEt)$_3$}$_3$]ClO$_4$		AgP$_3^+$	$^1J_{PAg}$		472	28
[Ag(PEt$_3$)$_4$]BF$_4$		AgP$_4^+$	$^1J_{PAg}$		218	28
[Ag(PPh$_3$)$_4$](pz)^b		AgP$_4^+$	$^1J_{PAg}$		223	30
[Ag(PPh$_3$)$_4$]BF$_4$		AgP$_4^+$	$^1J_{PAg}$ 260		230	21
[Ag{P(OEt)$_3$}$_4$]ClO$_4$		AgP$_4^+$	$^1J_{PAg}$		341	28
[Ag{Ph$_2$P(CH$_2$)$_2$PPh$_2$}$_2$]NO$_3$		AgP$_4^+$	$^1J_{PAg}$ 231		266	20
[Ag(cis-Ph$_2$PCH=CHPPh$_2$)$_2$]NO$_3$		AgP$_4^+$	$^1J_{PAg}$ 271		231	7, 20
[Ag{Et$_2$P(CH$_2$)$_2$PEt$_2$}$_2$]NO$_3$		AgP$_4^+$	$^1J_{PAg}$ 226		260	20

TABLE 3.   (*continued*)

Compound or ion	Coordination	Coupling constants(Hz)			Reference
		$^1J_{EAg}$	^{109}Ag	^{107}Ag	
[Ag{Ph$_2$P(CH$_2$)$_3$PPh$_2$}$_2$]NO$_3$	AgP$_4^+$	$^1J_{PAg}$	220	253	20
Ł[Ag{Ph$_2$P(CH$_2$)$_2$S(CH$_2$)$_2$S(CH$_2$)$_2$PPh$_2$}]$^+$	AgP$_2$S$_2$	$^1J_{PAg}$	510	445	19
Ł[Ag{Ph$_2$P(CH$_2$)$_2$S(o-C$_6$H$_4$)$_2$ S(CH$_2$)$_2$PPh$_2$}]$^+$	AgP$_2$S$_2$	$^1J_{PAg}$	535	470	5
[Ag(S$_2$CPh)(PPh$_3$)]	AgP$_n$S$_2^c$	$^1J_{PAg}$	355^c		31
[Ag(S$_2$CPh)(P(p-Tol)$_3$)]	AgP$_n$S$_2^c$	$^1J_{PAg}$	352^c		31
[Ag(S$_2$CPh)(P(o-Tol)$_3$)]	AgP$_n$S$_2^c$	$^1J_{PAg}$	360^c		31
[Ag(pz)(PPh$_3$)$_3$]^b	AgP$_3$N	$^1J_{PAg}$	292	253	30
Ag(μ-1,2,3-C$_2$N$_3$H$_2$)(PPh$_3$)$_2$	AgP$_2$N$_2$	$^1J_{PAg}$	~280^c		6
Ag(μ-1,2,4-C$_2$N$_3$H$_2$)(PPh$_3$)$_2$	AgP$_2$N$_2$	$^1J_{PAg}$	~280^c		6
[{AgCl(PCx$_3$)}$_2$]^b	AgP(μ-Cl)$_2$	$^1J_{PAg}$	690	595	32
[{AgBr(PCx$_3$)}$_2$]^b	AgP(μ-Br)$_2$	$^1J_{PAg}$	679	584	32
[{AgI(PCx$_3$)}$_4$]^b	AgP(μ_3-I)$_3$	$^1J_{PAg}$	505	582	32
[{Ag(μ-pz)$_2$(PPh$_3$)}$_2$]^b	AgPN$_2$	$^1J_{PAg}$	592	513	30
[Ag(PCx$_3$)$_2$ClO$_4$]^b	AgP$_2$O	$^1J_{PAg}$	505^e		33
[Ag(PCx$_3$)$_2$NO$_3$]^b	AgP$_2$O	$^1J_{PAg}$	470, 475^{d,e}		33
[Ag(PCx$_3$)$_2$NCO]^b	AgP$_2$N	$^1J_{PAg}$	410,415^{d,e}		33
[Ag(PCx$_3$)$_2$SCN]^b	AgP$_2$S	$^1J_{PAg}$	404^e		33
[Ag(PCx$_3$)$_2$Cl]^b	AgP$_2$Cl	$^1J_{PAg}$	400, 410^{d,e}		33
[Ag(PCx$_3$)$_2$Br]^b	AgP$_2$Br	$^1J_{PAg}$	396^e		33
[Ag(PCx$_3$)$_2$I]^b	AgP$_2$I	$^1J_{PAg}$	386^e		33
[Ag(PCx$_3$)$_2$CN]^b	AgP$_2$C	$^1J_{PAg}$	322^e		33
[Ag{P(2,4,6-C$_6$H$_2$(OMe)$_3$}$_2$]ClO$_4$	AgP$_2^+$	$^1J_{PAg}$	665	576	34
[Ag{P(2,4,6-C$_6$H$_2$(OMe)$_3$}Cl]	AgPCl	$^1J_{PAg}$	821	711	34
[Ag{P(2,4,6-C$_6$H$_2$(OMe)$_3$}Br]	AgPBr	$^1J_{PAg}$	796	690	34
[AgBr(μ-p-TolNCHNMe)-Pt{2,6-(Me$_2$NCH$_2$)$_2$C$_6$H$_3$}]	AgBrNPt	$^1J_{PtAg}$	173^a		35
[AgBr(μ-p-TolNCHNEt)-Pt{2,6-(Me$_2$NCH$_2$)$_2$C$_6$H$_3$}]	AgBrNPt	$^1J_{PtAg}$	165^a		35
[AgBr(μ-p-TolNCHN p-Tol)-Pt{2,6-(Me$_2$NCH$_2$)$_2$C$_6$H$_3$}]	AgBrNPt	$^1J_{PtAg}$	170^a		35
[Ag$_2$Ru$_4$(μ_3-H)$_2${μ-Ph$_2$PCH$_2$ PPh$_2$}(CO)$_{12}$]^f	AgPAgRu$_2$	$^1J_{AgP}$	500		23
	AgPAgRu$_3$-(μ_3-H)$_2$	$^1J_{AgAg}$ $^1J_{AgAg}$	40.3 35.0	35.0 30.4	
[AgRu$_4$(μ_3-H)$_3$(PPh$_3$)(CO)$_{12}$]	AgPRu$_3$-(μ_3-H)$_3$	$^1J_{PAg}$ $^1J_{HAg}$	678 34		23

^{a} Averaged coupling constant due to exchange broadening or solid state measurements.
^{b} pz = pyrazolate; Cx = cyclohexyl.
^{c} Solution equilibrium of two or more species in rapid exchange.
^{d} Two molecules per triclinic unit cell.
^{e} Solid state MAS spectra; linewidths preclude resolution of the ^{109}Ag and ^{107}Ag coupling constants.
^{f} The two silver environments equilibrate in solution; coupling constants are 109–109; 109–107; 107–107.

bisphosphine complex, there are four possible orientations for the two phosphines: R,R and L,L constitute an enantiomeric pair (C_2 symmetry), and the R,L and L,R are super-imposable *meso* structures (C_i when the mesityl groups are staggered on opposite sides of the P—Au—P axis and/or C_s when they are eclipsed). All three complexes exhibit two phosphine resonances at low temperature and a single peak at higher temperature where the two configurations interchange by a concerted rearrangement. In the case of silver, both low temperature signals ($\delta_P = -28.9, -29.0$ ppm) are split into quartets by coupling to the two silver isotopes ($^1J_{PAg} = 586, 508$ Hz). The retention of the coupling to silver at 50 °C, where the signals have coalesced ($\delta_P = -27.5$ ppm; $^1J_{PAg} = 591, 517$ Hz), demonstrates conclusively that the interchange is a concerted intramolecular process that does not entail dissociation of the phosphine[29].

The $^1J_{AgC}$ coupling constants for $[Ag(CO)]_2[Zn(OTeF_5)_4]$ and $[Ag(CO)_2]_2[Zn(OTeF_5)_4]$ provide evidence that supports the assignment of the Ag—C interactions as primarily σ-bonded with insignificant π back-bonding[25]. The average coupling constants (264 ± 6 and 189 ± 6 Hz, respectively) are larger than for $[AgPh_2]^-$ or $[Ag(CH_2PPh_2)_2]^+$ ($J_{AgC}^{109} = 132$ and 103 Hz, respectively)[18,27] and decrease from $[Ag(CO)]^+$ to $[Ag(CO)_2]^+$, although the bonds are long. The reduced coupling constants ($J_{AgC}/\gamma_{Ag}\gamma_C$) are considerably larger than the $J_{RhC}/\gamma_{Rh}\gamma_C$ value for $Rh_2Cl_2(CO)_4$, where π back-bonding is significant. Thus the coupling constants strongly suggest covalent interactions between CO and the silver 5s orbital. Consistent with this is the increase in ν_{CO} from that of free CO[19], compared to the decrease when back bonding is important.

Silver(I) is used as a probe in bioinorganic chemistry. Recent studies of a yeast metal-lothionein by Armitage and coworkers[14,15] demonstrate the advantage of substituting Ag(I) for Cu(I) and using $^1H-^{109}Ag$ HMQC spectra to solve the protein structure. Metallothioneins are ubiquitous metal-binding proteins that exhibit a wide range of metal-binding capacities dependent on the organism, the primary structure of the protein and the metal-exposure history of the organism[36]. The *Saccharomyces cerevisiae* protein is isolated with seven or eight copper(I) ions bound by the cysteine residues among the 53 amino acids in the polypeptide chain, but is subject to unwanted oxidation. Substitu-tion of Ag^+ for Cu^+ circumvents the oxidation and provides an NMR-active nucleus that can be examined through the protons of the amino acids bound to it. Detailed analysis of the HMQC couplings for the intact Ag_7MT revealed that silver is bound exclusively by cysteine residues, but only 10 of the 12 cysteines are required[14]. This was confirmed by further studies of a truncated protein, T48, from which the last five residues including the two free thiols have been removed. The anti-phase HMQC spec-trum in Figure 6 provides the details of the connectivity between the silver ions (ω_1 axis) and the cysteine H_β protons (ω_2 axis); the cross peaks represent $^3J_{AgH}$ coupling constants. For example, cysteine 9 is coordinated only to Ag VII, while cysteine 30 bridges between Ag II and Ag V. The metal coordination in the truncated protein is the same as in the intact protein (shown in the diagrams at the right of Figure 6). In both, the seven metal ions form a single large cluster, unlike mammalian and crustacean MTs which group metals into two independent clusters at the C- and N-terminal ends of the proteins. Based on the connectivities from the HMQC spectra, Ag ions I and II, with $\delta_{Ag} = 788$ and 888, were assigned as AgS_2 coordination. Ag ions III, IV, V and VII, with shifts of 994, 1033, 1184 and 1249, are each coupled to three thiolates. It is likely that Ag VI is also three-coordinate, since the δ_{Ag} value, 1220 ppm, falls high in the range of the AgS_3 shifts[14,15], although the coupling to the third cysteine was not detected. These assignments have been confirmed by model studies on silver thiolates in the solid state[10-13].

FIGURE 6. ^{109}Ag–^{1}H HMQC spectrum of Ag$_7$T48 yeast metallothionein residues 1–48 from *Saccharomyces cerevesiae* obtained at 500 MHz with preparation period of 40 ms. ω_1 is ^{109}Ag and ω_2 is ^{1}H. The seven principal resonances corresponding to the bound silver ions are shown on the left axis by Roman numerals, and the cysteine β hydrogen resonances (2 per residue) are designated by the position of the cysteines in the amino acid sequence. The upper right figure shows the connectivities observed previously for the complete 53 residue protein, while the lower figure presents the complete amino acid sequence and the relationship of the Ag–S bonds to the primary structure. Reprinted with permission from References 14 and 15. Copyright (1991, 1993) American Chemical Society

FIGURE 7. X-band ESR spectra of $[Ag([15]aneS_5)]^{2+}$. Left: anisotropic spectrum at 77 K in H_2SO_4 glass; $g_1 = 2.043$; $g_2 = 2.020$; $g_3 = 2.009$. Right: isotropic spectrum at 298 K in H_2SO_4 solution: $g_{iso} = 2.030$ and $A_{iso} = 32$ G. Reproduced by permission of the Royal Society of Chemistry from Reference 37

B. ESR Studies of Silver(II) Complexes

Silver(II) is a d^9 ion which contains an unpaired electron, usually in the $d_{x^2-y^2}$ orbital of square-planar complexes. This renders the complex paramagnetic and makes ESR a useful tool for identifying and characterizing Ag(II)[37−41], but causes difficulties for NMR studies. Silver(II) complexes can be formed by direct chemical oxidation of Ag(I) with species such as peroxydisulfate or ozone and by electrochemical oxidation at controlled potentials. Many complexes exhibit intense colors ranging from dark red to dark blue depending on the ligands present. The absorption originates from a d–d transition. For example, $[Ag\{[15]aneS_5\}]^{2+}$ (cf Figure 7) absorbs strongly at 565 nm ($\epsilon = 7700$ M^{-1} s^{-1})[41].

Isotropic ESR spectra, sometimes exhibiting coupling to the ^{109}Ag and ^{107}Ag nuclear spins, are often observed at room temperature. Spectra observed at lower temperature in glasses are generally more complicated because the complexes are in an anisotropic environment (Figure 7)[37].

Radiation of complex silver polymers of pyrene and perylene generates ESR signals with $g = 2.003$, characteristic of organic radical cations. Thus, the process is better described as an internal redox reaction leading to silver(0) and a radical cation, rather than oxidation to silver(II)[38]. Ketoximes, nitroso and isonitroso compounds are oxidized by silver(II) complexes such as $[Ag(bipy)_2]^{2+}$ and $[Ag(phen)_2]^{2+}$ to form nitroxide radicals. ESR can be used to follow the course of the reaction since both the nitroxides and the oxidant exhibit characteristic ESR spectra[39]. On the other hand, radiation of silver dissolved in aliphatic alcohols generates silver complexes which have been formulated as having a single-electron bond between silver and carbon[40]. The unpaired electron gives an ESR signal with g values much smaller than those of Ag(II) complexes where the electron resides in the metal $d_{x^2-y^2}$ orbital (Table 4).

TABLE 4. Representative ESR parameters for silver(II) complexes

Compound	Conditions	g Values				Hyperfine coupling (G)[a]			Reference
		g_{iso}	$g_\parallel, g_1$	$g_\perp, g_2$	g_3	A_1	A_2, A_{iso}	A_3	
$[Ag[[9]aneS_3]]^{2+}$	149 K, MeNO$_2$	2.030							41
$[Ag[[15]aneS_5]]^{2+}$	298 K, H$_2$SO$_4$	2.030					29		37
$[Ag[[15]aneS_5]]^{2+}$	77 K, H$_2$SO$_4$		2.043	2.020	2.009	45.0	24.0	33.0	37
$[Ag[[18]aneS_6]]^{2+}$	77 K, H$_2$SO$_4$		2.054	2.029	2.010				37
$[Ag(bipy)_2](NO_3)_2$	solid		2.168	2.047	2.037				42
$[Ag(picolinate)_2]$	solid		2.244	2.072	2.044				42
$[Ag(pyridine)_4]S_2O_8$	doped 1 : 100 in $[Cd(pyridine)_4]S_2O_8$		2.18	2.04		42.4	19.2		43
$Ag(SO_3F)_2$	80 K, solid	2.187							44
$Ag(SO_3F)_2$	80 K, BrSO$_3$F	2.198	2.407	2.086					44
$AgPt(SO_3F)_6$	80 K, solid	2.258	2.486	2.134					44
$K_2Ag(SO_3F)_4$	80 K, solid	2.173							44
$AgSnF_6$	80 K, solid	2.315	2.610	2.135					45
$[Ag (bipy)_2] (SO_3F)_2$	80 K, solid	2.091	2.170	2.051					44
$[Ag (bipy)_2](SO_3F)_2$	80 K, MeCN	2.092	2.166	2.054					44
$[Ag (bipy)_2](SO_3CF_3)_2$	80 K, MeCN	2.092	2.160	2.057					44
$[Ag^I·CH_2OH]^+$	120 K, MeOH		2.009	2.006	2.002		128		40

[a]Hyperfine constants reported with the approximation that $1\ G \sim 10^{-4}\ cm^{-1} = 3\ MHz/3.000\ cm·s^{-1}$.

III. GOLD COMPLEXES

Gold has two principal oxidation states, gold(I) and gold(III), which are stable under a wide variety of conditions. In addition, the minor oxidation states, Au(-I), Au(II), Au(IV) and Au(V), are known. Gold(I) has a $5d^{10}$ electronic configuration and, like silver(I), forms two-coordinate linear, three-coordinate trigonal-planar and four-coordinate tetrahedral complexes. However, due to the strong relativistic effect on the 6s orbital, gold has a much greater propensity to form two-coordinate complexes. Indeed, many ligands such as thiolates and cyanide which form three- and four-coordinate complexes with Ag(I) generate only the two-coordinate gold(I) analogues even in the presence of excess ligands. Four coordination is usually achieved using three or four neutral ligands such as phosphines and thioether ligands. Gold(III) has a $5d^8$ configuration and forms principally square-planar four-coordinate complexes. Weak interactions at the axial position sometimes generate complexes that approach five coordination. Both oxidation states are diamagnetic and therefore amenable to NMR studies. Gold(II) and gold(IV) have d^9 and d^7 electronic configurations, respectively, which make them potentially ESR-active oxidation states.

A. NMR Studies of Gold(I) and Gold(III) Complexes

As described in the introduction, the ^{197}Au nucleus is 100% abundant and has a quadrupole moment (Table 1). Yet, in practice, the measurement of ^{197}Au NMR spectra is not feasible. Thus, all NMR studies of gold complexes are based on the detection of other NMR-active nuclei present in the organic ligands. The literature is too extensive for a complete review here, but representative applications of ^{1}H, ^{13}C and ^{31}P NMR are described in the following sections.

1. ^1H NMR studies of methylgold(I) and methylgold(III) complexes

Gold(I) and gold(III) have extensively developed organometallic chemistries. Proton NMR studies are important in characterizing the compounds and describing their reactions. Methyl derivatives of both oxidation states are among the more stable organometallic compounds of gold. The sharp signals of the methyl resonances are crucial spectroscopic probes for the complexes. Table 5 collects some typical chemical shifts and coupling constants for the gold-bound methyl groups of such compounds. Several applications to the determination of structure and reactivity are described below.

[Me$_2$Au(μ-CN)]$_4$ is a planar tetramer in which each cyanide forms a linear bridge to the dimethylgold(III) centers at the corners of a square. The crystal structure was interpreted in terms of a C_{4h} structure in which each gold has one N and one C coordinated. But in solution, four methyl resonances appear in approximately $1 : 3 : 3 : 1$ intensity[50] (Table 5). This is inconsistent with the presence of exclusively the C_{4h} structure with cyanides organized in head-to-tail fashion around the ring, which would generate only two resonances (one for four methyls opposite N and one for four methyls opposite C). Nor is it consistent with completely statistical organization of the cyanides in solution[50], which would generate four equal intensity signals: one for methyls on gold with two C donor atoms and one for methyls with two nitrogen donor atoms; and two more of the same intensity for methyls opposite C and N on golds with one of each bound. The observed intensity $1 : 3 : 3 : 1$ ratio for [Me$_2$Au(μ-CN)]$_4$ is consistent with a high proportion of the C_{4h} structure in equilibrium with other possible cyanide-flip isomers.

The first example of a reductive elimination reaction from a dimethylgold(III) complex was discovered through NMR spectroscopy[48]. The methyl resonances ($\delta = 1.18$ ppm) of [*cis*-Me$_2$Au(PPh$_3$)$_2$]$^+$ cations, which exhibit coupling to the *cis* and *trans* phosphines,

TABLE 5. ^{1}H chemical shifts and $^3J_{PH}$ coupling constants for gold-bound methyl groups

Compound, solvent		δ_H(ppm)	$^3J_{PH}$(Hz)	Reference
Li[Au^{I}Me$_2$], Et$_2$O		−0.28		46
Ph$_3$PAu^{I}Me, CDCl$_3$		0.53	8	46
Me$_3$PAu^{I}Me, CDCl$_3$		0.09	8.6	47
Li[Au^{III}Me$_4$], Et$_2$O		−0.05		46
Me$_3$PAu^{III}Me$_3$, CDCl$_3$	cis P	0.08	7.7	47
	trans P	0.80		
Me$_3$AsAu^{III}Me$_3$, CDCl$_3$	cis P	0.04	9.5	47
	trans P	0.96		
Ph$_3$PAu^{III}Me$_3$, CDCl$_3$	cis P	0.04	8	47
	trans P	1.11	7	
[(Me$_3$P)$_2$Au^{III}Me$_2$]Cl, CDCl$_3$		0.96	6.2, 7.8	48
[(Ph$_3$P)$_2$Au^{III}Me$_2$]ClO$_4$, CDCl$_3$		1.18	6.9, 8.4	48
[Me$_2$Au^{III}{MeS(CH$_2$)$_2$SMe}]NO$_3$, CHCl$_3$, 30 °C		1.47		49
CHCl$_3$, −40 °C		1.48,1.52		49
[Me$_2$Au^{III}(μ-CN)]$_4^-$, CHCl$_3$		0.83 (1.3)^a		50
		0.91 (2.8)^a		
		1.07 (3.0)^a		
		1.15 (1)^a		
[Me$_2$Au^{III}(CH$_2$S(=O)Me$_2$)Cl]	trans CH$_2$	−0.01		51
	trans Cl	0.57		

^{a}Relative intensities

are gradually replaced by a singlet (δ_H = 0.85) ppm, which results from the elimination of ethane, and the formation of the linear [Au(PPh$_3$)$_2$]$^+$ cation[48]. Examination of other phosphine analogues showed that the steric bulk of the PPh$_3$ ligands provides the driving force for the room temperature reaction[48], which proceeds by phosphine dissociation followed by reductive elimination.

The [Me$_2$Au(MeSCH$_2$CH$_2$SMe)]$^+$ ion exhibits interesting fluxional behavior based on the chirality of the sulfur centers[49]. The uncoordinated lone pair, the methyl group and the methylene group may be arranged in R or S configurations around the S−Au bonds. At −40 °C, two resonances are observed for the Au−methyl groups (δ = 2.67 and 2.93 ppm) and two for the S−methyl groups (δ = 1.48 and 1.52 ppm). One of each is associated with the R, R and S, S enantiomers, while the second resonance of each pair corresponds to the *meso* structure (R, S and S, R). At 30 °C, a single resonance for the Au−methyl groups (δ = 1.47 ppm) and another for those bound to sulfur (δ = 2.72) are observed[49]. The effective inversion of sulfur between the R and the S forms can be achieved by its dissociation and reassociation through the second lone pair, or by inversion at sulfur without dissociation.

2. NMR studies of ^{13}C- or ^{15}N-enriched cyano gold complexes

Carbon-13 NMR spectroscopy is also widely used to characterize gold compounds. Measurements at the natural abundance (1.11%) require moderately high concentrations, but in many cases specific sites can be enriched to increase the sensitivity of measurement. Cyanides of gold(I) have been studied because of their technological importance

TABLE 6. $^{13}CN^-$ and $C^{15}N^-$ NMR parameters for gold cyanide complexes

Compound	Conditions	δ_C (ppm)	$\delta_N{}^a$ (ppm)	Coupling Constants (Hz)	Reference
KCN	D$_2$O, RT	166.2			53
			274.7	$^1J_{CN} = 6.1$	54
HCN	D$_2$O, RT	114.7^c			55
[Au(CN)$_2$]$^-$	D$_2$O, RT	154.1			53
	D$_2$O, 300 K		265.9^b		56
			266.5	$^1J_{CN} = 11.1$	54
[Me$_3$PAuCN]	CH$_3$OD, 298 K	156.0^c		$^2J_{PC} = 129.4$	57
			263.0	$^3J_{PN} = 3.6$	56
[Et$_3$PAuCN]	CH$_3$OD, 298 K	158.1^c		$^2J_{PC} = 122.4$	57
			262.5	$^3J_{PN} = 2.9$	56
[(*i*-Pr)$_3$PAuCN]	CH$_3$OD, 298 K	158.6^c		$^2J_{PC} = 116.4$	57
			262.2		56
[Cx$_3$PAuCN]^d	CH$_3$OD, 298 K	158.6^c		$^2J_{PC} = 116.4$	57
[Ph$_3$PAuCN]	CH$_3$OD, 298 K	153.8^c		$^2J_{PC} = 126$	58
			265.5	$^3J_{PN} = 4.0$	56
[Au(CH$_2$PPh$_3$)CN]	CDCl$_3$, 198 K	153.8			59
[Au(thioglucose-*S*)CN]$^-$	D$_2$O, RT	153.2			60
			260.3		61
[Au(*cis*-captopril-*S*)CN]$^-$	D$_2$O, RT	143.8			62
[Au(*trans*-captopril-*S*)CN]$^-$	D$_2$O, RT	152.2			62
[Au(thiomalate-*S*)CN]$^{3-}$		~153.4			63
		~153.6^c			55
			260.3		63
Au(glutathione-*S*)CN]$^{2-}$		153.1^c			55
Albumin° [Au(CN)$_2$]$^-_{1-7}$		152.5^c			64
[Au^{III}(CN)$_4$]$^-$	D$_2$O, RT	104.5			53
cis-[Au^{III}(Me$_2$NCH$_2$C$_6$H$_4$)(CN)$_2$]	DMSO, RT				
trans N		109.8			65
trans C		144.2			65

^{a}Downfield relative to external Na^{15}NO$_3$, except as noted.
^{b}Relative to external NH$_4$^{15}NO$_3$.
^{c}Corrected from internal trimethylsilyl propionate (TSP) to TMS, δ_C(Au(CN)$_2$$^-$) = 154.1 ppm.
^{d}Cx = cyclohexyl

in electroplating and in extraction of gold from ores. Recently, the role of cyanide in the metabolism of gold antiarthritic drugs and the finding that aurocyanide ([Au(CN)$_2$]$^-$) inhibits HIV infection of T cells has given new importance to their study[52]. Gold cyanides can be prepared using enriched K^{13}CN, a readily available starting material, which confers up to a 99-fold increase in sensitivity. The chemical shifts of diamagnetic metal cyanide complexes typically are upfield of CN$^-$ (δ_c = 166.2) and sometimes even upfield of HCN (δ_C = 114.7 ppm) (Table 6). The upfield shifts are greater for the higher oxidation states of a given metal[53]. Thus, Au(CN)$_2$$^-$ and Au(CN)$_4$$^-$ have shifts of 154 and 104 ppm, respectively[53]. There are extensive studies, typically using enriched ^{13}CN$^-$, of substituted gold(I) cyanides, but relatively few of gold(III) cyanides. The chemical shift

range of gold(I) cyanides with neutral (L) and anionic (X) ligands, LAuCN and XAuCN$^-$, respectively, is rather small (Table 6). Thiolate ligands generate a small upfield shift, typically less than 2 ppm from Au(CN)$_2{}^-$. A single exception is the assignment of a broad resonance at 143.8 ppm to the *cis*-captopril complex. Phosphine ligands in R$_3$PAuCN, on the other hand, cause a downfield shift, which increases with the basicity of the phosphine as measured by the Tolman ν_{CO} parameter[66]:

$$i\text{-Pr}_3\text{P (160.9 ppm)} > \text{Et}_3\text{P (160.4 ppm)} > \text{Me}_3\text{P (158.3 ppm)} > \text{Ph}_3\text{P (156.2 ppm)}$$

$$\text{2059 cm}^{-1} \qquad\qquad \text{2062 cm}^{-1} \qquad\qquad \text{2064 cm}^{-1} \qquad\qquad \text{2069 cm}^{-1}$$

The spectra of phosphine gold(I) cyanides must be interpreted carefully. For example, Ph$_3$PAuCN undergoes a ligand scrambling reaction[58,67],

$$[\text{R}_3\text{PAuCN}] \rightleftharpoons \tfrac{1}{2}[(\text{R}_3\text{P})_2\text{Au}]^+ + \tfrac{1}{2}[\text{Au(CN)}_2]^-$$

which is obscured by rapid ligand exchange at room temperature, but clearly evident from the ^{31}P and ^{13}C NMR spectra obtained at 200 K with 30% enriched ^{13}CN$^-$. At room temperature (Figure 8a), the ^{31}P spectrum exhibits a single broad resonance [38.1 ppm *vs* trimethylphosphate (TMP)] while the ^{13}C spectrum consists of two singlets (156.7 ppm for Ph$_3$PAuCN and 152.1 ppm for [Au(CN)$_2$]$^-$). At 200 K (Figure 8b), the ^{31}P spectrum is resolved into two components: a singlet at 41.6 ppm for [(Ph$_3$P)$_2$Au]$^+$ and a complex signal centered at 36.0 ppm for Ph$_3$PAuCN. The Ph$_3$Pau^{13}CN resonance exhibits sidebands due to coupling with the 26% enriched ^{13}CN$^-$ ($^2J_{PC} = 126$ Hz). The coupling between the ^{13}C resonance of the Ph$_3$PAu^{13}CN ($^2J_{PC} = 126$ Hz) and ^{31}P observed at 200 K confirms the assignments. Investigation of complexes with various aliphatic

FIGURE 8. ^{31}P and ^{13}C NMR spectra of 26% enriched Ph$_3$PAu^{13}CN dissolved in CH$_3$OD and measured at (a) 297 K and (b) 200 K. The ligand scrambling reaction is rapid at room temperature and only the averaged signals of species present are observed, but under slow exchange conditions at 200 K additional species are clearly evident in the ^{31}P and ^{13}C NMR spectra. Reprinted with permission from Reference 58. Copyright (1986) American Chemical Society

phosphines showed that this is a general phenomenon. The equilibrium constants ($K_{eq} = [(R_3P)_2Au^+][Au(CN)_2{}^-]/[R_3PAuCN]^2$) for the scrambling reactions were subsequently measured by integration of the ^{31}P spectra for R = Ph (0.112), Me (0.37), Et (0.24), i-Pr (0.29) and Cx (0.49)[58,67]. Interestingly, Ph$_3$PAuCN, Et$_3$PAuCN and most other complexes exist as such in the solids and scramble in solution. In contrast 'tris(cyanoethyl)phosphine cyanogold(I)' is ionic in the solid state, $[\{(NCCH_2CH_2)_3P\}_2Au][Au(CN)_2]$[57], but equilibrates to form the neutral species, $(NCCH_2CH_2)_3PAuCN$, in solution. Thus, these interesting systems demonstrate the importance of NMR methods in assessing the differences between the solution chemistry and the solid state structures of substances.

3. ^{31}P NMR studies of gold phosphine complexes

Phosphine complexes of gold are even more numerous than those of silver and are important due to their current and potential medicinal uses.[68,69] Auranofin, an antiarthritic agent which contains a thiolate and a phosphine as ligands, is used clinically, and bis(diphosphine)gold(I) complexes show promise in a number of applications[70]. ^{31}P NMR spectroscopy provides a way to examine the structures and reactivity of these compounds. Coupling of the ^{31}P nucleus to ^{197}Au is not observed due to the effective relaxation arising from the large quadrupole moment of the nucleus (Table 1). ^{31}P NMR studies in solution have been routine for several decades and the increasing availability of the CP-MAS technique now allows solids to be easily studied. The solid state method avoids ligand exchange problems, which sometimes affect solution studies at room temperature[71].

Two different sign conventions have been used for ^{31}P NMR chemical shifts, δ_P. In this chapter, the resonances downfield of aqueous H_3PO_4 are taken as positive. In the older literature the opposite convention was often used. The chemical shifts of gold phosphine complexes and the corresponding free phosphines are listed in Table 7. The resonances are sensitive to the organic residues attached to the phosphine and one must be careful to compare the same ligand in discussing changes in chemical shifts. These considerations are simplified somewhat by considering the coordination chemical shift defined as

$$\Delta\delta_P{}^{coord} = \delta_P{}^{complex} - \delta_P{}^{ligand}$$

The $\Delta\delta_P{}^{coord}$ values reflect the electronic changes in the ligand when different phosphines are considered.

For a homoleptic series of gold(I) complexes, $AuL_2{}^+$, $AuL_3{}^+$, $AuL_4{}^+$, the $\delta_P{}^{complex}$ values shift upfield toward that of the free phosphine as the number of bound ligands increases and, consequently, the coordination chemical shift, $\Delta\delta_P{}^{coord}$, decreases in the order[74,75]

$$\delta_P{}^{complex} \text{ and } \Delta\delta_P{}^{coord}: \quad AuL_2{}^+ > AuL_3{}^+ > AuL_4{}^+ > L$$

See, for example, the values for $[Au(PEt_3)_x]^+$ and $[Au(PPh_2Bu-n)_x]^+$ in Table 7. The pattern is consistent with the increasing bond lengths for gold–phosphorous bonds, as the coordination number increases. That is, as additional phosphines bind, their electronic structure more closely resembles that of free ligand. One might expect a similar trend to apply when an anionic ligand is present, but for the series $AuXL_x$ ($x = 1, 2, 3, 4$), there is a consistent irregularity[72,74]:

$$\delta_P{}^{complex} \text{ and } \Delta\delta_P{}^{coord}: \quad AuXL < AuXL_2 > AuXL_3 > [AuL_4]X > L$$

C. Frank Shaw III

TABLE 7. ^{31}P NMR shifts^a and coordination chemical shifts for gold–phosphine complexes

Compound	Conditions	$\delta_P^{complex}$	$\Delta\delta_P^{coord\,b}$	Reference
[Au^I(PPh$_3$)Cl]	solid state	30		71
[Au^I(PPh$_3$)Br]	solid state	32		71
[Au^I(PPh$_3$)I]	solid state	36		71
[Au^I(PPh$_3$)$_2$Cl]	solid state	37		71
[Au^I(PPh$_3$)$_2$Br]	solid state	38		71
[Au^I(PPh$_3$)$_2$I]	solid state	36		71
[Au^I(P(Bu-n)$_3$)Br]	CH$_2$Cl$_2$, 160 K	24.5	55.0	72
[Au^I(P(Bu-n)$_3$)$_2$Br]	CH$_2$Cl$_2$, 160 K	32.6	63.1	72
[Au^I(P(Bu-n)$_3$)$_3$Br]	CH$_2$Cl$_2$, 160 K	28.3	58.8	72
[Au^I(P(Bu-n)$_3$)$_4$]Br	CH$_2$Cl$_2$, 160 K	−13.3	17.2	72
P(Bu-n)$_3$	CH$_2$Cl$_2$, 160 K	−30.5	0.0	72
[(Au^{I}Cl)$_2$(Ph$_2$PCH$_2$CH$_2$PPh$_2$)]	CDCl$_3$, 302 K	31.5		73
[(Au^{I}Ph$_2$PCH$_2$CH$_2$PPh$_2$)$_2$]$^+$	CDCl$_3$, 302 K	20.8		73
[Au^I(PPh$_2$(Bu-n))$_2$]$^+$		41.3	58.6	74
[Au^I(PPh$_2$(Bu-n))$_3$]$^+$		33.1	50.4	74
[Au^I(PPh$_2$(Bu-n))$_4$]$^+$		9.2	26.5	74
[Au^I(PPh$_2$(Bu-n))Br]		31.9	49.2	74
[Au^I(PPh$_2$(Bu-n))$_2$Br]		36.1	53.4	74
[Au^I(PPh$_2$(Bu-n))$_3$Br]		33.6	50.9	74
PPh$_2$Bu-n		−17.3	0.0	74
[Au^I(PEt$_3$)$_2$]PF$_6$	CH$_2$Cl$_2$, 175 K	43.3	62.4	75
[Au^I(PEt$_3$)$_3$]PF$_6$	CH$_2$Cl$_2$, 175 K	38.3	57.4	75
[Au^I(PEt$_3$)$_4$]PF$_6$	CH$_2$Cl$_2$, 175 K	−5.7	13.4	75
[Au^I(PEt$_3$)Cl]	CH$_2$Cl$_2$, 175 K	29.0	48.1	75
PEt$_3$	CH$_2$Cl$_2$, 175 K	−19.1	0.0	75
[Au^I(PEt$_3$)(phthalimide-N)]	CDCl$_3$	29.6		76
[Au^I(PEt$_3$)(riboflavin-N^3)]	3 : 1 DMSO:EtOH	32.9		76
[Au^I(PEt$_3$)(5,5′-diphenylhydantoin-N)]	CDCl$_3$	30.0		76
[Au^I(PEt$_3$)(saccharin-N)]	CDCl$_3$	28.9		76
[Au^{III}(PEt$_3$)Br$_3$]	CDCl$_3$	47.6		76
trans-[Au^{III}(PEt$_3$)(phthalimide-N)Br$_2$]	CDCl$_3$	35.4		76
cis-[Au^{III}(PEt$_3$)Br(phthalimide-N)$_2$]	CDCl$_3$	41.5		76
[Au^{III}(PEt$_3$)Cl$_3$]	CDCl$_3$	66.0		77
cis-[Au^{III}(PEt$_3$)Cl$_2$Br]	CDCl$_3$	60.8		77
trans-[Au^{III}(PEt$_3$)Cl$_2$Br]	CDCl$_3$	61.6		77
cis-[Au^{III}(PEt$_3$)ClBr$_2$]	CDCl$_3$	56.8		77
trans-[Au^{III}(PEt$_3$)ClBr$_2$]	CDCl$_3$	55.6		77
[Au^{III}(PEt$_3$)Br$_3$]	CDCl$_3$	51.9		77
cis-[Me$_2$Au^{III}(PMe$_3$)$_2$]ClO$_4$	CDCl$_3$	15.5		47

^{a}Relative to external 85% H$_3$PO$_4$.
^{b}$\Delta\delta_P^{coord} = \delta_P^{complex} - \delta_P^{ligand}$.

Data for L = P(Bu-n)$_3$ and X = Br$^-$ in Table 7 illustrate the trend. It applies, as well, to bulky ligands where the $x = 3$ complex can be ionic, [AuL$_3$]X; for example, L = PPh$_2$Bu-n and X = Br (Table 7).

Chemical shifts of gold(III) complexes are typically larger than those of gold(I) complexes with similar ligands: for example, 66 ppm for [Au(PEt$_3$)Cl$_3$] *vs* 29 ppm for [Au(PEt$_3$)Cl][77]. In addition, they also exhibit *cis* and *trans* effects, due to the square-planar structure of the compounds. Thus, the shifts are 61.6 ppm for PEt$_3$ when it is opposite to Br$^-$ in *trans*-[Au(PEt$_3$)BrCl$_2$], and 60.6 when it is opposite to Cl$^-$ in *cis*-[Au(PEt$_3$)BrCl$_2$][77].

4. NMR studies of biologically active gold complexes

^{31}P NMR studies have been important for elucidating the metabolism and pharmacology of the anti-arthritic drug auranofin: triethylphosphine(2,3,4,6-tetra-*O*-acetylglucopyranosato-*S*)gold(I) or Et$_3$PAuSAtg[68,69]. Table 8 lists the ^{31}P chemical shifts in aqueous solution of complexes related to auranofin including analogues with Me$_3$P, *i*-Pr$_3$P and (NCCH$_2$CH$_2$)$_3$P replacing the Et$_3$P ligand and various biological ligands replacing the tetraacetylthioglucose ligand. There is a general pattern to the shifts (δ_P) as the ligands *trans* to phosphorous in the two-coordinate complexes are varied:

$$R_3P < R_3PAuCl < R_3Pau-N_{His}-albumin < R_3PAuSAtg$$

$$< R_3PAuS_{34}-albumin < R_3P=O$$

From studies with isolated proteins, red cells and low molecular weight metabolites, a great deal of information has been derived about the succession of reactions that generate gold complexes from which one or both carrier ligands have been displaced. Figure 9

TABLE 8. ^{31}P NMR chemical shifts of trialkylphosphine gold complexes of biological interest[a]

Compound	δ_P(ppm)[a]			
R =	Me	Et	*i*-Pr	CH$_2$CH$_2$CN
References	78	79–81	82	83
R$_3$P		−20	18.0	−27.4
R$_3$PAuCl	−13.1	31.3	60.5	21.6
R$_3$PAuCN		35.5	64.7	26.8
R$_3$PAu(2,3,4,6-tetraacetylthioglucose-*S*)	−1.7	37.0	66.5	28.8
R$_3$PAu(albumin-S_{34})	−2.3	38.8	68.5	27.0
(R$_3$PAu)$_2$(μ-albumin-S_{34})	−13.7	35.9	—	—
(R$_3$PAu)$_x$(albumin-N_{His})	−12 to −15	∼25 to ∼28	∼58 to ∼60	∼17 to ∼20
[(R$_3$P)$_2$Au]$^+$		44.1	73.7	29.4
R$_3$P=O	49.7	61.7[b]	66.7	49.2
R$_3$P=S			71.0	48
R$_3$PAu(thioglucose-*S*)		36.3		
R$_3$PAu(glutathione-*S*)		35.8		
(R$_3$PAu)$_{1.7}$(hemoglobin-$S_{\beta-93}$)		34.0		
R$_3$P$^+$SCH$_2$(HSCH$_2$)Albumin			75.5	

[a]In aqueous 100 mM NH$_4$HCO$_3$ buffer, pH 7.9, measured and reported relative to internal trimethylphosphate ($\delta =$ −2.74 ppm *vs* external 85% H$_3$PO$_4$).
[b]$\delta_O = 40.6$ ppm; $^1J_{PO} = 156$ Hz[84].

Albumin—S$^-$ + Et$_3$PAuSAtg $\longrightarrow$ Albumin—S—Au—PEt$_3$ + AtgSH
            37.0 ppm   38.8 ppm

Albumin—S—Au—PEt$_3$ + AtgSH $\rightleftharpoons$ Albumin—S—Au—SAtg + Et$_3$P
            38.8 ppm

$$\text{Et}_3\text{P} + \begin{array}{c} \text{S—CH}_2 \\ | \quad\quad \text{Albumin} \\ \text{S—CH}_2 \end{array} \xrightarrow{\text{H}_2{}^{17}\text{O}} \begin{array}{c} \text{HS—CH}_2 \\ \quad\quad \text{Albumin} + \text{Et}_3\text{P}^{17}\text{O} \\ \text{HS—CH}_2 \end{array}$$

                                                                    61.7 ppm
                                                                    $^1J_{PO}$ = 156 Hz

                        + Et$_3$PAuSAtg $\longrightarrow$ No Reaction

Albumin—S—Au—PEt$_3$
      38.8 ppm

                        + xs Et$_3$PAuCl $\xrightarrow{x \leq 17}$
                              31.3 ppm

              (Et$_3$P—Au—N$_{His}$)$_x$Albumin—μ—S—(Au-PEt$_3$)$_2$
                    25–28 ppm   35.6 ppm

                                    (a)

Albumin—S$^-$ + (i-Pr)$_3$PAuSAtg $\longrightarrow$ Albumin—S—Au—P(Pr-i)$_3$ + AtgSH
                  66.5 ppm   68.5 ppm

Albumin—S—Au—P(Pr-i)$_3$ + AtgSH $\longrightarrow$ No Reaction
            68.5 ppm

Albumin—S—Au—P(Pr-i)$_3$ + 2 HCN $\longrightarrow$ Albumin—S$^-$ + Au(CN)$_2$$^-$ + (i-Pr)$_3$P
            68.5 ppm

$$(i\text{-Pr})_3\text{P} + \begin{array}{c} \text{S—CH}_2 \\ | \quad\quad \text{Albumin} \\ \text{S—CH}_2 \end{array} \longrightarrow \begin{array}{c} \text{HS—CH}_2 \\ \quad\quad \text{Albumin} \\ (i\text{-Pr})_3\text{P}^+\text{S—CH}_2 \end{array}$$

                                                        75.5 ppm $\searrow k = 7 \times 10^{-5}$ s^{-1}

                              (i-Pr)$_3$PS + S$\begin{array}{c}\text{—CH}_2\\ \quad\quad\text{Albumin}\\ \text{—CH}_2\end{array}$
                                    71.0 ppm

                        + (i-Pr)$_3$PAuSAtg $\longrightarrow$ No Reaction

Albumin—S—Au—P(Pr-i)$_3$
          68.5 ppm

                        + xs(i-Pr)$_3$PAuCl
                              60.5 ppm

              (i-Pr)$_3$P—Au—N$_{His}$)$_x$Albumin—S—Au—P(Pr-i)$_3$
                    58–60 ppm   68.5 ppm

                                    (b)

FIGURE 9. Scheme showing the reactions of auranofin (Et$_3$PAuSAtg) and its chloride and (i-Pr)$_3$P analogues with serum albumin under biomimetic conditions. ^{31}P, ^{17}O, ^{13}C and ^{1}H NMR have been used to characterize various reactions and products

shows the reactions of auranofin and its triisopropyl analogue which have been detected and described through NMR studies, primarily by monitoring ^{31}P. The exchange of low molecular weight thiols such as glutathione, cysteine, homocysteine, thioglucose or penicillamine with AtgSH is rapid on the NMR timescale[85,87], while exchange at protein thiolates such as cysteine 34 of albumin or the β-93 cysteine of hemoglobin is slow.

Sadler and coworkers[86,87] assigned a band at 38.8 ppm (*vs* TMP) to the albumin−gold−triethylphosphine complex formed by reaction of albumin with auranofin, which was confirmed by EXAFS studies and analysis of the isolated product[79]. No further reaction occurs with excess auranofin. The drug metabolite Et$_3$PO (61.6 ppm) is generated as a minor product when auranofin is used, but not when Et$_3$PAuCl (31.3 ppm) is used, to generate albumin−S−AuPEt$_3$[79]. The chloride ion, unlike the AtgSH ligand released from auranofin, cannot displace phosphine and generate Et$_3$P=O. The reaction of Et$_3$PAuCl with albumin exhibits another important difference. For example, when sufficient excess is used, a second Et$_3$PAu$^+$ moiety binds to cysteine 34 and up to 17 histidine residues will bind to the imidazole nitrogens of the histidine side chains, because chloride is a weaker ligand than a thiolate[80]. Figure 10 (left side) shows the titration of bovine serum albumin with Et$_3$PAuCl which initially forms albumin−S−AuPEt$_3$ and then populates many histidines ($\delta_P = 25-28$ ppm) and converts the cysteine 34 site from albumin−S−AuPEt$_3$ ($\delta_P = 38.8$ ppm) to albumin−μ−S−(AuPEt$_3$)$_2^+$ ($\delta_P = 35.9$ ppm) as additional Et$_3$PAuCl is added. If cysteine 34 is alkylated with iodoacetate, Figure 10 (right side), binding at cysteine 34 is blocked, demonstrating that the 35.9 ppm resonance is indeed due to formation of the digold complex at this site[80]. Model studies using tetraacetylthioglucose show that complexation to form the thiolate-bridged digold species is feasible (Figure 11)[80]. When auranofin and Et$_3$PAuCl react at 1 : 1 ratio, the resulting complex shows two ^{31}P NMR signals due to the diastereotopically inequivalent Et$_3$PAu$^+$ groups bound to the chiral thiosugar ligand (Figure 11). But when an excess of either gold species is present, rapid exchange of all species present is observed. In the case of albumin, the protein environment inhibits exchange of Et$_3$PAu$^+$ on the NMR time scale[80].

Further studies of albumin−S−AuPEt$_3$ (Figure 9) defined the mechanism of Et$_3$PO formation in which tetraacetylthioglucose (liberated from auranofin) or another thiol displaces Et$_3$P[84,88]. The free phosphine is not detected because it reassociates rapidly unless it is immediately oxidized by one of the seventeen disulfide bonds in albumin, which is concomitantly reduced to two cysteine residues. The role of water as the primary source of oxygen for the reaction (Figure 9) was confirmed by incorporation of ^{17}O from enriched water into Et$_3$P=^{17}O ($\delta_O = 40.6$ ppm; $^1J_{PO}$ 156 Hz)[84].

Structure−function relationships defined the tendency of thiols to displace the phosphine. The unfavorable displacement of phosphine depends on the thiol's affinity for gold(I), which is related to the pK_{SH} of the thiol[89], which in turn correlates with the chemical shift of the particular Et$_3$PAuSR compound[81]:

$$\delta_P(Et_3PAuSR): RSH = \text{tetraacetylthioglucose} > \text{1-thioglucose}$$
$$> \text{glutathione} > \text{ergothionine}$$
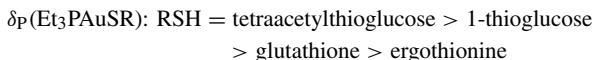
Similarly, the ease of displacement of the phosphine (R$_3$P) leading to the corresponding oxide was found to increase from R = isopropyl to ethyl to methyl[78,82,88]. *i*-Pr$_3$P requires cyanide, which has an even higher affinity for gold than thiolates and phosphines, to initiate the oxidation[82]. Et$_3$P is slowly displaced and oxidized over 24 to 48 hours with added thiols[83], but Me$_3$P is readily displaced by the tetraacetylthioglucose released from the auranofin analogue, Me$_3$PAuSAtg, and rapidly oxidized[78]. This series of 3 phosphines

Et$_3$PAuCl : AlbSCH$_2$CO$_2^-$

Et$_3$PAuCl   BSA

G   G

F   F

E   E

D   D

C   C

B   B

A   A

          40   30   40   30
               ppm   ppm
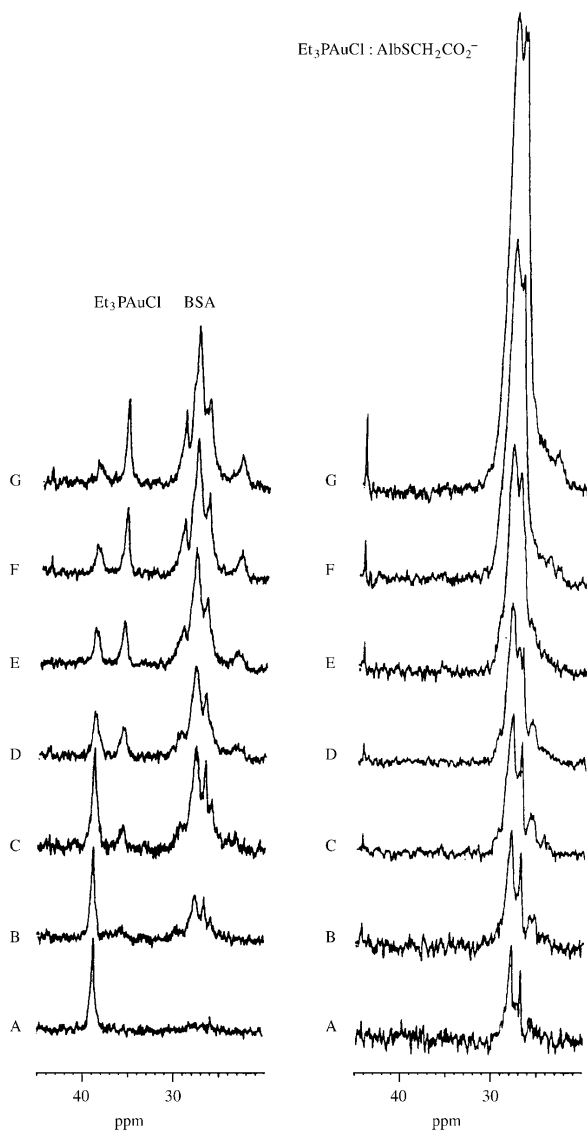
FIGURE 10. ^{31}P {^{1}H} NMR(101.3 MHz) spectral titrations of bovine serum albumin with Et$_3$PAuCl in 60 : 40 D$_2$O:MeOH. δ_P measured and reported *vs* TMP. Native albumin (A, left) reacts initially with Et$_3$PAuCl to form Alb$-$S$_{34}-$AuPEt$_3$ (38.8 ppm) and (B$-$G, left) reacts further with additional Et$_3$PAuCl to form up to 17 histidine adducts (23$-$29 ppm). Simultaneously, Alb$-$S$_{34}-$(AuPEt$_3$)$_2^+$ (35.6 ppm) is formed at the expense of Alb$-$S$_{34}-$AuPEt$_3$ (B$-$G, left). (A$-$G, right) Spectra for titration of cysteine-34-modified bovine serum albumin with 0.94 to 17.1 equiv of Et$_3$PAuCl lack the peaks at 38.8 and 35.6 ppm assigned to cysteine-34-bound gold species; only the Et$_3$PAuN$_{His}$ adducts are observed. Reprinted with permission from Reference 80. Copyright (1986) American Chemical Society
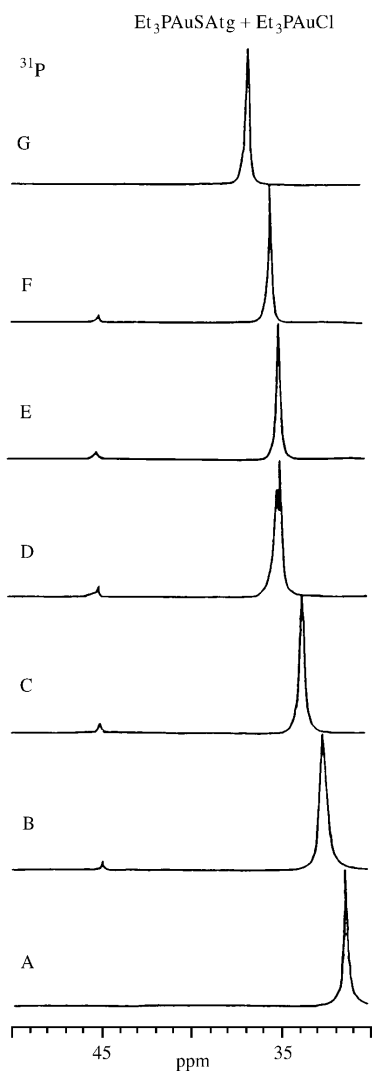
FIGURE 11. Auranofin (Et$_3$PAuSAtg) and Et$_3$PAuCl form a digold complex, [(Et$_3$PAu)$_2$(μ-SAtg)]$^+$, in which the two Et$_3$PAu$^+$ moieties are diastereotopically inequivalent. But the inequivalence is observable only when the stoichiometry is close to 1 : 1 (spectrum D). An excess of either Et$_3$PAuCl (A−C) or Et$_3$PAuSAtg (E−G) causes rapid exchange of Et$_3$PAu$^+$ among the three environments and observation of a single, averaged resonance. ^{31}P {^{1}H} NMR spectra (101.3 MHz) in 60 : 40 D$_2$O:MeOH. δ_P measured and reported *vs* trimethylphosphate (TMP). Mole fractions of Et$_3$PAuCl:Et$_3$PAuSAtg: (A) 1.00 : 0; (B) 0.69 : 0.31; (C) 0.55 : 0.45; (D) 0.51 : 0.49; (E) 0.42 : 0.58; (F) 0.20 : 0.80; (G) 0 : 1.00. Reprinted with permission from Reference 80. Copyright (1986) American Chemical Society

cannot distinguish whether the effect was steric, due to the environment of the phosphine in the protein, or electronic due to its basicity, since both decrease in the same order. Therefore, tris(cyanoethyl)phosphine, which has a cone angle similar to Et_3P, but is a much weaker base, was investigated[83]. It is displaced and oxidized as easily as Me_3P, consistent with electronic effects as the dominant factor[83]:

$$(NCCH_2CH_2)_3P \sim Me_3P > Et_3P \gg i\text{-}Pr_3P$$

Examination of reactions with the more basic and sterically hindered triisopropylphosphine analogue led to spectroscopic characterization of an intermediate that reacts too quickly to be detected when auranofin itself is studied[82] (Figure 9). When $(i\text{-}Pr)_3P$ is displaced from albumin$-$S$-$Au$-$P(Pr-i)$_3$ by cyanide, it reacts to generate $i\text{-}Pr_3P^+SCH_2$ (HSCH$_2$)albumin, the key intermediate for the oxidation of the phosphine by disulfide bonds. This long-lived triisopropylphosphonium thiolate intermediate was detected at 75.5 ppm in the ^{31}P NMR spectrum. In this case it is long-lived because the bulky isopropyl groups hinder water attack at the P atom, whereas it is short-lived for R_3P, where R = Me, Et, $(NCCH_2CH_2)_3P$. The first-order rate constant (7×10^{-5} s^{-1}) for its decay to $(i\text{-}Pr)_3P=S$ and a trace of $(i\text{-}Pr)_3P=O$ was measured by monitoring the decay of the signal. The formation of the sulfide due to attack at the cysteine β carbon instead of the oxide by attack at the P atom is also a consequence of the bulky isopropyl groups[82].

These studies (Figure 9), using NMR studies of ^{31}P and other nuclei, have developed a detailed picture of the reactions of auranofin and its metabolites in blood. They demonstrate the applicability of NMR to elucidating metallodrug pharmacology and reactivity.

B. ESR Studies of Gold(II) Complexes

Gold(II) complexes fall into three distinctly different categories. The first consists of pseudogold(II) compounds, which are salts or dinuclear complexes containing equal amounts of gold(I) and gold(III) and can be dismissed. The largest class consists of digold species formed by the oxidation of gold(I) or the reduction of gold(III) juxtaposed to one another in ring systems. The two gold(II) centers have square-planar coordination and are linked by gold$-$gold bonds, which render the complexes diamagnetic. Mononuclear gold(II) complexes, which are less common and less stable, contain paramagnetic gold(II) centers. They are formed with ligands such as malononitriledithiolate, $((NC)_2C_2S_2{}^{2-})$ or [15]aneS$_5$, by reduction of the corresponding gold(III) complexes. The unpaired electron occupies an orbital that contains metal $d_{x^2-y^2}$ and ligand character. Table 9 lists the g values and hyperfine constants for a number of such complexes.

Gold(IV) ions should also exhibit ESR spectra, since they have a d^7 electronic configuration, which is paramagnetic regardless of whether it is high spin or low spin. The only compound reported to date, bis(benzene-1,2-dithiolato)gold(IV), $Au(S_2C_6H_4\text{-}o)_2$[96,97], was characterized crystallographically in 1990. Magnetic studies showed that it exhibits antiferromagnetic coupling in the solid state, but no ESR data have been reported.

Comparison of Tables 4 and 9 reveals that the chemistry of silver(II) provides a template for directing the investigation of new gold(II) species. Recently reported examples of mononuclear gold(II) complexes[90,92] include $Au^{II}(SO_3F)_x{}^{2-x}$ and $[Au^{II}([9]aneS_3)]^{2+}$ for which there are silver precedents[37,41,44]. $Au^{II}(SO_3F)_x{}^{2-x}$ can be prepared by mild pyrolysis of $Au^{III}(SO_3F)_3$ in the solid state or by its reduction with metallic gold in HSO_3F solution[92]. The ESR spectra of the solid state defects at 100 K is isotropic (Table 9). The solution spectrum, measured at 100 K, reveals a well defined quartet due to hyperfine interaction with the 100% abundant ^{197}Au nucleus (A_{iso} = 44.6 G)[92]. $[Au^{II}([9]aneS_3)]^{2+}$,

TABLE 9. ESR parameters for paramagnetic gold compounds

Compound	Conditions	g Values				Hyperfine constants(G)^a				Reference
		g_{iso}	$g_{\parallel}$, g_1	$g_{\perp}$, g_2	g_3	A_{iso}	A_1	A_2	A_3	
[Au^{II}([9]aneS$_3$)$_2$]$^{2+}$	MeCN, 77 K	2.010				57.3				90
[Au^{II}{1,2-S$_2$C$_2$(CN)$_2$}$_2$]$^{2-}$	doped, 295 K	2.000	2.016	2.006	1.978	40.5	41.5	40.7	39.2	91
[Au^{II}(SO$_3$F)$_{3-x}$]	defects, 103 K	2.359	2.882	2.103	2.093					92
Au^{II}(solvate)		2.362	2.890	2.103	2.093	44.6	48.3	48.3	40.0	92
Au^{II}(phthalocyanine)	1-C$_{10}$H$_7$Cl, 77 K	2.065		1.996		60.1				93
[Au^{II}(o-aminobenzenethiolate)$_2$(DMF)$_2$]	MeCN, 298 K	2.0032				5.50				94
[Au^{II}(o-aminobenzenethiolate)$_2$]$_2$	MeCN, 298 K	2.0033				4.24				94
[cis-Au^{II}{o-(methylthio)analine}$_2$Cl]Cl	CH$_2$Cl$_2$, RT	2.0033				6.5				95
[{Au^{II}[o-(methylthio)analine]$_2$}$_2\mu^2$-Cl$_2$]	CH$_2$Cl$_2$, RT	2.0033				4.0				95

^{a}Hyperfine constants reported with the approximation that 1 G $\sim$ 10^{-4} cm^{-1} = 3 MHz/3.000 cm·s^{-1}.

98
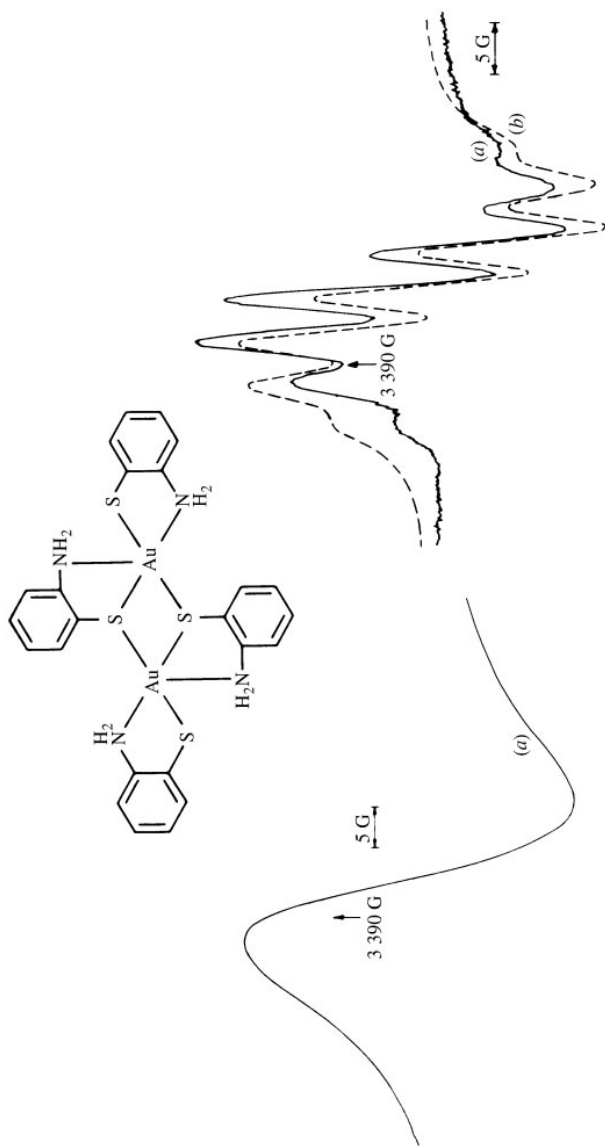
FIGURE 12. Structure and X-band ESR spectra of tetrakis(*o*-aminobenzenethiolato)digold(II), [Au^{II}(*o*-H$_2$NC$_6$H$_4$S)]$_2$. Left: powder spectrum at room temperature. Right: solution spectrum in DMF at room temperature: (a) experimental and (b) simulated by assuming coupling to two ^{197}Au nuclei. g_{iso} = 2.0033 and A_{iso} = 4.25 G. The small hyperfine constant indicates that the unpaired electron occupies an orbital with relatively small metal character, but symmetrically distributed over both metal ions. Reproduced by permission of the Royal Society of Chemistry from Reference 94

prepared by *in situ* oxidation of the gold(I) precursor, exhibits a *g* value of 57.3 G[90]. These *g* values are comparable to those reported earlier for mononuclear gold(II) complexes such as $[Au\{S_2C_2(CN)_2\}_2]^{2-}$, 41.5 G[91] (Table 9).

Dinuclear complexes exhibiting hyperfine coupling to two independent gold(II) centers have been reported[94,95] (Figure 12). In these systems, S,N bidentate chelate complexes of ligands such as *o*-dimethylaminobenzenethiolate bridge between the two ligands. The ESR spectrum exhibits a septuplet due to coupling to the two gold ions. The hyperfine coupling constants (4–7 G) are almost an order of magnitude smaller than those described above, indicating that relatively little of the electron density resides on the metal ions, and the *g* values are closer to those of an organic radical than of an electron with substantial gold 5d character[94,95].

IV. CONCLUSIONS

The practical utility of NMR as a tool for studying inorganic species is not in doubt. Clearly, the development of gold and silver chemistry has profited enormously from it. The greatest utility is for the diamagnetic oxidation states M(I) and M(III). In the case of silver, the spin-$\frac{1}{2}$ ^{109}Ag and ^{107}Ag nuclei provide an additional advantage through the coupling constants that confirm Ag–heteroatom bonding and chemical shifts that probe the environment in silver complexes. Gold chemistry, despite the lack of detectable NMR resonances or coupling to other nuclei, is at least as well developed, however.

ESR has application primarily to the rather rare and somewhat unstable M(II) oxidation states of gold and silver, but is an important tool for demonstrating their presence unambiguously.

V. ACKNOWLEDGMENT

VI. REFERENCES

1. B. E. Mann, *Annu. Rep. NMR Spectrosc.*, **23**, 141 (1991).
2. R. G. Kidd, *Annu. Rep. NMR Spectrosc.*, **23**, 85 (1991).
3. J. R. Black, N. R. Champness, W. Levason and G. Reid, *Inorg. Chem.*, **35**, 1820 (1996).
4. J. R. Black, N. R. Champness, W. Levason and G. Reid, *J. Chem. Soc., Dalton Trans.*, 3439 (1995).
5. A. R. J. Genge, A. M. Gibson, N. K. Guymer and G. Reid, *J. Chem. Soc., Dalton Trans.*, 4099 (1996).
6. K. Nomiya, K. Tsuda and N. C. Kasuga, *J. Chem. Soc., Dalton Trans.*, 1653 (1996).
7. S. J. Berners-Price, P. J. Sadler and C. Brevard, *Magn. Reson. Chem.*, **28**, 145 (1990).
8. F. Lianza, A. Macchioni, P. Pregosin and H. Rüegger, *Inorg. Chem.*, **33**, 4999 (1994).
9. R. Eujen, B. Hoge and D. J. Brauer, *Inorg. Chem.*, **36**, 3160 (1997).
10. H. G. Fijolek, P. González-Duarte, S. H. Park, S. L. Suib and M. J. Natan, *Inorg. Chem.*, **36**, 5299 (1997).
11. H. G. Fijolek, J. R. Grohal, J. L. Sample and M. J. Natan, *Inorg. Chem.*, **36**, 622 (1997).
12. H. G. Fijolek, T. A. Oriskovich, A. J. Benesi, P. González-Duarte and M. J. Natan, *Inorg. Chem.*, **35**, 797 (1996).
13. P. González-Duarte, J. Sola, J. Vives and X. Solans, *J. Chem. Soc., Chem. Commun.*, 1641 (1997).
14. S. S. Narula, R. K. Mehra, D. R. Winge and I. M. Armitage, *J. Am. Chem. Soc.*, **113**, 9354 (1991).
15. S. S. Narula, D. R. Winge and I. M. Armitage, *Biochemistry*, **32**, 6773 (1993).
16. R. Eujen, B. Hoge and D. J. Brauer, *Inorg. Chem.*, **36**, 1464 (1997).
17. K. Endo, K. Yamamoto, K. Matsushita, K. Deguchi, K. Kanda and H. Nakatusji, *J. Magn. Reson.*, **65**, 268 (1985).

18. J. Blenkers, H. K. Hofstee, J. Boersma and G. M. van der Kerk, *J. Organomet. Chem.*, **168**, 251 (1979).
19. C. L. Doel, A. M. Gibson, G. Reid and C. S. Frampton, *Polyhedron*, **14**, 3139 (1995).
20. S. J. Berners-Price, C. Brevard, A. Pagelot and P. J. Sadler, *Inorg. Chem.*, **24**, 4278 (1985).
21. A. M. Hill, W. Levason and M. Webster, *Inorg. Chem.*, **35**, 3428 (1996).
22. F. Lianza, A. Macchioni, P. Pregosin and H. Rüegger, *Inorg. Chem.*, **33**, 4999 (1994).
23. S. S. D. Brown, I. D. Salter, V. Sik, I. J. Colquhoun, W. McFarlane, P. A. Bates, M. B. Hursthouse and M. Murray. *J. Chem. Soc., Dalton Trans.*, 2177 (1988).
24. L. J. Baker, G. A. Bowmaker, D. Camp, Effendy, P. C. Healy, H. Schmidbaur, O. Steigelmann and A. H. White, *Inorg. Chem.*, **31**, 3656 (1992).
25. P. K. Hurlburt, J. J. Rack, S. F. Dec., O. P. Anderson and S. H. Strauss, *Inorg. Chem.*, **32**, 373 (1993).
26. S. M. Socol, R. A. Jacobson and J. G. Verkade, *Inorg. Chem.*, **23**, 88 (1984).
27. Y. Yamamoto and H. Schmidbaur, *J. Organomet. Chem.*, **96**, 133 (1975).
28. S. M. Socol and J. G. Verkade, *Inorg. Chem.*, **23**, 3487 (1984).
29. A. Bayler, G. A. Bowmaker and H. Schmidbaur, *Inorg. Chem.*, **35**, 5959 (1996).
30. G. A. Adrizzoia, G. La Monica, A. Maspero, M. Moret and N. Masciocchi, *Inorg. Chem.*, **36**, 2321 (1997).
31. A. M. M. Lanfredi, F. Ugozzoli, F. Asaro, G. Pellizer, N. Marisch and A. Camus, *Inorg. Chim. Acta*, **190**, 71 (1991).
32. G. A. Bowmaker, Effendy, P. J. Harvey, P. C. Healy, B. W. Skelton and A. H. White, *J. Chem. Soc., Dalton Trans.*, 2459 (1996).
33. G. A. Bowmaker, Effendy, P. J. Harvey, P. C. Healy, B. W. Skelton and A. H. White, *J. Chem. Soc., Dalton Trans.*, 2449 (1996).
34. L. J. Baker, G. A. Bowmaker, D. Camp, Effendy, P. C. Healy, H. Schmidbaur, O. Steigelmann and A. H. White, *Inorg. Chem.*, **31**, 3656 (1992).
35. A. F. M. J. van der Ploeg, G. Van Kotyen and C. Brevard, *Inorg. Chem.*, **21**, 2878 (1982).
36. M. J. Stillman, C. F. Shaw III and K. Suzuki, *Metallothioneins: Synthesis, Structures and Properties of Metallothioneins, Phytochelatins, and Metal–Thiolate Complexes*, VCH Publishers, New York, 1992.
37. A. J. Blake, D. Collison, R. O. Gould, G. Reid and M. Schröder, *J. Chem. Soc., Dalton Trans.*, 974 (1990).
38. M. Munakata, L. P. Wu, T. Kuroda-Sowa, M. Maekawa, Y. Suenaga and K. Sugimoto, *Inorg. Chem.*, **36**, 4903 (1997).
39. A. Jezierski, *Magn. Reson. Chem.*, **27**, 130 (1989).
40. M. C. R. Symons, R. Janes and A. D. Stevens, *Chem. Phys. Lett.*, **160**, 386 (1989).
41. P. J. Blower, J. A. Clarkson, S. C. Rawle, J. R. Hartman, R. E. Wold, Jr., R. Yagbasan, S. G. Bott and S. R. Cooper, *Inorg. Chem.*, **28**, 4040 (1989).
42. J. A. McMillan and B. Samller, *J. Chem. Phys.*, **35**, 1698 (1961).
43. H. G. Hecht and J. B. Frazier, III. *J. Inorg. Nucl. Chem.*, **29**, 613 (1967).
44. P. C. Leung and F. Aubke, *Inorg. Chem.*, **17**, 1765 (1978).
45. G. C. Allen and R. F. McMeeking, *J. Chem. Soc., Dalton Trans.*, 1062 (1976).
46. G. W. Rice and R. S. Tobias, *Inorg. Chem.*, **14**, 2402 (1975).
47. C. F. Shaw III and R. S. Tobias, *Inorg. Chem.*, **12**, 965 (1973).
48. C. F. Shaw III, J. W. Lundeen and R. S. Tobias, *J. Organomet. Chem.*, **51**, 365 (1973).
49. K. C. Dash, *Ind. J. Chem.*, **24A**, 265 (1985); A. Lowenstein and T. M. Conner, *Ber. Bunsenges Phys. Chem.*, **67**, 280 (1963).
50. F. Stocco, G. C. Stocco, W. M. Scovell and R. S. Tobias, *Inorg. Chem.*, **10**, 2639 (1971).
51. J. P. Fackler, Jr. and C. Paparizos, *J. Am. Chem. Soc.*, **99**, 2363 (1977).
52. G. G. Graham, G. D. Campion and J. B. Ziegler, *Metal Based Drugs*, **1**, 395 (1994); C. F. Shaw III, S. Schraa, E. Gleichmann, Y. P. Grover, L. Dunemann and A. Jagarlamudi, *Metal Based Drugs*, **1**, 351 (1994); K. Tepperman, Y. Zhang, P. W. Roy, R. Floyd. Z. Zhao, J. G. Dorsey and R. C. Elder, *Metal Based Drugs*, **1**, 433 (1994); R. C. Elder, W. B. Jones, Z. Zhao, J. G. Dorsey and K. Tepperman, *Metal Based Drugs*, **1**, 363 (1994).
53. J. J. Pesek and R. W. Mason, *Inorg. Chem.*, **18**, 924 (1979).
54. M. Sano, Y. Yosikawa and H. Hideo, *Inorg. Chem.*, **21**, 2521 (1982).
55. G. Lewis and C. F. Shaw III, *Inorg. Chem.*, **25**, 58 (1986).

56. M. N. Akhtar, I. H. Gazi, A. A. Isab, A. R. Al-Arfaj, M. I. M. Wazeer and M. S. Hussain, *J. Coord. Chem.*, **36**, 149 (1995).
57. M. S. Hussain, A. R. Al-Arfaj, M. N. Akhtar and A. A. Isab, *Polyhedron*, **15**, 2781 (1996).
58. A. L. Hormann, C. F. Shaw III, D. W. Bennett and W. M. Reiff, *Inorg. Chem.*, **25**, 3953 (1986).
59. G. A. Bowmaker and H. Schmidbaur, *J. Chem. Soc., Dalton Trans.*, 2859 (1984).
60. A. A. Isab, *J. Inorg. Biochem.*, **46**, 145 (1992).
61. A. A. Isab, I. H. Ghazi, I. M. Wazeer and H. P. Perzanonwski, *J. Inorg. Biochem.*, **50**, 299 (1993).
62. A. A. Isab, I. H. Ghazi and A. R. Al-Arfaj, *J. Chem. Soc., Dalton Trans.*, 841 (1993).
63. G. G. Graham, J. R. Bales, M. C. Grootveld and P. J. Sadler, *J. Bioinorg. Chem.*, **25**, 163 (1985).
64. A. Canumalla, S. Schraa, A. A. Isab, C. F. Shaw III, E. Gleichmann, L. Dunemann and F. Turfeld. *J. Biol. Inorg. Chem.*, **3**, 9 (1998).
65. R. V. Parish, B. P. Howe, J. P. Wright, J. Mack, R. Pritchard, R. G. Buckley, A. Elsome and S. P. Fricker, *Inorg. Chem.*, **35**, 1659 (1996).
66. C. A. Tolman, *Chem. Rev.*, **77**, 313 (1977).
67. A. L. Hormann-Arendt and C. F. Shaw III, *Inorg. Chem.*, **29**, 4683 (1990).
68. C. F. Shaw III, *Comments Inorg. Chem.*, **8**, 233 (1989).
69. S. L. Best and P. J. Sadler, *Gold Bull.*, **29**, 87 (1996).
70. S. J. Berners-Price and P. J. Sadler, *Struct. Bonding*, **70**, 27 (1998).
71. G. A. Bowmaker, J. C. Dyasson, P. C. Healy, L. M. Englehardt, C. Pakawatchai and A. H. White, *J. Chem. Soc., Dalton Trans.*, 1089 (1987).
72. S. Al-Baker, W. E. Hill and C. A. McAuliffe, *J. Chem. Soc., Dalton Trans.*, 1297 (1986).
73. S. J. Berners-Price, M. A. Mazid and P. J. Sadler, *J. Chem. Soc., Dalton Trans.*, 969 (1984).
74. S. Al-Baker, W. E. Hill and C. A. McAuliffe, *J. Chem. Soc., Dalton Trans.*, 2655 (1985).
75. M. J. Mays and P. A. Vergano, *J. Chem. Soc., Dalton Trans.*, 1112 (1979).
76. S. J. Berners-Price, M. J. DiMartino, D. T. Hill, R. Kuroda, M. A. Mazid and P. J. Sadler, *Inorg. Chem.*, **24**, 3425 (1985).
77. B. T. Heaton and R. J. Kelsey, *Inorg. Nucl. Chem.*, **11**, 363 (1975).
78. A. A. Isab, C. F. Shaw III, J. D. Hoeschele and J. Locke, *Inorg. Chem.*, **27**, 3588 (1988).
79. M. T. Coffer, C. F. Shaw III, M. K. Eidsness, J. W. Watkins II and R. C. Elder, *Inorg. Chem.*, **25**, 333 (1986).
80. J. Xiao and C. F. Shaw III, *Inorg. Chem.*, **31**, 3706 (1992).
81. C. F. Shaw III, M. T. Coffer, J. Klingbeil and C. K. Mirabelli, *J. Am. Chem. Soc.*, **110**, 729 (1988).
82. C. F. Shaw III, A. A. Isab, J. D. Hoeschele, M. Starich, J. Locke, P. Schulteis and J. Xiao, *J. Am. Chem. Soc.*, **116**, 2254 (1994).
83. M. Starich, Senior Honors Thesis, University of Wisconsin-Milwaukee, 1990.
84. A. A. Isab, C. F. Shaw and J. Locke, *Inorg. Chem.*, **27**, 3406 (1988).
85. M. T. Razi, G. Otiko and P. J. Sadler, *ACS Symp. Ser.*, **209**, 371 (1983).
86. N. A. Malik, G. Otiko and P. J. Sadler, *J. Inorg. Biochem.*, **12**, 317 (1980).
87. D. T. Hill, G. R. Girard, O. D. Stringer, B. M. Sutton, D. E. Griswold, M. T. Razi, P. J. Sadler, A. L. Arendt and C. F. Shaw III, submitted (1998).
88. M. T. Coffer, C. F. Shaw III, A. L. Hormann, C. K. Mirabelli and S. T. Crooke, *J. Inorg. Biochem.*, **30**, 177 (1987).
89. A. A. Isab and P. J. Sadler, *J. Chem. Soc., Dalton Trans.*, 135 (1982).
90. A. J. Blake, J. A. Grieg, A. J. Holder, T. I. Hyde, A. Taylor and M. Schröder, *Angew. Chem., Int., Ed. Engl.*, **29**, 197 (1990).
91. R. I. Schlupp and A. H. Maki, *Inorg. Chem.*, **13**, 44 (1974).
92. F. G. Herring, G. Hwang, K. C. Lee, F. Mistry, P. S. Phillips, H. Willner and F. Aubke, *J. Am. Chem. Soc.*, **114**, 1271 (1992).
93. A. MacCragh and W. S. Koski, *J. Am. Chem. Soc.*, **87**, 2496 (1965).
94. A. P. Koley, S. Purohit, S. Ghosh, L. S. Prasad and P. T. Manoharan, *J. Chem. Soc., Dalton Trans.*, 2607 (1988).
95. A. P. Koley, S. Purohit, L. S. Prasad, S. Ghosh and P. T. Manoharan, *Inorg. Chem.*, **31**, 305 (1992).
96. G. Rindorf, N. Thorup, T. Bjørnholm and K. Bechgaard, *Acta Crystallogr.*, **C46**, 1437 (1990).
97. N. C. Schiødt, T. Bjørnholm, K. Bechgaard, J. J. Neumeier, C. Allgeier, C. J. Jacobson and N. Thorup, *Phys. Rev. B*, **53**, 1773 (1996).

CHAPTER **5**

The photoelectron spectroscopy of organic derivatives of gold and silver

IGOR NOVAK

Department of Chemistry, National University of Singapore, Singapore 119260, Singapore
Fax: 65-779-1691; e-mail: chmigorn@nus.edu.sg

I. INTRODUCTION

The electronic structure, i.e. the distribution of electron density throughout the material (atom, molecule, solid), is of fundamental importance, because it strongly influences its chemical reactivity and physical properties. The photoelectron spectroscopy (PES) is the

most widely used experimental method for studying the electronic structure of materials. PES is in fact not a single method, but a family of rather diverse methods.

The experimental techniques and theoretical interpretations of PES data have been discussed in detail in numerous articles and books. Some detailed reviews were published recently in this series[1]. Other reviews are too numerous to list so we shall mention only some of the more recent ones[2-4]. Our aim is not to give a detailed coverage of PES, but rather to provide a summary of PES methods which were used in studies of the electronic structure of gold and silver compounds. What all PES methods have in common is the basic phenomenon of photoionization, in which a photon of known energy $h\nu$ becomes absorbed by the material and induces subsequent ejection of an electron (photoionization). The law of conservation of energy applied to the process can be expressed by equations 1 and 2,

$$h\nu = E_k + E_b + \Phi \qquad \text{solid state} \qquad (1)$$

$$h\nu = E_k + IE \qquad \text{gas phase} \qquad (2)$$

where E_b is the binding energy, IE the ionization energy, E_k the measured kinetic energy of the outgoing photoelectron and Φ the work function of the material; E_b represents the energy required to remove the electron from the intramolecular (intraatomic) attractive potential, while Φ represents the energy required to eject the electron from the external, interatomic or intermolecular potential created by material units surrounding the atom or molecule being ionized and is measured with respect to the Fermi edge of the sample material.

Expressions similar to equation 1 can be written for the conservation of linear and angular momenta, but they are not commonly used because of experimental difficulties associated with measuring such momenta for photoelectrons[5].

The photoionization can be achieved by utilizing photons in the vacuum UV or X-ray energy ranges. In the former case the method is called UPS and, in the latter, XPS or ESCA. The UPS method often uses a He discharge source with two principal photon energies: HeI (21.22 eV) and HeII (40.8 eV). Both methods can in principle be applied to samples in different aggregation states (gas, liquid, solid). However, very few UPS or XPS studies of liquid samples have been reported. Table 1 below compares the two methods in terms of sample handling and the type of information which they can provide.

The ejected photoelectron is the primary *information carrier* and measurement of its properties (mostly E_k) represents the physical basis of PES. In spite of the conceptual simplicity of photoionization experimentation, it is not straightforward to obtain useful information from E_k values.

The photoionization process can be represented as a transition between the initial and final states characterized by their energies (E_i and E_f, respectively) and wavefunctions (equation 3):

$$\{\Psi_i E_i\} \Rightarrow \{\Psi_f E_f\} \qquad (3)$$

The measured E_k value is directly proportional to the difference $E_b(IE) = E_f - E_i$. The final state in PES consists of an ion *and* the outgoing photoelectron. The electronic structure of material is often described by approximate, one-electron wavefunctions (MO theory). MO approximation neglects electron correlation in *both* the initial and final states, but fortunately this often leads to a cancellation of errors when E_b is calculated. A related problem arises when one tries to use the *same* wavefunctions to describe Ψ_i and Ψ_f. This frozen orbital approximation is embedded in the Koopmans approximation (or the Koopmans theorem as it is most inappropriately called), equation 4,

$$IE_i = -\epsilon_i^{SCF} \qquad (4)$$

where IE_i is the i-th ionization energy and ϵ_i^{SCF} is the orbital energy obtained from MO-type calculations. In UPS, the Koopmans approximation is approximately valid because, when an outer, valence electron is ejected, the remaining electrons are not significantly affected by its loss. In XPS an inner, core electron is removed, the nuclear shielding by the 'electron cloud' is significantly changed and the remaining electrons quickly rearrange themselves according to the new Coulomb potential (relaxation effect). This implies that in XPS the Koopmans approximation is totally inadequate, and so is the simple picture of ionization in which a single electron is removed from a particular 'frozen MO'. The practical consequence is that in XPS one can observe more bands than there are orbitals, or that some bands are shifted in energy. The broad, additional (satellite) bands may also appear in UPS but are usually confined to the IE >25 eV region. Another important point stemming from strong relaxation effects in XPS is that the lifetime of the hole state (a hole generated by the ejected electron) is shorter than in UPS. The Heisenberg uncertainty principle, $\Delta E \Delta t \geqslant h/4\pi$, indicates that states with short lifetimes (small Δt) will have large bandwidths (ΔE). This is the fundamental reason why a natural linewidth (and hence spectral resolution) is inferior in XPS when compared to UPS. There has been some progress recently in improving the resolution of XPS (at least in the soft X-ray region). Vibrationally resolved C1s ionizations in methane and ethane have been observed[6] (measured at photon energies of 316 eV in the gas phase), but this does not imply that the resolution of XPS can routinely match that of UPS. The resolution when measured as the FWHM of the calibrant peak can reach 10–15 meV in UPS(g), while in XPS(s) it is around 350 meV at best[6].

In XPS the primary information is not E_b itself, but rather the *chemical shift*. It represents changes in binding energy for a particular atomic core level as a result of changes in the chemical environment of the atom.

Figure 1 illustrates chemical shifts. It shows that C1s ionizations from the same molecule appear at slightly different energies, depending on the electron affinity of neighboring atoms (e.g. a carbon atom bonded to a high electron affinity chlorine atom has the highest binding energy among three carbons in EtOCOCl). XPS or ESCA is thus very useful in determining charge distributions and oxidation states for particular atoms in the material. Although the chemical shift is easy to measure in principle, two considerations must be taken into account when its numerical values are considered:

(a) the binding energies must not be influenced by any other effects if the chemical shift is to be meaningful,

(b) the reference E_b for an atom of a particular element must be well specified when chemical shifts in different molecules are compared.

Unfortunately, chemical shift measurements are prone to additional effects (shifts): relaxation shifts, surface-core level shifts and shifts due to surface charging. The relaxation effects are sometimes not easy to distinguish from chemical shifts. Furthermore, the removal of electrons from the initially neutral nonconducting solid sample causes it to acquire nonuniform positive charge along the surface. This charge (potential) introduces a 'drag' on the outgoing photoelectrons. As a result the spectral peaks may be shifted to higher E_b with concomitant band broadening and distortion. Flooding the sample surface with low energy electrons (from an electron gun) and ensuring good electrical contact between the sample and the spectrometer chamber (earth potential) may alleviate charging shifts. Surface-core level shifts can usually be identified more easily and originate from the different environment (extramolecular potential) experienced by centers located on the sample surface and inside the bulk of material. Although all these effects may seem to make chemical shift measurements too difficult, they can (if carefully analyzed) provide additional information in XPS studies. This additional information enriches the data analysis similarly to the way the vibrational fine structure extends the information provided by UPS(g).
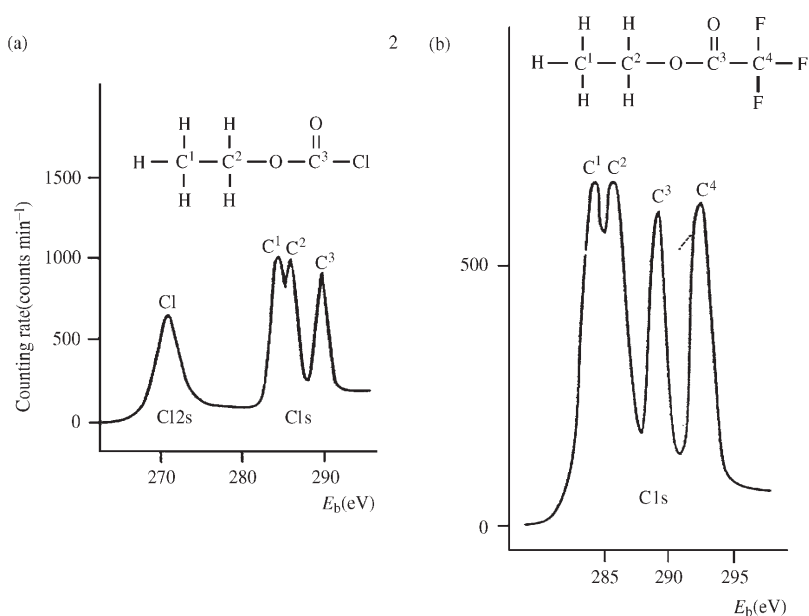
FIGURE 1. ESCA spectra of some esters showing C1s chemical shifts. Reproduced by permission of the Royal Society of Chemistry from Reference 3b

The magnitudes of chemical shifts are often interpreted semiempirically in the first instance; a chemical shift observed for a particular element is approximated by the sum of group shifts for functional groups bonded to that element. The group shifts can be obtained by regression analysis of XPS data for a series of related compounds.

Knowledge of the work function and Fermi (reference) level of the spectrometer is important if one wishes to obtain meaningful absolute E_b values. The ESCA spectrometer should be periodically checked by measuring the energy of photoelectrons emitted from a sample with a well-established E_b (e.g. the Au4f$_{7/2}$ level at 83.96 eV).

Core level photoionization cross-sections in molecules are similar to the cross-section for single atoms, which indicates that relative XPS line intensities can be used directly for elemental analysis of the sample. A comparison of UPS and XPS methods is presented in Table 1.

As the subsequent sections show, most gold and silver derivatives were studied by the XPS(s) rather than the UPS(g) method. There are two principal reasons for the XPS bias:

(a) UPS(g) requires vaporization of the sample at elevated temperatures, where many such compounds will undergo thermal decomposition. This favors XPS as the method of choice for involatile samples, even though some care still needs to be taken to prevent sample damage caused by the high energy X-ray source.

(b) The organic ligands present in silver or gold complexes are often large and possess numerous valence energy levels in the energy region of 7–12 eV. As a result, the ligand orbitals mix (interact) strongly with ns and nd orbitals on Ag or Au. Furthermore, the large number of ligand levels gives rise to many overlapping spectral bands, which significantly complicates the assignment of UPS spectra (see e.g. Figure 2).

TABLE 1.   Comparison of UPS and XPS methods[a]

UPS(g)	XPS(s)
High energy resolution	Low energy resolution
No sample charging problems	Sample charging of nonconducting samples
'Koopmans compatible'	'Koopmans noncompatible'
Sample destructive	Sample nondestructive
Requires sample vaporization (heating)	No sample vaporization (heating)
Valence electron ionization	Core electron ionization
Not sensitive to surface contamination	Sensitive to surface contamination
$\Phi = 0$	$\Phi \neq 0$
Not useful as an analytical method	Useful as an analytical method
Information: ionization energies	Information: chemical shifts

[a]If UPS is used for solid samples, then sample charging and surface contamination problems also occur.
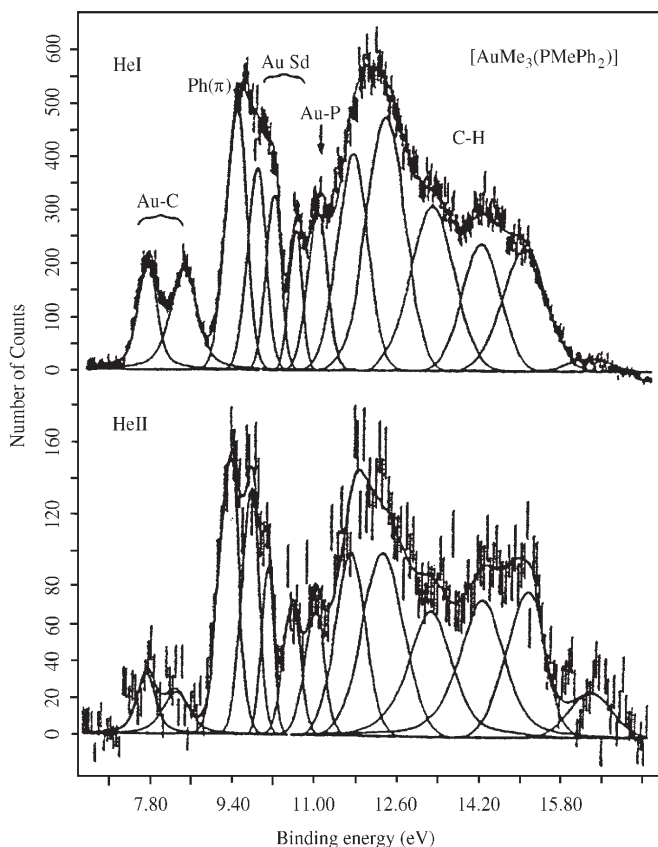
FIGURE 2. HeI/HeII UPS of $AuMe_3(PPh_2Me)$ showing the band manifold for ionizations from metal and ligand orbitals. Reprinted with permission from Reference 8b. Copyright 1983 American Chemical Society

Figure 2 shows an example of a UPS spectrum where the overlap between bands associated with ligand (Me, PPh$_3$) and metal (Au5d) moieties is pronounced. On the other hand, metal core level ionizations in XPS spectra produce few distinct and easily recognizable peaks.

The selection of compounds reviewed in this chapter deviates from the 'Patai rule', which states[7] that only compounds containing C−Au and C−Ag bonds should be discussed. The aim is to describe how the electronic structure of silver and gold is affected by the presence of organic ligands, irrespective of whether or not the formal donor atom is carbon.

II. PES OF GOLD COMPOUNDS

A. UPS Studies

The study of bonding in gold complexes has wide significance. Gold(III) complexes, like AuMe$_3$L (L = phosphine ligand), act as catalysts for coupling between alkyllithium reagents and alkyl halides. The thermal stability of these complexes depends on the strength of the Au−L bond, which can in turn be related to the electron distribution along the Au−L bond. The alkyl−gold bond in Au(I) complexes may undergo electrophilic addition which leads to the formation of Au(III) complexes. An important question concerning the reaction mechanism is whether the electrophile attacks the metal center or the alkyl−gold bond first. Since electrophiles usually attack (interact with) HOMO orbitals, a knowledge of energies and types of HOMOs in Au(I) complexes is of interest. Bancroft and coworkers[8] have reported a UPS(g) study, with variable photon energy, of gold(I) and gold(III) complexes: AuMe(PMe$_3$), AuMe$_3$(PMe$_3$), AuMe$_3$(PPhMe$_2$) and AuMe$_3$(PMePh$_2$). The analysis of spectra is complicated and was based on the results of Xα calculations, relative HeI/HeII band intensities, bandwidths and comparison with spectra of related molecules like HgMe$_2$. We shall describe the analysis of the HeI/HeII spectra of AuMe(PMe$_3$) in some detail in order to convey the arguments used and conclusions reached concerning Au−ligand bonding. The spectra are shown in Figure 3.

The bands A and B appear at the lowest ionization (binding) energies and exhibit a decrease in relative intensity on going from HeI to HeII radiation. On the other hand, the high energy bands C−E show an increase in relative intensity under the same conditions. Bancroft and coworkers[8] concluded, on the basis of this observation as well as the Xα calculations and comparison with UPS of Me$_2$Hg, that bands C−E correspond to Au5d ionizations. This conclusion is supported by the consideration of atomic photoionization cross-sections[9] given in Table 2. The atomic energy levels in Table 2 were deduced from the first ionization energies and emission spectra of the corresponding atoms[10].

Table 2 clearly shows that the pronounced increase in intensity observed for bands C−E vs bands A−B is related to changes in photoionization cross-sections. Bands F−I were assigned to ligand-based orbital ionizations on the basis of comparison with the UPS spectrum of PMe$_3$. Bancroft and coworkers[8a] have attributed bands A and B to ionization from orbitals with Au−C and Au−P characters, respectively, on the basis of Xα calculations and comparison with the spectrum of HgMe$_2$. More recent calculations[11] using the relativistic LCGTO-LDF method have provided more details about orbital compositions in AuMePMe$_3$ (Table 3). They have also indicated that the role of Au6p orbitals in bonding is minimal.

Data presented in Tables 2 and 3 can be used for a qualitative explanation of two other details observed in the spectra (Figure 3):

(a) Bands A and B have similar relative intensities in HeI and HeII spectra.
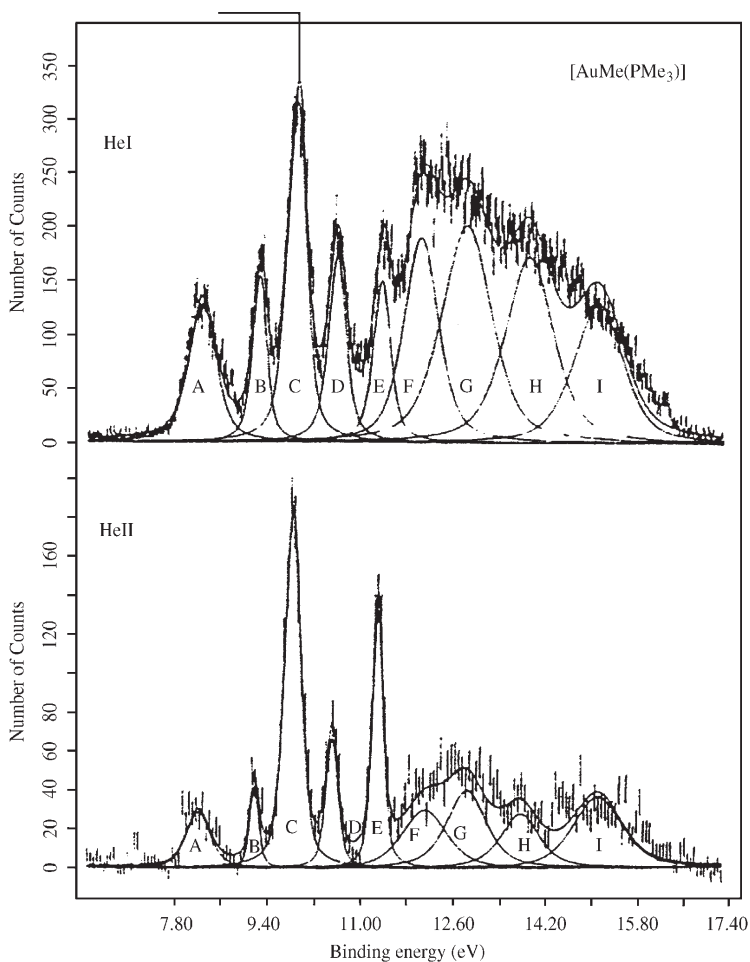
FIGURE 3. HeI/HeII UPS of AuMe(PMe$_3$). Reprinted with permission from Reference 8a. Copyright 1982 American Chemical Society

TABLE 2. Atomic energy levels (ϵ/eV) and photoioniza-
tion cross-section (σ/Mb)

Atom/orbital	ϵ	σ (HeI)	σ (HeII)
Au6s	9.22	0.01881	0.02865
Au5d	11.85	25.95	38.67
P3p	10.48	1.232	0.5061
C2p	11.26	6.121	1.881

TABLE 3.   Characters of some MOs in AuMe(PMe$_3$)

Band	Principal MO characters
A	42% Me + 37% Au6s
B	18% Au6s + 29% Au5d + 40% PMe$_3$
C	99% Au5d
D	20% Me + 72% Au5d
E	35% Au5d + 44% PMe$_3$

(b) The intensity of band D decreases relative to C and E intensities on going from HeI to HeII radiation.

Bands A and B show similar HeI/HeII intensity variations, because their corresponding MOs have contributions from atomic orbitals whose photoionization cross-sections increase at higher photon energies (Au5s, Au6s) as well as those whose cross-sections decrease (Me, PMe$_3$). The relative decrease in the intensity of band D can be attributed to the fact that the corresponding MO contains more Me and less PMe$_3$ character than either band C or E orbitals. The C2p (and hence Me) cross-section shows the most pronounced decrease on going from HeI to HeII radiation.

These qualitative explanations are based on the Gelius model[12] according to which the MO photoionization cross-section (and the corresponding band intensity) $\sigma_i{}^{MO}$ can be expressed by equation 5,

$$\sigma_i{}^{MO} = \Sigma_i P_{ij}\sigma_i{}^{AO} \qquad (5)$$

where P_{ij} is the electron population of the i-th AO and $\sigma_i{}^{AO}$ are the atomic orbital cross-sections. The different bandwidths of A and B can be related to geometry changes upon ionization (the Franck–Condon principle) and corresponding differences in bonding characters; the broad band A is associated with the orbital which has more bonding character than the orbital related to the narrow band B. Why? The band A orbital has (among other contributions) significant Au6s character while the band B orbital has Au5d. Gold is the most 'relativistic' of all the common elements and one must take into consideration the effects of relativity on the electronic structure of its derivatives. The principal effect would be an expansion of 4f and 5d orbitals and subsequent contraction of the 6s orbital[13]. The 6s contraction is not a direct relativistic effect, but rather a shell-structure effect caused by relativistically induced 4f and 5d expansions. The expansions reduce the nuclear shielding of the 6s electron, leading to the final 6s contraction. What has all this to do with A and B bandwidths? We suggest that a more compact Au6s orbital overlaps better (forms a stronger bond) with C2p than does an expanded Au5d with P3p orbital.

Degeneracy of Au5d orbitals is lifted by both ligand field and spin–orbit coupling (SOC) effects in the 5d^9 final ionic state. The SOC effect in atomic gold is large (1.52 eV) and must certainly be taken into consideration. The final order of the 5d ionic states was rationalized in terms of both effects and the assignment was given using double group notation[8a]. However, such notation does not carry much useful information for inorganic chemists. They often use pseudo-axial terminology where orbitals are labeled according to their local symmetry with respect to the metal–ligand bond:

$$\{5d_{x^2-y^2} \quad 5d_{xy}\} \Rightarrow 5d_\delta$$
$$\{5d_{xz} \quad 5d_{yz}\} \Rightarrow 5d_\pi$$
$$\{5d_{z^2}\} \Rightarrow 5d_\sigma$$

The $5d_\sigma$ orbitals will be stabilized (with respect to $5d_\pi$ and $5d_\delta$) by interactions with ligands. In linear Au(I) complexes $5d_\sigma$ corresponds to the $5d_{z^2}$ orbital while in square-planar Au(III) it corresponds to $5d_{x^2-y^2}$. Using the value of 1.52 eV for SOC in atomic gold and vertical ionization energies of bands C−E, Bancroft and coworkers[8a] estimated $5d_\sigma$, $5d_\pi$ and $5d_\delta$ orbital energies. The $5d_\sigma$ orbital was found to be stabilized by 0.71 eV due to ligand bonding and 5d/6s hybridization. This stabilization (which reflects participation of Au5d in bonding) is slightly larger than in HgMe$_2$, where it amounts to 0.45 eV. On the other hand, both $5d_\pi$ and $5d_\delta$ energies were found to be approximately equal to 10.73 eV.

The correlation within the series of complexes has allowed Bancroft and coworkers to conclude[8b] that the σ-donor strength of ligands increases along the sequence: PMe$_3$< PMe$_2$Ph<PMePh$_2$ (Figure 4). Good σ-donors will increase the electron density on a gold atom and reduce the binding energies of Au5d and Au−C orbitals. Simultaneously, the binding energies of the phosphorus lone pair can be expected to increase. The Au−P orbital stabilization energy can be defined as the difference between the Au−P orbital energy in the complex and the P lone-pair energy in the phosphine ligand. The UPS data indicate that the Au−P stabilization energy in an Au(I) complex (0.66 eV) is much smaller than in Au(III) complexes, where it is 2.35−2.64 eV. The increased stabilization is in keeping with the known tendency of gold(I) complexes to undergo oxidative addition, which produces square-planar Au(III) complexes.

One may conclude that Au5d orbitals should not be regarded as core, but rather as valence orbitals which contribute significantly to bonding in gold−phosphine complexes.

The stabilizing effect of phosphine ligands is due in large measure to their ability to 'induce' Au5d orbital participation in bonding.
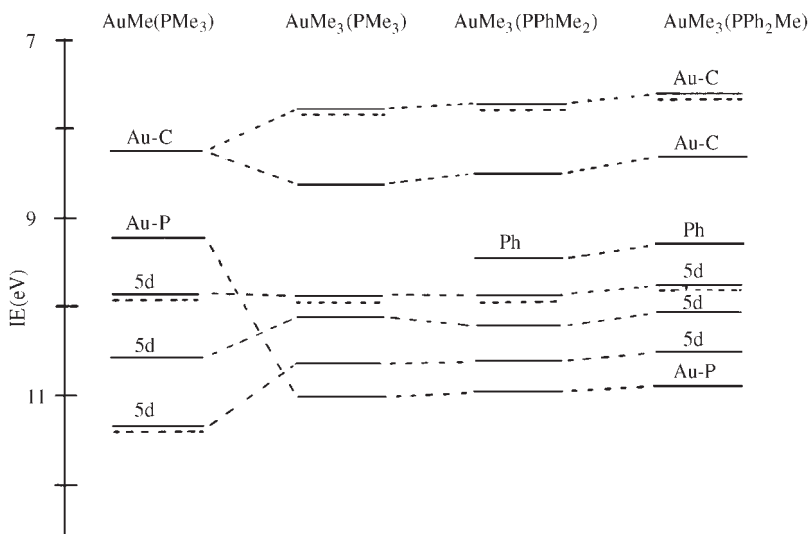
FIGURE 4. Energy level correlation diagram and MO characters for Au(I) and Au(III) complexes deduced from HeI/HeII photoelectron spectra[8a]. The levels indicated by dotted lines correspond to unresolved ionic states. Ph designates the manifold of π-orbitals from phenyl groups

B. XPS Studies

We shall classify the studies of mono- and polynuclear gold complexes according to the types of atoms coordinated to gold. The numbers incorporated into structural formulae show binding energies of core levels: C1s, N1s, P2p, S2p, Au4f$_{7/2}$, O1s, Cl2p$_{3/2}$ for the respective atoms.

1. Complexes with Au−C coordination

Several reports of organo-gold compounds have been published. In these studies, the main concern was to establish the oxidation state of gold atoms and to deduce whether the XPS data are consistent with the proposed molecular structure. Some of the compounds studied are shown below.
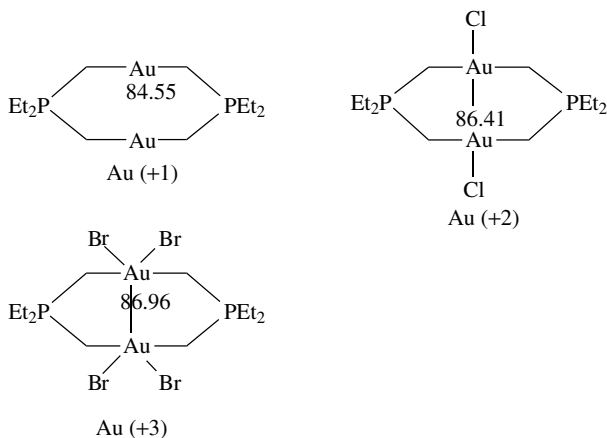
The XPS results[14] clearly demonstrate how the oxidation state of gold increases with increasing Au4f$_{7/2}$ binding energy. On the other hand, there is no correlation between the Au oxidation state of gold and C1s, P2p or Br3p energies. The reason behind the correlation between the Au oxidation state and Au4f$_{7/2}$ binding energy is that the higher E_b corresponds to more positive charge on gold atom, which is reflected in the higher oxidation number. The magnitude of E_b is determined by the electron distribution around the gold atom and is usually summarized by attributing an effective (partial) charge to the atom. The partial charge of an atom, I, depends on the number, type and electronegativity of atoms bonded to it. On the other hand, the formal oxidation state (number) is a fictitious number determined by the set of arbitrary rules[15].

The concept of an oxidation state in inorganic chemistry is as ubiquitous and useful for rationalizing a large number of observations as is the concept of aromaticity in organic chemistry. However, neither concept is a physical observable *per se* nor can it be rigorously defined. In order to reduce arbitrariness, attempts were made to link both concepts to experimental parameters. Aromaticity can be related to the exalted diamagnetic susceptibility[16], while oxidation states may be correlated with ESCA shifts or binding energies[3b].

The nature of oxidation numbers makes it impossible to assign a specific binding energy to a particular oxidation state. Instead, one must study a series of related compounds

in which the oxidation number of a particular atom varies, and then deduce oxidation numbers from the correlation with measured E_b. This approach has been very fruitful in the analysis of gold complexes. It not only helped to establish common oxidation states of gold, e.g. Au(I), Au(II) and Au(III), but it also lead to the identification of the rare oxidation state Au(-1), which is present in CsAu and RbAu compounds[14c]. This finding may seem surprising, but one should remember that gold is not only 'the most relativistic stable element'[13] but also 'the most electronegative' among metals. Its electronegativity (2.50) is comparable to that of iodine (2.57) or phosphorus (2.46)[17], both of which appear in negative oxidation states.

Fackler and coworkers[18] have identified the mixed-valence Au(I)/Au(III) complex [Au(CH$_2$)$_2$PPh$_2$]$_2$Br$_2$ with the aid of XPS and X-ray diffraction analysis. The identification is the result of comparing Au4f$_{7/2}$ binding energies in [Au(CH$_2$)$_2$PPh$_2$]$_2$Br$_2$ with those in the Au(I) complex [Au(CH$_2$)$_2$PPh$_2$]$_2$ and in the Au(III) complex [Au(CH$_2$)$_2$PPh$_2$]$_2$Br$_4$.

Au(I)/Au(I) complex

mixed valence Au(I)/Au(III)

Au (III)/Au(III) complex
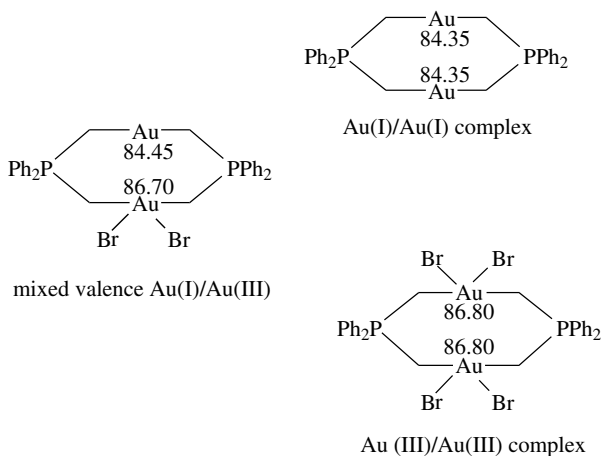
The Au(I)/Au(I) complex exhibits, as expected, only a single Au4f$_{7/2}$ peak in the XPS spectrum. The Au(III)/Au(III) complex shows two peaks of unequal intensity which were resolved with the aid of a deconvolution procedure. The high intensity peak at 86.80 eV accounts for the presence of gold in the ($+3$) oxidation state. The presence of a low intensity peak at 85.25 eV was explained by the assumption that a strong X-ray beam from the source induces a reduction in gold from the $+3$ to the $+2$ state. The mixed valence complex showed three Au4f$_{7/2}$ peaks at 86.70 eV [strong, Au(III)], 85.85 eV [medium, Au(II)] and 84.45 eV [weak, Au(I)]. Once again, the presence of a peak at 85.85 eV could be explained by the reduction of Au(III) by the X-ray beam. However, the fact that the Au(I) peak had a very low intensity compared to Au(III) was not explained. One would expect, on stoichiometrical grounds, that Au(III) and Au(I) peaks should have equal intensities. If some Au(III) is subsequently reduced to Au(II) by the source X-ray beam, the intensity of Au(I) should in fact be higher than Au(III). The X-ray diffraction study confirmed that gold atoms have two different coordination environments, thus supporting XPS data.

Yamamoto and Konno[19] used the XPS method to determine bonding in ylide–metal complexes. Initially, they established that triphenylmethylenephosphorane ligand assumes

the $R_3P^+-CH_2^-$ (ylide) rather than the $R_3P=CH_2$ (ylene) form. This conclusion follows from a comparison of XPS data for triphenylmethylenephosphorane **3** with related compounds **1** and **2**.

285.0 131.3   285.0 132.6
$(C_6H_5)_3P$ $[(C_6H_5)_3PCH_3]Br$

(1)   **(2)**

285.0 132.6 283.9
$(C_6H_5)_3P=CH_2$

(3)
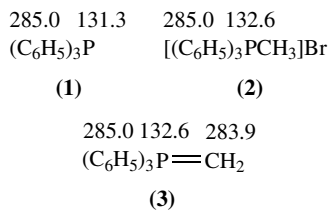
A comparison of P2p binding energies indicates that the phosphorus atom contains a positive charge in **3**. On the other hand, the values of C1s energies indicate the presence of negative partial charge (excess electron density) on the CH_2 group in triphenylmethylenephosphorane. Consequently, these data are consistent with the ylide structure $(C_6H_5)_3P^+-CH_2^-$ for triphenylmethylenephosphorane. Next, Konno and Yamamoto[19a] considered the structure of the complex **4** between gold and triphenylmethylenephosphorane and compared XPS data for the complex **4** with similar complexes, i.e. **5** and **6**.

132.4
$(C_6H_5)_3P-CH_2$
                          84.9   197.5
                          Au—Cl
385.0   283.8
$(C_6H_5)_3P-CH_2$

(4)

285.0 132.9
$(C_6H_5)_3PCH_2$
                    85.0 197.7
                    Au—Cl
285.0 131.6
$(C_6H_5)_3P$

(5)

285.0 131.8   85.2   197.8
$[(C_6H_5)_3P]_2Au-Cl$

(6)
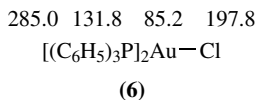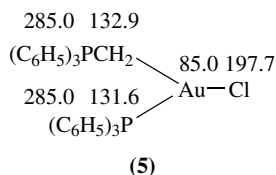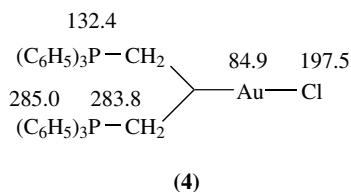
The data strongly suggest that Au is in oxidation state $+1$ and that the bis-triphenylmethylenephosphorane–gold has the structure given by **4**. However, the distinction between C1s peaks for normal carbon (285.0 eV) and for carbanion carbon (283.8 eV) was difficult due to a 18 : 1 intensity ratio between the two. Therefore, Yamamoto and Konno measured XPS spectra of another ylide–gold complex, namely bis(dimethylsulfoxonium methylide)gold[19b], where the intensity ratio between normal

$$[(CH_3)_2-S(O)-CH_2-Au-CH_2-(O)S-(CH_3)_2]Cl$$

(7a)

$$(CH_3)_2-S(O)-CH_2$$
$$(CH_3)_2-S(O)-CH_2$$ Au—Cl
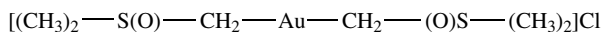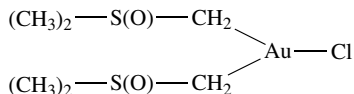
(7b)

carbon and carbanion was expected to be 2 : 1. This complex can have two possible structures, **7a** or **7b**, both of which contain ligands in the ylide form.

The XPS spectrum of complex **8** showed (upon deconvolution) two C1s peaks at 285.1 and 284.0 eV which can be readily assigned to methyl and methylene carbons. This observation vindicated the proposed ylide structure for **4**. The distinction between structures **7a** and **7b** was made on the basis of combined XPS and X-ray data. X-ray diffraction has shown that in complex **6** an Au−Cl bond exists. Cl2p$_{3/2}$ energies in **4**, **8** and **7b** are similar, suggesting that structure **7b** is the correct one. Finally, a comparison of O1s and S2p energies in **8** and **9** shows that the sulfur and oxygen atoms have higher electron density in complex **8**, possibly due to electron delocalization (transfer) from the electron-rich neighboring methylene group. The complex **8** contains gold in the Au(I) state.

285.1   167.7   284.8 84.4   197.7
$$[(CH_3)_2-S(O)-CH_2]_2Au-Cl$$
531.5   **(8)**

285.4   168.4   67.5
$$(CH_3)_2-S(O)-Br$$
532.3
(9)
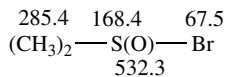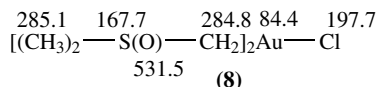
2. Complexes with Au−N coordination

Very few XPS studies of this coordination have been reported[20]. The coordinating ligands were pyrazole derivatives. Belonosov and coworkers[20a] measured XPS for complexes of AuCl$_3$ and AuCl$_4$ with free and protonated 3(5)-methylpyrazole and 3,5-dimethylpyrazole. The Au4f$_{7/2}$ energies were 88.1 and 88.2 eV, respectively, which confirms that these are Au(III) complexes. N1s bands are shifted by 1.6 eV toward lower binding energies (when compared with a free ligand), which suggests that an electron density transfer from ligand to metal takes place. Raptis and Fackler[20b] studied the formation of mixed valence Au(I)/Au(III) pyrazolato complex **12**, which is formed by oxidation of **10** in aqua regia. They also obtained complex **11** by trimerization reaction from the AuCl$_3$–pyrazoline complex.

Complexes **10** and **11** were subjected to XPS analysis. The existence of Au(I)/Au(III) states in complex **11** was inferred from the broadening of the Au4f$_{7/2}$ band (compared with **10**), which was attributed to the appearance of a shoulder at the higher energy side of the main peak. The charging effects (common in XPS) prevented the authors from measuring absolute values of E_b. The reaction of **10** with aqua regia is unusual because the product of the reaction, **12**, contains gold in the Au(I)/Au(III) states. This implies
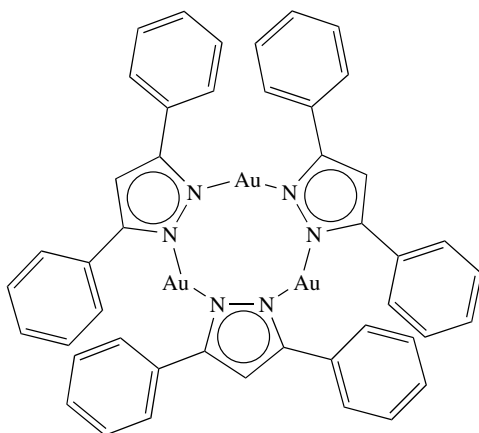
(10)
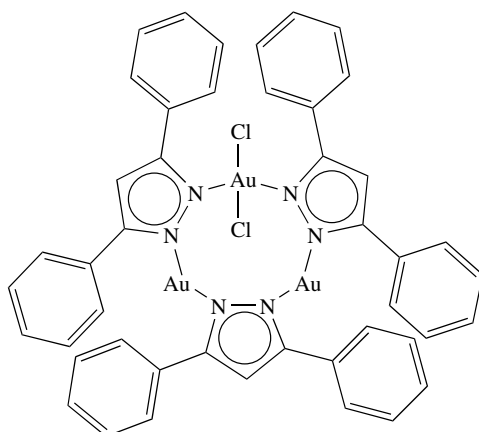
(11)

that the oxidation of the complex does not proceed fully to the Au(III)/Au(III) state. The electron delocalization in the 9-membered planar metallocyclic ring may be responsible for preventing complete oxidation. The delocalization may also be invoked to explain why (upon oxidation) a shoulder develops on the Au4f$_{7/2}$ band instead of a fully resolved additional band. However, the shoulder formation was also observed in XPS of a similar mixed valence complex $[Au(CH_2)_2PPh_2]_2Br_2$ where no such delocalization is apparent.

3. Complexes with Au–S coordination

The number of XPS studies of complexes with this coordination is small. A possible reason lies in the instability of some complexes when illuminated by the high energy
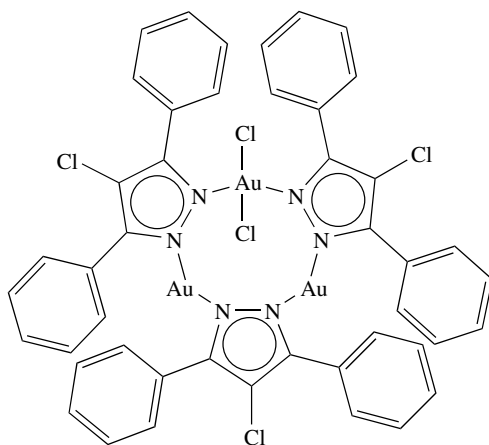
(12)

X-ray beam. Van Attekum and Trooster[21] used gold(III) dithiocarbamates as a test case on which to evaluate factors which may influence decomposition during XPS measurements. They observed that the nature of the substrate supporting the sample during measurement and the temperature are as important as the intensity of the X-ray radiation. The use of graphite-supporting substrate together with measurements conducted at low sample temperature considerably reduce the rate of decomposition.

   X-ray induced decomposition entails conversion (reduction) of gold from the Au(III) to the Au(I) state, which can be readily monitored by XPS. The magnitude of binding energy change for Au4f electrons during decomposition depends on the ligand group's electronegativity. This conclusion agrees with the reported sensitivity of Au4f energies to the electronegativity of the ligand as a whole and not just that of the coordinating atoms[22].
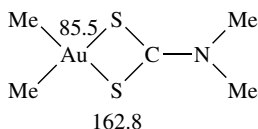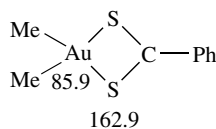
(13)   **(14)**

   The data for **13** and **14** show that the $Au4f_{7/2}$ energy decreases by 0.4 eV when the ligand is changed from a weaker electron donor to a stronger electron donor. The S $\Rightarrow$ Au π-interaction between S3p and Au5d orbitals is greater in dithiocarbamate complexes than in dithiocarboxylates or xanthates. The sulfur atom appears to be a better 'relay' of electron density than carbon, nitrogen or phosphorus. Matsubayashi and Yokozawa[23] have studied several Au(III) complexes **(15)** containing planar $[Au(C_3S_5)_2]^{n-}$ and $[Au(C_3Se_5)_2]^{n-}$ anions.

$$\left[\begin{array}{c} S \end{array} \right]^{n-}$$
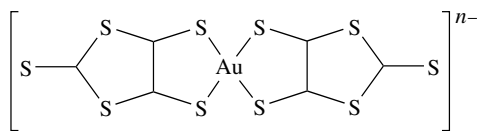
(15)

When such complexes are partially oxidized, they often become good electrical conductors and some of them even exhibit superconductivity. The study of their molecular and electronic structure utilized various techniques: cyclic voltammetry, X-ray diffraction, XPS, ESR and electrical conductivity measurements. The XPS data have shown that, in spite of the variations in the anionic charges, the Au4f energies remain almost constant. This leads to the conclusion that during the oxidation, it is ligand and not gold atoms which are being oxidized. There were no reported measurements of S2p or Se3p binding energies, although they would have shed more light on the processes taking place during partial oxidation.

Thiols are another class of complexes with Au−S coordination, which was studied by XPS[24]. Complexes with octanethiol, cysteine, glutathione and penicillamine show rather interesting properties. The complexes containing the last three ligands exhibit broadening of Au4f bands, which was attributed not to decomposition but rather to the effects associated with the presence of polymeric species. McNeillie and coworkers[24] compared various complexes of gold with tetraethylammonium, phosphine and thiol ligands. The comparison of binding energies for P2p, S2p, C12p and Br3p coordinating atoms in Au(I) and Au(III) complexes revealed an interesting fact. All ligand atom energies, except S2p, showed an increase when going toward higher oxidation states of gold. This can be expected, because when gold atom is in a higher oxidation state it has higher charge, which stimulates transfer of electron density from the ligand atoms to gold. The behavior of S2p energies can be tentatively rationalized by assuming that bonding in an Au(III)−S complex is more ionic than in Au(I)−S complexes.

4. Complexes with mixed coordination

Manoharan and coworkers[25] have studied several complexes of gold(II) with *N*-(2-pyridylmethyl)-2-mercaptoaniline (pma) **(16)**. The pma ligand is a reduced form of Schiff base and generates rare paramagnetic Au(II) complexes. Manoharan and coworkers[25] succeeded in isolating mono- and binuclear gold complexes, but not in the form of single crystals which are suitable for X-ray diffraction analysis. Their studies were therefore performed on powders or in solution using a combination of techniques: IR, UV, cyclic voltammetry, XPS, ESR. The ESCA results for the two complexes **17** and **18** are shown below.

(16)

198.5
163.78 Cl
S
Au   400.26
86.38 N
NH—CH₂
398.27

(17)

198.10
KAuCl₄
87.59

(19)

Cl
Cl   Cl   198.21
Au
163.98 88.94
S   Cl   199.35
86.14
Au
400.34
N
NH—CH₂
398.5

(18)
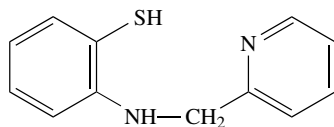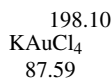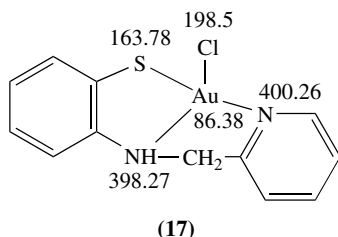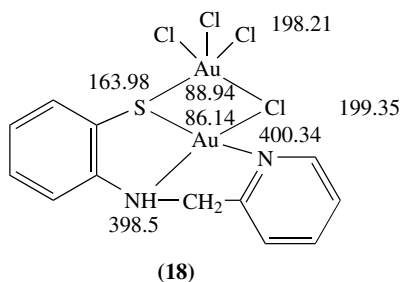
Spectral bands were resolved by deconvolution. The band shapes suggest that in the Au$_2$(pma)Cl$_4$ complex **(18)** the gold is present in oxidation states Au(II) and Au(III). The Au(II) center has $4f_{7/2}$ binding energy which is typical for Au(I) complexes, but the Au(III) value of 88.94 eV is higher than in KAuCl$_4$ **(19)**. The XPS results for **18** thus indicate that electron densities on the Au(III) atom and on the bridging Cl atom are lower than in **19**. N1s energies (and electron densities) are different for pyridine and mercaptoaniline nitrogens, the pyridine nitrogen being more electron-donating.

C. Cluster Compounds

The importance of metal clusters stems from our efforts to understand the 'clusters-to-bulk' problem, i.e. the correlation between properties of molecular and solid states of matter (mononuclear complex ⇒ polynuclear complex (cluster) ⇒ bulk metal). A considerable research effort (theoretical and PES)[26] has been expended on trying to obtain the following information about gold clusters:

(a) structural information (in cases when X-ray diffraction data are not available due to difficulties in obtaining crystals suitable for measurements),

(b) bonding information (the role of stabilizing organic ligands and metal–metal inter-actions),

(c) information about the oxidation state of gold atoms in different parts of the cluster (surface, bulk) and the influence of cluster size on the above.

Au$_{55}$ is one of the most frequently studied larger clusters and it can be used as a model for small gold particles. The cluster had been a subject of extensive investigation by a variety of techniques (Mössbauer, EXAFS, UV, UPS, XPS, specific heat, electrical con-ductivity and magnetic susceptibility measurements). The cluster contains gold core with cuboctahedral (fcc; face-centered cubic) structure which is different from the icosahedral geometry observed in smaller clusters (e.g. Au$_{11}$). The ligand's organic shell serves only

to stabilize and insulate the metal core and one must conclude that the amount of charge transfer (and bonding) between gold atoms and ligands is very small. This raises the possibility that such clusters may be better thought of as metal–adsorbate systems. Can gold clusters be considered 'organic derivatives of gold'? Many large clusters (e.g. Au_{55}) are essentially metallic in character and stand on the very boundary of the 'organic derivative of gold' category.

D. Adsorption studies

XPS is one of the best available techniques for studying adsorption processes of organic ligands on metal surfaces. However, the XPS method is often employed as only one of several complementary techniques with the purpose of answering the following two questions:

(a) Which species exist in the adsorbate layer and under what conditions of temperature, concentration, pH, electrode potential are they stable?

(b) What is the nature of adsorbate–metal interactions?

In the *ex-situ* XPS method, the metal surface is coated with adsorbate under specific conditions, rinsed with water and quickly inserted into the spectrometer. Study of the adsorption of the organic ligand thymine on single-crystal gold electrode by this method revealed some interesting facts[27]. Three adsorption states were detected and their relative amounts shown to depend on ambient conditions. The chemisorbed state was formed via charge transfer from deprotonated thymine to the metal surface. This conclusion was deduced from the observed splitting of the N1s band and a shift of one of its components toward lower binding energies. In an XPS study of the adsorption of thiols and disulfides on gold surfaces the simultaneous presence of two species was detected[28]. The measured $S2p_{3/2}$ binding energy of 162 eV was attributed to bound thiol species (gold–thiolate bonds), while the $S2p_{3/2}$ energy of 163.5–164 eV corresponded to unbound thiol/disulfide species. The reduction of binding energy suggests formation of an Au−S bond, but the details of bond formation are unclear. The mechanism is unlikely to be a simple charge transfer from ligand to gold because in that case one would expect an increase in $S2p_{3/2}$ energy rather than the observed decrease.

III. PES OF SILVER COMPOUNDS

A. XPS Studies

The organic derivatives of silver were studied mainly by the XPS method and we have again classified the compounds studied on the basis of coordinating atoms. The numbers incorporated into chemical formulae again indicate core binding energies of relevant atoms.

1. Complexes with Ag−N coordination

The complexes with this coordination can be divided into two classes:

(a) complexes with heterocyclic ligands (pyridine, bipyridine, phenanthroline) and (b) complexes with macrocyclic ligands (crowns, cryptands, porphyrins).

Walton and coworkers[29,30] have reported an extensive study of complexes of silver with heterocyclic ligands (pyridine, bipyridine and phenanthroline derivatives). The aim of their study was threefold: to establish whether the metal binding energies vary with changes in the oxidation state, to analyze and compare bandwidths for diamagnetic Ag(I) complexes with those of paramagnetic Ag(II) and to determine whether binding energies

show any dependence on the coordination number. Their results showed that Ag3d ener-
gies are generally insensitive to the oxidation state of silver and fall within the ranges
of $374.1-374.5$ eV (Ag3d$_{3/2}$) and $368.0-368.5$ eV (Ag3d$_{5/2}$). It is interesting that Ag3d
energies are slightly higher in Ag(I) than in Ag(II) complexes, although one would expect
the opposite to be the case. However, the differences between Ag3d energies in Ag(I)
and Ag(II) complexes are small, which indicates that XPS is not the best technique for
determination of oxidation states of silver.

The insensitivity of Ag3d energies can be illustrated by the fact that in the mixed
Ag(I)−Ag(II) complex with pyrazine-2,3-dicarboxylic acid, no band doubling was
observed. Such doubling could be expected when two different oxidation states of silver
are present. The insensitivity of Ag3d can be compared with the sensitivity of Au4f
binding energies. It demonstrates that core level shifts for heavy metals in low oxidation
states are not always sufficiently large to be detected by XPS.

The coordination stereochemistry has a small but noticeable effect on the Ag3d energies.
The silver atoms in complexes with higher coordination numbers tend to have lower
Ag3d energies. This trend can be attributed to the increase in electron density on the
silver atom (due to the presence of donor ligands) which in turn results in lower binding
energies. Walton and coworkers mentioned in their original report[29] that Ag3d bands are
significantly broader in paramagnetic Ag(II) than in diamagnetic Ag(I) complexes. This
effect was attributed to 'multiplet splittings due to the coupling of 3d core hole with 4d
valence shell'. However, a later study by the same workers[30] showed that the broadening
was partly due to surface charging effects. This example illustrates vividly the inherent
experimental difficulties and caveats pertaining to the XPS method.

XPS studies of Ag(II) complexes containing aza crown **20** and cryptand **21** were also
reported[31,32]. Tolentino and Po[31] and Siegbahn, Lehn and coworkers[32] have observed that
the Ag3d energies in macrocyclic and heterocyclic complexes fall within the same energy
range; i.e. the ring structure of the ligand (whether it is monocyclic or polycyclic) does not
influence the charge density on the silver center. However, the ring size does influence
the Ag3d energies. Thus the Ag3d$_{5/2}$ energies in the complexes with [14]aneN$_4$ and
[15]aneN$_4$ were found to be 368.2 and 369.3 eV, respectively. The variation in energies
was attributed to different metal−donor atom distances. The [15]aneN$_4$ ligand **20** can
accommodate an Ag(II) atom, while at the same time imposing least ring strain on the
complex.

(20)   **(21)**
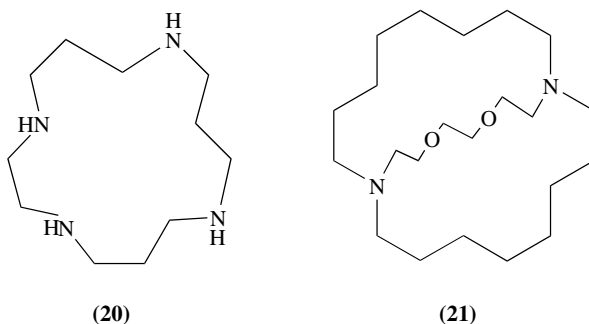
Tolentino and Po[31] have also observed N1s satellite bands (with ionization energies
2 eV higher than the principal N1s band) in the spectra of aza macrocycles. The origin of
these satellite bands is not clear[33a] and various explanations related to electronic structure

and coordination geometries were proposed. However, considering all available evidence, the explanation related to final-state electronic structure effects seems most plausible. N1s energies in complexes of silver with aza macrocycles, cryptands and porphyrin[33] ligands are also very similar, although they are lower than in analogous complexes containing heterocyclic ligands. This similarity suggests that the presence of an unsaturated π-ring system (e.g. in porphyrins) has little influence on the electron density at the silver atom.

Knowledge of the electronic structure of metalloporphyrins is useful, because such compounds can serve as models for biological redox systems. In this context one may wish to know whether, during a redox process, the electron is transferred directly from the metal center or whether porphyrin ligands are also involved in the process. Further, an understanding of the influence of the oxidation state of the metal on the porphyrin ring's charge and reactivity is of interest.

In their XPS studies Winograd and coworkers[33b,c] analyzed complexes containing octaethylporphyrin (OEP, **22**), tetraphenylporphyrin (TTP, **23**), tetraphenylchlorin (TPC, **24**) and tetraphenylbacteriochlorin (TPBC, **25**). They reached several important conclusions regarding the electronic and molecular structure of the free ligands and their complexes. The ligands are easily polarizable and can stabilize metal ions in high oxidation states by electron transfer via metal–nitrogen σ-bonds. The free bases (ligands) show two N1s peaks in XPS spectra which arise from two protonated and two unprotonated

(22)

(23)

(24)

(25)
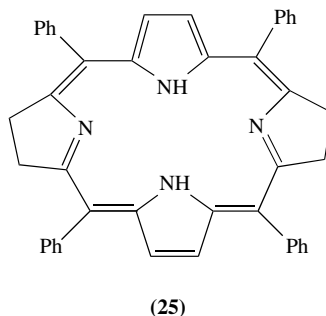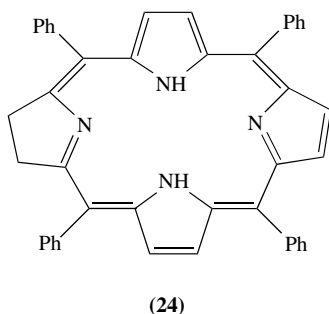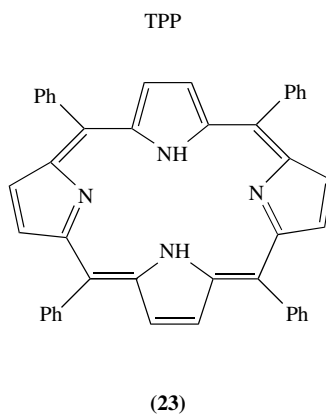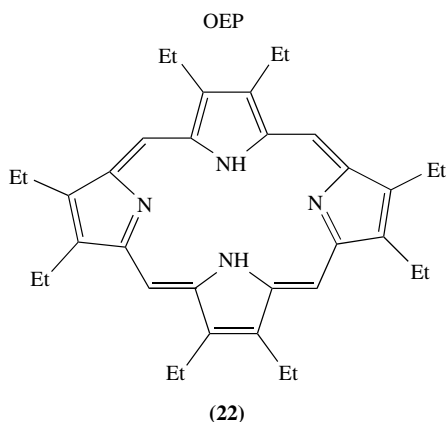
pyrrole nitrogens. The Ag3d and N1s, but not the C1s bands were primarily used for the analysis. Nitrogen atoms are involved both in σ-bonding to metal as well as in π-bonding to carbon. Also, there are 44 carbon atoms present in the ligand skeleton which may reduce the apparent magnitude of electronic structure effects. The free ligands were analyzed first and it was observed that on going from **22** to **25**, the electron density at the four nitrogens is slightly diminished. When two protons in the free base are removed by the introduction of a metal ion to generate metalloporphyrins, only a single N1s peak with binding energy higher than in the free base is observed. This is due to the increase in molecular symmetry which makes all four nitrogens equivalent. Besides this 'nitrogen equalization', the porphyrin skeleton becomes polarized after the transfer of σ electron density from the nitrogens to the metal, as can be seen from the correlation between N1s energies and metal ion electronegativities. Polarization of the ligand skeleton effected by this electron density transfer is also reflected in the lengthening of ring C−C bonds. In metallochlorins both effects (symmetry change and electron density transfer) are combined.

Figure 5 shows how the two N1s bands (in 1 : 3 intensity ratio) reappear on going from Ag−**24** and Ag−**23** to **23**. This indicates that in the Ag−**24** complex two distinct types of nitrogen atom exist and that the introduction of a silver atom does not increase the symmetry as it did in Ag−**23**. Different N1s energies for metalloporphyrins and metallochlorins containing paramagnetic and diamagnetic metal ions were measured. The N1s peaks in diamagnetic metallochlorins or metalloporphyrins have approximately 0.9 eV higher binding energies than in their paramagnetic counterparts. The reasons for this behavior are not quite clear. The differences between Ag3d energies for Ag(0), Ag(I) and Ag(II) oxidation states are not very pronounced (*vide supra*). However, in XPS spectra of Ag(III)−**22** complexes Winograd and coworkers[33b] have measured Ag3d binding energies which were 2.7 eV higher than in the Ag(II) analogue. This observation not only confirmed the presence of the Ag(III) state, but also demonstrated that during oxidation of metalloporphyrins, the electron transfer originates from the metal and not from the porphyrin system. The N1s energies are also larger in Ag(III)−**22** than in the free base. This is not surprising in view of the greater electron affinity of Ag(III) compared with silver ions in lower oxidation states. What is somewhat unusual is the observation of a small C1s shift toward lower binding energies[33b].

2. Complexes with mixed coordination

Nefedov and coworkers have reported XPS studies of silver complexes with cyanamido derivatives **26**–**30** and the uncomplexed **31**[34]. They have also recorded XPS spectra of the cyano silver complexes **32** and **33**. The *N*-acylthiourea silver complex **34** was compared with the *N*-acylthiourea (**35**)[35].

The following conclusions were reached from the analysis of binding energies and comparison between core energies in complexes and free ligands:

(a) Ag3d energies are similar to those in other silver complexes.

(b) The nitrogen atom in the amido group has a higher binding energy than the one in the cyano group. This is expected because of the electron density transfer which takes place upon complex formation. The transfer from the amide nitrogen to the metal leads to the formation of a σ donor bond.

(c) The net flow of electron density is indicated by arrows which are collinear with the chemical bonds. The proposed flows are only tentative because additional data on O1s and C1s energies were not reported for some of the complexes. In the thiourea complex **34**, the S2p energy increases upon complex formation. This indicates that formation of a Ag−O σ-bond and a Ag−S donor bond takes place. There was no change in N1s energy
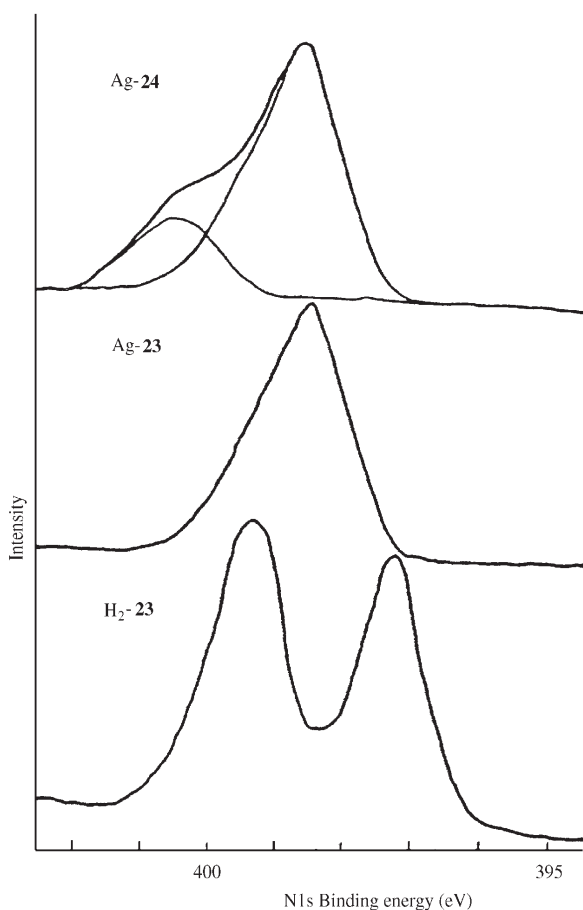
FIGURE 5. N1s peaks for some porphyrins and chlorins. Reprinted with permission from Reference 33c. Copyright 1976 American Chemical Society

of the amido group (vs free ligand) which suggests that a backbonding metal → ligand mechanism cannot be invoked as the explanation of the electronic structure and bonding.

A very interesting study of the adsorption of dithizone (H_2Dz, **36**) on the surface of a silver electrode has been reported[36]. Dithizone is an excellent chelating agent for transition metals and in strongly alkaline solution it exists in HDz^- form. Electrooxidation of HDz^- yields the disulfide which in turn may disproportionate into HDz^- and the tetrazolium species **38**. The latter can be regarded as a product of further oxidation of HDz^-. The XPS data for these species and for the Ag(I) dithizonate complex **(39)** are summarized below.

The HDz^-/pH 12/Ag system (i.e. a dithizone anion in alkaline solution in which a silver electrode was immersed) was studied by XPS[36]. The study was not performed *in*

(26)

$$Ph_2P(=O)-N(-Ag)-CN \quad 399.7 \quad 398.7$$

Ph, Ph, O, P—N—CN, Ag   399.7 398.7

(27)

Ph, Ph, S, P—N—CN, Ag   399.7 398.6

(28)

oCl—C$_6$H$_4$—S(=O)(=O)—N(—Ag)—CN   399.5 399.5   168.5

(29)

Ph—O—CH$_2$—C(=O)—N(—Ag)—CN   400.84 399.54

(30)

Ag—N(CN)$_2$ 399.1   400.4

(31)

Ph—O—CH$_2$—C(=O)—N(—Me)—CN   401.65 399.85

(32)

pMe—C$_6$H$_4$—S(=O)(=O)—C(—Ag)(CN)$_2$ 399.54   168.1

(33)

AgC(CN)$_3$ 399.1

(34)

Ph—C(=N)(O)...(S)—C(=N)—NEt$_2$, Ag   399.9 398.2   368.7   162.8

(35)

Ph—C(=O)—NH—C(=S)—N(Et)(Et)   400.0 400.0   162.3

(36)

Ph—N=N—C(=S)—N(H)—N(H)—Ph   161.8   400.6

(37)

Ph—N=N—C(=N—NH—Ph)—S—S—C(—N=N—Ph)(—N—NH—Ph)   163.8   400.6

(38)

Ph, Ph — tetrazolium — S$^-$ 402.8   161.3   399.7

(39)

Ph—N—N=...—C—S—Ag ... =N—NH—Ph   399.5   368.3 162.0
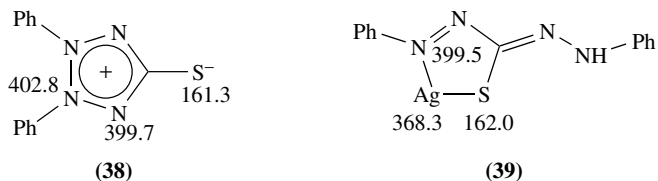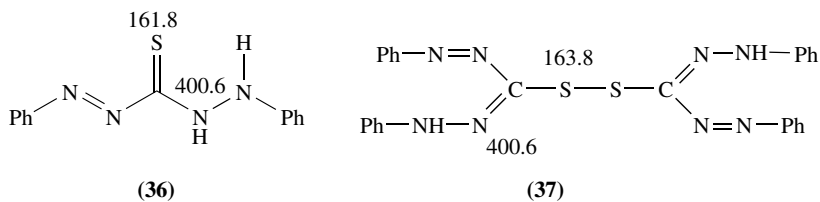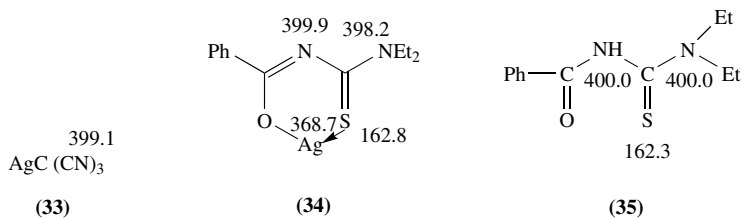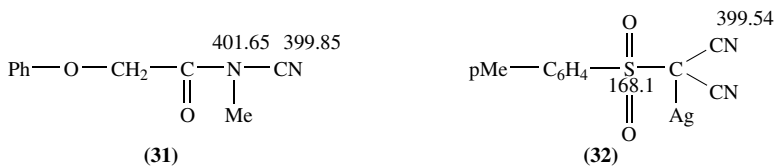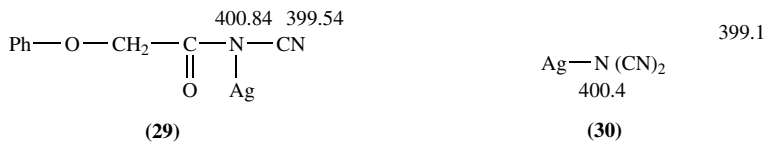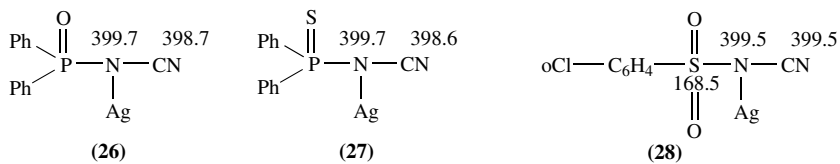
situ (in solution). The silver electrode was allowed to equilibrate in solution for 15 min, after which it was taken out of solution, rinsed with deionized water, dried and quickly inserted into the probe of the XPS instrument. The adsorption of dithizone anion on the silver electrode was studied at different electrode potentials and the results obtained were compared with previously reported voltammetric and surface Raman spectroelectrochemical data. The interpretation of the previously reported data was complicated by the possible presence of HDz$^-$ in solution and on the electrode surface. Pemberton and Buck[36] have classified XPS data into three sets, each of which covers a particular range of potentials applied to the silver electrode. In the first potential range (-1.2V to -0.5V) XPS data showed N1s peaks at 393.7 and 399.7 eV and S2p at 161.5 eV. Comparison of these energies with XPS of individual species (*vide supra*) helped to identify the presence of adsorbed HDz$^-$ species in this potential regime. The peak at 393.7 eV was attributed (tentatively) to the presence of the inorganic species Ag$_3$N. In the potential regime -0.5V to 0.0 V, single N1s and S2p peaks at 400.2 eV and 161.8 eV were observed and identified (from the similarity with E_b of H$_2$Dz) as belonging to an HDz$^-$ species adsorbed on the silver surface. In the potential regime $\geqslant$0.0 V, N1s peaks at 400.4 eV and 403.0 eV appeared. S2p peaks at 163.9 and 162.1 eV were also observed. The comparison with stable compounds (shown above) again allowed the identification of species present as HDz$^-$, **37** and **38**. Ag3d peaks were observed at 368.3 and 374.3 eV, which indicated that some Ag$^+$ was also detected by XPS.

The XPS data have pinpointed the existence of nitride and tetrazolium species, which Raman scattering method was unable to do. This is a good example of the power and versatility of the XPS (ESCA) method for studies performed in unusual experimental environments. However, in some cases like the adsorption of xanthate on silver, XPS could not (on the basis of chemical shifts) discern the presence of chemisorbed species[37].

B. UPS Studies

Reported UPS studies of organic silver derivatives are very scarce. However, if one stretches the meaning of 'organic derivative' somewhat, the recent UPS study of chemisorption of quaterthiophene **(40)** ligand on silver surface provides an interesting example of the application of PES methods[38]. The UPS (Figure 6) was employed in combination with LEED and NEXAFS techniques to establish the nature of ligand–silver interactions and spatial arrangement of the adsorbed ligand molecules on Ag(III) surface.

The results suggest that **40**, when adsorbed at a monolayer thickness, forms covalent bonds with Ag. The bonding involves the ligand's π-orbitals and Ag4d and Ag5s orbitals. The orbital overlap, and hence the strength of bonding, can be expected to be favored by 'flat-lying' molecules of **40** on the silver surface. This structural suggestion had been confirmed independently by LEED and NEXAFS.
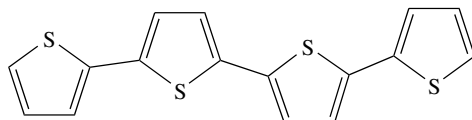
(40)
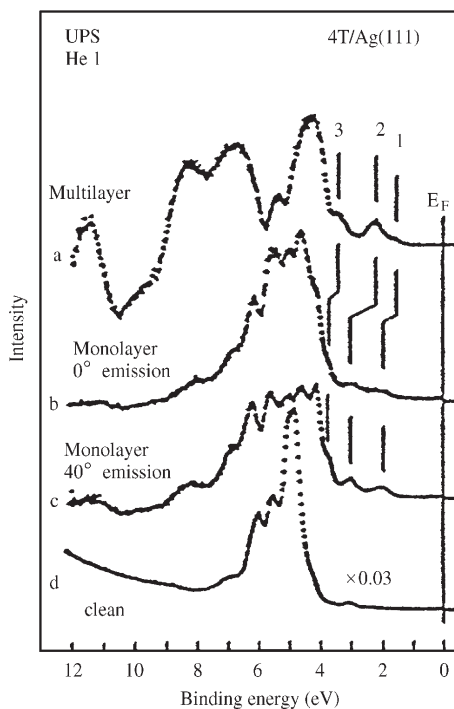
FIGURE 6. UPS spectra of a film of **40** on Ag(lll) surface. Vertical lines mark shifts of the topmost orbitals. Reproduced by permission of Elsevier Science SA from Reference 38.

IV. CONCLUSIONS

The PES techniques provide valuable information about structure and bonding in organic derivatives of silver and gold. Sometimes, the relevant information could not be obtained by any other method. This statement does not imply that PES methods are the best choices in all cases. PES methods have problems and limitations which must be taken into consideration (charging effects, inadequate resolution etc.), but they are still very useful. Quantum chemical studies are often performed first when analyzing electronic structures of metallic complexes. In the case of gold and silver derivatives, these studies can make predictions about various properties like electronic structure, metallic oxidation states and the nature of bonding between the metal and ligands. Such predictions[39] could and should be tested by PES techniques, which are indispensable for any complete study of bonding and structure. XPS data can be correlated with Mössbauer spectra[14a] and with ^{13}C NMR chemical shifts[40]. It is worth remembering, though, that such correlations must be treated with caution because the measurements are performed on systems in different physical states. Mössbauer spectra are measured for species in the ground electronic states, while XPS (ESCA) refer to excited states of the ionized species. As for comparison between NMR and XPS data, one must bear in mind that NMR shifts depend on several factors including shielding terms, which are strongly dependent on interatomic potentials.

V. ACKNOWLEDGMENTS

VI. REFERENCES

1. L. Klasinc, I. Novak and S. P. McGlynn, in *The Chemistry of Halides, Pseudo-halides and Azides, Supplement D2, Part 1* (Eds. S. Patai and Z. Rappoport), Wiley, Chichester, 1995, p. 123.
2. (a) U. Becker and D. A. Shirley (Eds.), *VUV and Soft X-ray Photoionization*, Plenum Press, New York, 1996.
   (b) S. Höfner, *Photoelectron Spectroscopy*, 2nd ed., Springer-Verlag, Berlin, 1996.
3. (a) T. L. Barr, *Modern ESCA, The Principles and Practice of X-ray Photoelectron Spectroscopy*, CRC Press, Boca Raton, 1994.
   (b) J. Furnemont, *Educ. Chem.*, **31**, 135 (1994).
4. Z. B. Maksic (Ed.), *Molecular Spectroscopy, Electronic Structure and Intramolecular Interactions*, Springer-Verlag, Berlin, 1991.
5. I. Novak and B. Kovač, in *The Chemistry of Hydrazo, Azo and Azoxy Groups, Vol. 2* (Ed S. Patai), Wiley, Chichester, 1997, p. 191.
6. S. J. Osborne, S. Sundin, A. Ausmees, S. Svensson, L. J. Saethre, O. Svaeren, S. L. Sorensen, J. Vegh, J. Karvonen, S. Aksela and A. Kikas, *J. Chem. Phys.*, **106**, 1661 (1997).
7. S. Patai, *Patai's Guide to the Chemistry of Functional Groups*, Wiley, Chichester, 1989.
8. (a) G. M. Bancroft, T. Chan, R. J. Puddephatt and J. S. Tse, *Inorg. Chem.*, **21**, 2946 (1982).
   (b) G. M. Bancroft, T. Chan and R. J. Puddephatt, *Inorg. Chem.*, **22**, 2133 (1983).
9. J.-J. Yeh, *Atomic Calculation of Photoionization Cross-sections and Asymmetry Parameters*, Gordon and Breach, Langhorne, 1993.
10. C. E. Moore, *NBS Circular 467*, Vol. 3, National Bureau of Standards, Washington, 1958.
11. O. D. Häberlen and N. Rösch, *J. Phys. Chem.*, **97**, 4970 (1993).
12. U. Gelius, in *Electron Spectroscopy* (Ed. D. A. Shirley), North-Holland, Amsterdam, 1972, p. 311.
13. N. Kaltsoyannis, *J. Chem. Soc., Dalton Trans.*, 1(1997).
14. (a) H. Schmidbaur, J. R. Mandl, F. E. Wagner, D. F. van de Vondel and G. P. van der Kelen, *J. Chem. Soc., Chem. Commun.*, 170 (1976)
   (b) D. F. van de Vondel, G. P. van der Kelen, H. Schmidbaur, A. Wolleben and F. E. Wagner, *Phys. Scr.*, **16**, 364 (1977).
   (c) J. Knecht, R. Fischer, H. Overhof and F. Hensel, *J. Chem. Soc., Chem. Commun.*, 905 (1978).
15. W. D. Perry and G. C. Vogel, *J. Chem. Educ.*, **69**, 222 (1992).
16. P. v. R. Schleyer and H. Jiao, *Pure Appl. Chem.*, **68**, 209 (1996).
17. D. Bergmann and J. Hinze, *Angew. Chem., Int. Ed. Engl.*, **35**, 150 (1996).
18. R. G. Raptis, L. C. Porter, R. J. Emrich, H. H. Murray and J. P. Fackler, *Inorg. Chem.*, **29**, 4408 (1990).
19. (a) H. Konno and Y. Yamamoto, *Bull. Chem. Soc. Jpn.*, **59**, 1327 (1986).
   (b) Y. Yamamoto and H. Konno, *Bull. Chem. Soc. Jpn.*, **60**, 2561 (1987).
20. (a) V. A. Belonosov, N. I. Ushakova, Ya. V. Salyn, V. G. Pleshakov, B. E. Zaitsev, V. I. Zelenov, A. M. El'bert and A. K. Molodkin, *Zh. Neorg. Khim.*, **26**, 963 (1981); *Chem. Abstr.*, **94**, 218813e (1981).
   (b) R. G. Raptis and J. P. Fackler, *Inorg. Chem.*, **29**, 5003 (1990).
21. P. M. Th. M. van Attekum and J. M. Trooster, *J. Chem. Soc., Dalton Trans.*, 201 (1980).
22. H. W. Chen, C. Paparizos and J. P. Fackler, *Inorg. Chim. Acta.*, **96**, 137 (1985).
23. (a) G. Matsubayashi and A. Yokozawa, *J. Chem. Soc., Dalton Trans.*, 3535 (1990).
   (b) G. Matsubayashi and A. Yokozawa, *Inorg. Chim. Acta*, **193**, 137 (1992).
24. A. McNeillie, D. H. Brown, W. E. Smith, M. Gibson and L. Watson, *J. Chem. Soc., Dalton Trans.*, 767 (1980).
25. A. P. Koley, R. Nirmala, L. S. Prasad, S. Ghosh and P. T. Manoharan, *Inorg. Chem.*, **31**, 1764 (1992).

26. (a) O. D. Häberlen, S.-C. Chung, M. Stener and N. Rösch, *J. Chem. Phys.*, **106**, 5189 (1997).
(b) C. Battistoni, G. Mattogno, F. Cariati, L. Naldini and A. Sgamellotti, *Inorg. Chim. Acta*, **24**, 207 (1977).
(c) C. Battistoni, G. Mattogno and D. M. P. Mingos, *J. Electron Spectrosc.*, **33**, 107 (1984) and references cited therein.
(d) P. M. Th. M. van Attekum, J. W. A. van der Velden and J. M. Trooster, *Inorg. Chem.*, **19**, 701 (1980).
(e) Y. M. Shul'ga, A. V. Bulatov, R. A. T. Gould, W. V. Konze and L. H. Pignolet, *Inorg. Chem.*, **31**, 4704 (1992).
(f) R. C. Thiel, R. E. Benfield, R. Zanoni, H. H. A. Smit and M. W. Dirken, *Z. Phys. D.*, **26**, 162 (1993).
(g) D. van der Putten, R. Zanoni, C. Coluzza and G. Schmid, *J. Chem. Soc., Dalton Trans.*, 1721 (1996) and references cited therein.
27. B. Roelfs, E. Bunge, C. Schröter, T. Solomun, H. Meyer, R. J. Nichols and H. Baumgärtel *J. Phys. Chem. B*, **101**, 754 (1997).
28. D. G. Castner, K. Hinds and D. W. Grainger, *Langmuir*, **12**, 5083 (1996).
29. D. P. Murtha and R. A. Walton, *Inorg. Chem.*, **12**, 368 (1973).
30. T. J. Smith and R. A. Walton, *J. Inorg. Nucl. Chem.*, **39**, 1331 (1977).
31. L. U. Tolentino and H. N. Po, *J. Coord. Chem.*, **13**, 341 (1984).
32. O. Bohman, P. Ahlberg, R. Nyholm, N. Mårtensson, K. Siegbahn and J. M. Lehn, *Chem. Scr.*, **18**, 44 (1981).
33. (a) S. Muralidharan and R. G. Hayes, *J. Am. Chem. Soc.*, **102**, 5106 (1980).
(b) D. Karweik, N. Winograd, D. G. Davis and K. M. Kadish, *J. Am. Chem. Soc.*, **96**, 591 (1974).
(c) D. H. Karweik and N. Winograd, *Inorg. Chem.*, **15**, 2336 (1976).
34. L. Jäger, V. I. Nefedov, K.-H. Richter, B. Freude and H. Köhler, *Z. Anorg. Allg. Chem.*, **605**, 125 (1991).
35. Von J. V. Salyn, E. K. Žumadilov, V. I. Nefedov, R. Scheibe, G. Leonhardt, L. Beyer and E. Hoyer, *Z. Anorg. Allg. Chem.*, **432**, 275 (1977).
36. J. E. Pemberton and R. P. Buck, *Anal. Chem.*, **54**, 1355 (1982).
37. A. N. Buckley and R. Woods, *Colloid Surface A*, **104**, 295 (1995).
38. A. Soukopp, C. Seidel, R. Li, M. Bässler, M. Sokolowski and E. Umbach, *Thin Solid Films*, **284−285**, 343 (1996).
39. L. F. Veiros and M. J. Calhorda, *J. Organomet. Chem.*, **510**, 71 (1996).
40. S. Hoste, C. T. Huys, J. Schaubroeck and G. P. van der Kelen, *Spectrochim. Acta A*, **38**, 709 (1982).

CHAPTER **7**

Synthesis and uses of organosilver compounds

HUBERT SCHMIDBAUR and ANGELA BAYLER

Lehrstuhl für Anorganische und Analytische Chemie, Technische Universität München, D-85747 Earching, Germany
Fax: 49-89-289-13125.   e-mail: H.Schmidbaur@lrz.tum.de

I. INTRODUCTION

A number of review articles dealing with organosilver chemistry have appeared since 1970[1−4]. The present chapter is confined to compounds in which the organic group is bound to silver as one-electron ligand.

II. ALKYLSILVER COMPOUNDS

The first, unsuccessful, attempts to prepare alkylsilver compounds were made as early as 1859 by Buckton[5a] and 1861 by Wanklyn and Carius[5b]. The reaction of silver chloride with diethylzinc yielded only metallic silver, and a mixture of ethylene, ethane and butane. Due to their low thermal stability alkylsilver compounds were entirely unknown until 1941, when Semerano and Riccoboni[6] reported the formation of some alkylsilver complexes by the reaction of silver nitrate with tetraalkyllead in alcoholic solution at low temperatures (equation 1). The yellow to brown precipitates of the formula RAg (R = methyl, ethyl, propyl) were stable at $-80\,^\circ$C for several hours, but upon warming to room temperature rapid decomposition took place with formation of metallic silver and

gaseous hydrocarbons (equation 2). The thermal stability of these compounds decreases with increasing chain length of $R^{1,2}$.

$$AgNO_3 + R_4Pb \longrightarrow AgR + R_3PbNO_3 \qquad (R = \text{alkyl, aryl}) \qquad (1)$$

$$4AgC_nH_{2n+1} \longrightarrow 4Ag^0 + C_nH_{2n+2} + (C_nH_{2n+1})_2 + C_nH_{2n} \qquad (2)$$
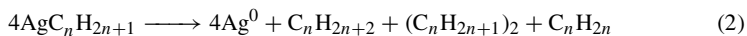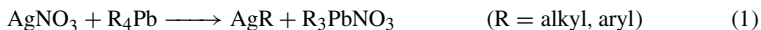
Other transmetallation reactions of silver halides or their complexes with phosphine ligands (e.g. [AgIP(Bu-n)$_3$]) with alkyllithium and alkylmagnesium reagents confirm the fleeting stability of the alkylsilver compounds. In each case the composition of the AgR intermediates has been derived from the analysis of the products formed in their thermal decomposition. So far, representatives of the class of simple alkylsilver complexes have not been isolated in pure form.

However, some interesting alkylsilver compounds, where the organic group is a di- or tri-substituted anionic (sp^3)C$^-$ ligand, have been reported.

The transmetallation reaction between AgBF$_4$ and a tertiary bis(silyl)pyridylmethyllithium compound afforded the dinuclear alkylsilver species (**1**), which is stable at room temperature for several days[7]. Despite the susceptibility of most organosilver compounds to hydrolysis, the argentate complex with a β-disulfone carbanion (**2**) can be obtained by the reaction of 1,3-dithiane 1,1,3,3-tetraoxide with silver nitrate in alkaline aqueous solution[8].
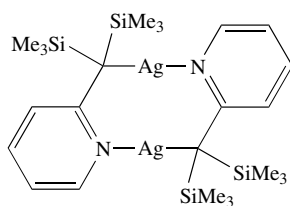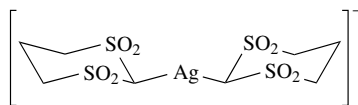
(1)   **(2)**

A. Complexes of Silver(I) with Ylide Ligands

Organosilver complexes with ylide ligands have been prepared in a variety of ways. Most of them are remarkably inert with respect to hydrolysis and thermal decomposition, representing some of the most stable organometallic compounds of silver. The identity and structure of the compounds have been determined either by X-ray diffraction or by multinuclear NMR spectroscopy, where the observation of large ^{13}C–, ^{1}H– and ^{3}P–$^{107/109}$Ag coupling constants is indicative for a structure with the ylide attached to the metal centre through the carbanionic donor atom.

Four types of ylide complexes of silver(I) have been reported so far: (a) mononuclear neutral [Ag(R)(ylide)], (b) mononuclear cationic [Ag(ylide)$_2$]X, (c) dinuclear neutral [Ag$_2${(CH$_2$)$_2$ERR'}$_2$] (E = P, As) and (d) dinuclear dicationic [Ag$_2${{CH(PPh$_3$)}$_2$CO}$_2$].

Stable mononuclear complexes of the type [AgCl(ylide)] have been obtained by reaction of equimolar amounts of AgCl and triphenylphosphonium methylide (Ph$_3$P=CH$_2$)[9] or the double ylide hexaphenylcarbodiphosphoran [C(PPh$_3$)$_2$][10]. In a similar way the reactions of AgC$_6$F$_5$ with the free ylides Ph$_3$P=CH$_2$, Ph$_2$MeP=CH$_2$ and Ph$_3$P=CHCO$_2$Me lead to the corresponding complexes [Ag(C$_6$F$_5$)(ylide)]. Haloarylsilver(I) ylide complexes of this type are obtained in better yields by the *in situ* reaction of AgO$_2$CCF$_3$ and LiC$_6$F$_5$ with the phosphonium salts [ER$_3$Me](CF$_3$CO$_2$) (ER$_3$ = PPh$_3$, PPh$_2$Me, PPhMe$_2$, AsPh$_3$)

(equation 3)[11]. These complexes have been used to transfer the ylide ligand (phosphorus or arsenic) to metal centres like gold(I) and thallium(I)[12].

$$AgO_2CCF_3 + 2\ LiC_6F_5 + [ER_3Me]O_2CCF_3 \xrightarrow[\substack{-2\ LiO_2CCF_3 \\ -C_6F_5H}]{} [Ag(C_6F_5)CH_2ER_3] \quad (3)$$
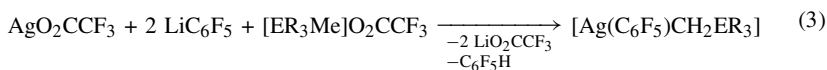
$ER_3 = PPh_3,\ PPh_2Me,\ PPhMe_2,\ AsPh_3$

Cationic bis(ylide) complexes $[Ag(ylide)_2]^+$ can be isolated only with aryl substituted ylide ligands of the formula $Ph_3P=CHR$. They have been synthesized by the reaction of silver salts AgX (X = Cl, ClO$_4$, NO$_3$) and free ylides in a 1 : 2 molar ratio. A large variety of different simple ylides (R = H, Me, CH(CH$_3$)$_2$)[11,13] and carbonyl stabilized ylides [R = C(O)Me, C(O)Ph, CO$_2$Me, CO$_2$Ph][14] have been employed in this reaction.

The reaction of alkyl substituted ylides like $Me_3P=CH_2$[15] or c-(CH$_2$)$_5$P(Me)=CH$_2$[16] with AgCl or (Me$_3$P)AgCl under the same reaction conditions yields dinuclear neutral ylide bridged complexes **3** and **4** in a transylidation process (equation 4). The corresponding tetraalkylphosphonium chlorides [R$_2$Me$_2$P]Cl are formed as by-products in these reactions. The analogous silver dimethylarsonium methylide complex **5** can be prepared in a similar way by the reaction of trimethylarsonium methylide and (Me$_3$As)AgCl (equation 5)[17].

$$4\ R_2MeP=CH_2\ +\ 2\ Me_3PAgCl \xrightarrow[\substack{-2\ Me_3P \\ -2\ [R_2Me_2P]Cl}]{} \qquad (4)$$

(**3**) R = Me

(**4**) RR = (CH$_2$)$_5$−c

$$4\ Me_3As=CH_2\ +\ 2\ Me_3AsAgCl \xrightarrow[\substack{-2\ Me_3As \\ -2\ [Me_4As]Cl}]{} \qquad (5)$$
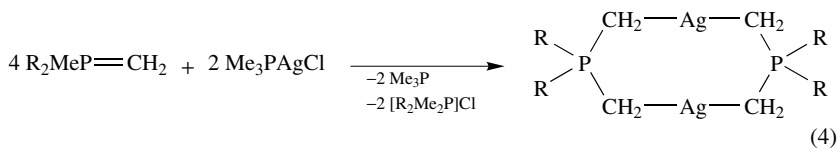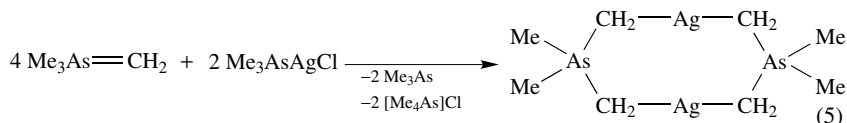
(**5**)

Related dinuclear complexes with carbonyl-stabilized phosphorus ylide ligands (**6**) are accessible from the reaction of the phosphonium chlorides [Ph$_2$P(CH$_2$CO$_2$R)$_2$]Cl (R = Me, Et) with Ag$_2$CO$_3$ (equation 6)[18]. The precipitation of AgCl is regarded as the driving force of these reactions.

$$2\ Ag_2CO_3\ +\ 2\ [Ph_2P(CH_2CO_2R)_2]Cl \xrightarrow[\substack{-2\ AgCl \\ -2\ CO_2 \\ -2\ H_2O}]{} \qquad (6)$$
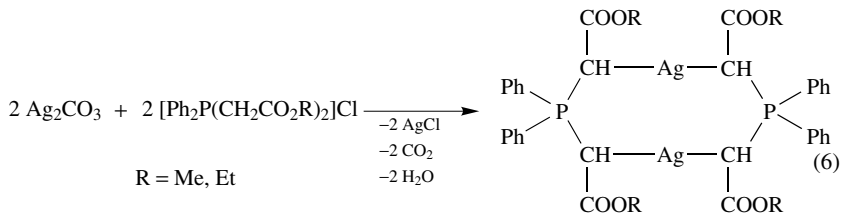
R = Me, Et

(**6**)

The dinuclear dicationic complex **7** with the di-ylide [(Ph$_3$PCH)$_2$CO] as a bridging ligand between two silver atoms has been obtained from a transylidation reaction between the diphosphonium salt [(Ph$_3$PCH$_2$)$_2$CO]ClO$_4$ and the bis(ylide) complex [Ag{(Ph$_3$P)CHC(O)CH$_3$}$_2$]ClO$_4$ described above (equation 7)[19].

$$\left[\begin{array}{c} \text{Ph}_3\text{P} \qquad\qquad \text{PPh}_3 \\ \text{CH}-\text{Ag}-\text{CH} \\ \text{Me}-\text{C} \qquad\quad \text{C}-\text{Me} \\ \parallel \qquad\qquad \parallel \\ \text{O} \qquad\qquad \text{O} \end{array} \right]^{+}$$

$$\xrightarrow[\;-4\,[\text{Ph}_3\text{PCH}_2\text{C(O)Me}]^{+}\;]{+2\,[(\text{Ph}_3\text{PCH}_2)_2\text{CO}]^{+}} \left[\begin{array}{c} \text{PPh}_3 \qquad\qquad \text{PPh}_3 \\ \text{CH}-\text{Ag}-\text{CH} \\ \text{O}= \qquad\qquad =\text{O} \\ \text{CH}-\text{Ag}-\text{CH} \\ \text{PPh}_3 \qquad\qquad \text{PPh}_3 \end{array} \right]^{2+} \qquad (7)$$

(7)
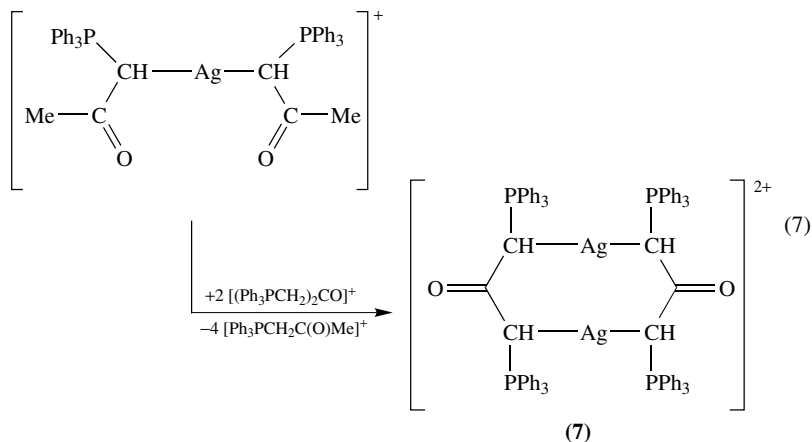
Silver(I) ylide complexes can also be generated from precursors such as [Ag(acac)PPh$_3$] by reaction with phosphonium salts. The reaction of [Ag(acac)PPh$_3$] with the phosphine-phosphonium salt [Ph$_2$PCH$_2$PPh$_2$CH$_2$CO$_2$Me]ClO$_4$ leads to monodeprotonation of the methylene group nearest to the ester group and formation of acetylacetone (equation 8). The chelating nature of the ligand in the mononuclear complex **8** has been confirmed by NMR spectroscopy[20]. Reactions of two equivalents of [Ag(acac)PPh$_3$] with the related phosphine oxide or phosphine sulphide derivatives [XPPh$_2$CH$_2$PPh$_2$CH$_2$CO$_2$Me]ClO$_4$ (X = O, S) give the doubly deprotonated complexes [Ag$_2$(PPh$_3$)$_2$(XPPh$_2$CHPPh$_2$CHCO$_2$Me)]ClO$_4$ (**9**)[20].

$$[\text{Ag(acac)PPh}_3] \;+\; [\text{Ph}_2\text{PCH}_2\text{PPh}_2\text{CH}_2\text{CO}_2\text{Me}]\text{ClO}_4 \xrightarrow[-\,\text{acacH}]{} \begin{array}{c} \text{Ph}_3\text{P} \quad \overset{+}{\text{P}}\text{Ph}_2 \\ \text{Ag} \\ \text{O}_3\text{ClO} \qquad \text{PPh}_2 \\ \text{COOMe} \end{array} \qquad (8)$$

(8)
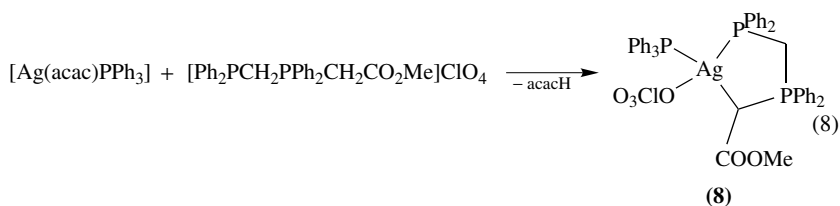
Other neutral or cationic dinuclear complexes with sulphur functionalized ylide ligands have been obtained from the reactions of AgNO$_3$ with Li(CH$_2$PPh$_2$S) (**10**)[21] and of AgClO$_4$ with the free ylide Ph$_2$PCH=PPh$_2$Me (**11**)[22], respectively. The latter complex can also be generated by a ligand exchange reaction between [Ag(ClO$_4$)PPh$_3$] and the corresponding gold(III) ylide complex or by the deprotonation with Na$_2$CO$_3$ of [Ag(SPh$_2$PCH$_2$PPh$_2$Me)][ClO$_4$]$_2$ prepared by the 1 : 1 reaction of AgClO$_4$ and [SPh$_2$PCH$_2$PPh$_2$Me]ClO$_4$.

(9)

X = O, S

(10)

(11)
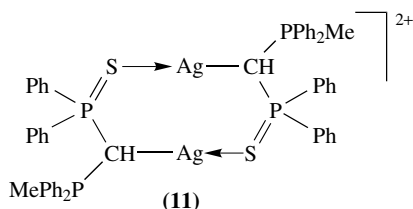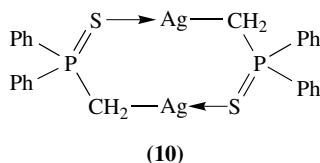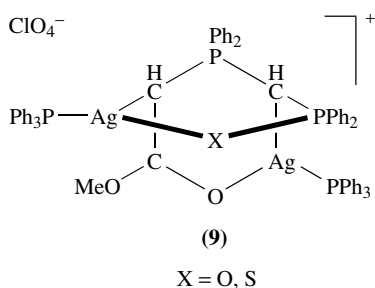
B. Complexes of Silver(I) and Silver(III) with Perfluoroalkyl Ligands

The silver–carbon bond in compounds containing a perfluoroalkyl group is considerably more stable than in non-fluorinated compounds. The synthesis can be accomplished by the nucleophilic addition of silver fluoride to fluoro-olefines. A typical example of this reaction is given in equation 9. The complexes are soluble in organic solvents and have been isolated as the 1 : 1 complexes with acetonitrile $[RAg(CH_3CN)]$[23].

(9)
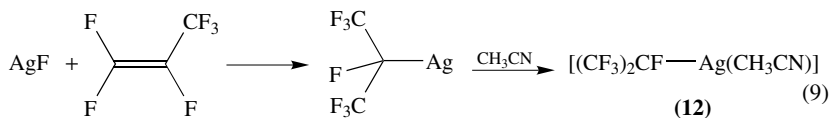
The perfluoroisopropylsilver complex **12** is heterolytically labile, existing in solution in dynamic equilibrium with solvated Ag^+ and the anionic bis(perfluoroisopropyl)silver anion, which can be isolated in the form of the tetraalkylammonium salt **13** (equation 10)[24].

(10)
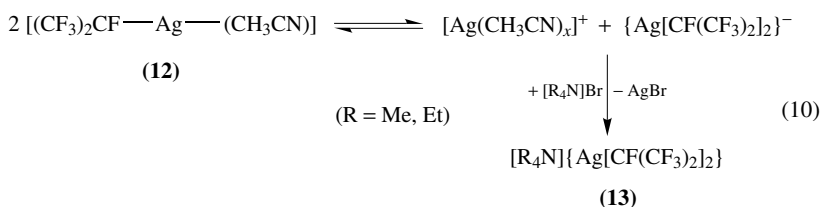
The formation of $AgCF_3$ from Ag atoms and CF_3I was indicated by the course of the hydrolysis reaction[25]. Spectroscopic data of $AgCF_3$ were registered for the co-condensation product of trifluoromethyl radicals and silver vapour at $-196\,^{\circ}C$ which, upon addition of PMe_3, yielded $AgCF_3(PMe_3)$[26]. The highly photosensitive trifluoromethyl silver complexes $[AgCF_3(PR_3)]$ (R = Me, Et) have also been prepared by ligand exchange reactions between $Cd(CF_3)_2 \cdot glyme$ (glyme = $MeOCH_2CH_2OMe$) and AgOAc, followed by addition of PR_3[27].

A surprisingly stable argentate(III) ion $[Ag(CF_3)_4]^-$ is readily formed when silver(I) salts like $AgNO_3$ or AgOAc are treated with $Cd(CF_3)_2 \cdot$ glyme in the absence of additional donor ligands. The intermittently observed bis(trifluoromethyl)argentate(I) ion disproportionates at ambient temperature to silver metal and the mixed silver(I)/silver(III) salt $Ag[Ag(CF_3)_4]$ (**14**) according to equation 11[28]. Alternatively, the oxidation of the argentate(I) to argentate(III) may be achieved with bromine or iodine. Compound **14** is essentially unaffected by water and air and exhibits an unusually high thermal and photolytic stability. The square-planar $[Ag(CF_3)_4]^-$ ion has attracted additional interest as the counterion in tetrathiofulvene-based organic superconductors[29,30].

$$Cd(CF_3)_2 + Ag^+ \longrightarrow [Ag(CF_3)_2]^- + Cd^{2+}$$

$$2[Ag(CF_3)_2]^- + Ag^+ \longrightarrow [Ag(CF_3)_4]^- + 2Ag^0 \qquad (11)$$
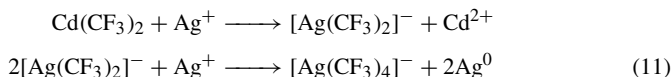
The CF_3 groups in $[Ag(CF_3)_4]^-$ can be replaced by other anionic or neutral ligands, although the stability of the resulting complexes decreases with decreasing number of CF_3 groups. Trifluoromethylation of $[Ag(CN)_2]^-$ with $Cd(CF_3)_2 \cdot$ glyme yields the air- and moisture-sensitive (trifluoromethyl)argentate(I) $[AgCF_3(CN)]^-$. The anion is readily oxidized by bromine to give the cyano(trifluoromethyl)argentates(III) $[Ag(CF_3)_n(CN)_{4-n}]^-$ ($n = 1-4$) (equation 12), which can be isolated as their tetraphenylphosphonium salts. Halogenation of these complexes with acetyl chloride or with bromine affords (halo)argentates(III) of the type $[Ag(CF_3)_nX_{4-n}]^-$ (X = Cl, Br), which can be isolated only for $n = 3$ (equation 13). Their dehalogenation with $AgNO_3$ in a donor solvent D gives the neutral adducts $[Ag(CF_3)_3D]$ (equation 14). The syntheses of methyl- or cyclohexylethynyl-substituted derivatives $[Ag(CF_3)_nR_{4-n}]^-$ (R = Me, C$\equiv$CC$_6$H$_{11}$-c, $n = 2, 3$) are accomplished by reaction of the related (cyano)argentates(III) with CH_3MgCl or $LiC\equiv CC_6H_{11}$-c, respectively[31].

$$2[Ag(CN)_2]^- \xrightarrow[-Cd(CN)_2]{+Cd(CF_3)_2} 2[Ag(CF_3)(CN)]^- \xrightarrow[\substack{-AgBr \\ -Br^-}]{+Br_2} [Ag(CF_3)_n(CN)_{4-n}]^- \qquad (12)$$
$$(n = 1-4)$$

$$[Ag(CF_3)_3(CN)]^- + CH_3C(O)Cl \longrightarrow [Ag(CF_3)_3Cl]^- + CH_3C(O)CN \qquad (13)$$
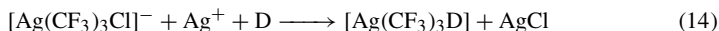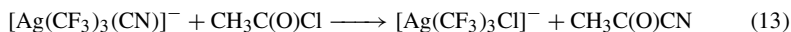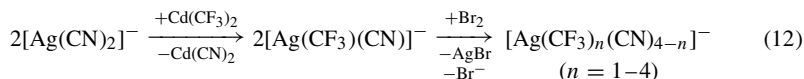
$$[Ag(CF_3)_3Cl]^- + Ag^+ + D \longrightarrow [Ag(CF_3)_3D] + AgCl \qquad (14)$$
$$(D = DMF, DMSO, CH_3CN, glyme, pyridine)$$

Analogous silver(III) complexes with CF_2H groups bound to the metal centre have been synthesized in a similar way using $Cd(CF_2H)_2$ as a difluoromethylating reagent. However, these compounds have a much reduced thermal stability, and only the complexes $[Ag(CF_2H)_4]^-$ and *trans*-$[Ag(CF_2H)_2(CF_3)_2]^-$ have been isolated in pure form[32].

III. ALKENYL- AND ALKYNYLSILVER COMPOUNDS

Alkenylsilver compounds are more thermally stable than alkylsilver compounds. This has allowed the isolation of a few genuine representatives of this class of compounds.

Reaction of silver nitrate with tetravinyllead at $-78\,°C$ yields vinylsilver as an almost insoluble material, which is stable up to about $-30\,°C$[33]. Other simple alkenylsilver compounds AgR, for example isobutenylsilver [R = $(CH_3)_2C=CH$][34,35] and styrylsilver (R = $C_6H_5-CH=CH$)[36], have been obtained by the reaction between silver ions and the corresponding alkenyltriethyllead compounds at low temperatures. Apparently, the

presence of a double bond adjacent to the silver atom causes an enhanced thermal stability of the complexes. Complete decomposition of styrylsilver requires several days at room temperature or several hours in boiling ethanol. The main products of the thermal decomposition are in most cases metallic silver and the corresponding dienes R—R.

The synthesis of alkenylsilver · tributylphosphine complexes [(Bu$_3$P)AgR], where R = *cis*- and *trans*-1-propenyl (CH$_3$CH=CH) or *cis*- and *trans*-2-butenyl [CH$_3$CH=C(CH$_3$)], have been accomplished by treatment of the tetrameric silver iodide · tributylphosphine complex with the relevant propenyl- and butenyllithium compounds[37].

Similar to perfluoroalkylsilver compounds perfluorinated alkenylsilver complexes possess a remarkably high thermal stability. The compounds can be obtained by addition of silver fluoride to perfluoroalkynes (equation 15)[38] or perfluoroallene (equation 16)[39]. Compound **15** has been used as precursor for the deposition of silver films by plasma-enhanced chemical vapour deposition[40] or thermal MOCVD[41].

$$F_3C-C\equiv C-CF_3 \;+\; AgF \;\longrightarrow\; \underset{\underset{Ag}{|}}{F_3C}C=\underset{\underset{CF_3}{|}}{C}F \tag{15}$$

(15)

$$\underset{\underset{F}{|}}{F}C=C=\underset{\underset{F}{|}}{C}F \;+\; AgF \;\longrightarrow\; \underset{\underset{Ag}{|}}{F_3C}C=\underset{\underset{F}{|}}{C}F \tag{16}$$
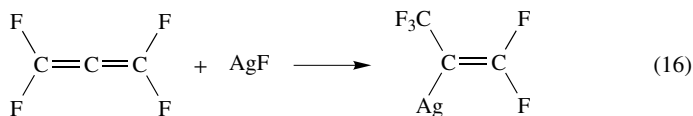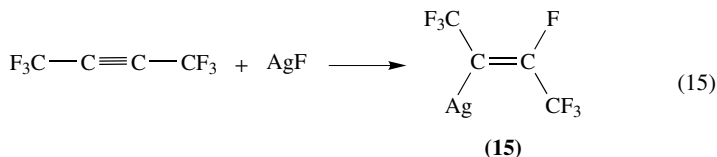
Several alkynylsilver compounds such as silver acetylide (AgC≡CAg)[42,43], propynyl-silver (CH$_3$C≡CAg)[44] and (phenylethynyl)silver (C$_6$H$_5$C≡CAg)[45,46] have been known since the second half of the nineteenth century. In general, alkynylsilver compounds of the type RC≡CAg are readily prepared by the reaction of silver nitrate or silver perchlorate in aqueous ammonia (equation 17). Propynyl- and (phenylethyny)silver have also been prepared by reacting silver nitrate with potassium acetylides in liquid ammonia (equation 18)[47], and (1-hexynyl)silver results from the addition of silver bromide to the relevant Grignard reagent[48].

$$RC\equiv CH + Ag(NH_3)_2{}^+ + OH^- \longrightarrow RC\equiv CAg + H_2O + 2NH_3 \tag{17}$$

$$RC\equiv CK + AgNO_3 \xrightarrow{\text{liquid NH}_3} RC\equiv CAg + KNO_3 \qquad (R = Me, Ph) \tag{18}$$
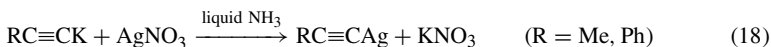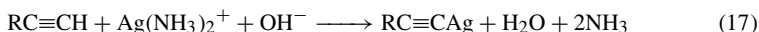
The insoluble alkynylsilver complexes are regarded as coordination polymers (RC≡CAg)$_\infty$ with cross-linking between the metal atoms and the ethynyls of adjacent RC≡CAg units. Donor molecules (L) such as tertiary amines, phosphines and arsines can partly break down the polymeric structure. Thus the reactions of PhC≡CAg with isopropylamine, trimethyl-, triethyl- or triphenylphosphine and triethylarsine yield the 1 : 1 complexes of the composition [(L)AgC≡CR][49−51].

The leaving group properties of the cyclopentadienyl group (Cp) have been employed in the reaction of lithium acetylides LiC≡CR (R = Ph, SiMe$_3$) with an *in situ* prepared solution of CpAgPR$'_3$ (R$'$ = Ph, Me) according to equation 19[52].

The 1 : 1 complexes of alkynylsilver compounds with tertiary phosphines build oligomeric or polymeric structures in which alternating [Ag(C≡CR)$_2$]$^-$ units π-donate to

adjacent $[Ag(PMe_3)]^+$ units rather than monomeric $[(R_3P)AgC \equiv CR]$ molecules[51,52].

$$AgNO_3 + PR'_3 + CpLi \longrightarrow CpAgPR'_3 + LiNO_3$$

$$+ LiC \equiv CR$$

$$(19)$$

$$(R = R' = Ph \quad or \quad R = SiMe_3, R' = Me)$$

$$R'_3PAgC \equiv CR + CpLi$$
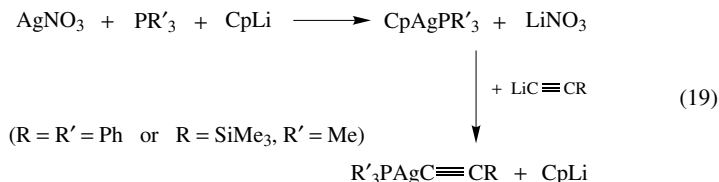
Bis(alkynyl)argentate anions $[Ag(C \equiv CR)_2]^-$ can be obtained in the form of the potassium[47] or the more stable bis(triphenylphosphine)iminium (PPN) salts[53] by the reaction of silver nitrate with an excess of $RC \equiv CK$ (equation 20) or by reacting [PPN][Cl], $AgC \equiv CPh$ and PPh_3 in $1:2:3$ mole ratio (equation 21), respectively. The complexes act as useful alkynylating agents for some gold(I) and platinum(II) compounds.

$$AgNO_3 + 2RC \equiv CK \longrightarrow K[Ag(C \equiv CR)_2] + KNO_3 \qquad (20)$$

$$[PPN][Cl] + 2AgC \equiv CPh + 3PPh_3 \longrightarrow [PPN][Ag(C \equiv CPh)_2] + (Ph_3P)_3AgCl \quad (21)$$
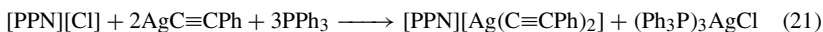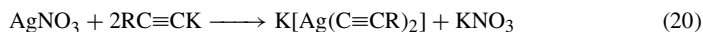
Various homo- and heteronuclear cluster species which contain both σ and π-bonded alkynyl groups have been synthesized and characterized, for example $[Ag_5(C \equiv CPh)_6]^-$ [54], $[Ag_3(C \equiv CPh)_2(dppm)_3]^+$ [dppm = bis(1,1-diphenylphosphino)methane][55], $[Au_2Ag_2(C \equiv CPh)_4(PPh_3)_2]$[56,57] and $[Ag_6Cu_7(C \equiv CPh)_{14}]^-$ [58].

Compounds with silver(I) bonded 'side-on' to olefins are rare[1,2] and are generally very unstable both thermally and chemically. No specific preparative methods have been established. Formation of such adducts has been included in other chapters on structure and bonding.

IV. ARYLSILVER COMPOUNDS

Arylsilver compounds are likewise air, moisture and light sensitive, but are sufficiently thermally stable and thus could be isolated and characterized in selected cases. The first synthesis of an arylsilver species was reported in 1919 by Krause and Schmitz, who studied the reaction of silver nitrate with alkyl aryllead or -tin compounds in alcohol solution and obtained bright yellow precipitates of the composition $(PhAg)_2 \cdot AgNO_3$ (equation 22)[59].

$$3AgNO_3 + 2EtPh_3Pb \longrightarrow (PhAg)_2 \cdot AgNO_3 + 2 EtPh_2PbNO_3 \qquad (22)$$
$$(or\ EtPh_3Sn) \qquad\qquad\qquad (or\ EtPh_2SnNO_3)$$
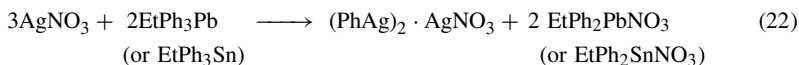
Several other early attempts to prepare phenylsilver had resulted in impure products[1,60−62]. In those preparations silver salts were treated with phenylmagnesium compounds, but in all cases the resulting phenylsilver was contaminated with either magnesium salts or silver salts. The presence of such contaminants, which could not easily be removed, generally resulted in products of low thermal stability.

It was only in 1972 that pure, uncomplexed phenylsilver was isolated for the first time[63]. The method used by Beverwijk and Van der Kerk employs the very slow addition of a solution of silver nitrate in ethanol to a solution of a large excess of trialkylphenyltin or trialkylphenyllead compounds in the same solvent. Although this route affords pure, stable PhAg as a colourless solid, it is cumbersome and restricted to small-scale preparations. These problems are overcome when diarylzinc compounds are used as arylating

agents. The reactions of finely divided solid silver nitrate with ether solutions of a diarylzinc reagent yield the corresponding arylsilver compounds almost quantitatively (equation 23)[64,65].

$$Ar_2Zn + AgNO_3 \xrightarrow{\text{ether}} ArAg + ArZnNO_3 \tag{23}$$

(Ar = phenyl, o-tolyl, m-tolyl, p-tolyl, 2, 6-xylyl)
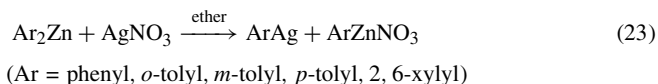
Subsequently, aryllithium and arylmagnesium compounds have been found to be convenient arylating reagents for the preparation of arylsilver compounds containing various substituents at the aryl nucleus. Mesitylsilver $[(2,4,6\text{-}Me_3C_6H_2)Ag]_4$ (**15**)[66,67] and the related complex with the bulkier phenyl substituted ligand $2,4,6\text{-}Ph_3C_6H_2$ (**16**)[68] have been prepared by the reaction of silver chloride with the relevant aryl Grignard reagents in THF (equation 24). The tetrameric formulation of **15** is based on X-ray analysis. The originally suggested monomeric structure of **16** has recently been disproved[69].

$$AgCl + R\text{—}\boxed{}\text{—MgBr} \xrightarrow{\text{THF}} R\text{—}\boxed{}\text{—Ag} + MgBrCl \tag{24}$$
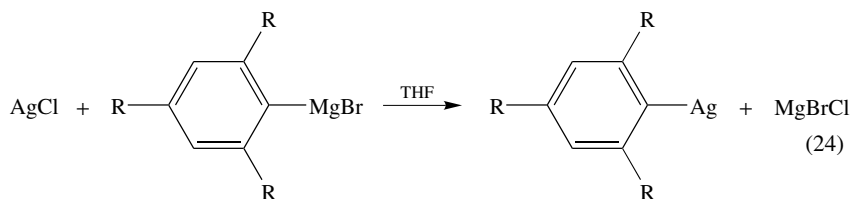
R = Me, Ph

(**15**) R = Me
(**16**) R = Ph
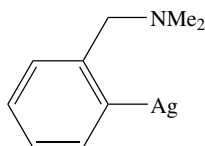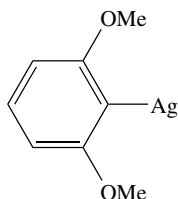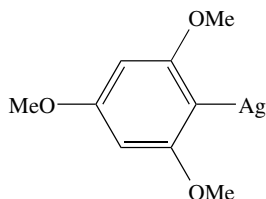
(**17**)   (**18**)   (**19**)

Arylsilver compounds ArAg, where the aryl group carries one or two substituents containing a heteroatom, have been obtained by transmetallation reactions of silver bromide with the corresponding organolithium compounds: {2-[(dimethylamino)methyl]phenyl}silver (**17**)[70], (2,6-dimethoxyphenyl)silver (**18**)[70,71] and (2,4,6-trimethoxyphenyl)silver (**19**)[70]. The compounds show an enhanced thermal stability with decomposition temperatures well above $150\,^{\circ}C$.

The reaction of N-benzyl C-imidazolyllithium with $[(Me_2S)AgNO_3]$ affords the corresponding trimeric (by molecular weight determination) C-imidazolylsilver compound **20** (equation 25)[72]. This compound is related to the (alkoxy)(arylimino)methylsilver compounds (**21**) obtained by the addition of alcoholic potassium hydroxide to an alcohol suspension of an (aryl isocyanide) chlorosilver(I) complex and for which the trimeric

structure shown in equation 26 has been suggested[73].

$$[(Me_2S)AgNO_3] \ + \quad \text{(20)} \quad \longrightarrow \quad \quad + \ LiNO_3 \ + \ Me_2S \qquad (25)$$

(20)

$$3 \ (Ar\!-\!N\!\equiv\!C)AgCl \ + \quad 3 \ ROH \quad \xrightarrow[-3 \ H_2O]{+3 \ OH^-} \qquad (26)$$

Ar = p-tolyl
R = n-Pr, n-Bu

(21)

Comparable with the situation in organocopper chemistry it was found that the arylsilver compounds react with aryllithium compounds to give lithium diarylargentates Ar_2AgLi [Ar = phenyl (**22**), o-tolyl, m-tolyl, p-tolyl, 2,5-xylyl[74], 2-[(dimethylamino)methyl]phenyl (**23**)[75]] (equation 27). The same compounds can be obtained by treating the organolithium compound with silver bromide in a 2 : 1 ratio in diethyl ether (equation 28). Molecular weight determinations and NMR spectroscopic data indicate that the Ar_2AgLi compounds are associated into dimers as tetranuclear mixed metal clusters containing aryl groups bridging the silver and lithium atoms.

(22)   **(23)**

$$ArLi + ArAg \longrightarrow Ar_2AgLi \qquad\qquad (27)$$

(Ar = phenyl, o-tolyl, m-tolyl, p-tolyl, 2,5-xylyl, 2-[(dimethylamino)methyl]phenyl)

$$2ArLi + AgBr \xrightarrow{\text{ether}} Ar_2AgLi + LiBr \qquad (28)$$

A mixed metal-cluster [$Ag_3Li_2Ph_6$] was prepared by treating a cold suspension ($0\,^\circ$C) of AgBr in diethyl ether with a solution of freshly prepared phenyllithium in a 1 : 3 molar ratio[76].

Di- and trinuclear gold(I)–silver(I) complexes containing mesityl groups acting as bridges between the two metal centres have also been described. Treatment of [Au(Mes)(PPh$_3$)] with [Ag(SO$_3$CF$_3$)L] (L = PPh$_3$, tetrahydrothiophene) in a 1 : 1 molar ratio leads to the formation of dinuclear complexes [(Ph$_3$P)Au(μ-Mes)AgL][SO$_3$CF$_3$] (24)[77]. A similar reaction involving [Au(Mes)(PPh$_3$)] and Ag(SO$_3$CF$_3$) in a 2 : 1 ratio affords the trinuclear Au$_2$Ag derivative [{(Ph$_3$P)Au(μ-Mes)}$_2$Ag]SO$_3$CF$_3$ (25)[78].

(L = PPh$_3$, tetrahydrothiophene)

(24)   **(25)**
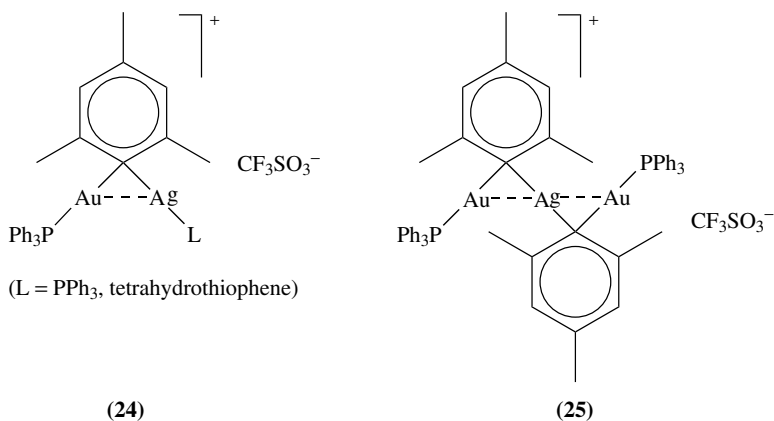
In the earlier preparative studies involving transmetallation with silver nitrate, products were often isolated which still contained silver nitrate starting material, for example (PhAg)$_2 \cdot$ AgNO$_3$[59]. Subsequent studies have revealed that in such mixed-ligand arylsilver compounds the inorganic anions form an integral part of larger aggregates containing both the organic and the inorganic components bound to a central array of silver atoms. Reaction of silver bromide with the arylsilver complex RAg (R = 2-[(dimethylamino)methyl]phenyl) afforded the rust-brown 1 : 1 complex RAg $\cdot$ AgBr in nearly quantitative yield[70]. A 2 : 1 complex of 2-(dimethylamino)phenylsilver (R$'$Ag) with silver bromide has been isolated from the 2 : 3 reaction of 2-(dimethylamino)phenyllithium with AgBr (equation 29)[70]. The molecular weight in benzene shows that this complex exists as a dimer, and thus has R$'_4$Ag$_6$Br$_2$ stoichiometry. Related mixed copper–silver complexes (such as R$'_4$Ag$_4$Cu$_2$Br$_2$ and R$'_4$Ag$_2$Cu$_4$Br$_2$)[70,79] and compounds in which the halide ligands are substituted by anions of low coordination ability (SO$_3$CF$_3{}^-$)[80] have also been described.

$$2R'Li + 3AgBr \longrightarrow (R'Ag)_2 \cdot AgBr + 2LiBr \qquad (29)$$

[R$'$ = 2-(dimethylamino)phenyl]
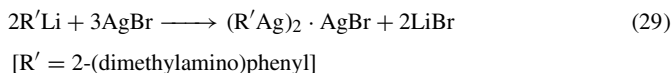
In contrast to the air and moisture sensitivity of most simple arylsilver compounds, perhalogenated aromatic silver compounds are usually stable to water and oxygen.

Neutral perfluorophenylsilver can be obtained from perfluorophenyl lithium and silver trifluoroacetate or by halogen–metal exchange between perfluorophenyl bromide and perfluoroisopropylsilver[81]. C_6F_5Ag with its decomposition temperature above $200\,^\circ C$ is much more stable than the non-fluorinated compound PhAg. The moisture-sensitive anionic bis(pentafluorophenyl)silver complex $Li[Ag(C_6F_5)_2]$ has been prepared from AgCl and C_6F_5Li at $-78\,^\circ C$[82]. The corresponding air- and moisture-stable tetrabutylammonium salts $Bu_4N[AgR_2]$ (R $= C_6F_5$, C_6Cl_5[83], $C_6F_3H_2$[84]) have been obtained by the reaction of silver trifluoroacetate with an excess of LiR followed by the addition of $CF_3CO_2[Bu_4N]$ (equation 30). Treatment of these ionic complexes with equimolar amounts of silver perchlorate lead to precipitation of $[Bu_4N]ClO_4$ and the formation of the neutral compounds RAg (equation 31)[83,84], which have been used as arylating reagents for the preparation of some haloaryl gold(I), gold(II) and gold(III) complexes[84,85].

$$AgO_2CCF_3 + 2LiR \xrightarrow{+CF_3CO_2[Bu_4N]} Bu_4N[AgR_2] + 2LiO_2CCF_3 \qquad (30)$$

$$(R = C_6F_5, C_6Cl_5, C_6F_3H_2)$$

$$Bu_4N[AgR_2] + AgClO_4 \longrightarrow [NBu_4]ClO_4 + 2AgR \qquad (31)$$
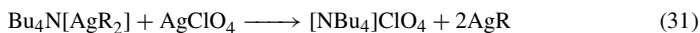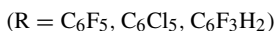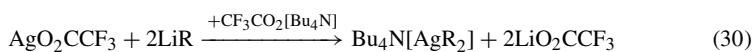
Stable organosilver derivatives of chloroferrocene have been prepared by the reaction of the corresponding boronic acid with silver salts in aqueous ammonia solution (equation 32)[86–88] 2-Silver(dimethylaminomethyl)ferrocene has been obtained by transmetallation between silver bromide and the corresponding lithium ferrocenyl compound[89].

(32)
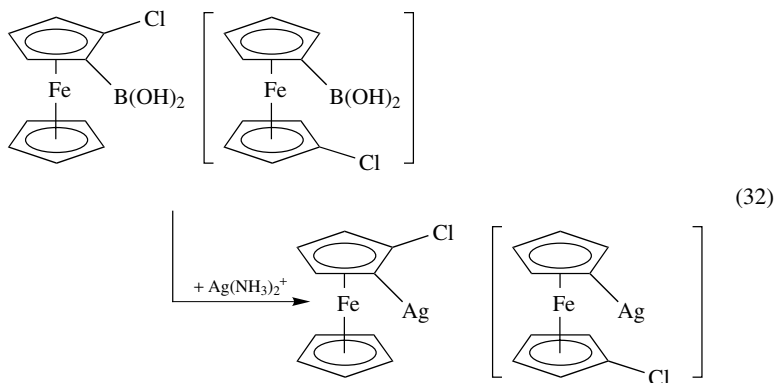
Silver(I) cations form only rather labile π-complexes with aromatic hydrocarbons. The nature of the complex formation may be described as 'solvation' of silver salts in arene solution. Supramolecular framework structures can be isolated upon concentration, and the structure of many of these solvates has been determined[2]. The Ag(I) cations are found to be mostly η^2 or η^3 bound to the arene, but the coordination is weak and arene may be removed already at ambient temperature in a vacuum. This class of compounds for which no 'synthetic strategy' is required, is no longer considered in this chapter which is orientated towards preparative methods. The adducts have not yet found any significant applications.

V. CARBENE−SILVER COMPLEXES

While stable carbene complexes of gold have been known for a long time, the analogues of the lighter group 11 elements could not be isolated, although copper and silver are used extensively as catalysts for reactions in which carbenes are believed to be intermediates[90]. The first stable carbene complex of Ag(I) was described in 1993 by Arduengo and coworkers. The reaction of the stable nucleophilic carbene 1,3-dimesitylimidazol-2-ylidene and silver triflate afforded the homoleptic bis(carbene) adduct of silver (**26**) in good yield (equation 33)[91]. 1,2,4-Triazole-3-,5-diylidene has been used as a building block for the synthesis of a bis(carbene)silver(I) organometallic polymer (equation 34)[92].

$$(33)$$

(26)

$$(34)$$
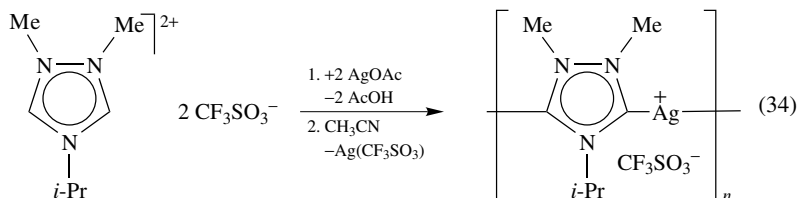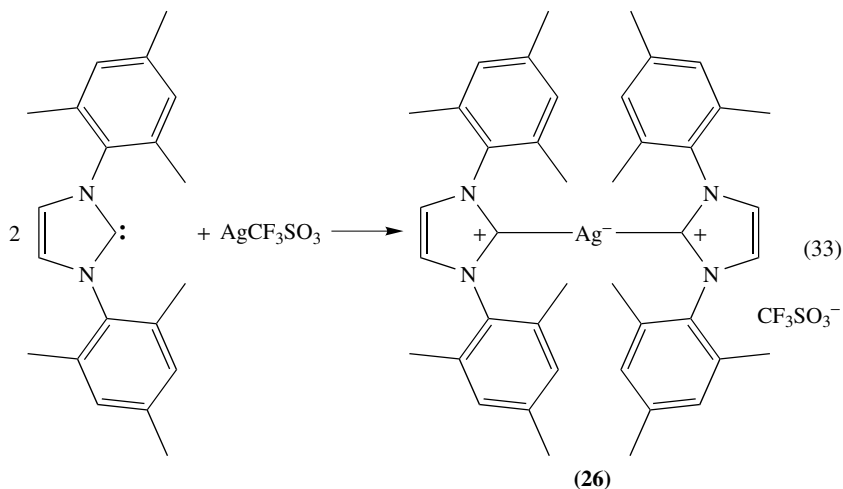
VI. REFERENCES

1. C. D. M. Beverwijk, G. J. M. Van der Kerk, A. J. Leusink and J. G. Noltes, *Organomet. Chem. Rev. (A)*, **5**, 215 (1970).
2. *Gmelin Handbuch der anorganischen Chemie*, Vol. 61, part B5, Springer, Berlin, 1975.
3. G. Van Koten and J. G. Noltes, in *Comprehensive Organometallic Chemistry* (Eds. G. Wilkinson, F. G. A. Stone and E. W. Abel), Vol. 2, Pergamon, Oxford, 1981, p. 709.
4. G. Van Koten, S. L. James and J. T. B. H. Jastrzebski, in *Comprehensive Organometallic Chemistry* (Eds. G. Wilkinson, F. G. A. Stone and E. W. Abel), Vol. 3, Pergamon, Oxford, 1995, p. 57.
5. (a) G. B. Buckton, *Ann. Chem.*, **109**, 225 (1859).
   (b) J. A. Wanklyn and L. Carius, *Ann. Chem.*, **120**, 70 (1861).
6. G. Semerano and L. Riccoboni, *Chem. Ber.*, **74**, 1089 (1941).
7. R. I. Papasergio, C. L. Raston and A. H. White, *J. Chem. Soc., Chem. Commun.*, 612 (1984).

8. J. R. DeMember, H. F. Evans, F. A. Wallace and P. A. Tariverdian, *J. Am. Chem. Soc.*, **105**, 5647 (1983).
9. Y. Yamamoto and H. Schmidbaur, *J. Organomet. Chem.*, **97**, 479 (1975).
10. H. Schmidbaur, C. E. Zybill, G. Müller and G. Kruger, *Angew. Chem., Int. Ed. Engl.*, **22**, 729 (1983).
11. R. Usón, A. Laguna, A. Usón, P. G. Jones and K. Meyer-Bäse, *J. Chem. Soc., Dalton Trans.*, 341 (1988).
12. R. Usón, A. Laguna, M. Laguna, A. Usón and M. C. Gimeno, *J. Chem. Soc., Dalton Trans.*, 701 (1988).
13. Y. Yamamoto and H. Schmidbaur, *J. Organomet. Chem.*, **96**, 133 (1975).
14. J. Vicente, M. T. Chicote, J. Fernandez-Baeza, J. Martin, I. Saura-Llamas and J. Turpin, *J. Organomet. Chem.*, **331**, 409 (1987).
15. H. Schmidbaur, J. Adlkofer and M. Heimann, *Chem. Ber.*, **107**, 3697 (1974).
16. H. Schmidbaur and H. P. Scherm, *Chem. Ber.*, **110**, 1576 (1977).
17. H. Schmidbaur and W. Richter, *Chem. Ber.*, **108**, 2656 (1975).
18. J. Vicente, M.-T. Chicote, I. Saura-Llamas and P. G. Jones, *Organometallics*, **8**, 767 (1989).
19. J. Vicente, M.-T. Chicote, I. Saura-Llamas, P. G. Jones, K. Meyer-Bäse and C. F. Erdbrügger, *Organometallics*, **7**, 997 (1988).
20. M. C. Gimeno, P. G. Jones, A. Laguna and M. D. Villacampa, *J. Chem. Soc., Dalton Trans.*, 805 (1995).
21. S. Wang, J. P. Fackler, Jr. and T. F. Carlson, *Organometallics*, **9**, 1973 (1990).
22. R. Usón, A. Laguna, M. Laguna, M. Nieves Fraile, I. Lázaro, M. C. Gimeno, P. G. Jones, C. Reihs and G. M. Sheldrick, *J. Chem. Soc., Dalton Trans.*, 333 (1990).
23. W. T. Miller and R. J. Burnard, *J. Am. Chem. Soc.*, **90**, 7367 (1968).
24. R. R. Burch and J. C. Calabrese, *J. Am. Chem. Soc.*, **108**, 5359 (1986).
25. K. J. Klabunde, *J. Fluorine Chem.*, **7**, 95 (1976).
26. M. A. Guerra, T. R. Bierschenk and R. J. Lagow, *J. Organomet. Chem.*, **307**, C58 (1986).
27. H. K. Nair and J. A. Morrison, *J. Organomet. Chem.*, **376**, 149 (1989).
28. W. Dukat and D. Naumann, *Rev. Chim. Miner.*, **23**, 589 (1986).
29. U. Geiser, J. A. Schlueter, J. D. Dudek, J. M. Williams, D. Naumann and T. Roy, *Acta Crystallogr.*, **C51**, 1779 (1995).
30. U. Geiser, J. A. Schlueter, J. M. Williams, D. Naumann and T. Roy, *Acta Crystallogr.*, **B51**, 789 (1995).
31. R. Eujen, B. Hoge and D. J. Brauer, *Inorg. Chem.*, **36**, 1464 (1997).
32. R. Eujen, B. Hoge and D. J. Brauer, *Inorg. Chem.*, **36**, 3160 (1997).
33. A. K. Holliday and R. E. Pendlebury, *J. Organomet. Chem.*, **7**, 281 (1967).
34. F. Glockling, *J. Chem. Soc.*, 716 (1955).
35. F. Glockling, *J. Chem. Soc.*, 3640 (1956).
36. F. Glockling and D. Kingston, *J. Chem. Soc.*, 3001 (1959).
37. G. M. Whitesides and C. P. Casey, *J. Am. Chem. Soc.*, **88**, 4541 (1966).
38. W. T. Miller and R. J. Burnard, *J. Am. Chem. Soc.*, **91**, 6532 (1969).
39. R. E. Banks, R. N. Haszeldine, D. R. Taylor and G. Webb, *Tetrahedron Lett.*, 5215 (1970).
40. C. Oehr and H. Suhr, *Appl. Phys. A*, **49**, 691 (1989).
41. P. M. Jeffries, S. R. Wilson and G. S. Girolami, *J. Organomet. Chem.*, **449**, 203 (1993).
42. R. Vestin and E. Ralf, *Acta Chim. Scand.*, **3**, 101 (1949).
43. R. Vestin and A. Somersalo, *Acta Chim. Scand.*, **3**, 125 (1949).
44. C. Liebermann, *Justus Liebigs Ann. Chim.*, **135**, 268 (1865).
45. C. Liebermann and F. Damerov, *Chem. Ber.*, **25**, 1096 (1892).
46. C. Glaser, *Justus Liebigs Ann. Chem.*, **154**, 137 (1870).
47. R. Nast and H. Schindel, *Z. Anorg. Allg. Chem.*, **326**, 201 (1963).
48. J. P. Danehy and J. A. Nieuwland, *J. Am. Chem. Soc.*, **58**, 1609 (1936).
49. D. Blake, G. Calvin and G. E. Coates, *Proc. Chem. Soc.*, 396 (1959).
50. G. E. Coates and C. Parkin, *J. Inorg. Nucl. Chem.*, **22**, 59 (1961).
51. P. W. R. Corfield and H. M. M. Shearer, *Acta Crystallogr.*, **20**, 502 (1966).
52. C. Brasse, P. R. Raithby, M.-A. Rennie, C. A. Russell, A. Steiner and D. S. Wright, *Organometallics*, **15**, 639 (1996).
53. O. M. Abu-Salah, A. R. Al-Ohaly and H. A. Al-Qahtani, *Inorg. Chim. Acta*, **117**, L29 (1986).

54. K. A. Al-Farhan, O. M. Abu-Salah, M. Mukhalalati and M. Jaafar, *Acta Crystallogr.*, **C51**, 1089 (1995).
55. C.-F. Wang, S.-M. Peng, C.-K. Chang and C.-M. Che, *Polyhedron*, **15**, 1853 (1996).
56. O. M. Abu-Salah and C. B. Knobler, *J. Organomet. Chem.*, **302**, C10 (1986).
57. O. M. Abu-Salah, *J. Organomet. Chem.*, **387**, 123 (1990).
58. O. M. Abu-Salah, M. Sakhawat Hussain and E. O. Schlemper, *J. Chem. Soc., Chem. Commun.*, 212 (1988).
59. E. Krause and M. Schmitz, *Chem. Ber.*, **52**, 2159 (1919).
60. E. Krause and B. Wendt, *Chem. Ber.*, **56**, 2064 (1923).
61. H. Gilman and J. M. Sraley, *Recl. Trav. Chim. Pays-Bas*, **55**, 821 (1936).
62. H. Hashimoto and T. Nakano, *J. Org. Chem.*, **31**, 891 (1966).
63. C. D. M. Beverwijk and G. J. M. Van der Kerk, *J. Organomet. Chem.*, **43**, C11 (1972).
64. H. K. Hofstee, J. Boersma and G. J. M. Van der Kerk, *J. Organomet. Chem.*, **168**, 241 (1978).
65. J. Boersma, F. J. A. des Tombe, F. Weijers and G. J. M. Van der Kerk, *J. Organomet. Chem.*, **124**, 229 (1977).
66. S. Gambarotta, C. Floriani, A. Chiesi-Villa and C. Guastini, *J. Chem. Soc., Chem. Commun.*, 1087 (1983).
67. E. M. Meyer, S. Gambarotta, C. Floriani, A. Chiesi-Villa and C. Guastini, *Organometallics*, **8**, 1067 (1989).
68. R. Lingnau and J. Strähle, *Angew. Chem., Int. Ed. Engl.*, **27**, 436 (1988).
69. A. Haaland, K. Rypdal, H. P. Verne, W. Scherer and W. R. Thiel, *Angew. Chem., Int. Ed. Engl.*, **33**, 2443 (1994).
70. A. J. Leusink, G. Van Koten and J. G. Noltes, *J. Organomet. Chem.*, **56**, 379 (1973).
71. O. Wennerström, *Acta. Chem. Scand.*, **25**, 2341 (1971).
72. F. Bonati, A. Burini, B. R. Pietroni and B. Bovio, *J. Organomet. Chem.*, **375**, 147 (1989).
73. G. Minghetti, F. Bonati and M. Massobrio, *Inorg. Chem.*, **14**, 1974 (1975).
74. J. Blenkers, H. K. Hofstee, J. Boersma and G. J. M. Van der Kerk, *J. Organomet. Chem.*, **168**, 251 (1979).
75. A. J. Leusink, G. Van Koten, J. W. Marsman and J. G. Noltes, *J. Organomet. Chem.*, **55**, 419 (1973).
76. M. Y. Chiang, E. Bohlen and R. Bau, *J. Am. Chem. Soc.*, **107**, 1679 (1985).
77. M. Contel, J. Jiménez, P. G. Jones, A. Laguna and M. Laguna, *J. Chem. Soc., Dalton Trans.*, 2515 (1994).
78. M. Contel, J. Garrido, C. Gimeno, P. G. Jones, A. Laguna and M. Laguna, *Organometallics*, **15**, 4939 (1996).
79. G. Van Koten and J. G. Noltes, *J. Organomet. Chem.*, **102**, 551 (1975).
80. G. Van Koten, J. T. B. H. Jastrzebski and J. G. Noltes, *Inorg. Chem.*, **16**, 1782 (1977).
81. K. W. Sun and W. T. Miller, *J. Am. Chem. Soc.*, **92**, 6985 (1970).
82. V. B. Smith and A. G. Massey, *J. Organomet. Chem.*, **23**, C9 (1970).
83. R. Usón, A. Laguna and J. A. Abad, *J. Organomet. Chem.*, **246**, 341 (1983).
84. R. Usón, A. Laguna, E. J. Fernandez, A. Mendia and P. G. Jones, *J. Organomet. Chem.*, **350**, 129 (1988).
85. R. Usón, A. Laguna, M. Laguna, M. N. Fraile, P. G. Jones and G. M. Sheldrick, *J. Chem. Soc., Dalton Trans.*, 291 (1986).
86. A. N. Nesmeyanov, V. A. Sazonova and N. S. Sazonova, *Dokl. Akad. Nauk SSSR*, **176**, 598 (1967); (Eng. transl.) *Proc. Acad. Sci. USSR*, **176**, 843 (1967).
87. V. A. Sazonova, N. S. Sazonova and V. N. Plyukhina, *Dokl. Akad. Nauk SSSR*, **177**, 1352 (1967); (Eng. transl.) *Proc. Acad. Sci. USSR*, **177**, 1193 (1967).
88. A. N. Nesmeyanov, *Pure Appl. Chem.*, **17**, 216 (1968).
89. A. N. Nesmeyanov, N. N. Sedova, Y. T. Struchkov, V. G. Andrianov, E. N. Stakheeva and V. A. Sazonova, *J. Organomet. Chem.*, **153**, 115 (1978).
90. W. Kirmse, *Carbene Chemistry*, Vol. 1, Academic Press, New York, 1971, 85.
91. A. J. Arduengo, III, H. V. R. Dias, J. C. Calabrese and F. Davidson, *Organometallics*, **12**, 3405 (1993).
92. O. Guerret, S. Solé, H. Gornitzka, M. Teichert, G. Trinquier and G. Bertrand, *J. Am. Chem. Soc.*, **119**, 6668 (1997).

CHAPTER **6**

Analytical aspects of organogold and organosilver compounds

JACOB ZABICKY and SARINA GRINBERG

Institutes for Applied Research, Ben-Gurion University of the Negev, Beer-Sheva, Israel
Fax: 972-7-6472969;   e-mail: zabicky@bgumail.bgu.ac.il;
sarina@bgumail.bgu.ac.il

I. ABBREVIATIONS

AAS	atomic absorption spectroscopy
AES	atomic emission spectroscopy
AFM	atomic force microscopy
ASV	anodic stripping voltammetry
CD	circular dichroism
CP-MAS-NMR	cross polarization−magic angle spinning NMR
DPSV	differential pulse stripping voltammetry
EDAX	energy dispersive analysis by X-rays
EPR	electron paramagnetic resonance
ET-AAS	electrothermal (atomization)-AAS
FAB-MS	fast-atom-bombardment MS
FIA	flow injection analysis
GF-...	(atomization by) graphite furnace-..., e.g. GF-AAS, GF-LIF
ICP	inductively coupled plasma AES (also ICP-AES)
ICP-MS	ICP combined with MS detection
ISE	ion-selective electrode
LEED	low-energy electron diffraction
LIF	laser-induced fluorescence
LLE	liquid−liquid extraction
LOD	limit(s) of detection
MIES	metastable induced electron spectroscopy
NAA	neutron activation analysis

NEXAFS	near edge X-ray absorption fine structure spectroscopy
PGE	platinum group elements
PIXE	particle-induced X-ray emission
QCM	quartz crystal microbalance
RAIRS	reflection-absorption infrared spectroscopy
REE	rare earth elements
RNAA	NAA with radiochemical separation
SAM	self-assembled molecular monolayer
SEM	scanning electron microscopy
SERS	surface-enhanced Raman spectroscopy
SNR	signal-to-noise ratio
SPE	solid-phase extraction
SPR	surface plasmon resonance
STM	scanning tunneling microscopy
TEM	transmission electron microscopy
TLC	thin layer chromatography
TPD	temperature programmed desorption
UVV	UV-visible spectroscopy/spectrophotometry
XPS	X-ray photoelectron spectroscopy
XRD	X-ray diffraction
XRF	X-ray fluorescence

II. INTRODUCTION
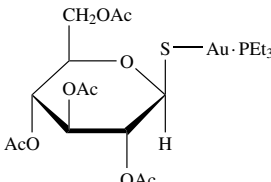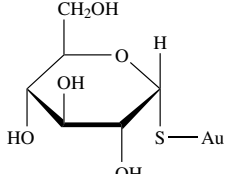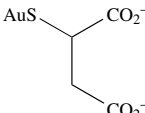
A. Gold, Silver and their Compounds

The choice of subject to celebrate the appearance of the hundredth volume of the series *The Chemistry of Functional Groups* is only an expression of the ancestral attitude toward gold and silver. These have been historically the materials of choice for economic transactions and the elaboration of ornamental objects of high esthetic value. Both are trace elements: The concentration of Au in sea water is about 0.5 ppb and that of Ag is about 10 ppb; Ag is ranked at about the 63rd place in the order of abundance of the elements on the earth crust[1]. The vertical distribution of Au content (ppb range) of certain pelagic marine sediments in Japan was attributed to migration of organometallics[2]. Published data suggest that the Au and Ag content in whole blood of a normal human individual can range up to the same values mentioned above for sea water; for urine it may be up to 0.5 μg Au L^{-1} and 1 μg Ag L^{-1}; the concentration of Pt in these fluids is not detectable[3].

The technological importance of silver as the prime material for photography and of gold plating as a protective shield against chemically agressive environments needs no further comment. An important field of application of gold compounds is as anti-inflammatory agents in the treatment of rheumatism (chrysotherapy). In Table 1 are presented some of these pharmaceuticals; it should be noted that all are Au(I) thiolates.

Some recent applications of gold organometallics are concerned with controlled deposition of the metal, for development of gold bodies of definite shape. Typical examples found in recent publications are fabrication of thin multilayers[5], high resolution lithography for fabrication and repair of wires of submicrometric width or thickness on various

TABLE 1.   Metallorganic drugs containing gold[a]

Name	Formula	CAS Reg. No.
Auranofin (**1**)	CH$_2$OAc ... S—Au·PEt$_3$ ... O ... OAc ... AcO ... H ... OAc	34031-32-8
Aurothioglucose (**2**)	CH$_2$OH ... H ... O ... OH ... HO ... S—Au ... OH	12192-57-3
Aurothioprol	Au—SCH$_2$CH(OH)CH$_2$SO$_3$Na	27279-43-2
Aurothioglycanide	Au—SCH$_2$CONHPh	16925-51-2
Gold keratinate		9078-78-8
Sodium aurothiomalate (**3**)	AuS ... CO$_2^-$ ... xNa$^+$ $(2-x)$H$^+$ ... CO$_2^-$	12244-57-4, 39377-38-3

[a]Taken from Reference 4.

surfaces[6−8] and fabrication of submicrometric cantilever tips for atomic force microscopy (AFM)[9]. The microstructure of gold films grown on a surface by ion-induced deposition, from dimethylgold hexafluoroacetylacetonate (**4**) vapor, was examined by transmission electron microscopy (TEM). The films consisted of segregated gold and carbon nanoscale particles, of morphology that varied with the temperature of deposition[10]. A scanning electron microscopy (SEM) study including energy dispersive analysis of X-rays (EDAX) confirmed the purity of the metal depositions attained on laser radiation of a metallorganic polymeric spread[11]. Polyimide precursors doped with organometallic compounds can lead to final materials endowed with useful mechanical, electrical, optical or other functional properties. For example, 3,3′,4,4′-benzophenonetetracarboxylic dianhydride (**5**) containing the 1,5-cyclooctadiene complex with hexafluoroacetylacetonatosilver(I) (**6**), produces, with various diamines, flexible polymeric films with good thermal stability and optical reflectivity as high as 65%. The films were characterized by differential scanning calorimetry, thermogravimetric analysis, X-ray photoelectron spectroscopy (XPS), TEM and AFM[12−14].

B. Analytical Aspects

1. General

Gold, silver and some of their compounds have found important analytical applications. Gold, silver and silver chloride electrodes are widely used in electrochemical methods.

(4)   **(5)**

(6)
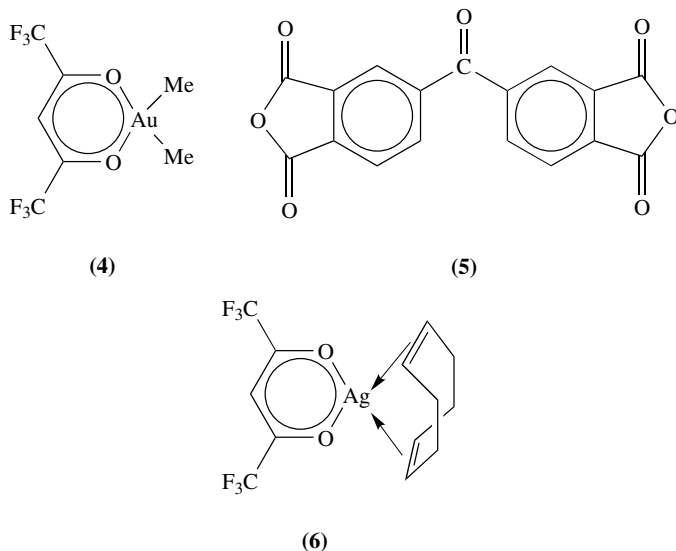
Silver chloride slabs are transparent to a useful range of IR wavelengths and are used as windows of IR sample cells for aqueous solutions. Surface-enhanced Raman spectroscopy (SERS) and allied techniques use silver colloidal suspensions as carriers for the analyte. Organogold compounds serve as a tool for biological investigation of cells and tissues, as illustrated by two examples taken at random from recently published literature: Identification of P-glycoprotein at the membrane of mast-cell secretory granules by the immunogold electron microscopy technique[15]; immunoprobes containing a covalently bonded 1.4 nm gold cluster and a fluorescent label, were applied for simultaneous detection of a pre-messenger-RNA splicing factor by both light and electron microscopy[16].

Analytical methods for gold and silver have been intensely investigated, leading to a large profusion of works in the literature on ore evaluation and on the determination of these metals and accompanying impurities in alloys and electroplating solutions. Gold and silver are discussed in a classical analytical opus published three decades ago[17]. Gold and silver appear in nature as the free metal, and many of their compounds have the tendency to become reduced into that form. It is helpful, therefore, to have an intuitive feeling of the size of a particle involving a certain amount of metal. Figure 1 presents the particle size of a spherical corpuscule of a given mass. Particles of either metal containing 1 ng or 1 nmol have a diameter of nearly 5 or 30 μm, respectively.

Speciation of organometallic compounds containing Au and Ag, on the other hand, was paid only scant attention as a subject for analytical research. The analytical methods that supported research on these compounds had to be dug out from the experimental sections of articles dealing with diverse aspects of chemistry, physics, biochemistry, etc. A review appeared on some of the antiinflammatory drugs shown in Table 1, discussing determination of Au in body fluids and pharmaceutical preparations, and speciation of the compounds and their metabolites. The methods included varieties of atomic absorption spectroscopy (AAS), varieties of neutron activation analysis (NAA), inductively coupled plasma spectrometry combined with mass spectrometric detection (ICP-MS),
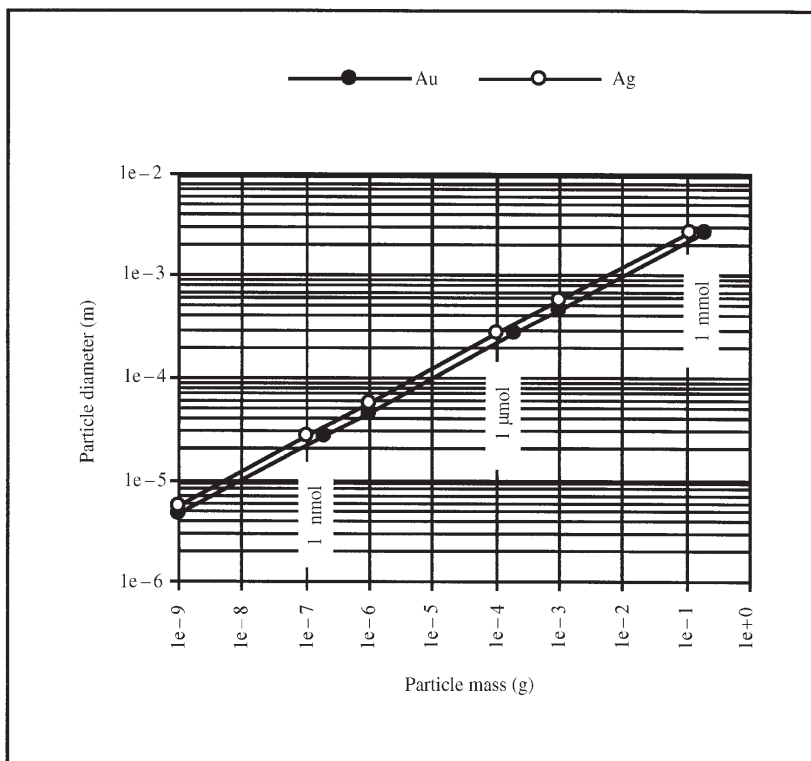
FIGURE 1. Size of spherical gold and silver particles

ultraviolet-visible (UVV) spectroscopy, electrochemical methods, LC, HPLC and post-column derivatization. Sample stability on strorage was also discussed[18].

2. Scope of the chapter

The present chapter is intented mainly for hard core organic chemists, who seldom encounter organometallics, and then, certainly not those of gold and silver. It should be pointed out that the valence-bond formalism of single, double and triple bonds that is customary in ordinary CHNOPS-halogen compounds, loses its sense when various transition metal atoms appear in close proximity in a molecule. A bond is considered to exist when the atoms are closer than the sum of their van der Waals radii. In some cases a bond is drawn even for larger distances, to emphasize a long-range interaction or a geometrical configuration. No fine descriptive details of nomenclature usually employed in organometallic chemistry, e.g. the μ or η nature of certain metal to ligand bonds, are mentioned here.

Although the literature sources of this chapter are mostly of the last five to six years, a fair coverage was made of the instrumental battery and the manipulation techniques

available for the determination and characterization of organometallic compounds containing gold and silver. The reader wishing to expand on a particular subject can easily do so, by retrieving the pertinent articles cited in the references listed here.

Section III presents an overview of the methods for elemental analysis. Frequently involved are matrices rarely encountered by organic chemists, such as rocks for ore evaluation or alloys. Nevertheless, many such methods may be adopted without or with slight changes for sample preparation and end analysis of organometallic samples. Sections IV. A–H deal with structural characterization by instrumental methods. Although other chapters in this book discuss in detail structure and its relation to chemical, electrochemical and spectral properties, the intention here is to awaken awareness of the existence of certain instrumental techniques and illustrate their power for solving certain analytical problems. Section IV. I deals briefly with molecular speciation by chromatographic techniques of organometallics and other compounds. Section V reviews the application of varied instrumental techniques for the molecular and supramolecular characterization of self-assembled monolayers (SAMs) on Au and Ag surfaces. The SAMs are viewed as a particular case of metallorganic compounds that are formed due to the great affinity of metallic Au and Ag for S and to a lesser extent for other atoms and π-electron systems.

III. ELEMENTAL ANALYSIS OF GOLD AND SILVER

A. General Aspects

Other volumes of the *Functional Groups* series contain brief reviews on the analysis of the *organic* elements C, H, N, S and O[19] and more detailed accounts on detection and determination of N[20,21], F, Cl, Br, I[22], Ge, Sn and Pb[23]. The elemental analysis of metallic Au and Ag and their compounds have been reviewed in the past[24,25]. Reviews appeared on methods for analytical speciation of the metallic elements[26] and on many general aspects and instrumental methods for the analysis of trace elements[27]. A brief review was published on various types of element-responsive GC detectors[19,28] and a more detailed one on plasma emission detectors for both GC and LC end analysis[29].

Two subjects of fundamental importance in analysis are sample preparation and end analysis. In many published articles emphasis is placed on one or the other when trying to find the optimal analytical conditions for a certain type of sample. For example, an article dealing with an improved method for trace concentrations of Au may be based on some additives to the usual digestion reagents; once the Au of the sample is converted to an adequate form, measurement can proceed either as described in the article or by alternative methods compatible with the nature of the elaborated sample. A book was published on methods for separation of trace elements, including Ag[30a] and Au[30b]. This section is mainly organized according to the type of end analysis whereas sample preparation methods are mentioned incidentally; however, in Section III.B.1 below some special preparation methods are addressed. Two trends for elemental analysis may be distinguished, the classical macro and semimicro methods and the modern approach, heavily based on expensive instrumentation, allowing faster and more accurate determinations, and extremely low limits of detection (LOD). It should be pointed out that in general the modern trend is much influenced by the stringent demands of environmental and occupational protection agencies.

Several alkyl phosphonates (**7**) were studied for their selectivity in liquid–liquid extraction (LLE) of gold from aqueous solutions. Thus, **7b** was found to be highly selective for aqueous Au(III) against Ag(I), Pd(II), Pt(IV) and Cu(II), in the presence of HCl concentrations larger than 3 M. Various solvents were evaluated as diluents for **7b**[31].

$n\text{-BuO}$ — P(=O) — R — P(=O) — $\text{OBu-}n$, with $n\text{-BuO}$ and $\text{OBu-}n$ substituents

(a) R = — $(CH_2)_n$ —, $n = 2,3,4$

(b) R = — CH_2 — (benzene ring) — CH_2 —

(7)
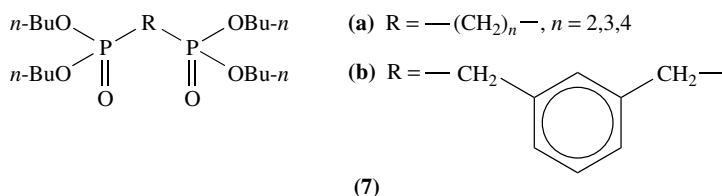
The presence of heteropoly anions in a matrix can have interfering effects on Au and Ag determination, due to possible sequestration of the analyte ions on precipitation of the heteropoly acid. Interference can be avoided by pH increase or addition of complexing agents such as CN^-, resorcinol, ethylenediamine or EDTA[32].

B. Atomic Absorption and Emission

1. General

Much of the research in AAS is concerned with removing or masking interferences present in the matrix in large excess. The tendency is minimization of sample pretreatment, and modification of the subsample in the atomizer immediately before or during atomization. Such operations can be efficiently performed in flow injection analysis (FIA) systems[33].

Some fundamental problems pertaining to elemental analysis by atomic spectroscopy are being investigated using novel approaches and techniques. Various matrix-dependent phenomena take place in the electrothermal unit, including vaporization, atomization and ionization. The influence of these processes on electrothermal (atomization)-AAS (ET-AAS) and ICP-MS analyses was investigated[34]. Profiles of the resonance lines of various elements, including Ag, emitted by hollow cathode lamps were measured. Self-absorption broadening, self-reversal, isotope effects and hyprefine structure, all influence in a complex manner the calibration curves. The absorption line widths and shifts were also measured in an air−acetylene flame, and were found to be in good agreement with calculated values found in the literature for Ag, Li, Mg and Mn[35]. It was proposed to carry out the trace element analysis of high purity samples using a combination of laser-enhanced ionization with the graphite furnace AAS (GF-AAS) method for liquid samples and rod-flame atomization AAS for solid samples without preparation. Avoidance of dilution significantly reduces the background signal and improves the LOD. The method was demonstrated for trace element analysis of high purity orthophosphoric acid, germanium, CdHgTe alloy and silver nitrate; LOD down to 0.001 ppt, which is about 100 times better than that obtained for solutions[36].

The characteristic mass m_0 values for ET-AAS can be calculated by the CHMASS computer program, using specifications such as atomizer type or dimensions and atomization temperature. A variety of theoretical and practical applications have been demonstrated: (i) the effect of atomization temperature on absorption and diffusion coefficients for Ag; (ii) effect of the sample injection hole on ET-AAS sensitivity for Cu as the tube length is increased; (iii) optimization of the atomization temperature for the determination of Cd; and (iv) a comparison of the efficiency of several commercial atomizer designs, using data from the manufacturers' literature. The latter comparison is in favor of platform atomization and integrated absorbance measurements over wall atomization combined with peak height evaluation[37]. A method for linearization of calibration curves in GF-AAS

with Zeeman background correction, based on Newton's method of successive approximations, was tested experimentally in an intermediate concentration region. The linear range of the calibration curves was extended by a factor of $2-3$ for the tested elements, including Ag[38].

Interference by rare earth elements (REE) can be selectively removed from aqueous matrices using a C_{18} cartridge impregnated with 2-ethylcyclohexyl dihydrogen phosphate **(8)** and bis(2-ethylcyclohexyl) hydrogen phosphate **(9)**. Of course, this is a good preconcentration method for the analysis of REE, attaining 200 to 1000-fold enrichment factors. End analysis of other elements in the matrix or the REE eluted from the cartridge is by AAS, ICP or a similar method[39]. An electrothermal vaporization sample introduction device made of tantalum filament was combined with microwave plasma torch atomic emission spectroscopy (AES), leading to reduced sample consumption, and sensitive trace analysis of Ag, Au and other elements. No matrix modifiers were required with this method[40].

(8)   **(9)**
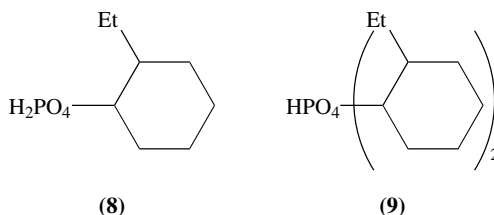
A sample preparation method developed by the US Bureau of Mines for determination of Au in ores consists of comminution to a powder, roasting to oxidize sulfides and carbonaceous materials, elimination of silica and other oxides from the matrix by acid digestion, bromine digestion and LLE of the bromoaurate complex with amyl acetate. The organic solution can be determined by AAS. The method was tested by various independent laboratories, and was found to be satisfactory for the range of 30 ppb up to several thousand ppm[41]. A sample preparation method, claimed to be matrix-independent and allowing high precision Au determinations, consists of roasting the sample at $600-700\,^\circ\text{C}$, dissolving the gold in 2 M HCl solution in the presence of MnO_2, coprecipitating the gold with a solution of K_2TeO_3 and $SnCl_2$, extracting the precipitate with toluene and stripping back with aqua regia for end analysis[42]. Sulfide ores of Ag, Au and other precious metals were digested by a method using aqua regia, Br_2, HF, $HClO_4$ and H_2O_2, without previous roasting. End analysis was by ICP-MS[43].

Sample preparation procedures involving reduction to the metal before redissolution and end analysis require certain precautions when several elements are involved. Au, Pd and Pt are only partially soluble in nitric acid, making their determination difficult in a silver matrix. For analysis of these elements as impurities of silver, two approaches were proposed. One consists of placing a small piece of the silver in the graphite furnace with HNO_3; a strong gas flow removes both the matrix and the analyte to atomization. Alternatively, the undissolved material is introduced to the atomizer as a slurry together with the solution containing the silver[44].

On-line solid-phase extraction (SPE) by ion-exchange and preconcentration using FIA techniques are becoming increasingly popular for trace analysis of heavy metals both by flame AAS and by hydride generation and cold vapor AAS[45−49].

Dynamic ranges of 3 to 6 orders of magnitude for simultaneous multielement analysis can be attained on performing AAS with a continuum source using a diode array UVV detector; LOD 2 μg L^{-1} for the 328 nm Ag absorption line[50].

2. Gold

Solutions of gold with high cyanide content can be preconcentrated by SPE, using a microcolumn packed with tri-n-octylphosphine oxide **(10)**. The high selectivity of this reagent allows separation of the aurocyanide complex from large excess of other metals[51]. A tungsten wire chemically modified with **10** was used for preconcentration of Au traces in waste water. After the extraction step the wire was placed in the hollow of a graphite furnace for direct atomization; LOD 0.2 μg L^{-1}, linearity range 0.4 to 18 μg L^{-1}[52]. Gold in natural waters was preconcentrated on a tungsten bar. End analysis was by ET-AAS, using a molybdenum tube atomizer. The absorption signal was unaffected by matrix elements in 10^5-fold concentrations; at the optimal conditions LOD 1.6 ng L^{-1}, at signal-to-noise ratio (SNR) 3[53]. For the same type of instrumentation, matrix modification by addition of copper nitrate served to eliminate the interferences from 10^4 to 10^5-fold concentrations of foreign elements, at the pyrolysis temperature. The absolute characteristic mass of gold, giving 0.0044 absorbance, was 0.26 pg, corresponding to LOD 38 ng L^{-1}[54]. A method for direct Au determination at ppb levels in plasma was developed, based on GF-AAS with Zeeman effect background correction[55]. The interfering effect of Na(I), K(I), Mg(II), Ca(II), Al(III), Cr(VI), Mn(II), Fe(II), Co(II), Ni(II), Cu(II), Zn(II), As(III), Ru(III), Rd(III), Pd(II), Ag(I), Ir(III), Pt(III) and U(VI) on the determination of aqueous Au(III) by AES, using the 242.795 and 267.595 nm emission lines, was investigated; LOD ca 6 ppb (3σ)[56]. The interference of complexing agents in the AAS determination of gold can be eliminated on addition of excess sodium N,N-diethyldithiocarbamate **(11)**. The mechanism of this effect was discussed[57]. Vanadyl chloride (VOCl$_3$) was found to be a good matrix modifier for Au determination in the presence of heavy metals, by flame AAS or GF-AAS. This was applied to ores digested with a mixture of HF and aqua regia; LOD 0.1 μg g^{-1} of ore or 1 μg L^{-1} after sample preparation; linear range 1 to 120 μg L^{-1}[58]. Au(III) in river bottom and sea floor was preconcentrated on activated carbon containing dithizone **(12)**, at pH 3.0; a suspension of the carbon was injected into a metal furnace AAS; LOD 0.4 μg Au L^{-1}, for 100 mL samples (SNR 3)[59].

$(n\text{-}C_8H_{17})_3PO$ Et_2NCS_2Na

$$S = C \begin{cases} NHNHPh \\ N = NPh \end{cases}$$

(10)   **(11)**   **(12)**
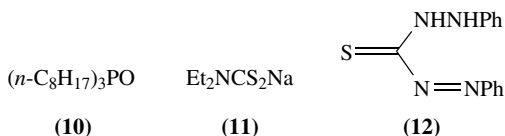
The interferences caused by high concentrations of NaCl in the matrix were investigated, for the AAS determination of Au and Fe in solution using atomization by cathodic sputtering in a glow discharge. Modification of the atomizing method effectively eliminates the interference for NaCl concentrations as high as 10% (w/v). This is important for trace analysis of sea water, and other NaCl-containing substances[60]. The atomization efficiency of GF-AAS approaches 100% for high temperature operation. This feature was applied to standardless Au determination of geological samples, using Pd as matrix modifier[61].

Gold in collected atmospheric particular matter was determined by digestion, LLE and two-color laser-induced fluorescence (LIF) with atomization in a graphite furnace (GF-LIF); absolute instrumental LOD 1 fg, corresponding to an atmospheric concentration of 50 fg m^{-3}. These LOD values increase by a 20-fold factor due to blank limited noise[62].

LOD in the $ng\,L^{-1}$ range were found for GF-LIF determinations of gold and Pt-group elements (PGE) dissolved in pure water[63].

Gold and platinum in a TRIS buffer were determined by ICP-AES, in the presence of blood plasma proteins (albumin and transferin, respectively), using direct injection nebulization; LOD 0.03 µg $^{195}Pt\,L^{-1}$ and 0.08 µg $^{197}Au\,L^{-1}$; precision *ca* 0.5% over the $1-100\,\mu g\,L^{-1}$ range, with linear dynamic range of four orders of magnitude with no interferences from the proteins. Bonding of the antiarthritic drug triethylphosphine gold(I) chloride **(13)** to albumin at various Au:albumin molar ratios was investigated using this method[64]. Preconcentration of gold from complex matrices, containing large amounts of alkaline and alkaline earth metals and other components, can be achieved by SPE with cotton fibers impregnated with thioacetic acid. After separation of the adsorbate with hot aqua regia, Au was determined by ICP-AES[65]. Solutions resulting from digestion of ores containing $0.1-10$ ppm of Au were preconcentrated in a FIA system using a microcolumn of Amberlite XAD-8 and eluted with ethanol into the AAS nebulizer[66].

$$Et_3PAuCl$$

(13)

Mineral samples containing PGE or gold in native or sulfide form were treated with dry chlorine and extracted with dilute HCl. The end analysis was by ICP-MS; LOD $<1\,ng\,g^{-1}$ with recoveries better than 90%[67]. After preconcentration by sorption on a foamed plastic column and desorbing with ammonium iodide solution, gold was determined by arc emission spectrometry, using specially developed gas chamber profile electrodes; LOD $0.2\,ng\,g^{-1}$, limits of quantation $0.5\,ng\,g^{-1}$ [68]. A method for gold determination in sea water at fM concentration levels involves preconcentration as $[Au(CN)_2]^-$ complex by ion exchange, using ^{195}Au as radiotracer to monitor recovery. End analysis by ICP-MS; LOD *ca* 10 fM for 4 L sea water preconcentrated to 1 mL, RSD 15% at 100 fM[69].

Scintillation emission spectral analysis provides information on the number and size of the particles containing a specific element being determined. It may be applied to ores, rocks, soil, ashed plants and other materials. The method is very fast and is sensitive to gold and the PGE $(3-30$ ppb)[70]. The spark spectrum of Au in the 54.0 to 208.0 nm region yields 745 new lines for Au(III), raising the number of classified lines to a total of 1040. As many as 134 new energy levels were added to a total of 196. The new levels belong to the doubly excited configurations $5d^76s^2$ and $5d^76s6p$ and to the mixed group $5d^8(6d+7s)$. The theoretical probabilities of selected strong transitions were calculated[71].

3. Silver

A method for direct Ag determination at ppb levels in blood plasma was developed, based on GF-AAS with Zeeman effect background correction[55]. Selective preconcentration of several metal ions can be accomplished with poly(chlorotrifluoroethylene). Thus, after SPE of the complexes of Ag(I), Cd(II) or Cu(II) with bismuthiol II **(14)** at pH 2 and elution with tetrabutylammonium chloride in acetone, the eluate was directly determined by AAS[72]. Sub $ng\,L^{-1}$ concentrations of Ag(I) may be preconcentrated by sorption on finely ground dithizone **(12)**, filtration, dissolution of the dithizone in $CHCl_3$ and end analysis by ET-AAS; LOD $1\,ng\,L^{-1}$ with no interference by humic acids, fulvic acids or soluble silica[73]. Ag(I) in river bottom and sea floor was preconcentrated on activated carbon containing dithizone **(12)**, at pH 1.5; a suspension of the carbon was injected into a metal furnace AAS; LOD 0.05 µg $Ag\,L^{-1}$, for 100 mL samples at SNR 3[59].

Ph
|
N—N
/ \\
S   SK
\\ /
S
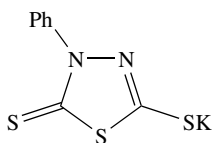
(14)

The palladium ion proved to be a good matrix modifier for trace analysis of silver in water solution, including sea water; LOD $0.5–1.1$ $\mu g\,L^{-1}$ (20 μL sample)[74]. Trace amounts of silver in high purity aluminum were determined after acid dissolution of the metal and LLE of silver N,N-diethyldithiocarbamate **(15)** with xylene at pH 2.5 to 4. The resulting solution was back-extracted into a small amount of aqueous nitric acid for end analysis by GF-AAS[75]. ET-AAS with a molybdenum tube atomizer was applied for Ag determination. The metal atomizer was protected from oxidation by adding hydrogen to the argon purge gas. Ammonium thiocyanate as chemical modifier eliminated matrix interferences[76]. The silver content of plants was determined after digestion with sulfonitric mixture, LLE of silver N,N-diethyldithiocarbamate **(15)** with methyl isobutyl ketone and AAS of this solution[77]. Silver in natural and spiked distilled water was determined after addition of Fe(III) ions, precipitation with sodium sulfide, redissolution of the precipitate, LLE of **15** with methyl isobutyl ketone and AAS of this solution; LOD 5 ng Ag L^{-1} (SNR 2)[78]. The Ag and Mn content of an organic matrix (cocaine and heroin) was determined by ET-AAS, after dissolving it in dilute nitric acid and adding palladium nitrate as chemical modifier to stabilize the analytes at the charring temperatures of $1000–1300\,^\circ C$; LOD 2.3 and 6.9 ng g^{-1} of solid alkaloid for Ag and Mn, respectively[79]. Silver and cesium in soil and fungal samples were determined by ET-AAS, after microwave-assisted digestion with aqua regia; LOD for soil: 0.02 mg Ag g^{-1} and 0.09 mg Cs g^{-1} [80]. A rapid method for determination of silver in blood consists of diluting the sample with a buffered solution of Triton X-100 **(16)** followed by ET-AAS using wall atomization with a pyrolytically coated tube; analytical recovery $98\pm3\%$, LOD 0.1 $\mu g\,L^{-1}$, which is sufficient for detection of occupational exposure[81].

Me   Me
| |
Me—C—CH$_2$—C—⟨ ⟩—(OCH$_2$CH$_2$)$_n$OH
| |
Me   Me
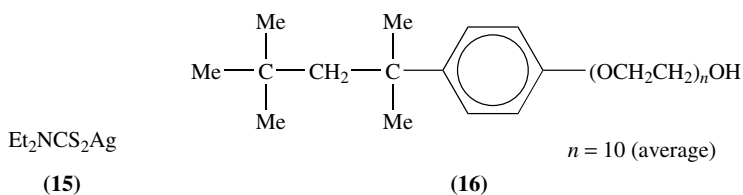
Et$_2$NCS$_2$Ag $n = 10$ (average)

(15)   **(16)**

Trace impurities present in high purity potassium hydrogen phthalate were separated from the matrix using Chelex-100 ion exchange resin. The desorbed elements were determined by ICP-MS, using electrothermal vaporization; LOD $1–10$ ng g^{-1} for eight elements, including silver, which is lower by 1 to 2 orders of magnitude than ICP-MS using a conventional nebulizer[82].

Atomic LIF in conjuction with a graphite tube of novel design was applied to ultratrace analysis of silver; LOD 4 ppt for solutions in pure water and 9 ppt for sea water at 1 : 1 dilution. A two-fold suppression of the fluorescence signal was observed for sea water

over a concentration range of 6 orders of magnitude. Certified soil reference samples were also tested with good results. A silver concentration of 14 $ng\,L^{-1}$ was found for a coastal Atlantic water sample[83].

C. Spectrophotometric and Colorimetric Methods

1. Gold

The tiresome sample preparation methods involved in gold determination digestions were overcome by extracting the sample with a $NaBr-H_2SO_4-H_2O_2$ solution at room temperature, concentrating the gold ions with plastic foam, desorbing the gold ions with a dilute Na_2SO_4-NaCl solution at pH 8 and forming a ternary complex with Michler's thioketone (17) and sodium dodecylbenzenesulfonate (18). End analysis for sample concentrations below 20 $ng\,g^{-1}$ was carried out by visual comparison with a set of standards, while for higher concentrations a fiber-optics colorimeter could be used; LOD 0.5 $ng\,g^{-1}$. The simplicity of the method makes it appropriate for field applications[84]. A bromine hydrobromic acid mixture was proposed as an alternative digestion system for gold analysis. The gold dissolved in bromine is coprecipitated with tellurium, redissolved in aqua regia and determined by AAS[85].

$$C_{12}H_{25}C_6H_4SO_3Na$$

                    (17)   **(18)**
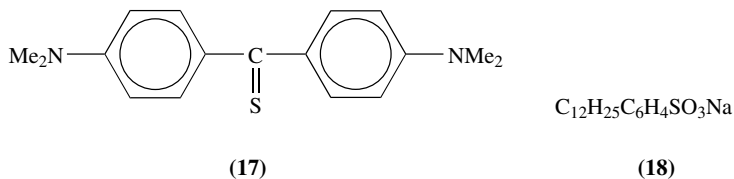
Dithizone (H_2Dz, 12) deserves special attention because of the wide variety of applications it has found in inorganic analysis. It forms intensely colored complexes with the so-called 'dithizone metals'. The dithizonate ion may assume two types of structure, namely a primary dithizonate (MHDz, 19) and a secondary dithizonate (MDz, 20). The metallic ions may have charges other than those shown in reaction 1, resulting in primary and secondary dithizonates of the appropriate metal-to-dithizone ratio. In some cases the metal ion may combine in either form, depending on the pH of the solution, as shown in reactions 1 and 2; however, the primary form is usually the most important one in analysis. Elaborate schemes have been devised for the analysis of mixtures of dithizone metals, including LLE, pH changes and the use of masking reagents[86,87]. Au(III) forms a primary complex $[Au(HDz)_3]$ at low pH, λ_{max} *ca* 405 nm, ε *ca* 24 000 ($CHCl_3$)[88].

    (MDz, **20**)   (H$_2$Dz, **12**)   (MHDz, **19**)

$$2MDz \xrightleftharpoons{+2H^+} M(HDz)_2 + M^{2+} \qquad (2)$$
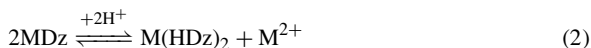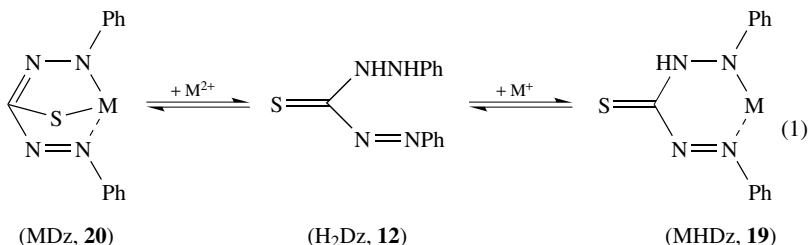
8-Hydroxy- and 8-aminoquinolines form stable bidentate complexes with many transition element ions. Further enhancement of UVV absorbance can be attained by introduction of azo chromophores. 7-(2-Pyridylazo)-5-chloro-8-hydroxyquinoline (PACHQ, **21**) yields a violet 2 : 1 ligand-to-Au(III) complex at pH 9.5; linearity range from 0 to 7.87 mg L^{-1} [89]. 5-(4-Sulfophenylazo)-8-aminoquinoline (SPAQ, **22**) forms a 1 : 3 Au(III)-to-ligand complex, λ_{max} 605 nm, ε 148 000, in alkaline solution, in the presence of cetyltrimethylammonium bromide; linearity range from 0 to 2 ppm[90]. Methylene blue (**23**) forms an association complex with $[AuI_2]^-$ of intense color; in MeOH λ_{max} 660 nm, $\varepsilon 1.9 \times 10^5$, obeying Beer's law at concentrations up to 1 ppm[91].
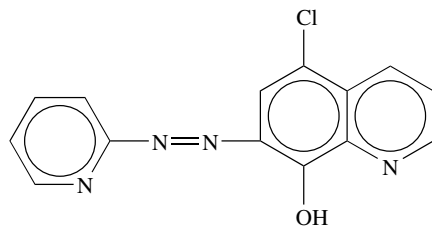
(21)
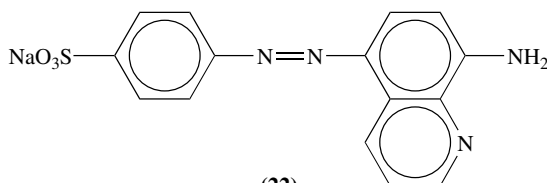
(22)
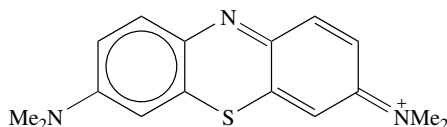
(23)

A simple and sensitive method for Au(III) determination is based on color development with the combination of N,N-dimethyl-p-phenylenediamine (**24**) and potassium persulfate ($K_2S_2O_8$) in acidic media; linearity range from 0 to 300 μg L^{-1}, λ 552 nm, $\varepsilon 1.9 \times 10^6$. The method was used for Au assay in the antirheumatic drugs auranofin (**1**) and gold sodium thiomalate (**3**) (Table 1)[92]. Au(III) in the aqueous solution resulting from digestion of the original sample was selectively extracted into CHCl$_3$ containing tri-n-octyl phosphine oxide (**10**). This solution was treated in a FIA system with a reverse micelle dispersion of luminol (**25**). The intensity of the chemiluminescence accompanying the Au-catalyzed oxidation of **25** is proportional to the Au concentration. No interference with the chemiluminescence induced by Au was found for Li(I), Na(I), K(I), Ca(II), Ba(II), Mn(II), Ni(II), Pd(II) and Pb(II); some ions had an enhancement effect: A moderate one by Cr(III), Co(II) and Cu(II), and an especially strong one by Fe(III). Some ions showed an inhibitory effect: Pt(II) and Ag(I). The interferences can be avoided by increasing the

extraction selectivity[93]. The luminol (25) luminescent reaction was directly measured after introducing in the chemiluminescence chamber a sample of $[AuCl_4]^-$ preconcentrated by SPE on foamed plastic[94].

Me$_2$N—⟨benzene ring⟩—NH$_2$

(24)

(25)
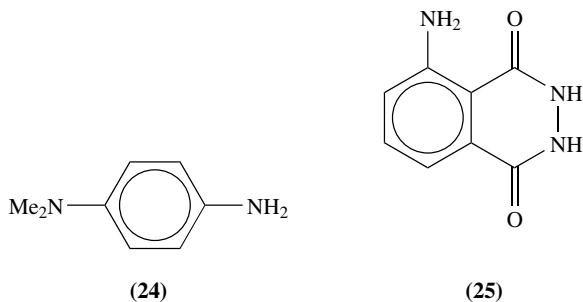
Au(III) can be extracted from bromide-containing media with triphenylphospine sulfide dissolved in toluene. This permits separation from Cu(II), Pb(II), Pd(II) and Pt(IV). End analysis was by UVV spectrophotometry[95]. Separation of $[Au(CN)_2]^-$ from cyano complexes of other metal ions was performed by anion chromatography of the cyano complexes. The elution order of the various species depended on the concentration of sodium perchlorate in the eluting solution. Higher selectivity for gold was achieved when the eluant contained ammonia. Measurement was at 215 nm; LOD 5 μg Au L^{-1} using direct injection[96].

2. Silver

The abatement of absorption of nickelocyanide ions (26), due to reaction with silver ions, measured at 275 nm at pH 10, was applied for a fast determination of Ag in a FIA system; linearity in the 10 to 400 μM range, RSD about 1%[97]. The anionic complex of Ag(I) with 2-carboxybenzaldehyde thiosemicarbazone (27) was extracted into a solution of Adogen 464 (28) in toluene and measured spectrophotometrically at 345 nm[98].

CO$_2$H

CH=NNHCNH$_2$
‖
S

$[Ni(CN)_4]^{2-}$

MeNR$_3$Cl$^-$

(R = C$_8$H$_{17}$ to C$_{10}$H$_{21}$)

(26)   (27)   (28)
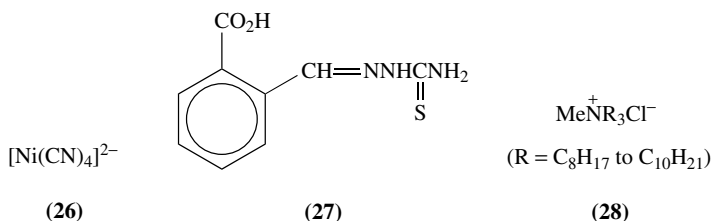
Silver(I) yields a primary dithizone complex (19 in reaction 1) at low pH, λ_{max} 460 nm, ε 30 500 (in CCl$_4$)[87]. This complex in the presence of cetyltrimethylammonium ions has λ_{max} 565 nm, ε 55 000 (in H$_2$O)[99]. Instead of densitometry of Ag deposited on X-ray film images and other gel matrices, analysis can be carried out by dissolution with nitric acid, neutralization, LLE with a dithizone solution and spectrophotometric determination; λ 600 nm, ε 32 800[100].

(29)

(30)

(31)

(32)

(33)

(34)

(35)   **(36)**   **(37)**
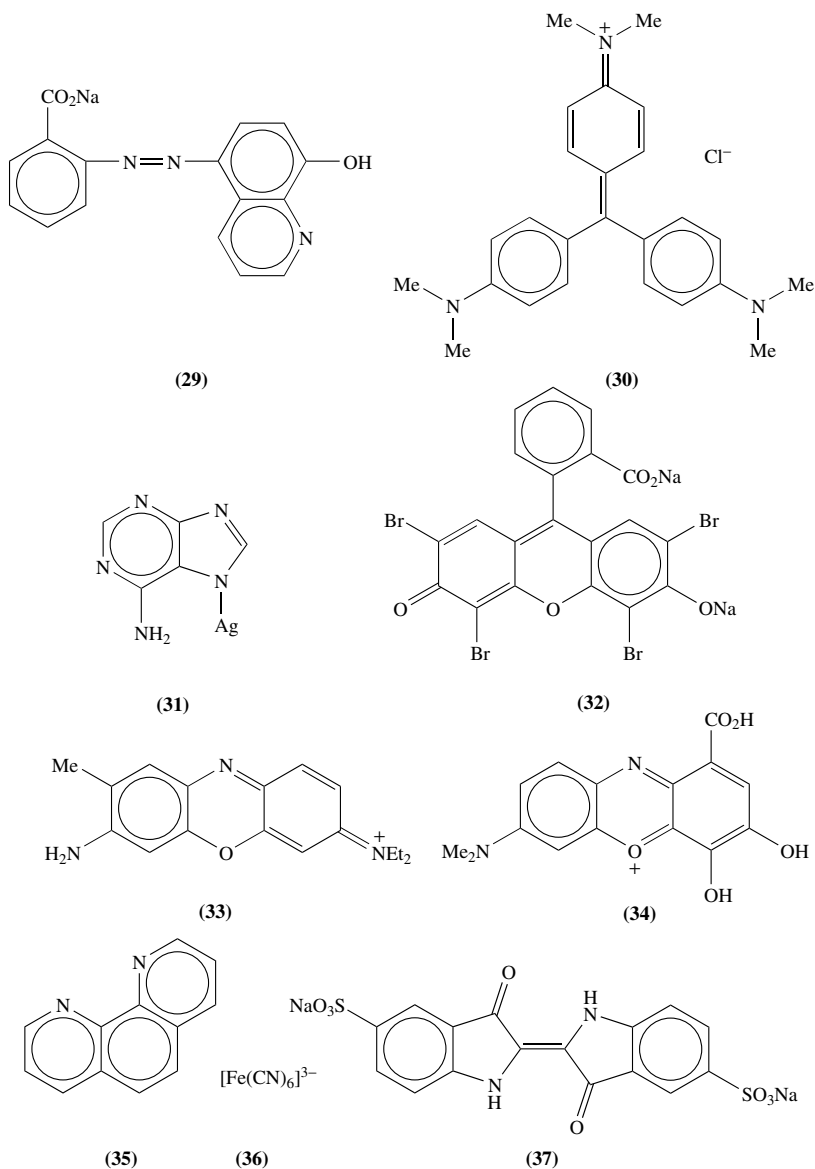
Silver ions yield an intensely purple complex with sodium 2-(8-hydroxyquinolin-5-ylazo)benzoate **(29)** in tartrate buffer at pH 5.2 to 6.1; λ 525 nm, ε 36 500[101]. A method involving a large multiplication factor consists of decomposition of ferrocyanide complex ions $[Fe(CN)_6]^{4-}$ with Ag(I) to give $[Ag(CN)_2]^-$. In the presence of crystal violet (CV,

30) a complex ionic associate of formula $\{(CV)^+[Ag(CN)_2]^-\}\cdot 3\{(CV)_4^+)[Fe(CN)_6]^{4-}\}$ is formed, with $\varepsilon 1.4 \times 10^6$ and Ag : CV molar ratio of 1 : 13[102]. Formation of an association complex between adenine siver **(31)** and eosin **(32)** affords a sensitive method for Ag(I) determination; $\varepsilon 1.1 \times 10^5$ at 560 nm. A further five- to ten-fold sensitivity enhancement may be achieved by third-order derivative spectrophotometry and by fluorescence quenching[103].

Kinetic spectrophotometric determination methods for Ag(I) were proposed, based on the strong catalytic effect of this ion on the controlled oxidation of various dyes, by measuring the rate of change of absorbance. Some recently published examples are Ag(I)-catalyzed peroxodisulfate oxidation of brilliant cresyl blue **(33)**[104] or gallocyanine **(34)**[105], both in the presence of 1,10-phenanthroline **(35)**; and hexacyanoferrate **(36)** oxidation of indigo carmine **(37)**[106].

A column of silver chloranilate was used for chloride ion determination in a FIA system. According to reaction 3, the column liberates into the solution violet chloranilate ions **(38)**, that are measured with a spectrophotometric detector at 530 nm. The method is fast (30 samples h^{-1}) and was applied to the analysis of fresh and waste waters (1–20 ppm Cl$^-$) with negligible interference of other anions[107].

$$+ 2Cl^- \longrightarrow \qquad\qquad + 2AgCl \qquad (3)$$

(38)
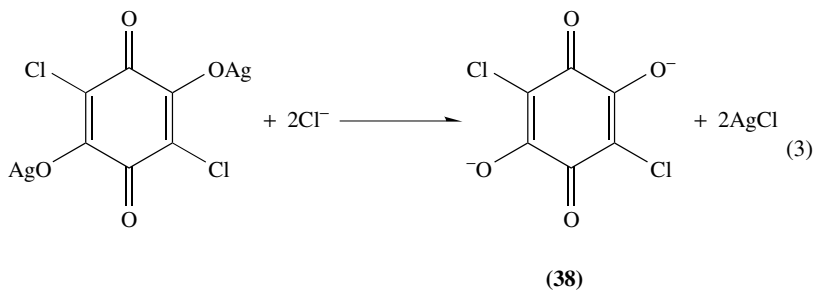
D. Miscellaneous Spectral Methods

1. Gold

Thiourea is used instead of cyanide for gold leaching[108, 109]. A method for determination of gold was based on leaching with thiourea, removing the gold from the leaching solution by SPE with activated charcoal and end analysis by energy dispersive X-ray fluorescence (XRF) of the charcoal; LOD 38 and 45 ng g^{-1} for the L_α and L_β lines, respectively[110]. XRF determination of gold in geological samples is hampered by the high content of elements that have energetically similar K and L series bands and by the strong absorption of the Au XRF emission by the base elements present in the matrix. A preconcentration and separation step for gold in digestion solutions was performed with tributyl phosphate, followed by elution with aqueous thiourea and XRF analysis using a ^{109}Cd radioisotope excitation source; LOD 10 ng g^{-1} ore for 25 g sample[111]. Gold was determined by XRF of the K X-rays that were excited using a ^{57}Co radioisotope source and a high purity Ge detector with a range of energies from 1 keV to 4 MeV. The source employed has an advantage over other possibilities to excite X-ray emission: High sensitivity at 1 ppm concentrations, lack of interference by other elements present in the matrix and performance of analysis using large samples[112]. Accelerator MS was applied for *in*

situ determination of Au and PGE in sulfide minerals[113]. Due to the toxic effects of gold-containing drugs on the kidney, a mobile XRF unit was proposed for *in vivo* monitoring of Au levels in patients undergoing chrysotherapy of rheumatoid arthritis[114,115].

2. Silver

EDAX coupled to SEM is a useful tool for elemental analysis of samples that are too small to handle or difficult to separate from the matrix. The average analysis of heavy elements contained in a field of *ca* 1 μm^2 area can be easily determined. The Ag content of the complex phases mentioned in entry S-3 of Table 3 could be estimated for each single crystal in the observation field, from the EDAX results for the heavy atoms S, Cl and Ag, gathered during SEM observations[116,117].

Electrospray MS may be developed into a simple low-cost method for elemental speciation. Thus, spectra with M^+ as the dominant species were obtained for aqueous and methanolic solutions containing the alkali metals and various transition metals, including M = Ag. A number of background ions, such as MH^+, MO^+, MOH^+ and $MOH(H_2O)^+$, also appeared[118,119].

E. Chemical and Electrochemical Methods

1. Gold

Gravimetric determinations by precipitation of pure gold with various reducing agents were proposed. Electrochemical precipitation was especially recommended[25]. A standard assay for Au in aurothioglucose (**2**, Table 1) consists of gravimetric determination by reduction to the metallic state[120]. A gravimetric method was proposed for Au and other precious metals, based on reduction with dipyrone (**39**)[121]. Quartz crystals can oscillate at a stable frequency when immersed in a solution, and may serve as central devices for the design of a quartz crystal microbalance (QCM). The frequency varies with the density, viscosity, specific conductivity of the solution and the mass adsorbed on the crystal. A sensitive piezoelectric method for Au(III) determination is based on measurement of the rate of change of the vibration frequency during Au electrodeposition on a gold-plated quartz crystal. The method is very fast, as the deposit need not be removed; linearity in the range of 0.15 to 2.50 ppm. Of the 21 possibly interfering metals tested with this method, only Ag(I), Hg(II), Pd(II) and Pt(IV) were codeposited with gold[122]. When such ions interfere, the $HAuCl_4$ complex can be previously extracted into Et_2O[123].
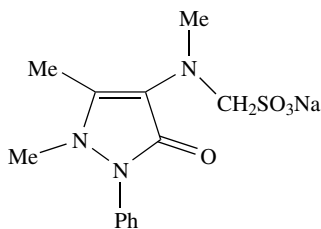
(39)

All gold titrations are based on reduction of Au(III) to either Au(I) or Au(0). Various reducing reagents have been proposed: Fe(II) sulfate, oxalic acid or an oxalate, ascorbic

acid and potassium iodide[25]. Titration with iodide precedes with gold iodide precipitation, as shown in reaction 4; the end-point can be detected by derivative potentiometry. Alternatively, the titration can be carried out in the presence of As(III) and Ce(IV), whence iodide is regenerated according to reaction 5 for participation in reaction 4; as long as Au(III) is present in solution the concentration of iodide ions is very low; the end-point can be detected by controlled current potentiometry, as the slow reaction 6 becomes accelerated in the presence of excess iodide ions acting as catalyst. This was applied for assay of the gold present in auranofin (**1**, Table 1), after the drug was oxidized to Au(III) by digestion with aqua regia[124]. Good results by the 'catalytic' method were claimed for the determination of Au(III) and other precious metals as main components of some alloys[125].

$$Au(III) + 3I^- \longrightarrow AuI(s) + I_2 \tag{4}$$

$$I_2 + As(III) \rightleftharpoons 2I^- + As(V) \tag{5}$$

$$2Ce(IV) + As(III) \rightleftharpoons 2Ce(III) + As(V) \tag{6}$$
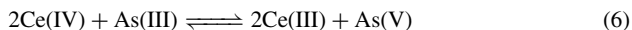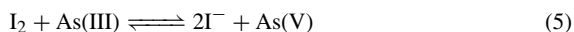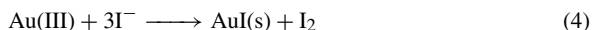
A potentiometric titration method was proposed based on the reduction of Au(III) with Co(II), according to reaction 7. The process takes place at 50 °C and pH 4 to 6, in the presence of excess ligand L, which may be either 2,2′-bispyridine (**40**) or 1,10-phenanthroline (**35**). No interference was observed for many common metal ions; interference by Ag(I) and Pd(II) could be overcome but not that of Hg(II), Fe(III) or Pt(IV)[126].

$$Au(III) + 3[Co(II)L_3] \longrightarrow Au(0) + 3[Co(III)L_3] \tag{7}$$
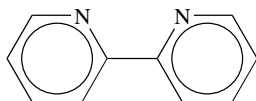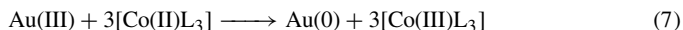
(**40**)

A selective anodic stripping voltammetry (ASV) method for Au(III) consists of previous activation of a glassy carbon electrode with small amounts of gold, and carrying out the reduction at +0.4 V *vs* Ag/AgCl electrode; linearity of the gold stripping peak current in the 0.05 to 1 μM range, LOD 4 nM, RSD 4.2% (*n* = 5) for 0.2 μM of HAuCl$_4$[127]. A gold-activated graphite electrode was used to eliminate or largely reduce the effect of other ions in the determination of trace concentrations of gold by ASV. Thus, a linear dependence for the gold stripping current on concentration was found for Au(III) from 5×10^{-8} to 1×10^{-6} M in the presence of 1 M of Cu(II) ions[128].

Various preconcentration agents were investigated as modifiers for working electrodes. Gold traces in aqua regia, hypochlorite-iodine solution and other solutions of high redox potential can be determined by direct current ASV, using as working electrode a graphite electrode impregnated with epoxy resin and polyethylene amine; RSD ≤0.2 for solutions with oxidation-reduction potential >0.9 V[129]. Carbon paste electrodes modified with tri-isooctylamine selectively extract gold from its solutions; after open circuit immersion in the stirred sample the electrode is transferred to an HCl solution for differential pulse voltametry[130]. Au(III) can be preconcentrated on carbon paste electrodes modified with

thiobenzanilide (PhCSNHPh) followed by voltammetric measurements[131]. Preconcentration of Au(III) with Adogen 464 **(28)** was investigated and applied to its determination in mud by ASV[132]. Rhodamin B **(41)** was proposed as modifier for carbon paste electrodes. After open circuit preconcentration, measurement is carried out by differential pulse voltametry; 5 μg L^{-1} could be analyzed, with linearity up to 10 mg L^{-1} [133].
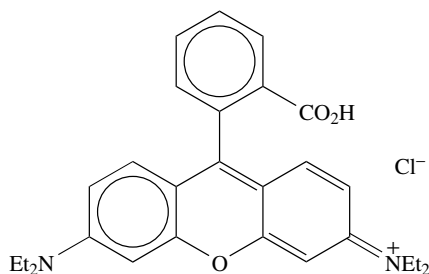
(41)

Capillary electrophoresis of cyanide[134] and chloride[135] complexes of Au(III) and Ag(I) and other transition metal ions have been investigated as a separation method; it gave good results in the mid ppb concentration range.

Some problems may arise in the determination of Au(I) when acetonitrile is present in the solution. Thus, instead of the expected disproportionation of Au(I) to yield a ratio Au(III) : Au(0) = 1 : 2, in the pH range from 2 to 12 only less than 2% was converted to Au(III) and the rest to Au(0). A study involving voltammetric reductions, alkalimetric titrations and UVV spectrophotometric measurements led to the postulation of the complexes $[Au(MeCN)_2]^+$, $[Au(OH)(MeCN)]$ and $[Au(OH)]$, e.g. as in reaction 8. The latter two species may decompose yielding hydroxy radicals and ultimately oxygen, as shown in reactions 9–11. Furthermore, at higher pH values, the presence of the gold hydroxide species shifted the onset potential of Au(I) reduction to more negative values and accelerated the nonelectrochemical reduction rate[136].

$$Au^+ + H_2O \rightleftharpoons Au(OH) + H^+ \qquad (8)$$

$$Au(OH) \longrightarrow Au(0) + OH^\bullet \qquad (9)$$

$$2OH^\bullet \longrightarrow H_2O_2 \qquad (10)$$

$$2H_2O_2 \longrightarrow 2H_2O + O_2 \qquad (11)$$
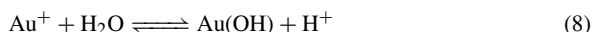
2. Silver

A gravimetric method was proposed for Ag and other precious metals, based on reduction with dipyrone **(39)**[121]. Determination of Ag(I) ions, strongly complexed with ammonia, sulfite, thiocyanate or thiosulphate, was carried out by potentiometric titration with sodium *N*,*N*-diethyldithiocarbamate **(11)**. The titration end-point was better defined when using a sulfide ion-selective electrode (ISE)[137]. Polypyrrole-based ISEs are poisoned by Ag(I) cations leading to modified selectivities. Ag(I) ions can be implanted

during fabrication of such electrodes against interferences from Cu(II), Pb(II) or less aggressive cations[138].

Trace analysis of Ag(I) was carried out by ASV using a carbon paste electrode, at pH ranging from 0.1 to 9.7. The electrode was cleaned by dipping in dilute nitric acid; dynamic range 0.05 to 150 μg L^{-1} [139]. A differential pulse ASV method for ultratrace concentrations of silver achieved effective preconcentration on a carbon paste electrode containing tricresyl phosphate (42) modified with sodium heptanesulfonate (43). Interference of copper (10 000-fold molar excess) and mercury (500-fold) could be masked with EDTA. At concentrations $\geqslant$0.5 μM of gold no interference was noted up to 100-fold molar excess; at higher gold concentrations [AuCl$_4$]$^-$ could be separated on a Dowex-1 column before ASV analysis of Ag(I); LOD 2.5 pM of Ag(I) for 15 min accumulation time, with linearity up to 20 μM, and good agreement with ICP-MS results[140].

(42)   **(43)**
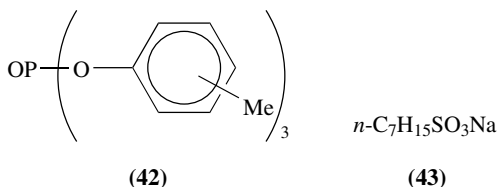
Modification of carbon paste electrodes with glyoxalbis(2-hydroxyanyl) (44) improved the determination of silver and mercury by differential pulse stripping voltammetry (DPSV); LOD for Ag(I) 0.10 μM and for Hg(II) 1.0 μM[123]. A tubular graphite paste electrode, modified with 2-mercaptobenzoxazole (45), was used for ASV in a continuous flow or FIA system, for determination of Ag(I), Hg(II) and Bi(III). For Ag(I) in continuous flow LOD 1.8×10^{-10} M, RSD 10.5% (5.00×10^{-9} M, $n = 6$), and in the FIA system 1.18 μg L^{-1} for 500 μL sample (SNR 3)[141]. The polished surface of a graphite electrode was treated with each of the ligands L = 46−50 and then covered with a Nafion membrane. The modified electrodes were tested for ASV duty. The stripping peak current I_p was proportional to the stability constant of the complexes Ag(I)L, which was in the order 46 < 47 < 48 < 49 < 50. Good ligands for Ag(I), such as cyanide or thiosulfate anions, had a diminishing effect on I_p that was proportional to their concentration[142]. DPSV was applied for multielement determination of gold, silver, copper and mercury in reactor moderator heavy water, at low μg L^{-1} levels. High concentrations of aluminum and iron precluded determination by ICP, whereas DPSV was unaffected by these elements[143].

Differential pulse polarography of water containing trace amounts of Ag(I) and Au(III), in the presence of 0.1 M ammonium tartrate as supporting electrolyte and 0.001% gelatin as maximum suppressor, gave a unique peak for both ions at $E_p = -0.08$ V *vs* standard calomel electrode. On addition of EDTA the signal could be resolved into two peaks, one at -0.04 V and the other at -0.2 V for silver and gold, respectively[144]. A piezoelectric method based on electrolytic deposition was described for Ag(I)[145].

Polyester membrane electrodes containing TCNQ units (51) were used for determination of Ag(I) in concentrations ranging from 10^{-8} to 1 M. The determination consists of various steps. First the membrane is brought to the reduced state in LiCl solution, as shown in reaction 12. The conditioned membrane is then dipped into the sample solution where ion exchange and a redox process take place, as shown in reaction 13; the existence of Ag(0) in the membrane was demonstrated by XPS, ESR and Raman spectra. Finally, silver is determined in the anodic stripping step 14[146].

(44)

(45)

(46)

(47)

$Et_2N-C-SS-C-NEt_2$ with $=S$ below each C

(48)

(49)

(50)

(51)

$$\{(TCNQ)\}_n + n e^- \xrightarrow{Li^+} \{(TCNQ)^-, Li^+\}_n \tag{12}$$

$$\{(TCNQ)^-, Li^+\}_n \xrightarrow{m Ag^+} \{(TCNQ)^-, Ag^+\}_m \longrightarrow \{(TCNQ), Ag^0\}_m \tag{13}$$

$$\{(TCNQ), Ag^0\}_m \xrightarrow{Cl^-} \{(TCNQ)\}_n + m AgCl + m e^- \tag{14}$$
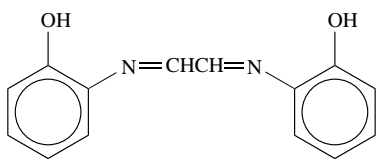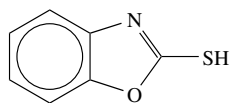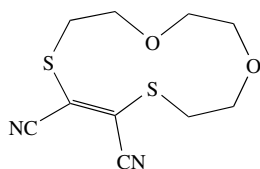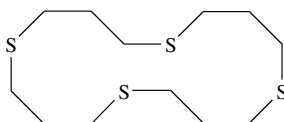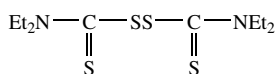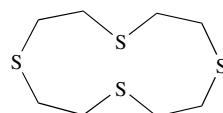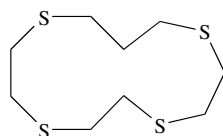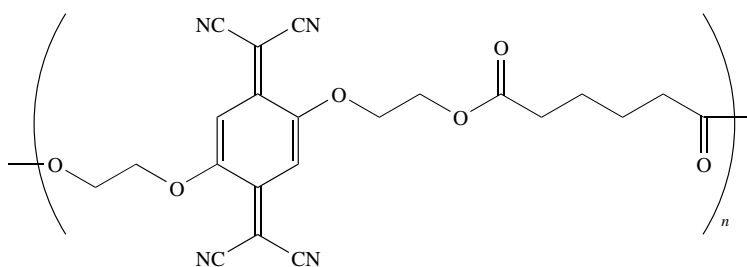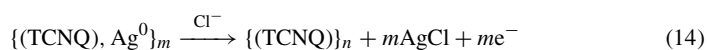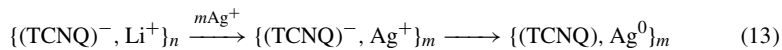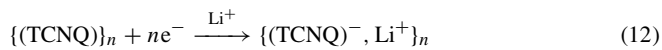
Various multidentate ligands were used as podands for the preparation of Ag^+ ISE membranes; LOD for **52** was 16 μM, for **53** and **54** *ca* 1 μM. The operation of these membranes was similar to that of the solid state Ag_2S electrode[147].

(52)   **(53)**   **(54)**
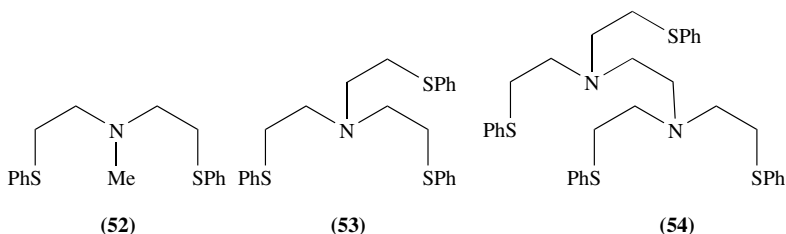
The carriers for silver ISEs were critically evaluated as anion sensors. The Ag(I) complex of silver ionophore III **(55)** was found to be sufficiently stable in the presence of Na^+ to serve as Cl^- sensor in complex matrices such as blood[148,149].

(55)
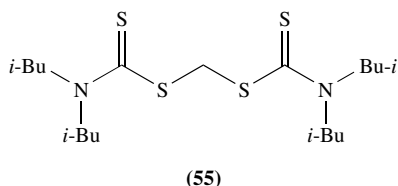
F. Radiation and Radio-isotopic Methods

1. Gold

A review appeared on speciation of trace elements using radioanalytical methods[150]. Particle-induced X-ray emission (PIXE) combined with X-ray spectrometry affords a sensitive multielement analytical method. An advantage of this radiation method is its capability to combine with microbeam techniques, allowing elemental mapping with 1 μm spatial resolution. Applications of PIXE in biology, medicine, geology, air pollution research, archeology and art have been demonstrated[26].

Thermal neutrons have energy somewhere under 0.5 eV whereas epithermal neutrons have energies in the range above thermal neutrons up to 0.5 eV. Epithermal neutron activation analysis was found to significantly underestimate gold when present in particles of diameter above 53 μm, as compared to the results of activation analysis by thermal neutrons (NAA)[151]. A method for determination of Au and PGE in rocks at ppb levels consists of irradiating the pulverized rock, fusing with Na_2O_2-NaOH, dissolving in dilute HCl and coprecipitating the noble metals with Te, using a Sn(II) salt as reductor. Some interference is expected from the simultaneous presence of Au and Pt in the sample, due to reactions 15 and 16 taking place during thermal neutron activation. ^{199}Au is the decay product we actually measure from activation of ^{198}Pt because of the relatively short lifetime of the intermediate ^{199}Pt; it is also the result of double neutron uptake of ^{197}Au. Standards need to be irradiated to correct for this interference[152].

$$^{198}Pt(n,\gamma) \ ^{199}Pt \xrightarrow{\beta^-} \ ^{199}Au \qquad (15)$$
$$\phantom{^{198}Pt(n,\gamma) \ } 30 \ m \phantom{\xrightarrow{\beta^-} \ } 3.15 \ d$$

$$^{197}Au(n,\gamma)\ ^{198}Au\ (n,\gamma)\ ^{199}Au \tag{16}$$
$$\text{2.693 d}\quad\text{3.15 d}$$
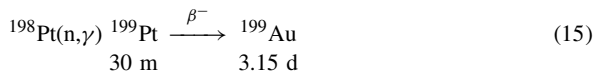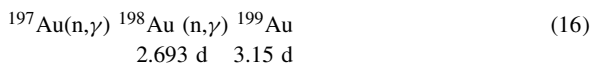
A method was described for the preparation of ^{199}Au radioisotopic standards, based on neutron activation of natural Pt (^{nat}Pt) in a reactor, as shown in reaction 17. An insignificant fraction (6×10^{-5}) of the ^{198}Au radioisotope was detected in the product[153].

$$^{nat}Pt(n,\gamma)^{199}Pt \xrightarrow{\beta^-} {}^{199}Au \tag{17}$$
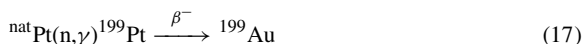
NAA as an ultratrace method for determination of gold may suffer interference by other elements present in the matrix. For example, in samples of biological origin Ca ions may interfere. Reciprocal separation factors of 7×10^6 are needed to reduce Ca to insignificance at the ultratrace level. This is difficult to achieve by extraction or precipitation without reducing the chemical yield of the nuclides of interest. An NAA method including radiochemical separation (RNAA) was developed consisting of sample irradiation, digestion to solubilize the metallic elements, electrolytic deposition of the dissolved gold on a niobium cathode, dissolution of the gold deposit with aqua regia and measurement of the radioactivity of this solution. RNAA was used to determine Au in bovine muscle and liver (7 to 8 ng g^{-1})[154]. An RNAA method was developed for trace and ultratrace determination of twelve elements in human blood serum. Gold was measured as ^{198}Au[155]. Multielement instrumental NAA (INAA) was applied to monitor the levels of gold and other elements in body fluids of patients undergoing chrysotherapy with auranofin (**1**, Table 1). Aliquots of a body fluid (e.g. 1.5 mL bile) were dried (*ca* 20 mg), irradiated in a reactor, let to 'cool down' for 5 to 10 d and the radioactivity measured (*ca* 10 or 90 μg Au L^{-1} of bile or plasma, respectively); LOD *ca* 20 ng Au L^{-1}. Up to 24 elements could be determined in one sample; however, some needed cooling down periods of 14 to 23 d and others of 30 to 40 d before measurement[156].

A sample of an iron meteorite was irradiated with thermal neutrons, dissolved in concentrated HCl in the presence of H_2O_2, evaporated to dryness, redissolved and submitted to SPE with a polyaniline column. Pt, Pd and Au were eluted from the resin with aqueous thiourea and Ir with aqueous ascorbic acid and measured. Polyaniline resin has great affinity for Pt(IV), Pd(II), Ir(IV) and Au(III) ions in 0.1 M HCl; as the acid concentration rises up to 10 M, only Au(III) remains strongly attached to the column[157].

Aliquots of a gold radioisotope can be used to monitor recovery percentage of Au on extraction or precipitation. An example using ^{195}Au for sea water analysis was mentioned in Section III.B.2 above[68]; the following method for Au determination in ores, at trace concentrations down to 0.02 μg g^{-1}, is another one. A sample of material milled to pass 200 mesh was treated with an aliquot of high-activity ^{198}Au and digested with aqua regia; after filtration and washing, the activity of the solid residue was insignificant; the filtrate was evaporated to dryness, redissolved with 6 N HCl and treated with AT-14 ion exchange resin; the residual activity of the treated solution was insignificant; the resin was washed with dilute HCl to eliminate Zn and with 4.5 N HNO_3 to eliminate Hg; the end analysis of the resin was carried out by XRF[158]. Determination of Au and the six PGE in iron meteorites was carried out by accelerator mass spectrometry[159].

2. Silver

NAA and radioisotopic methods are less frequently applied to Ag than to Au determination. An example for the application of ultraclean laboratory techniques is described for the determination of silver and other chalcophile elements in Antarctic ice, by isotope

dilution-thermal ionization MS[160]. Silver traces in platinum were determined by converting to the hydroxylamine silver complex, adding ^{110m}Ag and applying substoichiometric extraction with dithizone **(12)** in CHCl$_3$; no interference by many ions was observed[161]. *In situ* measurement of ^{107}Ag : ^{109}Ag isotope ratio variations was carried out by accelerator mass spectrometry[162].

IV. CHARACTERIZATION AND DETERMINATION OF ORGANOGOLD AND ORGANOSILVER COMPOUNDS

Section III deals with analytical procedures for the elemental analysis of gold and silver. Many such methods actually involve the analysis of salts and complexes of these elements, which were extant in the sample or were obtained during the sample preparation prior to the end analysis. The present section is concerned with speciation and characterization methods of metallorganic compounds, comprising salts and complexes of gold and silver in which bonding of the metal atoms to the organic residue is effected through a hetroatom, most frequently O, N, S and P, and of organometallic compounds, where the metal is bonded to the organic residue at a C atom. Cyanide ion and carbon monoxide are usually considered as inorganic ligands, whereas a compound with direct bonding to Si and other group 14 elements is taken as organometallic.

A review appeared on the synthesis of organometallic gold compounds in which some attention is also given to the structural analysis of systems such as triphenylphosphinegold oxonium salts, cyclopentadienylgold compounds, the aureated derivative of malononitrile and cationic carbametallacyclic complexes of gold including a carbon bridge. A smaller section is dedicated to compounds containing only gold to heteroatom bonds[163].

Although crystallographic analysis may be considered the best proof for the structure of a solid compound, it is often accompanied by additional spectroscopic evidence. This is helpful for better understanding the chemistry of the compound and its behavior in solution, molten or vapor phase. Often, certain structural features undergo changes on passing from the crystalline state to states that require analytical tools other than XRD for their study. The brief accounts on structural assignment of the present section are focussed mainly on the metallic atoms and their influence on the spectral properties of the organic ligands.

A comprehensive review appeared on the chemistry and structure of polynuclear clusters containing triphenylphosphine-stabilized Au and Pd or Pt. Many of the clusters contain also additional metals, such as Ag, Cu or Hg. The nuclearity (number of metal atoms) of the clusters ranges from 3 (e.g. **56**) to 25 (e.g. **57**). The spectroscopic techniques used for structural characterization of these entities were NMR, fast-atom-bombardment MS (FAB-MS), UVV and XPS. Several applications in catalysis were also reviewed[164].

$$[Pt(NO_3)(PPh_3)_2(AuPPh_3)_2]^+ \qquad [Pt_2Ag_{13}(AuPPh_3)_{10}Cl_7]$$
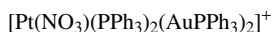
$$\textbf{(56)} \qquad\qquad\qquad \textbf{(57)}$$

A. Crystallographic Methods

The most frequently applied method for structural determination of Au and Ag compounds is single crystal X-ray diffraction (XRD) analysis. Some limitations to this approach are encountered when suitable crystals are difficult to obtain or when the compounds are unstable. A review appeared on nearly 140 crystallographic structures

of Ag complexes and organometallics where at least one other metal is present, including many compounds containing both Au and Ag atoms[165]. An interesting feature of compounds containing several atoms of transition metal elements is the tendency of such atoms to group together in clusters. In Tables 2 and 3 are summarized some crystallographic analyses of gold and silver compounds that appeared in recent years, ordered according to the atoms linking to the organic residues; when more than one binding element is present the order of descending priority is C, halogen, N, O, S and P. The examples illustrate the enormous variety of coordination modes and structural features attainable with organic compounds containing transition metal elements.

TABLE 2.   Crystallographic (XRD) analysis of organogold compounds

No.	Complexes and comments

C−Au bonds

C-1   Complex $[Au(C_5H_8N_2)_2]Cl \cdot H_2O$ (58) is obtained by reaction 18 via a carbene intermediate. Nearly linear C−Au−C bond angle, with C−Au distances from 0.2012 to 0.2016 nm. 58 forms a nearly eclipsed dimer with Au−Au distance of 0.3372 nm. Water molecules and chloride ions bridge between neighboring dimers by hydrogen bonding with NH groups[168].

(18)
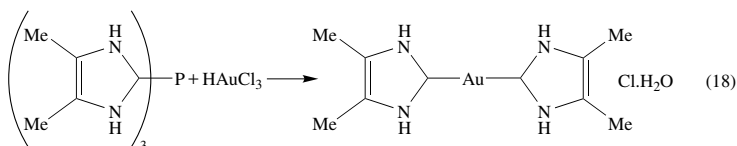
(58)

C-2 $Au_{10}(PPh_3)_5(C_6F_5)_4$ is a neutral cluster of 10 gold atoms, at the vertices of a toroidal ring of face- and edge-sharing tetrahedra with a common vertex[169]

X = Au——C_6F_5

Y = Au——PPh_3
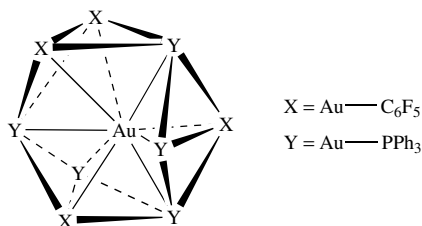
C-3[a]   Au(I) complexes 59–61 have nearly linear P−Au−C configuration. The intermolecular Au−Au distance in 59 is too long for effective bonding; intramolecular Au−Au distance of 0.3251 and 0.3154 nm for 60 and 61, respectively[170].

Ph_3P——Au——Ph
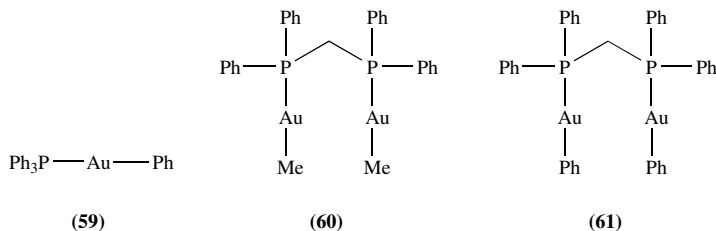
(59)   (60)   (61)

TABLE 2. (*continued*)

No.	Complexes and comments
C-4[b,c]	Square-planar geometry at the Au atom of complexes **62**. No π coordination of the allylic C=C groups with Au atoms[171].

$$\text{Me}$$
$$|$$
$$\text{Me}\!-\!\text{Au}\!-\!\text{R}$$
$$|$$
$$\text{PPh}_3$$
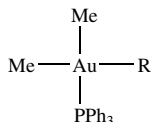
(a) R = $CH_2CH=CH_2$

(b) R = $CH_2CH=CHMe$

(c) R = $CH_2C(Me)=CH_2$

(62)

C-5 A mixed trinuclear cluster complex $[Ag\{Au(2,4,6\text{-}Me_3C_6H_2)\}_2(dppm)_2]ClO_4$ (**63**, dppm = bis(diphenylphosphino)-methane). Interatomic distances: Au−C 0.2080 nm, Au−P 0.2315 nm, Au−Ag 0.2944 nm and Ag−P 0.2413 nm; no bonding between Au atoms[172].

$$2,4,6\text{-}Me_3C_6H_2\!-\!Au$$
$$\text{PPh}_2$$
$$\text{Ag}$$
$$\text{PPh}_2$$
$$2,4,6\text{-}Me_3C_6H_2\!-\!Au$$
$$\text{PPh}_2$$
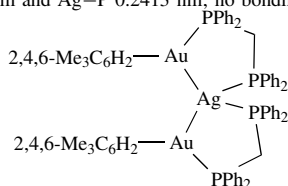
(63)

C-6 A drastic change in the structure of the trinuclear complex takes place in complexes **65** when a far off Me group in the ylide ligands of **64** is replaced by a more bulky Ph group. See also item S-7 below[173].

$$\text{MePh}_2\text{PCH}_2\!-\!Au\!-\!-\!-\!M\!-\!-\!-\!Au\!-\!CH_2\text{PMePh}_2$$

(with S, S bridges above and S, S below)

(64)   M = Mo, W

$$\text{AuCH}_2\text{PPh}_3$$

$$\text{Ph}_3\text{PCH}_2\text{Au}\!-\!-\!-\!M$$

(with S, S above and S, S below)

(65)
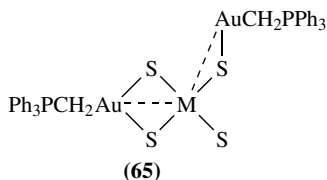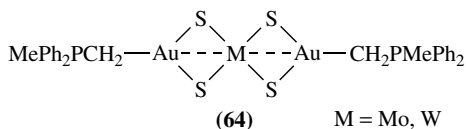
C-7 The first reported case of a carborane complex with direct Au−C links $[Au_2(1,7\text{-}C_2B_{10}H_{10})(PPh_3)_2]0.5CH_2Cl_2$ (**66**). The P−Au−C bonds of **66** are nearly linear, with distances Au−C 0.2047−0.2054 nm and Au−P 0.2265−0.2271 nm. The circle represents the $1,7\text{-}C_2B_{10}H_{10}$ core[174].

TABLE 2.   (*continued*)

No.	Complexes and comments
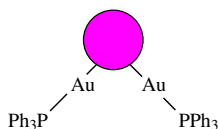
(66)

C-8[b]   Various Au(I) acetylide complexes **(67)** have an almost linear arrangement of atoms from P through the anchoring atom of group X at the *para* position. These compounds showed nonlinear optical properties, as discussed in Section IV.B.1[175].

$$[Ph_3P \longrightarrow Au \longrightarrow C \equiv C \longrightarrow C_6H_4X\text{-}p]$$
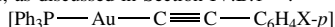
(67)

C-9   Compound **68** is noteworthy because it contains Au atoms having three degrees of oxidation. In the cation the cental atom is Au(I) and the other four are Au(II), whereas that of the anion is Au(III). The cation is centrosymmetric and its five Au atoms are almost collinear. All the Au atoms have square-planar coordination. Compounds **69** and **70** contain only Au(II) atoms[176−178].
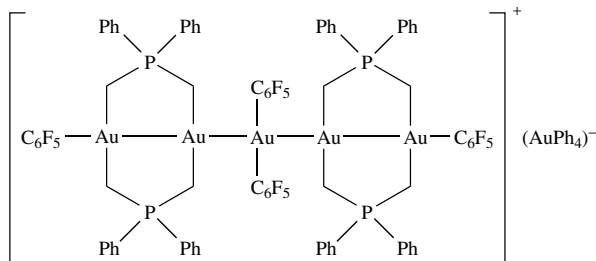
(68)
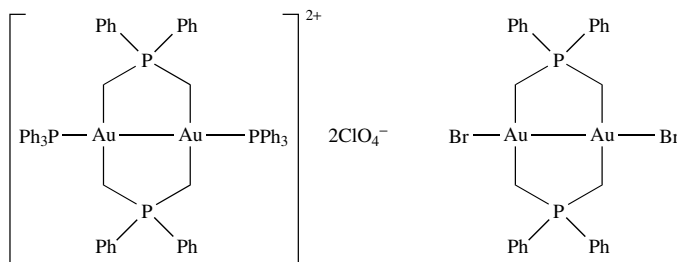
(69)   **(70)**

N−Au bonds

N-1   Condensation of 1,2-diaminoethane, nitroethane and formaldehyde in the presence of Au(III) ions leads to the formation of a salt of the gold-colored complex cation **(71)**. Note that one of the nitrogens has lost a proton and both nitro groups are *cis* to each other. The geometry at the gold atom is square planar, with the bond to the deprotonated N atom shorter than the other three. On dissolving the solid in strong acid the complex gains a proton and loses its color[179].

TABLE 2.   (*continued*)

No.	Complexes and comments
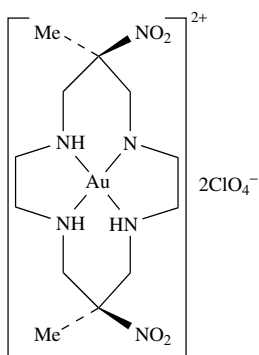
(71)

N-2   The square-planar geometry of Au in cation **72**, with Au−Cl distances of 0.2275 nm, is turned to pseudo-square pyramidal by the third chlorine atom at a distance of 0.3229 nm. This atom is also H-bonded to the two hydroxyls of a neighboring cation, producing a polymeric chain[180].
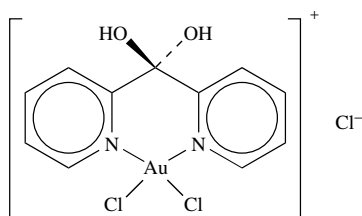
(72)

N-3   Phosphine-stabilized Au(I) ions can replace protons of amino groups. The Au(I) clusters in complexes **73** and **74** have pyramidal geometry with N atoms at the apex; in each triangular cluster Au−Au distances are 0.30±0.01 nm[181]. See also items N-4 and P-6 below.

R = *n*-Bu, *n*-octyl

(73)   (74)

TABLE 2.   (*continued*)

No.	Complexes and comments

N-4[c,d] Complex **75**, derived from 8-aminoquinoline and a trinuclear Au(I) cluster, has a pyramidal structure similar to those shown in the preceding entry, with the quinolinyl group perpendicular to the plane of the cluster. Interatomic distances: Au−Au 0.2928–0.3207 nm, Au−N(amino) 0.2040–0.2071 nm, Au−N(ring) 0.2805 nm and Au−P 0.2233–0.2242 nm. Only the amino nitrogen is involved in N−Au bonding, as the distance from the quinoline N to the nearest Au atom is too long. The Au−N−Au angles (97.1°) are much smaller than the nearly tetrahedral angles (109.4°) prevalent in ordinary quaternary ammonium compounds. Complex **76** involves a nearly planar rhombic cluster. Interatomic distances: Au−Au 0.2940–0.3023 nm, Au−N(amino) 0.2074–0.2103 nm, Au−N(ring) 0.2115 nm and Au−P 0.2242–0.2253 nm. The amino N is involved in a pyramidal structure with three Au atoms, while the fourth one is strongly bonded to the heterocyclic N atom[182]. See also item P-6 below.

(75)   **(76)**
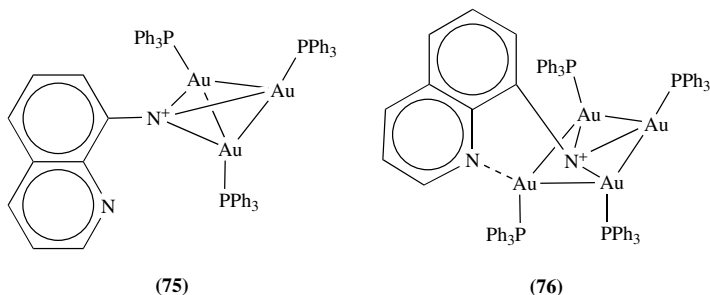
O−Au bonds

O-1 Compound **77** contains centrosymmetric dimeric units with Au−Au contact distance of about 0.376 nm. Compound **78** is monomeric due to steric hindrance by the phenyl groups. Coordination at the Au atoms is nearly linear in both cases. See the S analog in item S-1 below[183].

Me$_3$P——Au——OSiMe$_3$ Ph$_3$P——Au——OSiPh$_3$

(77)   **(78)**
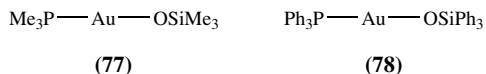
O-2 The O$_{(1)}$−Au−P angle is nearly linear (176.9°). The crystal of the dichloroacetato (R = CHCl$_2$) complex is not isostructural with the complexes **79** having R = Me or F$_3$C[184].

RCO$_2$——Au——PPh$_3$

(79)
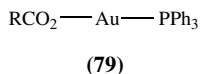
S−Au bonds

S-1 Compound **80** is monomeric due to steric hindrance by the phenyl groups. Coordination at the Au atom is nearly linear and the angle at S (95.0°) is narrow. See the O and Me analogs in item O-1 above[183].

Ph$_3$P——Au——SSiPh$_3$

(80)
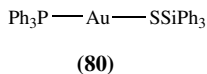
S-2[b] Various Au(I) arylthiolates, stabilized with chiral phosphine ligands derived from saccharides, were prepared and characterized. Complex **81** showed antitumor activity[185,186].

TABLE 2. (*continued*)

No.	Complexes and comments

(81)
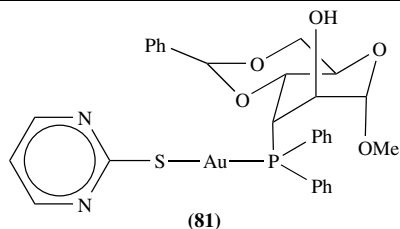
S-3^c In complex **82** there is no bonding interaction between Au and the carboxylate group. The P−Au−S angle is nearly linear[187].

$$c\text{-Hex}_3\text{P} \longrightarrow \text{Au} \longrightarrow \text{SC}_6\text{H}_4\text{CO}_2\text{H-}o$$

(82)
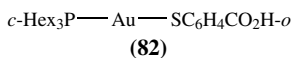
S-4^d 1,2-Disulfanyl-1,2-dicarba-*closo*-dodecaborane and certain chloroaurates yield under basic conditions salts of the **83** anion, where the circles represent the $C_2H_{10}B_{10}$ polyhedral carborane core. Coordination at the Au(III) atom has square-planar geometry, with Au−S distances of *ca* 0.232 nm[188,189].

(83)
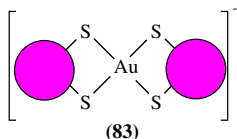
S-5^c The dinuclear complex **84** presents two different Au−S−P environments (S−Au distances 0.23216 and 0.2575 nm), one with nearly linear P−Au−S and the other a distorted trigonal-planar configuration of the P_2AuS group[190].

(84)
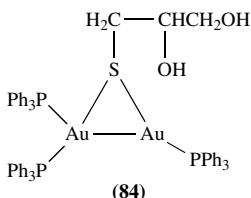
S-6   The Au(I) dinuclear complex **85**, derived from a dithiol ligand, forms a helical polymeric chain via Au to Au contacts, with eight Au atoms per turn[191].

(85)
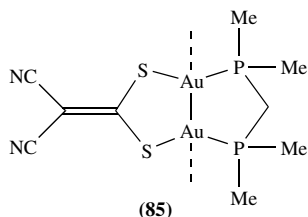
TABLE 2.   (*continued*)

No.	Complexes and comments

S-7   The structure of the trinuclear clusters **86** remains similar to that of **64** (item C-6 above) despite the proximity of the more bulky Ph$_3$P ligands to the Au(I) atoms[173].

$$Ph_3Y - Au \overset{S}{\underset{S}{\cdots}} M \overset{S}{\underset{S}{\cdots}} Au - YPh_3$$
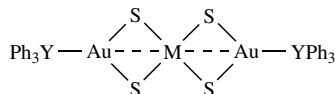
Y = P, As; M = Mo, W

(86)

P–Au bonds

P-1[a]   Some of the interatomic distances in the heteronuclear Au–Pt–W cluster **87** (Cp = cyclopentadienyl anion) involving Au atoms: Au–W 0.2738 nm, Au–Pt 0.2858 nm and Au–P 0.2289 nm; some of the angles are: Au–Pt–P 77.3 and 103.3°, W–Au–Pt 59.7°, W–Au–P 146.5°, Pt–Au–P 152.6°, Au–W–P 77.9° and Au–W–C 71.2° [192].

PPh$_3$
|
Au   PPh$_2$
OC
Cp — W — Pt — W — Cp
Ph$_2$P   C   CO
|
O
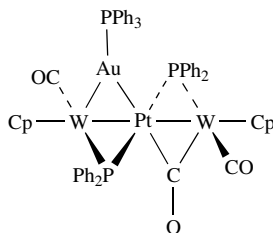
(87)

P-2   Small crystals of complex **88**, inadequate for single-crystal XRD analysis, were analyzed with synchrotron radiation in the 0.024–0.065 nm range, using Laue's method for recording diffraction data. The complex consists of an AuOs$_3$ cluster with Au bonded to a PPh$_3$ ligand and the Os atoms to the other ligands, including a σ bond to C–O[193].

[AuOs$_3$H(CO)$_8$(Ph$_2$PCH$_2$PPhC$_6$H$_4$-o)(PPh$_3$)]PF$_6$·0.5PhCl

(88)

P-3   In the 16-electron clusters **89** every Au atom is bonded to the M atom, three other Au atoms and a phosphine ligand; the geometry is toroidal. The 18-electron clusters **(90, 91)** have a more compact spheroidal geometry[194].

[M(AuPPh$_3$)$_8$]$^{2+}$ [M(CO)(AuPPh$_3$)$_8$]$^{2+}$ [M(H$_2$)(AuPPh$_3$)$_8$]$^{2+}$

M = Pd, Pt

(89)   **(90)**   **(91)**

P-4   A salt combining a complex Au(I) cation **(92)** with a complex trigermylgold(I) anion **(93)**. The eight-membered ring of **92** has boat conformation and the Au atoms are in close proximity (0.29736 nm). Anion **93** is between T- and Y-shaped planar with Au–Ge distances from 0.241 to 0.254 nm[195]. See also item P-11 below.

TABLE 2.   (*continued*)

No.	Complexes and comments
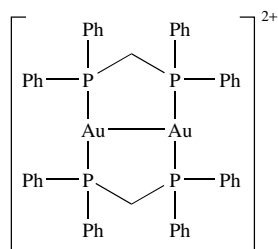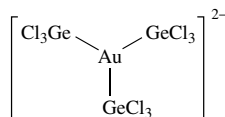
(92)   **(93)**

P-5[a]   Au(I) complex cation **94** has tetrahedral geometry (average Au−P distances 0.2404 nm), and is water-soluble. Complex cation **95** has distorted trigonal-planar geometry and is soluble in nonpolar solvents and alcohols with large alkyl groups[196]. Analogous bidentate phosphines were found to yield uninuclear (**96**, Au−P distances 0.2354−0.2378 nm) and dinuclear (**97**, Au−P distances 0.2300−0.2316 nm) complex cations, that are soluble in water and alcohol[197].
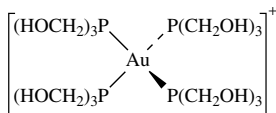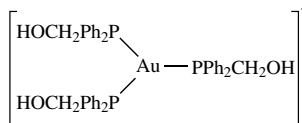
(94)   **(95)**
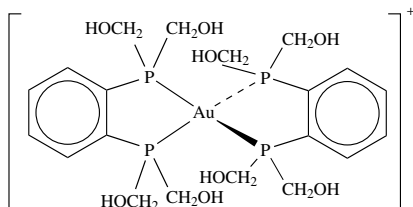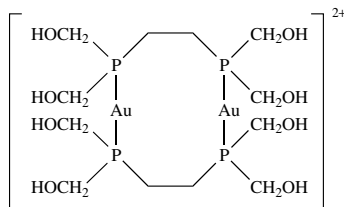
(96)   **(97)**

P-6   Au(I) can form uninuclear complexes with tris(dimethylamino)phosphane (**98**), or can form trinuclear cluster cations with oxide (**99**) or imido (**100**) divalent anions. The P−Au−X atoms are nearly collinear in complexes **99** and **100**, the O and N atoms are at the apex of a pyramid with Au$_3$ basis[198]. See also items N-3 and N-4 above.

(98)

TABLE 2.   (*continued*)

No.	Complexes and comments

(99)
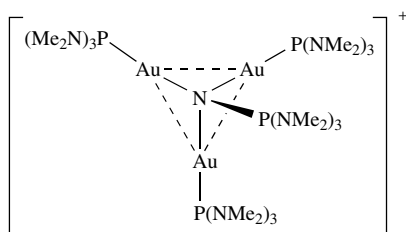
(100)

P-7   Complex **101** affords an unusual nine-membered chelate ring, with a C_2 pseudo-axis of symmetry along the Au(I)−Cl bond[199].
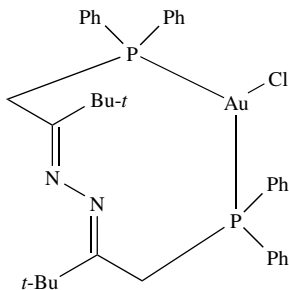
(101)

P-8[a]   Tridentate phosphine ligands yield trinuclear complexes with Au(I) halides of structure depending on both the ligand and the halide. Tris(diphenylphosphino)methane (tppm) yields neutral homostructural [Au$_3$X$_3$(tppm)] complexes **(102)**, while bis(diphenylphosphinomethyl) phenylphosphine (dpmp) yields cationic [Au$_3$X$_2$(dpmp)$_2$]$^+$ of structure depending on the halogen **(103, 104)**[200]. For a clearer representation, in formulas **102** to **104**, P = PPh$_2$, P^* = PPh.

TABLE 2.   (*continued*)

No.	Complexes and comments
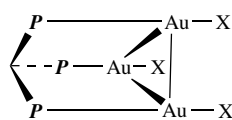
(a) X = Cl; (b) X = I

(102)
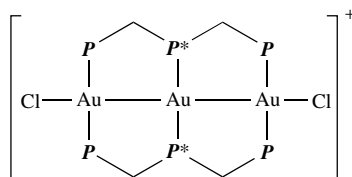
(103)
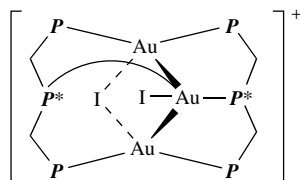
(104)

P-9   Pseudo-tetrahedral Au cluster with Au−Au distances from 0.26036 to 0.29148 nm. The circles in complex **105** represent $C_2B_{10}H_{10}$ carborane groups[201].
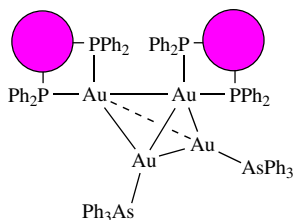
(105)

P-10   Complexes **106, 107** and others in the same family consist of multinuclear clusters, where the W atom occupies the center of an incomplete icosahedron and the Au atoms are at certain vertices of the icosahedron. Distances between proximate Au atoms vary in the approximate range from 0.276 to 0.305 nm and Au−W distances from 0.275 to 0.284 nm[202].

$$[W(CO)_4(AuPPh_3)_5]^+[PF_6^-]   [W(CO)_4(AuPPh_3)_7]^+[PF_6^-]$$

(106)   **(107)**

P-11   The complex cation in **108** has chair conformation. Interatomic distances: Au−P 0.2289 nm, Au−Au 0.3045 nm. Although the Au−Au distance is somewhat larger than typical Au−Au single bonds (0.2757−0.2780 nm), the contact is closer than twice the van der Waals radius and bonding can be considered to exist[203]. See item X-2 in Table 3 for a similar case with silver, where no metal-to-metal bonding exists. See also item P-4 above.

(*continued overleaf*)

TABLE 2. (*continued*)

No.	Complexes and comments

(108)

P-12   Interatomic distances in complex anion **109**: Au−Au 0.29220−0.30889 nm, Au−P
0.02313−0.2351 nm, Au−Cl 0.2642 nm; Au−Au−Au angles 56.46−61.67°. The close silver
analog (item P-6 of Table 3) has longer metal−metal distances in the cluster, precluding
metal-to-metal bonding[204].

(**109**, **P** = PPh₂)

[a] See Section IV.C.1 for structural evidence based on electronic spectra.
[b] See Section IV.B.1 for structural evidence based on vibrational spectra.
[c] See Section IV.D.1 for structural evidence based on NMR spectra.
[d] See Section IV.F.1 for structural evidence based on MS.

The breakdown of organosilver(I) and organocopper(I) polymers $[MR]_n$, M = Ag(I),
Cu(I), where R is a single organic or inorganic ligand, was reviewed. The structural
features of oligomeric complexes $[M(I)R]_n$, $1 \leqslant n \leqslant 4$, were also discussed[166]. Silver
behenate (n-$C_{21}H_{43}CO_2Ag$) powder was proposed as a standard for low-angle X-ray
powder diffraction (XRPD)[167].

B. Infrared Region

1. Gold

The C=C groups show no special features in the IR spectra of Au complexes **62** (item
C-4 in Table 2), pointing to the lack of conjugation of these groups with the Au atom. See
also Section IV.D.1 below[171]. IR spectroscopy was used to elucidate the structure of gold
complexes with azobenzene compounds (**165–167**), including formation of N−metal and
C−metal bonds[237]. The resonance Raman spectra of bilirubin (**168**) and its complexes
with Cu(II), Ag(I) and Au(III) show that the complexes have different structures, due to
the different ionic charge and ionic radius of the metal ions[238].

TABLE 3.   Crystallographic (XRD) analysis of organosilver compounds

No.	Complexes and comments

C−Ag bonds

C-1[a]   In its complex with deltaphane **(110)** Ag(I) lies on the C_3 pseudorotation axis but off the center of the cavity[205].
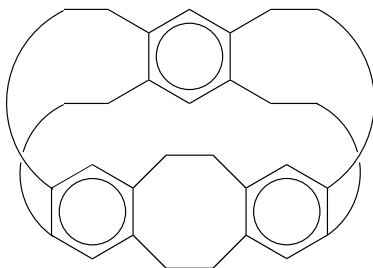
(110)

C-2[b,c]   In the cationic Ag(I) arylacetylide complexes $[Ag_3(dppm)_3L]^{2+}$ **(111)** and $[Ag_3(dppm)_3L_2]^+$ **(112)** the trinuclear silver cluster has triangular pyramidal or bipyramidal geometry, with acetylenic C atoms in apical positions. Interatomic distances, **111**: Ag−Ag 0.29850−0.34080 nm, Ag−C 0.2224−0.2269 nm; **112**: Ag−Ag 0.28946−0.31948 nm, Ag−C 0.2323−0.2981 nm[206a]

$$L = C \equiv C - \!\!\!\!\bigcirc\!\!\!\!\!- NO_2$$

(111)   **(112)**
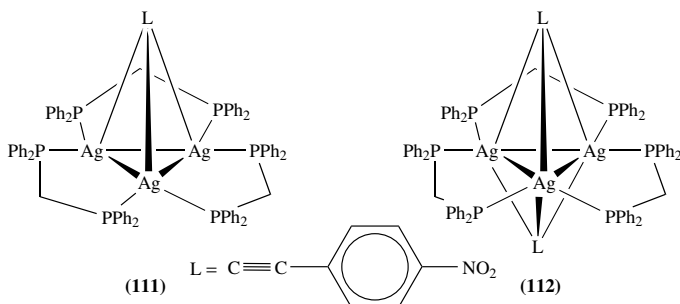
C-3[c]   In complex $[\{Ag_3(dppm)_2\}_2\{1,4\text{-}(C_2)_2C_6H_4\}]\cdot 4BF_4$ each pair of Ag atoms in a trinuclear Ag cluster is bridged by a dppm bidentate ligand, and two such clusters are bridged together by a diacetylide ligand, to give a cation **(113)**. Excitation with $\lambda > 350$ nm at room temperature or 77 K gives intense green-yellow luminescence[206b]

P = PPh$_2$

(113)

TABLE 3.   (*continued*)

No.	Complexes and comments

C-4   The phosphine complex of Ag(I) acetylide disproportionates into $[Ag(PR_3)_2]^+$ cationic units and $[Ag(C{\equiv}CR')_2]^-$ anionic units that reassemble according to the steric hindrance exerted by the R and R′ groups. For bulky R = R′ = Ph, the tetrameric solvate complex $[(Ph_3P)AgC{\equiv}CPh]_4{\cdot}3.5THF$ is formed, with 'flat butterfly' geometry (**114**). For the less hindered R = Me, R′ = $SiMe_3$, polymer **115** is formed, with nearly linear anionic and cationic units and the C≡C groups π-bonded to the neighboring Ag atoms. The Ag−Ag distances in both cases are rather long, *ca* 0.3 nm[207].

(114)   (115)

C-5   The silver atom in compound **116** is trigonally coordinated to one mesityl group and to the π-electrons of two acetylenic groups[208]. See also the analogous compound **172** in Section IV.B.2.

(116)

C-6   The Ag(I) ion of complex $[(oetp)AgO_3SCF_3]_2$ (**117**)^d lies in the cavity of oetp, coordinated with two O atoms and two C=C groups. Dimerization is achieved by bridging Ag ions with triflate anions[209].

TABLE 3.   (*continued*)

No.	Complexes and comments

(**117**)

C-7   Ag(I) salts and 1,8-diisocyano-*p*-menthane (dipm, **118**) yield a 1-D polymeric structure
[Ag(dipm)$_2$(Y)]$_n$, Y = PF$_6$, BF$_4$ (**119**), where every tetracoordinated Ag(I) is double bridged
to the two adjacent Ag atoms. All dipm bridges are oriented in the same direction. No direct
Ag−Ag bonding exists (distance *ca* 0.5 nm) with the Ag atoms forming a zig-zag line
(Ag−Ag−Ag angle 137.15°). When irradiating the polymer in EtOH solution, at 77 K, a
blue luminescence appears (λ_{max} 385 nm)[210].
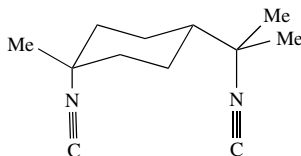
(**118**)
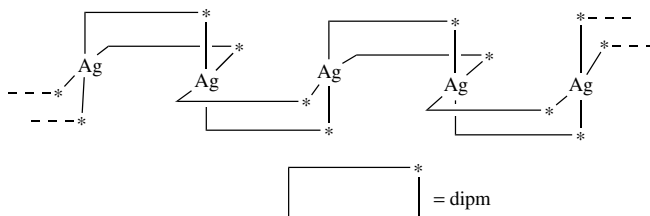
(**119**)

C-8[a]   Stable Ag(III) salts of PNP (**120**) could be isolated. The nearly planar geometry of the
complex argentate anions allows in some cases stable *cis* (**121**) and *trans* (**122**)
configurations. Ag−C distances in **120** range from 0.207 to 0.210 nm[211].

TABLE 3. (*continued*)
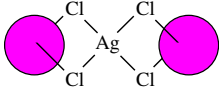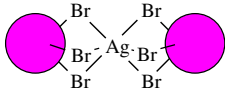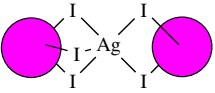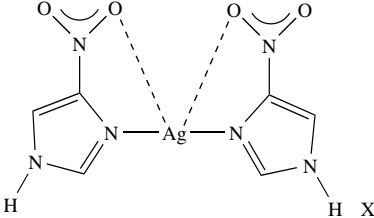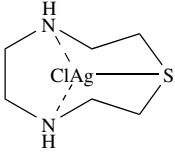
No.	Complexes and comments

$$[Ph_3P = N = PPh_3]^+ [Ag(CHF_2)_4]^-$$

(**120**)

$$\begin{bmatrix} F_2HC & CF_3 \\ & Ag \\ F_2HC & CF_3 \end{bmatrix}^-$$

(**121**)

$$\begin{bmatrix} F_2HC & CF_3 \\ & Ag \\ F_3C & CHF_2 \end{bmatrix}^-$$

(**122**)

Hal−Ag bonds

X-1   Hexahalogenocarborane silver salts, $Ag^+(CH_6B_{11}X_6)^-$, X = Cl, Br, I, crystallize as
unidimensional coordination polymers, where Ag^+ cations and hexahalogenocarborane anions
are consecutively linked to each other by coordination via nonbonding electrons of the halogen
atoms. However, the mode of coordination of the silver atom varies according to the halogen,
as depicted in **123–125**, where circles represent CH_6B_{11} polyhedral cores[212].

(**123**)   (**124**)   (**125**)

N−Ag bonds

N-1[a,b]   In complex **126** N−Ag−N is nearly linear and the imidazole rings are nearly coplanar; Ag−N
distances 0.2127 to 0.2135 nm. The secondary bonds to O atoms of the nitro groups approach
the equatorial plane. Anions X are bonded to NH groups and have no direct contact with the
metal[213].

$$X = BF_4^-, NO_3^-$$

(**126**)

N-2   Ag(I) in **127** is tetracoordinated to the tridentate ligand and to the chloride ion forming a
neutral complex; Ag−S distance is 0.2611 nm[214].

(**127**)

TABLE 3.   (*continued*)

No.	Complexes and comments

N-3   Acyclic multidentate amine ligands yield polymeric solid complexes with Ag(I). Thus, diethylenetetramine and tris(2-aminoethyl)amine give **128** and **129**, respectively. In the presence of unidentate ligands such as PPh$_3$, PMe$_3$ and *t*-BuNC polymer formation may be hampered, as in **130**[215].
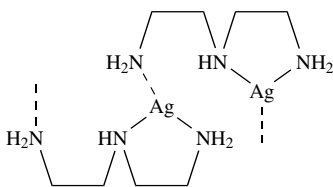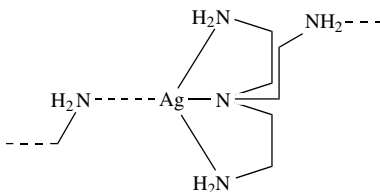
(**128**)   (**129**)
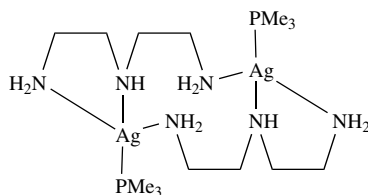
(**130**)

N-4^a Silver(I) triflate yields dimeric units with multidentate ligands such as **131**–**133**. Such units are bound to each other by triflate anions through the silver cation, forming a polymer as illustrated by **134** for the complex with ligand **133**[216].

(**131**)   (**132**)

(**133**)
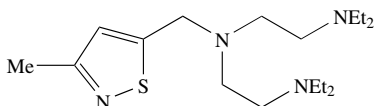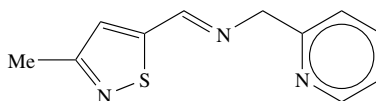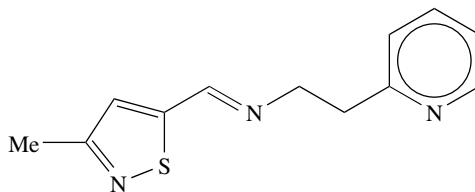
TABLE 3.   (*continued*)

No.	Complexes and comments
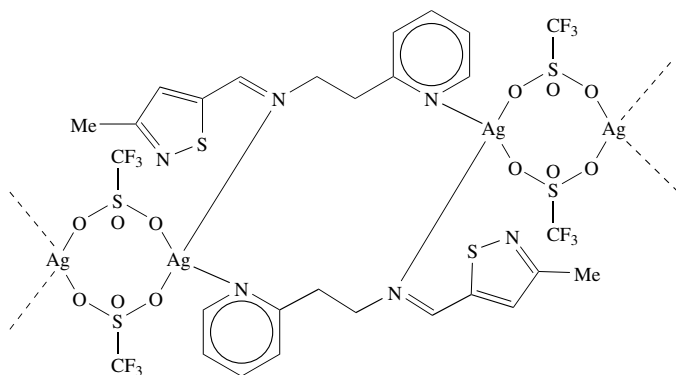
(**134**)

N-5   Silver(I) salts form solid coordination networks with bidentate bis(3-cyanophenyl)acetylene
      (**135**), the topology of which depends both on the counterion and the solvent. Thus, silver(I)
      triflate in benzene consists of a polymeric network of pentacoordinated binuclear silver clusters
      (**136**). Changing solvent to toluene, the coordination number of Ag rises to six (**137**) and the
      network attains the geometry of an undulating sheet[217].
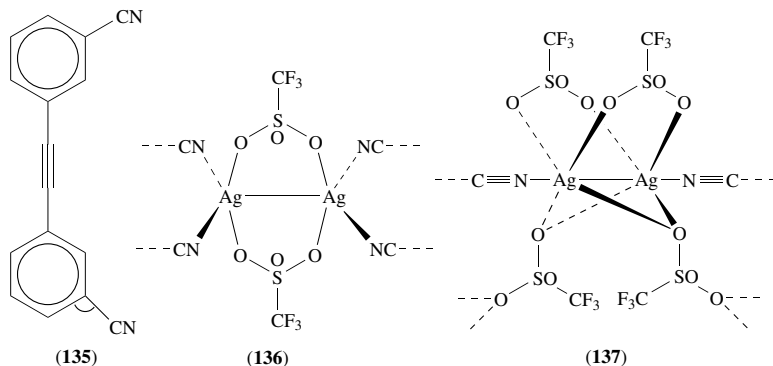
(**135**)   (**136**)   (**137**)

N-6   Polymer **138** is an abbreviated representation of the complex of Ag(I) with bis[3-(2-pyridyl)
      pyrazol-1-yl][phosphinate anions (**139**). Ag(I) is coordinated to the N atoms with
      pseudotetrehedral geometry. The strand is helical, with all the anionic phosphinate groups
      aligned along one face, yielding a strand with one polar and one nonpolar face. This allows
      two types of supramolecular association: In the 'face-to-face' one of the phosphinate groups of
      one strand are H-bonded to those of a facing strand by means of water molecules; in the
      'back-to-back' association heterocyclic groups of one strand lie parallel to those of the other,
      with π bonding one, interactions. The long distance between contiguous Ag atoms (0.5450 to
      0.6857 nm) allows no bonding between them[218].

TABLE 3.   (*continued*)

No.	Complexes and comments

(**138**)   (**139**)
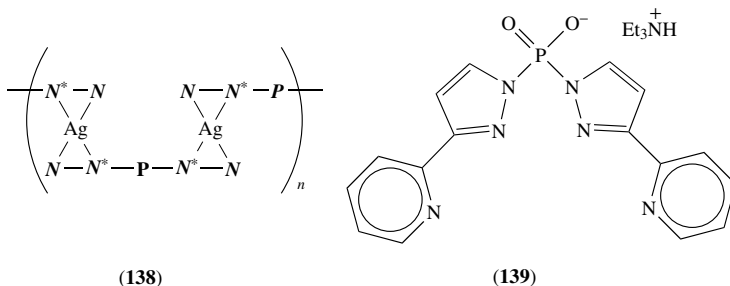
N-7   In the linear polymeric structure **140** the two close Ag atoms (Ag−Ag distance 0.3078 nm) replaced H-bonding protons of the 4,7-dihydro-5-methyl-7-oxo[1,2,4]triazolo[1,5-*a*]pyrimidine ligand, neutralizing their charges. Such dimeric units are linked by a third Ag atom, held by nonbonding electron pairs. Bonding to inorganic anions and solvating water is not shown[219].
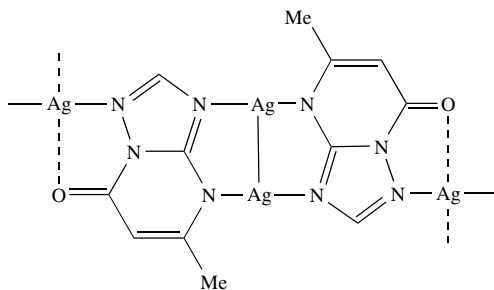
(**140**)

N-8   Complex [Ag$_4${Sb$_2$(NHex-*c*)$_2$}$_2$] (**141**) consists of a double cage combining four Sb(III) atoms with a cluster of four Ag(I) atoms. All N atoms are tetracoordinated and every Ag atom is coordinated to two Ag atoms and three N atoms[220].

R = *c*-HeX
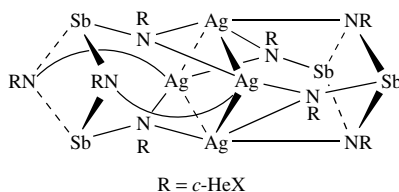
(**141**)

N-9^a The polymeric complex [Ag$_2${C$_6$H$_4$-1,2-(CO$_2$)$_2$}(C$_8$H$_6$N$_2$)$_2$(H$_2$O)] (**142**) is formed by dimeric planar Ag-phthalazine units that are linked in a chain through the Ag atoms by phthalate anions. In the latter, one of the carboxylate groups bonds two Ag atoms in successive dimeric units, whereas the second one forms a seven-membered chelate ring with one of the Ag atoms and is H-bonded to a solvating water molecule[221].

TABLE 3.   (*continued*)

No.	Complexes and comments

(142)
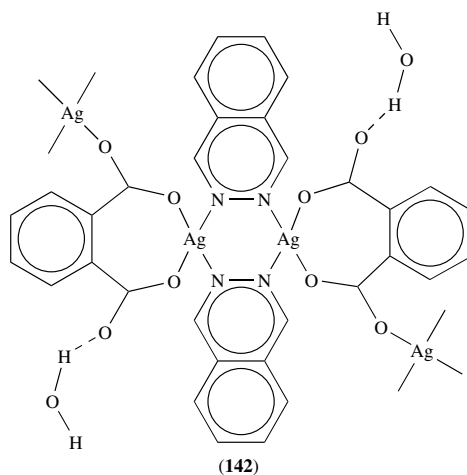
O−Ag bonds

O-1   In solid silver(I) chloroacetate the dimeric units **(143)** are almost planar, and the Cl atoms in
trans conformation; the Ag atoms have further long-range interactions with neighboring O and
Cl atoms. A thermally induced solid-state polymerization leads to AgCl elimination and
polyglycolide formation[222].

(143)
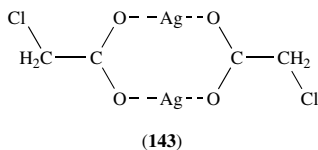
O-2   Mercury(II) acetate and silver(I) nitrate in MeOH in the presence of 2-oxazolidone or
β-propiolactam yield polymeric complexes $[AgHg(L)_2NO_3]_n$, where Hg(II) is neutralized by
two deprotonated anions derived from the organic ligand **(144, 145)**. The N−Hg−N bonding is
nearly linear. In the complex incorporating **144** Ag is bonded to two exocyclic O atoms,
forming a four-membered Ag_2O_2 ring and a dimeric structure. These dimers are further paired
to produce a stepped Ag_4O_4 species, where Ag atoms are of coordination 6. Further weak
interaction of the tetrameric units leads to loosely linked polymeric sheets. In the complex
incorporating **145** Ag atoms are linked in a helical chain. Each turn of the helix is bridged by a
nitrate ion linking between adjacent Ag atoms, forming a 12-membered metallamacrocycle,
with tetrahedrally coordinated Ag[223].

(144)   **(145)**
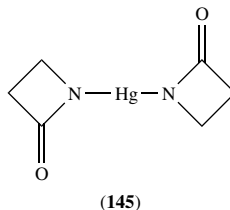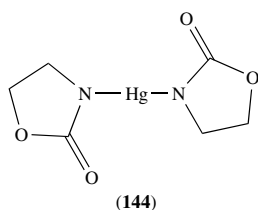
TABLE 3.   (*continued*)

No.	Complexes and comments

O-3[e]   Complex [*trans*-Os(CO)$_3$(PPh$_3$)$_2$] (**146**) has a distorted trigonal bipyramidal configuration, with Ag approaching Os in the equatorial plane; Ag−Os distance is 0.2712 nm[224].

$$PPh_3$$

$$OC - Os \overset{CO}{\underset{CO}{\diagup}} - AgO_2CF_3$$

$$PPh_3$$

(**146**)
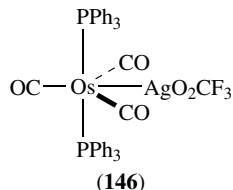
S−Ag bonds

S-1   Silver(I) butanethiolate (*n*-BuSAg) crystallizes as a polycrystalline layered solid (**147**), forming slabs of plane-trigonally coordinated S and Ag atoms, with rows of the alkyl groups alternatively sticking out on one side (▲) or the other (▼) of the slab. Using UVV reflectance, ^{13}C and ^{109}Ag CP-MAS-NMR and Raman spectroscopies, three structural types of crystals could be distinguished, according to the conformation **148** adopted by the C(1)−C(2) link of the butyl groups: the white all-*trans*, the bright yellow all-*gauche* and a phase containing both conformational species. The all-*trans* phase is thermodynamically the less stable one. The analogies of these structures and self-assembled monolayers on Ag surfaces (see Section V) were discussed[225].

(**147**)   (**148**)
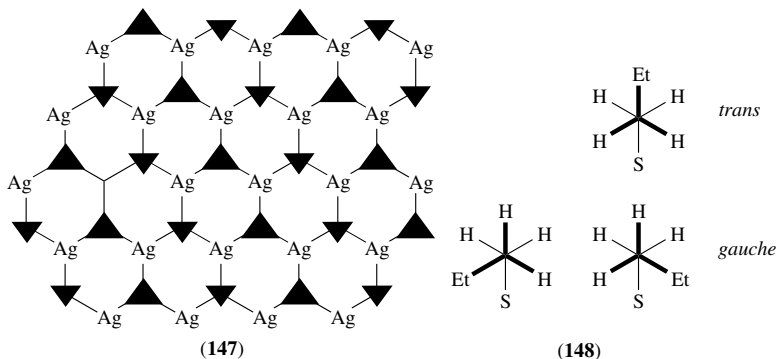
S-2   In the dimeric version of the complex each Ag(I) ion binds three 4,5-ethylenedithio-1,3-di-thiole-2-thione molecules (**149**) through the thiono S atoms (Ag−S distance *ca* 0.25 nm), and two such units become paired as shown in **150** (Ag−S′ distance between paired units is *ca* 0.30 nm)[226]. A polymeric complex [Ag(C$_5$H$_4$S$_5$)$_2$NO$_3$]$_n$ (**151**) also exists, where every Ag atom coordinates two thiono and two heterocyclic S atoms of four different **149** molecules. The Ag atoms have distorted tetrahedral coordination, with two distinct Ag−S bond distances, 0.25612 nm (to thiono) and 0.28268 nm[227]. In both the dimeric and the polymeric versions supramolecular organization is attained by S···S contacts between neighboring units.

(**149**)   (**150**)
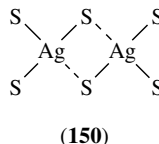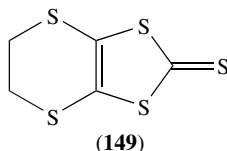
TABLE 3. (*continued*)

No.	Complexes and comments
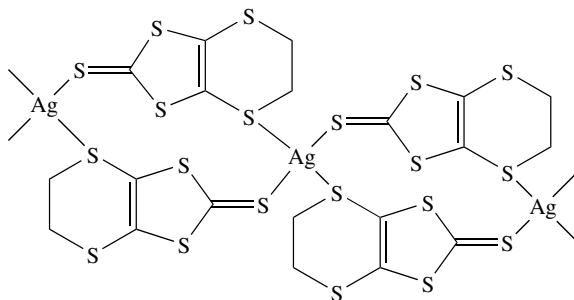
(151)

S-3 Bis(ethylenedithio)tetrathiafulvalene (ET, **152**) forms with the square-planar organometallic ion [Ag(CF$_3$)$_4$]$^-$, in 1,1,2-trichloroethane (TCE) solution, by the electrocrystallization technique, at least four crystalline phases. Three of these phases are solvates of formula ET$_2$Ag(CF$_3$)$_4$•TCE and the fourth one does not contain solvent. The three solvated phases are superconductive at very low temperatures[115,116].
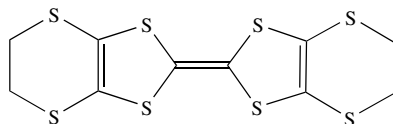
(ET, **152**)

S-4 A cubane-like structure was found for the heteronuclear complex [(MoAg$_3$S$_3$)(PPh$_3$)$_3$(O)(Cl)] **(153)**. The Mo−Ag and Ag−Cl distances (0.2980 and 0.2810 nm) are too long for effective bonding between such pairs of atoms[228].
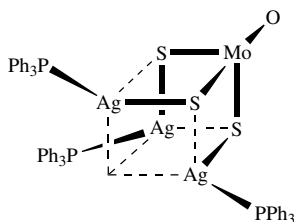
(153)

S-5 Complex **154** was the first example of a dodecanuclear heterobimetallic cage cluster with a central S ligand. Three Ag−Ag pairs are bound to the central S atom in a propeller-like disposition and three M−M pairs are bound to the Ag−Ag pairs through SCH$_2$CH$_2$S bridges[229].

$$[\{M_2Ag_2S_2O_2(S_2C_2H_4)_2\}_3(S)]\cdot(NEt_4)_2\cdot CH_2Cl_2\cdot MeCN$$
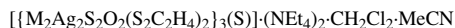
(**154**, M = Mo, W)

TABLE 3.   (*continued*)

No.	Complexes and comments

S-6   Bimetallic clusters of Ag(I) and Rh(III) (**155, 156**) contain the bidentate anionic ligand 2-aminoethanethiolate (aet, $H_2NCH_2CH_2S^-$). In complex **155** the Rh_2Ag_3 cluster has trigonal bipyramidal geometry with Rh atoms in apical positions, each Ag atom being chelated by an aet ligand[230].

$$[Ag_3\{Rh(aet)_3\}_2]^{3+}(BF_4^-)_3 \qquad [Ag_5\{Rh(aet)_3\}_4]^{5+}(BF_4^-)_5$$

(155) **(156)**

P−Ag bonds

P-1[a,b]   Adducts **157** with X = Cl, Br are isomorphic of the tetragonal space group, where P−Ag−X is slightly nonlinear, with the Ag displaced toward one of the MeO oxygen atoms. No structural assignment could be found for XRD when X = I[231].
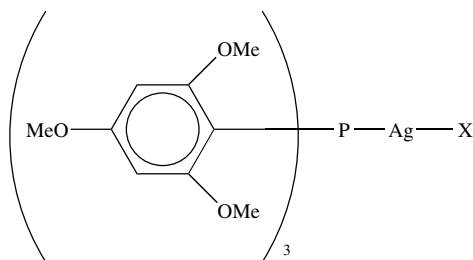
(157, X = Cl, Br, I)

P-2[a]   Ag(I)X salts yield two types of solid complexes with 1,3-bis(diphenylphosphino)propane (dppp): A cationic complex [Ag(dppp)$_2$]$^+$ (**158**) is obtained for X = SCN$^-$, NO$_3^-$; when X = Cl$^-$, Br$^-$, I$^-$, CN$^-$, neutral complexes [Ag(dppp)X] (e.g. **159**) are formed[232].
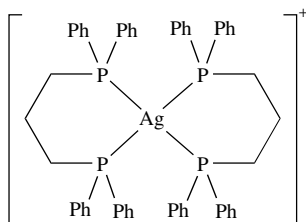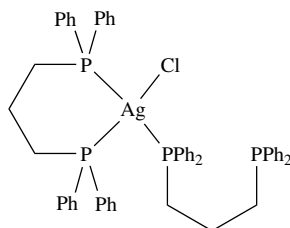
(158) **(159)**

P-3   The silver cluster in complex **160** has a square-planar Ag$_4$ ring geometry with the chalcogenide atom E sitting off this plane; this deviation is largest for Te. The range of some distances in nm units for E = S, Se, and Te, respectively: Ag−Ag 0.3038 to 0.3160, 0.3055 to 0.3232, 0.3071 to 0.3357; Ag−E 0.2508 to 0.2513, 0.2613 to 0.2622, 0.2745−0.2765; Ag−P 0.242 to 0.251 for all three. The Ag−Ag distances point to a progressively weakening Ag−Ag interaction with increasing atomic number of E[233].

TABLE 3.   (*continued*)

No.	Complexes and comments
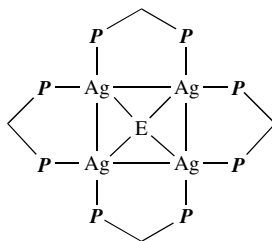
P = PPh$_2$; E = S, Se, Te

(160)

P-4   A series of multinuclear phosphinidine-bridged silver clusters were prepared, where many of
the neighboring Ag atoms are at distances of about 0.29 to 0.30 nm, but some of them are at
shorter distances[234]. For example,

$$[Ag_{18}(PPh)_8(PhSiMe_3)_2(PPr_3)_8]$$

$$[Ag_{45}(PPh)_{18}(PhSiMe_3)_2(PPr_3)_{12}Cl_7] \qquad [Ag_{50}(PPh)_{20}(PPr_3)_{13}Cl_7]$$
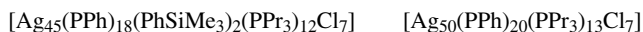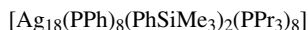
P-5   A phosphinic calixarene is complexed to four Ag(I)Cl molecules and one additional chloride
ion to give an anion **(161)** that can act as host for alkali metal cations, Hg(II) and Pb(II)[235,236].
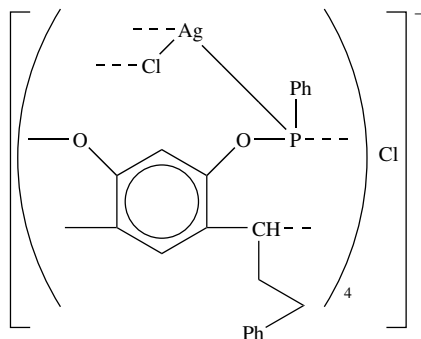
(161)

P-6   Interatomic distances in complex anion **162**: Ag—Ag 0.31618–0.32228 nm, Ag—P
0.2427–0.2485 nm, Ag—N 0.2592–0.3161 nm; Ag—Ag—Ag angles 56.46–61.67°. The
solvating acetonitrile molecules are differently attached to the cluster by weak coordination of
the N atoms. The close gold analog (item P-12 of Table 2) has shorter metal–metal distances
in the cluster, allowing metal-to-metal bonding[204].

TABLE 3.   (*continued*)

No.	Complexes and comments
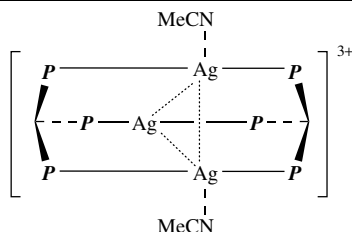
(**162**, ***P*** = PPh$_2$)

P-7   Compound **163** crystallizes in linear polymeric chains (**164**) where **163** units are linked by Br bridges, with the eight-membered rings at right angles to the four-membered rings. Interatomic distances: Ag–Br 0.27431–0.29453 nm, Ag–P 0.24229–0.24339 nm, Ag–Ag 0.3605 nm (8-ring), 0.3912 nm (4-ring). The Ag–Ag distances are too long for bonding[203]. See item P-11 of Table 2 for a similar case where metal-to-metal bonding exists.
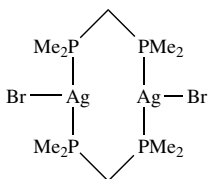
(**163**)
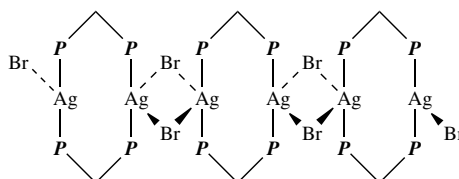
(**164**, ***P*** = PMe$_2$)

P-8   A mixed trinuclear cluster complex [Ag{Au(2,4,6-Me$_3$C$_6$H$_2$)}$_2$(dppm)$_2$]ClO$_4$ (**63**) T^c. Interatomic distances: Au–C 0.2080 nm, Au–P 0.2315 nm, Au–Ag 0.2944 nm and Ag–P 0.2413 nm; no bonding between Au atoms[172].
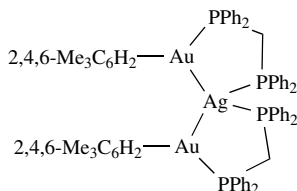
(**63**)

^{a}See Section IV.D.2 for further structural evidence based on NMR spectroscopy.
^{b}See Section IV.B.2 for further structural evidence based on vibrational spectra.
^{c}dppm = bis(diphenylphosphino)methane.
^{d}oetp = *meso*-octaethyltetraoxaporphyrinogen.
^{e}See Section IV.E for further structural evidence based on ESR spectroscopy.

OBu-*n*

X

X

N=N Au Cl / Cl

Cl

OBu-*n*

N=N Au Cl / Cl

X

N=N Au Cl / CH₂COCH₃

X

(165)

(166)
X = OBu, Bu, *n*-C₁₀H₂₁

(167)
X = OBu, Bu, *n*-C₁₀H₂₁

CH₂= OH HO Me

Me N N HO CH₂

N N

HN Me

Me

HO₂C CO₂H

(168)
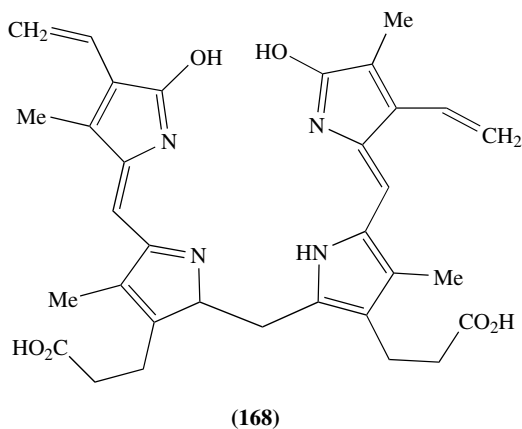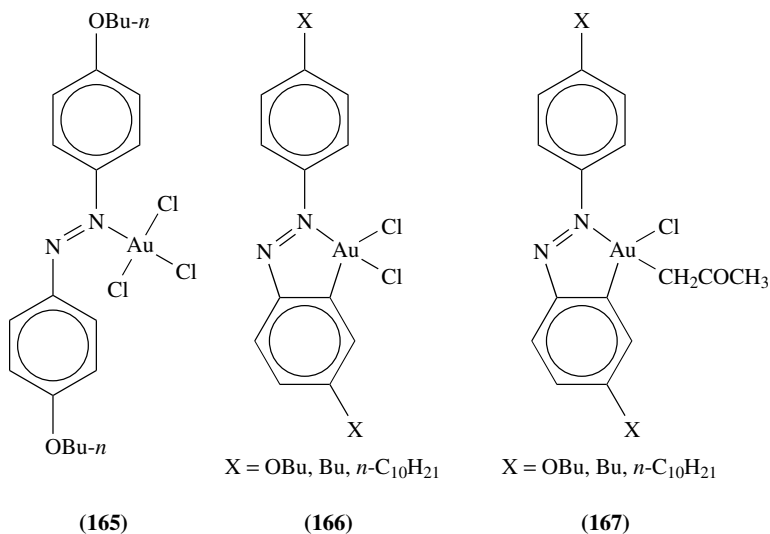
Gold reacts with nitrosyl tetrafluoroborate or hexafluorostibnate in nitrile solvents (RCN) to yield solvated Au(I) salts, according to reaction 19. Bonding with acetonitrile (R = Me) is too weak to enable characterization of the complex cation at room temperature. However, for benzonitrile (R = Ph) or pivalonitrile (R = *t*-Bu) the solvated salts **169** could be isolated and used as synthons for a wide variety of Au(I) complexes. In the IR spectrum of the product obtained from benzonitrile solution the $\nu(C{\equiv}N)$ stretching band appears at 2295–2299 cm^{-1}, a frequency higher than that of plain benzonitrile, pointing to the involvement of the cyano group in the complex (see also Section IV.F.1 below)[239]. The bands at 326–315 cm^{-1} of complex **81** (item S-2 in Table 2) were attributed to $\nu(Au{-}S)$ stretching vibrations[185].

$$\text{Au} + \text{NOBF}_4 \xrightarrow[R = Me, Ph, \textit{t}-Bu]{R-CN} [\text{Au(NC-R)}_2]^+ \text{ BF}_4{}^- \tag{19}$$

(169)
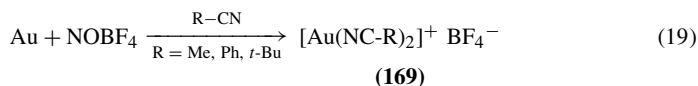
The nonlinear optical properties of complex Au(I) arylacetylides (**67**, item C-8 of Table 2) were determined by hyper-Raleigh scattering at 1064 nm. The following structural changes caused a significant increase in nonlinearity: introduction of a nitro group (**a** to **b**), chain lengthening (**b** to **c** to **d**), replacing biphenyl or yne linkage to ene linkage (**c** or **f** to **d**), replacing *zusammen* by *entgegen* configuration (**e** to **d**) and repacing a C=C by an N=C linkage (**d** to **g**)[175].

(67)

(a) X = H

(b) X = NO$_2$

(c) X = C$_6$H$_4$NO$_2$-*p*

(d) X = (with C=C, H and C$_6$H$_4$NO$_2$-*p* substituents)

(e) X = (with C=C, C$_6$H$_4$NO$_2$-*p* and H substituents)

(f) X = —C≡C—C$_6$H$_4$NO$_2$-*p*

(g) X = —N=C—C$_6$H$_4$NO$_2$-*p* (with H)
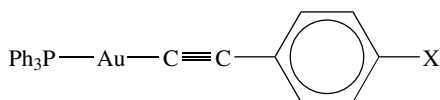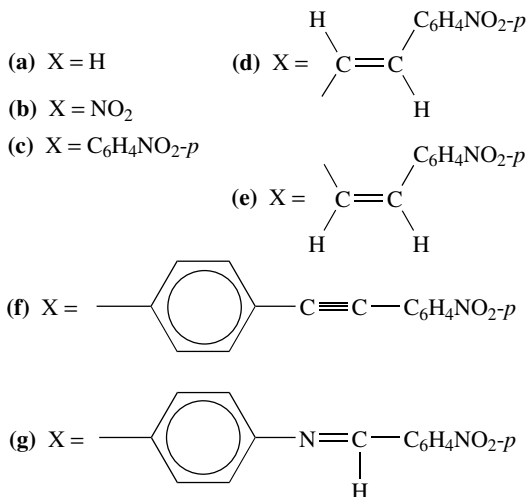
2. Silver

IR spectroscopy was used to elucidate detection of the structure of gold and silver complexes (**170**) with azobenzene compounds , including formation of N—metal bonds (compare to complexes **165–167** above)[237]. The resonance Raman spectra of bilirubin (see **168** above) and its complexes with Cu(II), Ag(I) and Au(III) showed that the complexes had different structures, due to differences in ionic charge and ionic radius between the metal ions[238]. IR spectra of complexes Ar$_3$P—Ag—X, with X = Cl, Br (**157**, item P-1 in Table 3) showed strong ν(Ag—X) stretching bands, whereas in the case of X = I no such vibrational mode could be assigned[231]. The IR spectrum of compound **126** (item N-1 in Table 3) points to the presence of H-bonding between the NH of the imidazole ring and the anion X[213]. *p*-Ethoxychrysoidine (**171**) is used as adsorption indicator for titration of

iodide with silver. Comparison of the $\nu(NH_2)$ stretching and $\delta(NH_2)$ deformation bands (3500–3100 and 1630–1615 cm^{-1} regions, respectively) of the free crystalline dye and of **171** adsorbed on AgI led to the conclusion that in the adsorbate bonding takes place through the amino groups. Adsorption arises from interaction of the partial charges on the amino groups and the partial negative charge on the silver iodide surface[240].

X = OBu-*n*, OC$_8$H$_{17}$-*n*
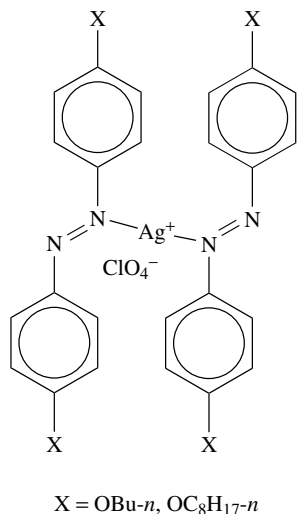
(170)
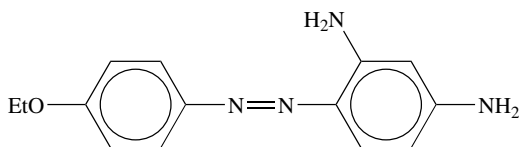
(171)

The UVV emission spectrum of arylacetylide complexes **111** and **112** (item C-2 of Table 3) shows a vibrionic structure in which the series of $\Delta\nu = 2080–1880$ cm^{-1} can be ascribed to superimposition of $\nu(C\equiv C)$ stretching vibrations[206]. The $\nu(C\equiv C)$ band at 1948–1912 cm^{-1} in the IR spectra of the titanocene complexes **172** pointed to the π-bonding of acetylenic moieties with Ag(I)[241]. See also Sections IV.D.2 and IV.F.2 below, and the analogous compound **116** (item C-5 of Table 3).
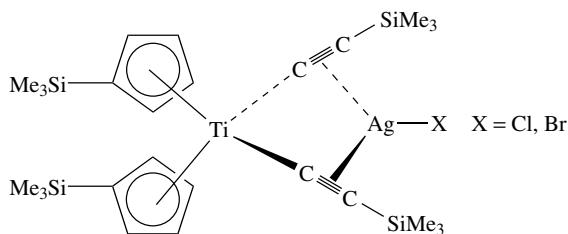
(172)

A film of Ag nanoparticles embedded in a polycrystalline C$_{60}$ matrix was grown by codeposition under high vacuum. The Raman spectrum shift to lower frequency observed

for the $A_g(2)$ pentagonal-pinch mode of C_{60} points to strong interfacial interaction and charge transfer from the Ag to C_{60}[242]. It was demonstrated by dispersive IR and FT-Raman spectroscopy that at the infinite dilution limit of silver triflate or perchlorate, the solvation number of Ag(I) ions in acetonitrile is 3. At higher concentrations this number decreases due to ionic pairing. The ion pair is bidentate with 2 molecules of acetonitrile in the first solvation shell of Ag(I)[243].

FTIR and NMR (see Section IV.D below) spectra showed that in the complex of poly[bis(alkylamino)phosphazene] **(173)** with silver nitrate, silver ions are bonded to N atoms of both the chain and the side groups. The conductivity of the complexes can rise up to four orders of magnitude higher than that of the uncomplexed polymer[244].

R = Pr, Bu
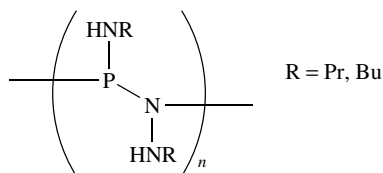
(173)

C. Ultraviolet−visible Region

1. Gold

Au−Au bonding can be adduced from UVV spectra of organogold compounds. Thus, complex **59** (item C-3 in Table 2) shows no such bonding either in solution or in the solid state. Some weak photoluminescence is observed for solutions of **60** and a stronger one for **61**. Photoexcitation of compound **174** at 320 nm in CH_2Cl_2 solution leads to an emission spectrum at 400−600 nm with well resolved vibrational spacing of 2100 nm, that was attributed to $\nu(C\equiv C)$ stretching[170]. Au(I) complex **175** has nearly no absorption in the $\lambda > 300$ nm region while the complex cations **103** and **104** (item P-8 in Table 2) display an appreciable absorption, ascribed to weak Au−Au interactions at distances less than 0.33 nm. Complexes **176** of bidentate ligand bis(diphenylphosphino)methane and of tridentate ligands **(102−104)**, both in solid state or in solution, display photoluminescence, related to the Au(d) → phosphine(π^*) transition, modified by Au−Au interactions, and for the iodine-containing complexes also the $I^- \rightarrow$ phosphine(π^*) transition. Complex **175** displays no photoluminescence[200].

$$(p\text{-MeOC}_6\text{H}_4)_3\text{P}\!-\!\!\text{Au}\!-\!\!\text{C}\!\equiv\!\text{C}\!-\!\!\text{Au}\!-\!\!\text{P(C}_6\text{H}_4\text{OMe-}p)_3$$

(174)

[AuI(PPh₃)]   [Au₂X₂(dppm)]
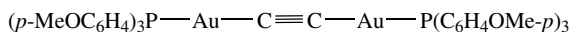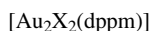
(175)   **(176)** **(a)** X = Cl
                                             (b) X = I

Two emission bands were observed for complex cation **97** (item P-5 of Table 2) on excitation at 280 nm: The one at 560 nm was attributed to a singlet-to-singlet transition for a ligand-to-metal excitation, and the second one at 310 nm to Au−Au interaction[197].

2. Silver

The SH groups of cysteine residues (**177**) in the rabbit liver protein metallothionein (MT) and two of its fractions (α-MT, β-MT) can bind transition metal ions. Thus, formation of the silver complexes Ag_{12}-MT, Ag_{18}-MT, Ag_6-α-MT and Ag_6-β-MT was determined by circular dichroism (CD), when zinc complexes of metallothionein and its fractions were titrated with Ag(I) ions. The intense CD spectrum of one of the silver complexes was attributed to supercoil formation[245]. The UVV spectra of bilirubin (**168**) and its complexes with Cu(II), Ag(I) and Au(III) showed that the complexes had different structures, due to differences of ionic charge and ionic radius between the metal ions[238].

$$CH_2SH$$
$$|$$
$$\cdots\cdots NH-CH-CO\cdots\cdots$$

(177)
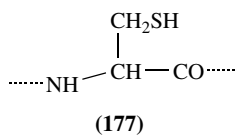
D. Nuclear Magnetic Resonance

1. Gold

The planar stereochemistry at the Au atom in complexes **62** (item C4 of Table 2) was demonstrated by ^{1}H NMR: The Me groups showed two different splitting constants due to coupling with ^{31}P, depending on the *cis* or *trans* configuration. The CH$_2$ of the R group showed coupling with ^{31}P too, but none of the olefinic protons or Me groups did. This points to absence of C=C coordination to Au[171]. ^{1}H and ^{13}C NMR of the complexes $R_3P-Au-SC_6H_4CO_2H$-*o*, R = Et, Ph, *c*-Hex confirmed the presence of the thiolate link to Au(I) and the absence of coordination to carboxylate (see item S-3 in Table 2)[187]. It was shown by ^{31}P NMR that compound **84** (item S-5 in Table 2) undergoes fast phosphine ligand interchange in solution, rendering equivalent all three ligands[190].

Compounds **178** and **179** were used for microlithographic deposition of Au and AuPd alloy with an electron beam. The alkyl groups were characterized by ^{1}H and ^{13}C NMR spectroscopy. The ^{19}F NMR spectrum of **178** showed a unique peak with no coupling, in accord with the D_{2h} symmetry of the F atom environment. The spectrum of compound **179** showed a dominant singlet and a set of smaller peaks; none of the H peaks of *i*-Bu or *c*-Hex showed coupling with the F nuclei[8].
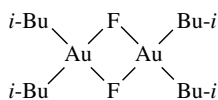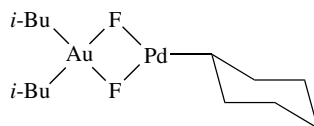
(178)   **(179)**

Phosphine-stabilized Au(I) ions can replace protons of amino groups, ultimately yielding analogs of quaternary ammonium compounds (**180**), as shown in reaction 20, where X represents an unreactive organic structure. A series of compounds of structure **180** were prepared according to reaction 20 and were characterized by their ^{1}H, ^{13}C and

^{31}P NMR spectra; e.g. the derivatives of aniline, *o*-, *m*- and *p*-diaminobenzene and 1,2-diaminoethane[246]. ^{31}P NMR evidence points to three equivalent P atoms in complex cation **75** (item N-4 of Table 2). This was interpreted as the quinolinyl group freely rotating around the $N-C_{(8)}$ axis. Also the four P atoms of complex **76** in solution are equivalent, suggesting that the N atoms change their coordination from one Au atom to another at a fast rate relative to the NMR time scale[181].

$$X-NH_2 + \{[Ph_3PAu]_3O]^+BF_4^-\} \xrightarrow[THF]{-H_2O} [X-N(AuPPh_3)_3]^+BF_4^- \tag{20}$$
$$\mathbf{(180)}$$
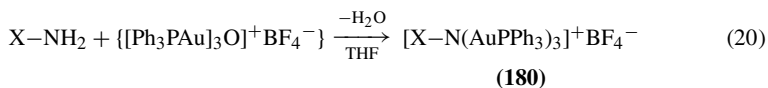
2. Silver

A review appeared on the chemistry of transition metal complexes with strained cyclophanes. NMR evidence was very important in the characterization of these complexes[247]. The solubility of $[2_3](1,4)$cyclophane **(181)** in $CHCl_3$ increases in the presence of silver triflate (AgO_3SCF_3) due to a π complex formation[248]. Deltaphane (**110**, item C-1 in Table 3) becomes soluble due to complex formation with Ag(I). The metal ion is interchanged; however, it does not cross the central cavity of **110**[249]. In the complex of Ag(I) with cyclophane **182** the ion is bonded only to the naphthalene ring as π electron donor[250].
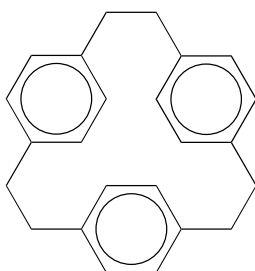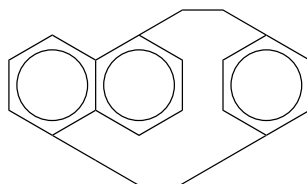
(181)   **(182)**

It was shown by ^{13}C and ^{31}P NMR and FTIR spectra that in the complex of poly[bis(alkylamino)phosphazene] **(173)** with sliver nitrate, silver ions are bonded to N atoms of both the chain and the side groups[244]. ^{1}H NMR and ^{19}F NMR spectra of complex polymer **134** (item N-4 in Table 3) and its analogs in solution are similar to those of the free ligands, pointing to dissociation of the polymer in solution[216]. The Ag(III) complex anion **120** (item C-8 of Table 3) was prepared by oxidation of the corresponding Ag(I) complex, as shown in reaction 21. The change of oxidation state could be demonstrated by [109]Ag NMR spectroscopy. Multinuclear NMR spectra of the nearly planar argentate complex anions **121** and **122** (item C-8 of Table 3) allowed *cis–trans* configuration assignments[211].

$$[Ag(CHF_2)_2]^- \xrightarrow{Br_2} [Ag(CHF_2)_4]^- \tag{21}$$
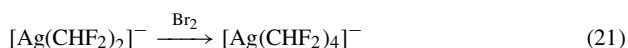
^{31}P NMR spectra of complexes **157** (item P-1 in Table 3) in CHCl$_3$ solution show two doublets due to coupling with [107]Ag and [109]Ag; $\delta - 67.2$, -66.4 and -64.6 ppm, [1]J([31]P–[107]Ag) 821, 796 and 745 Hz for X = Cl, Br and I, respectively. The [1]J values are larger than those reported for complexes with analogous triarylphosphines, pointing to the high base strength of the ligand used here. [31]P cross polarization–magic angle spinning NMR (CP-MAS-NMR) spectra of the solids were similar to those of the solutions. Complex **183** is obtained in solution from **157** in the presence of excess ligand. The ionic nature of the silver-to-halogen bond is demonstrated by the independence of the ^{31}P NMR spectra of the nature of the X$^-$ anion[231].
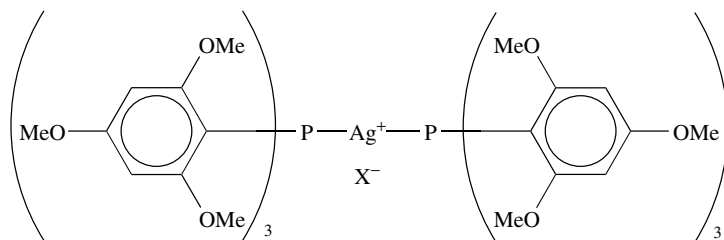
(183)

^{31}P CP-MAS-NMR spectra of the solid complexes of various Ag(I)X salts with 1,3-bis(diphenylphosphino)propane (dppp) pointed to two different types of complex, [Ag(dppp)$_2$]$^+$ and [Ag(dppp)X] (item P-2 in Table 3). ^{31}P NMR of the dissolved complexes showed that equilibration takes place between both complex types[208]. ^{13}C CP-MAS-NMR spectra of the polymeric complex **142** (item N-9 in Table 3) pointed to two different types of carboxylate groups in the phthalate anion[221].

Compound **126** (item N-1 in Table 3) undergoes decomposition in DMSO solution as its ^{1}H NMR and ^{13}C NMR spectra coincided with that of the ligand 4-nitroimidazole. The ^{13}C NMR spectrum of the 1 : 1 complex **184** points to its polymeric nature, including deprotonated 4-nitroimidazole units[213].

(184)

The behavior of aurothioglucose (**2**, Table 1) in the presence of cyanide ion was studied by ^{13}C NMR spectroscopy. The presence of an association species **2**-CN$^-$ could be

detected only when cyanide-^{13}C was used; when the **2**:CN$^-$ molar ratio was 1 : 2 the only product detected was the [Au(CN)$_2$]$^-$ complex anion[251].

E. Electron Spin Resonance

Complex **146** (entry O-3 of Table 3) forms a free radical in THF solution and the electron paramagnetic resonance (EPR) spectrum shows a weak triplet signal with hyperfine splitting by coupling with the P ligands. The triplet disappears when Ag(0) precipitates[224]. The presence of covalent radicals [Ag−CH(R)OH]$^{\bullet+}$, R = H, Me, in Ag(I)-containing molecular sieves loaded with MeOH or EtOH was detected by EPR and electron spin echo envelope modulation spectroscopies[252].

F. Mass Spectrometry

1. Gold

The gas-phase reactions of Au$^+$ ions with small alkenes, such as ethene, propene, 1-butene, *cis*-2-butene and *trans*-2-butene, was studied with quadrupole MS. In the case of propene, for example, the main processes are reaction 22, of 5% yield, and reaction 23, of 95% yield. The species denoted by (∗) were actually detected[253a].

$$C_3H_6 \xrightarrow{Au^+} H{-}Au{-}+ \Big\rangle\!\!\Big\rangle \longrightarrow Au^+ \diamondsuit \xrightarrow{C_3H_6} (AuC_6H_{12})^+ \tag{22}$$

$$C_3H_6 \xrightarrow{Au^+} H{-}Au\ ++ \Big\rangle\!\!\Big\rangle \xrightarrow{C_3H_6} \tag{23}$$

$$C_2H_4 + C_4H_7^+ \xrightarrow{C_3H_6} C_7H_{13}^+$$

$$C_6H_{11}^+$$

FAB-MS of gold phenylacetylide complex **185** shows a fragmentation pattern involving loss of PPh$_3$, Ph and PhC$_2$ groups and intermediate formation of clusters of formula **186**. It should be pointed out that **185** exists in the crystalline state as a polymer with Au−Au long-range contacts[253b].

$$Ph{-}C{\equiv}C{-}Au{-}PPh_3$$

(185)

$$[Au_a(C_2P)_b(PPh_3)_c]^+$$

$$1 \leq a \leq 4;\ a \geq b \geq c$$

(186)

The MS of compound **178** showed a molecular peak with m/z 661 and fragmentation peaks typical of the alkyl groups[8]. The peak corresponding to cation **75** (item N-4 of Table 2) is the parent peak of the field desorption MS of its salts[182]. The peak for [Au(S$_2$C$_2$B$_{10}$H$_{10}$)$_2$], corresponding to the carborane complex anion **83** (entry S-4 of Table 2), appeared in the negative ion FAB-MS of its salts[188]. The FAB-MS spectrum of the complex salt **169** (R = Ph), produced according to reaction 19, showed the parent

peak of $[Au(NC-Ph)_2]^+$ (m/z 403) and the derived cation $[Au(NC-Ph)]^+$ (m/z 300)[239]. The existence of reactive carbene intermediates such as $[Au(=CPh_2)(C_6H_5)]$ was detected by FAB-MS[254].

The relative affinity series 24 was found for bare Au^+ ions binding with various molecules M, to yield complex ions $[AuM]^+$. This took place in the low-pressure regime of a Fourier transform ion cyclotron resonance MS. The absolute bond dissociation energies were evaluated by means of *ab initio* MO calculations at the MP2 level of theory[255].

$$C_6F_6 < H_2O < CO < C_2H_4 < C_6H_6 < NH_3 < C_3H_6 < C_4H_6 \qquad (24)$$
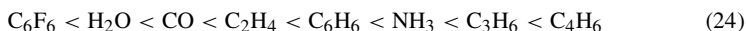
2. Silver

Adding $AgNO_3$ to solutions of hydrocarbon polymers before analysis by laser-desorption FT-MS allows efficient Ag ion chemical ionization. This was applied to polystyrene **(187)**, polyisoprene **(188)**, polybutadiene **(189)** and polyethylene **(190)**. Oligomers attached to Ag^+ were observed with m/z values ranging from 400 to 6000 D, with unit mass resolution[256].

$$n\text{-Bu}-(CH_2-CH)_n-H \qquad s\text{-Bu}-(CH_2CH=CCH_2)_n-H$$
$$\underset{Ph}{|} \qquad\qquad\qquad\qquad \underset{Me}{|}$$

(187)   **(188)**

$$s\text{-Bu}-(CH_2CH=CHCH_2)_n-H \qquad H-(CH_2CH_2)n-H$$
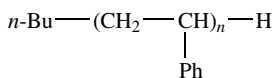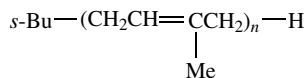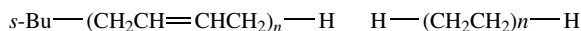
(189)   **(190)**

FAB-MS of silver phenylacetylide complex **191** shows a fragmentation pattern involving loss of PPh_3, Ph and PhC_2 groups and intermediate formation of clusters of formula **192**. It should be pointed out that **191** exists in the crystalline state as a disproportionation copolymer, analogous to **115** (item C-4 of Table 3)[253].

$$[Ag_a(C_2P)_b(PPh_3)_c]^+$$

$$Ph-C\equiv C-Ag-PPh_3 \qquad 1 \leq a \leq 3; \ a \geq b \geq c$$
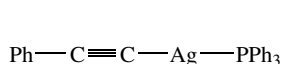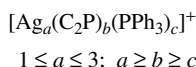
(191)   **(192)**

Field desorption MS of the titanocene complex **172** with X = Cl (Section IV.B.2 above) showed the molecular peak at m/z 660, besides other fragmentation peaks[241]. Ag(I) yields complexes in solution with sulfur and nonsulfur containing peptides. Although S atoms are a good anchoring site for Ag(I) in solution, electrospray tandem MS of these complexes pointed to a different situation for the breakdown species, where Ag is chelated by N and O atoms[257].

G. Miscellaneous Optical and Spectral Methods

The validity of the methods for background correction when using XPS was investigated. Significantly large errors were found for various methods when applied to Ag,

Au and Pt compounds. The Tougaard method gave approximately 3% RSD from theory, which is of the order of the expected uncertainty due to the effects of instrumental stability and the errors in the ratio of photoionization cross-sections[258]. Additional considerations for background correction were made from reflection electron energy-loss spectroscopy (REELS) measurements at different take-off angles[259].

The structure of the bis(triphenylphosphine)gold(I) complex **(193)** in pyridine solution was examined by large angle X-ray scattering (LAXS). The bond distances (Au−P 0.2325 nm and Au to the six closest C atoms 0.344 nm) were in agreement with those found for the solid state complex. No coordination of Au with pyridine was observed[260].

$$[Ph_3P\!-\!\!\!-Au\!-\!\!\!-PPh_3]^+$$

(193)

The state of adsorption of aurocyanide anions on various types of anion exchangers was investigated using XPS. Two weak bases were used, cross-linked poly(diallylamine) **(194)** and Duolite A7 **(195)**, and a strong base, IRA 400 **(196)**. The photoelectron peaks of $N(1s)$ pointed to two states for the nitrogen atom of resins **194** and **195**. The $Au(4f)$ photoelectron peaks pointed to three well defined states: Au(0), AuCN and $Au(CN)_2{}^-$. When a solution containing $Au(CN)_2{}^-$ anions was placed in contact with the quaternary ammonium resin **196**, equilibrium was reached by anion exchange. A different reaction scheme took place when the aurocyanide solution was placed in contact with the weak base resins **194** and **195** in their protonated form $R^+\!-\!H$. First a chemisorption step occurred, according to reaction 25; this is in accord with the absence of XPS evidence for $Au(CN)_2{}^-$ ions in the resin. On elution with base, part of the gold remains in the resin as elementary gold whereas the eluted complex anion may contain one or several gold atoms. The process is believed to take place reductively, as depicted in reaction 26, with $n = 2, 3, 4, \ldots$. This is in accord with the energies of the photoelectron peaks of the elution products showing a spread of values between that of AuCN and that of $Au(CN)_2{}^-$. The disproportionation reaction 27 can leave some gold attached to the resin too[261].

(194)   **(195)**   **(196)**

$$R^+\!-\!H + Au(CN)_2{}^- \longrightarrow R\!-\!AuCN + HCN \qquad (25)$$

$$nR\!-\!AuCN + e^- \longrightarrow Au(0) + [Au_{n-1}(CN)_n]^- \qquad (26)$$

$$2R\!-\!AuCN + e^- \longrightarrow RAu(I) + R + Au(CN)_2{}^- \qquad (27)$$
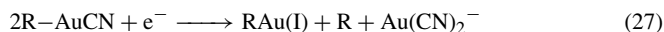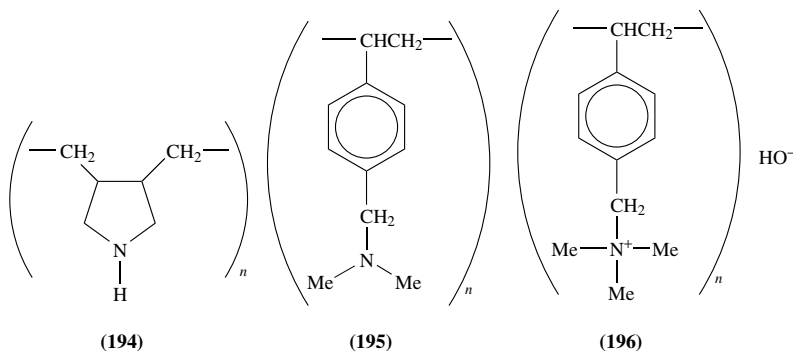
A review appeared on the interactions observed between polyimide surfaces and metallic films developed on them by vapor deposition. Coverage includes several monolayers, but special attention is given to chemical and nonchemical effects observed at very low coverage by the metal on applying Fourier transform infrared reflection absorption spectroscopy and near edge X-ray absorption fine structure (NEXAFS) spectroscopy. Except for K deposits, only attenuation of the IR bands was observed. In the case of Au, Cu, Ag and Pd this attenuation can be explained by purely physical interaction mechanisms, such as dynamical dipole screening and changes in the intermolecular dipole−dipole coupling between the polymer macromolecules[262].

A silver layer 0.3−1.5 nm thick was deposited on boron-doped diamond and thermally annealed until it disappeared. In contrast to other metals, no evidence for intermixing, graphitization or carbide formation was observed at the interface by Auger electron spectroscopy, ionization loss spectroscopy and low energy electron diffraction[263]. It was shown by Auger electron spectroscopy that no Ag−Si bonds are formed at the interface of silver deposited on or annealed with silica, in contrast to Ti deposited on or annealed with silica[264].

H. Electrochemical Methods

The composition and formation constants of silver complexes with 6-phenyl-2,2′-bipyridine (bpp, **197**), in propylene carbonate solution (**198**), were determined potentiometrically. Cyclic voltametry and galvanostatic coulometry were used to determine the normal potential of the reduction processes of Ag(II) to Ag(I), as depicted in reactions 28 and 29[265].

(197)   **(198)**

$$[Ag(bpp)_2]^{2+} + e^- \rightleftharpoons [Ag(bpp)_2]^+ \qquad (E_f^\circ = 1.555 \text{ V}) \qquad (28)$$

$$[Ag(bpp)_2]^{2+} + e^- \rightleftharpoons [Ag(bpp)]^+ + (bpp) \qquad (E_f^\circ = 1.300 \text{ V}) \qquad (29)$$
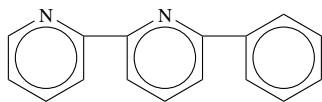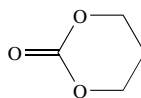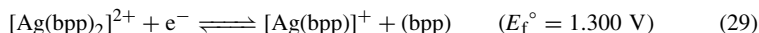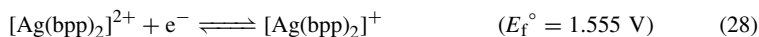
The oxidation potential of the osmium complex [*trans*-Os(CO)$_3$(PPh$_3$)$_2$] in the presence of silver trifluoroacetate in CH$_2$Cl$_2$ solution is higher by 0.51 V than that of the complex [*trans*-Os(CO)$_3$(PPh$_3$)$_2$] alone. This points to the formation of the intermediate complex **146** (item O-3 of Table 3), that can serve as a model for the intermediate electron transfer stage in oxidation reactions by Ag(I)[224].

I. Chromatography

1. LC of gold pharmaceuticals and their metabolites

Aurothioglucose (**2**, Table 1) was identified by TLC on a plate impregnated with silicic acid and a fluorescent compound, according to the R_f value and fluorescence quenching[120]. Various studies were published for the speciation of auranofin (**1**)[266,267] and sodium aurothiomalate (**3**)[268] in urine, blood and plasma. Using an ICP-MS detector it was possible to detect five gold-containing metabolites of **1**[269,270].

2. LC aided by silver ions

The interaction by π coordination of Ag(I) between silver ions and C=C double bonds or aromatic groups is the basic principle for many effective chromatographic separations. Silver trifluoroacetate and silver trifluoromethanesulfonate are very soluble in poly(methylphenylsiloxane), due to the presence of phenyl groups. Such stationary phases were studied for the GC separation of benzene–cyclohexene–cyclohexane mixtures. The salting-out effects and formation constants of the complex of Ag(I) with various olefinic and aromatic compounds were estimated based on retention time measurements[271].

Silver ion chromatography of unsaturated lipids have been reviewed[272,273]. Ag(I) is usually part of the stationary phase, as in GC[273,274], TLC[275] or HPLC using cation-exchange columns[273,276]. However, the silver ions may be part of the mobile phase, as in reversed-phase HPLC[274,277]. HPLC combined with atmospheric-pressure chemical ionization MS detection has been applied for characterization of the eluted lipid fractions[273]. Supercritical fluid chromatography using argentated columns was investigated for triglyceride separation. The mobile phase consisted of a mixture of carbon dioxide, acetonitrile and isopropanol. A UVD or an evaporative light-scattering detector was used[278]. A study of the performance of silver ion chromatographic columns on saturated fatty acid methyl esters and triglycerides showed that the effect of the silver ions is that of π-bonding with olefinic unsaturations[279]. A rapid silver ion HPLC procedure was developed for the isolation of the Me ester of *trans*-monoenoic fatty acids[280].

V. SELF-ASSEMBLED MONOLAYERS

A. General

A field of growing activity and relevance is the investigation of the chemical nature, supramolecular structure and development mechanism of layers of organic compounds, as they become adsorbed on surfaces of known structure. Under easily controlled conditions it is possible to develop the so-called self-assembled monolayers (SAMs) of organic compounds. A general mechanisms for SAM development can be depicted as follows: On exposing a clean surface to a medium containing the species of interest (say a solution or a vapor chamber) molecules of the species begin to cover the surface by physisorption, followed if possible by chemisorption. At low degrees of surface coverage the molecules attain almost random conformations. However, as coverage increases, the conformations become restricted due to mutual interaction of the sorbed molecules, and definite supramolecular patterns begin to develop. For strongly chemisorbed molecules more than one defined SAM structure may be recognized as the coverage density increases to its maximum. It should be pointed out that SAM development is a reversible process governed by the laws of chemical equilibrium. A great variety of analytical tools has been applied in SAM investigation to probe structural features at the molecular and supramolecular level, including microscopic, optical, spectral, electromechanical, electrochemical and other physicochemical methods.

Of special interest in general, and for the present chapter in particular, are SAMs grown on gold and silver surfaces. These elements have a face-centered cubic crystalline structure, with lattice parameter of 0.40789 and 0.40862 nm, respectively. The surface growing normal to the (111) crystalline direction, denoted by Au(111) or Ag(111), is the one of lowest surface energy, and is the one that develops faster when thin layers of the metal are grown. (111) surfaces show the closest 2-D packing of atoms in the crystal, namely every atom is surrounded by six equidistant closest neighbors in the plane.

SAMs developed on Au(111) thin layer surfaces, single crystals or polycrystalline gold have attracted the widest attention. In contrast to gold surfaces, only meager attention has been paid to analogous phenomena taking place on silver surfaces, despite their important function in surface-enhanced Raman spectroscopy (SERS) and related spectroscopic techniques. Raman spectra enhancement techniques involving adsorption on colloidal silver surfaces are now widely applied. Enhancement factors over unenhanced Raman spectra of several orders of magnitude are observed, e.g. 1×10^6 for p-aminobenzoic acid on a silver/alumina substrate[281].

Monolayers of enzymes, proteins and lipids were developed on SAMs derived from thiols on gold; they can serve as models for the physiological functions of cell membranes[282]. A series of thiols $HS(CH_2)_{15}X$ (X = CH_2OH, CO_2Me, Me, CO_2H) was used to prepare functionalized SAMs on gold. They were investigated for the adsorption and elutability of two serum proteins, albumin (Alb, a nonadhesive or growth blocking protein) and fibronectin (Fn, an adhesive protein). Bovine aortic endothelial cells grown on the SAM became attached to it by means of a protein layer. Cell growth depended on the functionality of the terminal group of the thiol as follows: $CH_2OH < CO_2Me < Me \ll CO_2H$. This was consistent with the fact that the SAMs with terminal CO_2H groups showed the highest Fn adsorption and the highest Alb elutability[283]. A similar preference for the CO_2H SAMs was shown by murine 3T3 fibroblast cells growth[284].

SAMs on Au may serve as cell membrane simulation surfaces endowed with hydrophobic and hydrophilic properties. They were prepared with hydrophobic 1-hexadecanethiol (HDT) and the hydrophilic compound **199** (EG_6OH). The SAMs were used to study effects on dissociation of proteins adsorbed on hydrophobic layers by four typical detergents: sodium dodecyl sulfate **(200)**, β-octyl glucoside **(201)**, Tween 20 **(202)** and Triton X **(16)**. The main analytical tool used was surface plasmon resonance (SPR) spectroscopy, measuring the shift in the resonance angle, $\Delta\Theta_m$, for the surface in the presence of various detergent concentrations relative to the clean solvent. The hydrophobic SAM showed strong association with the detergents whereas the hydrophilic one showed lower $\Delta\Theta_m$ values that were proportional to the detergent concentration. The latter results were interpreted as due to weak detergent interaction with the SAM[285].

$HO(CH_2CH_2O)_6(CH_2)_{11}SH$ $n\text{-}C_{12}H_{25}OSO_3Na$

(199)   **(200)**   **(201)**

$w + x + y + z = 20$

(202)
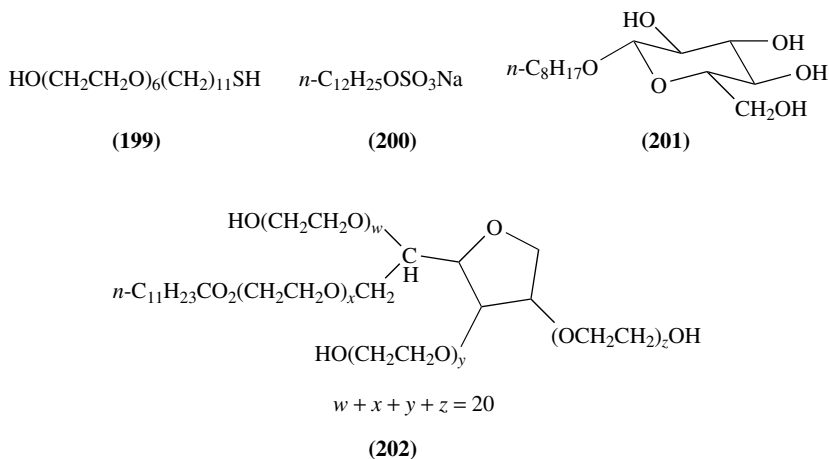
The characteristic electrochemical behavior of enzyme, protein and lipid monolayers adhered to SAMs derived from thiols on gold surfaces may be applied to the development of biosensors. The gold electrodes resulting from incorporation of monensin (**203**) and valinomycin (**204**) into bilayers, consisting of the SAMs of alkanethiol covered by a lipid monolayer, have high sensitivity for monovalent ions[282]. A gold electrode with a SAM of a modified β-cyclodextrin was proposed for electrochemical detection of organic compounds[286].
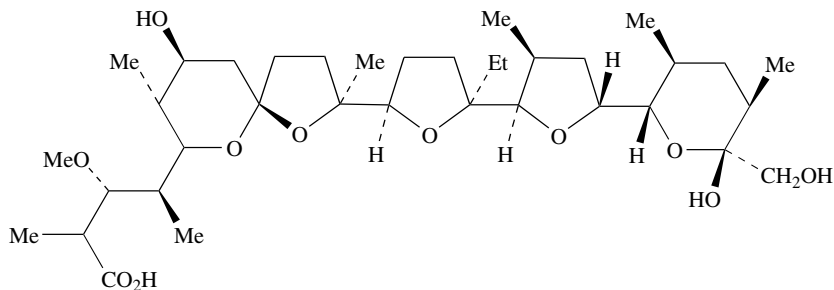
(203)
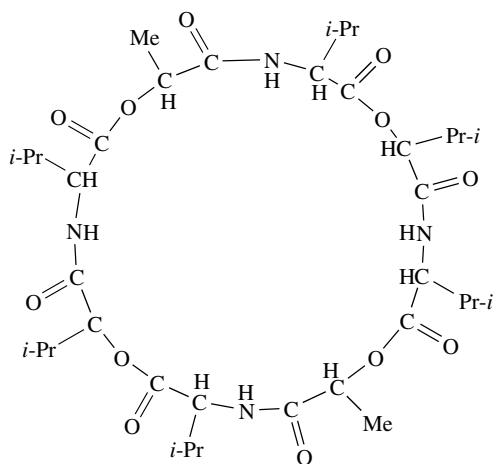
(204)

The strong chemical interaction of a lipid thiol monolayer developed on a gold disk electrode yields a structure resembling a biological membrane. The blocking ability of various substances was tested for the cyclic voltametry redox reaction of $[Fe(CN)_6]^{3-}$ ions, upon adsorption on the thiol monolayer. This was applied to measure the threshold concentrations for detection of various odor substances. The order of response shown in series 30 was the same as the one followed by the human olfactory sense, pointing to

the potential usefulness of thiol on gold monolayer membranes as transducers for an odor sensor[287].

$$< \quad < CHCl_3 \leq AcOC_5H_{11}\text{-}n \quad (30)$$

β-ionone   Neral
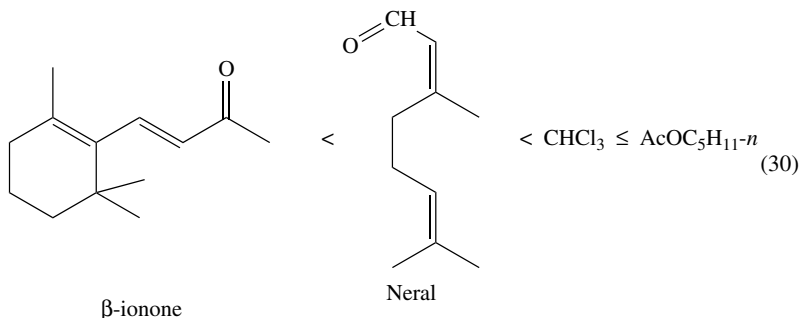
SAMs derived from $Me_2NCH_2CH_2SH$ on a Au(111) surface were used for strong immobilization of the DNA molecule, at pH values of the solution sufficiently low to achieve protonation of the amino groups. The adsorbed DNA was visualized by scanning tunneling microscopy (STM)[288]. Alkanethiol SAMs may be used for controlling the size of gold clusters. Thus, it was shown by MS that colloidal gold had a high incidence of cluster particles containing *ca* 150 atoms, when synthesized in the presence of thiols with chain length between C_4 to C_{14}. With C_{18}, clusters of *ca* 75 atoms were very abundant[289].

B. SAM Structure: Straight-chain Molecules on Au and Ag Surfaces

Various reviews appeared on the structure of SAM derived from thiols on gold surfaces[290−293]. Thiols of general formula $HS(CH_2)_nX$, $0 \leq n \leq 21$, $X = Me$, OH, CO_2H, have been investigated. Various factors affect the SAM structure: The thiol group provides chemisorption anchoring on the corrugated Au(111) surface, the alkyl chains interact by dispersion forces and the groups at the other end of neighboring molecules may interact by H-bonding. At the first stage of SAM development strips of parallel-lying molecules cover the surface and gold vacancies start to nucleate at specific sites of the Au surface. Once the stripped phase reaches saturation a transition to molecules with the alkyl groups in parallel alignment off the surface takes place, until the end of the SAM development[293]. Better control of the surface coverage was claimed for SAMs developed from alkanethiol vapors of various chain lengths, studied by low-energy electron diffraction (LEED). The unit cell size of the SAM showed a linear dependence on the chain length, pointing to parallel alignment to the Au(111) surface, up to about 12 methylene groups. The alkyl axes at the final stage of SAMs prepared from solutions were aligned in close packing at an angle of about 30° from the normal to the Au(111) surface, independently of the chain length[294]. An STM study of SAMs on Au(111) derived from a mixture of C_{18} and C_4 alkanethiols showed a tendency of the long-chain alkanethiol molecules to associate together. Thus, side diffusion in SAMs is a phenomenon to be investigated in addition to sorption and desorption[295]. The thickness, refractive index and tilt angle of SAMs derived from 1-*n*-alkanethiols developed on Ag and Au, as a function of alkyl chain length, was studied by SPR spectroscopy. Refractive indices gradually increased from 1.33 for C_{12} to 1.44 for C_{20} on Ag. A similar increase was noted for Au up to C_{18} with a slight drop taking place for C_{20}. For Ag the tilt angle began to increase from 0° on, starting at C_{16}; with Au an average tilt of 41° was obtained, independently of chain length[296]. Metastable induced electron spectroscopy (MIES) is

a pure surface technique, capable of distinguishing various functional groups as seen from above the surface. Thus, taking a well-developed SAM of nonanethiol on Au(111) as a standard for upright standing molecules, where only methyl groups are seen, and decane on graphite as a standard for molecules lying parallel to the surface, where both methyl and methylene groups can be seen, increasing disorder was observed for SAMs on Au(111) with increasing chain length, as measured by MIES, and in accordance with LEED, UV photoelectron spectroscopy and XPS results[297].

The peak potential (E_p) of the reductive desorption in basic solution of thiols from a gold(111) surface is shifted by -15 mV per methylene group for both Me- and carboxyl-terminated chains. This suggests that the chemical interaction of the thiol group with the gold atoms and the chain–chain attractive interactions add up to make adsorption stronger. On replacing a terminal Me by a carboxylate group a change of $+110$ mV in the E_p is observed, caused by the repulsive interaction between the carboxylate groups[298]. A voltammetric study with single-crystal electrodes showed that adsorption of alkanethiolate monolayers is stronger on Au(110) than on Au(111) surfaces. This is in accord with results of XPS and IR reflection spectroscopy, showing only one type of S–Ag bonding by thiolate groups, and the similar structure of the adlayers on Au(111) and Au(110) surfaces[299]. The size, number and chemical characteristics of the defect sites of a SAM derived from (3-mercaptopropyl)trimethoxysilane **(205)** on gold can be reproduced. The diameters of electrochemically produced defects on the monolayer were estimated to be in the range of 1.5 to 20 nm, based on the change of electron transfer kinetics. The modified gold surfaces served as molecular recognition devices and have potential for application in the study of single molecule electrochemistry[300].

$$HSCH_2CH_2CH_2Si(OMe)_3$$

(205)
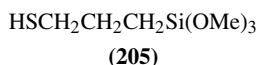
The influence of pH and other factors on the reductive desorption and oxidative reformation of a hexadecanethiol SAM on a gold electrode was studied by reflection-absorption infrared spectroscopy (RAIRS) and cyclic voltammetry. At low pH the lack of solubility of desorbed molecules was problematic; however, after three adsorption-desorption cycles the process was reproducible[301]. The reductive desorption in alkaline solution of an alkanethiol SAM on a single-crystal Au(111) electrode involves a one-electron process to yield a thiolate. Oxidative removal is a complicated process, involving up to eleven electrons per alkanethiol molecule[302].

SERS was proposed as a method for assessing the orientation of some simple molecules, such as MeOH, n-BuOH, s-BuOH, i-BuOH, n-BuSH and s-BuSH, on a silver surface, and n-BuSH on gold. The method is based on the modification of the isotropic intensity ratio of two vibrational modes of known spacial relation, as a function of the radiation intensity existing at the surface[303]. SAM electrodeposition of ethanethiolate on a Ag(111) surface was investigated by *in situ* SERS of the C–S stretching band region, electrochemical QCM and voltammetric methods. The electrochemical process is depicted in reaction 31, where the right-hand side represents the surface-bound molecule. The intensity of the SERS band showed adsorption or desorption at various applied potentials, pointing to the reversibility of the process. The adsorption isotherm could be measured with the electrochemical QCM and was potential-dependent. A supramolecular arrangement of the SAM at various degrees of coverage was proposed[304].

$$Ag(111) + EtS^- \rightleftharpoons Ag(111)/-SEt^{(\lambda-1)} + \lambda e^- \tag{31}$$

Monolayers derived from 1-octadecanethiol are penetrated by organic adsorbed vapors, while those derived from 11-mercapto-1-undecanol are not, as determined by ellipsometry

and adsorbed mass measurements[305]. A study based on AFM, XPS and cyclic voltammetry of a Au(111) electrode modified by polyamides containing disulfide groups on the chain (206) showed that the surface modified with polymer 206b was much rougher than that modified by polymer 206a. In the latter case the polymeric chain lays flat on the surface between the disulfide anchoring points, whereas in the case of 206b the longer polymethylene chains protrude from the surface, causing the roughness[306].

$$\text{-}(\text{NHCO(CH}_2)_2\text{---SS---(CH}_2)_2\text{CONH(CH}_2)_n)_x\text{-}$$

(206) (a) $n = 4$; (b) $n = 12$
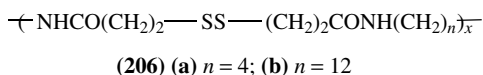
Silver electrodes become hydrophobic in the presence of ethyl xanthate ions ($EtOCS_2^-$), as they undergo a chemisorption process followed by silver xanthate formation. This phenomenon was studied by voltammetry, FTIR, UVV spectroscopy and contact angle measurements under controlled potential[307].

A functional protein labeled with ^{125}I was adsorbed on a SAM of cysteine (207) on gold. From the interference fringes of the monochromatic radiation of ^{125}I, it was concluded that the adsorbed protein molecules had uniform 2-D orientation[308].

$$HSCH_2 \diagdown \quad \diagup CO_2H$$
$$C$$
$$H_2N \diagup \quad \diagdown H$$

(207)
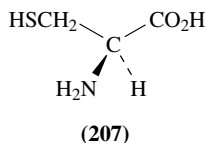
Monolayers and multilayers of CF_3I were developed on Au(111) and subjected to temperature programmed desorption (TPD) in the absence or presence of electron radiation. The nature of the adsorbed molecules was investigated by RAIRS, and the species produced during TDP were characterized by quadrupole MS[309].

C. SAM Structure: Nonlinear Molecules on Au and Ag Surfaces

The SAM derived from 7-(10-thiodecoxy)coumarin (208) on polycrystalline gold surfaces undergoes photodimerization by irradiation at 350 nm. The photochemical process was followed by the changes observed before and after irradiation in the grazing angle surface FTIR spectra, contact angles measured by the sessile drop method and UVV fluorescence spectra. The process can be reversed by irradiation at 300 nm. Of the four possible results, the desorbed nonfluorescent product had the *syn* (head-to-head) configuration (209), pointing to a parallel *syn* arrangement of 208 in the SAM[310].

The development and structure of the SAMs derived from (3-mercaptopropyl)trimethoxysilane (205) on Au and Ag surfaces were characterized using Raman, FTIR and XPS spectroscopies, ellipsometry and electrochemistry. In the fully developed stage the alkyl chain is in nearly all-*trans* conformation, with the trimethoxysilyl groups parallel to and off the surface. SAM permeability, as a measure of the coverage defects and disorder, was probed by cyclic voltammetric underpotential deposition of Pb(II) as compared with the bare surface. After hydrolysis of the SAM a highly crosslinked polysiloxane layer was developed, relatively free of gross defects, that was attached to the gold surface by alkylthio residues[311]. The SAM of thiophene (210) on Au(111) was shown by STM to have a striped structure, similar to those of alkanethiols or alkyl disulfides at an early stage

$HS(CH_2)_{10}$ $(CH_2)_{10}SH$

(**208**)   (**209**)
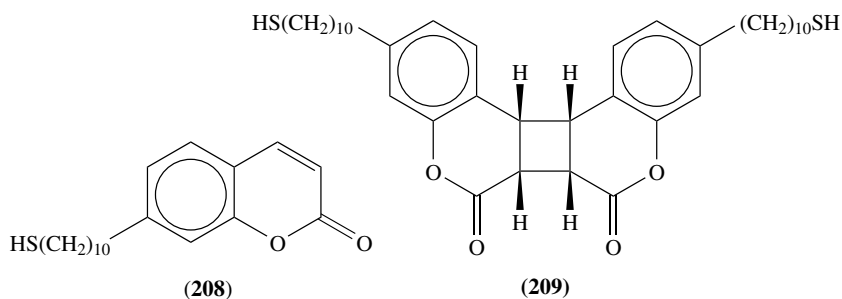
of their developement. The stability of the thiophene SAM casts doubts on SAM formation mechanisms involving redox processes, proposed for other sulfur compounds[312].

(**210**)

Various ways of accommodation on the metal surface were found for complicated molecules, as illustrated by the following examples. The SAMs formed from dilute solutions of various disk-shaped molecules on gold were investigated by contact angle measurements, polarized grazing angle FTIR, QCM and AFM. The QCM showed only a small change of frequency with compound **211**, endowed with weakly chemisorbing groups. This response served as a blank and was taken for poor surface coverage. Compound **212**, with a good anchoring SH group at the end of an alkyl chain, caused a fast QCM response and asymptotic stabilization. This was taken for fast adsorption ending at a well-developed SAM at equilibrium. Compounds **213b** and **214a** caused a slower QCM frequency change than compound **212**, but the change was larger when they reached equilibrium. This was interpreted as face-on adsorption and formation of multiple layers instead of a SAM. Evidence from FTIR and AFM at the end stage pointed to edge-on and parallel orientation of the aromatic groups of adsorbed **212**. Compounds **215** and **216** showed a behavior similar to that of **212**. Grazing angle FTIR spectra of SAM derived from the disk-like compounds **213** and **214** showed only weak CH_2 stretching bands, pointing to a disordered arrangement of the alkyl groups away from the Au(111) surface, in contrast to the parallel arrangement on and off the surface, mentioned above for alkanethiol SAMs. Contact angle measurements showed increased SAM hydrophobicity for the longer alkyl substituents[313].

It was shown by *in situ* STM that highly ordered SAMs of the porphyrin compound **217** in face-on disposition were formed on iodine-modified Au(111) surfaces, whereas disordered adlayers were formed on bare Au(111) surfaces[314]. Two periodicities were found by AFM for the SAM on Au(111) of a thioether derivative of calix[4]resorcinarene (**218**), one with lattice constant of *ca* 0.42 nm, attributed to the alkyl chain packing of the four thioether anchors on the metal surface, and the second one with lattice constant of *ca* 1.16 nm, attributed to the calixarene macrocycles[315,316].

The SAMs on a gold substrate of terthiophenes (**219**), where X-R-T$_3$ is either a thiol (**220**) or a dithio (**221**) anchoring group were characterized by ellipsometry, contact angle goniometry, IR spectroscopy, XPS and cyclic voltametry. **220** organized in a few minutes

OR
OR
RO
RO

R = C$_5$H$_{11}$

OR
OR

(211)

OR
OR
RO
RO

R = C$_5$H$_{11}$

OR
O(CH$_2$)$_{10}$SH

(212)

SR
SR
RS
RS

(**a**) = C$_5$H$_{11}$
(**b**) = C$_6$H$_{13}$

SR
SR

(213)

SR
SR
RS
N
N
RS
N
N

(**a**) R = C$_{12}$H$_{25}$
(**b**) R = C$_{16}$H$_{33}$

SR
SR

(214)

OR   OR
OR RO
RO   OR
RO   OR
RO

OR RO
O(CH$_2$)$_{10}$S——S(CH$_2$)$_{10}$S

R = C$_5$H$_{11}$

(215)

OR

OR

RO

RO

OR

R = C$_5$H$_{11}$

O(CH$_2$)$_{10}$S——S(CH$_2$)$_{11}$OH

(216)

Me

Me

O——CH$_2$- - -

CH- - -

Me

N
H

N   N

H
N

Me

Me

(4-MeC$_6$H$_4$SO$_3^-$)$_4$

S
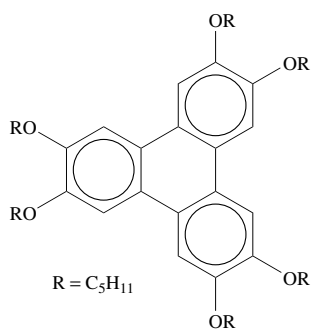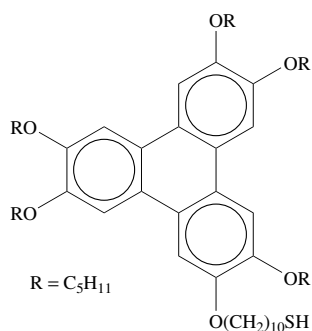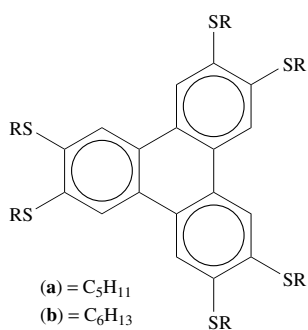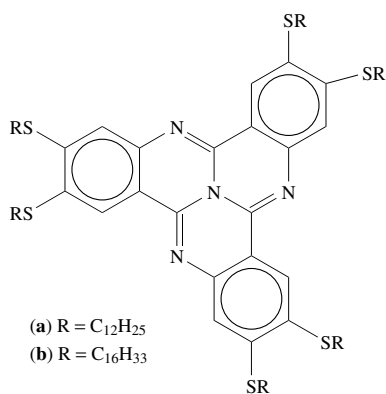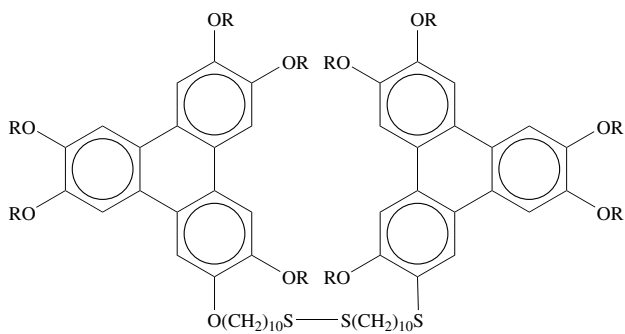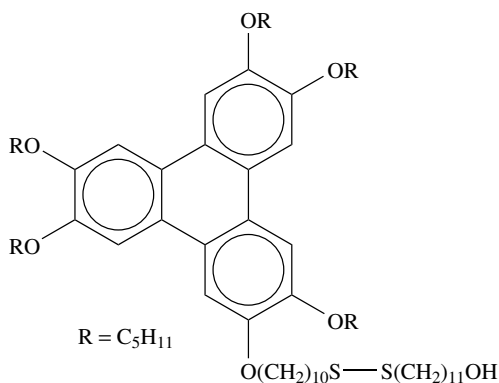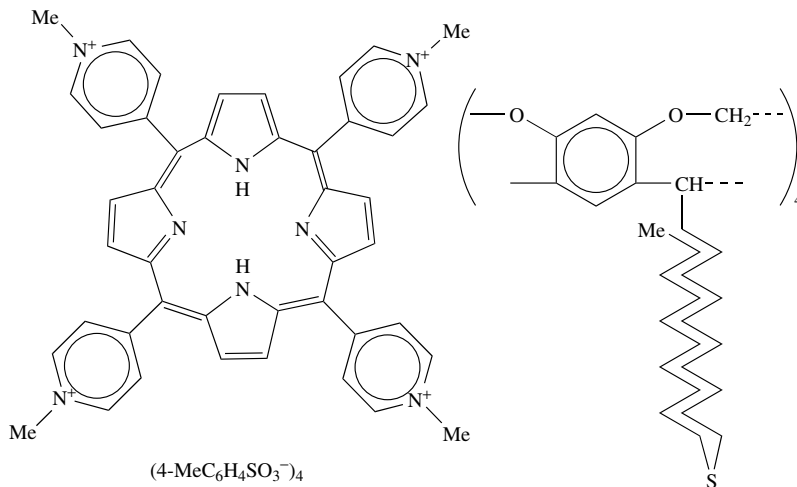
(217)   **(218)**

into a densely packed adlayer, with the alkyl groups in almost perfect all-*trans* conforma-
tion and the T$_3$ groups slightly tilted away from the metal surface. The electrochemical
response of the covered gold electrode was much reduced as compared to the bare one.
With **221**, SAM formation was slower and the tilt of the T$_3$ groups was larger; the hetero-
geneous electron transfer rate was almost equal to that of the bare gold surface, suggesting
abundant defects, or alternatively, π-electron involvement[317].

NEXAFS, a synchrotron-based soft X-ray spectroscopy, can be used for surface analysis
with an information depth of a few nanometers. It was applied for the investigation of
the electronic structure of ultrafine films of substituted poly-*p*-phenylenes **(222–225)**

(**219**)

$HS(CH_2)_{11}T_3$

(**220**)

$T_3(CH_2)_{11}SS(CH_2)_{11}T_3$

(**221**)

(**222**)

(**223**)

(**224**)

(**225**)
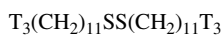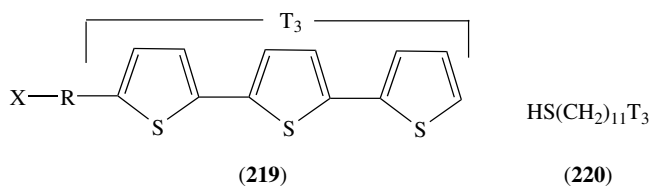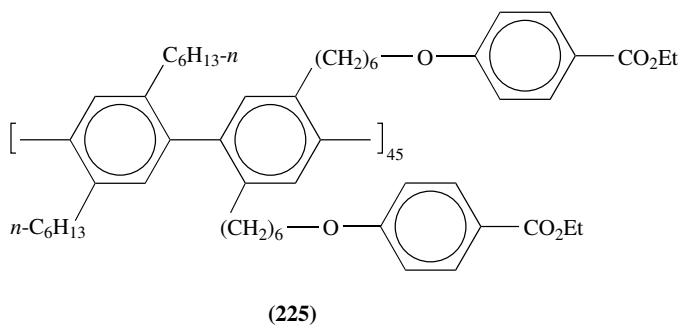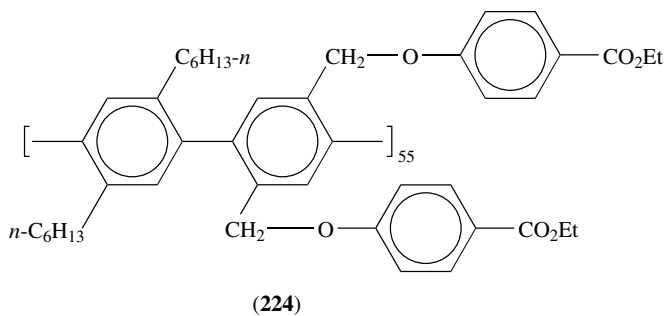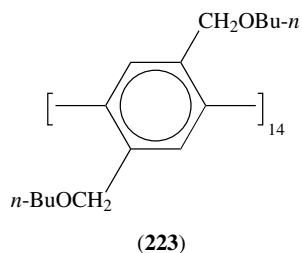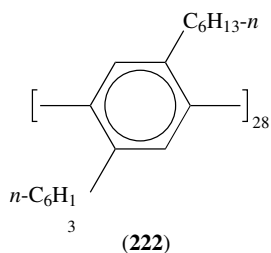
adsorbed on a gold surface. The multiplicity numbers shown in the formulas are poly-merization number averages of the investigated substances. It was found that the aromatic rings have a tilt angle of *ca* 50° relative to the gold surface[318].

Uracil can form four types of SAM films on the Au(111) surface of a single-crystal gold electrode, as was observed by *in situ* STM. These coincide with four stability regions appearing in cyclic voltammograms. It was proposed that the uracil molecules undergo deprotonation and become attached edge-on to the surface via an N^- atom **(226)**, as shown in reaction 32[319]. Similar results were reported for thymine **(227)**[320]. *In situ* elec-tromodulated reflectance FTIR spectroscopy showed that adsorbed 4-cyanopyridine **(228)** is coordinated to the Au(111) electrode surface through the heterocyclic N atom[321]. Laser-activated desorption of 4-vinylbenzoic acid **(229)** adsorbed on colloidal silver showed the existence of a population of molecules that desorb and one that does not. SERS evidence indicates that the desorbing molecules lie with the carboxyl and benzene ring face-on the silver surface, while the vinyl group sticks out; in the nondesorbing population the vinyl group lies flat on the surface too[322].

(32)

(226)

(227)

(228)

(229)
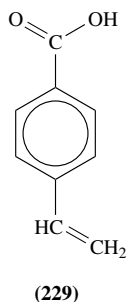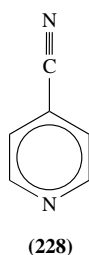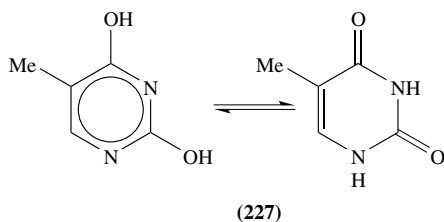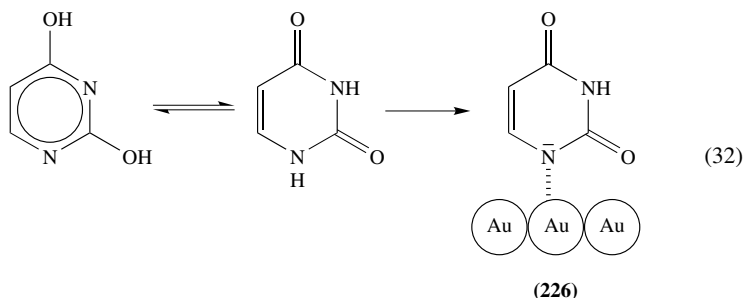
VI. REFERENCES

1. M. C. Snead, J. L. Maynard and R. C. Brasted, *Comprehensive Inorganic Chemistry*, Vol. 2, Van Nostrand, Toronto, 1954.
2. S. Terashima, S. Nakao, N. Mita, Y. Inouchi and A. Nishimura, *Appl. Geochem.*, **10**, 35 (1995).
3. G. Perrelli and G. Piolatto, *Sci. Total Environ.*, **120**, 93 (1992)
4. J. E. F. Reynolds (Ed.), *Martindale—The Extra Pharmacopoeia*, 13th ed., Pharmaceutical Press, London, 1993, pp. 1–36.
5. G. Carter, M. J. Nobes and M. G. McLaren, *Rad. Effects and Defects Solids*, **133**, 267 (1995).
6. L. M. Schiavone, H. G. Craighead and S. Divita, *Thin Solid Films*, **208**, 156 (1992).
7. D. Tonneau, J. E. Bouree, A. Correia, G. Roche, G. Pelous and S. Verdeyme, *J. Appl. Phys.*, **78**, 5139 (1995).
8. G. J. Berry, J. A. Cairns and J. Thomson, *Sensors Actuators A*, **51**, 47 (1995).
9. K. L. Lee, D. W. Abraham, F. Secord and L. Landstein, *J. Vacuum Sci. Technol. B*, **9**, 3562 (1992).
10. J. S. Ro, C. V. Thompson, and J. Melngailis, *Thin Solid Films*, **258**, 333 (1995).
11. A. M. M. Lanfredi, F. Ugozzoli, A. Camus and N. Marsich, *J. Chem. Crystallogr.*, **25**, 37 (1995).
12. A. F. Rubira, J. D. Rancourt, M. L. Caplan, A. K. St. Clair and L. T. Taylor, *Chem. Mater.*, **6**, 2351 (1994).
13. R. K. Boggess, L. T. Taylor, D. M. Stoakley and A. K. St. Clair, *J. Appl. Polym. Sci.*, **64**, 1309 (1997).
14. R. E. Southward, D. W. Thompson and A. K. St. Clair, *Chem. Mater.*, **9**, 1691 (1997).
15. E. Crivellato, L. Travan, L. Candussio, F. B. Klugmann and G. Decorti, *Histochem. J.*, **29**, 193 (1997).
16. R. D. Powell, C. M. R. Halsey, D. L. Spector, S. L. Kaurin, J. McCann and J. F. Hainfeld, *J. Histochem. Cytochem.*, **45**, 947 (1997).
17. I. M. Kolthoff, P. J. Elving and E. B. Sandell (Eds.), *Treatise on Analytical Chemistry*, Interscience, New York, 1966.
18. R. R. Barefoot and J. C. Van Loon, *Anal. Chim. Acta*, **334**, 5 (1996).
19. J. Zabicky, in *The Chemistry of Sulfenic Acids and Their Derivatives* (Ed. S. Patai), Wiley, Chichester, 1990, pp. 83ff.
20. J. Zabicky, in *The Chemistry of the Amino Group* (Ed. S. Patai), Interscience Publishers, New York, 1968, pp. 79ff.
21. J. Zabicky and S. Bittner, in *Supplement F: The Chemistry of Amino, Nitroso and Nitro Compounds* (Ed. S. Patai), Wiley, Chichester, 1996, pp. 1041ff.
22. J. Zabicky and S. Erlich-Rogozinski, in *The Chemistry of Carbon–Halogen Compounds* (Ed. S. Patai), Interscience Publishers, New York, 1973, pp. 63ff.
23. J. Zabicky and S. Grinberg, in *The Chemistry of Organic Germanium, Tin and Lead Compounds* (Ed. S. Patai), Wiley, Chichester, 1995, pp. 339ff, 365ff, 429ff.
24. E. P. Przybylowicz and C. W. Zuehlke, in Refernce 17, Part II, Vol. 4, pp. 1ff.
25. N. Herz, in Reference 17, Part II, Vol. 4, pp. 71ff.
26. S. A. E. Johansson, *Analyst*, **117**, 259 (1992).
27. Z. B. Alfassi (Ed.), *Determination of Trace Elements*, VCH, Weinheim, 1994.
28. J. Zabicky, in *Supplement C: The Chemistry of Triple-bonded Functional Groups*, Vol. 2 (Ed. S. Patai), Wiley, Chichester, 1994, pp. 191ff.
29. P. C. Uden, in Reference 27, pp. 425ff.
30. J. Korkish, *Modern Methods for the Separation of the Rarer Metal Ions*, Pergamon, Oxford, 1969: (a) pp. 375ff, (b) pp. 388ff.
31. D. A. Chowdhury and S. Kamata, *Solvent Extract. Ion Exchange*, **15**, 231 (1997).
32. A. M. Abdallah, M. El-Shahawi, M. M. El-Defrawy and E. E. Askar, *Chem. Anal. (Warsaw)*, **37**, 589 (1992).
33. J. F. Tyson, S. R. Bysouth, E. A. Grzeszczyk and E. Debrah, *Anal. Chim. Acta*, **261**, 75 (1992).
34. D. C. Gregoire, M. Lamoureux, C. L. Chakrabarti, S. Al-Maawali and J. P. Byrne, *J. Anal. Atom. Spectrom.*, **7**, 579 (1992).
35. P. L. Larkins, *J. Anal. Atom. Spectrom.*, **7**, 265 (1992).
36. N. V. Chekalin and I. I. Vlasov, *J. Anal. Atom. Spectrom.*, **7**, 225 (1992).
37. M. Berglund and D. C. Baxter, *J. Anal. Atom. Spectrom.*, **7**, 461 (1992).

38. A. I. Yuzefovsky, R. F. Lonardo, J. X. Zhou and R. G. Michel, *Appl. Spectrosc.*, **51**, 738 (1997).
39. M. B. Shabani, T. Akagi and A. Masuda, *Anal. Chem.*, **64**, 737 (1992).
40. Q. Jin, H. Zhang, W. Yang, Q. Jin and Y. Shi, *Talanta*, **44**, 1605 (1997).
41. R. A. Davidson, *At. Spectrosc.*, **13**, 199 (1992).
42. P. Chattopadhyay and M. Mistry, *Fresenius J. Anal. Chem.*, **357**, 308 (1997).
43. V. Balaram. S. M. Hussain, B. U. Raj, S. N. Charan, D. V. S. Rao, K. V. Anjaiah, S. L. Ramesh and S. Ilangovan, *At. Spectrosc.*, **18**, 17 (1997).
44. M. W. Hinds, *Spectrochim. Acta, Part B*, **48**, 435 (1993).
45. M. Valcárcel and M. D. Luque de Castro, *J. Chromatogr.*, **393**, 3 (1987).
46. B. Karlberg, *Anal. Chim. Acta*, **214**, 243 (1989).
47. S. Zhang, S. Xu and Z. Fang, *Quim. Anal., (Barcelona)*, **8**, 191 (1989); *Chem. Abstr.*, **113**, 51713 (1990).
48. J. Ruzicka and A. Arnald, *Anal. Chim. Acta.*, **216**, 29 (1988).
49. J. F. Tyson, *Anal. Chim. Acta*, **234**, 3 (1990).
50. R. Fernando, C. P. Calloway, Jr. and B. T. Jones, *Anal. Chem.*, **64**, 1556 (1992).
51. A. G. Coedo, M. T. Dorado, F. J. Alguacil and I. Padilla, *Talanta*, **43**, 313 (1996).
52. G. H. Lu, J. Y. Xu, T. M. Xu, L. T. Jin and Y. Z. Fang, *Talanta*, **39**, 51 (1992).
53. K. Ohta, M. Yokoyama, J. Ogawa and T. Mizuno, *Analysis*, **24**, 22 (1996).
54. K. Ohta, M. Yokoyama, J. Ogawa and T. Mizuno, *Mikrochim. Acta*, **122**, 61 (1996).
55. L. Thunus and J. F. Dauphin, *Anal. Chim. Acta*, **235**, 393 (1990).
56. K. Smolander and M. Kauppinen, *Anal. Chim. Acta*, **248**, 569 (1991).
57. M. A. Mostafa, *Analusis*, **20**, 283 (1992).
58. C. García-Ollalla and A. J. Aller, *Anal. Chim. Acta*, **252**, 97 (1991).
59. A. Uzawa, W. Yoshimura and T. Okutani, *Bunseki Kagaku*, **44**, 391 (1995). *Chem. Abstr.*, **123**, 24742 (1995).
60. G. Absalan, C. L. Chakrabarti and K. L. Headrick, *Can. J. Appl. Spectrosc.*, **41**, 51 (1996).
61. W. M. Yang and Z. M. Ni, *Spectrochim. Acta, Part B, Atomic Spectrosc.*, **51**, 65 (1996).
62. H. Beissler, G. A. Petrucci, K. Bachmann, U. Panne, P. Cavalli and N. Omenetto, *Fresenius J. Anal. Chem.*, **355**, 345 (1996).
63. E. Masera, P. Mauchien and Y. Lerat, *Spectrochim. Acta, Part B, Atom. Spectrosc.*, **51**, 543 (1996).
64. J. Christodoulou, M. Kashani, B. M. Keohane and P. J. Sadler, *J. Anal. Atom. Spectrom.*, **11**, 1031 (1996).
65. L. Xu and P. Schramel, *Fresenius J. Anal. Chem.*, **342**, 179 (1992).
66. S. Xu, L. Sun and Z. Fang, *Anal. Chim. Acta*, **245**, 7 (1991).
67. B. J. Perry, J. C. Van Loon and D. V. Speller, *J. Anal. At. Spectrom.*, **7**, 883 (1992).
68. P. Xu, *J. Anal. Atom. Spectrom.*, **7**, 775 (1992).
69. K. K. Falkner and J. M. Edmond, *Anal. Chem.*, **62**, 1477 (1990).
70. A. L. Kovalevskii and S. I. Prokopchuk, *J. Geochem. Explor.*, **55**, 145 (1995).
71. J. F. Wyart, Y. N. Joshi, L. Tchang-Brillet and A. J. J. Raassen, *Phys. Scr.*, **53**, 174 (1996).
72. T. Yamaguchi, L. P. Zhang, K. Matsumoto and K. Terada, *Anal. Sci.*, **8**, 851 (1992).
73. M. Hiraide, S. H. Zhou and H. Kawaguchi, *Analyst*, **118**, 1441 (1993).
74. P. Bermejo-Barrera. J. Moreda-Pineiro, A. Moreda-Pineiro and A. Bermejo-Barrera, *Talanta*, **43**, 35 (1996).
75. Y. Shijo, E. Yoshimoto, T. Kitamura, H. Ono, N. Uehara and T. Shimizu, *Anal. Sci.*, **12**, 959 (1996).
76. K. Ohta, S. Kaneco, S. Itoh and T. Mizuno, *Anal. Chim. Acta*, **267**, 131 (1992).
77. S. Saeki, M. Kubota and T. Asami, *Int. J. Environ. Anal. Chem.*, **64**, 179 (1996).
78. S. Saeki, M. Kubota and T. Asami, *Int. J. Environ. Anal. Chem.*, **64**, 185 (1996).
79. P. Bermejo-Barrera, A. Moreda-Pineiro, J. Moreda-Pineiro and A. Bermejo-Barrera, *Talanta*, **43**, 1783 (1996).
80. P. Anderson, C. M. Davidson, D. Littlejohn, A. M. Ure, C. A. Shand and M. V. Cheshire, *Anal. Chim. Acta*, **327**, 53 (1996).
81. S. A. Armitage, M. A. White and H. K. Wilson,, *Ann. Occup. Hyg.*, **40**, 331 (1996).
82. N. Shibata, N. Fudagawa and M. Kubota, *Anal. Chim. Acta*, **265**, 93 (1992).
83. I. B. Gornushkin, B. W. Smith and J. D. Winefordner, *Spectrochim. Acta Part B*, **51**, 1355 (1996).
84. Y. Lu and X. Wang, *J. Geochem. Explor.*, **55**, 49 (1995).

85. G. S. Reddi, S. Ganesh, C. R. M. Rao and V. Ramanan, *Anal. Chim. Acta*, **260**, 131 (1992).
86. G. Iwantscheff, *Das Dithizon und seine Anwendung in der Mikro- und Spurenanalyse*, Verlag Chemie, Weinheim, 1972.
87. J. Fries and H. Getrost, *Organic Reagents for Trace Analysis*, E. Merck, Darmstadt, 1977.
88. J. J. Cox and D. M. Servant, *Anal. Chim. Acta*, **74**, 200 (1975).
89. A. Z. Abu Zuhri and A. H. Rady, *J. Chem. Technol. Biotechnol.*, **54**, 39 (1992).
90. Z. Zeng and Q. Xu, *Talanta*, **39**, 409 (1992).
91. M. Balcerzak, *Chem. Anal. (Warsaw)*, **37**, 683 (1992).
92. I. Mori, H. Tominaga, Y. Yujita and T. Matsuo, *Anal. Lett.*, **30**, 953 (1997).
93. F. T. Imdadullah and T. Kumamaru, *Anal. Chem.*, **65**, 421 (1993).
94. J. Lu, X. Zhang, W. Fan and Z. Zhang, *Anal. Chim. Acta*, **262**, 225 (1992).
95. P. B. Shetkar, J. S. Gaudh and V. M. Shinde, *Sep. Sci. Technol.*, **32**, 1937 (1997).
96. E. O. Otu, C. W. Robinson and J. J. Byerley, *Analyst*, **117**, 1145 (1992).
97. A. T. Haj-Hussein, *Talanta*, **42**, 2053 (1995).
98. F. Salinas, A. Espinosa-Mansilla and P. L. López de Alba, *Analyst*, **120**, 2857 (1995).
99. R. Shah and S. Devi, *Indian J. Chem., Sect. A*, **34**, 925 (1995).
100. R. I. Sánchez, M. J. Darsley and M. T. Martin, *Anal. Biochem.*, **224**, 190 (1995).
101. N. R. Saran, V. Umashanker and G. V. Ramanaiah, *Bull. Chem. Soc. Jpn.*, **65**, 2291 (1992).
102. N. N. Ishchenko, L. I. Ganago and I. F. Ivanova, *J. Anal. Chem.*, **52**, 768 (1997).
103. Y. Fujita, I. Mori, M. Toyoda and T. Matsuo, *Anal. Sci.*, **9**, 829 (1993).
104. A. A. Ensafi and S. Abbasi, *Anal. Lett.*, **30**, 237 (1997).
105. A. A. Ensafi and K. Zarei, *Fresenius J. Anal. Chem.*, **358**, 475 (1997).
106. A. Safavi and B. Haghighi, *Fresenius J. Anal. Chem.*, **357**, 870 (1997).
107. F. Sagara, T. Tsuji, I. Yoshida, D. Ishii and K. Ueno, *Anal. Chim. Acta*, **270**, 217 (1992).
108. A. I. Zoubulis, K. A. Kydros and K. A. Matis, *Hydrometallurgy*, **36**, 39 (1994).
109. V. Gaspar, A. S. Mejerovich, M. A. Meretukov and J. Schiedl, *Hydrometallurgy*, **36**, 369 (1994).
110. S. Peraniemi, J. Parkkinen, K. Smolander, H. Mustalahti and M. Ahlgren, *Fresenius J. Anal. Chem.*, **343**, 292 (1992).
111. S. N. Dimitriev, T. V. Shishkina, E. L. Zhuravleva and J. Chimeg, *Anal. Chim. Acta*, **243**, 81 (1991).
112. B. Decelis, *Appl. Spectrosc.*, **50**, 572 (1996)
113. G. Chai, A. J. Naldrett, J. C. Rucklidge and L. R. Kilius, *Can. Mineral.*, **31**, [March] 19 (1993).
114. J. Shakeshaft, A. Clarke, K. Anthony, M. J. Evans and S. C. Lillicrap, *Basic Life Sci.*, **60**, 307 (1993).
115. J. Shakeshaft and S. C. Lillicrap, *Br. J. Radiol.*, **66**, 714 (1993).
116. J. A. Schlueter, K. D. Carlson, U. Geiser, H. H. Wang, J. M. Williams, W. K. Kwok, J. A. Fendrich, U. Welp, P. M. Keane, J. D. Dudek, A. S. Komosa, D. Naumann, T. Roy, J. E. Schirber, W. R. Bayless and B. Dodrill, *Physica C*, **233**, 379 (1994).
117. J. A. Schlueter, J. M. Williams, U. Geiser, J. D. Dudek, A. A. Sirchio, M. E. Kelly, J. S. Gregar, W. H. Kwok, J. A. Fendrich, J. E. Schirber, W. R. Bayless, D. Naumann and T. Roy, *J. Chem. Soc., Chem. Commun.*, 1311 (1995).
118. G. R. Agnes and G. Horlick, *Appl. Spectrosc.*, **46**, 401 (1992).
119. G. R. Agnes, I. I. Stewart and G. Horlick, *Appl. Spectrosc.*, **48**, 1347 (1994).
120. *The United States Pharmacopeia*, 21st rev., United States Pharmacopeial Convention, Rockville, MD, 1985, p. 81.
121. M. Wisniewski, *Fresenius J. Anal. Chem.*, **343**, 360 (1992).
122. C. Sanchez-Pedreño, J. A. Ortuño and D. M. Martinez, *Anal. Chim. Acta*, **263**, 143 (1992).
123. M. S. Won, D. W. Moon and Y. B. Shim, *Electroanalysis*, **7**, 1171 (1995).
124. B. F. Abramović, M. M. Marinković and F. F. Gaál, *Analyst*, **115**, 79 (1990).
125. B. F. Abramović, K. S. Horváth, F. F. Gaál and O. P. Gaál, *Microchem. J.*, **48**, 137 (1993).
126. B. V. Rao, *Anal. Chim. Acta*, **258**, 167 (1992).
127. M. Korolczuk, *Fresenius J. Anal. Chem.*, **356**, 480 (1996).
128. M. Korolczuk, *Chem. Anal. (Warsaw)*, **41**, 641 (1996).
129. E. A. Viltchinskaia and L. L. Zeigman, *Electroanalysis*, **8**, 92 (1996).
130. T. Peng, H. Li and S. Wang, *Analyst*, **118**, 1321 (1993).
131. X. Cai, K. Kalcher, C. Neuhold, W. Diewald and R. J. Magee, *Analyst*, **118**, 53 (1993).

132. S. Biswas, H. K. Mondal and S. Basu, *Indian J. Chem. Sect. A, Inorg. Bioinorg. Phys. Theor. Anal. Chem.*, **35**, 804 (1996).
133. G. Kolbl, K. Kalcher and A. Voulgaropoulos, *Fresenius J. Anal. Chem.*, **342**, 83 (1992).
134. M. Aguilar, A. Farrán and V. A. Martí, *J. Chromatogr. A*, **767**, 319 (1997).
135. A. V. Pirogov and J. Havel, *J. Chromatogr. A*, **772**, 347 (1997).
136. R. Kissner, G. Welti and G. Geier, *J. Chem. Soc., Dalton Trans.*, 1773 (1997).
137. M. Mojski, M. Jarosz and I. Gluch, *Analusis*, **20**, 567 (1992).
138. S. H. Chou, J. R. Rau and S. C. Chen, *Electrochim. Acta*, **42**, 2313 (1997).
139. C. Labar and L. Lamberts, *Talanta*, **44**, 733 (1997).
140. I. Svancara, K. Kalcher, W. Diewald and K. Vytras, *Electroanalysis*, **8**, 336 (1996).
141. R. D. Ye and S. B. Khoo, *Electroanalysis*, **9**, 481 (1997).
142. J. Labuda and M. Vaníčková, *Electroanalysis*, **5**, 141 (1993).
143. A. C. Almon, *Anal. Chim. Acta*, **249**, 447 (1991).
144. J. Shukla and K. S. Pitre, *Analyst*, **121**, 79 (1996).
145. T. Nomura and K. Tsuge, *Anal. Chim. Acta*, **169**, 257 (1985).
146. R. D. Shelton and J. Q. Chambres, *J. Electroanal. Chem.*, **305**, 217 (1991).
147. S. Chung, W. Kim, S. B. Park, I. Yoon, S. S. Lee and D. D. Sung, *Chem. Commun.*, 965 (1997).
148. M. Lerchi, E. Reitter, W. Simon, E. Pretsch, D. A. Chowdhury and S. Kamata, *Anal. Chem.*, **66**, 1713 (1994).
149. E. Bakker, *Sensors Actuators B*, **35**, 20 (1996).
150. H. A. Das, in Reference 27, pp. 461ff.
151. H. Malik and S. J. Parry, *Analyst*, **117**, 1945 (1992).
152. H. W. Stockman, *J. Radioanal. Chem.*, **78**, 307 (1983).
153. M. Gallorini, C. Birattari, M. Bonardi, L. Magon and E. Sabbioni, *J. Radioanal. Nucl. Chem.*, **160**, 549 (1992).
154. B. Rietz and K. Heydorn, *J. Radioanal. Nucl. Chem.*, **174**, 49 (1993).
155. D. van Renterghem, R. Cornelis and R. Vanholder, *Anal. Chim. Acta*, **257**, 1 (1992).
156. C. Schnier and H. P. Benn, *J. Radioanal. Nucl. Chem.*, **142**, 433 (1990).
157. S. Kumar, R. Verma and S. Gangadharan, *Analyst*, **118**, 1085 (1993).
158. V. Cojocaru and S. Spiridon, *J. Radioanal. Nucl. Chem.*, **170**, 259 (1993).
159. G. C. Wilson, J. C. Rucklidge, L. R. Kilius, G. J. Ding and R. G. Cresswell, *Nucl. Instrum. Methods Phys. Res., Sect. B*, **123**, 583 (1997).
160. A. Matsumoto and T. K. Hinkley, *Geochem. J.*, **31**, 175 (1997).
161. V. Jedinakova-Krizova, *J. Radioanal. Nucl. Chem.*, **183**, 93 (1994).
162. G. J. Ding, L. R. Kilius, G. C. Wilson, X. L. Zhao and J. C. Rucklidge, *Nucl. Instrum. Methods Phys. Res., Sec. B*, **123**, 414 (1997).
163. K. I. Grandberg and V. P. Dyadchenko, *J. Organomet. Chem.*, **474**, 1 (1994).
164. L. H. Pignolet, M. A. Aubart, K. L. Craighead, R. A. T. Gould, D. A. Krogstad and J. S. Wiley, *Coord. Chem. Rev.*, **143**, 219 (1995).
165. C. E. Holloway, W. A. Nevin and M. Melnik, *J. Coord. Chem.*, **31**, 191 (1994).
166. H. Lang, K. Köhler and S. Blau, *Coord. Chem. Rev.*, **143**, 113 (1995).
167. T. C. Huang, H. Toraya, T. N. Blanton and Y. Wu, *J. Appl. Crystallogr.*, **26**, 180 (1993).
168. J. F. Britten, C. J. L. Lock and Z. Wang, *Acta Crystallogr., Sect. C*, **48**, 1600 (1992).
169. A. Laguna, M. Laguna, M. C. Gimeno and P. G. Jones, *Organometallics*, **11**, 2759 (1992).
170. X. Hong, K. K. Cheung, C. X. Guo and C. M. Che, *J. Chem. Soc., Dalton Trans.*, 1867 (1994).
171. T. Sone, S. Ozaki, N. C. Kasuga, A. Fukuoka and S. Komiya, *Bull. Chem. Soc. Jpn.*, **68**, 1523 (1995).
172. M. Contel, J. Garrido, M. C. Gimeno, J. Jiménez, P. G. Jones, A. Laguna and M. Laguna, *Inorg. Chim. Acta*, **254**, 157 (1997).
173. F. Canales, M. C. Gimeno, P. G. Jones and A. Laguna, *J. Chem. Soc., Dalton Trans.*, 439 (1997).
174. O. Crespo, M. C. Gimeno, P. G. Jones and A. Laguna, *J. Organomet. Chem.*, **531**, 87 (1997).
175. I. R. Whittall, M. G. Humphrey, S. Houbrechts, A. Persoons and D. C. R. Hockless, *Organometallics*, **15**, 5738 (1996).
176. R. Usón, A. Laguna, M. Laguna, J. Jiménez and P. G. Jones, *Angew. Chem., Int. Ed. Engl.*, **30**, 198 (1991).

177. R. Usón, A. Laguna, M. Laguna, J. Jiménez and P. G. Jones, *J. Chem. Soc., Dalton Trans.*, 1361 (1991).
178. A. Laguna, M. Laguna, J. Jiménez, F. J. Lahoz and E. Olmos, *J. Organomet. Chem.*, **435**, 235 (1992).
179. M. Rossignoli, P. V. Bernhardt, G. A. Lawrance and M. Maeder, *J. Chem. Soc., Dalton Trans.*, 323 (1997).
180. S. O. Sommerer, A. J. Jircitano, B. L. Westcott, K. A. Abboud and J. A. K. Bauer, *Acta Crystallogr., Sect. C*, **53**, 707 (1997).
181. J. M. López-de-Luzuriaga, A. Sladek, A. Schier and H. Schmidbaur, *Inorg. Chem.*, **36**, 966 (1997).
182. H. Schmidbaur, A. Kolb and P. Bissinger, *Inorg. Chem.*, **31**, 4370 (1992).
183. A. Bauer, W. Schneider, K. Angermaier, A. Schier and H. Schmidbaur, *Inorg. Chim. Acta*, **251**, 249 (1996).
184. J. Skoweranda, W. Wieczorek, M. Bukowska-Strzyzewska, A. Grodzicki and E. Szlyk, *J. Crystallogr. Spectrosc. Res.*, **22**, 527 (1992).
185. J. C. Shi, L. J. Chen, X. Y. Huang, D. X. Wu and B. S. Kang, *J. Organomet. Chem.*, **535**, 17 (1997).
186. J. C. Shi, T. B. Wen, G. T. Lu, D. X. Wu, Q. T. Liu and B. S. Kang, *J. Coord. Chem.*, **41**, 199 (1997).
187. P. D. Cookson and E. R. T. Tiekink, *J. Coord. Chem.*, **26**, 313 (1992).
188. O. Crespo, M. C. Gimeno, P. G. Jones and A. Laguna, *J. Chem. Soc., Dalton Trans.*, 1099 (1997).
189. O. Crespo, M. C. Gimeno, P. G. Jones, B. Ahrens and A. Laguna, *Inorg. Chem.*, **36**, 495 (1997).
190. J. M. López de Luzuriaga, A. Sladek and H. Schmidbaur, *J. Chem. Soc., Dalton Trans.*, 4511 (1996).
191. S. S. Tang, C. P. Chang, I. J. B. Lin, L. S. Liou and J. C. Wang, *Inorg. Chem.*, **36**, 2294 (1997).
192. P. Braunstein, E. de Jesús, A. Tiripicchio and F. Ugozzoli, *Inorg. Chem.*, **31**, 411 (1992).
193. I. M. Dodd, Q. A. Hao, M. M. Harding and S. M. Prince, *Acta Crystallogr., Sect. B*, **50**, 441 (1994).
194. M. A. Aubart, B. D. Chandler, R. A. T. Gould, D. A. Krogstad, M. F. J. Schoondergang and L. H. Pignolet, *Inorg. Chem.*, **33**, 3724 (1994).
195. A. Bauer and H. Schmidbaur, *J. Chem. Soc., Dalton Trans.*, 1115 (1997).
196. D. E. Berning, K. V. Katti, C. L. Barnes and W. A. Volkert, *Chem. Ber.-Recl.*, **130**, 907 (1997).
197. D. E. Berning, K. V. Katti, C. L. Barnes, W. A. Volkert and A. R. Ketring, *Inorg. Chem.*, **36**, 2765 (1997).
198. A. Bauer, N. W. Mitzel, A. Schier, D. W. H. Rankin and H. Schmidbaur, *Chem. Ber.-Recl.*, **130**, 323 (1997).
199. P. A. Cooke, S. D. Perera, B. L. Shaw, M. Thornton-Pett and J. D. Vessey, *J. Chem. Soc., Dalton Trans.*, 435 (1997).
200. H. Xiao, Y. X. Weng, W. T. Wong, T. C. W. Mak and C. M. Che, *J. Chem. Soc., Dalton Trans.*, 221 (1997).
201. O. Crespo, M. C. Gimeno, P. G. Jones, A. Laguna and M. D. Villacampa, *Angew. Chem., Int. Ed. Engl.*, **36**, 993 (1997).
202. T. G. M. M. Kappen, A. C. M. van den Broek, P. P. J. Schlebos, J. J. Bour, W. P. Bosman, J. M. M. Smits, P. T. Beurskens and J. J. Steggerda, *Inorg. Chem.*, **31**, 4075 (1992).
203. D. Perreault, M. Drouin, A. Michel, V. M. Miskowski, W. P. Schaefer and P. D. Harvey, *Inorg. Chem.*, **31**, 695 (1192).
204. C. M. Che, H. K. Yip, V. W. W. Yam, P. Y. Cheung, T. F. Lai, S. J. Shieh and S. M. Peng, *J. Chem. Soc., Dalton Trans.*, 427 (1992).
205. P. C. Cohen-Addad, P. Baret, P. Chautemps and J. L. Pierre, *Acta Crystallogr., Sect., C*, **39**, 1346 (1983).
206. (a) V. W. W. Yam, W. K. M. Fung and K. K. Cheung, *Organometallics*, **16**, 2032 (1997).
     (b) V. W. W. Yam, W. K. M. Fung and K. K. Cheung, *Chem. Commun.*, 963 (1997).
207. C. Brasse, P. R. Raithby, M. A. Rennie, C. A. Russell, A. Steiner and D. S. Wright, *Organometallics*, **15**, 639 (1996).
208. M. D. Janssen, K. Köhler, M. Herres, A. Dedieu, W. J. J. Smeets, A. L. Spek, D. M. Grove, H. Lang and G. van Koten, *J. Am. Chem. Soc.*, **118**, 4817 (1996).

209. C. M. Kretz, E. Gallo, E. Solari, C. Floriani, A. Chiesivilla and C. Rizzoli, *J. Am. Chem. Soc.*, **116**, 10775 (1994).
210. D. Perreault, M. Drouin, A. Michel and P. D. Harvey, *Inorg. Chem.*, **31**, 3688 (1992).
211. R. Eujen, B. Hoge and D. J. Brauer, *Inorg. Chem.*, **36**, 3160 (1997).
212. Z. Xie, B. M. Wu, T. C. W. Mak, J. Manning and C. A. Reed, *J. Chem. Soc., Dalton Trans.*, 1213 (1997).
213. I. Segalas and A. L. Beauchamp, *Can. J. Chem.*, **70**, 943 (1992).
214. U. Heinzel and R. Mattes, *Polyhedron*, **11**, 597 (1992).
215. E. C. Plappert, D. M. P. Mingos, S. E. Lawrence and D. J. Williams, *J. Chem. Soc., Dalton Trans.*, 2119 (1997).
216. M. Konrad, F. Meyer, M. Büchner, K. Heinze and L. Zsolnai, *Chem. Ber.-Recl.*, **130**, 95 (1997).
217. K. A. Hirsch, S. R. Wilson and J. S. Moore, *Inorg. Chem.*, **36**, 2960 (1997).
218. E. Psillakis, J. C. Jeffery, J. A. McCleverty and M. D. Ward, *J. Chem. Soc., Dalton Trans.*, 1645 (1997).
219. J. A. R. Navarro, M. A. Romero, J. M. Salas, R. Faure and X. Solans, *J. Chem. Soc., Dalton Trans.*, 2321 (1997).
220. M. A. Beswick, N. L. Cromhout, C. N. Harmer, M. A. Paver, P. R. Raithby, M. A. Rennie, A. Steiner and D. S. Wright, *Inorg. Chem.*, **36**, 1740 (1997).
221. D. R. Whitcomb and R. D. Rogers, *Inorg. Chim. Acta*, **256**, 263 (1997).
222. M. Epple and H. Kirschnick, *Chem. Ber.-Recl.*, **130**, 291 (1997).
223. D. M. L. Goodgame, S. P. W. Hill and D. J. Williams, *Polyhedron*, **11**, 1841 (1992).
224. L. Song and W. C. Trogler, *Angew. Chem., Int. Ed. Engl.*, **31**, 770 (1992).
225. H. G. Fijolek, J. R. Grohal, J. L. Sample and M. J. Natan, *Inorg. Chem.*, **36**, 622 (1997).
226. J. Dai, T. Kuroda-Sowa, M. Munakata, M. Maekawa, Y. Suenaga and Y. Ohno, *J. Chem. Soc., Dalton Trans.*, 2363 (1997).
227. J. Dai, M. Munakata, T. Kuroda-Sowa, Y. Suenaga, L. P. Wu and M. Yamamoto, *Inorg. Chim. Acta*, **255**, 163 (1997).
228. J. Wu, N. Zhu, S. Du, X. Wu and J. Lu, *Polyhedron*, **11**, 1201 (1992).
229. P. Lin, X. Wu, W. Zhang, J. Guo, T. Sheng, Q. Wang and J. Lu, *Chem. Commun.*, 1349 (1997).
230. T. Konno and K. Okamoto, *Inorg. Chem.*, **36**, 1403 (1997).
231. L. J. Baker, G. A. Bowmaker, D. Camp, Effendy, P. C. Healy, H. Schmidbaur, O. Steigelmann and A. H. White, *Inorg. Chem.*, **31**, 3656 (1992).
232. D. Affandi, S. J. Berners-Price, Effendy, P. J. Harvey, P. C. Healy, B. E. Ruch and A. H. White, *J. Chem. Soc., Dalton Trans.*, 1411 (1997).
233. V. W. W. Yam, K. K. W. Lo, C. R. Wang and K. K. Cheung, *Inorg. Chem.*, **35**, 5116 (1996).
234. D. Fenske and F. Simon, *Angew. Chem., Int. Ed. Engl.*, **36**, 230 (1997).
235. W. Xu, J. P. Rourke, J. J. Vittal and R. J. Puddephatt, *J. Chem. Soc., Chem. Commun.*, 145 (1993).
236. W. Xu, J. J. Vittal and R. J. Puddephatt, *Inorg. Chem.*, **36**, 86 (1997).
237. J. Vicente, M. D. Bermúdez, F. J. Carrión and G. Martínez Nicolás, *J. Organomet. Chem.*, **480**, 103 (1994).
238. J. M. Hu, E. J. Liang, F. Duschek and W. Kiefer, *Spectrochim. Acta, Part A*, **53**, 1431 (1997).
239. J. Yau and D. M. P. Mingos, *J. Chem. Soc., Dalton Trans.*, 1103 (1997).
240. V. P. Izvekov, E. Pungor and K. Tóth, *Anal. Chim. Acta*, **119**, 409 (1980).
241. M. Herres and H. Lang, *J. Organomet. Chem.*, **480**, 235 (1994).
242. J. G. Hou, Y. Wang, W. Xu, S. Y. Zhang, Z. Jian and Y. H. Zhang, *Appl. Phys. Lett.*, **70**, 3110 (1997).
243. J. M. Alia, H. G. M. Edwards, Y. Díaz de Mera and E. E. Lawson, *J. Solution Chem.*, **26**, 497 (1997).
244. Y. W. Chen-Yang, J. J. Hwang and J. Y. Kau, *J. Polym. Sci., Part A*, **35**, 1023 (1997).
245. A. J. Zelazowski and M. J. Stillman, *Inorg. Chem.*, **31**, 3363 (1992).
246. A. Grohmann and H. Schmidbaur, *Inorg. Chem.*, **31**, 3378 (1992).
247. J. Schulz and F. Vogtle, in *Cyclophanes* (Ed. E. Weber), *Topics in Current Chemistry*, Vol. 172, Springer, Berlin, 1994, pp. 41ff.
248. J. L. Pierre, P. Baret, P. Chautemps and M. Armand, *J. Am. Chem. Soc.*, **103**, 2986 (1981).
249. H. C. Kang, A. W. Hanson, B. Eaton and V. Boekelheide, *J. Am. Chem. Soc.*, **107**, 1979 (1985).
250. H. Schmidbaur, W. Bublak, M. W. Haenel, B. Huber and G. Müller, *Z. Naturforsch. B*, **43**, 702 (1988).

251. A. A. Isab, *J. Inorg. Biochem.*, **46**, 145 (1992).
252. J. Michalik, J. Sadlo, A. van der Pol and E. Reijerse, *Acta Chem. Scand.*, **51**, 330 (1997).
253. (a) W. S. Taylor, A. S. Campbell, D. F. Barnas, L. M. Babcock and C. B. Linder, *J. Phys. Chem. A*, **101**, 2654 (1997).
     (b) M. I. Bruce and M. J. Liddell, *J. Organomet. Chem.*, **427**, 263 (1992).
254. R. Bertani, R. A. Michelin, M. Mozzon, P. Traldi, R. Seraglia, L. Busetto, M. C. Cassani, P. Tagliatesta and G. D'Arcangelo, *Organometallics*, **16**, 3229 (1997).
255. D. Schröder, J. Hrušák, R. H. Hertwig, W. Koch, P. Schwerdtfeger and H. Schwarz, *Organometallics*, **14**, 312 (1995).
256. M. S. Kahr and C. L. Wilkins, *J. Am. Soc. Mass Spectrom.*, **4**, 453 (1993).
257. H. B. Li, K. W. M. Siu, R. Guevremont and J. C. Y. Leblanc, *J. Am. Soc. Mass Spectrom.*, **8**, 781 (1997).
258. S. Tougaard and C. Jansson, *Surface Interface Anal.*, **19**, 171 (1992).
259. H. Yoshikawa, T. Tsukamoto, R. Shimizu and V. Crist, *Surface Interface Anal.*, **18**, 757 (1992).
260. S. Ahrland, S. Balzamo and I. Persson, *Acta Chem. Scand.*, **46**, 259 (1992).
261. C. F. Vernon, P. D. Fawell and C. Klauber, *Reactive Polym.*, **18**, 35 (1992).
262. T. Strunskus, M. Grunze, G. Kochendoerfer and C. Woll, *Langmuir*, **12**, 2712 (1996).
263. M. Pitter, M. B. Hugenschmidt and R. J. Behm, *Appl. Phys. Lett.*, **70**, 4035 (1996).
264. K. Takahashi, H. Ishii, Y. Takahashi and K. Nishiguchi, *Thin Solid Films*, **221**, 98 (1992).
265. M. Ignaczak, A. Grzejdziak and G. Andrijewski, *Soviet Electrochem.*, **27**, 795 (1991); *Chem. Abstr.*, **115**, 242342 (1991).
266. S. G. Matz, R. C. Elder and K. Tepperman, *J. Anal. At. Spectrom.*, **4**, 767 (1989).
267. R. Kizu, M. Kaneda, Y. Yamaguchi and M. Miyazaki, *Chem. Pharm. Bull.*, **41**, 1261 (1993).
268. M. H. Rayner, M. Grootveld and P. J. Sadler, *Int. J. Clin. Pharmacol. Res.*, **9**, 377 (1989).
269. R. C. Elder, K. Tepperman, M. L. Traver, S. Matz, W. B. Jones and E. V. Heiss, *J. Liq. Chromatogr.*, **13**, 1191 (1990).
270. R. C. Elder, W. B. Jones and K. Tepperman, in *Element-Specific Chromatographic Detection by Atomic Emission Spectroscopy*, (Ed. P. C. Uden), American Chemical Society, Washington, DC, 1992, pp. 309ff.
271. A. M. Soto, N. Yanagihara and T. Ogura, *J. Coord. Chem.*, **38**, 65 (1996).
272. G. Dobson, W. W. Christie and B. Nikolova-Damyanova, *J. Chromatogr. B*, **671**, 197 (1995).
273. P. Laakso and P. Voutilainen, *Lipids*, **31**, 1311 (1996).
274. T. Rezanka and P. Mares, *J. Cromatogr.*, **542**, 145 (1991).
275. W. M. N. Ratnayake, D. G. Mathews and R. G. Ackman, *J. Am. Oil Chem. Soc.*, **66**, 966 (1989).
276. F. Santinelli, P. Damiani and W. W. Christie, *J. Am. Oil Chem. Soc.*, **69**, 552 (1992).
277. B. Petersson, O. Podhala and B. Jirskog-Hed, *J. Chromatogr. A*, **653**, 25 (1993).
278. L. B. Blomberg, M. Demirbüker and P. E. Andersson, *J. Am. Oil Chem. Soc.*, **70**, 939 (1993).
279. R. O. Adlof, *J. Chromatogr. A*, **764**, 337 (1997).
280. T. G. Toschi, P. Capella, C. Holt and W. W. Christie, *J. Sci. Food Agric.*, **61**, 261 (1993).
281. A. Ibrahim, P. B. Oldham, D. L. Stokes and T. Vodinh, *J. Raman Spectros.*, **27**, 887 (1996).
282. S. J. Dong and J. H. Li, *Bioelectrochem. Bioenerg.*, **42**, 7 (1997).
283. C. D. Tidwell, S. I. Ertel, B. D. Ratner, B. J. Tarasevich, S. Atre and D. L. Allara, *Langmuir*, **13**, 3404 (1997).
284. E. Cooper, R. Wiggs, D. A. Hutt, L. Parker, G. J. Leggett and T. L. Parker, *J. Mater. Chem.*, **7**, 435 (1997).
285. G. B. Sigal, M. Mrksich and G. M. Whitesides, *Langmuir*, **13**, 2749 (1997).
286. P. He, Y. Ye, Y. Fang, I. Suzuki and T. Osa, *Electroanalysis*, **9**, 68 (1997).
287. Y. Miyazaki, K. Hayashi, K. Toko, K. Yamafuji and N. Nakashima, *Jpn. J. Appl. Phys., Part 1*, **31**, 1555 (1992).
288. L. A. Bottomley, J. N. Haseltine, D. P. Allison, R. J. Warmack, T. Thundat, R. A. Sachleben, G. M. Brown, R. P. Woychik, K. B. Jacobson and T. L. Ferell, *J. Vacuum Sci. Technol. A*, **10**, 591 (1992).
289. M. M. Alvarez, J. T. Khoury, T. G. Schaaff, M. Shafigullin, I. Vezmar and R. L. Whetten, *Chem. Phys. Lett.*, **266**, 91 (1997).
290. G. M. Whitesides and C. G. Gorman, in *Handbook of Surface Imaging and Visualization* (Ed. A. T. Hubbard), CRC Press, Boca Raton, FL, 1995, pp. 713ff.
291. G. M. Whitesides, *Trends Biotechnol*, **13**, 228 (1995).
292. A. Ulman, *Chem. Rev.*, **96**, 1533 (1996).

293. G. E. Poirier, *Chem. Rev.*, **97**, 1117 (1997).
294. F. Balzer, R. Gerlach, G. Polanski and H. G. Rubahn, *Chem. Phys. Lett.*, **274**, 145 (1997).
295. K. Tamada, M. Hara, H. Sasabe and W. Knoll, *Langmuir*, **13**, 1558 (1997).
296. T. T. Ehler, N. Malmberg and L. J. Noe, *J. Phys. Chem. B*, **101**, 1268 (1997).
297. B. Heinz and H. Morgner, *Surf. Sci.*, **372**, 100 (1997).
298. S. Imabayashi, M. Iida, D. Hobara, Z. Q. Feng, K. Niki and T. Kakiuchi, *J. Electroanal. Chem.*, **428**, 33 (1997).
299. C. J. Zhong, J. Zak and M. D. Porter, *J. Electroanal. Chem.*, **421**, 9 (1997).
300. G. L. Che and C. R. Cabrera, *J. Electroanal. Chem.*, **417**, 155 (1996).
301. D. F. Yang, C. P. Wilde and M. Morin, *Langmuir*, **13**, 243 (1997).
302. D. F. Yang, H. Al-Maznai and M. Morin, *J. Phys. Chem. B*, **101**, 1158 (1997).
303. J. E. Pemberton, M. A. Bryant, R. L. Sobocinski and S. L. Joa, *J. Phys. Chem.*, **96**, 3776 (1992).
304. D. W. Hatchett, K. J. Stevenson, W. B. Lacy, J. M. Harris and H. S. White, *J. Am. Chem. Soc.*, **119**, 6596 (1997).
305. D. S. Karpovich and G. J. Blanchard, *Langmuir*, **13**, 4031 (1997).
306. H. Tsutsumi, K. Takeoka and T. Oishi, *J. Colloid Interface Sci.*, **185**, 432 (1997).
307. R. Woods, C. I. Basilio, D. S. Kim and R. H. Yoon, *J. Electroanal. Chem.*, **328**, 179 (1992).
308. Y. C. Sasaki, K. Yasuda, Y. Suzuki, T. Ishibashi, I. Satoh, Y. Fujiki and S. Ishiwata, *Biophys. J.*, **72**, 1842 (1997).
309. J. E. Fieberg, A. Szabo and J. M. White, *J. Chem. Soc., Faraday Trans.*, **92**, 4739 (1996).
310. W. Li, V. Lynch, H. Thompson and M. A. Fox, *J. Am. Chem. Soc.*, **119**, 7211 (1997).
311. W. R. Thompson, M. Cai, M. K. Ho, and J. E. Pemberton, *Langmuir*, **13**, 2291 (1997).
312. M. H. Dishner, L. C. Hemminger and F. J. Feher, *Langmuir*, **12**, 6176 (1996).
313. H. Schönherr, F. J. B. Kremer, S. Kumar, J. A. Rego, H. Wolf, H. Ringsdorf, M. Jaschke, H. J. Butt and E. Bamberg, *J. Am. Chem. Soc.*, **118**, 13051 (1996).
314. M. Kunitake, U. Akiba, N. Batina and K. Itaya, *Langmuir*, **13**, 1607 (1997).
315. E. U. T. van Velzen, J. F. J. Engbersen and D. N. Reinhoudt, *Synthesis*, **8**, 989 (1995).
316. H. Schönherr, G. J. Vancso, B. H. Huisman, F. C. J. M. van Veggel and D. N. Reinhoudt, *Langmuir*, **13**, 1567 (1997).
317. B. Liedberg, Z. Yang, I. Engquist, M. Wirde, U. Gelius, G. Gotz, P. Bauerle, R. M. Rummel, C. Ziegler and W. Gopel, *J. Phys. Chem. B*, **101**, 5951 (1997).
318. G. Hähner, A. Marti, N. D. Spencer, S. Brunner, W. R. Caseri, U. W. Suter and M. Rehahn, *Langmuir*, **12**, 719 (1996).
319. T. Dretschkow, A. S. Dakkouri and T. Wandlowski, *Langmuir*, **13**, 2843 (1997).
320. B. Roelfs, E. Bunge, C. Schröter, T. Solomun, H. Meyer, R. J. Nichols and H. Baumgärtel, *J. Phys. Chem. B*, **101**, 754 (1997).
321. A. C. Chen, S. G. Sun, D. F. Yang, B. Pettinger and J. Lipkowski, *Can. J. Chem.*, **74**, 2321 (1996).
322. N. H. Jang, J. S. Suh and M. Moskovits, *J. Phys. Chem. B*, **101**, 1649 (1997).

CHAPTER **8**

Synthesis and uses of organogold compounds

HUBERT SCHMIDBAUR, ANDREAS GROHMANN, M. ELENA OLMOS and ANNETTE SCHIER

Lehrstuhl für Anorganische und Analytische Chemie, Technische Universität München, D-85747 Garching, Germany
Fax: 49-89-289-13125.   E-mail: H.Schmidbaur@lrz.tum.de

I. INTRODUCTION

Organogold chemistry is one of the oldest sub-disciplines of organometallic chemistry and the first successful syntheses date back to the first decade[1,2] of this century and to the

late 1950s[3]. It has developed only slowly, but has matured considerably after the 1970s. This evolution is reflected also by this summary of the syntheses and uses of organogold compounds.

The presentation of the material in this chapter largely follows an order of increasing oxidation states, except where a classification of ligand type (as in the case of the ylide complexes) facilitates a generalizing treatment. Reviews published during the last fifteen years include general surveys of organogold chemistry[4,5] as well as more specialized accounts on topics such as coordination chemistry[6-10] and arylgold chemistry [11,12]. For further information, the reader is also referred to the classical book on Gold Chemistry[13] and to the *Dictionary of Organometallic Compounds* as another highly useful compilation of data concerning the organic chemistry of gold[14]. This article concentrates on the *progress* in the syntheses of organogold compounds since 1980[15], i.e. it complements the Organogold Gmelin volume which is comprehensive up to 1980. As in previous treatises, cyanide and isocyanide complexes of gold are excluded.

II. SYNTHESIS OF σ-BONDED ORGANOGOLD COMPLEXES

A. Complexes of the Type [RAuL]

Complexes of this type may contain a variety of organic residues R, such as alkyl, vinyl, alkynyl or aryl. The neutral donor group L is most commonly a tertiary phosphine or an isocyanide ligand, and polynuclear complexes with bridging polyfunctional donor ligands are also known[4,13,15]. From a practical point of view, the series of organogold(I) and isocyanide complexes is of particular interest since some of its members hold promise as precursors for the chemical vapour deposition of gold films. A selection of these and other compounds of the type [RAuL] is presented in Tables 1–3.

Alkylgold(I) phosphine complexes are usually synthesized by reaction of an alkyl-lithium or a Grignard reagent with a complex gold(I) halide, and the corresponding isocyanide complexes are accessible by analogous routes. Typical examples for the preparation of this type of complexes are given in equations 1 and 2[16,13c]. In a modified synthesis of alkylgold(I) phosphine complexes, tris(phosphinegold(I))oxonium tetrafluoroborates are used instead of (phosphine)gold(I) halides and considerably shorter reaction times and generally higher yields of organogold compounds have been reported (equations 3 and 4, R = e.g. $C_6H_5CH_2$). In addition, the separation of starting materials and final products is facilitated by the low solubility of the oxonium salt in common solvents such as ether or tetrahydrofuran[31,32]. Photophysical and luminescence properties[33,34], photoelectron spectra[35] and the electronic structure[36,37] of alkylgold(I) complexes have been investigated.

$$\qquad\qquad (1)$$

$$[AuCl(SMe_2) + MeMgCl + CNMe \xrightarrow{-MgCl_2, \ -SMe_2} [AuMe(CNMe)] \qquad (2)$$

$$[(Ph_3PAu)_3O][BF_4] \xrightarrow[\text{2. H}_2\text{O}]{\text{1. RLi}} [AuR(PPh_3)] \qquad (3)$$

$$[(Ph_3PAu)_3O][BF_4] \xrightarrow[\text{2. H}_2\text{O}]{\text{1. RMgCl}} [AuR(PPh_3)] \qquad (4)$$
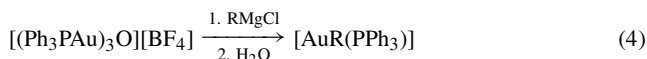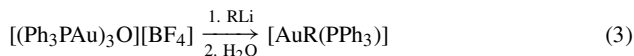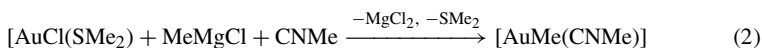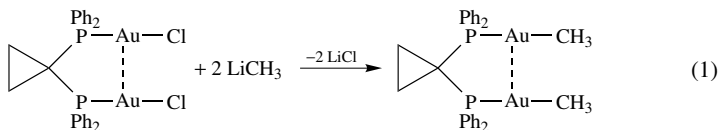
TABLE 1. Gold(I) complexes of the type [RAuL]

Complex	M.p.($^\circ$C)	Reference
R = alkyl		
[{AuMe}$_2${(Ph$_2$P)$_2$C̄CH$_2$C̄H$_2$}]	203(d)	16
[AuMe(TPA)]^a	143(d)	17
[AuMe{(Ph$_2$PCH$_2$PPh$_2$)Fe(CO)$_2$(η^4-MeC$_5$H$_5$)}]	141–142	18
[AuMe(AsPh$_3$)]	—	19
[AuMe(CNMe)]	95(d)	13c
[AuMe(CNPr-i)]	<40(d)	13c
[AuMe(CNC$_6$H$_{11}$-c)]	88(d)	13c
[AuMe(CNPh)]	102(d)	13c
R = functionalized alkyl and related ligands		
[Au(CCl$_3$)(PPh$_3$)]	>200(d)	20
[Au(CF$_3$)(PMe$_3$)]	191–193(d)	21, 22
[Au(CH$_2$CN)(PPh$_3$)]	141–142	23
[Au(CCl$_2$CN)(PPh$_3$)]	172–173	23
[Au{CH(CN)(COOEt)}(PPh$_3$)]	147–149	24, 25
[Au{C(=N(C$_6$H$_3$Me$_2$-2,6))(CH$_2$COPh)}]	160(d)	26
[Au(C̄=NC(Me)=CHS̄)]	—	27
[Au(C̄=NC$_6$H$_4$S̄-o)(PPh$_3$)]	155–156	27
[Au(C̄=CHCH=NS̄)(PPh$_3$)]	157–158	28
[Au$_2${(CH$_2$)$_3$PPh$_2$}$_2$]	—	29
[Au$_2${2-C(SiMe$_3$)$_2$(C$_5$H$_4$N)}$_2$]	122(d)	30
[Au{2-(1-Ph-$closo$-1,2-C$_2$B$_{10}$H$_{10}$)}(PPh$_3$)]	—	19
[Au{2-(1-Ph-$closo$-1,2-C$_2$B$_{10}$H$_{10}$)}(AsPh$_3$)]	—	19
R = vinyl		
[Au(HC=CH$_2$)(CNMe)]	—	13c
[Au(HC=CH$_2$)(CNBu-t)]	—	13c

^{a}TPA: 1,3,5-triaza-7-phosphaadamantane.

Haloalkylgold(I) complexes can be prepared by photochemical insertion of fluoro-alkenes into the gold–carbon bond of methylgold(I) complexes and this and related processes involving other metals have been reviewed[38]. In addition, several new routes to haloalkylgold(I) complexes have been established[39,40]. These include the direct auration of halocarbons such as chloroform with tris(triphenylphosphinegold(I))oxonium tetrafluoroborate (see also above) to give the halomethylgold(I) derivatives (equation 5)[20,23] and the reaction of bis(trifluoromethyl)cadmium with (phosphine)gold(I) halides (equation 6)[21,22]. The auration product of chloroform is unstable with respect to decomposition into (triphenylphosphine)gold(I) chloride and dichlorocarbene, as has been ascertained by scavenging experiments with olefins[20]. An unusual reaction is reported for the chloromethyl complex [Au(CH$_2$Cl)(PPh$_3$)]: Interaction with [PtMe$_2$(2,2$'$-bipy)] (2, 2$'$-bipy = 2, 2$'$-bipyridine) results in oxidative addition to give

[PtClMe$_2$(CH$_2$AuPPh$_3$)(2,2′-bipy)], a rare example of a heteronuclear μ-methylene complex that does not contain either a metal–metal bond or an additional bridging ligand[41].

$$CHCl_3 \xrightarrow[\text{NaH}]{[(Ph_3PAu)_3O][BF_4]} [Au(CCl_3)(PPh_3)] \tag{5}$$

$$2\,[AuCl(PEt_3)] + (CF_3)_2Cd \cdot DME \longrightarrow 2[AuCF_3(PEt_3)] + CdCl_2 \tag{6}$$

$$(DME = CH_3OCH_2CH_2OCH_3)$$
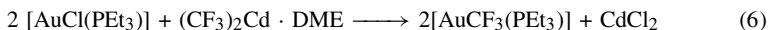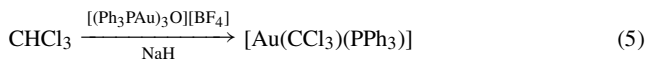
Alkylgold(I) complexes in which the alkyl group carries a donor functionality represent a special class of compounds in that they often form di- or oligonuclear arrays. Pertinent examples include the complex [Ph$_2$P(CH$_2$)$_3$Au]$_2$, which is prepared according to equation 7 and for which a dimeric structure is proposed[29]. The cyclic structure of the compound [{2-C(SiMe$_3$)$_2$(C$_5$H$_4$N)}Au]$_2$ has been established by X-ray crystallography[30]. By contrast, the complex Pt[C$_6$H$_4${2-CH(AuPPh$_3$)PPh$_2$}]$_2$ represents a heterobimetallic species in which gold(I) is not part of a cyclic arrangement[42].

$$[Ph_2P(CH_2)_3]_2Zn + 2\,[AuCl(CO)] \xrightarrow{-ZnCl_2,\, -2\,CO} \tag{7}$$
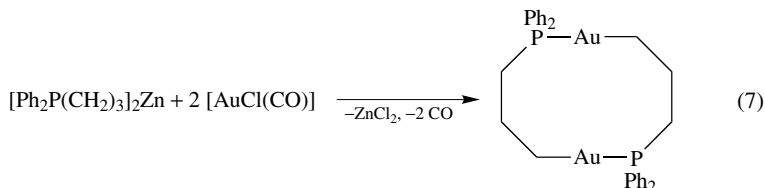
Several alkyl ligands derived from organic molecules in which the functional groups induce α-hydrogen acidity have been used to prepare the respective gold(I) complexes. Particularly interesting are thiazolyl and isothiazolyl compounds, which are precursors for the synthesis of gold(I) carbene complexes[27,28]. Recently reported examples include various ketone and sulphonic acids derivatives, and C-coordination is observed in all cases[43]. The syntheses have been carried out by one of the following four methods:

(1) The original 'alkyllithium route' (cf equation 1)[27,28,31,43,44].

(2) The modified alkyllithium route (cf equation 3)[46].

(3) Deprotonation and subsequent auration with stable gold(I) alkoxides (equation 8)[47].

$$[Au\{OCH(CF_3)_2\}(PPh_3)] + CH_2(CN)COOEt \longrightarrow [Au\{CH(CN)COOEt\}(PPh_3)]$$

$$+(CF_3)_2CHOH \tag{8}$$
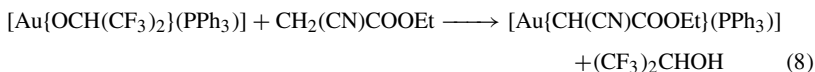
(4) Reaction of silyl enol ethers with complex (phosphine)gold(I) halides in the presence of caesium fluoride (equation 9)[26], or of enol ethers with [(Ph$_3$PAu)$_3$O][BF$_4$][25].
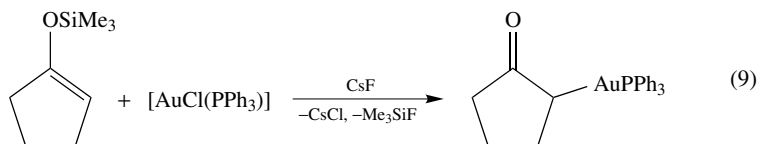
Silylcyclopropyl ethers have been used for the preparation of (phosphine)gold(I) homoenolate complexes (equation 10)[48].

$$\triangleright\!\!\!<\begin{array}{l}\text{Ph}\\\text{OSiMe}_3\end{array} \quad + \quad [\text{AuCl(PPh}_3)] \xrightarrow[-\text{CsCl, }-\text{Me}_3\text{SiF}]{\text{CsF}} [\text{Au(CH}_2\text{CH}_2\text{COPh)(PPh}_3)] \quad (10)$$
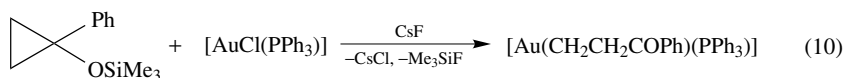
Less general reactions include the C-auration of pyrazolone derivatives with (phosphine)gold(I) halide in the presence of an aqueous base[49], and the auration of a palladium(II) phosphinoenolate complex with [AuCl(PPh$_3$)] in the presence of AgBF$_4$, resulting in the metallation of the C$_\alpha$ carbon atom of the former enolate moiety (equation 11)[50] (Table 2)

(11)
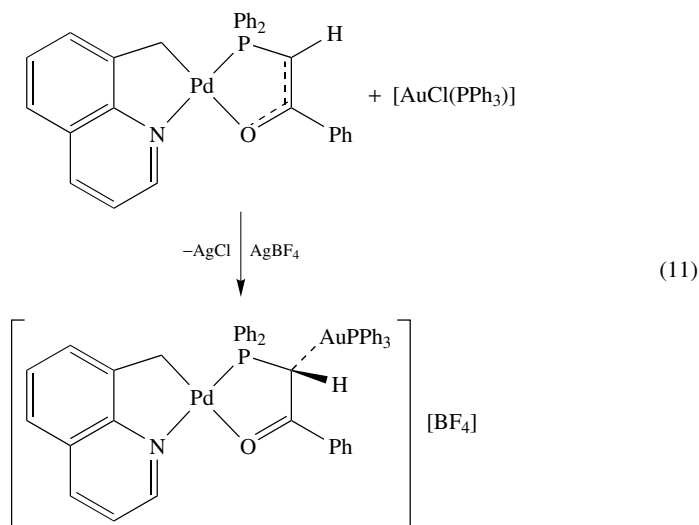
Finally, there are numerous complexes in which one or both protons in the methylene bridge of geminal diphosphine disulphides such as bis(diphenylphosphino)methane disulphide have been substituted with a (phosphine)gold(I) unit, as illustrated by the reaction products of equation 12[51]. Deprotonation and subsequent auration can be accomplished by using gold(I) complexes containing basic ligands, such as [Au(acac)(PPh$_3$)][51]

TABLE 2. Alkylgold(I) complexes with carbonyl or sulphonyl functional groups

Complex	Reference
[Au{CH(Ph)SO$_2$Bu-t}(PPh$_3$)]	44
[Au{(CCH$_2$CH$_2$)CO(CHCH$_2$CH$_2$)}(PPh$_3$)]	45
[Au{CH$_2$COC$_5$H$_4$Mn(CO)$_3$}(PPh$_3$)]	46
[Au{CH(CN)$_2$}(PPh$_3$)]	47
[Au(CH$_2$COCH$_2$CH$_2$CH=CH$_2$)(PPh$_3$)]	48

or $[(Ph_3PAu)_3O][BF_4]$[52], which are displaced as the conjugate acid in the process. Even a tetranuclear gold(I) complex, $[Au_2(PPh_2CH\{Au(acac)\}Ph_2P)_2]$, with two basic ligands, can be used as a base for the deprotonation and this allows the synthesis of hexanuclear gold derivatives, such as the one represented in equation 13[53]. Since the diphosphine ligands offer the possibility of further gold coordination at the phosphorus centres, they are versatile building blocks for the preparation of homo- and heteropolynuclear complexes and a large variety of structural types have been prepared[54−57].

$$(12)$$

$$(13)$$
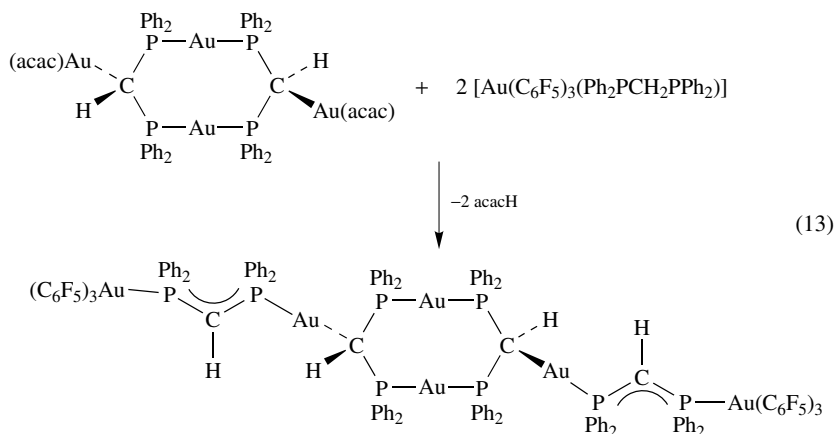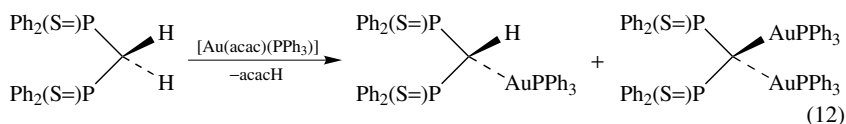
There has been considerable activity concerning the synthesis and exploration of possible applications[58] of alkynylgold(I) compounds in recent years and a number of X-ray structural (see below) as well as Mössbauer[59] studies have appeared. Previous routes to such complexes generally start with $HAuCl_4$, which is reduced by SO_2 in the presence of acetate, followed by addition of the terminal acetylene. In this way polymeric gold(I) acetylides $[Au(C\equiv CR)]_n$ are obtained. The oligomeric compound of general formula $[Au(C\equiv CBu\text{-}t)]_n$ has also recently been prepared by treatment of $[Au(NH_3)_2]^+$ with $t\text{-}BuC\equiv CH$[60,61].

Compounds of the type $[Au(C\equiv CR)]_n$ have been used for the introduction of the acetylide ligand into heterobimetallic complexes of the late transition metals[62−64]. They react with electron-rich metal complexes by incorporation of the $[Au(C\equiv CR)]$ unit to form neutral gold–metal clusters[65,66], and they can be transformed into alkynylgold(I) complexes of the type $[Au(C\equiv CR)(L)]$ simply by addition of suitable donor ligands, such as amines, tertiary phosphines or isocyanides[14,67]. The reaction of $[Au(C\equiv CPh)]_n$ with bis(diphenylphosphino)methane affords the photoluminescent trinuclear complex $[Au_3(C\equiv CPh)_2(\mu\text{-}dppm)_2][Au(C\equiv CPh)_2]$ (dppm $= Ph_2PCH_2PPh_2$) (Figure 1). Not only neutral ligands, but also halide ions have recently been added to $[Au(C\equiv CR)]_n$, giving anionic species of the general type $[Au(C\equiv CR)(X)]^-$ [68−70].
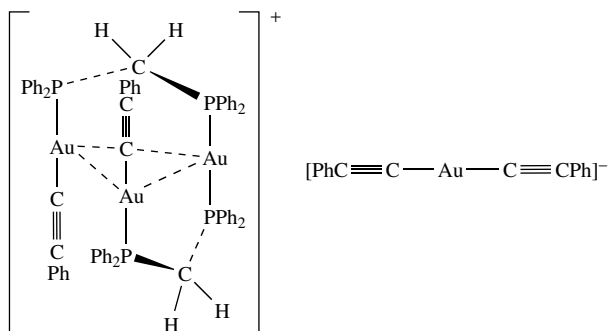
FIGURE 1. Structure of $[Au_3(C\equiv CPh)_2(\mu\text{-}Ph_2PCH_2PPh_2)_2][Au(C\equiv CPh)_2]$

However, the preparation of complexes of the type $[Au(C\equiv CR)(L)]$ as outlined above often fails, since the initially formed $[Au(C\equiv CR)]_n$ compounds may readily decompose, depending on the nature of the acetylide ligand. Several novel synthetic routes to alkynylgold(I) compounds that circumvent this problem have been established. Complex gold(I) chlorides containing a variety of tertiary phosphines have been found to react with a wide range of terminal acetylenes, either in diethylamine in the presence of copper(I) halides[71], or in alcoholic solution in the presence of sodium alkoxide[71–74], to afford the corresponding alkynylgold(I) complexes in good yield. These transformations are equally applicable to unsubstituted acetylene, which gives dinuclear gold(I) acetylides $[Au_2(C\equiv C)(PR_3)_2]^{72-74}$. Examples are shown in equations 14 and 15.

$$[AuCl(PPh_3)] + HC\equiv CC_6F_5 \xrightarrow[-[Et_2NH_2]Cl]{Et_2NH/Cu(I)Cl} [Au(C\equiv CC_6F_5)(PPh_3)] \quad (14)$$

$$[AuCl\{P(C_6H_4Me\text{-}4)_3\}] + HC\equiv CMe \xrightarrow[-HCl]{EtOH/NaOEt}$$
$$[Au(C\equiv CMe)\{P(C_6H_4Me\text{-}4)_3\}] \quad (15)$$
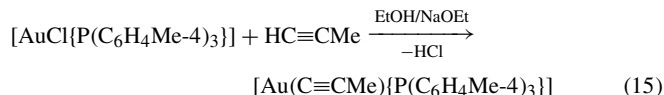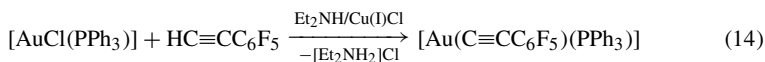
An alternative high-yield method for preparing gold(I) phenylacetylides involves the electrochemical oxidation of gold metal in an acetonitrile solution of the acetylene[75], with the target compounds precipitating during electrolysis. The measured current efficiency of about 1 mol Faraday^{-1} implies the following simple electrode processes:

Cathode: $\quad e^- + (PhC\equiv CH) \rightarrow (PhC\equiv C)^- + 1/2H_2(g)$

Anode: $\quad Au \rightarrow Au^+ + e^-$

Overall reaction: $\quad Au + (PhC\equiv CH) \rightarrow (PhC\equiv C)Au + \frac{1}{2}H_2$
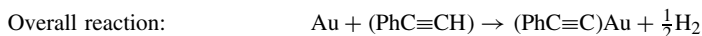
Other routes that have led to alkynylgold(I) complexes have employed acetylacetonatogold(I) derivatives[76], alkylgold(I) complexes[26] and N-substituted (phosphine)gold(I) imidazoles[77], respectively. The anionic ligands in these reagents are sufficiently basic to deprotonate the acetylene moiety, thus forming acetylide complexes such as those shown in Figure 2[77]. Also NH_3 can act as a deprotonating base, as demonstrated in
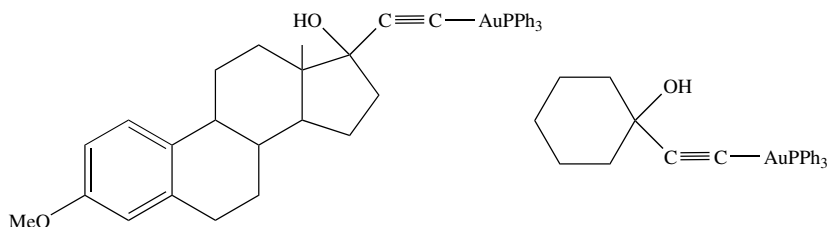
FIGURE 2. Alkynylgold(I) complexes[77]

the reaction of $[Au(NH_3)_2]^+$ with phenylacetylene to give $[Au(C{\equiv}CPh)(NH_3)]$ in excellent yield[60]. Finally, compounds of the type $[Au(C{\equiv}CH)(PR_3)]$ (R = Ph, C_6H_4OMe-4) have been obtained by treating the bis(acetylide)aurate(I) with bis(phosphine)gold(I) derivatives[76]. A collection of other alkynylgold complexes is listed in Table 3. The alkynylgold(I) complexes of the type $[Au(C{\equiv}CBu$-$t)(R_2PCH_2PR_2)]$ contain monodentate diphosphine ligands and can undergo ligand exchange reactions[78]. Thermolysis of the dinuclear $[Au_2(C{\equiv}CBu$-$t)_2(Ph_2PCH_2PPh_2)]$ in refluxing toluene leads to intermolecular elimination of t-$BuC{\equiv}CH$ and formation of the stable tetragold(I) complex represented in equation 16[79].

(16)
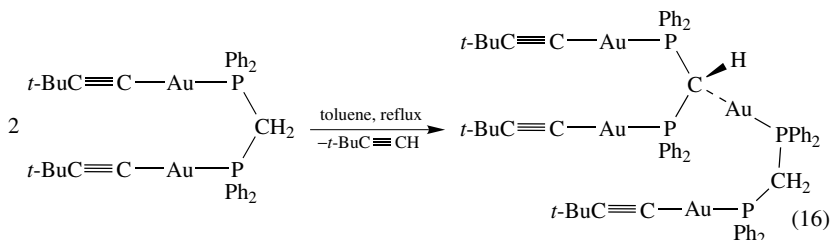
Alkynylgold(I) halide anion complexes have been prepared from suitable gold(I) acetylide precursors by addition of halide ion, as illustrated in equation 17[70], or reacting a bis(acetylide)aurate(I) with a dihalogenoaurate(I) (equation 18)[76].

$$1/n[Au(C{\equiv}CPh)]_n + [NEt_4]Cl \longrightarrow [NEt_4][Au(C{\equiv}CPh)Cl] \qquad (17)$$

$$[N(PPh_3)_2][Au(C{\equiv}CH)_2] + [N(PPh_3)_2][AuCl_2] \longrightarrow 2[N(PPh_3)_2][Au(C{\equiv}CH)Cl] \,(18)$$
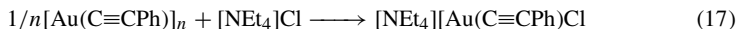
Bifunctional acetylene ligands such as $R_2PC{\equiv}CH$ or p-$C{\equiv}N$-C_6H_4-$C{\equiv}CH$ have been employed in the synthesis of novel classes of metal-containing polymers. The polymer backbone contains both unsaturated organic fragments and inorganic elements, such as gold or a combination of gold and phosphorus. These materials are therefore expected to show electrical conductivity or optical non-linearity[81,83–85]. Modes of preparation of such compounds have been summarized in equation 19 and Scheme 1.

$$[AuCl(Ph_2PC{\equiv}CH)] \xrightarrow{\text{NaOMe}} [\{Au(Ph_2PC{\equiv}C-\}_x] \qquad (19)$$
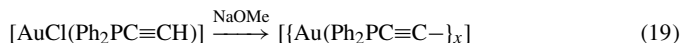
Polymers have also been prepared from diphosphines and diacetylides, both of which act as bridging ligands and alternate along the polymeric chain (Figure 3). The synthesis

TABLE 3. Alkynylgold(I) complexes

Complex	M.p.($^\circ$C)	Reference
[Au(C≡CPh)]$_n$	180(d)	75
[Au(C≡CH)(PPh$_3$)]	168	72, 76
[Au(C≡CH)(PPh$_2$Np)]^a	—	74
[Au(C≡CH)(PPh$_2$Bp)]^b	—	74
[Au(C≡CH)(NH$_3$)]	—	60
[Au(C≡CMe)(PMe$_3$)]	123(d)	13c, 71
[Au(C≡CMe)(PPh$_3$)]	173–175	71
[Au(C≡CCF$_3$)(PPh$_3$)]	155	72
[Au(C≡CEt)(PPh$_3$)]	154–155	72
[Au(C≡CPr-n)(PPh$_3$)]	256–259	71
[Au(C≡CBu-n)(PPh$_3$)]	279–281	71
[Au(C≡CBu-t)(PMe$_3$)]	183–186	71
[Au(C≡CBu-t)(PPh$_3$)]	181–182	71
[Au(C≡CCH$_2$OH)(PPh$_3$)]	234–235	71
[Au(C≡CCH$_2$OMe){P(C$_6$H$_4$Me-4)$_3$}]	—	80
[Au(C≡CCH$_2$CH$_2$OH)(PPh$_3$)]	248–250	71
[Au(C≡CCO$_2$Me)(PPh$_3$)]	239–240	71
[Au(C≡CPh)(PMe$_3$)]	196–198	71
[Au(C≡CPh){PPh(OMe)$_2$}]	212–215	71
[Au(C≡CPh)(PPhFc$_2$)]^c	—	74
[Au(C≡CPh)(PPh$_3$)]	163–165	72, 75
[Au(C≡CPh){P(C$_6$H$_4$Me-4)$_3$}]	146–148	72
[Au(C≡CPh)(phen)]^d	95–97	75
[Au(C≡CC$_6$F$_5$)(PPh$_3$)]	235–236	71
[Au(C≡CBu-t)(Me$_2$PCH$_2$PMe$_2$)]	165(d)	78
[Au(C≡CBu-t)(Ph$_2$PCH$_2$PPh$_2$)]	99(d)	78
[Au(C≡CPPh$_2$)]$_x$	—	81
[Au$_2$(C≡C)(PPh$_3$)$_2$]	—	72
[Au$_2$(C≡C){P(C$_6$H$_4$Me-4)$_3$}$_2$]	110–115	72, 82
[Au$_2$(C≡C){P(C$_6$H$_4$OMe-4)$_3$}$_2$]	125	72, 82
[Au$_2${p-C≡C−(C$_6$H$_4$)$_n$−C≡C}(PMe$_3$)$_2$], n = 1, 2	—	83
[Au$_2$(C≡CBu-t)$_2$(Ph$_2$PCH$_2$PPh$_2$)]	—	79
[Au$_2$(C≡CPh)$_2$(Ph$_2$PC$_6$H$_4$PPh$_2$-p)]	—	83
[Au$_2$(C≡CPh)$_2$(Ph$_2$PCH$_2$CH$_2$PPh$_2$)]	—	58
[Au(C≡CMe)(CNMe)]	140(d)	13c
[Au(C≡CBu-t)(CNMe)]	180–181(d)	13c
[Au(C≡CH)Cl]$^-$	192	76
[Au(C≡CH)Br]$^-$	186	76
[Au(C≡CPh)Cl]$^-$	—	70
[Au(C≡CPh)Br]$^-$	—	70
[Au(C≡CPh)I]$^-$	—	70

^{a}Np, 1-naphthyl.
^{b}Bp, 4-biphenylyl.
^{c}Fc, ferrocenyl.
^{d}phen, 1,10-phenanthroline.
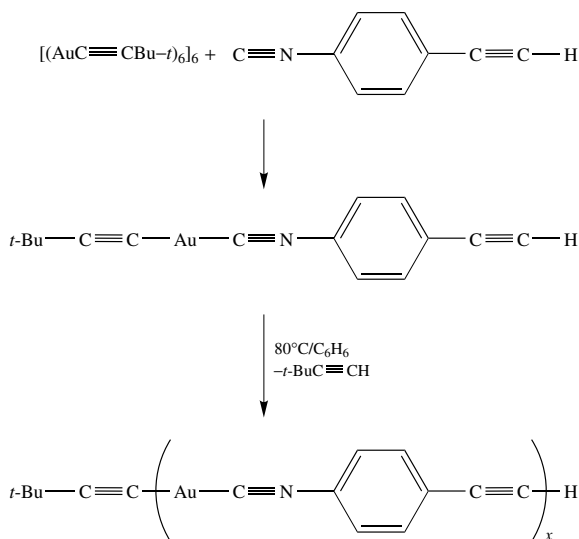
SCHEME 1. Synthesis of (isocyano)gold(I) acetylide polymers

starts from digold(I) acetylides $[(AuC{\equiv}CArC{\equiv}CAu)_x]$ (Ar = e.g. 1,4-C$_6$H$_4$), prepared by reaction of the diacetylene with $[AuCl(SMe_2)]$ in the presence of sodium acetate as base. Reaction of the starting material with diphosphine, PP, gives polymers of the general formula $[(C{\equiv}CArC{\equiv}C-Au-PP-Au-)_x]$.
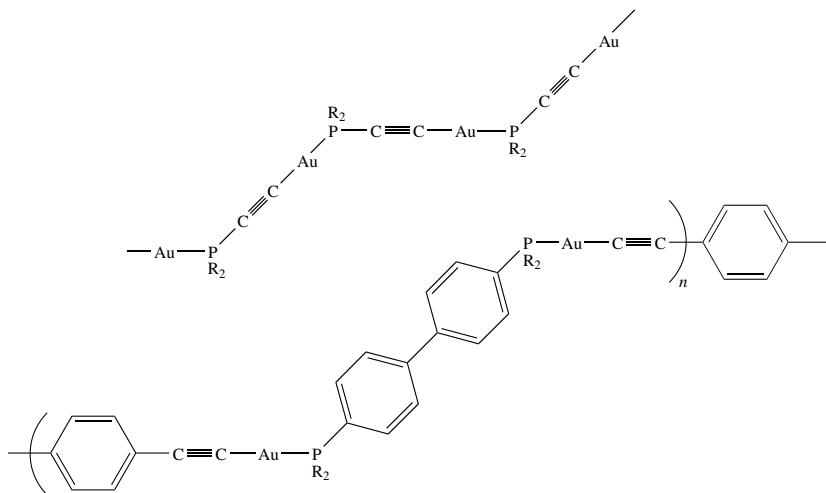
FIGURE 3. Suggested structures of $[\{Au(R_2P-C{\equiv}C)\}]_n$ and $[(Ar-C{\equiv}C-Au-C{\equiv}C)_n]$
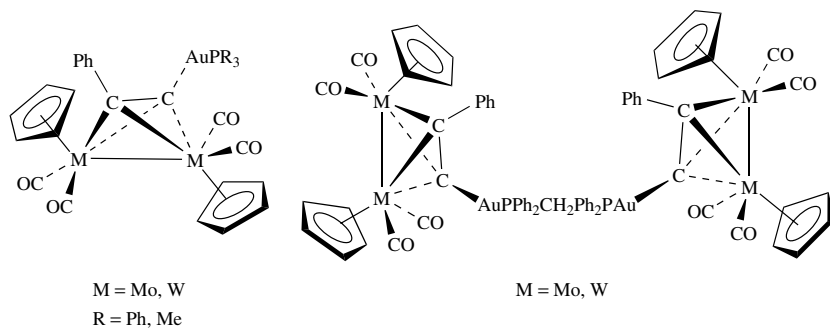
FIGURE 4. Heteropolynuclear complexes with bridging alkynylphosphinegold(I) units

Some heteropolynuclear gold-containing acetylides are also known, such as the dinuclear [Fe{(C≡C)Au(PPh$_3$)}(η^5-C$_5$H$_5$)(Ph$_2$PCH$_2$PPh$_2$)] and [Ru{(C≡C)Au(PPh$_3$)}(η_5-C$_9$H$_7$)L$_2$] (L$_2$ = (PPh$_3$)$_2$; (PPh$_3$)(PMe$_3$); (PPh$_2$)$_2$(CH$_2$)$_n$, n = 1, 2), obtained from the corresponding ethynyl complexes of iron or ruthenium and (triphenylphosphine)gold(I) chloride in the presence of Tl(acac)[86], or the tri- or hexanuclear gold(I) and group 6 metal complexes represented in Figure 4[87−90].

The chemistry of *arylgold(I) complexes* [ArAuL] has developed rapidly in recent years and two reviews have appeared[11,12]. The available synthetic methods allow the preparation of complexes with a diverse range of ligands L, including tertiary phosphines, amines, isocyanides, tetrahydrothiophene, and tertiary arsines. Difunctional phosphines such as bis(diphenylphosphino)amine give the corresponding dinuclear arylgold(I) complexes[91,92], and a dimeric orthometallated phenylphosphine complex of formula [Au$_2${C$_6$H$_4$(PPh$_2$)}$_2$] has also been prepared[93]. Both types of complexes undergo two-centre oxidative addition reactions reminiscent of those described for the structurally related gold(I) ylide complexes (see below). Also trinuclear arylgold(I) phosphine derivatives have been described[33,94,95], and some of these are luminescent materials[33].

In analogy to the synthesis of the alkyl derivatives, arylgold compounds [ArAuL] (L being a neutral donor ligand) can be prepared from complex gold(I) halides via the organolithium or the Grignard route[96,97]. [ArAuL] complexes can also be synthesized with ligands L that are only weakly coordinating (such as tetrahydrothiophene, SC$_4$H$_8$)[92−100] (equation 20); derivatives may then be obtained through displacement of this ligand by a variety of other, more strongly coordinating donors (equation 21)[101]. These may include unusual species such as alkylidyne complexes [W(≡CR)(CO)$_2$(Me$_2$PCH$_2$CH$_2$PMe$_2$)Cl], which react to give heteronuclear complexes with bridging carbyne ligands between tungsten and gold[102]. Several tricoordinate arylgold(I) diphosphine complexes have recently been prepared by displacement of tetrahydrothiophene with the metallodiphosphine 1,1′-bis(diphenylphosphino)octamethylferrocene or with bis(diphenylphosphino)-*o*-carborane[103].

$$[Au(SC_4H_8)_2]ClO_4 + [NBu_4][Au(C_6H_2F_3\text{-}2,4,6)_2] \longrightarrow$$

$$2[Au(C_6H_2F_3\text{-}2,4,6)(SC_4H_8)] + [NBu_4]ClO_4 \quad (20)$$

$$[Au(C_6F_5)(SC_4H_8)] + H_2NCH_2CH_2NH_2 \longrightarrow [Au(C_6F_5)(H_2NCH_2CH_2NH_2)] \quad (21)$$
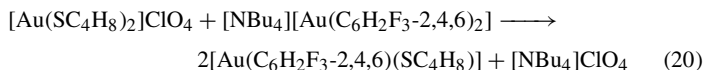
Treatment of (phosphine)gold(I) halides or tris(phosphinegold(I))oxonium salts with sodium tetraphenylborate affords arylgold(I) phosphine species through an unusual phenyl transfer reaction. Examples of this novel synthetic route are given in equations 22^{104} and 23^{105}.

$$[Au(TPA)_3]Cl + Na[BPh_4] \longrightarrow [AuPh(TPA)] + NaCl + 2TPA + BPh_3 \qquad (22)$$

TPA = 1,3,5-triaza-7-phosphaadamantane

$$[(t\text{-}Bu_3PAu)_3O][BF_4] + Na[BPh_4] \longrightarrow 3[AuPh(PBu\text{-}t_3)] + Na[BF_4] + PhBO \quad (23)$$
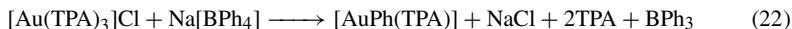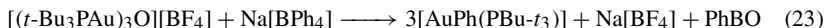
TABLE 4.　Arylgold(I) complexes of the type [ArAuL]

Complex	M.p.($^{\circ}$ C)	Reference
[AuPh(CNMe)]	—	13c
[Au$_2$Ph$_2${C$_6$H$_4$(CH$_2$PPh$_2$)$_2$-1,4}]	135(d)	105
[Au{C$_6$H$_5$(η^6-Cr(CO)$_3$)}(PPh$_3$)]	—	109
[Au{C$_6$H$_4$NO$_2$-2}(AsPh$_3$)]	—	108
[Au{C$_6$H$_4$NO$_2$-2}(SbPh$_3$)]	120(d)	108
[Au{C$_6$H$_4$NO$_2$-2}(phen)]^a	100(d)	108
[Au{C$_6$H$_2$(NO$_2$)$_3$-2,4,6}(dmphen)]^a	—	110
[Au$_2${C$_6$H$_4$PPh$_2$-2}$_2$]	—	93
[Au$_2${C$_6$H$_4$AsPh$_2$-2}$_2$]	—	111
[Au(C$_6$H$_2$F$_3$-2,4,6)(SC$_4$H$_8$)]	73(d)	93
[Au(C$_6$F$_5$){N(=CPh$_2$)N=CPh$_2$}]	—	112
[Au$_2$(C$_6$F$_5$)$_2${(Ph$_2$P)$_2$CH$_2$}]	—	113
[Au$_2$(C$_6$F$_5$)$_2${Ph$_2$As)$_2$CH$_2$}]	189(d)	107
[Au$_2$(C$_6$F$_5$)$_2${(Ph$_2$PC$_5$H$_4$)$_2$Fe}]	245(d)	114
[Au$_2$(C$_6$F$_5$)$_2${Ph$_2$PC(Ph$_2$PAuPPh$_2$)$_2$CPPh$_2$}]	170	94
[Au$_2$(C$_6$F$_5$)$_2${Au(Ph$_2$PCHPPh$_2$Me)$_2$}]$^+$	—	115
[Au$_2$(C$_6$F$_5$)$_2${(Ph$_2$P)$_2$Mn(CO)$_4$}]$^-$	—	116
[Au$_2$(C$_6$F$_5$)$_2${(Ph$_2$P)$_2$NH}]	205	92
[Au$_2$(C$_6$Cl$_5$)$_2${(Ph$_2$P)$_2$NH}]	144(d)	92
[Au$_2$(C$_6$F$_5$)$_2$(S$_2$CPEt$_3$)]	144	117
[Au$_2$(C$_6$F$_5$)$_2${(Ph$_2$PS)$_2$CH$_2$}]	185	118
[Au$_2$(C$_6$F$_5$)$_2$(L)]^b	195	119
[Au$_2$(C$_6$F$_5$)$_2$(L')]^b	143	119
[Au$_3$(C$_6$F$_5$)$_3${(Ph$_2$P)$_3$CH}]	220(d)	94
[Au(C$_6$F$_5$){[W](CC$_6$H$_4$Me-4)}]^c	—	102
[(AuC$_3$N$_2$Me)$_3$]^d	272–275(d)	120
[Au(C$_6$F$_5$)Cl]$^-$	—	121
[Au(C$_6$F$_5$){Ph$_2$PC(PPh$_2$)$_2$}Mo(CO)$_4$]$^-$	108	99
[Au(C$_6$H$_2$F$_3$-2,4,6)Br]$^-$	—	122
[Au(C$_6$H$_2$F$_3$-2,4,6)(SCN)]$^-$	—	122
[Au{C$_6$H$_2$(NO$_2$)$_3$-2,4,6}Cl]$^-$	—	110

^{a}phen, 1,10-phenanthroline; dmphen, 2,9-dimethyl-1,10-phenanthroline.
^{b}HL, C$_3$H$_5$NS$_2$(1,3-thiazolidine-2-thione); HL', C$_5$H$_5$NS(pyridine-2-thione).
^{c}[W], [W(CO)$_2$(Me$_2$PCH$_2$CH$_2$PMe$_2$)Cl].
^{d}C$_3$N$_2$, C^2-imidazolyl.

A selection of arylgold(I) complexes that have recently been prepared is presented in Table 4. Complexes of the type [ArAuL] readily undergo oxidative addition of halogen, acyl halides or similar reagents to give gold(III) complexes of the type [ArAu(X)$_2$L][106−108]. Mesityl(triphenylphosphine)gold(I) (mesityl = C$_6$H$_2$Me$_3$-2,4,6) reacts with [Ag(OSO$_2$CF$_3$)L] (L = PPh$_3$, SC$_4$H$_8$), giving rise to polynuclear derivatives in which the mesityl group acts as a bridge between a gold and a silver centre[98].

Anionic complexes [ArAuX]$^-$, in which X is a halide or pseudohalide donor ligand, have so far only been isolated if the aryl group is strongly electron-withdrawing, as in nitrophenyl or pentafluorophenyl derivatives[11,12,121]. Two methods of preparation have been reported: One relies on the displacement of weakly coordinating ligands, such as tetrahydrothiophene, SC$_4$H$_8$[122] or triphenylarsine[97] by halide or pseudohalide ions, while the other involves the arylation of dihalogenoaurate ions with dialkylmercury compounds[110]. Examples of both types of reactions are presented in equations 24 and 25, respectively.

$$[Au(C_6H_2F_3\text{-}2,4,6)(SC_4H_8)] + [N(PPh_3)_2]SCN \longrightarrow$$
$$[N(PPh_3)_2][Au(C_6H_2F_3\text{-}2,4,6)(SCN)] + SC_4H_8 \qquad (24)$$
$$[PPh_3(CH_2Ph)][AuCl_2] + [Hg\{C_6H_2(NO_2)_3\text{-}2,4,6\}_2] \longrightarrow$$
$$[PPh_3(CH_2Ph)][Au\{C_6H_2(NO_2)_3\text{-}2,4,6\}Cl] + [Hg\{C_6H_2(NO_2)_3\text{-}2,4,6\}Cl] \qquad (25)$$
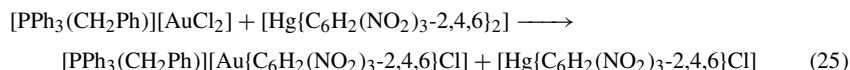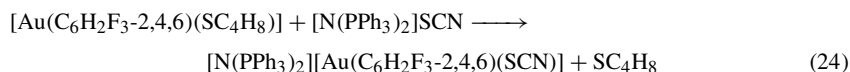
(Phosphine)gold(I) complexes containing a cyclopentadienyl or related ligand have been the subject of a number of studies, the major question being the degree of fluxionality in such molecules. Several cyclopentadienyl complexes have been prepared (Table 5) either by the organolithium method[123] or by direct auration of the parent cyclopentadiene with tris(triphenylphosphinegold(I))oxonium tetrafluoroborate[124,125] (equations 26 and 27). A unique reaction is that of pentakis(methoxycarbonyl)cyclopentadiene (**1**)[126], which is a strong acid and will displace weaker organic acids upon interaction with their metal salts (equation 28)[127].

$$[AuCl(PPr\text{-}i_3)] + LiC_5H_5 \longrightarrow [Au(C_5H_5)(PPr\text{-}i_3)] + LiCl \qquad (26)$$
$$[(Ph_3PAu)_3O][BF_4] + 3C_5Ph_4H_2 \longrightarrow 3[Au(C_5Ph_4H)(PPh_3)] + [H_3O][BF_4] \qquad (27)$$
$$[Au(CO_2Me)(PPh_3)] + C_5(CO_2Me)_5H \longrightarrow [Au\{C_5(CO_2Me)_5\}(PPh_3)] +$$
$$MeCO_2H \qquad (28)$$

(**1**)
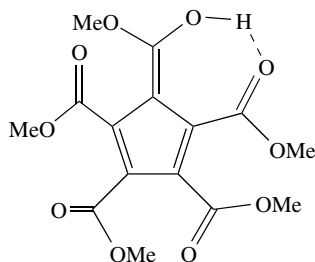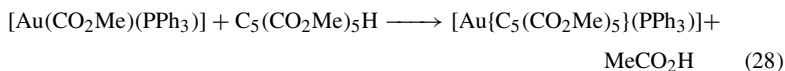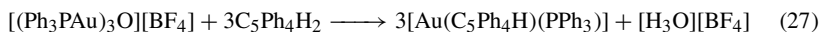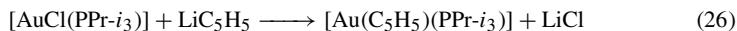
Cyclopentadienyl- and pentamethylcyclopentadienylgold(I) complexes react with terminal acetylenes such as HC≡CH, HC≡CPh and HC≡CCO$_2$Me to give the corresponding alkynylgold(I) compounds[123]. A most unusual reactivity towards aurating agents such as (triphenylphosphine)gold(I) tetrafluoroborate is observed with the tetraphenylcyclopentadienylgold(I) phosphine complex, which can add one or even two (triphenylphosphine)gold(I) units to form dinuclear compounds containing 3-centre−2-electron bonds[124−130].

Gold(I) complexes of Cp-related ligands have also been prepared. 9-Fluorenyl (triphenylphosphine)gold(I) (**2**)[131] can be obtained via the oxonium salt route, but the reduced C−H acidity of fluorene requires the use of an additional base, such as sodium hydride, to deprotonate the hydrocarbon.
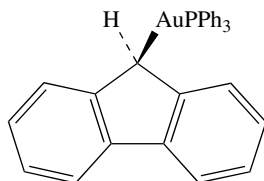
(**2**)

Ferrocenylgold compounds have been prepared by the organolithium method and auration of one or both of the cyclopentadienyl rings could be achieved[24]. Similar to tetraphenylcyclopentadienylgold(I) phosphine complexes, these compounds can incorporate additional (phosphine)gold(I) units upon interaction with (triphenylphosphine)gold(I) tetrafluoroborate to give electron-deficient species as described below.

Reaction of C-imidazolyllithium derivatives with (triphenylphosphine)gold(I) chloride results in the formation of C-aurated imidazolylgold(I) compounds[106,120,132]. In these, the imidazole ring can act as a donor ligand towards other imidazolylgold(I) units and displacement of phosphine leads to the formation of cyclic trimers like **3**. These kinds of species undergo oxidative addition reactions to give trinuclear gold(III) derivatives or gold(I) carbene complexes.
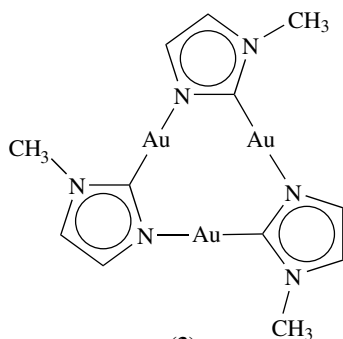
(**3**)

Several metallocene complexes of cobalt and rhodium have been studied in which one cyclopentadienyl ring is replaced by a diborole moiety[133]. Under suitable conditions, auration of the C-2 carbon atom occurs (equation 29). Cyclopentadienyl and related gold(I) complexes are given in Table 5.

(29)
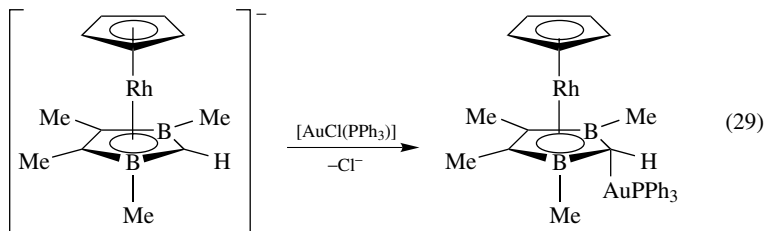
Iminoalkyl complexes of gold(I) can be prepared by the simultaneous treatment of a (phosphine)gold halide [AuX(PR$_3$)] with isocyanides and alcohols in the presence of alkali (equation 30)[134]. In some cases, an intermolecular reaction similar to that observed for imidazolylgold(I) compounds results in the displacement of the phosphine ligands by the iminoalkyl moiety to form cyclic oligomers[135].

$$[AuCl(PBu\text{-}t_3)] + CNCH_2Ts + MeOH + KOH \longrightarrow$$

$$[Au\{C(OMe)\equiv NCH_2Ts\}(PBu\text{-}t_3)] + KCl + H_2O \quad (30)$$
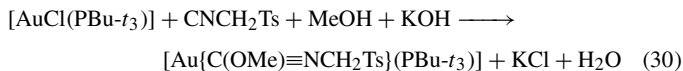
A related compound is obtained upon auration of an unusual tungsten carbene thioketene adduct, as shown in equation 31[136].

TABLE 5. Cyclopentadienyl and related gold(I) complexes

Complex	M.p.(°C)	Reference
[Au(C$_5$H$_5$)(PMe$_3$)]	87(d)	123
[Au(C$_5$H$_5$)(PPr-i_3)]	105(d)	123
[Au(C$_5$Me$_5$)(PPr-i_3)]	92(d)	123
[Au(C$_5$Me$_5$)(PPh$_3$)]	83(d)	123
[Au(C$_5$HPh$_4$)(PPh$_3$)]	159–160(d)	125
[Au{C$_5$(CH$_2$Ph)$_5$}(PPh$_3$)]	—	128
[Au{C$_5$Me(CO$_2$Me)$_4$}(PPh$_3$)]	157–159	129
[Au{C$_5$(CO$_2$Me)$_5$}(PPh$_3$)]	145	127
[Au(C$_{13}$H$_9$)(PPh$_3$)]^a	135–137(d)	131
[Au$_2$(C$_5$H$_4$FeC$_5$H$_4$)(PPh$_3$)$_2$]	105–106(d)	24
[Au{$\overline{C}$(NMe)CHCH$\overline{N}$}]$_3$	—	120
[Au{(C$_3$B$_2$HMe$_4$)Co(C$_5$H$_5$)}(PPh$_3$)]^b	190(d)	133

^{a}C$_{13}$H$_9$, 9-fluorenyl.
^{b}C$_3$B$_2$HMe$_4$, 2,3,4,5-tetramethyl-2,3-dihydro-1H-1,3-diborol-2-yl.

$$\left[\begin{array}{c} (OC)_5W-C \begin{array}{c} Ph \\ OEt \\ \end{array} \\ C=C=S \\ Ph \end{array} \right] Li + [AuCl(PPh_3)]$$

$$\downarrow -LiCl$$

$$(OC)_5W \leftarrow S=C \begin{array}{c} AuPPh_3 \\ Ph \\ C=C \\ Ph \qquad OEt \end{array}$$

(31)
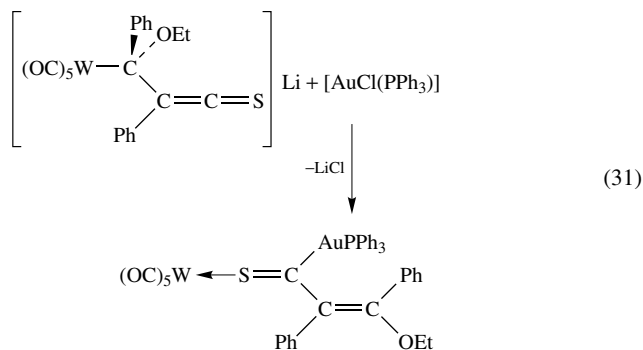
B. Gold(I) Complexes Containing the Structural Building Block C(AuL)$_n$, $n \geqslant 2$

The first compounds to be characterized in which a single carbon atom acts as a bridging ligand between two gold(I) units are the tolyl and ferrocenyl derivatives $[4\text{-MeC}_6\text{H}_4(\text{AuPPh}_3)_2][\text{BF}_4]$ and $[\{(C_5H_5)Fe(C_5H_4)\}(\text{AuPPh}_3)_2][\text{BF}_4]$, respectively, prepared as shown in equation 32[137].

$$2[4\text{-MeC}_6\text{H}_4(\text{AuPPh}_3)] + \text{H}[\text{BF}_4] \longrightarrow [4\text{-MeC}_6\text{H}_4(\text{AuPPh}_3)_2][\text{BF}_4] + C_6H_5Me \quad (32)$$
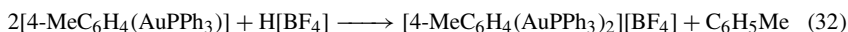
Protonation of the aryl moiety in the starting material liberates the electrophilic species $[\text{Au(PPh}_3)]^+$, which subsequently attacks a second molecule of the arylgold(I) complex.

Similar complexes have subsequently been prepared. One example is the tolyl complex $[4\text{-MeC}_6\text{H}_4\{\text{Au}_2(\text{Ph}_2\text{PCH}_2\text{CH}_2)_2\}][\text{BF}_4]$, in which the two independent PPh$_3$ groups have been replaced by the bidentate chelating ligand 1,4-bis(diphenylphosphino)butane[138]. The reaction leading to such species is obviously not affected by the accumulation of positive charges within the same molecule, as indicated by the facile preparation of stable $[\{C_5H_4(\text{AuPPh}_3)_2\}Fe\{C_5H_4(\text{AuPPh}_3)_2\}][\text{BF}_4]_2$ (equation 33)[24]. The syntheses of unusual trinuclear complexes $[\text{Ph}_4\text{C}_5(\text{AuPPh}_3)_3][\text{BF}_4]$[124,130] and $[(\text{CN})_2\text{C}(\text{AuPPh}_3)_3][\text{BF}_4]$[25] along a similar route provide other cases in point.

(33)
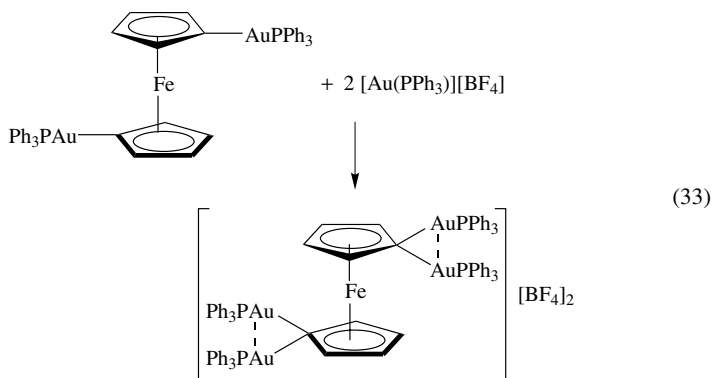
There has also been a report of dinuclear gold(I) alkynyl complexes, $[RC{\equiv}C(AuPPh_3)_2][BF_4]$ (R = Ph, *i*-Pr), which are prepared in the same way[139−141].

A related group of compounds has aryl groups bridging gold atoms or gold and a second metal, thus giving cyclic oligomers like $[Au(C_6H_2F_3-2,4,6)]_4$ (prepared by the interaction of the diarylaurate with $H[PF_6]$) or $[Au(C_6H_2Me_3-2,4,6)]_5$ (equation 34 and Figure 5)[142−144]. $[Au(C_6H_2Me_3-2,4,6)]_5$ will react with mono- and bidentate phosphine ligands to give the respective mesitylgold(I) phosphine complexes[145].

$$5\ [AuCl(CO)] + 5\ [MgBr(C_6H_2Me_3-2,4,6)] \longrightarrow [Au(C_6H_2Me_3-2,4,6)]_5 +$$

$$5\ CO + 5\ MgBrCl \quad (34)$$
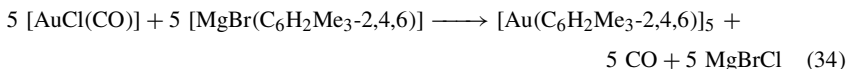
Complexes in which an *aliphatic* carbon atom acts as a bridging ligand between two gold(I) units are well represented[146]. Several of these can be considered to be derived from the simplest hydrocarbon, methane, by formal substitution of two hydrogen atoms with isolobal (phosphine)gold(I) units. A few examples of these diaurio(I)methanes and related complexes are shown in Figure 6, and Table 6 offers a more comprehensive
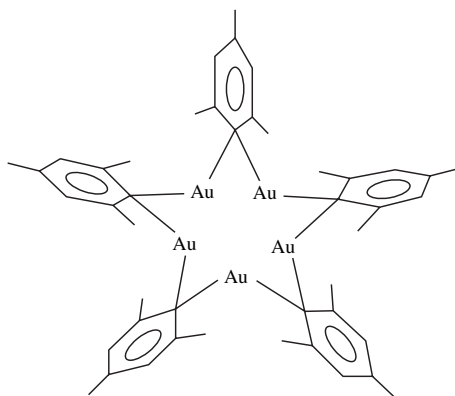
FIGURE 5. Structure of $[Au(C_6H_2Me_3-2,4,6)]_5$
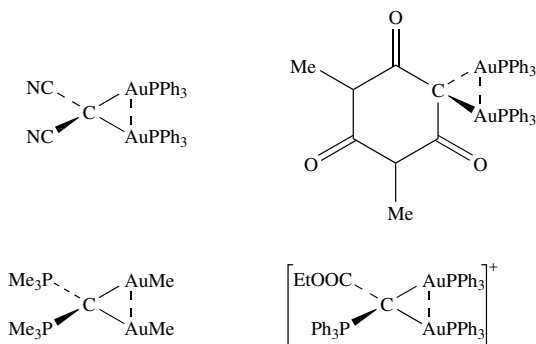
FIGURE 6. Structures of some diaurio(I)methanes and related complexes

TABLE 6.   Compounds containing the structural building block $C(AuL)_2$

Complex	Reference
$[(Ph_3PAu)_2\{-C(CN)_2\}]$	25
$[(Ph_3PAu)_2(-\overline{C.CO.NMe.CO.NMe.\dot{C}O})]$	147
$[(Ph_3PAu)_2(-\overline{C.CMe.N.NPh.\dot{C}O})]$	49, 153a
$[(Ph_3PAu)_2(-CHPPh_3)]^+$	153c
$[(MeAu)_2\{-C(PMe_3)_2\}]$	149
$[(Ph_3PAu)_2\{-C(PMePh_2)_2\}]^{2+}$	154
$[(Ph_3PAu)_2\{-C(PPh_3)(CONMe_2)\}]$	151
$[(Ph_3PAu)_2\{-\overline{C.B(NPr\text{-}i_2).C(SiMe_3)_2.\dot{B}}(NPr\text{-}i_2)\}]$	155
$[(Ph_3PAu)_2\{-\overline{C.PPh_2(Fe(CNPh)_3Cl)\dot{P}Ph_2})\}]^+$	156
$[(Ph_3PAu)_2(-C\{PPh_2AuPh_2P\}_2C-)(AuPPh_3)_2]^{2+}$	53, 55
$[\{(PhMe_2PAu)_2(-CPPh_3)_2\}C=O]$	157
$[(Ph_3PAu)_2\{-C(COOEt)PPh_2CH(COOEt)(AuPPh_3)\}]^+$	158

listing. $[(NC)_2C(AuPPh_3)_2]$ can be prepared by auration of C−H acidic maleodinitrile with tris(triphenylphosphinegold(I))oxonium tetrafluoroborate, $[(Ph_3PAu)_3O][BF_4]^{25}$. In a similar way, the methylene group of N-alkylated barbituric acid can be doubly aurated by reaction with sodium methoxide/methanol in the presence of $[AuCl(PPh_3)]^{147,148}$. A hexanuclear gold(I) complex featuring two $C(AuPPh_3)_2$ units can be obtained through two alternative synthetic methods, one of them involving an intramolecular deprotonation of the starting material when treated with $[Au(PPh_3)_2]ClO_4$, as shown in equation 35[53]. The bis(ylide) derivative $[(Me_3P)_2C(AuMe)_2]$ has been prepared by reaction of hexamethylcarbodiphosphorane with methyl(trimethylphosphine)gold(I)[149].

(35)

A number of other diaurated ylide derivatives have been obtained from the interaction of functionalized phosphonium salts such as $[Ph_3PCH_2(C_5H_4N\text{-}2)]ClO_4$ with two equivalents of (triphenylphosphine)gold(I) acetylacetonate, which induce double deprotonation and subsequent auration of the methylene group (Scheme 2)[150−152].

SCHEME 2. Synthesis and adduct formation of diaurated ylide derivatives

Triple auration is achieved in the reaction of the silylated ylide $Me_3P=CHSiMe_3$ with $[AuCl(PPh_3)]$ in the presence of caesium fluoride, as shown in equation 36[154]. For other compounds with triply aurated elements, see elsewhere[159−161].

(36)
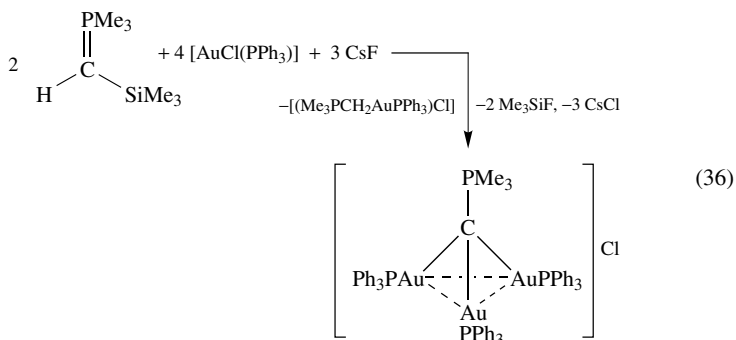
Bis(trimethylsilyl)methyl (triphenylphosphine)gold(I) reacts with the oxonium salt $[(Ph_3PAu)_3O][BF_4]$ to give a mixture of two products (equation 37)[162]. One has been identified as a disilyl diauriomethane, while the major product is found to be the stable trinuclear complex $[(Ph_3PAu)_3\{\mu\text{-}C(SiMe_3)_2\}][BF_4]$. Clearly, this compound forms from the diauriomethane precursor by incorporation of yet another $[Au(PPh_3)]^+$ unit, even though the result is a positively charged species with a hypercoordinate carbon atom.

$$[(Me_3Si)_2CH(AuPPh_3)] + [(Ph_3PAu)_3O][BF_4] \longrightarrow [(Me_3Si)_2C(AuPPh_3)_2] +$$

$$[(\mu\text{-}Me_3Si)_2C(AuPPh_3)_3][BF_4] \quad (37)$$
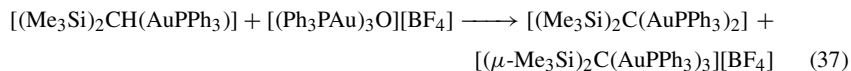
A different triauriomethane derivative is an important intermediate in an unusual transformation which provides access to gold–carbon compounds of even higher nuclearity, containing the structural fragment $[RC(AuL)_4]^+$. The overall reaction is depicted in Scheme 3[163].
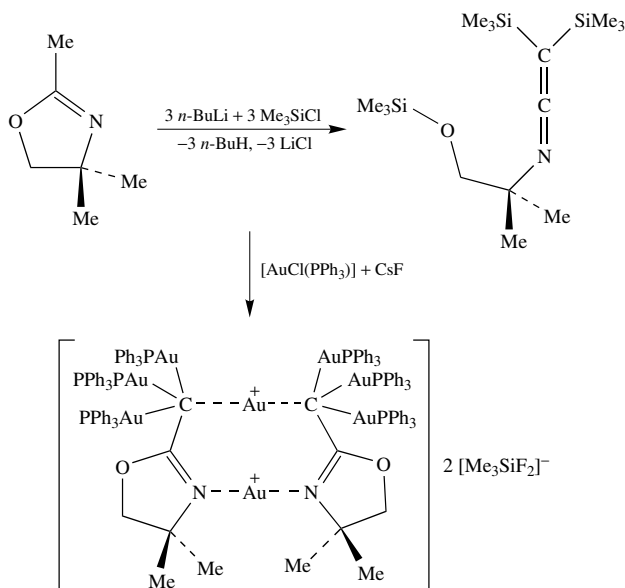
SCHEME 3. Synthesis of a polynuclear organogold(I) cluster featuring tetraaurated, pentacoordinate carbon atoms

The synthesis starts from 2,4,4-trimethyl-4,5-dihydrooxazole, a compound with marked C−H acidity in the exocyclic methyl group. Triple lithiation followed by derivatization with chlorotrimethylsilane affords a triply silylated, open-chain ketenimine which is reacted with [AuCl(PPh$_3$)] in the presence of caesium fluoride to give a dimeric, octanuclear gold(I) cluster. The reaction proceeds beyond the stage of a triauriomethyl oxazolinyl derivative which, in fact, can only be observed as a side product.

The simplest tetra-aurated carbon-centred complex is the cation in [HC(AuPPh$_3$)$_4$][BF$_4$], which is formed in the reaction of (trimethylsilyl)diazomethane with tris(triphenylphosphinegold(I))oxonium tetrafluoroborate together with two by-products (equation 38)[153c]. Formally, it represents the product of the protonation of the neutral tetra-auriomethane molecule. This indicates that the species [C(AuPPh$_3$)$_4$] is a strong Lewis base[153d].

$$[(Ph_3PAu)_3O][BF_4] + Me_3SiCHN_2 \xrightarrow{-N_2} [HC(AuPPh_3)_4][BF_4] + \cdots \qquad (38)$$
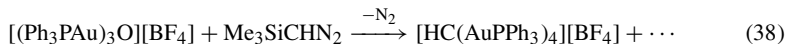
Hypercoordinate, tetra-aurated carbon centres in which all gold(I) atoms carry a phosphine ligand have also been realized in the ethane-derived complexes of the type [H$_3$C−C(AuPR$_3$)$_4$][BF$_4$][164]. The common starting material for this series of compounds is 1,1,1-tris(dimethoxyboryl)ethane, which is reacted with (phosphine)gold(I) halides in the presence of caesium fluoride to give the pentacoordinate organogold(I) clusters as air-stable substances (equation 39). Complexes containing four monodentate phosphine ligands PR$_3$ (R = Ph, c-C$_6$H$_{11}$) or two intramolecularly bridging bidentate diphosphine

ligands 1,2-(Ph$_2$PCH$_2$CH$_2$)$_2$C$_6$H$_4$ have been prepared.

$$H_3C\text{-}C[B(OMe)_2]_3 + 4\,[AuCl\{P(c\text{-}C_6H_{11})_3\}] + 4\,CsF$$

$$\left[\begin{array}{c} CH_3 \\ | \\ (c\text{-}C_6H_{11})_3PAu\diagup \overset{}{C} \diagdown AuP(C_6H_{11}\text{-}c)_3 \\ (c\text{-}C_6H_{11})_3PAu \qquad AuP(C_6H_{11}\text{-}c)_3 \end{array} \right] [BF_4] + 4\,CsCl + 2\,B(OMe)_3 \qquad (39)$$
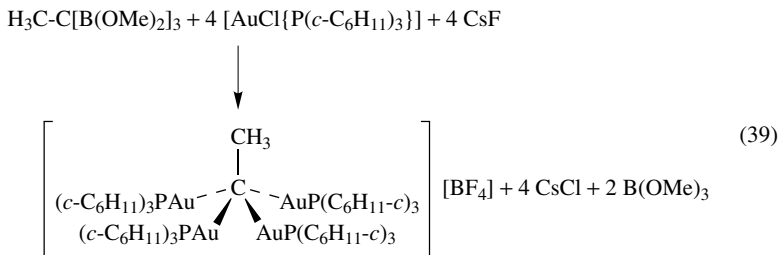
In the many attempts to synthesize *homoleptic* polyauriomethanes C(AuPR$_3$)$_4$, the preparation has only been successful if phosphine ligands of sufficient steric bulk were employed. Tetrakis[(tricyclohexylphosphine)gold(I)]methane is obtained from a mixture of C[B(OMe)$_2$]$_4$, [AuCl\{P(c-C$_6$H$_{11}$)$_3$\}] and CsF as a colourless crystalline solid with the expected tetrahedral array of gold atoms around the central carbon atom[165].

In the presence of sterically less demanding phosphine ligands L [such as PPh$_3$ or P(C$_6$H$_4$Me-4)$_3$] the reactions (equation 40)[166] proceed beyond the stage of tetra-auration at carbon and homoleptic penta-aurated cations [C(AuPR$_3$)$_5$]$^+$ are produced in high yield.

$$H_2C\{B(OMe)_2\}_2 + [AuCl(PPh_3)]/CsF + [P(O)(NMe_2)_3] \longrightarrow [C(AuPPh_3)_5][BF_4]$$
$$(40)$$
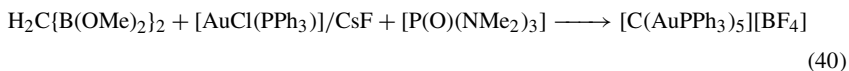
Dications [C(AuPR$_3$)$_6$]$^{2+}$ with a large variety of phosphine ligands have been characterized (R = Et, *i*-Pr, Ph, C$_6$H$_4$X-4 with X = Cl, Br, NMe$_2$, OMe, Me) and the isolation of species containing tailor-made chelating phosphine ligands is equally straightforward[167−170]. The salts are stable, colourless, crystalline substances. They are accessible in high yields and have been found to be diamagnetic in all cases. A typical reaction is given in equation 41. For further information on this general class of compounds the reader is referred elsewhere[171−181].

$$C\{B(OMe)_2\}_4 + 6\,[AuCl(PPh_3)] + 6\,CsF \longrightarrow [C(AuPPh_3)_6][MeOBF_3]_2 +$$
$$6\,CsCl + 2\,B(OMe)_3 \quad (41)$$
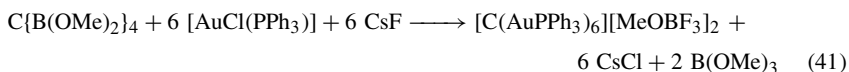
C. Gold(I) Complexes with Two Gold−Carbon Bonds

Simple dialkylaurates(I) are best prepared by the interaction of an alkylgold(I) phosphine adduct with an organolithium reagent[13a]. This method has also been used for the preparation of complexes containing functionalized alkyl groups, as shown in equation 42[31], although these can alternatively be obtained by treatment of (tetrahydrothiophene)gold(I) chloride with two equivalents of alkyllithium, as in the case of thiazolyl[27] or isothiazolyl[28] complexes (equation 43). Treatment of the product of reaction 42 with potassium carbonate affords the analogous potassium bis(diethylcarbamoylcyclopropyl)aurate, which possesses a dimeric structure in the

solid state[31].

(42)

(43)
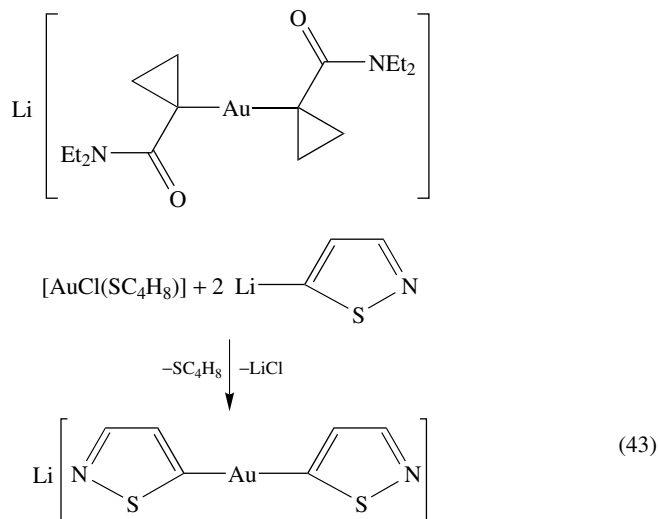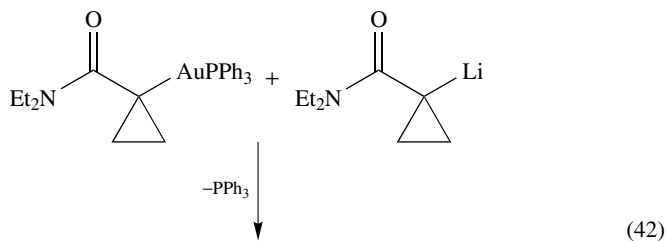
The stabilization of dialkylaurate(I) by means of functionalized alkyl groups appears to be a general phenomenon. An example is provided by the complex [Ph$_3$P=N=PPh$_3$][Au(acac)$_2$] which is a versatile precursor for other dialkylaurate derivatives and related compounds[76,182]. Some relevant reactions are summarized in Scheme 4. Similar products have also been obtained from complex gold(I) halides by reaction with carbanionic ligands such as bis(diphenylphosphino)methanide[115].

Related dialkynylaurates(I) are accessible from dialkylaurates by treatment with terminal acetylenes (Scheme 4). Alternatively, the bis(phenylacetylide) complex [PPN][Au(C≡CPh)$_2$] may be prepared by metathesis of the organocuprate [PPN][Cu(C≡CPh)$_2$] with various gold(I) complexes such as [Au(C≡CPh)(PPh$_3$)], [AuCl(PPh$_3$)], [AuCl(C≡CPh)]$^-$ or [Au(C≡CPh)]$_n$[183]. A less straightforward synthesis of dialkynylaurates(I) starts from gold(I) iodide and potassium acetylide, requiring liquid ammonia as the reaction medium[184]. Metal−metal contacts are the dominating feature in the solid state structures of a series of related (in most cases heterometallic) organogold compounds, prepared from the alkynylgold(I) complexes [PPN][Au(C≡CPh)$_2$] or [Au(C≡CPh)(PPh$_3$)] by reaction with the coinage metal acetylides [Cu(C≡CR)]$_n$,

[PPN][AuCl$_2$]

+2 Tl(acac) $\Big|$ −2 TlCl

[PPN][Au(acac)$_2$]

i

ii

[PPN][Au(C≡CSiMe$_3$)$_2$]

iii   iv   v

[Au{CH(PPh$_2$)$_2$}]$_n$

[PPN][Au(C≡CH)$_2$]

$$[PPN]\left[\begin{array}{c} R' \\ \diagdown \\ R \end{array} CH-Au-CH \begin{array}{c} R \\ \diagup \\ R' \end{array}\right]$$

R = R′ = CN
R = R′ = CO$_2$Me
R = CN, R′ = CO$_2$Me

$$\left[R_3P-CH-Au-CH-PR_3 \right] ClO_4$$

R = C$_6$H$_4$Me-4
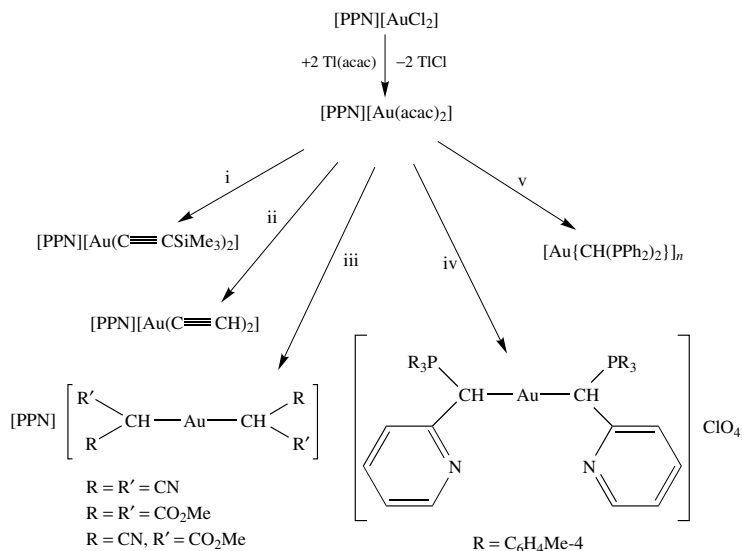
SCHEME 4. Preparation and reactions of homoleptic dialkylaurates with functionalized ligands. Conditions: i, 2HC≡CSiMe$_3$, −2 acacH; ii, 2 HC≡CH, −2 acacH; iii, 2 CH$_2$RR′, −2 acacH; iv, 2 [R$_3$P{CH$_2$(2-C$_5$H$_4$N)}]ClO$_4$, −2 acacH, - [PPN]ClO$_4$; v, CH$_2$(PPh$_2$)$_2$, - acacH, -[PPN]acac

[Ag(C≡CR)]$_n$ or [Au(C≡CR)]$_n$ (R = Ph or C$_6$H$_4$Me-4)[185−191]. The structure of a heterometallic pentanuclear cluster is given in Figure 7.

The reaction of polymeric long-chain gold(I) acetylides with isocyanides results in the formation of alkynylgold(I) isocyanide complexes, as represented in equation 44, some of them displaying liquid-crystalline properties ($m = 6, 8, 10, 12$; X = H, OC$_n$H$_{2n+1}$; $n = 4, 6, 8, 10$).
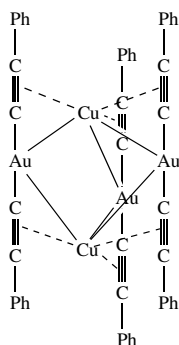
FIGURE 7. Structure of the pentanuclear cluster [Au$_3$Cu$_2$(C≡CPh)$_6$]$^-$

$$\left[AuC\equiv C-\left\langle\bigcirc\right\rangle-C_mH_{2m+1} \right]_n + C\equiv N-\left\langle\bigcirc\right\rangle-X$$

$$X-\left\langle\bigcirc\right\rangle-N\equiv C-Au-C\equiv C-\left\langle\bigcirc\right\rangle-C_mH_{2m+1}$$

(44)
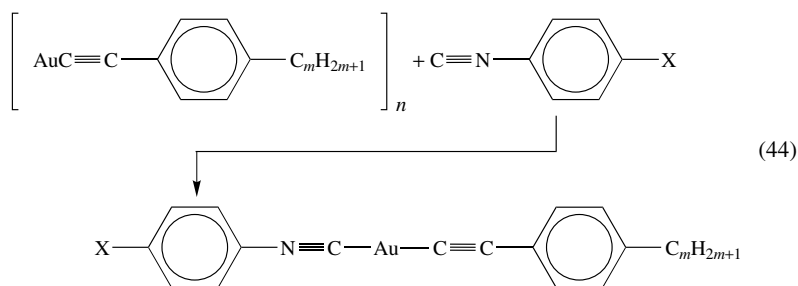
Diarylaurate(I) complexes have been prepared by a variety of methods, depending on the nature of the aromatic ligands[11,12,192,193]. While diarylaurates as such are generally more stable than their unfunctionalized dialkyl analogues, this stability is particularly enhanced with aryl groups bearing a number of strongly electron-withdrawing ligands. Polyhalophenylaurates(I) have been much studied recently and their preparation and properties have been the subject of two reviews[11,12]. The most versatile method for the preparation of such compounds is the arylation of a complex gold(I) halide with two equivalents of aryllithium (equation 45). These compounds show a propensity for metal–metal aggregation when treated with reagents such as $AgClO_4$ (equation 46)[194,195].

$$[AuCl(SC_4H_8)] + 2Li(C_6H_2F_3\text{-}2,4,6) + NBu_4Cl \longrightarrow NBu_4[Au(C_6H_2F_3\text{-}2,4,6)_2] +$$

$$2LiCl + SC_4H_8 \quad (45)$$

$$NBu_4[AuR_2] + AgClO_4 + L \longrightarrow 1/n[AuR_2AgL]_n + NBu_4ClO_4 \quad (46)$$
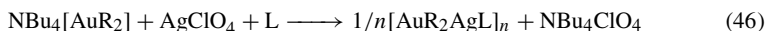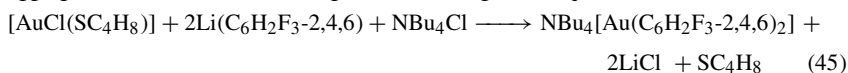
$R = C_6H_5, C_6Cl_5, C_6H_2F_3\text{-}2,4,6;$
$L = N, P, O, S$ donors, olefin, acetylene, arene

There are a number of compounds in which an arylgold(I) moiety is bonded to a bis(diphenylphosphino)methanide group, which in turn acts as a bridging ligand in a polynuclear gold or gold/silver complex[11,12,196]. An example is shown in Scheme 5[197,198].

$$2\,[AuCl(CH_2PPh_3)] + 2\,CH_2(PPh_2)_2 \xrightarrow{-2\,[PPh_3Me]Cl}$$
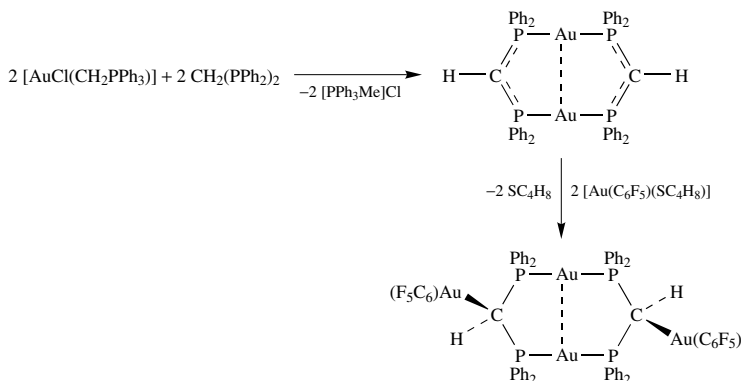
SCHEME 5. Synthesis of a polynuclear gold complex containing bis(diphenylphosphino)methanide ligands
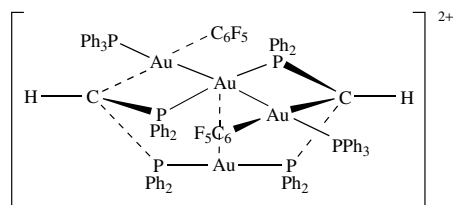
FIGURE 8. Structure of the tetranuclear $[Au_4(C_6F_5)_2\{(Ph_2P)_2CH\}_2(PPh_3)_2]$ $(ClO_4)_2$

The product thus obtained undergoes oxidative addition of halogens, leading to unusual tetranuclear species, which give cationic complexes by substitution of the halogen atoms by a neutral ligand (Figure 8)[199−202].

D. Complexes of Gold(I), Gold(II) and Gold(III) with Ylide Ligands

There now exists a large number of methods for the synthesis of organogold complexes with various ylide ligands. In an extensive reaction chemistry, successive oxidation of the gold centres [Au(I) → Au(II) → Au(III)] can often be accomplished. Ylide complexes of gold have therefore been summarized in the following sections regardless of their oxidation state.

1. Mononuclear ylide complexes

Mononuclear ylide complexes of gold(I) and gold(III) have been obtained in a variety of ways[203,204], as detailed below. The largest number of complexes of both gold(I) and gold(III) has been prepared with phosphorus ylides, but species containing arsenic or sulphoxonium ylides have also been reported. Some prototypes are summarized in Table 7.

The reaction of alkylgold(I) phosphine complexes with ylides leads to alkylgold monoylide species with concomitant liberation of phosphine, as illustrated in equation 47[15].

$$[AuR(PR_3''')] + R_3''P{=}CR_2' \longrightarrow [AuR(CR_2'PR_3'')] + PR_3''' \qquad (47)$$

R = alkyl
R$'$ = H, alkyl, aryl
R$''$, R$'''$ = alkyl, aryl

Haloarylgold(I) ylide complexes have been generated from suitable precursors via an indirect route: The interaction of phosphonium halides with $[Au(C_6F_5)(SC_4H_8)]$ leads to phosphonium organo(halo)aurates which can subsequently be reacted with base to give the respective ylide derivatives (Scheme 6). Gold(III) ylide complexes of the type $[Au(C_6F_5)_3(ylide)]$ have been prepared analogously from $[Au(C_6F_5)_3(SC_4H_8)]$[210].

$$[Au(C_6F_5)(SC_4H_8)] + [H_3CPPh_3]Cl$$

$$\downarrow {\scriptstyle -SC_4H_8}$$

$$[H_3CPPh_3][AuCl(C_6F_5)] \xrightarrow[-H_2,\ -NaCl]{NaH} [Au(C_6F_5)(CH_2PPh_3)]$$
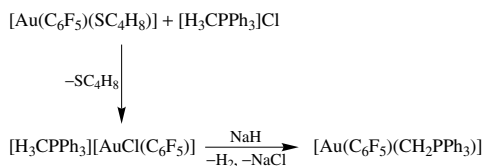
SCHEME 6. Synthesis of haloarylgold(I) ylide complexes

TABLE 7.   Mononuclear ylide complexes of gold(I) and gold(III)

Complex	M.p. ($^{\circ}$C)	Reference
Gold(I)		
$[AuCl(CH_2PPh_2Me)]$	148(d)	205
$[AuCl\{CH(PPh_3)C(=O)CH_3\}]$	154	206
$[AuCl\{CH(PPh_3)CO_2Me\}]$	180	207
$[AuCl(Ph_3P=C=PPh_3)]$	250(d)	208
$[AuBr(CH_2PPh_3)]$	164(d)	205
$[Au(CN)(CH_2PPh_3)]$	185–188	209
$[Au(C_6F_5)(CH_2PPh_3)]$	157	210
$[Au(C_6F_5)(CH_2AsPh_3)]$	144	210
$[Au(C\equiv CPh)(CH_2PPh_3)]$	—	211
$[Au\{Co(CO)_4\}(CH_2PPh_3)]$	—	211
$[Au(CH_2PPh_3)(SC_4H_8)]ClO_4$	—	211
$[Au(CH_2PPh_3)(SbPh_3)]ClO_4$	—	211
$[Au(CH_2PPh_3)(phen)ClO_4]^a$	—	211
$[Au(CH_2AsPh_3)(SC_4H_8)]ClO_4$	—	211
$[Au\{CH(PPh_3)C(=O)CH_3\}(PPh_3)]ClO_4$	125	206
$[Au\{CH(PPh_3)CO_2CH_3\}(PPh_3)]ClO_4$	97	207
$[Au(CH_2PMe_3)_2]BF_4$	214(d)	205
$[Au(CH_2PMe_3)_2][Au^{III}(1,2-Me_2C_2B_9H_9)_2]$	—	212
$[Au\{CH(PPh_3)C(=O)CH_3\}_2]ClO_4$	128	206
$[Au\{CH(PPh_3)CO_2CH_3\}_2]ClO_4$	125	207
$[Au\{CH_2S(=O)Me_2\}_2]Cl$	—	213
$[Ph_3P=N=PPh_3][Au\{CH_2P(S)Ph_2\}_2]$	—	214
Gold(III)		
$[AuCl_3\{CH(PPh_3)C(=O)CH_3\}]$	120	206
$[AuCl_3\{CH(PPh_3)CO_2CH_3\}]$	161	207
$[AuCl_2\{CH(PPh_3)C(=O)CH_3\}_2]ClO_4$	130	206
$[AuCl_2\{CH(PPh_3)CO_2CH_3\}_2]ClO_4$	150	207
$[AuBr\{CH_2P(S)Ph_2\}_2]$	—	215
$[Au(S_2CNEt_2)_2\{CH_2P(S)Ph_2\}]$	156	215
$[AuI_3(CH_2PPh_3)]$	133(d)	216
trans-$[AuI_2(CN)(CH_2PPh_3)]$	165–170	209
$[Au(SCN)_3(CH_2PPh_3)]$	140(d)	216
$[AuMe_3(CH_2PPh_3)]$	—	217
$[AuMe_3\{CH_2S(=O)Me_2\}]$	—	217
$[AuMe_2(\eta^2-CH_2PMe_2BH_2PMe_2CH_2)]$	—	218
$[Au(C_6F_5)_3(CH_2PPh_3)]$	252	210
$[Au(C_6F_5)_3(CH_2PPh_2Me)]$	—	219
$[Au(C_6F_5)_3(CH_2AsPh_3)]$	231	210
cis-$[Au(C_6F_5)_2Cl(CH_2PPh_3)]$	214(d)	220
trans-$[Au(C_6F_5)Cl_2(CH_2PPh_3)]$	135(d)	216

^{a}phen, 1,10-phenanthroline.

$$[AuCl(PR'''_3)] \xrightarrow{R''_3P=CR'_2} [Au(CR'_2PR''_3)(PR'''_3)]Cl \xrightarrow[-PR'''_3]{R''_3P=CR'_2} [Au(CR'_2PR''_3)_2]Cl$$
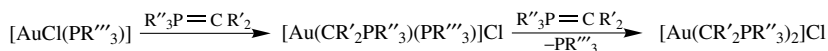
$R' = H$, alkyl, aryl

R'', $R''' = $ alkyl, aryl

SCHEME 7. Synthesis of bis(ylide)gold(I) complexes
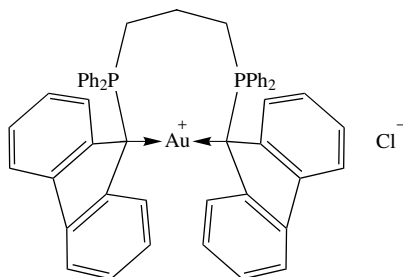
FIGURE 9. A chelated bis(ylide)gold(I) complex

The reaction of (phosphine)gold(I) halides with ylides of the type $R'_2C=PR''_3$ proceeds in two steps: Initial displacement of halide gives an isolable monoylide species, which can be transformed into a bis(ylide)gold(I) complex if an excess of ylide is employed (Scheme 7)[15]. In some instances, however, the reaction produces the bis(ylide) species directly, regardless of the relative ratios of gold(I) halide and ylide employed, as in the case of the bis(cyclopropylide) complex $[Au\{C(c\text{-}CH_2)_2PPh_3\}_2]Cl^{221}$. Obviously, bis(ylide) complexes form particularly easily with a chelating bis(ylide) ligand, an example being the compound 1,3-propanediylbis[(9-fluorenylidene)diphenylphosphorane]gold(I) chloride (Figure 9)[222]. Facile double substitution also occurs with amino-substituted phosphorus ylides and sulphoxonium ylides to give complexes such as $[Au\{CH_2P(NMe_2)_3\}_2]Cl^{222-224}$ and $[Au\{CH_2S(=O)(CH_3)_2\}_2]Cl^{213}$.

Carbonyl-stabilized phosphorus ylides are less nucleophilic and hence do not react with (phosphine)gold(I) halides, but their gold(I) complexes can be generated from precursors such as $[Au(acac)(PPh_3)]$ or $[AuCl(SC_4H_8)]$ by reaction with phosphonium salts and ylides, respectively, and again both mono- and bis(ylide) complexes have been obtained (equation 48 and Scheme 8)[206,207]. The ylide carbon atoms in these complexes are centres of chirality, but no stereospecificity was observed in the coordination process and racemic mixtures are formed throughout.

(48)

R = Me, Ph, OMe, OEt

$$[AuCl(SC_4H_8)] \; + \; Ph_3PCHC(\!=\!O)R$$

$$R = Me, Ph, OMe, OEt$$
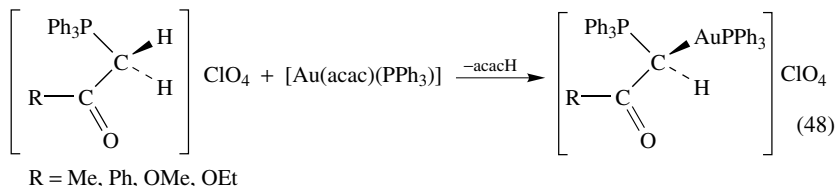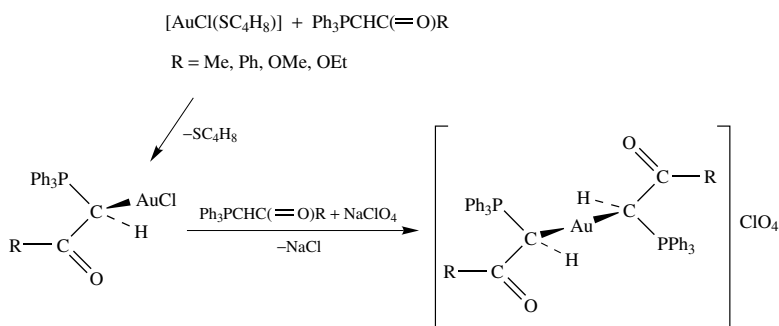
SCHEME 8. Synthesis of gold(I) complexes containing carbonyl-stabilized phosphorus ylides

An alternative strategy for the preparation of mononuclear ylide complexes is to start from gold(I) precursors which already contain an ylide ligand. Displacement in such complexes of tetrahydrothiophene, SC_4H_8, by neutral or anionic ligands (including polyfunctional phosphines, acetylides, carbonyl metalates and methanide complexes) leads to a variety of mono-, di- and tetranuclear compounds of remarkable stability (Scheme 9)[55,114,211].
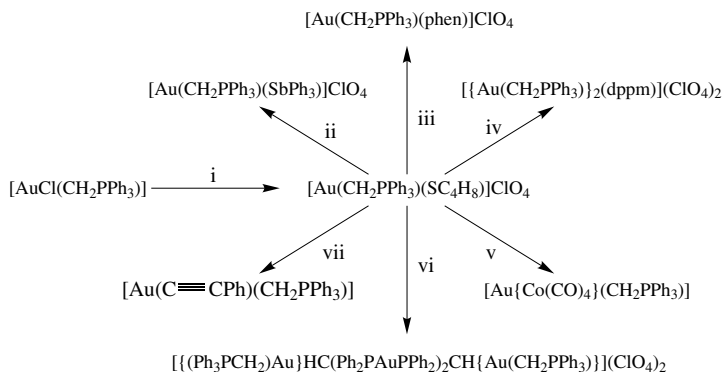
SCHEME 9. Preparation of phosphorus ylide gold(I) complexes by displacement of tetrahydrothiophene (SC_4H_8). Conditions; i, $[Ag(ClO_4)(SC_4H_8)]$; ii, $SbPh_3$; iii, phen (1,10-phenantroline); iv, dppm (bis(diphenylphosphino)methane); v, $[N(PPh_3)_2][Co(CO)_4]$; vi, $[HC(Ph_2PAuPPh_2)_2CH]$; vii, $PhC\!\equiv\!CH$, KOH

Interaction of gold(I) ylide dimers such as $[Au(CH_2)_2PPh_2]_2$[225,226] or gold(I) ylide monomers such as $[Au(C_6F_5)(CH_2PPh_3)]$[205] with HCl, HBr or acetyl bromide gives gold(I) mono(ylide) complexes in which a halide is the second ligand. Acids with weakly coordinating anions X^- ($BF_4{}^-$, $ClO_4{}^-$) convert the haloarylgold(I) ylide complexes into bis(ylide) species of the type $[Au(ylide)_2]X$[205].

Conversely, certain mono(ylide) complexes are accessible from the respective bis(ylide) compounds. Reaction between complexes of the type $[Au(ylide)_2]ClO_4$ and aurates(I) such as $NR_4[AuX_2]$ ($X = Cl, Br, C_6F_5, C_6Cl_5$) affords neutral halogold(I) and (haloaryl)gold(I)

ylide species, respectively (equation 49). Related gold(III) complexes have been prepared in a similar manner[220].

$$[Au(CH_2PPh_3)_2]ClO_4 + NBu_4[Au(C_6F_5)_2] \longrightarrow 2[Au(C_6F_5)(CH_2PPh_3)] +$$

$$NBu_4ClO_4 \quad (49)$$
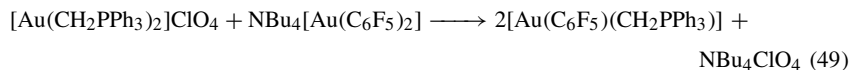
A few mono(ylide) complexes of gold(I) have been obtained from the interaction of phosphorus ylides with [Au(CO)Cl] and AuCN. The complex [AuCl(Ph$_3$P=C=PPh$_3$)] forms readily when carbonylgold(I) chloride is reacted with hexaphenylcarbodiphosphorane. It is stable to oxygen and water and also thermally stable up to 250° C[208]. Similarly, the reaction of gold(I) cyanide with triphenylphosphonium methylide yields the complex [Au(CN)(CH$_2$PPh$_3$)]. The complex undergoes oxidative addition reactions with halogens X_2 to give the gold(III) complexes trans-[AuX$_2$(CN)(CH$_2$PPh$_3$)] (X = Cl, Br, I)[209].

A number of mononuclear gold(III) ylide complexes may be similarly prepared by oxidative addition of halogens to suitable gold(I) ylide precursors. This approach is exemplified by complexes of the general types [AuX$_3$(ylide)][216], trans-[Au(C$_6$F$_5$)X$_2$(ylide)][216] and trans-[AuX$_2$(ylide)$_2$]ClO$_4$ (X = Cl, Br)[206,207], some of which may be further converted into the related iodo or thiocyanato complexes by reaction with potassium iodide or potassium thiocyanate[216]. Additionally, a few methods for the direct synthesis of gold(III) ylide complexes have been described. Thus, interaction of trimethylgold(III) phosphine complexes with phosphonium or sulphoxonium ylides results in the displacement of phosphine to yield complexes such as [AuMe$_3$(CH$_2$PPh$_3$)] and [AuMe$_3${CH$_2$S(=O)Me$_2$}], respectively, which are again of remarkable stability[217]. A gold(III) complex containing a chelating bis(ylide) ligand is represented by the species [AuMe$_2$(η^2-CH$_2$PMe$_2$BH$_2$PMe$_2$CH$_2$)], obtained from the reaction of dimethylgold(III) chloride with lithium boranato-bis(dimethylphosphonium methylide), as shown in equation 50[218].
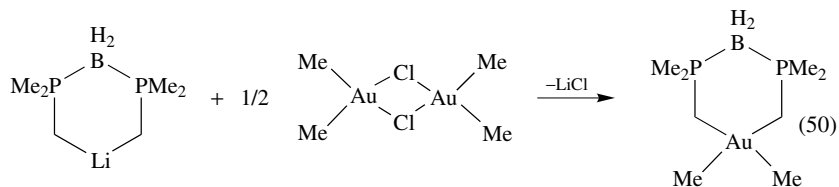
The reaction chemistry of both mono- and bis(ylide) complexes of gold(I) has been explored for several cases. In carbonyl-stabilized ylide ligands, the acidic proton of the α-methylene group can be replaced by yet another gold(I) unit leading to polynuclear species (equations 51 and 52)[206,207].
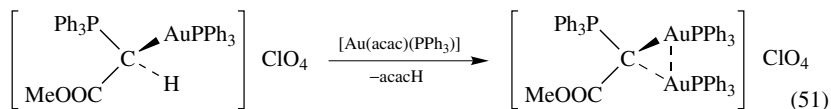
The haloarylgold(I) ylide complexes were also investigated regarding their reactivity towards chlorobis(pentafluorophenyl)thallium(III). Partial oxidation of gold(I) to give chloro-substituted haloarylgold(III) ylide complexes was observed, together with formation

of bis(ylide) complexes of monovalent gold (equation 53)[227].

$$\text{(52)}$$

$$[Tl(C_6F_5)_2Cl] + [Au(C_6F_5)(CH_2PPh_3)] \longrightarrow trans\text{-}[Au(C_6F_5)_2Cl(CH_2PPh_3)] +$$

$$[Au(CH_2PPh_3)_2][Au(C_6F_5)_4] + Tl(C_6F_5)_3 + TlCl \quad (53)$$
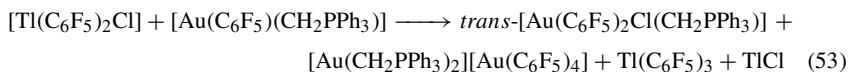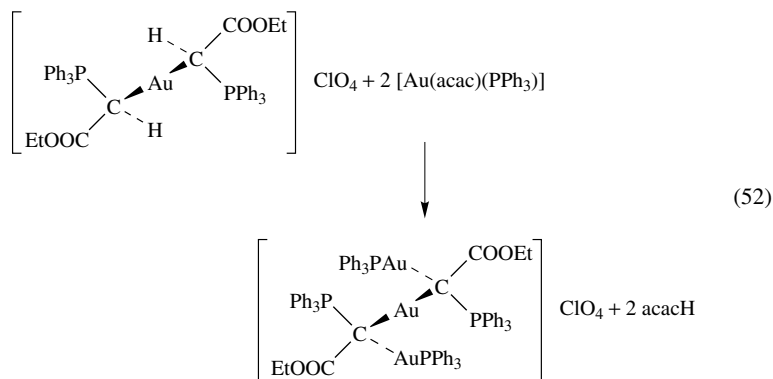
Bimetallic gold–silver complexes may be prepared from gold(I) bis(ylide) species such as $[Au(CH_2PPh_3)_2]ClO_4$ and $AgClO_4$ (leading to neutral clusters, equation 54) or $[Ag(ClO_4)(PPh_3)]$ (leading to dicationic species)[228].

$$2[Au(CH_2PPh_3)_2]ClO_4 + 2AgClO_4 \longrightarrow$$

$$[(Ph_3PCH_2)_2Au\{\mu\text{-}Ag(OClO_3)_2\}_2Au(CH_2PPh_3)_2] \quad (54)$$
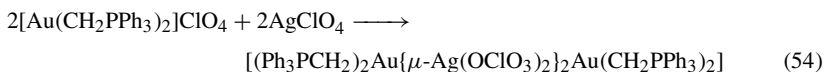
2. Di- and polynuclear ylide complexes

In addition to the mononuclear gold(I) ylide complexes described above, a large number of dinuclear compounds have been prepared in which the ylide moiety functions as a bridging ligand. Complexes with two bridging ylide groups and two gold atoms in a metallacyclic array are by far the most numerous, but variants containing one ylide and one diphosphine or thiolate bridge as well as open-chain compounds with one bridging ylide ligand between two gold centres have also been reported. A selection of complexes of this type is shown in Table 8.

Five general methods for the preparation of such complexes have been established, their applicability depending on the nature of the ylide ligand: Complexes such as $[Au_2\{(CH_2)_2PR_2\}_2]$ or $[Au_2\{CH_2P(S)Ph_2\}_2]$ are accessible by transylidation of the corresponding mononuclear bis(ylide) compounds (equation 55)[203,204,230,231], while species of the type $[Au_2\{(CHPPh_3)_2CO\}_2]^{2+}$ and $[Au_2\{(CH_2PMe_2)_2BH_2\}_2]$ have been prepared from complex gold chlorides by reaction with the lithium salt of the appropriate ligand[157,158,218]. The third method employs symmetric diphosphine precursors, from which the asymmetric complexes $[Au_2\{(CH_2)_2PR_2\}\{PPh_2CHPPh_2\}]$ and $[Au_2\{(CH_2)_2S(O)NMe_2\}\{PPh_2CH_2PPh_2\}]^+$ can be made by reaction with one equivalent of ylide ligand[146,232]. Most of the asymmetric complexes as well as open-chain di- and trinuclear derivatives have been obtained treating the bis(ylide) complex $[Au_2\{(CH_2)_2PPh_2\}_2]$ with a gold(I) precursor containing the second ligand through ylide transfer reactions (equation 56)[233−237]. Some other asymmetric derivatives with one or two bridging ligands can be synthesized from open-chain $[Au_2X_2(ylide)]^-$

TABLE 8. Dinuclear Au(I) complexes with bridging ylide ligands

Complex	Reference
$[Au_2\{(CH_2)_2PEt_2\}_2]$	203, 204
$[Au_2\{(CH_2)_2P(CH_2)_4\}_2]$	203, 204
$[Au_2\{(CH_2)_2PPh_2\}_2]$	203, 204
$[Au_2\{(CH_2)_2PMePh\}_2]$	229
$[Au_2\{(CH_2)_2PMePh\}_2(SO_2)_2]$	229
$[Au_2\{CH_2P(S)Ph_2\}_2]$	230
$[Au_2\{CH(PPh_2Me)P(S)Ph_2\}_2]^{2+}$	231
$[Au_2\{(CHPPh_3)_2CO\}_2]^{2+}$	157
$[Au_2\{(CH(CO_2R))_2PPh_2\}_2]$	158
$[Au_2\{(CH_2PMe_2)_2BH_2\}_2]$	218
$[Au_2\{(CH_2)_2PBu\text{-}t_2\}\{PPh_2CHPPh_2\}]$	232
$[Au_2\{(CH_2)_2S(O)NMe_2\}\{PPh_2CH_2PPh_2\}]^+$	246
$[Au_2\{(CH_2)_2PPh_2\}\{PPh_2NHPPh_2\}]^+$	233
$[Au_2\{(CH_2)_2PPh_2\}\{PPh_2(C_5H_4N\text{-}2)\}]$	233
$[Au_2\{(CH_2)_2PPh_2\}\{S_2CNEt_2\}]$	233
$[Au_2\{(CH_2)_2PPh_2\}\{S_2COPr\text{-}i\}]$	234
$[Au_2\{(CH_2)_2PPh_2\}\{S_2CP(c\text{-}C_6H_{11})_3\}]^+$	235
$[Au_2\{(CH_2)_2PPh_2\}\{SC_5H_4N\text{-}2\}]$	236
$[Au_2Cl_2\{(CHPPh_3)_2CO\}]$	157
$[Au_2Cl_2\{(CH_2)_2PPh_2\}]^-$	237
$[Au_2\{(CH_2)_2PPh_2\}(PPh_3)_2]^+$	237
$[Au_2\{(CH_2)_2PPh_2\}(SC_4H_8)_2]^+$	237
$[Au_3\{(CH_2)_2PPh_2\}_2(PPh_2Me)_2]^+$	237

complexes by precipitation of silver halide[233,237] or displacement of a highly stable gold species (such as $[Au(C_6F_5)(PPh_3)]^{233}$) when reacted with the appropriate silver salt, which contains the second ligand. A less general route has been used for the preparation of $[Au_2Cl_2\{(CHPPh_3)_2CO\}]$, starting from the appropriate diphosphonium salt and $[AuCl(ylide)]^{157}$. Other data are given elsewhere[238−242].

$$2\,[Au(CH_2PMeR_2)_2]X \longrightarrow \underset{\underset{+}{R_2P}}{\overset{\overset{+}{PR_2}}{\left[\begin{array}{c}\overset{-}{Au}\\Au\end{array}\right]}} + 2\,[PMe_2R_2]X \qquad (55)$$

$$[Au_2\{(CH_2)_2PPh_2\}_2] + 2/n\,[Au(S_2COR)]_n \longrightarrow 2[Au_2\{(CH_2)_2PPh_2\}\{S_2COR\}] \qquad (56)$$
$$R = Me,\ Et,\ i\text{-}Pr$$

Dinuclear bis(ylide) complexes are characterized by a rich reaction chemistry which involves the [Au$\cdots$Au] structural unit and, to a lesser extent, the bridging ylide ligands. The attractive Au$\cdots$Au interactions facilitate oxidative addition to the metal centres which, depending on the type of substrate, may lead to bicyclic Au(II) compounds containing a discrete transannular Au−Au bond, conventional Au(III) complexes as well as Au(III) 'A-frame' species containing bridging methylene groups, and mixed-valence Au(I)/Au(III) complexes[243]. In some cases, further derivatization of the resulting compounds by ligand exchange is also possible. An overview of these reactions in given in Schemes 10–14 for the example of $[Au_2\{(CH_2)_2PPh_2\}_2]$ and derivatives, and Tables 9–11 contain examples

SCHEME 10. Preparation of dinuclear Au(I) and Au(III) complexes from $[Au_2\{(CH_2)_2PPh_2\}_2]$ by oxidative addition

ClO_4

$X' = C_6F_5$; L = PPh_3, SC_4H_8, $P(C_6H_4Me-4)_3$, $AsPh_3$, C_5H_5N

$X' = C_6H_3F_3-2,4,6$; L = PPh_3, SC_4H_8

[Ag(ClO_4)L]

[Au(PPh_3)L]ClO_4
[L = PPh_3, SC_4H_8]
[X' = C_6F_5, $C_6H_3F_3-2,4,6$]

[Au$_2$Cl$_2${(CH$_2$)$_2$PPh$_2$}$_2$]
[X' = C_6F_5, $C_6H_3F_3-2,4,6$]

PPh_2

$X' = C_6F_5$, $C_6H_3F_3-2,4,6$

AgX

$X = F_5$; X = NO_3, MeCOO, ClO_4
$X' = C_6H_3F_3-2,4,6$; X = ClO_4

[Au(NO_3)(PPh_3)]
[X' = C_6F_5]

Cd(CF_3)$_2$
[X = Br]

CF_3 ... CF_3

2 AgX'
[X = Cl]

$X' = Br$, SCN, NO_3,
MeCO$_2$, $C_6H_3F_3-2,4,6$,
C_6F_5, S_2CN(CH$_2$Ph)$_2$

SSC(NPh)(NHPh) ... SSC(NPh)(NHPh)

H$_2$S
[X = PhCOO]

2 SC(NHPh)$_2$
O$_2$, OH$^-$
[X = Cl]

2 [AgX'(L)]
[X = Cl]

X' = ClO_4, L = SC_4H_8; PPh$_3$
X' = NO_3, L = PMe_3

(X')$_2$

S$_2$CNR$_2$ ... S$_2$CNR$_2$
R = Me, Et

2 NaS$_2$CNR$_2$
[L = SC_4H_8]

2 L'
[L = SC_4H_8]

(ClO$_4$)$_2$

L' = C_5H_5N, AsPh$_3$, CH$_2$PPh$_3$,
S(MeS)CHNR (R = C_6H_4Me-4, C_6H_4Me-2,
C_6H_4OMe-4, $C_6H_3Me_2-3,5$)

SCHEME 11. Derivatization of dinuclear Au(II) complexes by ligand substitution

$$2+$$

Ph$_2$P—Au—L ... L—Au—PPh$_2$ (dinuclear gold complex)

$$+$$

$$2+$$

Ph$_3$P—Au—PPh$_3$ (dinuclear gold complex)

$$2+$$

Ph$_2$P—Au—SC$_4$H$_8$ ... H$_8$C$_4$S—Au—PPh$_2$ (dinuclear gold complex)

[Ag(ClO$_4$)(PR$_3$)]

$$2+$$

Ph$_3$P—Au—L ... L—Au—PPh$_2$ (dinuclear gold complex)

L = C$_5$H$_5$N, AsPh$_3$, PPh$_2$Me

$$2+$$

R$_3$P—Au—SC$_4$H$_8$ ... Au—PPh$_2$ (dinuclear gold complex)

$$\dfrac{L}{[R = Ph]}$$

PR$_3$ = PPh$_3$, PPh$_2$Me, P(C$_6$H$_4$OMe-4)$_3$

S(MeS)CHNR′
[R = Ph]

MX

$$2+$$

Ph$_3$P—Au—PPh$_3$ ... Au—PPh$_2$ (dinuclear gold complex)

$$\dfrac{[Au(PR_3)(SC_4H_8)]^+}{\text{or } [Au(C_6F_5)(SC_4H_8)]}$$

[Ag(ClO$_4$)(PPh$_3$)]

$R' = C_6H_4Me-2, C_6H_4OMe-4,$
$C_6H_3Me_2-3,5$

$PR_3 = PPh_3, X = Cl, S_2CN(CH_2Ph)_2$
$PR_3 = PPh_2Me, X = Cl$

$PR_3 = PPh_3, PPh_2Me$

SCHEME 12. Preparation of asymmetric cationic Au(II) complexes by ligand substitution

CH$_2$CF$_3$
Ph$_2$P
Br
Au
Br
Au
P
Ph$_2$

CH$_3$
Ph$_2$P
H$_3$C
Au
Au
P
Ph$_2$

Ph$_2$P
Au
Br
Au
Br
P
Ph$_2$

B$_2$
[R = CH$_2$CF$_3$]

LiCH$_3$
[R = CH$_3$]

R = CH$_3$, CH$_2$Ph

Ph$_2$P
Au
CCl$_3$
Cl
Au
Cl
P
Ph$_2$

CCl$_4$/THF

Ph$_2$P
Cl
Au
CCl$_3$
Au
Cl
P
Ph$_2$

CCl$_4$

Ph$_2$P
Au
R
I
Au
R
P
Ph$_2$

R = CH$_3$, CH$_2$CH$_3$,
CH$_2$CF$_3$, CH$_2$SiMe$_3$

RBr

RI

Ph$_2$P
H$_2$C
Au
X
Au
X'
P
Ph$_2$

Ph$_2$P
H$_2$C
Au
X
Au
X'
P
Ph$_2$

CH$_2$X$_2$ or
1. X$_2$; 2. CH$_2$N$_2$
[X = Cl, Br, I]

Ph$_2$P
Au
Au
P
Ph$_2$

CH$_2$XX'
[X = Cl, X' = Br, I
or X = CN, X' = Br
or X = C(O)Ph, X' = Br]

CH$_2$ClBr

AgCN

Ph$_2$P
Au
CH$_2$X
Au
X'
P
Ph$_2$

[X = Cl
X = Br, I]

Ph$_2$P
H$_2$C
Au
CN
Au
NC
P
Ph$_2$

Ph$_2$P
Cl
Au
CHCl$_2$
Br
Au
Br
P
Ph$_2$

CHCl$_2$Br

Ph$_2$P
Br
Au
CHBr$_2$
Au
P
Ph$_2$

CHBr$_3$

SCHEME 13. Preparation of Au(II) and Au(III) complexes from [Au$_2$((CH$_2$)$_2$PPh$_2$)$_2$] by oxidative addition of alkyl halides

SCHEME 14. Derivatization of Au(III) 'A-frame' complexes by ligand substitution

TABLE 9.   Dinuclear Au(II) complexes with bridging ylide ligands

$[Au_2X_2\{(CH_2)_2PR_2\}_2]$	R	X	Reference
	Me	Cl	247
	Me	Br	247
	Ph	Cl	153b, 248a
	Ph	Br	249
	Ph	SCN	249
	Ph	NO_2	250
	Ph	NO_3	249
	Ph	$MeCO_2$	249, 251
	Ph	$PhCO_2$	252
	Ph	S_2CNMe_2	253
	Ph	S_2CNEt_2	253
	Ph	$S_2CN(CH_2)_4$-c	253
	Ph	$S_2CN(CH_2Ph)_2$	249
	Ph	S_4	254
	Ph	SSC(NPh)(NHPh)	255
	Ph	CF_3	256
	Ph	$C_6H_2F_3$-2,4,6	249
	Ph	C_6F_5	249, 256
	Ph	CN	257
$[Au_2X_2\{(CH_2)P(S)Ph_2\}_2]$		X	
		Cl	258
		I	230
$[Au_2X_2\{(CH_2)_2PPh_2\}\{L-L\}]$	L−L	X	
	S_2COMe	Br	234
	S_2COEt	Cl	234
	S_2COPr-i	I	234
	S_2CNMe_2	Cl	259
	S_2CNEt_2	I	259
	$S_2CN(CH_2Ph)_2$	Br	259
	SC_5H_4N-2	Br	266
	SC_5H_4N-2	SCN	266
$[Au_2XX'\{(CH_2)_2PPh_2\}_2]$	X	X'	
	C_6H_5Se	Cl	260
	$C_6H_2F_3$-2,4,6	Cl	261
	$C_6H_2F_3$-2,4,6	ClO_4	201
	C_6F_5	Cl	261
	C_6F_5	NO_3	261
	C_6F_5	SCN	261
	C_6F_5	MeCOO	261
	C_6F_5	ClO_4	201
	S_4	S_5	254

$[Au_2R'X\{(CH_2)_2PR_2\}_2]$	R	R'	X	
	Me	CH_2Ph	Br	262
	Me	Me	I	262, 263
	Me	CH_2SiMe_3	I	262

TABLE 9.   (*continued*)

	Ph	Me	ClO_4	201
	Ph	Me	Br	262
	Ph	CH_2Ph	Br	262
	Ph	Me	I	262
	Ph	CH_2CH_3	I	264
	Ph	CH_2SiMe_3	I	262
	Ph	CH_2CF_3	I	264
	Ph	CH_2Cl	Br	265, 266
	Ph	CH_2CN	Br	267
	Ph	$CH_2C(O)Ph$	Br	267
	Ph	CH_2Cl	I	268
	Ph	$CHBr_2$	Br	269
	Ph	CCl_3	Cl	153b, 248a
$[Au_2X_2\{(CH_2)_2PPh_2\}\{L-L\}](ClO_4)$		L−L	X	
		$S_2CP(c\text{-}C_6H_{11})_3$	Cl	235
		$S_2CP(c\text{-}C_6H_{11})_3$	C_6F_5	235
		$Ph_2PCH_2PPh_2$	Br	259
		$Ph_2PNHPPh_2$	I	259
$[Au_2XL\{(CH_2)_2PPh_2\}_2][X']$	X	L	X'	
	I	CH_2PMe_3	I	270
	Cl	PPh_2Me	ClO_4	271
	ClO_4	PPh_2Me	ClO_4	271
	$C_6H_2F_3$-2,4,6	SC_4H_8	ClO_4	261
	C_6F_5	C_5H_5N	ClO_4	261
	C_6F_5	PPh_3	ClO_4	261
	C_6F_5	$AsPh_3$	ClO_4	261
$[Au_2L_2\{(CH_2)_2PPh_2\}_2][X']_2$		L	X'	
		CH_2PMe_3	I	270
		CH_2PPh_3	ClO_4	261
		$S(MeS)CHN(C_6H_4Me\text{-}4)$	ClO_4	253
		$S(MeS)CHN(C_6H_3Me_2\text{-}3,5)$	ClO_4	253
		SC_4H_8	ClO_4	249
		C_5H_5N	ClO_4	249
		PPh_3	ClO_4	249
		$AsPh_3$	ClO_4	249
		$SbPh_3$	ClO_4	249
		PMe_3	NO_3	249
$[Au_2LL'\{(CH_2)_2PPh_2\}_2]\ (ClO_4)_2$		L	L'	
		PPh_3	SC_4H_8	271
		PPh_3	C_5H_5N	271
		PPh_3	PPh_2Me	271
		PPh_3	$AsPh_3$	271
		PPh_2Me	SC_4H_8	271
		PPh_2Me	OH_2	271
		$P(C_6H_4OMe\text{-}4)_3$	SC_4H_8	271

(*continued overleaf*)

TABLE 10.   Dinuclear Au(III) complexes with bridging ylide ligands

$[Au_2(X_2)_2\{(CH_2)_2PR_2\}_2]$	R	X_2	Reference
	Me	Cl_2	247
(*cis/trans*)	Ph	Cl_2	244
(*trans/trans*)	Ph	Cl_2	272
(*cis/cis*)	Ph	Br_2	273
(*trans/trans*)	Ph	Br_2	244, 274
(*cis/cis*)	Ph	$C_6H_4S_2$	275

$[Au_2X_2(RY)\{(CH_2)_2PPh_2\}_2]$	X_2	R	Y	
(*trans/trans*)	Cl_2	CCl_3	Cl	153b, 248
(*cis/trans*)	Br_2	CH_2CF_3	Br	276
(*trans/trans*)	Br_2	$CHCl_2$	Cl	276

$[Au_2(\mu\text{-}CH_2)X_2\{(CH_2)_2PR_2\}]$	R	X	Reference
	Me	Cl	277
	Me	Br	277
	Me	I	277
	t-Bu	Cl	247
	Ph	Br	265, 266
	Ph	I	278
	Ph	CN	257, 268
	Ph	PhCOO	268
	Ph	SCN	268, 278
	Ph	S_2CNMe_2	278
	Ph	CH_3	279
	Ph	C_6F_5	278

$[Au_2(\mu\text{-}CHY)X_2\{(CH_2)_2PPh_2\}_2]$	Y	X	Reference
	NO_2	PhCOO	250, 280

$[Au_2(\mu\text{-}CH_2)XX'\{(CH_2)_2PR_2\}_2]$	R	X	X'	Reference
	Ph	Cl	Br	268
	Ph	Cl	I	268
	Ph	Br	CH_3	279

$[Au_2(\mu\text{-}CH_2)LX\{(CH_2)_2PPh_2\}_2][X']$	L	X	X'	Reference
	CH_2PMe_3	Br	Br	281
	PPh_3	I	ClO_4	278
	$AsPh_3$	I	ClO_4	278
	C_5H_5N	I	ClO_4	278
	SC_4H_8	I	ClO_4	278
	phen	I	ClO_4	278

$[Au_2(\mu\text{-}CH_2)L_2\{(CH_2)_2PPh_2\}_2][X]_2$	L	X	Reference
	CH_2PMe_3	Br	281
	PPh_3	ClO_4	278
	$AsPh_3$	ClO_4	278
	C_5H_5N	ClO_4	278
	SC_4H_8	ClO_4	278
	phen	ClO_4	278

TABLE 11. Dinuclear mixed-valence Au(I)/Au(III) complexes with bridging ylide ligands

Complex	Reference
$[Au\{AuBr_2\}\{(CH_2)_2PPh_2\}_2]$	282
$[Au\{AuMe_2\}\{(CH_2)_2PPh_2\}_2]$	279
$[Au\{AuCl_2\}\{CH_2P(S)Ph_2\}_2]$	215
$[Au\{AuI_2\}\{CH_2P(S)Ph_2\}_2]$	230, 283
$[Au_2Cl_2\{(CH_2)_2PPh_2\}\{\mu\text{-}(CH_2)_2PPh_2\}]$	283
$[Au_2(C_6F_5)_2\{(CH_2)_2PPh_2\}\{S_2CNMe_2\}]$	259
$[Au_2\{(CH_2)_2PPh_2\}\{S_2CNMe_2\}(PPh_3)_2]^{2+}$	259
$[Au_2\{(CH_2)_2PPh_2\}\{S_2CN(CH_2Ph)_2\}(PPh_3)_2]^{2+}$	259

of the various types of products thus obtained. Conversions involving the bridging ylide ligands include isomerizations[229,244], acid-induced cleavage reactions to give mononuclear species[245], oxidative cleavage to give ring-opened dimeric complexes[246] and replacement of acidic protons with further gold(I) units to give polynuclear complexes reminiscent of the polyauriomethanes[146,157,158].

Some substrates (e.g. halogens) react with dinuclear gold(I) ylide complexes by two-centre two-electron oxidative addition to give the corresponding gold(II) complexes as isolable species (Scheme 10). Further oxidative addition of halogens to the dihalide complexes cleaves the metal–metal bond, leading to dimeric gold(III) ylide complexes as geometrical isomers with ligands in a *trans/trans*[273,274], *cis/trans*[244] or *cis/cis*[275] geometry, which have all been structurally characterized (Figure 10). Interestingly, some of these species interconvert in solution upon prolonged standing[244].

With benzoyl peroxide, the dimer $[Au_2\{(CH_2)_2PPh_2\}_2]$ gives a dinuclear gold(II) ylide complex containing oxygen-bound carboxylate ligands[250]. This compound shows interesting reactivity in the presence of nitromethane as co-solvent. If kept at $0°C$, a dibenzoate complex (with A-frame geometry) can be isolated wherein a $CHNO_2$ group bridges two Au(III) centres[280], while at ambient temperature and upon prolonged standing the reaction gives a nitritogold(II) complex, as illustrated in Scheme 10. The latter compound may also be prepared directly by reacting $[Au_2\{(CH_2)_2PPh_2\}_2]$ with N_2O_4[250].

As can be seen in Scheme 11, various procedures have been established for the further derivatization of dinuclear gold(II) ylide complexes by ligand substitution. Halide ligands can be substituted by neutral donor ligands such as tetrahydrothiophene or pyridine (giving the corresponding cationic complexes)[249], or with other anionic ligands (such as

trans/trans   *cis/trans*   *cis/cis*
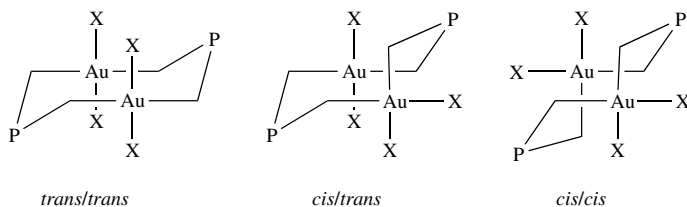
FIGURE 10. The possible geometrical isomers of Au(III) ylide dimers: *trans/trans*, *cis/trans*, *cis/cis*

pseudohalides, carboxylates or dithiocarbamates)[249,253]. The digold(II) dibenzoate complex reacts with hydrogen sulphide in tetrahydrofuran to give macrocyclic complexes in which two [Au$_2${(CH$_2$)$_2$PPh$_2$}$_2$] units are bridged by two polysulphide chains[254]. The introduction of carbanionic groups is also straightforward, leading to organogold(II) complexes with exocyclic trifluoromethyl[256], pentafluorophenyl[249,256], or phosphorus ylide ligands[261,270]. While substitution usually occurs at both gold(II) centres simultaneously, some asymmetric derivatives have been prepared from pentafluorophenyl complexes[261].

A number of asymmetric cationic Au(II) complexes with a phosphine ligand have been synthesized starting from the symmetric triphenylphosphine or tetrahydrothiophene derivatives (Scheme 12)[253,271]. In solution, some of these products are in equilibrium with an equimolecular mixture of the corresponding symmetric derivatives.

Considerable effort has been expended to elucidate the course of oxidative addition reactions of haloalkanes to dinuclear gold(I) bis(ylide) complexes[39], experimental evidence supporting the notion that the order of reactivity of such substrates is inversely proportional to the carbon−halogen bond dissociation energies[269]. As shown in Scheme 13, [Au$_2${(CH$_2$)$_2$PPh$_2$}$_2$] reacts with alkyl halides RX (X = Br, I) to give asymmetrically substituted bicyclic digold(II) complexes[262−264,284,285]. The reaction is reversible if R bears no electron-withdrawing substituents[264]. Further, [Au$_2${(CH$_2$)$_2$PPh$_2$}$_2$] catalyzes S$_N$2 halogen exchange between CH$_3$Br and CD$_3$I in a process which is thought to involve an S$_N$2 reaction between the free alkyl halide and the postulated intermediate [Au$_2${(CH$_2$)$_2$PPh$_2$}$_2${C(H or D)$_3$}]X[262,285]. There is no indication that alkyl halides RX add to [Au$_2${(CH$_2$)$_2$PPh$_2$}$_2$] by two-electron oxidation of a single gold centre, although asymmetric gold(I)/gold(III) complexes do form when complexes such as [Au$_2$(CH$_3$)(I){(CH$_2$)$_2$PPh$_2$}$_2$] are reacted with LiCH$_3$ (Scheme 13)[263]. As may be expected, digold(II) haloalkyl halide complexes are susceptible to further oxidative addition when treated with halogen. The reaction, which can be used to prepare digold(III) haloalkyl trihalide complexes (Scheme 13)[276], apparently proceeds via an intermediate cationic μ-halogeno A-frame species, as suggested by the isolation of small quantities of [Au$_2$(μ-Br){(CH$_2$)$_2$PPh$_2$}$_2$][IBr$_2$] from the mixture of [Au$_2$(CH$_2$CF$_3$)(I){(CH$_2$)$_2$PPh$_2$}$_2$] and Br$_2$[273]. Several geometrical isomers of the digold(III) haloalkyl trihalide complexes have been studied by X-ray techniques[276].

With methylene dihalides CH$_2$X$_2$ (X = Cl, Br, I), dimeric gold(I) ylide complexes undergo a two-centre four-electron oxidative addition reaction to give gold(III) 'A-frame' complexes in which a methylene group bridges two gold centres (Scheme 14)[247,277]. Alternatively, such complexes have been prepared by the reaction of [Au$_2${(CH$_2$)$_2$PPh$_2$}$_2$] first with a halogen and then with diazomethane[268]. While no dinuclear gold(II) haloalkyl halide complexes are isolated from the reactions of symmetrical methylene dihalides, the intermediacy of such species is documented for asymmetric substrates, as exemplified by the reactions of [Au$_2${(CH$_2$)$_2$PPh$_2$}$_2$] with CH$_2$ClBr[265], CH$_2$ClI[268], CH$_2$Br(CN)[267], or CH$_2$Br{C(=O)Ph}[267] (Scheme 13). There is structural evidence for the formation of a carbene intermediate preceding the formation of an 'A-frame' complex containing a bridging methylene group[265,266]. The formulation of the final product as the mixed halogenated μ-methylene 'A-frame' species is tentative (Scheme 13); at least in the case of CH$_2$ClBr, further halide exchange with solvent molecules leads to the formation of the symmetrically substituted μ-methylene dibromo complex [Au$_2$(μ-CH$_2$)Br$_2${(CH$_2$)$_2$PPh$_2$}$_2$], which has been structurally characterized[265,266]. A related reaction is the treatment of [Au$_2${(CH$_2$)$_2$PPh$_2$}$_2$] first with CH$_2$ClBr and then with silver salts such as AgCN, AgSCN or AgOOCPh to give the symmetrically disubstituted μ-methylene complexes[257,268]. Derivatization of digold(III) μ-methylene dihalide

complexes with other reagents to introduce carbanionic ligands[278,279], pseudohalides[278], phosphorus ylides[281] or neutral donor ligands[278] has also been reported (Scheme 14). The treatment with organolithium compounds gives several well-defined products, including a partially alkylated intermediate and a mixed-valence Au(I)/Au(III) species. The doubly methylated complex $[Au_2(CH_3)_2\{(CH_2)_2PPh_2\}_2]$ undergoes thermally induced reductive elimination of alkane, the dinuclear gold(I) bis(ylide) complex being regenerated in the process[279].

The reaction of $[Au_2\{(CH_2)_2PPh_2\}_2]$ with trihalomethanes can afford two products (Scheme 13): Initially, a digold(II) halomethyl halide species is formed, as exemplified by the isolation of $[Au_2(CHBr_2)(Br)\{(CH_2)_2PPh_2\}_2]$ from a mixture of $[Au_2\{(CH_2)_2PPh_2\}_2]$ and $CHBr_3$[269]. In a second step, renewed oxidative addition leads to the formation of digold(III) halomethyl trihalide complexes, as shown in Scheme 13 for the substrate $CHCl_2Br$[276]. Tetrahalomethanes react in an analogous way, the interaction of $[Au_2\{(CH_2)_2PPh_2\}_2]$ with CCl_4 having been studied in some detail[248]: Oxidative addition of one equivalent of the reagent leads to the isolable digold(II) halomethyl halide species $[Au_2(CCl_3)(Cl)\{(CH_2)_2PPh_2\}_2]$ which, in the presence of tetrahydrofuran, reacts a second time with CCl_4 to give the digold(III) trichloromethyl trichloride complex $[Au_2(CCl_3)Cl_3\{(CH_2)_2PPh_2\}_2]$. By contrast, prolonged interaction of $[Au_2\{(CH_2)_2PPh_2\}_2]$ and CCl_4 in the absence of tetrahydrofuran generates the digold(II) dichloride complex $[Au_2Cl_2\{(CH_2)_2PPh_2\}_2]$ and it has been noted that the two products do not interconvert in the presence of CCl_4. Reactions in the CCl_4/tetrahydrofuran solvent mixture are accompanied by the formation of chloroform, suggesting a radical pathway with tetrahydrofuran as a hydrogen source for CCl_3 radicals.

Two-electron oxidative addition of reagents to dinuclear gold(I) ylide complexes usually involves both gold centres to yield Au(II)/Au(II) complexes. Remarkably, both Au(I)/Au(III) and Au(II)/Au(II) complexes have been obtained from the reaction of dimeric Au(I) methylenethiophosphinate complexes with iodine. As illustrated in Scheme 15, the isovalent isomer contains both bridging ligands in a geometry which is *trans* to S, while the mixed-valence isomer exhibits a linear S−Au(I)−S and a square-planar *trans*-$[Au^{III}I_2C_2]$ unit[230]. A related mixed-valence dichloride is also known[215].

SCHEME 15. Synthesis of isovalent and mixed-valent isomers of $[Au_2I_2\{CH_2P(S)Ph_2\}_2]$

Methylenethiophosphinate ligands have also been used to synthesize dinuclear gold/mercury complexes which show a similar isomerism: Depending on the synthetic procedure, species containing S−Au−C/S−Hg−C or S−Au−S/C−Hg−C structural units are obtained[286]. The latter isomer undergoes an interesting ring expansion reaction upon treatment with diazomethane, in the course of which one methylene group inserts into each gold−sulphur bond to give a ten-membered heterobimetallic ring[287]. Oxidative addition of chlorine gives the symmetrical complex containing a metal−metal bonded [Cl−Au−Pt−Au−Cl] unit, rather than a mixed-valence species[214].

A number of other procedures have led to mixed-valence Au(I)/Au(III) ylide complexes, but these do not involve oxidative addition in the key step. Thus, reaction of digold(II) bis(ylide) dihalide complexes such as $[Au_2I_2\{(CH_2)_2PPh_2\}_2]$ with various phosphorus ylides in a 1 : 2 molar ratio leads to the formation of dicationic complexes with a Au(I)/Au(III) constitution[270], as shown by Mössbauer spectroscopy[288]. This result is in agreement with the finding that oxidative addition of CH_3I to $[Au_2\{(CH_2)_2PPh_2\}_2]$ yields the asymmetrically substituted digold(II) complex, whereas attempts to carry out further alkylation with $LiCH_3$ afford only a mixed-valence isomer (Scheme 13). Apparently, the strong *trans* influence of two alkyl groups at the Au−Au bond results in the destabilization of this structural unit and induces disproportionation (Scheme 16).

SCHEME 16. Preparation of mixed-valent gold ylide complexes from a digold(II) precursor

Treatment of the digold(III) complex $[Au_2Br_4\{(CH_2)_2PPh_2\}_2]$ with AgCN under suit-able conditions has been reported to produce in a single-centre reduction process the mixed-valence complex $[Au(AuBr_2)\{(CH_2)_2PPh_2\}_2]$, which was characterized by X-ray

crystallography and photoelectron spectroscopy[282]. Neutral or dicationic open-chain di-nuclear Au(I)/Au(III) complexes with one ylide bridging the gold atoms and another ylide or dithiocarbamate ligand in a chelating mode can be obtained by disproportiona-tion of $[Au_2Cl_2\{(CH_2)_2PPh_2\}_2]$ in polar solvents such as nitromethane (equation 57)[283] or by treating $[Au_2I_2\{(CH_2)_2PPh_2\}\{S_2CNMe_2\}]$ with $[Ag(C_6F_5)]$ or $[Ag(OClO_3)(PPh_3)]$[259]. For the dithiocarbamate complexes it is not clear which one of the difunctional ligands is acting as a chelate and which one acts as a bridge.

$$(57)$$
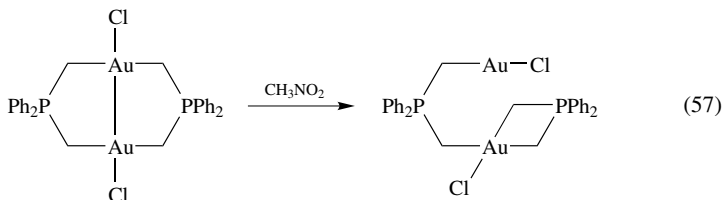
Complexes containing direct bonds between gold(I) and gold(III) or gold(II) which are unsupported by other ligands could be prepared in straightforward reactions, as illustrated in equations 58[289], 59[200] and 60[201].

$$(58)$$

$$(59)$$

$$2 \left[F_5C_6\!\!-\!\!Au\!\!-\!\!\!-\!\!Au\!\!-\!\!SC_4H_8 \right] ClO_4 \; + \; Au\!-\!-\!-\!Au$$

(with bridging $\overset{Ph_2}{P}$ ligands above and $\underset{Ph_2}{P}$ below each Au–Au unit)

$$(60)$$

$$\left[F_5C_6\!\!-\!\!Au\!\!-\!\!\!-\!\!Au\!\!-\!\!Au\!-\!-\!-\!Au\!\!-\!\!Au\!\!-\!\!\!-\!\!Au\!\!-\!\!C_6F_5 \right] (ClO_4)_2$$

(with bridging $\overset{Ph_2}{P} \cdots \underset{Ph_2}{P}$ ligands across each Au–Au unit)
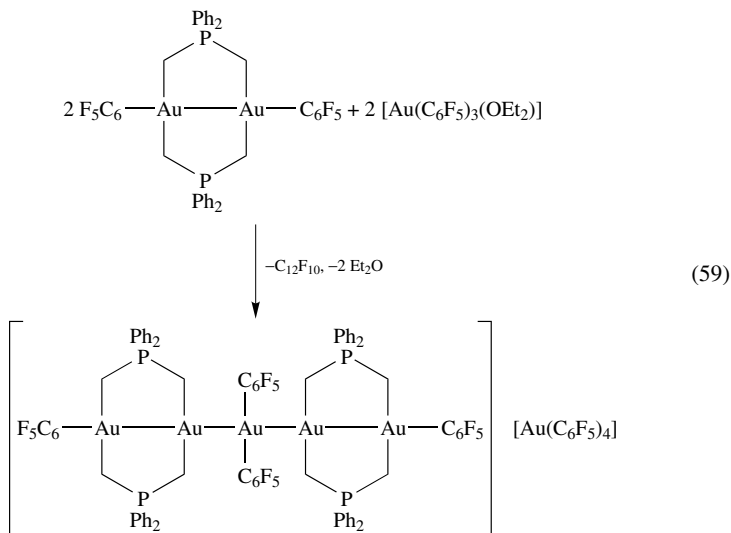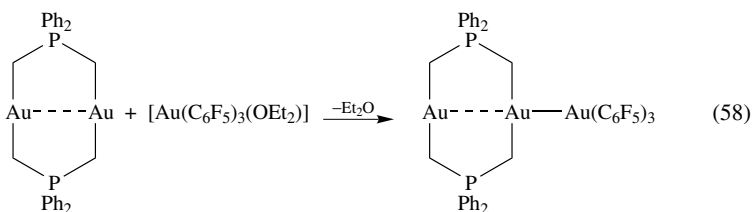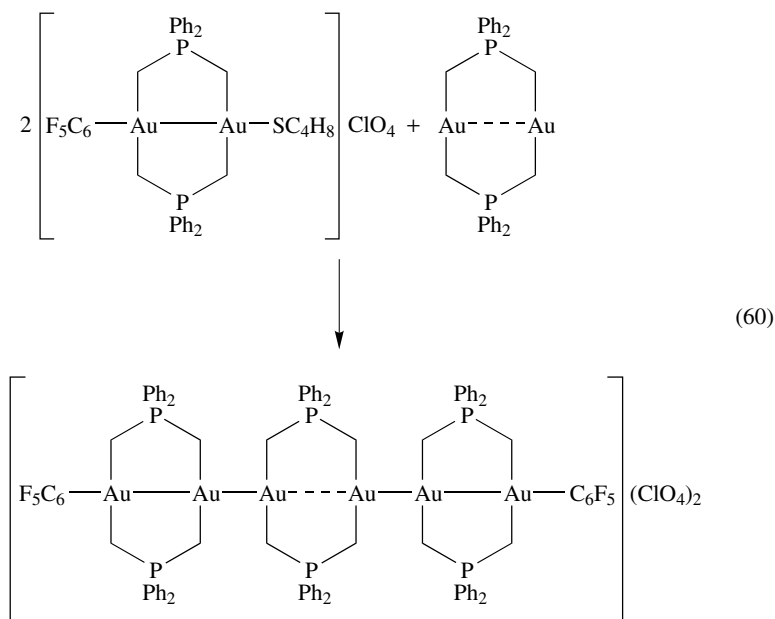
E. Gold(III) Complexes with One Gold–Carbon Bond

Alkylgold(III) complexes containing one gold–carbon bond are still rare[13a,290], and only a few trifluoromethyl compounds of the type $[Au(CF_3)X_2(PR_3)]$ (X = Br, I; R = Me, Et, Ph) have been reported, which are formed by oxidative addition of halogen to the respective trifluoromethyl(phosphine)gold(I) complex[21]. By contrast, various methods now exist for the synthesis of monoarylgold(III) species. One of the earliest established procedures involves the electrophilic substitution by gold(III) at the aromatic ring of benzene derivatives ('auration')[13]. Recently, systems such as the trichloro(phenyl)aurate anion have been investigated with respect to their ligand substitution kinetics and the *trans* influence of the aryl ligand has been assessed[291].

Another synthesis of monoarylgold(III) compounds starts from pentahaloaryl or mesityl-gold(I) complexes, which are sufficiently stable to undergo oxidative addition of halogen without cleavage of the gold–carbon bond, as illustrated in equation 61[11,12,97]. In these products, the thiophene ligand may then be substituted by other neutral or anionic ligands (e.g. phosphine, isocyanide, 1,10-phenanthroline, halide) and a wide variety of derivatives has thus been obtained, examples of which are given in Table 12[96]. This type of compound may be further derivatized by treatment with $AgClO_4$, giving four-coordinate cationic complexes of the types $[Au(C_6F_5)X(phen)]ClO_4$ (X = Cl, Br) and $[Au(C_6F_5)(PPh_3)(phen)](ClO_4)_2$[292].

$$[Au(C_6F_5)(SC_4H_8)] + Cl_2 \longrightarrow [Au(C_6F_5)Cl_2(SC_4H_8)] \qquad (61)$$
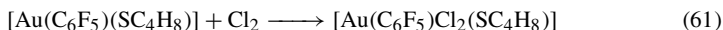
Some pentafluorophenyl dithiolate complexes have recently been synthesized from $[Au(C_6F_5)Cl_2L]$ (L = PR_3, $AsPh_3$, SC_4H_8) using tin or zinc derivatives as dithiolate

TABLE 12.   Some monoarylgold(III) complexes

Complex	M.p.($^\circ$C)	Reference
$[Au(C_6F_5)Cl_2(SC_4H_8)]$	—	11
$[Au(C_6Cl_5)Cl_2(SC_4H_8)]$	—	11
$[Au(C_6F_5)Br_2(CNC_6H_4Me-4)]$	148(d)	11
$[Au(C_6F_5)Cl_2(phen)]^a$	149(d)	292
$[Au(C_6F_5)Cl_2(pdma)]^b$	100	292
$[Au(C_6F_5)(3,4-S_2C_6H_3Me)]_3$	—	293
$[Au(C_6F_5)(1,2-S_2C_6H_4)(1,2-SC_6H_4SPPh_3)]$	—	293
$[Au(C_6F_5)(1,2-S_2C_6H_4)(PPh_3)]$	222	294
$[Au(C_6F_5)(dmit)(AsPh_3)]^c$	190(d)	294
$[Au(C_6F_5)Br_2Cl]^-$	—	11
$[Au(C_6F_5)(dmit)(SCN)]^{-c}$	—	293
$[Au(C_6F_5)Cl(phen)]^{+a}$	195(d)	292
$[Au(C_6F_5)(PPh_3)(phen)]^{2+a}$	147(d)	292
$[Au\{C_6H_4(N=NPh)-2\}Cl_2]$	218(d)	295
$[Au\{C_6H_4(N=NPh)-2\}(CH_3COO)_2]$	140(d)	296
$[Au\{C_6H_4(N=NPh)-2\}(OOC-COO)]$	129(d)	296
$[Au\{C_6H_4(N=NPh)-2\}Cl_2(PPh_3)]$	181(d)	295
$[\{Au\{C_6H_4(N=NPh)-2\}Cl_2\}_2(Ph_2PCH_2CH_2PPh_2)]$	169	295
$[Au\{C_6H_4(N=NPh)-2\}Cl_3]^-$	83	295
$[Au\{C_6H_4(N=NPh)-2\}Cl(PPh_3)_2]^+$	136(d)	295
$[Au\{C_6H_4(N=NPh)-2\}(C_5H_5N)_2]^{2+}$	210(d)	296
$[\{Au\{C_6H_4(N=NPh)-2\}(PPh_3)_2\}_2]^{4+}$	185(d)	297
$[Au\{C_6H_4(CH_2NMe_2)-2\}Cl_2]$	185(d)	298
$[Au\{C_6H_4(CH_2NMe_2)-2\}I_2]$	105(d)	298
$[Au\{C_6H_4(CH_2NMe_2)-2\}Cl(PPh_3)]^+$	174	298
$[Au\{C_6H_4(CH_2NMe_2)-2\}(phen)]^{2+a}$	—	11
$[Au\{C_6H_4(CH_2NMe_2)-2\}(CN)(phen)]^{+a}$	125(d)	299
$[Au\{C_6H_4(CH_2NMe_2)-2\}(phen)(PPh_3)]^{2+a}$	145	299
$[Au\{C_6H_4(2-C_5H_4N)-2\}Cl_2]$	—	300
$[Au\{C_6H_4\{2-(CMe_2)C_5H_4N\}-2\}Cl_2]$	283–284	301
$[Au\{C_6H_4\{2-(CHMe)C_5H_4N\}-2\}Cl(dppe)]^{+d}$	100–102	301
$[Au\{C_6H_4\{2-(CH_2)C_5H_4N\}-2\}(dppe)]^{2+d}$	175(d)	301
$[Au\{4-MeOC_6H_4-(Phbipy)\}Cl]^{+e}$	—	302
$[Au\{C_6H_3\{N=NC_6H_4(C_4H_9-4')-2\},C_4H_9-5\}Cl_2]$	137	303
$[Au\{C_6H_3\{N=NC_6H_4(C_{10}H_{21}-4')-2\},C_{10}H_{21}-5\}Cl_3]^-$	118	303
$[Au(C_6H_2Me_3-2,4,6)\}Cl_3]^-$	—	97
$[Au(C_6H_2Me_3-2,4,6)\}Br_3]^-$	—	97

[a] phen, 1,10-phenanthroline.
[b] pdma, phenylene-1,2-bis(dimethylarsine).
[c] dmit, 1,3-dithiol-2-thione-4,5-dithiolate.
[d] dppe, 1,2-bis(diphenylphosphino)ethane.
[e] 4-MeOPh-(Phbipy), 4′-(4-methoxyphenyl)-6′-phenyl-2,2′-bipyridine.

transfer agents[293,294]. Tetrahydrothiophene as the neutral ligand is also displaced and a trinuclear complex is isolated (equation 62)[293]. Further reaction of these trinuclear compounds with neutral or anionic ligands breaks the Au_3S_3 ring, leading to mononuclear complexes[293].

$$3[Me_2Sn(S_2C_6H_4)] + 3 \text{ } trans\text{-}[C_6F_5Au(SC_4H_8)Cl_2] \longrightarrow [C_6F_5Au(S_2C_6H_4)]_3 +$$

$$3 \text{ } Me_2SnCl_2 \quad (62)$$
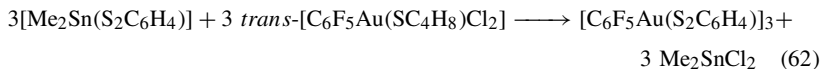
Arylgold(III) complexes $[Au(Ar)X_2L]$ may also be obtained by arylation of $[AuCl_3(SC_4H_8)]$ or $[AuCl_4]^-$ with arylmercury(II) compounds. Two examples of this conversion are presented in equations 63 and 64[295,298]. With 4,4′-disubstituted azobenzenes as aryl groups, the reaction with $[AuCl_4]^-$ follows the same pathway, but when chloroarylmercurials are treated with $[AuCl_3(SC_4H_8)]$, anionic aryltrichloroaurates(III) are obtained[303]. The derivatization of $[Au(Ar)X_2L]$ (by substitution of the chloride ligands or displacement of the N-donor) is straightforward and examples of products obtained from reactions with neutral or anionic ligands are listed in Table 12. These may again be transformed in subsequent conversions. Specifically, $[Au(C_6H_4\{CH_2NMe_2\}\text{-}2)(phen)](ClO_4)_2$ reacts with triphenylphosphine to give the pentacoordinated complex $[Au(C_6H_4\{CH_2NMe_2\}\text{-}2)(phen)(PPh_3)](ClO_4)_2$[299].

$$2 [AuCl_3(SC_4H_8)] + 2 [Hg\{C_6H_4(N=\!\!=NPh)\text{-}2\} Cl]$$

2 NMe$_4$Cl

$$\quad + [NMe_4]_2[Hg_2Cl_6] + 2 \text{ } SC_4H_8 \quad (63)$$

$$4 [AuCl_4]^- + 2 [Hg\{C_6H_4(CH_2NMe_2)\text{-}2\}_2]$$

$$\quad + [Hg_2Cl_6]^{2-} + 2 \text{ } Cl^- \quad (64)$$
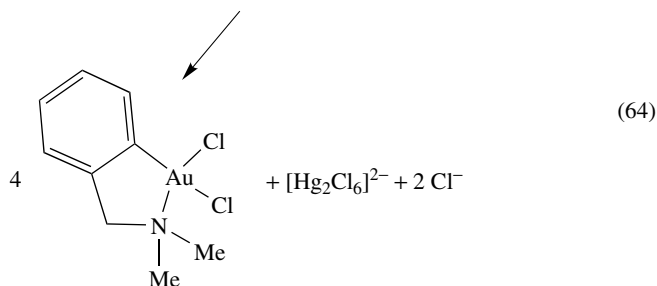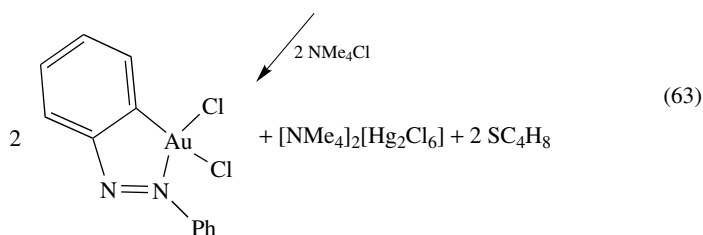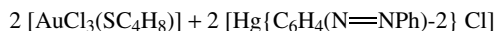
Several closely related arylgold(III) complexes have also been formed in the course of cyclometalation processes. The reaction of substituted pyridine ligands such as 2-phenylpyridine or 2-benzylpyridines (denoted HL) with $[AuCl_4]^-$ at ambient temperature

yields non-metallated gold(III) complexes which, upon heating, are transformed into the metallated compounds $[Au(L)Cl_2]$[300,301]. The process with 2-phenylpyridine is illustrated in equation 65. This product has also been prepared by transmetallation of the appropriate arylmercury(II) chloride with $[AuCl_4]^-$, a reaction resembling that depicted in equation 63. With 2-benzylpyridine, other metallated and non-metallated species can be prepared by substitution of the chlorine atoms[301]. The ligand 6-(2-thienyl)-2,2′-bipyridine gives analogous reactions with $Na[AuCl_4]$[304−306]. The structure of the product is given in Figure 11.

$$(65)$$
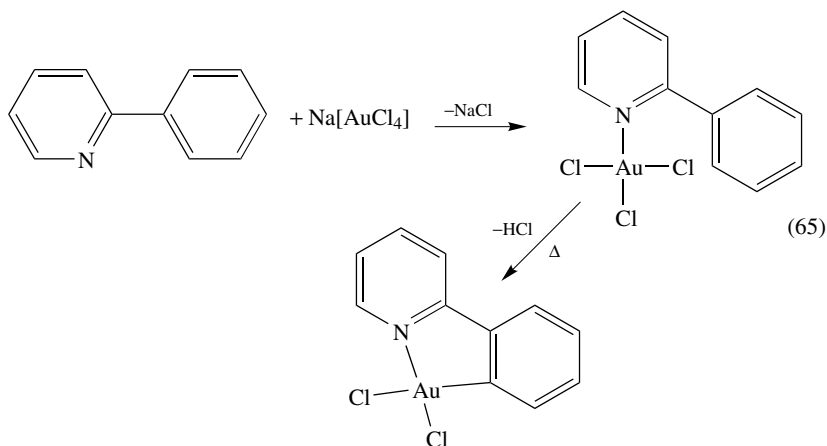
Several metallated cationic compounds with bipyridine and phenanthroline derivatives as aryl groups have been described in recent years. The ligand (HL) is treated with
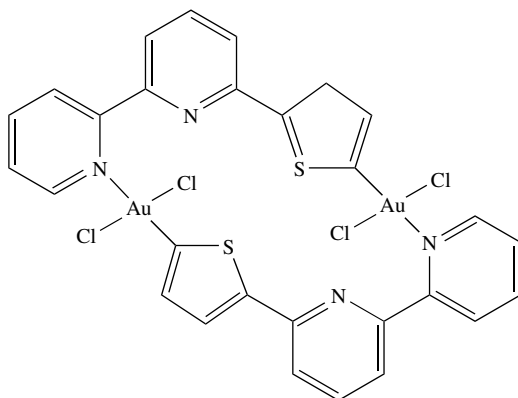
FIGURE 11. Structure of the dimeric complex $[\{Au(thbipy)Cl_2\}_2]$ [thbipy = 6-(2-thienyl)-2,2′-bipyridine]

$[AuCl_4]^-$ and a silver salt in acetonitrile at reflux temperature as shown in equation 66[307].

$$+ K[AuCl_4] + 2\ AgX$$

CH$_3$CN, reflux -2 AgCl, $-$KCl

(66)

X = C$_7$H$_7$SO$_3$
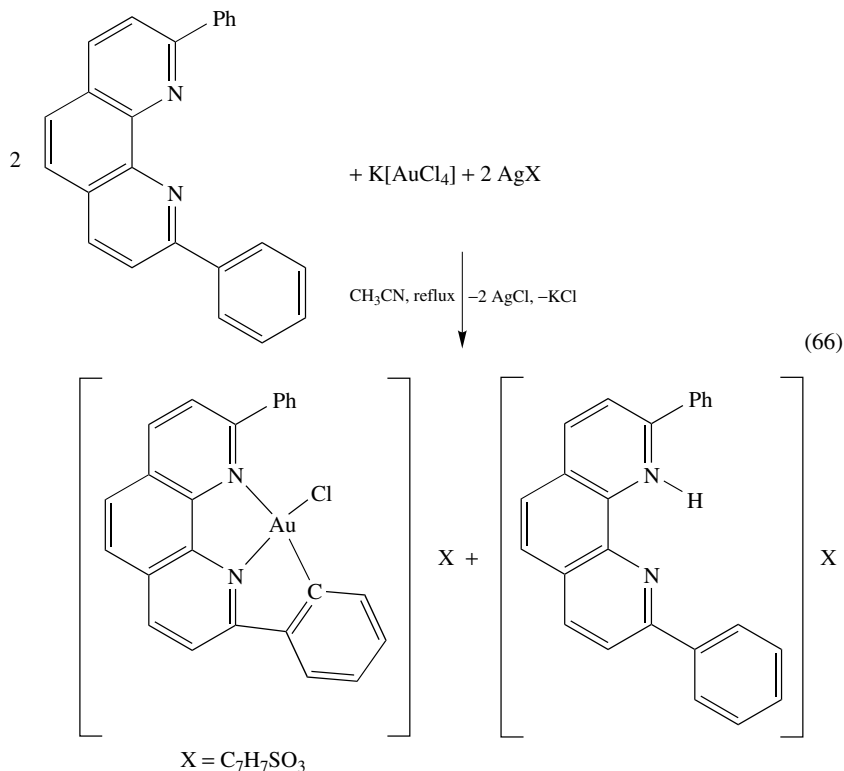
F. Gold(III) Complexes with Two Gold−Carbon Bonds

1. Diorganylgold(III) halides and pseudohalides

Compounds of the type $[AuR_2X]_2$ have been known for a long time, the organic ligands being unsubstituted alkyl groups in the majority of cases[13]. One of the simplest representatives is the dimethylchlorogold(III) $[Au_2(\mu\text{-}Cl)_2Me_4]$, whose traditional synthesis with Grignard reagents or methyllithium gives very low yields. An improved synthetic method using SnMe$_4$ as alkylating agent, which affords higher yields under better reaction conditions, has recently been published (equation 67)[308,309].

$$2\ HAuCl_4\ +\ 4\ SnMe_4\ \xrightarrow{-2\ HCl}\ \underset{Me}{\overset{Me}{}}Au\underset{Cl}{\overset{Cl}{}}Au\underset{Me}{\overset{Me}{}}\ +\ 4\ SnMe_3Cl \quad (67)$$
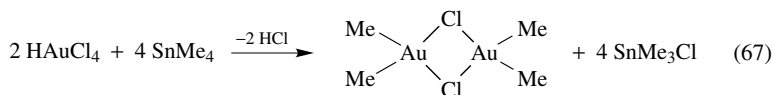
Trifluoromethylated complexes are potentially useful precursors for chemical vapour deposition studies as they are expected to show enhanced volatility[310]. This is indeed

observed for the dimeric complexes $[Au_2(\mu\text{-}Br)_2(CF_3)_4]$ and $[Au_2(\mu\text{-}I)_2(CF_3)_4]$, which are accessible by cocondensation of gold with CF_3Br and CF_3I, respectively, and may be sublimed at room temperature $(10^{-2}$ Torr$)$[311]. $cis\text{-}[Au(CF_3)_2I(PMe_3)]$ is formed in quantitative yield by oxidative addition of trifluoromethyl iodide to $[Au(CF_3)(PMe_3)]$, the reaction being assumed to proceed via a radical intermediate[21,22].

Diarylaurate(III) complexes of the type $[AuR_2X_2]^-$ $(R = C_6F_5, C_6F_3H_2\text{-}2,4,6; X = Cl, Br, I)$ were first prepared by oxidative addition of halogen to the corresponding organogold(I) complexes $[AuR_2]^-$[11−13]. Reaction of these compounds with $AgClO_4$ results in the abstraction of halide anion to give the dimeric diarylgold(III) halides $[Au_2(\mu\text{-}X)_2(C_6F_5)_4]$ $(X = Cl, Br)$ which, in turn, can react with sodium azide or potassium thiocyanate to give the corresponding dinuclear pseudohalide derivatives. Treatment of the dimeric chloride complex with Tl(acac) results in the formation of monomeric $[Au(C_6F_5)_2(acac)]$, while the cleavage of the chloro bridges with neutral ligands yields complexes of the types $[Au(C_6F_5)_2(L\text{-}L)][Au(C_6F_5)_2Cl_2]$ (L-L = 1, 10-phenanthroline and related ligands) or $[Au(C_6F_5)_2Cl(L)]$ (L = pyridine)[312].

The preparation of diarylaurate(III) complexes of the type $[AuR_2X_2]^-$ by oxidative addition of halogens as described above is not generally applicable, as less stable organogold(I) derivatives usually react with cleavage of the gold–carbon bonds under the given conditions. An alternative synthesis of diarylgold(III) halides uses organomercurials as arylating reagents and compounds of the type $[NMe_4][cis\text{-}AuR_2Cl_2]$ can be prepared where $R = C_6H_4NO_2\text{-}2$ or $C_6H_3Me\text{-}2$, $NO_2\text{-}6$ (equation 68)[313]. The complexes may then be derivatized by substitution of one or both halide ligands with various reagents. Thus, reaction with KCN results in substitution of both halide ligands by cyanide, while treatment with neutral mono- or bidentate ligands leads to neutral or cationic complexes, as illustrated in equations 69–71[313].

$$2[Hg(C_6H_4NO_2\text{-}2)_2] + [AuCl_4]^- \longrightarrow [Au(C_6H_4NO_2\text{-}2)_2Cl_2]^- +$$

$$2[Hg(C_6H_4NO_2\text{-}2)Cl] \qquad (68)$$

$$[NMe_4][Au(C_6H_4NO_2\text{-}2)_2Cl_2] + 2\ KCN \longrightarrow [NMe_4][Au(C_6H_4NO_2\text{-}2)_2(CN)_2] +$$

$$2\ KCl \qquad (69)$$

$$[NMe_4][Au(C_6H_4NO_2\text{-}2)_2Cl_2] + PPh_3 \longrightarrow [Au(C_6H_4NO_2\text{-}2)_2Cl(PPh_3)] +$$

$$[NMe_4]Cl \quad (70)$$

$$[NMe_4][Au(C_6H_4NO_2\text{-}2)_2Cl_2] + Ph_2PCH_2CH_2PPh_2 + NaClO_4 \longrightarrow$$

$$[Au(C_6H_4NO_2\text{-}2)_2(\eta^2\text{-}Ph_2PCH_2CH_2PPh_2)]ClO_4 + [NMe_4]Cl + NaCl \qquad (71)$$
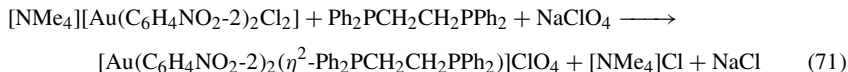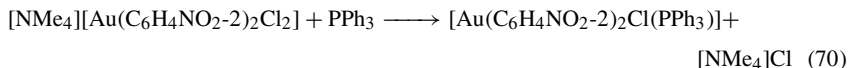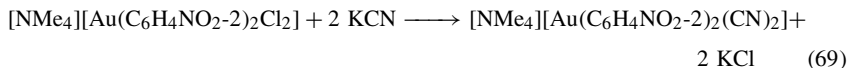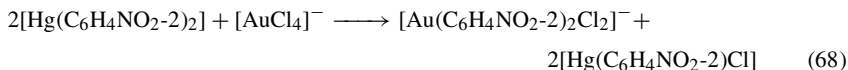
Gold is incorporated in a carbocyclic ring in the auracyclopentadiene derivative $[Au_2(\mu\text{-}Cl)_2(C_4Ph_4)_2]$. The reaction with various anionic and neutral ligands leads to cleavage of the chloride bridges and some of the resulting products are illustrated in Scheme 17[314].

2. Diorganylgold(III) complexes with group 16 donor ligands

Dimethyl(acetylacetonato)gold(III), $[AuMe_2(acac)]$ (**4**), is of great interest as a precursor for the chemical vapour deposition of gold[315].

The complex $[Au(C_4Ph_4)(acac)]$ can be prepared from the auracyclopentadiene species $[AuCl(C_4Ph_4)(SC_4H_8)]$ or $[Au_2(\mu\text{-}Cl)_2(C_4Ph_4)_2]$ by reaction with Tl(acac) and has been
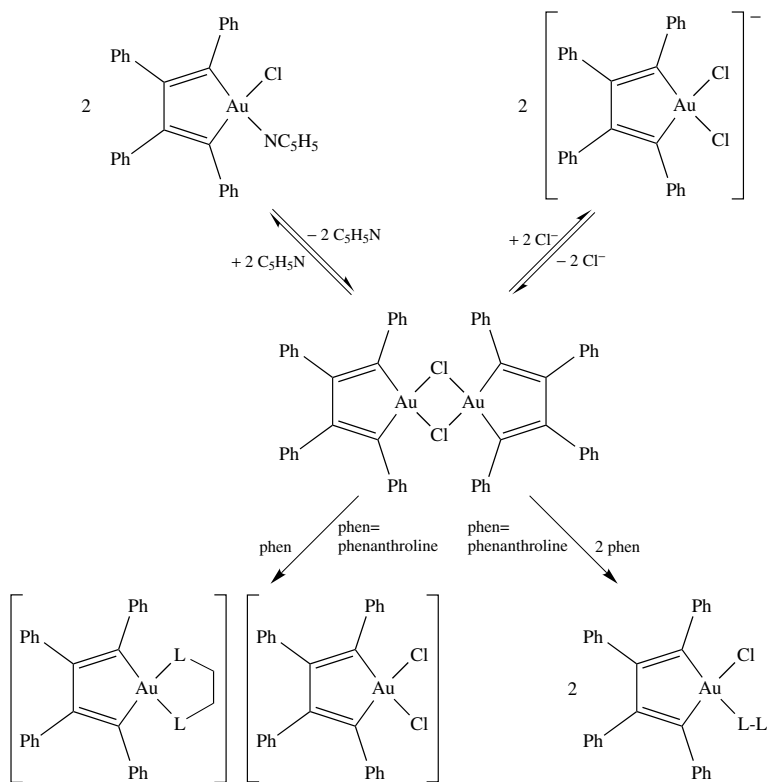
SCHEME 17. Reactions of [Au$_2$(μ-Cl)$_2$(C$_4$Ph$_4$)$_2$] with mono- and bidentate ligands
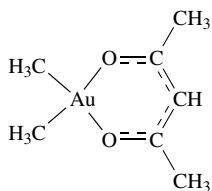
(4)

used as the starting material in the synthesis of several other complexes with oxygen donor ligands, as illustrated in Scheme 18[316].

Sulphur donor ligands have also been employed in the synthesis of several types of dialkyl- and diarylgold(III) complexes. A dimeric dimethylgold(III) thiolate may be prepared from [Au$_2$(μ-I)$_2$Me$_4$] by reaction of either sodium thiolate or sodium thioxanthate, the latter reaction proceeding through an intermediate which decomposes with liberation of carbon disulphide (Scheme 19)[317]. With other chelating
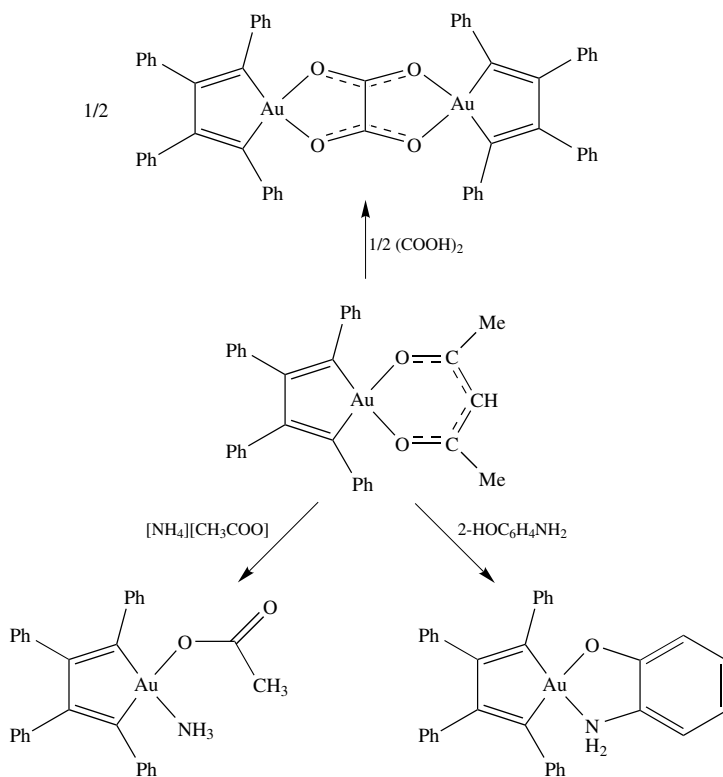
SCHEME 18. Preparation of auracyclopentadiene derivatives with O donor ligands
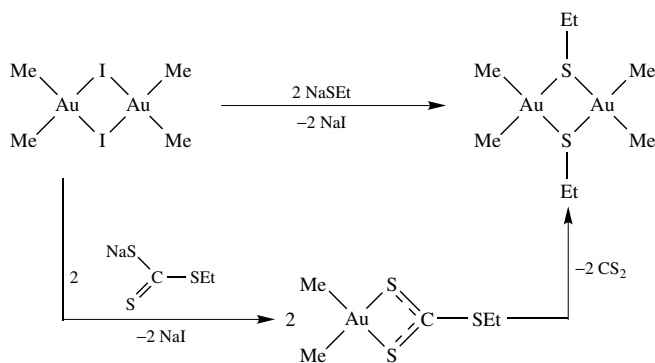
SCHEME 19. Synthesis of [Au$_2$(μ-SEt)$_2$Me$_4$]

S,S donor ligands, $[Au_2(\mu\text{-}I)_2Me_4]$ gives a variety of stable mononuclear, neutral dimethylgold(III) complexes, examples being the compounds $[Au(CH_3)_2\{S_2P(CH_3)_2\}]$ and $[Au(CH_3)_2\{(CH_3)_2P(S)NP(S)(CH_3)_2\}]$[317]. An analogous reaction is that of $[Au_2(\mu\text{-}Cl)_2(C_6F_5)_4]$ with dialkyldithiocarbamates, which leads to complexes such as $[Au(C_6F_5)_2(S_2CNMe_2)]$[318]. Diorganogold(III) dialkyldithiocarbamates have also been obtained together with other products from the oxidative addition of tetraalkylthiuram disulphides to organogold(I) complexes $[AuR(PPh_3)]$ (R = alkyl, phenyl, ferrocenyl), as illustrated in equation 72[319].

$$[Au(Fc)(PPh_3)] + Me_2NC(=S)S-SC(=S)NMe_2 \longrightarrow [Au(Fc)\{SC(=S)NMe_2\}_2]+$$
$$[Au(Fc)_2\{SC(=S)NMe_2\}] + \cdots \quad (72)$$
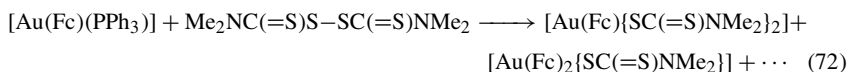
Several other compounds with chelating sulphur-containing ligands are known[320]. Treatment of cis-$[Au(C_6F_5)_2Cl(\eta^1\text{-}Ph_2PCH_2PPh_2)]$ with elemental sulphur leads to oxidation of the non-coordinated phosphorus centre to give the phosphine sulphide, which adopts a chelating bonding mode upon further reaction of the complex with $AgClO_4$. The resulting compound can be deprotonated with sodium hydride to give the methanide derivative. The reactions of these products with a variety of gold and silver compounds readily give polynuclear complexes containing carbon–metal bonds (Scheme 20)[321].
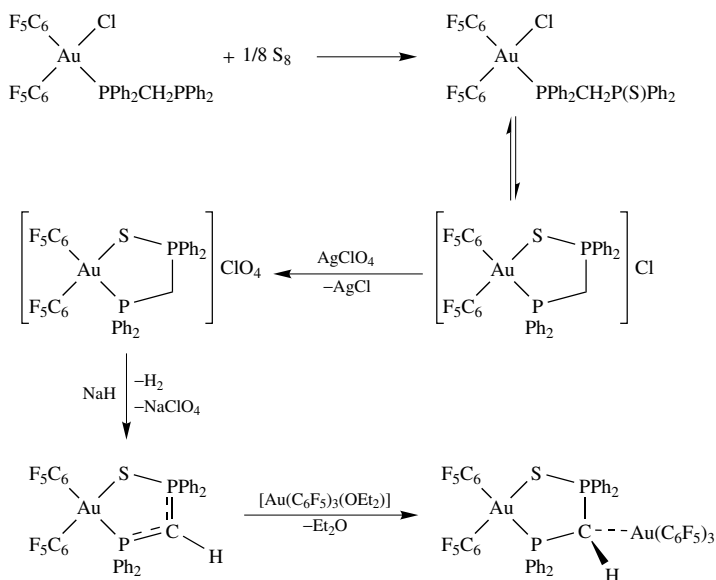
SCHEME 20. Diarylgold(III) complexes with a chelating P, S donor ligand

3. Diorganylgold(III) complexes with group 15 donor ligands

Complexes with amide ligands may be prepared by reaction of $[Au_2(\mu\text{-}I)_2Me_4]$ with metal amides. Depending on the reaction conditions, Au−N heterocycles of varying ring size are obtained (Scheme 21)[322−324].

$$[Au_2(\mu\text{-}I)_2Me_4] \begin{cases} \xrightarrow[\text{NH}_3\,(1)]{\text{KNH}_2} & \begin{array}{l}[Au_4(\mu\text{-}NH_2)_4Me_8]\,+ \\ [Au_3(\mu\text{-}NH_2)_3Me_6]\end{array} \\[2mm] \xrightarrow[\text{C}_6\text{H}_{12}/\text{Et}_2\text{O}]{\text{LiNHMe}} & [Au_2(\mu\text{-}NHMe)_2Me_4] \\[2mm] \xrightarrow[\text{Et}_2\text{O}]{\text{LiNMe}_2} & [Au_2(\mu\text{-}NMe_2)_2Me_4] \end{cases}$$
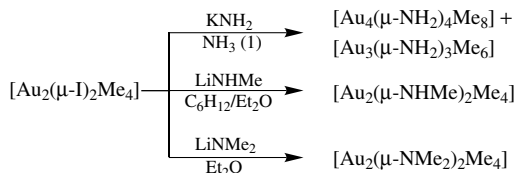
SCHEME 21. The synthesis of dimethylgold(III)amides

Dimethylgold(III) nitrate forms mononuclear complexes with a wide range of polynuclear nitrogen-donor ligands (L) containing imidazole (cf **5**)[325,326], pyridine[325−327], pyrazole (cf **6**)[325,327,328] and other functionalities[329]. A complex (**7**) with an ambidentate N,P-donor ligand derived from 1,3,5-triaza-7-phosphoniaadamantane salts has been obtained by reaction of dimethylchlorogold(III) with an equimolecular quantity of the ligand[330]. By contrast, simple pyrazole ligands (pzH) react with dimethylgold(III) nitrate in water to give dimeric complexes of the type $[AuMe_2(pz)]_2$ (**8**)[331].

(5)　　　　　　　　　　　　　(6)

(7)　　　　　　　　　　　　　(8)
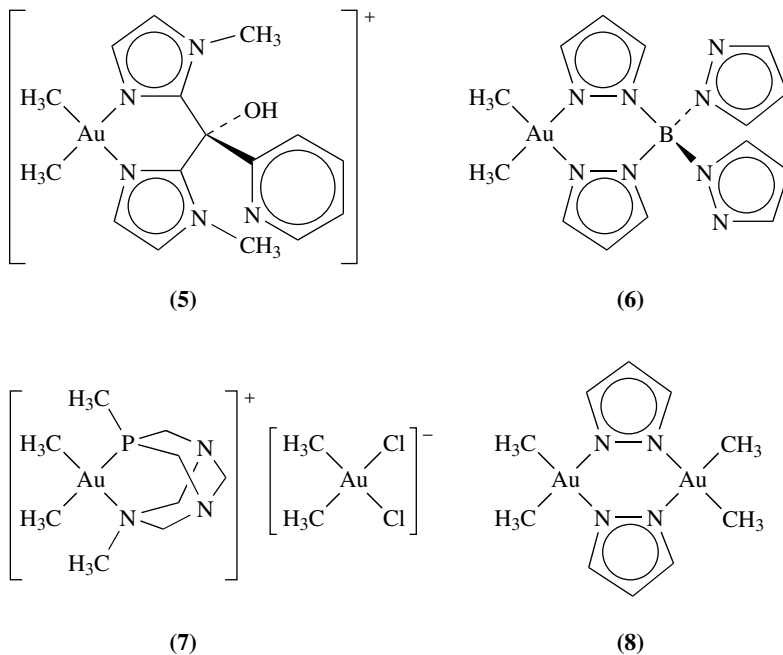
Structurally related complexes can also be prepared by the reaction of gold(III) dihalide precursors with Grignard reagents (equation 73)[332] and by treatment of the auracyclopentadiene derivative $[Au(C_4Ph_4)(acac)]$ with protonated nitrogen ligands, similar to the reactions depicted in Scheme 18[316]. The complexes prepared according to equation 73

show interesting luminescence properties[332].

(73)
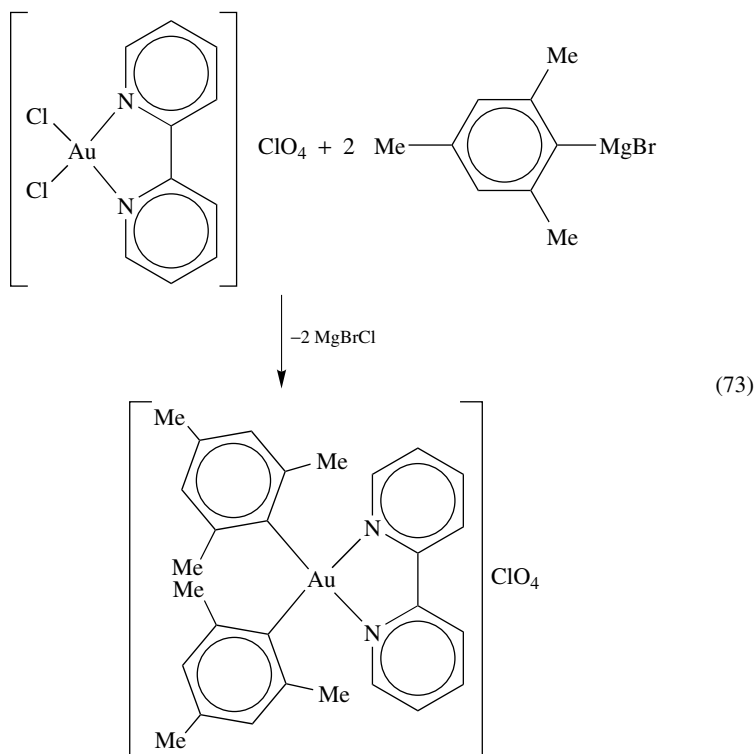
Several types of diarylgold(III) complexes with chelating C,N-donor ligands are known which can be prepared by arylation of suitable gold(III) precursors with organomercury(II) reagents[11,12]. An example is shown in Scheme 22[333]. The analogous complexes with Ar $= \eta^2$-{C$_6$H$_4$(CH$_2$NMe$_2$)-2} have also been prepared[334]. Sequential arylation allows the synthesis of complexes with two different aryl ligands, as illustrated in Scheme 23[335]. The doubly C,N-chelated cationic complexes can be derivatized further by reactions with anionic (halide, cyanide, acetate) or neutral ligands (pyridine).

Sequential arylation has also been used to prepare diarylgold(III) complexes in which the second aryl ligand does not carry a potential donor group, and complexes such as **9** and **10** have been obtained from reactions analogous to the first step in Scheme 23[336−339]. The chlorine ligand in these complexes is readily substituted and bromide, iodide and acetate derivatives as well as a cationic pyridine adduct have been synthesized, together with other related species.

Upon treatment with phosphine or chloride, some of the C,N-chelated diarylgold(III) chloride complexes undergo reductive elimination of the aryl ligands to give biaryls. The high-yield reaction proceeds at room temperature and can be used for the synthesis of

$[NMe_4][AuCl_4] \ + \ [Hg\{C_6H_4(N{=\!=}NPh)\text{-}2\}_2]$

$- \ 1/2 \ [NMe_4]_2[Hg_2Cl_6]$
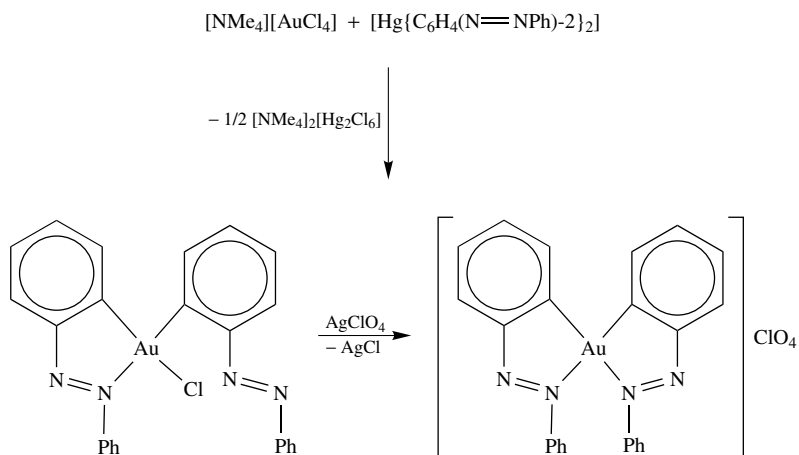
SCHEME 22. Synthesis of diarylgold(III) complexes using organomercury(II) reagents

$+ \ [Hg\{C_6H_4(N{=\!=}NPh)\text{-}2\}_2]$

$- \ [Hg\{C_6H_4(N{=\!=}NPh)\text{-}2\}Cl]$
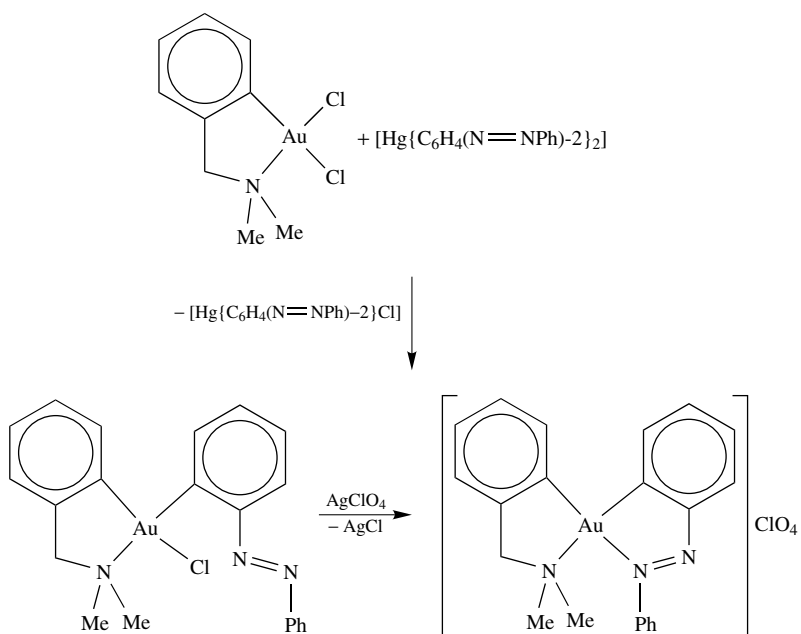
SCHEME 23. Synthesis of diarylgold(III) complexes using organomercury(II) reagents

(9)   **(10)**
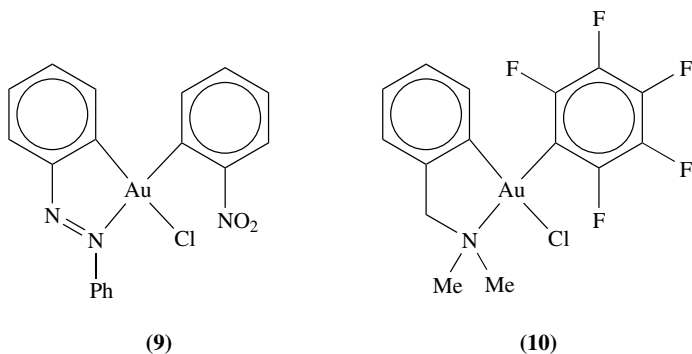
both symmetrical and asymmetrical products. An example is given in equation 74[340].

$$\xrightarrow[-[\text{AuCl(PPh}_3)]]{\text{PPh}_3}$$

(74)
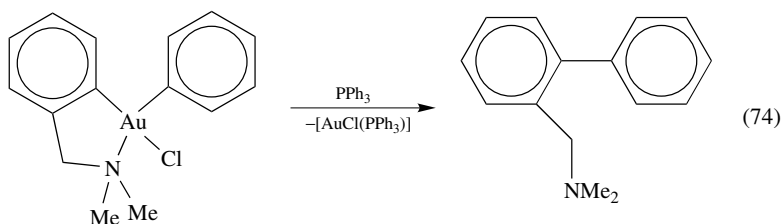
Gold(III) complexes with one aryl and one acetonyl ligand form as products of an unusual auration of acetone[341]. Thus $[\text{Au}\{\eta^2\text{-C}_6\text{H}_4(\text{N}=\text{NPh})\text{-2}\}\text{Cl}_2]$, when treated in acetone with various reagents such as Tl(acac), KCN, AgClO$_4$, 1,10-phenanthroline or diarylmercury(II) compounds (e.g. [Hg(C$_6$F$_5$)$_2$]), gives $[\text{Au}\{\eta^2\text{-C}_6\text{H}_4(\text{N}=\text{NPh})\text{-2}\}(\eta^1\text{-CH}_2\text{COMe})\text{Cl}]$ as the final product[297]. Some intermediates of this process have been isolated (Scheme 24) and the C−H activation of other ketones has also been studied[342]. Like the diaryl complexes described above, the aryl acetonyl complexes can be derivatized in various ways, either by substitution of the chloride ligand or by cleavage of the gold–nitrogen bond with other donor ligands[343]. Some of these chloro or triphenylphosphine derivatives undergo a reductive elimination of both aryl and acetonyl ligands in a similar way as shown in equation 74[344].

Several diarylgold(III) complexes with monodentate alkyldiphenylphosphonio(diphenylphosphino)methanide ligands have been prepared. These compounds react with sodium hydride to give the corresponding methanide complexes, which in turn may be transformed into polynuclear gold(III)/gold(I) complexes upon treatment with gold(I) reagents containing labile ligands (Scheme 25)[320].

Most other reported diorganylgold(III) complexes with phosphorus donor ligands contain difunctional phosphines such as bis(diphenylphosphino)methane (dppm) or closely related species[56,239,320,345−347]. Dimeric $[\text{Au}_2(\mu\text{-Cl})_2(\text{C}_6\text{F}_5)_4]$ may be cleaved with dppm to give [Au(C$_6$F$_5$)$_2$Cl(dppm)], which upon reaction with AgClO$_4$ forms the cationic complex [Au(C$_6$F$_5$)$_2$(dppm)]ClO$_4$. This is transformed into the deprotonated complex [Au(C$_6$F$_5$)$_2$(Ph$_2$PCHPPh$_2$)] by treatment with sodium hydride. This compound as well as the related complex with tris(diphenylphosphino)methane can be alternatively prepared by direct reaction of the phosphine with [Au(C$_6$F$_5$)$_2$(acac)] under mild reaction
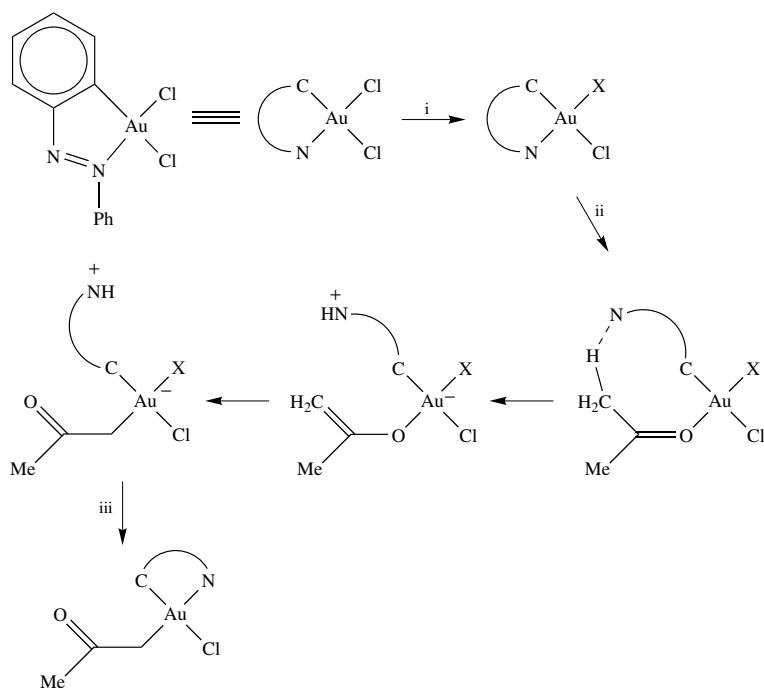
SCHEME 24. Proposed mechanism for the C−H activation of ketones with 2-(phenylazo)-phenyl-gold(III) complexes; (i) +HX; X = acac-C, CN, $C_6H_4(N=NPh)$-2, C_6F_5 or $C_6H_4NO_2$-2; (ii) +Me_2CO; (iii) - HX
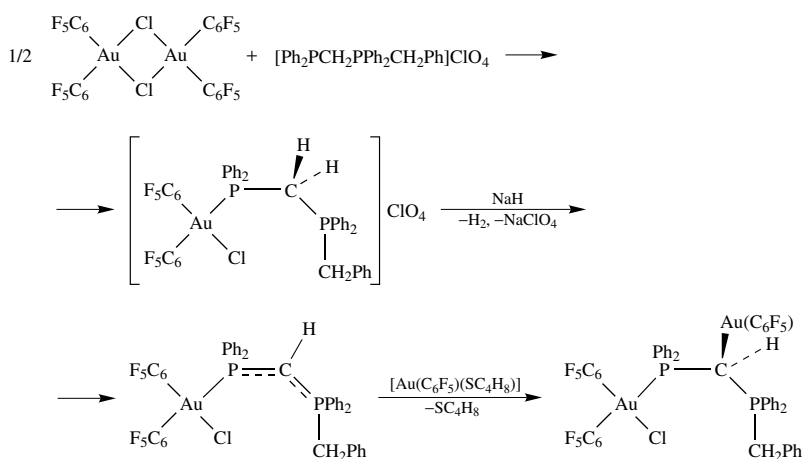
SCHEME 25. Synthesis of alkyldiphenylphosphonio(diphenylphosphino)methanide complexes of gold(III)

conditions[345]. The methanide derivatives can then react further with gold(I) or gold(III) complexes to yield di- or trinuclear complexes such as $[(C_6F_5)_2Au\{(Ph_2P)_2CHAu(C_6F_5)\}]$ or cis-$[\{(C_6F_5)_2Au\{(Ph_2P)_2CPPh_2\}\}_2Au(C_6F_5)_2]ClO_4$. The preparation of the latter is summarized in Scheme 26. A hexanuclear gold(III)/gold(I) complex with four methanide bridging units has also been described[353]. Deprotonation and metallation to give polynuclear methanediide derivatives is also possible with dppm. A comprehensive review of these complexes has appeared[320].
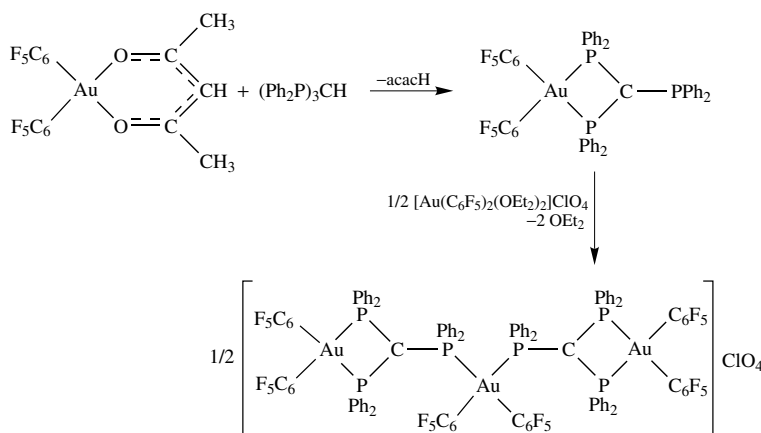
SCHEME 26. Synthesis of polynuclear diarylgold(III) complexes containing diphosphinomethanide ligands

G. Gold(III) Complexes with Three Gold−Carbon Bonds

The principal methods available for the synthesis of compounds containing three alkyl and/or aryl ligands are the reactions of suitable gold(III) halide complexes with organolithium or Grignard reagents and the oxidative arylation of gold(I) complexes with organothallium(III) compounds[11−13]. Specific examples for these reactions are given in equations 75[348], 76[349] and 77[350] and a selection of complexes of this type is presented in Table 13.

$$Au_2Br_6 \xrightarrow[\text{2. 2 PMe}_3]{\text{1. 6 MeLi; −6 LiBr}} 2[AuMe_3(PMe_3)] \tag{75}$$

$$cis\text{-}[AuIMe_2(PPh_3)] + PhMgBr \longrightarrow cis\text{-}[AuMe_2Ph(PPh_3)] + MgBrI \tag{76}$$

$$[Au(C_6F_5)(SC_4H_8)] + [Tl(C_6F_5)_2Cl] \longrightarrow [Au(C_6F_5)_3(SC_4H_8)] + TlCl \tag{77}$$
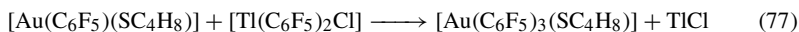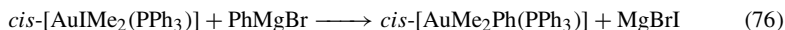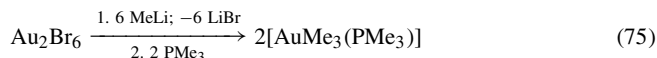
Some tris(trifluoromethyl)gold(III) complexes are also known. $[Au(CF_3)_3(PMe_3)]$ can be synthesized in high yield by treatment of $[AuI(CF_3)_2(PMe_3)]$ with $[Cd(CF_3)_2] \cdot DME$ (DME $= 1, 2$-dimethoxyethane) in the presence of an excess of trifluoromethyl iodide (equation 78)[21]. The complex has also been obtained by donor ligand stabilization of $[Au(CF_3)_3]$, which can be generated by cocondensation of gold atoms with CF_3 radicals[356]. The related complex $[Au(CF_3)_3(PEt_3)]$ is reported to form when CF_3I and

TABLE 13.   Some gold(III) complexes of the types [AuR$_3$L] and [AuR$_2$R$'$L]

Complex	M.p.($^\circ$C)	Reference
[AuMe$_3$(PMe$_3$)]	—	348
[Au(CF$_3$)$_3$(PMe$_3$)]	—	21
[Au(CF$_3$)$_3$(PEt$_3$)]	—	22
cis-[AuMe$_2$Et(PPh$_3$)]	—	351
cis-[AuMe$_2$\{η^1-CH$_2$C(Me)=CH$_2$\}(PPh$_3$)]	—	352
cis-[AuMe$_2$ (trans-MeCH=CH)(PPh$_3$)]	—	351
cis-[AuMe$_2$(C≡CPh)(PPh$_3$)]	—	351
cis-[AuMe$_2$Ph(PPh$_3$)]	101(d)	351
cis-[AuMe$_2$Ph\{P(C$_6$H$_4$OMe-4)$_3$\}]	113(d)	349
cis-[AuMe$_2$Ph\{P(C$_6$H$_4$F-4)$_3$\}]	115(d)	349
cis-[AuMe$_2$(COOMe)(PPh$_3$)]	124(d)	353
cis-[AuMe$_2$(COOEt)(PPh$_3$)]	130(d)	353
cis-[AuMe$_2$(COOPr-i)(PPh$_3$)]	120(d)	353
[Au(C$_6$F$_5$)$_3$(SC$_4$H$_8$)]	190	350
[Au(C$_6$F$_5$)$_3$\{S(MeS)CNH(C$_6$H$_4$Me-4)\}]	131	100
[Au(C$_6$F$_5$)$_3$(OEt$_2$)]	—	354
[Au(C$_6$F$_5$)$_3$(O=CMe$_2$)]	—	354
[Au(C$_6$F$_5$)$_3$(OAsPh$_3$)]	157	354
[Au(C$_6$F$_5$)$_3$(η^1-Ph$_2$AsCH$_2$AsPh$_2$)]	197	107
[Au(C$_6$F$_5$)$_3$(η^1-SPh$_2$PCH$_2$PPh$_2$Me)]$^+$	138	331
[Au$_2$(C$_6$F$_5$)$_6$(μ-Ph$_2$P-\{Fc$'$\}-PPh$_2$)]^a	260	114
[Au$_2$(C$_6$F$_5$)$_6$(μ-S$_2$CNEt$_2$)]$^-$	203	318
[Au$_2$(C$_6$F$_5$)$_6$(μ-S$_2$CPBu$_3$)]	152	117
[\{(C$_6$F$_5$)$_3$Au(μ-Ph$_2$PCHPPh$_2$)\}$_2$Au]$^-$	80(d)	196
[\{(C$_6$F$_5$)$_3$Au\{μ-Ph$_2$PC(AuPPh$_3$)$_2$PPh$_2$\}\}$_2$Au]$^+$	99(d)	196
[Au(C$_6$Cl$_5$)$_3$(SC$_4$H$_8$)]	150(d)	355
[Au(C$_6$Cl$_5$)$_3$Cl]$^-$	145(d)	355

^{a}\{Fc$'$\}; 1,1$'$-ferrocenediyl.

[Au(CF$_3$)(PEt$_3$)] are reacted over extended periods of time (>10 days)[22].

$$2[AuI(CF_3)(PMe_3)] + [Cd(CF_3)_2] \cdot DME + 2\,CF_3I \longrightarrow 2[Au(CF_3)_3(PMe_3)]+$$

$$+DME + CdI_2 \quad (78)$$
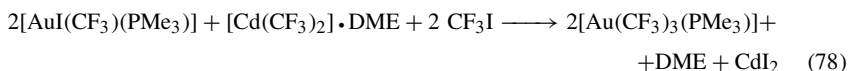
The mixed compounds of the type [AuMe$_2$R(PR$'_3$)] (R = alkyl, alkenyl, alkynyl, aryl; R$'$ = alkyl, aryl) often have cis stereochemistry, as indicated by NMR data[349,352,357,358]. When heated, both the trimethyl- and the mixed cis-dimethyl(organyl)(phosphine)gold(III) complexes undergo reductive elimination of two organic groups after dissociation of the phosphine ligand, a reaction which is important for the catalytic coupling between alkyl-lithium reagents and alkyl halides[348]. As illustrated in Scheme 27, two types of product may form in the case of the mixed complexes. While reductive elimination of R−Me is predominant when R = alkenyl or aryl, the formation of ethane is favoured when R is

Me
|
Me — Au — L $\rightleftharpoons$ Me — Au + L → RMe + [AuMeL]
|
R   R

→ C$_2$H$_6$ + [AuRL]
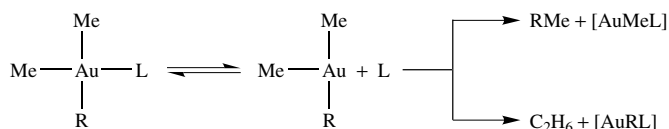
SCHEME 27. Mechanism of thermolysis of *cis*-dimethylorganylgold(III) compounds

an alkynyl or an electron-withdrawing alkyl group[351]. In addition to electronic effects, the selectivity of the process also depends on the steric demand of both the phosphine ligand and R[349,357]. In another type of reaction, dimethylarylgold(III) complexes undergo selective cleavage of the gold–aryl bond when treated with electrophiles such as HCl, HgCl$_2$ or [PtI$_2$(PMe$_2$Ph)$_2$], the gold-containing products being complexes of the type *cis*-[AuXMe$_2$(PPh$_3$)] (X = Cl or I)[358]. Similar processes take place with dimethylallylgold(III) derivatives and their reaction with aldehydes and ketones gives homoallyl alcohols, with C–C bond formation selectively at the γ-position of the η^1-allyl moiety[352]. An example of these reactions is represented in equation 79.

(79)

R = CH(CN)$_2$, C≡CPh
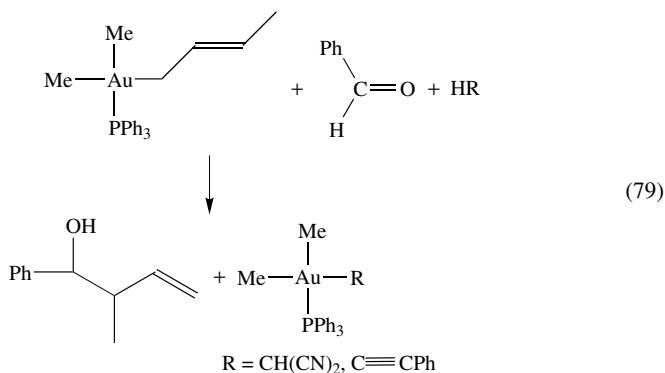
A related group of compounds is that of the gold(III) dimethyl(alkoxycarbonyl) complexes, accessible by the reaction of carbon monoxide with dimethyl(alkoxy)(triphenylphosphine)gold(III), which is prepared *in situ* from *cis*-[AuIMe$_2$(PPh$_3$)] and sodium alkoxide in methanol (equation 80)[353,359]. Thermolysis of the methoxycarbonyl complex in benzene leads to the reductive elimination of methyl acetate and ethane, indicating competition between the two modes of decomposition illustrated in Scheme 27. The reaction of the same complex with electrophiles such as hydrogen chloride proceeds with liberation of carbon monoxide and methanol, as illustrated in equation 81.

$$cis\text{-}[AuIMe_2(PPh_3)] + NaOMe/MeOH + CO \longrightarrow cis\text{-}[AuMe_2(COOMe)(PPh_3)] \quad (80)$$

$$cis\text{-}[AuMe_2(COOMe)(PPh_3)] + HCl \longrightarrow cis\text{-}[AuClMe_2(PPh_3)] + MeOH + CO \quad (81)$$
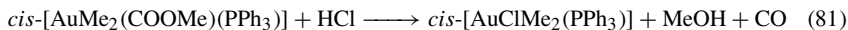
As regards triarylgold(III) complexes, only polyhalophenyl derivatives are known. [Au(C$_6$F$_5$)$_3$(SC$_4$H$_8$)] is a useful precursor for the preparation of a wide variety of other compounds by ligand substitution. It reacts with neutral [L = NH$_3$, C$_5$H$_5$N, P(OPh)$_3$,

$$[NBu_4] \begin{bmatrix} (F_5C_6)_3AuS & & Et \\ & C = N & \\ (F_5C_6)_3AuS & & Et \end{bmatrix}$$

(11)

$$\begin{array}{c} (F_5C_6)_3AuS \\ \diagdown \\ C \equiv\!\!= PEt_3 \\ \diagup \\ (F_5C_6)_3AuS \end{array}$$

(12)

2 [AuR$_3$(Ph$_2$PCH$_2$PPh$_2$)] $\xrightarrow[-2\ SC_4H_8]{[Au(SC_4H_8)_2]ClO_4}$ 1/2
R = C$_6$F$_5$
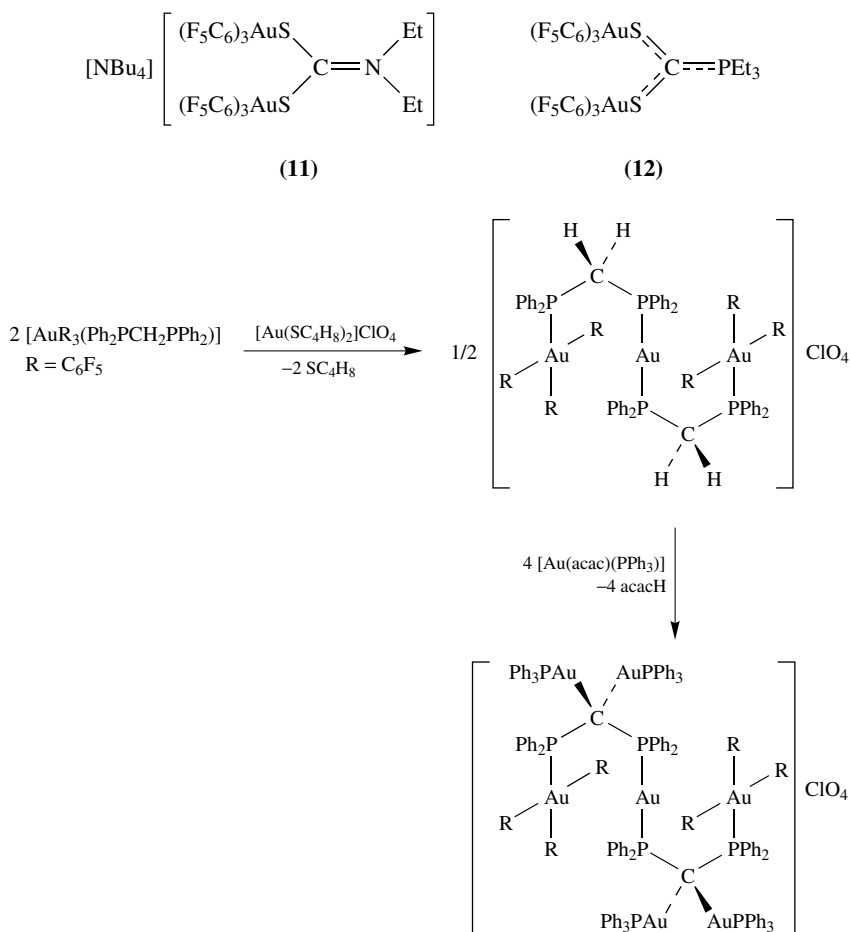
SCHEME 28. Preparation of a heptanuclear trialkylgold complex with two C(AuPPh$_3$)$_2$ units

AsPh$_3$, SbPh$_3$, CNC$_6$H$_4$Me-4][350] or anionic ligands (X = Cl, Br, I, SCN, N$_3$)[350,355] to give complexes of the types [Au(C$_6$F$_5$)$_3$L] and [Au(C$_6$F$_5$)$_3$X]$^-$, and dinuclear derivatives (for example **11** and **12**[117]) have been similarly obtained from the reaction with bridging ligands[107,114,117,350]. The diphosphine complex [Au(C$_6$F$_5$)$_3$(Ph$_2$PCH$_2$PPh$_2$)] can be used as a precursor for the preparation of polynuclear gold(III)/gold(I) phosphino and methanide complexes[53,196]. The synthesis of a heptanuclear product with two [C(AuPPh$_3$)$_2$] units is illustrated in Scheme 28. The complex [Au(C$_6$F$_5$)$_3$(OEt$_2$)][354], prepared according to equation 82, is another useful starting material as the ether molecule is displaced even more readily, allowing the synthesis of compounds which are inaccessible
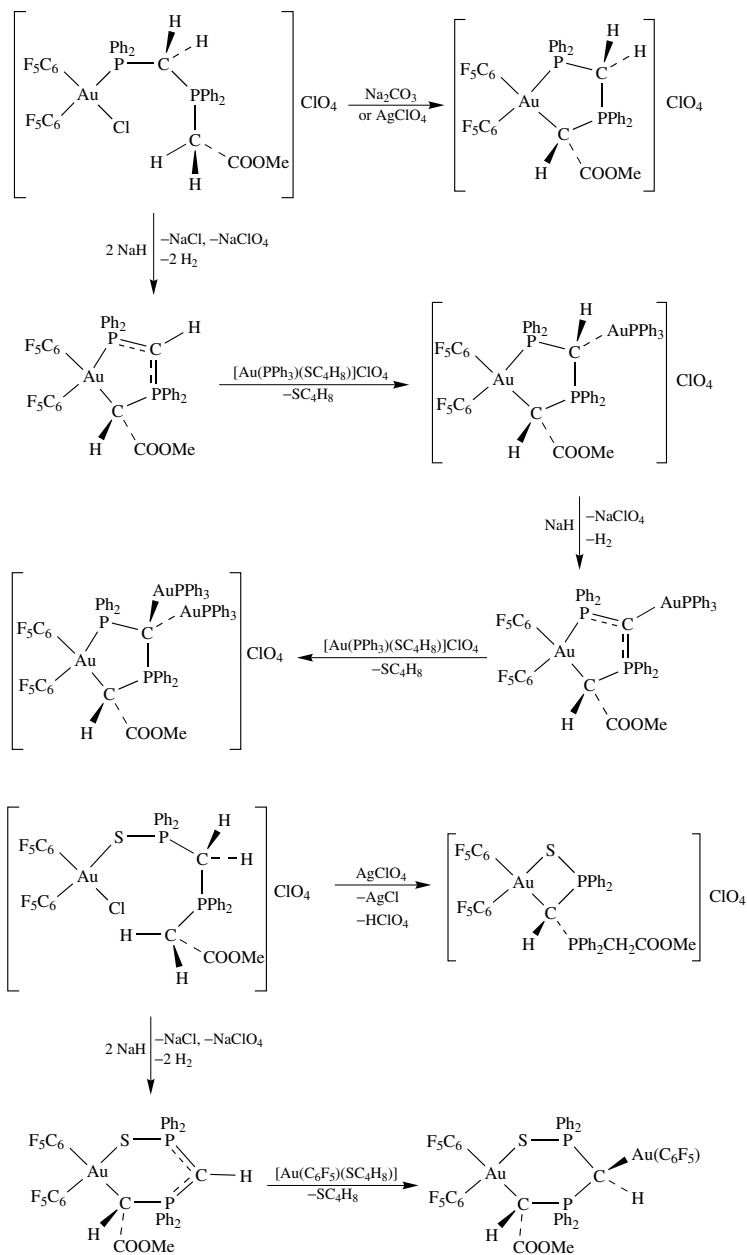
SCHEME 29. Preparation of methanide auracycles from different diarylgold(III) phosphinophosphonium salts

from the thiophene adduct (equation 83)[100,119,231].

$$[NBu_4][Au(C_6F_5)_3Br] + AgClO_4 \xrightarrow[\substack{- AgBr \\ -[NBu_4]ClO_4}]{Et_2O} [Au(C_6F_5)_3(OEt_2)] \qquad (82)$$

$$[Au(C_6F_5)_3(OEt_2)] + C_5H_5NS \xrightarrow{-Et_2O} \qquad (83)$$
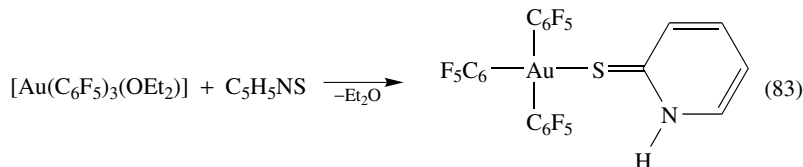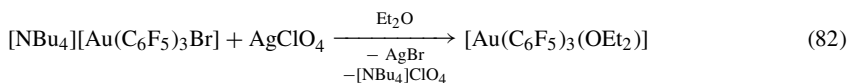
Gold(III) complexes with two aryl ligands and one methanide ligand have also been prepared, as illustrated in Scheme 29[320,360,361]. The synthesis starts from diarylgold(III) precursors containing substituted phosphinophosphonium ligands, which adopt a chelating bonding mode upon deprotonation. Depending on the reaction conditions, chelate rings of varying size may be obtained. Thus, Na_2CO_3 or $AgClO_4$ as deprotonating agents effect single deprotonation and simultaneous halide abstraction, leading to cationic four- or five-membered auracycles, while NaH deprotonates both CH_2 groups to give neutral complexes containing five- or six-membered rings, whose methanide carbon atoms can serve as electron donors to other metal centres, thus forming polynuclear derivatives. Sequential deprotonation and metallation of the same methylene group is also possible, giving five-membered methanediide auracycles with a $[>C(AuPPh_3)_2]$ structural unit which resembles that found in certain diauriomethanes[362]. Analogous reactions have also been carried out with gold(III) complexes of bis(diphenylphosphino)methane disulphide[118].

H. Gold(III) Complexes with Four Gold−Carbon Bonds

The simplest compounds of this type are the tetraalkylaurates(III), prepared by the reaction of trialkyl(triphenylphosphine)gold(III) complexes with alkyllithiums, which proceeds by phosphine displacement as illustrated in equation 84. Recent studies have shown the reaction to be stereoselective, with *cis-* (or *trans-*) dimethylalkylgold(III) complexes giving square planar *cis-* (or *trans-*) tetraalkylaurates and an associative mechanism involving a pentacoordinate gold(III) intermediate has been postulated[363].

$$cis\text{-}[AuMe_2Et(PPh_3)] + LiEt \longrightarrow Li\{cis\text{-}[AuMe_2Et_2]\} + PPh_3 \qquad (84)$$
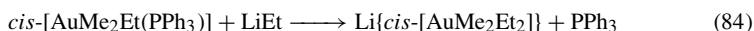
The novel tetrakis(trifluoromethyl)aurate(III) anion has been employed to prepare two distinct phases of $\kappa\text{-}(ET)_2Au(CF_3)_4 \cdot (TCE)$ [ET = bis(ethylenedisulphanyl) tetrathiafulvalene, TCE = 1,1,2-trichloroethane], which are superconductors at ambient pressure at low temperatures[363].

Several tetraaurates(III) are known[364,256]. Tetraarylaurate(III) complexes containing polyhalophenyl ligands[11,12] are best prepared by further arylation of triarylhaloaurates(III) with $Ag(C_6F_5)$ (equation 85)[350].

$$[N(PPh_3)_2][Au(C_6F_5)_3Cl] + Ag(C_6F_5) \longrightarrow [N(PPh_3)_2][Au(C_6F_5)_4] + AgCl \qquad (85)$$
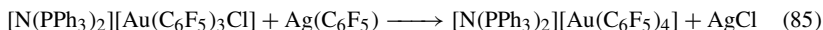
The stable hydrogen dimethyl-bis(2-pyridyl)-aurate(III) is prepared by the reaction of *cis*-dimethyliodo(triphenylphosphine)gold(III) with 2-pyridyllithium at low temperature

and subsequent hydrolysis (equation 86)[365].

$$(86)$$
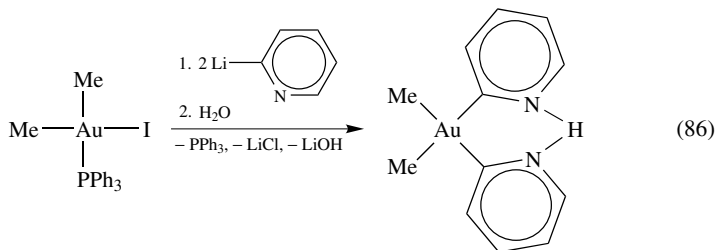
III. HOMO- AND HETEROMETALLIC GOLD CLUSTERS CONTAINING GOLD−CARBON BONDS

Of the many gold cluster compounds in which the metal has an oxidation state between 0 and +1, only very few also feature bonds between gold and carbon[4,13]. A recent example is the neutral cluster $[Au_{10}(C_6F_5)_4(PPh_3)_5]$, prepared selectively by the reaction of $[Au_9(PPh_3)_8](NO_3)_3$ with $[NBu_4][Au(C_6F_5)_2]$ in a 1 : 3 molar ratio[366].

Species such as $[Au_8(PPh_3)_7(CNBu\text{-}t)](NO_3)_2$ and $[Au_9(PPh_3)_6(CNBu\text{-}t)_2](NO_3)_3$ have been prepared by the addition of one equivalent of isocyanide to the starting material $[Au_8(PPh_3)_7](NO_3)_2$ and by isocyanide-induced displacement of phosphine ligands in $[Au_9(PPh_3)_8](NO_3)_3$, respectively. The reactivity of the products towards halide ions and amines has been studied[367]. Ligand displacement in related platinum−gold clusters has led to species such as $[PtAu_8(PPh_3)_7(CNBu\text{-}t)_2](NO_3)_2$[368].
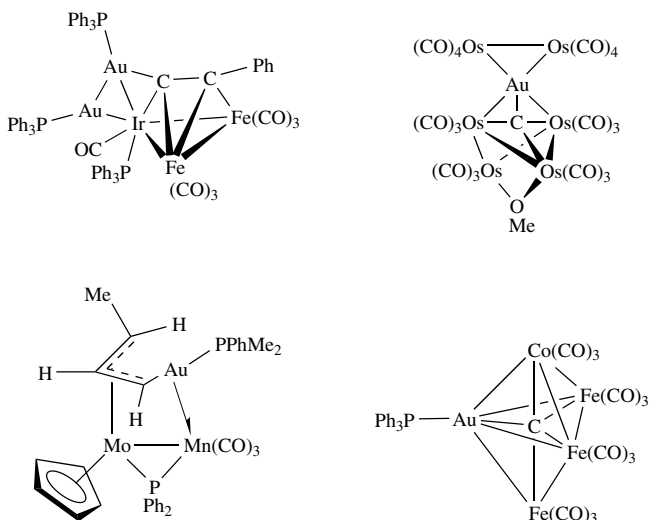
FIGURE 12. Heterometallic cluster compounds of monovalent gold containing gold−carbon bonds

Heterometallic cluster compounds of gold can often be prepared by treating suitable substrates with aurating agents such as [AuCl(PPh$_3$)] or [O(AuPPh$_3$)$_3$][BF$_4$][369]. The reaction has served to determine the extent of structural analogies between isolobal hydrido and L−Au clusters. A variety of substrates has been studied in this context, some of them containing alkyne[370] or carbido ligands[371]. Auration may involve the metal framework and/or the organic ligand[372]. In a related reaction, it was possible to replace an agostic hydrogen atom of a metal-coordinated allyl group by an isolobal gold ligand[373]. Examples of the various kinds of compounds which have recently been prepared are collected in Figure 12[370,371,373,374].

IV. SYNTHESIS AND PROPERTIES OF ALKENE, ALKYNE, CARBENE AND RELATED COMPLEXES OF GOLD

Complexes of zero valent gold (in the form of atoms or at the surface of the bulk metal) and unsaturated molecules such as alkenes[375,376], alkynes[376,377], allenes[378], arenes[379] or fullerenes[380] were the subject of a number of experimental studies. Molecular species which are formed by low-temperature cocondensation of gold atoms with unsaturated organic substrates have been characterized by their infrared/Raman, UV-visible absorption and ESR spectra, but the interpretation of these data is not without contradictions[377,378,381].

Olefin complexes of gold(I) can be prepared either by the reaction of tetrachloroauric acid with the olefin or directly from the olefin and gold(I) halide[13,15]. While such species usually have poor stability and decompose in solution at room temperature, the *cis*-cyclooctene and norbornene complexes of AuCl, obtained from the reaction of [AuCl(CO)] with the corresponding olefin by a CO displacement reaction, have been found to be less prone to decomposition[382]. An (olefin)gold(I) complex featuring a tetracoordinate environment for the gold centre bonded to the olefin has recently been obtained according to the procedure shown in equation 87[383].

(87)
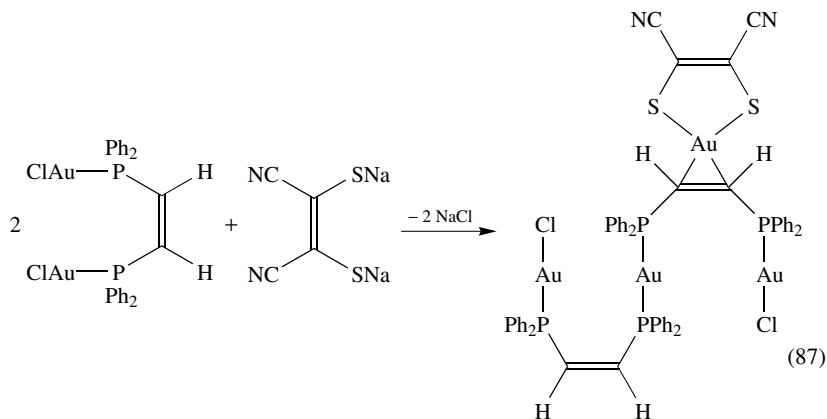
It has been noted that metal−carbon triple bonds behave in a similar way as alkynes with respect to π-complex formation[13,15]. Various heterometallic gold complexes with bridging carbyne ligands reflect this analogy. Alkylidyne complexes like [W(≡CR)(CO)$_2$(η^5-C$_5$H$_5$)], [W(≡CR)(CO)$_2$(η^5-C$_2$B$_9$H$_9$R$_2'$)]$^-$ (R = alkyl, aryl, amino; R$'$ = H, Me) readily
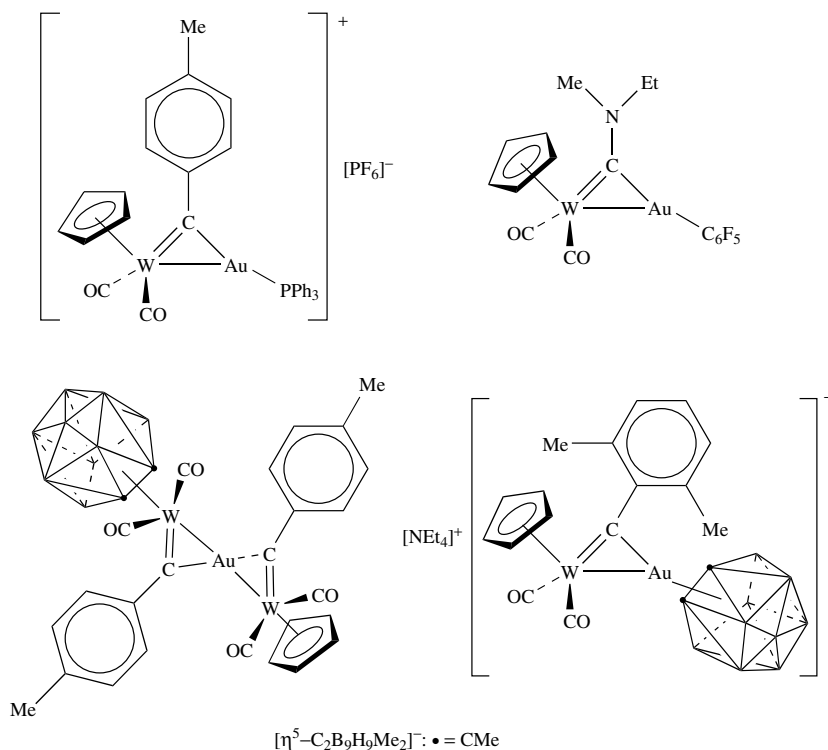
$[\eta^5-C_2B_9H_9Me_2]^-: \bullet = CMe$

FIGURE 13. Dimetallacyclopropene complexes obtained in the addition of gold(I) fragments to metal alkylidyne complexes

react with [AuCl(PPh$_3$)] or [AuX(SC$_4$H$_8$)]$^{n-}$ ($n = 0$, X = Cl, C$_6$F$_5$; $n = 1$, X = C$_2$B$_9$H$_9$Me$_2$) to give cationic, neutral or anionic dimetallacyclopropene species, formed by addition of a gold(I) fragment to the metal–ligand multiple bond (Figure 13)[384−387]. Trinuclear compounds in which an alkylidyne ligand caps a triangle of metal atoms have been obtained in an analogous way[386−388]. A review of these gold complexes and related copper species has appeared[389].

Four main methods have been established for the preparation of gold carbene complexes and a large number of compounds are known.

(a) The most important preparation uses the nucleophilic addition of alcohols or amines to gold-coordinated isocyanides (equation 88)[390]:

$$p\text{-MeC}_6\text{H}_4\text{NCAuCl} + \text{CH}_3\text{OH} \longrightarrow \begin{array}{c} p\text{-MeC}_6\text{H}_4\text{NH} \\ \diagdown \\ \text{C-Au-Cl} \\ \diagup \\ \text{CH}_3\text{O} \end{array} \qquad (88)$$
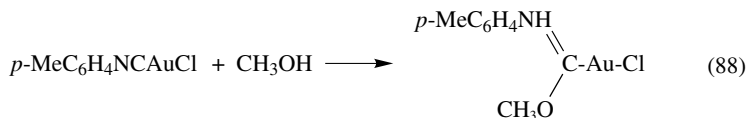
Similarly, diisocyanide compounds, $[Au(R^1NC)_2]^+$ (R^1 = aryl), give cationic bis(carbene) complexes, which can be further oxidized with I_2 to gold(III) carbene complexes (equation 89)[391−394]:

$$\left[\begin{array}{c} X \\ \diagdown \\ C{-}Au{-}C \\ \diagup \qquad \diagdown \\ R'HN \qquad\qquad NHR' \end{array}\right]^+ \;+\; I_2 \;\longrightarrow\; \left[\begin{array}{c} X \quad\; I \quad\; X \\ \diagdown \;\;|\;\; \diagup \\ C{-}Au{-}C \\ \diagup \;\;|\;\; \diagdown \\ R'HN \quad I \quad NHR' \end{array}\right]^+ \tag{89}$$
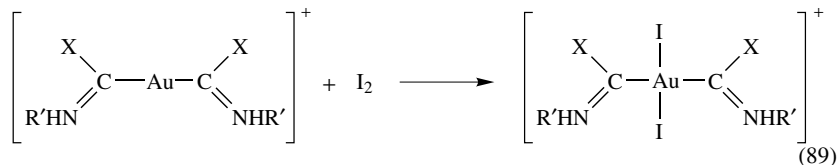
where $X = NR^2R^3$ or OR^4 and R^2, R^3 and R^4 are organic groups.

Amines react in general more readily than alcohols and aromatic isocyanides are more reactive than aliphatic ones. The ionic diisocyanide complexes react under milder conditions than the neutral monoisocyanide complexes[395,396]. No reactions with mercaptanes have been reported. Acyclic aminocarbene complexes occur as isomers when $R^1 \neq R^2$ due to restricted rotation around the C(carbene)−N bond[397]. Dinuclear carbene complexes are formed when the amine complexes $[Au(C_6F_5)NH_2(CH_2)_nNH_2]$ (n = 1 or 2) or the carbene complexes $[(C_6F_5)_mAuC(NHR)NH(CH_2)_nNH_2]$ (m = 1 or 3) are treated with the isocyanide compound $[(C_6F_5)_mAuCNR]$ (R = Ph or p-tolyl)[398].

The same principle is also utilized, albeit in somewhat modified form, when $[AuCl_4]^-$ is treated with isocyanides and an excess of amine to yield bis(carbene) complexes (equation 90)[399].

$$AuCl_4^- \;+\; R'NC \;+\; R''NH_2 \;\longrightarrow\; \left[Au\left(C{\begin{array}{c} NHR'' \\ \diagup \\ \diagdown \\ NHR' \end{array}}\right)_2\right]^+ \;+\cdots \tag{90}$$
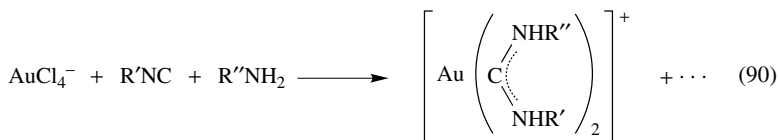
The aliphatic derivatives have been oxidized with I_2 to their gold(III) analogues. In a further unique application of this method, isocyanides with OH groups in position 2 or 3 become activated by $[AuCl_4]^-$ and undergo an internal attack by the OH group on the isocyanide to give heterocyclic carbene complexes. Excess isocyanide leads to reduction of the initially formed gold(III) complex to afford both mono- and bis(carbene) complexes of gold(I) (Scheme 30)[400].

In a modification of this reaction, the use of isocyanide becomes unnecessary when $H[Au(CN)_2]$ reacts with propene oxide or styrene oxide to yield (cyano)carbene complexes of the same family (Scheme 31)[401].

Organogold carbene compounds $[Au(carbene)(CN)_{m-1}R_n]$ can be obtained from complexed cyanides $[Au(CN)_m(C_6F_5)_n]^-$ (n = 1 or 3, m = 1 and n = m = 2) by sequential alkylation (to form isocyanide complexes) and nucleophilic attack of amine[402]. Gold(III) diisocyanides $[Au(CNR)_2(C_6F_5)_2]^+$ (R = Ph or p-tolyl), which can also be obtained by isocyanide substitution of ether in $[Au(C_6F_5)_2(OEt_2)_2]^+$, react with hydrazobenzene NH(Ph)NHPh and hydrazine or phenylhydrazine according to the reactions in Scheme 32 to furnish cyclic bis(carbene) and cyclic carbene-imidoyl compounds[403].

The amine addition to a coordinated isocyanide finds application for a cyclization reaction[404]. μ-(1,2-Diisocyanobenzene)bis(chlorogold) reacts with methylamine, aniline

$$AuCl_4^- \ + \ HO(CH_2)_nNC \ \longrightarrow \ Cl_3Au-C \underset{O-CH_2}{\overset{NH-(CH_2)_n}{\diagdown}}$$

n = 2 or 3   n = 1 or 2

excess isocyanide ↓

$$ClAu-C \underset{O-CH_2}{\overset{NH-(CH_2)_n}{\diagdown}} \ + \ Cl_2Au \left(C \underset{O-CH_2}{\overset{NH-(CH_2)_n}{\diagdown}} \right)_2^+$$
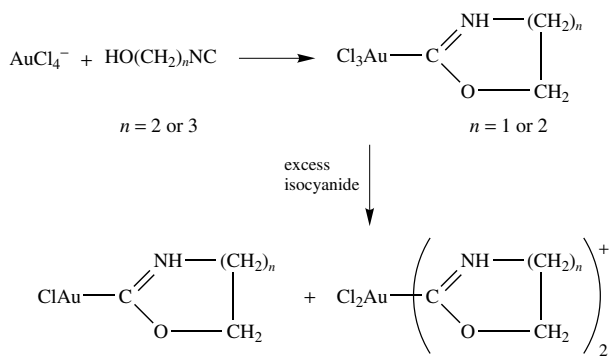
SCHEME 30. Carbene complexes from ω-hydroxyisocyanides

$$CNAuCNH \ + \ \underset{R \quad R'}{\triangle^O} \ \longrightarrow \ CNAu-C\equiv N-CHR-CHR'OH$$

R = Me and R′ = H
R = H and R′ = Ph

$$CNAu-C \underset{O-CHR'}{\overset{NH-CHR}{\diagdown}}$$
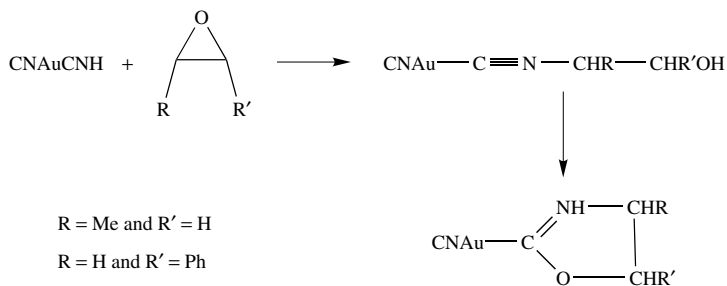
SCHEME 31. Carbene complexes from epoxides

$$\left[\underset{C_6F_5}{\overset{C_6F_5}{\diagdown}} Au \underset{CNR}{\overset{CNR}{\diagup}} \right]^+ \ + \ \underset{NHPh}{\overset{NHPh}{|}} \ \longrightarrow \ \left[\underset{C_6F_5}{\overset{C_6F_5}{\diagdown}} Au \underset{NPh}{\overset{NPh}{}} \underset{NHR}{\overset{C}{\diagdown}} \right]^+ \ + \cdots$$

↓ NHR′ / NH₂

$$\underset{C_6F_5}{\overset{C_6F_5}{\diagdown}} Au \underset{C=N}{\overset{C-NR'}{}} \underset{NHR}{\overset{NHR}{}} \ + \ H^+$$
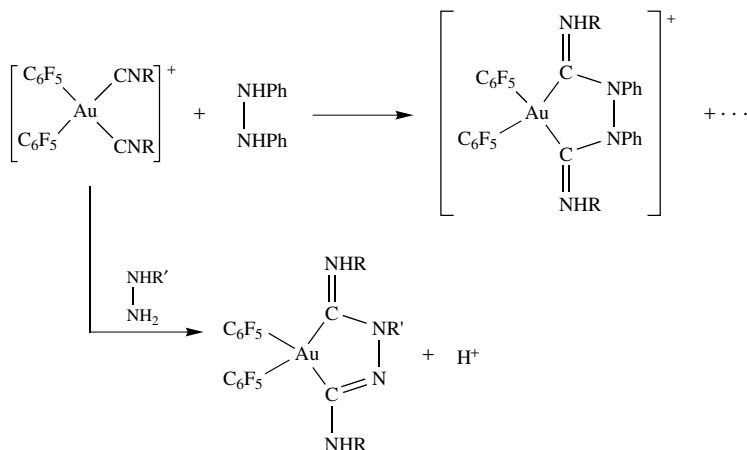
SCHEME 32. Cyclic bis(carbenes)

SCHEME 33. Cyclic carbene complexes from bis(isocyanides)
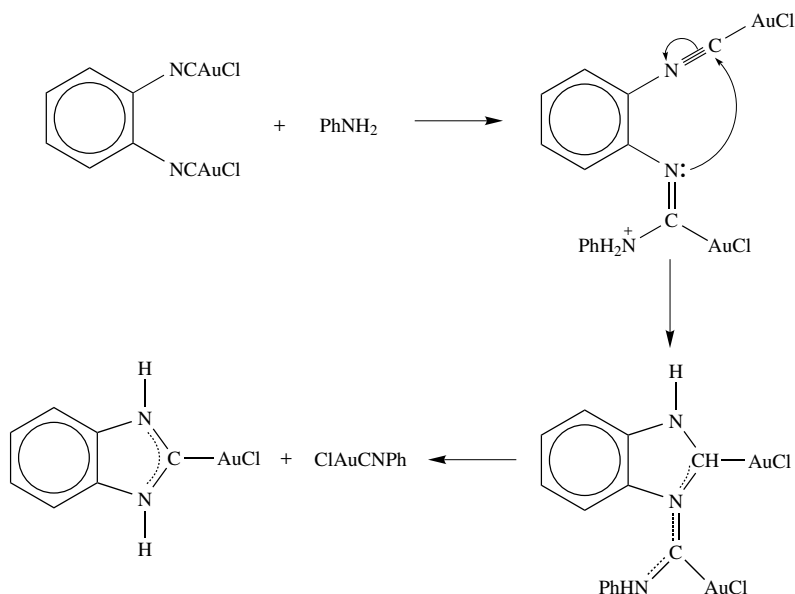
(see Scheme 33), 1,2-diaminobenzene or 1,8-diaminonaphthalene to form benzimidazolin-2-ylidene(chloro)gold complexes.

In the process the nucleophilic attack by the amine is followed by an imine attack on the second isocyanide functionality to give a heterocyclic ring by the elimination of [Au(Cl)CNPh].

(b) Electron-rich olefins can be used as nucleophilic carbene transfer reagents to give, e.g., bis(imidazolinylidene) complexes (equation 91)[405].

$$ \text{(equation 91)} \tag{91} $$
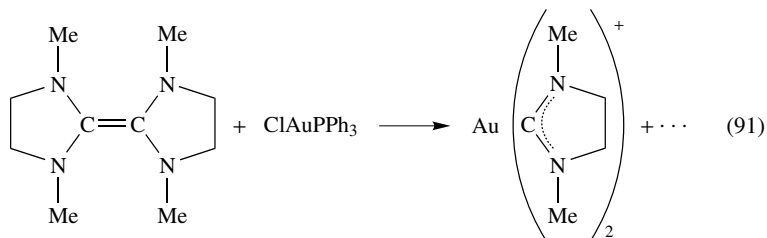
(c) Carbene groups can also be introduced via a transfer from group 6 metals. Typical Fischer-type alkoxy-organo or amino-organo carbene complexes of gold(I) and gold(III) are formed when $H[AuCl_4]$ reacts with pentacarbonyl carbene complexes of chromium, molybdenum or tungsten (equation 92)[406,407].

$$ (CO)_5M{=}C(Y)R + H[AuCl_4] \longrightarrow ClAu{=}C(Y)R + Cl_3Au{=}C(Y)R \tag{92} $$

$$ Y = OMe, NH_2, NHMe, NMe_2 $$
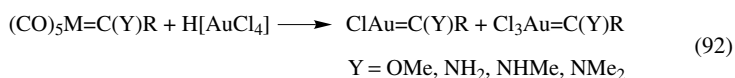
The carbene transfer occurs with retention of the aminocarbene configuration, indicating that an sp^3 transition state is not formed. With H[AuBr$_4$] and [W(CO)$_5$\{C(NMe$_2$)Ph\}], only the reductive substitution reaction occurs to give the gold(I) compound [Au(Br)C(NMe$_2$)Ph].

(d) Protonation or alkylation of gold azolyl compounds is another straightforward approach to carbene complexes. An azolyl lithium is used to substitute one or more ligands of gold and then one or two of these is protonated or alkylated[408−411] (Scheme 34).

ClAu(SC$_4$H$_8$) + 2 $^-$C ... → Au ...

+ 2 R$^+$

+R$^+$

R = H or Me
X = N or S
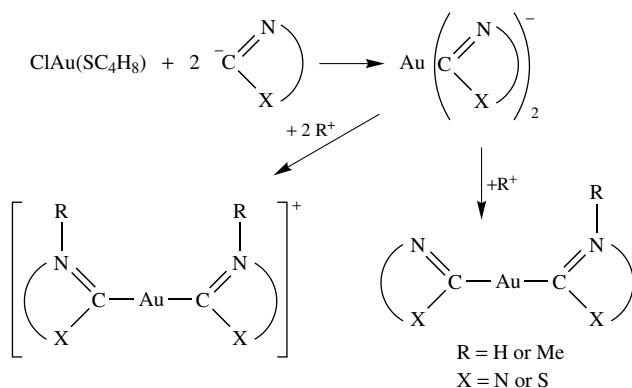
SCHEME 34. Carbene complexes via azolyl lithium reagents

With lithiated imidazoles, only bis(carbene) complexes are formed, although careful adjustment of the conditions can lead to a compound which contains carbene ligands resulting from both alkylation and protonation[411]. A similar methodology is applicable with isothiazolyl lithium. In the product the nitrogen atom occupies a position remote from the coordinated carbon (equation 93)[412].

C$_6$F$_5$Au(SC$_4$H$_8$) + ... → ... Li

CF$_3$SO$_3$Me   (93)

Me ... AuC$_6$F$_5$
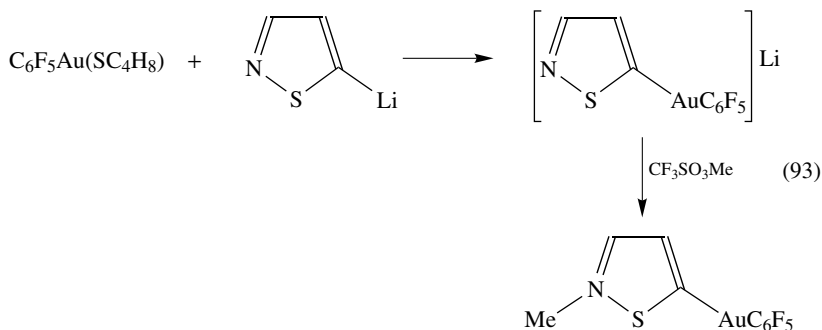
Sequential transmetallation and protonation of 2-(2′-oxazolinyl)thien-3-yl lithium affords the *mono*- and *bis*-carbene complexes **13**, **14** and **15**. These complexes contain only distant (albeit conjugated) heteroatoms[413].

(13)   **(14)**   **(15)**
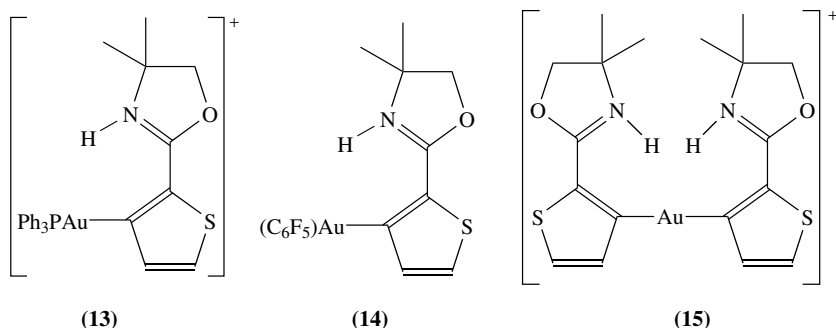
Other compounds belonging to this family are formed when a stable gold trimer is treated, for example, with ClCOOEt or EtI (equation 94)[414,415].

$$ \tfrac{1}{3} \left\{ Au-C \right\}_3 \xrightarrow{\text{EtI}} I-Au-C \tag{94} $$
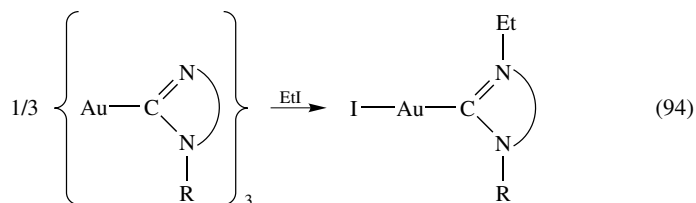
The general pattern is the same if a gold halide is reacted with 2-lithiated pyridine followed by a protonating or an alkylating agent[416]. Both the gold pyridyl trimer[417,418] which precipitates upon treatment with one molar amount and the aurate which forms with an excess of 2-pyridyl lithium may be protonated, but only the latter can be alkylated readily (Scheme 35).

Mixed ligand gold(I) complexes are prone to homoleptic rearrangement. This reaction may either occur in solution or during crystallization (equation 95)[412].

$$ 2 \left[(Ph_3P)Au-\!\!\!\begin{array}{c}\\ S\end{array}\!\!\!-N-Me \right]^+ \longrightarrow \left(Au-\!\!\!\begin{array}{c}\\ S\end{array}\!\!\!-N-Me \right)_2^+ + Au(PPh_3)_2^+ \tag{95} $$
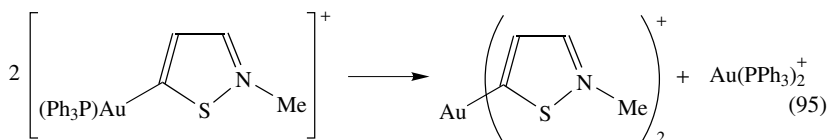
Treatment of $[Au(Cl)[C(OEt)NMe_2]]$ with Lewis acids does not lead to carbyne complex formation. Reactions with BBr_3 and BI_3 yield only the substitution products $[Au(X)\{C(OEt)NMe_2\}]$[419,420].

Liquid-crystalline gold isocyanide complexes $[C_nH_{2n+1}O-(C_6H_4)-O-C(O)-(C_6H_4)-NCAuCl]$ react with alcohols $C_mH_{2m+1}OH$ ($n = 10$ or 11; $m = 2$ to 5) to form Z/E isomeric mixtures of carbene complexes [isomerism occurs around the C(carbene)−N bond] with mesomorphic properties and provide the first examples of liquid-crystalline metal–carbene complexes[421]. The isomers can also be separated, with the E form being slightly more stable than the Z form.
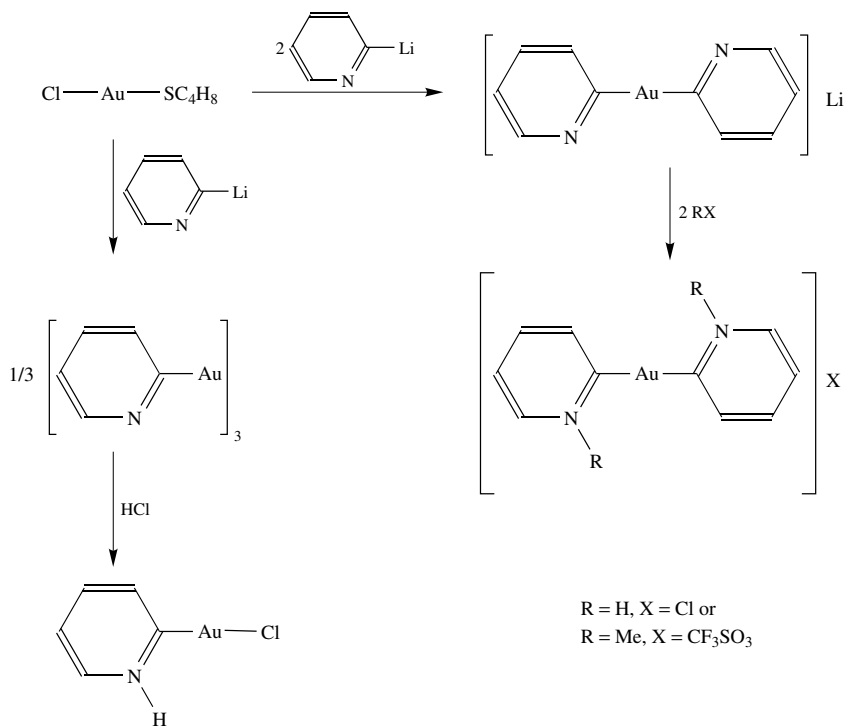
SCHEME 35. Pyridyl and pyridinium complexes of gold(I)

V. REFERENCES

 1. W. J. Pope and C. S. Gibson, *J. Chem. Soc.*, 2061 (1907).
 2. W. J. Pope and C. S. Gibson, *Proc. Chem. Soc.*, **23**, 245 (1908).
 3. G. Calvin, G. E. Coates and P. S. Dixon, *Chem. Ind.*, 1628 (1959).
 4. G. K. Anderson, *Adv. Organomet. Chem.*, **20**, 39 (1982).
 5. K. I. Grandberg and V. P. Dyadchenko, *J. Organomet. Chem.*, **474**, 1 (1994).
 6. C. E. Housecroft, *Coord. Chem. Rev.*, **127**, 187 (1993).
 7. C. E. Housecroft, *Coord. Chem. Rev.*, **115**, 117 (1992).
 8. W. E. Smith, *Coord. Chem. Rev.*, **67**, 311 (1985).
 9. W. E. Smith, *Coord. Chem. Rev.*, **45**, 319 (1982).
10. W. E. Smith, *Coord. Chem. Rev.*, **35**, 259 (1981).
11. R. Usón and A. Laguna, *Coord. Chem. Rev.*, **70**, 1 (1986).
12. A. Laguna and M. C. Gimeno, *Trends Organomet. Chem.*, **1**, 231 (1994).
13. (a) R. J. Puddephatt, in *Comprehensive Organometallic Chemistry* (Eds. G. Wilkinson, F. G. A. Stone and E. W. Abel), 1st ed., Vol. 2, Pergamon Press, Oxford, 1982; p. 765.
     (b) R. J. Puddephatt, *The Chemistry of Gold*, Elsevier, Amsterdam, 1978.
     (c) R. J. Puddephatt and I. Treurnicht, *J. Organomet. Chem.*, **319**, 129 (1987).
14. J. Buckingham and J. E. Macintyre (Eds.), *Dictionary of Organometallic Compounds*; Chapman and Hall, London, 1984–1990.
15. H. Schmidbaur, *Gmelin Handbuch der Anorganischen Chemie. Organogold Compounds*, Springer-Verlag, Berlin, 1980.

16. H. Schmidbaur, T. Pollok, R. Herr, F. E. Wagner, R. Bau, J. Riede and G. Müller, *Organometallics*, **5**, 566 (1986).
17. Z. Assefa, B. G. McBurnett, R. J. Staples, J. P. Fackler, Jr., B. Assmann, K. Angermaier and H. Schmidbaur, *Inorg. Chem.*, **34**, 75 (1995).
18. L.-K. Liu, L.-S. Luh, Y.-S. Wen, U. B. Eke and M. A. Mesubi, *Organometallics*, **14**, 4474 (1995).
19. B. D. Reid and A. J. Welch, *J. Organomet. Chem.*, **438**, 371 (1992).
20. E. G. Perevalova, E. I. Smyslova and K. I. Grandberg, *Bull. Acad. Sci. USSR, Chem. Ser.*, 2506 (1982).
21. R. D. Sanner, J. H. Satcher Jr. and M. W. Droege, *Organometallics*, **8**, 1498 (1989).
22. H. K. Nair and J. A. Morrison, *J. Organomet. Chem.*, **376**, 149 (1989).
23. E. G. Perevalova, Y. T. Struchkov, V. P. Dyadchenko, E. I. Smyslova, Y. L. Slovokhotov and K. I. Grandberg, *Bull. Acad. Sci. USSR, Chem. Ser.*, 2529 (1983).
24. E. G. Perevalova, T. V. Baukova, M. M. Sazonenko and K. I. Grandberg, *Bull. Acad. Sci. USSR, Chem. Ser.*, 1726 (1985).
25. E. I. Smyslova, E. G. Perevalova, V. P. Dyadchenko, K. I. Grandberg, Y. L. Slovokhotov and Y. T. Struchkov, *J. Organomet. Chem.*, **215**, 269 (1981).
26. M. Murakami, M. Inouye, M. Suginome and Y. Ito, *Bull. Chem. Soc. Jpn.*, **61**, 3649 (1988).
27. H. G. Raubenheimer, F. Scott, G. J. Kruger, J. G. Toerien, R. Otte, W. van Zyl, I. Taljaard, P. Olivier and L. Lindford, *J. Chem. Soc., Dalton Trans.*, 2091 (1994).
28. H. G. Raubenheimer, M. Desmet and G. J. Kruger, *J. Chem. Soc., Dalton Trans.*, 2067 (1995).
29. J. Dekker, J. W. Münninghoff, J. Boersma and A. L. Spek, *Organometallics*, **6**, 1236 (1987).
30. R. I. Papasergio, C. L. Raston and A. H. White, *J. Chem. Soc., Dalton Trans.*, 3085 (1987).
31. E. G. Perevalova, I. G. Bolesov, Y. S. Kalyuzhnaya, T. I. Voyevodskaya, L. G. Kuzmina, V. I. Korsunsky and K. I. Grandberg, *J. Organomet. Chem.*, **369**, 267 (1989).
32. E. G. Perevalova, K. I. Grandberg, E. I. Smyslova and E. S. Kalyuzhnaya, *Bull. Acad. Sci. USSR, Chem. Ser.*, 191 (1985).
33. V. W. W. Yam and S. W. K. Choi, *J. Chem. Soc., Dalton Trans.*, 2057 (1994).
34. X. Hong, K. K. Cheung, C. X. Guo and C. M. Che, *J. Chem. Soc., Dalton Trans.*, 1867 (1994).
35. G. M. Bancroft, T. Chan, R. J. Puddephatt and J. S. Tse, *Inorg. Chem.*, **21**, 2946 (1982).
36. R. L. DeKock, E. J. Baerends, P. M. Boerrigter and R. Hengelmolen, *J. Am. Chem. Soc.*, **106**, 3387 (1984).
37. A. Haaland, J. Hougen, H. V. Volden and R. J. Puddephatt, *J. Organomet. Chem.*, **325**, 311 (1987).
38. J. Sykora and J. Sima, *Coord. Chem. Rev.*, **107**, 1 (1990).
39. H. B. Friedrich and J. R. Moss, *Adv. Organomet. Chem.*, **33**, 235 (1991).
40. J. A. Morrison, *Adv. Inorg. Chem. Radiochem.*, **27**, 293 (1983).
41. G. J. Arsenault, M. Crespo and R. J. Puddephatt, *Organometallics*, **6**, 2255 (1987).
42. H.-P. Abicht, P. Lehniger and K. Issleib, *J. Organomet. Chem.*, **250**, 609 (1983).
43. S. Bruni, A. L. Bandini, F. Cariati and F. Speroni, *Inorg. Chim. Acta*, **203**, 127 (1993).
44. H.-J. Kneuper, K. Harms and G. Boche, *J. Organomet. Chem.*, **364**, 275 (1989).
45. E. G. Perevalova, I. G. Bolesov, Y. T. Struchkov, I. F. Leschova, Y. S. Kalyuzhnaya, T. I. Voyevodskaya, Y. L. Slovokhotov and K. I. Grandberg, *J. Organomet. Chem.*, **286**, 129 (1985).
46. E. G. Perevalova, M. D. Reshetova and G. M. Kokhanyuk, *J. Gen. Chem. USSR*, 2424 (1984).
47. S. Komiya, M. Iwata, T. Sone and A. Fukuoka, *J. Chem. Soc., Chem. Commun.*, 1109 (1992).
48. Y. Ito, M. Inouye, M. Suginome and M. Murakami, *J. Organomet. Chem.*, **342**, C41 (1988).
49. F. Bonati, A. Burini, B. R. Pietroni and M. Felici, *J. Organomet. Chem.*, **273**, 275 (1984).
50. P. Veya, C. Floriani, A. Chiesi-Villa, C. Guastini, A. Dedieu, F. Ingold and P. Braunstein, *Organometallics*, **12**, 4359 (1993).
51. M. C. Gimeno, A. Laguna, M. Laguna, F. Sanmartin and P. G. Jones, *Organometallics*, **12**, 3984 (1993).
52. M. I. Bruce, P. J. Low, B. W. Skelton and A. H. White, *J. Chem. Soc., Dalton Trans.*, 3145 (1993).
53. E. J. Fernández, M. C. Gimeno, P. G. Jones, A. Laguna, M. Laguna, J. M. López-de-Luzuriaga and M. A. Rodríguez, *Chem. Ber.*, **128**, 121 (1995).
54. E. J. Fernández, M. C. Gimeno, P. G. Jones, A. Laguna, M. Laguna and E. Olmos, *Inorg. Chim. Acta*, **238**, 173 (1995).
55. E. J. Fernández, M. C. Gimeno, P. G. Jones, A. Laguna, M. Laguna and J. M. López-de-Luzuriaga, *Angew. Chem., Int. Ed. Engl.*, **33**, 87 (1994).

302 Hubert Schmidbaur, Andreas Grohmann, M. Elena Olmos and Annette Schier

56. E. J. Fernández, M. C. Gimeno, P. G. Jones, A. Laguna, M. Laguna and J. M. López-de-Luzuriaga, *J. Chem. Soc., Dalton Trans.*, 3365 (1992).
57. N. C. Payne, R. Ramachandran, I. Treurnicht and R. J. Puddephatt, *Organometallics*, **9**, 880 (1990).
58. D. Li, X. Hong, C.-M. Che, W.-C. Lo and S.-M. Peng, *J. Chem. Soc., Dalton Trans.*, 2929 (1993).
59. F. Bonati, A. Burini, B. R. Pietroni, E. Torregiani, S. Calogero and F. E. Wagner, *J. Organomet. Chem.*, **408**, 125 (1991).
60. D. M. P. Mingos, J. Yau, S. Menzer and D. J. Williams, *Angew. Chem., Int. Ed. Engl.*, **34**, 1894 (1995).
61. A. Grohmann, *Angew. Chem., Int. Ed. Engl.*, **34**, 2107 (1995).
62. X. L. R. Fontaine, S. J. Higgins, C. R. Langrick and B. L. Shaw, *J. Chem. Soc., Dalton Trans.*, 777 (1987).
63. A. J. Deeming, S. Donovan-Mtunzi and K. Hardcastle, *J. Chem. Soc., Dalton Trans.*, 543 (1986).
64. A. T. Hutton, P. G. Pringle and B. L. Shaw, *Organometallics*, **2**, 1889 (1983).
65. G. J. Arsenault, L. Manojlovic-Muir, K. W. Muir, R. J. Puddephatt and I. Treurnicht, *Angew. Chem., Int. Ed. Engl.*, **26**, 86 (1987).
66. L. Manojlovic-Muir, K. W. Muir, I. Treurnicht and R. J. Puddephatt, *Inorg. Chem.*, **26**, 2418 (1987).
67. R. Nast, *Coord. Chem. Rev.*, **42**, 89 (1982).
68. C. M. Cheng, H. K. Yip, W. C. Lo and S. M. Peng, *Polyhedron*, **13**, 887 (1994).
69. O. M. Abu-Salah, A.-R. A. Al-Ohaly, S. S. Al-Showiman and I. M. Al-Najjar, *Transition Met. Chem.*, **10**, 207 (1985).
70. O. M. Abu-Salah and A. R. Al-Ohaly, *Inorg. Chim. Acta*, **77**, L159 (1983).
71. M. I. Bruce, E. Horn, J. G. Matisons and M. R. Snow, *Aust. J. Chem.*, **37**, 1163 (1984).
72. R. J. Cross and M. F. Davidson, *J. Chem. Soc., Dalton Trans.*, 411 (1986).
73. R. J. Cross, M. F. Davidson and A. J. McLennan, *J. Organomet. Chem.*, **265**, C37 (1984).
74. T. E. Müller, S. W. K. Choi, D. M. P. Mingos, D. Murphy, D. J. Williams and V. W. W. Yam, *J. Organomet. Chem.*, **484**, 209 (1994).
75. A. T. Casey and A. M. Vecchio, *Appl. Organomet. Chem.*, **4**, 513 (1990).
76. J. Vicente, M. T. Chicote and M. D. Abrisqueta, *J. Chem. Soc., Dalton Trans.*, 497 (1995).
77. F. Bonati, A. Burini, B. R. Pietroni, E. Giorgini and B. Bovio, *J. Organomet. Chem.*, **344**, 119 (1988).
78. N. C. Payne, R. J. Puddephatt, R. Ravindranath and I. Treurnicht, *Can. J. Chem.*, **66**, 3176 (1988).
79. N. C. Payne, R. Ramachandran and R. J. Puddephatt, *Can. J. Chem.*, **73**, 6 (1995).
80. G. A. Carriedo, V. Riera, X. Solans and J. Solans, *Acta Crystallogr., Sect. C*, **C44**, 978 (1988).
81. G. Jia, R. J. Puddephatt and J. J. Vittal, *J. Organomet. Chem.*, **449**, 211 (1993).
82. M. I. Bruce, K. R. Grundy, M. J. Liddell, M. R. Snow and E. R. T. Tiekink, *J. Organomet. Chem.*, **344**, C49 (1988).
83. G. Jia, R. J. Puddephatt, J. D. Scott and J. J. Vittal, *Organometallics*, **12**, 3565 (1993).
84. G. Jia, R. J. Puddephatt, J. J. Vittal and N. C. Payne, *Organometallics*, **12**, 263 (1993).
85. G. Jia, N. C. Payne, J. J. Vittal and R. J. Puddephatt, *Organometallics*, **12**, 4771 (1993).
86. M. P. Gamasa, J. Gimeno, I. Godefroy, E. Lastra, B. M. Martín-Vaca, S. García-Granda and A. Gutierrez-Rodriguez, *J. Chem. Soc., Dalton Trans.*, 1901 (1995).
87. M. Ferrer, O. Rossell, M. Seco, M. A. Pellinghelli and A. Tiripicchio, *Organometallics*, **14**, 57 (1995).
88. M. I. Bruce and D. N. Duffy, *Aust. J. Chem.*, **39**, 1697 (1986).
89. S. J. Shieh, X. Hong, S. M. Peng and C. M. Che, *J. Chem. Soc., Dalton Trans.*, 3067 (1994).
90. T. E. Müller, D. M. P. Mingos and D. J. Williams, *J. Chem. Soc., Chem. Commun.*, 1787 (1994).
91. L. S. Moore, R. V. Parish, R. Usón, A. Laguna, M. Laguna and M. N. Fraile, *J. Chem. Soc., Dalton Trans.*, 23 (1988).
92. R. Usón, A. Laguna, M. Laguna, M. N. Fraile, P. G. Jones and G. M. Sheldrick, *J. Chem. Soc., Dalton Trans.*, 291 (1986).
93. M. A. Bennett, S. K. Bhargava, K. D. Griffiths and G. B. Robertson, *Angew. Chem., Int. Ed. Engl.*, **26**, 260 (1987).
94. E. J. Fernández, M. C. Gimeno, P. G. Jones, A. Laguna, M. Laguna and J. M. López-de-Luzuriaga, *J. Chem. Soc., Dalton Trans.*, 3401 (1993).
95. P. G. Jones, *J. Organomet. Chem.*, **345**, 405 (1988).
96. R. Usón, A. Laguna, M. Laguna, I. Colera and E. de Jesús, *J. Organomet. Chem.*, **263**, 121 (1984).

97. M. Contel, J. Jiménez, P. G. Jones, A. Laguna and M. Laguna, *J. Chem. Soc., Dalton Trans.*, 2515 (1994).
98. R. Usón, A. Laguna, A. Navarro, R. V. Parish and L. S. Moore, *Inorg. Chim. Acta*, **112**, 205 (1986).
99. E. J. Fernández, M. C. Gimeno, P. G. Jones, A. Laguna, M. Laguna and E. Olmos, *J. Chem. Soc., Dalton Trans.*, 2891 (1994).
100. M. Bardají, A. Laguna, M. Laguna and F. Merchán, *Inorg. Chim. Acta*, **215**, 215 (1994).
101. R. Usón, A. Laguna and M. D. Villacampa, *Inorg. Chim. Acta*, **81**, 25 (1984).
102. G. A. Carriedo, G. Sánchez, V. Riera, C. Bois, Y. Jeannin and D. Miguel, *J. Chem. Soc., Dalton Trans.*, 3355 (1990).
103. O. Crespo, M. C. Gimeno, A. Laguna and P. G. Jones, *J. Chem. Soc., Dalton Trans.*, 1601 (1992).
104. J. M. Forward, J. P. Fackler, Jr. and R. J. Staples, *Organometallics*, **14**, 4194 (1995).
105. A. Sladek, S. Hofreiter, M. Paul and H. Schmidbaur, *J. Organomet. Chem.*, **501**, 47 (1995).
106. F. Bonati, A. Burini, B. R. Pietroni and B. Bovio, *J. Organomet. Chem.*, **408**, 271 (1991).
107. A. Laguna, M. Laguna, J. Fañanas, P. G. Jones and C. Fittschen, *Inorg. Chim. Acta*, **121**, 39 (1986).
108. J. Vicente, A. Arcas, M. Mora, X. Solans and M. Font-Altaba, *J. Organomet. Chem.*, **309**, 369 (1986).
109. P. H. van Rooyen, M. Schindehutte and S. Lotz, *Organometallics*, **11**, 1104 (1992).
110. J. Vicente, A. Arcas, P. G. Jones and J. Lautner, *J. Chem. Soc., Dalton Trans.*, 451 (1990).
111. M. A. Bennett, S. K. Bhargava, K. D. Griffiths, G. B. Robertson, W. A. Wickramasinghe and A. C. Willis, *Angew. Chem., Int. Ed. Engl.*, **26**, 258 (1987); **27**, 589 (1988).
112. S. Bordoni, L. Busetto, M. C. Cassani, V. G. Albano and P. Sabatino, *Inorg. Chim. Acta*, **222**, 267 (1994).
113. P. G. Jones and C. Thöne, *Acta Crystallogr., Sect. C*, **C48**, 1312 (1992).
114. M. C. Gimeno, A. Laguna, C. Sarroca and P. G. Jones, *Inorg. Chem.*, **32**, 5926 (1993).
115. R. Usón, A. Laguna, M. Laguna, I. Lázaro, A. Morata, P. G. Jones and G. M. Sheldrick, *J. Chem. Soc., Dalton Trans.*, 669 (1986).
116. G. A. Carriedo, V. Riera, M. L. Rodríguez, P. G. Jones and J. Lautner, *J. Chem. Soc., Dalton Trans.*, 639 (1989).
117. R. Usón, A. Laguna, M. Laguna, M. L. Castilla, P. G. Jones and C. Fittschen, *J. Chem. Soc., Dalton Trans.*, 3017 (1987).
118. A. Laguna, M. Laguna, A. Rojo and M. N. Fraile, *J. Organomet. Chem.*, **315**, 269 (1986).
119. R. Usón, A. Laguna, M. Laguna, J. Jiménez, M. P. Gómez, A. Sainz and P. G. Jones, *J. Chem. Soc., Dalton Trans.*, 3457 (1990).
120. F. Bonati, A. Burini, B. R. Pietroni and B. Bovio, *J. Organomet. Chem.*, **375**, 147 (1989).
121. D. A. Briggs, R. G. Raptis and J. P. Fackler Jr., *Acta Crystallogr., Sect. C*, **C44**, 1313 (1988).
122. A. Laguna, M. Laguna, J. Jiménez and A. J. Fumanal, *J. Organomet. Chem.*, **396**, 121 (1990).
123. H. Werner, H. Otto, T. Ngo-Khac and C. Burschka, *J. Organomet. Chem.*, **262**, 123 (1984).
124. E. G. Perevalova, K. I. Grandberg, V. P. Dyadchenko and T. V. Baukova, *J. Organomet. Chem.*, **217**, 403 (1981).
125. T. V. Baukova, Y. L. Slovokhotov and Y. T. Struchkov, *J. Organomet. Chem.*, **220**, 125 (1981).
126. M. I. Bruce and A. H. White, *Aust. J. Chem.*, **43**, 949 (1990).
127. M. I. Bruce, J. K. Walton, B. W. Skelton and A. H. White, *J. Chem. Soc., Dalton Trans.*, 809 (1983).
128. H. Schumann, F. H. Görlitz and A. Dietrich, *Chem. Ber.*, **122**, 1423 (1989).
129. M. I. Bruce, P. A. Humphrey, M. L. Williams, B. W. Skelton and A. H. White, *Aust. J. Chem.*, **42**, 1847 (1989).
130. T. V. Baukova, Y. L. Slovokhotov and Y. T. Struchkov, *J. Organomet. Chem.*, **221**, 375 (1981).
131. Y. T. Struchkov, Y. L. Slovokhotov, D. N. Kravtsov, T. V. Baukova, E. G. Perevalova and K. I. Grandberg, *J. Organomet. Chem.*, **338**, 269 (1988).
132. B. Bovio, A. Burini and B. R. Pietroni, *J. Organomet. Chem.*, **452**, 287 (1993).
133. K. Geilich, K. Stumpf, H. Pritzkow and W. Siebert, *Chem. Ber.*, **120**, 911 (1987).
134. G. Banditelli, A. L. Bandini, F. Bonati, R. G. Goel and G. Minghetti, *Gazz. Chim. Ital.*, **112**, 539 (1982).
135. M. Lanfranchi, M. A. Pellinghelli, A. Tiripicchio and F. Bonati, *Acta Crystallogr., Sect. C*, **C41**, 52 (1985).

136. H. G. Raubenheimer, G. J. Kruger, C. F. Marais, J. T. Z. Hattingh, L. Linford and P. H. van Rooyen, *J. Organomet, Chem.*, **355**, 337 (1988).
137. A. N. Nesmeyanov, E. G. Perevalova, K. I. Grandberg, D. A. Lemenovskii, T. V. Baukova and O. B. Afanassova, *J. Organomet. Chem.*, **65**, 131 (1974).
138. H. Schmidbaur and Y. Inoguchi, *Chem. Ber.*, **113**, 1646 (1980).
139. E. G. Perevalova, E. I. Smyslova, V. P. Dyadchenko and K. I. Grandberg, *Bull. Acad. Sci. USSR, Chem. Ser.*, 883 (1984).
140. V. I. Korsunsky, *J. Organomet. Chem.*, **311**, 357 (1986).
141. V. I. Korsunsky, K. I. Grandberg, E. I. Smyslova and T. V. Baukova, *J. Organomet. Chem.*, **335**, 277 (1987).
142. R. Usón, A. Laguna and P. Brun, *J. Organomet. Chem.*, **197**, 369 (1980).
143. S. Gambarotta, C. Floriani, A. Chiesi-Villa and C. Guastini, *J. Chem. Soc., Chem. Commun.*, 1304 (1983).
144. E. M. Meyer, S. Gambarotta, C. Floriani, A. Chiesi-Villa and C. Guastini, *Organometallics*, **8**, 1067 (1989).
145. G. van Koten, J. T. B. H. Jastrzebski, C. H. Stam and N. C. Niemann, *J. Am. Chem. Soc.*, **106**, 1880 (1984).
146. I. J. B. Lin, C. W. Liu, L.-K. Liu and Y.-S. Wen, *Organometallics*, **11**, 1447 (1992).
147. F. Bonati, A. Burini, B. R. Pietroni and B. Bovio, *J. Organomet. Chem.*, **317**, 121 (1986).
148. F. Bonati, A. Burini, B. R. Pietroni and E. Giorgini, *Inorg. Chim. Acta*, **137**, 81 (1987).
149. H. Schmidbaur and O. Gasser, *Angew. Chem., Int. Ed. Engl.*, **15**, 502 (1976).
150. J. Vicente, M.-T. Chicote, M.-C. Lagunas and P. G. Jones, *J. Chem. Soc., Chem. Commun.*, 1730 (1991).
151. J. Vicente, M.-T. Chicote, M.-C. Lagunas and P. G. Jones, *J. Chem. Soc., Dalton Trans.*, 2579 (1991).
152. J. Vicente, M.-T. Chicote and M.-C. Lagunas, *Inorg. Chem.*, **32**, 3748 (1993).
153. (a) F. Bonati, A. Burini, M. Felici and B. R. Pietroni, *Gazz. Chim. Ital.*, **113**, 105 (1983).
    (b) S. Bommers, H. Beruda, N. Dufour, M. Paul and H. Schmidbaur, *Chem. Ber.*, **128**, 137 (1995).
    (c) H. Schmidbaur, F. P. Gabbaï, A. Schier and J. Riede, *Organometallics*, **14**, 4969 (1995).
    (d) P. Pyykkö and T. Tamm, *Organometallics*, **17**, 4842 (1998).
154. H. Schmidbaur, F. Scherbaum, B. Huber and G. Müller, *Angew. Chem., Int. Ed. Engl.*, **27**, 419 (1988).
155. G. Karger, P. Hornbach, A. Krämer, H. Pritzkow and W. Siebert, *Chem. Ber.*, **122**, 1881 (1989).
156. V. Riera, J. Ruiz, X. Solans and E. Tauler, *J. Chem. Soc., Dalton Trans.*, 1607 (1990).
157. J. Vicente, M.-T. Chicote, I. Saura-Llamas, P. G. Jones, K. Meyer-Bäse and C. Freire Erdbrügger, *Organometallics*, **7**, 997 (1988).
158. J. Vicente, M.-T. Chicote and I. Saura-Llamas, *J. Chem. Soc., Dalton Trans.*, 1941 (1990).
159. A. N. Nesmeyanov, E. G. Perevalova, Y. T. Struchkov, M. Y. Antipin, K. I. Grandberg and V. P. Dyadchenko, *J. Organomet. Chem.*, **201**, 343 (1980).
160. C. Lensch, P. G. Jones and G. M. Sheldrick, *Z. Naturforsch.*, **37b**, 944 (1982).
161. P. G. Jones, G. M. Sheldrick and E. Hädicke, *Acta Crystallogr., Sect. B*, **B36**, 2777 (1980).
162. N. Dufour, A. Schier and H. Schmidbaur, *Organometallics*, **12**, 2408 (1993).
163. F. Scherbaum, B. Huber, G. Müller and H. Schmidbaur, *Angew. Chem., Int. Ed. Engl.*, **27**, 1542 (1988).
164. O. Steigelmann, P. Bissinger and H. Schmidbaur, *Z. Naturforsch.*, **48b**, 72 (1993).
165. H. Schmidbaur and O. Steigelmann, *Z. Naturforsch.*, **47b**, 1721 (1992).
166. F. Scherbaum, A. Grohmann, G. Müller and H. Schmidbaur, *Angew. Chem., Int. Ed. Engl.*, **28**, 463 (1989).
167. F. Scherbaum, A. Grohmann, B. Huber, C. Krüger and H. Schmidbaur, *Angew. Chem., Int. Ed. Eng.*, **27**, 1544 (1988).
168. O. Steigelmann, P. Bissinger and H. Schmidbaur, *Angew. Chem., Int. Ed. Engl.*, **29**, 1399 (1990).
169. H. Schmidbaur, B. Brachthäuser and O. Steigelmann, *Angew. Chem., Int. Ed. Engl.*, **30**, 1488 (1991).
170. H. Schmidbaur, B. Brachthäuser, O. Steigelmann and H. Beruda, *Chem. Ber.*, **125**, 2705 (1992).
171. C. J. McNeal, R. E. P. Winpenny, J. M. Hughes, R. D. Macfarlane, L. H. Pignolet, L. T. J. Nelson, T. G. Gardner, L. H. Irgens, G. Vigh and J. P. Fackler Jr., *Inorg. Chem.*, **32**, 5582 (1993)

172. P. L. Bellon, M. Manassero, L. Naldini and M. Sansoni, *J. Chem. Soc., Chem. Commun.*, 1035 (1972).
173. P. L. Bellon, M. Manassero and M. Sansoni, *J. Chem. Soc., Dalton Trans.*, 2423 (1973).
174. D. G. Evans and D. M. P. Mingos, *J. Organomet. Chem.*, **232**, 171 (1982).
175. C. E. Briant, K. P. Hall and D. M. P. Mingos, *J. Organomet. Chem.*, **254**, C18 (1983).
176. C. E. Briant, K. P. Hall, D. M. P. Mingos and A. C. Wheeler, *J. Chem. Soc., Dalton Trans.*, 687 (1986).
177. E. D. Jemmis, J. Chandrasekhar, E.-U. Würthwein, P. v. R. Schleyer, J. W. Chinn Jr., F. J. Landro, R. J. Lagow, B. Luke and J. A. Pople, *J. Am. Chem. Soc.*, **104**, 4275 (1982).
178. D. M. P. Mingos, *Nature*, **345**, 113 (1990).
179. D. M. P. Mingos, *J. Chem. Soc., Dalton Trans.*, 1163 (1976).
180. N. Rösch, A. Görling, D. E. Ellis and H. Schmidbaur, *Angew. Chem., Int. Ed. Engl.*, **28**, 1357 (1989).
181. D. M. P. Mingos and R. P. F. Kanters, *J. Organomet. Chem.*, **384**, 405 (1990).
182. J. Vicente, M.-T. Chicote, I. Saura-Llamas and M.-C. Lagunas, *J. Chem. Soc., Chem. Commun.*, 915 (1992).
183. O. M. Abu-Salah and A. R. Al-Ohaly, *J. Organomet. Chem.*, **255**, C39 (1983).
184. R. Nast, P. Schneller and A. Hengefeld, *J. Organomet. Chem.*, **214**, 273 (1981).
185. O. M. Abu-Salah, A. R. A. Al-Ohaly and Z. F. Mutter, *J. Organomet. Chem.*, **391**, 267 (1990).
186. O. M. Abu-Salah, A. R. A. Al-Ohaly and Z. F. Mutter, *J. Organomet. Chem.*, **389**, 427 (1990).
187. O. M. Abu-Salah, *J. Organomet. Chem.*, **387**, 123 (1990).
188. O. M. Abu-Salah and A. R. A. Al-Ohaly, *J. Chem. Soc., Dalton Trans.*, 2297 (1988).
189. O. M. Abu-Salah and C. B. Knobler, *J. Organomet. Chem.*, **302**, C10 (1986).
190. O. M. Abu-Salah, A.-R. A. Al-Ohaly and C. B. Knobler, *J. Chem. Soc., Chem. Commun.*, 1502 (1985).
191. O. M. Abu-Salah, *J. Organomet. Chem.*, **270**, C26 (1984).
192. R. Usón, A. Laguna, E. J. Fernández, M. E. Ruiz-Romero, P. G. Jones and J. Lautner, *J. Chem. Soc., Dalton Trans.*, 2127 (1989).
193. H. G. Raubenheimer, J. G. Toerien, G. J. Kruger, R. Otte, W. van Zyl and P. Olivier, *J. Organomet. Chem.*, **466**, 291 (1994).
194. R. Usón, *J. Organomet. Chem.*, **372**, 171 (1989).
195. R. Usón, A. Laguna, M. Laguna, B. R. Manzano, P. G. Jones and G. M. Sheldrick, *J. Chem. Soc., Dalton Trans.*, 285 (1984).
196. E. J. Fernández, M. C. Gimeno, P. G. Jones, A. Laguna, M. Laguna and J. M. López-de-Luzuriaga, *Organometallics*, **14**, 2918 (1995).
197. R. Usón, A. Laguna, M. Laguna and M. C. Gimeno, *J. Chem. Soc., Dalton Trans.*, 1883 (1989).
198. R. Usón, A. Laguna, M. Laguna, M. C. Gimeno, P. G. Jones, C. Fittschen and G. M. Sheldrick, *J. Chem. Soc., Chem. Commun.*, 509 (1986).
199. M. C. Gimeno, J. Jiménez, P. G. Jones, A. Laguna and M. Laguna, *Organometallics*, **13**, 2508 (1994).
200. R. Usón, A. Laguna, M. Laguna, J. Jiménez and P. G. Jones, *Angew. Chem., Int. Ed. Engl.*, **30**, 198 (1991).
201. A. Laguna, M. Laguna, J. Jiménez, F. J. Lahoz and E. Olmos, *Organometallics*, **13**, 253 (1994).
202. C. King, D. D. Heinrich, G. Garzon, J. C. Wang and J. P. Fackler, Jr., *J. Am. Chem. Soc.*, **111**, 2300 (1989).
203. H. Schmidbaur, *Angew. Chem., Int. Ed. Engl.*, **22**, 907 (1983).
204. W. C. Kaska, *Coord. Chem. Rev.*, **48**, 1 (1983).
205. R. Usón, A. Laguna, M. Laguna, A. Usón and M. C. Gimeno, *Inorg. Chim. Acta*, **114**, 91 (1986).
206. J. Vicente, M. T. Chicote, I. Saura-Llamas, J. Turpin and J. Fernández-Baeza, *J. Organomet. Chem.*, **333**, 129 (1987).
207. J. Vicente, M. T. Chicote, J. A. Cayuelas, J. Fernández-Baeza, P. G. Jones, G. M. Sheldrick and P. Espinet, *J. Chem. Soc., Dalton Trans.*, 1163 (1985).
208. H. Schmidbaur, C. E. Zybill, G. Müller and C. Krüger, *Angew. Chem., Int. Ed. Engl.*, **22**, 729 (1983).
209. G. A. Bowmaker and H. Schmidbaur, *J. Chem. Soc., Dalton Trans.*, 2859 (1984).
210. R. Usón, A. Laguna, M. Laguna and A. Usón, *Inorg. Chim. Acta*, **73**, 63 (1983).
211. C. J. Aguirre, M. C. Gimeno, A. Laguna, M. Laguna, J. M. López-de-Luzuriaga and F. Puente, *Inorg. Chim. Acta*, **208**, 31 (1993).

212. M. C. Gimeno, A. Laguna, M. Laguna and P. G. Jones, *Inorg. Chim. Acta*, **189**, 117 (1991).
213. H. Konno and Y. Yamamoto, *Bull. Chem. Soc. Jpn.*, **60**, 2561 (1987).
214. H. H. Murray, D. A. Briggs, G. Garzón, R. G. Raptis, L. C. Porter and J. P. Fackler Jr., *Organometallics*, **6**, 1992 (1987).
215. H. H. Murray, G. Garzón, R. G. Raptis, A. M. Mazany, L. C. Porter and J. P. Fackler Jr., *Inorg. Chem.*, **27**, 836 (1988).
216. R. Usón, A. Laguna, M. Laguna, M. C. Gimeno, A. de Pablo, P. G. Jones, K. Meyer-Bäse and C. Freire Erdbrügger, *J. Organomet. Chem.*, **336**, 461 (1987).
217. J. Stein, J. P. Fackler Jr., C. Paparizos and H.-W. Chen, *J. Am. Chem. Soc.*, **103**, 2192 (1981).
218. H. Schmidbaur, G. Müller, K. C. Dash and B. Milewski-Mahrla, *Chem. Ber.*, **114**, 441 (1981).
219. P. G. Jones, *Acta Crystallogr., Sect. C*, **C48**, 1209 (1992).
220. R. Usón, A. Laguna, M. Laguna, A. Usón and M. C. Gimeno, *Organometallics*, **6**, 682 (1987).
221. A. Schier and H. Schmidbaur, *Z. Naturforsch.*, **37b**, 1518 (1982).
222. N. Holy, U. Deschler and H. Schmidbaur, *Chem. Ber.*, **115**, 1379 (1982).
223. Y. Yamamoto, *Bull. Chem. Soc. Jpn.*, **57**, 43 (1984).
224. Y. Yamamoto and H. Konno, *Bull. Chem. Soc. Jpn.*, **59**, 1327 (1986).
225. L. C. Porter, H. Knachel and J. P. Fackler Jr., *Acta Crystallogr., Sect. C*, **C43**, 1833 (1987).
226. L. C. Porter, H. Knachel and J. P. Fackler Jr., *Acta Crystallogr., Sect. C*, **C42**, 1125 (1986).
227. R. Usón, A. Laguna, M. Laguna, A. Usón, and M. C. Gimeno, *J. Chem. Soc., Dalton Trans.*, 701 (1988).
228. R. Usón, A. Laguna, M. Laguna, A. Usón, P. G. Jones and C. Freire Erdbrügger, *Organometallics*, **6**, 1778 (1987).
229. D. D. Heinrich, R. J. Staples and J. P. Fackler, Jr., *Inorg. Chim. Acta*, **229**, 61 (1995).
230. A. M. Mazany and J. P. Fackler Jr., *J. Am. Chem. Soc.*, **106**, 801 (1984).
231. R. Usón, A. Laguna, M. Laguna, M. N. Fraile, I. Lázaro, M. C. Gimeno, P. G. Jones, C. Reihs and G. M. Sheldrick, *J. Chem. Soc., Dalton Trans.*, 333 (1990).
232. H. Schmidbaur, J. R. Mandl, J.-M. Bassett, G. Blaschke and B. Zimmer-Gasser, *Chem. Ber.*, **114**, 433 (1981).
233. M. Bardají, N. G. Connelly, M. C. Gimeno, J. Jiménez, P. G. Jones, A. Laguna and M. Laguna, *J. Chem. Soc., Dalton Trans.*, 1163 (1994).
234. M. Bardají, P. G. Jones, A. Laguna and M. Laguna, *Organometallics*, **14**, 1310 (1995).
235. M. Bardají, A. Laguna and M. Laguna, *J. Organomet. Chem.*, **496**, 245 (1995).
236. M. Bardají, N. G. Connelly, M. C. Gimeno, P. G. Jones, A. Laguna and M. Laguna, *J. Chem. Soc., Dalton Trans.*, 2245 (1995).
237. E. Cerrada, M. C. Gimeno, J. Jiménez, A. Laguna and M. Laguna, *Organometallics*, **13**, 1470 (1994).
238. Y. Jiang, S. Alvarez and R. Hoffmann, *Inorg. Chem.*, **24**, 749 (1985).
239. B. Chaudret, B. Delavaux and R. Poilblanc, *Coord. Chem. Rev.*, **86**, 191 (1988).
240. C. King, J.-C. Wang, M. N. I. Khan and J. P. Fackler Jr., *Inorg. Chem.*, **28**, 2145 (1989).
241. H.-R. C. Jaw, M. M. Savas, R. D. Rogers and W. R. Mason, *Inorg. Chem.*, **28**, 1028 (1989).
242. W. Ludwig and W. Meyer, *Helv. Chim. Acta*, **65**, 934 (1982).
243. J. P. Fackler Jr. and J. D. Basil, In *'Inorganic Chemistry: Towards the 21st Century' (ACS Symp. Ser. No. 211)* (Ed. M. H. Chisholm), 1983; 201 pp.
244. D. S. Dudis and J. P. Fackler Jr., *Inorg. Chem.*, **24**, 3758 (1985).
245. H. C. Knachel, C. A. Dettorre, H. J. Galaska, T. A. Salupo, J. P. Fackler Jr. and H. H. Murray, *Inorg. Chim. Acta*, **126**, 7 (1987).
246. R. G. Raptis, J. P. Fackler Jr., J. D. Basil and D. S. Dudis, *Inorg. Chem.*, **30**, 3072 (1991).
247. H. Schmidbaur and P. Jandik, *Inorg. Chim. Acta*, **74**, 97 (1983).
248. H. H. Murray III, J. P. Fackler Jr., L. C. Porter and A. M. Mazany, *J. Chem. Soc., Chem. Commun.*, 321 (1986).
249. R. Usón, A. Laguna, M. Laguna, J. Jiménez and P. G. Jones, *J. Chem. Soc., Dalton Trans.*, 1361 (1991).
250. B. Trzcinska-Bancroft, M. N. I. Khan and J. P. Fackler Jr., *Organometallics*, **7**, 993 (1988).
251. L. C. Porter and J. P. Fackler Jr., *Acta Crystallogr., Sect. C*, **C42**, 1646 (1986).
252. L. C. Porter and J. P. Fackler Jr., *Acta Crystallogr., Sect. C*, **C42**, 1128 (1986).
253. M. Bardají, A. Blasco, J. Jiménez, P. G. Jones, A. Laguna, M. Laguna and F. Merchán, *Inorg. Chim. Acta*, **223**, 55 (1994).

254. J. P. Fackler Jr. and L. C. Porter, *J. Am. Chem. Soc.*, **108**, 2750 (1986).
255. D. D. Heinrich and J. P. Fackler Jr., *J. Chem. Soc., Chem. Commun.*, 1260 (1987).
256. H. H. Murray, J. P. Fackler Jr., L. C. Porter, D. A. Briggs, M. A. Guerra and R. J. Lagow, *Inorg. Chem.*, **26**, 357 (1987).
257. H. H. Murray, A. M. Mazany and J. P. Fackler Jr., *Organometallics*, **4**, 154 (1985).
258. L. C. Porter and J. P. Fackler Jr., *Acta Crystallogr., Sect. C*, **C43**, 587 (1987).
259. M. Bardají, M. C. Gimeno, P. G. Jones, A. Laguna and M. Laguna, *Organometallics*, **13**, 3415 (1994).
260. L. C. Porter and J. P. Fackler Jr., *Acta Crystallogr., Sect. C*, **C43**, 29 (1987).
261. A. Laguna, M. Laguna, J. Jiménez, F. J. Lahoz and E. Olmos, *J. Organomet. Chem.*, **435**, 235 (1992).
262. J. D. Basil, H. H. Murray, J. P. Fackler Jr., J. Tocher, A. M. Mazany, B. Trzcinska-Bancroft, H. Knachel, D. Dudis, T. J. Delord and D. O. Marler, *J. Am. Chem. Soc.*, **107**, 6908 (1985).
263. J. P. Fackler Jr. and J. D. Basil, *Organometallics*, **1**, 871 (1982).
264. H. H. Murray, J. P. Fackler Jr. and B. Trzcinska-Bancroft, *Organometallics*, **4**, 1633 (1985).
265. H. H. Murray III, J. P. Fackler Jr. and D. A. Tocher, *J. Chem. Soc., Chem. Commun.*, 1278 (1985).
266. H. H. Murray III, J. P. Fackler Jr. and D. A. Tocher, *J. Chem. Soc., Chem. Commun.*, 580 (1986).
267. H. H. Murray, J. P. Fackler Jr., A. M. Mazany, L. C. Porter, J. Shain and L. R. Falvello, *Inorg. Chim. Acta*, **114**, 171 (1986).
268. H. H. Murray, J. P. Fackler Jr. and A. M. Mazany, *Organometallics*, **3**, 1310 (1984).
269. H. H. Murray and J. P. Fackler Jr., *Inorg. Chim. Acta*, **115**, 207 (1986).
270. H. Schmidbaur, C. Hartmann, G. Reber and G. Müller, *Angew. Chem., Int. Ed. Engl.*, **26**, 1146 (1987).
271. M. C. Jimeno, J. Jiménez, A. Laguna, M. Laguna, P. G. Jones and R. V. Parish, *J. Organomet. Chem.*, **481**, 37 (1994).
272. L. C. Porter, H. H. Murray and J. P. Fackler Jr., *Acta Crystallogr., Sect. C*, **C43**, 877 (1987).
273. R. G. Raptis, H. H. Murray, R. J. Staples, L. C. Porter and J. P. Fackler Jr., *Inorg. Chem.*, **32**, 5576 (1993).
274. R. G. Raptis, J. P. Fackler Jr., H. H. Murray and L. C. Porter, *Inorg. Chem.*, **28**, 4057 (1989).
275. D. D. Heinrich and J. P. Fackler Jr., *Inorg. Chem.*, **29**, 4402 (1990).
276. H. H. Murray III, L. C. Porter, J. P. Fackler Jr. and R. G. Raptis, *J. Chem. Soc., Dalton Trans.*, 2669 (1988).
277. P. Jandik, U. Schubert and H. Schmidbaur, *Angew. Chem., Int. Ed. Engl.*, **21**, 73 (1982).
278. M. Bardají, M. C. Gimeno, J. Jiménez, A. Laguna, M. Laguna and P. G. Jones, *J. Organomet. Chem.*, **441**, 339 (1992).
279. H. Schmidbaur, C. Hartmann, J. Riede, B. Huber and G. Müller, *Organometallics*, **5**, 1652 (1986).
280. H. C. Knachel, D. S. Dudis and J. P. Fackler Jr., *Organometallics*, **3**, 1312 (1984).
281. H. Schmidbaur and C. Hartmann, *Angew. Chem., Int. Ed. Engl.*, **25**, 575 (1986).
282. R. G. Raptis, L. C. Porter, R. J. Emrich, H. H. Murray and J. P. Fackler Jr., *Inorg. Chem.*, **29**, 4408 (1990).
283. J. P. Fackler Jr. and B. Trzcinska-Bancroft, *Organometallics*, **4**, 1891 (1985).
284. R. J. H. Clark, J. H. Tocher, J. P. Fackler Jr., R. Neira, H. H. Murray and H. Knachel, *J. Organomet. Chem.*, **303**, 437 (1986).
285. J. P. Fackler Jr., H. H. Murray and J. D. Basil, *Organometallics*, **3**, 821 (1984).
286. S. Wang and J. P. Fackler Jr., *Organometallics*, **7**, 2415 (1988).
287. S. Wang and J. P. Fackler Jr., *Organometallics*, **8**, 1578 (1989).
288. H. Schmidbaur, C. Hartmann and F. E. Wagner, *Angew. Chem., Int. Ed. Engl.*, **26**, 1148 (1987).
289. R. Usón, A. Laguna, M. Laguna, M. T. Tartón and P. G. Jones, *J. Chem. Soc., Chem. Commun.*, 740 (1988).
290. M. A. Bennett, *J. Organomet. Chem.*, **300**, 7 (1986).
291. E. Ahmed, R. J. H. Clark, M. L. Tobe and L. Cattalini, *J. Chem. Soc., Dalton Trans.*, 2701 (1990).
292. R. Usón, A. Laguna, M. U. de la Orden, R. V. Parish and L. S. Moore, *J. Organomet. Chem.*, **282**, 145 (1985).
293. E. Cerrada, E. J. Fernández, P. G. Jones, A. Laguna, M. Laguna and R. Terroba, *Organometallics*, **14**, 5537 (1995).
294. E. Cerrada, E. J. Fernández, M. C. Gimeno, A. Laguna, M. Laguna, R. Terroba and M. D. Villacampa, *J. Organomet. Chem.*, **492**, 105 (1995).
295. J. Vicente, M. T. Chicote and M.-D. Bermúdez, *Inorg. Chim. Acta*, **63**, 35 (1982).

296. J. Vicente, M. T. Chicote, M.-D. Bermúdez and M. Garcia-Garcia, *J. Organomet. Chem.*, **295**, 125 (1985).
297. J. Vicente, M.-D. Bermúdez, M.-T. Chicote and M.-J. Sánchez-Santano, *J. Chem. Soc., Dalton Trans.*, 1945 (1990).
298. J. Vicente, M. T. Chicote and M.-D. Bermúdez, *J. Organomet. Chem.*, **268**, 191 (1984).
299. J. Vicente, M. T. Chicote, M.-D. Bermúdez, P. G. Jones, C. Fittschen and G. M. Sheldrick, *J. Chem. Soc., Dalton Trans.*, 2361 (1986).
300. E. C. Constable and T. A. Leese, *J. Organomet. Chem.*, **363**, 419 (1989).
301. M. A. Cinellu, A. Zucca, S. Stoccoro, G. Minghetti, M. Manassero and M. Sansoni, *J. Chem. Soc., Dalton Trans.*, 2865 (1995).
302. H. Q. Liu, T. C. Cheung, S. M. Peng and C. M. Che, *J. Chem. Soc., Chem. Commun.*, 1787 (1995).
303. J. Vicente, M.-D. Bermúdez, F. J. Carrión and G. Martínez-Nicolás, *J. Organomet. Chem.*, **480**, 103 (1994).
304. E. C. Constable, R. P. G. Henney, P. R. Raithby and L. R. Sousa, *J. Chem. Soc., Dalton Trans.*, 2251 (1992).
305. E. C. Constable, R. P. G. Henney, P. R. Raithby and L. R. Sousa, *Angew. Chem., Int. Ed. Engl.*, **30**, 1363 (1991).
306. E. C. Constable, R. P. G. Henney and T. A. Leese, *J. Organomet. Chem.*, **361**, 277 (1989).
307. C. W. Chan, W. T. Wong and C. M. Che, *Inorg. Chem.*, **33**, 1266 (1994).
308. M. Paul and H. Schmidbaur, *Z. Naturforsch.*, **49b**, 647 (1994).
309. Y. Mizuno and S. Komiya, *Inorg. Chim. Acta*, **125**, L13 (1986).
310. J. A. Morrison, *Adv. Organomet. Chem.*, **35**, 211 (1993).
311. J. L. Margrave, K. H. Whitmire, R. H. Hauge and N. T. Norem, *Inorg. Chem.*, **29**, 3252 (1990).
312. R. Usón, A. Laguna, M. Laguna and M. Abad, *J. Organomet. Chem.*, **249**, 437 (1983).
313. J. Vicente, M. T. Chicote, A. Arcas, M. Artigao and R. Jimenez, *J. Organomet. Chem.*, **247**, 123 (1983).
314. R. Usón, J. Vicente, M. T. Chicote, P. G. Jones and G. M. Sheldrick, *J. Chem. Soc., Dalton Trans.*, 1131 (1983).
315. S. Shibata, K. Iijima and T. H. Baum, *J. Chem. Soc., Dalton Trans.*, 1519 (1990).
316. R. Usón, J. Vicente and M. T. Chicote, *J. Organomet. Chem.*, **209**, 271 (1981).
317. H. W. Chen, C. Paparizos and J. P. Fackler Jr., *Inorg. Chim. Acta*, **96**, 137 (1985).
318. R. Usón, A. Laguna, M. Laguna, M. L. Castilla, P. G. Jones and K. Meyer-Bäse, *J. Organomet. Chem.*, **336**, 453 (1987).
319. E. G. Perevalova, K. I. Grandberg, V. P. Dyadchenko and O. N. Kalinina, *J. Organomet. Chem.*, **352**, C37 (1988).
320. A. Laguna and M. Laguna, *J. Organomet. Chem.*, **394**, 743 (1990).
321. R. Usón, A. Laguna, M. Laguna, M. N. Fraile, P. G. Jones and C. Freire Erdbrügger, *J. Chem. Soc., Dalton Trans.*, 73 (1989).
322. U. Grässle, W. Hiller and J. Strähle, *Z. Anorg. Allg. Chem.*, **529**, 29 (1985).
323. H.-N. Adams, U. Grässle, W. Hiller and J. Strähle, *Z. Anorg. Allg. Chem.*, **504**, 7 (1983).
324. U. Grässle and J. Strähle, *Z. Anorg. Allg. Chem.*, **531**, 26 (1985).
325. P. K. Byers, A. J. Canty, N. J. Minchin, J. M. Patrick, B. W. Skelton and A. H. White, *J. Chem. Soc., Dalton Trans.*, 1183 (1985).
326. P. K. Byers, A. J. Canty, L. M. Engelhardt, J. M. Patrick and A. H. White, *J. Chem. Soc., Dalton Trans.*, 981 (1985).
327. A. J. Canty, N. J. Minchin, P. C. Healy and A. H. White, *J. Chem. Soc., Dalton Trans.*, 1795 (1982).
328. A. J. Canty, N. J. Minchin, J. M. Patrick and A. H. White, *Aust. J. Chem.*, **36**, 1107 (1983).
329. A. J. Canty, R. Colton and I. M. Thomas, *J. Organomet. Chem.*, **455**, 283 (1993).
330. B. Assmann, K. Angermaier, M. Paul, J. Riede and H. Schmidbaur, *Chem. Ber.*, **128**, 891 (1995).
331. P. K. Byers, A. J. Canty, K. Mills and L. Titcombe, *J. Organomet. Chem.*, **295**, 401 (1985).
332. V. W.-W. Yam, S. W.-K. Choi, T.-F. Lai and W.-K. Lee, *J. Chem. Soc., Dalton Trans.*, 1001 (1993).
333. J. Vicente, M.-T. Chicote, M.-D. Bermúdez, X. Soláns and M. Font-Altaba, *J. Chem. Soc., Dalton Trans.*, 557 (1984).
334. J. Vicente, M.-D. Bermúdez, M. J. Sánchez-Santano and J. Payá, *Inorg. Chim. Acta*, **174**, 53 (1990).

335. J. Vicente, M.-T. Chicote, M.-D. Bermúdez, M. J. Sanchez-Santano, P. G. Jones, C. Fittschen and G. M. Sheldrick, *J. Organomet. Chem.*, **310**, 401 (1986).
336. J. Vicente, M.-D. Bermúdez, J. Escribano, M. P. Carrillo and P. G. Jones, *J. Chem. Soc., Dalton Trans.*, 3083 (1990).
337. J. Vicente, M.-D. Bermúdez, M. T. Chicote and M. J. Sanchez-Santano, *J. Organomet. Chem.*, **381**, 285 (1990).
338. J. Vicente, M.-D. Bermúdez, M. T. Chicote and M. J. Sanchez-Santano, *J. Organomet. Chem.*, **371**, 129 (1989).
339. J. Vicente, M. T. Chicote, M.-D. Bermúdez, M. J. Sanchez-Santano and P. G. Jones, *J. Organomet. Chem.*, **354**, 381 (1988).
340. J. Vicente, M.-D. Bermúdez and J. Escribano, *Organometallics*, **10**, 3380 (1991).
341. J. Vicente, M.-D. Bermúdez, M.-T. Chicote and M.-J. Sánchez-Santano, *J. Chem. Soc., Chem. Commun.*, 141 (1989).
342. J. Vicente, M.-D. Bermúdez, M.-P. Carrillo and P. G. Jones, *J. Chem. Soc., Dalton Trans.*, 1975 (1992).
343. J. Vicente, M.-D. Bermúdez, M.-P. Carrillo and P. G. Jones, *J. Organomet. Chem.*, **456**, 305 (1993).
344. J. Vicente, M.-D. Bermúdez and F. J. Carrión, *Inorg. Chim. Acta*, **220**, 1 (1994).
345. E. J. Fernández, M. C. Gimeno, P. G. Jones, B. Ahrens, A. Laguna, M. Laguna and J. M. López-de-Luzuriaga, *J. Chem. Soc., Dalton Trans.*, 3487 (1994).
346. R. Usón, A. Laguna, M. Laguna, B. R. Manzano, P. G. Jones and G. M. Sheldrick, *J. Chem. Soc., Dalton Trans.*, 2417 (1985).
347. R. Usón, A. Laguna, M. Laguna, B. R. Manzano, P. G. Jones and G. M. Sheldrick, *J. Chem. Soc., Dalton Trans.*, 839 (1984).
348. G. M. Bancroft, T. C. S. Chan and R. J. Puddephatt, *Inorg. Chem.*, **22**, 2133 (1983).
349. S. Komiya and A. Shibue, *Organometallics*, **4**, 684 (1985).
350. R. Usón, A. Laguna, M. Laguna, E. Fernandez, P. G. Jones and G. M. Sheldrick, *J. Chem. Soc., Dalton Trans.*, 1971 (1982).
351. S. Komiya, S. Ozaki and A. Shibue, *J. Chem. Soc., Chem. Commun.*, 1555 (1986).
352. T. Sone, S. Ozaki, N. C. Kasuga, A. Fukuoka and S. Komiya, *Bull. Chem. Soc. Jpn.*, **68**, 1523 (1995).
353. S. Komiya, T. Sone, S. Ozaki, M. Ishikawa and N. Kasuga, *J. Organomet. Chem.*, **428**, 303 (1992).
354. R. Usón, A. Laguna, M. Laguna, J. Jiménez and M. E. Durana, *Inorg. Chim. Acta*, **168**, 89 (1990).
355. R. Usón, A. Laguna and M. D. Villacampa, *Inorg. Chim. Acta*, **122**, 81 (1986).
356. M. A. Guerra, T. R. Bierschenk and R. J. Lagow, *J. Organomet. Chem.*, **307**, C58 (1986).
357. S. Komiya, A. Shibue and S. Ozaki, *J. Organomet. Chem.*, **319**, C31 (1987).
358. J. K. Jawad, R. J. Puddephatt and M. A. Stalteri, *Inorg. Chem.*, **21**, 332 (1982).
359. S. Komiya, M. Ishikawa and S. Ozaki, *Organometallics*, **7**, 2238 (1988).
360. R. Usón, A. Laguna, M. Laguna, I. Lázaro, P. G. Jones and C. Fittschen, *J. Chem. Soc., Dalton Trans.*, 2323 (1988).
361. R. Usón, A. Laguna, M. Laguna, I. Lázaro and P. G. Jones, *Organometallics*, **6**, 2326 (1987).
362. M. C. Gimeno, P. G. Jones, A. Laguna, M. Laguna and I. Lázaro, *J. Chem. Soc., Dalton Trans.*, 2223 (1993).
363. (a) S. Komiya, S. Ozaki, I. Endo, K. Inoue, N. Kasuga and Y. Ishizaki, *J. Organomet. Chem.*, **433**, 337 (1992). (b) J. A. Schlueter, J. M. Williams, U. Geiser, J. D. Dudek, S. A. Sirchio, M. E. Kelly, J. S. Gregar, W. H. Kwok, J. A. Fendrich, J. E. Schirber, W. R. Bayless, D. Naumann and T. Roy, *J. Chem. Soc., Chem. Commun.*, 1311 (1995).
364. A. J. Markwell, *J. Organomet. Chem.*, **293**, 257 (1985).
365. S. Komiya, S. Meguro, A. Shibue and S. Ozaki, *J. Organomet. Chem.*, **328**, C40 (1987).
366. A. Laguna, M. Laguna, M. C. Gimeno and P. G. Jones, *Organometallics*, **11**, 2759 (1992).
367. W. Bos, R.P. F. Kanters, C. J. van Halen, W. P. Bosman, H. Behm, J. M. M. Smits, P. T. Beurskens, J. J. Bour and L. H. Pignolet, *J. Organomet. Chem.*, **307**, 385 (1986).
368. R. P. F. Kanters, P. P. J. Schlebos, J. J. Bour, J. Wijnhoven, E. van den Berg and J. J. Steggerda, *J. Organomet. Chem.*, **388**, 233 (1990).
369. A. M. Mueting, W. Bos, B. D. Alexander, P. D. Boyle, J. A. Casalnuovo, S. Balaban, L. N. Ito, S. M. Johnson and L. H. Pignolet, *New J. Chem.*, **12**, 505 (1988).
370. M. I. Bruce, G. A. Koutsantonis and E. R. T. Tiekink, *J. Organomet. Chem.*, **408**, 77 (1991).

371. C. M. Hay, B. F. G. Johnson, J. Lewis, N. D. Prior, P. R. Raithby and W. T. Wong, *J. Organomet. Chem.*, **401**, C20 (1991).
372. M. I. Bruce, *J. Organomet. Chem.*, **400**, 321 (1990).
373. A. D. Horton, M. J. Mays and M. McPartlin, *J. Chem. Soc., Chem. Commun.*, 424 (1987).
374. C. Thöne and H. Vahrenkamp, *J. Organomet. Chem.*, **485**, 185 (1995).
375. P. H. Kasai, *J. Am. Chem. Soc.*, **106**, 3069 (1984).
376. P. H. Kasai, *J. Am. Chem. Soc.*, **105**, 6704 (1983).
377. J. H. B. Chenier, J. A. Howard, B. Mile and R. Sutcliffe, *J. Am. Chem. Soc.*, **105**, 788 (1983).
378. J. H. B. Chenier, J. A. Howard and B. Mile, *J. Am. Chem. Soc.*, **107**, 4190 (1985).
379. A. J. Buck, B. Mile and J. A. Howard, *J. Am. Chem. Soc.*, **105**, 3381 (1983).
380. R. L. Garrell, T. M. Herne, C. A. Szafranski, F. Diederich, F. Ettl and R. L. Whetten, *J. Am. Chem. Soc.*, **113**, 6302 (1991).
381. G. Nicolas and F. Spiegelmann, *J. Am. Chem. Soc.*, **112**, 5410 (1990).
382. D. Belli Dell'Amico, F. Calderazzo, R. Dantona, J. Strähle and H. Weiss, *Organometallics*, **6**, 1207 (1987).
383. R. M. Dávila, R. J. Staples and J. P. Fackler, Jr., *Organometallics*, **13**, 418 (1994).
384. J. E. Goldberg, D. F. Mullica, E. L. Sappenfield and F. G. A. Stone, *J. Chem. Soc., Dalton Trans.*, 2495 (1992).
385. G. A. Carriedo, V. Riera, G. Sánchez, X. Solans and M. Labrador, *J. Organomet. Chem.*, **391**, 431 (1990).
386. V. G. Albano, L. Busetto, M. C. Cassani, P. Sabatino, A. Schmitz and V. Zanotti, *J. Chem. Soc., Dalton Trans.*, 2087 (1995).
387. J. C. Jeffery, P. A. Jelliss and F. G. A. Stone, *Organometallics*, **13**, 2651 (1994).
388. J. C. Jeffery, P. A. Jelliss and F. G. A. Stone, *J. Chem. Soc., Dalton Trans.*, 1073 (1993).
389. F. G. A. Stone, *Adv. Organomet. Chem.*, **31**, 53 (1990).
390. F. Bonati and G. Minghetti, *Synth. React. Inorg. Metal-Org. Chem.*, **1**, 299 (1971).
391. G. Minghetti and F. Bonati, *J. Organomet. Chem.*, **54**, C62 (1973).
392. G. Minghetti, F. Bonati and G. Banditelli, *Inorg. Chem.*, **15**, 1718 (1976).
393. G. Banditelli, A. L. Bandini, G. Pacchioni, G. Minghetti, R. Seraglia and P. Traldi, *Org. Mass Spectrom.*, **26**, 945 (1991).
394. A. L. Bandini, G. Banditelli, G. Minghetti, B. Pelli and P. Traldi, *Organometallics*, **8**, 590 (1989).
395. F. Bonati and G. Minghetti, *J. Organomet. Chem.*, **59**, 403 (1973).
396. G. Banditelli, F. Bonati and G. Minghetti, *Gazz. Chim. Ital.*, **107**, 267 (1977).
397. J. A. McCleverty and M. M. M. Da Mota, *J. Chem. Soc., Dalton Trans.*, 2571 (1973).
398. R. Usón, A. Laguna and M. D. Villacampa, *Inorg. Chim. Acta*, **81**, 25 (1984).
399. J. E. Parks and A. L. Balch, *J. Organomet. Chem.*, **71**, 453 (1974).
400. K. Bartel and W. P. Fehlhammer, *Angew. Chem., Int. Ed. Engl.*, **13**, 599 (1974).
401. W. Beck, W. Weigand, U. Nagel and M. Schaal, *Angew. Chem., Int. Ed. Engl.*, **23**, 377 (1984).
402. R. Usón, A. Laguna, P. Brun, M. Laguna and M. Abad, *J. Organomet. Chem.*, **218**, 265 (1981).
403. R. Usón, A. Laguna, M. D. Villacampa, P. G. Jones and G. M. Sheldrick, *J. Chem. Soc., Dalton Trans.*, 2035 (1984).
404. W. P. Fehlhammer and W. Finck, *J. Organomet. Chem.*, **414**, 261 (1991).
405. B. Cetinkaya, P. Dixneuf and M. F. Lappert, *J. Chem. Soc., Dalton Trans.*, 1827 (1974).
406. G. Minghetti and F. Bonati, *J. Organomet. Chem.*, **73**, C43 (1974).
407. R. Aumann and E. O. Fischer, *Chem. Ber.*, **114**, 1853 (1981).
408. F. Bonati, A. Burini, B. R. Pietroni and B. Bovio, *J. Organomet. Chem.*, **375**, 147 (1989).
409. H. G. Raubenheimer, F. Scott, M. Roos and R. Otte, *J. Chem. Soc., Chem. Commun.*, 1722 (1990).
410. H. G. Raubenheimer, F. Scott, G. J. Kruger, J. G. Toerien, R. Otte, W. van Zyl, I. Taljaard, P. Olivier and L. Linford, *J. Chem. Soc., Dalton Trans.*, 2091 (1994).
411. H. G. Raubenheimer, L. Lindeque and S. Cronje, *J. Organomet. Chem.*, **511**, 177 (1996).
412. H. G. Raubenheimer, M. Desmet and G. J. Kruger, *J. Chem. Soc., Dalton Trans.*, 2067 (1995).
413. M. Desmet, H. G. Raubenheimer and G. J. Kruger, unpublished.
414. F. Bonati, A. Burini, B. R. Pietroni and B. Bovio, *J. Organomet. Chem.*, **408**, 271 (1991).
415. B. Bovio, A. Burini and B. R. Pietroni, *J. Organomet. Chem.*, **452**, 287 (1993).
416. H. G. Raubenheimer, J. G. Toerien, G. J. Kruger, R. Otte, W. van Zyl and P. Olivier, *J. Organomet. Chem.*, **466**, 291 (1994).

417. L. G. Vaughan, *J. Am. Chem. Soc.*, **92**, 730 (1970).
418. P. Jutzi and H. Hensler, *J. Organomet. Chem.*, **8**, 829 (1976).
419. E. O. Fischer and M. Boeck, *J. Organomet. Chem.*, **287**, 279 (1985).
420. E. O. Fischer, M. Boeck and R. Aumann, *Chem. Ber.*, **116**, 3618 (1983).
421. R. Ishii, T. Kaharu, N. Pirio, S. W. Zhang and S. Takahashi, *J. Chem. Soc., Chem. Commun.*, 1215 (1995).

CHAPTER **9**

The electrochemistry of gold and silver complexes

AHMED A. MOHAMED, ALICE E. BRUCE and MITCHELL R. M. BRUCE

Department of Chemistry, University of Maine, Orono, Maine 04469-5706, USA
Fax: 207-581-1191;   e-mail: mbruce@maine.maine.edu

I. INTRODUCTION

Gold and silver belong to the group known as coinage metals. They occupy positions near the bottom of the electrochemical series and so they are difficult to oxidize. Silver oxidizes to Ag^+ at +0.7996 V *vs* NHE while $Au^0 \rightarrow Au^I$ oxidation takes place at +1.692 V and $Au^I \rightarrow Au^{III}$ occurs at +1.498 V (Table 1). In contrast, metals near the top of the electrochemical series, such as Na, are very active, i.e. Na oxidizes to Na^+ at −2.71 V *vs* NHE[1]. The reactivity of Cu, Ag and Au decreases down the group[2]. Although gold and silver are often grouped together, their chemical and physical properties differ significantly, partly as a result of increased relativistic effects for gold[3]. The effects of solvent interaction

TABLE 1.   Standard reduction potentials of gold and silver compounds[1]

Reaction							E^0, V vs NHE^a
AgI	+	e$^-$	=	Ag	+	I$^-$	−0.15224
Ag$_2$CO$_3$	+	2 e$^-$	=	2 Ag	+	CO$_3{}^{2-}$	−0.017
AgBr	+	e$^-$	=	Ag	+	Br$^-$	+0.07133
AgCl	+	e$^-$	=	Ag	+	Cl$^-$	+0.22233
AgNO$_2$	+	e$^-$	=	Ag	+	NO$_2{}^-$	+0.564
AgF	+	e$^-$	=	Ag	+	F$^-$	+0.779
Ag$^+$	+	e$^-$	=	Ag			+0.7996
AuBr$_4{}^-$	+	3 e$^-$	=	Au	+	4 Br$^-$	+0.854
AuBr$_2{}^-$	+	e$^-$	=	Au	+	2 Br$^-$	+0.959
AuCl$_4{}^-$	+	3 e$^-$	=	Au	+	4 Cl$^-$	+1.002
Au^{3+}	+	2 e$^-$	=	Au$^+$			+1.401
Au^{3+}	+	3 e$^-$	=	Au			+1.498
Au$^+$	+	e$^-$	=	Au			+1.692
Ag^{2+}	+	e$^-$	=	Ag$^+$			+1.980

^{a}At 25 °C and 1 atm.

and ligand stabilization on redox properties are also quite pronounced. The most common oxidation state of silver is +1 while for gold the +1 and +3 states are most common. In aqueous solution, Ag^{II}, Ag^{III} and Au^I are either unstable or form insoluble compounds. However, in nonaqueous solvents, Au^I can be stabilized by the appropriate ligand set. Linear Au^I compounds containing a combination of trialkyl or triaryl phosphine ligands with an anionic ligand, such as thiolate or halide, are especially prevalent.

There is no doubt that the chemistry of gold and silver has expanded dramatically since 1980. However, electrochemical studies are still fairly limited compared with those of other transition metals of biological importance. To our knowledge, no extensive reviews have appeared on the electrochemistry of gold and silver complexes. Several reviews that are more limited in scope have appeared in the literature and these are referenced in the appropriate sections.

This chapter is organized by ligand type. This organization recognizes the importance that ligand–metal interactions play in the redox chemistry of gold and silver compounds. The general approach has been to offer an interpretation of trends in redox potentials as a function of each ligand type. An extensive tabulation of physical and spectroscopic properties has not been included. The chapter is built around several core sections concerning gold and silver interactions with carbon (phosphorus ylides and organometallics), biologically active molecules (drugs and phosphine gold thiolates) and complexes with promising commercial applications (dithiolenes and dithiocarbamates). Other sections such as L$_2$Au and L$_n$Ag, phosphine gold halides, and imides and anilides are provided to give coverage to ligand types that are related to the core sections. Although comprehensive literature citation of electrochemical studies was not the major goal, we hope that reasonably good coverage of the core sections was achieved. Finally, we have also included a brief survey of a few other ligands and structural types where electrochemistry of gold and silver have been reported.

The electrochemical investigations of gold and silver have employed a range of electrochemical techniques, working electrodes, solvents and reference electrodes. In compiling the tables that appear in this chapter, a decision was made to report all potentials as

TABLE 2.   Conversion of reference electrodes and couples[a].

	SCE[b]	Ag/AgCl[c]	Fc/Fc[+d]	NHE	Ag/Ag[+e]
SCE[b]	—	+0.045 V	−0.307 V	+0.241 V	−0.559 V
Ag/AgCl[c]	−0.045 V	—	−0.352 V	+0.197 V	−0.604 V
Fc/Fc[+d]	+0.307 V	+0.352 V	—	+0.549 V	−0.252 V
NHE	−0.241 V	−0.197 V	−0.549 V	—	−0.800 V
Ag/Ag[+e]	+0.559 V	+0.604 V	+0.252 V	+0.800 V	—

[a]Read across table and add voltage factor to convert from one reference electrode or couple to another. All data taken from Reference 4.
[b]Hg/Hg_2Cl_2, KCl (sat'd).
[c]KCl (sat'd).
[d]Reference 4, p. 701, Fc/Fc[+] couple in 0.2 M $LiClO_4$/MeCN = +0.307 V *vs* SCE.
[e]Reference 4, p. 699.

published using the reference system employed, and not to also report the potentials in a common reference scale. An obvious disadvantage of this omission is that it makes direct comparison between studies employing different reference systems somewhat cumbersome. However, we believe the decision is sound because a significant proportion of the redox processes reported in this chapter involve irreversible electrochemical processes measured in nonaqueous solvents. These redox processes are particularly sensitive to a host of factors such as electrode, solvent, electrolyte and cell configuration, which in turn affect capacitance, adsorption and cell resistance (*i*R drop).

Despite the caveat expressed above, it is still often useful to convert from one reference system to another when discussing studies involving closely related compounds. Table 2 presents the conversion factors employed in discussions in the chapter. A survey of the electrochemical literature reveals that differences in conversion factors exist. Thus, Table 2 is provided only for the purpose of approximating potentials in different reference systems. The reader is referred to a number of excellent reference which discuss the complications involved in rigorously converting reference systems[5].

In compiling the redox couples for tables that appear in this chapter, we have routinely rounded peak potentials to the nearest 10 mV. Redox potential values that appear to occur outside the normal useful working range of a solvent at a particular electrode[4] were not, in general, included in the tables. For ligands that have common or easily recognized abbreviations, these are also provided in the tables and may also be used in the text and equations. For many of the entries in the tables, notations have been made about reversible (rev), quasi-reversible (qr) or irreversible (ir) processes.

II. DITHIOLENES AND DISELENOLENES

In 1,2-dithiolene complexes (or the selenium analogs), there is extensive delocalization of the electrons through the π system of the ligand as well as with metal $d\pi$ orbitals of the corresponding symmetry[6]. This extensive delocalization makes it possible for dithiolene complexes to exist with a range of electron populations. It also makes assignment of the metal oxidation states ambiguous. The 1,2-dithiolenes are expected to have more metal−ligand π-bonding than 1,1-dithiolenes (e.g. dithiocarbamates), which is evidenced by the short M−S bond lengths and facile reversible redox reactions in the former. In contrast, 1,1-dithiolene complexes, with strained four-membered chelate rings and deviation from ideal coordination geometries, are expected to show less reversible redox behavior and have weaker M−S bonds than 1,2-dithiolenes[6]. Monomeric bis(1,2-dithiolene)

complexes may undergo one, two or three redox processes according to equation 1, where the two dithiolene ligands are represented simply by S_4.

$$[M-S_4]^{2-} \rightleftharpoons [M-S_4]^{-} \rightleftharpoons [M-S_4]^{0} \rightleftharpoons [M-S_4]^{+} \qquad (1)$$
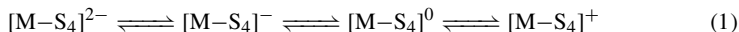
The expansion in dithiolene chemistry is due to a wide variety of applications of this type of compound in fungicides, pesticides, fingerprint developers, specific analytical reagents and highly electrical conductors. There are a number of examples of 1,2-dithiolene and diselenolene gold complexes, but to our knowledge there are no examples of silver for which electrochemical data are available.

Electrochemical potentials obtained from cyclic voltammetry studies of gold 1,2-dithiolene and diselenolene complexes are listed in Table 3[7−21]. These studies reveal

TABLE 3. Cyclic voltammetry data (V) of 1,2-dithiolenes and 1,2-diselenolenes

Compound	Alternative formula	Redox couples				Ref. couple	Solvent	Ref.
		1/0	0/1−	1−/2−	2−/3−			
[Au(1a)$_2$]^n	[Au(mnt)$_2$]^n		+1.51 (rev)	−0.54 (rev)	−1.33 (ir)	Ag/AgCl	CH$_2$Cl$_2$	7
				−0.96 (rev)[a]		Ag/AgClO$_4$	DMF	8
				−0.42 (rev)[a]		SCE	MeCN	9
				−0.61[a]		SCE	MeCN	10
[Au(1b)$_2$]^n	[Au(tfd)$_2$]^n		+1.32 (rev)	−0.97 (rev)[a]		SCE	CH$_2$Cl$_2$	11
			+1.20 (rev)[a]	b		SCE	MeCN	9
[Au(1c)$_2$]^n	[Au(tds)$_2$]^n		+1.04 (ir)	−1.10		SCE	MeCN	12
[Au(2a)$_2$]^n	[Au(C$_3$S$_5$)$_2$]^n		+0.72 (qr)	−0.52		SCE	DMF	13
[Au(2b)$_2$]^n	[Au(C$_3$Se$_5$)$_2$]^n		+0.34 (ir)	−0.70 (rev)		SCE	DMF	13
[Au(3)$_2$]^n	[Au(dddt)$_2$]^n	+0.82 (qr)	+0.41 (rev)	−1.32 (rev)		SCE	CH$_2$Cl$_2$	14
[Au(4)$_2$]^n	[Au(oxdt-dt)$_2$]^n		+0.41 (rev)			SCE	CH$_2$Cl$_2$	15
[Au(5)$_2$]^n	[Au(C$_8$H$_4$S$_8$)$_2$]^n		+0.10			SCE	DMF	16
[Au(6)$_2$]^n	[Au(dpdt)$_2$]^n		+1.28 (ir)	+0.63 (ir)		SCE	MeCN	17
[Au(7)$_2$]^n	[Au(diod)$_2$]^n		+0.64 (ir)	c		SCE	MeCN	18
[Au(8a)$_2$]^n	[Au(bdt)$_2$]^n		+0.53 (qr)	−1.57 (rev)		SCE	MeCN	19
			+0.37 (rev)			Fc/Fc$^+$	DMF	20
[Au(8b)$_2$]^n	[Au(tdt)$_2$]^n		+0.46 (qr)	−1.61 (rev)		SCE	MeCN	19
				−1.95 (rev)		Ag/AgClO$_4$	DMF	8
[Au(8c)$_2$]^n	[Au(Bu-t-bdt)$_2$]^n		+0.59 (ir)	−1.59 (rev)		SCE	MeCN	19
[Au(9a)$_2$]^n	[Au(xdt)$_2$]^n		+0.22 (rev)			Fc/Fc$^+$	DMF	20
[Au(9b)$_2$]^n			+0.25 (rev)			Fc/Fc$^+$	DMF	20
[Au(9c)$_2$]^n			+0.06 (rev)			Fc/Fc$^+$	DMF	20
[Au(9d)$_2$]^n			+0.26 (rev)			Fc/Fc$^+$	DMF	20
[Au(9e)$_2$]^n			+0.15 (ir)			Fc/Fc$^+$	DMF	20
[Au(9f)$_2$]^n			+0.43 (ir)			Fc/Fc$^+$	DMF	20
[Au(9g)$_2$]^n			+0.29 (rev)			Fc/Fc$^+$	DMF	20
[Au(10a)$_2$]^n	[Au(Me$_4$bdt)$_2$]^n		+0.13 (rev)			Fc/Fc$^+$	DMF	20
[Au(10b)$_2$]^n	[Au(tcdt)$_2$]^n			−1.67[a]		Ag/AgClO$_4$	DMF	21
[Au(11)$_2$]^n	[Au(Naph-dt)$_2$]^n		+0.51 (rev)			Fc/Fc$^+$	DMF	20

[a]Polarography at dme.
[b]No wave found in the range 0 to −1.5 V.
[c]Not observed.

a rich redox chemistry, consistent with the behavior of many other metal dithiolene complexes. There are several prominent features of the data; the redox couples are highly ligand dependent and many of the redox processes are reversible. Transition metal complexes with the maleonitriledithiolate ligand (mnt, **1**) have been intensely studied since the mid-1960s when reports began to appear describing the ability of mnt to form highly colored transition metal complexes in interesting oxidation states. Cyclic voltammetry studies of square planar, $[Au(mnt)_2]^-$ complexes have measured the potentials for the $0/1^-$, $1^-/2^-$ and $2^-/3^-$ couples. The first two redox couples are reversible in CH_2Cl_2[7], DMF[8] and MeCN[9,10] (see equations 2 and 3)[7]. A seemingly wide range of redox potentials has been reported for the $1^-/2^-$ couple. However, inspection of Table 3 reveals that the reference electrode/solvent systems employed are largely responsible for this difference. For example, the $1^-/2^-$ couple at -0.96 V *vs* $Ag/AgClO_4$ would be approximately -0.4 V *vs* SCE, which compares favorably with other values reported for this couple. While the $2^-/3^-$ couple of the $[Cu(mnt)_2]^{2-}$ analog is electrochemically reversible, $[Au(mnt)_2]^-$ shows an irreversible electrochemical process in CH_2Cl_2 at 200 mV s^{-1} (equation 4)[7]. This was further investigated by infrared spectroelectrochemistry which indicates that a chemically reversible process occurs at longer timescales. These differences were attributable to kinetics of the reactions and the electronic structure of the complexes.

$$[Au(mnt)_2] + e^- \rightleftharpoons [Au(mnt)_2]^- \qquad E_{1/2} = +1.51 \text{ V} \qquad (2)$$

$$[Au(mnt)_2]^- + e^- \rightleftharpoons [Au(mnt)_2]^{2-} \qquad E_{1/2} = -0.54 \text{ V} \qquad (3)$$

$$[Au(mnt)_2]^{2-} + e^- \longrightarrow [Au(mnt)_2]^{3-} \qquad E_c = -1.33 \text{ V} \qquad (4)$$

(1a) E = S, X = CN   **(2a)** E = S   **(3)**   **(4)**
(1b) E = S, X = CF$_3$ **(2b)** E = Se
(1c) E = Se, X = CF$_3$
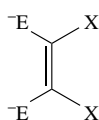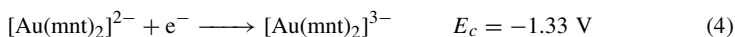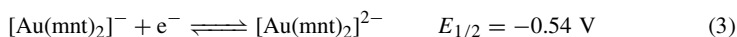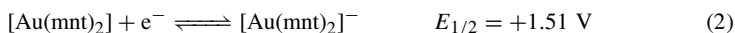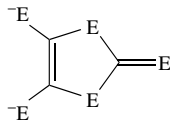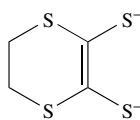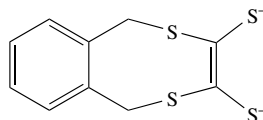
The $0/1^-$ couple in $[Au(tfd)_2]^-$ (tfd = bis(trifluoromethyl)ethylenedithiolate, **1b**) occurs at a slightly lower potential ($+1.32$ V *vs* SCE in CH_2Cl_2) than the mnt counterpart[9,11]. This is in accord with observations that in other transition metal 1,2-dithiolene complexes the ease of oxidation is dependent on X with X = Ph > CF$_3$ > CN[9]. Replacing sulfur with the less electronegative atom, selenium, results in a lower oxidation potential for $[Au(tds)_2]^-$ (tds = bis(trifluoromethyl)ethylenediselenolate, **1c**) relative to $[Au(tfd)_2]^-$[12]. More electronegative substituents make a complex easier to reduce, as expected. Thus, the $1^-/2^-$ couple for $[Au(mnt)_2]^-$ occurs approximately 500 mV more positive than the same couple for $[Au(tds)_2]^-$.

Similar electronic effects are observed for the cyclic ligands, **2a** and **2b**. The sulfur complex, $[Au(C_3S_5)_2]^-$, is oxidized quasi-reversibly at $+0.72$ V *vs* SCE (Figure 1a) while the selenium complex, $[Au(C_3Se_5)_2]^-$, undergoes an irreversible oxidation at $+0.34$ V (Figure 1b)[13]. Assignment of the $0/1^-$ couple as a ligand-based oxidation was made on
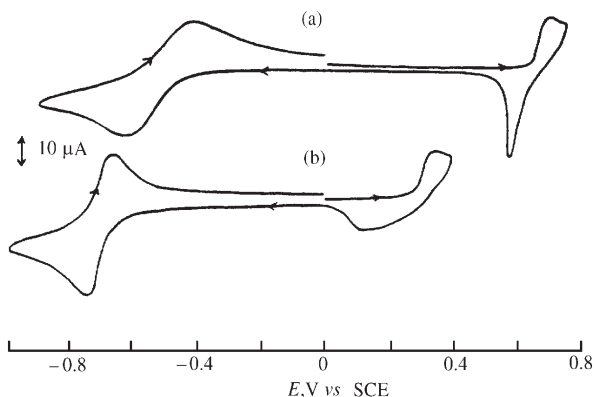
FIGURE 1. Cyclic voltammograms for 4.7×10^{-4} M compound in 0.1 M [Bu$_4$N]ClO$_4$/DMF at room temperature and scan rate of 100 mV s^{-1}: (a) **2a**; (b) **2b**. Reproduced by permission of the Royal Society of Chemistry from Reference 13

the basis of ESR data, and is consistent with the electrochemical potentials observed. The $1^-/2^-$ couple for the selenium complex is reversible (Figure 1b) and occurs at a lower potential than for the sulfur counterpart. The reason for the differences in reversibility for the sulfur and selenium derivatives is not apparent.

An interesting feature concerning the redox properties of the complex, [Au(dddt)$_2$]$^-$ (dddt = 5,6-dihydro-1,4-dithiine-2,3-dithiolate, **3**), is that the one-electron oxidized product, [Au(dddt)$_2$]^0, can be isolated[14]. An X-ray analysis of the neutral complex reveals a square planar gold structure stacked in 'dimeric' units as a result of intermolecular S - - - S contacts. Extended Hückel calculations predict that the odd electron resides primarily in a π^* orbital of the ligand and suggests that oxidation of the monoanion is ligand based. Oxidation of the neutral complex to the monocation was also reported to occur at +0.82 V *vs* SCE[14].

Incorporation of two of the sulfurs in an eight-membered ring has no apparent effect on the 0/1$^-$ couple, i.e. [Au(oxdt-dt)$_2$]$^-$ (oxdt-dt = *ortho*-xylenedithiodithiolate, **4**) oxidizes at the same potential as [Au(dddt)$_2$]$^-$, +0.41 V *vs* SCE. The one-electron oxidized product, [Au(oxdt-dt)$_2$]^0, was also isolated and characterized by elemental analysis[15].

Gold complexes of dithiolene ligands containing many sulfur atoms are expected to be oxidized at lower potentials. This is demonstrated by [Au(C$_8$H$_4$S$_8$)$_2$]$^-$ (C$_8$H$_4$S$_8$ = 2-(4,5-ethylenedithio)-1,3-dithiole-2-ylidene-1,3-dithiole-4,5-dithiolate, **5**), which oxidizes very readily to the neutral complex at +0.10 V *vs* SCE[16]. The partially oxidized complex, [Au(C$_8$H$_4$S$_8$)$_2$]$^{\delta+}$, could also be obtained, which is of interest for molecular conductivity.

(5)   **(6)**   **(7)**
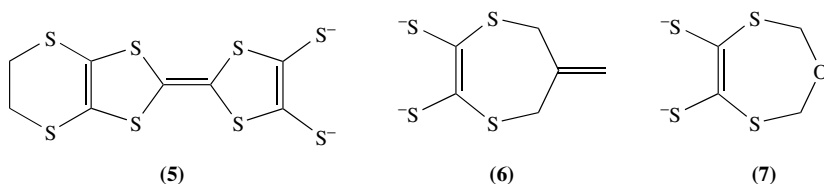
The 0/1$^-$ couple for [Au(dpdt)$_2$]$^-$ (dpdt = 6,7-dihydro-6-methylene-5H-1,4-dithiepine-2,3-dithiolate, **6**) occurs at +1.28 V *vs* SCE, which suggests that the electronic properties of dithiolene **6** are intermediate between mnt **(1a)** and tfd **(1b)**[17]. However, the 1$^-$/2$^-$ couple is reported at +0.63 V *vs* SCE, which is significantly more positive than the 1$^-$/2$^-$ couples for the other gold dithiolene complexes listed in Table 3. In addition, reduction of the monoanion, [Au(dpdt)$_2$]$^-$, is irreversible, in contrast to the other complexes, suggesting that in this case the product dianion is unstable.

A dithiolene ligand incorporating an oxygen atom in the ring backbone has recently been prepared and the corresponding nickel, copper and gold complexes were studied[18]. The gold complex, [Au(diod)$_2$]$^-$ (diod = 1,4-dithia-6-oxa-2,3-dithiolate, **7**), which was difficult to prepare, shows only a single irreversible oxidation at +0.64 V *vs* SCE. Reduction to the dianion was not observed up to −1.5 V *vs* SCE. Apparently, this dithiolene ligand is less able to delocalize negative charge.

A large number of derivatives of [Au(bdt)$_2$]$^-$ (bdt = benzene dithiolate, **8a**) with different substituents on the aromatic part of the ligand have been prepared **(8−11)**. The monoanionic gold complexes are typically green and contain square planar Au^{III}. Oxidation to the neutral complexes occurs at low, positive potentials and is dependent on the electronic properties of the aromatic substituents[19−21]. The stability of the monoanion relative to the dianion is greater for [Au(**8**)$_2$]^n than for [Au(mnt)$_2$]^n. An SCF-HF calculation using LANL1DZ core pseudopotentials was carried out on [Au(bdt)$_2$]$^-$ [20]. The calculation predicts that the HOMO is primarily a ligand-based π orbital while the LUMO is a mixed ligand/metal (*ca* 50% Au d$_{xy}$) orbital (see Figures 2a and 3). The HOMO should therefore be destabilized by electron-releasing substituents while the LUMO may be less sensitive to substituent electronic effects. The electrochemical data are consistent with this orbital description. Within series **9**, the complex which is easiest to oxidize is [Au(**9c**)$_2$]$^-$ with two methoxy groups, while the complex which is hardest to oxidize is [Au(**9f**)$_2$]$^-$. Note that the CV data for this series of complexes are referenced against the Fc/Fc$^+$ couple and the sweep rate necessary to achieve chemical reversibility varied[20]. Oxidation of [Au(**9e**)$_2$]$^-$ and [Au(**9f**)$_2$]$^-$ was irreversible even at ν = 1000 V s^{-1}, suggesting that the neutral species was chemically unstable.

(8a) R = H
(8b) R = Me
(8c) R = *t*-Bu

(9a) X = Me
(9b) X = SCH$_3$
(9c) X = OCH$_3$
(9d) XX = —SCH$_2$CH$_2$S—
(9e) XX = —OCH$_2$CH$_2$O—
(9f) XX = —SC(S)S—
(9g) XX = —SC(O)S—

(10a) X = Me
(10b) X = Cl

(11)

(a)

(b)

(1)   (1a)
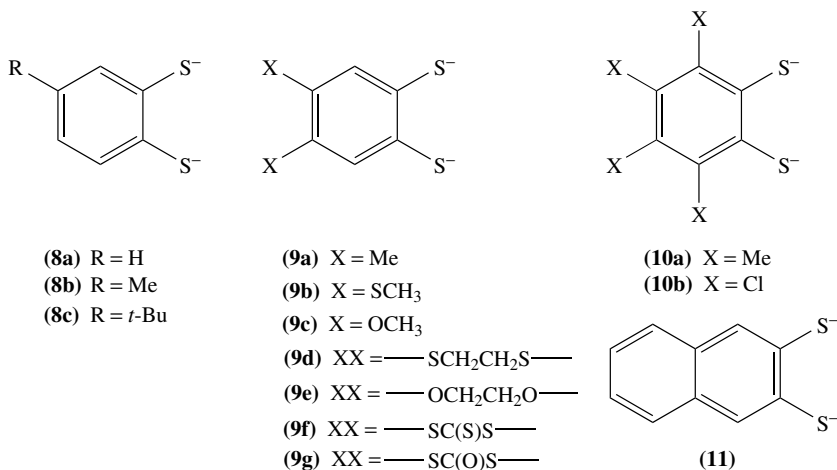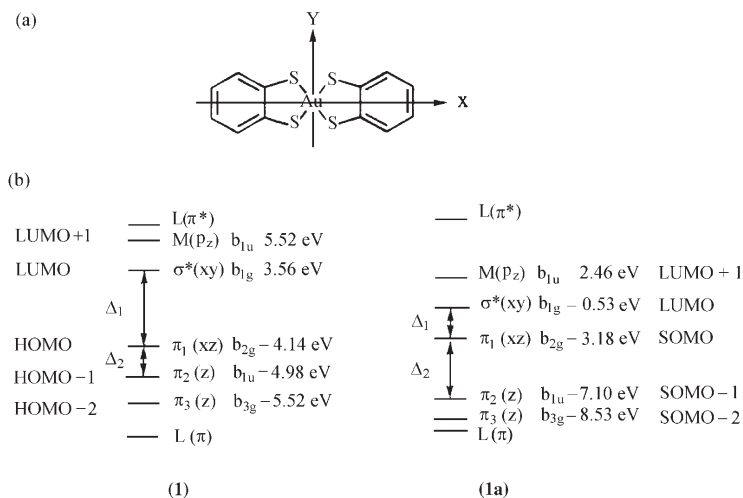
FIGURE 2. (a) Coordinate system of $[Au(\mathbf{8a})_2]^-$ used in the *ab initio* calculation; (b) electronic structure in the valence region of $\mathbf{I} = [Au(\mathbf{8a})_2]^-$ (left) and $\mathbf{Ia} = [Au(\mathbf{8a})_2]$ (right). Reprinted with permission from Reference 20. Copyright (1995) American Chemical Society

0.69 Au(d_{xy})

0.27 S(p_x) + 0.30 S(p_y) + 0.15S(s: not shown)

−0.16 C (p_x)

0.11C (p_y) − 0.21 C(s)

− 0.18C(s)

LUMO (b_{1g})

−0.21 Au(d_{zx})

0.34 S(p_z)

−0.21C(p_z)

−0.07 C(p_z)

0.16 C(p_z)

HOMO (b_{2g})

−0.11 Au(p_z)

0.27 S(p_z)

−0.24 C(p_z)

−0.06 C(p_z)

0.19 C(p_z)

HOMO-1 (b_{1u})

0.22 Au(d_{yz})

−0.29 S(p_z)

0.24 C(p_z)

0.15 C(p_z)

HOMO-2 (b_{3g})
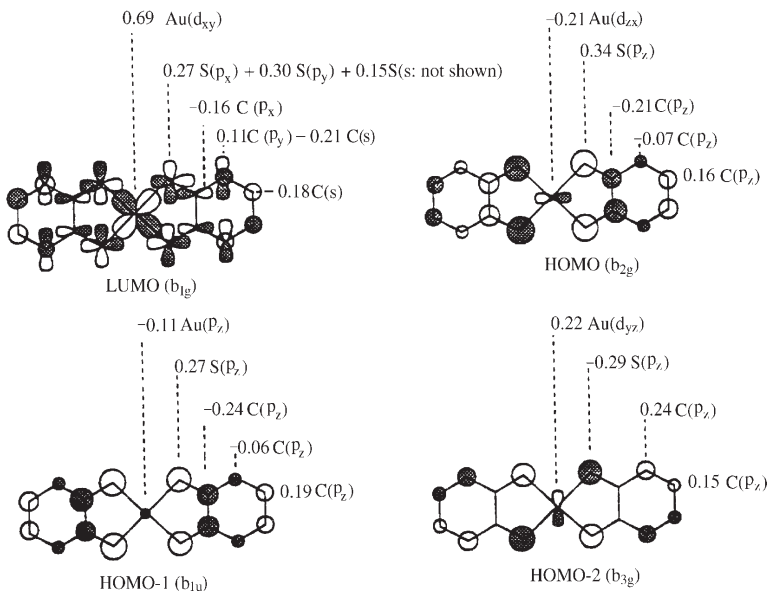
FIGURE 3. Valence molecular orbital basis function coefficients according to the *ab initio* calculations on $[Au(\mathbf{8a})_2]^-$. Reprinted with permission from Reference 20. Copyright (1995) American Chemical Society

The $1^-/2^-$ couple has been reported for only a few members of the $[Au(bdt)_2]^-$ series. However, the available data suggest that substituent electronic properties also affect the reduction potential of the monoanion. The complex, $[Au(tcdt)_2]^-$ (tcdt = 3,4,5,6-tetrachlorobenzene-1,2-dithiolate, **10b**), with four electron-withdrawing chlorine atoms, is easier to reduce (-1.67 V *vs* Ag/Ag$^+$)[21] than $[Au(tdt)_2]^-$ (tdt = toluene-3,4-dithiolate, **8b**) with one electron-releasing methyl group (-1.95 V *vs* Ag/Ag$^+$)[8].

An SCF-HF calculation on the neutral complex, $[Au(bdt)_2]$, reveals a similar ordering of the frontier orbitals compared to $[Au(bdt)_2]^-$ but with significantly different energies (see Figure 2b)[20]. Thus the calculation predicts that the odd electron in $[Au(bdt)_2]$ resides in a ligand-based orbital, consistent with experimental results from other laboratories which suggest that the $0/1^-$ couple in Au^{III} dithiolenes is a ligand-based oxidation (*vide supra*).

III. DITHIOCARBAMATES

Electrochemical data for gold dithiocarbamate (dtc) complexes are listed in Table 4. Van der Linden and coworkers studied a series of square planar Au^{III} dithiocarbamates, $[Au(12)_2]^+$ and mixed 1,2-dithiolene and dithiocarbamate complexes, Au(mnt)(dtc) and Au(tdt)(dtc)[10,22]. Note that the potentials in these studies were all obtained using a rotating

TABLE 4. Electrochemical data (V) of 1,1-dithiolenes and mixed 1,1- and 1,2-dithiolenes

Compound	Alternative Formula	Redox couples		Ref. Couple	Solvent[d]	Reference
		1/0	0/1$^-$			
$[Au(12a)_2]^+$	$[Au(dtc)_2]^+$	-0.29^a		SCE	CH_2Cl_2	10
$[Au(12b)_2]^+$	$[Au(Me_2dtc)_2]^+$	-0.22^a		SCE	CH_2Cl_2	22
$[Au(12c)_2]^+$	$[Au(Et_2dtc)_2]^+$	-0.26^a		SCE	CH_2Cl_2	22
$[Au(12d)_2]^+$	$[Au(Pr_2dtc)_2]^+$	-0.28^a		SCE	CH_2Cl_2	22
$[Au(12e)_2]^+$	$[Au(Bu_2dtc)_2]^+$	-0.29^a		SCE	CH_2Cl_2	22
$[Au(12f)_2]^+$	$[Au(Ph_2dtc)_2]^+$	-0.19^a		SCE	CH_2Cl_2	22
$[Au(1a)(12a)]$	$[Au(mnt)(dtc)]$		-0.46^a	SCE	CH_2Cl_2	10
$[Au(1a)(12f)]$	$[Au(mnt)(Ph_2dtc)]$		-0.41 (rev)^a	SCE	CH_2Cl_2	22
$[Au(1a)(12c)]$	$[Au(mnt)(Et_2dtc)]$		-0.45 (rev)^a	SCE	CH_2Cl_2	22
$[Au(1a)(12e)]$	$[Au(mnt)(Bu_2dtc)]$		-0.46 (rev)^a	SCE	CH_2Cl_2	22
$[Au(8b)(12a)]$	$[Au(tdt)(dtc)]$		-0.87^a	SCE	CH_2Cl_2	10
$[Au(12c)_3]$	$[Au(Et_2dtc)_3]$		-0.80 (rev)^b	SCE	PC	23
			-0.77^c	SCE	PC	23
$[Au(12d)_3]$	$[Au(Pr_2dtc)_3]$		-0.82^b	SCE	PC	23
			-0.84^c	SCE	PC	23
$[Au(12e)_3]$	$[Au(Bu_2dtc)_3]$		-0.79^b	SCE	PC	23
			-0.75^c	SCE	PC	23
$[Au(12g)_3]$	$[Au(Bn_2dtc)_3]$		-0.76^b	SCE	PC	23
$[Ag\{Co(12d)_3\}]^+$	$[Ag\{Co(Pr_2dtc)_3\}]^+$	-1.10^c		Fc/Fc$^+$	Tol^e/CH_2Cl_2	24

^{a}Rotating disk.
^{b}Polargraphy.
^{c}Cyclic voltammetry.
^{d}PC = propylene carbonate.
^{e}Tol = toluene

Pt disk electrode[10,22]. In contrast to the gold 1,2-dithiolene complexes, only one redox couple has been reported for the complexes containing dithiocarbamates. The monocations reduce at less negative potentials than the neutral, mixed complexes. The 1/0 couple for $[Au(12)_2]^+$ is irreversible and is fairly insensitive to the substituents bonded to nitrogen. Similarly, in the mixed 1,1- and 1,2-dithiolene complexes, the $0/1^-$ couple is more sensitive to the nature of the 1,2-dithiolene ligand rather than to the substituents on the 1,1-dithiolene ligand.

$$\begin{array}{c} S \\ \diagdown \\ \diagup \diagdown N \diagdown \\ {}^-S \end{array} \begin{array}{c} R \\ \diagup \\ \diagdown R \end{array}$$
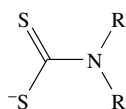
(12a) R = H
(12b) R = Me
(12c) R = Et
(12d) R = Pr
(12e) R = Bu
(12f) R = Ph
(12g) R = Bn

Reduction of a series of Au^{III} dithiocarbamates, $[Au(S_2CNR_2)_3]$, R = Et (12c), Pr (12d), Bu (12e) and Bn (12g), was investigated by polarography, chronoamperometry and cyclic voltammetry at a mercury electrode[23]. All the complexes show one main reduction wave in the polarogram in a fairly narrow potential range, -0.76 V to -0.82 V vs SCE. Constant potential coulometry gave n values of $2.27-2.93$ for the series. The nonintegral values for n are indicative of a chemical reaction coupled to the electron transfer process. Cyclic voltammograms of the series were more complex than the polarograms. For example, the cyclic voltammogram for $[Au(12c)_3]$ is shown in Figure 4. The major reduction peak at ca -1.4 V vs Ag/Ag^+ (-0.8 vs SCE) is assigned as the $0/1^-$ couple.
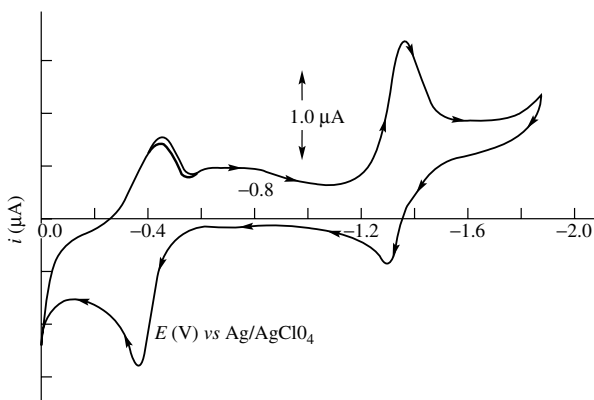
FIGURE 4. Cyclic voltammogram for 4.0×10^{-4} M $[Au(12c)_3]$ in 0.2 M $NaClO_4$/propylene carbonate at $25\,^\circ$C and scan rate of 50 mV s^{-1}. Reproduced by permission of The Australian Journal of Chemistry from Reference 23

There are also two smaller reduction waves at more positive potentials. Similar cyclic voltammograms displaying three cathodic reduction peaks and two anodic oxidation peaks were obtained for the other complexes in this series. The main reduction peak for each gold complex is similar to the peak obtained from the polarographic study (see Table 4, values labeled c). The nonintegral n values and the complex CVs were attributed to dissociation of the dithiocarbamate ligand upon reduction of $Au^{III}(dtc)_3$ to $[Au^I(dtc)_3]^{2-}$, followed by reaction of free dtc with the mercury electrode (see Scheme 1).

$$[Au^{III}(dtc)_3]^0 + 2e^- \longrightarrow [Au^I(dtc)_3]^{2-} \text{ (unstable)}$$

$$[Au^I(dtc)_3]^{2-} \longrightarrow Au^I(dtc) + 2(dtc)^-$$

$$(dtc)^- + Hg^0 \longrightarrow Hg^I(dtc) + e^-$$

$$2\,Hg^I(dtc) \rightleftharpoons Hg^{II}(dtc)_2 + Hg^0$$
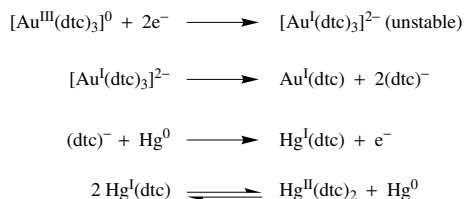
SCHEME 1

The final entry of Table 4 represents the only example we found of a silver dithiocarbamate complex for which electrochemical data have been reported[24]. Addition of $AgBF_4$ to cobalt tris dithiocarbamate complexes has been reported by Bond and coworkers. In the absence of silver, a fully reversible redox couple occurs which is assigned to the $[Co(S_2CNR_2)_3]^+/Co(S_2CNR_2)_3$ couple. When R = Pr (**12d**), this redox couple occurs at +0.355 V (*vs* Fc/Fc^+). Upon addition of $AgBF_4$ to the toluene/CH_2Cl_2 solution of Co(**12d**)$_3$ several new redox couples appear. The electrochemical data are consistent with the existence and stability of the complex cation, $[Ag\{Co(\textbf{12d})_3\}_2]^+$, in solution. Reduction of the complex cation occurs at *ca* −1.1 V and this is assigned to a process involving reduction of the silver ion. Oxidation occurs at +0.83 V which is assigned as involving one of the cobalt dtc ligands. The solid state structure of $[Ag\{Co(\textbf{12d})_3\}_2]BF_4$ reveals a central Ag^+ ion in a highly distorted tetrahedral geometry coordinated by four sulfurs from the dtc ligands, bridging between Ag and Co. There is no direct Ag−Co bond. The solution interactions of a number of cobalt, rhodium and iridium tris dtc complexes with Ag^+ were also investigated[24].

IV. L₂Au AND L_nAg COMPLEXES

The series of gold(I) bis(diphenylphosphine) compounds, $[Au(\textbf{13a–d})_2]^+$, shown in Table 5, was studied extensively by McArdle and Bossard[25]. Cyclic voltammetry at a gold electrode shows diffusion controlled, reversible or quasi-reversible behavior consistent with a two-electron process ($Au^{I/III}$ redox couple) occurring at potentials *ca* +0.6 V ± 0.2 V *vs* SCE. Bulk electrolysis studies on $[Au(\textbf{13a})_2]PF_6$ indicate that 2 electrons (1.81 and 1.83) are removed during oxidation at +0.7 V, while the peak-to-peak splitting in the CV study was 37 mV, indicative of near-idealized two-electron behavior (0.591/n). The other complexes showed similar CV peak-to-peak separations. The bulk electrolysis experiment for $[Au(\textbf{13b})_2]PF_6$ was complicated by decomposition of the oxidized product and the generation of another redox active compound. This prevented the authors from completing the electrolysis and resulted in an estimate for the n value of >1.7 before the secondary process became significant. The oxidation products of $[Au(\textbf{13c})_2]PF_6$ and $[Au(\textbf{13d})_2]PF_6$ were too unstable for the authors to attempt bulk electrolysis experiments. McArdle and Bossard were also able to gain significant insight into the electrochemical process by performing UV-vis-spectroelectrochemistry

TABLE 5.   Cyclic voltammetry data (V) of L_2Au and L_nAg complexes (L = phosphine or arsine, $n = 1,2$)

Compound	Alternative Formula	Oxidations	Reductions	Ref. couple	Solvent	Reference
[Au(**13a**)$_2$]$^+$	[Au(dppb)$_2$]$^+$	+0.46 (rev)		SCE	MeCN	25
[Au(**13b**)$_2$]$^+$	[Au(dppen)$_2$]$^+$	+0.57 (qr)		SCE	MeCN	25
[Au(**13c**)$_2$]$^+$	[Au(dppe)$_2$]$^+$	+0.46 (qr)		SCE	MeCN	25
[Au(**13d**)$_2$]$^+$	[Au(dppp)$_2$]$^+$	+0.75 (qr)		SCE	MeCN	25
Au[P(C$_6$H$_5$)$_3$]$_2^+$		+0.78 (ir)		SCE	MeCN	26
Au[P(OC$_2$H$_5$)$_3$]$_2^+$		+1.10		SCE	MeCN	26
Ag(**14**)$^+$		+1.17 (qr)		Ag/AgCl	Acetone	27
Au(**15a**)$_2^{3+}$			−0.45 (ir)	Ag/AgClO$_4$	MeCN	28
Au(**15b**)$_2^{3+}$			−0.17 (ir)	Ag/AgClO$_4$	MeCN	28
Ag(**15a**)$_2^{3+}$			−0.03 (ir)	Ag/AgClO$_4$	MeCN	28
Ag(**15b**)$_2^{3+}$			+0.26 (ir)	Ag/AgClO$_4$	MeCN	28

on [Au(**13a**)$_2$]PF$_6$[25]. During oxidation at +1.26 V they found clean conversion of one species to another as evidenced by a series of isosbestic points. They proposed that during oxidation, tetrahedral gold(I) is converted to square-planar gold(III). The differences in the electrochemical behavior of the series were proposed to be a consequence of the lability of the gold–phosphorus bond and the overall rigidity of the four-coordinate gold compounds.
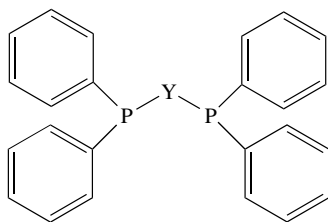
(13a) Y = o-C$_6$H$_4$
(13b) Y = CH=CH
(13c) Y = (CH$_2$)$_2$
(13d) Y = (CH$_2$)$_3$
(13e) Y = CH$_2$
(13f) Y = (CH$_2$)$_4$
(13g) Y = (CH$_2$)$_5$
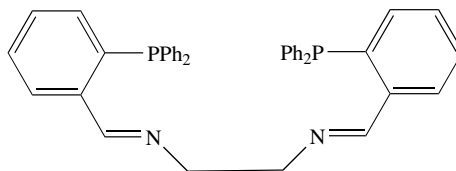
(14)
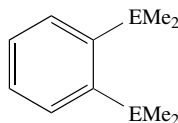
(15a) E = P
(15b) E = As

Anderson and coworkers investigated the effect of added phosphine to solutions of Au(PR$_3$)Cl[26], which results in additional phosphine ligands attaching to a central gold(I) atom as shown in equation 5.

$$Au(PR_3)Cl + (n-1)PR_3 \rightleftharpoons Au(PR_3)_n{}^+ + Cl^- \qquad (5)$$

$$PR_3 = PPh_3 \text{ or } P(OC_2H_5)_3, \quad n = 2\text{--}4$$
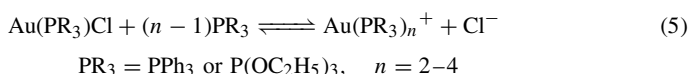
Conductivity data show that adding PPh_3 to the nonelectrolyte solution of $Au(PPh_3)Cl$ in MeCN produces a weakly conducting solution at $1-2$ equivalents of PPh_3, and a strongly conducting solution at >4 equivalents of PPh_3, indicative of the presence of a $1:1$ electrolyte. By keeping the amount of added phosphine low, Anderson and coworkers ensured that the multiple equilibria implied in equation 5 involved predominantly $n = 1$ and 2, thereby allowing them the opportunity to investigate the electrochemical oxidation of $[Au(PPh_3)_2]^+$ and $[Au(P(OC_2H_5)_3)_2]^+$ (see Table 5). Interestingly, the cationic complex, $[Au(PPh_3)_2]^+$, is easier to oxidize than $Au(PPh_3)Cl$ ($+1.54$ V vs SCE)[26] suggesting that the Cl^- ligand stabilizes and 'protects' the gold from oxidation. Substituting the triphenylphosphine ligand by the electron-withdrawing triethylphosphite shifts the $Au^{I/III}$ couple to higher potentials, as expected.

The silver diiminodiphosphine complex, $Ag(14)^+$, was investigated electrochemically by using a Pt working electrode in 0.1 M tetraethylammonium perchlorate/acetone solution[27]. The quasi-reversible redox couple, $Ag(14)^+/Ag(14)^{2+}$, occurs at $+1.17$ V (vs Ag/AgCl). Comparison of the oxidation potentials of the four-coordinate gold(I) bis-phosphine complexes, $[Au(13a-d)_2]^+$, shown in Table 5, indicates that the silver complex is on average 0.5 V harder to oxidize, which is in line with expectations from comparisons of the $Au^{I/III}$ and $Ag^{I/II}$ redox couples discussed in the introduction. Rauchfuss and coworkers also reported that the fully reversible $Cu^{I/II}$ redox couple found for the copper analog, $Cu(14)^+$, occurs at $+0.77$ V (vs Ag/AgCl)[27].

Reduction of the gold and silver complexes of **15a,b** was investigated by cyclic voltammetry at a Pt electrode[28]. These data afford an interesting comparison of the electrochemical behavior of Au vs Ag and P vs As. The Au^{III} complexes are harder to reduce than the corresponding Ag^{III} complexes, which reflects the relative chemical stability of Au^{III} and Ag^{III}. The Ag^{III} complex, $[Ag(15b)_2](ClO_4)_3$, decomposes readily in the presence of water, chloride and many organic solvents[23]. A qualitative comparison of the reduction potential of $[Au(15a)_2]^{3+}$ (-0.45 V vs Ag/Ag$^+$ or ca $+0.15$ V vs SCE) with the reversible redox couple for $[Au(13a)_2]^+$ ($+0.46$ V vs SCE) is also in line with the difference in electronic properties of methyl vs phenyl groups on P.

V. PHOSPHINE GOLD HALIDES

The electrochemical properties of phosphine gold halide compounds have been the subject of a number of investigations. Anderson and coworkers[26] reported that $Au(PPh_3)Cl$ and $Au(PEt_3)Cl$ undergo oxidations at $+1.54$ V and $+1.51$ V, respectively (vs SCE), in MeCN solutions at 100 mV s^{-1} (see Table 6). The oxidation process for $Au(PEt_3)Cl$ involves a broad irreversible oxidation wave, is diffusion controlled (i.e. $i_p/v^{1/2}$ is constant) and the value of E_{pa} shifts positively with an increase in scan rate. On the basis of cyclic voltammetry, bulk electrolysis and UV-vis spectroelectrochemistry studies, the authors conclude that an overall two-electron oxidation of $Au^I \rightarrow Au^{III}$ occurs, followed by a fast chemical reaction. The n value for bulk electrolysis of $Au(PEt_3)Cl$ was 2.0 ± 0.5. Cyclic voltammetry studies for $Au(PEt_3)Cl$ show no reduction process out to -2.0 V, except when the oxidation wave at $+1.51$ V is first scanned, whereby a reduction wave at $+0.20$ V is observed. The observation is made that the presence of a reduction wave at ca 0.2 V implies formation of a gold(III) ionic species, similar to the reduction wave which appears for $K[AuCl_4]$[26]. In addition, reduction of $[AuCl_4]^-$ in the presence of phosphine, PR_3, regenerates $Au(PR_3)Cl$. Spectroelectrochemical data show that upon oxidation of $Au(PEt_3)Cl$ at $+1.45$ V (vs Pt pseudoreference) a band at 310 nm appears. This band is assigned to $AuCl_4^-$. The electrochemistry of $Au(PPh_3)Cl$ was found to be very similar.

TABLE 6. Electrochemical data (V) of phosphine gold halide complexes

Compound	Ox.	Red.	Ref. couple	Solvent	Reference
Au(PPh$_3$)Cl	+1.58	−1.76	Ag/AgCl	MeCN	29
Au(PPh$_3$)Cl	+1.54	+0.03^a	SCE	MeCN	26
Au(PPh$_3$)Cl	+1.13		Fc/Fc$^+$	CH$_2$Cl$_2$	30
Au(PPh$_3$)Cl	+1.52		SCE	MeCN	31
Au(PPh$_3$)Br	+1.31	−1.71	Ag/AgCl	MeCN	29
Au(PPh$_3$)Br	+1.14		Fc/Fc$^+$	CH$_2$Cl$_2$	30
Au(PEt$_3$)Br	+1.38	−1.76	Ag/AgCl	MeCN	29
Au(PPh$_3$)I	+1.05	−1.54	Ag/AgCl	MeCN	29
Au(PEt$_3$)Cl	+1.51	+0.20^a	SCE	MeCN	26
Au[P(OC$_2$H$_5$)$_3$]Cl	+1.86		SCE	MeCN	26
Au[P(OC$_6$H$_5$)$_3$]Cl	+1.76		SCE	MeCN	26
Au(**16**)Cl	+1.07		Fc/Fc$^+$	CH$_2$Cl$_2$	30
Au(**16**)Br	+1.03		Fc/Fc$^+$	CH$_2$Cl$_2$	30
Au(PPh$_3$)Cl$_3$		−0.49	Fc/Fc$^+$	CH$_2$Cl$_2$	30
Au(PPh$_3$)Br$_3$		−0.31	Fc/Fc$^+$	CH$_2$Cl$_2$	30
Au(**16**)Cl$_3$		−0.49	Fc/Fc$^+$	CH$_2$Cl$_2$	30
Au(**16**)Br$_3$		−0.37	Fc/Fc$^+$	CH$_2$Cl$_2$	30
Au(**17**)Cl	+1.75		SCE	MeCN	31
Au(**17**)$_2$Cl	+1.12		SCE	MeCN	31

^{a}Reduction wave appearing after oxidation.

Two other studies have appeared which also assign the oxidation of Au(PPh$_3$)Cl as involving a two-electron Au^I → Au^{III} irreversible process[30,31]. In contrast, Rakhimov and coworkers have recently suggested that the oxidation of Au(PPh$_3$)Cl is a one-electron process involving phosphine[29]. Their analysis is based, in part, on similar oxidation currents observed in cyclic voltammetry experiments of Au(PPh$_3$)Cl solutions containing equal concentrations of ferrocene, a well-known one-electron redox couple[31].

Substituting alkyl phosphines for aromatic phosphines or phosphites has only a minor effect on the oxidation potentials in two separate studies[26,29]. Substitution of less electronegative halides for chloride might be expected to make the oxidation of gold(I)−halide moieties easier. This was indeed observed in cyclic voltammetry studies in 0.05 M [Et$_4$N]BF$_4$/MeCN solution at a Pt working electrode where Au(PPh$_3$)Br and Au(PPh$_3$)I are 27 mV and 53 mV, respectively, easier to oxidize than Au(PPh$_3$)Cl[29]. However, Nelson and coworkers found little change when Br$^-$ is substituted for Cl$^-$ in cyclic voltammetry experiments run in 0.1 M [Bu$_4$N]ClO$_4$/CH$_2$Cl$_2$ solution at a Pt working electrode: oxidation of Au(PPh$_3$)Br occurs at +1.14 V and for Au(PPh$_3$)Cl at +1.13 V vs Fc/Fc$^+$ (see Table 6)[30]. The oxidation potentials of gold(I) 1-phenyldibenzophosphole (**16**) halide compounds are also insensitive to halide substitution. Oxidation of Au(**16**)Cl occurs at +1.07 V vs Fc/Fc$^+$ and for Au(**16**)Br at +1.03 V[30]. In fact, all four compounds investigated by Nelson and coworkers are reported to oxidize within a narrow range 1.09 V ± 0.06 V (vs Fc/Fc$^+$)[30]. Substitution of more electronegative halides for bromide might be expected to result in making reduction of gold(III) easier. Nelson and coworkers

observe this for AuLX$_3$ compounds (L = PPh$_3$, **16**; X = Cl, Br) where substitution of Br$^-$ for Cl$^-$ decreases the average Au(III) reduction potential by 150 mV[30].
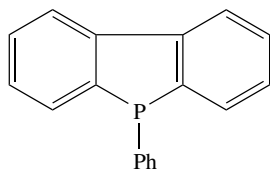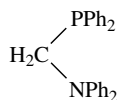
(16)   **(17)**

Ligand **17** is believed to act as a monodentate ligand for Au^I, coordinated through the phosphine only, on the basis of ^{13}C NMR data which show that the aromatic carbon atoms bonded to nitrogen remain practically unchanged, in contrast to the carbon atoms bonded to phosphorus which are shielded after complexation. The oxidation of Au(**17**)Cl and Au(**17**)$_2$Cl complexes was studied by Castan and coworkers[31]. The major anodic process of Au(**17**)Cl is an irreversible wave occurring at +1.75 V (see Table 6) which is assigned as Au^I to Au^{III}. A shoulder at +0.95 V occurs which is assigned to oxidation of the free ligand (+0.87 V *vs* SCE). In the cyclic voltammogram of Au(**17**)$_2$Cl, there is also a shoulder at *ca* 0.95 V and a major oxidation wave at +1.12 V, which is assigned as a Au^I → Au^{III} oxidation. The authors suggest that increasing the coordination number around gold from two in Au(**17**)Cl to three in Au(**17**)$_2$Cl is responsible for decreasing the oxidation potential. This observation is further supported by comparison with the redox couple for the four-coordinate Au^I complex, [Au(**13a**)$_2$]$^+$, found in Table 5. This simple relationship is illustrated in Figure 5.
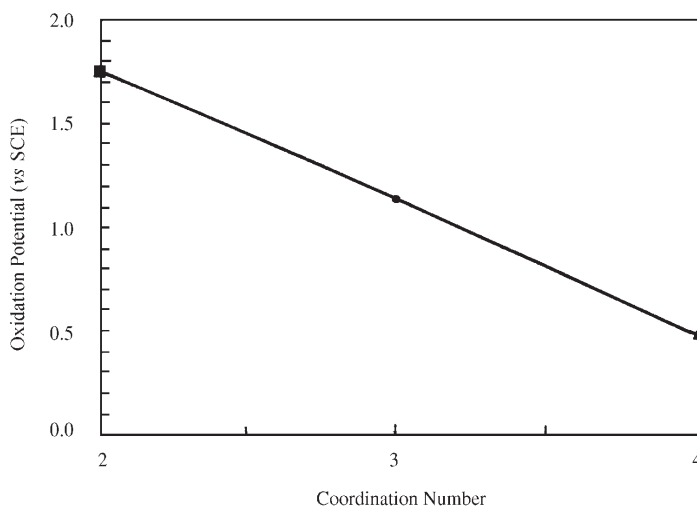
FIGURE 5. Oxidation potentials *vs* coordination number: ■ Au(**17**)Cl, +1.75 V; ● Au(**17**)$_2$Cl, +1.12 V; ▲ [Au(**13a**)$_2$]$^+$, +0.46 V. All potentials *vs* SCE

VI. PHOSPHINE GOLD THIOLATES AND MIXED DONOR LIGANDS

The electrochemistry of a series of neutral phosphine gold(I) thiolate complexes has been investigated[32,33]. The series includes cyclic dinuclear gold(I) complexes formed from 1,2-propanedithiolate (pdt, **18**) and bis-chelating phosphines, Au_2(**13c,g**)(**18**), open dinuclear gold(I) complexes formed from *para*-thiocresolate (*p*-tc, **19**) and bis-chelating phosphines, Au_2(**13c-g**)(**19**)$_2$, and a mononuclear complex, Au(PPh$_3$)(**19**). Oxidative cyclic voltammetry experiments were performed at Pt and glassy carbon electrodes in 0.1 M [Bu$_4$N]PF$_6$/MeCN and CH$_2$Cl$_2$ solutions. Adsorption effects occurred in all electrode/solvent combinations investigated and were minimized by wiping the electrode between each CV experiment. Scan rates between 50 and 500 mV s^{-1} were employed and several replications at each scan rate were obtained. Table 7 shows the results of the oxidative cyclic voltammetry experiments at a Pt working electrode in 0.1 M [Bu$_4$N]PF$_6$/CH$_2$Cl$_2$ solution.

(18)   (19)
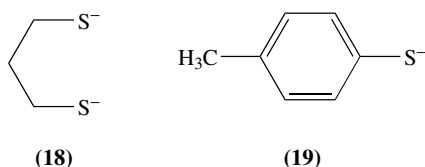
The position and wave shape of the oxidation processes were somewhat dependent on the electrode/solvent combination. The effect of changing the solvent from CH$_2$Cl$_2$ to

TABLE 7.   Cyclic voltammetry data(V) of phosphine gold thiolate and mixed donor ligand complexes[a]

Compound	Alternative formula	Oxidations		Reductions	Solvent	Reference
Au$_2$(**13c**)(**18**)	Au$_2$(dppe)(pdt)	+0.77[b] (ir)	+1.20 (ir)		CH$_2$Cl$_2$	32
Au$_2$(**13g**)(**18**)	Au$_2$(dpppn)(pdt)	+0.63 (ir)	+1.23 (ir)		CH$_2$Cl$_2$	32
Au(PPh$_3$)(**19**)	Au(PPh$_3$)(*p*-tc)	+0.82 (ir)	+1.52 (ir)		CH$_2$Cl$_2$	32
Au$_2$(**13e**)(**19**)$_2$	Au$_2$(dppm)(*p*-tc)$_2$	+0.58[c] (ir)	+1.52[c] (ir)		MeCN	33
Au$_2$(**13c**)(**19**)$_2$	Au$_2$(dppe)(*p*-tc)$_2$	+0.72 (ir)	+1.54 (ir)		CH$_2$Cl$_2$	32
Au$_2$(**13d**)(**19**)$_2$	Au$_2$(dppp)(*p*-tc)$_2$	+0.77 (ir)	+1.54 (ir)		CH$_2$Cl$_2$	32
Au$_2$(**13f**)(**19**)$_2$	Au$_2$(dppb)(*p*-tc)$_2$	+0.83 (ir)	+1.59 (ir)		CH$_2$Cl$_2$	32
Au$_2$(**13g**)(**19**)$_2$	Au$_2$(dpppn)(*p*-tc)$_2$	+0.78 (ir)	+1.56 (ir)		CH$_2$Cl$_2$	32
[Au$_2$(**13e**)(**20**)]$^+$		+1.42 (ir)			CH$_2$Cl$_2$	34
[Au$_2$(**13c**)(**20**)]$^+$		+1.46 (ir)			CH$_2$Cl$_2$	34
[Au(**21**)$_2$]$^+$				−0.86 (rev)	MeCN	35
22a		+0.26 (rev)	+0.59 (rev)	−1.22 (ir)	MeCN	36
22b		+0.32 (rev)	+0.68 (rev)	−1.18 (ir)	MeCN	36
22c		+0.65 (rev)		−1.0 (ir)	MeCN	36
23a		+1.2 (ir)		+0.08 (rev)	MeCN	37
23b		+1.2 (ir)		−0.10 (rev)	MeCN	37

[a]All studies employed a Pt working electrode except as noted. Reference was SCE in all studies, except Reference 35 which was Fc/Fc$^+$.
[b]Adsorption wave appears at +0.47 V.
[c]Glassy carbon working electrode.

MeCN in cyclic voltammetry experiments of Au$_2$(**13c**)(**18**) at glassy carbon is illustrated in Figure 6. The broadness of the irreversible oxidation wave shown in Figure 6b was noted in the study[32]. The difference between the potential maximum and half currents ($E_{pa} - E_{pa/2}$) was found to be 150 mV. A similar observation about broadness in the oxidation wave of phosphine gold halide complexes was made by Anderson and coworkers during investigation of the oxidation of Au(PEt$_3$)Cl[26]. The first oxidation process of all complexes shown in Table 7 occurs at +0.7 V ± 0.1 V (*vs* SCE), with the possible exception of Au$_2$(**13c**)(**18**) for which the presence of an adsorption wave at +0.47 makes the exact potential of the first oxidation process somewhat difficult to determine. The first oxidation process is followed by a second one which occurs between +1.2 V and +1.6 V (see Table 7). With the exception noted for Au$_2$(**13c**)(**18**), substituting aromatic thiolate, **19**, for alkyl thiolate, **18**, shifts both the first and second oxidation processes to lower potentials. Figure 7 shows the 0.0 V to +2.0 V cyclic voltammograms for Au$_2$(**13c**)(**18**) and Au$_2$(**13g**)(**18**) in CH$_2$Cl$_2$ or MeCN solutions. Lengthening the bis-chelating phosphine from **13c** to **13g** has only a small effect on the overall cyclic voltammogram waveshape (compare Figure 7a and 7c). It has been noted that for a particular solvent/electrode combination the first oxidation wave broadens as the length of the bis-chelating phosphine becomes very short (i.e. **13e**, not shown) and may indicate weak coupling of the two gold(I) redox centers[33].

Comparison of the oxidation processes of Au(PPh$_3$)X (see Figure 8, X = halide) shows an inverse linear relationship between the oxidation potentials and the electronegativity of the X ligand. Since the electronegativity of sulfur is similar to iodine, oxidation of phosphine gold thiolate complexes may be expected to occur near +1.0 V. However, as shown in Table 7, the first oxidation occurs at *ca* 200–400 mV lower potential. In addition, constant potential electrolysis studies at +1.0 V result in formation of the disulfide, *p*-CH$_3$C$_6$H$_4$S-SC$_6$H$_4$CH$_3$-*p* and *n* values of 1 and 0.5 for the dinuclear and mononuclear gold(I) complexes, respectively. The lowest transition state energy of phosphine gold(I) thiolate complexes has been assigned as a sulfur-to-metal charge transfer[38]. This assignment and the formation of disulfide are consistent with sulfur-based oxidation, in contrast to Au(PPh$_3$)X where gold-based oxidation was suggested by several authors[26,30,31]. This

Publisher's Note:
Permission to reproduce this image online was not granted by the copyright holder. Readers are kindly requested to refer to the printed version of this chapter.

FIGURE 6. Cyclic voltammograms at a glassy carbon electrode at room temperature and scan rate of 50 mV s^{-1}: (a) 4.7×10^{-4} M Au$_2$(**13c**)(**18**) in 0.1 M [Bu$_4$N]PF$_6$/MeCN; (b) 4.8×10^{-4} M Au$_2$(**13c**)(**18**) in 0.1 M [Bu$_4$N]PF$_6$/CH$_2$Cl$_2$. Reproduced by permission of Freund Publishing House from Reference 32

Publisher's Note:
Permission to reproduce this image
online was not granted by the
copyright holder. Readers are kindly
requested to refer to the printed version
of this chapter.

FIGURE 7. Cyclic voltammograms at a glassy carbon electrode at room temperature: (a) 4.8×10^{-4} M Au$_2$(**13c**)(**18**) in 0.1 M [Bu$_4$N]PF$_6$/CH$_2$Cl$_2$ at scan rate 200 mV s^{-1}, (b) 4.7×10^{-4} M Au$_2$(**13c**)(**18**) in 0.1 M [Bu$_4$N]PF$_6$/MeCN at scan rate 50 mV s^{-1}, (c) 4.8×10^{-4} M Au$_2$(**13g**)(**18**) in 0.1 M [Bu$_4$N]PF$_6$/CH$_2$Cl$_2$ at scan rate 100 mV s^{-1}. Reproduced by permission of Freund Publishing House from Reference 32

difference may be significant for the biological activity of phosphine gold thiolate complexes such as Auranofin, since the redox chemistry of gold(I) centers interacting with thiol groups of proteins and enzymes may be critical to the mechanism of action of a drug.

The electrochemistry of gold(I) complexes with pyridine-2-thiolate, **20**, was investigated by Laguna and coworkers[34]. The gold(I) cationic complexes [Au$_2$(**13e**)(**20**)]$^+$ and [Au$_2$(**13c**)(**20**)]$^+$ undergo irreversible oxidations at +1.42 V and +1.46 V, respectively, during cyclic voltammetry experiments at a Pt disk working electrode recorded at 200 mV s^{-1} in 0.1 M [Bu$_4$N]PF$_6$/CH$_2$Cl$_2$ solution. No reduction waves were observed out to −1.8 V. The reference electrode was SCE, which was standardized against either the [Fe(η-C$_5$H$_5$)$_2$]$^+$–[Fe(η-C$_5$H$_5$)$_2$] or the [Fe(η-C$_5$Me$_5$)$_2$]$^+$–[Fe(η-C$_5$Me$_5$)$_2$] couple as an internal standard (E^0 = 0.47 and −0.09 V, respectively).

The electrochemistry of a square-planar gold(III) complex with 2-(diphenylphosphino) benzenethiolate (**21**) was reported by Dilworth and coworkers[35]. Cyclic voltammetry experiments on [Au(**21**)$_2$]BPh$_4$ indicate a reversible redox couple at −0.862 V (*vs* the Fc/Fc$^+$ reference couple) in 0.2 M [Bu$_4$N]BF$_4$/MeCN solution. Peak-to-peak separation of the redox waves was 84.2 mV and convolution methods were used to establish that the redox couple was reversible and involved the same number of electrons as the ferrocene/ferrocenium couple under identical conditions. The reductive scan was assigned
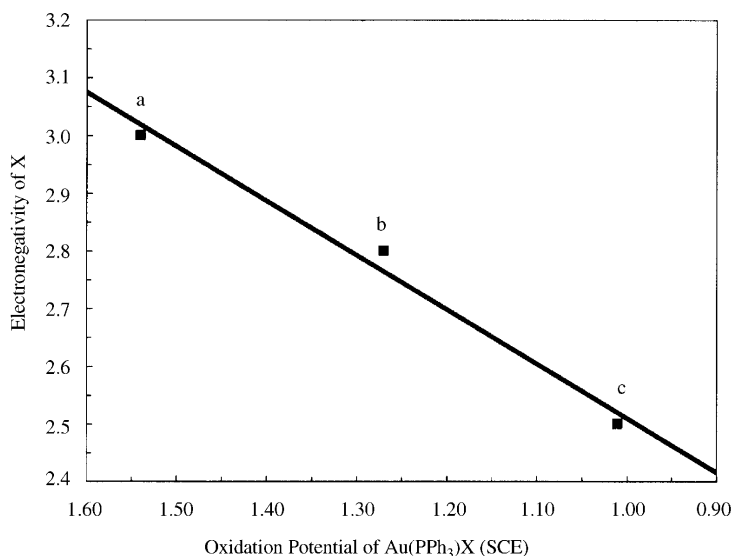
FIGURE 8. Electronegativity of halides vs oxidation potentials of phosphine gold(I) halides: (a) Au(PPh$_3$)Cl, +1.54 V[26]; (b) Au(PPh$_3$)Br, +1.27 V[29]; (c) Au(PPh$_3$)I, +1.01 V[29]. The oxidation potentials of Au(PPh$_3$)Br and Au(PPh$_3$)I were converted to the SCE scale using Table 2
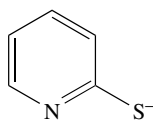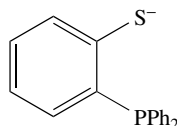
(20)   **(21)**

as Au$^{III} \rightarrow$ Au^{II}. The reversibility of the redox couple under slow scan rate conditions (50 mV s^{-1}) indicates that the gold(II) complex is stable over the time scale of the electrochemical experiment. In contrast, the neutral Pt(II) and Pd(II) analogs, Pt(**21**)$_2$ and Pd(**21**)$_2$, are electrochemically inactive over the accessible range of DMF (-2.4 V to $+1.2$ V relative to ferrocene).

The synthesis, characterization and electrochemical investigation of an interesting series of gold(II) complexes with o-aminobenzenethiolate ligands has been reported by Gosh, Manoharan and coworkers[36]. The ligands are noteworthy, because they have both hard and soft donor atoms which may contribute to stabilizing gold(II) complexes. The dinuclear gold(II) complex, **22a**, is prepared by the reaction of NaAuCl$_4$ with o-aminobenzenethiol. The isomer, **22b**, forms after refluxing **22a** for 2 hours in dry, degassed methanol, while the mononuclear complex, **22c**, is formed upon dissolution, refluxing and workup of **22a** in DMF. ESR measurements in DMF solution on **22a** and **22b** show a seven-line pattern ($1 : 2 : 3 : 4 : 3 : 2 : 1$) assigned as two interacting gold(II) nuclei (Au, $I = \frac{3}{2}$, 100%). The

mononuclear complex, **22c**, shows a four-line pattern. Close agreement between the ESR experimental results and simulation was found. Cyclic voltammetry experiments at a Pt working electrode in 0.1 M [Et$_4$N]ClO$_4$/MeCN solution at 50 mV s^{-1} show two sets of reversible redox couples for **22a** and **22b** and one for **22c** (see Table 7). The small shifts in the pairs of redox couples for **22a** and **22b** support the idea that these complexes are isomers with gold(II) atoms in slightly different electronic environments. The complexes **22a–c** all display a broad irreversible reduction wave at *ca* −1.0 V, presumably due to reduction of Au^{II} to Au^{I}. The *o*-aminobenzenethiol ligand does not show any redox behavior in this region.
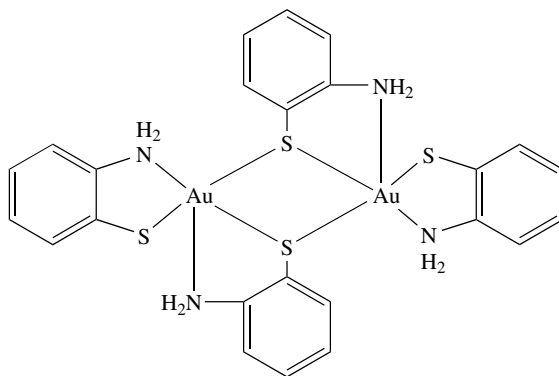
(22a)
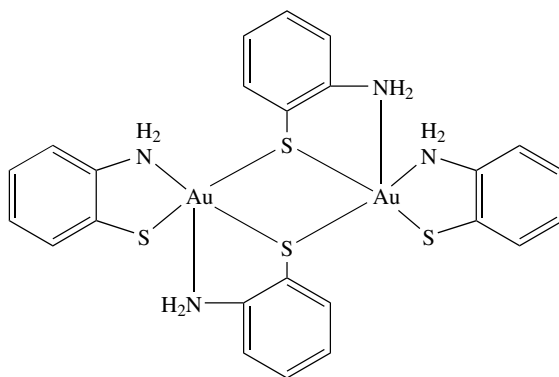
(22b)

Ghosh, Manoharan and coworkers have also reported on a pair of isomers formulated as shown below, **23a** and **23b**[37]. Four-line patterns were observed in the ESR of each of these complexes which appear to originate from one interacting gold nucleus. The authors
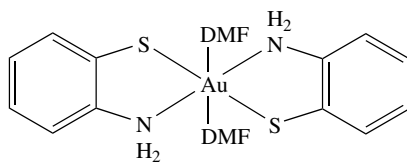
(22c)

suggest that the complexes have Au(II)-stabilized radical structures containing oxidized ligands where the unpaired electron is highly delocalized onto the ligand. Cyclic voltammetry experiments demonstrate that the redox behavior of these complexes is somewhat complicated, in contrast to the relatively well-behaved features found in **22a** and **22b**. On oxidative scans, both complexes show irreversible oxidation processes occurring at about $+1.2$ V. On reductive scans, a reversible couple occurs near $+0.1$ V, but there is also a broad reduction wave at *ca* $+0.35$ V that appears coupled to two successive oxidative processes occurring near $+0.4$ V and $+0.6$ V. The origin of these redox features is not discussed.
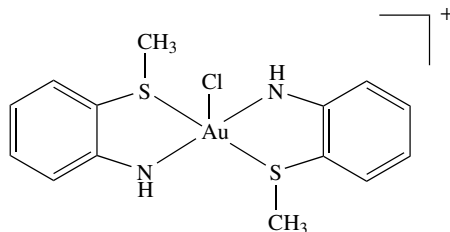
(23a)
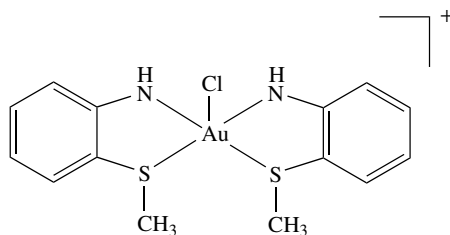
(23b)

VII. PHOSPHORUS YLIDES

Dinuclear gold(I) and gold(II) phosphorus ylide complexes have been the subject of several separate electrochemical investigations by Fackler and coworkers[39] and Laguna and coworkers[34,40]. The neutral, cyclic bis-ylide, gold(I) complex, **24**, undergoes two quasi-reversible, stepwise oxidations at $+0.11$ and $+0.24$ V (*vs* Ag/AgCl) (see Table 8)[39]. The stepwise oxidations presumably involve one electron each, to form a gold(II)–gold(II)

complex. Precipitation of a yellow compound complicated efforts of further electrochemical analysis. The cyclic gold(II)–gold(II) halogen adducts, **25a–c**, all show one irreversible reduction wave and the potentials are dependent on the nature of the halogen ligands[39]. The reductions are followed by a chemical reaction that generates **24**, which can be clearly detected electrochemically. Bulk electrolysis of the Au(II) halogen adducts yields an *n* value of 2 electrons per molecule. For **25c** two quasi-reversible oxidation waves are seen, whereas for **25a** and **25b** only ill-defined, irreversible oxidation processes are observed. The electrochemistry of **25d** and **25e** is complicated by an equilibrium that involves **24** which results in deteriorating electrochemical signals[39]. Therefore, the potentials listed in Table 8 for **25d** and **25e** were obtained under conditions of excess alkyl halide.

(24)

(25a) X = Y = Cl
(25b) X = Y = Br
(25c) X = Y = I
(25d) X = Me, Y = Br
(25e) X = Me, Y = I
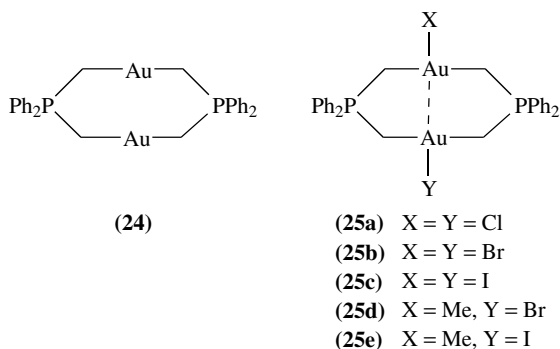
Cyclic voltammetry experiments on cyclic, dinuclear gold(I) ylide dithiocarbamate complexes, **26a–c**, show irreversible oxidation processes between +0.30 V and +0.4 V (see Table 8)[40]. Electrochemical analysis was complicated by formation of a coating on the Pt electrode surface. These complexes oxidize at potentials which are intermediate between

TABLE 8.   Cyclic voltammetry data (V) of phosphorus ylide complexes

Compound	Ox1	Ox2	Red1	Red2	Ref.couple	Solvent	Reference
24	+0.24	+0.11			Ag/AgCl	THF	39
25a		+1.5	−0.92 (ir)		Ag/AgCl	THF	39
25b		+1.22	−0.69 (ir)		Ag/AgCl	THF	39
25c	+1.12	+0.88	−0.58 (ir)		Ag/AgCl	THF	39
25d		+0.38	−0.75	−1.18	Ag/AgCl	THF	39
25e		+0.42	−0.68	−1.14	Ag/AgCl	THF	39
26a		+0.30 (ir)			SCE	CH$_2$Cl$_2$	40
26b		+0.37 (ir)			SCE	CH$_2$Cl$_2$	40
26c		+0.42 (ir)			SCE	CH$_2$Cl$_2$	40
27		+0.53 (ir)			SCE	CH$_2$Cl$_2$	34
28a		*a*	−0.44 (ir)		SCE	CH$_2$Cl$_2$	34
28b		*a*	−0.43 (ir)		SCE	CH$_2$Cl$_2$	34

[a]Oxidation wave observed at +0.55 (ir) after reduction.
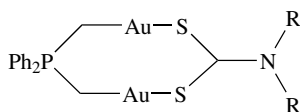
(26a) R = Me
(26b) R = Et
(26c) R = Bn

those of $[Au_2\{\mu - S_2CN(CH_2Ph)_2\}_2]$ (irreversible wave at +1.15 V)[40] and **24**. Increasing the electron-donating ability of the substituent groups on the dithiocarbamate ligands from Bz to Me leads to a decrease in the oxidation potential.

Dinuclear gold(I) and gold(II) complexes of pyridine-2-thiolate, **27**, **28a** and **28b**, were studied by cyclic voltammetry at a Pt working electrode in CH_2Cl_2[34]. The dinuclear gold(I) complex, **27**, has an irreversible, extended oxidation process at +0.53 V *vs* SCE. No reduction wave was observed out to −1.8 V. The cyclic voltammograms for the dinuclear gold(II) complexes show irreversible reduction waves at −0.44 V **(28a)** and −0.43 V **(28b)**. After reduction, the return oxidation scan shows an irreversible oxidation process at +0.55 V, indicative of the presence of **27**.
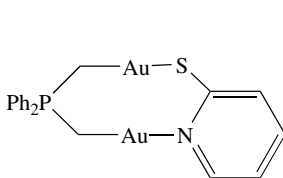
(27)
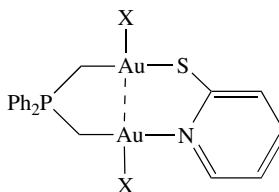
(28a) X = Cl
(28b) X = Br

VIII. ORGANOMETALLICS

The electrochemistry of a fairly large number of organometallic gold compounds has been studied (Table 9). With few exceptions, these complexes also contain a triphenylphosphine (or a derivative) ligand. Many of the compounds exhibit 'typical' linear, two-coordinate gold, with the organometallic ligand coordinated to gold through a Au−C single bond. Gold–gold bonding is also possible, and there are several examples of three-coordinate gold organometallic compounds that have been investigated.

The prototypical gold(I) organometallic compounds are $Au(PPh_3)R$ (R = Me, Ph). They are oxidized at +1.6 V (*vs* Ag/AgCl) and reduced at *ca* −1.6 V (see Table 9)[29]. Comparing these potentials with those for $Au(PPh_3)X$ (X = Cl, Br and I, Table 6) suggests that the alkyl and aryl groups in $Au(PPh_3)Me$ and $Au(PPh_3)Ph$, respectively, are electronically similar to the chloride anion. The effects of different substituent groups on the oxidation potentials of a series of $Au(PPh_3)R$ compounds can be explained on the basis of simple electronegativity arguments. Placing an electron-donating methoxy group in the *para* position of the aryl group makes oxidation of $Au(PPh_3)(4\text{-MeOC}_6H_4)$ *ca* 300 mV easier than for $Au(PPh_3)R$ (R = Me, Ph), while a *para* fluoride makes $Au(PPh_3)(4\text{-FC}_6H_4)$ *ca* 400 mV harder to oxidize. Cyanide has a similar effect (R = CN, CH_2CN etc.), as do the other electron-withdrawing groups, $CH(COR)_2$ (R = Me, Ph or *t*-Bu). Note that the

TABLE 9.   Cyclic voltammetry data (V) of organometallic complexes

Compound	Oxidations	Reductions	Conditions	Reference
$Au(PPh_3)Me$	+1.59	−1.63	a	29
$Au(PPh_3)Ph$	+1.61, +1.97	−1.73	a	29
$Au(PPh_3)(4\text{-}MeOC_6H_4)$	+1.28, +1.71	b	a	29
$Au(PPh_3)(4\text{-}FC_6H_4)$	+2.00	b	a	41
$Au(PPh_3)CN$	+2.25	-0.78^b	c	29
$Au(PPh_3)CH_2CN$	+2.24	-0.98^b	c	29
$Au(PPh_3)CH(COOEt)CN$	+2.17	-0.79^b	c	29
$Au(PPh_3)CMe(CN)_2$	+2.30	−1.00, −1.91	c	29
$Au(PPh_3)CH(COMe)_2$	+2.00	−1.64	a	29
$Au(PPh_3)CH(COMe)(COPh)$	+2.05	−1.60	a	29
$Au(PPh_3)CH(COPh)_2$	+1.96	−1.56	a	29
$Au(PPh_3)CH(COBu\text{-}t)_2$	+1.86	−1.60, −1.78	a	29
$Au(PPhFc_2)(4\text{-}FC_6H_4)^d$	+0.61, +0.80, +2.09	b	a	41
$Au(PFc_3)(4\text{-}FC_6H_4)^d$	+0.57, +0.72, +0.86, +2.13	b	a	41
29a	+0.76 (ir), +1.01 (qr)		e	42
29b	+0.74 (ir), +1.03 (qr), +2.05		e	42
29c	+0.78 (ir), +1.05 (qr), +1.66, +1.73, +1.88		e	42
29d	+0.74 (ir), +1.05 (qr), +1.27, +1.39, +1.54, +1.70		e	42
29e	+0.66 (ir), +1.08 (qr), +1.97		e	42
29f	+0.95 (ir), +1.11 (qr)		e	42
29g	+0.93 (ir), +1.11 (qr)		e	42
29h	+0.98 (rev)		f	43
29i	+1.03 (rev)		f	43
30a	+0.24	b	a	44
30b	+0.81	-1.66^g	a	44
31a	+0.68, +1.62	−1.62	a	44
31b	+0.88, +1.81	−1.77	a	44
32	+0.72, +2.21	−2.21	a	44
33	+0.48, +1.36, +1.97	−1.84	a	29
34	+1.52, +1.94	b	h	29
35	+0.79, +1.08, +1.41, +2.04, +0.84	−1.36	h	29
36		−0.62, −0.84	i	45

^{a}Pt working electrode, 0.05 M [Et$_4$N]BF$_4$/MeCN, Ag/AgCl reference couple.
^{b}No reduction observed at a Pt working electrode.
^{c}Dropping mercury electrode.
^{d}Fc = ferrocenyl.
^{e}Glassy carbon working electrode, Ag/AgCl reference couple in CH$_2$Cl$_2$, potentials reported vs SCE.
^{f}SCE reference in CH$_2$Cl$_2$.
^{g}Reduction of the nitro group.
^{h}Ag/AgCl reference couple in MeCN/CH$_2$Cl$_2$ (1:10).
^{i}SCE reference in MeCN.

electron-releasing t-butyl groups in $Au(PPh_3)CH(COBu-t)_2$ have only a modest effect on the oxidation potential.

Replacing triphenylphosphine with ferrocenyl-derivatized phosphines adds additional redox centers with very rich organometallic chemistry of their own[46]. The cyclic voltammogram of $Au(PPhFc_2)(4-FC_6H_4)$ shows an oxidation process at *ca* +2 V, similar to that of $Au(PPh_3)(4-FC_6H_4)$, and two additional redox processes at +0.61 V and +0.80 V that appear to be associated with coupled, iron-based redox processes.

A number of dinuclear gold(I) complexes containing the 1,1′-bis(diphenylphosphino)ferrocene (dppf) ligand, **29a–i**, have been analyzed electrochemically[42,43]. On the basis of the above discussion, two oxidation processes are expected, one that is ferrocenyl-based and the other associated with the organogold fragment. Indeed, this is what is reported for **29a**. However, the situation is obviously more complicated for the other dinuclear gold(I) complexes **(29b–i)**, where up to six anodic processes are reported in the range of 0–2 V (see Table 9). In the dppf chemistry of other transition metals, the dppf ligand is often found chelated to a single metal[46]. This suggests that in solution the two $Au^I R$ redox centers might easily encounter each other to produce redox coupling, resulting in splitting of peaks, or perhaps initiating a facile chemical reaction, following the electron transfer process.

There are several other factors that make it difficult to assign the redox processes in **29b–i**. The oxidation potential of the dppf ligand is somewhat solvent-dependent[46]. The dppf redox couple is generally reversible; however, in the presence of water, the dppf ligand undergoes a fast chemical reaction following oxidation[47]. In cyclic voltammetry experiments run under similar conditions but employing different electrodes, the oxidation potentials reported for dppf are +0.68 V[43] (*vs* SCE at Pt in 0.1 M $[NBu_4]PF_6/CH_2Cl_2$ at 100 mV s^{-1}) and +0.97 V[42] (*vs* SCE at glassy carbon in 0.1 M $[NBu_4]PF_6/CH_2Cl_2$ at 100 mV s^{-1}), which suggests that the nature of the electrode also significantly affects the oxidation potential.
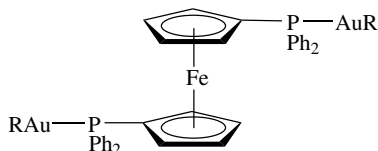
(29a) R = Me	**(29d)** R = $C_{14}H_9$, 9-anthryl	**(29g)** R = C≡CBu-t
(29b) R = Ph	**(29e)** R = $C_{16}H_9$, 1-pyrenyl	**(29h)** R = C_6F_5
(29c) R = $C_{10}H_7$, 1-naphthyl	**(29f)** R = C≡CPh	**(29i)** R = CH_2PPh_2Me

In compounds **29a–g**, the quasi-reversible oxidations at *ca* +1.0–1.1 V occur almost identically where dppf oxidizes at a glassy carbon electrode, which suggests that the redox process at this potential is iron (dppf) based. The anodic waves occurring at lower potentials in the range between +0.66 V and +0.95 V have been assigned as one-electron oxidations of gold in **29a–g**[42]. Comparing the first oxidation potential of $Au(PPh_3)Ph$ (+1.61 V) *vs* $Au(PPh_3)(4-FC_6H_4)$ (+2.00 V), it is expected that the pentafluorinated phenyl substituent in **29h** would push gold-based oxidation to much higher potentials, possibly switching the lowest energy oxidation process to a dppf-based oxidation. In cyclic voltammetry experiments on **29h**, the first oxidation process (+0.98 V at a Pt electrode) is reversible with peak-to-peak splitting of 60 mV, suggesting that this is indeed what has occurred. Until more data are available, e.g. bulk electrolyses as a function of

potential, it is prudent to reserve judgment about the assignment of these redox processes. Nevertheless, what is evident is the rich electrochemistry of these complexes.

(30a) X = H
(30b) X = NO$_2$

(31a) X = H
(31b) X = COOMe

(32)
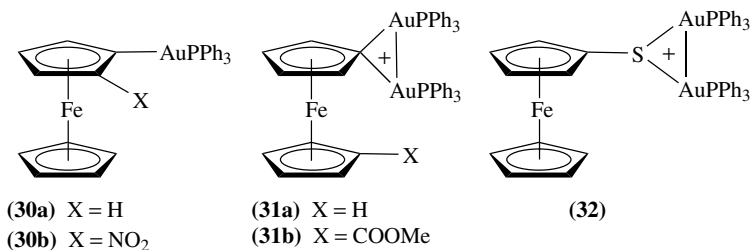
The electrochemistry has been reported for a variety of other structural types, notably compounds where one AuPPh$_3$ is directly attached to a Cp ligand in ferrocene **(30a,b)**[44], two AuPPh$_3$ units are bonded to the same carbon of a Cp ring stabilized by intramolecular gold–gold interactions **(31a,b)**[44], two AuPPh$_3$ units are coordinated to a sulfur substituent on a Cp ring **(32)** and a series of compounds where AuPPh$_3$ is sequentially added to cyclopentadiene **(33–35)**[29]. The reduction potentials for **30–35** occur in a fairly narrow range (see Table 9). However, the oxidation processes vary tremendously (e.g. compare **33** vs **34**) suggesting significantly different electrochemical properties that would be quite interesting to investigate further.

(33)

(34)

(35)
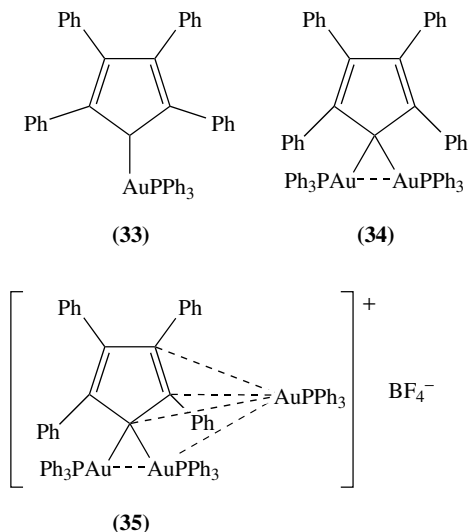
Finally, the electrochemistry of the organometallic gold(III) carborane complex, **36**, has been reported[45]. The cyclic voltammogram of **36** in MeCN solution shows two redox processes. The first is a reversible redox couple (-0.62 V vs SCE) that has been assigned as a one-electron reduction to a stable gold(II) complex. The second reduction process

involves a quasi-reversible redox couple, presumably to the gold(I) carborane. Strong evidence that the intermediate redox compound is a gold(II) complex was found by investigating the electrochemistry of an isolated gold(II) compound made by reduction of **36** with sodium amalgam. The dianionic gold(II) compound displays an initial cathodic process (-0.92 V *vs* SCE) similar to that found in the second reduction process of **36** (-0.84 V *vs* SCE). In addition, a reversible redox process is observed at -0.62 V *vs* SCE for oxidation of the gold(II) compound.

(36)
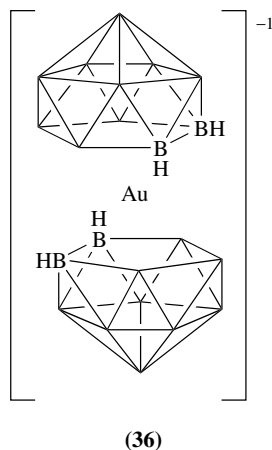
IX. DRUGS

Although the antibacterial effects of silver and the biological activity of gold have long been known, few electrochemical studies have appeared on the redox properties of gold and silver complexes of biological importance. Gold complexes such as $[Au(\mathbf{13c})_2]^+$ have been shown to be potent cardiovascular toxins[25] while complexes such as Auranofin, **37**, have been used successfully to treat rheumatoid arthritis. While the mechanism of action of anti-inflammatory gold drugs is not clear, the interaction of gold(I) centers with the thiol groups of proteins and enzymes is believed to play a role.

(37)
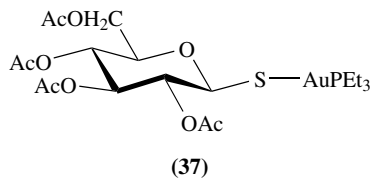
Pérez and coworkers investigated the reduction of **37** at a dropping mercury electrode[48]. Figure 9 shows the electrochemical behavior of **37** in deoxygenated alkaline 0.06 M K_3PO_4 ethanol/water (1 : 1) solution using dc polarography (a) and differential pulse polarography (b) techniques. The polarographic techniques were used to establish that the electrochemical processes are diffusion controlled and reversible in alkaline media. Bulk electrolysis at -0.8 V leads to an *n* value of 0.9 electrons per molecule and suggests
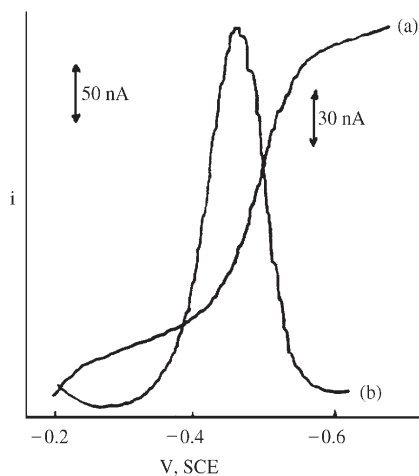
FIGURE 9. Electrochemical behavior of Auranofin, **37**, in deoxygenated alkaline 0.06 M K_3PO_4 ethanol/water (1 : 1) solution: (a) direct current polarography; (b) differential pulse polarography. Reproduced by permission of the American Pharmaceutical Association from Reference 48
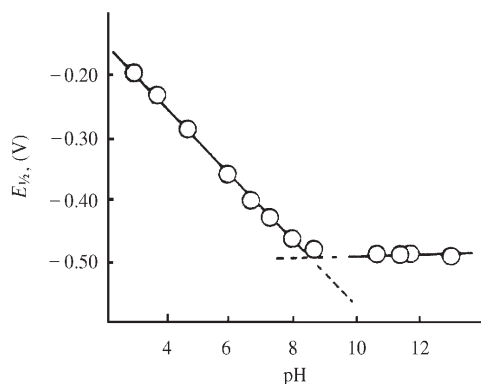
FIGURE 10. The pH dependence on $E_{1/2}$ of Auranofin, **37**. Reproduced by permission of the American Pharmaceutical Association from Reference 48

that the reduction involves the $Au^{I/0}$ redox couple. Interestingly, the reduction potential is strongly sensitive to the pH values below 8.5 as shown in Figure 10. Above a pH of 9, there is no proton-dependent pathway and the redox couple appears at -0.5 V *vs* SCE (see Table 10). Below a pH of *ca* 8.5, a proton-dependent reduction pathway is indicated. Protonation of triethylphosphine (equation 6, $pK_a = 8.69$) is believed to be responsible for the shift in potential as a function of pH. A linear relationship between the limiting current and Auranofin concentration was also noted in the concentration range 3.63×10^{-5} to 5.1×10^{-4} M. Effects of adsorption processes at the electrode surface

TABLE 10.   Electrochemical data (V) of gold drugs

Compound	Alternative formula	Oxidations	Reduction	Conditions	Solvent	pH	Reference
37	Auranofin		−0.5	a	EtOH/H$_2$O	> 9	48
Au(**41**)	Au[*L*-cysteine]	+1.19		b	H$_2$O	1.67	49
Au(**42**)	Au[*D*-penicillamine]	+1.14, +1.35		b	H$_2$O	1.67	49

^{a} Polarography, SCE reference, dropping mercury working electrode.
^{b}Cyclic voltammetry, SCE reference, Pt working electrode.

appear at concentrations above 3×10^{-4} M.

$$P(C_2H_5)_3 + H^+ \rightleftharpoons [P(C_2H_5)_3H]^+ \qquad (6)$$
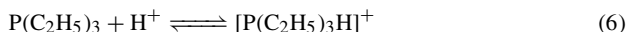
The reducing properties of antiarthritic drugs such as Auranofin, **37**, sodium aurothiomalate (myocrisin), **38**, sodium aurothiopropanol sulfonate (allocrysin), **39**, and aurothioglucose (solganol), **40**, were investigated by Huck and coworkers[50]. The standard redox potentials of drugs which instantly react with the oxidant, 5,5′-dithiobis-(2-nitrobenzoic acid), were determined by titration with potassium hexacyanoferrate(III) in a 0.1 M phosphate buffer (pH 7.0, 25 °C), at a dropping mercury electrode using a SCE reference. Unfortunately, none of the gold-containing compounds reacted very quickly with the oxidant and the standard potentials could not be measured directly even after long incubation periods in phosphate buffer at 37 °C[50].

(**38**)   (**39**)   (**40**)
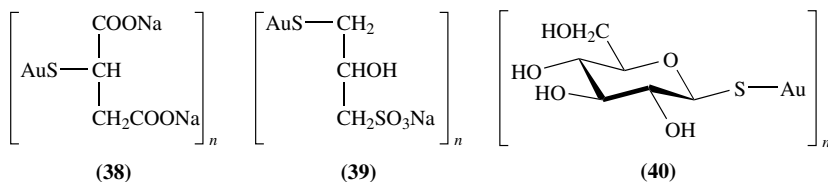
Anderson and Sawtelle have investigated the aqueous redox processes for the electrogenerated gold(I) species, [AuCl$_2$]$^-$, complexed by biologically relevant ligands such as cysteine, **41**, and penicillamine, **42**[49]. They propose an aqueous reduction mechanism that begins with [AuCl$_4$]$^-$ as illustrated in equations 7–9. The progress of these electron transfer and coupled chemical reactions can be followed by cyclic voltammetry and UV-vis spectroelectrochemistry. Upon formation of [AuCl$_2$]$^-$, addition of **41** or **42** leads to complexation and changes in the electrochemistry which allows an estimation of the oxidation potentials (see Table 10) of the Au[cysteine] and Au[penicillamine] complexes. Cyclic voltammetry control experiments with cysteine, cystine and penicillamine indicate that the observed electrochemical responses do not originate from these free species in solution.

$$[AuCl_4]^- \rightleftharpoons [AuCl_2]^+ + 2\ Cl^- \qquad (7)$$

$$[AuCl_2]^+ + 2\ e^- \rightleftharpoons [AuCl_2]^- \qquad (8)$$

$$[AuCl_2]^- + e^- \rightleftharpoons Au + 2\ Cl^- \qquad (9)$$
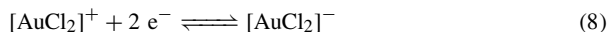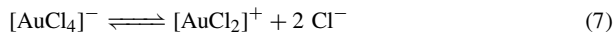
The mechanisms of a wide range of bactericidal agents, including silver sulfadiazine, **43**, which has an extended polymeric structure[51], were examined by Ames, Ryan and
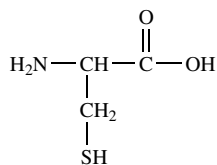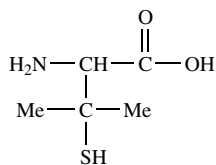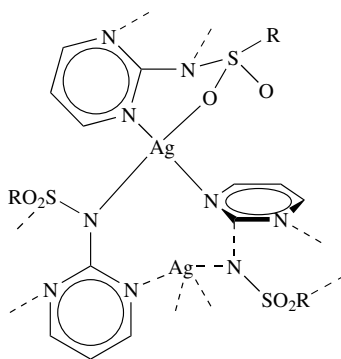
(41)   **(42)**   [**(43)** R = p-C$_6$H$_4$NH$_2$]

Kovacic using cyclic voltammetry measurement at either Pt or dropping mercury working electrodes[52]. Unfortunately, because of the low solubility of **43** in 0.1 M KH$_2$PO$_4$/0.1 M NaOH solution (pH 7.0), no reduction wave was observed.

X. IMIDES AND ANILIDES

Two series of linear silver salts of imides and anilides, formulated as [Ag(L)$_2$]NEt$_4$ (amide = **44a–h**) and [Ag(L)$_2$]Ag (L = **44a–e**), have been studied using linear voltammetry, cyclic voltammetry and coulometry at Pt and vitreous electrodes in acetonitrile[53,54]. The linear voltammograms obtained for [Ag(L)$_2$]Ag show two cathodic waves and one anodic wave (see Table 11). The first cathodic wave at ca −0.2 V vs Ag/Ag$^+$ for [Ag(**44a**)$_2$]Ag corresponds to reduction of the loosely bound silver ion (equation 10) and the second wave at ca −1.3 V vs Ag/Ag$^+$ corresponds to reduction of the tightly bound silver ion (equation 11). As expected, there is only one reduction wave at −1.35 V for [Ag(**44a**)$_2$]NEt$_4$ which corresponds to reduction of the tightly bound silver ion.

$$[\text{Ag}(\mathbf{44a})_2]\text{Ag} + e^- \xrightarrow{\ ca\ -0.2\ \text{V}\ } [\text{Ag}(\mathbf{44a})_2]^- + \text{Ag}^0 \qquad (10)$$

$$[\text{Ag}(\mathbf{44a})_2]^- + e^- \xrightarrow{\ ca\ -1.3\ \text{V}\ } 2[\mathbf{44a}]^- + \text{Ag}^0 \qquad (11)$$
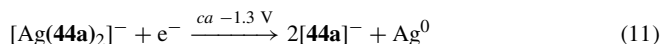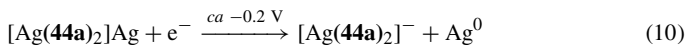
The second cathodic process in [Ag(**44e**)$_2$]Ag is broad and occurs at a very low potential (−0.5 V vs Ag/Ag$^+$) compared to the other silver salts in this series. This anomalous behavior was attributed to the lower stability of the silver complex and the presence of several isomeric forms of the acyclic imide ligand.

Both the silver salts and the mixed silver/tetraethylammonium salts show anodic waves that are similar in potential and amplitude, demonstrating similar oxidation processes in both salts. Coulometric measurements and n values show that the oxidation process is irreversible and involves one electron. This process was assigned as a ligand-based oxidation. In general, the complexes with cyclic imide ligands (**44a–d**) oxidize at ca +1.5 V vs Ag/Ag$^+$. The oxidation potentials of the silver complexes with acyclic ligands (**44e–h**) are more sensitive to changes in ligand composition. The presence of two electron-withdrawing carbonyl groups in **44e** gives rise to a higher oxidation potential than those with only one carbonyl group (**44f–h**). Placing an electron donating methoxy group

TABLE 11.   Electrochemical data (V) of imides and anilides[a]

Compound	Alternative formula	Oxidations[b]	Reductions[b]		Reference
[Ag(**44a**)$_2$]NEt$_4$	[Ag(succinimide$^-$)$_2$]NEt$_4$	+1.48[c]		−1.35[c]	53,54
[Ag(**44a**)$_2$]Ag	[Ag(succinimide$^-$)$_2$]Ag	+1.48[c]	−0.18[c]	−1.30[c]	53
		0.0[d]	−0.25[d]	−1.50[d]	53
[Ag(**44b**)$_2$]NEt$_4$	[Ag(Me$_4$succinimide$^-$)$_2$]NEt$_4$	+1.56[c]			54
[Ag(**44b**)$_2$]Ag	[Ag(Me$_4$succinimide$^-$)$_2$]Ag	+1.50[c]	−0.16[c]	−1.52[c]	53
		0.0[d]	−0.26[d]	−1.70[d]	53
[Ag(**44c**)$_2$]NEt$_4$	[Ag(phthalimide$^-$)$_2$]NEt$_4$	+1.52[c]			54
[Ag(**44c**)$_2$]Ag	[Ag(phthalimide$^-$)$_2$]Ag	+1.52[c]	−0.17[c]	−1.30[c]	53
		0.0[d]	−0.22[d]	−1.46[d]	53
[Ag(**44d**)$_2$]NEt$_4$	[Ag(glutarimide$^-$)$_2$]NEt$_4$	+1.47[c]			54
[Ag(**44d**)$_2$]Ag	[Ag(glutarimide$^-$)$_2$]Ag	+1.45[c]	−0.18[c]	−1.38[c]	53
		0.0[d]	−0.48[d]	−1.66[d]	53
[Ag(**44e**)$_2$]NEt$_4$	[Ag(benzoylimide$^-$)$_2$]NEt$_4$	+1.01[c]			54
[Ag(**44e**)$_2$]Ag	[Ag(benzoylimide$^-$)$_2$]Ag	+1.04[c]	−0.20[c]	−0.5[c]	53
		0.0[d]	−0.30[d]	−0.54[d]	53
[Ag(**44f**)$_2$]Ag	[Ag(formanilide$^-$)$_2$]Ag	+0.41[c]	−0.27[c]	−1.38[c]	53
		−0.1[d]	−0.30[d]	−1.74[d]	53
[Ag(**44g**)$_2$]NEt$_4$		+0.27[c]			54
[Ag(**44h**)$_2$]NEt$_4$		+0.65[c]			54
45a	Au(PPh$_3$)NHCOMe	+1.89[d]	−1.77[d]		29
45b	Au(PPh$_3$)NHCOCH$_2$Cl	+1.99[d]	−1.80[d]		29
45c	Au(PPh$_3$)NHCOPh	+2.27[d]	−1.92[d]		29
45d	Au(PPh$_3$)NHC$_6$H$_4$NO$_2$-o	+1.54[d]	−1.65[d]		29
45e	Au(PPh$_3$)NHC$_6$H$_4$NO$_2$-p	+1.44[d]	−1.37[d]	−1.76[d]	29
46	[(AuPPh$_3$)$_2$NHC$_6$H$_4$NO$_2$-p]$^+$	+1.36[d]	−1.43[d]	−1.65[d]	29
47	[(AuPPh$_3$)$_2$NC$_6$H$_4$NO$_2$-p]	+2.50[d]	−1.43[d]	−1.84[d]	29
48a	[(AuPPh$_3$)$_3$NC$_6$H$_4$NO$_2$-p]$^+$	+1.41[d]	−1.51[d]	−1.75[d]	29
48b	[(AuPPh$_3$)$_3$NC$_6$H$_4$Me-p]$^+$	+0.95[d]	−1.87[d]		29

[a]Electrochemical studies reported at Pt working electrode and Ag/Ag$^+$ reference couple in MeCN.
[b]Values reported in Reference 29 as $E_{1/2}$ and References 53 and 54 as E_{pc}.
[c]Linear rotating disc voltammetry at $\omega = 600$ rpm.
[d]Cyclic voltammetry.

in the *para* position of the phenyl ring (**44g**) makes the silver complex, [Ag(**44a**)$_2$]NEt$_4$, easier to oxidize (+0.27 V *vs* Ag/Ag$^+$) than the parent complex, [Ag(**44f**)$_2$]Ag (+0.41 V *vs* Ag/Ag$^+$). The silver complex, [Ag(**44h**)$_2$]NEt$_4$, with an electron-withdrawing cyanide substituent, is harder to oxidize (+0.41 V *vs* Ag/Ag$^+$).

Finally, in the cyclic voltammetry studies of the silver salts, there are two cathodic waves, with similar potential values as observed in the linear voltammetry studies. However, on the return sweep in the CV, there was an anodic peak at 0 V *vs* Ag/Ag$^+$ which was attributed to oxidation of electrodeposited silver[53].

A series of triphenylphosphine gold amide complexes (**45–48**) was studied by Rakhimov and coworkers[29]. The anodic process was in general assigned to a one-electron

(44a)   **(44b)**   **(44c)**   **(44d)**

(44e)   **(44f)**   **(44g)**   **(44h)**
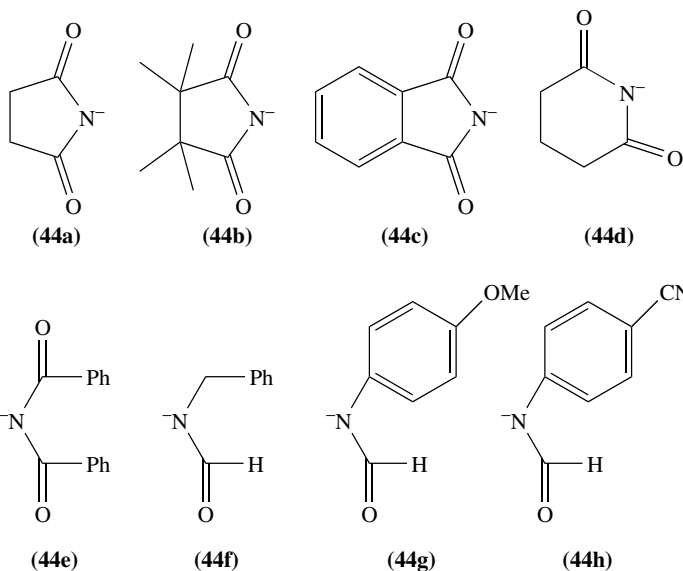
oxidation of the amide or anilide ligands, followed by a series of chemical reactions that resulted in deposition of Au^0 on the platinum electrode. The aniline derivatives can be doubly and triply 'aurated' **(46–48)** by addition of two or three $(AuPPh_3)^+$ groups. Auration does not have a predictable effect on the oxidation potential (see Table 11). However, changing the substituent on the phenyl ring appears to have a significant effect on the oxidation potential. For example, $[(AuPPh_3)_3NC_6H_4Me\text{-}p]^+$ with an electron-donating methyl in the *para* position of the ring oxidizes at +0.95 V *vs* Ag/AgCl, while the *para*-nitro derivative is harder to oxidize by 560 mV.

(45a) R = COMe
(45b) R = COCH$_2$Cl
(45c) R = COPh
(45d) R = C$_6$H$_4$NO$_2$-o
(45e) R = C$_6$H$_4$NO$_2$-p

(46) R = C$_6$H$_4$NO$_2$-p

(47) R = C$_6$H$_4$NO$_2$-p

(48a) R = C$_6$H$_4$NO$_2$-p
(48b) R = C$_6$H$_4$Me-p
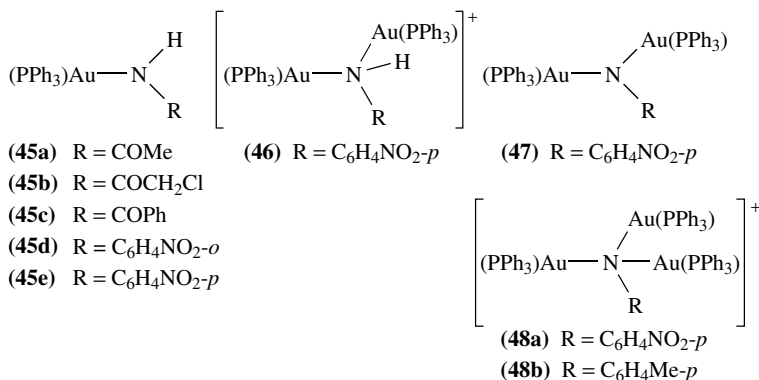
The first cathodic process for the amide gold complexes is proposed to be a one-electron reduction. As the number of $(AuPPh_3)^+$ groups increases, the reduction process

becomes less reversible[29]. The *para*-nitroaniline complexes also show a second cathodic process with n values of 2.8−4. A scheme was proposed that included initial one-electron reduction of the *p*-nitroaniline ligand followed by formation of metallic gold and regeneration of a molecule that is electrochemically active in the same potential range[29].

XI. OTHER LIGANDS AND STRUCTURAL TYPES

This section includes selected examples of electrochemistry of gold and silver complexes with other ligands and structural types that were not included in previous sections. We have also included a list of references divided into the following areas that can be consulted for additional information: sulfur- and nitrogen-containing macrocycles[55−79], porphyrins[80−96] and clusters[97−116].

A. Macrocycles

Macrocycles are well known to bind to a variety of metals in several oxidation states and the macrocycle cavity size can be varied to electronically tune redox couples. A number of electrochemical investigations have been conducted on gold and silver macrocycles[55−79].

Electrochemical data for complexes with the sulfur-coordinated macrocycles, [9]aneS$_3$ (**49**) and [18]aneS$_9$ (**50**) are listed in Table 12[57,62]. Silver(I) and gold(I) coordinate to two molecules of **49** but only one molecule of **50**. In [Ag(**49**)$_2$]$^+$, the silver atom is six coordinate. In contrast, the X-ray structure of [Au(**50**)]$^+$ shows a distorted tetrahedral

TABLE 12. Cyclic voltammetry data (V) of other ligands and structural types

Compound	Oxidations	Reductions	Conditions	Reference
Macrocycles — Sulfur				
[Au(**49**)$_2$]$^+$	+0.12, +0.46		*a*	62
[Ag(**49**)$_2$]$^+$	+0.75	−0.57	*a*	57
[Au(**50**)]$^+$	+0.36, +0.56		*a*	62,66
[Ag(**50**)]$^+$	+1.00	−0.42	*a*	57
Macrocycles — Nitrogen				
[Au(**51**)]$^{3+}$		−0.16, −0.62, −0.98	*b*	70
[Au(**52**)]$^{3+}$		−1.28, −1.42, −1.89	*b*	70
[Ag(**51**)]$^{2+}$	+0.86		*b*	68
Porphyrins				
Ag(**53**)	+0.55, +1.64	−1.1	*c*	80
[Au(**53**)]$^+$	+1.68	−0.59	*c*	80
Clusters				
[Ag$_{13}$\{μ_3 − Fe(CO)$_4$\}$_8$]$^{3−}$		−0.37(rev),−0.65(rev)	*b*	107
[Pd(AuPPh$_3$)$_8$]$^{2+}$		−1.80(rev),−1.98(rev)	*d*	110
[Pt(AuPPh$_3$)$_8$]$^{2+}$		−1.57(rev),−1.72(rev)	*d*	111
[Au(AuPPh$_3$)$_8$]$^{3+}$		−1.03(rev),−1.11(rev)	*d*	111

[a]MeCN, *vs* Fc/Fc$^+$ couple.
[b]MeCN, *vs* SCE.
[c]CH$_2$Cl$_2$, referenced to Ag/AgCl but reported *vs* SCE.
[d]CH$_2$Cl$_2$, *vs* Fc/Fc$^+$.

geometry with Au^I coordinated to four of the sulfurs in the ring[62]. Figure 11 shows a cyclic voltammetry experiment on $[Au(\mathbf{50})]^+$ in MeCN solution[66]. Two redox couples occur at $+0.36$ V and $+0.56$ V (*vs* Fc/Fc$^+$) which were assigned as two successive one-electron oxidations: $Au^I \rightarrow Au^{II}$ followed by $Au^{II} \rightarrow Au^{III}$. The corresponding Ag^I macrocycle complexes, $[Ag(\mathbf{49})_2]^+$ and $[Ag(\mathbf{50})]^+$, show one oxidation process at higher potentials that have been assigned as the $Ag^{I/II}$ couples. The influence of the macrocycle ring size can be illustrated by comparing the oxidation potentials for the complexes with **49** and **50**. The gold and silver complexes with **50** are harder to oxidize reflecting the increased stability of Au^I and Ag^I coordinated to the larger macrocycle.

(49)   **(50)**
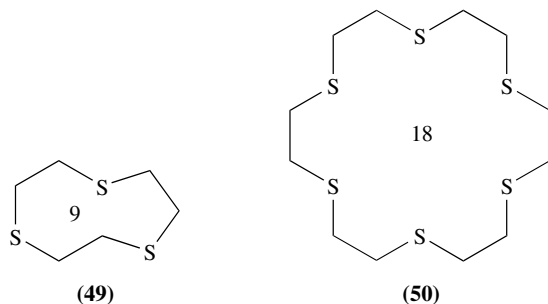
Examples of the electrochemistry of nitrogen-containing gold and silver macrocycles are listed in Table 12. Kimura and coworkers have investigated a series of complexes based on cyclams such as [14]aneN$_4$ (**51**)[70]. Cyclic voltammetry experiments of $[Au(\mathbf{51})]^{3+}$ in 0.1 M [Bu$_4$N]PF$_6$/MeCN solution at a glassy carbon working electrode shows three irreversible reduction waves. The reductions which occur at -0.16 V, -0.62 V and -0.98 V *vs* SCE were assigned as successive one-electron processes. The Au^{III} complex with the triphenylphosphine-pendant cyclam, **52**, shows dramatic shifts in the reduction potentials, indicating that this gold complex is greatly stabilized toward reduction (see Table 12)[70]. Po and coworkers investigated the Ag^{II} complex, $[Ag(\mathbf{51})]^{2+}$ [68]. Cyclic voltammetry experiments at a Pt electrode in 0.1 M [Et$_4$N]ClO$_4$/MeCN solution show a quasi-reversible redox couple at $+0.86$ V *vs* SCE assigned to the $Ag^{II/III}$ couple.

+ 0.05   + 1.05 V *vs* FC / FC$^+$
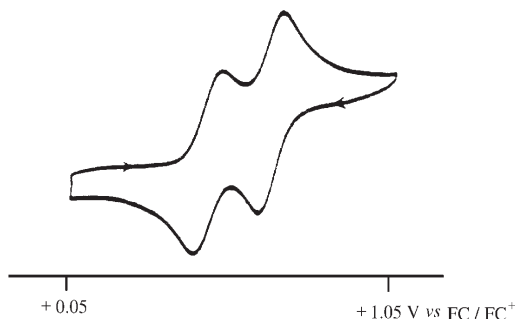
FIGURE 11. Cyclic voltammetry experiment on $[Au(\mathbf{50})]^+$ in MeCN. Reproduced by permission of Kluwer Academic Publishers from Reference 66

(51)   (52)
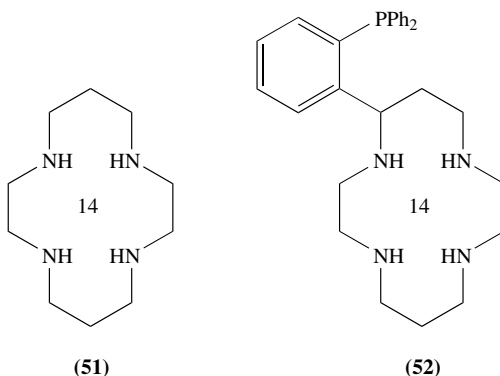
B. Porphyrins

There is great interest in studying the electrochemistry of gold and silver porphyrins in aqueous and nonaqueous solutions[80−96]. The redox reactions for metalloporphyrins include changes in the oxidation state of the porphyrin nucleus and, in some cases, changes in the oxidation state of the metal. The porphyrin ring tends to stabilize the higher oxidation states of silver and gold.

The electrochemical data for many gold and silver porphyrins can be exemplified by considering their complexes with the tetraphenylporphyrin ring, **53** (see Table 12). The metal-based oxidation (Ag$^{II/III}$ couple) of Ag(**53**) at +0.55 V vs SCE occurs between the porphyrin ring oxidation (+1.64 V) and reduction (−1.1 V) processes. In contrast, in the Au^{III} analog, [Au(**53**)]$^{+}$, gold is inert and only ring-based redox processes are observed.

(53)

(54)
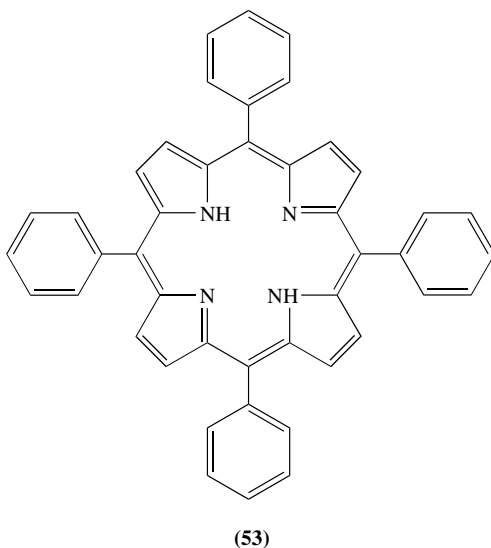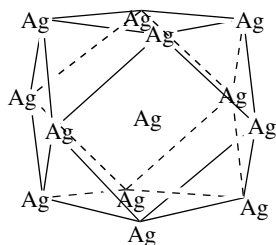
C. Clusters

The tendency of clusters to undergo facile rearrangements or decomposition upon electron transfer, as well as the presence of a large number of redox centers, can make the assignment of the redox behavior of clusters a challenge[97–116]. An interesting example is provided by $[Ag_{13}\{\mu_3\text{-Fe(CO)}_4\}_8]^{3-}$, a cluster composed of a core of 12 silver atoms arranged in a cuboctahedron structure, with an additional silver atom at the center bridging to the other 12 silver atoms **(54)**[107]. Eight μ_3-Fe(CO)$_4$ units cap each triangular face of the cuboctahedron (not shown in **54**). Cyclic voltammetry experiments of $[Ag_{13}\{\mu_3\text{-Fe(CO)}_4\}_8]^{3-}$ at low concentrations (0.1 mM/MeCN) display two reversible cathodic processes (see Table 12). Controlled potential bulk electrolysis at -0.5 V yields an n value equal to one electron per cluster molecule. However, at higher concentrations (2.1 mM), the first redox process remains reversible, but the second becomes irreversible, suggesting a second order following reaction. Figure 12 shows the cyclic voltammogram recorded at the higher concentration using a Pt working electrode and a scan rate of 200 mV s^{-1}. The large wave that appears in the cathodic scan at *ca* -0.2 V *vs* SCE appears to be a silver surface wave, i.e. the result of oxidation of silver metal deposited at the electrode in the reduction scan. The wave is similar in shape and potential to that seen in the analysis of silver during a stripping voltammetry experiment[117].
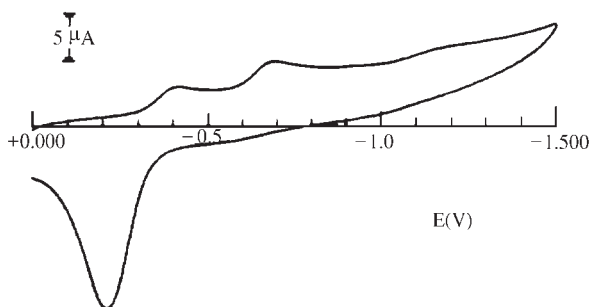
FIGURE 12. Cyclic voltammogram for 2.1 × 10^{-4} M [Et$_4$N][Ag$_{13}$\{μ_3-Fe(CO)$_4$\}$_8$] at a platinum electrode in 0.2 M [Et$_4$N]ClO$_4$/MeCN at scan rate 200 mV s^{-1}. Reproduced by permission of Plenum Press from Reference 107
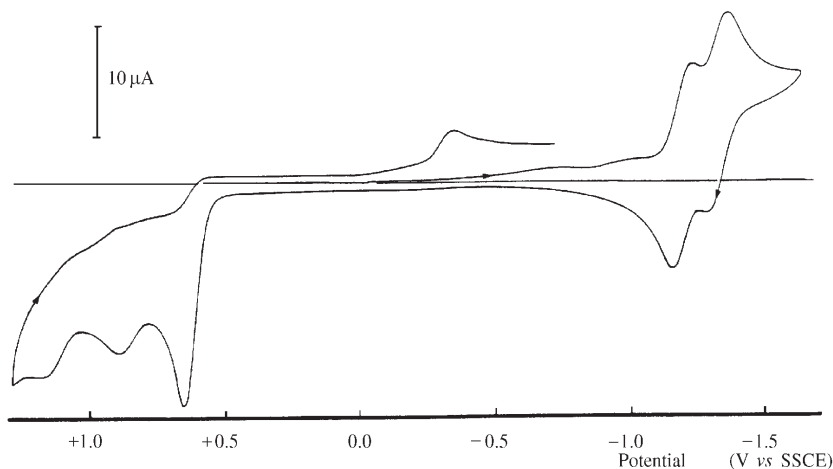
FIGURE 13. Cyclic voltammogram for $[Pt(AuPPh_3)_8]^{2+}$ in 0.1 M $[Bu_4N]PF_6/CH_2Cl_2$ at scan rate 200 mV s^{-1}. Reprinted with permission from Reference 111. Copyright (1989) American Chemical Society

The electrochemistry of $[Pd(AuPPh_3)_8]^{2+}$ was investigated by cyclic voltammetry and differential pulse polarography in CH_2Cl_2 and MeCN solutions[110]. This cluster undergoes two stepwise, reversible one-electron transfers, thus showing an EE reduction mechanism (see equations 12 and 13, and Figure 13). It is interesting to note the large shift to more positive potentials as the central metal atom in $[M(AuPPh_3)_8]^{n+}$ changes from Pd^{II} to Pt^{II} to Au^{II} (see Table 12)[110,111].

$$[Pd(AuPPh_3)_8]^{2+} + e^- \rightleftharpoons [Pd(AuPPh_3)_8]^+ \quad E_{1/2} = -1.80 \text{ V } vs \text{ Fc/Fc}^+ \quad (12)$$

$$[Pd(AuPPh_3)_8]^+ + e^- \rightleftharpoons Pd(AuPPh_3)_8 \quad E_{1/2} = -1.98 \text{ V } vs \text{ Fc/Fc}^+ \quad (13)$$
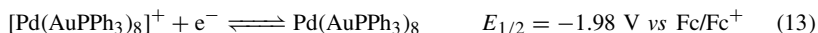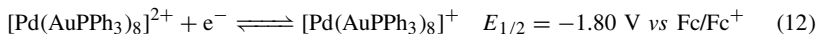
XII. REFERENCES

1. P. Vanysek, in *CRC Handbook of Chemistry and Physics*, 71st edn. (Ed. D. R. Lide), Table 1, CRC Press, Boca Raton, 1990–1991, pp. 8–16.
2. N. Greenwood and A. Earnshaw, in *Chemistry of the Elements*, Chap. 28, Pergamon Press, Oxford, 1984, pp. 1368–1372.
3. F. A. Cotton and G. Wilkinson, in *Advances in Inorganic Chemistry*, Chap. 19, Wiley, New York, 1988, p. 937.
4. A. J. Bard and L. R. Faulkner, in *Electrochemical Methods Fundamentals and Applications*, Wiley, New York, 1980.
5. (a) D. J. G. Ives and G. J. Janz, in *Reference Electrode Theory and Practice*, Chap. 1, Academic Press, New York, 1969, pp. 1–70.
   (b) B. Tremillon, in *Chemistry in Non-Aqueous Solvents*, Chap. 4, D. Reidel, Boston, 1974, pp. 157–198.
   (c) H. Strehlow, in *The Chemistry of Non-Aqueous Solvents Principles and Techniques*, Vol. 1, Chap. 4, Academic Press, 1966, pp. 129–171.
   (d) O. Popovych and R. P. T. Tomkins, in *Non-Aqueous Solution Chemistry*, Chap. 9, Wiley, New York, 1981, pp. 372–422.

6. R. Eisenberg, in *Progress in Inorganic Chemistry* (Ed. S. J. Lippard), Vol. 12, Interscience, New York, 1970, pp. 295–369.

7. S. P. Best, S. A. Ciniawsky, R. J. H. Clark and R. C. S. McQueen, *J. Chem. Soc., Dalton Trans.*, 2267 (1993).

8. R. Williams, E. Billig, J. H. Waters and H. B. Gray, *J. Am. Chem. Soc.*, **88**, 43 (1966).

9. A. Davison, D. V. Howe and E. T. Shawl, *Inorg. Chem.*, **6**, 458 (1967).

10. J. G. M. van der Linden and H. G. J. van de Roer, *Inorg. Chem. Acta*, **5**, 254 (1971).

11. A. L. Balch, I. G. Dance and R. H. Holm, *J. Am. Chem. Soc.*, **90**, 1139 (1968).

12. W. B. Heuer, A. E. True, P. N. Swepston and B. M. Hoffman, *Inorg. Chem.*, **27**, 1474 (1988).

13. G. Matsubayashi and A. Yokozawa, *J. Chem. Soc., Dalton Trans.*, 3535 (1990).

14. A. J. Schultz, H. H. Wang, L. C. Soderholm, T. L. Sifter, J. M. Williams, K. Bechgaard and M. Whangbo, *Inorg. Chem.*, **26**, 3757 (1987).

15. A. E. Underhill, B. Girmay and J. D. Kilburn, *Synth. Met.*, **55–57**, 1920 (1993).

16. M. Nakano, A. Kuroda and G. Matsubayashi, *Inorg. Chim. Acta*, **254**, 189 (1997).

17. A. Charlton, A. E. Underhill, A. Kobayashi and H. Kobayashi, *J. Chem. Soc., Dalton Trans.*, 1285 (1995).

18. C. F. Cleary, N. Robertson, M. Takahashi, A. E. Underhill, D. E. Hibbs, M. B. Hursthouse and K. M. Abdul Malik, *Polyhedron*, **16**, 1111 (1997).

19. M. Nakamoto, *Kagaku to Kogyo (Osaka)*, **68**, 463 (1994); *Chem. Abstr.*, **122**, 95110K (1995).

20. N. C. Schiodt, P. Sommer-Larsen, T. Bjornholm, M. Folmer Nielsen, J. Larsen and K. Bech-gaard, *Inorg. Chem.*, **34**, 3688 (1995).

21. M. J. Baker-Hawkes, E. Billig and H. B. Gray, *J. Am. Chem. Soc.*, **88**, 4870 (1966).

22. J. G. M. van der Linden, *J. Inorg. Nucl. Chem.*, **34**, 1645 (1972).

23. M. Ahmed and R. J. Magee, *Aust. J. Chem.*, **34**, 1861 (1981).

24. A. M. Bond, R. Colton, B. M. Gatehouse and Y. A. Mah, *Inorg. Chim. Acta*, **260**, 61 (1997).

25. J. V. McArdle and G. E. Bossard, *J. Chem. Soc., Dalton Trans.*, 2319 (1990).

26. J. E. Anderson, S. M. Sawtelle and C. E. McAndrews, *Inorg. Chem.*, **29**, 2627 (1990).

27. J. C. Jeffery, T. B. Rauchfuss and P. A. Tucker, *Inorg. Chem.*, **19**, 3306 (1980).

28. L. F. Warren and M. A. Bennett, *Inorg. Chem.*, **15**, 3126 (1976).

29. R. D. Rakhimov, K. P. Butin and K. I. Grandberg, *J. Organomet. Chem.*, **464**, 253 (1994).

30. S. Attar, J. H. Nelson, W. H. Bearden, N. W. Alcock, L. Solujic and E. B. Milosavljevic, *Polyhedron*, **10**, 1939 (1991).

31. A. M. Larsonneur-Galibert, P. Fabre, C. Bresson and P. Castan, *J. Chem. Res, (S)*, 168 (1996).

32. T. Jiang, G. Wei, C. Turmel, A. E. Bruce and M. R. M. Bruce, *Metal-Based Drugs*, **1**, 419 (1994).

33. A. E. Bruce and M. R. M. Bruce, unpublished results.

34. M. Bardaji, N. G. Connelly, M. C. Gimeno, P. G. Jones, A. Laguna and M. Laguna, *J. Chem. Soc., Dalton Trans.*, 2245 (1995).

35. J. R. Dilworth, A. J. Hutson, J. Zubieta and Q. Chen, *Trans. Met. Chem.*, **19**, 61 (1994).

36. A. P. Koley, S. Purohit, S. Ghosh, L. S. Prasad and P. T. Manoharan, *J. Chem. Soc., Dalton Trans.*, 2607 (1988).

37. A. P. Koley, S. Purohit, L. Prasad, S. Ghosh and P. T. Manoharan, *Inorg. Chem.*, **31**, 305 (1992).

38. (a) R. Narayanaswamy, M. A. Young, E. Parkhurst, M. Ouellette, M. E. Kerr, D. M. Ho, R. C. Elder, A. E. Bruce and M. R. M. Bruce, *Inorg. Chem.*, **32**, 2202 (1993).
(b) W. B. Jones, J. Yuan, R. Narayanaswamy, M. A. Young, R. C. Elder, A. E. Bruce and M. R. M. Bruce, *Inorg. Chem.*, **34**, 1996 (1995).

39. J. D. Basil, H. H. Murray, J. P. Fackler, Jr., J. Tocher, A. M. Mazany, B. T. Bancroft, H. Knachel, D. Dudis, T. J. Delord and D. O. Marler, *J. Am. Chem. Soc.*, **107**, 6908 (1985).

40. M. Bardaji, N. G. Connelly, M. C. Gimeno, J. Jimenez, P. G. Jones, A. Laguna and M. Laguna, *J. Chem. Soc, Dalton Trans.*, 1163 (1994).

41. R. D. Rakhimov, K. P. Butin, K. I. Grandberg and E. I. Smyslova, *Metalloorg. Khim.*, **4**, 650 (1991); *Chem. Abstr.*, **115**, 585 (1991).

42. V. W. W. Yam, S. W. K. Choi and K. K. Cheung, *J. Chem. Soc., Dalton Trans.*, 3411 (1996).

43. M. C. Gimeno, A. Laguna, C. Sarroca and P. G. Jones, *Inorg. Chem.*, **32**, 5926 (1993).

44. R. D. Rakhimov, K. P. Butin, K. I. Grandberg, E. I. Smyslova and V. P. Dyadchenko, *Metalloorg. Khim.*, **5**, 1212 (1992); *Chem. Abstr.*, **118**, 827 (1993).

45. L. F. Warren, Jr. and M. F. Hawthorne, *J. Am. Chem. Soc.*, **90**, 4823 (1968).

46. P. Zanello, in *Ferrocenes* (Eds. A. Togni and T. Hayashi), Chap. 7, VCH, Weinheim, 1995, pp. 317–430.
47. G. Pilloni, B. Longato and B. Corain, *J. Organomet. Chem.*, **420**, 57 (1991).
48. J. Hernandez Mendez, A. Sanchez Pérez and M. Delgado Zamarreno, *J. Pharm. Sci.*, **78**, 589 (1989).
49. J. E. Anderson and S. M. Sawtelle, *Inorg. Chim. Acta*, **194**, 171 (1992).
50. F. Huck, R. de Medicis, A. Lussier, G. Dupuis and P. Federlin, *J. Rheum.*, **11**, 605 (1984).
51. N. Farrell, in *Transition Metal Complexes as Drugs and Chemotherapeutic Agents*, Chap. 9, Kluwar Academic Publishers, Dordrecht, 1989, p. 212.
52. J. R. Ames, M. D. Ryan and P. Kovacic, *J. Free Radicals Biol. Med.*, **2**, 377 (1986).
53. J. Y. Hout, D. Serve and J. Lessard, *Can. J. Chem.*, **61**, 1890 (1983).
54. J. Y. Hout, D. Serve and J. Lessard, *Can. J. Chem.*, **66**, 35 (1988).
55. P. J. Blower, J. A. Clarkson, S. C. Rawle, J. R. Hartman, R. E. Wolf, Jr., R. Yagbasan, S. G. Bott and S. R. Cooper, *Inorg. Chem.*, **28**, 4040 (1989).
56. J. A. Clarkson, R. Yagbasan, P. J. Blower, S. C. Rawle and S. R. Cooper, *J. Chem. Soc., Chem. Commun.*, 950 (1987).
57. A. J. Blake, R. O. Gould, A. J. Holder, T. I. Hyde and M. Schroder, *Polyhedron*, **8**, 513 (1989).
58. R. J. Smith, S. N. Salek, M. J. Went, P. J. Blower and N. J. Bernard, *J. Chem. Soc., Dalton Trans.*, 3165 (1994).
59. B. de Groot, H. A. Jenkins and S. J. Loeb, *Inorg. Chem.*, **31**, 203 (1992).
60. B. de Groot and S. J. Loeb, *Inorg. Chem.*, **30**, 3103 (1991).
61. A. J. Blake, D. Collison, R. O. Gould, G. Reid and M. Schroder, *J. Chem. Soc., Dalton Trans.*, 521 (1993).
62. A. J. Blake, A. Taylor and M. Schroder, *J. Chem. Soc., Chem. Commun.*, 1097 (1993).
63. A. J. Blake, J. A. Greig, A. Holder, T. I. Hyde, A. Taylor and M. Schroder, *Angew. Chem., Int. Ed. Engl.*, **29**, 197 (1990).
64. A. J. Blake, G. Reid and M. Schroder, *J. Chem. Soc., Dalton Trans.*, 615 (1991).
65. G. Reid and M. Schroder, *Chem. Soc. Rev.*, **19**, 239 (1990).
66. A. J. Blake, R. O. Gould, A. J. Hoder, T. I. Hyde, G. Reid, A. Taylor, M. Schroder and D. Collison, *Molecular Electrochemistry of Inorganic, Bioinorganic and Organometallic Compounds*, NATO ASI Series, **385**, 1992, p. 121.
67. A. J. Blake, R. O. Gould, C. Radek, G. Reid, A. Taylor and M. Schroder, in *The Chemistry of the Copper and Zinc Triads* (Eds. A. J. Welch and S. K. Chapman), Royal Society of Chemistry, Cambridge, 1993.
68. H. N. Po, J. Kiang, E. Brinkman and R. Trismitro, *Bull. Soc. Chim. Fr.*, 325 (1988).
69. V. E. Marquez and J. R. Anacona, *Polyhedron*, **16**, 2375 (1997).
70. E. Kimura, Y. Kodama, M. Shionoya and T. Koike, *Inorg. Chim. Acta*, **246**, 151 (1996).
71. E. Kimura, Y. Kurogi, T. Koike and M. Shionoya, *J. Coord. Chem.*, **28**, 33 (1993).
72. E. K. Barefield and M. T. Mocella, *Inorg. Chem.*, **12**, 2829 (1973).
73. M. Kodama, A. B. Mahatma, T. Koike and E. Kimura, *Bull. Chem. Soc. Jpn.*, **63**, 2803 (1990).
74. I. J. Clark and J. M. Harrowfield, *Inorg. Chem.*, **23**, 3740 (1984).
75. H. Takemura, N. Kon, K. Tani, K. Takehara, J. Kimoto, T. Shinmyozu and T. Inazu, *J. Chem. Soc., Perkin Trans. 1*, 239 (1997).
76. A. Grzejdziak, *Polish J. Chem.*, **68**, 1395 (1994).
77. A. Grzejdziak, *Polish J. Chem.*, **67**, 2133 (1993).
78. A. Grzejdziak, *Polish J. Chem.*, **68**, 1223 (1994).
79. A. Grzejdziak, *Monatsh. Chem.*, **125**, 107 (1994)
80. A. Antipas, D. Dolphin, M. Gouterman and E. C. Johnson, *J. Am. Chem. Soc.*, **100**, 7705 (1978).
81. J. H. Fuhrhop, *Structure and Bonding*, **18**, 1 (1974).
82. P. Bhyrappa and V. Krishnan, *Inorg. Chem.*, **30**, 239 (1991).
83. A. S. Hinman and T. Olorunyolemi, *Can. J. Chem.*, **71**, 1975 (1993).
84. D. J. Morano and H. N. Po, *Inorg. Chim. Acta*, **31**, L421 (1978).
85. J. H. Fuhrhop, K. M. Kadish and D. G. Davis, *J. Am. Chem. Soc.*, **95**, 5140 (1973).
86. A. Harriman, M. C. Richoux and P. Neta, *J. Phys. Chem.*, **87**, 4957 (1983).
87. Z. Abou-Gamra, A. Harriman and P. Neta, *J. Chem. Soc., Faraday Trans. 2*, **82**, 2337 (1986).
88. S. E. Jones and H. N. Po, *Inorg. Chim. Acta*, **42**, 95 (1980).
89. T. Shimidzu, H. Segawa, T. Iyoda and K. Honda, *J. Chem. Soc., Faraday Trans. 2*, **83**, 2191 (1987).

90. T. Shimidzu, T. Iyoda, H. Segawa and K. Honda, *New J. Chem.*, **10**, 213 (1986).
91. A. Giraudeau, A. Louati, H. J. Callot and M. Gross, *Inorg. Chem.*, **20**, 769 (1981).
92. K. M. Kadish, X. Q. Lin, J. Q. Ding, Y. T. Wu and C. Araullo, *Inorg. Chem.*, **25**, 3236 (1986).
93. J. C. Chambron, V. Heitz and J. P. Sauvage, *New J. Chem.*, **21**, 237 (1997).
94. G. Fu, Y. Fu, K. Jayaraj and A. B. P. Lever, *Inorg. Chem.*, **29**, 4090 (1990).
95. M. E. Jamin and R. T. Iwamoto, *Inorg. Chim. Acta*, **27**, 135 (1978).
96. K. Kadish, D. G. Davis and J. H. Fuhrhop, *Angew. Chem., Int. Ed. Engl.*, **11**, 1014 (1972).
97. C. H. Hay, B. F. G. Johnson, J. Lewis, R. C. S. McQueen, P. R. Raithby, R. M. Sorrell and M. J. Taylor, *Organometallics*, **4**, 202 (1985).
98. M. Fajardo, M. P. Gomez-Sal, H. D. Holden, B. F. G. Johnson, J. Lewis, R. C. S. McQueen and P. R. Raithby, *J. Organomet. Chem.*, **267**, C25 (1984).
99. D. A. Kaner, *PhD Thesis*, University of Cambridge (1984).
100. M. D. Vargas, *PhD Thesis*, University of Cambridge (1984).
101. G. A. Moehring, P. E. Fanwick and R. A. Walton, *Inorg. Chem.*, **26**, 1861 (1987).
102. J. D. Allison and R. A. Walton, *J. Am. Chem. Soc.*, **106**, 163 (1984).
103. P. D. Boyle, D. C. Boyd, A. M. Mueting and L. H. Pignolet, *Inorg. Chem.*, **27**, 4424 (1988).
104. G. A. Moehring and R. A. Walton, *J. Chem. Soc., Dalton Trans.*, 1701 (1988).
105. J. D. Allison, C. J. Cameron, R. E. Wild and R. A. Walton, *J. Organomet. Chem.*, **218**, C62 (1981).
106. V. G. Albano, R. Aureli, M. C. Iapalucci, F. Laschi, G. Longoni, M. Monari and P. Zanello, *J. Chem. Soc., Chem. Commun.*, 1501 (1993).
107. V. G. Albano, F. Calderoni, M. C. Iapalucci, G. Longoni, M. Monari and P. Zanello, *J. Cluster Sci.*, **6**, 107 (1995).
108. C. E. Housecroft, M. S. Shongwe, A. L. Rheingold and P. Zanello, *J. Organomet. Chem.*, **408**, 7 (1991).
109. O. Rossell, M. Seco, G. Segales, R. Mathieu and D. de Montauzon, *J. Organomet. Chem.*, **509**, 241 (1996).
110. L. N. Ito, A. M. P. Felicissimo and L. H. Pignolet, *Inorg. Chem.*, **30**, 988 (1991).
111. J. G. M. van der Linden, A. M. Roelofsen and G. H. W. Ipskamp, *Inorg. Chem.*, **28**, 967 (1989).
112. J. J. Bour, R. P. F. Kanters, P. P. J. Schlebos and J. J. Steggerda, *Recl. Trav. Chim. Pays-Bas*, **211**, 107 (1988).
113. J. G. M. van der Linden, M. L. H. Paulissen and J. E. J. Schmitz, *J. Am. Chem. Soc.*, **105**, 1904 (1983).
114. T. G. M. M. Kappen, J. G. M. van der Linden, A. M. Roelofsen, J. J. Bour, P. P. J. Schlebos and J. J. Steggerda, *Inorg. Chim. Acta*, **245**, 133 (1996).
115. S. Watase and M. Nakamoto, *Kagaku to Kogyo (Osaka)*, **69**, 402 (1995); *Chem. Abstr.*, **123**, 765 (1995).
116. J. J. Steggerda, J. G. M. van der Linden and J. E. F. Gootzen, *Mat. Res. Soc. Symp. Proc.*, **272**, 127 (1992).
117. Kh. Z. Brainina, *Stripping Voltammetry in Chemical Analysis*, Wiley, New York, 1974.

CHAPTER **10**

The organic photochemistry of silver and gold

WILLIAM M. HORSPOOL

Department of Chemistry, The University of Dundee, Dundee DD1 4HN, Scotland
Fax: 44(0)1382 345517;   e-mail: w.m.horspool@dundee.ac.uk

I. INTRODUCTION

The photochemical reactivity of organic silver and gold compounds has been reviewed in the earlier editions of this series where five volumes have been devoted to the study of organometallic systems in all their many guises. Throughout these volumes there are several, but not many, references to the organic photochemical activity of silver and gold systems[1,2]. This seems to be the case in the literature in general. It is very dependent upon how the term 'organic photochemistry of gold and silver' is defined. The simplest definition is one where the photoreactions mainly involve the photochemical transformation of the organic moiety or the photochemical fission of a gold or a silver covalent bond. Using this it soon becomes clear that there is a scarcity of such processes. Thus the scope has been widened to include a variety of different processes, such as the catalytic activity of these metals. This review has endeavoured to highlight some of the areas that are currently of interest or have been studied to some extent in the past. There has been no attempt to ensure that the coverage is encyclopaedic. Thus photochemical processes relating to the deposition of silver and gold to form printed circuits and such like have been omitted.

II. REACTIONS INVOLVING SILVER AS FILMS OR IN SOLUTION

The photochemical processes occurring in thin films deposited on metal surfaces such as Ag and Au has been reviewed[3]. In general, the photochemistry is subject to quenching of the photoprocess by the surface or the reverse of this where an electron transfer process becomes important. The films on the metal surface can be either physisorbed as in Langmuir–Blodgett systems or can be chemisorbed as in thin films of thiols or carboxylic acids, for example.

A. Alkyl Halides

There is little doubt that considerable research effort has been put into the study of the catalytic effect induced on compounds spread as thin films on silver surfaces. The means of activation of these molecules can either be by photonic processes or by electron bombardment. As would be expected much work has been devoted to the study of halo compounds on silver. For example, the UV irradiation at 254 nm (4.9 eV) of ethyl chloride adsorbed at 100 K on a silver(111) surface brings about C−Cl bond fission[4]. Usually the halide remains attached to the surface accumulating as silver chloride. There is also some desorption of the haloalkane and of the hydrocarbon fragments formed during the irradiation. The ethyl radicals that remain on the surface combine to form butane. There is catalytic activity due to the silver surface and this usually manifests itself as a red shift, from that observed in the gas phase processes, in the onset of the C−Cl bond fission. The C−Cl bond in ethyl chloride is also dissociated when monolayers are subjected to low-energy electron bombardment[5a]. Irradiation with 50 eV electrons has also shown that ethyl radicals, ethane and ethene are formed from ethyl chloride monolayers on silver. Many other products, such as butene and butadiene, are formed when multilayers are irradiated[5b]. Methyl chloride is also reactive on irradiation under the same conditions. Again there is a dependence on the coverage of the silver surface. With a coverage of up to one monolayer methyl and ethyl radicals are detected, as are methane and ethane. The product formation does show a dependence upon the intensity of the irradiation[5c].

Irradiation of methyl bromide, again on a silver(111) surface, follows the same pattern. The principal photochemical event is the fission of the C−Br bond with the bromide being retained on the surface and with expulsion of the methyl fragment. The study reports that the threshold energy for the C−Br bond fission was higher for multilayer systems

(>3.5 eV) than for the monolayer (3.0 eV). Both of these are lower than the same event in the gas phase and this suggests that the mechanism involves a metal/ligand charge transfer from the silver surface to the C—Br bond within the monolayer[6,7]. Desorption of the methyl fragments affords ethane[7].

Others[8−10] have reported that a photoinduced charge transfer is involved in the dissociation of the C—halogen bond in the series of alkyl halides, carbon tetrachloride, chloroform, methylene dichloride, methyl chloride and methyl bromide. The activation of these was by UV laser irradiation of the halides as films adsorbed on a silver(111) surface. The process is proposed to follow the path outlined in equation 1 in which a substrate electron brings about the dissociation of the RCl. Again the electron transfer process involves the formation of the radical anion of the halo compound that collapses into halide and the corresponding alkyl radical.

$$RCl/Ag(111) \xrightarrow{\text{light}} RCl^{\bullet-}/Ag(111) \longrightarrow Cl^- + R^{\bullet}/Ag(111) \qquad (1)$$
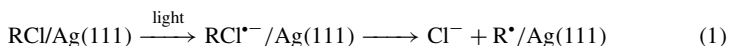
Studies in two-layer systems have also shown the involvement of electron transfer processes from the metal surface. The two-layer system is made by deposition of an alkyl halide on the silver surface and then the deposition of the next reactant as an additional monolayer. Thus irradiation (at 193, 248 or 350 nm) of the $CH_3X/RCl/Ag(111)$ system, where $X = Br$ or I and $R = CCl_3$, $CHCl_2$ or CH_2Cl, brings about C—X bond fission. This operates via an electron transfer process from the metal to the RCl layer affording the RCl radical anion. Collision of this, an ion molecule process that is thought to be concerted (i.e. loss of X^- from CH_3X occurs concomitantly with the formation of the C—Cl bond in methyl chloride), with CH_3X brings about the C—X bond fission (equation 2)[11]. At one monolayer thickness, the yield of methyl chloride is enhanced but decreases at higher CH_3X coverage.

$$Ag/RCl \xrightarrow{\text{light}} Ag/RCl^{\bullet-} + CH_3X \longrightarrow Ag/R^{\bullet} + CH_3Cl + X^- \qquad (2)$$
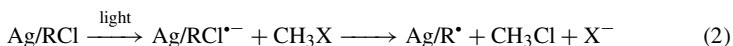
Both neutral and charge-transfer photochemistry is involved in the photodissociation at 248 nm of methyl iodide as a monolayer (1 ML) or up to 10 ML on a silver(111) surface. Such reactivity involves the fission of the C—I bond and the formation of methyl radicals and iodide adsorbed at the surface[12,13a]. Dissociation also occurs during X-ray photoelectron spectroscopy[13b]. Multilayers of methyl iodide on silver(111) surfaces undergo C—I bond fission on irradiation at 248 nm. Several products such as ethane, ethyl iodide and iodoform are formed but the principal reaction path, which is somewhat time-dependent, yields methane and methylene di-iodide[14].

At 95 K a monolayer of trifluoromethyl iodide on a silver(111) surface undergoes C—I bond fission when irradiated at 193 nm or 248 nm. While some desorption occurs during the irradiation, chemisorbed CF_3 and I are produced. Three mechanisms are observed in this reaction system: (i) direct absorption of light by the CF_3I, (ii) absorption by clustered CF_3I and (iii) photoabsorption by the silver surface and electron transfer to the CF_3I with the formation of the CF_3I radical anion[15,16]. Irradiation by low energy electrons of a film of CF_3I on silver(111) also involves electron transfer from the metal surface as well as other processes. Again C—I bond fission is dominant with desorption of the methyl radical. Difluoro-diiodomethane and trifluoro-iodoethene are also formed when the coverage of the metal surface is greater than 0.3 monolayers[17].

Decomposition of alkyl halides also occurs in solution under the influence of silver. Thus it is possible to bring about photochemical C—halogen bond fission in chloroform on irradiation in aqueous solutions with titanium dioxide catalysts. The efficiency of the process is enhanced by up to 25% when the catalyst is loaded with silver[18].

B. Arenes

1. Haloarenes

Not only halogens bonded to tetrahedral carbons are reactive under such conditions, but haloarenes are also photoreactive. The effect of irradiation of monolayers of chlorobenzene on a silver surface has been studied by high resolution electron energy loss spectroscopy. Irradiation by UV brings about cleavage of the C−Cl bond. The resultant carbon-based fragments produce biphenyl after irradiation at 110 K and the spectroscopy shows that the aryl rings are parallel to the surface. Multilayers of chlorobenzene, however, undergo polymerization upon irradiation[19]. Roughened metal surfaces or silver islands[20] have also been used and this introduces the possibility of a catalytic effect at the defect sites. Under these different conditions chlorobenzene also undergoes C−Cl bond fission. Again biphenyl is produced and it can be desorbed from the surface by annealing to 400 K. Similar behaviour is reported for 3-chloropyridine. The authors[21,22] observed that there is a definite red shift in the photodissociation threshold from that observed on smooth silver. This shift to longer wavelength and therefore lower energy is due, perhaps, to the excitation of a surface/adsorbate complex near the defect sites.

2. Heterocyclic compounds

While pyridine is unreactive both pyrazine (**1**) and triazine (**2**) are photochemically reactive and irradiation on a silver surface follows a biphotonic path with the production of graphitic carbon[23]. Phthalazine (**3**) as a thin film on colloidal silver undergoes N−N bond fission. This yields nitrogen groups that are firmly bound to the silver surface[24]. Irradiation of 1,10-phenanthroline (**4**) adsorbed on a silver colloid has also been studied[25]. It appears that irradiation brings about the fission of C−N bonds forming groups, perhaps C=N groups, that become attached to the surface.

| (1) | (2) | (3) | (4) |
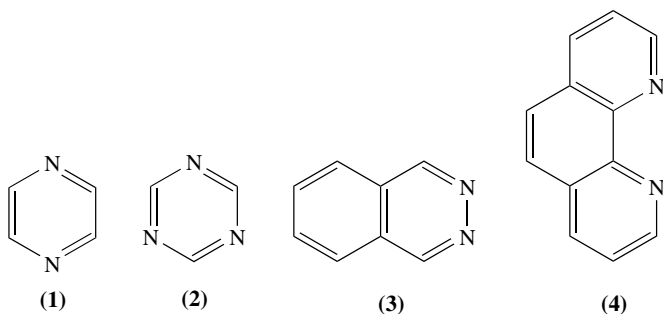
C. Carbonyl Compounds

The photochemical behaviour of other halogenated systems such as phosgene have also been investigated on silver(111) either as monolayers or multilayers. The UV irradiation of this system brings about C−Cl bond fission. The Cl remains chemisorbed to the surface while the CO is desorbed. Again, the data collected suggest that the mechanism involves excitation of an adsorbate/substrate complex. There is evidence that the silver has a catalytic effect with the onset of the reaction red-shifted by 2.6−2.8 eV from the gas

phase process[26]. Others have studied the same reaction and have measured the energetics of the surface reaction[27].

The behaviour of simple carbonyl compounds has also been studied. Thus formaldehyde, as a sub-monolayer coverage on silver(111), undergoes polymerization at 80 K when it is irradiated at 355 nm by a pulsed laser source. The photopolymerization arises by the formation of formyl radicals formed by C−H bond fission. These radicals add to neighbouring molecules to induce the polymerization[28]. The polymerization occurs over a wide range of surface coverage from one monolayer downwards. Temperature effects have also been studied and show that polymerization decreases with decreasing temperature between 35 K and 85 K[29]. A study of the geometry of the adsorbed formaldehyde has shown it to lie with the carbonyl group tilted away from the surface[29c]. Acetone does not undergo photolysis, using 193 nm and 248 nm, when multilayer systems with over five layers were irradiated on a silver surface. Interestingly, when the layers were formed by dosing with hexadeuterioacetone and then by acetone, extensive mixing was observed. However, 100 eV irradiation does bring about C−C bond fission processes. The outcome of the reaction is dependent on the orientation of the molecule on the surface. Usually the carbonyl axis is always parallel to the silver surface. Thus one observes ejection of a methyl fragment and retention of the acetyl fragment on the surface, or *vice versa*[30]. Analogous to acetone, no thermal decomposition of biacetyl occurs on silver(111) surfaces, implying that silver(111) surfaces are inert to the breaking of C−C, C−O and C−H bonds. During low energy electron irradiation carbon monoxide, methyl radicals, ketene and ethane can be detected[31,32]. UV irradiation at 193 nm using a laser source of a monolayer of biacetyl brings about C−C bond fission and methyl radicals are ejected from the surface. Irradiation of multilayers gives carbon monoxide, methyl radicals, ketene and acetyl radical fragments[33]. Irradiation at 266 nm also affords acetyl and methyl fragments[34]. Methyl formate has also been studied under similar conditions. The induced decomposition affords hydrogen, methane, formaldehyde, carbon dioxide and glycolaldehyde (**5**). From the data collected, the mechanism for product formation appears to follow two paths as outlined in equation 3 where fission of a C−O bond affords methyl and formyloxy radicals or methoxy and formyl radicals[35].

$$\text{(i) HCOOCH}_3 \longrightarrow \overset{\bullet}{\text{C}}\text{H}_3 + \text{HCO}\overset{\bullet}{\text{O}}$$

$$\text{(ii) HCOOCH}_3 \longrightarrow \text{CH}_3\overset{\bullet}{\text{O}} + \overset{\bullet}{\text{H}}\text{CO}$$
(3)
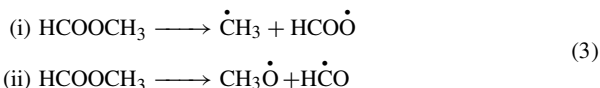
D. Alcohols

Low energy (55 eV) electron irradiation of multilayers of methanol on silver has been used in conjunction with temperature-programmed desorption of the products as a method to identify radiolysis products. In this case several products such as methoxymethanol were identified[36a]. The primary photochemical process in the methanol system is thought to involve the fission of a C−H bond forming a heteroatom stabilized cation such as **6**. In addition to methoxymethanol glycolaldehyde (**5**) or methyl formate are also detected. Apparently the methanol system is unreactive to UV irradiation either at 240 nm or at 355 nm[36b].

Silver also has an enhancing effect on the photocatalytic dehydrogenation of aqueous ethanol by the Pt/CdS system. Apparently, the silver acts as a promoter and transfers s and d electrons from itself to the Pt component of the system[37]. Electron transfer also occurs on γ-irradiation of Ag$^+$ in frozen aqueous, ethanol or ethyl tetrahydrofuran solutions[38]. Liquid propan-2-ol can be oxidized to propanone on irradiation with visible light in the

presence of a Ag^+-doped CdS semiconductor surface[39]. Small amounts of silver deposited on TiO_2 have also been shown to have a catalytic effect on the oxidation of propan-2-ol. The oxidations arise by way of hydroxy radicals. The effect of silver could be the result of enhanced trapping of electrons[40]. Silver-loaded TiO_2 can also be used as a catalyst to oxidize various phenols[41].

E. Organized Systems: Cycloaddition and Related Reactions

The organization of the molecules within the thin layers on the silver surface can also be important in the determination of the outcome of the reactions. Apparently, there are three types of hydrogen bonding when cinnamic acid is spread as a Langmuir–Blodgett film on silver. Lateral hydrogen bonding occurs in monolayers and irradiation of this does not bring about dimerization. However, in a multilayer film both the *cis*-hydrogen bonded form **(7)** and the *trans*-form **(8)** are present and these do undergo dimerization, a conventional $(2+2)$ photochemical process to afford a cyclobutane, on UV irradiation[42]. Dimerization is also observed within Langmuir-Blodgett films of the stilbazolium cations **(9)** embedded in perdeuteriated arachidic acid ($C_{20}H_{40}O_2$) on a silver film. The dimerization yielding **10** proceeds mainly on irradiation at 340 nm. There is a temperature dependence and dimerization is successful at 300 K, but below 200 K the reaction fails. An analysis of the results suggest that there is a non-radiative energy transfer from the photoexcited film to the silver surface[43]. Photochemical dimerization of stilbazole **(11)** and diarylbuta-1,3-dienes, embedded in deuteriated arachidic acid, also can be brought about on a silver surface. Both dimerization processes were shown to be two-step processes[44a]. The product formed is a cyclobutane of the type illustrated in **12** that is formed on irradiation of **11** in the crystalline phase. Such photochemical dimerization is common in ordered systems whether they are in the crystal or on a surface[44b]. Prolonged irradiation at $\lambda > 420$ nm of the Langmuir–Blodgett films of a benzothiazolium styryl dye containing a crown ether group complexed with Ag^+ results in cycloaddition and the formation of a cyclobutane adduct. The dimerization is reversible using irradiation of $\lambda = 310$ nm[45].
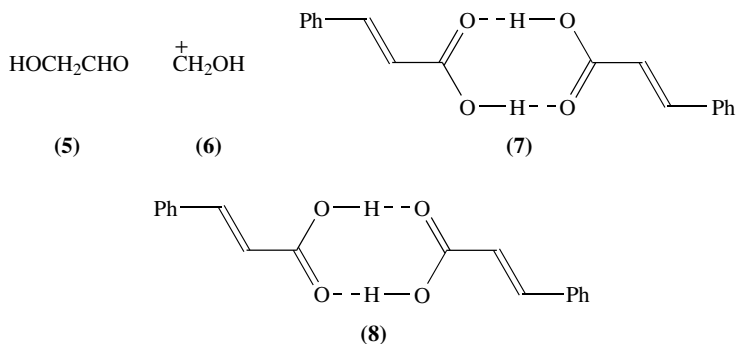
Self-assembled monolayers on silver where the compounds are chemisorbed to the surface have also been studied. Typical of this is the irradiation of alkanethiol films **(13)** on silver in the presence of oxygen, which results in their oxidation to alkyl sulphonates. There is also some sulphur–carbon bond fission[46]. A study of the photooxidation process

Ph—CH=CH—(pyridinium)—$C_{18}H_{37}$-n

(9)

(cyclobutane with Ar, Ph, Ph, R^1, R^2)

(10)

$R^1 =$ (pyridinium with $C_{18}H_{37}$-n) , $R^2 = H$

or vice versa

Ph—CH=CH—(pyridinium)—N—CH$_3$

(11)

(cyclobutane with Ph, Ph and two pyridyl groups)

(12)

$CH_3(CH_2)_nCH_2SH$

(13)

$n = 4, 6, 8, 10$ or 16
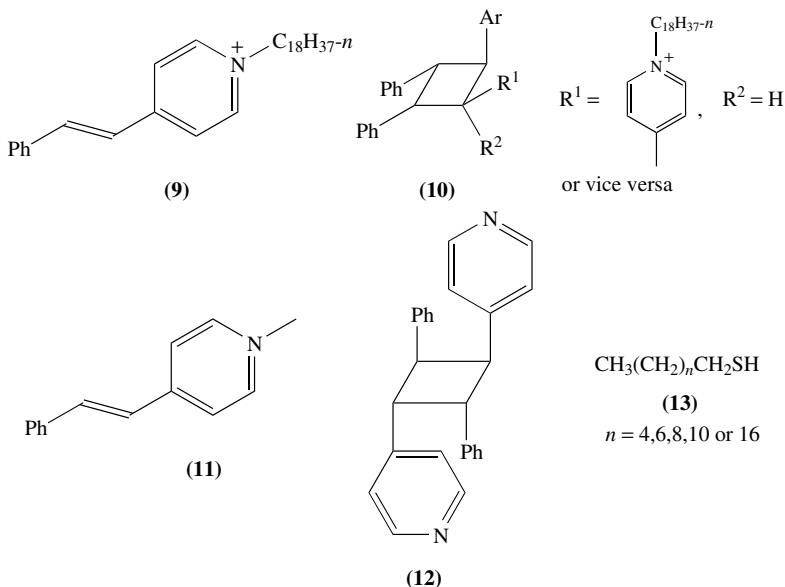
has also been carried out. This has been interpreted as demonstrating that the inorganic sulphur left on the film after the S−C bond fission undergoes oxidation[47].

F. Miscellaneous Compounds

Methyl nitrite on an Ag(111) surface undergoes decomposition on irradiation at $\lambda >$ 365 nm or by 50 eV electrons. The decomposition involves the extrusion of NO from both irradiation methods but X-ray irradiation (50 eV) also supplies evidence for the formation of methyl radicals, formaldehyde and methanol[48]. The orientation of the methyl nitrite monolayer on the silver is consistent with the NO extrusion process[49]. *t*-Butyl nitrite also undergoes loss of NO when a thin film assembled on silver(111) is irradiated at 355 nm[50].

Azomethane undergoes loss of nitrogen on irradiation with low energy electrons[51]. The photochemical decomposition of azo compounds **14** and **15** on silver island films has been studied. The thin film coatings of the organic compounds are deposited on the silver and irradiation is carried out by excimer laser irradiation at 308 nm. The rate of the photochemical decomposition of azosulphonates such as **15** is enhanced by an order of magnitude. This is a further example of surface-enhanced photochemistry[52]. Photochemistry of carbon disulphide on silver(111) has also been studied[53].

Low-energy electron bombardment of monolayers of ethylene on a silver(111) surface brings about C−H bond fission. The H is absorbed on the surface and the vinyl radical dimerizes to yield buta-1,3-diene. Higher doses of electrons lead to the formation of ethyne[54]: Olefins can undergo catalytic oxidation when they are irradiated in the presence of silver catalysts either as silver powder or supported silver metals on anatase titania, silica and porous glass. Irradiation under these conditions increases the reaction rate[55]. When the surface is coated with ethene and deuterium, partly deuteriated ethene is formed on irradiation, presumably as a result of a vinyl radical reacting with deuterium. UV
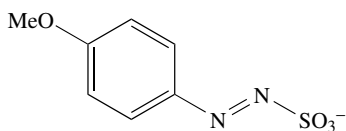
(14)
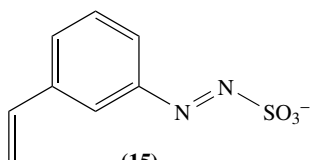
(15)
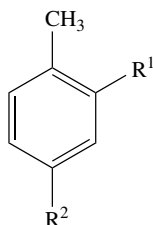
(16)
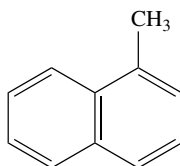
(17)

$R^1 = H, \quad R^2 = Me, MeO$
$R^1 = Me, R^2 = MeO$

irradiation of polystyrene as a thin film of silver leads to degradation[56]. Photoinduced polymerization of styrene can be induced by irradiation of thin films of the monomer on a silver(110) surface[57]. X-ray irradiation of thiophene on a silver(111) surface brings about polymerization within the multilayers assembled on the metal[58].

Others have observed that silver salts can have a beneficial effect on some oxidation reactions. Typical of this is the photooxygenation of methylarenes **16** and **17** to the corresponding benzaldehydes and benzoic acids using TiO_2/Ag_2SO_4 in acetonitrile solution under air. The yields from this reaction system are moderate with the best being the conversion of *p*-methoxytoluene into the corresponding aldehyde in a yield of 30%[59a]. Another example of this is the oxidation of the benzyl trimethylsilanes **18** into the 1,2-diphenylethanes **19** (equation 4)[59b]. This beneficial effect arises from the greater ability of silver sulphate to capture a photogenerated hole in the TiO_2.
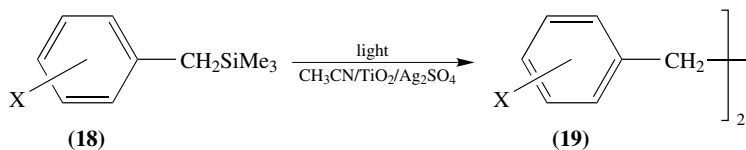
(18)   **(19)**

(4)

X	Yield (%)
H	74
p-Me	71
m-Me	51
m-Cl	58
m-CF$_3$	50

G. Some Electron Transfer Reactions

As has been illustrated earlier, electron transfer processes, often referred to as charge transfer processes, are important steps in the determination of the outcome of the irradiation of many systems on silver. These occur under vacuum on the surface of the metal or in solution where ions are involved. An example of another gas-phase process is the irradiation in the wavelength range 260–385 nm of complexes of silver clusters, and adsorbed species such as benzene, toluene or acetone yield organic ions by electron transfer. These results are among the first dealing with photoinduced charge transfer dissociation for gas-phase metal complexes. The authors[60] concede that it is difficult to arrive at a mechanism for the photoprocess. *p*-Nitrobenzoic acid also undergoes a photochemical reaction and is reduced to *p*-aminobenzoic acid when it is irradiated as a film on roughened silver surfaces. A charge transfer mechanism is thought to be involved[61]: When the distance from the silver is increased, for example when the benzoate is adsorbed onto a silver island film (a rough silver surface) pre-coated with self-assembled monolayers of hexadecylmercaptans, the benzoate does not undergo reduction on irradiation[62].

Electron transfer is also common at electrodes. An example of such a process is the laser irradiation at 406.7 nm of methylviologen **(20)** as a thin film on a roughened silver electrode at liquid nitrogen temperatures which results in its reduction by electron transfer to its radical cation **(21)**. Again, electron transfer from the metal to the dication of **20** is considered to be a reasonable mechanism for the process[63]. Apparently, the radical

(20)   (21)   (22)
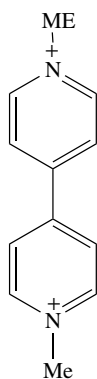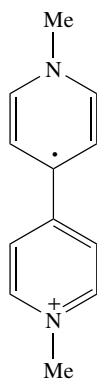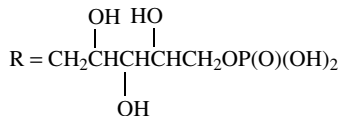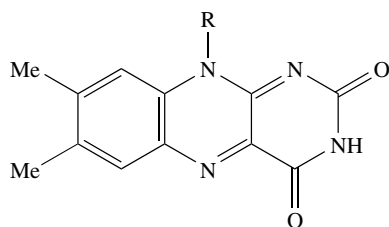
R = CH_2CHCHCHCH_2OP(O)(OH)_2
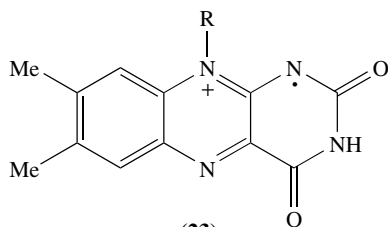
(23)

cation is less strongly absorbed to the surface than is the dication. *p*-Nitrothiophenol also undergoes reduction, presumably by electron transfer from the electrode, to the *p*-aminothiophenol when it is irradiated as a self-assembled monolayer on a smooth silver electrode[64]. Single electron transfer, the reverse of the previous examples, occurs on irradiation of an adsorbed flavin mononucleotide (**22**) on a silver electrode. This results in the formation of the flavin mono radical cation **23**[65].

III. PHOTOCHEMISTRY OF SILVER COMPLEXES OF ALKENES

Silver also has been demonstrated to be reactive in solution systems. Thus, silver perchlorate has been shown to influence the photochemical reactivity of stilbene in acetonitrile and methanol. The fluorescence of the stilbene is quenched on addition of the perchlorate and this is good evidence for the enhancement of the S_0-T_1 crossing induced by the heavy ion Ag^+. It seems likely that an Ag^+/stilbene complex is formed. The perturbation of the system is better in methanol than in acetonitrile. However, *cis,trans* isomerism of the stilbene is reduced within the excited Ag^+/stilbene complex since it is difficult for the geometrical isomerism to occur. Enhanced isomerism is observed with the Ag^+/azobenzene system. In this complex there are steric problems encountered in the nitrogen rehybridization process that is operative in the isomerism[66]. Enhanced S_0-T_1 crossing is also seen in the Ag^+/1 : 1 complex with tryptophan where the fluorescence is quenched and there is a threefold increase in phosphorescence[67]. Complexes between Ag^+ and polynucleotides and DNA cause quenching of the fluorescence. Enhancement of phosphorescence and a 20-fold increase in the dimerization of thymine moieties has also been observed when silver ions are added to the reaction system[68].

As mentioned above, some arylalkenes, such as stilbene, form complexes with Ag^+. Such complexes are also formed between Ag^+, as added silver perchlorate, and simpler alkenes. Typical of this is the interaction with 1-methylenecyclohexane when a crystalline complex is formed. Irradiation of this complex in the polycrystalline state or in solution in methanol affords isomerization to 1-methylcyclohexene by a 1,3-hydrogen migration path. Further irradiation brings about the stereospecific formation of the *exo,trans,exo*-dimer (**24**) of 1-methylcyclohexene. Less specific photodimerization is also reported for the irradiation of the β-pinene (**25**)/silver perchlorate complex[69]: The mechanism was thought to involve a silver/cyclohexenyl radical similar in type to that observed in the γ-radiolysis of silver/cycloalkene complexes[70,71].

(24)   **(25)**
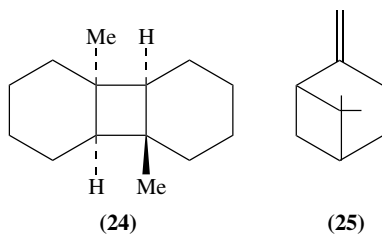
Crystalline Ag^+/norbornene (**26**) complexes can be prepared readily. Excitation of these at 313 nm, where only the complexes absorb, in acetonitrile solution, results in the formation of the norbornene radical cation (**27**). The formation of this radical cation species involves electron transfer from the alkene moiety to the silver, resulting in the formation of metallic silver. The resultant radical cation reacts with solvent to yield the

(26)   (27)   (28)

(29)   (30)   (31)

(32)   (33)
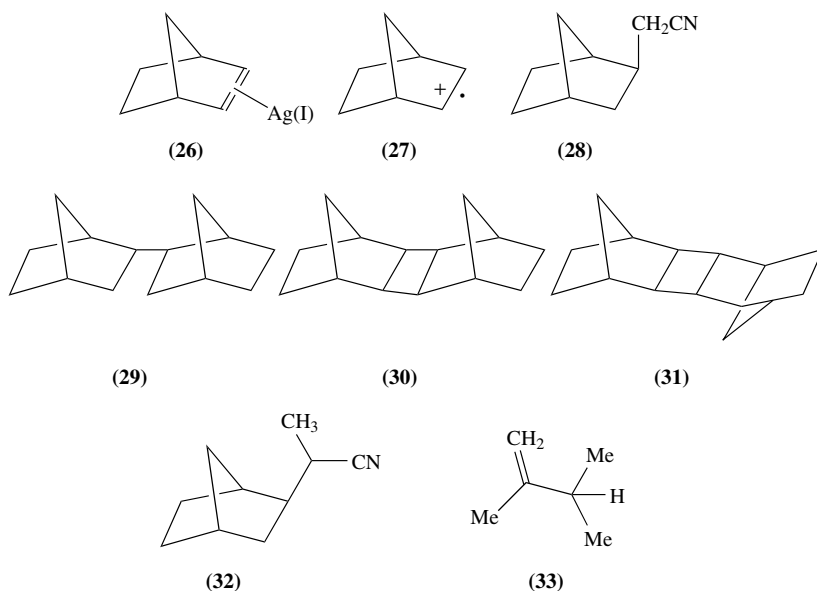
principal product **(28)**, obtained in 93% yield. This is accompanied by small amounts of the dimer **(29)** and the adducts **30** and **31**. Additional work has shown that other solvents such as EtCN are also reactive, leading to an analogous adduct **(32)**[72,73]. The influence that silver ions can have on the *trans,cis*-isomerism of simple alkenes has been studied in some detail. The experiments studied the enhancement of the $E-Z$ or $Z-E$ isomerism of a series of alkenes (Table 1) in the presence of silver triflate. The authors[74] suggest that the considerable enhancement of isomerization is again due to the heavy atom effect of the silver ion on the intersystem crossing to the triplet state of the alkene, as has been shown by others for stilbene.

Interestingly, the irradiation of 2,3-dimethylbut-2-ene under the same conditions is also thought to bring about triplet state enhancement. The outcome of this reaction, since *cis,trans*-isomerism is a degenerate process, is the formation of the alkene **33** by way of a 1,3-hydrogen migration similar to that observed by Wan and coworkers[70,71].

TABLE 1. Irradiation of alkenes in the presence and absence of silver triflate[74]

Alkene	% isomerization	
	Ag^+	Control
Z-Hept-2-ene	45.7	9.0
E-Hept-2-ene	5.6	1.5
Z-Piperylene	18.4	8.7
E-Piperylene	22	40
Z-Stilbene	13.3	15.8
E-Stilbene	11.6	8.2

IV. SILVER−CARBON BOND FISSION ON PHOTOLYSIS

In early studies it was demonstrated that irradiation of the silver compound **34** in ether at −60 °C brings about cleavage of the Ag−C bond and the liberation of butyl radicals. The products from this are illustrated in equation 5. The behaviour observed under the photochemical conditions is considerably different from the thermal reactivity. A study of **35** showed that only a slow photochemical reaction cleaving the C−Ag bond took place. The faster reaction was cyclization to a cyclopentane derivative[75].

n-BuAgP(Bu-n)$_3$

(34)

(5)

(35)
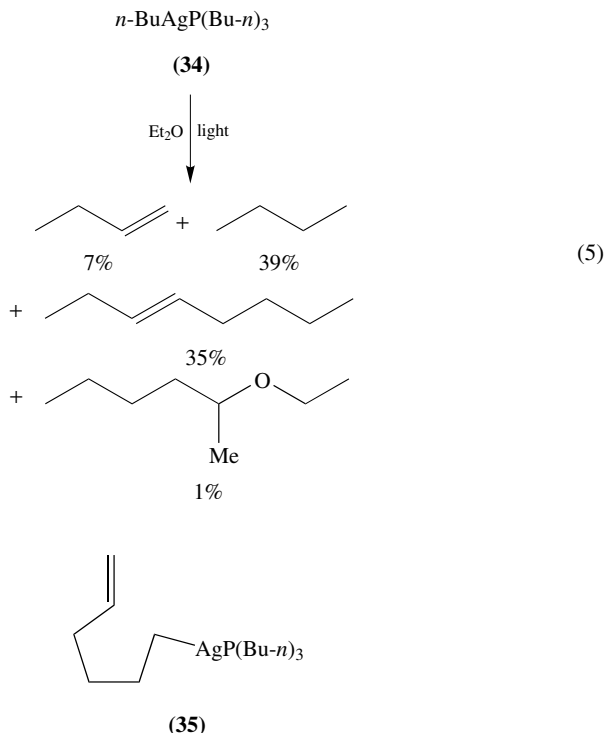
V. SILVER SALTS OF CARBOXYLIC ACIDS

Decarboxylation of silver carboxylates is a well known thermal process and is involved in the Hunsdiecker[76] or Kolbe[77] reactions. The Hunsdiecker reaction is the thermal decarboxylation of silver salts of acids and is used for the formation of bromoalkanes and related compounds, while the Kolbe process involves electrolysis of carboxylates as a route to decarboxylated radicals that can dimerize. Silver carboxylates are also photochemically reactive and the irradiation has been described as a facile process for the formation of alkyl radicals, as illustrated in equation 6[78]. Later experimentation has shown that the irradiation of silver trifluoroacetate can serve as a route to trifluoromethyl radicals. This development uses irradiation of silver trifluoroacetate in the presence of titanium dioxide as a photocatalyst. The reaction follows the usual path with the formation of metallic silver and the formation of radicals. However, in this instance the formation of metallic

silver is not a technical problem in that it deposits on the titanium dioxide and therefore does not impede the outcome of the reaction. Substitution of aromatic substrates can be brought about using this method. The yields from the process vary from moderate to good and some of these are shown in Table 2[79]. Other studies have examined the photo-Kolbe reaction of carboxylic acids in the presence of silver fluoride and colloidal TiO_2. This reaction is a two-electron process involving the formation of cations. This particular study examined the mechanism of the reaction using laser flash photolysis[80]. 4-Nitrobenzoic acid undergoes decarboxylation on Ag(111) surfaces[81].

$$CF_3COOAg \xrightarrow{\text{C}_6\text{H}_6,\text{ light}} \dot{C}F_3 \longrightarrow \text{(C}_6\text{H}_5\text{CF}_3) + CO_2 + Ag^0 \tag{6}$$

57% mol yield
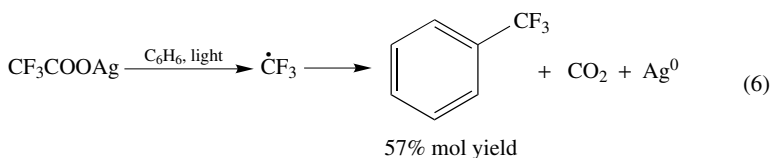
Several examples of the decarboxylation of silver carboxylates have been used as a means of forming patterns that could be used in the formation of printed circuits. From the several examples studied, the authors[82] report that disilver glutamate is the best salt and has good photosensitivity. There is evidence that the ionization potential of the carboxylate is a key to the decomposition path. Further study has shown that the sensitivity of the decomposition can be enhanced by the use of 'chemical sensitizers' such as zinc oxide. Silver oxalate undergoes irradiation in the crystalline phase. An analysis has shown that the photolysis occurs in a thin film on the surface and the crystal structure of the silver oxalate is unaffected[83]. The photocatalytic oxidation of oxalate ion by peroxodisulphate ion can be catalyzed by the presence of silver salts[84]. More complex systems also undergo decomposition. Thus, the irradiation at 253.7 nm of the cellulose derivative **36** in wet air results in the deposition of a silver mirror, presumably by a path analogous to that involved in the simpler carboxylate photochemistry[85]. There are many examples whereby the irradiation of silver salts in the presence of reducing substrates provides a path to the formation of colloidal silver. Presumably all of the reactions involve electron transfer processes from the substrate to the metal to permit the precipitation. Thus silver perchlorate can be irradiated in the presence of sodium alginate to yield colloidal silver with particle diameters of 10–30 nm[86]. Furthermore, irradiation of silver alginate, the silver salt of a polysaccharide, as a thin film provides a method for the formation of small silver particles[87]. Silver clusters can be formed on the irradiation of silver alginate at 77 K[88].

TABLE 2. Products from trifluoromethylation of some arenes[79]

Starting material	Products			Yield (%)
C_6H_6	$C_6H_5CF_3$			50
$1,4\text{-}Cl_2C_6H_4$	$2\text{-}CF_3\text{-}1,4\text{-}Cl_2C_6H_3$			45
C_6H_5Br	$p\text{-}CF_3C_6H_4Br$	: $o\text{-}CF_3C_6H_4Br$	: $m\text{-}CF_3C_6H_4Br$	46
	2	: 1	: 1	
C_6H_5Me	$p\text{-}CF_3C_6H_4Me$	: $o\text{-}CF_3C_6H_4Me$	: $m\text{-}CF_3C_6H_4Me$	38
	2	: 1	: 1	
$4\text{-}ClC_6H_4COOMe$	$4\text{-}Cl\text{-}3\text{-}CF_3C_6H_3COOMe$	$4\text{-}Cl\text{-}2\text{-}CF_3C_6H_3COOMe$		20
	2	: 1		

Silver pectate is also reactive under such conditions[88]. The silver salt of polyacrylic acid in an aqueous solution undergoes pulse radiolysis leading to the deposition of silver and the formation of Ag^{2+} ions[89]. γ-Irradiation of the Ag^+/polyacrylic acid/water system leads to the formation of metallic silver clusters[90]. Irradiation at 253.7 nm (where both the benzophenone and silver ions absorb) of silver perchlorate/sodium dodecyl sulphate in water with benzophenone also affords silver colloids[91]. Similar behaviour is reported for the irradiation at 253.7 nm of silver perchlorate in solutions of acetone and propan-2-ol[92,93] in the presence of poly(vinylpyrrolidone). The average particle size obtained is in the 3–9 nm range, dependent upon the concentration of silver perchlorate used[92]. Irradiation at 355 nm of Ag^+ aggregates with carboxymethanethiol or carboxyethanethiol results in decomposition and the deposition of silver[94]. Colloidal silver is also deposited when amine-stabilized silver ions are irradiated in the UV region[95].
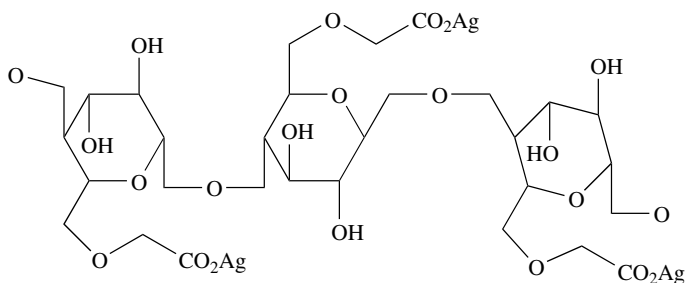
(36)

VI. REACTIONS WITH SILVER TRIFLATE

Silver trifluoromethanesulphonate (triflate) apparently catalyzes the photochemical reaction of 2-chloroacetophenone **(37)** with olefins $R^1R^2C=CHR^3$. The irradiation yields naphthalenone derivatives with high regio- and stereoselectivity. The reactions are best carried out in acetonitrile solution in Pyrex apparatus. The reaction is truly photochemical and there is no similar dark reaction. A single electron transfer process is involved and the authors suggest that a complex, alkene/Ag^+/chloroacetophenone, exists that transforms the starting material into the cation or radical **(38)**. An aromatic substitution completes the process[96,97]. An extension of the study has used the same acetophenone derivative with a variety of alkenes. This yields variously substituted naphthalenones **(39)**. This study demonstrated that the reaction could be carried out in solvents other than acetonitrile and benzene was also effective. Indeed, the reaction is more selective in benzene, but this solvent has the drawback that a silver mirror is produced and silver chloride is suspended in the solvent. In acetonitrile no silver mirror is detected and the silver chloride formed coagulates at the bottom of the reactor. The yields from the process are good and some results illustrating the variety of alkenes that can be used are shown in Table 3[98].

The process has been the subject of a patent[99]. Further study on the same system has clearly established the single electron transfer (SET) involvement of the Ag^+ ion. This report gives additional evidence for the generation of the radical **40**, formed from **41** by irradiation in benzene solution through a Pyrex filter of the enone/alkene/silver triflate system. The radical thus formed adds to the alkene, which then cyclizes to yield the

(37) (39)
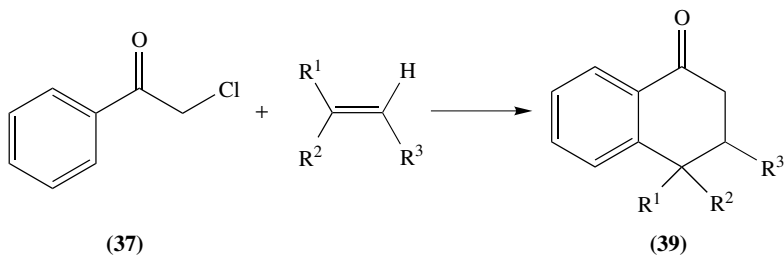
TABLE 3. Naphthalenones formed on irradiation of **37** with various alkenes[98]

R^1	R^2	R^3	Yield (%)
CH_2CN	H	N	69
CH_2OMe	H	H	45
$(CH_2)_3COMe$	H	H	65
Me	Me	CH_2OMe	50
H	CH_2OCH_2		31
CH_2CH_2Br	H	H	50
$CH_2CH_2CH_2Br$	H	H	67
$(CH_2)_2SiMe_3$	H	H	66
$PhCH_2$	H	H	64
$PhCH_2CH_2$	H	H	63
CO_2Me	H	H	53

final products. The reaction is affected by the addition of some additional reagents to the reaction system. In fact, the best yields are obtained when thiophenol is added. This could be further evidence for the involvement of free radicals. Some examples of the efficiency of the reaction are shown in Scheme 1[100].

(38) (40) (41)
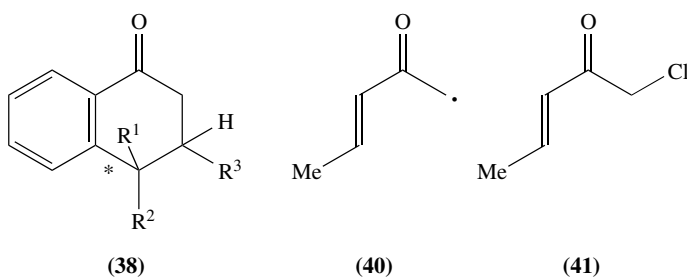
* = • or +

Cationic polymerization of THF can be brought about by its irradiation at 254 nm with various silver(I) salts. The salts studied were $AgPF_6$, $AgBF_4$, AgO_3SCF_3 and $AgSbF_6$ and their reactivity is in the order given. As the reaction proceeds, silver metal is deposited
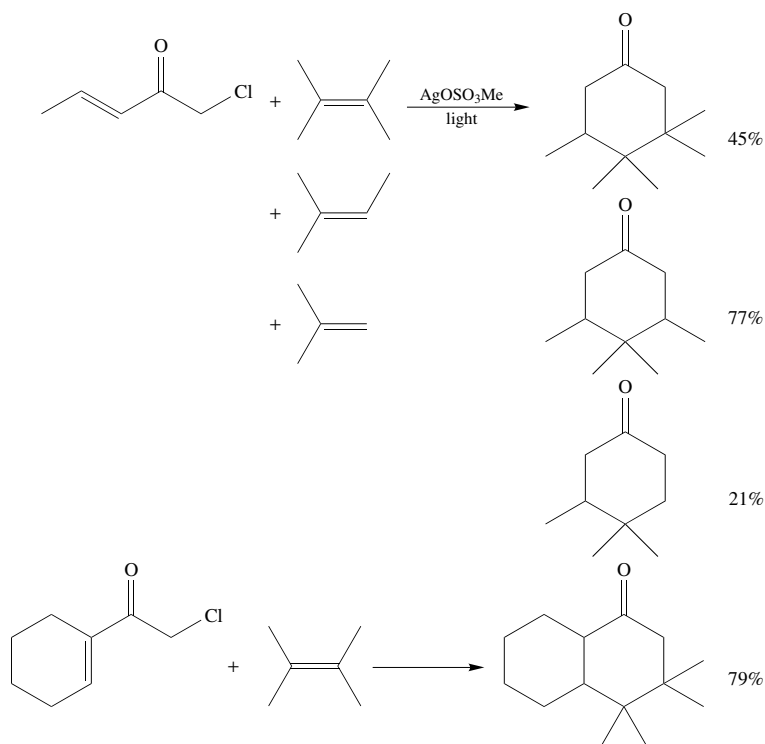
SCHEME 1

implying that a SET process is involved. Interestingly, all of the silver salts that brought about polymerization yielding **42** are insoluble in the reaction system and soluble silver salts fail to bring about the polymerization[101].
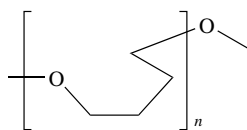
(42)

VII. AMINE COMPLEXES OF SILVER

Electron transfer processes are also involved in the photochemistry of silver(II) complexes such as **43a** or **43b** of macrocyclic amines. The use of such ligands is important since nitrogen ligands stabilize the higher valencies of silver. Irradiation in sunlight in acetonitrile solution brings about photobleaching. This involves conversion from the silver(II) complex to a silver(I) species. These could not be isolated. Prolonged irradiation brings about the deposition of metallic silver[102]. Others have shown that the photo-oxidation of

the tetraazacyclotetradecane ligand in the silver complex **(43a)** occurs with a rate faster than that of the corresponding copper complex. The study used both pulse radiolysis and flash photolysis to examine the electron transfer processes[103].
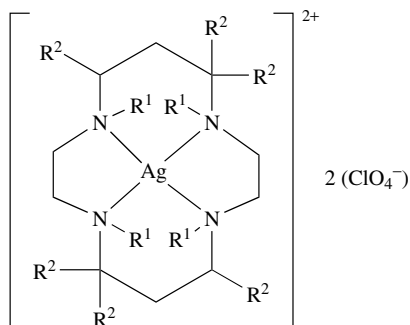
(43)

(**a**) $R^1 = R^2 = H$

(**b**) $R^1 = Me, R^2 = H$

VIII. MISCELLANEOUS REACTIONS INVOLVING SILVER

Dimerization of alkanes can be brought about by the irradiation of zeolite-Y with added silver atoms and silver clusters lead to dimerization on irradiation at $220-300$ nm[104]. Selective fluorination of di- and triphenyl methane in acetonitrile as solvent and TiO_2 as catalyst can be effected using AgF. Di- and triphenylacetic acid as well as alkenes can be fluorinated in the same way. A single electron transfer reaction is thought to be involved, followed by attack of fluoride[105]. It could be that the reaction is one that arises on the TiO_2 surface and that the Ag^+, to which the electron transfer could take place, is not involved[106].

IX. MONOLAYERS ON GOLD

A. Disulphides and Thiols

One of the areas that is currently receiving attention is the assembling of monolayers on gold substrates. These self-assembled monolayers, referred to as SAMS, have a variety of uses such as patterned SAMS for material science, biotechnology or microelectronics. The potential of the practical applications of such systems has been reviewed[107]. Once assembled, a variety of photochemical reactions can take place within the monolayer dependent upon the compounds used. Typical of this is the oxidation of a monolayer of 8-chloro-octyl disulphide. When the layer is formed, the chains are chemisorbed via the sulphur groups. This can then undergo photo-oxidation and photoreduction on the gold surface on irradiation. Oxidation occurs at the gold/sulphur interface and reduction at the chlorine/air interface. The oxidation is mediated by the gold surface and photoexcitation of 'hot' electrons on the gold surface is considered to be the primary process[108]. Another photosensitive SAMS can be obtained by assembling films of bis(undecanyl-4-azidobenzoate) disulphide **(44)** on polycrystalline gold[109]. The monolayers of this sulphide undergo photoreaction with amines such as diethyl and di-*n*-butylamine. Products formed

by this treatment have been identified as the hydrazine derivative **(45)** and the azepine
derivative **(46)**. These products are typical of those obtained from the ring expansion
reactions of azidobenzene derivatives. The products obtained from the irradiation of the
self-assembled monolayers with diethylamine are identical to photoproducts obtained by
irradiation of methyl 4-azidobenzoate with the same amine[109]. Aniline derivatives are
also formed. Controlled irradiation can also result in surface attachment of ferrocenyl
units when the monolayer is irradiated through a thin film of *N*-(2,2,2-trifluoroethyl)-*N*-
(2-ferrocenylethyl)amine **(47)**[110,111]. This yields a surface modified by the addition of the
ferrocenyl moiety **(48, 49)**.
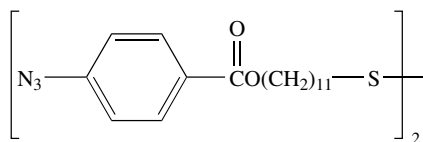
(44)
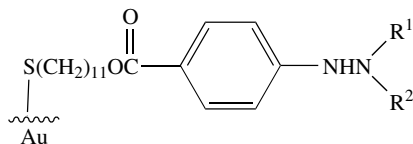
(45) **(a)** R^1 = R^2 = Et
       (b) R^1 = R^2 = *n*-Bu
(48) R^1 = CF$_3$CH$_2$; R^2 = Fc
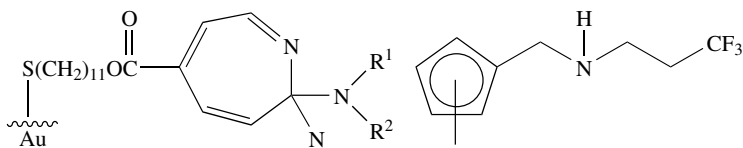
(46) **(a)** R^1 = R^2 = Et
       (b) R^1 = R^2 = *n*-Bu
(49) R^1 = CF$_3$CH$_2$; R^2 = Fc
Fc = Ferrocenyl

(47)

Chemisorption to gold surfaces via gold alkanethiolate bonds occurs with poly[methyl
(mercaptopropyl)siloxane]. The chemiadsorbed film has two distinct sulphur moieties
resulting from bonded and unbonded thiolate groups. Photochemical modification of these
surface layers can be brought about resulting in a variety of derivatives[112]. Alkanethiol
monolayers on gold can be patterned photochemically. For example, these SAMS have

been used to culture Murine 3T3 cells. The cells apparently attach to the acid functional-ized regions of the patterned surface[113]. Alkanethiol monolayers **(50)** can also be desorbed from the gold surface by irradiation at 193 nm[114].

Irradiation by UV of the self-assembled monolayer of n-dodecanethiol on a gold(111) surface in the presence of air converts the monolayer to the n-dodecanesulphonate quantitatively. The oxidation destroys the ordered structure of the monolayer[115]. Some alkanethiol monolayers formed from **50** have also been oxidized during X-ray photoelectron spectroscopy. The thiol group is oxidized to the sulphonate, probably by the intervention of singlet oxygen. The rate of this oxidation varies with the length of the alkyl chain and the shorter-chain systems [$CH_3(CH_2)_6CH_2SH$ or smaller] oxidize more rapidly[116]. Other self-assembled monolayers have been formed using the diacetylene derivatives **(51)**. Irradiation of these brings about polymerization. During the polymerization some reorganization of the monolayer occurs[117]. Some SAMS of alkanethiols or thiophenols such as p-chlorothiophenol on gold can be used as photoresists. The systems used here oxidize the thiol to a sulphonate. The sulphonate can then be washed off leaving a clean gold substrate[118]. Octadecanethiol self-assembled films on polycrystalline gold can be modified by ionizing radiation. This brings about the fission of S−Au bonds and the formation of disulphides[119].

$$CH_3(CH_2)_nCH_2SH$$

(50)

$$n = 2,4,6,7,10 \text{ or } 16$$

$$—S(CH_2)_2COO(CH_2)_9C\equiv CC\equiv C(CH_2)_{13}CH_3$$
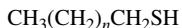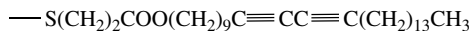
(51)
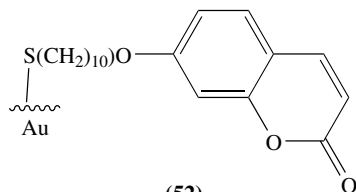
(52)

Another interesting photochemical reaction that occurs with the monolayers is dimerization. This is exemplified by the photochemical behaviour of the SAM of 7-(10-thiodecoxy)coumarin **(52)** on polycrystalline gold. Irradiation at 350 nm results in the (2 + 2)-cycloaddition of the coumarin moieties. The photodimerization is a reversible process by irradiating at 254 nm. Better regioselectivity in the cycloaddition is obtained when the solid monolayer is irradiated rather than when it is in contact with benzene. The dimer formed is the *syn*-head-to-head dimer identified as **53**[120]. Self-assembled monolayers of *cis*- and *trans*-4-cyano-4′-(10-thiodecoxy)stilbene **(54)** are also photochemically reactive. Irradiation of a thin film in benzene solution using λ > 350 nm results in the formation of a photostationary state with 80% of the *cis*-isomer present. Irradiation in the solid shows that *cis,trans* isomerism occurs but that *trans,cis*-isomerism fails. Prolonged irradiation brings about (2 + 2)-cycloaddition of the stilbene units to afford cyclobutane adducts. Such dimerization is a well established process[121,122]. The influence of irradiation at 254 nm or 350 nm of self-assembled monolayers of 10-thiodecyl 2-anthryl ether on polycrystalline

William M. Horspool

gold has been studied[123]. Silyl derivatives have also been used for the construction of monolayers on gold. The layers are composed of the amine **55** where the amine moiety is protected by a photoremovable group such as in the derivatives **56** or **57**. The amino groups can be released by irradiation of the surface[124].

(53)

(54)

(55)

R =

(56)

Fc = Ferrocenyl

(57)
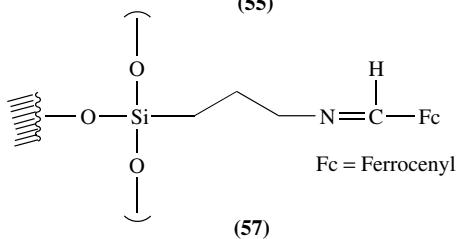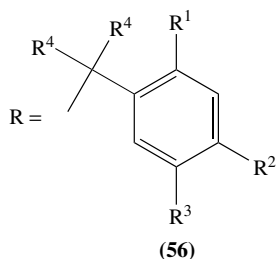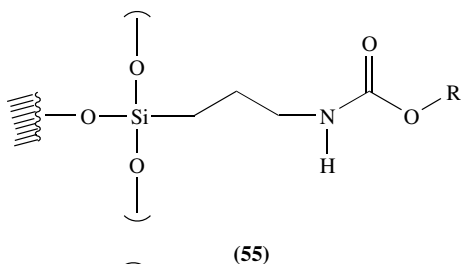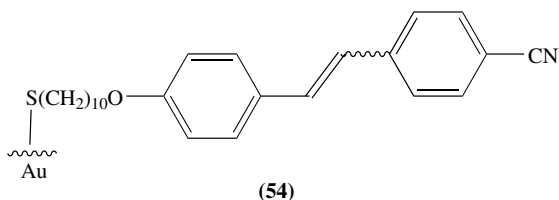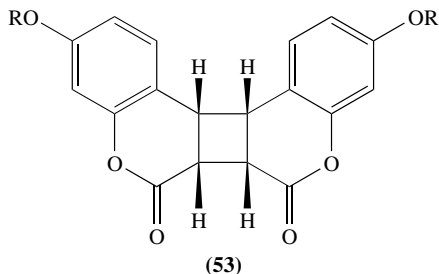
R^1	R^2	R^3	R^4
NO$_2$	MeO	MeO	H
NO$_2$	H	H	H
H	MeO	MeO	Me

B. Modified Gold Electrode Surfaces

The ability to change the monolayer attached to the surface of the gold has been used as a means of altering the behaviour of gold electrodes that are commonly used for electrochemical processes. A self-assembled monolayer of (mercaptobutyl)nitrospiropyran

on a gold electrode exhibits reversible photochemistry. Irradiation between 320 nm and 350 nm brings about the formation of a protonated species. Irradiation of this charged monolayer at 495 nm regenerates the neutral species. The authors[125] claim that these light-induced photochemical transformations permit control of the electron transfer processes at the electrode surface. Other examples of spiropyran amphiphiles have been described[126]. Other modified gold electrodes have been used to study the influence of photoinduced electron transfer between porphyrins and flavins deposited as physisorbed Langmuir–Blodgett films[127]. The influence of spacers has also been investigated. In this example the quinone (58) was anchored to the gold electrode via a SAM of aminoalkanethiols (59). The redox behaviour of the quinone under those conditions was studied and the electron transfer rate constants were measured. This electron transfer rate decreased with increasing chain length of the monolayer[128]. The photolysis of p-chloronitrobenzene in aqueous ethanol in the presence of hydroxide ion has been studied using a gold electrode in channel electrode voltammetry. The irradiation brings about the formation of the stable radical cation (60) by a photochemical electron transfer process[129].

$HS(CH_2)_n NH_2$

$n = 2, 5$ or 8

(58)   (59)   (60)

(61)

^-O_2C

$(CH_2)_7 CH_3$
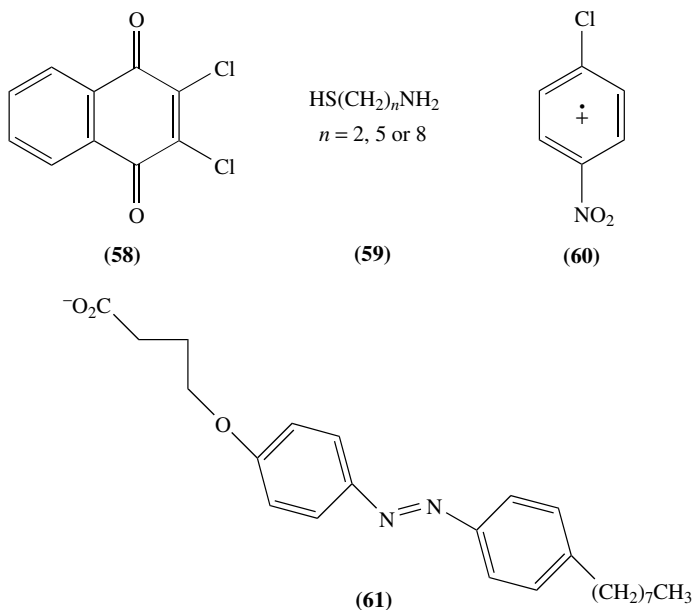
Several examples of oxidation at the positively charged monolayer surface were demonstrated[130]. Others have used similar photochemical isomerization to modify the behaviour of electrodes[131]. Other modified gold electrodes have been prepared by the modification of the SAM of hexadecylthiolate[132] and by the photoisomerism at 432 nm of cis-azobenzene as the monolayer on gold[133]. Irradiation of azobenzene films at 350 nm allows for a study of the photochromic behaviour of the azobenzene on the gold surface[134]. Others have studied the modification of the azobenzene derivative (61) deposited as a Langmuir–Blodgett film of gold that previously had been coated with a thiol self-assembled monolayer[135]. In this instance the azobenzene undergoes a two-electron reduction.

C. Miscellaneous Reactions

Liquid crystalline azobenzene polymers can undergo photoisomerization on irradiation at 360 or 450 nm on gold films. This permits changing the refractive index of the film depending upon the wavelength used[136]. A study has examined the photopolymerization of *p*-styrene sulphonate counteranions associated with monolayers of disulphide amphiphiles as self-assembled monolayers on gold[137].

The influence of X-ray irradiation of monolayers of the amide **62** on gold has been studied. The work demonstrated that the trifluoroacetamido groups lose fluorine under these conditions[138,139]. This study and that reported earlier confirm that electrons and not X-rays are the principal cause of damage[140]. Decomposition of perfluoropolyether applied to a gold film has been brought about by X-ray photons. The fission occurs at the ether linkages[141].

$$Au \left\{ \!\!\!\!— S — (CH_2)_{11}NHCOCF_3 \right.$$

(62)
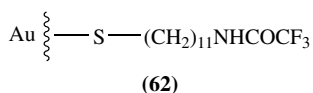
X. GOLD COMPLEXES

A. Luminescent Compounds

Considerable interest has built up over the years in the synthesis of luminescent gold complexes. Within this study most of the gold(I) complexes, that can contain one or more gold atoms, are made with phosphine and thiolate ligands since these ligands are particularly good in the stabilization of gold(I) complexes. A few examples of these will be illustrated to give a sample for the extensive work that has been and is being carried out.

Both sodium aurothiomalate hydrate and 2,3,4,6-tetra-*O*-acetyl-1-thio-D-glucopyrano-sato-S)(triethylphosphine)gold(I) are luminescent in ethanol glasses at 77 K. This arises from a metal-centred *ds* excited state with partial ligand-to-metal charge transfer. Both compounds undergo decomposition that is thought to arise from ligand-to-metal charge transfer excitation. Aqueous solutions undergo decomposition on irradiation[142]. In one series of complexes benzenethiolate ligands have been used where substituents have been placed on the *ortho, meta* and *para* positions. The phosphine ligands were either triphenylphosphine, as in **63**, or 1,3,5-triaza-7-phosphaadamantanetriylphosphine, as in **64**. All of these compounds exhibit phosphorescence at low temperatures. The excitation is assigned to a ligand metal charge transfer from sulphur to the gold[143]. Even in neutral dinuclear gold(I) complexes **65** and **66**, again with phosphine and thiolate ligands, the luminescence arises from a sulphur-to-gold charge transfer in the excited state[144]. The luminescence of the related complexes **(67)** in solution has also been studied[145]. Subtle variations in the ligands, such as in the xanthate phosphine gold(I) complexes **(68)**, also give luminescent compounds that emit in the solid phase. The luminescence for such complexes in the solid phase is of several nanoseconds in duration and is thought to arise from an nπ* transition within the ligand[146,147].

Some interesting effects are also observed with the gold complex **69** that shows a long-lived emission at 640 nm. This complex exhibits solvent effects and the emission is quenched by polar solvents such as acetonitrile, methanol, ethanol and tetrahydrofuran. Again the luminescence arises from a thiolate gold charge transfer process[148]. The gold complex **70** with a linear array of three gold atoms is also luminescent[149] as are the related gold complexes $[Au(PPh_3)]_2[(HS)_2C=C(CN)_2]$ and **71**[150].

Ph₃PAuSAr

(63)

Ar = Ph, o-MeOC₆H₄, o-ClC₆H₄

(64)

Y=H, X=H, o-MeO, m-MeO, o-Cl, m-Cl, p-Cl; X=Y=Cl

(65)

n = 2,3,4; R = Ph or cyclohexyl

(66)

n = 2,3,4,5

(67)

(68)

R¹=Me, Et, n-Bu; R²=Ph, CH₂CH₂CN
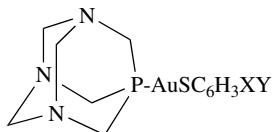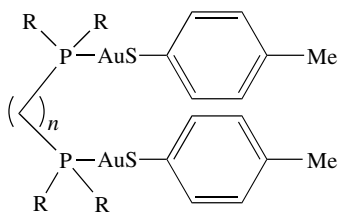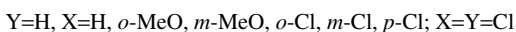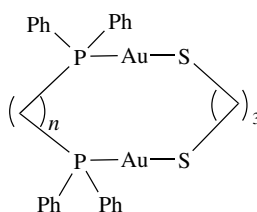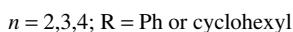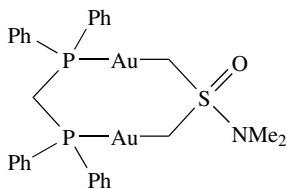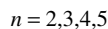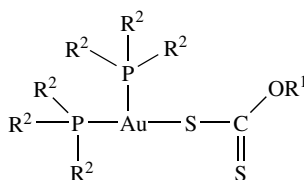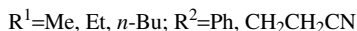
Other more complex systems such as the compound **72**, formed from KAuCl₄ and bis(dimethylphosphinomethyl)methylphosphine, are phosphorescent on irradiation at 300–370 nm in a degassed acetonitrile solution. It is interesting to note that there are few polynuclear gold complexes with long-lived excited states in fluid solution[151]. A reinvestigation of the gold complex **73**[152], synthesized earlier by Parker and Balch[153], has demonstrated the remarkable luminescence of the compound. Apparently the luminescence at 422 nm is stimulated by contact of the solid with solvents such as methylene chloride. A brief overview of such systems has been published[154].

Luminescent gold(I) acetylides **(74–76)** with a rigid rod-like structure have been synthesized. Their photochemical and photophysical properties have been studied in some detail[155]. The emission properties of the gold acetylides **77** have been studied. This

(69)

(70)

(71)

(72)

(73)

(74) R=H, Me

Me—(aryl)—N≡C—Au—C≡C—(aryl)—NO₂

Me

(75)

PhC≡C—Au—C≡N—(aryl)—N≡C—Au—C≡CPh

(76)

$$\left[\text{AuC}\equiv\text{CPh} \right]_4 \text{L}$$

(77)

complex is one of gold(I) with the supramolecular phosphine ligand **78**[156]. Many other luminescent alkyne gold complexes, for example those illustrated in **79**, have been synthesized and studied[157].

L ≡

PPh₂ (CH₂)₃ PPh₂
N N
(CH₂)₂ (CH₂)₂
Ph₂P N N PPh₂
(CH₂)₃

(78)

$$\left[\text{Au}_2(\text{dppn})(\text{C}\equiv\text{CPh})_2 \right]$$

$$\left[\text{Au}_2(\text{dppn})(\text{C}\equiv\text{CC}_6\text{H}_{13}\text{-}n)_2 \right]$$

$$\left[\text{Au}(\text{PPh}_3)(\text{C}\equiv\text{C-l-naphthyl}) \right]$$

(79)

dmpm =

Me   Me
  P—P
Me   Me

dppn =

Ph   Ph
  P   P
Ph   Ph

Methods have been developed for the determination of gold(I) from its luminescent properties[158].

B. Electron Transfer Photochemistry

The luminescent gold complexes with long-lived emission are clearly of interest, since they can be involved in bimolecular redox processes and can be used to either accept or transfer an electron from or to an organic substrate. The complex **80**, for example, has been estimated to have an excited state reduction potential of 2.2 V (vs. NHE). A demonstration of this reactivity is shown by the formation of the 1,4-dimethoxybenzene cation radical on ultraviolet irradiation in acetonitrile solution with the gold complex. When the complex is irradiated with visible light (406 nm) in the presence of tetrahydrofuran, reduction occurs[159]. Electronically excited $[Au(II)(1,2\text{-bis(dicyclohexylphosphino)ethane})_3]^{2+}$ undergoes electron transfer to N-alkylpyridinium acceptors in acetonitrile solution. The quenching rates were measured by conventional Stern–Volmer techniques[160]. Electron transfer photochemistry takes place between gold acetylide complexes and suitable acceptors such as pyridinium salts or methyl viologen (Scheme 2). The reaction is redox in type and this has been verified by time-resolved transient absorption spectroscopy[157]. The gold(I) acetylide complex **81** has a long-lived emissive triplet $\pi\pi^*$ excited state (equation 7)[161]. The synthesis and the photochemistry of the pentanuclear gold(I) complex ion (**82**) has been carried out. This luminescent compound also undergoes electron transfer to methylviologen[162]. Photoredox studies of gold porphyrins have established that chlorogold *meso*-tetrakis(4-N-methylpyridyl)porphine tetrachloride is a useful reductive electron transfer catalyst and is useful for SET processes in water[163]. Cleavage of the plasmid pBR322 DNA can also be brought about by the long-lived triplet excited state of the gold complex **83**[164].

(80)

$$\left[Au(PPh_3)(C{\equiv}CPh)\right]$$

(81)

$$\left[[Au_5L_3(Ph_3PCH_2PPh_3)_2]\right]^{2+}$$

(82)

L =

$$\left[Au_3 \, dmmp \, (C\!\!\equiv\!\!CPh)_3 \right] \xrightarrow{\text{light}} [Au \, complex]^* \; + \;$$

CO$_2$Me

$$[Au \, complex]^+ \; + \;$$

CO$_2$Me

$$\left[Au_2 \, dppm \, (C\!\!\equiv\!\!CC_6H_4OMe\text{-}p)_2 \right] \xrightarrow{\text{light}} [Au \, complex]^* \; + \;$$

$$[Au \, complex]^+ \; + \;$$

SCHEME 2

$$\left[Au^I(PPh_3)(C \equiv\!\!\equiv CPh)\right] \; + \quad \xrightarrow{\quad light \quad} \quad \left[Au^{II}(PPh_3)(C \equiv\!\!\equiv CPh)\right]^+ \; + \qquad (7)$$

$$\left[[Au_3(dmmp)_2]\right]^{3+} \quad dmmp =$$

(83)

XI. GOLD AS A CATALYST

Aqueous solutions of ethylene glycol undergo photocatalytic formation of hydrogen when irradiated in the presence of a gold-doped titanium dioxide catalyst[165]. Gold, deposited in a range of 1–2 wt%, on titanium dioxide can also be used as a catalyst system for the photochemical generation of hydrogen from ethanol in water. The main products obtained from the irradiation are hydrogen, methane, carbon dioxide and acetaldehyde[166]. Acrolein, as a film on gold, undergoes photochemical polymerization. The authors[167] suggest that the existence of the gold may enhance the formation of free radicals in the surface absorbed layer. Xanthate-based monolayers on gold have been used to control the photopolymerization of methacrylic acid in aqueous solutions. The photopolymerization is initiated by the xanthate groups[168].

Sodium tetrachloroaurate catalyzes the photo-oxidation of hydrocarbons in solution. Typical of this is the irradiation with wavelengths >310 nm of aerated solutions of cyclohexane in acetonitrile or methylene chloride. The principal isolable products formed from this treatment are cyclohexanol and cyclohexanone[169]. A mechanism that might involve the formation of a metal peroxo or metal oxo complex has been suggested. Such complexes are known to react with alkanes to yield hydroxy derivatives[170]. The principal organic intermediate is the unstable cyclohexylhydroperoxide that readily decomposes to afford cyclohexanone and cyclohexanol[171]. Further study has shown that the hydroperoxide accumulates during the oxidation[172,173]. The influence of wavelength (λ 300, 365 or 436 nm) on the reaction has also been studied[170]. Hexane and ethylbenzene can be similarly oxidized to yield analogous products[169].

XII. CARBON−GOLD BOND FISSION

The methyl(trisubstituted phosphine)gold(I) complexes **84** undergo photochemical reactions when irradiated in the presence of perfluoroethene derivatives. Typical of the reaction

encountered is that with tetrafluoroethene when the derivative **85** is formed. Other per-fluoroalkenes **86** are also reactive. The process is thought to involve an insertion reaction perhaps via an intermediate such as **87**[174]. Irradiation using wavelengths <360 nm of the gold compound **84** co-condensed with chloroform results in the formation of 1,1,1-trichloroethane via a radical mechanism[175]. Fission of the Au−C bond results on irradiation of MeAu(PPh$_3$) in CDCl$_3$. The reaction was followed by CIDNP. The main products formed are MeD and ClAu(PPh$_3$) and the reaction involves the triplet state. It is suggested that the first step involves the formation of ClAu(PPh$_3$), a methyl radical and CDCl$_2$ as a triplet[175]. Some side reactions involve the attack by methyl radicals in an S_H2 reaction at gold. Others have used the photochemical decomposition at 257 nm of the methyl(triphenylphosphine)gold as a means of depositing gold-bearing tracks[176].

<div align="center">

R
|
Ph$_2$PAuMe   Ph$_3$PAuCFXCF$_2$Me   FXC=CF$_2$

(84) R = Me, Ph   **(85)** X = F, Cl   **(86)** X = F, Cl

</div>

<div align="center">

Ph$_3$P⟍ ⟋CF$_2$
    Au |
Me⟋ ⟍CF$_2$

(87)

</div>
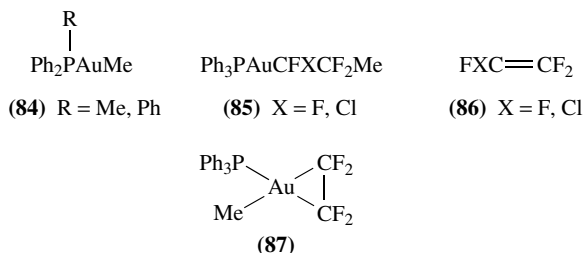
XIII. MISCELLANEOUS REACTIONS INVOLVING GOLD

Irradiation of gold and silver in the presence of films of alkanes at 15 K results in the formation of compounds such as those shown in equation 8. The compounds were identified by IR spectroscopy, showing absorptions at 1725.8 cm^{-1} for Ag−H and at 2195.8 cm^{-1} for Au−H bonds[177].

$$\text{Au or Ag} + \text{CH}_4 \xrightarrow{\text{15 K}} \text{HAuCH}_3 \text{ or } \text{HAgCH}_3 \qquad (8)$$
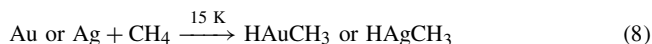
Bibenzyl is formed in a yield of 22% when a degassed solution in acetonitrile of benzyl chloride, an electron donor such as triethylamine and a catalytic amount of the gold complex **88**, is irradiated. The gold complex **(88)** is described as a potent new photocatalyst for such systems and performs better than existing catalysts. The mechanism of the process has been shown to involve direct halogen transfer as shown in equation 9. The resultant alkyl radicals then yield the final product. A similar reaction operates with 1-bromopentane when it is irradiated under the same conditions; This yields n-decane[178].

$$[\text{Au}_2\text{Ph}_3\text{PCH}_2\text{PPh}_3]_2{}^{2+}(\text{CF}_3\text{SO}_3{}^-) \ + \ \text{RX} \longrightarrow [\text{Au complex}]^{2+} + \text{R}^{\bullet} \qquad (9)$$

(88)
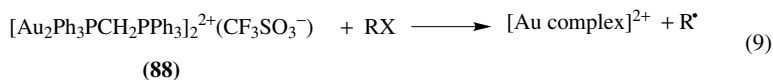
Thin films of chloroauric acid salt of chitosan on irradiation at 253.7 nm in air at room temperature bring about the formation of colloidal gold[179]. Colloidal gold is also produced on irradiation of the dimethylgold(III) complex **89**. The decomposition occurs via the triplet state of the complex[180]. The water-insoluble gold complexes **90** are also photochemically reactive and irradiation brings about the reduction of the tetrachloroaurate anion to yield colloidal gold[181].

(89)

(90)
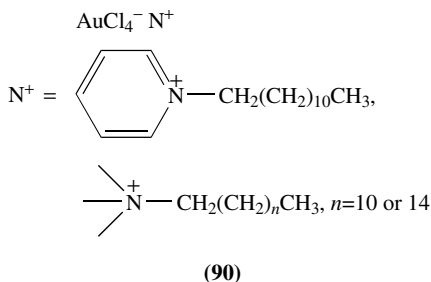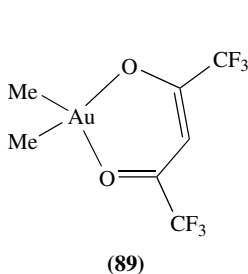
XIV. REFERENCES

1. F. R. Hartley and S. Patai (Eds.), *The Chemistry of the Metal – Carbon Bond*, Wiley, Chichester, Volume 1, 1982; Vol. 2, 1985; Vol. 3, 1985.
2. F. R. Hartley (Ed.), *The Chemistry of the Metal – Carbon Bond*, Wiley, Chichester, Vol. 4, 1987; Vol. 5, 1989.
3. W. Ho, in *Desorption Induced by Electronic Transitions*, DIET IV (Eds. D. Betz and P. Varga), Springer-Verlag, Berlin, 1990, p. 48.
4. X. L. Zhou and J. M. White, *Surf. Sci.*, **241**, 244 (1991).
5. (a) Z. M. Liu, X. L. Zhou and J. M. White, *Chem. Phys. Lett.*, **198**, 615 (1992).
   (b) X. L. Zhou, P. M. Bass, B. E. Koel and J. M. White, *Surf. Sci.*, **271**, 452 (1992).
   (c) X. L. Zhou, P. M. Bass, B. E. Koel and J. M. White, *Surf. Sci.*, **271**, 427 (1992).
6. X. L. Zhou and J. M. White, *Chem. Phys. Lett.*, **167**, 205 (1990).
7. X. L. Zhou and J. M. White, *Surf. Sci.*, **241**, 259 (1991).
8. St. J. Dixon-Warren, E. T. Jensen and J. C. Polanyi, *J. Chem. Phys.*, **98**, 5938 (1993).
9. St. J. Dixon-Warren, E. T. Jensen and J. C. Polanyi, *Phys. Rev. Lett.*, **67**, 2395 (1991).
10. St. J. Dixon-Warren, E. T. Jensen, J. C. Polanyi, C. G. Xu, S. H. Yang and C. Z. Hua, *Faraday Discuss. Chem. Soc.*, **91**, 451 (1991).
11. St. J. Dixon-Warren, D. V. Heyd, E. T. Jensen and J. C. Polanyi, *J. Chem. Phys.*, **98**, 5954 (1993).
12. E. T. Jensen and J. C. Polanyi, *J. Phys. Chem.*, **97**, 2257 (1993).
13. (a) X. L. Zhou and J. M. White, *Surf. Sci.*, **235**, 270 (1991).
    (b) X. L. Zhou and J. M. White, *Surf. Sci.*, **241**, 270 (1991).
14. S. R. Coon, K. B. Myli and V. H. Grassian, *J. Phys. Chem.*, **99**, 16416 (1995).
15. Z. J. Sun, A. L. Schwaner and J. M. White, *J. Chem. Phys.*, **103**, 4279 (1995).
16. Z. J. Sun, A. L. Schwaner and J. M. White, *Chem. Phys. Lett.*, **219**, 118 (1994).
17. J. E. Fieberg, A. Szabo and J. M. White, *J. Chem. Soc., Faraday Trans.*, **92**, 4739 (1996).
18. M. M. Kondo and W. F. Jardim, *Water Res.*, **25**, 823 (1991).
19. Y. Song, P. Gardner, H. Conrad, A. M. Bradshaw and J. M. White, *Surf. Sci.*, **248**, L279 (1991).
20. S. Garoff, D. A. Weitz and M. S. Alvarez, *Chem. Phys. Lett.*, **93**, 283 (1982).
21. K. B. Myli and V. H. Grassian, *J. Phys. Chem.*, **98**, 6237 (1994).
22. K. B. Myli, S. R. Coon and V. H. Grassian, *J. Phys. Chem.*, **99**, 16407 (1995).
23. R. A. Wolkow and M. Moskovits, *J. Chem. Phys.*, **87**, 5858 (1987).
24. J. S. Suh, N. H. Jang, D. H. Jeong and M. Moskovits, *J. Phys. Chem.*, **100**, 805 (1996).
25. N. H. Jang, J. S. Suh and M. Moskovits, *J. Phys. Chem. B*, **101**, 8279 (1997); N. H. Jang, J. S. Suh and M. Moskovits, *J. Phys. Chem. B*, **102**, 759 (1998).
26. X. L. Zhou and J. M. White, *J. Phys. Chem.*, **94**, 2643 (1990).
27. Q. S. Xin and X. Y. Zhu, *J. Chem. Phys.*, **104**, 4274 (1996).
28. L. E. Fleck, W. F. Feehery, E. W. Plummer, Z. C. Ying and H. L. Dai, *J. Phys. Chem.*, **95**, 8428 (1991).
29. (a) L. E. Fleck, Z. C. Ying and H. L. Dai, *J. Vac. Sci. Tech. A — Vac. Surfaces and Films*, **11**, 1942 (1993).
    (b) L. E. Fleck, J. S. Kim and H. L. Dai, *Surf. Sci.*, **356**, L417 (1996).
    (c) L. E. Fleck, Z. C. Ying, M. Feehery and H. L. Dai, *Surf. Sci.*, **296**, 400 (1993).

30. S. C. Sparks, A. Szabo, G. J. Szulczewski, K. Junker and J. M. White, *J. Phys. Chem. B*, **101**, 8315 (1997).
31. E. D. Pylant, M. J. Hubbard and J. M. White, *J. Phys. Chem.*, **100**, 15890 (1996).
32. E. D. Pylant, K. H. Junker, G. Szulczewski, M. J. Hubbard and J. M. White, *J. Phys. Chem. B*, **101**, 4803 (1997).
33. E. D. Pylant, M. J. Hubbard and J. M. White, *J. Vac. Sci. Tech. A — Vac. Surfaces and Films*, **14**, 1684 (1996).
34. X. J. Yang, Z. M. Zhang and Q. Z. Qin, *J. Photochem. Photobiol. A — Chem.*, **101**, 229 (1996).
35. A. L. Schwaner and J. M. White, *J. Phys. Chem. B*, **101**, 11119 (1997).
36. (a) T. D. Harris, D. H. Lee, M. Q. Blumberg and C. R. Arumainayagam, *J. Phys. Chem.*, **99**, 9530 (1995).
    (b) A. L. Schwaner and J. M. White, *J. Phys. Chem. B*, **101**, 10414 (1997).
37. Z. Fang, L. Zhao and Q. Zhuang, *Xiamen Daxue Xuebao, Ziran Kexueban*, **33**, 202 (1994); *Chem. Abstr.*, **122**, 42455 (1995).
38. H. Hase, Y. Miyatake, M. Hoshino, M. Taguchi and S. Arai, *Radiat. Phys. Chem.*, **49**, 59 (1997).
39. K. J. Green and R. Rudham, *J. Chem. Soc., Faraday Trans.*, **88**, 3599 (1992).
40. A. Sclafani, M. N. Mozzanega and P. Pichat, *J. Photochem. Photobiol., A*, **59**, 181 (1991).
41. R. M. Alberici and W. F. Jardim, *Water Res.*, **28**, 1845 (1994).
42. M. Yamamoto, N. Furuyama and K. Itoh, *J. Phys. Chem.*, **100**, 18483 (1996).
43. M. Yamamoto, K. Itoh, A. Nishigaki and S. Ohshima, *J. Phys. Chem.*, **99**, 3655 (1995).
44. (a) K. Itoh, M. Yamamoto, N. Furuyama and A. Saito, *Mikrochim. Acta*, **S14**, 33 (1997).
    (b) G. Kaupp, in *CRC Handbook of Organic Photochemistry and Photobiology*, (Eds. W. M. Horspool and P.-S. Song), CRC Press, Boca Raton, 1995, p. 50.
45. I. K. Lednev and M. C. Petty, *Langmuir*, **10**, 4190 (1994).
46. D. A. Hutt, E. Cooper and G. J. Leggett, *J. Phys. Chem. B*, **102**, 174 (1998).
47. M. Lewis, M. Tarlov and K. Carron, *J. Am. Chem. Soc.*, **117**, 9574 (1995).
48. L. A. Pressley, E. D. Pylant and J. M. White, *Surf. Chem.*, **367**, 1 (1996).
49. J. E. Fieberg and J. M. White, *J. Vac. Sci. Tech. A — Vac. Surfaces and Films*, **15**, 1674 (1997).
50. H. G. Jenniskens, W. Van Essenberg, M. Kadodwala and A. W. Kleyn, *Chem. Phys. Lett.*, **268**, 7 (1997).
51. M. E. Castro, L. A. Pressley and J. M. White, *Surf. Sci.*, **256**, 227 (1991).
52. D. Franzke and A. Wokaun, *J. Phys. Chem.*, **96**, 6377 (1992).
53. X. L. Zhou and J. M. White, *Surf. Sci.*, **235**, 259 (1990).
54. X. L. Zhou and J. M. White, *J. Phys. Chem.*, **96**, 7703 (1992).
55. M. Funakoshi, T. Kawamura, K. Nakano and S. Koda, *Kagaku Kogaku Ronbunshu*, **21**, 95 (1995); *Chem. Abstr.*, **122**, 133 931 (1995).
56. L. O'Toole, R. D. Short, F. A. Bottino, A. Pollicino and A. Recca, *Polym. Degrad. Stabil.*, **38**, 147 (1992).
57. S. R. Carlo and V. H. Grassian, *Langmuir*, **13**, 2307 (1997).
58. K. M. Baumgartner, M. Volmeruebing, J. Taborski, P. Bauerle and E. Umbach, *Int. J. Phys. Chem.*, **95**, 1488 (1991).
59. (a) E. Baciocchi, G. C. Rosato, C. Rol and G. V. Sebastiani, *Tetrahedron Lett.*, **33**, 5437 (1992).
    (b) E. Baciocchi, C. Rol, G. C. Rosato and G. V. Sebastiani, *J. Chem. Soc., Chem. Commun.*, 59 (1992).
60. K. F. Willey, P. Y. Cheng, M. B. Bishop and M. A. Ducan, *J. Am. Chem. Soc.*, **113**, 4721 (1991).
61. S. C. Sun, R. L. Birke, J. R. Lombardi, K. P. Leung and A. Z. Genack, *J. Phys. Chem.*, **92**, 5965 (1988).
62. H. Bercegol and F. J. Boerio, *J. Phys. Chem.*, **99**, 8763 (1995).
63. H. Feilchenfeld, G. Chumanov and T. M. Cotton, *J. Phys. Chem.*, **100**, 4937 (1996).
64. W. Zhang, A. Vivoni, J. R. Lombardi and R. L. Birke, *J. Phys. Chem.*, **99**, 12846 (1995).
65. N. Matsuda, T. Sawaguchi, M. Osawa and I. Uchude, *Chem. Lett.*, 145 (1995).
66. P. Bortolus, L. Flamigni, S. Monti, M. Bolte and G. Guyot, *J. Chem. Soc., Faraday Trans.*, **87**, 1303 (1991).
67. R. F. Chen, *Arch. Biochem. Biophys.*, **166**, 584 (1975).
68. R. O. Rahn and L. C. Landry, *Photochem. Photobiol.*, **18**, 29 (1973); R. O. Rahn, J. K. Setlow and L. C. Landry, *Photochem. Photobiol.*, **18**, 39 (1973).
69. F. Leh, S. K. Wong and J. K. S. Wan, *Can. J. Chem.*, **49**, 2760 (1971).
70. D. R. Gee and J. K. S. Wan, *Can. J. Chem.*, **49**, 160 (1971).

71. D. R. Gee, K. E. Russell and J. K. S. Wan, *Can. J. Chem.*, **48**, 2740 (1970).
72. J. W. Bruno, T. J. Marks and F. D. Lewis, *J. Am. Chem. Soc.*, **103**, 3608 (1981).
73. J. W. Bruno, T. J. Marks and F. D. Lewis, *J. Am. Chem. Soc.*, **104**, 5580 (1982).
74. H. Morrison and C. Koviak, *Tetrahedron Lett.*, **27**, 2711 (1986).
75. G. M. Whitesides, D. E. Bergbreiter and P. E. Kendal, *J. Am. Chem. Soc.*, **96**, 2806 (1974).
76. R. G. Johnson and R. K. Ingham, *Chem. Rev.*, **56**, 219 (1957).
77. L. Eberson, in *The Chemistry of Carboxylic Acids and Esters* (Ed. S. Patai), Wiley, New York, 1969, p. 53.
78. E. K. Fields and S. Meyerson, *J. Org. Chem.*, **41**, 916 (1976).
79. C. W. Lai and T. E. Mallouk, *J. Chem. Soc., Chem. Commun.*, 1359 (1993).
80. C. Lai, Y. I. Kim, C. M. Wang and T. E. Mallouk, *J. Org. Chem.*, **58**, 1393 (1993).
81. P. G. Roth, R. S. Venkatachalam and F. J. Boerio, *J. Phys. Chem.*, **85**, 1150 (1986).
82. S. Sugihara, A. Iwasawa, H. Tabei and J. Yamaki, *Nippon Kagaku Kaishi*, 992 (1994); *Chem. Abstr.*, **122**, 118723 (1995).
83. D. Y. Naumov, N. V. Podberezskaya, A. V. Virovets and E. V. Boldyreva, *J. Struct. Chem.*, **35**, 890 (1994).
84. S. Yamazaki-Nishida and M. Kimura, *Nippon Kagaku Kaishi*, 963 (1994); *Chem. Abstr.*, **122**, 132258 (1995).
85. Y. Yonezawa, T. Miyama and T. Sato, *Chem. Lett.*, 2455 (1992).
86. T. Sato, S. Kuroda, A. Takami, Y. Yonezawa and H. Hada, *Appl. Organomet. Chem.*, **5**, 261 (1991).
87. Y. Yonezawa, T. Sato, T. Miyama, A. Takami, J. Umemura and T. Takenaka, *Surf. Rev. Lett.*, **3**, 1109 (1996).
88. Y. Yonezawa, Y. Konishi, H. Hada, K. Yamamoto and H. Ishida, *Thin Solid Films*, **218**, 109 (1992); Y. Yonezawa, M. Kijima and T. Sato, *Int. J. Phys. Chem.*, **96**, 1828 (1992).
89. N. Keghouche, M. Mostafavi, M. O. Delcourt and G. Picq, *J. Chim. Phys. Phys.-Chim. Biol.*, **90**, 777(1993); M. Mostafavi, M. O. Delcourt, N. Kegouche and G. Picq, *Rad. Phys. Chem.*, **40**, 445 (1992).
90. N. Keghouche, M. Mostafavi and M. O. Delcourt, *J. Chim. Phys.-Chim. Biol.*, **88**, 855 (1991).
91. T. Sato, N. Maeda, H. Ohkoshi and Y. Yonezawa, *Bull. Chem. Soc. Jpn.*, **67**, 3165 (1994).
92. K. Esumi, M. Wakabayashi and K. Torigoe, *Colloids Surf. A — Physicochem. Eng.*, **109**, 55 (1996).
93. Y. Yonezawa, T. Sato, S. Kuroda and K. Kuge, *J. Chem. Soc., Faraday Trans.*, **87**, 1905 (1991); A. Henglein, *Chem. Mater.*, **10**, 444 (1998).
94. A. Foitik, P. Mulvaney, T. Linnert, M. Giersig and A. Henglein, *Ber. Buns. Gesell.-Phys. Chem. Chem. Phys.*, **95**, 770 (1991).
95. M. Mennig, J. Spanhel, H. Schmidt and S. Betzholz, *J. Non-Cryst. Solids*, **147**, 326 (1992).
96. S. H. Oh, K. Tamura and T. Sato, *Tetrahedron*, **48**, 9687 (1992).
97. T. Sato and K. Tamura, *Tetrahedron Lett.*, **25**, 1821 (1984).
98. S.-H. Oh and T. Sato, *J. Org. Chem.*, **59**, 3744 (1994).
99. T. Sato, K. Tamura, K. Kurebayashi and H. Otsuka, *Jpn. Kokai Tokkyo Koho*, JP 61 00, 040; *Chem. Abstr.*, **104**, 206950 (1986).
100. Y. Sawayanagi, T. Sato and I. Shimizu, *Chem. Lett.*, 843 (1997).
101. M. E. Woodhouse, F. D. Lewis and T. J. Marks, *J. Am. Chem. Soc.*, **100**, 996 (1978).
102. I. J. Clark and J. MacB. Harrowfield, *Inorg. Chem.*, **23**, 3740 (1984).
103. S. Ronco, B. Van Vlierberge and G. Ferraudi, *Inorg. Chem.*, **27**, 3453 (1988).
104. G. A. Ozin and F. Hugues, *J. Phys. Chem.*, **86**, 5174 (1982).
105. C. M. Wang and T. E. Mallouck, *J. Am. Chem. Soc.*, **112**, 2016 (1990).
106. Y. Li, in *Molecular and Supramolecular Photochemistry, Organic Photochemistry*, (Eds. V. Ramamurthy and K. S. Schranze), Marcel Dekker, New York 1997, p. 295.
107. B. R. Heywood and S. Mann, *Chem. Mater.*, **6**, 311 (1994).
108. H. Rieley, N. J. Price, T. L. Smith and S. H. Yang, *J. Chem. Soc., Faraday Trans.*, **92**, 3629 (1996); H. Rieley, N. J. Price, R. G. White, R. I. R. Blyth and A. W. Robinson, *Surf. Sci.*, **333**, 189 (1995).
109. E. W. Wollman, D. Kang, C. D. Frisbie, I. M. Lorkovic and M. S. Wrighton, *J. Am. Chem. Soc.*, **116**, 4395 (1994).

110. C. D. Frisbie, E. W. Wollman and M. S. Wrighton, *Langmuir*, **7**, 2563 (1995); L. F. Rozsnyai and M. S. Wrighton, *Langmuir*, **11**, 3913 (1995); C. D. Frisbie, E. W. Wollman, J. R. Martin and M. S. Wrighton, *J. Vac. Sci. Technol. A*, **11**, 2368 (1993).
111. E. W. Wollman, C. D. Frisbie and M. S. Wrighton, *Langmuir*, **9**, 1517 (1993).
112. F. Sun, D. W. Grainger, D. G. Castner and D. K. Leachs-Campavia, *Macromolecules*, **27**, 3053 (1994).
113. E. Cooper, R. Wiggs, D. A. Hutt, L. Parker, G. J. Leggett and T. L. Parker, *J. Mater. Chem.*, **7**, 435 (1997).
114. Y. Z. Li, J. Y. Huang, R. T. McIver, Jr. and J. C. Hemminger, *J. Am. Chem. Soc.*, **114**, 2428 (1992).
115. M. H. Dishner, F. J. Feher and J. C. Hemminger, *J. Chem. Soc., Chem. Commun.*, 1971 (1996).
116. D. A. Hutt and G. J. Leggett, *J. Phys. Chem.*, **100**, 6657 (1996).
117. D. N. Batchelder, S. D. Evans, T. L. Freeman, L. Haussling, H. Ringsdorf and H. Wolff, *J. Am. Chem. Soc.*, **116**, 1050 (1994).
118. J. Y. Huang, D. A. Dahlgren and J. C. Hemminger, *Langmuir*, **10**, 626 (1994); J. Y. Huang and J. C. Hemminger, *J. Am. Chem. Soc.*, **115**, 3342 (1993).
119. M. Wirde, U. Gelius, T. Dunbar and D. L. Allara, *Nucl. Instr. Methods Phys. Res. Sect. B — Beam Interactions*, **131**, 245 (1997).
120. W. J. Li, V. Lynch, H. Thompson and M. A. Fox, *J. Am. Chem. Soc.*, **119**, 7211 (1997).
121. M. O. Wolf and M. A. Fox, *J. Am. Chem. Soc.*, **117**, 1845 (1995).
122. M. O. Wolf and M. A. Fox, *Langmuir*, **12**, 955 (1996).
123. M. A. Fox and M. D. Wooten, *Langmuir*, **13**, 7099 (1997).
124. J. Jennane, T. Boutros and R. Gaisson, *Can. J. Chem.*, **74**, 2509 (1996).
125. A. Doron, E. Katz, G. L. Tao and I. Willner, *Langmuir*, **13**, 1783 (1997); E. Katz, B. Willner and I. Willner, *Biosens. Bioelectron.*, **12**, 703 (1997).
126. K. Nishiyama, K. Matsuura and M. Fujihara, *Thin Solid Films*, **210**, 384 (1992).
127. S. Isoda, S. Nishikawa, S. Ueyama, Y. Hanazato, H. Kawakubo and M. Maeda, *Thin Solid Films*, **210**, 290 (1992).
128. F. Mukae, H. Takemura and K. Takehara, *Bull. Chem. Soc. Jpn.*, **69**, 2461 (1996).
129. S. Kumbhat, R. Webster, F. Marken, J. C. Eklund and R. G. Compton, *Electroanal.*, **8**, 515 (1996).
130. E. Katz, M. Lion-Dagan and I. Willner, *J. Electroanal. Chem.*, **382**, 25 (1995).
131. K. Nishiyama, K. Matsumura and M. Fujihira, *Thin Solid Films*, **210**, 384 (1992).
132. M. Ohtani, T. Sunagawa, S. Kuwabata and H. Yoneyama, *J. Electroanal. Chem.*, **396**, 97 (1995).
133. R. G. Compton, R. G. Wellington, D. Bethell, P. Lederer and D. M. O'Hare, *J. Electroanal. Chem.*, **322**, 183 (1992).
134. Y.-Q. Wang, J. Wang, H. Z. Yu, S. M. Cai and Z.-F. Liu, *Chem. J. Chin. Univ.-Chinese*, **17**, 1130 (1996); *Chem. Abstr.*, **127**, 168088 (1997)
135. K. Morigaki, Z.-F. Liu, K. Hashimoto and A. Fujishima, *J. Phys. Chem.*, **99**, 14771 (1995); H. Takano, Z.-F. Liu, K. Hashimoto and A. Fujishima, *Chem. J. Chin. Univ.-Chinese*, **16**, 246 (1995); *Chem. Abstr.*, **124**, 215804 (1996).
136. J. H. Gu, Y. W. Chen, B. J. Liang, B. Lu and Z. H. Lu, *Chin. Phys. Lett.*, **14**, 849 (1997).
137. M. Niwa, T. Mori and N. Nigashi, *J. Mater. Chem.*, **2**, 245 (1992).
138. P. E. Laibinis, R. L. Graham, H. A. Biebuyck and G. M. Whitesides, *Science*, **254**, 981 (1991).
139. R. L. Graham, C. D. Bain, H. A. Biebuyck, P. E. Laibinis and G. M. Whitesides, *J. Phys. Chem.*, **97**, 9456 (1993).
140. C. J. Powell and M. P. Seah, *J. Vac. Sci. Technol. A*, **8**, 735 (1990).
141. F. M. Pan, Y. L. Lin and S. R. Horng, *Appl. Surf. Sci.*, **47**, 9 (1991).
142. H. Kunkely and A. Vogler, *Z. Naturforsch. B — J. Chem. Sci.*, **51**, 1067 (1996).
143. J. M. Forward, D. Bohmann, J. P. Fackler, Jr. and R. J. Staples, *Inorg. Chem.*, **34**, 6330 (1995).
144. W. B. Jones, J. Yuan, R. Narayanaswamy, M. A. Young, R. C. Elder, A. E. Bruce and M. R. M. Bruce, *Inorg. Chem.*, **34**, 1996 (1995).
145. D.-F. Feng, S. S. Tang, C. W. Liu, I. J. B. Lin, Y.-S. Wen and L.-K. Liu, *Organometallics*, **16**, 901 (1997).
146. Z. Assefa, R. J. Staples and J. P. Fackler, Jr., *Inorg. Chem.*, **33**, 2790 (1994).
147. C. King, J. C. Wang, M. N. I. Khan and J. P. Fackler, Jr., *Inorg. Chem.*, **28**, 2145 (1989).
148. B.-C. Tzeng, C.-K. Chan, K. K. Cheung, C.-M. Che and S.-M. Peng, *J. Chem. Soc., Chem. Commun.*, 135 (1997).

149. S. D. Hanna, S. I. Khan and J. I. Zink, *Inorg. Chem.*, **35**, 5813 (1996).
150. M. Khan, I. Nazrul, J. P. Fackler, Jr., C. King, J. C. Wang and S. Wang, *Inorg. Chem.*, **27**, 1672 (1988).
151. V. W.-W. Yam, T.-F. Lai and C.-M. Che, *J. Chem. Soc., Dalton Trans.*, 3747 (1990).
152. J. C. Vickery, M. M. Olmstead, E. Y. Fung and A. L. Balch, *Angew. Chem., Int. Ed. Engl.*, **36**, 1179 (1997).
153. J. E. Parker and A. L. Balch, *J. Organomet. Chem.*, **71**, 453 (1974).
154. L. H. Gade, *Angew. Chem., Int. Ed. Engl.*, **36**, 1171 (1997).
155. M. J. Irwin, J. J. Vittal and R. J. Puddephatt, *Organometallics*, **16**, 3541 (1997).
156. B.-C. Tzeng, W. C. Lo, C.-M. Che and S.-M. Peng, *J. Chem. Soc., Chem. Commun.*, 181 (1996).
157. V. W.-W. Yam and S. W.-K. Choi, *J. Chem. Soc., Dalton Trans.*, 4227 (1996).
158. A. P. Golovina, I. M. Ivanova, V. M. Ivanova and P. N. Neterenko, *J. Anal. Chem. USSR*, **40**, 640 (1985); *Chem. Abstr.*, **103**, 134077 (1985).
159. C.-W. Chan, W.-T. Wong and C.-M. Che, *Inorg. Chem.*, **33**, 1266 (1994); see also T. J. Wallace and R. J. Gritter, *J. Org. Chem.*, **27**, 3067 (1962).
160. T. M. McCleskey, J. R. Winkler and H. B. Gray, *Inorg. Chim. Acta*, **225**, 319 (1994).
161. D. Li, X. Hong, C.-M. Che, W. C. Lo and S.-M. Peng, *J. Chem. Soc., Dalton Trans.*, 2929 (1993).
162. B.-C. Tzeng, C.-M. Che and S.-M. Peng, *J. Chem. Soc., Dalton Trans.*, 1769 (1996).
163. T. Shimizdu, H. Segawa, T. Iyoda and K. Honda, *J. Chem. Soc., Faraday Trans. 2*, **83**, 2191 (1987).
164. V. W.-W. Yam, S. W. K. Choi, K. K. W. Lo, W. F. Dung and R. Y. C. Kong, *J. Chem. Soc., Chem. Commun.*, 2379 (1994).
165. G. R. Bamwenda, S. Tsubota, T. Kobayashi and M. Haruta, *J. Photochem. Photobiol. A — Chem.*, **77**, 59 (1994).
166. G. R. Bamwenda, S. Tsubota, T. Nakamura and M. Haruta, *J. Photochem. Photobiol. A — Chem.*, **89**, 177 (1995).
167. F. C. Chen and H. S. Lackritz, *Macromolecules*, **30**, 5986 (1997).
168. M. Niwa, M. Date and N. Higashi, *Macromolecules*, **29**, 3681 (1996).
169. G. B. Shul'pin and G. V. Nizova, *Petrol. Chem.*, **32**, 36 (1992).
170. P. Lederer, G. V. Nizova, M. M. Kats and G. B. Shul'pin, *Collect. Czech. Chem. Commun.*, **57**, 107 (1992).
171. G. B. Shul'pin and G. V. Nizova, *Petrol. Chem.*, **33**, 107 (1993).
172. G. B. Shul'pin and G. V. Nizova, *Petrol. Chem.*, **33**, 118 (1993).
173. G. B. Shul'pin and A. N. Druzhinina, *Petrol. Chem.*, **33**, 256 (1993).
174. C. M. Mitchell and F. G. A. Stone, *J. Chem. Soc., Dalton Trans.*, 102 (1972).
175. P. W. N. M. Van Leeuwen, R. Kaptein, R. Huis and C. F. Roobeek, *J. Organomet. Chem.*, **104**, C44 (1976).
176. J. L. Davidson, P. John, P. G. Roberts, M. G. Jubber and J. I. B. Wilson, *Chem. Mater.*, **6**, 1712 (1994).
177. W. E. Billups, M. M. Konarski, R. H. Hauge and J. L. Margrave, *J. Am. Chem. Soc.*, **102**, 7393 (1980).
178. D. Li, C.-M. Che, H.-L. Kwong and V. W.-W. Yam, *J. Chem. Soc., Dalton Trans.*, 3325 (1992); see also C.-M. Che, H.-L. Kwong, C. K. Poon and V. W. W. Yan, *J. Chem. Soc., Dalton Trans.*, 3205 (1990); C. King, J. C. Wang, N. I. Md. Khan and J. P. Fackler, Jr., *Inorg. Chem.*, **28**, 2145 (1989).
179. Y. Yonezawa, I. Kawabata and T. Sato, *Ber. Buns. Gesell.-Phys. Chem., Chem. Phys.*, **100**, 39 (1996).
180. R. Krasnansky, S. Yamamura, J. K. Thomas and R. Dellaguardia, *Langmuir*, **7**, 2881 (1991).
181. K. Torigoe and K. Esumi, *Langmuir*, **8**, 59 (1992).

CHAPTER **11**

Pyrolysis of organic derivatives of silver and gold

R. ALAN AITKEN

School of Chemistry, University of St. Andrews, St. Andrews, Fife, KY16 9ST, UK
Fax: 44-1334-463808;   e-mail: raa@st-and.ac.uk

I. INTRODUCTION

The organic compounds of silver and gold are, in general, rather thermally unstable and in most cases they decompose to deposit the metallic elements. Many previous reviews of organogold chemistry, in particular, contain extensive listings of decomposition temperatures without any attempt having been made to identify the organic products[1]. This chapter concentrates on studies in which isolable organic compounds of silver and gold are heated at temperatures significantly above room temperature. There has recently been renewed interest in this area owing to the need to develop suitable volatile precursors for 'metal-organic chemical vapour deposition' (MOCVD) of microscopic conducting strips of these metals for electronic circuits.

II. ORGANOSILVER COMPOUNDS

A. Alkyl- and Alkenylsilver Compounds

The interaction of EtMgBr with AgBr in ether at $0\,^\circ$C leads to the generation of EtAg and upon warming to room temperature this was observed to decompose to give metallic silver together with butane, ethane and ethene, products expected from combination and disproportionation of ethyl radicals[2]. The kinetics of decomposition of MeAg[3] and EtAg[4,5] generated from the corresponding tetraalkylleads and silver nitrate in ethanol solution have been studied in the range -50 to $-20\,^\circ$C. The simple alkylsilvers can be filtered off at low temperature and decomposition of MeAg, EtAg and Pr^{n}Ag as damp solids upon warming up to room temperature has been reported to give silver together with, in the first case, ethane, in the second, butane, ethane and ethene, and in the third, hexane, propane and propene[6]. A later study showed the dry solids MeAg and EtAg to decompose with zero-order kinetics at temperatures of $-30\,^\circ$C and $-38\,^\circ$C, respectively[7].

Simple alkylsilvers are greatly stabilized by coordination of a tertiary phosphine and this has allowed Whitesides to study their decomposition at and above room temperature. Heating a solution of **1** in ether at $20\,^\circ$C led to decomposition within 5 minutes to give silver, tributylphosphine and octane (93%), butane (5%) and butene (2%)[8]. The low proportion of butene was taken to indicate that free radicals in solution are not involved and the joining of two butyl groups to form octane is concerted with Ag—C bond cleavage. Under comparable conditions, the isomeric s-butyl compound **2** decomposes by a different more complex mechanism to give a high proportion of butenes and butane[8]. On the other hand, the products formed from thermolysis of an ether solution of neophylsilver tributylphosphine complex **3** at $65\,^\circ$C were consistent with the intermediacy of the neophyl radical, PhC(Me)$_2$CH$_2{}^\bullet$, which could rearrange to PhCH$_2$C$^\bullet$(Me)$_2$ on a time scale comparable to the coupling and disproportionation processes[9].

Bu^n——Ag◄——PBu$^n_3$ Bu^s——Ag◄——PBu$^n_3$ Me   Me   PBu$^n_3$
                                                                                        Ag
                                                                       Ph

(1)   **(2)**   **(3)**
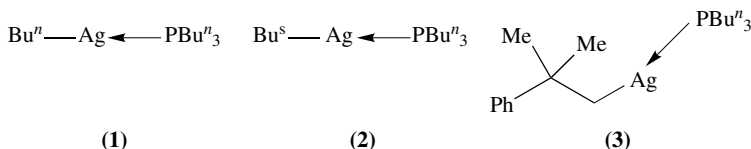
The decomposition of the E- and Z-isomers of MeCH=CH—Ag and MeCH=C(Me)—Ag, both as such and as the tributylphosphine complexes, occurs at room temperature over 4–6 hours to give the expected isomers of the hexadienes MeCH=CH—CH=CHMe and MeCH=C(Me)—C(Me)=CHMe with complete retention of the double bond configurations[10]. The styrylsilver, PhCH=CHAg, generated from the corresponding organolead compound is quite stable at room temperature but decomposes upon heating under reflux in ethanol overnight to give silver and a polymer[11].

B. Arylsilver Compounds

The arylsilver compounds formed by interaction of an aryl Grignard reagent with a silver(I) halide can be isolated as solids which are stable for a short time at room temperature. Thus, for example, PhAg was first obtained as a dark solid which upon drying out decomposed, sometimes with explosive violence, to give silver metal and biphenyl[12]. The

reaction could be achieved in a controlled manner by boiling a suspension of the material in toluene to give a high yield of biphenyl. In the same way *p*-tolyl- and *p*-anisylsilver were decomposed without isolation by boiling in benzene to afford the corresponding disubstituted biphenyls[13]. In an attempt to elucidate the mechanism of this process, Gardner and coworkers heated a solution containing phenyl- and *p*-tolylsilver and obtained not only biphenyl and 4,4'-dimethylbiphenyl, but also the cross-over product 4-methylbiphenyl[14]. Heating a mixture of *p*-anisyl- and *p*-tolylsilver as the dry solids at 100 °C for 30 minutes similarly gave all three possible biaryl products[15]. However, the high selectivity for coupling, as opposed to other reactions typical of aryl radicals, led to the suggestion that free aryl radicals are not involved and the reactions rather involve bimolecular coupling. This was supported by the fact that decomposition of PhAg in such reactive solvents as CCl_4, chlorobenzene and nitrobenzene gave only biphenyl with no products from reaction with the solvent[15]. Despite this, a more recent paper has claimed that radicals are involved based on the observation of the cross-over product upon thermolysis of phenyl- and *p*-tolylsilver in ether or pyridine[16]. Wittig attempted to use *o*-fluorophenylsilver as a source of benzyne but, when it was generated by treatment of *o*-bromofluorobenzene with Bu^nLi and then AgBr at low temperature, it decomposed upon warming to room temperature to give silver together with 2,2'-difluorobiphenyl in 77% yield[17].

C. Other Organosilver Compounds

The thermal decomposition of silver acetylide, $(Ag^+)_2{}^-C{\equiv}C^-$, is unusual in that it is a potentially explosive reaction in which no gases are evolved[18]. The material explodes when dropped on to a surface at 195–200 °C but the reaction may be carried out in a controlled way by heating the solid at 115–135 °C to give silver and carbon, and there has been some interest in the microcrystalline structure of the silver formed in this way[19].

Perhaps the most commonly used preparative reaction involving an organosilver compound is the Hunsdiecker reaction in which the silver salt of a carboxylic acid **4** is heated with a halogen to give the alkyl halide **5**. Although this is commonly carried out by heating the components in boiling carbon tetrachloride or benzene[20], it is clear that the heat is only required to bring about homolysis of the intermediate acylhypohalite **6**. The reaction is the subject of a comprehensive review[21] and more recent studies have confirmed that it proceeds by way of a radical mechanism[22].

$$RCO_2{}^-Ag^+ + X_2 \xrightarrow[-\,AgX]{} \underset{\textbf{(6)}}{\underset{R}{\overset{O}{\diagup\!\!\diagup}}\!\!C\!\!-\!\!O\!\!-\!\!X} \xrightarrow[-\,CO_2]{\Delta} RX$$

$$\textbf{(4)} \qquad\qquad\qquad \textbf{(6)} \qquad\qquad\qquad \textbf{(5)}$$
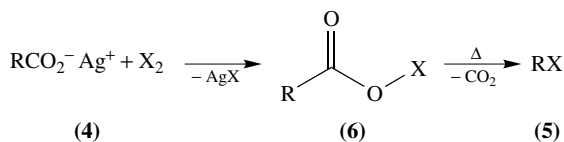
The thermal decomposition of silver oxalate proceeds readily to give silver and CO_2 and the kinetics of the process and how they are influenced by the presence of additives have been examined in detail[23]. Destructive distillation of the silver salts of simple aliphatic carboxylic acids, RCO_2Ag, gives the acids, RCO_2H, together with silver, CO_2 and carbon[24,25]. A number of early studies describe the destructive distillation of the silver salts of aromatic and heteroaromatic carboxylic acids, $ArCO_2Ag$, which proceeds with loss of CO_2 to give the corresponding aromatics, ArH, and a residue of metallic silver. Examples include **7**[26], **8**[27], **9**[28], **10**[29], **11**[30] and **12**[31]. For **13** or **14**[32] and **15**[33]

the process is accompanied by aromatization to give pyrazole and triphenylimidazole, respectively.

(7)   (8)   (9)

(10)   (11)   (12)

(13)   (14)   (15)
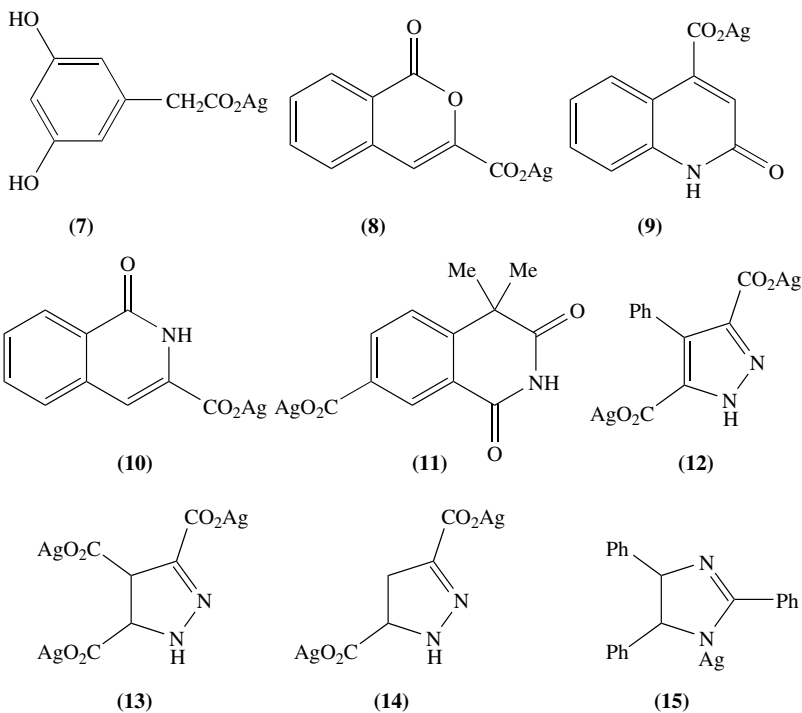
In an early study on the mechanism of the Beckmann rearrangement, Jones and Hurd showed that the silver salts of *N*-acylhydroxamic acids **16** decomposed upon heating in the solid state to produce the corresponding isocyanates **17**[34]. The silver derivative of propane-1,2-diol-3-thiol ('thiovanol') **18** undergoes thermal decomposition to deposit

$R^1 \!\!-\!\! NCO \; + \; R^2CO_2^- \, Ag^+$

(17)

(16)

(18)
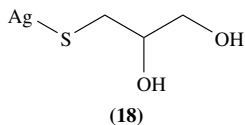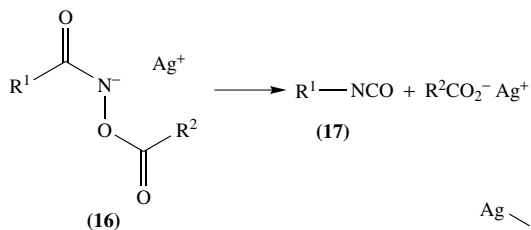
metallic silver and this has been examined in detail over the temperature range up to 500 °C using thermogravimetric analysis and IR spectroscopy[35].

III. ORGANOGOLD COMPOUNDS

A. Alkylgold(I) Compounds

The complexes between alkylgolds and tertiary phosphines are more stable than their silver analogues and are generally stable indefinitely at room temperature. A detailed study of the thermal decomposition of a series of compounds **19** led in each case to the quantitative formation of gold and triphenylphosphine together with the following hydrocarbon products at the temperatures noted: R = Me, 118 °C, ethane; R = Et, 100 °C, butane; R = Pr^n, 69 °C, hexane and a small amount of propene; R = Pr^i, 100 °C, propane and propene; R = Bu^t, 118 °C, isobutane, isobutene and C_8 hydrocarbons[36]. The kinetics of these processes were also examined. A comparative study of the thermolysis of **19** (R = Me) and the anionic dimethylgold complex **20** has also been carried out both by heating in boiling THF and by heating the solids at 140 °C[37]. The decomposition of **20** was found to be significantly faster particularly at the higher temperature.

R—Au ⟵ PPh₃

(19)

$[Me—Au—Me]^-$ Li⁺ - - - NMe (with Me₂N and Me₂N groups)

(20)

(cyclopentadienyl with Ph groups)—Au ⟵ PPh₃

(21)

ClH₂C—Au ⟵ PPh₃

(22)

(cyclohexen-3-ol with OH)

(23)

(bicyclic compound with OH)

(24)

Me—Au ⟵ :C≡NR

(25) R = Me, Bu^t, Ph

R———Au ⟵ :C≡NMe
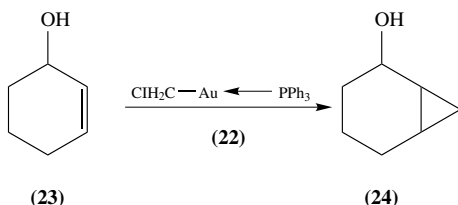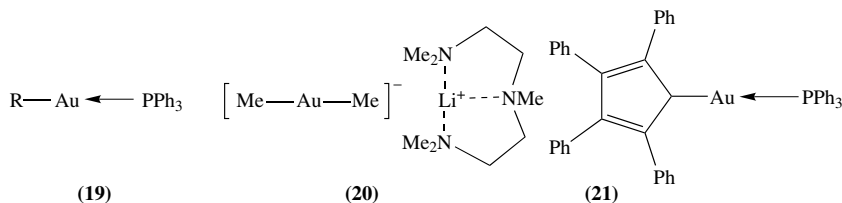
(26) R = Me, Bu^t

The cyclopentadienylgold complex **21** is reported to decompose under mass spectrometric conditions at 150 °C to give gold, triphenylphosphine and tetraphenylcyclopentadiene[38]. The Ph₃P complex of AuCl reacts with diazomethane to give **22** and this reacts with cyclohexen-3-ol **23** upon prolonged boiling in benzene solution with transfer of a methylene group to give **24**[39]. Isocyanides are also effective in stabilizing alkylgold(I) compounds and the compounds **25** and **26** have been examined as volatile gold precursors for MOCVD at 200 °C under vacuum[40].

B. Other Organogold(I) Compounds

Reaction of the triphenylarsine complex of AuCl with 2-pyridyllithium gives the stable 2-pyridylgold **27** which probably has a polymeric structure in the solid state. When this is heated at $120-150\,^{\circ}$C there is clean decomposition to give gold and 2,2′-bipyridyl[41]. This method has been extended to substituted pyridyl compounds **28** which give the corresponding substituted bipyridyls **29** upon heating at $160-220\,^{\circ}$C under vacuum in 70–85% yield[41].

Complexation of 2-trimethylsilylpyridine with AuCl gives the compound **30** and, when this is heated in boiling benzene, trimethylsilyl chloride is eliminated to give **27**[42]. The benzothiazole complex **31** reacts under the same conditions to give Me$_3$SiCl, gold and the coupling product **32** in 88% yield. For *N*-methylbenzimidazole, elimination of Me$_3$SiCl is spontaneous to give **33** in polymeric form and, when this is heated under vacuum at $150\,^{\circ}$C, gold is eliminated and the 2,2′-bi(benzimidazole) is formed in 85% yield[42].

(27)

(28) R = 3-Me, 4-Me, 5-Me, 6-Me, 4,6-Me$_2$

(29)

(32)

(31)

(33)

(30)
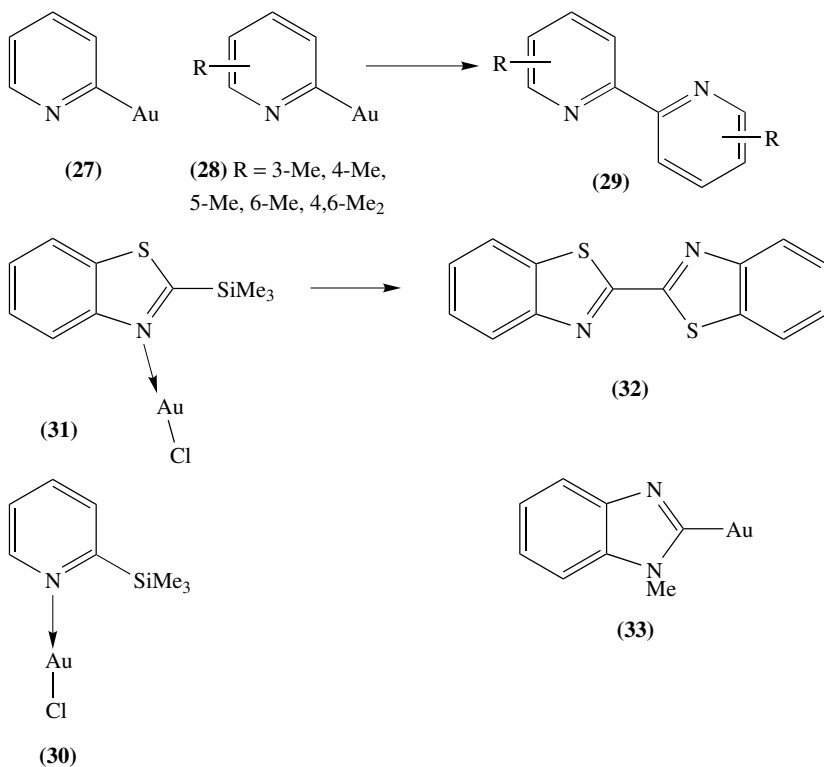
In a very recent study, the titanocene–alkynylgold complex **34** was found to decompose upon heating at $80\,^{\circ}$C in toluene to give **35**, gold metal and the 1,3-diyne **36**[43]. The thermal decomposition of **37** and the anionic complex **38** have also been examined by heating in air or nitrogen up to $500\,^{\circ}$C[35]. Both compounds give gold in air but gold sulfides under nitrogen.

(34)

(35)

+

(36)

(37)

(38)
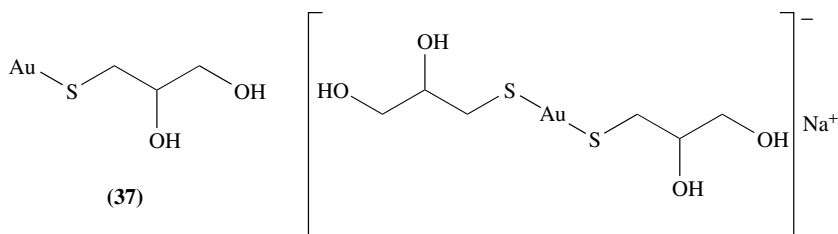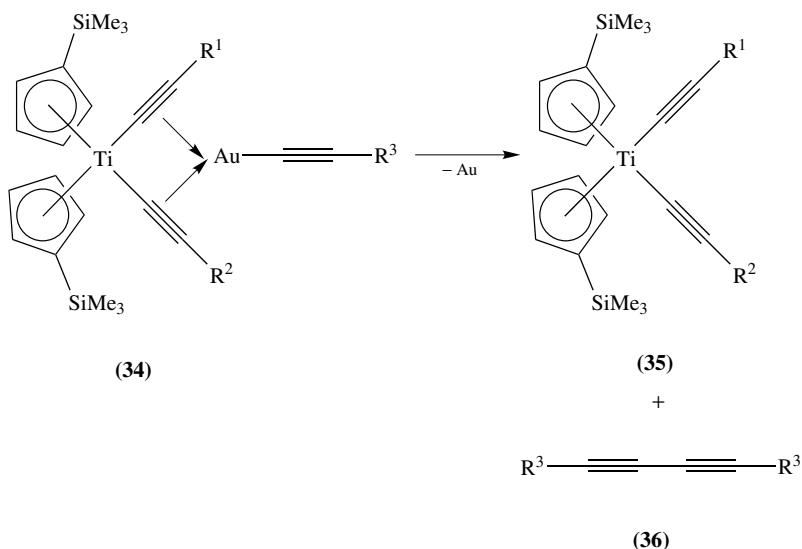
C. Alkylgold(III) Halides and Related Compounds

When diethylgold bromide, Et_2AuBr, was first prepared, it was found to explode on warming above $0\,^\circ C$ to give metallic gold but the organic products were not identified[44]. A later paper described the preparation of a wide range of dialkylgold halides and alkylgold dihalides and the decomposition temperature was noted for each example of the former type, but again the organic products were not identified[45]. It was, however, noted that the corresponding dialkylgold cyanides were significantly more stable. A series of studies in the 1930s showed that alkylgold dibromides, $RAuBr_2$, decompose cleanly at $80-85\,^\circ C$ to give the alkyl bromides, RBr, and $AuBr$ for $R = Et$[46] and Pr^n [47]. In the latter case, the compound readily formed a 2 : 1 adduct **39** with ethylenediamine and, when this was heated in boiling chloroform, hexane was cleanly eliminated to give **40**. Further heating of **40** resulted in an explosion at $140\,^\circ C$. In 1941, Gilman reported that Me_2AuBr decomposed upon boiling in ether to give mainly gold and ethane but the fate of the bromine was unclear[48]. The dialkylgold cyanides which have a tetrameric structure, $(R_2AuCN)_4$, were

found to lose two equivalents of the alkane R−R upon heating in boiling chloroform to give $(R_2AuCN)_2(AuCN)_2$[49]. Heating these materials at a higher temperature led to further loss of R−R to give AuCN. Diethylgold cyanide forms an analogous complex to **39** with ethylenediamine and, when this was heated at $100\,°C$, it underwent loss of one equivalent of butane to give **41**[49]. The thiocyanate, Et_2AuSCN, explodes when heated rapidly to give butane, gold and a thiocyanogen polymer. When the decomposition is carried out in a controlled way by boiling in benzene, toluene or xylene, the products are butane and $AuSCN$[50]. Oxygen containing ligands also have a beneficial effect on stability and $Me_2Au−OSiMe_3$ can be heated to $135\,°C$ before it decomposes with deposition of gold[51], while $Me_2Au−OSO_2CF_3$ undergoes smooth reductive elimination of ethane upon heating in benzene at $45\,°C$ to give $AuOSO_2CF_3$[52]. A study of the relative ease of elimination of ethane from a series of phosphine-stabilized compounds, $Me_2AuX•PR_3$, as a function of X showed a range of rates with $X = OSO_2CF_3$ giving the fastest elimination and $X = OCOMe$ giving the slowest[53].

(39)   **(40)**

(41)
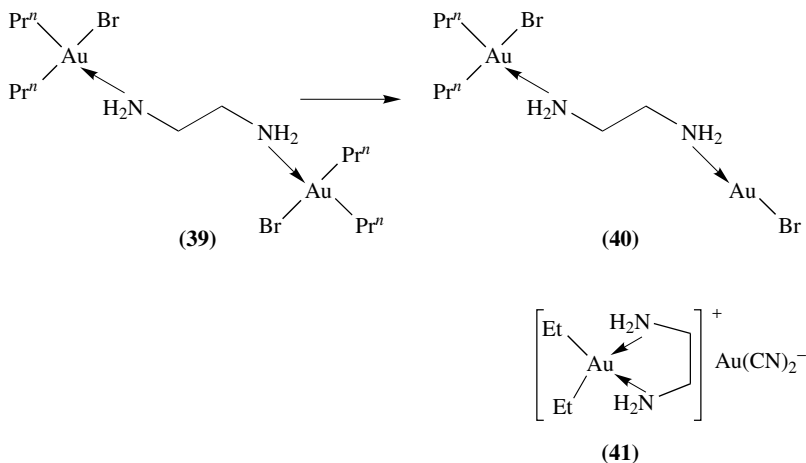
D. Trialkylgold(III) Compounds

Trimethylgold was first prepared by Gilman in 1948 by reaction of $AuBr_3$ with MeLi at $−65\,°C$[48]. Upon warming up it decomposed at $−40$ to $−35\,°C$ to give gold, methane and ethane. The 2 : 1 adduct with ethylenediamine analogous to **39** was stable at room temperature but exploded upon warming in an open crucible. Complexation with triphenylphosphine affords the square-planar adduct **42** which is stable at room temperature. When this was heated in xylene at $120\,°C$, reductive elimination occurred to give ethane and $MeAu•PPh_3$[54]. Heating at $175\,°C$ in biphenyl or at $120\,°C$ in the absence of solvent gave ethane, gold and Ph_3P. This reaction has since been the subject of detailed mechanistic studies since it is an unusual example of reductive elimination from a transition metal centre which does not involve β-elimination. Kochi and coworkers studied the elimination from the *cis* and *trans* isomers of $RMe_2Au•PPh_3$ in decalin at $70–90\,°C$ and found a preference for elimination of *cis* alkyl groups[55,56]. A more recent study of a range of compounds, $RMe_2Au•PPh_3$, in benzene at $70\,°C$ found that mainly RMe is eliminated for $R = Ph$, while mainly ethane is eliminated for $R = PhC≡C$. For $R = PhCH_2$ and

$PhCH_2CH_2$, both processes occur[57]. A detailed kinetic and mechanistic study, including the use of $CD_3Me_2Au\cdot PPh_3$, showed that the reaction is likely to proceed by initial decomplexation of Ph_3P to give a 'T'-shaped trialkylgold which may undergo isomerization in competition with the elimination[58]. In non-polar solvents such as benzene and decalin the elimination is intermolecular, while in polar solvents such as DMF and DMSO it is intramolecular.
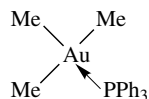
(42)

E. Dialkylgold(III) Acetylacetonides

Although the thermal decomposition of **43** to deposit metallic gold was noted when it was first prepared in 1930[59], it is only in the last 10 years that there has been renewed interest in compounds of this type as volatile gold sources for MOCVD. A study of the three compounds **44−46** using differential scanning calorimetry showed that decomposition begins at around $160\,°C$ and the rate of deposition of gold at $300\,°C$ and 0.5 Torr increased in the order $44 < 45 < 46$[60]. The use of laser-induced pyrolysis to trace out fine patterns of gold in films of these materials has also been described[61]. The kinetics of decomposition of **44** have been examined in solution[62], and this compound has also been used very recently to prepare a thin layer of gold on a surface of titanium dioxide, of interest for catalytic oxidation of CO[63].
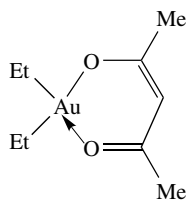
(43)
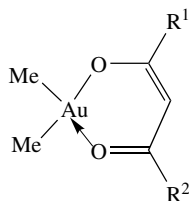
(44) $R^1 = R^2 = Me$

(45) $R^1 = Me, R^2 = CF_3$

(46) $R^1 = R^2 = CF_3$

F. Other Organogold(III) Compounds

The arylgold dichlorides, $ArAuCl_2$, undergo reaction upon heating at between 90 and $155\,°C$ to give mainly gold and the aryl chlorides, $ArCl$[64]. The absence of biaryls, $Ar−Ar$, in these reactions was taken to mean that aryl radicals are not involved. The compounds $(C_6F_5)_2AuOAc\cdot AsPh_3$ and $(C_6F_5)_2AuONO_2\cdot AsPh_3$ can be isolated but decompose at room temperature after a few hours to give $C_6F_5Au\cdot AsPh_3$[65]. An unusual thermal process is observed upon heating **47** in toluene at $50\,°C$: the isomeric compounds **48** are formed[66].

Azobenzene forms a stable complex with $AuCl_3$ and, when this is heated at 205 °C in 1,2,4,5-tetrachlorobenzene, gold is formed together with 2-chloroazobenzene and several isomers of dichloroazobenzene[67]. Vacuum sublimation of the same material at 140–190 °C and 0.05 Torr gives 2-chloroazobenzene and (mainly) 2,2′-dichloroazobenzene. These reactions are thought to involve intermediates such as **49**.

(47)

R = Ph, Et
X = Cl, Br, I

(48)

(49)
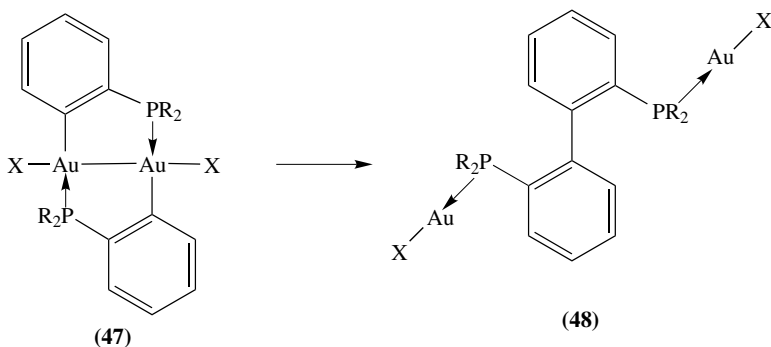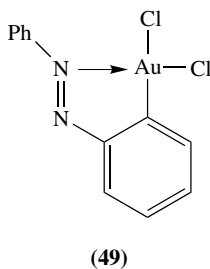
Thermal decomposition of a variety of ionic organogold(III) compounds has also been described. Reductive elimination of the hydrocarbon R−R from a variety of compounds **50** has been examined as a function of L and X and occurs with a range of rates between room temperature and 240 °C[68,69]. The anionic tetramethylgold complex **51** was found to decompose much more rapidly than **42** both in boiling THF at 65 °C and in the solid state at 140 °C[37].

(50) L = Ar_3P, Ar_3As
X = BF_4, ClO_4, PF_6

(51)
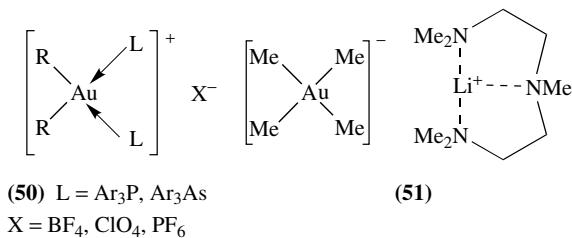
Phosphorus ylides react with organogold halides to give a variety of interesting structures whose thermal decomposition has been studied. The compound **52** is stable at its melting point of 205 °C but decomposes at higher temperatures with clean elimination of ethane to afford **53**[70]. Bulky groups also lead to considerable stabilization and compounds such as **54** and **55** have decomposition temperatures above 150 °C[71]. Finally, the cyclic compound **56** cleanly eliminates ethane at 153–155 °C to give **57**[72].
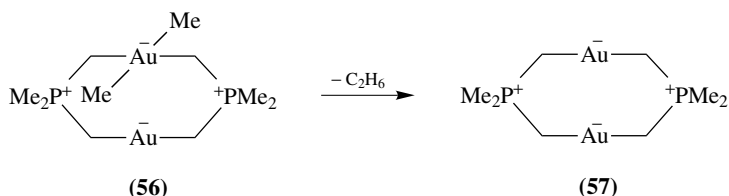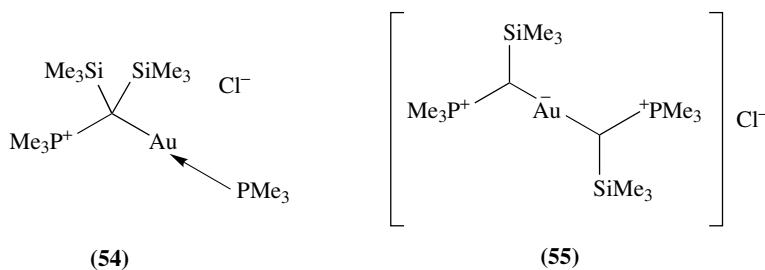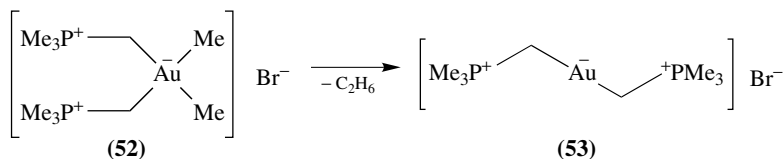
IV. REFERENCES

1. B. Armer and H. Schmidbaur, *Angew. Chem., Int. Ed. Engl.*, **9**, 101 (1970).
2. H. Gilman and R. G. Jones, *J. Am. Chem. Soc.*, **62**, 2357 (1940).
3. C. E. H. Bawn and F. J. Whitby, *Trans. Faraday Soc.*, **2**, 228, (1947).
4. C. E. H. Bawn and R. Johnson, *J. Chem. Soc.*, 3923 (1960).
5. G. Semerano, L. Riccobani and F. Callegari, *Ber. Dtsch. Chem. Ges.*, **74**, 1297 (1941).
6. G. Semerano and L. Riccobani, *Ber. Dtsch. Chem. Ges.*, **74**, 1089 (1941).
7. B. S. Rabinovitch, D. H. Dills and N. R. Larson, *J. Phys. Chem.*, **63**, 1523 (1959).
8. G. M. Whitesides, D. E. Bergbreiter and P. E. Kandall, *J. Am. Chem. Soc.*, **96**, 2806 (1974).
9. G. M. Whitesides, E. J. Panek and E. R. Stedronsky, *J. Am. Chem. Soc.*, **94**, 232 (1972).
10. G. M. Whitesides, C. P. Casey and J. K. Krieger, *J. Am. Chem. Soc.*, **93**, 1379 (1971).
11. F. Glockling and D. Kingston, *J. Chem. Soc.*, 3001 (1959).
12. E. Krauss and B. Wendt, *Ber. Dtsch. Chem. Ges.*, **56**, 2064 (1923).
13. J. H. Gardner and P. Borgstrom, *J. Am. Chem. Soc.*, **51**, 3375 (1929).
14. J. H. Gardner, L. Joseph and F. Gollub, *J. Am. Chem. Soc.*, **59**, 2583 (1937).
15. E. A. Bickley and J. H. Gardner, *J. Org. Chem.*, **5**, 126 (1940).

16. H. Hashimoto and T. Nakano, *J. Org. Chem.*, **31**, 891 (1966).
17. G. Wittig and K. Niethammer, *Chem. Ber.*, **93**, 944 (1960).
18. J. Eggert and H. Schimank, *Ber. Dtsch. Chem. Ges.*, **51**, 454 (1918).
19. J. D. McCowan, *Trans. Faraday Soc.*, **59**, 1860 (1963).
20. A. Lüttringhaus and D. Schade, *Ber. Dtsch. Chem. Ges.*, **74**, 1565 (1941).
21. C. V. Wilson, *Org. React.*, **9**, 332 (1957).
22. N. J. Bunce and N. G. Murray, *Tetrahedron*, **27**, 5323 (1971).
23. A. G. Leiga, *J. Phys. Chem.*, **70**, 3260 (1966).
24. F. Iwig and O. Hecht, *Ber. Dtsch. Chem. Ges.*, **19**, 238 (1886).
25. J. Kachler and A. Lieben, *Monatsh. Chem.*, **12**, 338 (1891).
26. H. Cornelius and H. von Pechmann, *Ber. Dtsch. Chem. Ges.*, **19**, 1446 (1886).
27. E. Bamberger and W. Frew, *Ber. Dtsch. Chem. Ges.*, **27**, 198 (1894).
28. W. Koenigs and G. Koerner, *Ber. Dtsch. Chem. Ges.*, **16**, 2152 (1883).
29. E. Bamberger and M. Kitschelt, *Ber. Dtsch. Chem. Ges.*, **25**, 1138 (1892).
30. F. Tiemann and P. Krüger, *Ber. Dtsch. Chem. Ges.*, **26**, 2675 (1893).
31. E. Buchner and A. Papendieck, *Ber. Dtsch. Chem. Ges.*, **28**, 221 (1895).
32. E. Buchner, M. Fritsch, A. Papendieck and H. Witter, *Justus Liebigs Ann. Chem.*, **273**, 214 (1893).
33. A. Claus and K. Elbs, *Ber. Dtsch. Chem. Ges.*, **16**, 1272 (1883).
34. L. W. Jones and C. D. Hurd, *J. Am. Chem. Soc.*, **43**, 2422 (1921).
35. V. P. Komarov, V. B. Lazarev and I. S. Shaplygin, *Zh. Neorg. Khim.*, **25**, 746 (1980); *Chem. Abstr.*, **92**, 190535 (1980).
36. A. Tamaki and J. K. Kochi, *J. Organomet. Chem.*, **61**, 441 (1973).
37. S. Komiya, T. A. Albright, R. Hoffmann and J. K. Kochi, *J. Am. Chem. Soc.*, **99**, 8440 (1977).
38. E. G. Perevalova, K. I. Grandberg, V. P. Dyadchenko and T. V. Baukova, *J. Organomet. Chem.*, **217**, 403 (1981).
39. A. N. Nesmeyanov, E. G. Perevalova, E. I. Smyslova, V. P. Dyadchenko and K. I. Grandberg, *Izv. Akad. Nauk SSSR, Ser. Khim.*, 2610 (1977); *Chem. Abstr.*, **88**, 105500 (1978).
40. R. J. Puddephatt and I. Treurnicht, *J. Organomet. Chem.*, **319**, 129 (1987).
41. L. G. Vaughan, *J. Am. Chem. Soc.*, **92**, 730 (1970).
42. P. Jutzi and H. Heusler, *J. Organomet. Chem.*, **114**, 265 (1976).
43. K. Köhler, S. J. Silverio, I. Hyla-Krispin, R. Gleiter, L. Zsolnai, A. Driess, G. Huttner and H. Lang, *Organometallics*, **16**, 4970 (1997).
44. W. J. Pope and C. S. Gibson, *J. Chem. Soc.*, **91**, 2061 (1907).
45. M. S. Kharasch and H. S. Isbell, *J. Am. Chem. Soc.*, **53**, 2701 (1931).
46. A. Burawoy and C. S. Gibson, *J. Chem. Soc.*, 860 (1934).
47. A. Burawoy and C. S. Gibson, *J. Chem. Soc.*, 219 (1935).
48. H. Gilman and L. A. Woods, *J. Am. Chem. Soc.*, **70**, 550 (1948).
49. A. Burawoy, C. S. Gibson and S. Holt, *J. Chem. Soc.*, 1024 (1935).
50. W. L. G. Gent and C. S. Gibson, *J. Chem. Soc.*, 1835 (1949).
51. H. Schmidbaur and M. Bergfeld, *Inorg. Chem.*, **5**, 2069 (1966).
52. S. Komiya, J. C. Huffmann and J. K. Kochi, *Inorg. Chem.*, **16**, 2138 (1977).
53. S. Komiya and J. K. Kochi, *J. Am. Chem. Soc.*, **98**, 7599 (1976).
54. G. E. Coates and C. Parkin, *J. Chem. Soc.*, 421 (1963).
55. A. Tamaki and J. Kochi, *J. Organomet. Chem.*, **40**, C81 (1972).
56. A. Tamaki, S. A. Magennis and J. K. Kochi, *J. Am. Chem. Soc.*, **95**, 6487 (1973); **96**, 6140 (1974).
57. S. Komiya, S. Ozaki and A. Shibue, *J. Chem. Soc., Chem. Commun.*, 1555 (1986).
58. S. Komiya, T. A. Albright, R. Hoffmann and J. K. Kochi, *J. Am. Chem. Soc.*, **98**, 7255 (1976).
59. C. S. Gibson and J. L. Simonsen, *J. Chem. Soc.*, 2531 (1930).
60. C. E. Larson, T. H. Baum and R. L. Jackson, *J. Electrochem. Soc.*, **134**, 266 (1987).
61. T. H. Baum, *J. Electrochem. Soc.*, **134**, 2616 (1987).
62. R. B. Klassen and T. H. Baum, *Organometallics*, **8**, 2477 (1989).
63. M. Okumura, K. Tanaka, A. Ueda and M. Haruta, *Solid State Ionics*, **95**, 143 (1997).
64. P. W. J. de Graaf, J. Boersma and G. J. M. van der Kerk, *J. Organomet. Chem.*, **105**, 399 (1976).
65. R. Uson, A. Laguna and J. Buil, *J. Organomet. Chem.*, **85**, 403 (1975).
66. M. A. Bennett, S. K. Bhargava, D. C. R. Hockless, L. L. Welling and A. C. Willis, *J. Am. Chem. Soc.*, **118**, 10469 (1996).

67. R. Hüttel and A. Konietzny, *Chem. Ber.*, **106**, 2098 (1973).
68. C. F. Shaw, J. W. Lundeen and R. S. Tobias, *J. Organomet. Chem.*, **51**, 365 (1973).
69. P. L. Kuch and R. S. Tobias, *J. Organomet. Chem.*, **122**, 429 (1976).
70. H. Schmidbaur and R. Franke, *Inorg. Chim. Acta*, **13**, 79 (1975).
71. H. Schmidbaur and R. Franke, *Angew. Chem., Int. Ed. Engl.*, **12**, 416 (1973).
72. H. Schmidbaur and R. Franke, *Inorg. Chim. Acta*, **13**, 85 (1975).

CHAPTER **12**

Acidity, basicity and H bonds

THOMAS M. KLAPÖTKE

*Institute of Inorganic Chemistry, University of Munich (LMU), Meiserstrasse 1,
D-80333 Munich, Germany*
Fax: +49 89 5902 382;   e-mail: tmk@anorg.chemie.uni-muenchen.de

I. ABBREVIATIONS/NOMENCLATURE

The following abbreviations are used in addition to the well known abbreviations which are listed in each volume.

a_0	Bohr radius
BDE	bond dissociation energy
B15C5	benzo-15-crown-5
c	speed of light
cyclam	1,4,8,11-tetraazacyclotetradecane
FAB	fast atom bombardment (mass spectrometry)
L	8-hydroxyquinolinate (LH, protonated form)
Mes	mesityl
non-rel.	non-relativistic
py	pyridine
Q	$[Ag(PPh_3)(C_9H_6NOH)(C_9H_6NO)]$
quasi-rel.	quasi-relativistic

II. OUTLINE

The aim of this review is to focus on the acidity, basicity and H bonds, especially but not exclusively, with organoelement compounds of compounds containing silver and gold atoms. This chapter is not exhaustive in scope but rather consists of surveys of the most recent 15 years of work in this still developing field. This chapter highlights the most fascinating developments in the area outlined above but also contains most of the relevant references covering the past 15 years in this large, rather diverse field of academic and industrially related research.

III. INTRODUCTION

Considering the recent developments in the area of acidity, basicity and H bonds of silver and gold compounds it can be stated that in both Ag and Au chemistry a comparable amount of research has been carried out (cf Table 1). Although our intention is to highlight

TABLE 1. Number of papers published [REFERENCES] in the area of acidity, basicity and H bonds of silver and gold compounds in the time between 1981 and March 1997[a]

	Silver compounds	Gold compounds
Acidity	33 [1–31]	44 [12, 14, 20, 27, 76–107]
Basicity	19 [16, 32–43]	9 [78, 108–113]
H bonds	38 [44–75]	41 [114–154]

[a]Some references in the list of references are subdivided into parts (a), (b), (c), ..., therefore the actual number of references is higher than the numbers shown in the Table.

recent topics in the field of research outlined in Section II rather than to cover the area comprehensively, Table 1 gives an overview of the most important papers published within the last 15 years and provides the corresponding references.

IV. SILVER COMPOUNDS

A. Acidity

In a recent study the acid dissociation constants of substituted 1-amino-4-aryl-2(1H)-pyrimidinethiones of the type **1** and stability constants of their silver complexes have been measured pH-potentiometrically in a 75% (v/v) mixture of dioxane/water[11]. The influence of the substituents R^1 and R^2 on pK_a and lgβ_n values has been discussed[11].

In an interesting recent study it has been found that the IR spectral measurements of the uptake of hydrogen cyanide by the protonic form of a number of zeolites are sensitive to the variety of acid sites and structural features of the zeolite[16b]. The uptake of hydrogen cyanide by silver(I) ion-exchanged Y zeolite results in the reversible formation of silver cyanide and zeolite Brønsted acid[16a]. The other changes brought about by the addition of hydrogen cyanide to silver(I)-exchanged NaY are also reversible, since the bands are due to the formation of silver cyanide [2166 cm^{-1}, cf. AgCN, 2160 cm^{-1}, Ag$^+$(HCN), 2138 cm^{-1}, Ag$^+$(HCN)$_2$, 2147 cm^{-1}][16c] along with bands due to HCN at diminished pressure.
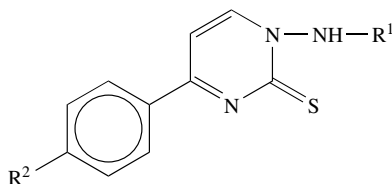
(1)

(1)   R^1 = H, PhCO, Ph, 4-O$_2$NC$_6$H$_4$ R^2 = H, n-C$_6$H$_{13}$O

B. Basicity

Silver ions promote the hydrolysis of thioacetals in dilute aqueous solutions (e.g. reaction 1)[34b,c].

$$RC_6H_4CH(SEt)_2 + 2Ag^+ + 3H_2O \longrightarrow RC_6H_4CHO + 2EtSAg + 2H_3O^+ \qquad (1)$$
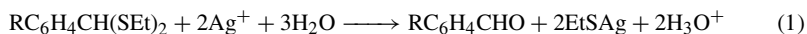
The reactions of open-chain thioacetals including **2** and **3** and others[34b,d] proceed at convenient rates for kinetic study at moderate silver ion concentrations and are very much faster than the corresponding hydrogen ion-catalyzed hydrolyses in dilute aqueous acid[34b]. Cyclic thioacetals, however, hydrolyze relatively very slowly and the silver ion-promoted hydrolysis of the cyclic analogues of **2** is inconveniently slow[34e]. Up to 1995 no cyclic S,S-acetal had been studied entirely satisfactorily from a kinetic viewpoint under silver ion promotion. Since acetal **3** was found[34d] to be significantly more reactive than **2** (R = H) Satchell and coworkers considered that appropriate 2-methyl-2-(substituted phenyl)-1,3-dithianes of the type **4** might prove to be sufficiently reactive for convenient kinetic study. This was found to be the case and, consequently, Satchell's group reported in a recent

paper on the behavior of the five acetals **4a−e** (equation 2)[34].

$$4 + 2Ag^+ + 3H_2O \longrightarrow RC_6H_4COCH_3 + AgS[CH_2]_3SAg + 2H_3O^+ \qquad (2)$$

(2)   **(3)**

(4)
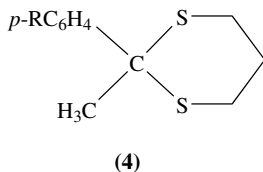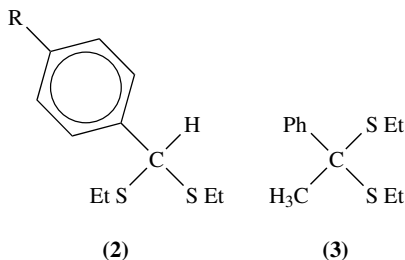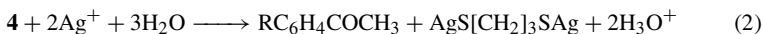
(4) **(a)** R = NO$_2$ **(b)** R = Cl **(c)** R = H **(d)** R = Me **(e)** R = MeO

It could be established that the hydrolysis of 1,3-dithianes derived from *para*-substituted acetophenones **(4)** is promoted by silver ions. Kinetic study using a 10% (v/v) dioxane/water solvent shows that, when [Ag$^+$] <0.2 mol L^{-1}, the *p*-NO$_2$, −Cl, −H and −Me derivatives hydrolyze via rapidly formed 1 Ag$^+$: 1 dithiane complexes, but that the *p*-MeO derivative forms an unreactive 1 : 1 complex and hydrolyses via a 2 Ag$^+$: 1 dithiane complex. Comparison of the kinetic parameters with those available for analogous open-chain *S,S*-acetals reveals that cyclization leads to a substantial (>10^4-fold) overall loss of reactivity and that this loss arises both from a lowering of acetal basicity toward Ag$^+$ and from a slower rate of hydrolysis of the 1 : 1 complex. The implications for hydrogen ion-catalyzed hydrolysis of cyclic acetals have been discussed, as have the reasons for the lower reactivity of the cyclic acetals[34a].

C. H Bonds

1. H bonded silver complexes

Interesting structural studies have concentrated on hydrogen bis[(8-quinolinol-N)(8-quinolinolato-N,O)(triphenylphosphine-P)silver(I)] complexes[45]. Crystallographic studies on AuL(LH), L = 8-hydroxyquinolinate, show the existence of short O···H···O′ hydrogen bonds [O···O 2.457 Å] between adjacent molecules[45b]. In the related Cu(II)L$_2$, a dimeric structure is found with the Cu atom forming a fifth bond to the O atom of a centrosymmetrically related molecule (Cu−O 2.830 Å)[45c]. The recent

structural study of the complex [Ag$_2$H(C$_9$H$_6$NO)$_2$(C$_9$H$_7$NO)$_2$(C$_{18}$H$_{15}$P)$_2$](C$_2$H$_3$O$_2$)H$_2$O (**5**) continues Othman's exploration of the reactions of the dimeric binuclear complex, bis[acetato(triphenylphosphine)silver(I)][45d,e].

(5)
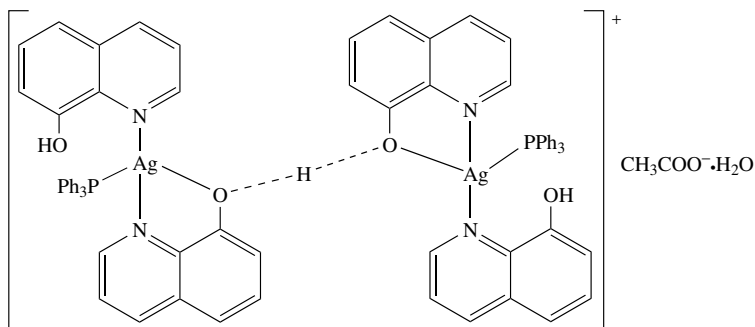
An interesting feature of compound **5** is the structure of the [QHQ]$^+$ cation. A displacement ellipsoid plot of one of the two independent Q residues is shown in Figure 1. In
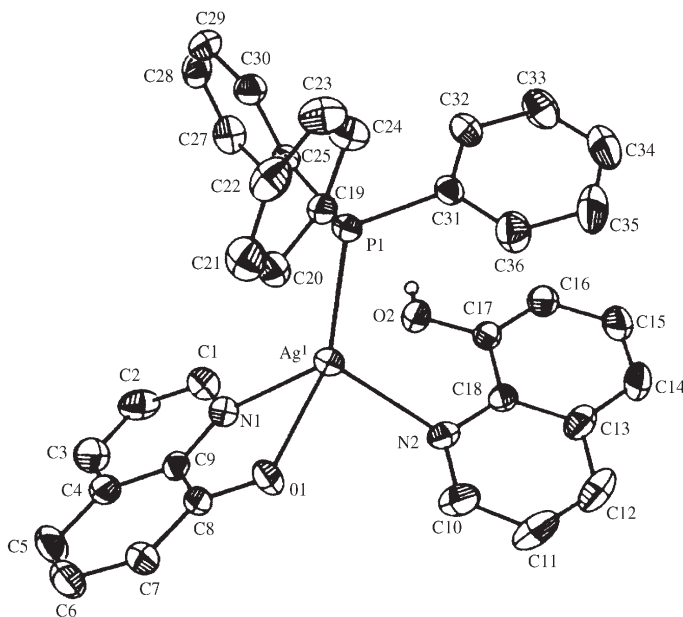
FIGURE 1. ORTEP diagram of an [Ag(PPh$_3$)(C$_9$H$_6$NO)(C$_9$H$_7$NO)] unit in **5**. Reproduced by permission of the International Union of Crystallography from Reference[45a]

each cation, equivalent Q residues are connected by a short hydrogen bond [O1A···O1A^i 2.452(5) and O1B···O1B^{ii} 2.463(6) Å]. In each case the proton lies on a center of inversion. The structure of compound **5** bears significant resemblance to that of hydrogen bis(1-methyl-2-quinolone)hexafluoroarsenate(V), where there is a similar short contact involving a hydrogen bond between the two quinolone moieties [O···O 2.439(12) Å][45f] although the hydrogen bond does not lie across a symmetry element.

In compound **5**, the quinoline ligands are planar. The acetate ion bridges the cations through O−H···O hydrogen bonds. There is also a short intermolecular contact between the solvent water molecule and one of the acetate O atoms. Hydrogen bonding involving the acatete ion and a water molecule has also been observed previously[45g].
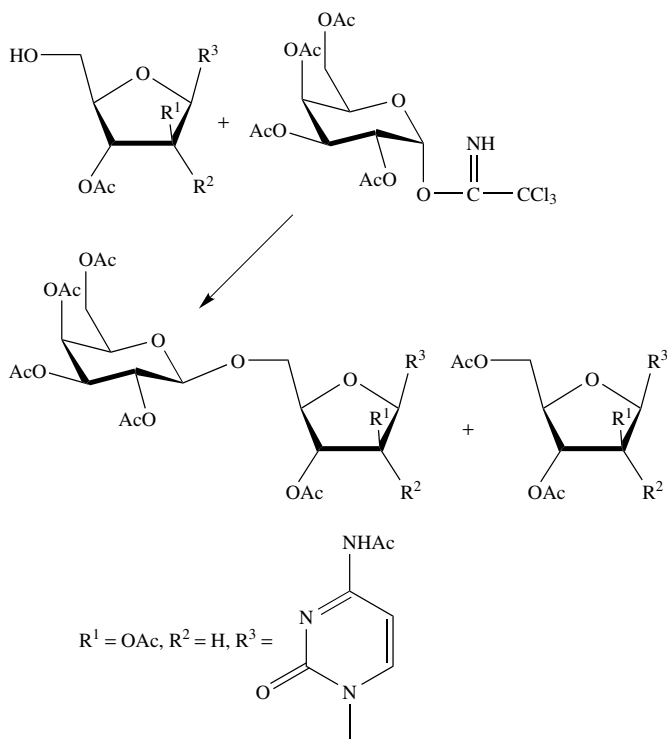
SCHEME 1. Galactosylation of nucleosidic O-5′H under silver triflate promotion. Reproduced by permission of the Canadian Chemical Society from Reference 64

2. Differential reactivity of carbohydrate hydroxyls in glycosylation reactions under silver triflate promotion

Quite recently, it has been established that silver triflate can be used as a promoter for direct galactosylation reactions[64]. Contrary to expectations, many primary hydroxy groups are completely unreactive in glycosylation reactions, or give the desired glycosides

in very low yields accompanied by products of many side reactions. Hydrogens such as primary hydroxyls are shown to be intramolecularly hydrogen bonded. Intermediates formed by nucleophilic attack by these hydroxyls on activated glycosylating agents may resist hydrogen abstraction. This resistance to proton loss is postulated to be the origin of the observed unreactivity. In the above-mentioned study[64] it has been shown that successful glycosylations take place under acidic conditions in which such hydrogen bonds cease to exist. Accordingly, direct galactosylations of the normally unreactive 5′-hydroxyls of nucleosides were accomplished for the first time with a galactose trichloroacetimidate donor in chloroform under silver triflate promotion (Scheme 1). It has been noted that such galactosylated anticancer nucleosides may have improved biological specificity[64].

V. GOLD COMPOUNDS

A. Acidity

1. General

Many homoleptic organogold compounds are Lewis acidic. For example, trimethylgold, prepared from gold(III) bromide and methyllithium, is stabilized by complexation with amines or tertiary phosphines, in $Me_3Au^{\bullet}L$. The dimeric compounds, $(R_2AuX)_2$, are prepared from $[Au(py)Cl_3]$ and methylmagnesium iodide[76].

Gold(I) derivatives, stabilized by complexation with tertiary phosphines, R_3PAuR, are obtained from the halides, $R_3P^{\bullet}AuX$, with organolithium or Grignard reagents. Examples are $(Me_3Si)_2CH-Au^{\bullet}L$ ($L = PPh_3$, $AsPh_3$). The triorganogold complexes, $R_3Au^{\bullet}L$, undergo reductive elimination, to form monovalent gold compounds, $RAu^{\bullet}L$[76].

The di- and tetramethylaurate anions, $[AuMe_2]^-$ and $[AuMe_4]^-$, are prepared from organolithium reagents (equations 3 and 4):

$$Me_3Au^{\bullet}PPh_3 + MeLi \longrightarrow Li^+[AuMe_4]^- \tag{3}$$

$$MeAu^{\bullet}PPh_3 + MeLi \longrightarrow Li^+[AuMe_2]^- \tag{4}$$
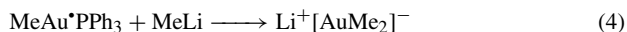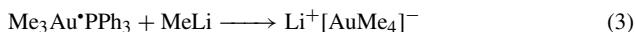
The former is linear, while the latter is square-planar. The anions are more thermally stable than neutral species, but less stable to oxidation.

The pentafluorophenyl derivatives of gold are also Lewis-acidic and include the neutral species, $(C_6F_5)_nA^{\bullet}PR_3$ ($n = 1$ or 3). The Lewis-basic phosphine ligand can be replaced either by a further C_6F_5 group or by a basic halide anion, X^-, to form the anionic species $[Au(C_6F_5)_n]^-$ ($n = 2$ or 4), $[(C_6F_5)_nAuX]^-$ ($n = 1$ or 3). Also the cationic complex, $[(PPh_3)(C_6F_5)_2Au-X-Au(C_6F_5)_2(PPh_3)]^+$, has been reported[76].

Gold compounds derived from phosphorus ylides also demonstrate the Lewis-basicity of (neutral) mono or tri coordinate gold(I) and gold(III) species. The following complexes have been reported: $Me_3Au-CH_2PMe_3$, $[Me_2Au(CH_2PMe_3)_2]Br$, $[Au(CH_2PMe_3)_2]^+X^-$ as well as several cyclic derivatives[76].

2. Gold(I) clusters

Reactions of $[Pt(AuPPh_3)_8](NO_3)_2$ with M(I) species (M = Cu, Au) under H_2-atmosphere yielded several new hydride-containing mixed-metal-gold phosphine cluster compounds. Two new hydride-containing PtAuCu clusters were obtained in this way: $[Pt(H)(CuCl)(AuPPh_3)_8](NO_3)$ (**6**) and $[Pt(H)(CuCl)_2(AuPPh_3)_8](NO_3)$ (**7**)[82]. Considerations of the solvent dependency show that the Brønsted acidity of the solvent used is crucial in controlling the formation of **6** and **7**. Clusters **6** and **7** were characterized

by elemental analyses, ICP analyses, and IR and NMR (^{31}P and ^{195}Pt) spectroscopy; their crystal structures have been determined by single-crystal X-ray analyses[82]. Compound **6** crystallizes in a monoclinic and compound **7** in a triclinic space group. Both clusters have a central platinum atom (Figures 2 and 3) surrounded by eight gold atoms and one (for **6**) or two (for **7**) copper atoms. The gold atoms are attached to triphenylphosphine ligands, whereas the copper atoms are attached to chlorine ligands. The crystal structures of **6** and **7** show that the copper atoms in these clusters are located trans to the hydride ligand.

The complex cation [Pt(H)(PPh$_3$)(CuCl)(AuPPh$_3$)$_6$]$^+$ (**8**) is obtained from the reaction of the cluster [Pt(H)(PPh$_3$)(AuPPh$_3$)$_7$](NO$_3$)$_2$ with [PPh$_3$CuCl]$_4$[82]. Compound **8** was characterized by IR, ^{1}H NMR, ^{31}P and ^{195}Pt NMR spectroscopy and by FAB-MS. Three different possible isomers for **8**, assuming its Pt(P)(M)$_7$ skeleton is derived from a spheroidal, cubic geometry, are shown in Figure 4.

3. MS studies on gold(I) and gold(III) derivatives

Fast atom bombardment (FAB) mass spectrometry of the gold(I) and gold(III) derivatives, {Au[C(Y)−NHAr]$_2$}$^+$X$^-$ and {Au[C(Y)−NHAr]$_2$I$_2$}$^+$X$^-$ (Y = −OC$_2$H$_5$ or −NHAr; X$^-$ = ClO$_4$$^-$ or BF$_4$$^-$; Ar = p-CH$_3$-C$_6H_4$) has led to the detection, for the alkoxyamino derivatives only, of [M − H]$^{+\bullet}$ molecular species[95a]. Both experimental
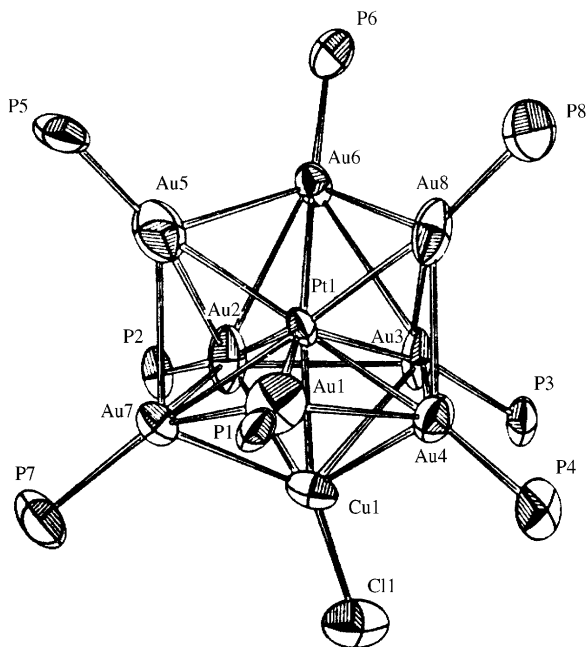
FIGURE 2. ORTEP plot of the structure of [Pt(H)(CuCl)(AuPPh$_3$)$_8$](NO$_3$) (**6**); phenyl rings and the NO$_3$$^-$ ion have been omitted for the sake of clarity. Reprinted with permission from Reference 82. Copyright 1995 American Chemical Society

FIGURE 3. ORTEP plot of the structure of $[Pt(H)(CuCl)_2(AuPPh_3)_8](NO_3)$ (**7**); phenyl rings and the NO_3^- ion have been omitted for the sake of clarity. Reprinted with permission from Reference 82. Copyright 1995 American Chemical Society

FIGURE 4. Three different possible isomers for compound **8**. Reprinted with permission from Reference 82. Copyright 1995 American Chemical Society

(mass spectrometry) and theoretical (*ab initio*) data indicate that $[M - H]^{+\bullet}$ formation is due to the reaction of M^+ with H^+-philic and/or $H^\bullet$-philic species produced from the matrix by FAB, whether the operative mechanism, the $[M - H]^{+\bullet}$ formation, is to be considered a FAB-induced oxidative process[95a].

When Au$^+$ is treated with acetyl fluoride, the predominant reaction channel corresponds to the formation of CH$_3$CO$^+$ and neutral AuF (Scheme 2a). This observation implies that BDE(AuF) >68 kcal mol^{-1}. Similarly, neutral AuF is formed in the reaction of Au$^+$ with methyl fluoroformate, which yields a lower bound for BDE(AuF) of 73 kcal mol^{-1} (Scheme 2b)[95b]. Since other reaction channels compete effectively with this reaction, abstraction from methyl fluoroformate is believed to occur near the threshold. However, because ΔH_f(FCO$_2$CH$_3$)[95c] is not as reliably known as ΔH_f(CH$_3$COF), the BDE value based on process (b) is subject to further refinement. The observation that various other R−F compounds do not give rise to neutral AuF and the corresponding organic cations R$^+$ (e.g. R = CH$_3$, C$_2$H$_5$, CFCl$_2$, CF$_2$Cl, CF$_2$Br, CHF$_2$, CF$_3$, c-C$_6$F$_5$, CH$_2$CH$_2$OH, and SF$_5$)[95d−f] permits an estimate of the upper limit of BDE(AuF). An upper bound for BDE(AuF) of 85 kcal mol^{-1} results from the absence of the formation of C$_2$H$_5$$^+$ in the ion−molecule reaction of Au$^+$ with ethyl fluoride (Scheme 2c). Furthermore, since in this reaction C$_2$H$_5$$^+$ is not even found if excited Au$^+$ cations are used, the upper bound of 85 kcal mol^{-1} will be considerably too high.

(a) Au$^+$ + CH$_3$COF
- $\xrightarrow{0.94}$ CH$_3$CO$^+$ + AuF
- $\xrightarrow{0.05}$ Au(CH$_2$CO)$^+$ + HF
- $\xrightarrow{0.01}$ AuCH$_2$$^+$ + HF + CO

(b) Au$^+$ + CH$_3$OCOF
- $\xrightarrow{0.02}$ COF$^+$ + AuOCH$_3$
- $\xrightarrow{0.18}$ CH$_3$OCO$^+$ + AuF
- $\xrightarrow{0.60}$ AuCH$_2$$^+$ + HF + CO$_2$
- $\xrightarrow{0.02}$ Au(CH$_2$O)$^+$ + HF + CO
- $\xrightarrow{0.18}$ Au(CH$_3$)F$^+$ + CO$_2$

(c) Au$^+$ + C$_2$H$_5$F
- $\xrightarrow{0.55}$ CH$_3$CHF$^+$ + AuH
- $\xrightarrow{0.45}$ Au(C$_2$H$_4$)$^+$ + HF
- $\xrightarrow{\times}$ C$_2$H$_5$$^+$ + AuF
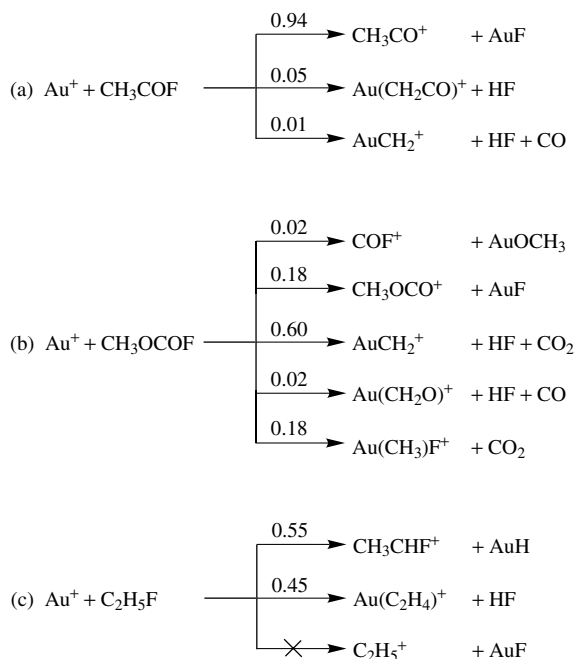
SCHEME 2. Ion−molecule reactions with Au$^+$. Reproduced by permission of VCH Verlagsgesellschaft mbH from Reference 95b

4. Gold(III) complexes

The hitherto unreported Au(III) macrocyclic polyamine complexes **18−23** with cyclam (1,4,8,11-tetraazacyclotetradecane, **9**), phenol-pendant cyclam **10**, pyridyl-pendant cyclam

11, monooxocyclam **12**, phenol-pendant monooxocyclam **13** and pyridyl-pendant monoox-ocyclam **14** have been synthesized and characterized[96]. Dissociation of a proton from one of the secondary amines in the Au(III) in cyclam complexes **18**, **19** and **20** readily occurs with pK_a values of 5.0–5.4 at 25 °C and $I = 0.1$ (NaClO$_4$). Although monoox-ocyclam **12** does not accommodate Au(III), the donor-pendant monooxocyclams **13** and **14** enclose Au(III) with concomitant dissociation of an amide proton to yield **22** and **23**, respectively[96]. As anticipated for the diamagnetic d^8 complexes, the pendant donors only weakly interact from an axial site. The extraordinary acidity of Au(III) over other com-mon metal ions in interaction with cyclam can be utilized for selective uptake of Au(III) with lipophilic cyclam derivatives **15** and **16**[96].

(9)   (10)   (11)

(12)   (13)   (14)
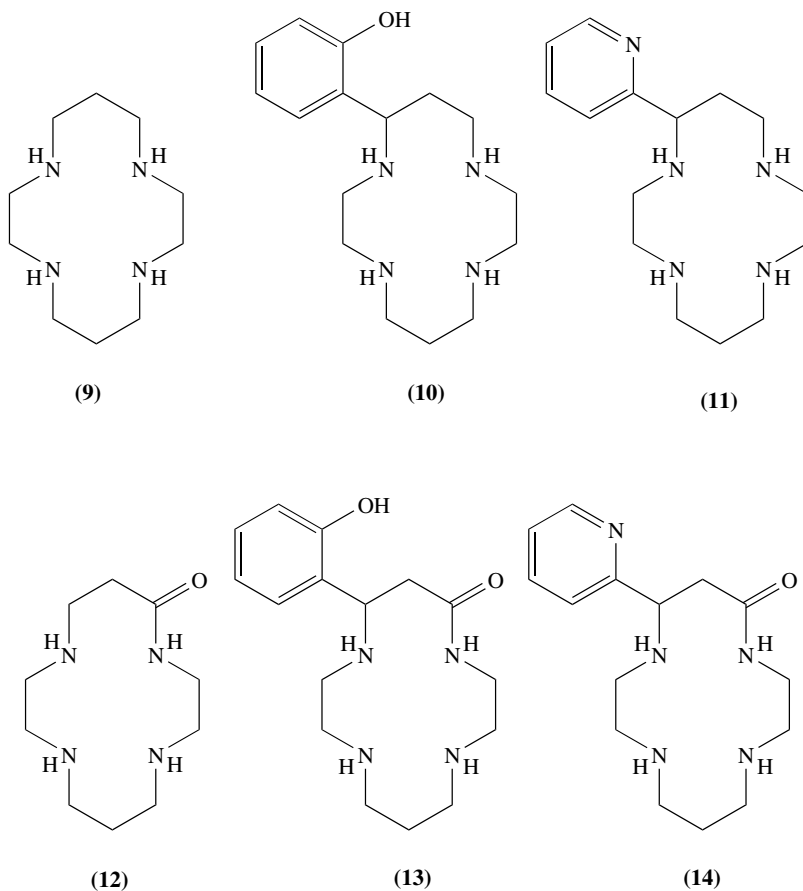
In another recent study it has been established that gold(III) can be extracted efficiently into 1,2-dichloroethane with benzo-15-crown-5 (B15C5) from an aqueous solution con-taining hydrochloric acid and potassium ion[97]. It was found that a bulky ion pair is formed
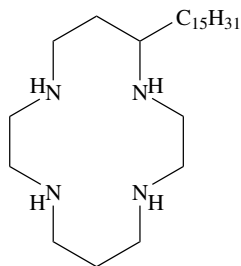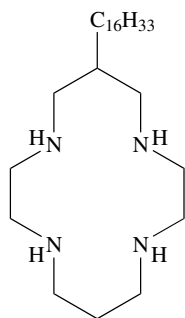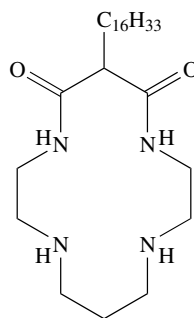
(15)   **(16)**   **(17)**
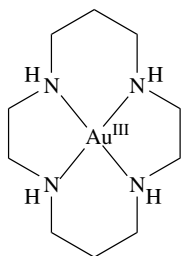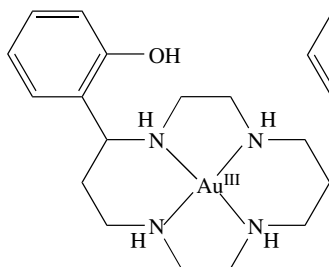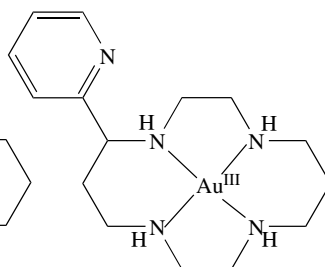
(18)   **(19)**   **(20)**
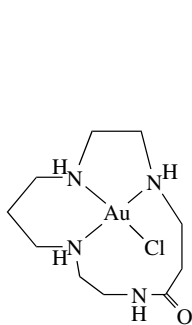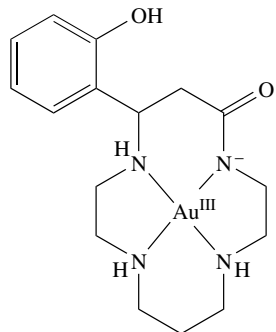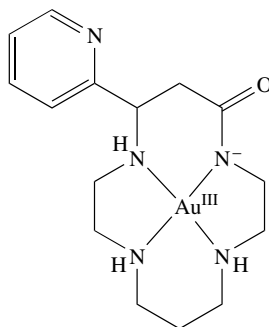
(21)   **(22)**   **(23)**

by association of a potassium–crown ether complex cation and complex anion $AuCl_4^-$ in the organic phase. The effects of acidity, temperature and other metal ions on the extraction have been studied. The apparent extraction equilibrium constant K_{ex} has been

measured to be 2.7×10^7 at 15 °C and the enthalpy change ΔH for the extraction process to be -28.4 kJ mol^{-1}. The crystalline extracted complex was characterized by elemental analysis, IR and UV-vis spectra, and its composition was found to be K(B15C5)$_2$AuCl$_4$[97].

5. Gold(I) carbonyl cations

No chapter on Lewis-acidic gold complexes would be complete without reference to the relatively recent and interesting work on gold carbonyl complexes[102]. Solutions of gold tris(fluorosulfate), Au(SO$_3$F)$_3$, in fluorosulfuric acid, HSO$_3$F, had been recognized previously[103] as strong monoprotonic acids, with the weakly basic tetrakis(fluorosulfato)aurate(III) ion, [Au(SO$_3$F)$_4$]$^-$, capable of stabilizing a number of strong electrophilic cations[104]. The seemingly low oxidizing power of Au(III) in this system suggested a possible use in the protonation of weakly basic, readily oxidizable carbon monoxide. In 1990 Aubke and Willner reported on the reaction behavior of carbon monoxide in the superacid HSO$_3$F−Au(SO$_3$F)$_3$[102]. While the interaction ultimately led to gold(I) carbonyl fluorosulfate, Au(CO)SO$_3$F, which was isolated and characterized, there was also strong evidence for the formation of the novel, linear cation [(OC)Au(CO)]$^+$[102].

In 1992 the synthesis of the bis(carbonyl)gold(I) salt, [Au(CO)$_2$][Sb$_2$F$_{11}$], was achieved in a two-step procedure: the reduction of gold(III) fluorosulfate, Au(SO$_3$F)$_3$, in HSO$_3$F to give Au(CO)SO$_3$F as an intermediate, followed by solvolysis in liquid antimony(V) fluoride in the presence of carbon monoxide[105]. The compound is thermally stable up to 130 °C. The cation is linear, and all seven fundamentals, three Raman and four IR active modes, have been observed. The near absence of gold to carbon π-back donation in [Au(CO)$_2$]$^+$ is manifested in strong carbon−oxygen bonds and consequently rather weak gold−carbon bonds, reflected in the highest CO-stretching frequencies so far observed for a metal carbonyl derivative with 2254(ν_1) and 2217(ν_3) cm^{-1}. In the ^{13}C NMR spectrum a single-line resonance at 174 ppm was attributed to [Au(CO)$_2$]$^+$[105]. Attempts to recrystallize [Au(CO)$_2$][Sb$_2$F$_{11}$] from acetonitrile resulted in the formation of single crystals of [Au(NC-CH$_3$)$_2$][SbF$_6$] instead[105,106a].

Whereas the original route to [Au(CO)$_2$][Sb$_2$F$_{11}$] is a multistep procedure that involves corrosive reagents and requires commercially unavailable starting materials (see above), quite recently the same authors reported two general simplifications: (i) the sole use of liquid antimony(V) fluoride as reaction medium in a single-step carbonylation process, and (ii) the use of the commercially available chloride AuCl$_3$ as starting material. The simplified route makes [Au(CO)$_2$][Sb$_2$F$_{11}$] more easily available for wider use in synthetic chemistry[106b].

6. Gold isocyanide and gold methanide complexes

The reaction of (MeNC)-, (PhNC)- and (MesNC)AuCl in tetrahydrofuran with an equimolar amount of the corresponding Lewis-basic isonitrile ligand and one equivalent of Ag$^+$X$^-$ (X$^-$ = BF$_4$$^-$ or CF$_3$SO$_3$$^-$) lead to the formation of the bis(isonitrile)gold(I) complexes (MeNC)$_2$Au$^+$ CF$_3$SO$_3$$^-$, (PhNC)$_2Au^+BF_4$$^-$ and (MesNC)$_2$Au$^+$BF$_4$$^-$. The crystal structures of all three compounds have been determined. In compound (MeNC)$_2$Au$^+$CF$_3$SO$_3$$^-$ there are rod-like cations with a parallel packing into meandering puckered layers, in which the gold atoms have alternating Au−Au contacts of 3.611 and 3.624 Å. In complex (PhNC)$_2$Au$^+$BF$_4$$^-$ the cations form long double-paddles, with the two paddles at an angle of 77.5°. The individual cations are well separated and have no sub-van-der-Waals Au−Au contacts. The crystal structure of compound

$(MesNC)_2Au^+BF_4^-$ is similar, but with a smaller dihedral angle between the planes of the two mesityl rings $(56.0°)^{107a}$.

Treatment of $[Au(\mu\text{-}Cl)(C_6F_5)_2]_2$ with vinylidenebis(diphenylphosphine), $(PPh_2)_2$ $C{=}CH_2$, leads to the compound $[Au(C_6F_5)_2Cl\{PPh_2C(=CH_2)PPh_2\}]$. The coordination of the diphosphine to a gold(III) center strongly activates the carbon–carbon bond, and this Lewis-acidic complex, therefore, undergoes Michael-type additions with several carbon-, sulfur- or oxygen-based nucleophiles. The complexes $[Au(C_6F_5)_2\{(PPh_2)_2CCH_2SPh\}]$, $[Au(C_6F_5)_2\{(PPh_2)_2CCH_2S_2CNEt_2\}]$ and $[\{Au(C_6F_5)_2\{(PPh_2)_2CCH_2\}\}_2O]$ have been structurally characterized by X-ray diffraction analysis. They show that the addition has taken place at the terminal carbon atom of the double bond, giving methanide-type complexes. Furthermore, the displacement of the ether molecules in $[Au(C_6F_5)_2(OR_2)_2]ClO_4$ (R = Et, i-Pr) by the diphosphine yielded, in a one pot synthesis, the complex $[Au(C_6F_5)_2\{(PPh_2)_2CHCH_2OR\}]ClO_4$ as a consequence of ether cleavage by water[107b].

B. Basicity

The gold(I) complexes $[(LAu)_3(\mu_3\text{-}O)]BF_4$ have recently been reported for L = $PMePh_2$, **24**; PPh_3, **25**; P(o-Tol)_3, **26** and were structurally characterized by single-crystal X-ray diffraction studies (Figure 5)[110]. The PPh_3 and the $PMePh_2$ structures consist of inversion-related edge-bridged $[(LAu)_3O]^+$ dimers held together by Au–Au interactions. The P(o-Tol)_3 structure consists of isolated $[(LAu)_3O]^+$ units.

The reaction of tris[(triphenylphosphane)gold]oxonium tetrafluoroborate with phosphane gas in tetrahydrofuran led to a mixture of products, one of which has been isolated and identified as the complex $\{[(Ph_3P)_6Au_5]P\}^{2+}(BF_4^-)_2$ **(27)**[109]. This cluster can be described as an adduct of $[(Ph_3PAu)_4P]^+$ and $[(Ph_3P)_2Au]^+$. Crystals of **(27)**_2 Et_2O contain two crystallographically independent formula units of very similar structure (Figure 6). The dications are centered by pentacoordinate phosphorus atoms in an irregular coordination geometry. In the crystal, one of the five gold atoms is attached to two triphenylphosphane ligands, while the other four bear one such ligand. In solution, rapid ligand exchange renders the ligands equivalent on the NMR time scale. The stoichiometry and structure of **27** are indicative of the strong basicity of the $[(Ph_3PAu)_4P]^+$ cation probably owing to its square-pyramidal structure with strong Au$\cdots$Au bonding, as suggested by the structure of its arsenic analogue[109].

Another interesting reaction is the carbon–carbon coupling via nucleophilic addition of a gold(I) methanide complex to heterocumulenes[113b]. The methanide carbon of $[Au(C_6F_5)(PPh_2CHPPh_2Me)]$ acts as a nucleophilic center toward reagents such as carbon disulfide and isothiocyanates, affording $[Au(III)\{PPh_2C(PPh_2Me)C(X)S\}_2][Au(I)(C_6F_5)_2]$ (X = S, 4-ClC_6H_4N, PhN) through a carbon–carbon coupling reaction. The X-ray structure of compound $[Au(III)\{PPh_2C(PPh_2Me)C(S)S\}_2][Au(I)(C_6F_5)_2]$ shows the ligand $PPh_2C(PPh_2Me)C(S)S$ acting as a bidentate P,S-chelate[113b].

C. H Bonds

Reaction of (t-BuNC)AuCl with sodium thiosalicylate in the two-phase system water/dichloromethane gave high yields of the corresponding (isocyanide)gold(I) complex **28**. The solid state structure of **28** has been determined by X-ray diffraction analysis (Figure 7)[115]. The supramolecular structure of compound **28** is governed by Au$\cdots$Au interactions [3.157(2) Å] and hydrogen bonding through the carboxylic acid groups.

(a)

(b)

(c)

FIGURE 5. ORTEP drawings of compounds (a) **24**, (b) **25**, (c) **26**. Reprinted with permission from Reference 110. Copyright 1993 American Chemical Society

FIGURE 6. Molecular structure of the gold/phosphorus core in the two crystallographically independent dications $\{[(Ph_3P)Au]_4PAu(PPh_3)_2\}^{2+}$. Reproduced by permission of VCH Verlagsgesellschaft mbH from Reference 109

FIGURE 7. Tetrameric unit of **28** aggregated via Au$\cdots$Au and hydrogen bonds. Reprinted with permission from Reference 115. Copyright 1996 American Chemical Society

Quite recently, Anderson and coworkers reported the synthesis and molecular structures of dppm-bridged complexes of Pt(II) with linear Au(I), trigonal Ag(I) and tetrahedral Hg(II) centers[124]. The complexes [PtR(dppm-P,P)(dppm-P)]PF$_6$ (R = Me, Et, Ph) react with [AuCl(SMe$_2$)] to generate the dppm-bridged Pt$-$Au complexes *trans*-[PtClR(μ-dppm)$_2$Au]PF$_6$ **(29)**. Addition of [PtR(dppm-P,P)(dppm-P)]Cl to a solution of Ag(I) acetate, followed by acetyl chloride, yielded the neutral Pt$-$Ag species *trans*-[PtClR(μ-dppm)$_2$AgCl] **(30)**[aa]. The crystal structures of the methyl derivatives of **29** and **30** (CHCl$_3$ solvates) have been determined by X-ray diffraction (Figure 8). Complex **29** exhibits approximate square-planar geometry at Pt and linear geometry at Au. The geometry of compound **30** is again square-planar at Pt, whereas the geometry at Ag is approximately trigonal planar. The pyramidal distortion taken together with a long Ag$-$Cl bond [2.610(4) Å] has been discussed in the context of C$-$H$\cdots$Cl hydrogen bonding and a possible incipient Pt$\cdots$Ag interaction.

A new synthesis of *cis*-Me$_4$N[Au(C$_6$H$_4$NO$_2$-2)$_2$Cl$_2$] **(31)** has been reported, involving the reaction of [Hg(C$_6$H$_4$NO$_2$-2)Cl] with Me$_4$N[AuCl$_4$] in the presence of Me$_4$NCl[129] (Scheme 3). Reaction of **31** with NaOPh or with Tlacac (acac = acetylacetonate) in the presence of NaClO$_4$ yields Na[Au(C$_6$H$_4$NO$_2$-2)$_2$(OPh)$_2$] **(32)** or *cis*-[Au(C$_6$H$_4$NO$_2$-2)$_2$(O,O-acac)] **(33)**, respectively. Complex **35** reacts with PPh$_3$ to give *trans*-[Au(C$_6$H$_4$NO$_2$-2)$_2$(C-acac)(PPh$_3$)] **(34)**. Treatment of **32** in acetone with NaOH gives [Au(C$_6$H$_4$NO$_2$-2)$_2$(μ-OH)]$_2$ **(37)**, which is also formed when a solution of **33** in CHCl$_3$/hexane is exposed to water. The crystal structure of **35**$\cdot$2Et$_2$O (Figure 9) shows that it is a centrosymmetric dimer with two hydroxo groups bridging two Au(C$_6$H$_4$NO$_2$-2) moieties. The features of the structure include short Au$-$C bond distances [1.992(5) Å, 1.995(5) Å] and hydrogen bonding between the bridging OH groups and diethyl ether molecules.

The compound [Ph$_3$PAu{SC(NHMe)$_2$}]$^+$Cl$^-\cdot$SC(NHMe)$_2$ **(36)** was prepared from the chloro(organophosphine)gold(I) complex and the urea homologue SC(NHMe)$_2$ in good

FIGURE 8. Molecular structures of **29** (top) and **30** (bottom) depicting H-bonding interactions. Reprinted with permission from Reference 124. Copyright 1996 American Chemical Society

$Me_4N(AuCl_4) + 2(Hg(C_6H_4NO_2\text{-}2)Cl) + 2\ Me_4NCl$

$\downarrow -\ (Me_4N)_2[Hg_2Cl_6]$

SCHEME 3. Synthesis of some (μ-hydroxo-, phenoxo- and O,O-acetylacetonato-arylgold(III) complexes. Reprinted from Reference 129 with kind permission from Elsevier Science S.A.

yield[68]. The crystal structure of **36** shows short N$\cdots$Cl and N$\cdots$S contacts that probably correspond to hydrogen bonding (Figure 10).

(Triphenylphosphine)(selenourea)gold(I) chloride $[Ph_3PAuSeC(NH_2)_2]^+Cl^-$ **(37)** and the corresponding dppm derivative $dppm[AuSeC(NH_2)_2]_2{}^{2+}\ 2\,Cl^-$ **(38)** were prepared from $SeC(NH_2)_2$ and the appropriate chloro(phosphine)gold(I) complex[151]. The reaction between **37** and aqueous Na_2CO_3 leads to the neutral complex (μ-selenido{bis[(triphenylphosphine)gold(I)]} $(Ph_3PAu)_2Se$ **(39)**. X-ray structure analyses of

FIGURE 9. The structure of compound **35** in the crystal. Reprinted from Reference 129 with kind permission from Elsevier Science S.A.

FIGURE 10. The cation of compound **36** in the crystal; H atoms are omitted. Reproduced by permission of Verlag der Zeitschrift der Naturforschung from Reference 68

37, **38** and **39** confirm the expected linear geometry at the gold atom (Figures 11–13) and reveal short intermolecular Au–Au contacts for **38** and **39**. Short nonbonding distances between the nitrogen atoms of the amino groups and the chloride ions in the crystal structures of **37** and **38** probably indicate hydrogen bonds.

FIGURE 11. One of the two independent cations of compound 37. Reproduced by permission of VCH Verlagsgesellschaft mbH from Reference 151

FIGURE 12. The dication of compound **38**. Reproduced by permission of VCH Verlagsgesellschaft mbH from Reference 151

FIGURE 13. The molecular structure of compound **39**. Reproduced by permission of VCH Verlagsge-sellschaft mbH from Reference 151

VI. RELATIVISTIC EFFECTS

It was not until the 1970s that the full relevance of relativistic effects in heavy-element chemistry was discovered. However, for the sixth row (W$\cdots$Bi), relativistic effects are comparable to usual shell-structure effects and therefore provide an explanation for many unusual properties of gold chemistry[155−159]. The main effects on atomic orbitals are (i) the relativistic radial contraction and energetic stabilization of the s and p shells, (ii) the spin−orbit splitting and (iii) the relativistic radial expansion and energetic destabilization of the outer d and f shells.

A. The Relativistic Contraction

Relativistic effects[160] increase, for all electrons, like Z^4 and, for valence shells, roughly like Z^2. For example, let us compare the radial 1s shrinkage for the elements Cu, Ag and Au (the latter two are the subject of this chapter). The nonrelativistic limit for a 1s electron is Z au (cf $c = 137$ au). Thus the 1s electron of copper has v/c of $29/137 \approx 0.21$, whereas these values are 0.34 for silver and 0.58 for gold [c is the finite speed of light and v is the average radial velocity of the electrons in the 1s shell (v is roughly Z au)]. As the relativistic mass increase is given by equation 5 with the effective Bohr radius defined by equation 6, the radial 1s shrinkage for copper and silver is 2 or 6%, respectively, whereas

TABLE 2.   M−C bond lengths (Å) in MCH$_3$, MC$_6$H$_5$ and M(CH$_3$)$_2$$^-$ for M = Cu, Ag and Au[161a]

M	Method	MCH$_3$	MC$_6$H$_5$	M(CH$_3$)$_2$$^-$
Cu	Relativistic calculation	1.866	1.850	1.922
	Nonrelativistic calculation	1.923		1.963
	Experimental			1.935
Ag	Relativistic calculation	2.111	2.091	
Au	Relativistic calculation	2.017	1.981	

it is as much as 19% (!) for gold.

$$m = \frac{m_0}{\sqrt{1 - (v/c)^2}} \tag{5}$$

$$a_0 = \frac{4\pi\varepsilon_0}{(\hbar^2/me^2)} \tag{6}$$

It was also proposed that the significant s and p orbital contraction at row four (Cu) is caused by the post-transition metal effect (d contraction), caused by an increase of the effective nuclear charge for the 4s electrons due to filling the first d shell (3d). A similar interpretation is possible for the row six (Au). This effect is commonly called lanthanoid contraction due to the effect of filling the 4f shell. The traditional explanation for the smaller size of gold (compared to Ag) is the lanthanoid contraction. However, this effect is only sufficient to cancel the shell-structure expansion, to make Au (nonrelativistic) similar to Ag (nonrelativistic).

A marked reduction in the lengths of covalent bonds involving gold atoms is often found on moving from nonrelativistic to relativistic calculations[161a]. In a density-functional study of MCH$_2$$^+$ (M = Ni, Pd, Pt, Ir and Au), Heinemann and coworkers[161b] calculated a nonrelativistic Au−C distance of 2.153 vs 1.867 Å relativistically. The DFT calculations on Au$_2$ find a 0.206 Å shortening of the Au−Au bond vs equivalent nonrelativistic Hartree−Fock−Slater (HFS) calculations[161c]. Furthermore, relativistic calculations consistently predict shorter gold covalent bond lengths than equivalent calculations on silver compounds. Table 2 presents M−C bond lengths in MCH$_3$, MC$_6$H$_5$ and M(CH$_3$)$_2$$^-$ for M = Cu, Ag and Au[161d]. The calculated Au−C distances in AuCH$_3$ and AuC$_6$H$_5$ are approximately 0.1 Å shorter than in the silver analogues.

B. The Spin−Orbit Splitting

In a relativistic treatment neither the orbital angular momentum l nor the spin angular momentum s of an electron are 'good' quantum numbers, but the vector sum still is (equation 7)[160].

$$\mathbf{j} = \mathbf{l} + \mathbf{s} \tag{7}$$

Thus we get for a p electron, $l = 1$, the two possible values $j = 1/2$ and $j = 3/2$, denoted as p$_{1/2}$ and p$_{3/2}$. The energetic splitting between these two j values is a relativistic effect and may rise up to a few eV for the valence electrons of the heaviest elements.

C. The Relativistic Self-consistent Expansion

The d and f electrons have high angular moment and seldom descend to the neighborhood of the nucleus where they would reach high velocities[161e]. The main relativistic effects are therefore indirect. Because the s and p AOs, both inside and outside the d and f AOs, have contracted, they screen the nuclear attraction more efficiently. Therefore, the d and f AOs 'see' a weaker attraction, expand radially, and are destabilized energetically.

D. Silver and Gold

Nowhere in the periodic table are the relativistic effects more pronounced than in gold chemistry[161a]. Figure 14 depicts the relativistic contraction of the 6s shell in the elements Cs ($Z = 55$) to Fm ($Z = 100$)[156,162]. The contraction increases considerably while the 4f shell is being filled and strikingly when the 5d shell is filled. The pronounced local maximum of the contraction at gold, $(5d)^{10}(6s)^1$, makes Au a unique element, even from this point of view. Figure 15 illustrates the nonrelativistic and quasi-relativistic energetic level of the Au frontier orbitals and demonstrates nicely how close the 6s and 5d orbitals are in energy in the relativistic picture. In agreement with this, the yellow color of gold can also be attributed to a relativistic effect[159]. The absorption is attributed to the 5d-to-Fermi level transitions which set in around 2.3 eV in Au. Thus gold reflects the red and yellow and strongly absorbs the blue and violet. The 4d–5s distance of silver is much larger, due to weaker relativistic effects (NB: The nonrelativistic electronic band structures of the two metals are very similar)[163].

The chemical difference between silver and gold has received a great deal of attention during the history of chemistry[164]. It seems to be mainly a relativistic effect[165]. The relativistic effects push the s and p AOs down in energy (effect i) and the d AOs up (effect iii, cf Figure 15). Moreover, the d AOs suffer a spin–orbit splitting (effect ii). All three effects are much larger for Au than for Ag. The relativistic contraction of the Au 6s
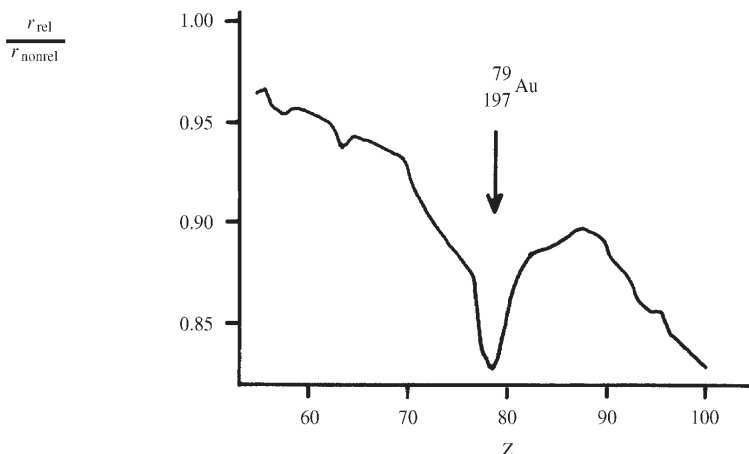
FIGURE 14. The relativistic contraction of the 6s shell in the elements Cs to Fm. Reproduced by permission of VCH Verlagsgesellschaft mbH from Reference 159
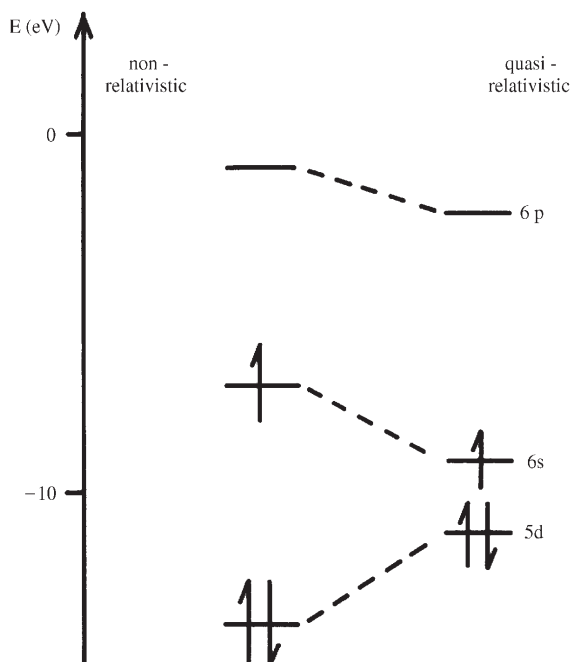
FIGURE 15. Non-relativistic and quasi-relativistic level of the gold frontier orbitals. Reproduced by permission of VCH Verlagsgesellschaft mbH from Reference[159]

shell explains qualitatively the shorter and stronger covalent bonds, as well as the larger ionization potential and electron affinity of gold[166a,b]. The relativistic destabilization of the Au 5d shell explains qualitatively the trivalence of gold. Besides this energetic effect, the larger radial extension of the 5d shell may also play a role[167].

E. The Aurophilicity of Gold

Though the strong aurophilicity of gold which leads to cluster formation may not be described by Lewis basicity in the classical definition, the formation of clusters containing direct Au–Au interactions falls within the scope of the relativistic discussion in this chapter[161a].

Closed-shell metal cations such as Au^I ($[Xe]4f^{14}5d^{10}$) would normally be expected to repeal one another. By the end of the 1980s, however, there was sufficient crystallographic evidence of attractions between gold(I) cations to lead Schmidbaur to introduce the term 'aurophilic attraction' or 'aurophilicity'[168]. Given that so much of gold chemistry is influenced by relativity, it was natural to inquire as to whether the aurophilic attraction is also a relativistic effect. Görling's group[169] used Ellis's DV-Xα density functional method to study the electronic structure of a fascinating series of gold cluster compounds, the main-group-element-centered octahedral complexes [{(H_3P)Au}$_6X_m$]$^{m+}$ ($X_1 = B$, $X_2 = C$, $X_3 = N$). These compounds, which may be formally regarded as containing gold(I)

cations, feature quite short 'aurophilic' Au−Au distances. Much of the study focused on the role of the gold 5d AOs in Au−Au bonding. d-Orbital participation can, of course, be achieved only if the formal d^{10} configuration is broken, e.g. through 6s/5d hybridization. The conclusion was that there is a prominent contribution of the gold 5d AOs to the Au−Au bonding within the cluster, via 6s/5d hybridization in the MOs of a_{1g} symmetry. Furthermore, it was argued that the effect has its origin in the relativistic modification of the gold valence AO energies, which brings the 5d and 6s orbitals into close energetic proximity.

VII. ACKNOWLEDGMENTS

VIII. REFERENCES

1. M. Ziyad, S. Arsalane, M. Kacimi, G. Coudurier, J. M. Millet and J. C. Vedrine, *Appl. Catal.*, **147**, 363 (1996).
2. X. C. Guo and R. J. Madix, *ACS Symp. Ser.*, **638**, 357 (1996).
3. A. N. Pestryakov, *Catal. Today*, **28**, 239 (1996).
4. A. S. L. Lee and Y. S. Li, *Spectrochim. Acta, Part A*, **52**, 173 (1996).
5. J. Ishikawa, H. Sakamoto, T. Mizuno and M. Otomo, *Bull. Chem. Soc. Jpn.*, **68**, 3071, (1995).
6. V. Gruver, A. Sun and J. J. Fripiat, *Catal. Lett.*, **34**, 359 (1995).
7. Y. Katayama, R. Hagiwara and Y. Ito, *J. Fluorine Chem.*, **74**, 89 (1995).
8. C. F. Mao and M. A. Vannice, *Appl. Catal.*, **122**, 61 (1995).
9. K. C. Sole, T. L. Ferguson and J. B. Hiskey, *Solvent Extraction and Ion Exchange*, **12**, 1033 (1994).
10. A. N. Pestryakov, M. I. Roznina and V. N. Belousova, *Russ. J. Appl. Chem.*, **66**, 1742 (1993).
11. S. Schmidt, F. Dietze, E. Hoyer, G. Zahn, J. Liebscher and B. Riemer, *J. Prakt. Chem.*, **336**, 500 (1994).
12. O. G. Vokina, L. P. Shaulina, I. P. Golentovskaya and S. V. Amosova, *Russ. J. Appl. Chem.*, **66**, 1629 (1993).
13. M. Noel and S. Chidambaram, *J. Fluorine Chem.*, **68**, 121 (1994).
14. K. Pyrzynska, *J. Anal. Atom. Spectrom.*, **9**, 801 (1994).
15. A. N. Pestryakov, V. N. Belousova and M. I. Roznina, *Russ. J. Appl. Chem.*, **66**, 941 (1993).
16. (a) C. J. Blower and T. D. Smith, *J. Chem. Soc., Faraday Trans.*, **90**, 931 (1994);
    (b) C. J. Blower and T. D. Smith, *J. Chem. Soc., Faraday Trans.*, **90**, 919 (1994).
    (c) M. F. A. Dove and J. G. Hallett, *J. Chem. Soc., A*, 2781 (1969).
17. T. Baba, M. Nomura, Y. Ono and Y. Ohno, *J. Phys. Chem.*, **49**, 12888 (1993).
18. V. M. Mastikhin, *Coll. Surf., Part A*, **78**, 143 (1993).
19. R. Garner, J. Yperman, J. Mullens and L. C. Vanpoucke, *Fresenius Z. Anal. Chem.*, **347**, 145 (1993).
20. W. J. Bruckard, G. J. Sparrow and J. T. Woodcock, *Hydrometallurgy*, **33**, 17 (1993).
21. R. Garner, J. Yperman, J. Mullens and L. C. Vanpouckle, *Bull. Soc. Chim. Belg.*, **102**, 3 (1993).
22. R. Garner, J. Yperman, J. Mullens and L. C. Vanpoucke, *Fresenius Z. Anal. Chem.*, **345**, 473 (1993).
23. H. K. Shin, M. J. Hampdensmith and E. N. Duesler, *Can. J. Chem.*, **70**, 2954 (1992).
24. L. Frunza, E. Pop, G. Pop, R. Ganea, R. Birjega, L. Milwa and I. Fota, *Rev. Roum. Chim.*, **37**, 803 (1992).
25. S. D. Nikolic, E. B. Milosavljevic, J. L. Hendrix and J. H. Nelson, *Analyst*, **117**, 47 (1992).
26. S. T. Oh, K. Kim and M. S. Kim, *J. Phys. Chem.*, **95**, 8844 (1991).
27. F. T. Awadalla and G. M. Ritcey, *Separation Sci. Technol.*, **26**, 1207 (1991).

28. P. K. Wrona, T. M. Krygowski and Z. Galus, *J. Phys. Org. Chem.*, **4**, 439 (1991).
29. A. G. Fogg, S. P. Scullion, T. E. Edmonds and B. J. Birch, *Analyst*, **116**, 573 (1991).
30. S. J. Xia and D. P. Cheng, *Acta Chim. Sinica*, **48**, 251 (1990).
31. V. N. Belousova, O. G. Kuznetsova and L. N. Kurina, *J. Appl. Chem. USSR*, **57**, 857 (1984).
32. T. Wakasugi, A. Hirota, J. Fukunaga and R. Ota, *J. Non-Cryst. Solids*, **210**, 141 (1997).
33. K. Yata, N. Hanyu and T. Yamaguchi, *J. Am. Ceram. Soc.*, **78**, 1153 (1995).
34. (a) T. F. Mohiuddin, D. P. N. Satchell and R. S. Satchell, *J. Chem. Soc., Perkin Trans. 2*, 163 (1995).
    (b) D. P. N. Satchell and R. S. Satchell, *Chem. Soc. Rev.*, **19**, 55 (1990).
    (c) D. P. N. Satchell and R. S. Satchell, *J. Chem. Res. (S)*, 102 (1989).
    (d) D. Penn, Z. Saidi, D. P. N. Satchell and R. S. Satchell, *J. Chem. Res. (S)*, 200 (1987).
    (e) D. P. N. Satchell and R. S. Satchell, *J. Chem. Soc., Perkin Trans. 2*, 513 (1987).
35. T. Murai, M. Yamamoto, S. Kondo and S. Kato, *J. Org. Chem.*, **58**, 7440 (1993).
36. M. Gabryszewski, *Pol. J. Chem.*, **67**, 1509 (1993).
37. M. P. Byfield, M. S. A. Hamza and J. M. Pratt, *J. Chem. Soc., Dalton Trans.*, 1641 (1993).
38. K. Yata and T. Yamaguchi, *J. Am. Ceram. Soc.*, **75**, 2910 (1992).
39. P. K. Wrona, T. M. Krygowski and Z. Galus, *J. Phys. Org. Chem.*, **4**, 439 (1991).
40. F. Fontana, F. Minisci, M. C. N. Barbosa and E. Vismara, *J. Org. Chem.*, **56**, 2866 (1991).
41. R. Ludwig, S. Fischer, R. Dreyer, R. Jacobi and J. Beger, *Polyhedron*, **10**, 11 (1991).
42. D. J. Min and R. J. Fruehan, *Metall. Trans. B*, **21**, 1025 (1990).
43. B. Barszcz, M. Gabryszewski, J. Kulig and B. Lenarcik, *J. Chem. Soc., Dalton Trans.*, 2025 (1986).
44. W. Schneider, A. Bauer and H. Schmidbaur, *J. Chem. Soc., Dalton Trans.*, 415 (1997)
45. (a) A. H. Othman, S. C. Goh, H. K. Fun and K. Sivakumar, *Acta Crystallogr., Sect. C*, **52**, 2760 (1996).
    (b) J. E. Fleming and H. Lynton, *Can. J. Chem.*, **46**, 471 (1968).
    (c) G. J. Palenik, *Acta Crystallogr.*, **17**, 687 (1964).
    (d) S. W. Ng and A. H. Othman, *Z. Kristallogr.*, **210**, 674 (1995).
    (e) A. H. Othman, H. K. Fun and K. Sivakumar, *Acta Crystallogr., Sect. C*, **52**, 843 (1996).
    (f) M. Calleri and J. C. Speakman, *J. Chem Soc., A*, 1644 (1969).
    (g) M. Perello, N. Verdaguer, J. Aymamie and I. Fita, *J. Chem. Cryst.*, **24**, 597 (1994).
46. Y. C. Chang and T. T. Chem, *Chin. J. Phys.*, **34**, 1352 (1996).
47. M. Yamamoto, N. Furuyama and K. Itoh, *J. Phys. Chem.*, **100**, 18483 (1996).
48. J. E. Pemberton, S. L. Joa, A. J. Shen and K. J. Woelfel, *J. Chem. Soc., Faraday Trans.*, **92**, 3683 (1996).
49. A. D. Burrows, D. M. P. Mingos, A. J. P. White and D. J. Williams, *J. Chem. Soc., Dalton Trans.*, 3805 (1996).
50. Q. Huang, X. T. Wu, T. L. Sheng, Q. M. Wang and J. X. Lu, *Polyhedron*, **16**, 217 (1997).
51. C. F. Xu, G. K. Anderson, L. Brammler, J. Braddockwilking and N. P. Rath, *Organometallics.*, **15**, 3972 (1996).
52. H. W. Schmalle, R. Pellaux and S. Decurtins, *Z. Kristallogr.*, **211**, 533 (1996).
53. A. Krasnopoler, N. Kizhakevariam and E. M. Stuve, *J. Chem. Soc., Faraday Trans.*, **92**, 2445 (1996).
54. T. Nabeshima, *Coord. Chem. Rev.*, **148**, 151 (1996).
55. Y. H. Zhang, Q. S. Li, Z. X. Xie, B. Z. Hua, B. W. Mao, Y. Z. Chen and Z. W. Tian, *Thin Solid Films*, **274**, 150 (1996).
56. Q. Huang, X. T. Wu, T. L. Sheng and Q. W. Wang, *Acta Crystallogr., Sect. C*, **52**, 29 (1996).
57. M. L. A. Temperini, M. R. Dossantos and V. R. P. Monteiro, *Spectrochim. Acta, Part A*, **51**, 1517 (1995).
58. S. E. Jayaraj and V. Ramakrishnan, *Spectrochim. Acta, Part A.*, **51**, 979 (1995).
59. A. Krasnopoler, A. L. Johnson and E. M. Stuve, *Surf. Sci.*, **328**, 186 (1995).
60. D. Philip and G. Aruldhas, *J. Solid State Chem.*, **116**, 427 (1995).
61. S. E. M. Colaianni, J. Aubard, S. H. Hansen and O. F. Nielsen, *Vibrational Spectrosc.*, **9**, 111 (1995).
62. D. Philip and G. Aruldhas, *J. Solid State Chem.*, **114**, 129 (1995).
63. T. Burchard, P. Firman, H. Schneider and B. G. Cox, *Ber. Bunsenges. Phys. Chem.*, **98**, 1534 (1994).

64.   D. M. Whitfield, S. P. Douglas, T. H. Tang, I. G. Csizmadia, H. Y. S. Pang, F. L. Moolten and J. J. Krepinsky, *Can. J. Chem.*, **72**, 2225 (1994).

65.   C. Y. Xu, T. S. Corbitt, M. J. Hampdensmith, T. T. Kodas and E. N. Duesler, *J. Chem. Soc., Dalton Trans.*, 2841 (1994).

66.   D. Philip, G. Aruldhas, T. Osaka and A. Miyazaki, *J. Solid State Chem.*, **110**, 92 (1994).

67.   E. Mieczynska, A. M. Trzeciak, J. J. Ziolkowski and T. Lis, *Polyhedron*, **13**, 655 (1994).

68.   W. Eikens, P. G. Jones, J. Lautner and C. Thone, *Z. Naturforsch., Sect. B*, **49**, 21 (1994).

69.   J. S. Gordon and D. C. Johnson, *J. Electroanal. Chem.*, **365**, 267 (1994).

70.   I. Weissbuch, J. Majewski, K. Kjaer, J. Alsnielsen, M. Lahav and L. Leiserowitz, *J. Phys. Chem.*, **97**, 12848 (1993).

71.   T. H. Ong, P. B. Davies and C. D. Bain, *Langmuir*, **9**, 1836 (1993).

72.   X. M. Chen and T. C. W. Mak, *J. Crystallogr. Spectrosc. Res.*, **23**, 291 (1993).

73.   J. M. Bello, V. A. Narayanan and T. Vodinh, *Spectrochim. Acta, Part A*, **48**, 563 (1992).

74.   M. Capdevila, W. Clegg, P. Gonzalezduarte and I. Mira, *J. Chem. Soc., Dalton Trans.*, 173 (1992).

75.   M. Buchner, *Phys. Rev. B*, **44**, 5309 (1991).

76.   I. Haiduc and J. J. Zuckerman, *Basic Organometallic Chemistry*, Walter de Gruyter, Berlin, New York, 1985, p. 373.

77.   (a) P. G. Fernandez, H. G. Linge and M. W. Wadsley, *J. Appl. Electrochem.*, **26**, 575 (1996).
      (b) M. Wells, D. L. Dermody, H. C. Yang, T. Kim, R. M. Crooks and A. J. Ricco, *Langmuir*, **12**, 1989 (1996).

78.   H. C. Yang, D. L. Dermody, C. J. Xu, A. J. Ricco and R. M. Crooks, *Langmuir*, **12**, 726 (1996).

79.   Z. Chang, L. Qiu, J. R. Chen, X. Lin and B. L. He, *Separation Sci. Technol.*, **30**, 3299 (1995).

80.   A. Arribas, C. G. Cunningham, J. J. Rytuba, R. O. Rye, W. J. Kelly, M. H. Podwysocki, E. H. McKee and R. M. Tosdal, *Econ. Geol. Bull. Soc. Econ. Geol.*, **90**, 795 (1995).

81.   Z. X. Su, Q. S. Pu, X. Y. Luo, X. J. Chang, G. Y. Zhan and F. Z. Ren, *Talanta*, **42**, 1127 (1995).

82.   T. G. M. M. Kappen, P. P. J. Schlebos, J. J. Bour, W. P. Bosman, J. M. M. Smits, P. T. Beurskens and J. J. Steggerda, *Inorg. Chem.*, **34**, 2133 (1995).

83.   L. P. Plyusnina, G. G. Likhoidov, G. P. Zaraisky and T. B. Afanaseva, *Petrology*, **3**, 189 (189).

84.   T. M. Salama, T. Shido, H. Minagawa and M. Ichikawa, *J. Catal.*, **152**, 322 (1995).

85.   F. Mistry and F. Aubke, *J. Fluorine Chem.*, **68**, 239 (1994).

86.   X. J. Chang, Z. X. Su, G. Y. Zhan, X. Y. Luo and W. Y. Gao, *Analyst*, **119**, 1445 (1994).

87.   S. D. T. Axford and T. M. Herrington, *J. Chem. Soc., Faraday Trans.*, **90**, 2085 (1994).

88.   B. W. Zhang, Y. Zhang, M. Grote and A. Kettrup, *Reactive Polymers*, **22**, 115 (1994).

89.   M. Parent, R. Cornelis, R. Dams and F. Alt, *Anal. Chim. Acta*, **281**, 153 (1993).

90.   S. Kumar, R. Verma and S. Gangadharan, *Analyst*, **118**, 1085 (1993).

91.   M. Nakazawa and G. A. Somorjai, *Appl. Surf. Sci.*, **68**, 517 (1993).

92.   T. M. Sun and W. T. Yen, *Minerals Eng.*, **6**, 17 (1993).

93.   V. V. Yakshin, O. M. Vilkova, L. T. Makarova, N. A. Tsarenko and A. A. Podmarenkov, *Sov. Radiochem.*, **34**, 382 (1992).

94.   G. Moutiers, M. Cassir and J. Devynck, *J. Electroanal. Chem.*, **315**, 103 (1991).

95.   (a) G. Banditelli, A. L. Bandini, G. Pacchioni, G. Minghetti, R. Seraglia and P. Traldi, *Org. Mass Spectrom.*, **26**, 945 (1991).
      (b) D. Schröder, J. Hrusak, I. C. Tornieporth-Oetting, T. M. Klapötke and H. Schwarz, *Angew. Chem., Int. Ed. Engl.*, **33**, 212 (1994).
      (c) S. W. Benson, *Thermochemical Kinetics*, 2nd ed., Wiley, New York, 1976.
      (d) W. L. Grady and M. M. Bursey, *Int. J. Mass Spectrom. Ion. Phys.*, **52**, 247 (1983).
      (e) D. A. Weil and C. L. Wilkins, *J. Am. Chem. Soc.*, **107**, 7316 (1985).
      (f) A. K. Chowdhury and C. L. Wilkins, *J. Am. Chem. Soc.*, **109**, 5336 (1987).

96.   E. Kimura, Y. Kurogi and T. Takahashi, *Inorg. Chem.*, **30**, 4117 (1991).

97.   Y. Hongwu, Z. Zhixian, Z. Mingrui, Z. Xianxin and R. Boyang, *Polyhedron*, **10**, 1025 (1991)

98.   S. K. Xu, L. J. Sun and Z. L. Fang, *Anal. Chim. Acta*, **245**, 7 (1991).

99.   G. Moutiers, M. Cassir, C. Piolet and J. Devynck, *Electrochim. Acta*, **36**, 1063 (1991).

100. Y. Fouquet, U. Vonstackelberg, J. L. Charlou, J. P. Donval, J. Erzinger, J. P. Foucher, P. Herzig, R. Muhe, S. Soakai, M. Wiedicke and H. Whitechurch, *Nature*, **349**, 6312 (1991).

101. F. Scherbaum, B. Huber, G. Müller and H. Schmidbaur, *Angew., Chem., Int. Ed. Engl.*, **11**, 1542 (1988).

102. H. Willner and F. Aubke, *Inorg. Chem.*, **29**, 2195 (1990).

103. K. C. Lee and F. Aubke, *Inorg. Chem.*, **18**, 389 (1979).
104. K. C. Lee and F. Aubke, *Inorg. Chem.*, **19**, 119 (1980).
105. H. Willner, J. Schaebs, G. Hwang, F. Mistry, R. Jones, J. Trotter and F. Aubke, *J. Am. Chem. Soc.*, **114**, 8972 (1992).
106. (a) F. Aubke, *J. Fluorine Chem.*, **72**, 195 (1995).
    (b) C. Q. Wang, S. C. Siu, G. Hwang, C. Bach, B. Bley, M. Bodenbinder, H. Willner and F. Aubke, *Can. J. Chem.*, **74**, 1952 (1996).
107. (a) W. Schneider, A. Sladek, A. Bauer, K. Angermaier and H. Schmidbaur, *Z. Naturforsch.*, **52b**, 53 (1997).
    (b) E. J. Fernandez, M. C. Gimeno, P. G. Jones, A. Laguna and E. Olmos, *Organometallics*, **16**, 1130 (1997).
    (c) G. A. Bowmaker, H. Schmisbaur, S. Krüger and N. Rösch, *Inorg. Chem.*, **36**, 1754 (1997).
    (d) D.-A. Feng, S. S. Tang, C. W. Liu, I. J. B. Lin, Y.-S. Wen and L.-K. Liu, *Organometallics*, **16**, 901 (1997).
108. K. Sugiyama, Y. Nakano, H. Souri, E. Konuma and T. Matsuda, *J. Mater. Chem.*, **4**, 1897 (1994).
109. H. Beruda, E. Zeller and H. Schmidbaur, *Chem. Ber.*, **126**, 2037 (1993).
110. Y. Yang, V. Ramamoorthy and P. R. Sharp, *Inorg. Chem.*, **32**, 1946 (1993).
111. A. S. Gunale, M. P. Jensen, D. A. Phillips, C. L. Stern and D.F. Shriver, *Inorg. Chem.*, **31**, 2622 (1992).
112. S. Ahrland, S. Balzamo and I. Persson, *Acta Chem. Scand.*, **46**, 259 (1992).
113. (a) L. Canovese, L. Cattalini, M. Tomaselli and M. L. Tobe, *J. Chem. Soc., Dalton Trans.*, 307 (1991).
    (b) M. Bardaji, M. C. Gimero, P. G. Jones, A. Laguna, M. Laguna, F. Merchan and I. Romeo, *Organometallics*, **16**, 1083 (1997).
114. M. Wells, D.L. Dermody, H.C. Yang, T. Kim, R.M. Crooks and A.J. Ricco, *Langmuir*, **12**, 1989 (1996).
115. W. Schneider, A. Bauer and H. Schmidbaur, *Organometallics*, **15**, 5445 (1996).
116. W. Schneider, A. Bauer and H. Schmidbauer, *J. Chem. Soc., Dalton Trans.*, 415 (1997).
117. H. Z. Yu, Y. Q. Wang, S. M. Cai and Z. F. Liu, *Ber. Bunsenges. Phys. Chem.*, **101**, 257 (1997).
118. J. M. Forward, R. J. Staples, C. W. Liu and J. P. Fackler, *Acta Crystallogr., Sect. C*, **53**, 195 (1997).
119. B. Roelfs, E. Bunge, C. Schroter, T. Solomun, H. Meyer, R. J. Nichols and H. Baumgartel, *J. Phys. Chem. B*, **101**, 754 (1997).
120. D. B. Yang and T. Wakamatsu, *Surf. Interface Anal.*, **24**, 803 (1996).
121. J. E. Pemberton, S. L. Joa, A. J. Shen and K. J. Woelfel, *J. Chem. Soc., Faraday Trans.*, **92**, 3683 (1996).
122. A. Wesch, O. Dannenberger, C. Woll, J. J. Wolff and M. Buck, *Langmuir*, **12**, 5330 (1996).
123. R. S. Clegg and J. E. Hutchison, *Langmuir*, **12**, 5239 (1996).
124. C. F. Xu, G. K. Anderson, L. Brammer, J. Braddockwilking and N. P. Rath, *Organometallics*, **15**, 3972 (1996).
125. F. Arias, L. A. Godinez, S. R. Wilson, A. E. Kaifer and L. Echegoyen, *J. Am. Chem. Soc.*, **118**, 6086 (1996).
126. M. Steinbeck and H. Ringsdorf, *J. Chem. Soc., Chem. Commun.*, 1193 (1996).
127. M. C. Parker, M. C. Davies and S. J. B. Tendler, *J. Vac. Sci. Technol., B*, **14**, 1432 (1996).
128. Y.Z. Gao, T. Zhu, M. Tang, S.M. Cai and Z.F. Liu, *Chem. J. Chin. Univ.*, **16**, 120 (1995).
129. J. Vicente, M. D. Bermudez, F. J. Carrion and P. G. Jones, *J. Organomet. Chem.*, **508**, 53 (1996).
130. M. Niwa, T. Mori and N. Higashi, *Macromolecules*, **28**, 7770 (1995).
131. M. L. A. Temperini, M. R. Dossantos and V. R. P. Monteiro, *Spectrochim. Acta, Part A*, **51**, 1517 (1995).
132. J. L. Keddie, R. A. L. Jones and R. A. Cory, *Faraday Discuss. Chem. Soc.*, **98**, 219 (1994).
133. S. E. Creager and C. M. Steiger, *Langmuir*, **11**, 1852 (1995).
134. T. Boland and B. D. Ratner, *Proc. Natl. Acad. Sci. U.S.A.*, **92**, 5297 (1995).
135. Y. Shibasaki, A. Seki and N. Takeishi, *Thermochim. Acta*, **253**, 103 (1995).
136. W. Kautek, M. Sahre and D.M. Soares, *Ber. Bunsenges. Phys. Chem.*, **99**, 667 (1995).
137. D. Philip and G. Aruldhas, *J. Solid State Chem.*, **116**, 427 (1995).
138. R. M. Crooks, O. Chailapakul, C. B. Ross, L. Sun and J. K. Schoer, *ACS Symp. Ser.*, **561**, 104 (1994).
139. J. A. Roush, D. L. Thacker and M. R. Anderson, *Langmuir*, **10**, 1642 (1994).

140. W. Eikens, P. G. Jones, J. Lautner and C. Thone, *Z. Naturforsch., Sect. B*, **49**, 21 (1994).
141. J. S. Gordon and D. C. Johnson, *J. Electroanal. Chem.*, **365**, 267 (1994).
142. L. M. Frostman, M. M. Bader and M. D. Ward, *Langmuir*, **10**, 576 (1994).
143. V. N. Morozov, N. C. Seeman and N. R. Kallenbach, *Scanning Micros.*, **7**, 757 (1993).
144. M. A. S. Goher, A. E. H. Abdou, W. H. Yip and T. C. W. Mak, *Polyhedron*, **12**, 1879 (1993).
145. T. H. Ong, P. B. Davies and C. D. Bain, *Langmuir*, **9**, 1836 (1993).
146. L. Sun, R. M. Crooks and A. J. Ricco, *Langmuir*, **9**, 1775 (1993).
147. P. D. Cookson and E. R. T. Tiekink, *J. Cryst. Spectrosc. Res.*, **23**, 231 (1993).
148. L. Bertilsson and B. Liedberg, *Langmuir*, **9**, 141 (1993).
149. L. Sun, L. J. Kepley and R.M. Crooks, *Langmuir*, **8**, 2101 (1992).
150. J. N. Glosli and M. R. Philpott, *J. Chem. Phys.*, **96**, 6962 (1992).
151. P. G. Jones and C. Thone, *Chem. Ber.*, **124**, 2725 (1991).
152. J. Hautman, J. P. Bareman, W. Mar and M. L. Klein, *J. Chem. Soc., Faraday Trans.*, **87**, 2031 (1991).
153. P. Zelenay, G. Horanyi, C. K. Rhee and A. Wieckowski, *J. Electroanal. Chem.*, **300**, 499 (1991).
154. H. A. O. Hill, D. J. Page and N. J. Walton, *J. Electroanal. Chem. Interfacial Electrochem.*, **208**, 395 (1986).
155. K. S. Pitzer, *Acc. Chem. Res.*, **12**, 271 (1979).
156. P. Pyykkö and J. P. Desclaux, *Acc. Chem. Res.*, **12**, 276 (1979).
157. P. Pyykkö, *Chem. Rev.*, **88**, 563 (1988).
158. T. M. Klapötke and A. Schulz, *Quantenmechanische Methoden in der Hauptgruppenchemie*, Spektrum, Heidelberg, 1996, pp. 79, 155, 174.
159. T. M. Klapötke and I. C. Tornieporth-Oetting, *Nichtmetallchemie*, VCH, Weinheim, 1994, p. 71.
160. A. Sommerfeld, *Ann. Phys.*, **51**, 1 (1916).
161. (a) N. Kaltsoyannis, *J. Chem. Soc., Dalton Trans.*, 1 (1997).
      (b) C. Heinemann, R. H. Hertwig, R. Wesendrup, W. Koch and H. Schwarz. *J. Am. Chem. Soc.*, **117**, 495 (1995).
      (c) T. Bastug, D. Heinemann, W. D. Sepp, D. Kolb and B. Fricke, *Chem. Phys. Lett.*, **211**, 119 (1993).
      (d) I. Antes and G. Frenking, *Organometallics*, **14**, 4263 (1995).
      (e) D. F. Mayers, *Proc. R. Soc. London, Ser. A*, **241**, 93 (1957).
162. J. P. Desclaux, *At. Data Nucl. Data Tables*, **12**, 311 (1973).
163. (a) K. E. Saeger and J. Rodies, *Gold Bull.*, **10**, 10 (1977).
      (b) N. E. Christensen and B. O. Seraphin, *Phys. Rev. B*, **4**, 3321 (1971).
164. E. v. Meyer, *Geschichte der Chemie*, von Weit, Leipzig, 1905.
165. J. P. Desclaux and P. Pyykkö, *Chem. Phys. Lett.*, **39**, 300 (1976).
166. (a) *Handbook of Chemistry and Physics*, 57th edn., CRC Press, Cleveland, OH, 1976.
      (b) E. C. M. Chen and W. E. Wentworth, *J. Chem. Educ.*, **52**, 486 (1975).
167. P. Schwerdtfeger, M. Dolg, W. H. E. Schwarz, G. A. Bowmaker and P. D. W. Boyd, *J. Chem. Phys.*, **91**, 1762 (1989).
168. (a) H. Schmidbaur, F. Scherbaum, B. Huber and G. Müller, *Angew. Chem., Int. Ed. Engl.*, **27**, 419 (1988).
      (b) H. Schmidbaur, *Gold Bull.*, **23**, 1 (1990).
169. A. Görling, N. Rösch, D. E. Ellis and H. Schmidbaur, *Inorg. Chem.*, **30**, 3986 (1991).

CHAPTER **13**

Rearrangement of gold and silver complexes

SUNING WANG

Department of Chemistry, Queen's University, Kingston, Ontario, K7L 3N6, Canada
Fax: 613-5456669;   e-mail: wangs@chem.queensu.ca

and

JOHN P. FACKLER, JR.

Department of Chemistry, Texas A&M University, College Station, TX 77843-3012, USA
Fax: 409-8452373;   e-mail: fackler@mail.chem.tamu.edu

I. INTRODUCTION

There has been an enormous growth in the volume of chemistry produced on organic derivatives of gold and silver during the past two decades. Interesting rearrangement reactions involving gold have been discovered, but to date very little detailed mechanistic understanding of these rearrangements has developed. Rearrangements of organic complexes of silver are even less well understood, although photographic film producers undoubtedly have observed many interesting examples[1]. The ready reduction of the gold

and silver compounds to the elements, especially in the presence of light, often makes detailed reaction mechanism studies difficult.

The developing interest in the potential of gold systems for catalysis[2] suggests that increased effort will take place over the next few years to understand special features of this element's chemistry, such as aurophilic behavior, lack of binary Au−H bonding, dynamic rearrangements of clusters and the effect of the relativistic contraction of the d-orbitals on ligand bonding. The rearrangement reactions that have been studied and which are described here are extremely varied. Much remains to be understood in this chemistry.

II. REARRANGEMENTS OF ORGANOGOLD COMPOUNDS

The rearrangement reactions of organogold compounds can be classified into three categories: (A) Rearrangements of gold(I) compounds; (B) Rearrangements of gold(III) compounds; (C) Rearrangement reactions involving a change in oxidation state. Some of the rearrangement reactions are dynamic and reversible while others are irreversible chemical rearrangements, both of which will be covered herein. The rearrangement reactions of gold compounds will be presented in the order of the three categories given above. In each category, the reactions are organized into subgroups with the emphasis on representative types of rearrangement reactions but not on all known facts of rearrangement reactions of gold compounds.

A. Rearrangements of Gold(I) Compounds

The common coordination geometry of gold(I) compounds is linear. Three-coordinate or four-coordinate gold(I) compounds, albeit not typical, have also been observed frequently[3]. The ability of the gold(I) ion to form two-, three- and even four-coordinate species is often responsible for many of the dynamic phenomena of gold(I) compounds.

(1)   **(2)**

(a) Au−S bonds: The shuttle motion of Au(ttp)Cl (ttp = trithiapentalene). Symmetrically substituted trithiapentalene molecules have a symmetrical structure **(1)** in solution and the solid state unless they are sterically crowded. Upon the coordination of a gold(I) moiety such as AuCl, Au(PPh$_3$)$^+$, an unsymmetrical structure **(2)** was observed in the solid state. In solution, however, the gold(I) complexes of ttp were found to be highly fluxional with an activation energy of *ca* 8 kcal mol^{-1}[4]. An intramolecular shuttle motion of the gold(I) moiety on the ttp ligand was proposed to be responsible for the observed fluxional process. Molecular orbital analyses by Ruiz and Alvarez suggested that a three-coordinate intermediate and a two-coordinate intermediate are likely involved in the process (Scheme 1)[5]. The high affinity of gold(I) toward sulfur atoms and its ability to be two- and three-coordinate obviously played a key role in the shuttle motion of the ttp complexes of gold(I).

SCHEME 1

(b) *Au−C bonds: The cyclic motion of* $Au(\eta^1\text{-}C_5H_4R)(PR'_3)$ *and* $Au(\eta^1\text{-}C_5R_5)(PR'_3)$. The cyclopentadienyl and its derivative gold(I) complexes, $Au(\eta^1\text{-}C_5H_4R)(PR'_3)$ and $Au(\eta^1\text{-}C_5R_5)(PR'_3)$ (R = H or Me; R′ = Me, Et, *i*-Pr or Ph), have a linear structure in the solid state[6]. However, in solution, they were found to be highly fluxional with the $Au(PR'_3)^+$ unit moving rapidly between carbon atoms of the η^1-cyclopentadienyl group, a phenomenon well known with other η^1-cyclopentadienyl metal derivatives (Scheme 2).
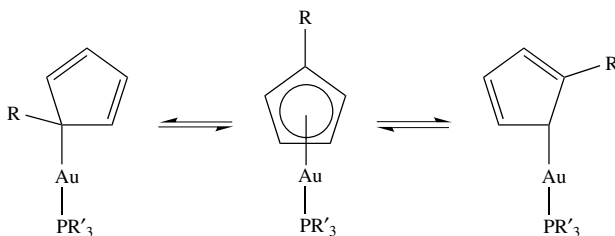
SCHEME 2

(c) *Au−C bonds: Metathesis of mononuclear gold(I) complexes.* Several examples of ligand metathesis involving gold(I) complexes have been reported, including[7] $Au(PR_3)(CN)$, $Au(mpt)(CN)$ (mpt = 1-methylpyridine-2-thione), $[Au(SR)(CN)]^-$ and gold(I) complexes of heterocyclic ligands such as isothiazolinylidene and 1-methylimidazolyl (Scheme 3)[8]. The species involved in the metathesis reactions are in equilibrium in solution. The metathesis of these gold(I) complexes has been attributed

to the labile nature of gold(I). Interesting metathesis of the anionic gold(I) complex $Au(mtp)_2^-$ [mtp $= CH_2P(S)Ph_2^-$] induced by a second metal center have also been observed. For example, the addition of Au(I) or Hg(II) ion to the $Au(mtp)_2^-$ anion results in the formation of dinuclear complexes and the rearrangement of the ligands on the gold(I) center (Scheme 4)[9].

$$2\ AuL(CN) \rightleftharpoons [AuL_2]^+ + [Au(CN)_2]^- \qquad L = PR'_3^-,\ mpt$$

SCHEME 3

SCHEME 4
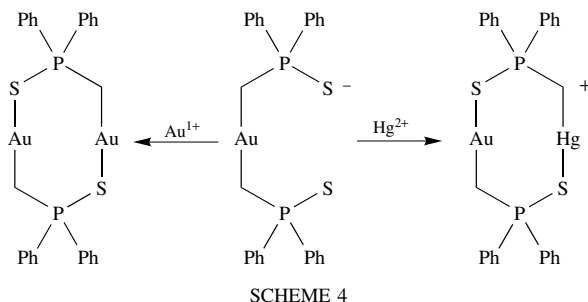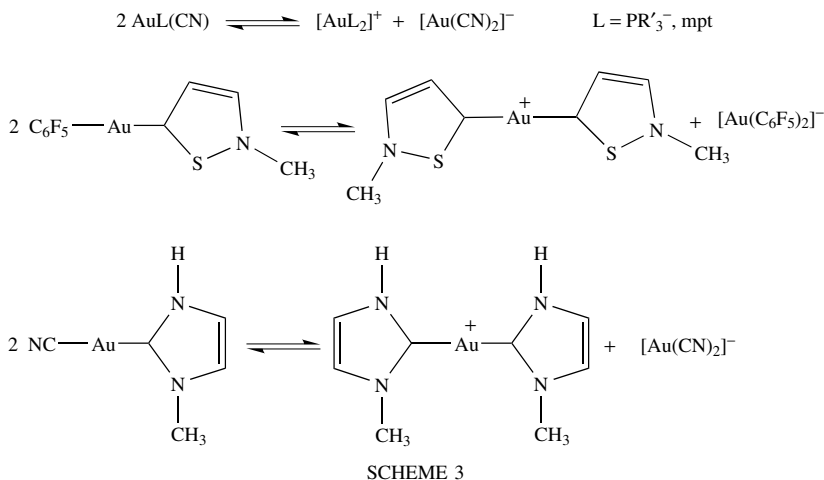
(d) Au−C bonds: Metathesis of dinuclear gold(I) complexes. An unusual ligand metathesis involving dinuclear gold(I) complexes, $Au_2[(CH_2)_2PR_2]_2$, has been reported by Jandik and Schmidbaur[10]. When two ylide gold(I) complexes $Au_2[(CH_2)_2PR_2]_2$ and $Au_2[(CH_2)_2PR'_2]_2$, where R and R′ are different substituents, are mixed in a CH_2Cl_2 solution, ligand exchanges occur, resulting in the formation of an equilibrium mixture of $Au_2[(CH_2)_2PR_2]_2$, $Au_2[(CH_2)_2PR'_2]_2$, and $Au_2[(CH_2)_2PR_2][(CH_2)_2PR'_2]$ (Scheme 5). The mechanism of this interesting metathesis has not been well understood.

(e) Au−C bonds: Isomerization of trans,cis-Au_2[(CH_2)_2PPh(CH_3)]_2. When the two substituents attached to the phosphorous atom of ylide ligand $(CH_2)_2PR_2^-$ are
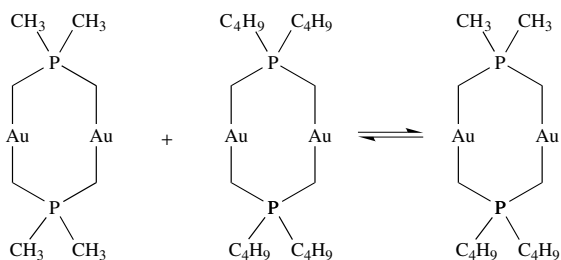
SCHEME 5

different, two structural isomers, *trans* and *cis*, are likely for the dinuclear gold(I) compound, $Au_2[(CH_2)_2PR_2]_2$. The isomerization between *trans* and *cis* isomers of $Au_2[(CH_2)_2PPh(CH_3)]_2$ has been observed. Weak acids and Lewis acids have been found to catalyze this isomerization process[11]. The activation energy for this isomerization process was determined to be $18.6\ kcal\,mol^{-1}$. A possible mechanism for the Lewis acid catalyzed isomerization proposed by Fackler and coworkers[11] is shown in Scheme 6 (where Y is a Lewis acid). They have suggested that a similar process may also be accountable for the intermolecular ligand exchange shown in Scheme 4.
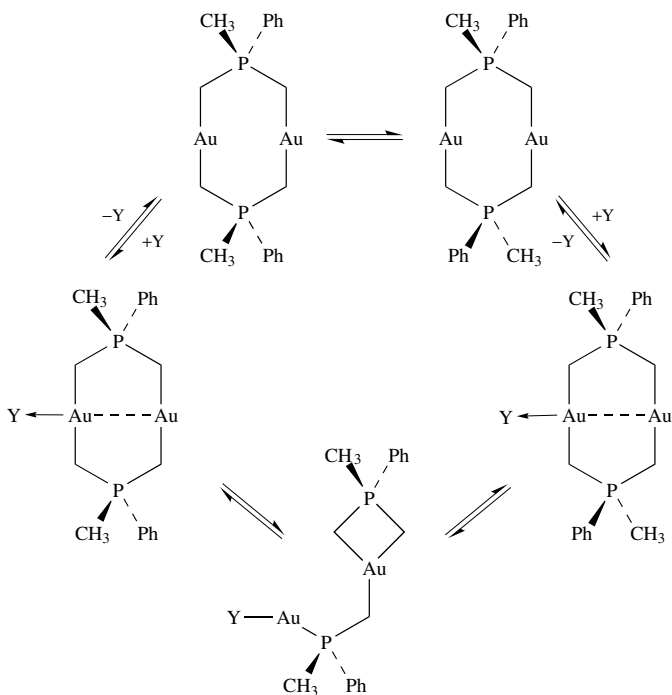
SCHEME 6

(f) Olefin isomerization. An olefin isomerization has been observed in a dinuclear gold(I) complex, $(AuCl)_2(Ph_2PCH=CHPPh_2)$ (Scheme 7). This isomerization is induced photochemically. In the absence of gold(I) moiety, the *cis* to *trans* isomerization does not occur. The gold(I) center is believed to activate the isomerization of the olefin via binding to the phosphorus center[12].

B. Rearrangements of Gold(III) Compounds

(a) Cis–trans isomerization: Monoarylgold(III) compounds. Two monoarylgold(III) complexes $AuCl_2(C_6Br_5)(PPh_3)$ and $AuCl_2(o\text{-}O_2NC_6H_4)(PPh_3)$, have been reported to undergo isomerization[13]. The *trans*-$AuCl_2(C_6Br_5)(PPh_3)$ was found to isomerize to the *cis* isomer[13a] when it is refluxed in $CHCl_3$. Similarly, the *trans*-$AuCl_2(o\text{-}O_2NC_6H_4)(PPh_3)$ isomer can be converted to the *cis* isomer[13b] when it is refluxed in CH_3CN. The *cis*-$AuCl_2(o\text{-}O_2NC_6H_4)(PPh_3)$ was reported to convert back to the *trans* isomer in the presence of Cl_2 (Scheme 8). The details of the isomerization mechanism have not been well understood.

(b) Cis–trans isomerization: Dialkylgold(III) compounds. $AuCl(CH_3)_2Py$ has been found to exist as a mixture of *cis* and *trans* isomers in pyridine[14]. The cationic ylide complex, *trans*-$\{AuX_2[(CH_2)P(CH_3)_3]_2\}^+$ (X = Br, I) is unstable in aqueous solution and isomerizes to the *cis* isomer[15]. In both cases, a five-coordinate intermediate may be involved in the isomerization process.
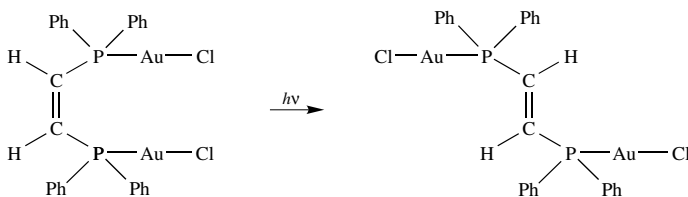
SCHEME 7
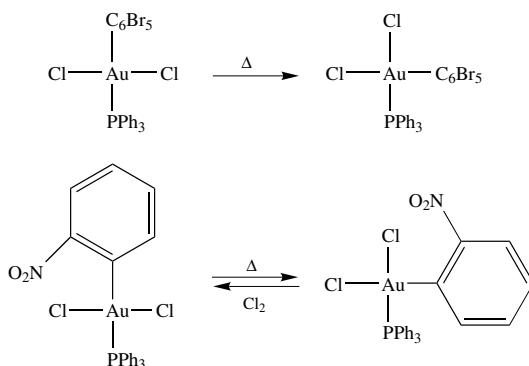
SCHEME 8

(c) Cis−trans isomerization of trialkylgold(III) compounds. Kochi and coworkers have examined the isomerization of trialkylgold(III) compounds extensively. The *cis* and *trans* isomers of $Au(CH_3)_2(C_2H_5)PPh_3$ were found to be in equilibrium in solution[16]. Based on the observation that tertiary phosphines retard the *cis−trans* isomerization of $Au(CH_3)_2(C_2H_5)PPh_3$, a dissociative pathway and a three-coordinate intermediate were proposed for the isomerization process (Scheme 9). The same intermediate was also proposed[16] to be involved in the reductive elimination of alkanes from $Au(CH_3)_2(C_2H_5)PPh_3$.
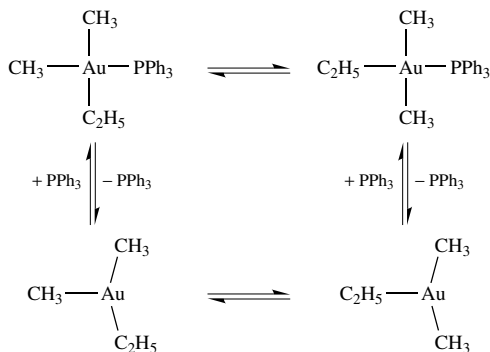
SCHEME 9

(d) Other isomerizations of mononuclear gold(III) compounds. A shuttle motion similar to that of Au(ttp)Cl has been observed in the gold(III) complex, $Au(CH_3)_2X(DMN)$ (DMN = 2,7-dimethyl-1,8-naphthyridine), X = halide, CN^-, OCN^-, SCN^-, $SeCN^-$, where the $Au(CH_3)_2X$ unit undergoes a rapid exchange between two nitrogen binding sites[15], resulting in the exchange of the two methyl environments on the DMN (Scheme 10). At temperatures above $25\,°C$, intermolecular halide or pseudohalide exchange occurs that averages the environments of the two methyl groups on the Au(III) center. The activation energies for the intra- and intermolecular exchange processes of $Au(CH_3)_2X(DMN)$ were determined to be *ca* $10.5\,\text{kcal}\,\text{mol}^{-1}$ and 16.3 to $17.4\,\text{kcal}\,\text{mol}^{-1}$, respectively[17].
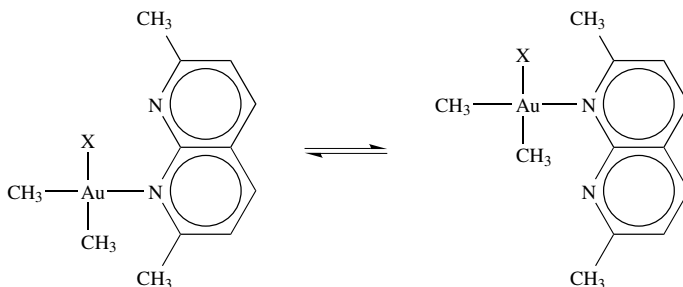
SCHEME 10

Komiya and Kochi have reported unusual dynamic processes exhibited by $Au(CH_3)_2(RC(O)CHC(O)R')$[18]. When $R = CH_3$, $R' = CF_3$, the gold(III) complex is highly fluxional in solution, averaging the ^1H resonances of the two methyl groups attached to the gold(III) center (Scheme 11). A dissociative mechanism was proposed to be likely responsible for the exchange process. When $R = CH_3$, $R' = Ph$, the gold(III) complex is not fluxional, but a similar exchange process can be induced by tertiary phosphines, where a five-coordinate intermediate is believed to be involved in the process. The addition of phosphines to $Au(CH_3)_2(RC(O)CHC(O)R')$ can also result in a reversible linkage isomerism between Au−O bonds and Au−C bonds of the acetylacetonato or substituted acetylacetonato ligand (Scheme 11).
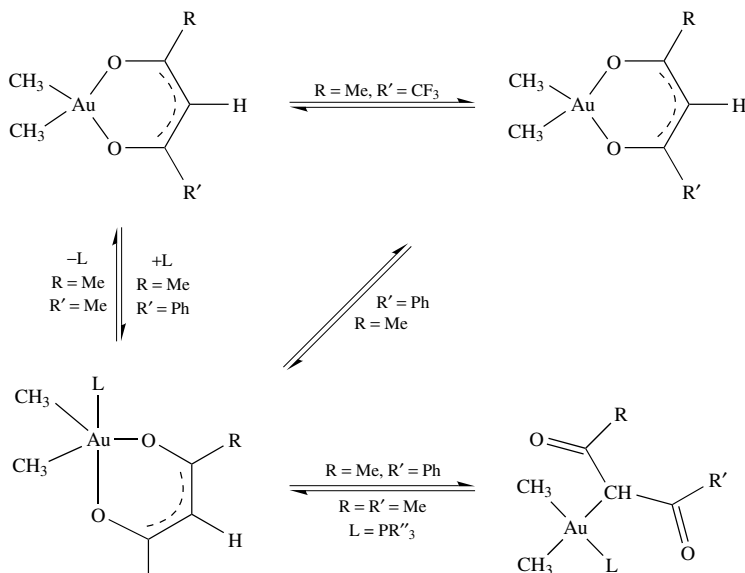
SCHEME 11

A conformational *cis–trans* isomerization has been observed in the cation $Au(S_2P(OH)Ph)_2{}^+$. The structures of both *cis* and *trans* stereoisomers have been determined by X-ray diffraction analyses. In solution, a facile isomerization occurs (Scheme 12)[19].
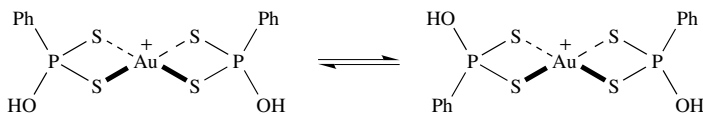
SCHEME 12

A facile isomerization of a *t*-butyl group to an isobutyl group σ-bonded to a gold(III) center has been observed in *trans*-$Au(CH_3)_2(C_4H_9)(PPh_3)$ (Scheme 13). The *t*-butyl to

isobutyl isomerization is irreversible. It was proposed that a three-coordinate intermediate similar to that in Scheme 9 could be involved in the isomerization process[16].
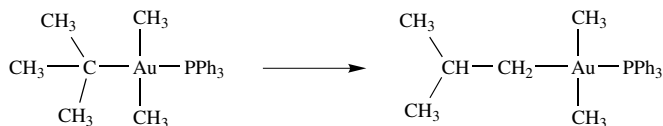
SCHEME 13

Canty and coworkers have reported dynamic behaviors of a series of dimethylgold(III) compounds $[Au(CH_3)_2L]NO_3$ where L is a tridentate ligand[20], as shown in Scheme 14. In the solid state, the gold(III) compounds have a typical square-planar geometry with two nitrogen atoms from the tridentate ligand L being coordinated to the gold(III) center. In solution, however, an exchange between the possible binding sites of the tridentate ligand occurs, resulting in the formation of structural isomers and the average of the two Au−CH3 environments [L = (mim)3COH **(3a)**, Py2(mim)COH **(3b)**, B(pz)3(Hpz) **(4)**, HB(pz)2(Hpz) **(5)**]. Five-coordinate species are proposed as likely intermediates involved in the exchange processes.

(3) (a) $n = 0$: (mim)3COH
  (b) $n = 1$: (py) (mim)2COH   **(4)** B(pz)3 (Hpz)   **(5)** HB(pz)2 (Hpz)
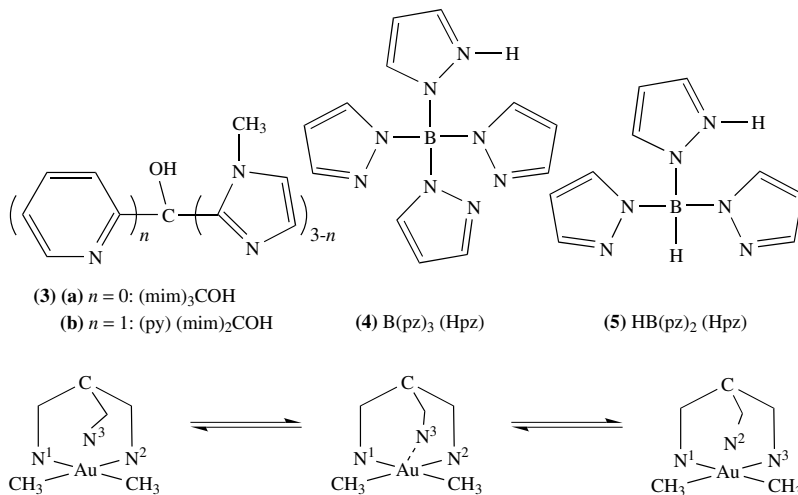
SCHEME 14

(e) Cis−trans isomerism of dinuclear gold(III) compounds. When two gold(III) centers are linked by two chelating ligands, three structural isomers are possible: *trans/trans-*, *cis/cis-* and *trans/cis-*, as shown in Scheme 15. All three isomers have been reported. An unusual isomerization of *trans/trans-*Au2[(CH2)2PPh2]2Br4 to *trans/cis-*Au2[(CH2)2PPh2]2Br4 has been observed[21].

(f) Isomerization of dinuclear gold(III) compounds to mononuclear gold(III) compounds. Bennett and coworkers have reported that the *trans/cis-*Au$_2^{III}$(o-C6H4PPh2)2X4 compounds (X = Br or I) are in equilibrium with the mononuclear compound
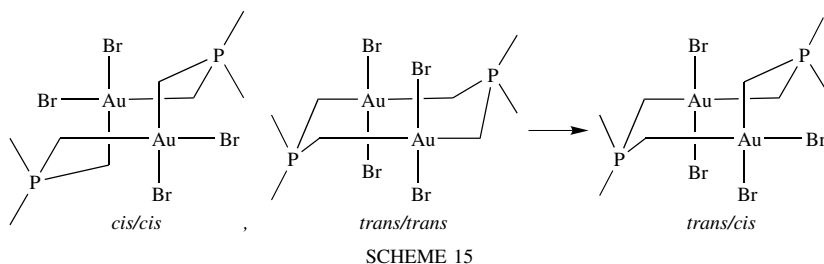
SCHEME 15

$Au^{III}(C_6H_4PPh_2)X_2$ in solution[22]. The latter can further isomerize to mononuclear gold(I) compounds $Au^I[PPh_2(o\text{-}C_6H_4X)]X$ via an intramolecular reductive elimination process (Scheme 16).

SCHEME 16
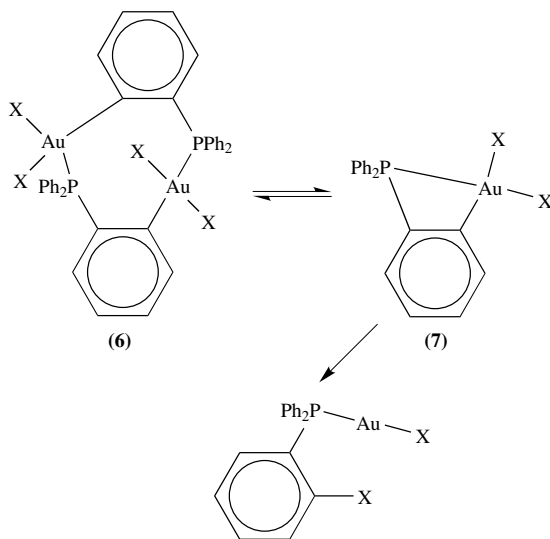
C. Rearrangements Involving a Change of Gold Oxidation State

(a) Disproportionation of dinuclear gold(II) compounds to gold(I) and gold(III) compounds. As an intermediate and least stable oxidation state, gold(II) compounds have a tendency to undergo a rearrangement or disproportionation reaction to yield the corresponding gold(I) and gold(III) species. In dinuclear gold(II) complexes where sulfur atoms are the donor atoms of the bridging ligand, the disproportionation reaction is always associated with the change of the thio-bridging ligands to chelating ligands. The first well-characterized examples of such rearrangements are dinuclear dithiocarbamate gold(II) compounds[23], $Au_2[S_2CN(C_2H_5)_2]_2X_2$, X = Br, I, SCN, SeCN (**8**). These dark green gold(II) compounds are stable at low temperature in the solid state, but disproportionate rapidly at ambient temperature to produce mixed valence compounds

(8)   **(9)**
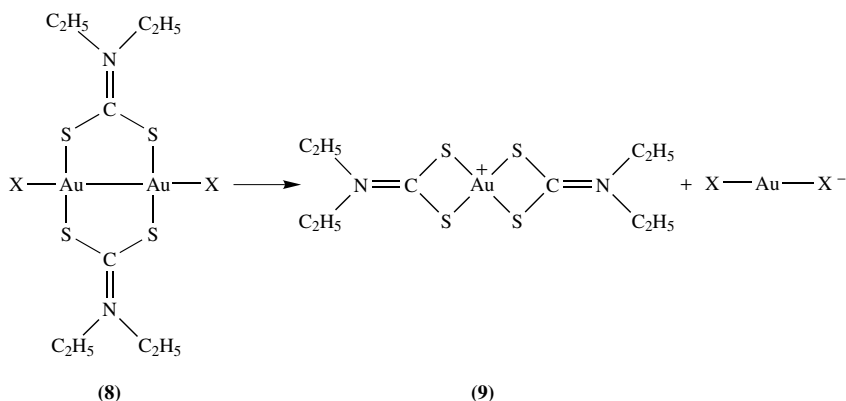
SCHEME 17

$[Au^{III}(S_2CN(C_2H_5)_2)_2][Au^I X_2]$ **(9)** (Scheme 17). In a related system, dark green gold(II) compounds $[Y]_2[Au_2(i\text{-MNT})_2X_2]$, $Y = AsPh_4^+$, or $N(Bu\text{-}n)_4^+$ (i-MNT = 1,1-dicyanoethylene-2,2-dithiolate), X = Cl, Br, I, are stable at ambient temperature in the solid state, allowing their structural characterization[24]. In solution, the $[Y]_2[Au_2(i\text{-MNT})_2X_2]$ compounds undergo a facile disproportionation reaction to yield $[Y]_2[Au^{III}(i\text{-MNT})_2]$ and $[Y][Au^I X_2]$ (Scheme 18). The activation energy for the disproportionation process increases in the order of $[Y]_2[Au_2(i\text{-MNT})_2I_2] < [Y]_2[Au_2(i\text{-MNT})_2Br_2] < [Y]_2[Au_2(i\text{-MNT})_2Cl_2]$.
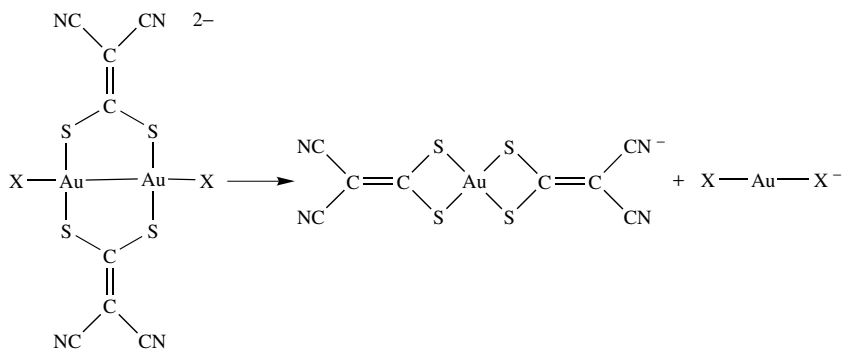
SCHEME 18

Di-phosphine bridged gold(II) dinuclear compounds, $Au_2(Ph_2PNHPPh_2)R_2X_2$, R = C_6F_5, C_6Cl_5, X = Cl, Br, are quite stable in the solid state. In solution, however, they rearrange to mixed valent dinuclear compounds[25], $Au^IAu^{III}((Ph_2PNHPPh_2)R_2X_2$, as shown in Scheme 19. When the bridging ligand in dinuclear gold(II) compounds is an ylide ligand, $(CH_2)_2PPh_2^-$, the gold(II) dimers are also quite stable. Isomerization of $Au_2[(CH_2)_2PPh_2]_2Cl_2$ **(10)** to a mixed valence compound $Au^IAu^{III}[(CH_2)_2PPh_2]_2Cl_2$ **(11)**, where one of the bridging ylide ligands becomes a chelating ligand, has been

observed (Scheme 20)[26]. The mixed valent compound $Au^IAu^{III}[(CH_2)_2PPh_2]_2I_2$ **(12)** exhibits a different structure from that of **(11)**, where both bridging ligands remain as bridging ligands[27]. It is conceivable that in the disproportionation process of dinuclear gold(II) compounds, the species with a structure similar to that of **(11)** acts as an intermediate which could lead to either the formation of mononuclear gold(III) and gold(I) species or a structure similar to that of **(12)** (Scheme 21).
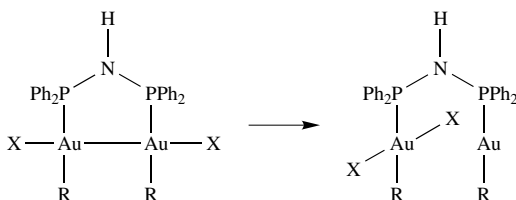
SCHEME 19
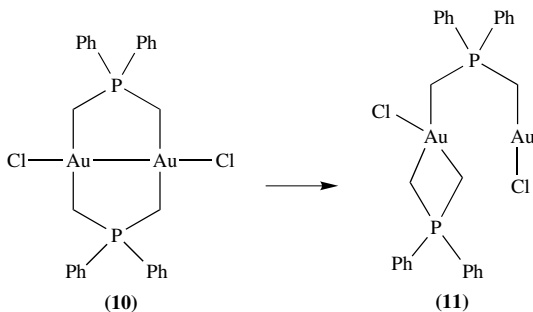
SCHEME 20
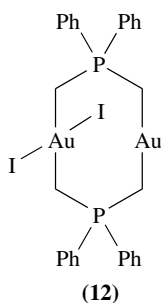
(12)

(b) Equilibrium between dinuclear gold(I) and dinuclear gold(II) compounds. The only example of reversible oxidative addition reaction of a dinuclear gold(I) compound to a dinuclear gold(II) compound was reported by Fackler and coworkers[28]. The dinuclear
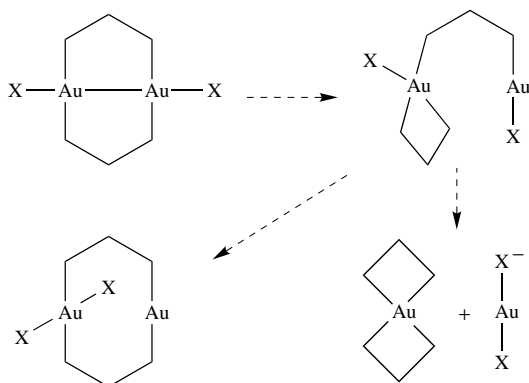
SCHEME 21

gold(I) compound, $Au_2[(CH_2)_2PR_2]_2$, R = Me, Ph, reacts with alkyl halides, $R'X =$ CH_3I, $(CH_3)_3SiCH_2I$, $PhCH_2Br$, to yield the dinuclear gold(II) compounds, $Au_2[(CH_2)_2$ $PR_2]_2(R')X$, $R' = CH_3$, $(CH_3)_3SiCH_2$, $PhCH_2$. The latter undergoes a reductive elimination to reproduce the gold(I) compound (Scheme 22). The Au(II) dimer catalyzes the halogen exchange reactions between alkyl halides via the equilibrium between $Au_2^I[(CH_2)_2PR_2]_2$ and $Au_2^{II}[(CH_2)_2PR_2]_2(R')X$. Thermodynamic parameters indicate that the equilibrium at 22 °C favors the gold(II) compound.
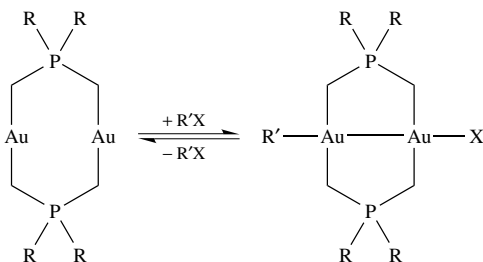
SCHEME 22

(c) Rearrangement of dinuclear gold(II) compounds to dinuclear gold(I) compounds. An irreversible rearrangement of a dinuclear gold(II) compound $Au_2^{II}(o\text{-}C_6H_4PPh_2)_2X_2$, X = Br, I, to a dinuclear gold(I) compound $Au_2^I[2,2'\text{-biphenylene-bis(diphenylphosphine}]X_2$ via an intramolecular reductive coupling of two aryl ligands has been reported by Bennett and coworkers[29] (Scheme 23). Mixed-valent dinuclear gold(I)–gold(III) intermediates are believed to be involved in the rearrangement[22].

(d) Rearrangement of a dinuclear gold(II) compound to a dinuclear gold(III) compound. Alkyl dihalides are capable of undergoing a four-electron oxidative addition reaction by breaking two carbon–halide bonds while a dinuclear ylide gold(I) compound is capable of providing four electrons. This is demonstrated by the reaction of a dinuclear ylide gold(I) compound, $Au_2[(CH_2)_2PPh_2]_2$, with alkyl dihalides to yield an A-frame dinuclear
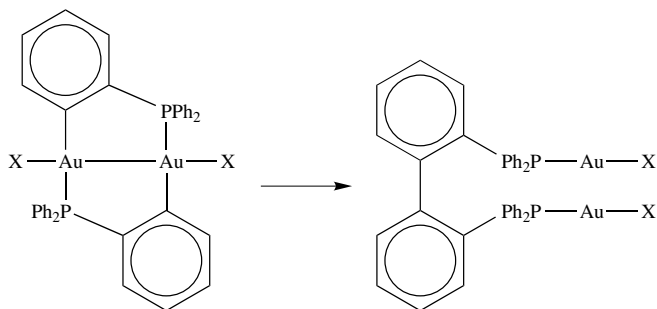
SCHEME 23

gold(III) compound (13)[30]. A dinuclear gold(II) compound has been found to be involved as an intermediate in the process[31]. Structural evidence also suggests a carbene species (14) as a possible intermediate (Scheme 24) for the rearrangement of the dinuclear gold(II) species to the dinuclear gold(III) species[32].
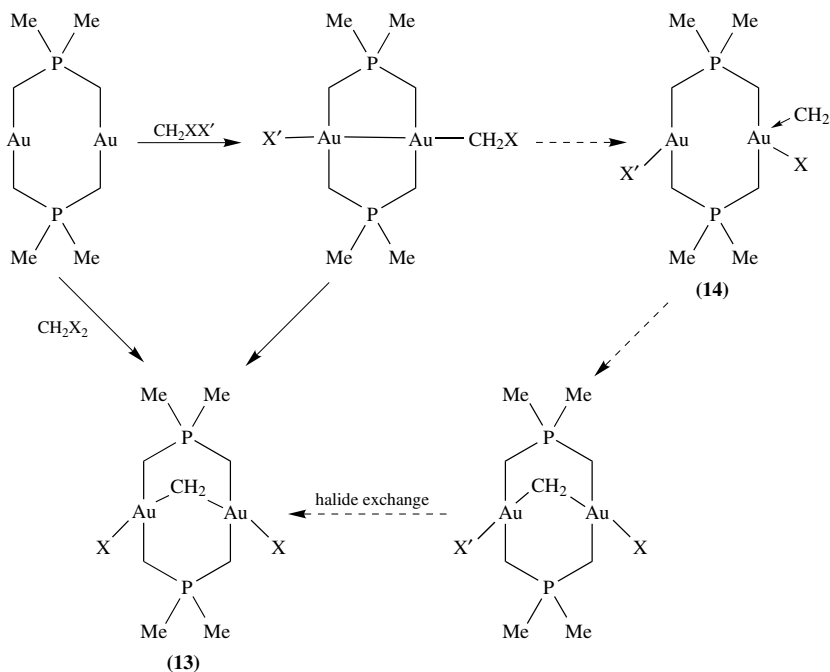
SCHEME 24

(e) Thermally induced reductive elimination of alkylgold(III) complexes. Thermally induced reductive elimination of alkyls from mononuclear gold(III) complexes

$AuR_3(PPh_3)$ has been examined extensively by Kochi and coworkers[16]. It was found that the reductive elimination of $AuR_3(PPh_3)$ produces *cis* elimination products only. A dissociative pathway involving a three-coordinate intermediate was proposed. A similar reductive elimination of ethane from *cis*-$Au(CH_3)_2[CH_2P(CH_3)_3]_2^+$ has also been observed by Schmidbaur and Franke[15]. Two interesting examples of thermally induced reductive elimination of alkanes involving gold(III) centers in dinuclear complexes were reported by Schmidbaur and coworkers. The first example (Scheme 25) involves the elimination of two methyls from a mixed valent ylide compound[33a], $Au^I Au^{III}(CH_3)_2[(CH_2)_2P(CH_3)_2]_2$ **(15)** to form ethane and a dinuclear gold(I) compound $Au_2^I[(CH_2)_2P(CH_3)_2]_2$ while the second example involves the elimination of two methyls and one methylene group from a dinuclear gold(III) complex[33b] $Au_2^{III}(CH_2)(CH_3)_2[(CH_2)_2PPh_2]_2$ **(16)** to produce propane and $Au_2^I[(CH_2)_2PPh_2]_2$ (Scheme 26). The mechanism of these two reductive elimination reactions remains to be understood.

(15)

SCHEME 25

(16)
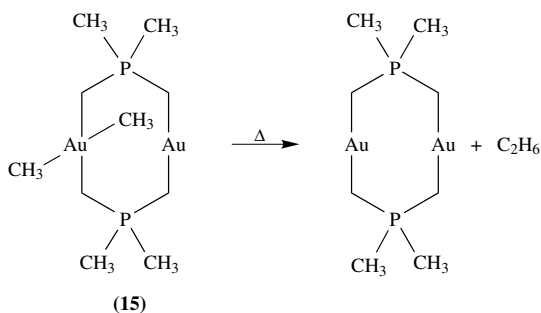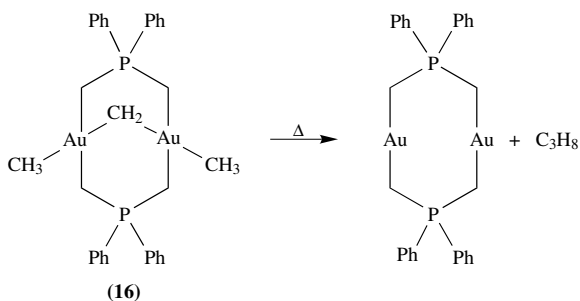
SCHEME 26

III. REARRANGEMENTS OF ORGANOSILVER COMPOUNDS

Examples of rearrangement involving organosilver compounds are scarce due to the rare occurrence of thermally stable organosilver compounds and the fact that Ag(I) is the only stable oxidation state.

A. Ag$_n$Ar$_n$ Compounds

This class of molecules has cyclic structures and is fluxional in solution due to either an intramolecular or an intermolecular dynamic process. Among the earliest examples[34] are Ag$_n$[2-(Me$_2$NCH$_2$)C$_6$H$_4$]$_n$, Ag$_n$[2,6-(CH$_3$O)$_2$C$_6$H$_3$]$_n$, Ag$_n$[2,4,6-(CH$_3$O)$_3$C$_6$H$_2$]$_n$. These compounds appeared to be polynuclear aggregates in solution, but n and the kinetic properties of these compounds were not conclusively determined. The structure of a copper(I) analog, Cu$_4$[2-(Me$_2$NCH$_2$)C$_6$H$_4$]$_4$, was determined recently[34b], which shows that the compound indeed has a cyclic structure. A trinuclear compound, Ag$_3$Ar$_3$, Ar = 2-methylphenyl **(17)**, was reported in 1978[35]. There are two possible conformational isomers, depending on the relative orientation of the methyl group: either all three methyl groups are up, or only two of them are up while the remaining one is on the opposite direction. The former would give one methyl chemical shift while the latter would have two methyl chemical shifts. At temperatures above −30 °C, only one methyl signal was observed in the ^{1}H NMR spectrum of the compound. At −60 °C, however, three methyl signals were observed, consistent with the presence of both isomers in solution. It was proposed that the interconversion between the two isomers is caused by the rotation of the phenyl ring along the Cl−C4 axis[35].

(17)　　　　　　　　　　　　**(18)**
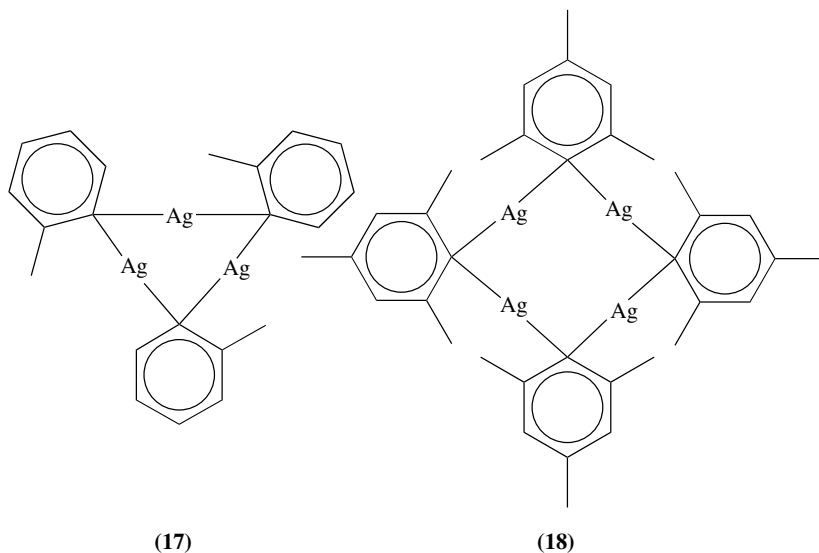
The structure of a cyclic tetranuclear compound, Ag$_4$Mes$_4$, Mes = 2,4,6-trimethylphenyl **(18)**, was reported[36] in 1983. Molecular weight and NMR spectroscopic studies suggested that this tetrameric compound converts to the dimeric compound, Ag$_2$Mes$_2$, in solution, rapidly[37]. The equilibrium between the tetramer and the dimer favors the dimer. The structure of the dimer remains uncharacterized. The structure of a related gold(I) compound, Au$_5$Mes$_5$, has also been determined, which was also found to exist largely as a dimeric compound, Au$_2$Mes$_2$, in solution[37].

B. Ag$_2$Li$_2$Ar$_4$ Compounds

The simplest member of this series is Ag$_2$Li$_2$Ar$_4$(Et$_2$O)$_2$ **(19)**, where Ar = phenyl, 2-methylphenyl, 3-methylphenyl, 4-methylphenyl or 2,6-dimethylphenyl[38]. Molecular weight measurements confirmed that these compounds remain as tetranuclear species in solution. NMR studies indicated that they have a nonplanar, cyclic structure which has been confirmed by the crystal structural determination of a copper(I) analog[38b], Cu$_2$Li$_2$Ph$_4$(Et$_2$O)$_2$. NMR studies also indicated that there is a rapid interconversion between different conformational/geometrical isomers of the Ag$_2$Li$_2$Ar$_4$(Et$_2$O)$_2$ compounds[38a]. To further establish the nature of dynamics in this class of molecules, Koten and coworkers introduced an internal donor group at the *ortho* position of the aryl ligand that replaces the ether ligand on the lithium ion. The tetranuclear compound, Ag$_2$Li$_2$(2-Me$_2$NCH$_2$C$_6$H$_4$)$_4$ **(20)**, and its copper(I) and gold(I) analogs have been examined[39]. A cyclic structure similar to that of **(19)** was proposed, which was supported by the crystal structure[39d] of Cu$_2$Li$_2$(2-Me$_2$NCH$_2$C$_6$H$_4$)$_4$, determined by X-ray diffraction analysis. Dynamic ^{1}H NMR and ^{13}C NMR studies revealed that these tetranuclear complexes are highly fluxional in solution. The bridging carbon atom of the aryl ligand in the tetramer is chiral. The dynamic process involves the dissociation of the Li−N nitrogen bond, the rotation of the C−N bond and finally the rotation of the aryl group around the C1−C4 axis, that causes the conversion of the configuration at the bridging carbon atom[39]. A similar C1−C4 rotation could also be responsible for the dynamic process observed in **(19)**.

(19)   (20)
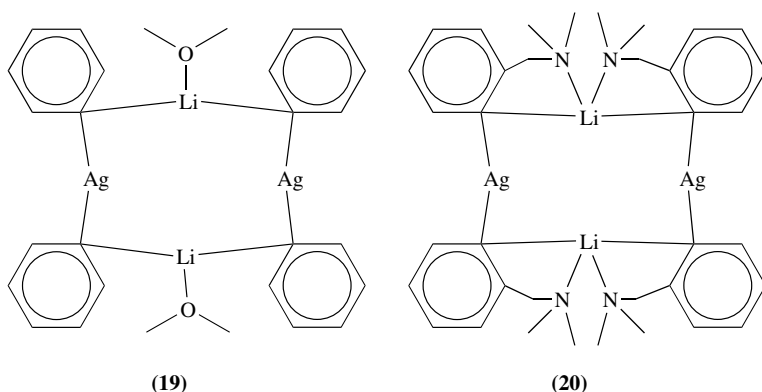
C. Ylide Complexes

Several ylide silver(I) complexes are known[40], but only one of them, the dinuclear compound, Ag$_2$(S(CH$_2$)PPh$_2$)$_2$, has been shown to be dynamic in solution[41]. Its ^{1}H NMR spectra are temperature-dependent. A doublet due to the CH$_2$ protons and $^2J_{P-H}$ coupling was observed at ambient temperature, while at −60 °C a triplet involving $^2J_{Ag-H}$ couplings was observed. The $^2J_{P-Ag}$ coupling was only observed at −40 °C. A dynamic process involving Ag−C bond rupture is likely to be responsible for the observed NMR spectra of Ag$_2$(S(CH$_2$)PPh$_2$)$_2$.

D. Rearrangement Involving C−C or C−N Bond Breaking/Formation

Although organosilver complexes are well known for their catalytic ability in a variety of organic syntheses[42], isolated or well-characterized silver species involved in the catalytic process are rare. Whitesides and coworkers reported the isomerization of a 5-hexenyl(tri-*n*-butylphosphine)silver(I) complex to cyclopentylcarbinyl(tri-*n*-butylphosphine)silver(I) complex via the formation of a C−C bond (Scheme 27)[43]. These silver(I) complexes also undergo a facile thermal decomposition to produce hydrocarbon products[43]. An interesting C−N bond coupling reaction was observed in the complex[44] of [Ag(aziridine)$_4$]NO$_3$ (21). NMR studies established that 21 isomerizes to [Ag(diin)$_2$NO$_3$] [diin = 1-(2-aminoethyl)aziridine)$_2$] (22) in which two aziridine ligands couple by the

SCHEME 27

(21)   (22)

SCHEME 28

(23)
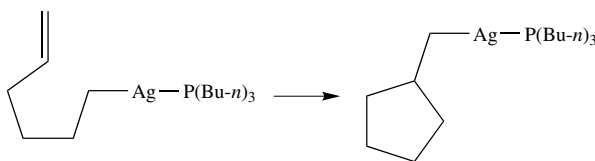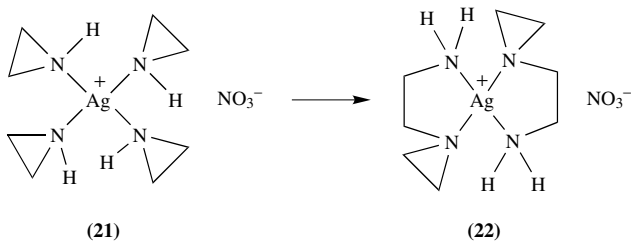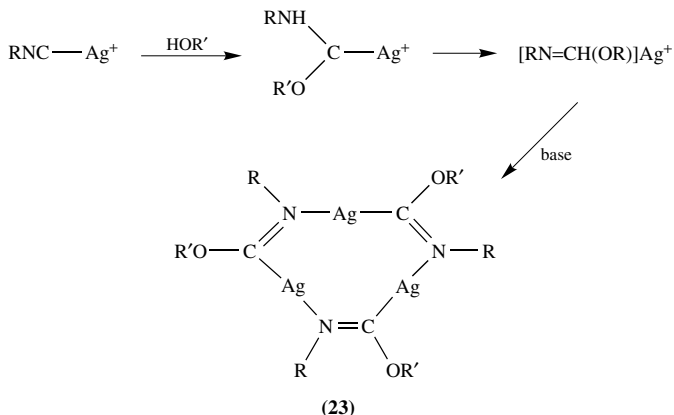
SCHEME 29

breaking and forming of a C−N and a N−H bond (Scheme 28). Similar coupling reactions were also observed in the analogous Zn(II), Cd(II) or Co(II) complexes of aziridine[44]. Silver chloride has been known to catalyze the addition reactions[45] of alcohols to isocyanides to produce RN=CH(OR). It is believed that a carbene intermediate, [(RNH(OR)C:]AgCl, is involved, which rearranges to form [RN=CH(OR)]AgCl. The latter forms a cyclic trimer (23) in the presence of base (Scheme 29)[46].

In summary, the dynamic process and rearrangements displayed by organogold and organosilver complexes are versatile. Detailed mechanistic studies are necessary for a better understanding of many of the unusual rearrangements described herein.

IV. REFERENCES

1. (a) Y. Sueishi, T. Mukai, K. Matsumoto, S. Yamamoto and N. Nishimura, *Bull. Chem. Soc. Jpn.* **67**, 3153 (1994).
   (b) R. Lok, R. Leone and A. J. Williams, *J. Org. Chem.*, **61**, 3289 (1996).
   (c) L. S. Meriwether, E. C. Breitner and C. L. Sloan *J. Am. Chem. Soc.* **87**, 4441 (1965).
   (d) L. S. Meriwether, E. C. Breitner and N. B. Colthup, *J. Am. Chem. Soc.*, **87**, 4448 (1965).
2. M. Valden, X. Lai and D. W. Goodman, *Science*, September 11 (1998).
3. (a) R. J. Puddephatt, *The Chemistry of Gold*, Elsevier, Amsterdam, (1978).
   (b) A. Grohmann and H. Schmidbaur, in *Comprehensive Organometallic Chemistry II* (Eds. E. W. Abel, F. G. A. Stone and G. Wilkinson), Vol. 3, Chap. 1, Pergamon Press, Oxford, 1995.
   (c) R. J. Puddephatt, in *Comprehensive Organometallic Chemistry*, (Eds. G. Wilkinson, F. G. A. Stone and E. W. Abel), Vol. 2, Chap. 15, Pergamon Press, Oxford, 1982.
4. S. Wang and J. P. Fackler, Jr., *J. Chem. Soc., Chem. Commun.*, 22 (1988).
5. E. Ruiz and S. Alvarez, *New J. Chem.*, **17**, 147 (1993).
6. (a) R. Hüttel, U. Raffay and H. Reinheimer, *Angew. Chem., Int. Ed. Engl.*, **6**, 862 (1967).
   (b) C. H. Campbell and M. L. H. Green, *J. Chem. Soc.*, (A), 3282 (1971).
   (c) H. Werner, H. Otto, T. Ngo-Khac and C. Burschka, *J. Organomet. Chem.*, **262**, 123 (1984).
7. (a) P. N. Dickson, A. Wehrli and G. Geier, *Inorg. Chem.*, **27**, 2921 (1988).
   (b) G. Lewis and C. F. Shaw III, *Inorg. Chem.*, **25**, 58 (1986).
   (c) A. L. Hormann, C. F. Shaw III, D. W. Bennett and W. M. Reiff, *Inorg. Chem.*, **25**, 3953 (1986).
   (d) A. L. Hormann-Arendt and C. F. Shaw III, *Inorg. Chem.*, **29**, 4683 (1990).
8. (a) H. G. Raubenheimer, F. Scott, G. J. Kruger, J. G. Toerien, R. Otte, W. Van Zyl, I. Taljaard, P. Olivier and L. Linford *J. Chem. Soc., Dalton Trans.*, 2091 (1994).
   (b) H. G. Raubenheimer, M. Desmet and G. J. Kruger, *J. Chem. Soc., Dalton Trans.*, 2067 (1995).
   (c) H. G. Raubenheimer, L. Lindeque and S. Cronje, *J. Organomet. Chem.*, **511**, 177 (1996).
9. S. Wang and J. P. Fackler, Jr., *Organometallics*, **7**, 2415 (1988).
10. P. Jandik and H. Schmidbaur, *J. Chromatogr.*, **213**, 55 (1981).
11. D. D. Heinrich, R. J. Staples and J. P. Fackler, Jr., *Inorg. Chim. Acta*, **229**, 61 (1995).
12. J. B. Foley, A. E. Bruce and M. R. M. Bruce, *J. Am. Chem. Soc.*, **117**, 9596 (1995).
13. (a) R. Usón and A. Laguna, *Syn. React. Inorg. Metal-Org. Chem.*, **5**, 17 (1975).
    (b) J. Vicente, A. Arcas, M. Mora, X. Solans and M. Font-Altaba, *J. Organomet. Chem.*, **309**, 369 (1986).
14. H. Hagnauer, G. C. Stocco and R. S. Tobias, *J. Organomet. Chem.*, **46**, 179 (1972).
15. H. Schmidbaur and R. Franke, *Inorg. Chim. Acta*, **13**, 79 (1975).
16. (a) A. Tamakai, S. A. Magennis and J. K. Kochi, *J. Am. Chem. Soc.*, **96**, 6140 (1974).
    (b) S. Komiya, T. A. Albright, R. Hoffmann and J. K. Kochi, *J. Am. Chem. Soc.*, **98**, 7255 (1976).
17. H. Schmidbaur and K. C. Dash *J. Am. Chem. Soc.*, **95**, 4855 (1973).
18. S. Komiya and J. K. Kochi, *J. Am. Chem. Soc.*, **99**, 3695 (1977).
19. H. H. Murray, G. Garzón, R. G. Raptis, A. M. Mazany, L. C. Porter and J. P. Fackler, Jr., *Inorg. Chem.*, **27**, 836 (1988).
20. (a) A. J. Canty, N. J. Minchin, P. C. Healy and A. H. White, *J. Chem. Soc., Dalton Trans.*, 1795 (1982).
    (b) P. K. Byers, A. J. Canty N. J. Minchin, J. M. Patrick, B. W. Skelton and A. H. White, *J. Chem. Soc., Dalton Trans.*, 1183 (1985).

21. D. Dudis and J. P. Fackler, Jr., *Inorg. Chem.*, **24**, 3758 (1985).
22. M. A. Bennett, S. K. Bhargava, D. C. R. Hockless, L. L. Welling and A. C. Willis, *J. Am. Chem. Soc.*, **118**, 10469 (1986).
23. D. C. Calabro, B. A. Harrison, G. T. Palmer, M. K. Moguel, R. L. Rebbert and J. L. Burmeiter, *Inorg. Chem.*, **20**, 4311 (1981).
24. (a) M. N. I. Khan, J. P. Fackler, Jr., C. King, J. C. Wang and S. Wang, *Inorg. Chem.*, **27**, 1673 (1988).
    (b) M. N. I. Khan, S. Wang and J. P. Fackler, Jr., *Inorg. Chem.*, **28**, 3579 (1989).
25. R. Usón, A. Laguna, M. Laguna, M. N. Fraile, P. G. Jones and G. M. Sheldrick, *J. Chem. Soc., Dalton Trans.*, 291 (1986).
26. J. P. Fackler, Jr. and B. Trzcinska-Bancroft, *Organometallics*, **4**, 1891 (1985).
27. A. M. Mazany and J. P. Fackler, Jr., *J. Am. Chem. Soc.*, **106**, 801 (1984).
28. J. D. Basil, H. H. Murray, J. P. Fackler, Jr., J. Tocher, A. M. Mazany, B. Trzcinska-Bancroft, H. Knachel, D. Dudis, T. J. Delord and D. O. Marler, *J. Am. Chem. Soc.*, **107**, 6908 (1985).
29. M. A. Bennett, S. K. Bhargava, K. D. Griffiths and G. B. Robertson, *Angew. Chem., Int. Ed. Engl.*, **26**, 260 (1987).
30. (a) P. Jandik, U. Schubert and H. Schmidbaur, *Angew. Chem., Int. Ed. Engl.*, **21**, 74 (1982).
    (b) H. Schmidbaur, *Angew. Chem., Int. Ed. Engl.*, **22**, 907 (1983).
    (c) P. Jandik and H. Schmidbaur, *Inorg. Chim. Acta*, **13**, 84 (1975).
31. (a) H. H. Murray, J. P. Fackler, Jr. and A. M. Mazany, *Organometallics*, **3**, 1310 (1984).
    (b) H. C. Knachel, D. S. Dudis and J. P. Fackler, Jr., *Organometallics*, **3**, 1312 (1984).
32. H. H. Murray, J. P. Fackler, Jr. and D. A. Tocher, *J. Chem. Soc., Chem. Commun.*, 1278 (1985).
33. (a) H. Schmidbaur and R. Franke, *Inorg. Chim. Acta*, **13**, 85 (1975).
    (b) H. Schmidbaur, C. Hartmann, J. Riede, B. Huber and G. Müller, *Organometallics*, **5**, 1652 (1986).
34. (a) A. J. Leusink, G. Van Koten and J. G. Noltes, *J. Organomet. Chem.*, **56**, 379 (1973).
    (b) M. D. Janssen, D. M. Grove, A. L. Spek and G. van Koten, in *XVth International Conference on Organometallic Chemistry*, Royal Society of Chemistry, 1994, Abstracts, p. OC9.
35. H. K. Hofstee, J. Boersma and G. J. M. Van Der Kerk, *J. Organomet. Chem.*, **168**, 241 (1978).
36. S. Gambarotta, C. Floriani, A. Chiesi-Villa and C. Guastin, *J. Chem. Soc., Chem. Commun.*, 1087 (1983).
37. E. M. Meyer, S. Gambarotta, C. Floriani, A. Chiesi-Villa and C. Guastin, *Organometallics*, **8**, 1067 (1989).
38. (a) J. Blenkers, H. K. Hofstee, J. Boersma and G. J. M. Van Der Kerk, *J. Organomet. Chem.*, **168**, 251 (1979).
    (b) N. P. Lorenzen and E. Weiss, *Angew. Chem., Int. Ed. Engl.*, **29**, 300 (1990).
39. (a) G. Van Koten, *J. Organomet. Chem.*, **171**, C39 (1979).
    (b) G. Van Koten and J. G. Noltes, *J. Organomet. Chem.*, **174**, 367 (1979).
    (c) G. Van Koten and J. G. Noltes, *J. Am. Chem. Soc.*, **101**, 6593 (1979).
    (d) G. Van Koten, J. T. B. H. Jastrebski, F. Fuller and C. H. Stam, *J. Am. Chem. Soc.*, **107**, 697 (1985).
40. (a) H. Schmidbaur, J. Adlkofer and W. Buchner, *Angew. Chem., Int. Ed. Engl.*, **12**, 415 (1973).
    (b) Y. Yamamoto and H. Schmidbaur, *J. Organomet. Chem.*, **96**, 133 (1975).
    (c) H. Schmidbaur, J. Adlkofer and W. Herrmann, *Chem. Ber.*, **107**, 3699 (1974).
    (d) H. Schmidbaur and J. Adlkofer, *Inorg. Synth.*, **18**, 142 (1978).
41. S. Wang, J. P. Fackler, Jr. and T. F. Carlson, *Organometallics*, **9**, 1973 (1990).
42. (a) G. Van Koten, S. L. James and J. T. B. H. Jastrzebski, in *Comprehensive Organometallic Chemistry II* (Eds. E. W. Abel, F. G. A. Stone and G. Wilkinson), Vol. 3, Chap. 2, Pergamon, Press, Oxford, (1995).
    (b) G. Van Koten and J. G. Noltes, in *Comprehensive Organometallic Chemistry* (Eds. G. Wilkinson, F. G. A. Stone and E. W. Abel), Vol. 2, Chap. 14, Pergamon Press, Oxford, 1982.
43. G. M. Whitesides, D. E. Bergbreiter and P. E. Kendall, *J. Am. Chem. Soc.*, **96**, 2806 (1974).
44. H. P. Fritz and G. Hierl, *Z. Naturforsch*, **26**, 476 (1971).
45. T. Saegusa and Y. Ito, in *Isonitrile Chemistry* (Ed. I. Ugi), Chap 4, Academic Press, New York, 1971.
46. G. Minghetti, F. Bonati and M. Massobrio, *Inorg. Chem.*, **14**, 1974 (1975).

CHAPTER **14**

Syntheses and uses of isotopically labelled compounds of silver and gold

MIECZYSŁAW ZIELIŃSKI

Isotope Laboratory, Faculty of Chemistry, Jagiellonian University, Cracow, Poland
Fax: 48-12-340515;   e-mail: zielinsk@trurl.ch.uj.edu.pl

MARIANNA KAŃSKA

Department of Chemistry, University of Warsaw, Warsaw, Poland
Fax: 48-22-8225996;   e-mail: mkanska@chem.uw.edu.pl

and

RYSZARD KAŃSKI

Department of Chemistry, University of Warsaw, Warsaw, Poland
Fax: 48-22-8230123;   e-mail: rkanski@chem.uw.edu.pl

I. ABBREVIATIONS

AD	Alzheimer disease
CINAA	cyclic instrumental neutron activation analysis
CP MAS	cross-polarization magic angle spinning
EC	electron capture
EELS	electron energy loss spectroscopy
EPR	electron paramagnetic resonance
ICP-MS	inductively coupled plasma-mass spectrometry
INAA	instrumental neutron activation analysis
INEPT	insensitive nuclei enhanced by polarization transfer
IP	ionization potential

IPA	inverse perturbation analysis
IR	infrared
IRRASS	infrared reflective adsorption spectra spectroscopy
KIE	kinetic isotope effect
LIF	laser-induced fluorescence
LLE	low level exposure
MAS	magic angle spinning
NCA	non-carrier added
NQR	nuclear quadrupole resonance
PCA	principal component analysis
R2PI	resonant two-photon ionization (spectroscopy)
SERS	surface-enhanced Raman scattering
TPRS	temperature-programmed reaction spectroscopy
TXRF	total X-ray reflection fluorescence
UHV	ultra-high vacuum

II. INTRODUCTION

Both organosilver and organogold chemistry are reviewed systematically in *Comprehensive Organometallic Chemistry* (Eds. G. Wilkinson, F. G. A. Stone and E. W. Abel, Pergamon Press, Oxford, New York, Toronto, Sydney, Paris, Frankfurt, 1982). The isotopically labelled silver and gold compounds described in these volumes are involved only in the reactions of o-$(BrAg_2)C_6H_4CH_2NMe_2$ with $D_2O/C_6H_6/25\,°C$ and of $MeCOOD/D_2O/25\,°C$. The mechanism of protonic acid cleavage of the Au−C σ-bond in the trialkylgold^{III} complexes is suggested to occur via bimolecular electrophilic substitution, S_E2, and to involve only the mutually *trans* methyl groups in $Me_2CD_3AuPPh_3$. The same is suggested for the S_E2 mechanism of methylation of gold^{III} by gold^{I} which proceeds with retention of stereochemistry of gold^{III}: $^{198}AuCD_3PPh_3 + $ *cis*-$[AuIMe_2PPh_3] \rightarrow$ *cis*-$[AuMe_2(CD_3)PPh_3] + {}^{198}AuIPPh_3$. Recent studies with isotopically labelled silver and gold compounds presented in this chapter increase significantly the number of scientific investigations of the dynamic behaviour of isotopic silver and gold compounds and their clusters in solutions. This increase is caused principally by the desire to understand and utilize silver and gold in catalytic processes. The role of gold is not restricted simply to geometric dilution of the main component (for instance Pt) of the bicomponent catalyst but has been considered recently also as a rich source of electrons in the catalytic systems. Several isotopically labelled gold compounds covered in this chapter have been synthesized for use in chrysotherapy (antiarthritic drugs) and in anticancer treatments. Radioanalytical, environmental, health and biomedical studies with silver and gold isotopes have also been given attention in this chapter since the non-invasive determinations of the concentrations of elements in fingernails, hair, saliva and in biological samples in general are of diagnostic value in contemporary medicine. The environmental aspects of $^{107,109}Ag(n,\gamma)\,^{108m,110m}Ag$ nuclear reaction and determinations of ^{108m}Ag and ^{110m}Ag concentrations in marine organisms have been stressed also. Parts of this chapter include radioanalysis as well as bioinorganic problems, and also problems in physical-spectroscopy and isotope effects. Thus this chapter, while mainly dealing with organometallic chemistry, has also partly an interdisciplinary character.

III. SYNTHESIS AND USES OF ISOTOPICALLY LABELLED COMPOUNDS OF SILVER

A. Isotopic Studies of Hydrocarbon Oxidations Catalyzed by Silver

1. Deuterium isotope effects in the oxidation of ethylene and propylene with oxygen over a silver sponge

A small *normal* kinetic deuterium isotope effect in the total oxidation of C_2D_4 (pressure of 5 to 15 torr) to CO_2 with oxygen (pressure of 65 torr) over a silver sponge, defined as the ratio of the oxidation rate for C_2H_4 relative to C_2D_4, has been found to be $r_H/r_D = 1.54 \pm 0.02$ at $145\,°C$ and 1.27 at $165\,°C$, and the *inverse* isotope effect $r_H/r_D = 1/1.75 = 0.571$ was found at $145\,°C$ and $r_H/r_D = 1/2.0 = 0.5$ at $165\,°C$ for epoxide formation[1].

Kinetic deuterium isotope effects (KIE) in propylene oxidation for $CH_3CH=CH_2$, $CD_3CH=CH_2$, $CH_3CH=CD_2$, $CH_3CD=CH_2$ and $CD_3CD=CD_2$ over silver at oxygen pressures of 120 to 150 torr and low olefin pressures of 5 to 10 torr have been determined also[1]. Within the overall experimental error all the above propylenes were oxidized to CO_2 and $H_2O/HDO/D_2O$ at the same rate ($r_H/r_D = 1.25$ at $166\,°C$ and 1.111 at $206\,°C$ for C_3H_6/C_3D_6; $r_H/r_D = 1.0$ at $166\,°C$ for $C_3H_6/CH_3CH=CD_2$ etc.). However, a very large apparent *inverse* deuterium KIE ($r_H/r_D = 1/2.5$ to $1/5$) has been found for propylene oxide formation from propylenes labelled with deuterium in the methyl group[1].

$$r_H/r_D = 1/3.5 \text{ at } 166\,°C \text{ for } C_3H_6/CD_3CH=CH_2$$

$$r_H/r_D = 1.0/1.0 \text{ at } 166\,°C \text{ for } C_3H_6/CH_3CD=CH_2$$

$$r_H/r_D = 1.0/5.0 \text{ at } 222\,°C \text{ for } C_3H_6/CD_3CH=CH_2$$

In the selective oxidation of $CD_3CH=CH_2$ to $CD_3\overset{\displaystyle \frown O \frown}{CH-CH_2}$ no deuterium could be detected in the propylene epoxide in positions other than the methyl group, and no hydrogen–deuterium transfer has been found in the unreacted $CD_3CH=CH_2$.

The stereochemistry of epoxide formation from ethylenes-d_2 was investigated also by taking the IR spectra of dideuterioethylene oxides prepared from *gem*-$C_2H_2D_2$, from *cis*-$C_2H_2D_2$ and from *trans*-$C_2H_2D_2$ over Ag. $\overset{\displaystyle \frown O \frown}{CH_2-CD_2}$ only was produced from *gem*-$C_2H_2D_2$, but substantial (about 54%) *cis–trans* equilibration, though without intra- or inter-molecular H/D transfer, was observed by IR of the products in the oxidation of *cis*- and *trans*-1,2-dideuterioethylenes similarly as in Reference 2.

The cooxidation at $199\,°C$ of C_2H_4 together with [1,2-^{14}C]ethylene oxide and the cooxidation at $215\,°C$ of C_3H_6 with [2-^{14}C]propylene oxide over a silver catalyst showed no oxygen exchange between olefin and epoxide, but a certain portion of CO_2 was produced by destruction of the product epoxide (2% of CO_2 was produced from oxidation of propylene oxide and about 10% from ethylene oxide).

The large *inverse* deuterium isotope effects, that is the ratio of the formation rates for C_3D_6O and C_3H_6O, r_D/r_H of 3–5, much greater than the possible range of the true deuterium *inverse* isotope effects[3], have been rationalized qualitatively within the framework of the reaction scheme (equation 1), by assuming that C—H versus C—D bond rupture determines the further total oxidation of the intermediate, common to both epoxide formation and full oxidation to CO_2.

Assuming that the isotope effects in adsorption are negligible and the concentration of intermediate is small, we obtain equation 2.

$$\begin{array}{cc}
C_3R_6 & O_2 \\
\end{array} \qquad\qquad\qquad\qquad C_3R_6O_{(gas)} + O_{(ads)}$$

$$C_3R_{6(ads)} \quad + \quad O_{2(ads)} \xrightleftharpoons[k_{-1}]{k_1} \text{[intermediate]} \xrightleftharpoons[k_{-2}]{k_2} \qquad\qquad (1)$$

$$\xrightarrow{k_3} \qquad CO_2 + R_2O$$

$$R = H \text{ or } D$$
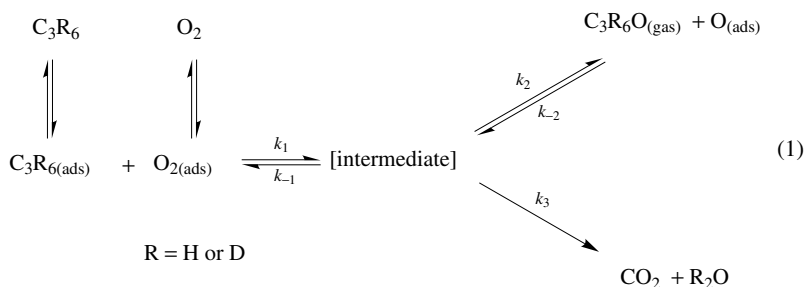
$$\frac{r_{(\text{for } CO_2 \text{ from } C_3H_6)}}{r_{(\text{for } CO_2 \text{ from } C_3D_6)}} = \frac{k_{3H}}{k_2 + k_{3H}} \cdot \frac{k_2 + k_{3D}}{k_{3D}} \qquad\qquad (2)$$

For propylene oxidation $k_{3H} \gg k_2$ and $k_{3D} \gg k_2$, therefore the ratio of rates of carbon dioxide formation should be near unity, whereas the ratio of rates of production of propylene oxides is approximated by equation 3.

$$\frac{r_{(\text{for } C_3D_6O \text{ from } C_3D_6)}}{r_{(\text{for } C_3H_6O \text{ from } C_3H_6)}} \cong \frac{k_2 + k_{3H}}{k_2 + k_{3D}} \approx \frac{k_{3H}}{k_{3D}} \qquad\qquad (3)$$

pointing directly to the oxidation of the intermediate to CO_2 as the rate-determining step. The experimental value of 4 indicates that C−H or C−D bond ruptures are rate limiting in this oxidation. The similarity of the rates of CO_2 production from $CD_3CD=CD_2$ and $CD_3CH=CH_2$ on the one hand and $CH_3CH=CH_2$, $CH_3CD=CH_2$ and $CH_3CH=CD_2$ on the other demonstrates that the hydrogen rupture (transfer) from the *methyl* group and not from the *vinyl* positions limits the further oxidation of the intermediate.

The analogous treatment of D KIE observed in the oxidation of ethylenes (equations 4 and 5) is less quantitative since in this case $k_2/(k_2 + k_{3H}) \approx 0.5$, $k_2 \approx k_{3H}$ and $k_2 \approx 2.5\, k_{3D}$.

$$\frac{r_{(\text{for } CO_2 \text{ from } C_2H_4)}}{r_{(\text{for } CO_2 \text{ from } C_2D_4)}} \approx \frac{1}{2}\left(1 + \frac{k_2}{k_{3D}}\right) \approx 1.7 \qquad\qquad (4)$$

$$\frac{r_{(\text{for } C_2D_4O \text{ from } C_2D_4)}}{r_{(\text{for } C_2H_4O \text{ from } C_2H_4)}} \approx \frac{2k_{3H}}{k_{3H} + k_{3D}} \approx 1.4 \qquad\qquad (5)$$

The above approximate assessments are in rather poor agreement with the experimental D KIE values corresponding to oxidation of isotopic ethylenes over Ag. Since the nature of the adsorbed oxygen species was unknown, the structures **1** and **2** have been proposed for the 'common' intermediates produced in the surface reaction between adsorbed molecular oxygen and olefin (equations 6 and 7).

The significantly higher rates of epoxidation of C_2D_4 than of C_2H_4 by O_2 catalyzed by Ag, observed by Cant and Hall[1], have been discussed subsequently by van Santen and coworkers[4] in terms of Worbs' mechanism of ethylene epoxidation[5], which assumes that diatomic adsorbed oxygen reacts with ethylene to give epoxide (EO) whereas monoatomic oxygen leads to total combustion of ethylene, and in terms of the mechanism proposed by Twigg[6], who assumed that EO is produced by the reaction of ethylene with monoatomic adsorbed oxygen. They found[4] that the EO depends selectively at 200 °C on the coverage of Ag powder surface by atomic Cl. A maximum selectivity of 74% was observed for an

atomic Cl/Ag surface ratio of 0.35 ± 0.10. The isotope effect α defined as

$$\alpha = \frac{k_{EO}^{D}}{k_{CO_2}^{D}} \Big/ \frac{k_{EO}^{H}}{k_{CO_2}^{H}}$$

$$(6a)$$

$$(6b)$$

$$(7)$$
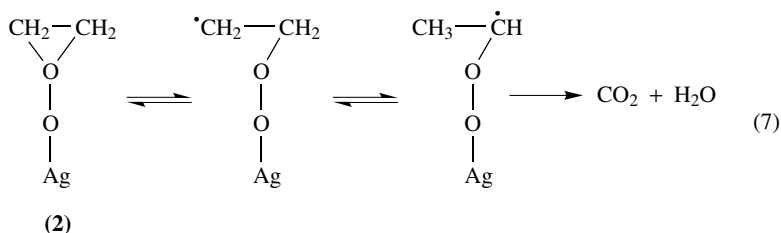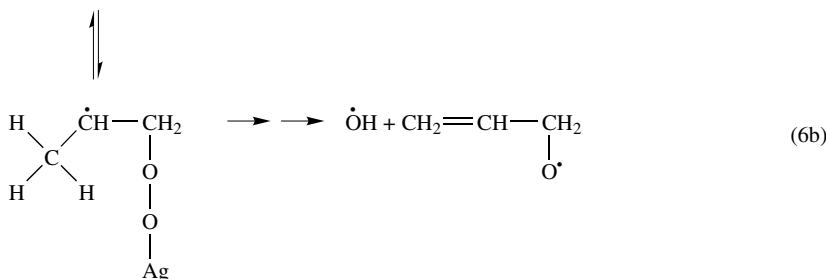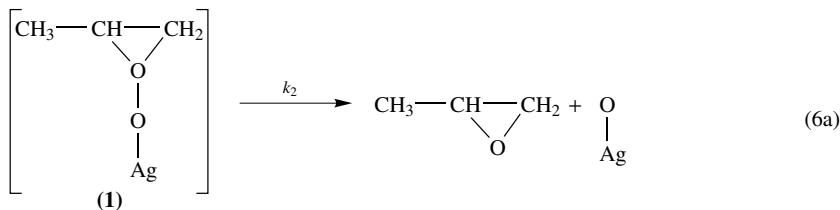
strongly decreases with increasing the selectivity caused by precovering of Ag surface with chlorine, and strongly increases with increasing temperature. In agreement with Cant and Hall[1] the replacement of C_2H_4 by C_2D_4 increases the rate of EO formation but decreases the rate of CO_2 formation.

2. Kinetic and deuterium isotope effect study of selective and total oxidation of ethylene catalyzed by Ag(111) single crystal surface

The detailed investigation of the oxidation of ethylene (C_2H_4 and C_2D_4) on Ag(111) single crystal surface in the temperature interval 300–700 K and at pressures of up to 50 torr has been carried out by Grant and Lambert[7] by MTPR (multimass temperature-programmed reaction) methodology. The chemisorbed atomic oxygen, $O_{(a)}$, reacts with adsorbed ethylene, in the absence of promotors and moderators, to produce ethylene oxide, EO, and ($CO_2 + H_2O$). The chemisorbed dioxygen, $O_{2(a)}$, does not play a direct role in the selective surface and total oxidations of ethylene. The subsurface oxygen, $O_{(d)}$, is

necessary for selective C_2H_4 oxidation but not for its total combustion. Oxidation of C_2H_4 and of C_2D_4 indicated that CD_3CDO, CD_3COOD and $(COOD)_2$ are intermediates in CO_2 formation. The yield of CD_3COOD was about 7 times greater than the yield of CH_3COOH. The total oxidations proceed by progressive stripping of the weakly acidic hydrogens' by basic $O_{(a)}$ species (equation 8), the $C-H/C-D$ scissions being the rate-determining ones in both pathways to carbon dioxide production. The Arrhenius activation energy for CO_2 production, E_a, was 50 ± 1 kJ mol^{-1} (at 10 torr pressure); E_a for selective oxidation was 45 ± 4 kJ mol^{-1}. The preexponential factors were approximately 4.5×10^{20} s^{-1} and 5.5×10^{18} s^{-1}, respectively.

$$
\begin{array}{ll}
& \text{CO}_2 + \text{H}_2\text{O} \qquad \text{C}_2\text{H}_4\text{O(g)} \\
\text{(1)} & \\
\text{O(a)} + \text{C}_2\text{H}_4 & \text{(3)} \\
\text{(2)} & \\
& \text{C}_2\text{H}_4\text{O(a)} \xrightarrow[\text{O(a)}]{4\text{(a)}} \text{CH}_3\text{CHO} \xrightarrow[\text{O(a)}]{4\text{(b)}} \text{CH}_3\text{COOH} \xrightarrow[\text{O(a)}]{4\text{(c)}} (\text{COOH})_2 \\
& \qquad\qquad\qquad\qquad\qquad\qquad\qquad\qquad\qquad\qquad\qquad \text{O(a)} \\
& \qquad\qquad\qquad\qquad\qquad\qquad\qquad\qquad\qquad\qquad\qquad\quad 4\text{(d)} \\
& \qquad\qquad\qquad\qquad\qquad\qquad\qquad\qquad\qquad\qquad \text{CO}_2 + \text{H}_2\text{O}
\end{array}
\tag{8}
$$
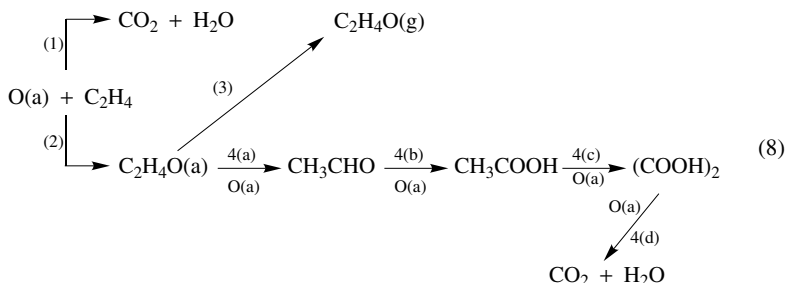
The apparent kinetic isotope effects for total and selective, partial oxidations of 1 : 1 (ethylene to O_2) mixtures (at 10 torr) at 500 K were found to be

$$
\frac{k_{(C_2D_4)}}{k_{(C_2H_4)}} = \frac{3.4 \times 10^{14}\,(\text{molecules s}^{-1}\,\text{cm}^{-2})}{7.2 \times 10^{14}\,(\text{molecules s}^{-1}\,\text{cm}^{-2})} \approx 0.5 \text{ for CO}_2 \text{ and}
$$

$$
\frac{4.0 \times 10^{14}}{6.1 \times 10^{13}} \approx 6.5 \text{ for epoxide production}
$$

Grant and Lamber[7,8] proposed that selective oxidation occurred by electrophilic attack by $O_{(a)}$ on the olefinic π-bond (charge transfer to $O_{(a)}$, equation 9), and that whole total oxidation is initiated by charge transfer from $O_{(a)}$ (equation 10).

$$\tag{9}$$
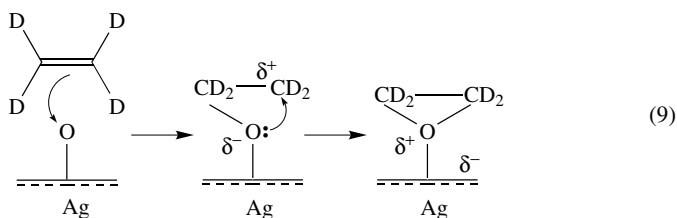
In the selective oxidation of ethylene over silver catalyst, the further oxidation of the product, ethylene oxide, EO, decreases the overall selectivity of the reaction. The isomerization of EO to acetaldehyde, AcH, has therefore been investigated[8] over a single crystal Ag(111) surface, which is an efficient catalyst for the isomerization EO $\rightarrow$ CH_3CHO, between 300 and 500 K and at pressures of up to 2 torr. Below about 410 K the rate of isomerization of the adsorbed reactant is rate limiting; at higher temperatures adsorption becomes rate controlling. The dissolved oxygen, $O_{(d)}$, enhances and the preadsorbed

Cs suppresses[9] the isomerization process, which is suggested to proceed as shown in equation 11.

(10)

(11)
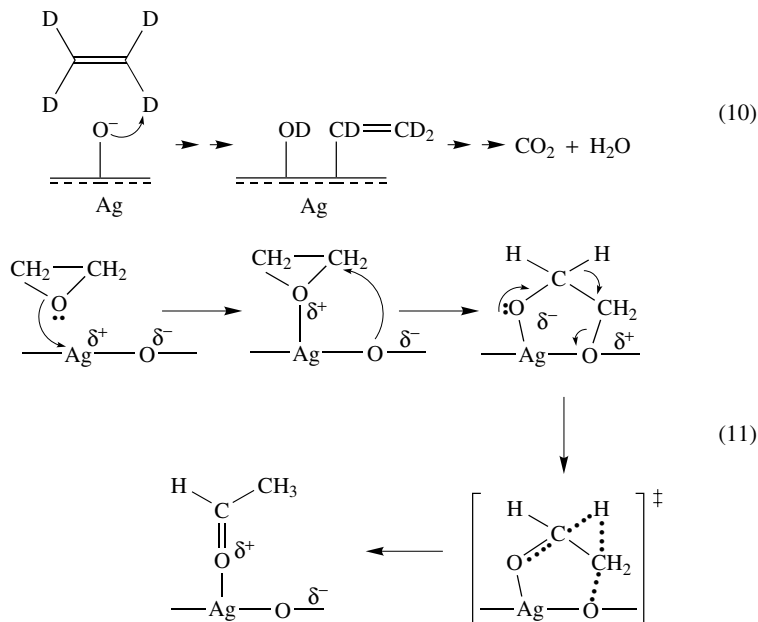
3. The relation between different oxygen species on the Ag surface and the deuterium isotope effects in the oxidation of ethylene on silver

Normal deuterium KIE for C_2H_4/C_2D_4 has been observed[1,4,7] in the complete total oxidation of ethylene on powdered silver and *inverse* D KIE has been found in the partial oxidation of C_2H_4/C_2D_4 to C_2H_4O/C_2D_4O (epoxyethane, ethylene oxide). The magnitude of D KIE in the oxidation of ethylene to EO depended on the initial composition of the gas mixture[7]. The above kinetic studies[1,4,7,10] have been supplemented[11,12] by passing $(He + C_2H_4 + O_2)$ mixtures over a powdered silver catalyst reduced with $(He + H_2)$ at 500 K or over a silver catalyst oxidized with $(He + O_2)$ mixture. In the initial period of oxidation of ethylene, catalyzed by reduced silver, the C_2H_4 interacts mainly with adsorbed surface O_s producing acetaldehyde CH_3CHO (involving hydrogen migration) which is oxidized[7] subsequently to AcOH, oxalic acid and CO_2. In the course of oxidation of ethylene (equations 12 and 13) the atoms of O_s oxygen insert into the bulk of silver and the subsurface, new species O_d oxygen are formed, producing $Ag^{\delta+}$ ions which bind ethylene molecules. This binding of π-systems by Ag^+ ions hinders the intramolecular hydrogen transfer and leads to production of epoxyethane not of AcH. Oxidations of $C_2H_4 : C_2D_4$, 1 : 1, mixtures showed no isotope scrambling in the reaction products and the rates of formation of C_2H_4O and C_2D_4O were the same. This means that no C—H bond rupture takes place in the course of epoxyethane production[13]. Both the (Ag_2O_s) and $Ag^{\delta+}$ $(-O^-{}_d)$ centres participate in the formation of epoxyethane (equations 14 and 15).

$$2Ag + O_2 \xrightarrow{k_1} 2Ag_2O_s \tag{12}$$

$$2Ag_2O_s \underset{k_{-2}}{\overset{k_2}{\rightleftharpoons}} Ag_2 + 2Ag^{\delta+}-O_d \tag{13}$$
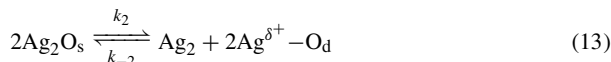
(diffusion of oxygen atoms into bulk of catalyst)

$$C_2H_4 + Ag_2O_s \xrightarrow{k_3} CH_3CHO-Ag_2 \xrightarrow{5Ag_2O_s} 2CO_2 + 2H_2O + 6Ag_2 \tag{14}$$

$$C_2H_4 + Ag_2O_s + Ag^{\delta+}-O_d \xrightarrow{k_4} C_2H_4O + Ag^{\delta+}-O_d + Ag_2 \tag{15}$$
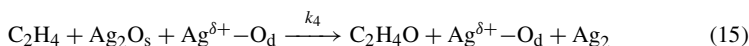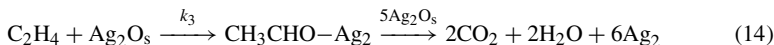
At large degrees of conversion of ethylene further oxidation of epoxyethane takes place on the $Ag^{\delta+}$ $(O^-{}_d)$ centres[8] at $T > 410$ K (equation 16).

$$C_2H_4O + Ag^{\delta+}-O_d \longrightarrow C_2H_4OAg^{\delta+}-O_d \xrightarrow{k_5} CH_3CHOAg^{\delta+}-O_d$$

$$\xrightarrow{5Ag_2O_s} 2CO_2 + 2H_2O + 5Ag_2 + Ag^{\delta+}-O_d \tag{16}$$
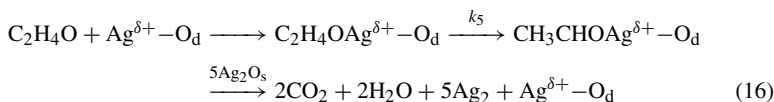
Equations 12–16 permitted one also to rationalize[11] the large *inverse* D KIE in the epoxidation of ethylene and their dependence on the inlet gas mixture. Since in the epoxyethane formation no C−H bond rupture takes place, the observed D KIEs are caused by the changes in the chemical composition of the surface layer of the catalyst controlling the catalytic reaction. In the presence of C_2D_4 the deep oxidation is slowed down, the concentration of $[Ag_2O_s]$ centres and subsequently also the $[Ag^{\delta+} (O^-{}_d)]$ centres increases and this results in the increase of the observed production of C_2D_4O.

Pinajeva and coworkers[11,12] tried to explain in a semiquantitative way the unusual deuterium isotope effects observed in the oxidation of ethylene on silver in terms of the inorganic parts of reactions 12–16 between oxygen and silver proceeding on the surface of the catalyst and also in the bulk of the catalyst, neglecting in their considerations the deuterium isotope effects in the adsorption of the C_2H_4/C_2D_4 and the contribution of the subsequent deep oxidation of the product, epoxide, to yield CO_2. Considering only reactions 14 and 15 the rate, r, of formation of epoxide is proportional to $[Ag_2O_s][Ag^{\delta+}-O_d]$ whereas the selectivity, s, is proportional to

$$\left(1 + \frac{k_3}{k_4} \cdot \frac{1}{[Ag^{\delta+}-O_d]}\right)^{-1}$$

Both r and s should increase with the degree of oxidation of surface Ag, but in different ways. In view of the reversibility of the process shown in equation 13, $[Ag^{\delta+}-O_d] \sim [Ag_2O_s]$, the rate of epoxidation $r \sim [Ag_2O_s]^2$, and the D KIE on r proportional to $\{[Ag_2O_s]^D/[Ag_2O_s]^H\}^2$ can reach large values. In the case of the reduced Ag catalyst the deuterium substitution leads to increase of $[Ag_2O_s]$ and of $[Ag^{\delta+}-O_d]$ and thus D KIE $= r_D/r_H$ increases greatly. In the stationary conditions when the surface of Ag is oxidized to a greater degree, the relative increase of the O_s and O_d silver oxides caused by the replacement of C_2H_4 with C_2D_4 is less pronounced and the D KIE is smaller. Similarly, the ratio $s^D/s^H \approx 70\%/30\%$ in the initial period diminishes to $72\%/57\%$ in the stationary conditions. At low O_2 pressures and low $\{P(O_2)/P(C_2H_4)\}$ ratios the concentrations of $[Ag_2O_s]$ and $[Ag^{\delta+}-O_d]$ are small, D KIE is large, whereas with increase of the $\{P(O_2)/P(C_2H_4)\}$ ratio the surface and subsurface layers are saturated with oxygen and the D KIEs are smaller. Moderate agreement between calculated and experimental D KIE

values was obtained by Pinajeva and coworkers[11,12] representing formally the catalytic epoxidation of ethylene by equations 12–16 only.

4. Oxygen-18 isotope effect in chemisorption of O_2 on Ag(111)

The oxygen-18 isotope effect in dissociative chemisorption of O_2 on the Ag(111) surface has been observed[14], when the Ag(111) crystal heated to 450 K was exposed to a 50% $^{16}O_2$–50% $^{18}O_2$ mixture at a total pressure of 0.05 mbar for 15 s in a high pressure cell[15] and then heated to 860 K in a linear fashion at simultaneous monitoring of desorbing $^{16}O_2$, $^{16}O^{18}O$ and $^{18}O_2$ molecules, formed by recombination of atomic oxygen on the Ag(111) surface[16]. The relative desorption yields for $^{16}O_2$, $^{16}O^{18}O$ and $^{18}O_2$ were 1 : 1.4 : 0.5 at 520 K. This distribution of isotopic dioxygen species indicates that oxygen is adsorbed dissociatively, the produced oxygen atoms are diffusing randomly on the surface and the dissociative adsorption probabilities for $^{18}O_2$ and $^{16}O_2$ are different. The authors[14] assessed that the dissociative adsorption probability for $^{16}O_2$ is 1.4 times larger than that of $^{18}O_2$. No reactions of adsorbed oxygen atoms with carbon monoxide adsorbed on the Ag surface yielding CO_2 were observed. The observed unusual ^{18}O isotope distribution between dioxygen molecules desorbed at 590 K has been ascribed rather arbitrarily to quantum mechanical tunnelling since the maximum ^{18}O KIE, calculated assuming that the $^{16}O-^{16}O$ and $^{18}O-^{18}O$ bonds are completely broken in the transition state of their dissociative adsorptions, equals 1.12 at 590 K [$\omega(^{16}O-^{16}O) = 1554.7$ cm^{-1}, $\omega(^{18}O-^{18}O) = 1465.59$ cm^{-1} and $\omega(^{16}O-^{18}O) = 1510.80$ cm^{-1}, respectively][17,18]. Using either the expression[19]

$$T = \exp\left\{-\frac{2}{h}\sqrt{2\mu(Q-E)a^2}\right\}$$

or the expression

$$T = \exp\left\{-\frac{2}{\hbar}\sqrt{2\mu(Q-E)a^2}\right\}$$

they found the ^{18}O isotope effect of 1.4 in agreement with their experimental assessments. The authors[14] did not test the precision of their MS determinations by reproducing the well-defined and studied equilibrium isotope effects for $^{18}O/^{16}O$ in the gas phase or in heterosystems[20]. The kinetics of the homomolecular ^{18}O isotope exchange in the $^{18}O_2/^{16}O_2$ system proceeding by the chain mechanism $^xO^\bullet + O_2 \rightarrow O^\bullet + {}^xO_2$ has been studied by Johnston and O'Shea[21a]. The dissociative mechanism of adsorption of $^{16}O_2$ and $^{18}O_2$ molecules leading to $^{16}O^{18}O$ molecules requires the formation of atomic ^{16}O and ^{18}O species, which recombine directly giving $^{16}O^{18}O$ molecules avoiding $Ag_2{}^*O$ and $^*O_3$ (ozone) formation which were indicated in other catalytic and gas-phase ^{18}O exchange studies[21].

Carbon-13 kinetic isotope effects in the oxidation of CO over Ag have been studied by I. Kobal and co-authors[21]. The experimental results have been reproduced assuming that CO reacts with only one adsorbed oxygen atom and by using the bent (CO_2) transition state structure with the interbond angle close to 110° in the rate determining step.

5. Final remarks

The deuterium isotope effect study[1] by Cant and Hall of the old catalytic process of epoxidation of ethylene[5] revealed the *unusual* deuterium KIE in the *olefin*/O_2/Ag reacting

system, which initiated the subsequent isotope and kinetic investigations aimed at the formal explanation of the observed isotope results and at understanding the nature of the hidden *organic/inorganic* catalytic processes[1]. It becomes obvious that the observed deuterium IEs are governed by D KIE in the C−H/C−D bond rupture and by changes in the concentration of individual oxygen species present on the surface and in the subsurface of the silver catalyst. Two mechanisms explaining qualitatively the observed D IEs have been proposed. In view of the importance of the industrial syntheses of oxygenated compounds the isotopic studies will undoubtedly be continued in spite of their complicated nature. The elegant explanation[1] of the role of deuteriation of the methyl group in propylene should mirror the ^{13}C KIE in the rupture of ^{13}C−H/^{12}C−H bonds.

B. Isotopic Studies of Oxidation of Oxygenated Compounds over Silver

1. Oxygen-18 study of the oxidation and decomposition of 1,2-ethanedioxy heterometallacycle by atomic oxygen on Ag(110)

The TPRS (temperature-programmed reaction spectroscopy) study of the products formed after exposure of $(CH_2{}^{16}OH)_2$ to the Ag(110) surface covered with $^{18}O_{(a)}$ showed[22] that in the reactions of adsorbed primary $OCH_2CH_2O_{(a)}$ species, with surface $^{18}O_{(a)}$ atoms besides $H_2{}^{18}O$, $(CH_2OH)_2$ and $(CHO)_2$ evolved at 255, 365 and 380 K, in addition, at 300 K $H_2C{}^{16}O$ and at 415 K $C{}^{16}O{}^{18}O$ and H_2 are also produced. Oxygen in the formaldehyde originates solely from the 1,2-ethanedioxy surface species, while in the surface formate one oxygen comes from $OCH_2CH_2O_{(a)}$, the second one from the coadsorbed ^{18}O oxygen atoms. The surface formate decomposes at 415 K to yield $C{}^{16}O{}^{18}O$ and hydrogen.

Two possible mechanisms can account for the observed distribution of ^{18}O between products: the first presented in equation 17 involving an initial nucleophilic attack of the adsorbed 1,2-ethanedioxy species by $^{18}O_{(a)}$ (with rate determining evolution of formaldehyde and water), and the second given in equation 18 involving the oxygen-assisted C−H bond breaking of $OCH_2CH_2O_{(a)}$ leading to formation of ethoxy-2-al species, $O=CHCH_2O_{(a)}$, and $OH_{(a)}$ which yields water by abstracting another hydrogen atom.

(17)

$$(18)$$
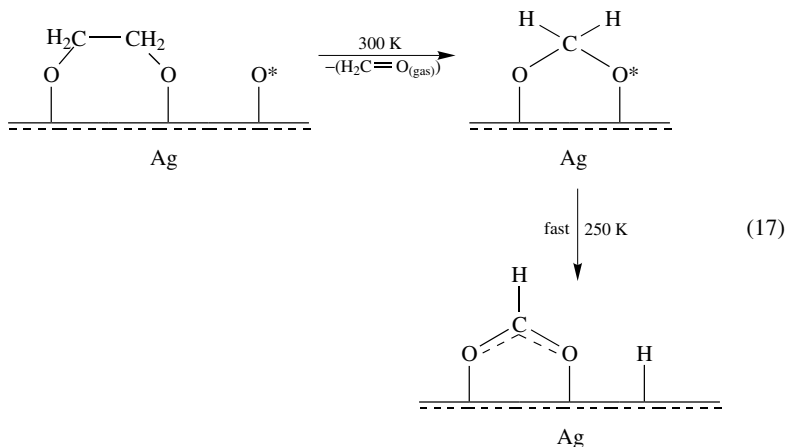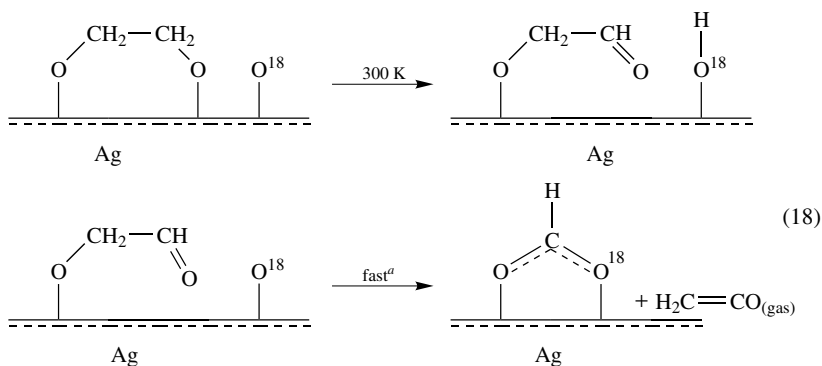
[a]Nucleophilic attack of ^{18}O at the carbonyl carbon

The TPR spectra following the exposure of $(CD_2OH)_2$ at 150 K to the Ag(110) surface covered with $O_{(a)}$ showed the desorption of H_2O at 250 K resulting in the reaction of $(CD_2OH)_2$ with $O_{(a)}$ (equation 19), similarly as in exposure of $(CH_2OH)_2$, but evolution of D_2CO and D_2O occurred at temperatures 20 K higher than that of H_2CO and H_2O. Such an upward shift of 20 K has also been observed[23] for the $CO_2/H_2(D_2)$ peak temperature when DCOOH was substituted for HCOOH. The k_H/k_D value of 8 ± 1 assessed from TPR spectra[24,25] is indicative of a primary D KIE[26]. Thus the reaction scheme given in equation 17 has been ruled out and the mechanism shown in equation 18, involving the rate-limiting abstraction of H/D from methylene carbon followed by C−C bond cleavage, release of $D_2C=O/H_2C=O$ and $DCOOH_{(a)}$ formation, has been selected as the favoured one. The vibrational spectra of $O_{(a)}$, $H_2O_{(a)}$, $OCH_2CH_2O_{(a)}$ and $OH_{(a)}$ on the Ag(110) surface following an exposure of $(CH_2OH)_2$ have been recorded by high resolution electron energy loss vibrational spectroscopy[27] (EELS).

$$(CD_2OH)_2 + O_{(a)} \longrightarrow OCD_2CD_2O_{(a)} + H_2O_{(a)} \qquad (19)$$
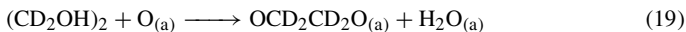
The oxidative decomposition of ethylene glycol, $(CH_2OH)_2$, on the Ag(110) surface covered with $O_{(a)}$ has been shown to proceed as given in equations 20. This differs from the mechanisms according to which 1,2-diols are cleaved in solutions by oxidizing agents such as HIO_4, $Pb(OAc)_4$[28] or Ag^{II} [29]. C−C bond cleavage on the Ag(110) surface in the presence of $O_{(a)}$ takes place via rate-limiting C−H bond activation followed by carbon−carbon bond scission to yield $H_2C=O$ and surface formate species. In solutions, the decomposition of the cyclic dialkoxy intermediates proceeds directly via carbon−carbon bond cleavage to yield two carbonyl fragments.

$$HOCH_2CH_2OH_{(a)} + O_{(a)} \longrightarrow HOCH_2CH_2O_{(a)} + OH_{(a)}$$

$$HOCH_2CH_2O_{(a)} + OH_{(a)} \longrightarrow OCH_2CH_2O_{(a)} + H_2O_{(a)} \qquad (20)$$

$$OCH_2CH_2O_{(a)} + {}^{18}O_{(a)} \longrightarrow O=CHCH_2O_{(a)} + {}^{18}OH_{(a)}$$

$$OCH_2CH_2O_{(a)} + {}^{18}OH_{(a)} \longrightarrow OCHCH_2O_{(a)} + H_2{}^{18}O_{(g)}$$

$$O=CHCH_2O_{(a)} + {}^{18}O_{(a)} \longrightarrow HCO^{18}O_{(a)} + H_2C=O_{(g)}$$

$$HCO^{18}O_{(a)} \longrightarrow CO^{18}O + H_{(a)}$$

$$2H_{(a)} \longrightarrow H_{2(g)}$$
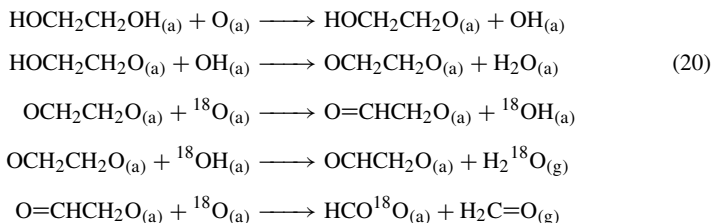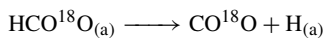
2. Deuterium and oxygen-18 study of the oxidation of t-butyl alcohol to isobutylene oxide on the Ag(110) surface

Me$_3$COD (*t*-BuOD), (CD$_3$)$_3$COH (*t*-BuOH-d$_9$) and ^{18}O have been applied[30,31] to study the mechanism of the reaction of *t*-butyl alcohol with preoxygenated Ag(110) surfaces by temperature-programmed reaction spectroscopy (TPRS). This differs from the oxidation of primary and secondary alcohols taking place in the temperature interval 275–300 K on Ag(110) or Cu(110) surfaces under ultra-high vacuum conditions (UHV) yielding aldehyde or ketone[32-36]. Below 200 K, *t*-BuOD reacts with oxygen adsorbed on Ag(110) to give *t*-BuO$_{(a)}$, adsorbed water and a hydroxyl group, similarly as do primary alcohols (equation 21). However, at further heating, *t*-BuO$_{(a)}$ reacts differently at 420–600 K providing *i*-butylene oxide (major product), *t*-butyl alcohol, water, *i*-butylene, acetone, CO and CO$_2$ (equation 22) by a process involving rate-limiting C–H bond rupture.

$$(21)$$
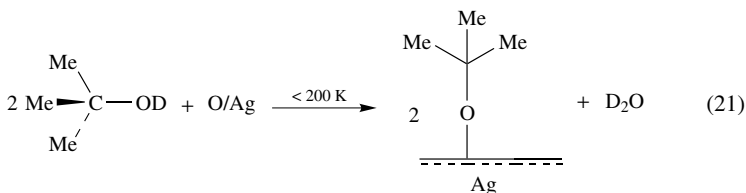
Clearly documented D KIEs with (CD$_3$)$_3$COH indicate that the process studied involves C–H/C–D bond breaking in the rate-limiting transition state[26,37]. No significant D KIE has been found in a process producing acetone which thus, probably, does not involve rate-limiting C–H/C–D bond breaking. The Arrhenius parameters had not been determined with sufficient accuracy to allow comparison of $A_{(Arrh)H}$ with $A_{(Arrh)D}$ or the differences in activation energy, E_a. Even so, the results show that the unactivated methyl C-bonds in *t*-BuO$_{(a)}$ are significantly more stable (98 kcal mol^{-1}) towards cleavage by the Ag surface than the activated C–H bond β to oxygen in MeO$_{(a)}$ or EtO$_{(a)}$ which are weaker by 4–7 kcal mol^{-1} due to their proximity to oxygen.

Experiments with ^{18}O$_2$ dosed on the Ag(110) surface showed that this oxygen added before the *t*-butyl alcohol dose does not incorporate into the *i*-butylene oxide, acetone or *t*-butyl alcohol products. The high-temperature reaction produces almost unlabelled water, indicating that the low-temperature reaction cleans off all the ^{18}O$_{(a)}$ and only the oxygen originating from *t*-BuO$_{(a)}$ and *i*-butylene formation is used for reaction above 500 K. The reactions occurring at 440 K and 510 K do not involve transfer of hydrogen atoms to the surface. No H$_2$ molecules have been noticed as a reaction product (H$_{(a)}$ reacts 100 times faster with itself than it does with *t*-BuO$_{(a)}$). Thus the cyclic TS **4** for reaction 23 has been rejected (path A in equation 23 compound **3**) and the direct proton transfer from the methyl group of *t*-BuO$_{(a)}$ to either O$_{(a)}$ at 440 K or to another *t*-BuO$_{(a)}$ at 510 K, as shown in equation 23 path B, has been suggested as the most likely bimolecular mechanism for the reaction proceeding at 510 K, consistent with the low preexponential factor (log A = 6.4), with the decrease of peak temperature with increasing *t*-BuO$_{(a)}$ coverage and with 'four-centered proton transfer reaction' common in the chemistry of metal alkoxides[38] and in methane activation[39].

$$\begin{array}{c}\text{CH}_2\\ \parallel\\ \text{Me}\diagup\text{C}\diagdown\text{Me}\end{array} + \text{CO}_2$$

$+$

$$\xrightarrow[\text{high O}_{(a)}]{440\text{ K}} \quad \text{CH}_2\!-\!\underset{\underset{\text{Me}}{|}}{\overset{\overset{\text{O}}{\diagup}\text{Me}}{\text{C}}} \quad + \text{ H}_2\text{O} \tag{22a}$$

$$\underset{\underset{\text{O}}{|}}{\overset{\text{Me}}{\underset{|}{\text{Me}}\!-\!\text{C}}}\cdots\overset{\text{Me}}{\underset{\underset{\text{Ag}}{\rule{2cm}{0.4pt}}}{\underset{|}{\text{O}}}}$$

$$\xrightarrow[\text{low O}_{(a)}]{510\text{ K}} \quad \text{CH}_2\!-\!\underset{\underset{\text{Me}}{|}}{\overset{\overset{\text{O}}{\diagup}\text{Me}}{\text{C}}} \quad + \text{ Me}_3\text{COH} \tag{22b}$$

$+$

$$\begin{array}{c}\text{CH}_2\\ \parallel\\ \text{Me}\diagup\text{C}\diagdown\text{Me}\end{array} + \text{H}_2\text{O} + \text{CO}_2$$

$$\xrightarrow{590\text{ K}} \quad \text{Me}_2\text{C}\!=\!\text{O} \tag{22c}$$

$$\underset{\underset{\text{CD}_3}{|}}{\overset{\overset{\text{O}}{\diagup}\text{CD}_3}{\text{CD}_2}} \quad + \text{ D}_{(a)} \qquad \overset{\text{D}_3\text{C}}{\underset{\text{D}_3\text{C}}{\diagup\diagdown}}\!=\!\text{CD}_2 + \text{O}_{(a)} + \text{D}_{(a)}$$

$$(23)$$

$$\text{(4)} \qquad \text{(3)}$$

$$\xrightarrow{\text{(B)}} \quad \longrightarrow \text{ 3 } + \text{ (CD}_3)_3\text{COD}$$
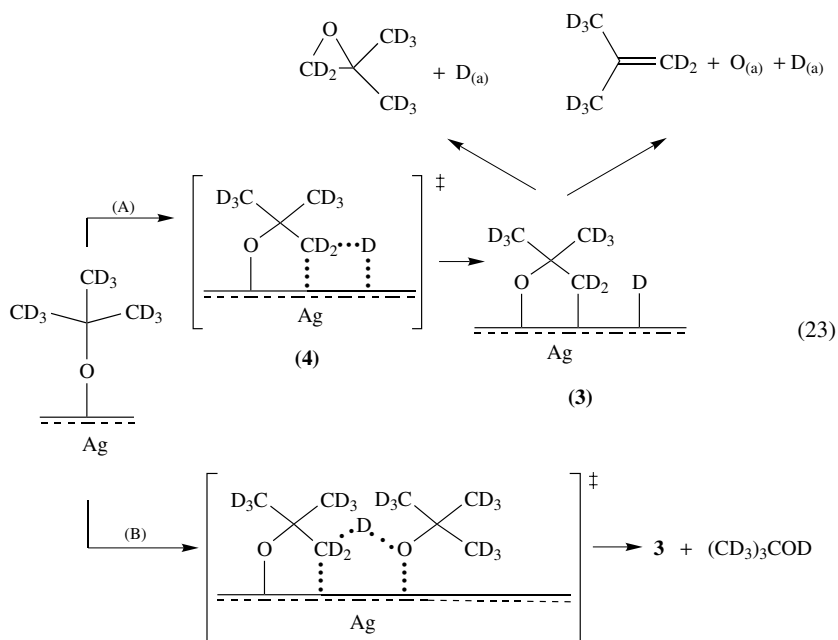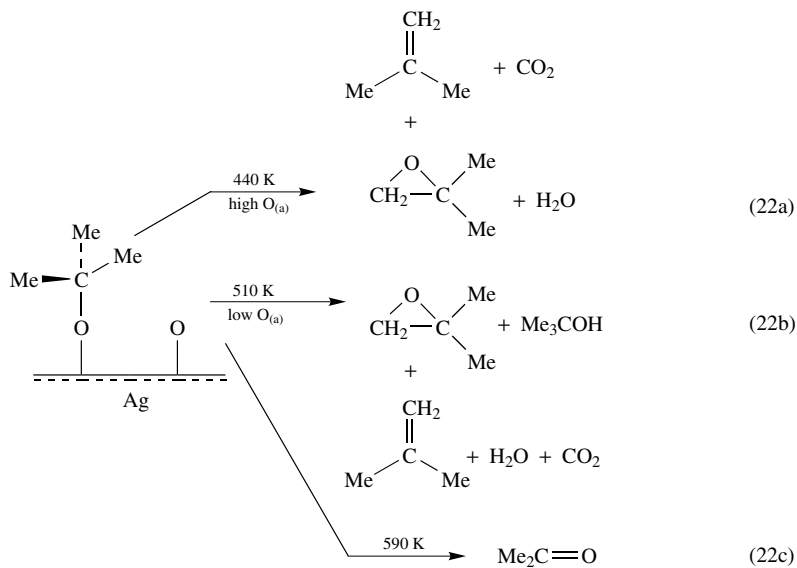
Mechanisms (C) and (D) have been proposed to rationalize the oxygen-assisted reaction at 440 K, shown in equation 24. It is impossible to distinguish the routes (C) and (D) since the hydroxyl disproportionation and the reaction of $H_{(a)}$ and $O_{(a)}$ to form water are fast at the reaction temperature. The role of oxygen in the C−H bond-breaking process has not been exposed precisely by Brainard and Madix[31].

$$\text{(24)}$$
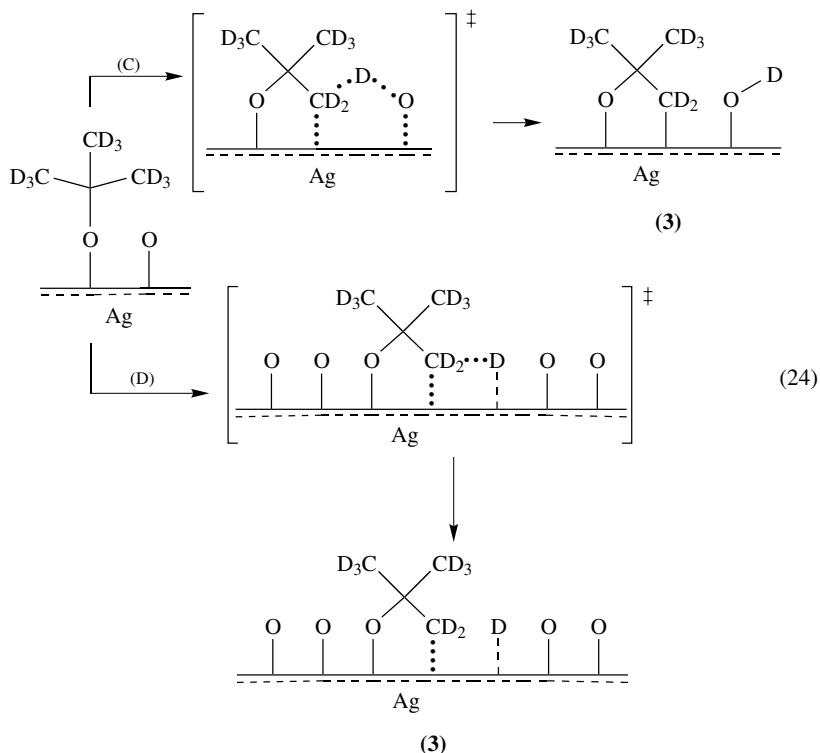
C. Isotopic Studies of Organic Reactions with Silver Salts

1. Vibrational spectra of $CH_2I_2 \cdot AgNO_3$ and $CD_2I_2 \cdot AgNO_3$

1 : 1 solid adducts have been obtained[40] in the reaction of aqueous silver nitrate with diiodoalkanes with adjacent iodine atoms like CH_2I_2, CHI_3, C_2I_4 or with diiodobenzenes (1,2, 1,4). Vibrational spectroscopy, solid state NMR spectra and powder X-ray diffraction indicated that the organic molecules act as donor ligands. The compounds, $[XAg_3](NO_3)_2$ (X = Br, I), have also been obtained from reactions of iodoorganic vapours with silver nitrate solutions. The numerical values of IR (and Raman) vibrations of diiodomethane, CH_2I_2, of its adduct, $CH_2I_2 \cdot AgNO_3$, and of its deuterated analogue $CD_2I_2 \cdot AgNO_3$ have been determined and their assignments given using Herzberg's descriptions[41]. The IR

spectrum of the $CH_2I_2 \cdot AgNO_3$ resembles the spectrum of the parent CH_2I_2. For instance, the symmetric, ν_1, and asymmetric ν_6, stretching modes of the methylene group, $-CH_2-$, equal 2967 cm^{-1} and 3096 cm^{-1} in CH_2I_2 (neat) and are located at 2980 cm^{-1} and 3075 cm^{-1} in IR of $CH_2I_2 \cdot AgNO_3$, respectively. They are shifted to 2200 cm^{-1} and 2320 cm^{-1} in $CD_2I_2 \cdot AgNO_3$. The symmetric, ν_3, and asymmetric, ν_9, modes for CI_2, located at 485 cm^{-1} and at 570 cm^{-1} in CH_2I_2 (neat), are shifted to 495 cm^{-1} and 570 cm^{-1} in $CH_2I_2 \cdot AgNO_3$. Thus the conclusion has been reached that CH_2I_2 retains its local C_{2v} symmetry in the adduct. The Raman adsorption at 132 cm^{-1} arises probably from Ag$-$I, since the ion $[AgI_2]^-$ has[42] ν_1 at 131 cm^{-1}. No $^{15}N/^{14}N$ or $^{18}O/^{16}O$ isotope shifts in the bonds corresponding to nitrate ion have been noted. The ^{127}I MAS (magic angle spinning) NMR spectra of solid AgI and of the CH_2I_2 silver adduct have also been recorded. The resonances are rather broad and do not permit one to prove the coordination of iodine to silver in the adduct, and they indicated only that silver is present in the local environment of iodine.

Silver salts catalyse organic reactions involving nucleophilic substitution by alkyl halides. A suggestion has been made that silver ion weakens the carbon–halogen bond before nucleophilic attack occurs (the 'pull' of the Ag$^+$ is greater than the 'push' of the nucleophile)[43].

2. Deuterium infrared study of the tetrahydroboratobis(triphenylphosphine)silver[l]

The vibrational IR modes of the title compound have been determined[44] during a comprehensive IR investigation of the $(Ph_3P)_2CuBH_4$ possessing mild reducing properties towards a number of organic functional groups[45−48]. Hydrogen–deuterium substitution has been utilized to facilitate the identification of the bond due to $CuBH_4/CuBD_4$ and $AgBH_4/AgBD_4$ portions of the $(Ph_3P)_2MBH_4$ and $(Ph_3P)_2MBD_4$ molecules (where M = Cu or Ag). The copper and silver borodeuterides were obtained[49,50] employing $NaBD_4$ in place of $NaBH_4$.

The infrared vibrational modes for $AgBH_4$ and $AgBD_4$ units in $(Ph_3P)_2AgBH_4$ and $(Ph_3P)_2AgBD_4$ have been recorded and assigned in Table 1. Substantial similarities of the fundamental frequencies for $CuBH_4$ and $AgBH_4$ have been observed. For instance, the bridge mode IR frequency (at *ca* 1380 cm^{-1}) and the skeletal M$-$B stretch frequency (360 cm^{-1}) in the case of Cu, and 312 cm^{-1} for Ag are comparable. The strengths of MBH_4 interactions for Cu and Ag complexes are found to be similar.

TABLE 1.   Infrared vibrational modes for $AgBH_4$ and $AgBD_4$ units in $(Ph_3P)_2AgBH_4$ and $(Ph_3P)_2AgBD_4$

ω_H/ω_D	$AgBH_4$ (cm^{-1})	$AgBD_4$ (cm^{-1})	Assignment
		1800 w	^{10}B$-$(H/D) terminal stretch
1.333	2378 s	1784 s	^{11}B$-$(H/D) terminal stretch
1.352	2343 s	1733 m	B$-$(H/D) terminal stretch
	2000 s		B$-$(H/D) bridge stretch
	1960		B$-$(H/D) bridge stretch
	1378 mw		Ag$-$(H/D)$-$B bridge mode
1.327$_4$	1115 s	840 mw	terminal BH_2/BD_2 deformation
1.076	312 mw	290 mw	Ag$-$B stretch

3. Infrared studies of Ag^I complexes with planar dithiooxamides (LH$_2$)

In the course of a detailed infrared study[51] of the structure of complexes of Cu^I formed in acid media with planar dithiooxamides (LH$_2$) of formula M(LH$_2$)$_1$X$_1$, where LH$_2$ is dithiooxamide (DTO), N-methyldithiooxamide (MDTO) and N,N'-dimethyldithiooxamide (DMDTO) and X is Cl, Br or I, the full vibrational analysis of the solid M(LH$_2$)$_1$X$_1$ products in the solid state with the use of NH/ND, CH$_3$/CD$_3$ and ^{63}Cu/^{65}Cu substitution has been performed. The in-plane deformation modes δNH$_2$ and δNH have been used to determine the S-*cis* or S-*trans* conformations of planar dithiooxamides. The position and number of metal–ligand vibration [single ν(MX) vibration in the case of terminal metal–halogen bonds and multiple ν(MX) vibrations in the case of bridging halogens between the metal atoms] served to determine the geometry around the metal[52]. These studies have been extended for the infrared study of Ag(DTO)$_1$Cl$_1$ and Ag(MDTO)$_1$Cl$_1$ complexes in which the terminal metal–halogen (νAgCl) bonds have been observed at 200 cm^{-1} for Ag(DTO)$_1$Cl$_1$ and at 205 cm^{-1} for Ag(MDTO)$_1$Cl$_1$ (see structure **5**). The νAgCl vibrations for Ag(DMDTO)$_1$Cl$_1$ are assigned to the bonds at lower frequencies: 188 and 149 cm^{-1}. The positions of these M−X−M vibrations are used as evidence of the presence of bridging halogen atoms in these compounds. The structure **6**, where the Ag atom is coordinated tetrahedrally with two S-*cis* and two halogen atoms, has been proposed for M(DMDTO)$_1$X$_1$ binuclear complexes[51].
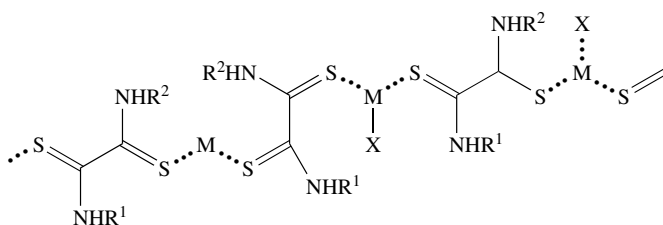
(5)

structure of the complexes Ag(DTO)$_1$Cl$_1$ and Cu(DTO)$_1$Cl$_1$, where R^1 = R^2 = H, and of the complexes Ag(MDTO)$_1$Cl$_1$ and Cu(MDTO)$_1$Br$_1$(black), where R^1 = H, R^2 = Me
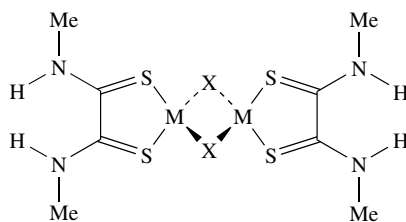
(6)

structure of the complex M(DMDTO)$_1$X$_1$, where M is Ag or Cu, X = Cl or Br

4. A correlation between the coupling constant $^1J(^{107}Ag-^{31}P)$ obtained by ^{31}P NMR and structural parameters in the $Ag(PPh_3)_3X$ series

The structure of tris(triphenylphosphine)silver^I tetrafluoroborate, $Ag(PPh_3)_3BF_4$, **7**, obtained in 73% yield from $AgBF_4$ with PPh_3 in CH_2Cl_2 at room temperature in darkness, and the structure of tris(triphenylphosphine)silver^I iodide, $Ag(PPh_3)_3I$, **8**, obtained in 62% yield from AgI with PPh_3 in CH_2Cl_2, have been determined[53] by X-ray diffraction. $Ag(PPh_3)_3NO_3$ has been prepared in 66% yield by mixing a solution of $AgNO_3$ in MeCN with a suspension of PPh_3 in MeCN, while $Ag(PPh_3)_3Cl$ was prepared as described by Cassel[54].

$$(Ph)_3P^1 \quad\quad\quad F-BF_3$$

$$Ag$$

$$(Ph)_3P^3 \quad\quad\quad (Ph)_3P^2$$

(7)

Distances (Å)	
Ag – F	2.82
Ag – P^1	2.577
Ag – P^2	2.506
Ag – P^3	2.543
<Ag – P>	2.54

Angles (deg)	
P^{1}AgP^2	114,9
P^{1}AgP^3	119.3
P^{2}AgP^3	119.0
P^{1}AgF	116.9
P^{2}AgF	89.8
P^{3}AgF	89.5

<P–Ag–P> 117.7, <P–Ag–F> 98.7

The parameters describing coordination about silver in $Ag(PPh_3)_3Cl$ and $^1J(^{107}Ag-^{31}P)$ in this complex have also been determined. The average values of Ag−P bond distances and the average values of P−Ag−P bond angles correlate with the $^1J(^{107}Ag-^{31}P)$ data in the series $Ag(PPh_3)_3X$, where X = BF_4, NO_3, Cl and I.

	X = BF$_4$	X = Cl	X = I
Ag–P distance (Å)	2.54	2.55	2.60
P–Ag–P angle (deg)	117.7	115.0	112.7
$^1J(^{107}Ag-^{31}P)^a$ (Hz)	318	277	262

$^a J(^{107}Ag-^{31}P)$ equals 309 Hz for $Ag(PPh_3)_3NO_3$, coupling constants measured at $-90\,^{\circ}C$.

The phosphorus atoms and one atom of the anion bind to metal in the distorted tetrahedral arrangement. The system is going from tetrahedral to a trigonal geometry at the metal.

		X = BF$_4$	X = Cl	X = I
Mean	P–Ag–P angle	98.7°	101.6°	108.6°

$$(Ph)_3P^1 \qquad\qquad I$$

$$Ag$$

$$(Ph)_3P^3 \qquad\qquad (Ph)_3P^2$$
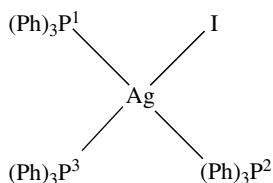
(8)

Ag $-$ P^1	2.582	P^{1}AgP^2	113.2	P^{1}AgI	104.9
Ag $-$ P^2	2.613	P^{1}AgP^3	114.1	P^{2}AgI	109.0
Ag $-$ P^3	2.616	P^{2}AgP^3	110.8	P^{3}AgI	104.1
<Ag $-$ P>	2.60	<PAgP>	112.7	<PAgI>	108.6

The changes of the P$-$Ag$-$P angle and the changes of the distance between metal$-$Ag and the plane determined by the three P atoms, changing from 0.39 to 0.72 Å, are also in agreement with this conclusion. The observed changes of the ^{107}Ag$-^{31}$P coupling constant are in agreement with a progressive decrease in the overlapping[55] of a bond orbital between Ag and P. The above data for the Ag(PPh$_3$)$_3$X series have been compared with the corresponding data for the Ag[P(p-Tol)$_3$]$_3$X series[56].

5. ^{31}P NMR and ^{109}Ag NMR study of [bis(phosphonio)isophosphindolide]silver complexes

The reactions of cations **9** [X] and **12** [X] (X $=$ Cl$^-$, Br$^-$, CF$_3$SO$_3^-$) with silver salts AgY (Y $=$ CF$_3$SO$_3^-$, CF$_3$COO$^-$, CH$_3$COO$^-$, 1/2SO$_4^{2-}$) (equation 25) and the equilibria observed in the reaction of cation **12** with CF$_3$COOAg (equation 26) have been studied[57] by ^{31}P and ^{109}Ag NMR. The ^{31}P and ^{109}Ag NMR data shown in Table 2 have been recorded for silver complexes **10a** and **11a** dissolved in CH$_2$Cl$_2$, for complexes **13** and **14** dissolved in THF and for complexes **15**$-$**17**. They were identical with NMR data for the crude reaction mixtures, thus indicating that all complexes dissociate partially forming a dynamic equilibrium involving mono- and di-silver complexes and free ligands. Identification of these species was possible by taking their ^{31}P NMR in the temperature interval -50 to $-120\,^{\circ}$C under slow exchange conditions. The species **10a**, **11a** and the dinuclear complex **15** were characterized also by ^{109}Ag NMR data derived from heteronuclear ^{31}P, ^{109}Ag shift correlations[58].

The values of $^1J(^{109}$Ag,^{31}P) given in last column are comparable with $^1J(^{109}$Ag, ^{31}P) $=$ 750$-$880 Hz values found in phosphane complexes of type (R$^1_3$P)AgR^2 (R$^2 =$ ligand not containing phosphorus)[59,60]. They indicate a σ-coordination of the cationic ligand via the phosphorus lone pair in agreement with the crystal structure of **13**, composed of separate [R^{1}Ag(THF)(OSO$_2$CF$_3$)]$^+$ cations and CF$_3$SO$_3^-$ anions, in which the two Ag$-$O distances correspond to a real bond connecting two atoms in the same molecule, and the Ag$-$P distance lies at the lower end of the normal silver$-$phosphorus bond lengths in related tertiary phosphane complexes[61$-$63].
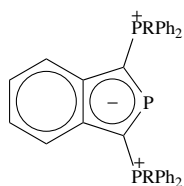
(9, 10a, 11a, 13, 14) R = Ph
(10b, 11b, 12) R = C$_2$H$_3$

$$\text{(25)}$$

9, 12 [CF$_3$SO$_3^-$]

$$\text{(26)}$$
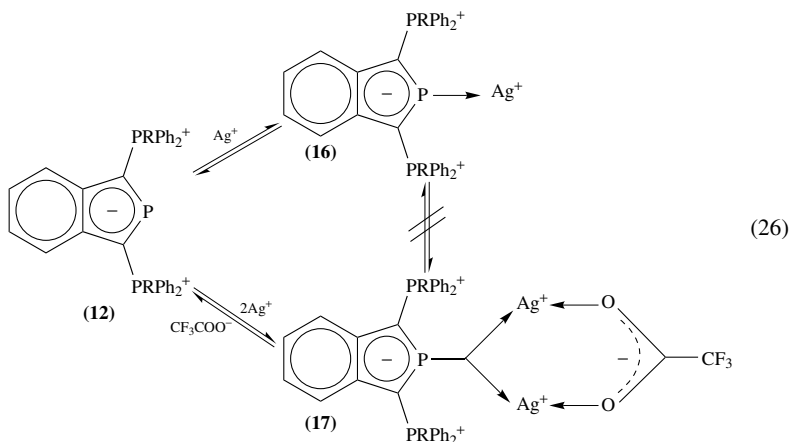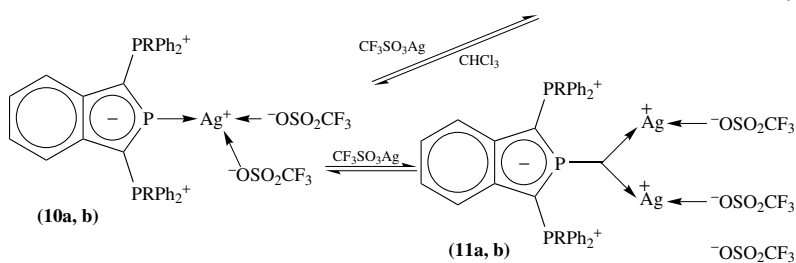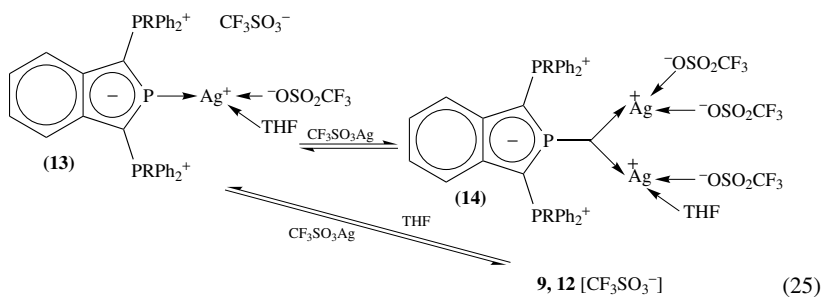
TABLE 2. ^{31}P and ^{109}Ag NMR data for the silver complexes **10**, **11**, **13**–**17** in solution^a

		T (°C)	δ^{31}P >P–Ag (ppm)	δ^{31}P –PPh$_3$ (ppm)	$^2J_{pp}$ (Hz)	δ^{109}Ag (ppm)	$^1J(^{109}$Ag$-^{31}$P) (Hz)
13 (in THF)	R^{1}Ag(CF$_3$SO$_3^-$)(THF)	–50	187.3	13.7	77.3	528.5	825 ($^3J_{AgP}$ = 1.4 Hz)
14 (in THF)	R^{1}Ag$_2$(CF$_3$SO$_3^-$)$_3$ (THF)	–110	102.9	11.8	69	—	492^b
10a (in CH$_2$Cl$_2$)	R^{1}Ag(CF$_3$SO$_3^-$)$_2$	–50	188.5	13.7	77.3	502.1	831.6 ($^3J_{AgP}$ = 2 Hz)
10b (in CH$_2$Cl$_2$)	R^{2}Ag(CF$_3$SO$_3^-$)$_2$	–100	193.3	9.5	79	—	808
11a (in CH$_2$Cl$_2$)	[R^{1}Ag$_2$(CF$_3$SO$_3^-$)$_2$]$^{+c}$	–120	98.8	10.6	70.4	—	520^b
11b (in CH$_2$Cl$_2$)	[R^{2}Ag$_2$(CF$_3$SO$_3^-$)$_2$]$^{+c}$	–100	104.7	8.1	70.5	—	519
15 (in CH$_2$Cl$_2$)	[R^{1}Ag$_2$(μ-CF$_3$COO)]$^{2+c}$	–70	131.0	12.3	73.8	764.3	440
16 (in CH$_2$Cl$_2$)	[R^{2}Ag]$^{2+b}$	–100	193.5	9.5	81.4	—	749^b
17 (in CH$_2$Cl$_2$)	[R^{2}Ag$_2$(μ-CF$_3$COO)]$^{2+c}$	–100	140.8	8.6	73.8	—	441

^{a}R^1 = **9**, R^2 = **12**. No coordination of **9** and **12** with Ag$^+$ took place when Y$^-$ = CH$_3$COO$^-$ and SO$_4^-$.
^{b}This value was calculated from the observed average coupling constant 0.5[$^1J(^{109}$Ag, ^{31}P) + $^1J(^{107}$Ag, ^{31}P)].
^{c}The additional ligands and coordination number three at silver are highly probable, but they are not detectable in the NMR spectra.
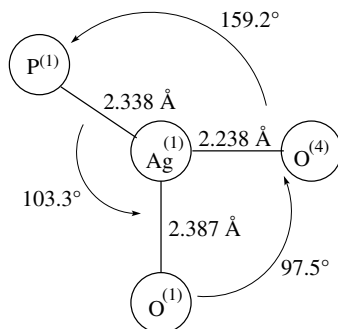
Structure **13** (oxygen atom $O^{(4)}$ belongs to a
THF ligand, $O^{(1)}$ to a triflate ligand)

6. Reactions of diaminophosphenium and 1,3,2-diazophospholenium triflates with silver salts

The multinuclear ^{1}H, ^{13}C, ^{31}P and ^{109}Ag NMR spectra served to establish the constitution and structure of neutral complexes $\{[(i\text{-}Pr_2N)_2(Y)P]Ag(OSO_2CF_3^-)\}$, **18**, **19**, **20**, **21** formed[64] in the reaction of bis(diisopropylamino)phosphenium triflate ($CF_3SO_3^-$), **22**, with silver salts AgY, where $Y^- = CF_3COO^-$, **23**, $CF_3SO_3^-$, **24**, CH_3COO^-, or in the reaction of 4-chloro-1,3-bis(2,6-dimethylphenyl)-1,3,2-diazaphospholenium triflate, **26**, with **23** and **25**, affording the equilibrium mixture **21** (equations 27 and 28).

Xyl
|
N
P$^+$ [CF$_3$SO$_3^-$] $\underset{\longleftarrow}{\overset{Ag(Y),\ \textbf{23, 25}}{\rightleftarrows}}$
N
|
Cl
Xyl

(26)

Xyl
|
N   Y
P
N   Ag
Cl   OSO$_2$CF$_3$
Xyl

(21)   **(21a)**   Y = CF$_3$COO
(21b)   Y = CH$_3$COO   **(28)**

Xyl =   (2,6-dimethylphenyl ring, Me, Me)
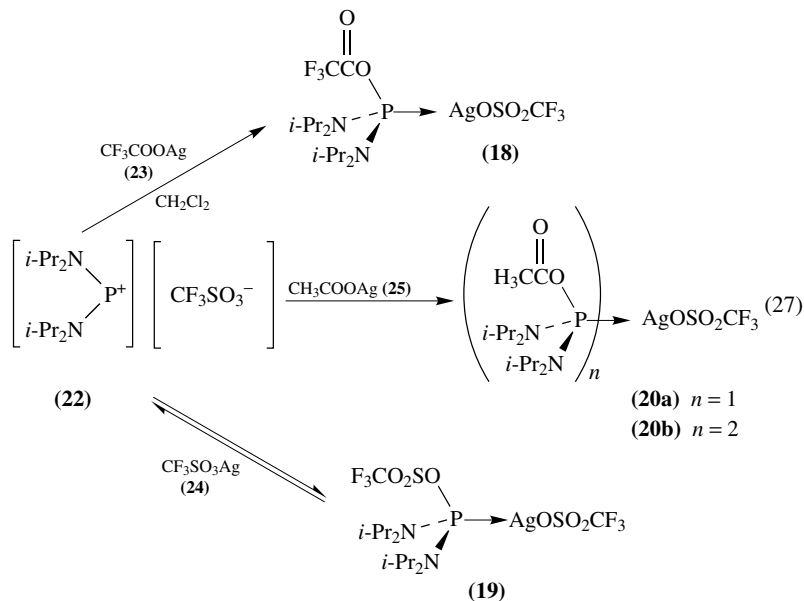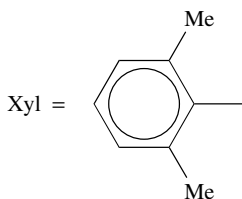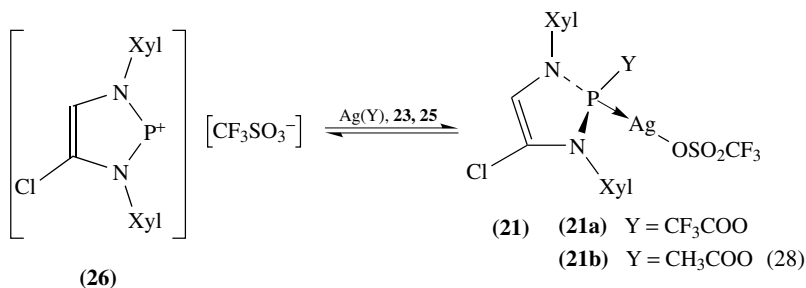
The AX spin systems (A = ^{31}P, X = ^{109}Ag) in the silver complexes (**18–20a**) associated with the 'AgP' core and A$_2$X spin system in **20b** have been revealed. The ^{31}P and ^{109}Ag NMR data in Table 3 have been obtained for **18–20** and **21a**, **b** compounds in CH$_2$Cl$_2$. These data suggested the presence of four-coordinate phosphorus centres and the attachment of the trifluoroacetate as the fourth substituent to phosphorus in **18**, **20a** and **20b**.

7. ^{109}Ag NMR spectroscopic studies of Ag^I complexes

^{107}Ag and ^{109}Ag both have $I = 1/2$ but ^{109}Ag is more suitable for NMR measurements[65]. The ^{109}Ag NMR spectra, using the INEPT (insensitive nuclei enhanced by polarization transfer) sequence [proton polarization transfer sequence between two J coupled spins $I(^{109}$Ag) and $s(^1$H), $^3J(^{107,109}$Ag$-^1$H-imine) = 9.3 Hz (δ 8.87) and 6.3 Hz (δ 8.69)], have been applied[66] to gain insight into the electronic environment and the structural and dynamic behaviour of Ag^I complexes in solutions[66,67]. The chemical shift of the ^{109}Ag^I nucleus is highly sensitive towards changes in its environment[68]. The

TABLE 3. ^{31}P and ^{109}Ag NMR data for compounds in CH$_2$Cl$_2$

Compound	$T(^\circ$C)	δ^{31}P	δ^{109}Ag	$J(^{109}$Ag,^{31}P)
18	−80	103.2	400.1	1140
19	−110	121.3	433	1116
20a	−40	93.0	385	1191
20b	−40	98.5	560	814
21a	−110	91.6	—	1040^a
21b	−100	86.1	469	1119

^{a}1/2[$J(^{107}$Ag, ^{31}P) + $J(^{109}$Ag, ^{31}P)].

[1]H decoupled INEPT spectra of dicationic complexes of the type {Ag^I$_2$[μ-(R,S)-1,2-[(6-R-2-C$_5$H$_3$N)C(H)=N]$_2$cyclohexane]$_2$}·(CF$_3$SO$_3^-$)$_2$ (27, R = H) have been studied[66,67]. The chemical shift value obtained for the binuclear silver (I, R = H) complex 27 equals +580 ppm relative to 2M aqueous AgNO$_3$. The δ^{109}Ag is very sensitive with respect to the ligand environment. Introduction of the Me group in the 6 position of the pyridine rings of the ligand caused a deshielding effect on the ^{109}Ag nucleus (downfield chemical shift) $\Delta\delta^{109}$Ag = 32 ppm with R = H and R = Me in 27. The $^1J(^{15}$N$-^{107,109}$Ag) values correlate with the Ag−N bond lengths[68]. Observation of $^1J(^{15}$N$-^{107,109}$Ag) and $^3J(^1$H$-^{107,109}$Ag) showed that the intermolecular exchange reactions of 27 are slow[68], but the exchanges of Ag$^+$ between Ag^I of 27 and the uncomplexed free radioactive $^{110m,111}Ag$ labelled silver cation in solutions have not been studied. Many organometallic complexes show long-range metal proton scalar coupling[70].
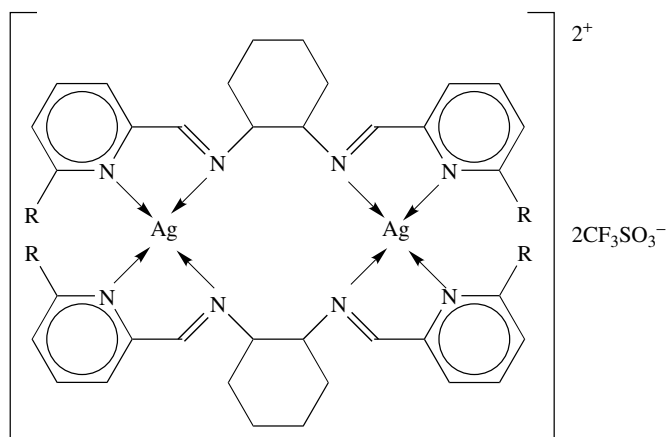
(27)

    Structural features of silver^I *bis*(thiophene-2-carbaldehyde imine)-trifluoromethane sulphonate complexes in solid state and in solution have also been investigated[69] by ^{109}Ag spectroscopy applying the INEPT pulse sequence (equation 29) where (R^1 = H, R^2 = *i*-Pr), (Me, *i*-Pr), (TBS, *i*-Pr), (H, S-CHMePh), (Me, S-CHMePh), (TBS, S-CHMePh).

    The cation 28 consists of a linearly coordinated sp-hybridized metal nucleus (d^{10} nuclei like Ag^I) with strong imine N−Ag bonds, caused by substantial hybrid overlap with an imine−N lone pair, resulting in a short Ag−N distance of 2.16 Å (av). The interaction of an empty perpendicular p orbital of Ag^I with the lone pairs of the thiophene S-group is extremely weak ('dipole-cation attraction'), with the Ag−S distance = 3.02 Å. The N−Ag−N angles are 174.6° (av). The S donor atoms are directed towards the silver nucleus. The ^{1}H, ^{19}F NMR experiments and ^{1}H$-^{109}$Ag decoupling experiment indicated that the Ag^I complexes are prone to intermolecular exchange processes (at 298 K) which become slow at low temperature (<255 K), whereas the intramolecular exchange processes are not eliminated even at 130 K. This can be corroborated by

isotope ligand exchange and [110]Ag exchange studies. No activation energy for intramolec-
ular ligand exchange was determined. The local environment of Ag^I in structure **29** of
$[Ag_2(N_2S_2)_2](OTf)_2$ was found to be similar[67]. The short N−Ag distances range from
2.15 to 2.17 (av), the thiophene−S−Ag distances equal 2.92−2.99 Å and indicate weak
or absent bonds. However, the S−Ag−S angles differ considerably, being 104.7° in the
monocation vs 82.1° (av) in the dication.

(28) 'Λ'

(29)

(28) 'Δ'
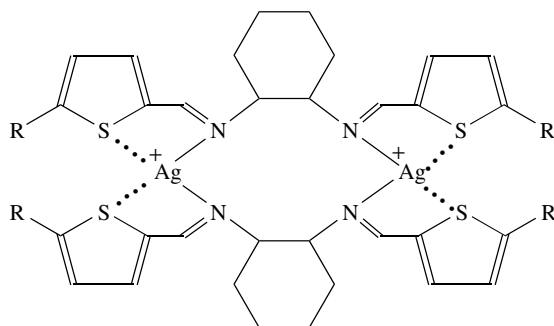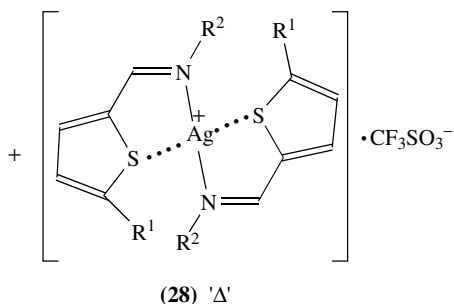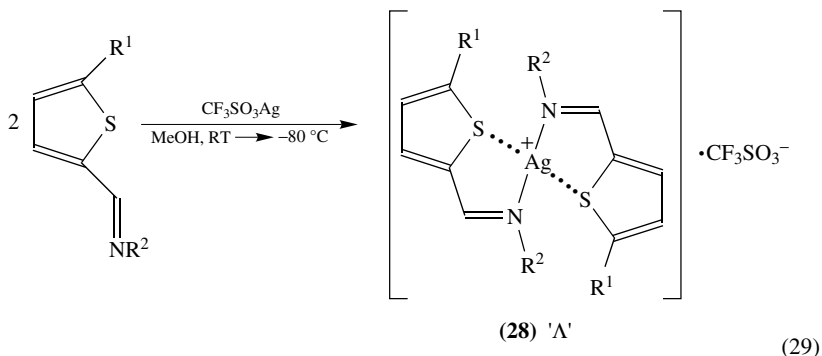
(29) $[Ag_2(N_2S_2)_2](CF_3SO_3)_2$

8. ^{109}Ag-[^1H] INEPT NMR studies of $\{Ag_2Ru_4(\mu_3\text{-}H)_2[\mu\text{-}Ph_2P(CH_2)_nPPh_2]\cdot(CO)_{12}\}$ (n = 1, 2 or 4) clusters

A spectroscopic and X-ray diffraction study[71] showed that the silver clusters $\{Ag_2Ru_4(\mu_3\text{-}H)_2[\mu\text{-}Ph_2P(CH_2)_nPPh_2]\cdot(CO)_{12}\}$ ($n = 1-6$) adopt the capped trigonal-bipyramidal metal core geometry, **30**, with two distinct silver sites in the ground-state structures, but the $^{109}Ag[^1H]$ INEPT NMR spectra of clusters in which $n = 1, 2$ or 4 have at ambient temperature a single averaged silver resonance indicating the stereochemical non-rigidity of the metal skeletons of the group 1B metal heteronuclear clusters in solutions[72]. The silver atoms exchange between these two different metal sites. The change in the ligands attached to the silver atom from two triphenylphosphine groups to $Ph_2PCH_2PPh_2$ ligand shortens the Ag–Ag distance by about 0.1 Å and lengthens the Ag–Ru separations. The ambient-temperature ^{109}Ag-[^1H] INEPT and ^{31}P-[^1H] NMR data have been determined for all compounds **30–35**. The coupling constants derived from ^{109}Ag-[^1H] INEPT and ^{31}P-[^1H] NMR spectra are in very good agreement[72].
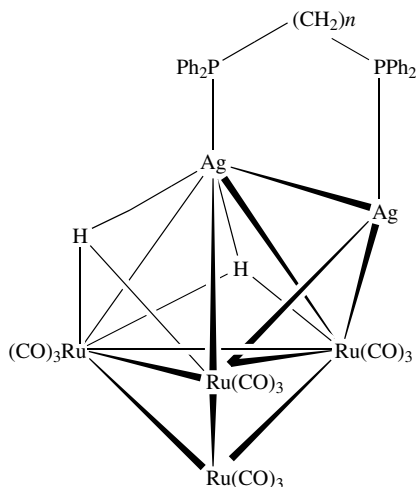
30-35 for $n = 1$ to 6, respectively

9. The dynamic behaviour of cluster compounds $\{Ag_2Ru_4(\mu_3\text{-}H)[\mu\text{-}Ph_2As(CH_2)_n EPh_2]\cdot(CO)_{12}\}$

In this investigation[73,74] the mixed-metal cluster compounds $\{Ag_2Ru_4(\mu_3\text{-}H)[\mu\text{-}Ph_2As(CH_2)_nEPh_2]\cdot(CO)_{12}\}$, where E = P, $n = 1$ or 2, **36**, and E = As, $n = 1$ or 2, **37**, have been synthesized[73]. Variable-temperature ^1H- and ^{31}P-[^1H] NMR studies demonstrated that the bidentate $Ph_2As(CH_2)_nPPh_2$ ligands undergo intramolecular site exchange between the two silver atoms in **36** and, as the temperature is raised further (decomposition at 70 °C), the bidentate ligands undergo intermolecular exchange between clusters. Clusters **37** containing $Ph_2As\,(CH_2)_nAsPh_2$ ligands also undergo a fluxional

process involving metal site exchange at ambient temperatures in solution as may be observed directly in {$Ag_2Ru_4(\mu_3$-H)$_2[\mu$-Ph$_2$AsCH$_2$AsPh$_2]\cdot(CO)_{12}$} by ^{109}Ag-[^{1}H] INEPT NMR spectroscopy. The signal for the ^{109}Ag^{109}Ag isotopomer of this compound is a singlet, and the ^{109}Ag chemical shift is about 650 ppm lower than in the analogous cluster containing Ph$_2$PCH$_2$PPh$_2$. The increase in shielding is attributed to the 'bulky substituent' effect of the more polarized arsenic atoms.

(36A)   **(36B)**
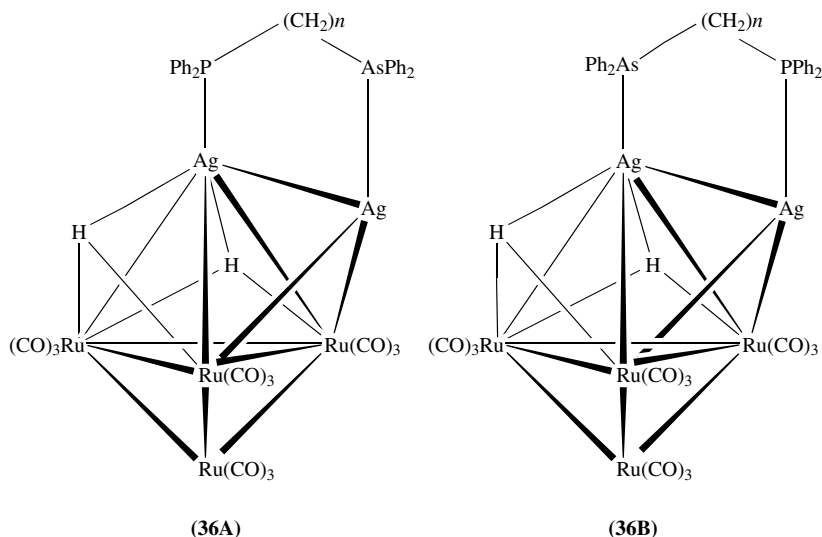
10. ^{31}P, ^{107}Ag and ^{109}Ag NMR spectroscopic study of [Ag(μ-R$_2$PhCH$_2$PR$_2$)$_3$Ag]$^{2+}\cdot$ (AsF$_6$)$_2^-$ complexes

^{107}Ag-enriched [Ag$_2[\mu$-R$_2$PCH$_2$PR$_2)_3]$(AsF$_6$)$_2$ compounds, where R = Ph **(38)** or Me **(39)**, have been obtained in the reaction of ^{107}AgAsF$_6$ with 1,2-bis(diphenylphosphino)methane or with 1,2-bis(dimethylphosphino)methane[75−77]. ^{107}Ag AsF$_6$ has been prepared[78] by treating isotopically enriched silver metal (98.22% ^{107}Ag) of 99.99% chemical purity with AsF$_5$ in SO$_2$. The ^{107}Ag-enriched complexes **38** and **39** were needed to simplify the detailed interpretation of the variable-temperature ^{31}P NMR spectra of **38** and **39** containing ^{107}Ag and ^{109}Ag at the natural abundance level. In the dimeric Ag$_2$ complex the statistical fractional populations[79] of the (^{107}Ag)$_2$, (^{107}Ag ^{109}Ag) and (^{109}Ag)$_2$ isotopomers are 0.269, 0.499 and 0.232, respectively. This makes the interpretation of NMR spectra of **38** and **39** rather difficult. The ^{31}P NMR spectra of a 1 : 1 mixture of ^{107}Ag$_2$-**38** and ^{107}Ag$_2$-**39** recorded at ambient temperature indicated the formation of a mixed ligand binuclear cation [^{107}Ag$_2$(Ph$_2$PCH$_2$PPh$_2$)$_{3-x}$(Me$_2$PCH$_2$PMe$_2$)$_x$]$^{2+}$ (x = 1 or 2), **40** (equation 30). The ^{31}P NMR spectra of **38**, **39** and **40** have been interpreted in terms of the manxane structure **41**.

(37)

$$^{107}Ag_2(dppm)_3(AsF_6)_2 \quad ^{107}Ag_2(dmpm)_3(AsF_6)_2$$

(38)   **(39)**

$$[^{107}Ag_2(dppm)_3]^{2+} + [^{107}Ag(dmpm)_3]^{2+} \longleftrightarrow [^{107}Ag_2(dppm)_{3-x}(dmpm)_x]^{2+} \quad (30)$$

(40)

(41) $P = PR_2, R = Ph$ or Me

The variable-temperature ^{31}P NMR spectra of **38** and **39** showed that the cations **38** and **39** have the same structure, contain symmetrical spin system, the expected couplings to ^{107}Ag (both having $I = 1/2$) and also that with the increase in the temperature, intramolecular exchange processes take place in **38** and **39** (faster for $R = Ph$ than for $R = Me$) through an 'end-over-end' exchange[80] of bridging $R_2PCH_2PR_2$ ligands as shown in equation 31. The anchored ligand exchange of equation 31 probably involves a short-lived complex **42** (equation 32).

(31)

(32)

(42)

The intramolecular ligand exchange (equation 31) in **38**, as determined from the temperature-dependence NMR study in the temperature range -4.1 to $22.4\,^\circ$C, proceeds with an enthalpy of activation of 58.7 ± 1.4 kJ mol^{-1}. The same Eyring plot covering the temperature range $36.0-54.4\,^\circ$C gives $\Delta H^{\neq} = 49.9 \pm 1.5$ kJ mol^{-1} for the ligand exchange of **39** in acetone, $[^{107}Ag(\mu\text{-Me}_2PCH_2PMe_2{}^{107}Ag)]^{2+}$. The difference in the entropies of activation between **38** and **39** favours the intramolecular ligand exchange in **38** (faster in **38** than in **39**).

11. Synthesis and ^{35}Cl nuclear quadrupole resonance study of (2,4,6-trichlorophenolato-O, Cl)bis(triphenylphosphine)silver^{l}

The title compound, $(Ph_3P)_2AgOC_6H_2Cl_3\text{-}2,4,6$, has been synthesized[81] as shown in equation 33:

$$Ag_2O + 2HOC_6H_2Cl_2X\text{-}2,4,6 + 4Ph_3P \longrightarrow 2(Ph_3P)_2AgOC_6H_2Cl_2X\text{-}2,4,6 + H_2O \quad (33)$$

(43)
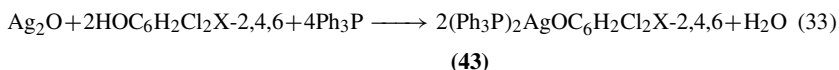
X-ray crystallographic study of the structure of **43** indicated[81] that Ag is coordinated in the trigonal planar geometry by the P atoms of the two PPh_3 ligands and one O atom of the chlorophenolate; Ag is additionally coordinated by the Cl one group at a distance of 3.160 Å, which is substantially shorter than the sum of van der Waals radii, $3.40-3.50$ Å. The five-membered chelate $[Ag-O^1-C^{37}-C^{38}-Cl^1]$ ring is not planar.

Supplementary spectroscopic data needed to clarify the bonding of Ag to the *ortho*-chlorine (Cl^1) atom have been provided by the ^{35}Cl NQR (nuclear quadrupole resonance) spectrum of **43**. According to previous studies[87−89] the ^{35}Cl NQR frequency of a coordinated chlorophenolate *ortho*-chlorine (Cl^1) should be lowered relative to that of the non-coordinated *ortho*-chlorine (Cl^2). The ^{35}Cl NQR spectrum of **43** taken at 77 K showed that the frequencies of the two *ortho*-chlorines of the trichlorophenolate ligand differ by 1.500 MHz ($35.039-33.539 = 1.500$ MHz). This indicates that the *o*-Cl is coordinated to the silver atom (the ^{35}Cl NQR frequency of *p*-Cl in **43** equals 35.100 MHz). The

(43)
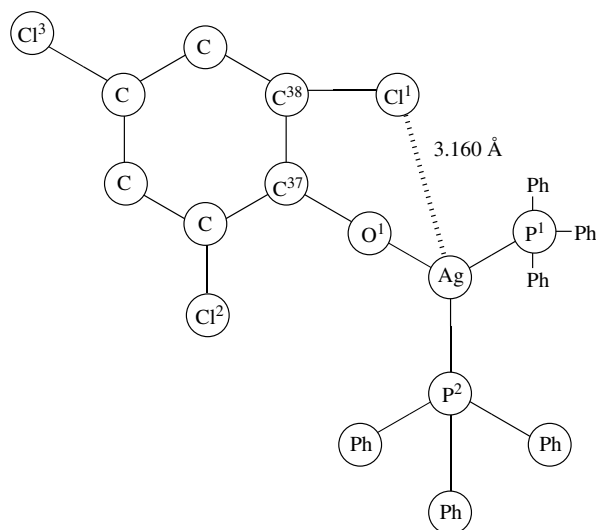
$Ag–P^1 = 2.444$ Å (or 244.4 pm)
$Ag–P^2 = 2.451$ Å (References 82–85)
$Ag–O^1 = 2.235$ Å (Reference 86)
$C–O^1 = 1.288$ Å; $C–Cl^1 = 1.748$ Å: $C^{38}–C^{37} = 1.410$ Å

^{35}Cl NQR spectra of 10 related chlorophenolates of Ag and Cu were presented and discussed[81] also.

The average NQR frequency difference $\nu(Cl^6) − \nu(Cl^2)$, in MHz, correlates with excess M−Cl distance, in Å, over the normal bond distance for a terminal metal–inorganic chlorine bond[90]. Excess M−Cl distance is defined as the observed metal–organochlorine distance minus the normal metal–terminal chlorine distance. No such correlation has been found between the average NQR frequency difference $\nu(Cl^6) − \nu(Cl^2)$, in MHz, and the M−Cl−C bond angle[81] in degrees.

12. ^{109}Ag and ^{29}Si NMR study of cyclo-tetrakis-[tri-t-butoxy]silanethiolatosilver[I]

The structure of this $[(t\text{-BuO})_3SiSAg]_4$ molecule, **44**, has been elucidated[91] by X-ray diffraction, by MS and by ^{29}Si NMR.

In the Ag_4S_4 ring the silver atoms are shifted slightly towards the centre of the ring, $S−Ag−S = 172.3°$. By analogy to Ag^I oxides where the binding interaction between Ag atoms was assumed to cause the unusual structural features[92], one could also assume that the spatial shift of the Ag atoms towards the centre of the ring is the result of silver–silver bonds between vicinal or between opposite Ag atoms. The ^{109}Ag NMR provides the decisive test for such Ag−Ag bonds in the $[SiSAg]_4$ core, since both silver nuclei ^{107}Ag and ^{109}Ag have spin $I = 1/2$ and hence very narrow NMR lines due to lack of quadrupole interactions.

In the eight-membered Ag_4S_4 ring, **45**, one can imagine the scalar [AgAg] coupling of the vicinal silver atom directly or through the S atom and also the direct coupling of the silver atoms situated at the opposite site of the central square. Detailed NMR investigation revealed[93] that the coupling constants, $^1J(Ag, Ag)$, of any [Ag, Ag] coupling in the $[SiSAg]_4$ molecule, $\{^1J(^{109}Ag, \, ^{109}Ag), \, ^1J(^{109}Ag, \, ^{107}Ag) \text{ and } ^1J(^{107}Ag, \, ^{107}Ag)\}$, are less than 1 Hz and any binding interactions between the Ag atoms in this molecule are very doubtful.

The ^{109}Ag and ^{29}Si NMR spectra have been investigated. In the ^{109}Ag spectra at 9.4 T and 2.1 T the single lines are shifted to higher frequency at the same field B_0 by $\delta = 725.8 \pm 1.5$ ppm relative to the resonance of the Ag^+ ion in aqueous solution at infinite dilution[94]. The coupling constants (at 9.4 T) were found to be $|J(^{29}Si, \, ^{109}Ag)| = 4.49 \pm 0.04$ Hz and $|J(^{29}Si, \, ^{107}Ag)| = 3.90 \pm 0.03$ Hz.
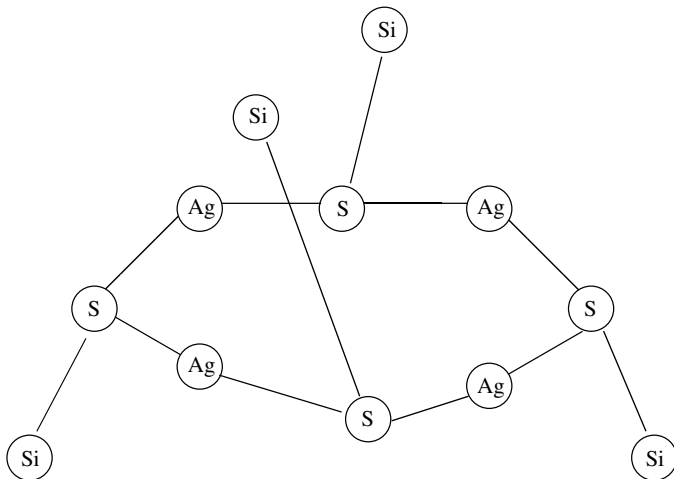
(44)

The 12 *t*-BuO ligands bonded to silicon are omitted; the four sulphur atoms are alternatingly slightly below and above the central plane defined by four silver atoms

The silver (^{109}Ag) relaxation in **44** (0.07 M in toluene), $T_1 = 20.2$ s (chemical shift anisotropy[95]), determined at 2.1 T and at 301 K, is shorter by nearly two orders of magnitude than T_1 of the Ag^+ ion in aqueous solution[96], which is extremely slowly relaxing ($T_1 > 1000$ s).

13. Synthesis and multinuclear NMR (^1H, ^{77}Se, ^{125}Te, ^{63}Cu, ^{109}Ag) spectrometry of Ag^I complexes with o-phenylene-backboned bis(thioethers), bis(selenoethers) and related crystal structure determinations.

Homoleptic silver^I complexes $[Ag(L-L)_2]X$ (where $X = BF_4$; $L-L = o\text{-}C_6H_4(EMe)_2$; $E = S$, Se, Te) have been prepared from the ligand with anhydrous $AgBF_4$ in acetone[97].
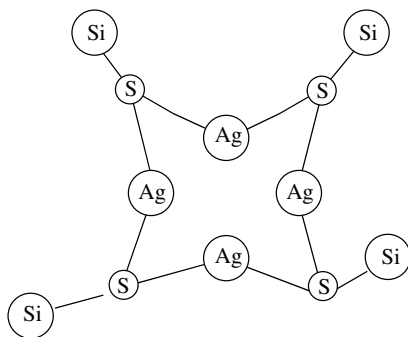
(45)

a. Single-crystal X-ray structural studies showed[97] that the single-crystal structure of {Ag[*o*-C₆H₄(SeMe)₂]₂}BF₄ (monoclinic, $a = 19.273$ Å, $b = 11.927$ Å, $c = 20.405$ Å, $\beta = 90.42°$, $P2_1/c$, $Z = 4$) comprises infinite chains of {Ag$_n$[μ-o-C₆H₄(SeMe)₂]$_n$•[*o*-C₆H₄(SeMe)₂]$_n$}$^{n+}$ cations, discrete BF₄⁻ anions maintaining electroneutrality and CH₂Cl₂ solvent molecules. The schematic view of the dinuclear Ag₂[μ-o-C₆H₄(SeMe)₂]₂ [*o*-C₆H₄(SeMe)₂]}$^{2+}$ cationic repeating unit is depicted as **46**. Each Ag¹ atom coordinates to both Se donors of one chelating bis(selenoether) and to one Se donor of each of two bridging bis(selenoethers). One of the bridging ligands links to the adjacent Ag atom above, while the other links to the Ag atom below as indicated schematically in **46**.
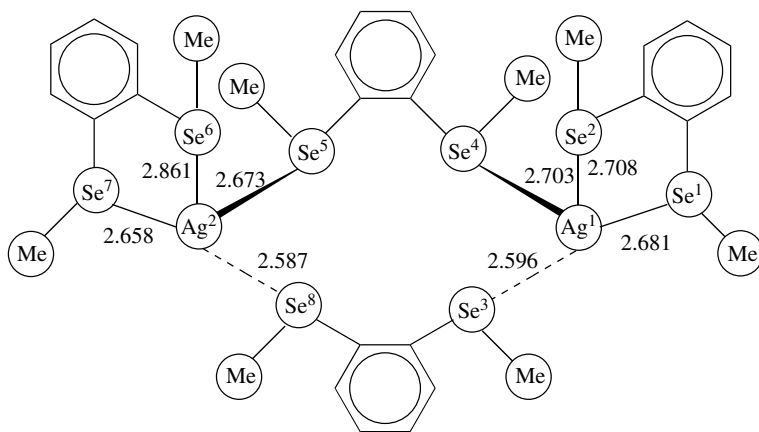
(46)

The Ag−Se bond lengths in **46** are within the range 2.59–2.86 Å, which is greater than, for instance, in [Ag$_n$(PhSe(CH₂)₃SePh)$_{2n}$]$^{n-}$, where d(Ag−Se) = 2.643–2.695 Å, or in [Ag(MeSe(CH₂)₂SeMe)₂]⁺, where d(Ag−Se) = 2.610–2.638 Å.

Examples of bond angles: $Se^1-A^1-Se^2 = 79.64°$; $Se^1-Ag^1-Se^4 = 115.51°$; $Se^1-Ag^1-Se^3 = 118.92°$; $Se^2-Ag^1-Se^3 = 128.67°$; $Se^2-Ag^1-Se^4 = 102.68°$; $Se^3-Ag^1-Se^4 = 108.76°$.

b. Multinuclear NMR studies. Single methyl resonances were observed in the ^1H NMR spectra of $\{Ag[o\text{-}C_6H_4(SeMe)_2]_2\}BF_4$ in CD_2Cl_2 and in the ^1H NMR spectra of $\{Ag[o\text{-}C_6H_4(TeMe)_2]_2\}BF_4$ in (CD_3CN), even on addition of the free ligand at 300 K, which demonstrates fast ligand exchange.

The $^{77}Se[^1H]$ and $^{125}Te[^1H]$ spectra showed a coordination shift in $\{Ag[o\text{-}C_6H_4(TeMe)_2]_2\}BF_4$ (in $MeNO_2/CD_3NO_2$) to high frequency, $\delta(^{125}Te) = +433$ ppm (300 K), +432 ppm (245 K) and fast exchange with added ligand down to the m.p. of solvent. In $\{Ag[o\text{-}C_6H_4(SeMe)_2]_2\}BF_4$ the $\delta(^{77}Se) = +180$ ppm (300 K), +180 ppm (180 K) and fast exchange with added ligand was observed also above *ca* 210 K in CH_2Cl_2/CD_2Cl_2. The suggestion was made[97] that the interaction of the 'free' lone pair in each coordinated Se or Te centre with the delocalized aromatic system is the cause of the observed $\delta(^{77}Se)$ or $\delta(^{125}Te)$ shifts. On cooling, the ligand exchange slows down and the separated resonances for free and bound ligand have been resolved below 210 K for ^{77}Se, and below 240 K for ^{125}Te, of the $\{Cu[o\text{-}C_6H_4(TeMe)_2]_2\}BF_4$ complex, but the poor solubility of $\{Ag[o\text{-}C_6H_4(TeMe)_2]_2\}BF_4$ in chlorocarbons prevented the low-temperature studies.

^{109}Ag NMR resonances have been observed[97] and the chemical shifts determined as follows: for $\{Ag[o\text{-}C_6H_4(SMe)_2]_2\}BF_4$, $\delta(^{109}Ag) = +788$ ppm (300 K), +846 ppm (180 K); with added free ligand $\delta(^{109}Ag) = +803$ ppm (300 K), +848 ppm (180 K); for $\{Ag[o\text{-}C_6H_4(SeMe)_2]_2\}BF_4$, $\delta(^{109}Ag) = +912$ ppm (300 K), +867 ppm with excess free ligand; for $\{Ag[o\text{-}C_6H_4(TeMe)_2]_2\}BF_4$, $\delta(^{109}Ag) = +1128$ ppm and +1164 ppm (300 K) with added ligand. The chemical shifts for Se and Te complexes are similar to those observed in $AgSe_4/Te_4$ species[98,99] but in the case of $\{Ag[o\text{-}C_6H_4(SMe)_2]_2\}BF_4$ the $\delta(^{109}Ag)$ observed at lower frequency than for AgS_4 species[98,99] may indicate that, on average, less than four sulphur atoms are coordinated with one Ag ion in solution. A conclusion has been reached that in labile complexes of silver the reversible chelate ring opening is significant even at low temperatures in spite of the initial expectation that the rigid *o*-phenylene backbone will reduce the ligand dissociation and the metal–donor spin–spin couplings to the $I = 1/2$ silver isotopes will be observable.

14. Synthesis and ^{119}Sn and ^{31}P NMR spectra of silver–tin complex salts with bis(diphenylarsenio)methane (dpam) and bis(diphenylophosphino)methane (dppm)

The title complex salts, $[Ag(dpam)_2][SnPh_2(NO_3)_3]$, $[Ag(dppm)_2][SnPh_2(NO_3)_3]$ and $[Ag_3Cl_2(dppm)_3][SnPh_2(NO_3)_2Cl]$, **47**, have been synthesized and their IR, and ^{31}P and ^{119}Sn NMR spectra, and conductivity recorded and discussed[100].

The X-ray structure of the trinuclear silver complex, $[Ag_3Cl_2(dppm)_3][SnPh_2(NO_3)_2Cl]\cdot CH_3OH$, **47**, containing bridging chlorine and dppm ligands, has been determined also. In all three complexes the separation of asymmetric and symmetric modes of NO_3^-, $\Delta\nu = [(1475 \text{ cm}^{-1})-(1285 \text{ cm}^{-1})]$, is indicative of bidentate behaviour of the NO_3^- groups towards the tin atom. The $\nu(Sn-Cl)$ band falls at 270 cm^{-1}, $\nu(Sn-C) = 295$ cm^{-1}, $\nu(NO_3)$ in-plane = 1010 cm^{-1} and $\nu(NO_3)$ out-of-plane = 803 cm^{-1}. The value of $\delta(^{119}Sn)$ equals -452 ppm for the $[SnPh_2(NO_3)_2Cl]^-$ anion and -662 ppm for the $[SnPh_2(NO_3)_3]^-$ anion, in agreement with the general tendency of the tin nucleus

to show increasing upfield shifts when the coordination number increases[101,102]. The ^{31}P NMR spectrum (233–303 K) of **47** exhibits an unresolved broad doublet centered at -2.0 ppm [$^{1}J(Ag^{31}P) = 436$ Hz], which compares well with silver compounds possessing distorted trigonal geometry[103].
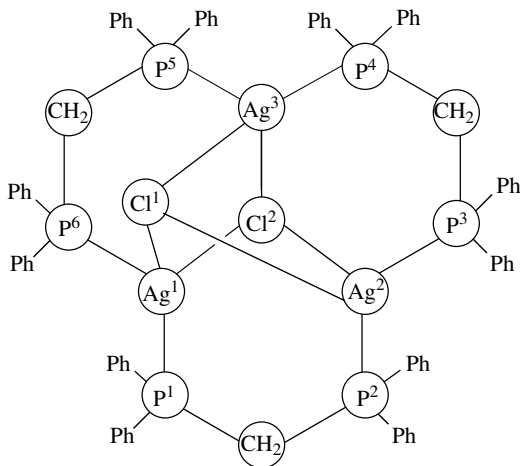
(47) $[Ag_3Cl_2(dppm)^3]^+$ cation; the 3 silver atoms are four-coordinated
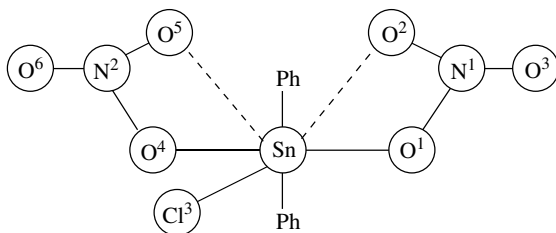
(47) $[SnPh_2(NO_3)_2Cl]^-$ anion

15. Isotopic EPR spectroscopic studies of the reaction of silver atoms with ethylene

a. EPR studies in rare-gas matrices. The first matrix isolation EPR study indicated[104] that at about 4 K silver atoms and ethylene condensed in rare-gas matrices form the $Ag(C_2H_4)_2$ diligand complex with D_{2h} structure. The mononuclear triligand complex was not observed. The EPR intensities of $Ag(C_2H_4)_2$ and $Ag(C_2D_4)_2$ have been dependent on the ethylene concentration[105]. This conclusion has been confirmed by the detailed analysis of the EPR spectra of the ^{13}C-enriched complex in the $Ag(^{13}C_2H_4)_2$/Ne system[106].

In the $H_2{}^{13}C=CH_2$ ethylene, only one of the two carbons was enriched with ^{13}C up to 90% and the resulting diethylene complex contained 81% $Ag(H_2{}^{13}C=CH_2)_2$, 18% $Ag(H_2{}^{13}C=CH_2)(C_2H_4)$ and 1% $Ag(C_2H_4)_2$. Computer simulation of the observed EPR spectra of $Ag(*C_2H_4)_2$ was achieved by assuming that the complex has eight equivalent protons and a 9 : 2 relative ratio of $Ag(H_2{}^{13}C=CH_2)_2$ and $Ag(H_2{}^{13}C=CH_2)C_2H_4$ isotopomers. [The additional peaks which could not be accounted for $Ag(C_2H_4)_2$ were assigned to ethylene oligomers $Ag(C_2H_4)_{\geqslant 3}$.] Agreement between the observed and computed EPR spectrum was obtained also in the isotopic experiments in which 60%−40% mixture of $H_2{}^{13}C=CH_2$ and C_2H_4 was used. The resulting diethylene complex contained in the last case 36% $Ag(H_2{}^{13}C=CH_2)_2$, 48% $Ag(H_2{}^{13}C=CH_2)C_2H_4$ and 16% $Ag(C_2H_4)_2$. A suggestion has been made that the complex is held together by the back-donation into antibonding bis(ethylene)silver^0 π-orbitals from Ag $4d_{xy}$ and $5p_x$ orbitals. The spin density in the Ag $5p_x$ orbital was concluded to be about 1/3, while the total spin density (unpaired electron distribution) in the ethylene moiety was 2/3, in agreement with earlier[105] work where the semi-filled orbital of complex was given by equation 34 and structure **48:**

$$\phi = a\phi_{Ag}(5p_x) + \frac{b}{\sqrt{2}}(\pi_y^* - \pi_y^{*'}) \tag{34}$$

(48)
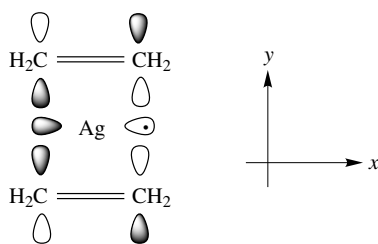
where π^* and $\pi^{*'}$ represent the antibonding π-orbital of the ethylene molecule[106].

   b. The reaction of Ag atoms with ethylene at 77 K in inert hydrocarbon matrices giving covalent silver–ethylene $Ag[C_2H_4]$ and $Ag[C_2H_4]_2$ complexes, and possibly the silver cluster–ethylene complexes, $Ag_3[C_2H_4]$ and $Ag_7[C_2H_4]_x$, $x \geqslant 1$, have been investigated by EPR spectroscopy[105] using isotopically enriched $^{107}Ag(98.22\%)$, C_2H_3D, $C_2H_2D_2$, C_2HD_3, C_2D_4, C_2H_4 and $^{13}CH_2=CH_2$. The magnetic parameters of the major paramagnetic products produced by ^{107}Ag atoms and C_2H_4 have been tabulated, discussed and taken as indicating that the species $Ag[C_2H_4]$ is the *bona fide* monoethylene silver complex and not the van der Waals $Ag\cdots C_2H_4$ complex observed in argon[107]. Spectra from the Ag atom and the deuterated ethylenes could not be resolved to give a hydrogen hyperfine interaction, but $^{13}CH_2=CH_2$ gave a doublet splitting confirming the ligand stoichiometry. The marked difference between the spectra of Ag_3 in N_2 and $Ag_3[C_2H_4]$ in adamantane is associated with the ethylene ligand. It has been concluded also that the mononuclear diligand complex has the symmetric D_{2h} geometry and that the unpaired electron is located largely in the 4p orbital on the metal. The bonding occurs due to overlap between the filled ligand π-orbitals and empty p_x or sp_x-hybridized orbitals on the metal and the semi-filled p_z orbital and the empty ligand π^*-orbitals. No explicit presentation of

the orbitals for the dative bonds was given in Reference 105 and no comments concerning the bonding in $Ag(C_2H_4)_2$ complex generated in argon are presented[106,107]. $Ag(C_2H_4)_2$ is about 100 times more concentrated than $Ag(C_2H_4)$ and the cluster ethylene complexes. The possible mechanisms of interactions between clusters Ag_3 and Ag_7 and the C_2H_4 ligand are considered in Reference 105.

16. Deuterium isotope effect in the association of NH_3 and ND_3 with Ag^+

The three-body association rate constants of CO, CH_4, CH_3F, NH_3, ND_3, CH_3Cl and CH_3Br with Ag^+ (and for NH_3, ND_3 and CH_3Cl with Cu^+) have been measured[108] at 298 K as a function of helium pressure and the k_o values were found to range from 2.5×10^{-30} $cm^6\,s^{-1}$ (for CO) to 3.9×10^{-27} $cm^6\,s^{-1}$ (for CH_3Br). The data have been analysed according to the Lindemann mechanism expressed by equations 35–37, where M^+ denotes Ag^+ (or Cu^+), LX the ligand and $(M \cdot LX)^{+*}$ denotes the metastable collision complex which either dissociates back to the original reactants or is stabilized by collision with helium.

$$M^+ + LX \underset{k_{-1}}{\overset{k_1}{\rightleftharpoons}} (M \cdot LX)^{+*} \xrightarrow{k_2,\,He} (M \cdot LX)^+ \tag{35}$$
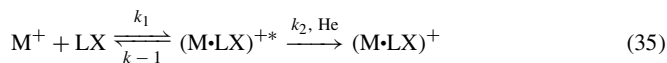
$$d[M^+]/dt = -k_3[M^+][LX][He] \tag{36}$$

$$k_3 = \frac{k_1 k_2}{k_{-1} + k_2[He]} \longrightarrow k_3^0 = \frac{k_1 k_2}{k_{-1}} \text{ (at low He pressure.)} \tag{37}$$

The $k_3^0 \times 10^{28}$ $cm^6\,s^{-1}$ values for LX = NH_3 and ND_3 have been found to be equal to 3.7 and 9.8, respectively, in the reaction with Ag^+ and 16 and 46 in the reaction with Cu^+. Thus the rate constants for association of ND_3 are about 2.7 and 2.9 times greater than for association of NH_3 with Ag^+ and Cu^+ cations, respectively. The calculated lifetimes of *(metal ion)–(ligand)* complexes are also three times larger for clustering of ND_3 with both silver and copper than for clustering of NH_3. Isotope effects of similar magnitude were found[108] also for association of ND_3 and NH_3 with Na^+ and in the reaction[109] of *n*-butane-d_{10} and *n*-butane with V^+. A nearly linear correlation has been found between the negative logarithm of the effective lifetimes of collision complexes [decomposing into clusters, for instance $(CuCH_3Cl)^+$, or into the insertion compound, for instance $(CH_3CuCl)^+$], and the lowest vibrational frequency of the ligand. This correlation indicates the contribution of vibrational motion to the energy distribution in ion–molecule collision complexes. The coupling between the vibrational frequency of the clustering ligand and the orbital motion of the ligand's trajectory was given also as the explanation of the longer lifetimes for ligands containing D, for both silver and copper (the smaller vibrations of heavier ND_3 are stimulated better than the higher frequencies of NH_3 at the expense of the potential energy between the ion and the molecule). The intermolecular relaxation is more probable the smaller the eigenfrequency of the interacting oscillator[108].

It should be noted that under the equilibrium conditions (equation 37) the heavier ND_3 should concentrate to a greater extent in the excited $(Ag \cdot ND_3)^{+*}$ metastable collision complex in which the translation and rotational degrees of freedom of the ND_3/NH_3 isotopic molecules are partly transformed into internal modes of motion. The deuterium isotope effect of 3 could be used to assess roughly the average force constant of vibrations between Ag^+ and NH_3 or ND_3 and eventually to assess the changes of the set of eigenfrequencies of free ND_3 molecules[110] into a new set of eigenfrequencies of the ND_3 unit

bound to Ag^+ in $(Ag^+ \cdots ND_3)$. No structures of either the metastable or the stabilized collision complexes $(Ag^+ \cdots ND_3)$ have been presented[108].

17. First examples of ^{109}Ag CP MAS spectroscopy

^{109}Ag CP MAS spectra have been obtained[111] and the δ^{109}Ag isotropic chemical shifts given below in parentheses relative to $AgNO_3$ water solution at infinite dilution of the selected solid silver compounds have been found to be as follows: silver lactate, $MeCH(OH)COOAg$ (345.9, 320.2 ppm, 219.7, 210.7 ppm); silver acetate, $MeCOOAg$ (401.2, 382.7 ppm); silver *p*-toluene sulphonate, $MeC_6H_4SO_3Ag$ (44.1 ppm); silver acetyl acetonate, $C_5H_7O_2Ag$ (471.6 ppm); $AgN(SO_2Me)_2$ (210.3 ppm); $AgN(SO_2Me)_2 \cdot 0.25$ H_2O (182.8, 130.7, 32.5 ppm).

A pronounced effect of a water molecule on the solid state structure of the $AgN(SO_2Me)_2$ compound has been shown. Many silver compounds are light sensitive and hence often no X-ray crystallographic information is available for them.

D. Silver and Deuterium Isotope Effects in Physical Studies

1. The ground state infrared spectra of ^{107}AgH and ^{109}AgH

Extending previous accurate laser studies of the IR spectra[112−122] of metal hydrides in gas phase, including NaH, CsH, BaH, SrH, RbH, GaH, InH, TlH CdH, ZnH, KH, MgH, CaH and LiH and also of diatomic hydride radicals[123], for instance SnH, NiH, FeH, CoH and GeH, the infrared spectra of two isotopic forms of silver hydride [^{107}Ag (51.35%) and ^{109}Ag (48.65%)] in its ground electronic state $(^1\Sigma)$ have been recorded[124,125]. Accurately known absorption lines of nitrogen dioxide[117] sulphur dioxide[126,127] and formaldehyde[127−129] served for wavenumber calibration; 21 transitions in the bands from $v = 1 \leftarrow 0$ up to $v = 3 \leftarrow 2$ have been measured for ^{109}AgH and ^{107}AgH respectively, their assignments and equation wavenumbers were presented explicitly and fitted to the Dunham[130] expression (equation 38) for the energy levels of diatomic molecules, and the parameters Y_{ij} for two isotopic forms of AgH were determined[124].

$$F = \sum_{ij} Y_{ij} \left(v + \tfrac{1}{2}\right)^i [J(J+1)]^j \tag{38}$$

The new data permitted one to obtain a new value of the equilibrium bond length of the AgH, which was found to be $r_e = 1.617798 (5)$ Å. The expected ^{107}Ag/^{109}Ag isotope effect in the *effective* bond length of AgH isotopomers, caused by the anharmonicity of the ^{i}Ag−H vibrations, is not discussed by Birk and Jones[124] as was done in the case of C−H/C−D bond distances and vibrations[131]. Subsequently[132], AgD was obtained from silver vapour with deuterium and 33 transitions have been recorded for ^{109}AgD and ^{107}AgD. As before, the rovibrational spectra have been fitted to the Dunham expression in equation 38 and the parameters Y_{ij} of two isotopic AgD species were determined[132], when Y_{10} was found to equal 1250.8912(15) for ^{107}AgD and 1250.676(30) for ^{109}AgD. The particular values of Y are greater for the lighter isotope species as required by equation 39, in which μ and μ^* are reduced masses of the two molecules. The values of Y_{10} in silver deuterides are smaller by a factor of 1.407 than the Y_{10} values for silver hydrides. The mean amplitudes of vibrations[133,134] of Ag−D and Ag−H stretches and the isotope effects on the size of isotopic ^{i}Ag^{i}H molecules have not been presented in

Reference 132. The problem of the relatively large anharmonicity in silver and related hydrides has been indicated only[132].

$$Y_{ij}^* = \left(\frac{\mu}{\mu^*}\right)^{(i+2j)/2} Y_{ij} \tag{39}$$

2. Spectroscopic and theoretical studies of the isotopic silver dimer molecules

The structure of metal clusters is of importance to organometallic chemistry, catalysis and surface science. Silver clusters form the latent photographic image[135].

a. Three disilver isotopomers are present at comparable natural isotope abundance levels (26.85 of ^{107}Ag$_2$, 49.93% of ^{107}Ag ^{109}Ag and 23.32% of ^{109}Ag$_2$). This causes the blending of spectral lines. Also in disilver, produced at high temperatures, the population of low-lying levels is reduced via the Boltzmann factor and it is difficult to establish the correct rotational line numbering[136]. Recently, the 0–0 and 2–0 bands of the $A(O_u^+)$–X($^1\Sigma_g^+$) system of Ag$_2$ have been analysed[137] by producing intense low-temperature beams of Ag$_2$ molecules via supersonic expansion and subsequent laser excitation of their fluorescence. The spectra over the range 22945–22978 cm^{-1} were recorded with 120-MHz resolution ($\equiv$0.0041 cm^{-1}). The A state was previously assigned as the $^1\Sigma_u^+$ state with a σ-bond formed by overlap of two singly occupied 5s atom orbitals or by 5s σ^*–5s σ promotion[138−140]. The analysis of the 2–0 band (resolution 90 MHz $\equiv$ 0.0030 cm^{-1}) range (23281.1849–23283.7088 cm^{-1}) has been restricted to ^{107}Ag$_2$ isotopomers. The rotational constants have been deduced from the LIF (laser-induced fluorescence) data by fitting the observed P and R line positions using the non-linear least-squares procedure[141]. The line positions have been calculated[142] using expression 40:

$$\nu(J) = \nu_{00} + F'(J + i) - F''(J) \tag{40}$$

where $i = -1$ refers to the P branch, $i = +1$ refers to the R branch and ν_{00} is the band origin. The rotational term values (measured from the rotational level having $J = 0$) are given by equation 41:

$$F(J) = BJ(J + 1) - DJ^2(J + 1)^2 \tag{41}$$

The mean value of rotational constant B_n in the given vibrational state, $B_n = (h/8\pi^2 c\mu)\cdot\overline{(1/r^2)}^n$, is related to the constant B_e corresponding to the equilibrium separation r_e, $B_e = h/8\pi^2 c\mu r_e^2 = h/8\pi^2 c I_e$, by relation 42:

$$B_n = B_e - \alpha_e(n + 1/2) + \cdots \tag{42}$$

where constant α_e is small compared to B_e, $\alpha_e/B_e \approx \omega_e X_e/\omega_e$. The mean rotational constant D_n, representing the influence of the centrifugal force, is related to D_n via equation 43:

$$D_n = D_e + \beta_e(n + 1/2) + \cdots \tag{43}$$

where constant β_e is much smaller than $D_e = 4B_e^3/\omega_e^2$. From equations 40–43 the following values of the spectroscopic constants for the $A(O_u^+) - X(^1\Sigma_g^+)$ system of Ag$_2$ have been deduced:

$$\nu_{00} = 22976.8308 \text{ cm}^{-1} (\text{for}^{107}\text{Ag}^{109}\text{Ag})$$

$$^{107}\text{Ag}^{109}\text{Ag}; A(n=0): \quad B_n(\text{cm}^{-1}) = 0.044224, D_n \ (\text{cm}^{-1}) = 10.3 \times 10^{-9},$$

$$r_n \ (\text{Å}) = 2.658115, \alpha_e \ (\text{cm}^{-1}) = 2.15 \times 10^{-4},$$

$$B_e \ (\text{cm}^{-1}) = 0.044331, r_e \ (\text{Å}) = 2.6549.$$

$$^{107}\text{Ag}_2; A(n=2): \quad B_n \ (\text{cm}^{-1}) = 0.0442000, r_n \ (\text{Å}) = 2.6711.$$

$$^{107}\text{Ag}^{109}\text{Ag}; X(n=0): \quad B_n \ (\text{cm}^{-1}) = 0.048682, D_n \ (\text{cm}^{-1}) = 7.6 \times 10^{-9},$$

$$r_n \ (\text{Å}) = 2.53350, \alpha_e \ (\text{cm}^{-1}) = 1.9520 \times 10^{-4},$$

$$B_e \ (\text{cm}^{-1}) = 0.048780, r_e \ (\text{Å}) = 2.53096.$$

$$^{107}\text{Ag}_2 : X(n=0): \quad B_n \ (\text{cm}^{-1}) = 0.049149, r_n \ (\text{Å}) = 2.5331,$$

The *ab initio* calculations of the ground-state bond length are in agreement with the above experimental determinations[143−148].

b. Rotationally resolved isotope-selective laser spectroscopy of Ag_2 molecules. The difficulties caused by the overlap of bands of three isotopomers of natural Ag_2 molecules and by limited spectral resolution specific for the conventional absorption spectroscopy have been overcome[148] by laser spectroscopic techniques based on resonant two-photon ionization of Ag_2 molecules in a collimated Ar/Ag_2 supersonic beam, separation of the three $Ag_2{}^+$ (ions) isotopomers in the time-of-flight (TOF) spectrometer and subsequent nearly simultaneous recording of their spectra behind TOF. Seven rotationally resolved bands $(0 \leftarrow 0)$ to $(6 \leftarrow 0)$ in the $B^1_{\pi_u} \leftarrow X^1\Sigma_g$ system of the three Ag_2 isotopomers have been measured, their analysis carried out, and band origins and the rotational constants of the upper and lower states determined. Due to adiabatic cooling during the expansion[149] the 'vibrational temperature' of Ag_2 molecules was $T_{vib} \approx 250$ K and the average rotational temperature, $T_{rot} = (40 + aJ^2)$K, was assessed to be $T_{rot} \approx 50$ K. In the $^1\pi - ^1\Sigma$ transitions, besides P and R branches, the Q branch ($i = 0$ in equation 40) is also present (equation 44):

$$Q_{\text{branch}}; \quad \nu = \nu_{00} + F'(J) - F''(J) = Q(J) \tag{44}$$

Band origins $\nu_0(n')$ and rotational constants B'_n and D'_n in the $B^1\Pi_u$ state of $^{107}\text{Ag}^{109}\text{Ag}$ have been determined for $n' = 0$–6. For $n' = 0$, $\nu_0 = 35808.343$ cm^{-1}, $B'_0 = 0.045286$ cm^{-1} and $D'_\nu = 1.73 \times 10^{-8}$ cm^{-1}; for $n' = 1$, $\nu_0 = 35958.335$ cm^{-1}, $B'_0 = 0.045048$ cm^{-1} and $D'_\nu = 1.87 \times 10^{-8}$ cm^{-1}. The most accurate rotational constants, B''_0 and D''_0 (equation 45) in the $X^1\Sigma_g^+$ ground state, have been obtained by fitting all 1400 observed line pairs $Q(J'' - 1) - P(J'')$ with a common upper level $J' = J'' - 1$ of all three isotopomers in all seven measured bands (equation 46):

$$\nu(n', J')J'' = \nu_0(n') + B'_n[J'(J'+1) - 1] - B''_0 J''(J''+1) + D''_0[J''(J''+1)]^2 \tag{45}$$

$$\nu_Q(J'' - 1) - \nu_P(J'') = 2\rho^2 B''_0 J'' = 4\rho^4 D''_0(J'')^3 \tag{46}$$

where $\rho^2 = \mu_i/\mu$, μ_i being the reduced mass of the *i*-isotopomer and μ the reduced mass of the mixed $^{107}\text{Ag}^{109}\text{Ag}$ isotopomer.

This fit gave the rotational constants $B_0'' = 0.04872$ cm^{-1} and $D_0'' = 1.2 \times 10^{-8}$ cm^{-1} and (for the $n'' = 0$ level) $B_0'' = 0.048703$ cm^{-1} and $D_0'' = 1.31 \times 10^{-8}$ cm^{-1}, respectively. The following values of the electronic term T_e, vibrational constants ω_e', $\omega_e \chi_e'$ and rotational constant B_e', α_e', D_n', r_e' for the $B^1 \Pi_u$ state of ^{107}Ag^{109}Ag (see equations 47 and 48) have been obtained: $T_e = 35828.9$ cm^{-1}, $\omega_e' = 151.388$ cm^{-1}, $\omega_e \chi_e' = 0.699$ cm^{-1}, $B_e' = 0.045413$ cm^{-1}, $\alpha_e' = 2.49 \times 10^{-4}$ cm^{-1}, $D_n' = 1.7 \times 10^{-8}$ cm^{-1}, $r_e = 2.6231$ Å. The above values satisfy the Kratzer relation (equation 49)

$$v_0(n') = T_e(B'\Pi_u) + G'(n') - G''(n'' = 0) = T_e + \omega_e'(n' + 1/2) - \omega_e \chi_e'$$

$$(n' + 1/2)^2 - G''(n'' = 0) \tag{47}$$

$$B_n' = B_e' - \alpha_e'(n' + 1/2) \tag{48}$$

$$D_e = 4\frac{B_e^3}{\omega_e^2} \tag{49}$$

which is exact for a Morse potential. Substituting[150] $T_e = 35828.9$ cm^{-1} and the atomic term value $T(P_{3/2}) = 30472.7$ cm^{-1} into equation 50, we obtain the difference in the dissociation energy, which indicates that the upper state is less tightly bound than the ground state.

$$D(X^1\Sigma_g) - D(B^1\Pi_u) = T_e - T(^2P_{3/2}) = 5356.2 \text{ cm}^{-1} \tag{50}$$

c. The potential of the Ag$_2$ B-1$^1\Pi_u$ state. The isotopically selective measurements of Beutel and coauthors[148] have been analysed theoretically[151] for each Ag$_2$ isotopomer by Müschenborn using Morse and RKR (Rydberg–Klein–Rees) potentials and then applying the IPA (inverse perturbation analysis) quantum mechanical method[152]. The final IPA procedure reproduced all measured values of every Ag$_2$ isotopomer with a standard deviation of 0.030 cm^{-1}, which compares very well with the experimental accuracy of 0.04 cm^{-1}. The mass independence of the final rotationless IPA potential energy curve has been demonstrated and the dissociation energy was estimated. The nuclear motion of a diatomic molecule has been approximated by the Schrödinger equation of the rotating vibrator (equation 51):

$$(H^0 + H^{\text{rot}})\Psi_{nJ} = E_{nJ}\Psi_{nJ} \left[\left(-\frac{h}{8\pi^2\mu c}\frac{\partial^2}{\partial r^2} + U^0(r) \right) \right.$$

$$\left. + \left(\frac{h}{8\pi^2\mu c}\frac{J(J+1) - \Lambda^2}{r^2} \right) \right] \Psi_{nJ} = E_{nJ}\Psi_{nJ} \tag{51}$$

where, as usual, H^0 denotes the rotationless Hamiltonian, H^{rot} the rotational Hamiltonian for a molecule with reduced mass μ, $U^0(r)$ is the rotationless intramolecular potential, Ψ_{nJ} are the wavefunctions of the state with vibrational quantum number n and rotation quantum number J, E_{nJ} are the energy eigenvalues, r is the internuclear distance, and Λ represents the quantum number of the resultant electronic angular momentum about the internuclear axis. Equation 51 has been solved[151,153,154] numerically for a given U^0. The Morse potential was the first step towards and IPA potential (equation 52):

$$U_{\text{Morse}}(r) = U_{\text{min}} + D_e\{1 - \exp[a(r_e - r)]\}^2 \tag{52}$$

where $U_{min} = T_e$, $r_e = \sqrt{h/8\pi^2 \mu c B_e}$, $a = \sqrt{8\pi^2 \mu c \omega_e \chi_e/h}$, $D_e = \omega_e^2/4\omega_e\chi_e$, with the Dunham coefficients $T_e \approx Y_{00}$, $B_e \simeq Y_{01}$, $\omega_e \approx Y_{10}$ and $\omega_e\chi_e \approx -Y_{20}$.

The parameters of the Morse potentials for the $Ag_2(B-1^1\Pi_u)$ states were found as follows (1 amu $= 1.6605402 \times 10^{-27}$ kg):

For$^{107}Ag_2$: $\mu = 53.452546$ (amu), $U_{min} = 35829.058$ (cm^{-1}), $D_e = 8211$ (cm^{-1}),

$$a = 1.4943 \text{ (Å}^{-1}), r_e = 2.6233 \text{ (Å)}.$$

For$^{107}Ag^{109}Ag$: $\mu = 53.947830$ (amu), $U_{min} = 35829.034$ (cm^{-1}), $D_e = 8203$ (cm^{-1}),

$$a = 1.4951 \text{ (Å}^{-1}), r_e = 2.6233 \text{ (Å)}.$$

For$^{109}Ag_2$: $\mu = 54.452379$ (amu), $U_{min} = 35829.019$ (cm^{-1}), $D_e = 8196$ (cm^{-1}),

$$a = 1.4957 \text{ (Å}^{-1}), r_e = 2.6231 \text{ (Å)}.$$

The values presented in Table 4 for the final IPA potential for the $Ag_2 B - 1^1\Pi_u$ state versus r (Å) were given elsewhere[151] for internuclear distances r ranging from 2.200 Å to 3.200 Å. These results have been compared with the recent *ab initio* calculation for 15 electronic states of Ag_2, including the X, A and B states[155].

3. Gas-phase spectroscopic studies of jet-cooled CuAg and AgAu molecules

Resonant two-photon ionization (R2PI) spectroscopy has been applied to study the nature of bonding of the diatomic copper group molecules: Cu_2, Ag_2, Au_2, CuAg, CuAu and AgAu. Since all the above six diatomics are formed from atoms with filled d subshells, it was expected that they would possess the electronic configuration of $d_{(A)}^{10} d_{(B)}^{10} \sigma_{(g)}^2$ giving the $^1\Sigma_{(g)}^+$ ground molecular term. They are thus bound only by the outer σ-electrons and are the transition metal analogues of H_2 molecules.

a. The R2PI spectroscopic study of the CuAg system. Four band systems of CuAg in the range 20000–27000 cm^{-1} have been recorded[156], three of which have been rotationally resolved and analysed with the use of equation 53:

$$\nu = \nu_0 + B'J'(J'+1) - B''J''(J''+1) \tag{53}$$

The values of ν_0, B'' and B' were obtained for each band. The multiply determined value of the B_0'' $(X^1\Sigma^+)$ ground state of CuAg, converted to bond lengths, gave:

TABLE 4.   Final IPA values

r (Å)	IPA (cm^{-1})
2.300	38811.943
2.500	36170.008
2.620	35830.095
2.624	35829.901
2.640	35833.942
2.700	35925.305
3.200	38016.161

$r_0''(^{63}\text{Cu}^{107}\text{Ag}) = 2.3734$ Å, $r_0''(^{63}\text{Cu}^{109}\text{Ag}) = 2.3734$ Å, $r_0''(^{65}\text{Cu}^{107}\text{Ag}) = 2.3671$ Å and $r_0''(^{65}\text{Cu}^{109}\text{Ag}) = 2.3740$ Å. The molecular configuration $3d_{\text{Cu}}^{10}\ 4d_{\text{Ag}}^{10}\sigma^2$ has been assigned to the ground state Ag ($^1\Sigma^+$ in character). Using the experimentally determined vibrational frequency and the bond length, the revised bond strength[157] was estimated to be D_0^0 (CuAg) $= 1.74 \pm 0.10$ eV. Three of the excited states (A0$^+$, A'1, and B'0$^+$) observed in the 20000–27000 cm^{-1} range correlate mainly to $3d_{\text{Cu}}^9\ 4d_{\text{Ag}}^{10}\sigma^2\sigma^*$-states of the molecule. This molecular configuration has been additionally supported by the observation of the unusually large electronic isotope shifts in the A–X, A'–-X and B'–X vibronic bands associated with the replacement of ^{63}Cu by ^{65}Cu. Such electronic isotope effects have been observed previously in A–X and B–X systems of Cu$_2$ caused by the s ← d excitations in atomic copper. For instance, in the band 5–0 of the (A'–X) system the isotope shifts (cm^{-1}) defined as ν(isotope modification) $-\nu(^{63}\text{Cu}^{107}\text{Ag})$ are found to be: -2.88 (for $^{63}\text{Cu}^{109}\text{Ag}$), -7.20 (for $^{65}\text{Cu}^{107}\text{Ag}$) and -9.36 (for $^{65}\text{Cu}^{109}\text{Ag}$). The highest energy state *B* observed in this study was suggested to be of ion-pair character[156].

b. The previous fragmentary studies of AgAu molecules[143,158−162] have been supplemented by R2PI spectroscopic investigation of AgAu and Au$_2$ spectra[163]. In spite of difficulties in producing the AgAu molecule, two excited electronic states, labelled as the A–X and B–X systems, have been located and assignments of *A* and *B* states of AgAu to $\Omega' = 0^+$ and $\Omega' = 1^+$, respectively, have been proposed. The A–X system consists of progression extending up to the 23–0 band. Although it was impossible to resolve the rotational structure of any of the AgAu bands, high-resolution scans over the 1–0, 2–0, 3–0, 4–0 and 5–0 bands have been performed and the isotope shifts $\nu_{n'-0}(^{107}\text{Ag}^{197}\text{Au}) - \nu_{n'-0}(^{109}\text{Ag}^{197}\text{Au})$ measured. The observed listed[163] band frequencies (vibronic bands) have been fitted to equation 54

$$\nu_{n'-0} = T_0 + n'\omega_e' - (n'^2 + n')\omega_e'\chi_e' \tag{54}$$

and the following values of $T_0(= \nu_{00})$, ω_e' and $\omega_e'\chi_e'$ for the electronic states of $^{107}\text{Ag}^{197}\text{Au}$ have been determined:

A–X : $T_0(\nu_{00}) = 21995.97$ cm^{-1}, $\omega_e' = 115.73$ cm^{-1}, $\omega_e'\chi_e' = 0.74$ cm^{-1},

   lifetime $= 0.040$ μs.

B–X : $T_0(\nu_{00}) = 24692.49$ cm^{-1}, $\omega_e' = 92.65$ cm^{-1}, $\omega_e'\chi_e' = 1.06$ cm^{-1},

   lifetime $= 1.14$ μs.

The observed band frequency and isotope shift used in the above calculations in the case of the $[A(0^+)–X^1\Sigma^+]$ system are shown below:

Band		Isotope shift:	
(0–0):	21993.50 cm^{-1}		-0.22 cm^{-1}
(1–0):	22110.18 cm^{-1}		-0.35 cm^{-1}
(2–0):	22223.32 cm^{-1}		-1.10 cm^{-1}
(3–0):	22334.85 cm^{-1}		-1.66 cm^{-1}
(4–0):	22445.03 cm^{-1}		-2.42 cm^{-1}
(5–0):	22553.34 cm^{-1}		-2.90 cm^{-1}

The 'A' state was described as an (Ag$^+$Au$^-$) 'ion pair state'.

Isotope shift $= \nu_{n'-0}(^{107}\text{Ag}^{197}\text{Au}) - \nu_{n'-0}(^{109}\text{Ag}^{197}\text{Au} = -1.52 \text{ cm}^{-1})$ in the low resolution of B−X system.

$B(1)-X^1\Sigma^+$, Band (0–0): 24693.10 cm^{-1}; isotope shift $= -1.52$ cm^{-1}, lifetime $=$ 1.13 μs.

The bond strength of AgAu, estimated[160] to be $D_0^0(\text{AgAu}) = 2.06 \pm 0.10$ eV, is weaker than these of CuAu and Au$_2$. The ionization potential[162] IP(AgAu) = 8.41 eV in agreement with this investigation[163], placing IP of AgAu below 9.15 eV.

4. Isotope selective laser spectroscopy of Ag₂ molecules

The relevant measurements, published[164−166] and analysed partly, allowed[167] the rotational analysis of the $X^1\Sigma_g^+$, $A^1\Sigma_u^+$, $B^1\Pi_u$, $C^1\Pi_u$, $D^1\Sigma_u^+$ and $E^1\Pi_u$ states of Ag$_2$, determination of the adiabatic ionization potential of Ag$_2$, namely IP(Ag$_2^+$) = 61747 ± 4 cm^{-1} = 7.6557 ± 0.0005 eV, and the vibrational constants of the ground state of Ag$_2$$^+$, all presented in Table 5.

Taking the value IP(Ag) = 61106 cm^{-1} from Reference 168, one finds that the ion ground state is more weakly bound than the neutral ground state, $D_0[\text{Ag}_2(^1\Sigma_g^+)] - D_0[\text{Ag}_2^+(^2\Sigma_g^+)] = 61747 - 61106 = 641$ cm^{-1}. With the absolute value $D_0[\text{Ag}_2(^1\Sigma_g^+)] = 13307$ cm^{-1} given in Reference 169, one obtains the absolute value of the dissociation energy of the ion ground state to be $D_0[\text{Ag}_2^+(^2\Sigma_g^+)] = 13307 - 641 = 12666 \pm 250$ cm^{-1}.

5. The resonant two-photon ionization spectral studies of ¹⁰⁷,¹⁰⁹Ag-rare gas van der Waals complexes

The spectroscopic studies of silver atom van der Waals complexes, Ag−Ar, Ag−Kr, Ag−Xe, presented in this section supplement the earlier investigations of silver dimer−rare gas complexes[170−172] and extend also previous studies of the laser-induced fluorescence of the Ag−Ar system[173]. New resonant two-photon ionization spectra of $^{107}\text{Ag}^{40}\text{Ar}$, $^{109}\text{Ag}^{86}\text{Kr}$, $^{107}\text{Ag}^{129}\text{Xe}$ complexes have been presented and the positions of bands (as well as their assignments to $^2\Pi \leftarrow {}^2\Sigma$ band systems) have been tabulated[174] as follows:

$$(^{107}\text{Ag}^{40}\text{Ar}, {}^{109}\text{Ag}^{40}\text{Ar}), \text{ (band systems } A^2\Pi_{1/2} \text{ and } A^2\Pi_{3/2})$$

$$(^{107}\text{Ag}^{40}\text{Ar}, {}^{109}\text{Ag}^{40}\text{Ar}), \text{ (band system } B^2\Pi_{3/2} \leftarrow X^2\Sigma)$$

$$(^{107}\text{Ag}^{83}\text{Kr}, {}^{109}\text{Ag}^{86}\text{Kr}), (A^2\Pi \leftarrow X^2\Sigma)$$

$$(^{107}\text{Ag}^{83}\text{Kr}, {}^{109}\text{Ag}^{86}\text{Kr}), (A^2\Pi_{3/2} \leftarrow X^2\Sigma)$$

$$(^{107}\text{Ag}^{83}\text{Kr}, {}^{109}\text{Ag}^{86}\text{Kr}), (B^2\Pi_{3/2} \leftarrow X^2\Sigma)$$

$$(^{107}\text{Ag}^{129}\text{Xe}, {}^{109}\text{Ag}^{136}\text{Xe}), (A^2\Pi_{1/2} \leftarrow X^2\Sigma)$$

$$(^{107}\text{Ag}^{129}\text{Xe}, {}^{109}\text{Ag}^{136}\text{Xe}), (A^2\Pi_{3/2} \leftarrow X^2\Sigma)$$

Analysis of the spectra provided vibrational constants, spin−orbit splittings and dissociation energies for the above-listed complexes. The vibrational frequencies in the excited $^2\Pi$ states correlating to ^2P are in the vicinity of 100 cm^{-1} for each of the complexes; the

TABLE 5. Vibrational and rotational constants and values of r_e of the mixed isotope $^{107,109}Ag_2$ in all important states (notation as used by Herzberg[17])

State Constant	$X^1\Sigma_g^+$	$A^1\Sigma_u^+$	$B^1\Pi_u$	$C^1\Pi_u$	$D^1\Sigma_u^+$	$E^1\Pi_u$	$H^1\Sigma_u^+$	$X^2\Sigma_g^+(Ag_2^+)$
T'_e (cm^{-1})	0.0	22996.4	35828.9	37631.6	39014.5	40158.64	58273.1	61775.3
ω'_e (cm^{-1})	192.4 192.0	154.6	151.388	171.0	168.2	146.41	165.9	135.8
$\omega_e\chi'_e$ (cm^{-1})	0.643 0.58	0.58	0.699	0.84	1.20	1.595	2.46	0.05
B'_e (cm^{-1})	0.048807	0.044354	0.045413	0.04858	0.048655	0.047171	—	—
α'_e (cm^{-1})	2.08×10^{-4}	2.19×10^{-4}	2.49×10^{-4}	2.68×10^{-4}	2.82×10^{-4}	4.16×10^{-4}	—	—
D'_e (cm^{-1})	1.27×10^{-8}	1.54×10^{-8}	1.7×10^{-8}	—	—	1.97×10^{-8}	—	—
r_e (Å)	2.5303	2.6543	2.6231	2.534	2.5341	2.5738	—	—

TABLE 6.   Spectroscopic constants (in cm^{-1})

	$A^2\Pi_{1/2}$	$A^2\Pi_{3/2}$	$B^2\Pi_{1/2}$
ν_{00}	(27404)	(28274)	30128.5 ± 1.1
ω'_e	121.6 ± 0.5	108.1 ± 0.7	19.6 ± 0.6
$\omega_e\chi'_e$	1.58 ± 0.02	1.26 ± 0.02	0.50 ± 0.07
D'_0	2286	2267	183
D''_0	138	68	69

vibrational frequencies in the $^2\Pi$ states correlating to ^2D are in the vicinity of 20 cm^{-1}. The spectroscopic constants (in cm^{-1}) derived, for instance, from spectroscopic data for $^{107}Ag^{83}Kr$ isotopomers in $A^2\Pi_{1/2}$, $A^2\Pi_{3/2}$ and $B^2\Pi_{3/2}$ states are given in Table 6. The dissociation energies are significantly greater in the $^2\Pi$ excited states than in the $^2\Sigma$ ground state $[D_0(Xe) > D_0(Kr) > D_0(Ar)]$. The excited states have much shorter bond distances than the ground states. The differences in bond distances between the two states in a band system are deduced to be: $\Delta r_e = -1.23 \pm 0.10$ Å (for Ag−Ar); $\Delta r_e = -1.32 \pm 0.15$ Å (for Ag−Kr); $\Delta r_e = -1.53 \pm 0.15$ Å (for Ag−Xe).

6. Photoionization spectroscopic studies of AgLi dimers

Photoionization spectra of isotopic metal dimer molecules provide information on their bond energies, bond distances and electronic configurations[169,175] which are essential for establishing the details of metal−metal bonding and important for understanding the chemical bond. Electronic spectra of alkali or coinage metal dimers have fewer over-lapping electronic states than the transition metals, and are easier to interpret[165]. The previous spectroscopic studies of homonuclear dimers[163,176−178] are followed by subse-quent R2PI studies of alkali−coinage mixed-metal dimers[176] such as AgK. The ground electron configuration of the Ag atom is $d^{10}s^1$, that of Li is s^1; thus the ground state of the mixed dimer, resulting from an s−s σ-bond, should be $^1\Sigma^+$, but due to the large electronegativity difference of the constituent atoms the partial ionic contribution to the (covalent) bonding of AgLi should be observed, as was found in the case of the AgK dimer[176].

Analysis of the R2PI excitation spectrum of various isotopic forms of the Ag−Li dimer, produced in a pulsed supersonic molecular beam by laser vaporization of a sil-ver rod containing lithium salt as an impurity, showed that the origin of the Ag^7Li electronic transition is located at 32893 ± 50 cm^{-1}, and the Ag^6Li origin is located at 32889 ± 50 cm^{-1}. The Ag^7Li excited state progression (vibrational band positions) is characterized by the vibrational frequency $\omega'_e = 247.8$ cm^{-1}, $\omega_e\chi'_e = 2.80$ cm^{-1} and $D'_0 = 5491$ cm^{-1}, while the ground state of Ag^7Li spectroscopic constants is given by $\omega''_e = 389.0$ cm^{-1}, $\omega_e\chi''_e = 2.27$ cm^{-1} and $D''_0 = 16648$ cm^{-1}. The excited state progres-sion of Ag^6Li is characterized by $\omega'_e = 259.2$ cm^{-1} and $\omega_e\chi'_e = 2.02$ cm^{-1}, but the value of the dissociation energy of Ag^6Li determined by extrapolation was not highly accurate. By comparing the ground state frequency[17] of Ag_2, equal to 192 cm^{-1} and the ground state frequency[17] of Li_2, equal to 351 cm^{-1}, with the measured AgLi ground state fre-quency, equal to 389 cm^{-1}. the conclusion was reached that the AgLi system has some ionic bonding character resulting from the difference in electronegativities of the con-stituent atoms. The ground state of AgLi is more strongly bound than those of Ag_2 and

Li$_2$, but the dissociation energies of AgLi assessed in this study[179] are of qualitative nature only.

7. Chlorine nuclear quadrupole coupling constants of AgCl isotopomers

The following Cl nuclear quadrupole coupling constants (NQCC in MHz) and $J = 2 - 1$ pure rotational transition frequencies (MHz) of AgCl isotopomers, obtained[180] by applying a pulsed high voltage to Ag wire electrodes in 2% Cl$_2$/Ar at a total pressure of $1-2$ atm, have been determined with great precision and compared with previously reported values[181−183]:

	Cl/NQCC (MHz)	ν_{rot} (MHz)
^{107}Ag^{35}Cl	−36.44089	14712.1127
^{109}Ag^{35}Cl	−36.44113	14645.6077
^{107}Ag^{37}Cl	−28.7213	14113.9164
^{109}Ag^{37}Cl	−28.7213	14047.4074

The new values of the quadrupole constants for ^{35}Cl of ^{107}Ag^{35}Cl and ^{109}Ag^{35}Cl isotopomers have been obtained with uncertainties by two orders of magnitude smaller than previously reported[181,184].

8. Effect of ethanol on surface-enhanced Raman scattering

The effect of ethanol on the surface-enhanced Raman scattering (SERS) of water molecules has been studied[185] both in water and in deuterated water. SERS intensities of OH/OD stretching bands in H$_2$O/D$_2$O water molecules (at 3500 cm^{-1} and at 2565 cm^{-1}, respectively), and the intensities of the SERS bands of the Ag^0−Cl stretching mode at around 240 cm^{-1}, are increased by factor of two when EtOH/EtOD is added to form a SERS solution of a 0.7 M KCl−EtOH (1.0)−water (2.8)/silver electrode system. This effect was explained by assuming that ethanol breaks the hydrogen-bonding network of water molecules, and thus increases their chance for surface adsorption and stabilizes also the surface adatomic complex[186,187] such as Ag^0−Cl$^-$.

E. Radioanalytical and Environmental Studies with Silver Isotopes

1. Environmental aspects of the ^{107}Ag(n,γ) ^{108m}Ag reaction in nuclear power reactors

Radionuclides produced in nuclear power plants may appear in the effluent to the environment in spite of extensive purification of the coolant water. Two long-lived silver radioisotopes, ^{108m}Ag ($T_{1/2} = 127$ y) and ^{110m}Ag ($T_{1/2} = 249.76$ days) have therefore been reinvestigated[188,189]. The rather accurately known[190] values $\sigma_\gamma^0 = 4.7 \pm 0.2$ barns and $I_\gamma = 72.3 \pm 4.0$ barns for ^{109}Ag(n,γ)^{110m} Ag reaction have been used for normalization of the counting data of ^{108m}Ag.

2. Retention of ^{110m}Ag by holm oak leaves

The forest canopy is an effective filter for atmospheric pollutants due to high specific leaf area[191−194]. The importance of the forest ecosystem as the radioactivity accumulator

has been demonstrated by the Chernobyl accident[195]. Therefore, radionuclide retention by holm oak leaves was studied in detail[196].

3. ^{110m}Ag in mushrooms

In 26 samples of mushrooms collected in a park forest in Hungary, four were found to contain ^{110m}Ag, besides ^{40}K and ^{137}Cs, emitted from a PWR-type power plant. It has been suggested[197,198] that these mushrooms bioaccumulate silver selectively and that *Macrolepiota* species could be used as suitable tools indicating the presence of ^{100m}Ag. The mushroom — soil transfer factor can reach[199] a value of 500–1000.

4. Studies of soil-to-plant transfer of ^{110m}Ag

The mobility and soil-to-plant transfer of ^{85}Sr, ^{134}Cs and ^{110m}Ag in two Mediterranean sandy and sandy-loam soils have been studied[200−205]. The relative transfer to plants of ^{134}Cs and ^{85}Sr follows the predictions[202,203] but radiosilver was found to be less mobile than expected. Silver complexation and reduction may play a certain role in its behaviour[206,207]. The behaviour of radionuclides in the Chernobyl area should be compared with theoretical schemes concerning the behaviour of accidentally released radionuclides in agricultural systems. In a study[208], silica gel bearing chemically immobilized humic acid was used to model the uptake of ^{110m}Ag$^+$ and ^{125}I$^-$ by humic matter. The absorptive properties of humic acid, as judged by the uptake of these radionuclides, are quite distinct from those of the parent silica gel.

Uptake experiments were carried out on cultures of a planctonic alga, *Scenedesmus obliquus*, exposed to ^{110m}Ag at different stages of development[209]. The accumulation of the radionuclide was rapid and intense, and equilibrium was reached in an exposure time of less than 24 hours. The uptake kinetics showed the algal concentration level to be dependent only on the medium concentration and on the cell development at the time of ^{110m}Ag addition. Passive uptake was described by Freundlich adsorption isotherms. During the depuration phase the ^{110m}Ag retention by *S. obliquus* developed in accordance with an exponential model based on the existence of two biological half-lives i.e. a very short one of a few seconds and a longer one of 115 h. In a similar study[210] the radioactivity of sea water was determined by studying the concentration of metals in squid livers and the distribution of ^{110m}Ag in them.

5. Concentrations of ^{108m}Ag, ^{110m}Ag, ^{137}Cs and ^{210}Pb in oysters on the Japanese coast

Knowledge of the distribution of radionuclides in coastal seas is important to human life. The determinations of low concentrations of radionuclides in sea water are possible due to 'bioindicators' which concentrate radioisotopes in their body from sea water[211]. Folsom investigated the distribution[212,213] of ^{108m}Ag and ^{110m}Ag using squid, yellow fin, lobster and albacore in the Pacific Ocean and also suggested the probability of dating of nuclear weapon tests using the ratio of ^{110m}Ag to ^{108m}Ag. Fukatsu, Higuchi and Umetsu[214,210] investigated the radiosilver in the sea around Japan using squid liver and mollusca. Beasley and Held[215] detected ^{108m}Ag in biota and sediments collected in 1964–1970 at Bikini and Eniwetok Atolls where nuclear explosions have been carried out several times. Changes of ^{110m}Ag contents were reported also in mussels, brown algae and limpets[216,217] after the Chernobyl accident.

According to several reports[218−221] the behaviours of ^{210}Pb and ^{108m}Ag in coastal sea water are similar. They are scavenged by suspended and organic particulates. Ishikawa and coworkers found[222] that the radiosilver concentration in cultivated oysters depends on the topographical conditions of the bay. The concentrations of ^{108m}Ag and ^{110m}Ag are lower in nearly-closed bays with narrow entrances than in open bays. The data on ^{108m}Ag (due to nuclear explosion tests carried out before 1963 in USA and USSR), on ^{110m}Ag (attributed to the 26th Chinese nuclear explosion test[214] in 1980 and the Chernobyl accident in 1986), on ^{210}Pb, on ^{137}Cs and on the ^{108m}Ag/Ag ratio collected at an open bay during the 1981–1993 period showed that the amount of ^{108m}Ag in *Crassostrea gigas* decreased exponentially from an initial value of about 30 mBq/kg flesh in the early 1980s to 10 mBq/kg flesh in the early 1990s. The ecological half-life of ^{108m}Ag in oysters was 5.6 ± 0.5 years, in agreement with the half-time value of 5.0 years for the decrease in concentration of ^{108m}Ag in the Pacific Ocean during the 1964–1977 period reported by Folsom[213].

The concentrations of ^{108m}Ag and ^{110m}Ag in oysters, cultivated in nearly closed bays, were remarkably lower than in open bays in the same sampling time. This trend was especially clear[223−230] in the Chernobyl-derived ^{110m}Ag. In an open bay 2780 [mBq/(kg flesh)] of ^{110m}Ag was detected in late 1986, 710 mBq/kg flesh in the inlet to a nearly closed bay and less than the detection limit at the end of this bay, in the same sampling time. The concentrations of ^{137}Cs in oysters cultivated in the open and nearly closed bays were similar. This has been related to the ionic chemical form of ^{137}Cs soluble in sea water[231], while silver is combined with highly polymeric organic compounds such as proteins or proteincarbohydrates.

Different concentrations of various metals are observed between open and nearly closed bays[232]. The effective half-life of ^{110m}Ag (equation 55) in squids after Chernobyl is $T_{(1/2)\text{eff}} = 130$ days, in oysters after the Chernobyl accident $T_{(1/2)\text{eff}} = 140$ days and in oysters after the 26th Chinese test $T_{(1/2)\text{eff}} = 160$ days. The $T_{(1/2)\text{eff}}$ value is shorter than the physical half-life, $T_{\text{phys}} = 249.76$ days. Taking $T_{\text{eff}} = 150$ days for ^{110m}Ag in oysters, we find that $T = 375$ days. This number probably reflects the half-residence time of ^{110m}Ag in the sea water rather than the biological half-life in the oysters. The $T_{(1/2)\text{eff}}$ values of ^{110m}Ag for oysters and squids are similar. The specific radioactivity of ^{108m}Ag for oysters was found to be 0.026 ± 0.008 Bq/mg silver at the open Japanese coast[222] which compares with value of 0.021 ± 0.005 Bq/mg silver for squid in the Pacific Ocean[214]. This coincidence suggests the similar behaviour of ^{108m}Ag in Pacific Ocean oysters and squids and also a uniform distribution of ^{108m}Ag in the Pacific Ocean water. Thus the present levels of ^{110m}Ag or ^{108m}Ag found in the above environmental studies do not ensue a health hazard. The ICRP recommended the value[233] of 2×10^7 Bq for ^{110m}Ag as an annual limit of intake.

$$\frac{1}{T_{\text{eff}}} = \frac{1}{T} + \frac{1}{T_{\text{phys}}} \tag{55}$$

F. Radioanalytical and Biomedical Studies with Silver Isotopes

1. ^{109}Cd/^{109m}Ag generator

Ultra-short-lived radionuclides are effectively used for visualizing veins, chambers of the heart and certain organs with gamma cameras. The short half-life of the nuclides

reduces the radiation exposure to the patient. They are easily obtained[234,235] by elution from a generator containing long-lived ^{109}Cd ($T_{1/2} = 453$ days). The ^{109m}Ag ($T_{1/2} = 39.6$ s) is eluted with 0.2 M NaCl physiologically compatible for human use[236,237]. ^{110m}Ag (needed also for measurement of the distribution coefficient of Ag) has been produced by a few hours of irradiation of AgNO$_3$ at neutron flux of about 2×10^{14} cm^{-2} s^{-1}, similarly as in the case of natural CdO targets 30 d irradiations. It was recently suggested that one use in the generator no-carrier-added ^{109}Cd parent[238].

2. Silver-stained polyacrylamide gels

Silver-stained polyacrylamide gels[239−243] have been used in quantitative and fast separations of individual proteins labelled with weak β-emitters (^{14}C, ^{3}H) by polyacrylamide gel electrophoresis[244]. The amount of radioactivity in a given band can be determined rapidly by liquid scintillation counting, which was found to be independent of the silver deposition and total protein content, but linear with respect to the amount of radioactivity in the given band, thus avoiding the lengthy exposures needed, for instance, in the autoradiography of [^{3}H]methionine-labelled proteins separated by polyacrylamide gel electrophoresis. The method was used to determine [^{3}H]mannose and [^{3}H]fucose incorporated into a cell adhesion protein[245].

3. Determination of silver concentration in fingernails

The concentration of essential, non-essential and toxic metals in the body is affected by such factors as age, nutrition, dose, retention, chemical form of the metals and their binding sites[246−248]. The relationships between the aging process and the trace element concentrations in normal human brain and the related studies of elemental imbalances in Alzheimer's disease and similar neurological disorders have received much attention recently. Imbalances in hair and fingernails of elderly patients are also under current study[249−252]. Middle-aged groups have been included in recent studies[249−251,253] applying modern instrumental neutron activation analysis (INAA) in which little sample preparation is needed, the possibility of contamination is minimized and sampling bias problems are avoided[253]. Studies of Ag, Ca, Co, Cr, Cs, Fe, Hg, Rb, Sb, Sc, Se and Zn have been carried out. Silver, gold, selenium and zinc concentrations have been found to be higher in females than in males[251,254] (for instance, 20.7 ng g^{-1} of Au in male and 51.9 ng g^{-1} of Au in female), possibly due to more frequent use of gold jewellery. In a population of a 30 year average age, 60.3 ng g^{-1} of Ag and 29.9 ng g^{-1} of Au was found[253]. No correlation with sex was given in this publication but earlier analytical data[255] indicated the decisively higher concentrations of Ag and Au in females than in males.

In the course of determinations of trace element concentrations in nails of a group of carpenters by cyclic instrumental neutron activation analysis (CINAA) using the PCA (principal component analysis[256−259]) method, the silver concentration in nails was determined[260] to be 0.027 ± 0.037 µg g^{-1}. The mean concentration of gold was 0.010 µg g^{-1}. Nails can be used as a dietary and environmental exposure monitor[261−267].

4. INAA study of trace elements in hair samples

About thirty elements, including silver and gold, have been determined quantitatively by the INAA method in hair samples taken from two children of different sex[268]. The radionuclides used in the INAA analysis of silver and gold were ^{198}Au and ^{110m}Ag. Scalp

hair has been found to be an attractive 'biological indicator' for monitoring environmental exposure, for evaluating heavy metal poisoning, assessing nutritional status and for diagnosing diseases. An earlier INAA study of elements in the hair of the Bulgarian urban population, compared with corresponding values from England and New Zealand, indicated a strong dependence on the washing procedures used[269]. More than 18 elements superficially attached to the hair surface were easily removed by water washing. Triton X 100 detergent has been effective in removing Ag, As, Au, Cl, Cs, K, Na and Pb, but not Hg. Only S and Zn have been strongly incorporated in the hair structure. Silver and gold contents in hair samples were as follows:

In unwashed scalp hair, 0.191 and 0.0951 μg g^{-1}, respectively, for Ag and Au; in distilled-water washed hair, 0.164 and 0.0662 μg g^{-1}, respectively; in acid/acetone/water washed hair, 0.144 and 0.0510 μg g^{-1}, respectively; in TritonX 100/water washed hair, 0.057 and 0.0363 μg g^{-1}, respectively.

The mean cadmium content of unwashed hair was 1.423 ± 0.508 and 1.559 ± 1.135 μg g^{-1} for non-smokers and smokers, respectively[270–272]. About 60 papers[273–324] which stress that the scalp hair is a valuable tissue recording the level and changes of many trace elements in the body have been reviewed[269].

5. Radiochemical NAA of trace metals in human blood serum using inorganic ion-exchangers

a. Thirteen trace elements in blood serum including silver, occurring in concentrations at the μg g^{-1} to pg g^{-1} level, have been determined quantitatively by two *Canberra* Ge(Li) calibrated detectors[325]. The concentrations of silver ([Ag] = 0.085 ng cm^{-3}) and antimony ([Sb] = 0.023 ng cm^{-3}) have been found to be much lower than the published data[326], equal to about 0.68 and 0.52 ng cm^{-3}, respectively. It has been assumed that the higher published values are due to contamination of the particular serum samples analysed[325].

b. Nuclear activation analytical methods (INAA) of detection of trace elements in pathological human blood serum have being suggested as a diagnostically useful characterization of blood[327,328]. The concentrations of 23 elements including Ag and Au have been determined in blood sera of patients with hereditary hemolytic anemias and compared with normal control subjects.

6. Ag and Au in human placental tissue as determined by neutron irradiation and gamma-ray spectrometry

The placenta functions as a barrier between fetus and mother[329–331]. The elemental content of the placenta provides an indication of the nutritional/excretory maintenance of the pregnancy. The concentrations of elements in placental tissue are at low μg^{-1}–ng g^{-1} levels and multi-element precise methods, including INAA, were applied to determine more than forty elements in this tissue[332,333]. The average contents of silver and gold [given in μg g^{-1} (dry wt)] in 100 hospitalized deliveries were found to be [Ag] = 0.0049 ± 0.0014 and [Au] = 0.00024 ± 0.00010. These two metals are neither essential trace metals nor are they toxic.

7. Identification of elemental status in Alzheimer's disease (AD)

Knowledge of trace element levels in the brain may be useful as a diagnostic aid for AD. The concentrations of silver in brain tissue in diseased and in control (C) individuals,

expressed in µg g^{-1} dry weight, have been found by INAA to be 0.0324 and 0.1086 in AD and 0.0277 and 0.0927 in C[334]. Observed variations in other elements strongly suggest multi-elemental involvement in Alzheimer's disease. Thus the possible effect of zinc deficiency on AD has been considered[335−339].

8. Determination of silver by INAA methods in biological materials

Trace element determination in biological materials (human erythrocytes, plasma, urine) by neutron activation analysis via long-lived isotopes has been investigated[340]. The method is particularly suitable for analysis of trace elements possessing isotopes having high ratios of resonance integral to thermal neutron cross-section (RI/σ_0) in the presence of interfering nuclides which are activated by thermal neutrons but have no resonance peaks in the epithermal region[341−350]. ^{110m}Ag has been used in this investigation[340]. The epithermal INAA of standard oyster tissue, containing the certified value of silver equal to 0.89 ± 0.9 µg g^{-1}, showed the value of 0.86 ± 0.09 µg g^{-1} comparable with the value of 0.93 ± 0.06 µg g^{-1} given by thermal INAA. Significantly, the irradiation and cooling times (48 h and 15−21 days) in epithermal NAA have been much shorter than those required by thermal NNA, which is important in clinical and environmental tracer element research.

A new irradiation facility suitable for the direct determination of several trace elements without pretreatment, which enables the neutron activation of large amounts of biological materials at liquid nitrogen temperature, has been constructed and tested[351].

The application of INAA analysis of saliva in clinical chemistry and in environmental and occupational technology has been discussed[352]. The contents of 21 chemical elements, including silver, have been assessed. Men involved in the clean-up operation after the Chernobyl accident had the same concentration of Ag in their saliva than uninvolved healthy men. However, a deficiency of Zn, Se, Rb in a cleaner's saliva was associated with the weakening of his immune response[353].

Radiochemical and INAA procedures for the determination of the low level trace elements in human livers established the limits of detection of seven critical low level trace elements (Cr, As, Se, Mo, Ag, Sn, ^{122}Sb and ^{124}Sb). For silver, the value 0.7 µg kg^{-1} is given[354]. These limits represent concentrations at which a sample would generate a detectable signal[355].

The INAA method is also used for biological and physical sediment transport studies[356]. Sediment particles are labelled (doped) with gold or silver that are present in only trace amounts in most natural settings and then these metals can be detected sensitively at [ng g^{-1}] levels by INAA.

The INAA method has been applied also for multi-element determination in water taken from wells near Riyadh in Saudi Arabia. The concentration of ^{110m}Ag in this water was determined[357] to be less than 5.5 ppm.

^{110m}Ag uptake from food, retention, elimination and tissue distribution were investigated in the fresh water fish *Cyprinus carpio*[358]. The biological half-life of ^{110m}Ag was relatively short (22 days). A tissue distribution study showed that ^{110m}Ag accumulation and retention by the liver and digestive tract accounted for 60−80% of the total radionuclide body load, although they represent only about 10% of the fish body mass.

The determination of metallothionein levels in rat tissues by a radiochemical method using ^{110m}Ag and ^{203}Hg as tracers was elaborated[359]. In all organs the ^{110m}Ag saturation procedure gave lower results than the ^{203}Hg procedure, and the latter also showed low specificity so should not be used for determining low levels of metallothioneins. The Hg

procedure, however, is more stable than the Ag method and may be useful for the assay of high concentrations of metallothionein. In a similar study[360] the Ag method was applied for measurements of metallothionein in animal tissues and found to be sensitive and valid.

The $^{105+106}$Au radioisotopes were applied[361] to label a pharmaceutical product (AGIPIV) which is used as a topical disinfectant and cicatrizant for the treatment of skin lesions. The amounts of Ag found in the tissues correspond to a maximal estimated retention of 0.01% of the dose of medicine. Although this value can be considered low, it represents an increase of $2-3$ times at the natural level of Ag in liver and other tissues.

IV. SYNTHESIS AND USE OF ISOTOPICALLY LABELLED GOLD-CONTAINING COMPOUNDS

A. Chemical and Physical Studies with Isotopically Labelled Compounds of Gold

1. Synthesis of ^{195}Au and ^{14}C-labelled antineoplastic gold^I phosphine complexes

Many gold^I phosphine complexes have been found to be potent cytotoxic agents, to have antitumor activity against P388 leukaemia and to be active against a spectrum of transplantable tumour models[362−366]. It has been of particular interest to obtain some of them labelled with radioactive isotopes of gold and carbon for cellular, binding, metabolism and biodistribution studies.

a. Synthesis of ^{14}C-labelled {[μ-1,2-bis(diphenylphosphino)[^{14}C$_2$]ethane]bis-(1-thio-β-D-glucopyranosato-S)gold^1}, **49**, SK&F 102912, bis{1,2-bis(diphenylphosphino[^{14}C$_2$] ethane}gold^I chloride, **50a**, SK&F 101772 and its lactate, **50b**, SK&F 104524, has been carried out[367] following the scheme[368,369] shown in equation 56. [^{14}C$_2$]Dppe, **51**, has been prepared by the double addition of diphenylphosphide anion to [^{14}C$_2$]acetylene.

b. Synthesis of bis[1,2-bis(diphenylphosphino)ethane][^{195}Au]gold^I-2-hydroxypropano-ate, **50c**.

The gold-195-labelled gold−dppe complex, **50c** (SK&F[^{195}Au] 104524), has been obtained using chloro[^{195}Au]auric acid (equation 57). The labelled product, **50c**, was diluted with unlabelled material. Radiogold ^{195}Au was produced in ^{195}Pt(p,n)^{195}Au nuclear reaction.

{μ-1,2-Bis(diphenylphosphino)ethane-bis[^{195}Au]gold^{I}chloride}, **52b**, the key interme-diate, has been prepared by diluting chloro[^{195}Au]auric acid with unlabelled chloroauric acid, reducing this solution with 2,2′-thiodiethanol in isopropanol under argon and sub-sequently treating it with unlabelled 1,2-bis(diphenylphosphino)ethane also under argon. After purification, **526** was isolated and used in the subsequent step.

2. Synthesis of complexes of gold^I with captopril and their ligand exchanges with thiomalate and cyanide

Captopril, **53**, is a drug used for treatment of high blood pressure[370−384], the action of which involves binding of the thiol group to the active site of the angiotensin I-converting enzyme[374−377]. Many studies of the interaction of this ligand with Zn^{2+}, Cd^{2+}, Au^+ etc. by ^{13}C NMR were performed[382−384]. Gold^I forms linear complexes of type LAuX, where L is a neutral Lewis base and X is an aryl, alkyl, halide or pseudohalide group[385−390]. Captopril, **53** (equation 58), forms with gold^I monomer or polymer complexes such as gold^I thiomalate, [Au(*tm*)], **54**, used as an antiarthritic drug[391−396]. The exchanges of [Au(*cap*)] with thiomalate, **55**, H*tm*, and with ^{13}CN$^−$ were studied[397] since the metabolism

of gold drugs deviates from the normal one for smokers[398−400] who absorb HCN.

$2AuCl_4^-$

(51)

n-BuLi, THF
HPPh$_2$

$HC\!\equiv\!CH$

(52a)

(49)
59% r.y. from 52a

(56)

Ph$_2$P   PPh$_2$
(51)

(50a) 81% r. y. from 51 and 52a

Dowex 1 x 8-50

(50b) sp. act. 49.2 mCi mmol^{-1}

* denotes ^{14}C label.
Lac$^-$ denotes d, l-CH$_3$CH(OH)COO$^-$

$2\overset{*}{A}uCl_4^-$

(52b)

Ag$^+$Lac$^-$

Ph$_2$P   PPh$_2$
(51a)

(57)

$\overset{*}{A}uCl_4^-$ - (34 mCi)
(sp. act. 4 kCi mmol^{-1}).

$\overset{*}{A}u$ denotes ^{195}Au.

(50c) 7 mCi, 96.4% radiochem. purity
(16 mCi crude product)

(53) *trans*   **(53)** H*cap*   **(53)** *cis*

$$(58)$$

(54) Au(*tm*)   **(55)** H(*tm*)

a. The captopril–gold^I complex, [Au(*cap*)], has been prepared[392] from AuCl$_4$$^-$ and 2,2′-thiodiethanol reduction of Au$^{III} \rightarrow$ Au^I, and subsequent treatment with captopril. The IR spectrum of the [Au(*cap*)] complex had no adsorption at 2500 cm^{-1} corresponding to SH. Thus the Au^I binds the ligand via the thiol group. The absorption at 345 cm^{-1} has been assigned to Au–S. No Au–Cl absorption within 310–320 cm^{-1} has been found, eliminating the possibility of formation of a [Au(*cap*)Cl]$^-$ complex[398,399].
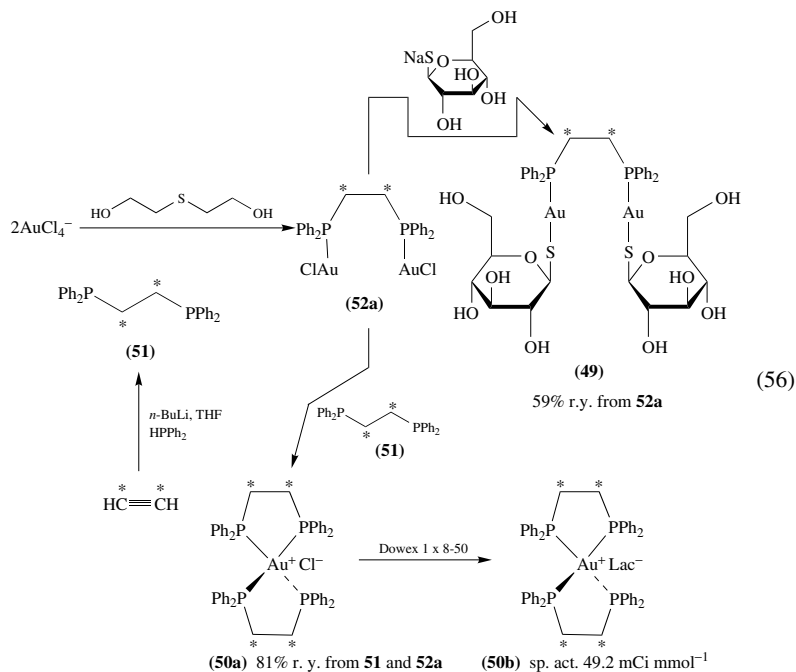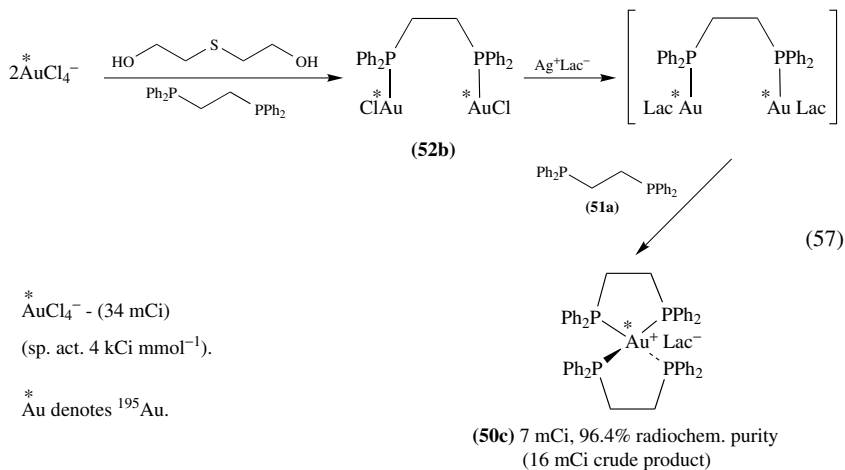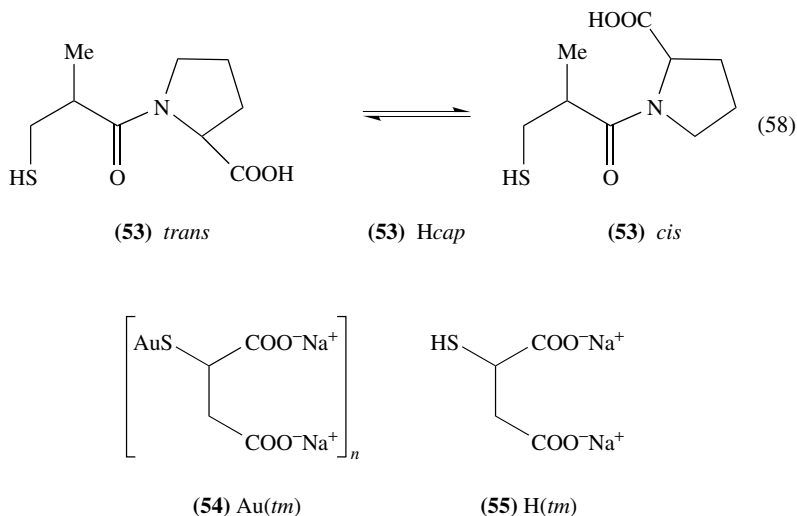
b. Study of the [Au(*cap*)] polymer complex with thiomalate by ^{13}C NMR indicated that *tm*$^-$ binds to the [Au(*cap*)]complex but does not displace all the captopril to form an [Au(*tm*)$_2$]$^-$ complex. Due to rapid ligand exchanges, various species like [Au(*cap*)(*tm*)]$^-$, [Au(*cap*)$_2$]$^-$ etc. are formed and only the exchange-averaged resonances are observed.

c. Interaction of [Au(*cap*)] with ^{13}CN$^-$. When solid K^{13}CN was added to the [Au(*cap*)] solution, three intense resonances appeared in the low-field region assigned to [Au{*cap*(*cis*)}(^{13}CN)]$^-$, [Au{*cap*(*trans*)}(^{13}CN)]$^-$ and [Au(^{13}CN)$_2$]$^-$, $\delta(^{13}$C) = 143.83, 152.18 and 154.06 ppm, respectively[378,397]. Cyanide binds to Au^I very strongly[401,402]. The affinity of the ligands for gold^I is found to be in the order: CN$^- \gg$ Et$_3$P > H*alb* (H*alb* = albumin) > thiols[403]. When [Au(*tg*)] reacted with ^{13}CN$^-$, a mixture of [Au(^{13}CN)$_2$]$^-$ and [Au(tg)^{13}CN]$^-$ was obtained[404] (*tg* = thioglucose).

The reaction of mercaptalbumin (*Alb*SH) with Et$_3$PAuCN and of *Alb*SAuPEt$_3$ with HCN have been also studied by Isab and coworkers[403] by ^{13}C and ^{31}P NMR spectroscopy, by ^{14}CN$^-$ (and H^{14}CN) radiotracer methods[405] and by ^{17}O. Et$_3$PAu^{13}CN (25% enriched) has been used in these studies. It has been demonstrated[403], as indicated in reaction 59, that oxygen-17 from H$_2$^{17}O incorporates into Et$_3$P = ^{17}O when *Alb*SAuPEt$_3$ reacts with H$_2$^{17}O.

Oxidation of Et$_3$P proceeds by reduction[403] of albumin disulphide bonds (*BSA* = any albumin species); see equation 60.

Reaction 61 has been also proposed as the competing alternate pathway of formation of Et$_3$P^{17}O.[403,405]

$AlbSAuPEt_3$ + HCN $AlbSH$ + Et_3PAuCN

$$\left[AlbS\!\!-\!\!Au\!\!\begin{array}{c} PEt_3 \\ CN \end{array} \right]^{\ddagger} \quad 1/2(Et_3P)_2Au^+ + 1/2Au(CN)_2$$

$$Et_3P + AlbSAuCN^-$$

$$1/2AlbSAuX + 1/2\ AlbSH + 1/2Au(CN)_2^-$$

$Et_3P^{17}O$ (X is the unknown ligand)

(59)

$$\begin{array}{c} S \\ | \\ S \end{array}\!\!BSA + Et_3P + H_2^{17}O \longrightarrow (HS)_2BSA + Et_3P\!\!=\!\!\overset{17}{O}$$

$$(HS)_2BSA + [(Et_3P)_2Au]^+ \longrightarrow (Et_3PAuS)BSA$$

(60)

$$[(Et_3P)_2Au]^+ + AlbSH \longrightarrow AlbSAuPEt_3 + Et_3P \xrightarrow{H_2^{17}O} Et_3P^{17}O \qquad (61)^{403,405}$$
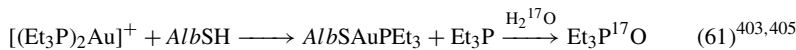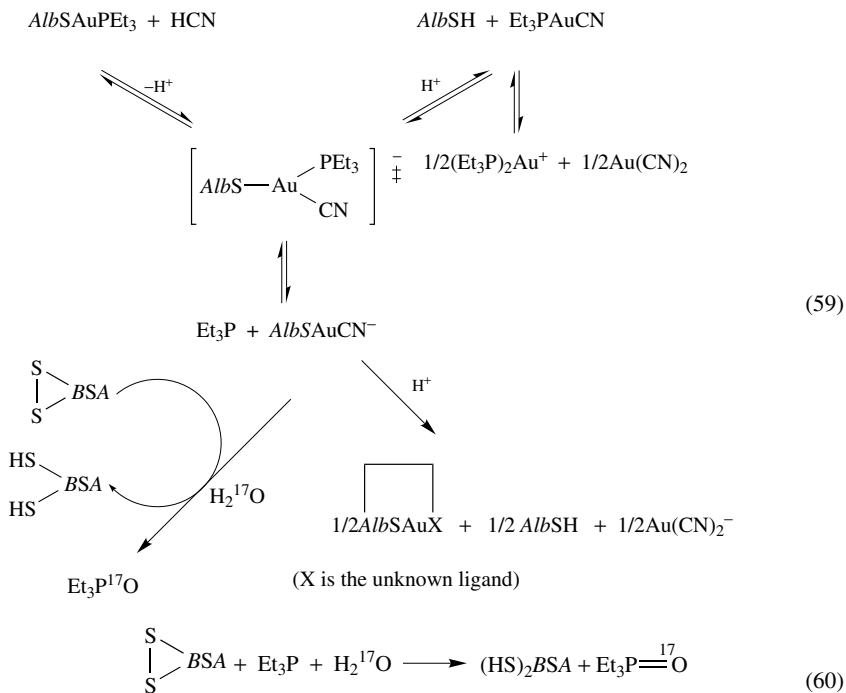
3. Synthesis of ^{13}C-labelled hexakis[phosphineaurio^I] methanium(2+) bistetrafluoroborates

^{13}C-labelled polyaureated carbon complexes of the type $[(L\text{-}Au)_6C]^{2+}$, **56**, with functionalized phosphine ligands have been synthesized[406,407] by the reaction of phosphinegold^I chlorides, RPh_2AuCl [where R = p-C_6H_4Cl, p-C_6H_4Br, p-C_6H_4Me, p-C_6H_4COMe, p-C_6H_4COOH, p-$C_6H_4NMe_2$, $R_2PhPAuCl$ (R = p-$C_6H_4NMe_2$) and R_3PAuCl (R = p-$C_6H_4NMe_2$)] with tetrakis(dimethoxyboryl)methane[^{13}C] in HMPT (equation 62). X-ray structure analyses of the compounds **56f**, **56g** and **56h** were given.

4. Synthesis of ^{13}C and ^{18}O-labelled bis(carbonyl)gold^I undecafluorodiantimonate

a. The synthesis of the bis(carbonyl)gold^I salt, $[Au(CO)_2][Sb_2F_{11}]$, **57**, involves[408] the preparation of gold^{III} fluorosulphate, $Au(SO_3F)_3$, **58** (equation 63), reduction of **58** with carbon monoxide in fluorosulphuric acid to produce carbonyl gold^I sulphate, $Au(CO)SO_3F$, **59**, via $[Au(CO)_2]^+$, **60**, as intermediate[409] (equation 64a), followed by its thermal decomposition (equation 64b) and conversion of **59** in the presence of CO to **57** (equation 65). By using in the above synthetic route isotopically labelled

carbon monoxides, ^{13}CO and $C^{18}O$ provided[408] the isotopomers $[Au(^{13}CO)_2][Sb_2F_{11}]$ and $[Au(C^{18}O)_2][Sb_2F_{11}]$, which permitted one to conduct the valence force field calculation and identification of $[Au(^{13}CO)_2]^+_{solv}$, **60**, and the monocarbonyl gold^I cation $[Au(^{13}CO)]^+_{solv}$ **59**, in the ^{13}C NMR spectra in strong protonic acid (HSO_3F) solutions[410,411]. Recrystallization of **57** from acetonitrile resulted in the formation of single crystals of $[Au(NCMe)_2][SbF_6]$ and evolution of the CO, which was displaced easily from **57** by the MeCN ligand due to the weak gold–carbon bond in **57**.

$$(62)$$

(56)

HMPT = $P(NMe_2)_3$　　　　L=$(R^1R^2R^3P)$

(56a) $R^1 = p\text{-}C_6H_4Cl$, $R^2=R^3=Ph$

(56b) $R^1 = p\text{-}C_6H_4Br$, $R^2=R^3=Ph$

(56c) $R^1 = p\text{-}C_6H_4Me$, $R^2=R^3=Ph$

(56d) $R^1 = p\text{-}C_6H_4OMe$, $R^2=R^3=Ph$

(56e) $R^1=p\text{-}C_6H_4COOH$, $R^2=R^3=Ph$

(56f) $R^1=p\text{-}C_6H_4NMe_2$, $R^2=R^3=Ph$

(56g) $R^1=R^2=p\text{-}C_6H_4NMe_2$, $R^3=Ph$

(56h) $R^1=R^2=R^3=p\text{-}C_6H_4NMe_2$
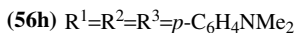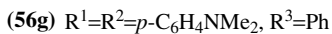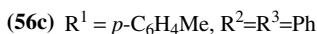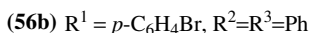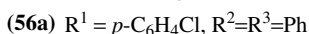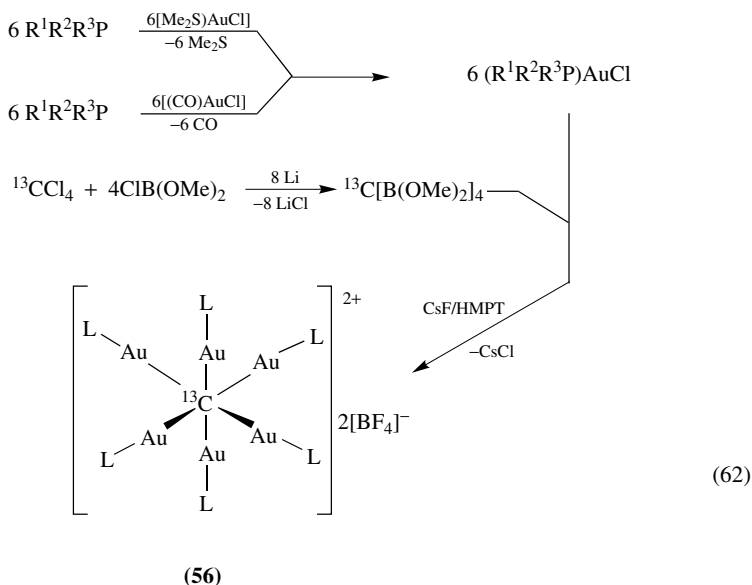
b. The Raman and IR spectra of $[Au(CO)_2][Sb_2F_{11}]$, $[Au(^{13}CO)_2][Sb_2F_{11}]$ and $[Au(C^{18}O)_2][Sb_2F_{11}]$ isotopomers and the IR and Raman spectra of $[Au(CO)_2]^+$, $[Au(^{13}CO)_2]^+$ and $[Au(C^{18}O)_2]^+$ in HSO_3F solution have been recorded and the correct band assignments given. The $\nu_1 = 2254$ cm^{-1} and $\nu_3 = 2217$ cm^{-1} strong CO stretching

vibrations due to solid $[Au(CO)_2][Sb_2F_{11}]$ are the highest so far observed in the metal carbonyl derivatives. These frequencies are located at 2199 cm^{-1} and 2165 cm^{-1} for $[Au(^{13}CO)_2][Sb_2F_{11}]$ and at 2203 cm^{-1} and 2165 cm^{-1} (and 2124 cm^{-1}, ν_3) for $[Au(C^{18}O)_2][Sb_2F_{11}]$ isotopomers, respectively. The IR active band at 354 cm^{-1} has been assigned as asymmetric Au−CO stretch ν_4. The symmetric Au−CO stretching vibrations ν_2 were observed at 400 cm^{-1} as very weak bands in the Raman spectrum of $[Au(CO)_2][Sb_2F_{11}]$. All observed fundamental frequencies (in cm^{-1}) of linear $[Au(CO)_2]^+$, **60**, and isotope shifts between **60** and its isotopomers $[Au(^{13}CO)_2]^+$, $[^{13}C]$-**60** and $[Au(C^{18}O)_2]^+$, $[^{18}O]$-**60** are collected in Table 7 with calculated isotope shifts from valence force fields given in parentheses[408].

$$Au + HSO_3F + S_2O_6F_2 \xrightarrow{80\,°C,\ 1\ h} Au(SO_3F)_3 \tag{63}$$

$$Au(SO_3F)_3 \xrightarrow{3CO} \underset{(60)}{[Au(CO)_2]^+} + CO_2(g) + S_2O_5F_2 + SO_3F^-$$

$$\underset{(58)}{} \qquad\qquad \tag{64a}$$

$$[Au(CO)_2]^+_{solv} + SO_3F^- \xrightarrow[HSO_3F]{80\,°C} \underset{(59)}{Au(CO)SO_3F_{solv}} + CO(g) \tag{64b}$$

$$Au(CO)SO_3F + CO + 4SbF_5 \xrightarrow{SbF_5(liquid)} \underset{(57)}{[Au(CO)_2][Sb_2F_{11}]} + Sb_2F_9SO_3F \uparrow \tag{65}$$

Using the data in Table 7, the following inner force constants (in 10^2 N m^{-1}) have been derived for $[Au(CO)_2]^+$: $f_{r(CO)} = 20.1 \pm 0.1$, $f_{R(AuC)} = 2.16 \pm 0.03$, $f_{rr} = 0.15 \pm 0.1$, $f_{RR} = 0.54 \pm 0.03$, $f_{Rr} = 0.45 \pm 0.2$, $f'_{Rr} = 0.0 \pm 0.02$, $f_\alpha = 0.77 \pm 0.09$, $f_\beta = 0.268 \pm 0.02$, $f_{\alpha\beta} = -0.015 \pm 0.015$ and $f_{\beta\beta} = 0.015 \pm 0.02$, where r, R, α and β correspond to the CO and AuC bonds and to the C−Au−C and O−C−Au angles, respectively. The above general valence force field (GVFF) data have been compared with isoelectronic and isosteric molecular species $Hg(CN)_2$ and $[Au(CN)_2]^-$. The C−X (where X = O or N) force constant f_r increases from the anion $[Au(CN)_2]^-$ over $Hg(CN)_2$ to $[Au(CO)_2]^+$, while the M−C (M = Au or Hg) force constant f_R decreases in the same direction[412] $\{f_{(Au-C)} = 2.78 \pm 0.03$ in $[Au(CN)_2]^+$, $f_{(Hg-C)} = 2.59 \pm 0.03$ in $Hg(CN)_2$, $f_{(Au-C)} = 2.16 \pm 0.03$ in $[Au(CO)_2]^+\}$ in agreement with metal-to-ligand π-back-donation, which is at a minimum for $[Au(CO)_2]^+$.

TABLE 7.   Fundamental frequencies [cm^{-1}] and ^{13}C and ^{18}O isotope shifts

$[Au(CO)_2]^+$	$[Au(^{13}CO)_2]^+$	$[Au(C^{18}O)_2]^+$	Assignments
2254	51.5 (52.4)	49 (50.7)	$\Sigma_g^+\ \nu_1$
400	6.5^a (6.5)	10^a (14.2)	$\Sigma_g^+\ \nu_2$
2217	50.5 (50.3)	52 (51.8)	$\Sigma_u^+\ \nu_3$
354	4.5 (4.6)	9 (9.6)	$\Sigma_g^+\ \nu_4$
312	9.0 (9.2)	3.5 (3.3)	$\Pi_g\ \nu_5$
406	14 (13.5)	3 (2.6)	$\Pi_u\ \nu_6$
105	0 (0.2)	5 (4.6)	$\Pi_u\ \nu_7$

^{a}Calculated from $[(\nu_2 + \nu_3) - \nu_3]$[408]

c. MAS NMR spectra of solid $[Au(^{13}CO)_2][Sb_2F_{11}]$ have a resonance at 174 ppm. In HSO_3F or SO_2 solvents, **57** shows a single peak of $[Au(^{13}CO)_2]^+$ at the same position. The NMR peak corresponding to $[Au(^{13}CO)]^+$ is located at 162 ppm. Fast CO exchange has been observed by vibrational spectroscopy when $[Au(^{12}CO)_2]^+$ was added to a solution of $[Au(^{13}CO)_2]^+$ in HSO_3F to give $[Au(^{12}CO)(^{13}CO)]^+$ isotopomer. Slow CO exchange between $[Au(^{13}CO)_2]^+$ and $[Au(^{13}CO)]^+$ was observed by ^{13}C NMR in the $17-52\,°C$ temperature range. The two peaks located at 174 and 162 ppm at $17\,°C$ gradually transform into a single resonance at 167 ppm with a line-width of 100 Hz in the course of heating the mixture of **59** and **60** from 17 to $52\,°C$. In magic acid solution (HSO_3F/SbF_5) the resonances for $[Au(^{13}CO)_2]^+$ and $[Au(^{13}CO)]^+$ coalesce at about $125\,°C$. The mechanism of CO exchange between **59** and **60** is under investigation and the ^{13}C NMR spectra indicated two distinct gold^I species, $[Au(^{13}CO)]^+_{(solv)}$ and $[Au(^{13}CO)_2]^+_{(solv)}$, in HSO_3F medium[408].

5. Synthesis of oxygen-17 labelled gold^I oxocomplexes, $[(LAu)_3\ (\mu_3\text{-}^{17}O)]BF_4$

Synthesis of $\{[(p\text{-}ClC_6H_4)_3PAu]_3(\mu_3\text{-}^{17}O)\}BF_4$, **61**, proceeds as shown in equation 66[413].

$$LAuCl \xrightarrow[\text{2. } K^{17}OH/NaBF_4/MeOH]{\text{1. } AgBF_4/MeOH} [(LAu)_3(\mu_3\text{-}^{17}O)]BF_4 + AgCl \qquad (66)$$
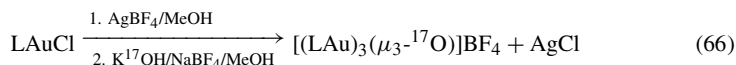
The synthesis of $\{[(Ph_3P)Au]_3\ (\mu_3\text{-}^{17}O)\}BF_4$, **62**, has been carried out in a similar manner. The title gold complexes with $L = PMePh_2$, PMe_2Ph, $PEtPh_2$, $P(o\text{-Tol})_3$, $P(OEt)Ph_2$, $P(OMe)_3$ have been obtained as shown in equation 67.

$$LAuCl + Ag_2O \xrightarrow{NaBF_4} [(LAu)_3(\mu_3\text{-}O)]BF_4 + AgCl \qquad (67)$$
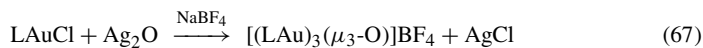
Fast ligand exchange and coincident chemical shifts have been observed by ^{31}P NMR (equation 68).

$$[(L^1Au)_3(\mu_3\text{-}O)]BF_4 + L^2AuCl \rightleftharpoons [(L^2Au)_3(\mu_3\text{-}O)]BF_4 + L^1AuCl \qquad (68)$$
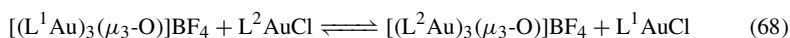
The fast ligand exchange up to $-80\,°C$ has been found[113] also by ^{31}P NMR for imido complexes[414], $[(L^1Au)_3\ (\mu_3\text{-}NR)]BF_4$, **63** ($R = t\text{-Bu}$, $L^1 = PPh_2Me$), with L^2AuCl [$L^2 = P(i\text{-Pr})Ph_2$], and also for the imido complexes with $R = t\text{-Bu}$, $L^1 = PPh_3$, $L^2 = PPh_2Me$. The exchange process slows with increasing steric pressure, suggesting associative pathways (equation 69).

The intermediacy of exchange structures, **64**, has also been discussed. Au–O distances in structures involving the $(LAu)_3O^+$, **65**, unit are equal to 2.05 Å, the Au–Au distances change with the size of phosphines in the range $3.054-3.069-3.086$ Å, whilst the Au–O–Au angles are 96.2, 97.0 and 97.6°. The nature of Au–O interaction is not clear. The ^{17}O NMR data of $[(LAu)_3(\mu_3\text{-}O)]BF_4$ show chemical shifts changing from $+19.7$ ppm (for $L = PPh_3$) to -36.0 ppm (for $L = PMe_2Ph$), with upfield shifts corresponding[415] to the increasing basicity of the phosphine, L. LAuCl complexes have been prepared by techniques described in the literature[416].

$$L^1Au \diagdown \underset{\overset{|}{AuL^1}}{\overset{+}{Y}} \diagdown AuL^1 + AuL^2 \;\; \rightleftharpoons \;\; \left[\underset{L^1Au \diagdown AuL^1}{L^1Au \diagup Y \diagdown AuL^2} \right]^{2+}$$

$$Y = O, NR$$

(69)

$$L^1Au \diagdown \underset{\overset{|}{AuL^1}}{\overset{+}{Y}} \diagdown AuL^2 \;\; + \;\; AuL^1$$

(64)

(65)
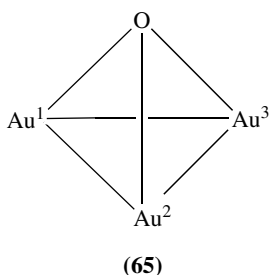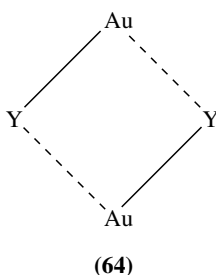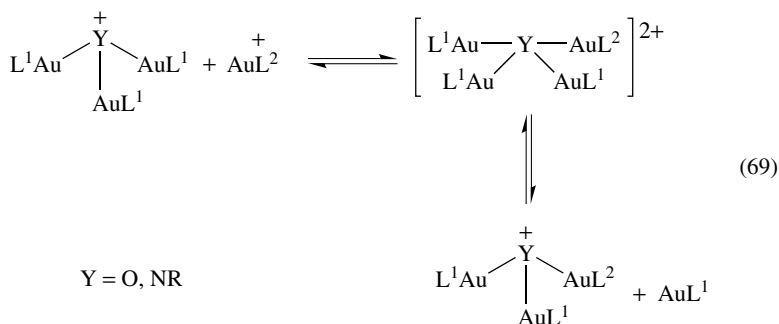
6. Synthesis of (ArN)₃TcAu(PPh₃)

This complex compound $(ArN)_3TcAu(PPh_3)$, **66**, containing the isotope $^{99}_{43}Tc$ (low energy β-emitter, $E_{max} = 0.292$ MeV, $<\beta^-> = 85$ keV, $T_{1/2} = 2.13 \times 10^5$ y), has been obtained[417] by reduction of tris(arylimido)technetium^{VII}, **67**, $Tc(NAr^1)_3I$ ($Ar^1 = 2,6$-dimethylphenyl or 2,6-diisopropylphenyl) and treating the anion **68** with $ClAuPPh_3$ (equation 70). The X-ray analysis of the new gold complex, **66**, gave the distances $Tc-Au = 2.589$ Å, $Tc-N = 1.758$ Å and $Au-P = 2.278$ Å, and the angles $Tc-Au-P = 180.0°$, $Au-Tc-N = 97.2°$ and $N-Tc-N = 118.4°$. The geometry around the technetium atom is best described as distorted trigonal-based pyramid with gold occupying the apex and the imido ligands occupying the base.

7. Synthesis and IR and Raman spectra of deuterium labelled complexes of Au^{III} with dithiooxamides

Complexes of Au^{III} with formula $A[Au(L)_2]$, **69**, where $A = $ Li, Na or K and LH_2 is N, N'-dimethyldithiooxamide (DMDTO) or N, N'-diethyldithiooxamide (DEDTO), have been prepared in alkaline media[418]. Complexes of Au^{III} with dithiooxamide (DTO) of formula $[Au(DTO)(DTO)-D]Cl_2$, **70**, and with N, N'-dimethyldithiooxamide (DMDTO) of formula $[Au(DMDTO-D)_1X_2]$ (where $X = $ Cl or Br), **71**, and $[Au(DMDTO)_1Br_2]Br$, **72**, have been prepared in acid media according to the literature[419].

Four possible ways of coordination in the $[Au(L)_2]$ ion can be imagined[419] (structures **69A−D**), but subsequent vibrational and crystallographic studies[420−424] showed

that dithiooxamides in acid media act solely as bidentate sulphur ligands. The thorough analysis of the vibrational spectra and NH/ND and CH_3/CD_3 substitution indicated that all complexes have a square-planar geometry around Au^{III} and in all cases the dithiooxamides act as bidentate ligands coordinating through both sulphur atoms forming chelate ring systems. The effect of hydrogen bonding on the IR spectra of the complexes has been studied in acid media, while in alkaline media the influence of the alkali counterion has been investigated.

`ethane like' dimer

$$(68) \xrightarrow[\text{THF}]{\text{ClAuPPh}_3}$$

(66)

(69)

(70)
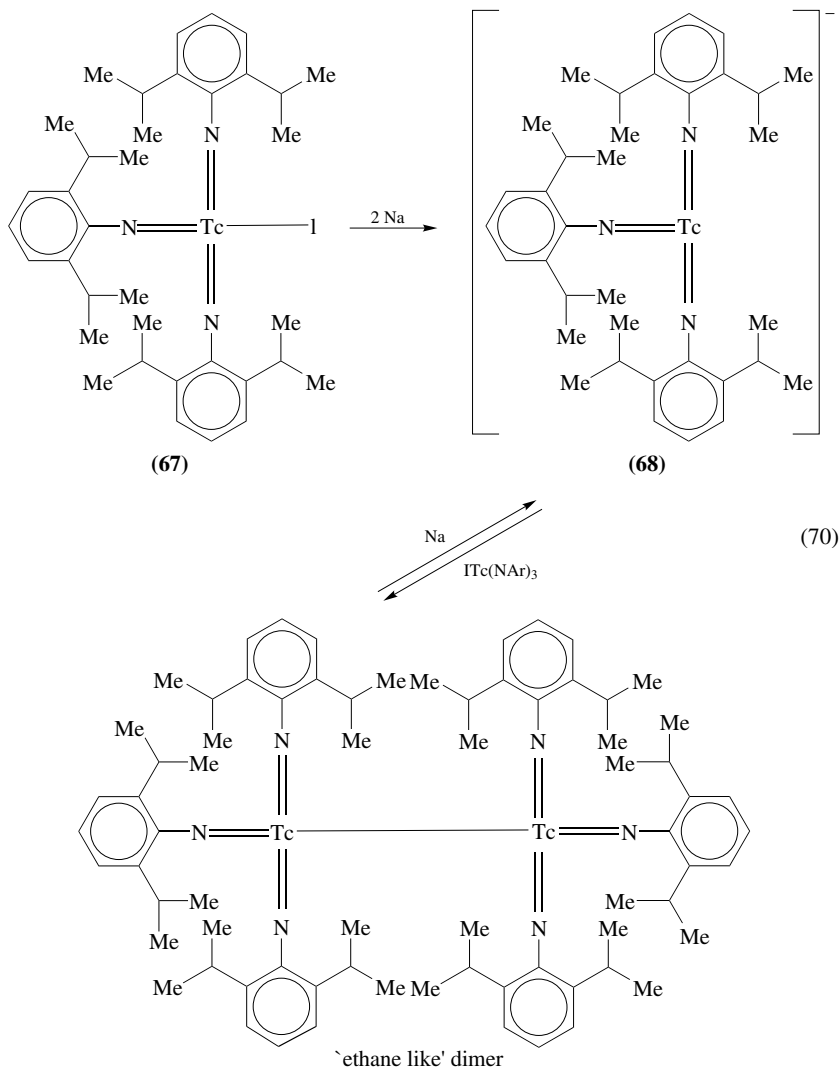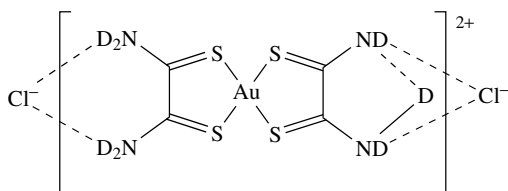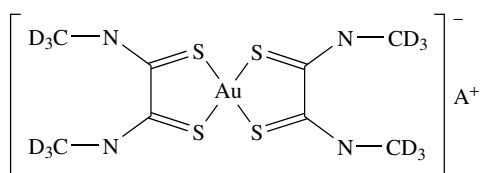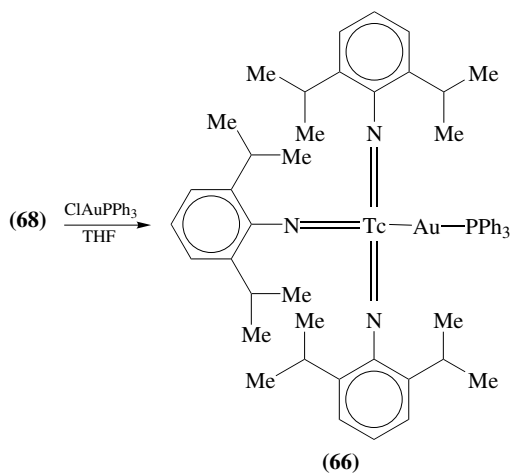
   The following IR data support the structure **69A** for the complex and support the formula A[Au(DMDTO-2H)$_2$]: absence of N−H vibrations and no bands in the 1500–1300 cm^{-1} region in the CH$_3$/CD$_3$ product. This indicates that δNH vibrations are also absent and it can be concluded that the complex is doubly deprotonated and possesses an anionic structure [Au(L)$_2$]$^-$ stabilized by an alkali counterion. A more stable bond is formed between the soft Au^{III} ion and the soft sulphur atom than between the Au^{III} ion and the hard nitrogen atom; ν AuS vibration situated around 410–370 cm^{-1}, found in Au^{III} complexes with sulphur-containing ligands, is also observed in the case of **69A** (at about 380 cm^{-1}). Only one ν(CN) and one ν(CS) is observed in the IR
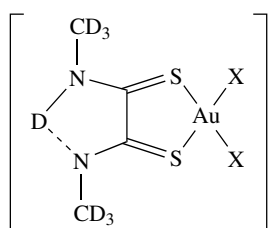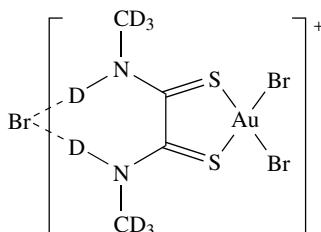
(71)   **(72)**
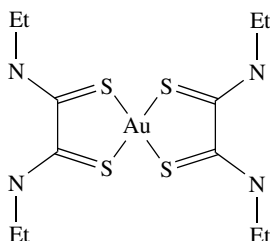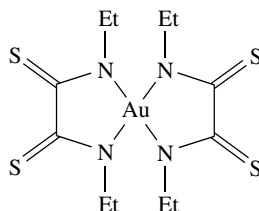
(69A)   **(69B)**
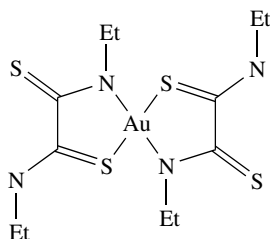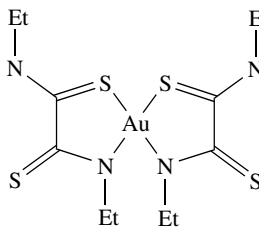
(69C)   **(69D)**

spectrum and not two (CN) and two (CS) bands, as required if structures **69C** and **69D** are present. The interionic vibration of $A^+[Au(L)_2]^-$ ion pairs shifts regularly from 500 cm^{-1} (for Li$^+$) to 180 cm^{-1} (for Na$^+$) and to 170–150 cm^{-1} (for K$^+$). The position of ν(CN) vibration is shifted upwards as the radius of the cation (Li→Na→K) increases, indicating again that the alkali ions are positioned near the nitrogen atom of the dithiooxamides. In acidic medium an intramolecular NH$\cdots$N$^{\delta-}$ hydrogen bond is present. In deuterated compounds ν(ND) is shifted to 2359 cm^{-1} and to 2342 cm^{-1}. The position of CS vibration is at 860 cm^{-1}, the ν(CC) vibration has been assigned to the band at 1112 cm^{-1}, the ν(AuS) to the bands at 399 cm^{-1} and 392 cm^{-1}, the δ (SAuS) vibration to 260 cm^{-1}, the δ(ClAuCl) vibration to 210 cm^{-1}, the δ(BrAuBr) vibration to 179 cm^{-1} and, finally, the ν_σ (NH$\cdots$N) at 120 cm^{-1} to the vibration of the intramolecular NH$\cdots$N hydrogen bond. The [Au(DMDTO-D)$_1$X$_2$] complexes therefore have structure **71** with singly deprotonated dithiooxamide in an S-*cis* conformation and *cis*-AuX$_2$ coordination around the metal atom.

The strong hydrogen bonding in **72** has been confirmed[425] by the very low ratio v NH/ND of 1.2, by the disappearance of the δNH bands at 1515 and 1475 cm^{-1} on NH/ND substitution and by S, S-coordination[420] of the ligand to Au^{III}. The v(CC) is assigned to the band at 1109 cm^{-1}, the v(CS) to the band at 874 cm^{-1} in **72**, the v(AuS) to 398 and 364 cm^{-1}, the v(AuBr) to 232 and 211 cm^{-1}, δ(SAuS) vibration to 246 cm^{-1} and v_σ(NH$\cdots$Br) to 187 cm^{-1} (this band is hardly influenced by NH/ND substitution).

The vibrational analysis of **70** has also been carried out. Strong hydrogen bonding with Cl$^-$ ions is also indicated by the low v(NH)/(ND) = 1.330 ratio. The out-of-plane vibration of the NH group (750 cm^{-1}) shifts to 599 cm^{-1} upon NH/ND substitution. Vibration v(CC) is located at 1036 cm^{-1}, v(AuS) at 416 cm^{-1} and at 345 cm^{-1}, v_σ(NH$\cdots$Cl) $\approx$200 cm^{-1}, whilst the vibration v at 146 cm^{-1} is probably the deformation mode of the NH$\cdots$Cl hydrogen bond. The above IR evidence is in agreement with S_4-coordination around Au in **70**.

8. Kinetic and deuterium labelling studies of the mechanism of decomposition of dimethyl(2,4-pentanedionato)gold^{III} in solution

Laser-induced decomposition of dimethyl(2,4-pentanedionato)gold^{III}, **73**, has been used[426,427] recently for selective formation of high quality and high purity thin gold metallic films[426−428]. An understanding of the mechanism of the thermal and photochemical decomposition of **73** is thus of scientific and practical interest.

(73)-(CH$_3$)$_2$ **(73)-(CD$_3$)$_2$**
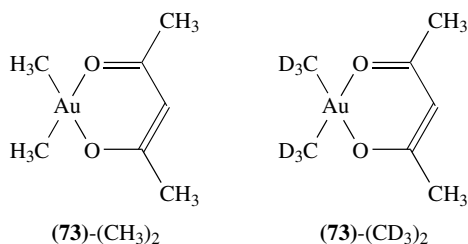
The isotopic studies of the mechanism of this reductive elimination process, involving breaking of M−C bonds followed by formation of C−C bonds, have been initiated by synthesis of (dimethyl-d$_6$)(2,4-pentanedionato)gold, **73**-(CD$_3$)$_2$, and identification of coupled reaction products produced in the pyrolytic decomposition carried out in sealed quartz NMR tubes in CD$_3$OD and C$_6$D$_{12}$ solvents.

a. The gold complex, **73**-(CD$_3$)$_2$, has been prepared following the procedure[429] elaborated for the synthesis of **73**-(CH$_3$)$_2$ using CD$_3$MgI in place of MeMgI. The methine protons of **73**-(CH$_3$)$_2$ and **73**-(CD$_3$)$_2$ rapidly exchange in CD$_3$OD, as shown by MS analysis and UV adsorbance through rapid ring opening followed by keto−enol deuteriation.

b. The decomposition of **73**-(CD$_3$)$_2$ in CD$_3$OD obeys first-order kinetics and is strongly solvent-dependent, with the rate of decomposition decreasing in the order (CF$_3$)$_2$CHOH ≫ Me$_2$CHOH > EtOH > MeOH. No decomposition of **73** was found in several nonpolar solvents including C$_6$D$_{12}$. Addition of AcOH to Me$_2$CHOH solvent accelerated the decomposition. Protonation of the pentanedione ligand was said to be the rate-determining step in the pyrolytic decomposition of **73**-(CH$_3$)$_2$ in solution.

c. The mechanism of decomposition of **73** has been investigated by observing by ^{1}H NMR the decomposition of 1 : 1, **73**-(CH$_3$)$_2$: **73**-(CD$_3$)$_2$ mixture in CD$_3$OD at 60 °C.

At 24% conversion of the substrate, the products contained 25% of C_2H_6, 7% of ethane-d_3, 61% of 2,4-pentanedione, 2% of 3-methyl-2,4-pentanedione, traces of CH_3D and 5% of unidentified products. The ethane to ethane-d_3 ratio is 3.6 : 1. In the absence of a deuterium isotope effect the statistical ratio 1 : 2 : 1 is expected for the formation of ethane-d_0, ethane-d_3 and ethane-d_6 in the case of a pure free radical mechanism. The presence of CH_3D in the products indicates that the radical abstraction of D from the solvent (equation 71), albeit small, is proceeding in the CD_3OD solution. The formation of 3-methyl-2,4-pentanedione has been suggested to proceed either via intermolecular mechanism or via radical–radical recombination. The last pathway was the best explanation of the experimental results[430]. The formation of ethane-d_3 indicates that besides the decomposition channels, shown in equations 72 and 73, leading to C_2H_6 and ethane-d_6 formation, there is a second decomposition pathway according to which methyl radicals, belonging initially to different **73** species, recombine leading to ethane-d_3 formation (equation 74). There are no ^{13}C KIE data which could distinguish the 'triangle like TS' shown in equations 72 and 73 from the TS structure for the production of free methyl radicals via homolysis of Au−CH_3 and Au−CD_3 bonds (equation 74) which diffuse from the reaction cage and react with a second free radical or with methyl groups present in solution (equations 74c and 74d). The presented[430] formation rates of ethane-d_0 and ethane-d_3 indicate clearly that recombinations of methyl groups within the reaction cage are more probable than recombinations of CH_3 and CD_3 produced by free radical decomposition of **73**-Me_2 or **73**-$(CD_3)_2$ or by decomposition of dinuclear dimeric gold intermediate species.

$$^\bullet CH_3 + ROD \longrightarrow CH_3D + RO^\bullet \qquad (71)$$

(72)

$\overset{*}{H}$ denotes D label
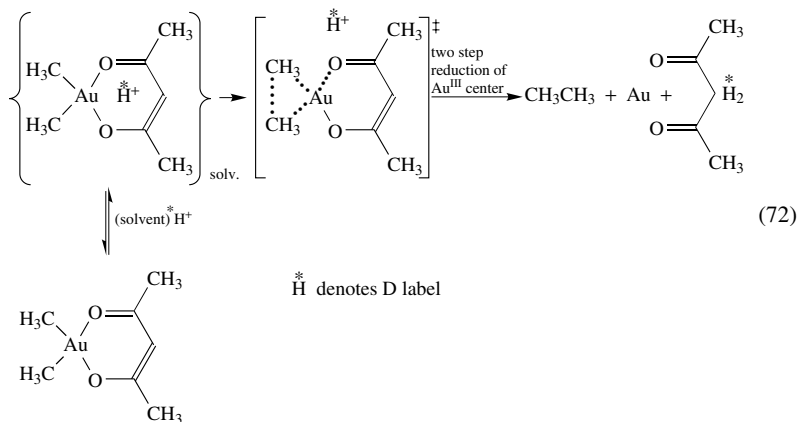
d. UV-irradiation of the 1 : 1 **73**-Me_2 : **73**-$(CD_3)_2$ mixture in CD_3OD provided ethane-d_0 (6%) and ethane-d_3 (5.5%) at roughly 16% conversion of the substrate. Ethane-d_6 could be formed either by recombination of free radicals or by decomposition of a binuclear complex in solution. Nevertheless, the nearly 1 : 1 ratio of isotopomeric ethanes, ethane-d_0 and ethane-d_3, indicates that the probability of homolysis of CH_3−Au and CD_3−Au bonds in the UV-excited electronic states of (**73**-Me_2)* and [**73**-$(CD_3)_2$]* are comparable, and the recombinations of two CH_3 or two CD_3 radicals within the reaction cage are less probable than in the pure thermal decomposition of **73** species, whilst the free $^\bullet CH_3$ and $^\bullet CD_3$ radicals diffuse from the reaction site or recombine yielding CH_3CD_3 species,

or recombine with liberated 2,4-pentanedione radical[431] or directly by a concerted mechanism in the excited state producing 3-methyl-2,4-pentanedione as a major photoproduct (28%). Photolysis of **73**-Me$_2$ and a 1 : 1 mixture of **73**-Me$_2$:**73**-(CD$_3$)$_2$ have been studied also in C$_6$D$_{12}$. Similar products as in CD$_3$OD have been produced, but in different yields. Free methyl radical formation has been stressed[432−435] as well as the differences between the pyrolytic and the photochemical decompositions of **73**.

(73)

* denotes D label
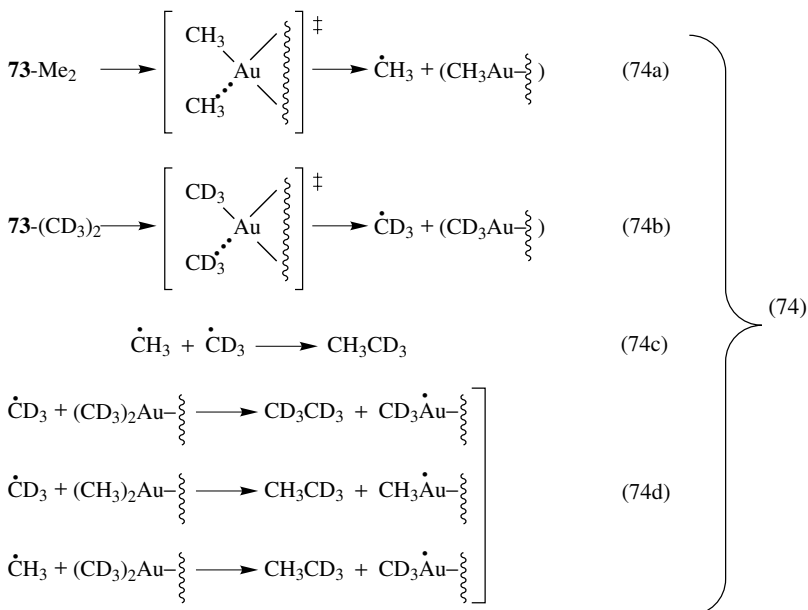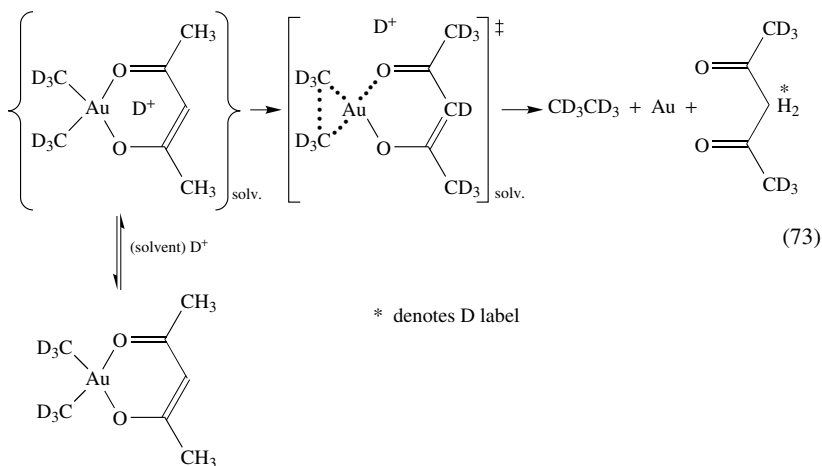
9. Deuterium studies of the cleavage of the dimeric complex [Au(CH$_2$)$_2$PPh$_2$]$_2$

The addition and elimination reactions of the first dimeric Au^I complex, [Au(CH$_2$)$_2$PPh$_2$]$_2$, **74**, synthesized by Schmidbauer[436,437] with halogens, alkyl halides, peroxides, disulphides and other reagents[438−449], have been extensively studied[450,451] recently. A mechanistic study of the reaction (equation 75) with DCl has also been performed[450]. The first fast step in reaction 75 was carried out in toluene at 80 °C for 3 h taking the reagents in a 2 : 1, DCl : **74**, ratio to avoid the subsequent much slower reaction which generates the fully cleaved and protonated salt, **75**. The X-ray diffraction, NMR spectrum and IR spectrum of intermediate **76** have been taken. The halogen, *trans* to methylene in **76**, reduces the shielding effect of gold upon methylene. The strong band at 290 cm^{-1} in **76** has been attributed to Au−Cl by analogy[439,440,452,453] to bands in Ph$_3$PAuCl (a force constant of 2.07 mdyn Å^{-1} for Au−Cl was taken from earlier works[454,455]). It has been suggested[450] that the initial attack of DCl on **74** gives the intermediate **77**.

$$D_2O(99.96\%) + PCl_5 \longrightarrow DCl + POCl_3$$

$$2[Ph_2(CH_2D)_2P^+][AuX_2^-] \tag{75}$$

(75)
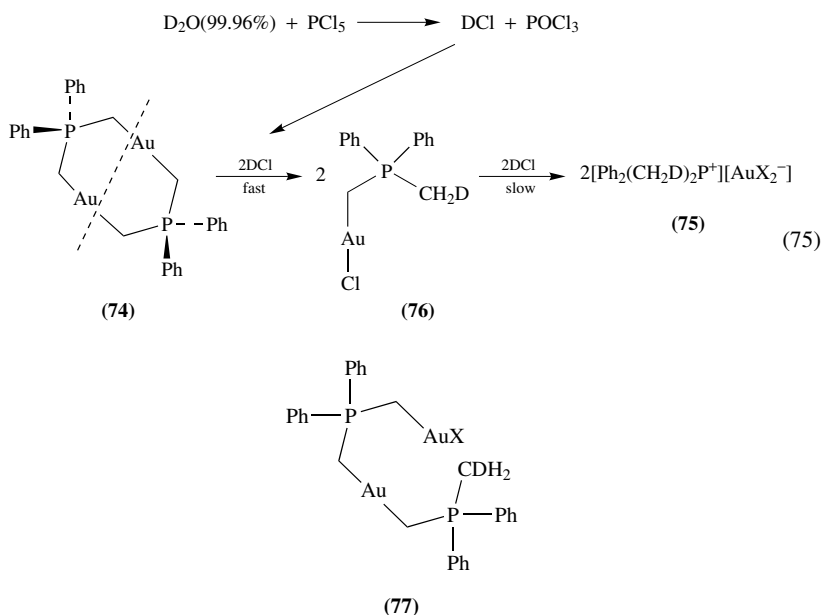
X-ray study of the structure of the crystal Br$_3$Au[μ-(CH$_2$)$_2$PPh$_2$]AuBr$_2$(CH$_2$PPh$_2$CH$_2$Br)·CDCl$_3$, **78**, obtained by evaporation of a CDCl$_3$ solution of the complex [Au(CH$_2$)$_2$PPh$_2$]$_2$Br$_4$, **79** (produced by addition of Br$_2$ to **74**), showed that the interstitial molecule of CDCl$_3$ is located at a position of no chemical importance[451].

10. ^{197}Au Mössbauer study of chlorogold derivatives of nitrogen-containing heterocycles

N-donor ligands have been considered suitable for modern chrysotherapy[393,456−458]. Since lack of suitable crystals is frequent in the field of gold chemistry ^{197}Au Mössbauer

spectroscopy[459] has been used for elucidating the structure and bonding of gold compounds in the solid state[460−462] needed to establish the 'structure biological activity' relationship for gold compounds applied in medical practice. Thus the co-ordinating behaviour of ligands **80** and **81** towards Au^{III} and Au^{I} have been investigated[463] by taking the Mössbauer spectra at 4.2 K of their complexes with Au^{III} and Au^{I} and calculating the ^{197}Au Mössbauer parameters such as isomer shift (IS), quadrupole splitting (QS) and line-width (LW) as well as the estimated percentage of the gold site, A. Two sites of types AuNCl$_3$ and [AuCl$_4$$^-$][HNR$^+$], or AuNCl and [AuCl$_2$$^-$][HNR$^+$], where N denotes the 3-nitrogen atom of the imidazole- or benzoxazole-type ligands, R, have been evidenced. Their ratio is governed by electronic and steric effects.
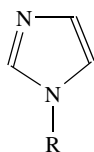
(80)-Im (N-alkylimidazole-type ligands)

N- methylimidazole; R = Me
N- ethylimidazole: R = Et
N- propylimidazole; R = Pr
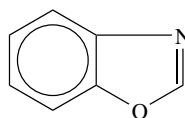
(81)-BO

(benzoxazole-type ligands)
2-methylbenzoxazole
2,5-dimethylbezoxazole

For example, the Mössbauer parameters for some samples are listed in Table 8[463]. The linear correlations QS = −0.22 + 1.74 IS (for Au^{III}) and QS = 5.05 + 1.06 IS (for Au^{I} compounds) have been deduced. The introduction of a hydrogen-bonded gold site into already existing structure should improve the interpretations of the Mössbauer spectra reported, for instance, for some chlorogold nucleosides[464]. A detailed discussion of the measured IS, QS and A values has been given. The relative area of the hydrogen-bonded site is larger in the presence of less hindered ligands {A = 54 for [AuCl$_4$$^-$][H-(N-MeIm)]} and decreases for more hindered ligands {A = 8 for [AuCl$_4$$^-$][H-(N-PrIm)$^+$]}. The given spectrum of Au(2,5-diMeBO)Cl$_3$, exhibiting one electric quadrupole interaction, has Mössbauer spectral parameters (IS = 1.39, QS = 2.14, LW = 1.99, A = 100) which are comparable[465] with those of C$_5$H$_5$NAuCl$_3$ (IS = 1.45 mm s^{-1}) and (C$_5$H$_5$)$_2$N$_2$AuCl$_3$ (QS = 2.22 mm s^{-1}). This suggests a similar stereochemistry (a more or less distorted square-planar site for AuNCl$_3$). The parameters of quadrupole splitting for a sample typical of linearly co-ordinated Au^{I} are in agreement with IR and ^{1}H NMR measurements and with theoretical predictions[463].

TABLE 8.   Mössbauer parameters

Site	IS (mm s^{-1})^a	QS (mm s^{-1})	LW (mm s^{-1})	A
Au(N-PrIm)Cl$_3$	1.40	2.20	2.13	75
[AuCl$_4$$^-$][H-(N-PrIm)$^+$]	0.85	1.20	2.11	8
Metallic gold	−1.25	0.00	2.10	17
Au(N-PrIm)Cl	1.97	7.58	1.96	58
[AuCl$_2$$^-$][H-(N-PrIm)$^+$]	0.22	5.79	2.05	42

^{a}The shifts are relative to Au(Pt); 1.25 mm s^{-1} must be added to refer these shifts to metallic gold.

11. Deuterium study of the surface reaction between pyrazine molecular ions and perdeuteriated hexadecanethiol covalently bound to gold film

The reaction shown in equation 76 has been observed by MS when pyrazine molecular ions, m/z 80, are scattered from the self-assembled monolayer[466–468] of perdeuteriated hexadecanethiol covalently bound to a gold film supported on a titanium layer on the silicon substrate[469]. The adduct ions appeared at m/z 82 (corresponding to deuteriated pyrazine ion) and m/z 98 (corresponding to d$_3$-methylated pyrazine ion). The loss of DCN from deuteriated pyrazine ions and HCN from pyrazine ions ($M^{•+}$) was detected. The ion/surface reactive collisions can provide information on the nature of the organic functional groups present at an interface. The product ions resulting when mass-selected $CD_3CD_2OD^{•+}$ (m/z 52) collides with a gold surface or with an ethanethiol/gold surface, both at a collision energy of 60 eV, have also been detected and discussed[470].

$$ (76) $$
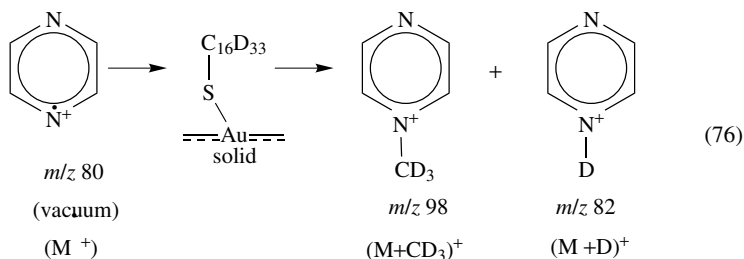
12. Spectroscopic properties of the $^1\Sigma^+$ ground state of $^{197}Au^{37}Cl$

The experimental vibrational harmonic frequencies ω_e for $^{197}Au^{35}Cl$ (and $^{197}Au^{37}Cl$ equal to 382.8 cm^{-1} (and 373.9 cm^{-1}, respectively) and anharmonicity constants $\omega_e\chi_e$ for the same pair of isotopomers equal to 1.30 cm^{-1} (and 1.21 cm^{-1}) have been found to be in good agreement with those calculated by the coupled cluster procedure theory QCISD(T)[471], which gives ω_e values of 369.5 cm^{-1} (and 360.9 cm^{-1}) and $\omega_e\chi_e$ values of 1.32 cm^{-1} (and 1.26 cm^{-1}), respectively, for $^{197}Au^{35}Cl$ (and $^{197}Au^{37}Cl$) isotopomers. The estimated[472,473] dissociation energy of 3.0 ± 0.7 eV and the value of 2.85 estimated at the QCISD level[471] indicate that the AuCl dissociation energy should be below 3.5 eV and that the experimentally obtained value[474] of 3.5 ± 0.1 eV is probably overestimated by about 0.5 eV. The vibrational-state dependencies of the molecular properties for $^{197}Au^{37}Cl$ have been established (equations 77–79):

distance : $\qquad\qquad\qquad r_n = 2.2515 + 0.0070n$ (Å) $\qquad\qquad$ (77)

dipole moment : $\qquad\qquad \mu_n = 4.0609 + 0.01888n$ (Debye) $\qquad$ (78)

dipole polarizability : $\qquad \alpha_n^{II} = 64.2415 + 0.446n + 0.0049n^2$ (au) $\quad$ (79a)

$\qquad\qquad\qquad\qquad\qquad \alpha_n^{\perp} = 37.6745 + 0.0310n + 0.0004n^2$ (au) $\quad$ (79b)

where n is the vibrational quantum number (for the $J \equiv 0$ rotation state). For the force constant $k_e = 2.375$ mdyn Å^{-1}, the vertical ionization potentials $^1\Sigma^+(AuCl) \rightarrow{}^2\Sigma^+(AuCl^+)$, IP$_v = 12.522$ eV, and the distance-dependent vibrational–rotational averaged[475,476] molecular properties, $P_{n,J} = <\Psi_{nJ}|P(r)|\Psi_{nJ}>$ for $n = J = 0$, $< r > =$

2.251 Å, $< \mu_e >= 4.061$ (Debye), $< \alpha_n^{II} >= 64.24$ (au) and $< \alpha_n^{\perp} >= 37.67$ (au), have been calculated and presented. The calculated Morse potential curves[477] for $^1\Sigma^+$(AuCl) have been presented also, and all Dunham parameters for the $^1\Sigma^+$ ground state of AuCl, ω_e (cm^{-1}), $\omega_e\chi_e$ (cm^{-1}), $\omega_e Y_e$ (10^{-3} cm^{-1}), B_e (cm^{-1}), centrifugal distortion constant D_e (10^{-7} cm^{-1}) and vibration–rotation coupling constants α_e (cm^{-1}), have been calculated on various [HF, MP2, MP3, MP4, QCISD and QCISD(T)] levels of theory (including relativistic effects) and presented[471].

13. The effect on dose of backscatter from gold

Radionuclide ^{125}I seeds backed by gold shield are used in brachytherapy treatment of opthalmic tumours. The effects of lead, silver and gold have been studied[478] since one of the protocols[479] of dose calculation calls for ignoring the effect of backscatter from the gold shield. The response of the two *p*-type silicon diodes has been measured at several distances from the seed with and without the high-*Z* backing relative to water and has been found to be the same for each diode, and the same for lead and gold. It decreased[479,480] from about 1.01 at 1.5 mm to about 0.92 at 20 mm. It has been demonstrated also that the contribution of 10-keV X-rays (induced L-shell fluorescence from gold) to the dose is negligible. The silver backing relative to water has been found to enhance the diode response by about 14% between 5 to 10 mm from the seed. The slight discrepancies between the present and earlier[480] results are discussed[478].

14. Homogeneous catalysis of $H_2 - D_2$ equilibration by Pt–Au phosphine stabilized cluster compounds

The homogeneous $H_2 - D_2$ equilibration, catalyzed by [Pt(AuPPh$_3$)$_8$](NO$_3$)$_2$ **82**, and other phosphine-stabilized platinum–gold cluster compounds, has been found[481] to be (equation 80) a convenient probe for studies of the activation of H_2, important in many industrial catalytic processes. The catalysis of the equilibration (equation 80) by **82** proceeds without any H/D exchange with solvent, water or ethanol. Olefins (1-hexene, ethylene, *c*-hexene) or nitrobenzene are not hydrogenated by **82**. No deuterium incorporation into the PPh$_3$ ligands has been observed, although such hydrogen exchange were reported for many monometallic systems[482−489] (equation 81).

$$H_2 + D_2 = 2HD; \qquad K = \frac{[HD]^2}{[H_2][D_2]} \tag{80}$$

$$(81)$$
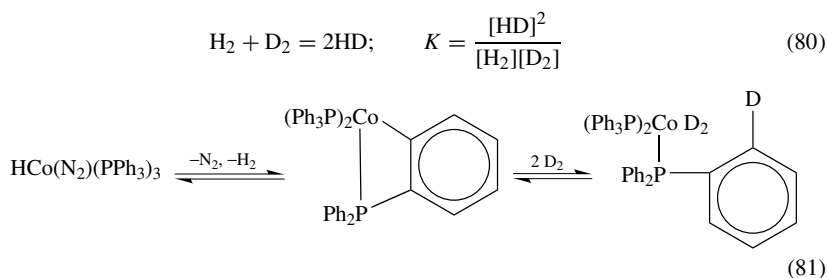
(*o*-C——H bonds add to a coordinately unsaturated' cobalt complex)

The above observations provide good evidence for the homogeneous nature of the H_2/D_2 equilibration in the presence of **82**, since the presence of heterogeneous platinum impurities would cause these reactions to occur[490−497]. Reaction 80 catalyzed by

82 results from H_2 and D_2 activation at the metal core of the cluster. Production of HD involves the addition of two molecules, H_2 and D_2, to the same cluster without heterolytic cleavage of H_2. Gold clusters are inactive for H_2–D_2 equilibration. The reaction is first order in cluster concentration. PPh_3 ligands shield the cluster cores and collisions between two clusters are not important. The H_2–D_2 experiments have been carried out by measuring the percentage of H_2, D_2 and HD as a function of time by gas chromatography. The percentage of H_2 and D_2 decreased at the same rate. It has been assumed[498−501] that within 2–3% there are no H/D isotope effects, neither on gas solubility nor on the thermodynamics and kinetics of reaction 80. The $[MH_2]/[M]$ ratio for reaction 80 with H_2 and D_2 studied by ^{31}P NMR (for nitrobenzene solvent, 0.5 atm and 6 °C), M = **82**, was found to be the same within ±5% experimental error. The k_{obs} values for catalytic H_2–D_2 equilibration (nitrobenzene/solvent, 1 atm, 30 °C) with 10 : 90 and 90 : 10 initial gas mixtures were found to be also the same, again within ±5% experimental error. The isotopic reaction 80 belongs to the best studied hydrogen exchange reactions, both experimentally and theoretically, in the older isotope literature[502]. The values of the equilibrium constant K (equation 80) calculated with the theoretically derived expression 82a, or the simpler expression 82b, reproduce well the experimental equilibrium constants K_{exp} (given in parentheses).

$$K = 4 \cdot 1.06 e^{-78/T} \tag{82a}$$

$$K = 4 e^{-79.1/T} \tag{82b}$$

T (K)	195	273	298	383
K	2.84(2.92 ± 0.08)	3.18 (3.24 ± 0.08)	3.26 (3.28)	3.46 (3.50 ± 0.06)

With rising temperature, K gradually approaches the value 4: at 741 K, $K = 3.87$ (3.70 ± 0.12); at 2000 K, $K = 3.97$.

The rate constants for HD productions (k_{obs}) have been determined by plotting equation 83:

$$k_{obs}t = \ln \frac{[HD]_e}{[HD]_e - [HD]_t} \tag{83}$$

where $[HD]_e$ and $[HD]_t$ are the mole fractions of HD at equilibrium and at time t, respectively. Concentration $[HD]_e$ has been calculated from the initial H_2 and D_2 concentrations taking[503] $K_{eq} = 3.28$ at 30 °C for equation 80. The turnover rates, defined as the rate of HD production divided by the number of moles of the cluster in the reactor and expressed as units $\{[\text{mol of HD produced}] [\text{mol of cluster}]^{-1} s^{-1}\}$, were determined with ±5 precision, and found to be equal[504] (at 30 °C) to 36×10^{-2} in acetonitrile, 15×10^{-2} acetonitrile/nitrobenzene 1 : 1 v/v and 7.5×10^{-2} in nitrobenzene solvent. The deuterium exchange kinetic data have been interpreted in terms of the consecutive reversible steps shown in equation 84:

$$M \underset{-(H,D)_2}{\overset{+(H,D)_2}{\rightleftharpoons}} M(H,D)_2 \underset{+PPh_3}{\overset{-PPh_3}{\rightleftharpoons}} M^*(H,D)_2 \underset{-(H,D)_2}{\overset{+(H,D)_2}{\rightleftharpoons}} M^*(H,D)_4 \tag{84}$$
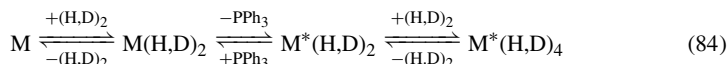
where M = $[Pt(AuPPh_3)_8](NO_3)_2$, **82**; (H, D) represents H_2, D_2 or HD, and M^* represents M minus one PPh_3.

The rate of the first step, the reversible addition of H_2 or D_2 to M directly observed by NMR, has been found to be 10^3 times faster than the observed rate of HD production, thus it is not rate determining. The second also denotes a reversible fast dissociation of a PPh_3 ligand and formation of a coordinatively unsaturated species M* which may accept a second $(H, D)_2$ molecule in the rate-limiting third step giving the 20-electron, tetrahydrido intermediate or activated complex[504]. The phosphine-stabilized clusters have deep and narrow hydrophobic channels leading into the metal core, preventing binding of large substrates and protecting the core from poisoning.

These studies of reaction 80 are of great interest for catalytic sciences, which try to understand how gold affects the reactivity of supported bimetallic catalysts[505−521].

15. IR reflectance−absorption spectra (IRRAS) of Langmuir−Blodgett stearic acid and deuteriated stearic acid monolayers on gold and aluminium

The IRRAS spectra of monolayers of $CH_3(CH_2)_{16}COOH$ and $CD_3(CD_2)_{16}COOH$ deposited on polycrystalline gold and native-oxide aluminium films have been recorded and analysed[522]. On aluminium, the acid molecules form a metal carboxylate structure characterized by peaks at 1590 and 1475 cm^{-1} assigned to asymmetric and symmetric vibrations of carboxylate groups tilted with respect to the surface (**83a**) so as to accommodate a nearly perpendicular orientation of the alkyl chain[523]. The observed peak at 1425 cm^{-1} is assigned to the symmetric stretch of a COO^- group in which the carboxylate oxygens are in a bidentate[524−526] configuration with respect to the surface (**83b**).
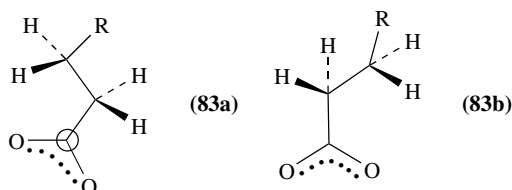
In the deuteriated acid spectrum, the vibrations associated with the carboxylate group are shifted to lower frequencies by several wavenumbers (1590 → 1575 cm^{-1}, 1475 → 1470 cm^{-1}). The presence of the small 1700 cm^{-1} band in the spectrum, assigned to the C=O stretch, indicates that the acid is not fully deprotonated[527,528]. Both the free acid and the carboxylate are present on gold [the carbonyl peak at 1795 cm^{-1} is found in both the deuteriated and the undeuteriated acid, the asymmetric carboxylate stretch is located at 1555 cm^{-1} ($C_{17}H_{35}COOH$) and at 1550 cm^{-1} ($C_{17}D_{35}COOH$)]. In the deuteriated acid spectrum, the two strong symmetric carboxylate stretches located at 1435 cm^{-1} and 1380 cm^{-1} are shifted to lower energies by 30 cm^{-1}. They indicate that on the gold surface the carboxylate is symmetrically bonded to the substrate and the alkyl chains are tilted with respect to the surface. As the film ages, changes of the IR spectra indicate that on aluminium the molecules realign to a more perpendicular orientation, while on gold they tend to aggregate into a three-dimensional crystal (where the acid molecules exist as hydrogen-bonded dimers and the methylene chains are packed in an orthorhombic structure), since the attractive energy[529] of the van der Waals interactions is about 8.4 $kcal\,mol^{-1}$, i.e. higher than the physisorption bonding energy which is equal to 2.5 $kcal\,mol^{-1}$. Thus IRRAS is of value in examining the orientation and surface bonding of organic films adsorbed on metal surfaces.

B. Radiochemical and Isotope Studies Related to Chrysotherapy

1. Production of radiotracers of high specific activity

a. Production of gold-199 via irradiation of platinum target of natural isotopic composition[530]. Non-carrier-added (NCA) ^{199}Au has been produced via the nuclear reaction 85. Neutron irradiation of Pt powder provided NCA ^{199}Au of 99.99% radionuclidic purity. After purification of ^{199}Au from inactive Sn impurities, the final radiochemical yield was greater than 98%.

$$^{198}_{78}\text{Pt}(n,\gamma)^{199}_{78}\text{Pt} \xrightarrow[\text{T}_{1/2} = 30.8 \text{ min}]{(\beta^-_{\max} = 1.69 \text{ MeV}, <\beta^-> = 514 \text{ keV})} {}^{199}_{79}\text{Au}(<\beta^-> = 87 \text{ keV},$$

$$T_{1/2} = 3.319 \text{ d}) \qquad (85)$$
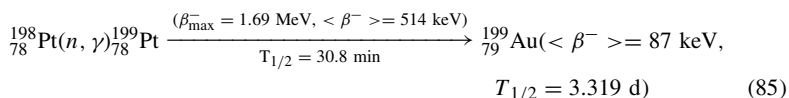
b. Synthesis of $^{195g,m}Hg$ and $^{197g,m}Hg$. These radioisotopes of mercury with specific activity of 0.9 and 1.4 GBq µg^{-1} have been obtained via (p, n) and (p, 3n) nuclear reactions by irradiating[531] ^{197}Au foils with cyclotron protons of $18 \rightarrow 7$ MeV and $33 \rightarrow 18$ MeV energy, respectively. The radiomercury has been recovered[532] from gold sheets by distillation at $700–800\,°C$ in 99% yield. No radionuclidic contaminants are present in ^{197g,m}Hg samples but ^{195g,m}Hg always contained a few percents of ^{197g,m}Hg. These radiotracers are needed to study the toxicology of trace elements on human health at low level exposure (LLE) and to study the incorporation of inorganic and methyl-Hg into metallothioneines in rats[530].

2. Synthesis of ^{199}Au- and ^{35}S-labelled myocrisin (GST, **84**) and auranofin (AF, **85**) and their distribution and kinetic studies in rats

The title antiarthritic agents, **84** and **85** are thiolate derivatives of gold[533,534], AuSR, with different solubility characteristics, as well as different chemical and toxic properties[535−539] and also different retentions of gold[537−540]. They have been synthesized[541] to obtain detailed distribution data both for the ^{199}Au−metal and for the [^{35}S]ligands and to study the biochemistry of these drugs[537−554].

(84) [^{35}S]GST or [^{199}Au]GST   **(85)** [^{35}S]AF or [^{199}Au]AF

*a. Synthesis of [^{199}Au]disodium[mercaptosuccinato(3-)S]aurate^I, **84**, and [^{199}Au](2,3,4, 6-tetra-O-acetyl-1-thio-β-D-glucopyranosato-S)(triethylphosphine)gold^I, **85**

a.i. ^{199}Au has been obtained by irradiating a platinum sponge of natural isotopic composition with a reactor neutron flux. After treatment with thiomalic acid and purification, the labelled drug **84** was obtained and, after isotopic dilution with unlabelled **84**, was ready for injection (equation 86).

$$H^{199}AuCl_4 \xrightarrow[\text{2. aq. HCl}]{\text{1. aq. NaCN}} H^{199}Au(CN)_4 \xrightarrow[\text{-cyanogen}]{110\,^{\circ}C} {}^{199}AuCN \xrightarrow{H_3STm} H^{199}AuSTm$$

$$\text{(EtOAc)} \qquad\qquad \text{(EtOAc)}$$

$$\xrightarrow{\text{aq. NaOH}} Na_2{}^{199}AuSTm \qquad\qquad (70\% \text{ purified yield}) \qquad\qquad (86)$$

$$\textbf{(84)} \qquad\qquad H_3STm = \text{thiomalic acid}$$

a.ii. [^{199}Au]auranofin, **85**, has been synthesized[541] according to the improved procedure[555,556] presented in equation 87.

$$H^{199}AuCl_4 \xrightarrow[\text{2. Et}_3\text{P}]{\text{1. (HOCH}_2\text{CH}_2)_2\text{S, (tdg)}} Et_3P^{199}AuCl \xrightarrow[0\,^{\circ}C\ 4\ h,\ dark]{\text{AgOAc/EtOH}} Et_3P^{199}AuOAc$$

$$\text{(aq. solution)} \qquad\qquad \text{(EtOH)}$$

$$\xrightarrow[0\,^{\circ}C,\ 1\ h]{\text{HSatg/water}} Et_3P\ {}^{199}AuSatg \qquad\qquad (87)$$

$$\textbf{(85)}$$

$$HS_{atg} = \text{tetraacetylthioglucose} \qquad\qquad >74\% \text{ overall crude yield}$$
$$\text{tdg} = \text{thiodiglycol} \qquad\qquad (66\% \text{ yield after purification})$$

b.i. Synthesis of [^{35}S]GST has been carried out as shown by equation 88.

$$\overset{\text{Br}}{\underset{\hphantom{x}}{|}}$$
$$\text{HOOCCH}_2\text{CHCOOH} \xrightarrow{[^{35}\text{S}]\text{Na}_2\text{S}} \text{NaOOCCH}_2\overset{^{35}\text{SNa}}{\underset{}{\text{CHCOONa}}}$$

$$\Big\downarrow \text{H}_2\text{SO}_4$$

$$(88)$$

$$\text{HOOCCH}_2\overset{^{35}\text{SAu}}{\underset{}{\text{CHCOOH}}} \xleftarrow{\text{AuCN}} \text{HOOCCH}_2\overset{^{35}\text{SH}}{\underset{}{\text{CHCOOH}}}$$

$$\Big\downarrow \substack{\text{1. isotope dilution} \\ \text{2. NaOH to pH 5.1}} \longrightarrow [^{35}\text{S}]\text{GST}, \ \textbf{84}$$

b.ii. The [^{35}S]AF, **85**, has been synthesized[541] from triethylphosphinegold acetate with [^{35}S]thioglucose as described previously[555].

c. Kinetic, biodistribution and biochemical studies with ^{35}*S- and* ^{199}*Au-labelled* **84** *and* **85**. The distribution of sulphur-35 and gold-199 in blood, skin, bone, joints and in all major organs of rats has been monitored over 7 days following the administration of a single dose of [^{199}Au or ^{35}S] gold sodium thiomalate, **84**, or triethylphosphinegold tetraacetylthioglucose, **85**. 168 hours after administration the largest percentage of the initial dose of ^{199}Au per gram was found in the kidney (12 ± 9% for GST and 6.6 ± 0.7% for AF). The amounts of sulphur in every organ are considerably less than those of

gold. This indicates that the cleavage of the Au−S bond takes place early in the metabolic process (probably in the stomach, intestine or in the blood stream), but the different rates of clearance of **84**- and **85**-gold from the blood indicate that at least part of the injected gold is present in different chemical forms for the **84** and **85** drugs and at least some of the administered gold retains the original ligands or their metabolites long enough to affect their biochemistry. The rapid and practically complete elimination of the ^{35}S-label suggests that the thiolate parts of the drugs are not responsible for the therapeutic action and the gold is the active component of the drugs. The unmetabolized AF does not pass through the intestinal wall[557]. Gold which passed this wall has been found to be in the deacylated form, Et$_3$PAuSR′ (HSR′ = 1-thio-β-D-glucopyranose). AF could be reformed by the addition of 2,3,4,6-tetra-O-acetyl-1-thio-β-D-glucopyranose to the metabolite mixture. *In vitro* experiments[558,559] showed that GST and AF react with albumin forming the *AlbSAuSTm* complex (S*Tm* = disodium thiomalate). *In vivo* the thiomalate ligand would probably be displaced from the complex by reaction with endogenous thiols (for instance, forming *AlbSAuSR″* with glutathione). Experiments with drug **85** labelled with ^{32}P showed that the ^{32}P label has a similar kinetic behaviour[550] to ^{35}S. In kidney, gold forms complexes with metallothionein by displacing zinc and cadmium[560−562]. The gold levels in the joints are 2−3 times higher than in the surrounding bone[563]. The therapeutic gold reaches the area of the affected tissue in rheumatoid arthritis and is retained there.

3. Complexes of gold^I with imidazoline-2-thione (Imt), with 1,3-diazinane-2-thione (Diaz) and with their N-substituted derivatives

Addition of *Imt*-type ligands to AuCl$_2{}^-$, obtained by reduction[564] of AuCl$_4{}^-$ with SO$_2$ resulted in the formation of the linear complexes of the type [L^1−Au−X], but addition of *Diaz* to AuCl$_2{}^-$ afforded a [L$_2^2$Au$_3$X$_2$]-type multinuclear complex (X = halide) instead of the [(*Diaz*)AuX] type complex[390]. Additions of excesses of ligands (*Imt, Diaz* and their N^1, N^2-derivatives) to suspensions of NH$_4$Au(SCN)$_4$ in methanol provided[390] complexes of the types L−Au^I−SCN (L = *Imt* and its derivatives) and L$_2^2$−Au^{I}SCN (where L^2 is *Diaz* and its derivatives).

(86) *Imt*   **(87)** *Diaz*
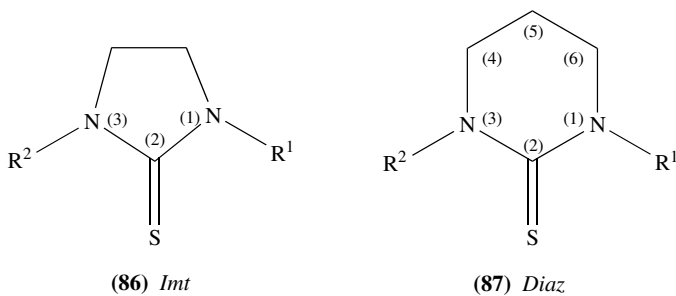
The following complexes have been obtained and characterized by elemental analysis, IR and ^{13}C NMR spectroscopy: [(*Imt*)AuSCN], [(Me*Imt*)AuSCN], [(Et*Imt*)AuSCN], [(Pr*Imt*)AuSCN], [(*i*-Pr*Imt*)AuSCN], [(Me$_2$*Imt*)AuSCN], [(*Diaz*)$_2$AuSCN], [(*Diaz*)$_2$AuCl], [(*Diaz*)$_2$AuBr] and [(Et*Diaz*)$_2$AuSCN]. These studies have been undertaken to understand the nature of complexes generated *in vivo* in reactions of AuSCN or Au(SCN)$_2{}^-$ with thiols (hemoglobin, glutathione) or with thione (ergothionine). Hydrogen

cyanide present in the blood of tobacco smokers[565] (at concentrations of 1600 ppm) binds in the absence of gold to *met*-hemoglobin or is irreversibly oxidized to thiocyanate[566], which in turn reacts with gold^I to form AuSCN or Au(SCN)$_2{}^-$. The gold^I thiolates, AuSR, are the commonly used antiarthritic gold complexes[567−569]. In IR spectra the shift of ν(S−C≡N) from 2130 to 2045 cm^{-1} was taken as evidence that −SCN is bonded[570] to Au^I in [(*Imt*)AuSCN]. The absorption at 321–350 cm^{-1} has been assigned[571] to the Au−S vibration. The low field shift of the ν(C=S) adsorption by about 30 cm^{-1} served also as an indication that Au^I is bonded to the ligand via the thione group[571−574]. The ^{13}C$_{(2)}$ NMR resonance of all the ligands has been high-field-shifted, the most after complexing with gold^I, due to back-donation of electrons from thione to Au^I, which is shielded after complexing with Au^I. The shielding of the C$_{(2)}$ resonance is greater for the linear system than for the three-coordinated system. In the [(*Imt*)AuSNC] complex the chemical shift difference between free and bound C$_{(2)}$ resonance is $185.04 - 175.47 = 9.57$ ppm relative to TMS, whereas in the [(*Diaz*)$_2$AuSCN] system this difference equals[575] $177.62 - 168.67 = 8.95$ ppm, relative to TMS.

4. Formation and disproportionation of thioglucose−gold^I −^{13}CN$^-$ complex

Gold^I thiolate complexes, **88**, are widely used in the treatment of rheumatoid arthritis[393,569,576]. These complexes have AuS$_2$ coordination environments and form oligomers[392,395,577−584] (AuSR)$_n$.

(88)
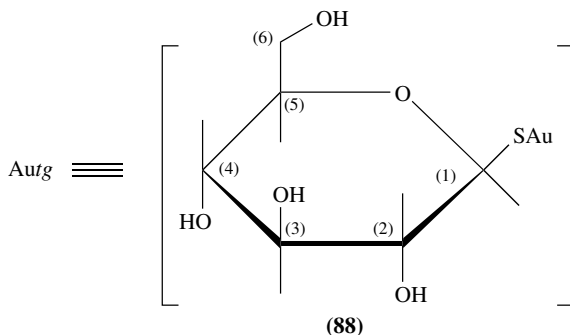
Chrysotherapy patients smoking cigarettes accumulate gold from injectable gold drugs in their red blood cells[398,585,586]. This observation initiated a series of NMR studies of reactions of gold^I thiolate complexes with isotopically labelled cyanides. The ^{13}C NMR study of the reaction of aurothioglucose (Au*tg*) with ^{13}CN$^-$ (30% ^{13}C enriched) permitted one to observe the *tg*−Au−^{13}CN$^-$ species. When the Au*tg*−^{13}CN$^-$ ratio reached 1 : 2, the Au(^{13}CN$^-$)$_2$ product was detected only. The observation of only one resonance in the NMR spectra in the course of titration of Au*tg* with ^{13}CN$^-$ is the result of fast ligand exchanges shown in equations 89−92.

$$\text{Au}tg + \text{H}^*\text{CN} \rightleftharpoons tg\text{−Au−}^*\text{CN}^- + \text{H}^+ \tag{89}$$

$$tg\text{−Au−}^*\text{CN}^- + \text{H}^*\text{CN} \rightleftharpoons \text{Au}(^*\text{CN})_2{}^- + \text{H}tg \tag{90}$$

$$\text{Au}tg + \text{H}tg \Longleftrightarrow \text{Au}(tg)_2{}^- + \text{H}^+ \tag{91}$$

$$2\text{Au}(tg{-}\text{Au}{-}{}^*\text{CN})^- \Longleftrightarrow \text{Au}({}^*\text{CN})_2{}^- + \text{Au}(tg)_2{}^- \tag{92}$$
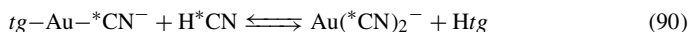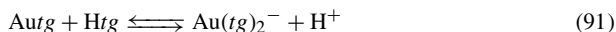
The disproportionation of asymmetric gold$^\text{I}$CN$^-$ complexes (for instance, of Et$_3$PAuCN which is a linear molecule in the solid state but disproportionates in solution as shown in equations 93a and 93b) is a known phenomenon[405,587].

$$2\text{Et}_3\text{PAuCN} \Longleftrightarrow (\text{Et}_3\text{P})_2\text{Au}^+ + \text{Au}(\text{CN})_2{}^- \tag{93a}$$

$$2\text{R}_3\text{PAuCN} \Longleftrightarrow (\text{R}_3\text{P})_2\text{Au}^+ + \text{Au}(\text{CN})_2^- \tag{93b}$$
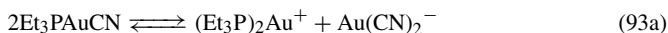
where R = Me, Et, Pr, *i*-Pr etc.

In the absence of HCN in the blood of a patient the drug Au*Tm* (gold$^\text{I}$-thiomalate) reacts with *Alb*SH to form[588,589] *AlbS*−Au$^\text{I}$−*Tm*. In the presence of HCN which accumulates in the blood of smokers, the *tg*−Au−CN$^-$ species are formed and disproportionate to Au(CN)$_2{}^-$, changing the metabolism of gold drugs and causing a sequence of toxic reactions[404].

5. ^{15}N NMR studies of the binding of C^{15}N$^-$ with gold^I drugs

Gold$^\text{I}$ complexes such as gold$^\text{I}$-thiomalate (Au*tm*) and gold$^\text{I}$-thioglucose (Au*tg*), used for treatment of rheumatoid arthritis[392,393,395,569,576,577,590], localize in intracellular organelles[591,592]. The mechanism of the cellular uptake of these complexes and of their interactions has been studied with labelled ^{13}CN$^-$ by ^{13}C NMR spectroscopy[404,593,594]. It has been shown that ^{13}CN$^-$ binds to Au$^\text{I}$, releasing thiols as free ligands into solution[403,404,593,594]. Unfortunately, the chemical shift difference for ^{13}C resonance of cyanide in Au(^{13}CN)$_2{}^-$ and RS−Au−^{13}CN$^-$ (RS = thiolates) complexes is small and no quantitative measurements were possible[404,593,594]. The interactions of CN$^-$ with gold$^\text{I}$ drugs have therefore been reinvestigated[595] using ^{15}N NMR. The interaction of cyanide with Au*tm* and Au*tg* has been studied at pH 7.40 by taking the 20.266-MHz ^{1}H noise-decoupled ^{15}N NMR spectra of 0.20 M Au*tm* and 0.20 M Au*tg* at different AuSR:C^{15}N$^-$ molar ratios. The spectra for *tg*−Au−C^{15}N$^-$ and *tm*−Au−C^{15}N$^-$ were similar. In both cases the ^{15}N chemical shifts are located at *ca* 260.30 ppm. Up to a 2 : 1 ratio of Au*tm*:C^{15}N$^-$ the resonance at 265 ppm attributed to Au(CN)$_2{}^-$ did not appear. At higher concentrations of C^{15}N$^-$ this resonance has been observed and was increasing in intensity. The similarity of ^{15}N chemical shifts indicates that electronic environments of CN$^-$ ligands are similar in both complexes, since the binding site of complex thiols is at a large distance. The following NMR data have been found:

At [AuSR] : [C^{15}N$^-$] = 0.20 M:0.15 M

$$\delta(^{15}\text{N}) = 260.12 \text{ ppm for } tg{-}\text{Au}{-}\text{C}^{15}\text{N}^-$$

$$= 260.70 \text{ ppm for } tm{-}\text{Au}{-}\text{C}^{15}\text{N}^-;$$

$$\delta(^{15}\text{N}) = 265.73 \text{ ppm for Au}(\text{C}^{15}\text{N})_2{}^-, \text{ RS} = tg$$

$$= 265.94 \text{ ppm for Au}(\text{C}^{15}\text{N})_2{}^-, \text{ RS} = tm;$$

$$Q = [\text{Au}(\text{C}^{15}\text{N})_2^-]^2/[\text{RS}{-}\text{Au}{-}\text{C}^{15}\text{N}^-]^2 = 3.08 \times 10^{-2} \text{ for RS} = tg,$$

$$= 5.38 \times 10^{-4} \text{ for RS} = tm,$$

The life-times for $RS-Au-CN^-$ ($tg-Au-CN^-$) and ($tm-Au-CN^-$) species at the above concentrations have been assessed to be $\tau = 0.0083$ s and 0.10 s, respectively, on the basis of the exchange model of equation 94

$$2(RS-(Au-C^{15}N)^- \rightleftharpoons Au(C^{15}N)_2{}^- + Au(SR)_2{}^- \tag{94}$$
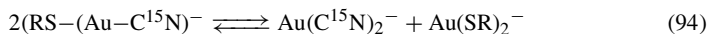
A suggestion has been made that the $tm-Au-C^{15}N^-$ linear complex is the gold carrier to the red blood cells of moderate smokers, while the $Au(CN)_2{}^-$ complex is the gold carrier to the red blood cells of heavy smokers, but further studies are required to establish the mechanism of gold transport into the red blood cells in the presence of CN^{-595}.

C. Radiochemical and Biomedical Studies with Radioactive Gold Isotopes

1. Developments of (Hg-195m) → (Au-195m) generators for the production of Au-195m for vascular imaging

Radiotracer ^{195m}Au has been found to be the ideal radionuclide for hemodynamic studies[596−599]. It decays with a 30.6-s half-life to ^{195}Au emitting predominantly 262-keV photons causing[600] a very low radiation dose[597]. Radionuclide ^{195m}Au is the daughter of the metastable mercury-195m (^{195m}Hg, $T_{1/2} = 41.6$ h), which is produced in the ^{197}Au(p, 3n)^{195m}Hg nuclear reaction by irradiating a gold target with 32-MeV cyclotron protons. Of the ^{195m}Au thus produced in the electron capture (EC) of ^{195m}Hg, about 80% of eluted carrier-free gold has been found in an ionic form and about 20% as an uncharged species. Pharmaceutical controls showed that the concentration of the mercury in the blood would be non-toxic, i.e. 1 ppb at the time of injection[601]. The first imaging observations in dogs showed the rapid build-up of the gold activity into highly vascular organs[599] (heart, brain, liver and kidneys). Animal studies carried out with the use of a tabletop (^{195m}Hg/^{195m}Au) generator[602] demonstrated a greatly increased left ventricular ejection fraction during iso-proterenol infusion[602], in excellent agreement with ejection fraction determinations using ^{99m}Tc-DTPA (diethylenetriaminepentaacetic acid). Multiple determinations of hemodynamic status are thus possible during a variety of physiological or pharmacological interventions at greatly reduced patient exposure to radiation[600,603]. Subsequent detailed measurements of ^{195m}Hg breakthrough[604] in the eluates of the ten bed-side ^{195m}Au generators over 3 days revealed a mercury breakthrough of 0.75 ± 0.09 µCi per 1 mCi of ^{195m}Au. 20 mCi injection of Au-195m results in 240 mrad to the kidney, or 1.5 rad to kidneys after six consecutive injections[605]. Approximately 20 to 25 mCi of ^{195m}Au in the $Na_3Au(S_2O_3)_2$ form has been produced per elution with $NaNO_3/Na_2S_2O_3$ solution from the commercial generator[604] containing 155 mCi of ^{195m}Hg (as mercury nitrate). The gamma camera energy spectrum of the eluate of ^{195m}Au generator taken immediately after elution shows, besides the 262-keV gamma photopeak, a low energy photon peak at 68 keV (Au-K_α) which allows the imaging of brain perfusion in both lateral views and computing calculation[606,607] of regional cerebral blood flow as well as generating images of high diagnostic value[608]. The quantitative mapping of cerebral blood flow in a patient after a stroke has been presented. The possibility of quantitative examinations of the influence of drugs on the cerebral blood flow has been stressed[608].

2. Biokinetics and dosimetry of ^{195m}Au

The diagnostically useful short-lived metastable Au-195m produced in ^{195m}Hg/^{195m}Au generator decays to long-lived Au-195 ($T_{1/2} = 183$ d). To assess correctly the dose from

this daughter radionuclide, its biodistribution and retention has been studied[609] by injecting the eluate from the ^{195}Hg/^{195m}Au generator into the ear vein of seven rabbits and subsequently measuring at regular intervals the whole body content[610] of ^{195m}Hg, ^{195}Au and ^{195}Hg. One animal was killed 1, 7, 21, 54, 121, 187 and 284 days after administration and the radioactivity content for each radionuclide was measured in the blood, liver, kidney, heart, spleen, lung, gonads, thyroid and bone morrow. The effective dose equivalent H_E defined by equation 95

$$H_E = \sum_i \omega_i H_i \qquad (95)$$

has been calculated to estimate the risk from irradiation in man[611], where ω_i is the weighting factor, H_i is the mean dose equivalent in tissue i calculated by multiplying the mean adsorbed dose, $\bar{D}$, by the 'quality factor', Q, depending on the nature of the primary radiation ($Q = 1$ for photons).

The major contributions to the adsorbed dose are caused by the radionuclide impurities in the eluate. The dose from ^{195m}Au is less than 7% of the total adsorbed dose. The activity accumulates mainly in the liver and in the kidneys. Transformation of the data from animal studies could be carried out using the effective dose equivalent H_E (equation 95) and also results from ^{99m}Tc-pertechnetate used for first pass studies[612].

3. Brief review of radiomedical studies with gold isotopes

Colloidal ^{199}Au is used in China for treatment of rheumatic arthritis and pleural, peritoneal metastases[613]. The migration of gold-198 has been evaluated also by radiometric scanning[614,615]. The sensitivity of neutron activation analysis (NAA) of biological molecules labelled with gold-197 has been greatly increased[616] by using colloidal gold as the label in the NAA. The particles of colloidal gold[617] amplify significantly the sensitivity of NAA, when attached to anti-human *IgG* antibodies to human immunodeficiency virus[618] type 1. Reactor neutron irradiations allow the detection of 2×10^{-16} mole of analyte in routine operations with possible extension of the detection capability to the 10^{-20} range.

The gold contents in two indigenous medicines, used in India, designated as TMF-14 and TMF-15, have been determined by NAA[619,620]. Gold has some toxic effects and strict control on standardization of these medicinal formulations is needed, since some shops tend to introduce higher gold contents based on a belief in the miraculous power of gold.

The rate of transport of ultra-fine particles less than 0.1 μm in diameter from the pulmonary region of lungs to the thoracic lymph nodes[621] has been studied[622] using ^{198}Au-colloid and ^{133}BaSO$_4$ particles. No significant differences between the quantities of the two particles which reached the regional lymph nodes have been found. This suggests that as they are both transported by alveolar macrophages migrating from lung to regional lymph nodes[623,624]. The deposition and clearance of inhaled or instilled gold-198 colloid particles are affected by the pathological condition of the lung[625].

The radioactive colloidal gold technique has been found to be a sensitive and reliable tool for pharmacological experiments to investigate small tissue samples[626]. The microvascular permeability was found to be increased with increasing doses of injected serotonin or histamine and has been inhibited by serotonine receptor antagonists and by H$_1$ antagonists[626]. Dosimetry calculations have been carried out for selected radionuclides (including Ag and Au) present in blood vessels of 3 representative sizes and were applied to determine the dose rates in the walls of blood vessels from radionuclides in the blood[627].

Gold micro-seeds irradiated in a nuclear reactor become useful radioactive isotopes clinically suitable for permanent implants in cancer patients to eradicate tumours[628]. The particle sizes of the colloidal dispersions of ^{198}Au, ^{99m}Tc-labelled S and ^{99m}Tc-labelled Sn produced in Hungary have been determined with an electron microscope and evaluated statistically[629]. The Au particle sizes of 2–10 nm agree with the information of the manufacturer, as did also the data found with ^{99m}Tc-labelled Sn, but not those with the dimensions of colloidal S particles. The radioactive impurities in commonly used radiopharmaceuticals have been determined to assess the additional doses to the total body from these impurities according to MIRD (Medical Internal Radiation Dosimetry) assuming each radionuclide to be uniformly distributed throughout the body. In the case of ^{198}Au the additional total body adsorbed dose from impurities was 5% of the ^{198}Au dose[630]. A method for the detection of the bacterial endotoxin in radiopharmaceuticals, particularly for ^{99m}TcO$_4{}^-$, ^{198}Au and ^{32}P, has been reported[631]. Gold has been detected[632] by NAA in 27 of 75 samples of natural drugs purchased from Chinese medical shops in Taiwan.

The determination of ^{196}Au and ^{198}Au isotopes in fallout samples produced in the ^{197}Au(n, 2n)^{196}Au and ^{197}Au(n, γ)^{198}Au neutron activation reactions has been described[633]. Fallout samples containing neutron activated nuclides and actinides have been collected with polyperchloroethylene filters. Counting procedures showed the concentrations of Au to be 0.24–0.42 ng g^{-1} in tumour-type tissues[634]. 1,2-Diarylethylenediamine Pt^{II} complexes have been examined by determining via NAA the content of platinum in tumour tissue and in the different organs of mice. The measurements of the induced radioactivity of ^{199}Au served as indications of the Pt concentration[635]. The contribution of this type of radiation is given. Irradiated platinum has been purified from ^{199}Au by extraction from acidic solutions with ethyl acetate[636]. The distribution of *cis*-dichlorodiamine platinum^{II} ('cisplatin') in various organs of mice has been determined[637].

4. Brief review of radioanalytical, health and environmental studies with gold isotopes[638a]

The slurry nebulization involving inductively coupled plasma mass spectrometry (ICP-MS) has been extended for the trace elemental analysis of biological samples. The method was tested[638b] by determining 24 trace elements in NIST (National Institute of Standards and Technology) biological samples. Thus, e.g. the certified value of Ag in bovine liver was 0.04 ± 0.01 µg g^{-1} while the slurry nebulization ICP-MS analytical result was 0.05 ± 0.01 µg g^{-1}. Twelve trace elements (As, Au, Cd, Cs, Cu, Fe, Hg, Mo, Rb, Sb, Se, Zn) have been determined[639] in the serum of patients with end-stage renal failure applying RNAA (radiochemical neutron activation analysis). The Au concentration of 73 ±12 pg g^{-1}, found in human blood serum, is much smaller than earlier reported[640,641]. The methods used for determination of platinum and gold in anticancer and antiarthritic drugs and metabolites, published in the period 1990–1995, have been reviewed[642,643]. It has been stressed that an understanding of the problems involved in treatments requires, besides RNAA, also data on the concentrations of total gold in blood and urine samples of patients, and on the behaviour and concentrations of intact drugs species and their metabolites.

Using the 411.8-keV γ-line of the ^{198}Au and the selective adsorption of gold on a chelating resin for the preconcentration of gold[644−647], the amounts of Au in the range of ng g^{-1} in river sediments from the Galicos river in North Greece have been determined[648]. INNA has been applied to test the reliability of different digestion procedures combined with ICP-MS and optical emission spectrometry as well as total reflection X-ray fluorescence spectrometry (TXRF) used for determination of 61 elements in sediments of the

river Elbe, including Ag and Au. The INAA determination showed 12.0 ± 0.6 mg kg^{-1} content of Ag compared with a value of 11.1 ± 4.4 mg kg^{-1} indicated by the TXRF method. The content of Au determined by INAA was only 0.048 ± 0.003 mg kg^{-1}. Microwave digestion procedures provided appropriate results for more than 50 elements in total[649]. MgO (1 g) as the preconcentration reagent has been applied in the analysis[650] by CNAA (chemical NAA) of seawater samples collected from the coast of Taiwan. The adsorption efficiency (in %) for Au^{3+} and Ag$^+$ by 1 g of MgO in 5 liters of seawater was 0.05 μg (58%) and 8 μg (58%) respectively. An increase in recovery of Au^{3+}, Ag^{2+}, Ni^{2+} etc., which form metal-chloro complexes with chloride ion, should be observed after acidification of seawater[651].

An accuracy of ± 0.2 ng has been reached in the analysis of biological and environmental samples containing about 4 ng Au on irradiation in the thermal neutron flux of 1×10^{13} n cm^{-2} s^{-1} during 6 days[652] and subsequent radiochemical separation. 4.7 ppb and 1.9 ppb of Au was detected[653] by INAA in two human kidney stones (one oxalate and one phosphate). There are indications that the trace element content of hair correlates with the body stores of these elements, particularly with those of bone[654]. The INAA of hair samples taken from osteoporosis patients showed 2.32 ± 1.32 ng g^{-1} content of Au in osteoporotic hair and 3.57 ± 1.90 ng g^{-1} in normal hair[655].

NAA has been applied recently to determine the level of 64 inorganic contaminants (elements at mg kg^{-1} concentrations) in the raw polymers and retail samples of plastic packaging used in contact with food[656]. The contents of Ag and Au have been found to be less than 0.19 ppm and 0.0038 ppm, respectively, in polyethylene terephthalate (PET); <0.0053 ppm and <0.0002 ppm in low density polyethylene (LDPE); <0.012 ppm and <0.0001 ppm in high density polyethylene (HDPE); <0.012 ppm and <0.0004 ppm in polystyrene (PS); and <0.039 ppm and 0.0002 ppm in polypropylene (PP).

The NAA method of monitoring the migration of additives into food is under development. The elemental contents in the human body change with changes of the health conditions. But the INAA analysis[657] of fingernails of pathologically diagnosed normal people (**N**), light esophageal epitheliosis patients (**A**), severe esophageal epitheliosis patients (**B**) and esophageal cancer patients (**C**) showed marked differences in the concentrations of Ca, Cl, K, Na, Mg, Se, Zn between the **N**, **A**, **B** and **C** groups. However, no significant differences have been found between the above four groups for the silver content (0.09 μg g^{-1} for **N**, 0.09 for **A**, 0.11 for **B** and 0.12 for **C**). No results for Au content have been published. The silver radioisotope ^{110m}Ag, a beta and gamma emitter, has been used[658] for determination by the autoradiographic method of cathodic silver depositions which are proportional to local current densities[659−663]. The optical density of the autoradiogram is proportional to the number of adsorbed β-particles. The local current densities have been found to decrease monotonically from a maximum value at the inner electrode boundary to the minimum value at the outer boundary of the electrode[658]. A column of silver powder labelled with ^{110m}Ag has been employed in the flow injection radiorelease analysis (FIRRA) of vanadium content in a solution containing vanadate^V (equation 96).

$$VO_3^- + 4H^+ + Ag^*(s) = VO^{2+} + Ag^{*+} + 2H_2O \qquad (96)$$

5. Brief review of the chemical application of gold isotopes in oncology

^{198}Au seeds have long been used as radiation sources in brachytherapy[664−666], to treat carcinoma of the prostate[667,668] and of the tongue[669]. The measurable dose anisotropy

around [198]Au seeds has been found to be too small to be of any clinical significance[670]. The dose distributions around [198]Au brachytherapy sources have been calculated[671] to be in good agreement with data available in the literature[670] and can be used in many computerized treatment planning systems. The use of monoclonal antibodies (*Ab*) radiolabelled with [211]At, [199]Au, ^{131}I and ^{90}Y for radioimmuno results in a large non-uniformity of the tumour dose[672−677]. Calculation of the energy deposition from radiolabelled *Ab* showed that the heterogeneity of antibody binding decreases the effectiveness of the radiation delivered, but enhanced cell killing is possible if the radiolabelled *Ab* binds to the cell surface membrane[678]. Energy deposition in tumour cell nuclei from membrane-bound radiolabelled antibody may be several times greater than the energy deposition estimated assuming uniform source distribution[678], including the short-range β-source [199]Au; with the latter, the calculated enhancement increases from 1.01 to 35[678]. The labelling of γ-globulin (*IgG*) with [199]Au was used as a model of the monoclonal antibody, for diagnosis and therapy of tumours[679]. Thiomalic acid (TMA) has been used as bifunctional conjugate to connect Au to *IgG*. S-Acetylmercaptosuccinic anhydride (AMSA) has been conjugated with *IgG* and the *IgG*-TMA conjugate reacted with [199]Au^I to form [199]Au-TMA-*IgG*. γ-Globulin has been labelled[680] with [199]Au also by reduction of the disulphide groups in the protein to free thiols with which [199]Au^I could bind. The behaviour of astatine-211 has been studied under various thermochromatographic conditions[681] on quartz, Pt, Pd, Au and Ag to find the best conditions for the separation of [211]At from a stream of the carrier gas.

The chemistry of gold drugs and gold complexes has been discussed[682,683]. Early introductory papers[684] concerning all dosimetric aspects of radiolabelled antibodies for tumour therapy[685] listed and classified radionuclides suitable for radioimmunotherapy (RIT) into:

(a) alpha emitters[686,687] ([211]At, [212]Bi),

(b) low-range beta sources [^{33}P, [121]Sn, ^{177}Lu, [191]Os and [199]Au produced in [198]Pt(n,γ)[199] reaction],

(c) medium-range beta sources ([47]Sc, [67]Cu, [77]As, [105]Rh, [109]Pd, [111]Ag, ^{131}I, [143]Pr, [161]Tb, [186]Re),

(d) long-range beta sources (^{32}P, ^{90}Y, [188]Re),

(e) electron capture (EC) and internal conversion (IC) decaying radionuclides ([71]Ge, [103]Pd, [119]Sb, [131]Cs, [193m]Pt and [197]Hg).

Assuming a tumour absorbed sterilization dose of 80 Gy and an antibody *IgG* molecular weight of 160000, Humm[685] calculated the weight of labelled *IgG* (1 : 1 labelling) required to deliver this specified radiation dose during 4 days as equal to 1.54 (μg g^{-1} tumour) for [199]Au labelled *IgG*.

Lucocq reviewed[688] the methods of absolute antigen quantitation in cellular structures in ultra-thin sections with colloidal gold. The absolute antigen quantitation is based on a knowledge of the relationship between the number of gold particles and the number of antigens (which is expressed as the labelling efficiency, LE).

D. Gold Isotopes in Natural Sciences

The solubility of tritium in copper and gold at high pressures in the temperature interval 473 K−700 K has been determined[689]. Gold annealed at 1273 K in air exhibited much higher solubility than samples annealed at 873 K. This effect has been explained by assuming that tritium has been trapped by oxygen which diffused into the sample

during the high temperature annealing treatment. The permeation of tritium through Au and Ag foils has been found to be dominated by the tritium transport along lattice defects at 323 K[690]. Deuterium interactions with ion-implanted oxygen in copper and gold have been examined[691]. In gold, the buried O sinks have been used to measure the permeability of D at 573 and 373 K when combined with the literature data[692]. ^{195}Au has been used[693] to study the distribution of Au during the mixing of basic and acid melts. In mixing of basaltic and granitic melts at 1200 °C and 1000 atm, ^{195}Au enrichment occurred in the hybrid, andesitic zone of melt. This has been explained by different activity coefficients of Au in andesitic, basaltic and granitic melts[693]. The resonant two-photon ionization spectrometry (R2PIS) applied to the jet-cooled ^{197}Au$_2$ molecules[163] confirmed previous high temperature Knudsen effusion measurements of the bond strength of ^{197}Au$_2$ that equal to D_0^0 (^{197}Au$_2$) = 2.290 ± 0.008 eV. The excited states of ^{197}Au$_2$ of O^+u symmetry have been shown to have partly Au$^+$ Au$^-$ ion pair character. The ionization potential of ^{197}Au$_2$ has been determined to be IP(^{197}Au$_2$) = 9.20 ± 0.210 eV. The last value combined with $D^0{}_0$(^{197}Au$_2$) and IP(^{197}Au) provides the value of the dissociation energy of the Au$_2^+$ ion equal to $D^0{}_0$(^{197}Au$_2$+) = 2.32 ± 0.21 eV. The B' state bond length of $r'_e[B'(1U)]$ = 2.570 ± 0.017 Å has been estimated; upon electronic excitation this bond length increased by 0.098 Å. The ground state and excited d-hole states of ^{63,65}Cu^{197}Au have been studied[694] by R2PIS applied to jet-cooled diatomic coinage metals ^{63}Cu ^{197}Au and ^{65}Cu^{197}Au.

V. ACKNOWLEDGEMENTS

VI. REFERENCES

1. N. W. Cant and W. K. Hall, *J. Catal.*, **52**, 81 (1978).
2. A. L. Larrabee and R. L. Kuczkowski, *J. Catal.*, **51**, 111 (1978).
3. L. C. Melander, *Isotope Effects on Reaction Rates*, Ronald Press, New York, 1960.
4. R. A. van Santen, J. Moolhuysen and W. M. H. Sachtler, *J. Catal.*, **65**, 478 (1980).
5. H. Worbs, Dissertation, Technische Hochschule, Breslau, Poland, 1942.
6. G. H. Twigg, *Trans. Faraday Soc.*, **42**, 208 (1946).
7. R. B. Grant and R. M. Lambert, *J. Catal.*, **92**, 364 (1985).
8. R. B. Grant and R. M. Lambert, *J. Catal.*, **93**, 92 (1985).
9. S. Andersson and V. Jostell, *Surf. Sci.*, **46**, 625 (1974).
10. C. Backx, J. Moolhuysen, P. Geenen and R. A. van Santen, *J. Catal.*, **72**, 364 (1981).
11. L. G. Pinajeva, Yu. A. Lokhov, B. S. Balzhinimajev, L. M. Karnatovskaya, A. A. Ivanov and K. I. Zamarajev, *Dokl. Acad. Sci. USSR*, **310**, 907 (1990); *Chem. Abstr.*, **116**, 129682s (1992).
12. L. G. Pinajeva, V. I. Bukhtiyarov, B. S. Balzhinimajev, A. I. Voronin, V. I. Savchenko, A. A. Ivanov and K. I. Zamarajev, *Unsteady State Processes in Catalysis, Proc. Int. Conf.* (Ed. Yu.

Sh. Matros), VSP, Zeist, The Netherlands, 1990, pp. 391–399; *Chem. Abstr.*, **116**, 129682s (1992).

13. G. K. Boreskov and A. V. Khasin, *Dokl. Acad. Sci. USSR*, **274**, 348 (1984). *Chem. Abstr.*, **100**, 191164X (1984).
14. P. H. F. Reijnen, A. Raukema, U. van Slooten and A. W. Kleyn, *J. Chem. Phys.*, **94**, 2368 (1991).
15. P. H. F. Reijnen, U. van Slooten, A. P. de Jongh, J. H. M. Kuijper and A. W. Kleyn, *Meas. Sci. Technol.*, **1**, 1224 (1990).
16. C. T. Campbell, *Surf. Sci.*, **157**, 43 (1985).
17. G. Herzberg, *'Spectra of Diatomic Molecules'*, in *Molecular Spectra and Molecular Structure*, D. van Nostrand, Toronto, London, 1957, p. 62.
18. K. W. F. Kohlrausch, *Gas Ramanspektren*, Akademische Verlagsgesellschaft, Becker and Erler, KOM-Ges, Leipzig, 1943, p. VI 65.
19. M. Zieliński, in *The Chemistry of Quinonoid Compounds* (Eds. S. Patai and Z. Rappoport), Wiley, London, 1974, p. 623.
20. H. C. Urey, H. Lowenstam, S. Epstein and C. R. McKinney, *Bull. Geol. Soc. Am.*, **62**, 399 (1951).
21. I. Kobal, U. Burghaus, M. Senegačnik and N. Ogrinc, manuscript submitted for publication in *J. Phys. Chem.*
21a. W. H. Johnston and C. J. O'Shea, *J. Chem. Phys.*, **21**, 2080 (1953).
22. A. J. Capote and R. J. Madix, *Surf. Sci.*, **214**, 276 (1989).
23. A. J. Capote and R. J. Madix, unpublished results.
24. C.-M. Chan, R. Aris and W. H. Weinberg, *Appl. Surf. Sci.*, **1**, 360 (1978).
25. D. Edwards, Jr., *Surf. Sci.*, **54**, 1 (1976).
26. L. Melander and W. H. Saunders, Jr., *Reaction Rates of Isotopic Molecules*, Wiley, New York, 1980.
27. E. M. Stuve, R. J. Madix and C. R. Brundle, *Surf. Sci.*, **146**, 155 (1984).
28. A. Streitwieser, Jr. and C. H. Heathcock, *Introduction to Organic Chemistry*, Macmillan, New York, 1985, p. 850.
29. A. Kumar, *J. Am. Chem. Soc.*, **103**, 517 (1981).
30. R. L. Brainard and R. J. Madix, *J. Am. Chem. Soc.*, **109**, 8082 (1987).
31. R. L. Brainard and R. J. Madix, *J. Am. Chem. Soc.*, **111**, 3826 (1989).
32. I. E. Wachs and R. J. Madix, *Surf. Sci.*, **76**, 531 (1978).
33. I. E. Wachs and R. J. Madix, *Appl. Surf. Sci.*, **1**, 303 (1978).
34. I. E. Wachs and R. J. Madix, *J. Catal.*, **53**, 208 (1978).
35. M. Bowker and R. J. Madix, *Surf. Sci.*, **95**, 190 (1980).
36. M. Bowker and R. J. Madix, *Surf. Sci.*, **116**, 549 (1982).
37. M. Zieliński, *Isotope Effects in Chemistry*, PWN, Warsaw, 1979.
38. D. C. Bradly, R. C. Mehrotra and D. P. Gaur, *Metal Alkoxides*, Academic Press, New York, 1978, pp. 27–28.
39. P. L. Watson, *J. Am. Chem. Soc.*, **105**, 6491 (1983).
40. H. N. Aliyu, R. D. Gillard, J. D. Honeywill, P. Lightfoot and J. Rocha, *Polyhedron*, **15**, 2409 (1996).
41. O. Reiner and H. Uehleke, *J. Physiol. Chem.*, **352**, 1048 (1971).
42. K. Nakamoto, *Infrared and Raman Spectra of Inorganic and Coordination Compounds*, Wiley, New York, 1986, p. 111.
43. R. P. Houghton, *Metal Complexes in Organic Chemistry*, Cambridge University Press, Cambridge, 1979, pp. 124, 130, 132, 144.
44. B. E. Smith and B. D. James, *Spectrochim. Acta*, **43A**, 383 (1987).
45. J. M. Davidson, *Chem. Ind.*, 2021 (1964).
46. S. J. Lippard and K. M. Melmed, *Inorg. Chem.*, **6**, 2223 (1967).
47. G. W. J. Fleet, C. J. Fuller and P. J. C. Harding, *Tetrahedron Lett.*, 1437 (1978).
48. S. Kano, S. Shibuya and T. Ebata, *J. Heterocycl. Chem.*, **18**, 1239 (1981).
49. F. Cariati and L. Naldini, *Gazz. Chim. Ital.*, **95**, 3 (1965).
50. F. Cariati and L. Naldini, *Gazz. Chim. Ital.*, **95**, 201 (1965).
51. B. Slootmaekers, A. C. Fabretti, H. O. Desseyn and S. P. Perlepes, *Spectrochim. Acta, Part A*, **52**, 1275 (1996).
52. A. Mosset, M. Abboudi and J. Galy, *Z. Kristallogr.*, **164**, 171, 181 (1983).

53. M. Camalli and F. Caruso, *Inorg. Chim. Acta*, **127**, 209 (1987).
54. A. Cassel, *Acta Crystallogr., Sect. B*, **37**, 229 (1981).
55. J. A. Pople and D. P. Santry, *Mol. Phys.*, **8**, 1 (1964).
56. E. L. Muetterties and C. W. Alegranti, *J. Am. Chem. Soc.*, **94**, 6386 (1972).
57. D. Gudat, M. Schrott, V. Bajorat, M. Nieger, S. Kotila and R. Fleischer, *Chem. Ber.*, **129**, 337 (1996).
58. J. S. Berners-Price, P. J. Sadler and C. Brevard, *Magn. Reson. Chem.*, **28**, 145 (1990).
59. S. M. Sokol, R. A. Jacobson and J. G. Verkade, *Inorg. Chem.*, **23**, 88 (1984).
60. R. G. Goel and P. Pilon, *Inorg. Chem.*, **10**, 2876 (1978).
61. T. S. A. Hor, S. P. Neo, C. T. Tan, T. C. W. Mak, K. W. P. Leung and R. J. Wang, *Inorg. Chem.*, **31**, 4510 (1992).
62. S. P. Neo, Z.-Y. Zhou, T. C. W. Mak and T. S. A. Hor, *Inorg. Chem.*, **34**, 520 (1995).
63. D. M. Ho and R. Bau, *Inorg. Chem.*, **22**, 4073 (1983).
64. D. Gudat, A. W. Holderberg, S. Kotila and M. Nieger, *Chem. Ber.*, **129**, 465 (1996).
65. E. Browne and R. B. Firestone, in *Table of Radioactive Isotopes* (Ed. V. S. Shirley), Wiley, Chichester, 1986.
66. C. Brevard, G. C. van Stein and G. van Koten, *J. Am. Chem. Soc.*, **103**, 6746 (1981).
67. G. C. van Stein, H. van der Poel, G. van Koten, A. L. Spek, A. J. M. Duisenberg and P. S. Pregosin, *J. Chem. Soc., Chem. Commun.*, 1016 (1980).
68. G. C. van Stein, G. van Koten, K. Vrieze, C. Brevard and A. L. Spek, *J. Am. Chem, Soc.*, **106**, 4486 (1984).
69. J. F. Modder, J.-M. Ernsting, K. Vrieze, M. de Wit, C. H. Stam and G. van Koten, *Inorg. Chem.*, **30**, 1208 (1991).
70. R. K. Harris and B. E. Mann (Eds.), *NMR and the Periodic Table*, Academic Press, New York, 1978, p. 248.
71. S. S. D. Brown, I. D. Salter and L. Toupet, *J. Chem. Soc., Dalton Trans.*, 757 (1988).
72. S. S. D. Brown, I. D. Salter, V. Sik, I. J. Colquhoun, W. McFarlane, P. A. Bates, M. B. Hursthouse and M. Murray, *J. Chem. Soc., Dalton Trans.*, 2177 (1988).
73. S. S. D. Brown, P. J. McCarthy, I. D. Salter, P. A. Bates, M. B. Hursthouse, I. J. Colquhoun, W. McFarlane and M. Murray, *J. Chem. Soc., Dalton Trans.*, 2787 (1988).
74. S. S. D. Brown, I. D. Salter, D. B. Dyson, R. V. Parish, P. A. Bates and M. B. Hursthouse, *J. Chem. Soc., Dalton Trans.*, 1795 (1988).
75. P. A. W. Dean, J. J. Vittal and R. S. Srivastava, *Can. J. Chem.*, **65**, 2628 (1987).
76. A. F. M. J. van der Ploeg and G. van Koten, *Inorg. Chim. Acta*, **51**, 225 (1981).
77. D. M. Ho and R. Bau, *Inorg. Chem.*, **22**, 4073 (1983).
78. P. A. W. Dean, D. G. Ibbott and J. B. Stothers, *Can. J. Chem.*, **54**, 166 (1976).
79. G. Calingaert and H. A. Beatty, *J. Am. Chem. Soc.*, **61**, 2748 (1939).
80. W. Bensch, M. Prelati and W. Ludwig, *J. Chem. Soc., Chem. Commun.*, 1762 (1986).
81. G. Wulfsberg, D. Jackson, W. Ilsley, S. Dou, A. Weiss and J. Gagliardi, Jr., *Z. Naturforsch.*, **47a**, 75 (1992).
82. A. Cassel, *Acta Crystallogr., Sect B*, **B35**, 174 (1979).
83. J. Howatson and B. Morosin, *Cryst. Struct. Commun.*, **2**, 51 (1973).
84. D. Coucouvanis, N. C. Baenzinger and S. M. Johnson, *Inorg. Chem.*, **13**, 1191 (1974).
85. H. Mueller, H. Boegge and E. Koeniger-Ahlborn, *Z. Naturforsch.*, **34B**, 1698 (1979).
86. J. E. Huheey, *Inorganic Chemistry: Principles of Structure and Reactivity*, Harper & Row, New York, 1983, p. 73.
87. G. Wulfsberg and A. Weiss, *Ber. Bunsenges. Phys. Chem.*, **84**, 474 (1980).
88. R. Meyer, J. Gagliardi, Jr. and G. Wulfsberg, *J. Mol. Struct.*, **111**, 311 (1983).
89. G. Wulfsberg, J. Yanisch, R. Meyer, J. Bowers and M. Essig, *Inorg. Chem.*, **23**, 715 (1984).
90. A. G. Orpen, L. Brammer, F. H. Allen, O. Kennard, D. G. Watson and R. Taylor, *J. Chem. Soc., Dalton Trans.*, S1 (1989).
91. W. Wojnowski, M. Wojnowski, K. Peters, E.-M. Peters and H. G. von Schnering, *Z. Anorg. Allg. Chem.*, **530**, 79 (1985).
92. M. Jansen, *J. Less-Common Met.*, **76**, 285 (1980).
93. A. Schwenk, U. Piantini and W. Wojnowski, *Z. Naturforsch.*, **46a**, 939 (1991).
94. W. Sahm and A. Schwenk, *Z. Naturforsch.*, **29a**, 1763 (1974).
95. A. Abragam, *The Principles of Nuclear Magnetism*, Oxford Univ. Press, New York, London, 1961, p. 315f.

96. H. Pfister, A. Schwenk and D. Zeller, *J. Magn. Reson.*, **68**, 138 (1986).
97. J. R. Black, N. R. Champness, W. Levason and G. Reid, *Inorg. Chem.*, **35**, 1820 (1996).
98. J. R. Black, N.R. Champness, W. Levason and G. Reid, *J. Chem. Soc., Chem. Commun.*, 1277 (1995).
99. J. R. Black, N. R. Champness, W. Levason and G. Reid, *J. Chem. Soc., Dalton Trans.*, 3439 (1995).
100. D. Franzoni, G. Pelizzi, G. Predieri, P. Tarasconi and F. Vitali, *J. Chem. Soc., Dalton Trans.*, 247 (1989).
101. J. Otera, T. Hinoishi and R. Okawara, *J. Organomet. Chem.*, **202**, C93 (1980).
102. A. G. Davies and P. J. Smith, in *Comprehensive Organometallic Chemistry* (Eds. G. Wilkinson, F. G. A. Stone and E. W. Abel), Vol. 2, Pergamon Press, Oxford, 1982, p. 527.
103. M. Camalli, F. Caruso, S. Chaloupka, P. N. Kapoor, P.S. Pregosin and L. M. Venanzi, *Helv. Chim. Acta*, **67**, 1603 (1984).
104. P.H. Kasai, D. McLeod, Jr. and T. Watanabe, *J. Am. Chem. Soc.*, **102**, 179 (1980).
105. J. A. Howard, H. A. Joly and B. Mile, *J. Phys. Chem.*, **94**, 6627 (1990).
106. P. H. Kasai, *J. Phys. Chem.*, **86**, 3684 (1982). *Chem. Abstr.*, **97**, 119354m (1982).
107. D. Cohen and H. J. Basch, *J. Am. Chem. Soc.*, **105**, 6980 (1983).
108. A. W. Castleman Jr., K. G. Weil, S. W. Sigsworth, R. E. Leuchtner and R. G. Keesee, *J. Chem. Phys.*, **86**, 3829 (1987).
109. M. A. Tolbert and J. L. Beauchamp, *J. Am. Chem. Soc.*, **108**, 7509 (1986).
110. G. Herzberg, *Molecular Spectra and Molecular Structure*, van Nostrand Reinhold, New York, 1966.
111. L. H. Merwin and A. Sebald, *J. Magn. Reson.*, **97**, 628 (1992).
112. U. Magg and H. Jones, *Chem. Phys. Lett.*, **146**, 415 (1988).
113. U. Magg and H. Jones, *Chem. Phys. Lett.*, **148**, 6 (1988).
114. U. Magg, H. Birk and H. Jones, *Chem. Phys. Lett.*, **149**, 321 (1988).
115. U. Magg, H. Birk and H. Jones, *Chem. Phys. Lett.*, **151**, 263 (1988).
116. U. Magg, H. Birk and H. Jones, *Chem. Phys. Lett.*, **151**, 503 (1988).
117. R.-D. Urban, U. Magg and H. Jones, *Chem. Phys. Lett.*, **154**, 135 (1989).
118. A. H. Bahnmaier, R.-D. Urban and H. Jones, *Chem. Phys. Lett.*, **155**, 269 (1989).
119. R.-D. Urban, A. H. Bahnmaier, U. Magg and H. Jones, *Chem. Phys. Lett.*, **158**, 443 (1989).
120. N. N. Haese, D. J. Liu and R. S. Altman, *J. Chem. Phys.*, **81**, 3766 (1984).
121. B. Lemoine, C. Demuynck, J. L. Destombes and P. B. Davies, *J. Chem. Phys.*, **89**, 673 (1988).
122. C. Yamada and E. Hirota, *J. Chem. Phys.*, **88**, 6702 (1988).
123. W. Urban, Spring Conference of the German Physical Society, Essen, March 1989.
124. H. Birk and H. Jones, *Chem. Phys. Lett.*, **161**, 27 (1989).
125. E. Bengtsson and E. Olsson, *Z. Phys.*, **72**, 163 (1931).
126. G. Guelachvili and K. N. Rao, *Handbook of Infared Standards*, Academic Press, New York, 1986.
127. G. Guelachvili, O. N. Ulenikov and G. A. Yshakova, *J. Mol. Spectrosc.*, **108**, 1 (1984).
128. C. Bréchignac, J. W. C. Johns, A. R. W. McKellar and M. Wong, *J. Mol. Spectrosc.*, **96**, 353 (1982).
129. S. Nadler, D. C. Reuter, S. J. Daunt and J. W. C. Johns, *NASA Technical Memorandum*, 100709 (1988).
130. J. L. Dunham, *Phys. Rev.*, **41**, 721 (1932).
131. W. A. Van Hook, Chapter 1, in *Isotope Effects in Chemical Reactions* (Eds. C. J. Collins and N. S. Bowman), van Nostrand Reinhold, New York, London, 1970, pp. 56–63.
132. R.-D. Urban, H. Birk, P. Polomsky and H. Jones, *J. Chem. Phys.*, **94**, 2523 (1991).
133. S. Shibata and L. S. Bartell, *J. Chem. Phys.*, **42**, 1147 (1965).
134. M. Zieliński, *Isotope Effects in Chemistry*, Polish Sci. Publ., Warsaw, 1979, pp. 144–153.
135. M. R. V. Sayhun, *Phot. Sci. Eng.*, **22**, 317 (1978).
136. D. S. Pesic and B. R. Vujisic, *J. Mol. Spectrosc.*, **146**, 516 (1991).
137. B. Simard, P. A. Hackett, A. M. James and P. R. R. Langridge-Smith, *Chem. Phys. Lett.*, **186**, 415 (1991).
138. H. Basch, *J. Am. Chem. Soc.*, **103**, 4657 (1981).
139. R. Grinter, *Chem. Phys.*, **102**, 187 (1986).
140. G. A. Ozin and W. E. Klotzbucher, *Inorg. Chem.*, **18**, 2101 (1979).
141. K. Levenberg, *Q. Appl. Math.*, **2**, 164 (1944).

142. G. Herzberg, *Molecular Spectra and Molecular Structure*, van Nostrand, Princeton, 1950, Vol. 1. pp. 168–182.
143. R. B. Ross and W. B. Ermler, *J. Phys. Chem.*, **89**, 5202 (1985).
144. K. Balasubramanian and M. Z. Liao, *Chem. Phys.*, **127**, 313 (1988).
145. P. J. Hay and R. L. Martin, *J. Chem. Phys.*, **83**, 5174 (1985).
146. H. Basch, *Faraday Symp. Chem. Soc.*, **14**, 149 (1980).
147. S. P. Walch, C. W. Bauschlicher and S. R. Langhoff, *J. Chem. Phys.*, **85**, 5900 (1986).
148. V. Beutel, M. Kuhn and W. Demtröder, *J. Mol. Spectrosc.*, **155**, 343 (1992).
149. G. Scoles (Ed.), *Atomic and Molecular Beam Methods*, Oxford Univ. Press, New York, Vol. 1, 1988; Vol. 2, 1992.
150. C. Moore, *Atomic Energy Levels*, in *Natl. Stand. Ref. Data Ser., Natl. Bur. Stand.* **35**, Washington, D.C., 1971.
151. H. J. Müschenborn, *J. Mol. Spectrosc.*, **179**, 1 (1996).
152. C. R. Vidal, *Comments At. Mol. Phys.*, **17**, 173 (1986).
153. B. Numerov, *Publ. Observ. Central Astrophys. Russ.*, **2**, 188 (1933).
154. J. W. Cooley, *Math. Comput.*, **15**, 363 (1961).
155. H. Zhang and K. Balasubramanian, *J. Chem. Phys.*, **98**, 7092 (1993).
156. G. A. Bishea, N. Marak and M. D. Morse, *J. Chem. Phys.*, **95**, 5618 (1991).
157. M. Ackerman, F. E. Stafford and J. Drowart, *J. Chem. Phys.*, **33**, 1784 (1960).
158. J. Ruamps, *Spectrochim. Acta, Suppl.*, **11**, 329 (1957).
159. J. Ruamps, *Ann. Phys. (Paris)*, **4**, 1111 (1959).
160. M. Ackerman, F. E. Stafford and J. Drowart, *J. Chem. Phys.*, **33**, 1784 (1960).
161. C. W. Bauschlicher, Jr., S. R. Langhoff and H. Partridge, *J. Chem. Phys.*, **91**, 2412 (1990).
162. H. Partridge, C. W. Bauschlicher, Jr. and S. R. Langhoff, *Chem. Phys. Lett.*, **175**, 531 (1990).
163. G. A. Bishea and M. D. Morse, *J. Chem. Phys.*, **95**, 5646 (1991).
164. V. Beutel, G. L. Bhale, M. Kuhn and W. Demtröder, *Chem. Phys. Lett.*, **185**, 313 (1991).
165. H -G. Krämer, V. Beutel, K. Weyers and W. Demtröder, *Chem. Phys. Lett.*, **193**, 331 (1992).
166. V. Beutel, M. Kuhn and W. Demtröder, *J. Mol. Spectrosc.*, **155**, 343 (1992).
167. V. Beutel, H.-G. Krämer, G. L. Bhale, M. Kuhn, K. Weyers and W. Demtröder, *J. Chem. Phys.*, **98**, 2699 (1993).
168. C. F. Moore, *Atomic Energy Levels*, in *Natl. Stand. Ref. Data Ser., Natl. Bur. Stand.*, (U.S.) Circ. no. 35, U.S. GPO, Washington, D. C., 1991.
169. M. D. Morse, *Chem. Rev.*, **86**, 1049 (1986).
170. P. Y. Cheng, K. F. Willey and M. A. Duncan, *Chem. Phys. Lett.*, **163**, 469 (1989).
171. K. F. Willey, P. Y. Cheng, C. S. Yeh, D. L. Robbins and M. A. Duncan, *J. Chem Phys.*, **95**, 6249 (1991).
172. D. L. Robbins, K. F. Willey, C. S. Yeh and M. A. Duncan, *J. Phys. Chem.*, **96**, 4824 (1992).
173. C. Jouvet, C. Lardeux-Dedonder, S. Martrenchard and D. Solgadi, *J. Chem. Phys.*, **94**, 1759 (1991).
174. L. R. Brock and M. A. Duncan, *J. Chem. Phys.*, **103**, 9200 (1995).
175. K. P. Huber and G. Herzberg, *Molecular Spectra and Molecular Structure*, Vol. 4, *Constants of Diatomic Molecules*, Van Nostrand Reinhold, New York, 1979.
176. C. S. Yeh, D. L. Robbins, J. S. Pilgrim and M. A. Duncan, *Chem. Phys. Lett.*, **206**, 509 (1993).
177. G. A. Bishea, N. Marak and M. D. Morse, *J. Chem. Phys.*, **95**, 5618 (1991).
178. G. A. Bishea, C. A. Arrington, J. M. Behm and M. D. Morse, *J. Chem. Phys.*, **95**, 8765 (1991).
179. J. S. Pilgrim and M. A. Duncan, *Chem. Phys. Lett.*, **232**, 335 (1995).
180. C. Jouvet, C. Lardeux-Dedonder and D. Solgadi, *Chem. Phys. Lett.*, **156**, 569 (1989).
181. J. Hoeft, F. J. Lovas, E. Tiemann and T. Törring, *Z. Naturforsch.*, **26A**, 240 (1971).
182. W. Gordy and R. L. Cook, *Technique of Organic Chemistry*, Vol. 9, *Microwave Molecular Spectra* (Ed. A. Weissberger), Interscience, New York, 1970, p. 665.
183. E. Pearson and W. Gordy, *Phys. Rev.*, **152**, 42 (1966).
184. C. Styger and M. C. L. Gerry, *Chem. Phys. Lett.*, **188**, 213 (1992).
185. M.-Y. Kwon, B.-W. Lee and J.-J. Kim, *Chem. Phys. Lett.*, **162**, 238 (1989).
186. F. Barz, J. G. Gordon II, M. R. Philpott and M. J. Weaver, *Chem. Phys. Lett.*, **94**, 168 (1983).
187. J. F. Owen and R. K. Chang, *Chem. Phys. Lett.*, **104**, 59 (1984).
188. M. Gavrilas and V. P. Guinn, *J. Radioanal. Nucl. Chem.*, **113**, 327 (1987).
189. E. Browne and R. B. Firestone, in *Table of Radioactive Isotopes*, (Ed. V. S. Shirley), Wiley, Chichester, 1986, pp. 108, 110–113.

190. S. F. Mughabghab, M. Divadeenam and N. E. Holden, *Neutron Cross Sections*, Vol. 1, *Neutron Resonance Parameters and Thermal Cross Sections, Part A* ($Z = 1-60$), Academic Press, New York, 1981.
191. A. Wyttenbach, S. Bajo and L. Tobler, in *Biological Trace Element Research* (Ed. G. N. Schrauzer), The Humana Press Inc., Totowa, N.J. 1990.
192. D. M. A. Al-Jaff, G. T. Cook, K. E. Carr and H. J. Duncan, in *The Plant Cuticle*, Academic Press, New York, 1980, p. 293.
193. G. M. Hunt and E. A. Baker, in *The Plant Cuticle*, Academic Press, New York, 1980, pp. 279–292.
194. P. J. Coughtrey and M. C. Thorne, *Radionuclide Distribution and Transport in Terrestrial Ecosystems*, Balkema, Rotterdam, 1983.
195. K. Bunzl and W. Schultz, *J. Radioanal. Nucl. Chem.*, **90**, 23 (1985).
196. J. Tent and G. Rauret, *J. Radioanal. Nucl. Chem.*, **204**, 321 (1996).
197. E. E. Vaszari, V. Tóth and S. Tarján, *Isotoptech. Diagn.*, **34**, 141 (1991) (in Hungarian); *Chem. Abstr.*, **117**, 10729a (1992).
198. E. E. Vaszari, V. Tóth and S. Tarján, *J. Radioanal. Nucl. Chem., Lett.*, **165**, 345 (1992).
199. R. O. Allen and E. Steinnes, *Chemosphere*, **4**, 371 (1978).
200. M. Vidal and G. Rauret, *J. Radioanal. Nucl. Chem.*, **181**, 85 (1994).
201. M. J. Frissel, H. Noordijk and K. E. van Bergeijk, in *The Transfer of Radionuclides in Natural and Semi-natural Environments*, Elsevier Applied Science, London, 1990.
202. G. Riise, H. E. Bjoernstad, H. N. Lien, D. H. Oughton and B. Salbu, *J. Radioanal. Nucl. Chem.*, **142**, 531 (1990).
203. D. H. Oughton, B. Salbu and P. Strand, *Mobility Factors for Estimating the Bioavailability of Radionuclides in Soil*, Biomovs, Sweden, 1990.
204. G. Rauret, M. Llaurado, M. Vidal and V. R. Vallejo in *The Transfer of Radionuclides in Natural and Semi-natural Environments*, Elsevier Applied Science, London, 1990.
205. M. Vidal and G. Rauret, *J. Radioanal. Nucl. Chem.*, **173**, 79 (1993).
206. M. Vidal and G. Rauret, *Int. J. Environ. Anal. Chem.*, **51**, 85 (1993).
207. J. Tent, M. Vidal, M. Llaurado, G. Rauret, J. Real and P. Misher, *J. Radioanal. Nucl. Chem.*, **173**, 377 (1993).
208. J. Guczi, A. Angelova, R. A. Bulman and G. Szabo, *React. Polym.*, **17**, 61 (1992); *Chem. Abstr.*, **117**, 35332w (1992).
209. J. Garnier and J. P. Baudin, *Water, Air, Soil Pollut.*, **45**, 287 (1989); *Chem. Abstr.*, **112**, 32678z (1990).
210. T. Umezu, *Hoshasen Kagaku (Tokyo)*, **35**, 369 (1992); *Chem. Abstr.*, **118**, 153865r (1993).
211. E. D. Goldberg, *Mar. Pollut. Bull.*, **6**, 111 (1975).
212. T. R. Folsom, R. Grismore and D. R. Young, *Nature* **227**, 450 (1970).
213. T. R. Folsom, *Isotope Marine Chemistry*, Uchida Rokakuho Publ. Co. Ltd., Tokyo, 1980, p. 51.
214. H. Fukatsu and H. Higuchi, *Radiological Sciences.*, (Hoshasen Kagaku in Jap.) **28**, 201 (1985); *Chem. Abstr.*, **104**, 125806q (1985).
215. T. M. Beasley and E. E. Held, *Nature*, **230**, 450 (1971).
216. N. E. Whitehead, S. Ballestra, E. Holm and L. Huynh-Ngoc, *J. Environ. Radioact.*, **7**, 107 (1988).
217. C. J. Martin and B. Heaton, *J. Environ. Radioact.*, **9**, 209 (1989).
218. S. A. Saňudo-Wilhelmy and A. R. Flegal, *Environ. Sci. Technol.*, **26**, 2147 (1992).
219. E. Matsumoto and C. S. Wong, *J. Geophys. Res.*, **82**, 5477 (1977).
220. W. R. Schell, *Geochim. Cosmochim. Acta*, **41**, 1019 (1977).
221. V. Kasemsupaya, M. Yashima, H. Tsubota and Y. Nozaki, *Geochem. J.*, **23**, 129 (1989).
222. Y. Ishikawa, N. Sato, E. Nakamura, T. Sekine and K. Yoshihara, *J. Radioanal. Nucl. Chem.*, **158**, 31 (1992).
223. H. van Dam, *Nature*, **324**, 216 (1986).
224. G. D. Jones, P. D. Forsyth and P. G. Appleby, *Nature*, **322**, 313 (1986).
225. S. B. Ballestra, E. Holm, A. Walton and N. E. Whitehead, *J. Environ. Radioact.*, **5**, 391 (1987).
226. J.-C. Roy, J.-E. Cote, A. Mahfaud, S. Villeneuve and J. Turcotte, *J. Environ. Radioact.*, **6**, 121 (1988).
227. H. Higuchi, H. Fukatsu, T. Hashimoto, N. Nonaka, K. Yoshimizu, M. Omine, N. Takano and T. Abe, *J. Environ. Radioact.*, **6**, 131 (1988).
228. J. Ishida, N. Miyanaga, H. Watanabe, T. Asano and Y. Kitahara, *J. Environ. Radioact.*, **7**, 17 (1988).

229. C. Papastefanou, M. Manolopoulou and S. Charalambous, *J. Environ. Radioact.*, **7**, 49 (1988).
230. N. E. Whitehead, S. Ballestra, E. Holm and A. Walton, *J. Environ. Radioact.*, **7**, 249 (1988).
231. Y. Ishikawa, T. Kikuchi, T. Sekine and K. Yoshihara, *J. Radioanal. Nucl. Chem.*, **197**, 343 (1995).
232. Y. Sugimura, Y. Suzuki and Y. Miyake. *Proc. of the 3rd NEA Seminar on Marine Radioecology*, Tokyo, 1979, p. 131.
233. *The International Commission on Radiological Protection, ICRP Publication No. 30*, Pergamon Press, Oxford, 1980.
234. Y. Yano and H. O. Anger, *J. Nucl. Med.*, **9**, 2 (1967).
235. G. Erdtmann and W. Soyka, *The Gamma Rays of the Radionuclides*, Verlag Chemie, New York, 1979.
236. G. S. Forbes and H. I. Cole, *J. Am. Chem. Soc.*, **43**, 2492 (1921).
237. K. H. Lieser, *Z. Anorg. Allg. Chem.*, **292**, 97 (1957).
238. M. S. Mansur, A. Mushtaq and A. Muhammad, *J. Radioanal. Nucl. Chem.*, **201**, 205 (1995).
239. R. C. Switzer III, C. R. Merril and S. Shifrin, *Anal. Biochem.*, **98**, 238 (1979).
240. B. R. Oakley, D. R. Kirsch and R. N. Morris, *Anal. Biochem.*, **105**, 361 (1980).
241. C. R. Merril, M. L. Dunau and D. Goldman, *Anal. Biochem.*, **110**, 201 (1981).
242. C. R. Merril, D. Goldman, S. A. Sedman and M. H. Ebert, *Science*, **211**, 1437 (1981).
243. J. H. Morrissey, *Anal. Biochem.*, **117**, 307 (1981).
244. W. R. Springer, *Anal. Biochem.*, **195**, 172 (1991).
245. W. R. Springer, *Dev. Biol.*, **133**, 447 (1989).
246. C. W. Bales, G. Freeland, H. Jeanne, S. Askey, F. Behmardi, R. S. Pobocik, J. Jacqueline and P. Greenlee, *Am. J. Clin. Nutr.*, **51**, 462 (1990).
247. A. Bush, G. Multhaup, R. D. Moir, T. G. Williamson, D. H. Small, B. Rumble, P. Pollwein, K. Beyreuther and C. L. Masters, *J. Biol. Chem.*, **268**, 22 (1993).
248. W. R. Markesbery, W. D. Ehmann, M. Alauddin and T. I. M. Hossain, *Neurobiol. Aging*, **5**, 19 (1984).
249. W. D. Ehmann, W. R. Markesbery, E. J. Kasarskis, D. E. Vance, S. S. Khare, J. D. Hord and C. M. Thompson, *Biol. Trace Elem. Res.*, **13**, 19 (1987).
250. D. E. Vance, W. D. Ehmann and W. R. Markesbery, *Biol. Trace Elem. Res.*, **17**, 109 (1988).
251. D. E. Vance, W. D. Ehmann and W. R. Markesbery, *Neurotoxicology*, **9**, 197 (1988).
252. *Activation Analysis of Hair as an Indicator of Contamination of Man by Environmental Trace Element Pollutants*, IAEA/RL/50, Vienna, 1978.
253. K. Chaudhary, W. D. Ehmann, K. Rengan and W. R. Markesbery, *J. Radioanal. Nucl. Chem.*, **195**, 51 (1995).
254. *Activation Analysis of Hair as an Indicator of Contamination of Man by Environmental Trace Element Pollutants*, IAEA/RL/50, Vienna, 1978, p. 135.
255. E. L. Kanabrocki, J. A. Kanabrocki, J. Greco, E. Kaplan and Y. T. Oester, *Sci. Total Environ.* **12**, 131 (1979).
256. A. Karlsson, *Meat Sci.*, **31**, 423 (1992).
257. P. J. Gemperline, K. H. Miller, T. L. West, J. E. Weinstein, J. C. Hamilton and J. T. Bray, *Anal. Chem.*, **64**, 523A (1992).
258. D. Vojnovic, G. Procida and F. L. Gabrielli, *Food Addit. Contam.*, **8**, 343 (1991).
259. Q. Yang, W. Pennickx, R. van Cauwenbergh, J. Smeyers-Verbeke, H. Keelstra and D. L. Massart, *Analusis*, **21**, 379 (1993).
260. T. B. Cheng, J. S. Morris, S. R. Koirtyohann, V. L. Spate and C. K. Baskett, *J. Radioanal. Nucl. Chem.*, **195**, 31 (1995).
261. W. Czarnowski and J. Krechniak, *Br. J. Ind. Med.*, **47**, 349 (1990).
262. B. Gammelgaard and N. K. Veien, *Acta Derm. Venereol.*, **70**, 417 (1990).
263. M. Hayashi, K. Yamamoto, M. Yoshimura, H. Hayashi and A. Shitara, *Bull. Environ. Contam. Toxicol.*, **50**, 547 (1993).
264. M. S. Nagra, B. S. Pallah, P. S. Sahota, H. Singh and H. S. Sahota, *J. Radioanal. Nucl. Chem.*, **162**, 283 (1992).
265. K. Peters, B. Gammelgaard and T. Menne, *Contact Dermatitis* **25**, 237 (1991).
266. A. Sukumar and R. Subramanian, *Biol. Trace Elem. Res.*, **34**, 89 (1992).
267. M. Wilhelm, D. Hafner, I. Lombeck and F. K. Ohnesorge, *Sci. Total Environ.*, **103**, 199 (1991).
268. L.-Y. Jin, G. Capannesi, L. Renzi and F. Sedda, *J. Radioanal. Nucl. Chem.*, **155**, 325 (1991).
269. N. I. Ward, N. M. Spyrou and A. A. Damyanowa, *J. Radioanal. Nucl. Chem.*, **114**, 125 (1987).

270. E. E. Menden and V. J. Elia, *Environ. Sci. Technol.*, **6**, 830 (1972).
271. G. P. Lewis, W. J. Juskow, L. L. Coughlin and S. Hartz, *Lancet*, **1**, 291 (1972).
272. C. G. Elinder, T. Kjellstrom, B. Lind, L. Linnman, M. Piscator and K. Sundstedt, *Environ. Res.*, **32**, 220 (1983).
273. V. Valkovic, *Trace Elements in Human Hair*, Garland STPM Press, New York and London, 1977.
274. D. J. Eatough, J. J. Christensen, R. M. Izatt and C. Hartley, *Level of Selected Trace Elements in Human Hair*, First Human Hair Symposium, Atlanta, 1973.
275. D. I. Hammer, J. F. Finklea, R. H. Hendricks and C. M. Shy, *Am. J. Epidemiol.*, **93**, 84 (1971).
276. R. E. Jervis, B. Tiefenbach and A. Chattopadhay, *J. Radioanal. Chem.*, **37**, 751 (1971).
277. P. Grandjean, *Int. Arch. Occup. Environ. Health*, **42**, 69 (1978).
278. S. Ohmori, H. Tsuji, Y. Kusaka, T. Takeuchi, T. Hayashi, J. Takada, M. Koyama, H. Kozuka, M. Shinogi, A. Aoki, K. Katayama and T. Tomiyama, *J. Radioanal. Chem.*, **63**, 269 (1981).
279. R. Cornelis, *J. Radioanal. Chem.*, **15**, 305 (1973).
280. A. Gordus, *J. Radioanal. Chem.*, **15**, 229 (1973).
281. R. Dybczyński and K. Boboli, *J. Radioanal. Chem.*, **31**, 267 (1976).
282. K. K. S. Pillay and R. L. Kuis, *J. Radioanal. Chem.*, **43**, 461 (1978).
283. R. E. Jervis, A. K. Perkons, W. D. Mackintosh and M. F. Kerr, *Proc. 1961 Int. Conf. on Modern Trends in Activation Analysis*, Texas A&M Univ., College Station, Texas, 1962, p. 107.
284. J. M. A. Lenihan and H. A. Smith, *Proc. 2nd Int. Conf. on the Peaceful Uses of Atomic Energy, Geneva, 1958*, Vol. 26, United Nations, New York, 1959, p. 233.
285. S. Forshufvud, H. Smith and A. Wassen, *Nature*, **192**, 103 (1961).
286. H. Al-Shahristani and I. K. Al-Haddad, *J. Radioanal. Chem.*, **15**, 59 (1973).
287. T. Giovanoli-Jakubczak, *Arch. Environ. Health*, **28**, 139 (1974).
288. L. M. Klevay, *Arch. Environ. Health*, **26**, 169 (1973).
289. H. G. Petering, D. W. Yeager and S. O. Witherup, *Arch. Environ. Health*, **27**, 327 (1973).
290. K. Noguchi, M. Shimizu and E. Sairenji, *J. Radioanal. Nucl. Chem.*, **90**, 217 (1985).
291. T. Suzuki, *J. Tokyo Dent. Assoc.*, **19**, 2 (1971).
292. K. Miyazawa, *Nihon Univ. Dent. J.*, **47**, 42 (1973).
293. L. E. Kopito and H. Schwachman, in *Alternation in the Elemental Composition of Hair in Some Diseases*, The First Human Hair Symposium (Ed. A. C. Brown), Medcom Press, Petach–Tikva, Ill. 1974, p. 83.
294. R. E. Jervis, R. G. V. Hancock, D. E. Hill and K. Isles, *J. Radioanal. Chem.*, **37**, 463 (1977).
295. C. A. Pankhurst and B. D. Pate, *Rev. Anal. Chem.*, **4**, 111 (1979).
296. D. E. Ryan, J. Holzbecher and D. C. Stuart, *Clin. Chem.*, **24**, 1966 (1978).
297. W. Wiesener, W. Goerner and S. Niese, *Proc. IAEA Symp. Nuclear Techniques in the Life Sciences*, Vienna, 1978, p. 307.
298. S. P. Moo and K. K. S. Pillay, *J. Radioanal. Chem.*, **77**, 141 (1983).
299. M. A. Tempero, M. M. Jacobs, H. T. Lynch, C. L. Graham and A. J. Blotcky, *Biol. Trace Element Res.*, **6**, 51 (1984).
300. N. I. Ward, D. Bryce-Smith, M. J. Minski and W. B. Matthews, *Biol. Trace Element Res.*, **7**, 153 (1985).
301. G. D. Renshaw, C. A. Pounds and E. F. Pearson, *Nature*, **238**, 162 (1972).
302. S. Gangadharan, V. V. Lakshmi and M. S. Das, *J. Radioanal. Chem.*, **15**, 287 (1973). *J. Indian Acad. Forensic Sci.*, **11**, 18 (1972).
303. I. Obrusnik, J. Gislason, D. K. McMillan, J. d'Auria and B. D. Pate, *J. Forensic Sci.*, **17**, 426 (1972).
304. E. A. Eads and C. E. Lambdin, *Environ. Res.*, **6**, 247 (1973).
305. R. K. Jolly, G. R. Pehrson, S. K. Gupta, D. C. Buckle and H. Aceto, *Proc. 3rd Conf. Appl. Small Accelerators*, Conf-741040-Pl, Denton, Texas, 1974, p. 203.
306. L. S. Chuang and J. F. Emery, *J. Radioanal. Chem.*, **45**, 169 (1978).
307. I. Obrusnik and V. Bencko, *Radiochem. Radioanal. Lett.*, **38**, 169 (1979).
308. H. A. Schroeder and A. P. Nason, *J. Invest. Dermatol.*, **53**, 71 (1969).
309. G. C. Verghese, R. Kishore and V. P. Guinn, *J. Radioanal. Chem.*, **15**, 329 (1973).
310. A. K. Perkons and R. E. Jervis, *Proc. 1965 Int. Conf. on Modern Trends in Activation Analysis*, Texas A&M Univ., College Station, Texas, 1965, p. 295.
311. L. C. Bate and F. F. Dyer, *Nucleonics*, **23**, 74 (1965).
312. F. W. Lima, H. Shibata and L. T. Atalla, *Proc. Symp. on Radiochemical Methods of Analysis*, Salzburg, Vol. 1, IAEA, Vienna, 1965, p. 119.

313. W. W. Harrison, J. P. Yurachek and C. A. Benson, *Clin. Chim. Acta*, **23**, 83 (1969).
314. K. M. Hambridge, M. L. Franklin and M. A. Jacobs, *Am. J. Clin. Nutr.*, **25**, 384 (1972).
315. I. Obrusnik, J. Gislason, D. Maes, D. K. McMillan, J. d'Auria and B. D. Pate, *J. Radioanal. Chem.*, **15**, 115 (1973).
316. D. C. Hilderbrand and D. H. White, *Clin. Chem.*, **20**, 148 (1974).
317. G. S. Assarian and D. Oberleas, *Clin. Chem.*, **23**, 1771 (1977).
318. D. Shapcott, *Clin. Chem.*, **24**, 391 (1978).
319. S. Salmela, E. Vuori and J. O. Kipio, *Anal. Chim. Acta*, **125**, 131 (1981).
320. *IAEA Advisory Group on Application of Nuclear Methods in Environmental Reasearch*, Report, Vienna, 22–26 March, 1976.
321. G. Chittleborough, *Sci. Total Environ.*, **14**, 53 (1980).
322. N. I. Ward and M. J. Minski, *Environ. Trace Subst. Res. Centre*, 16th Ann. Conf., Univ. of Missouri, 1982, p. 252.
323. N. I. Ward, *Conf. New Zealand Trace Element Group*, Massey Univ., Palmerston North, New Zealand, 1984.
324. E. J. Underwood, *Trace Elements in Human and Animal Nutrition*, Academic Press, New York, 1977.
325. L. Xilei, D. van Renterghem, R. Cornelis and L. Mees, *Anal. Chim. Acta*, **211**, 231 (1988).
326. J. Versieck and R. Cornelis, *Anal. Chim. Acta*, **116**, 217 (1980).
327. E. A. Preoteasa, M. Salagean, A. Pantelica, D. Plostinaru, B. Constantinescu and S. Berceanu, *J. Radioanal. Nucl. Chem.*, **151**, 261 (1991).
328. M. Salagean, A. Pantelica, E. A. Preoteasa, S. Berceanu, A. Vilcu and V. Lungu, *2nd Balkan Conf. Activation Analysis and Nuclear Related Analytical Techniques*, Bled, Yougoslavia, 1989.
329. G. H. Bell, D. Emslie-Smith and C. R. Paterson, in *Textbook of Physiology and Biochemistry*, Chap. 44, *Reproduction*, Churchill Livingston, Edinburgh, New York N.J. US 1976, p. 661.
330. J. S. Garrow and S. F. Hawes, *J. Obstet. Gynaecol. Br. Commonw.*, **78**, 22 (1971).
331. A. A. Fanaroff and R. J. Martin, *Behrman's Neonatal Perinatal Medicine, Diseases of the Fetus and Infant*, Mosby, St. Louis, Toronto, 1983.
332. G. V. Iyengar, W. E. Kollmer and H. J. M, Bowen, *The Elemental Composition of Human Tissues and Body Fluids*, Verlag Chemie, Weinheim, New York, 1978, p. 94.
333. N. I. Ward, T. D. Macmahon and J. A. Mason, *J. Radioanal. Nucl. Chem.*, **113**, 501 (1987).
334. N. I. Ward and J. A. Mason, *J. Radioanal. Nucl. Chem.*, **113**, 515 (1987).
335. A. Sahgal, *Trends Neurosci.*, **3**, 116 (1985).
336. I. L. Crawford and J. D. Connor, *Nature*, **244**, 442 (1973).
337. J. Storm-Mathisen, *'Glutamate in Hippocamal Pathways.'* in *Glutamate as a Neurotransmitter* (Eds G. di Ghiara and G. L. Gessa), Raven Press, New York, 1981, p. 43.
338. I. E. Dreosti, S. J. Manuel, R. A. Buckley, F. J. Fraser and I. R. Record, *Life Sci.*, **28**, 2133 (1981).
339. R. I. Henkin, B. Patten, P. K. Re and D. A. Bronzert, *Arch. Neurol.*, **32**, 745 (1975).
340. F. Chisela and P. Brätter, *Anal. Chim. Acta*, **188**, 85 (1986).
341. E. Steinnes and J. J. Rowe, *J. Radioanal. Chem.*, **37**, 849 (1977).
342. Z. Randa, *Radioanal. Lett.*, **24**, 157 (1976).
343. P. A. Baedecker, *J. Radioanal. Chem.*, **40**, 115 (1977).
344. A. G. Hanna and H. Al-Shahristani, *J. Radioanal. Chem.*, **37**, 581 (1977).
345. Z. Prouza and M. Rakovic, *Isotopenpraxis*, **3**, 389 (1967).
346. D. C. Borg, R. E. Segel, P. Kienle and L. Campbell, *Int. J. Appl. Radiat. Isot.*, **11**, 10 (1960).
347. T. Bereznai, D. Bodizs and G. Keömley, *J. Radioanal. Chem.*, **36**, 509 (1977).
348. H. Bem and D. E. Ryan, *Anal. Chim. Acta*. **124**, 373 (1981).
349. J. A. Davies, P. A. Hart and A. C. Jefferies, *J. Radioanal. Chem.*, **98**, 275 (1986).
350. F. Chisela, D. Gawlik and P. Brätter, *Analyst*, **111**, 405 (1986).
351. D. Gawlik, K. K. Berthold, F. Chisela and P. Brätter, *J. Radioanal. Nucl. Chem.*, **112**, 309 (1987).
352. V. Zaichick, A. Tsyb and S. Bagirov, *J. Radioanal. Nucl. Chem.*, **195**, 123 (1995).
353. R. K. Chandra, *Immunology Today*, **4**, 322 (1983).
354. R. Zeisler, R. R. Greenberg and S. F. Stone, *J. Radioanal. Nucl. Chem.*, **124**, 47 (1988).
355. L. A. Currie, *Anal. Chem.*, **40**, 586 (1968).
356. I. Olmez, F. X. Pink and R. A. Wheatcroft, *Environ. Sci. Technol.*, **28**, 1487 (1994).
357. A. Naeem, *J. Radioanal. Nucl. Chem.*, **118**, 79 (1987).
358. J. P. Baudin and J. Garnier-Laplace *Arch. Environ. Contam. Toxicol.*, **27**, 459 (1994).

359. M. Skrzypińska-Gawrysiak, J. K. Piotrowski and K. Jaroń, *Bromatol. Chem. Toksykol.*, **21**, 274 (1988); *Chem. Abstr.*, **111**, 36143y (1989).
360. W. Junguang, C. Ziyuan, W. Meiwen and S. Hui., *Henong Xuebao*, **4**, 235 (1990); *Chem. Abstr.*, **117**, 22633r (1992).
361. A. E. Sabbioni, R. Pietra, J. Edel, A. di Nucci, L. Manzo, E. Candioli, G. Tolu and M. Bonardi, *Comm. Eur. Communities Rep. EUR 12058*, 1989, p. 21; *Chem. Abstr.*, **112**, 104674r (1990).
362. T. M. Simon, D. H. Kunishima, G. J. Vilbert and A. Lorber, *Cancer Res.*, **41**, 94 (1981).
363. C. K. Mirabelli, R. K. Johnson, D. T. Hill, L. F. Faucette, G. R. Girard, G. Y. Kuo, C. M. Sung and S. T. Crooke, *J. Med. Chem.*, **29**, 218 (1986).
364. C. K. Mirabelli, D. T. Hill, L. F. Faucette, F. L. McCabe, G. R. Girard, D. B. Bryan, B. M. Sutton, J. O. Bartus, S. T. Crooke and R. K. Johnson, *J. Med. Chem.*, **30**, 2181 (1987).
365. D. Lewis, H. A. Capell, C. J. McNiel, M. S. Iqbal, D. H. Brown and W. E. Smith, *Ann. Rheum. Dis.*, **42**, 566 (1983).
366. A. P. Intaccia, T. L. Flanagan, D. T. Walz, L. Gutzait, J. E. Swagzdis, J. Flagiello, Jr., B. Y. H. Hwang, R. H. Dewey and H. Noguchi, in *Bioorganic Chemistry of Gold Coordination Compounds* (Ed. B. M. Sutton), Smith Kline and French Laboratories, Philadelphia, 1983, pp. 21–33,
367. K. T. Garnes, J. R. Heys and S. W. Landvatter, *J. Organometal. Chem.*, **378**, 293 (1989).
368. S. J. Berners-Price, M. A. Mazid and P. J. Sadler, *J. Chem. Soc., Dalton Trans.*, 969 (1984).
369. A. M. Aguiar and T. G. Archibald, *Tetrahedron Lett.*, **54**, 71 (1966).
370. M. A. Ondetti, B. Rubin and D. W. Cushman, *Science*, **196**, 441 (1977).
371. D. W. Cushman, H. S. Cheung, E. F. Sabo and M. A. Ondetti, *Biochemistry*, **16**, 5484 (1977).
372. D. W. Cushman, H. S. Cheung, E. F. Sabo and M. A. Ondetti, *Prog. Cardovasc. Dis.*, **21**, 176 (1978).
373. C. R. W. Edwards and P. L. Padfield, *Lancet*, **1**, 30 (1985).
374. S. J. Lan, S. H. Weinstein and B. H. Migdalof, *Drug. Metab. Dispos.*, **10**, 306 (1982).
375. B. K. Park, P. S. Grabowski, J. H. K. Yeung and A. M. Breckenridge, *Biochem. Pharmacol.*, **31**, 1755 (1982).
376. O. H. Drummer, P. J. Worland and B. Jarrott, *Biochem. Pharmacol.*, **32**, 1563 (1983).
377. J. H. K. Yeung, A. M. Breckenridge and B. M. Park, *Biochem. Pharmacol.*, **32**, 2467 (1983).
378. D. L. Rabenstein and A. A. Isab, *Anal. Chem.*, **54**, 526 (1982).
379. A. A. Isab, *J. Chem. Soc., Dalton Trans.*, 449 (1991).
380. D. A. Keire and D. L. Rabenstein, *Bioorg. Chem.*, **17**, 257 (1989).
381. D. L. Rabenstein and Y. Theriault, *Can. J. Chem.*, **63**, 33 (1985).
382. A. A. Isab, *J. Inorg. Biochem.*, **30**, 69 (1987).
383. M. A. Hughes, G. L. Smith and D. R. Williams, *Inorg. Chim. Acta*, **107**, 247 (1985).
384. G. L. Christie, M. A. Hughes, S. B. Rees and D. R. Williams, *Inorg. Chim. Acta*, **151**, 215 (1988).
385. P. L. Bellon, M. Manassero and M. Sansoni, *Ric. Sci.*, **39**, 173 (1969).
386. P. D. Gavens, J. J. Guy, M. J. Mays and G. M. Sheldrick, *Acta Crystallogr., Sect. B*, **33**, 137 (1977).
387. A. A. Isab and C. F. Shaw III, *J. Inorg. Biochem.*, **38**, 95 (1990).
388. A. A. Isab and M. S. Hussain, *Polyhedron*, **4**, 1683 (1985).
389. M. S. Hussain and A. A. Isab, *Transition Met. Chem.*, **9**, 398 (1984).
390. A. A. Isab, *Polyhedron*, **8**, 2823 (1989).
391. D. H. Brown, G. McKlinley and W. W. Smith, *J. Chem. Soc., Dalton Trans.*, 1874 (1977).
392. D. T. Hill, B. M. Sutton, A. A. Isab, T. Razi, P. J. Sadler, J. M. Trooster and G. H. M. Callis, *Inorg. Chem.*, **22**, 2936 (1983).
393. P. J. Sadler, *Struct. Bonding (Berlin)*, **29**, 171 (1976).
394. C. F. Shaw III, *Inorg. Perspect. Biol. Med.*, **2**, 287 (1979).
395. A. A. Isab and P. J. Sadler, *J. Chem. Soc., Dalton Trans.*, 1657 (1981).
396. L. F. Larkworthy and D. Sattari, *J. Inorg. Nucl. Chem.*, **42**, 551 (1980).
397. A. A. Isab, I. Ghazi and A. R. Al-Arfaj, *J. Chem. Soc., Dalton Trans.*, 841 (1993).
398. G. G. Graham, T. M. Haavisto, P. J. McNaught, C. D. Browne and G. D. Champion, *J. Rheum.*, **9**, 527 (1982).
399. D. W. James, N. W. Ludvigsen, L. G. Clelend and S. C. Milazzo, *J. Rheum.*, **9**, 532 (1982).
400. G. G. Graham, T. M. Haavisto, H. M. Jones and G. D. Champion, *Biochem. Pharmacol.*, **33**, 1257 (1984).

401. G. Lewis and C. F. Shaw III, *Inorg. Chem.*, **25**, 58 (1986).
402. R. D. Hancock, N. P. Finklestein and A. J. Avres, *J. Inorg. Nucl. Chem.*, **34**, 3747 (1972).
403. A. A. Isab, A. L. Hormann, M. T. Coffer and C. F. Shaw III, *J. Am. Chem. Soc.*, **110**, 3278 (1988).
404. A. A. Isab, *J. Inorg. Biochem.*, **46**, 145 (1992).
405. A. L. Hormann, C. F. Shaw III, D. W. Bennett and W. M. Reiff, *Inorg. Chem.*, **25**, 3953 (1986).
406. H. Schmidbaur, B. Brachthäuser and O. Steigelmann, *Angew. Chem.*, **103**, 1552 (1991).
407. H. Schmidbaur, B. Brachthäuser, S. Gamper, A. Schier and O. Steigelmann, *Z. Naturforsch.*, **47b**, 1725 (1992).
408. H. Willner, J. Schaebs, G. Hwang, F. Mistry, R. Jones, J. Trotter and F. Aubke, *J. Am. Chem. Soc.*, **114**, 8972 (1992).
409. H. Willner and F. Aubke, *Inorg. Chem.*, **29**, 2195 (1990).
410. R. C. Thompson in *Inorganic Sulphur Chemistry* (Ed. G. Nickless), Elsevier, Amsterdam, 1968, p. 821.
411. R. J. Gillespie, *Acc. Chem. Res.*, **1**, 202 (1968).
412. L. H. Jones, *Inorganic Vibrational Spectroscopy*, Vol. 1, Marcel Dekker, New York, 1971, p. 122.
413. Y. Yang, V. Ramamoorthy and P. R. Sharp, *Inorg. Chem.*, **32**, 1946 (1993).
414. V. Ramamoorthy and P. R. Sharp, *Inorg. Chem.*, **29**, 3336 (1990).
415. M. M. Rahman, H. Y. Liu, A. Prock and W. P. Giering, *Organometallics*, **6**, 650 (1987).
416. D. R. Williamson and M. C. Baird, *J. Inorg. Nucl. Chem.*, **34**, 3393 (1972).
417. A. K. Burrell, D. L. Clark, P. L. Gordon, A. P. Sattelberger and J. C. Bryan, *J. Am. Chem. Soc.*, **116**, 3813 (1994).
418. B. Slootmaekers, E. Manessi-Zoupa, S. P. Perlepes and H. O. Desseyn, *Spectrochim. Acta, Part A*, **52**, 1255 (1996).
419. A. C. Fabretti, G. C. Pellacani, G. Peyronel and B. Scapinelli, *J. Inorg. Nucl. Chem.*, **36**, 1067 (1974).
420. H. Hofmans, H. O. Desseyn, R. Dommisse and M. A. Herman, *Bull. Soc. Chim. Belg.*, **91**, 175 (1982).
421. H. Hofmans, H. O. Desseyn and M. A. Herman, *Spectrochim. Acta, Part A*, **38**, 1307 (1982).
422. H. Hofmans, P. Geboes and H. O. Desseyn, *Spectrochim. Acta, Part A*, **42**, 969 (1986).
423. P. Geboes and H. O. Desseyn, *Spectrochim. Acta, Part A*, **44**, 963 (1986).
424. B. Slootmaekers, S. P. Perlepes and H. O. Desseyn, *Spectrochim. Acta, Part A*, **45**, 1211 (1989).
425. T. Saitoh, K. Mori and R. Itoh, *Chem. Phys.*, **60**, 161 (1982).
426. T. H. Baum, *J. Electrochem. Soc.*, **134**, 2616 (1987).
427. T. H. Baum and C. R. Jones, *J. Vac. Sci. Technol.*, **4**, 1187 (1986).
428. T. H. Baum, E. E. Marinero and C. R. Jónes, *Appl. Phys. Lett.*, **49**, 1213 (1986).
429. C. S. Gibson and W. M. Colles, *J. Chem. Soc.*, 2407 (1931).
430. R. B. Klassen and T. H. Baum, *Organometallics*, **8**, 2477 (1989).
431. R. L. Lindvedt, in *Concepts in Inorganic Photochemistry* (Eds. A. W. Adamson and P. D. Fleischauer), Wiley, New York, 1975, pp. 299–322.
432. D. H. Volman and L. W. Swanson, *J. Am. Chem. Soc.*, **82**, 4141 (1960).
433. D. Mickewich and J. Turkevich, *J. Phys. Chem.*, **72**, 2703 (1968).
434. T. D. Son and J. Sutton, *J. Phys. Chem.*, **75**, 851 (1971).
435. K. I. Goldberg and R. G. Bergman, *J. Am. Chem. Soc.*, **111**, 1285 (1989).
436. H. Schmidbaur and M. Heimann, *Z. Naturforsch., Teil B*, **29**, 485 (1974).
437. H. Schmidbaur, *Angew. Chem., Int. Ed. Engl.*, **22**, 907 (1983).
438. J. P. Fackler, Jr., H. H. Murray and J. D. Basil, *Organometallics*, **3**, 821 (1984).
439. H. Schmidbaur and R. Franke, *Inorg. Chim. Acta*, **13**, 84 (1975).
440. H. Schmidbaur, J. R. Mandl, A. Frank and G. Huttner, *Chem. Ber.*, **109**, 466 (1976).
441. J. P. Fackler, Jr. and J. D. Basil, in *Inorganic Chemistry: Toward the 21st Century* (Ed. M. H. Chisholm), JACS Symposium Series, No. 211, 1983, p. 201.
442. J. P. Fackler, Jr. and J. D. Basil, *Organometallics*, **1**, 871 (1982).
443. J. D. Basil, H. H. Murray, J. P. Fackler, Jr., J. Tocher, A. M. Mazany, T. J. Delord, B. Trzcin-ska-Bancroft, H. C. Knachel and D. S. Dudis, *J. Am. Chem. Soc.*, **107**, 6908 (1985).
444. H. C. Knachel, D. S. Dudis and J. P. Fackler, Jr., *Organometallics*, **3**, 1312 (1984).
445. H. Schmidbaur and J. R. Mandl, *Naturwissenschaften*, **63**, 585 (1976).
446. H. H. Murray, J. P. Fackler, Jr. and A. M. Mazany, *Organometallics*, **3**, 1310 (1984).
447. H. H. Murray, J. P. Fackler, Jr. and A. M. Mazany, *Organometallics*, **4**, 154 (1985).

448. H. Schmidbaur and P. Jandik, *Inorg. Chim. Acta*, **74**, 97 (1983).
449. H. Schmidbaur and R. Franke, *Inorg. Chim. Acta*, **13**, 85 (1975).
450. H. C. Knachel, C. A. Dettorre, H. J. Galaska, T. A. Salupo, J. P. Fackler, Jr. and H. H. Murray, *Inorg. Chim. Acta*, **126**, 7 (1987).
451. R. G. Raptis, J. P. Fackler, Jr., J. D. Basil and D. S. Dudis, *Inorg. Chem.*, **30**, 3072 (1991).
452. C. A. McAuliffe, R. V. Parish and P. D. Randall, *J. Chem. Soc., Dalton Trans.*, 1730 (1979).
453. A. D. Westland, *Can. J. Chem.*, **47**, 4135 (1969).
454. K. Nakamoto, *Infrared and Raman Spectra of Inorganic and Coordination Compounds*, Wiley, New York, 1978, p. 114.
455. P. Braunstein and R. J. H. Clark, *J. Chem. Soc., Dalton Trans.*, 1845 (1973).
456. I. Haiduc and C. Silvestri, *Coord. Chem. Rev.*, **99**, 253 (1990).
457. B. M. Sutton, in *Platinum, Gold and Other Metal Chemotherapeutic Agents* (Ed. S. J. Lippard), ACS Symposium Series 209, Washington D.C., 1983, p. 355.
458. A. Lorbel and T. M. Simon, *Gold Bull.*, **12**, 149 (1979).
459. R. V. Parish, in *Mössbauer Spectroscopy Applied to Inorganic Chemistry* (Ed. G. J. Long), Plenum Press, New York, 1984, p. 577.
460. F. Bonati, A. Burini, B. R. Pietroni, S. Calogero and F. E. Wagner, *J. Organomet. Chem.*, **309**, 363 (1986).
461. F. Bonati, A. Cingolani, S. Calogero and F. E. Wagner, *Inorg. Chim. Acta*, **127**, 87 (1987).
462. F. Bonati, A. Burini, B. R. Pietroni, S. Calogero and F. E. Wagner, *J. Organomet. Chem.*, **408**, 125 (1991).
463. S. Calogero, F. E. Wagner and G. Ponticelli, *Polyhedron*, **12**, 1459 (1993).
464. G. H. M. Calis and N. Hadjiliadis, *Inorg. Chim. Acta*, **91**, 203 (1984).
465. P. G. Jones, A. G. Maddock, M. J. Mays, M. M. Muir and F. A. Williams, *J. Chem. Soc., Dalton Trans.*, 1434 (1977).
466. R. G. Nuzzo and D. L. Allara, *J. Am. Chem. Soc.*, **105**, 4481 (1983).
467. C. D. Bain, E. B. Troughton, Y.-T. Tao, J. Evail, G. M. Whitesides and R. G. Nuzzo, *J. Am. Chem. Soc.*, **111**, 321 (1989).
468. M. D. Porter, T. B. Bright, D. Allara and C. E. D. Chidsey, *J. Am. Chem. Soc.*, **109**, 3559 (1987).
469. B. E. Winger, R. K. Julian, Jr. and R. G. Cooks, *J. Am. Chem. Soc.*, **113**, 8967 (1991).
470. V. H. Wysocki, J. L. Jones and J.-M. Ding, *J. Am. Chem. Soc.*, **113**, 8969 (1991).
471. P. Schwerdtfeger, *Mol. Phys.*, **86**, 359 (1995).
472. D. Andrea, U. Häussermann, M. Dolg and H. Stoll, *Theor. Chim. Acta*, **77**, 123 (1990).
473. M. Dolg and H. Stoll, *Theor. Chim. Acta*, **75**, 369 (1989).
474. W. F. C. Ferguson, *Phys. Rev.*, **31**, 969 (1928).
475. D. M. Bishop, *Rev. Mod. Phys.*, **62**, 343 (1990).
476. S. Wilson, in *Methods in Computational Chemistry* (Ed. S. Wilson), Vol. 4, Plenum Press, New York, 1987, p. 1.
477. P. M. Morse, *Phys. Rev.*, **34**, 57 (1929).
478. J. A. Meli and K. A. Motakabbir, *Med. Phys.*, **20**, 1251 (1993).
479. *Manual of Procedures*, Chap. 12, Collaborative Ocular Melanoma Study Coordination Center, Baltimore, 1992.
480. J. Cygler, J. Szanto, M. Soubra and D. W. O. Rogers, *Med. Phys.*, **17**, 172 (1990).
481. M. A. Aubart and L. H. Pignolet, *J. Am. Chem. Soc.*, **114**, 7901 (1992).
482. D. M. Heinekey and W. J. Oldham, Jr., *Chem. Rev.*, **93**, 913 (1993).
483. G. G. Hlatky and R. H. Crabtree, *Coord. Chem. Rev.*, **65**, 1 (1985).
484. A. C. Albeniz, D. M. Heinekey and R. H. Crabtree, *Inorg. Chem.*, **30**, 3632 (1991).
485. S. W. Carr, E. H. Fowles, X. L. R. Fontaine and B. L. Shaw, *J. Chem. Soc., Dalton Trans.*, 573 (1990).
486. M. S. Chinn, D. M. Heinekey, N. G. Payne and C. D. Sofield, *Organometallics*, **8**, 1824 (1989).
487. G. K. Anderson, S. E. Saum, R. J. Cross and S. A. Morris, *Organometallics*, **2**, 280 (1983).
488. G. Parshall, *J. Am. Chem. Soc.*, **90**, 1669 (1968).
489. B. R. James, *Homogeneous Hydrogenations*, Wiley-Interscience, New York, 1973.
490. G. A. Somorjai, *Chemistry in Two Dimensions: Surfaces*, Cornell Univ. Press, Ithaca, New York, 1981.
491. D. R. Anton and R. H. Crabtree, *Organometallics*, **2**, 855 (1983).
492. P. N. Rylander, *Catalytic Hydrogenation over Platinum Metals*, Chap. 11, Academic Press, New York, 1967.

493. M. Hudlicky, *Reductions in Organic Chemistry*, Halstead Press, New York, 1984, pp. 71–76.
494. B. S. Gudkov, *Russ. Chem. Rev.*, **55**, 259 (1986).
495. G. C. Bond, *Catalysis by Metals*, Chap. 8, Academic Press, New York, 1962.
496. P. Nazario and A. Brenner, in *Proc. 9th Int. Congr. Catal.* (Eds. M. J. Phillips and M. Ternan), 1988, *Chem. Inst. Can.: Ottawa, Ont.*; (*Chem. Abstr.*, **111**, 84701a (1989)) p. 1020.
497. C. Kemball, *J. Chem. Soc.*, 735 (1956).
498. P. G. T. Fogg and W. Gerrard, *Solubility of Gases in Liquids*, Wiley, Chichester, 1991.
499. M. W. Cook, D. N. Haxson and B. J. Alder, *J. Chem. Phys.*, **26**, 748 (1957).
500. C. L. Young, *Solubility Data Series. Hydrogen and Deuterium*, Vol. 516, Pergamon Press, Oxford, 1981.
501. M. J. Hostetler and R. G. Bergman, *J. Am. Chem. Soc.*, **114**, 7629 (1992).
502. S. Z. Roginsky, *Theoretical Principles of Isotopic Methods of Investigation of Chemical Reactions*, Edition of Academy of Science of USSR, Moscow, 1956, pp. 73–103.
503. J. J. Steggerda, J. J. Bour and J. W. A. van der Velden, *Recl. Trav. Chim. Pays-Bas*, **101**, 164 (1982).
504. M. A. Aubart, B. D. Chandler, R. A. T. Gould, D. A. Krogstad, M. F. J. Schoondergang and L. H. Pignolet, *Inorg. Chem.*, **33**, 3724 (1994).
505. K. Balakrishnan and J. Schwank, *J. Catal.*, **132**, 451 (1991).
506. D. Rouabah and J. Fraissard, *J. Catal.*, **144**, 30 (1993).
507. A. Sachdev and J. Schwank, *J. Catal.*, **120**, 353 (1989).
508. P. A. Sermon, J. M. Thomas, K. Keryou and G. R. Millward, *Angew. Chem., Int. Ed. Engl.*, **26**, 918 (1987).
509. K. Balakrishnan, A. Sachdev and J. Schwank, *J. Catal.*, **121**, 441 (1990).
510. R. C. Yates and G. A. Samorjai, *J. Catal.*, **103**, 208 (1987).
511. J. K. A. Clarke, L. Manninger and T. Bair, *J. Catal.*, **54**, 230 (1978).
512. P. Braunstein and J. Rose, *Gold Bull.*, **18**, 17 (1985).
513. G. Suss-Fink and G. Meister, *Adv. Organomet. Chem.*, **35**, 41 (1993).
514. M. Ichikawa, *Adv. Catal.*, **38**, 283 (1992).
515. G. Munteanu, L. Ilieva and D. Andreeva, *Thermochim. Acta*, **291**, 171 (1997).
516. D. Andreeva, V. Idakiev, T. Tabakova, A. Andreev and R. Giovanoli, *Appl. Cat., A: General*, **134**, 275 (1996)
517. D. Andreeva, V. Idakiev, T. Tabakova and A. Andreev, *J. Catal.*, **158**, 354 (1996).
518. L. I. Ilieva, D. H. Andreeva and A. Andreev, *Thermochim. Acta*, **292**, 169 (1997).
519. D. Andreeva, T. Tabakova, V. Idakiev, R. Giovanoli and A. Andreev, *3rd European Congress on Catalysis, EuroCat. 3*, Krakow, 1997, p. 703.
520. A. Donato, A. M. Visco, G. Neri, C. Milone and S. Galvagno, *3rd European Congress on Catalysis, EuroCat. 3*, Krakow, 1997, p. 13.
521. D. Nazimek and J. Ryczkowski, *3rd European Congress on Catalysis, EuroCat. 3*, Krakow, 1997, p. 54.
522. J. L. Dote and R. L. Mowery, *J. Phys. Chem.*, **92**, 1571 (1988).
523. D. L. Allara and R. G. Nuzzo, *Langmuir*, **1**, 45 (1985).
524. J. F. Rabolt, F. C. Burns, N. E. Schlotter and J. D. Swalen, *J. Chem. Phys.*, **78**, 946 (1983).
525. D. L. Allara and J. D. Swalen, *J. Phys. Chem.*, **86**, 2700 (1982).
526. D. D. Saperstein, *J. Phys. Chem.*, **90**, 1408 (1986).
527. L. H. Dibois, B. R. Zegarski and R. G. Nuzzo, *Langmuir*, **2**, 412 (1986).
528. D. Hadzi, B. Orel and A. Novak, *Spectrochim. Acta, Part A*, **29 A**, 1745 (1973).
529. L. Salem, *J. Chem. Phys.*, **37**, 2100 (1962).
530. M. Gallorini, C. Birattari, M. Bonardi, L. Magon and E. Sabbioni, *J. Radioanal. Nucl. Chem.*, **160**, 549 (1992).
531. C. Birattari and M. Bonardi, *Excitation Functions for $^{195m,g}Hg/^{195m}Au$ Generator Production*, Proc. 3rd World Congress on Nuclear Medicine and Biology, Paris, 1982, Pergamon Press, Paris, 1982, p. 1119.
532. M. Bonardi, F. Groppi, C. Birattari and G. Alberti, *J. Labelled Compd. Radiopharm.*, **26**, 185 (1989).
533. T. N. Fraser, *Ann. Rheum. Dis.*, **4**, 71 (1961).
534. J. W. Sigler, G. B. Bluhm, H. Duncan, J. T. Sharp, D. C. Ensign and W. R. McCrum, *Ann. Intern. Med.*, **80**, 21 (1974).
535. B. M. Sutton, E. McGusty, D. T. Walz and M. J. DiMartino, *J. Med. Chem.*, **15**, 1095 (1972).

536. D. T. Walz, M. J. DiMartino, L. W. Chakrin, B. M. Sutton and A. Misher, *J. Pharmacol. Exp. Ther.*, **197**, 1 (1976).
537. D. T. Walz, M. J. DiMartino, D. E. Griswold, A. P. Intoccia and T. L. Flanagan, *Am. J. Med.*, **75**, 90 (1983).
538. R. H. Freyberg, M. Ziff and J. Baum, in *Arthritis and Allied Conditions* (Eds. J. L. Hollander and D. J. McCarty), 8th edn., Lea and Febiger, Philadelphia, 1972, p. 455.
539. N. J. Zvaifler, in *Arthritis and Allied Conditions* (Ed. D. J. McCarty), 9th edn., Lea and Febiger, Philadelphia, 1979, pp. 355–367.
540. H. Zeidler, *Rheumatology*, **8**, 175 (1983).
541. S. M. Cottrill, H. L. Sharma, D. B. Dyson, R. V. Parish and C. A. McAuliffe, *J. Chem. Soc., Perkin Trans. II*, 53 (1989).
542. A. Lorbel and T. M. Simon, *Gold Bull.*, **12**, 149 (1979).
543. R. V. Parish, *Gold Bull.*, **20**, 3 (1987).
544. E. Jellum, E. Munthe, G. Guldaal and J. Aaseth, *Scand. J. Rheumatol., Suppl.*, **28**, 28 (1979).
545. E. Jellum, E. Munthe, G. Guldaal and J. Aaseth, *Ann. Rheum. Dis.*, **39**, 155 (1980).
546. E. Jellum and E. Munthe, *Ann. Rheum. Dis.*, **41**, 431 (1982).
547. I. Jaffé, *Ann. Rheum. Dis.*, **27**, 14 (1963).
548. E. Arigoni-Martelli, E. Bramm and L. Binderup, *Eur. J. Rheumatol. Inflamm.*, **1**, 197 (1978).
549. A. Taylor, L. J. King and V. Marks, *Xenobiotica*, **15**, 221 (1985).
550. A. P. Intoccia, T. L. Flanagan, D. T. Walz, L. Gutzail, J. E. Swagdis, J. Flagiello, B. Y.-H. Hwang, R. H. Dewey and H. Noguchi, *J. Rheumatol., Suppl. 8*, **9**, 90 (1982).
551. R. C. Blodgett, *Am. J. Med.*, **75**, 86 (1983).
552. K. Blocka, S. Dromgoole, D. Furst and H. Paulis, *Arthritis Rheum.*, **23**, 654 (1980).
553. D. T. Walz, D. E. Griswold, M. J. DiMartino and E. E. Bumbier, *J. Rheumatol., Suppl. 5*, **6**, 81 (1982).
554. J. D. Herlinger, C. Alsen, R. Beress, U. Hecker and W. Weikert, *J. Rheumatol., Suppl. 8*, **9**, 110 (1982).
555. D. T. Hill, B. M. Sutton, S. H. Levinson, J. Meier, A. J. Villani and C. B. Spainhour, *J. Labelled Compd. Radiopharm.*, **20**, 363 (1983).
556. A. K. Al-Sa'ady, C.A. McAuliffe, R. V. Parish and J. A. Sandbank, *Inorg. Synth.*, **23**, 191 (1985).
557. K. Tepperman, R. Finer, S. Donovan, R. C. Elder, J. Doi, D. Ratliff and K. Ng, *Science*, **255**, 430 (1984).
558. C. F. Shaw, N. A. Schaeffer, R. C. Elder, M. K. Eidsness, J. M. Trooster and G. H. M. Calis, *J. Am. Chem. Soc.*, **106**, 3511 (1984).
559. M. T. Coffer, C. F. Shaw, M. K. Eidsness, J. W. Watkins and R. C. Elder, *Inorg. Chem.*, **25**, 333 (1986).
560. E. M. Mogilnicka and M. Webb, *Biochem. Pharmacol.*, **32**, 134 (1983).
561. R. P. Sharma and E. G. McQueen, *Biochem. Pharmacol.*, **31**, 2153 (1983).
562. J. E. Laib, C. F. Shaw, D. H. Petering, M. K. Eidsness, R. C. Elder and J. S. Garvey, *Biochemistry*, **24**, 1977 (1985).
563. B. Vernon-Roberts, J. L. Dove, J. D. Jessop and W. Henderson, *Ann. Rheum. Dis.*, **39**, 477 (1976).
564. A. A. Isab and P. J. Sadler, *Biochim, Biophys. Acta*, **492**, 322 (1977).
565. *Smoking and Health*, Chap. 6, Report of the Advisory Commitee of the Surgeon General of the Public Health Service, U.S. Public Health Service Publication 1103, Washington D.C., 1964, p. 60.
566. A. R. Pettigrew and G. S. Fell, *Clin. Chem.*, **19**, 466 (1973).
567. P. J. Sadler, *Struct. Bond.*, **29**, 171 (1976).
568. C. F. Shaw, *Inorg. Perspect. Biol. Med.*, **2**, 287 (1979).
569. D. H. Brown and W. E. Smith, *Chem. Soc. Rev.*, 217 (1980).
570. A. A. Isab and M. S. Hussain, *J. Coord. Chem.*, **15**, 125 (1986).
571. A. A. Isab and M. S. Hussain, *Polyhedron*, **4**, 1688 (1985).
572. A. A. Isab and M. S. Hussain, *Transition Met. Chem.*, **9**, 398 (1984).
573. M. S. Hussain and A. A. Isab, *J. Coord. Chem.*, **14**, 17 (1985).
574. M. S. Hussain and A. A. Isab, *Transition Met. Chem.*, **10**, 178 (1985).
575. R. Faure, E. J. Vincent, G. Assef, J. Kister and J. Metzger, *Org. Magn. Reson.*, **9**, 688 (1977).
576. C. F. Shaw III, *Comments Inorg. Chem.*, **8**, 233 (1989).

577. L. F. Larkworthy and D. Sattari, *J. Inorg. Nucl. Chem.*, **42**, 551 (1980).
578. A. A. Isab and P. J. Sadler, *J. Chem. Soc., Chem. Commun.*, 1051 (1976).
579. A. A. Isab and P. J. Sadler, *J. Chem. Soc., Dalton Trans.*, 135 (1982).
580. A. A. Isab, *J. Inorg. Biochem.*, **30**, 69 (1987).
581. C. F. Shaw, G. Schmitz, H. O. Thompson and P. J. Witkiewicz, *J. Inorg. Biochem.*, **10**, 317 (1979).
582. C. F. Shaw, J. Eldridge and M. P. Cancaro, *J. Inorg. Biochem.*, **14**, 267 (1981).
583. C. J. Danpure, *Biochem. Pharmacol.*, **25**, 2343 (1976).
584. A. A. Isab and A. P. Arnold, *J. Coord. Chem.*, **20**, 95 (1989).
585. D. Lewis, A. H. Capell, C. J. McNiel, M. S. Iqbal, D. H. Brown and W. E. Smith, *Ann. Rheum. Dis.*, **42**, 566 (1983).
586. D. W. James, N. W. Ludvigsen, L. G. Clelend and S. C. Milazzo, *J. Rheum.*, **9**, 532 (1982).
587. A. L. Hormann-Arendt and C. F. Shaw III, *Inorg. Chem.*, **29**, 4683 (1990).
588. C. F. Shaw III, N. S. Memmel and D. Krawczak, *J. Inorg. Biochem.*, **26**, 185 (1986).
589. C. F. Shaw III, N. A. Schaeffer, R. C. Elder, M. K. Eidness, J. M. Trooster and G. H. M. Callis, *J. Am. Chem. Soc.*, **106**, 3511 (1984).
590. D. H. Brown, G. McKinlay and W. E. Smith, *J. Chem. Soc., Dalton Trans.*, 1874 (1977).
591. F. N. Ghadially, A. F. Oryschak and D. M. Mitchell, *Ann. Rheum. Dis.*, **35**, 67 (1976).
592. B. Vernon Roberts, J. L. Dore, J. D. Jessop and W. J. Henderson, *Ann. Rheum. Dis.*, **35**, 477 (1976).
593. G. G. Graham, J. R. Bales, M. C. Grootveld and P. J. Sadler, *J. Inorg. Biochem.*, **25**, 163 (1984).
594. G. Lewis and C. F. Shaw III, *Inorg. Chem.*, **25**, 58 (1986).
595. A. A. Isab, I. H. Ghazi, M. I. M. Wazeer and H. P. Perzanowski, *J. Inorg. Biochem.*, **50**, 299 (1993).
596. E. Lebowitz and P. Richards, *Semin. Nucl. Med.*, **4**, 257 (1974).
597. E. Garcia, I. Mena and R. de Jong, *J. Nucl. Med.*, **22**, P71 (1981).
598. R. Bett, G. H. Coleman and J. G. Cuninghame, *Nucl. Med. Commun.*, **2**, 75 (1981).
599. C. Brihaye, M. Guillaume, N. Lavi and M. Cogneau, *J. Nucl. Med.*, **23**, 1114 (1982).
600. R. Loeringer and M. Berman, *A Revised Scheme for Calculating the Absorbed Dose from Biologically Distributed Radionuclides*, Pamphlet 1, Society of Nuclear Medicine, New York, 1976.
601. E. J. Underwood, *Trace Elements in Human and Animal Nutrition*, Chap. 14, *Mercury*, Academic Press, New York, 1977, pp. 375–387.
602. F. J. Wackers, R. W. Giles, P. B. Hoffer, R. C. Lange, H. J. Berger, B. L. Zaret, L. Pytlik and M. Plankey, *Am. J. Cardiol.*, **50**, 89 (1982).
603. A. Gottschalk and E. J. Potchen, *Diagnostic Nuclear Medicine*, Ross Golden Series in Diagnostic Radiology, Williams & Wilkins, Baltimore, 1976.
604. I. Mena, K. A. Narahara, R. de Jong and J. Maublant, *J. Nucl. Med.*, **24**, 139 (1983).
605. J. G. Ackers and R. de Jong, *J. Nucl. Med.*, **23**, P68 (1982).
606. P. Lindner, *Eur. J. Nucl. Med.*, **8**, 358 (1983).
607. P. Lindner, F. Wolf and N. Schad, *Eur. J. Nucl. Med.*, **5**, 229 (1980).
608. O. Nickel, P. Lindner and N. Schad, *Eur. J. Nucl. Med.*, **8**, 431 (1983).
609. L. Andersson, L. Hallstadius and S.-E. Strand, *Eur. J. Nucl. Med.*, **14**, 393 (1988).
610. *Radionuclide Transformations, Energy and Intensity of Emission*, ICRP Publication 38, 1983, p. 932, pp. 946–949. Pergamon Press, Oxford, England.
611. *Recommendations of the International Commission on Radiological Protection*, Publication 26, 1977, pp. 21–22. Pergamon Press, Oxford, England.
612. L. Johansson, S. Mattson and B. Nosslin, *Eur. J. Nucl. Med.*, **9**, 485 (1984).
613. J. Xiao-Hai, *J. Radioanal. Nucl. Chem.*, **206**, 17 (1996).
614. M. Neves and L. Patricio, *Int. J. Appl. Radiat. Isot.*, **39**, 183 (1988).
615. K. Nagai, I. Yasuhito and O. Nobuaki, *Int. J. Nucl. Med. Biol.*, **9**, 108 (1982).
616. R. Zeisler, S. F. Stone, R. P. Viscidi and E. H. Cerny, *J. Radioanal. Nucl. Chem.*, **167**, 445 (1993).
617. G. Frens, *Nature Phys. Sci.*, **241**, 20 (1973).
618. J. R. de Mey, *'The Preparation of Immunoglobulin Gold Conjugates (IGS Reagents) and Their Use as Markers for Light and Electron Microscopic Immunocytochemistry', in Immunohistochemistry* (Ed. A. C. Cuello), Wiley, New York, 1983, p. 347.
619. U. Myint, W. Than, H. Htay and K. O. Myint, *J. Radioanal. Nucl. Chem.*, **187**, 399 (1994).
620. U. Myint and S. S. Yi, *J. Radioanal. Nucl. Chem.*, **201**, 269 (1995).

621. S. Takahashi and G. Patrick, *Lab. Anim.*, **21**, 31 (1987).
622. S. Takahashi, S. Asaho, Y. Kubota, H. Sato and O. Matsuoka, *J. Radiat. Res.*, **28**, 227 (1987).
623. A. G. Harmsen, B. A. Muggenburg, B. A. Snipes and D. D. Brice, *Science*, **230**, 1277 (1985).
624. A. G. Harmsen, N. A. Gillett and B. Stegelmeir, *Annual Report of Inhalation Toxicology Research Institute*, Lovelace Biomedical and Environmental Research Institute, LMF-115, Albuquerque, 1986, pp. 101–104.
625. Y. Kubota, S. Takahashi, H. Sato, Y. Yamada and O. Matsouka, *Hoken Butsuri*, **23**, 295 (1988); *Chem. Abstr.*, **110**, 227789c (1989).
626. A. Verheyen, E. Vlaminkx, F. Lauwers, M. Borgers and L. Wouters, *Int. J. Microcirc. Clin. Exp.*, **5**, 321 (1987); *Chem. Abstr.*, **106**, 208206m (1987).
627. R. E. Faw and K. J. Shultis, *Health Phys.*, **62**, 334 (1992); *Chem. Abstr.*, **117**, 65578y (1992).
628. J. Ching, *Precious Met.*, **16**, 129 (1992); *Chem. Abstr.*, **120**, 182517a (1994).
629. M. Knihova, M. Novak, M. Vodak and L. Sprincl, *Cesk. Farm.*, **35**, 359 (1986); *Chem. Abstr.*, **106**, 164148n (1987).
630. T. Muto, *Tokyo-Toritsu Aisotopu Sogo Kenkyusho Kenkyu Hokoku*, **3**, 7 (1986); *Chem. Abstr.*, **106**, 80956m (1987).
631. R. Zhang, S. Bai and Z. Xia, *Zhongguo Haiyang Yaowu*, **9**, 16 (1990); *Chem. Abstr.*, **115**, 35809r (1991).
632. K.-S Chen, C.-L. Tseng and T.-H. Lin, *J. Radioanal. Nucl. Chem.*, **170**, 265 (1993).
633. L. Zhaoda, L. Yinming, D. Yuzheng, Q. Ruisheng, C. Da and Z. Zebo, *J. Radioanal. Nucl. Chem.*, **151**, 113 (1991).
634. M. M. Rajadhyaksha and Z. R. Turel, *J. Radioanal. Nucl. Chem.*, **156**, 341 (1992).
635. S. T. Haeberlin, F. Lux, J. Karl, T. Spruss and H. Schönenberger, *J. Radioanal. Nucl. Chem.*, **113**, 461 (1987).
636. A. B. Malinin, N. V. Kurenkov, M. D. Kozlova and A. S. Sevastyanova, *J. Radioanal. Nucl. Chem., Lett.*, **126**, 17 (1988).
637. M. Esposito, P. Collecchi, M. Oddone and S. Meloni, *J. Radioanal. Nucl. Chem.*, **113**, 437 (1987).
638. (a) *Highlights-97*, International Atomic Energy Agency Annual Report, 4 (1957–1997), IAEA/PI/A22E 97-02553, IAEA, September 1997.
      (b) T. Mochizuki, A. Sakashita, H. Iwata, Y. Ishibashi and N. Gunji, *Fresenius J. Anal. Chem.*, **339**, 889 (1991).
639. D. van Renterghem, R. Cornelis and R. Vanholder, *Anal. Chim. Acta*, **257**, 1 (1992).
640. G. V. Iyengar, W. E. Kollmer and H. J. M. Bowen, *The Elemental Composition of Human Tissues and Body Fluids*, Verlag Chemie, Weinheim, New York, 1978.
641. K. Jørstad, B. Salbu and A. C. Pappas, *Anal. Chem.*, **53**, 1398 (1981).
642. J. C. van Loon and R. R. Barefoot, *Determination of the Precious Metals*, Wiley, New York, 1991.
643. R. R. Barefoot and J. C. van Loon, *Anal. Chim. Acta*, **334**, 5 (1996).
644. C. F. Chai, S. L. Ma, X. Y. Mao, K. N. Liao and W. C. Liu, *J. Radioanal. Nucl. Chem.*, **114**, 281 (1987).
645. L. L. Sundberg, *Anal. Chem.*, **47**, 2037 (1975).
646. G. Koster and G. Schmucker, *Anal. Chim. Acta*, **38**, 179 (1967).
647. K. Kritsotakis and H. J. Tobschall, *Fresenius Z. Anal. Chem.*, **320**, 15 (1985).
648. K. M. Ochsenkühn, M. Ochsenkühn-Petropulu, N. N. Papadopulos and G. Parissakis, *J. Radioanal. Nucl. Chem.*, **212**, 121 (1996).
649. P. Krause, B. Erbslöh, R. Niedergesäß, R. Pepelnik and A. Prange, *Fresenius J. Anal. Chem.*, **353**, 3 (1995).
650. J. M. Lo, K. S. Lin, J. C. Wei and J. D. Lee, *J. Radioanal. Nucl. Chem.*, **216**, 121 (1997).
651. C. L. Tseng, J. M. Lo and S. J. Yeh, *Anal. Sci.*, **3**, 437 (1987).
652. B. S. Shanbhag and Z. R. Turel, *J. Radioanal. Nucl. Chem.*, **197**, 417 (1995).
653. C. Koeberl, P. M. Bayer and K. Höbarth, *J. Radioanal. Nucl. Chem.*, **169**, 270 (1993).
654. V. Valkovic, *Trace Elements in Human Hair*, Garland STPM Press, London, New York, 1977, p. 50.
655. L. G. Stephens-Newsham, M. J. M. Duke, T. R. Overton and D. Ng, *J. Radioanal. Nucl. Chem.*, **113**, 495 (1987).
656. D. Thompson, S. J. Parry and R. Benzing, *J. Radioanal. Nucl. Chem.*, **195**, 209 (1995).

657. L. Xiao, Y. H. Zhang, Q. G. Li, Q. X. Zhang and K. Wang, *J. Radioanal. Nucl. Chem.*, **195**, 43 (1995).
658. M. Šimek, I. Roušar and B. Štverák, *J. Appl. Electrochem.*, **21**, 6 (1991).
659. R. E. W. Jansson, *Electrochim. Acta*, **23**, 1345 (1978).
660. R. E. W. Jansson and R. J. Marshall, *J. Appl. Electrochem.*, **8**, 287 (1978).
661. M. Šimek and I. Roušar, *Collect. Czech. Chem. Commun.*, **49**, 1122 (1984).
662. A. B. Ferreira and R. E. W. Jansson, *Trans. Inst. Chem. Eng.*, **57**, 262 (1979).
663. K. Grudpan and D. Nacapricha, *Anal. Chim. Acta*, **246**, 329 (1991).
664. J. J. Hodt, W. K. Sinclair and D. W. Smithers, *Br. J. Radiol.*, **25**, 419 (1952).
665. U. K. Henschke, A. G. James and W. G. Myers, *Nucleonics*, **11**, 46 (1953).
666. L. L. Meisberger, R. J. Keller and R. J. Shalek, *Radiology*, **90**, 953 (1968).
667. P. T. Scardino, J. M. Frankel, T. M. Wheeler, R. B. Meacham, G. S. Hoffman, C. Searle, J. W. Wilbanks, J. Easley and C. E. Carlton, *J. Urol.*, **132**, 510 (1986).
668. S. A. Loening and S. J. Rosenberg, *Urology*, **29**, 250 (1987).
669. J. Slanina, M. Wannenmacher, K. Kuphal, H. Knufermann, C. Beck and W. Schilli, *Int. J. Radiat. Oncol. Biol. Phys.*, **8**, 1683 (1982).
670. S. K. Jani, E. C. Pennington and B. M. Knosp, *Med. Phys.*, **16**, 632 (1989).
671. L. Sakelliou, K. Sakellariou, K. Sarigiannis, A. Angelopoulos, A. Perris and G. Zarris., *Phys. Med. Biol.*, **37**, 1859 (1992).
672. R. K. Jain and L. T. Baxter, *Cancer Res.*, **48**, 7022 (1988).
673. L. M. Cobb, *Cancer Immunol. Immunother.*, **28**, 235 (1989).
674. P. A. W. Edwards, *Br. J. Cancer*, **51**, 149 (1985).
675. P. Enblad, B. Glimelius, C. Busch, J. Ponten and L. Pahlman, *Br. J. Cancer*, **55**, 503 (1987).
676. R. M. Ludatsher, B. Gellei and D. Barzilai, *J. Pathol.*, **128**, 57 (1979).
677. L. M. Cobb, J. A. Humphreys and A. Harrison, *Br. J. Cancer*, **55**, 53 (1987).
678. J. L. Humm and L. M. Cobb, *J. Nucl. Med.*, **31**, 75 (1990).
679. Z. Liu, Y. Wu and Y. Liu, *Beijing Daxue Xuebao, Ziran Kexueban*, **26**, 147 (1990); *Chem. Abstr.*, **113**, 207504g (1990).
680. L. Zhaogung, W. Yonghui and L. Yuanfang, *He Huaxue Yu Fangshe Xuaxue*, **13**, 18 (1991); *Chem. Abstr.*, **116**, 54724W (1992).
681. O. Scheibe and S. Fisher, *ZfI - Mitt.*, **165**, 69 (1991); *Chem. Abstr.*, **116**, 160607v (1992).
682. P. J. Sadler and R. E. Sue, *Met. - Based Drugs*, **1**, 107 (1994); *Chem. Abstr.*, **121**, 131152r (1994).
683. N. Dubhghaill, M. Orla and P. J. Sadler, *'Gold Complexes in Cancer Chemotherapy', in Metal Complexes in Cancer Chemotherapy* (Ed. B. K. Keppler), VCH Weinheim, Germany, 1993, pp. 221–248,
684. D. Pressman, *Radiolabeled antibodies Ann. N. Y. Acad. Sci.*, **69**, 644 (1957).
685. J. L. Humm, *J. Nucl. Med.*, **27**, 1490 (1986).
686. M. Zieliński and M. Kańska, *'Synthesis and Uses of Isotopically Labelled Compounds of Bismuth, Antimony and Arsenic'*, Chap. 15 in *The Chemistry of Organic Arsenic, Antimony and Bismuth Compounds* (Ed. S. Patai), Wiley, Chichester, 1994.
687. M. Zieliński and M. Kańska, *'Synthesis and Uses of Isotopically Labelled Organic Halides'*, Chap. 10 in *Supplement D2: The Chemistry of Halides, Pseudo-Halides and Azides* (Eds. S. Patai and Z. Rappoport), Wiley, Chichester, 1995.
688. J. Lucocq, *J. Anat.*, **184**, 1 (1994).
689. W. A. Swansiger, *Fusion Technol.*, **14**, 631 (1988); *Chem. Abstr.*, **110**, 200931f (1989).
690. J. L. Maienschein, F. E. McMurphy and V. L. Duval, *Fusion Technol.*, **14**, 701, (1988); *Chem. Abstr.*, **110**, 200937n (1989).
691. S. M. Myers and W. A. Swansiger, *J. Appl. Phys.*, **67**, 1334 (1990).
692. D. R. Begeal, *J. Vac. Sci. Technol.*, **15**, 1146 (1978).
693. E. G. Kounikov, M. B. Epel'baum, A. G. Mirnov and A. G. Kanakin, *Geokhimiya*, **12**, 1736 (1986); *Chem. Abstr.*, **106**, 53453p (1987).
694. G. A. Bishea, J. C. Pinegar and M. D. Morse, *J. Chem. Phys.*, **95**, 5630 (1991).

CHAPTER **16**

Medicinal chemistry of gold compounds

SIMON P. FRICKER

AnorMED Inc. #100 20353-64th Avenue, Langley, BC, V2Y 1N5, Canada
Fax: (604) 530 0976   Email: sfricker@anormed.com

I. METALS IN BIOLOGY

Living organisms range from simple unicellular organisms to sophisticated multicellular, highly organized animals such as man. Within each cell there is a complex, interactive, series of chemical reactions involving both synthesis of new molecules and breakdown of

others. In multicellular organisms there also has to be communication and coordination between cells. Within this plethora of biochemical and physiological events inorganic elements play a vital and fundamental role.

Metals have structural, communication and active functional roles. They are important in maintaining structural integrity, the most obvious example being calcium, as hydroxyapatite, $[3Ca_3(PO_4)_2 \cdot Ca(OH)_2]$, in bone. The tertiary structure of many proteins is maintained by metal ions coordinating to specific amino acid residues within the protein molecule, thus stabilizing its three-dimensional folding. Metals also play a part in communication between different components of an organism. Transmembrane concentration gradients of sodium and potassium ions create a potential difference across nerve cell membranes. Changes in this potential caused by movement of ions across the membrane are responsible for the transmission of nerve impulses. Hormone-induced changes in intracellular calcium concentration are important in the regulation of cell function, often by activating enzymes via the calcium binding protein calmodulin. Metals such as zinc, copper, manganese and iron are also important active constituents of many enzymes participating directly in the catalytic mechanism, for example by stabilizing reaction intermediates or acting as Lewis acids[1].

Metals are therefore essential for the normal functioning of living organisms, hence it is not surprising that metal compounds, either fortuitously or by design, occupy an important niche in modern pharmacopoeias. Metals and their compounds have been used as medicines since the early days of civilization. The ancient Egyptians used copper to sterilize water, the Greek physician Hippocrates was using mercury as a drug in 400 BC, and in the sixteenth century Paracelsus used mercurous chloride as a diuretic. The beginning of the twentieth century saw metals making an impact on modern medicine with Ehrlich's discovery of arsenic organometallic drugs for the treatment of syphilis. Antimony compounds were developed for the treatment of the parasitic disease leishmaniasis and gold compounds introduced for the treatment of arthritis in 1929. Modern medicine makes use of a diverse range of metal-based drugs for a variety of medical applications. Magnesium and aluminium oxides are widely used as antacids both as over-the-counter and prescription medicines and colloidal bismuth subcitrate is used to treat peptic ulcers. Lithium salts are used for the treatment of depression, silver sulphadiazine for topical prophylactic treatment of burn wounds and the platinum compounds cisplatin and carboplatin for cancer therapy[2,3].

II. HISTORICAL USE OF GOLD IN MEDICINE

Gold has been exploited for its putative medical properties throughout the history of civilization[4,5]. The earliest medical use of gold can be traced back to the Chinese in 2500 BC. In medieval Europe alchemists had numerous recipes for an elixir known as *aurum potabile*, many of which contained little gold! A gold cordial could be found in the 'new' pharmacopoeias of the 17th century and was advocated by Nicholas Culpepper for the treatment of ailments caused by a decrease in the vital spirits, such as melancholy, fainting, fevers and falling sickness. Later in the 19th century a mixture of gold chloride and sodium chloride, 'muriate of gold and soda,' $Na[AuCl_4]$, was used to treat syphilis.

The use of gold compounds in modern, twentieth century, medicine began with the discovery in 1890 by the German bacteriologist Robert Koch that gold cyanide $K[Au(CN)_2]$ was bacteriostatic towards the tubercle bacillus[6]. Gold therapy for tuberculosis was subsequently introduced in the 1920s. The suggestion that the tubercle bacillus was a causative agent for rheumatoid arthritis led to the use of gold therapy for this disease[7,8]. Gold therapy soon proved to be ineffective for tuberculosis but, after a thirty-year debate, a clinical study sponsored by the Empire Rheumatism Council confirmed the effectiveness of gold

compounds against rheumatoid arthritis. The early gold compounds used were gold(I) thiolates such as sodium aurothiomalate (**1**) and aurothioglucose (**2**). In 1985 a new compound, auranofin, [tetra-*O*-acetyl-β-D-(glucopyranosyl)thio](triethylphosphine)gold(I) (**3**), was introduced as an orally active gold drug for arthritis[9]. Chrysotherapy, treatment with gold-based drugs (from the Greek word for gold, *chrysos*) is now an accepted part of modern medicine.

(1)   **(2)**

(3)
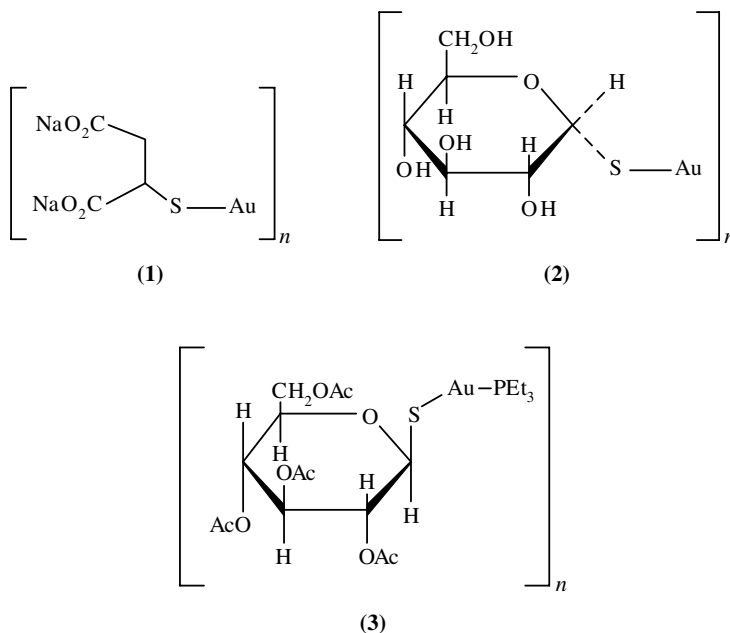
III. GOLD THERAPY FOR RHEUMATOID ARTHRITIS

A. Rheumatoid Arthritis

Rheumatoid arthritis is an inflammatory disease characterized by progressive erosion of the joints resulting in deformities, immobility and a great deal of pain. It is an autoimmune disease in which the body's immune system turns against itself[10]. The immune system is a complex, multi-component system which is strictly controlled by an intricate, interactive network of intercellular protein messenger molecules known as cytokines. In rheumatoid arthritis there is a breakdown of this control and an autoimmune response is mounted against 'self' components known as autoantigens. This results in pannus formation, a malign growth of the synovial cells (the cells lining the joint), and infiltration of the joint space by cells of the immune system, primarily macrophages, and associated production of immunoglobulin proteins, called rheumatoid factors.

Raised levels of chemical mediators, such as prostaglandins, leukotrienes and cytokines, mediate this progressive inflammatory response. There is an upregulation of adhesion molecules leading to further recruitment of phagocytic cells into the inflammatory site. The latter release degradative enzymes such as collagenase, and generate reactive oxygen species OH$^{\bullet}$ and O_2^{-}. Elevated levels of nitric oxide are also produced[11] which can

combine with superoxide to form peroxynitrite[12]. All of these mediators contribute to the resulting tissue damage.

Though there are several new strategies under development for the treatment of rheumatoid arthritis, at present there is no complete cure. The initial therapeutic approach is to treat the symptoms with non-steroidal anti-inflammatory drugs (NSAID) such as aspirin and ibuprofen. Corticosteroids are also used, but their long-term use is discouraged because of adverse side effects. More aggressive therapy is required as the disease progresses in the form of the disease-modifying anti-rheumatic drugs (DMARD)[10]. The first-line DMARD is the immunosuppressant methotrexate. This is followed by a raft of chemically diverse drugs including penicillamine, chloroquine and gold compounds. New strategies include COX-2 selective NSAIDs, immunomodulators, cytokine inhibitors and cytokine therapy, and matrix metalloproteinase inhibitors[13].

B. Chrysotherapy

The gold compounds used to treat arthritis are all linear, two-coordinate gold(I) thiolates[5,14]. The thiolate ligand stabilizes the gold(I) against disproportionation to gold(0) and toxic gold(III) whilst still allowing exchange reactions with biological ligands. These compounds have been shown to exist as polymeric structures both in solution and in the solid state by X-ray techniques such as WAXS and EXAFS[15]. This type of structure requires an extra SR group to cap the 'bare' gold atom at the end of the chain, and the normal preparation of aurothiomalate gives a compound with a typical formula of $[Au_8(STM)_9]^-$.

These drugs are administered by an intramuscular injection[16]. The drug is rapidly absorbed into the bloodstream at a dose which initially gives a serum level of $4-10 \ \mu g \ ml^{-1}$. Some of the gold is rapidly cleared to give a level of $2-3 \ \mu g \ ml^{-1}$, which is then maintained. The drug is distributed to organs throughout the body, particularly the kidney where it eventually accumulates, resulting in nephrotoxicity, one of the major side effects of these drugs. Other adverse reactions include skin reactions, blood disorders and occasional liver toxicity.

The problems inherent in administering a drug on a regular basis by intramuscular injection provided the impetus for the development of a drug with an improved toxicological and pharmacological profile[16]. The main requirement for an improved gold drug was a compound that could be administered orally in low daily doses, giving stable serum levels of active drug at therapeutic concentrations, resulting in an improved therapeutic response and reduced toxicity. Coordination of gold(I) with phosphine ligands stabilizes this oxidation state. A series of compounds with the general formula R_3PAuSR^1, where R is an alkyl group and SR^1 a diverse range of ligands such as thioglucose, acetylated thioglucose, 2-mercaptoethanol and thiocyanate, were investigated. Complexes of this type are monomeric, two-coordinate, linear species and generally non-ionic and lipophilic, and are therefore readily absorbed after oral administration. The triethylphosphine complexes were found to have the optimum pharmacological activity in models of rheumatoid arthritis, and as a result [tetra-O-acetyl-β-D-(glucopyranosyl)thio](triethylphosphine)gold(I), auranofin, was developed as an orally bioavailable drug.

Auranofin has a number of advantages over previous gold drugs. Primarily it can be administered orally, with approximately 25% of the administered gold being absorbed[16]. Gold levels in the blood are lower and can be sustained for longer periods of time with less retention of the gold in the tissues. This results in a reduction in the toxicity of auranofin, although this is offset by a reduction in efficacy.

There has been much debate over the efficacy of gold drugs in rheumatoid arthritis[17,18]. The gold drugs are slow-acting and responses are not seen until about three months after the start of treatment. It is now generally accepted that these drugs are efficacious as DMARDS, though they are not as effective as methotrexate which is now regarded as the DMARD of first choice. The gold compounds, however, are as active as any of the other second-line disease-modifying agents and still make up an important part of the clinician's armamentarium against rheumatoid arthritis.

C. Other Inflammatory Disorders

Gold drugs have been used to treat a variety of other rheumatic diseases including psoriatic arthritis[19], a form of arthritis associated with psoriasis, juvenile arthritis, palindromic rheumatism and discoid lupus erythematosus[20]. Gold therapy has also been investigated as a treatment for various inflammatory skin disorders such as psoriasis[21], pemphigus[22] and urticaria[23].

IV. MECHANISM OF ACTION OF ANTIARTHRITIC GOLD DRUGS

A. Biological Chemistry of Gold

The mechanism of action of the antiarthritic gold compounds is unclear, in part due to the lack of understanding of the disease process. An appreciation of the chemical interaction of gold complexes with naturally occurring ligands in a biological environment is helpful in our understanding of their pharmacological activity.

There are several excellent reviews on the biological chemistry of gold[24-27] so only a brief overview will be given here of selected aspects pertinent to the pharmacology of gold drugs. Gold can exist in a number of oxidation states: $-I$, 0, I, II, III, IV and V; however, only gold 0, I and III are stable in aqueous, and therefore biological, environments. Both gold(I) and gold(III) are unstable with respect to gold(0) and are readily reduced by mild reducing agents (equations 1 and 2).

$$Au^{1+} + 1e^- \longrightarrow Au(0) \qquad E^0 = +1.68 \text{ V} \tag{1}$$

$$Au^{3+} + 3e^- \longrightarrow Au(0) \qquad E^0 = +1.42 \text{ V} \tag{2}$$
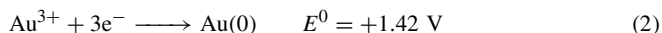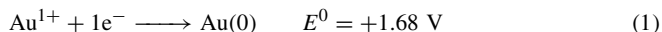
Gold(I) can be stabilized by cyanide or thiolate ligands, including naturally occurring thiols such as the amino acid cysteine (CysSH), e.g. equation 3.

$$[Au(CysS^-)_2]^- + 1e^- \longrightarrow Au(0) + 2CysS^- \qquad E^0_{1/2} = -0.14 \text{ V} \tag{3}$$
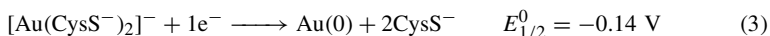
This means that gold(I) compounds can undergo associative ligand exchange reactions with cysteine-rich peptides and proteins such as glutathione, metallothionein and albumin[28,29], particularly where the pK_{SH} is low, e.g. the Cys-34 of albumin[30].

Gold(I) is thermodynamically more stable than gold(III). Many gold(III) complexes are strong oxidizing agents, being reduced to Au(I), and this means that they are generally toxic. This reduction can be driven by biologically occurring reductants such as thiols (equations 4 and 5).

$$Au(III)L_4 + 2RSH \longrightarrow Au(I)L_2 + 2L + 2H^+ + RSSR \tag{4}$$

$$Au(III)L_4 + RSR + H_2O \longrightarrow Au(I)L_2 + RS(O)R + 2L + 2H^+ \tag{5}$$
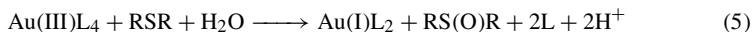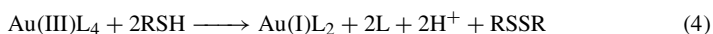
B. Gold–Protein Interactions

The ability of gold thiol compounds to undergo ligand exchange reactions with biological ligands such as the amino acid cysteine may contribute to their pharmacological activity. One proposal is that gold drugs inhibit the interaction of the degradative enzymes by reacting with thiol groups in metalloproteinases such as collagenase (see Section IV.C)[31]. Gold(I) also undergoes ligand exchange with other biological proteins including albumin, and metallothioneins forming aurothioneins[29]. Gold–peptide interactions may also account for some of the immunopharmacology of gold compounds, including some of their side effects (see Section IV.E)[32]. The precise pharmacological significance of these interactions is unclear but may well provide a focus for the development of third-generation antiarthritic drugs.

C. Biochemical Mechanisms

There are numerous hypotheses to explain the biochemical mechanism of gold drugs. As discussed in Section IV.B, one proposal is that gold drugs inhibit the interaction of the degradative enzymes by reacting with essential thiol groups on the protein. Gold compounds will also inhibit enzymes where there are no free sulphhdryl groups, and this is reflected in the wide and varied range of enzymes that can be inhibited by gold compounds[25]. The gold concentration required for inhibition is frequently in the millimolar range, much higher than the serum levels found in patients undergoing chrysotherapy, and at best not less than 50 µM. In some instances K_i values for purified enzymes have been reported, but these are difficult to interpret when extrapolated to the *in vivo* context. In these cases gold has been shown to be a non-competitive inhibitor. Though inhibition of sulphhydryl-containing proteolytic enzymes may occur *in vivo*, a careful consideration of the evidence indicates that this is unlikely to be the primary action of gold drugs[33]. Gold drugs produce a number of effects on the immune system and a number of alternative hypotheses have been proposed to explain these observations.

There is evidence to suggest that auranofin inhibits the production of reactive oxygen species such as superoxide and the hydroxyl radical produced during the oxidative burst of activated polymorphonuclear cells (a phagocytic cell of the immune system)[34]. One proposed mechanism for this observation is that gold complexes may react with the cyanide released during phagocytosis to form aurocyanide. This metabolite can readily enter cells and has been shown to inhibit the oxidative burst[20]. Gold compounds also exert a number of effects on the immune response. The gold(I) thiolates have been demonstrated to inhibit mitogen and IL-2 stimulated T cell proliferation[35,36]. This phenomenon is only seen at high gold concentrations and is not observed *in vivo*. One possible suggestion for the immunopharmacologic action is that the gold complexes may interfere with antigen presentation by forming chelates with antigenic peptides containing two or more cysteines (also Section IV.E)[37]. Treatment with gold drugs also leads to a reduction in cytokine levels[38,39]. Recent data suggest that this may be due to inhibition of transcription of the genes responsible for control of cytokine expression (Section IV.D)[33].

There is some evidence to suggest that auranofin may have a different mechanism of action to aurothiomalate[40]. Much of this work, however, has been performed *in vitro* using intact auranofin, which *in vivo* is rapidly metabolized. Upon oral administration it is deacylated in the intestine prior to absorption. The thioglucose ligand can then be replaced by ligand exchange with other thiols, and one proposal for the mechanism of gold transfer across cell membranes is ligand exchange with membrane associated thiols. Once inside cells the triethylphosphine ligand is readily lost, where it is oxidized to the

triethylphosphine oxide, thus leaving a gold(I) thiol as the possible active species[31]. The mechanism of action of auranofin could therefore be similar to that of the simple gold(I) thiolates.

D. Transcription

One of the most interesting new findings arising from the studies on the interactions of gold drugs with biological systems is their apparent ability to down-regulate transcription. Transcription is the copying of the DNA sequence encoding genes into the RNA messenger molecule. This is then subsequently translated into the protein product encoded by the gene. The process of transcription is carried out by the enzyme RNA polymerase and is controlled and directed by a number of ancillary proteins called transcription factors. These ancillary proteins bind to specific DNA sequences and initiate transcription of specific genes. Regulation of gene transcription plays an important part in a number of diseases including oncogene expression in cancer and cytokine production in inflammatory disease such as rheumatoid arthritis[41].

Many transcription factors contain cysteine, such as the Bzip transcription factors *jun* and *fos* oncogenes, whilst others require zinc, including steroid receptors and the so-called zinc finger proteins[42]. In these proteins the secondary structure of the protein is folded into loops or fingers stabilized by zinc tetrahedrally coordinated to either four cysteines or two cysteines and two histidines (Section I). Gold(I) thiolate drugs could potentially interact with transcription factors in two ways. Gold could bind to the sulphur of cysteine residues by ligand exchange of a thiolate ligand for the cysteine sulphur, alternatively the displaced thiolate ligand could chelate the zinc in a zinc-containing transcription factor.

Targeting gene transcription has been proposed as a new strategy for treating cancer. The overexpression of the *c-erb*B-2 oncogene has been implicated in a number of cancers including breast, stomach, ovarian and bladder. Transcription of this oncogene appears to be regulated by a positively acting transcription factor OB2-1. Aurothiomalate has been shown to diminish OB2-1-dependent *c-erb*B-2 transcription by inhibiting the binding of the transcription factor to DNA[43]. There is some evidence to suggest that OB2-1 may be a zinc finger protein and that the zinc may be the target. Support for this as a possible mechanism comes from the observation that aurothiomalate can decrease the binding of the progesterone receptor to DNA and it has been proposed that the mechanism of action may be chelation of the zinc in the receptor zinc finger[44]. A more likely explanation in both cases is ligand exchange with a specific cysteine residue in the protein structure.

The transcription factors encoded by the oncogenes *jun* and *fos* contain cysteine residues flanked by the basic amino acids lysine and arginine. This results in the lowering of the pK_{SH} thus favouring ligand exchange with gold(I) thiolates (Section IV.A). These transcription factors are known to control the transcription of a gene known as AP-1, which in turn is involved in the expression of genes for collagenase and the cytokine IL-2. It has been shown that aurothiomalate can inhibit AP-1 transcription via interaction with *jun* and *fos* at a concentration of 5 μM[45]. This has important implications for rheumatoid arthritis as another transcription factor NF-κB, which controls transcription of other inflammatory mediators including Tumour Necrosis Factor (TNF), also contains a cysteine flanked by lysine and arginine. Gold(I) thioglucose has been shown to inhibit IL-1 induced expression of NF-κB and AP-1, and to inhibit binding of NF-κB to DNA *in vitro*. Expression of the adhesion molecules ICAM-1 and VCAM-1 is also regulated by NF-κB and it has been demonstrated that expression of these adhesion molecules in vascular endothelial cells is inhibited by gold(I) thiomalate[33]. It is therefore possible that one molecular mechanism for the gold antiarthritic drugs is inhibition of transcription of the genes for crucial mediators of the inflammatory process.

E. Immunotoxicity

The most common side effects associated with gold therapy are inflammatory responses, primarily dermatitis, which accounts for 60% of all adverse reactions to the gold drugs. This is a delayed-type hypersensitivity reaction which appears to be genetically linked with increased risk being associated with the HLA-B35, DR2 and DR3 HLA antigens[20]. One proposal is that the inflammatory response is in part caused by contamination of the gold drugs with nickel[46]. The precise mechanism is unknown, but what is of great interest is that the hypersensitivity reaction is to gold(III) formed by the oxidation of gold(I), rather than the parent drug. This has been demonstrated both in patients and in animal models[47,48].

The antigen-specific immune response is mediated by activated CD4$^+$ T lymphocytes. Metals themselves cannot act as antigens to trigger the immune response but have to first bind to a carrier peptide. Antigenic peptides are processed by antigen present-ing cells (APC) where they become associated with a relevant major histocompatibility (MHC) class II protein on the surface of the APC. The antigen–MHC protein com-plex is then recognized by the CD4$^+$ T lymphocyte. Metal hypersensitivity may be the result of the metal interacting with the antigen–MHC protein complex. Pretreatment of antigen-presenting cells with gold compounds has been shown to inhibit peptide-induced proliferation of CD4$^+$ T lymphocytes, and gold has been shown to directly bind to MHC class II proteins[49].

An alternative hypothesis is that the gold may bind directly to the antigenic peptide, and it has been proposed that the formation of cryptic peptides may be induced by the binding of gold(III) to antigens[50]. In order for this to take place the gold(I) drugs have to be metabolized to gold(III). The inflammatory site is a highly oxidizing environment. During the oxidative burst hypochlorite is produced by the enzyme myeloperoxidase from H_2O_2 and Cl^-, which can oxidize gold(I) to gold(III)[20,51]. Gold is also known to accumulate in lysosomes where antigen processing takes place. The feasibility of this hypothesis is supported by the evidence for gold(III) to form complexes both with cysteine-containing peptides, and more recently with N-donor ligands including the tripepetide Gly-Gly-His[52].

V. ANTITUMOUR

A. Gold(I) Phosphine Complexes

The potential antitumour activity of gold compounds has been demonstrated in a number of experimental models, but as yet no gold compound has entered clinical trials[53,54]. Auranofin was shown to be cytotoxic towards HeLa cells. It was also active against P388 leukaemia *in vivo*, a standard and well-documented primary screen for anticancer activity, whereas the oligomeric gold(I) thiolates were inactive. Studies on the possible mechanism of action of auranofin indicated a preferential inhibition of DNA synthesis similar to the platinum anticancer drug cisplatin. Auranofin, however, was inactive in subsequent tests using solid tumour models. This initial activity of auranofin led to the testing of numerous related compounds in the former Smith Kline Beckman laboratories. A class of tertiary phosphine gold(I) complexes with thiosugar ligands was found to be active against both the P388 leukaemia and B16 melanoma *in vitro* and P388 *in vivo*. Again, these compounds were inactive against a range of solid tumour models.

Effort was then focused on the [μ-bis(diphenylphosphine)ethane]digold complexes such as [dppe(AuCl)$_2$] (**4**)[55]. The dppe ligand is active alone, but the digold complexes were shown to have increased activity. These complexes rearrange to give tetrahedral com-plexes of the type [Au(dppe)$_2$]$^+$ (**5**), which are of equal if not greater activity than their

(4)

(5)
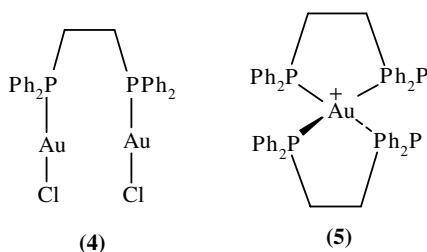
precursors[56]. The tetrahedral arrangement is more stable for two reasons. The chelate effect stabilizes the compound, and the phosphine ligand is more inert to substitution by potential thiolate ligands that could be encountered in a biological environment. The proposed mechanism of action for [Au(dppe)$_2$]Cl was the formation of DNA-protein crosslinks[57], the lack of affinity for Au(I) for O- and N-containing ligands resulting in poor reactivity with the bases of DNA. Though this compound had marked activity against peritoneal cancer cells, [Au(dppe)$_2$]Cl was still only slightly active against solid tumour models (see Section V.C). This compound failed to enter clinical trials due to problems with cardiotoxicity highlighted during pre-clinical toxicology studies[58].

The toxicity of the gold(I) phosphine complexes was found to be due to their inhibition of mitochondrial function. It has been reported that mitochondrial dysfunction is associated with platinum resistance in some tumour lines[59]. A series of gold(I) compounds containing the chiral ligands (2-aminophenyl)methylphenylphosphine, 1,2-phenylenebis(methylphenylphosphine) and bis{(2-diphenylphosphinoethyl)phenylphosphino}ethane has been synthesized and found to be cytotoxic towards both P388 leukaemia cells and human ovarian cell lines resistant to cisplatin[60]. The above compounds are hydrophobic cations and are readily taken up by the mitochondria of tumour cells. In addition, these compounds have reduced lipophilicity compared with [Au(dppe)$_2$Cl] which may reduce their toxicity. A series of gold(I) complexes with bidentate pyridylphosphine ligands [R$_2$P(CH$_2$)$_2$PR$_2$ where R = 2-pyridyl, 3-pyridyl or 4-pyridyl] has recently been reported to have selective antitumour activity. The gold(I) 4-pyridyl derivative was found to be active against a cisplatin-resistant ovarian tumour cell line, and to have *in vivo* activity against the colon 38 tumour[61].

B. Gold Complexes of Ligands with Antitumour Activity

One avenue of investigation has been to synthesize gold complexes containing ligands with known antitumour activity[54]. Examples of this are a series of Ph$_3$PAu(I)–nucleotide complexes containing ligands such as 5-fluorouracil and 6-mercaptopurine; phosphinogold(I) ferrocene complexes such as [μ-1,1-bis(diphenylphosphino)ferrocene]bis(chloro-gold(I)), and more recently a series of novel nitrogen-containing phosphinogold(I) ferrocenes[62]; and a gold(III) complex of streptonigrin, a substituted 7-aminoquinoline-5,8-dione[54].

C. Gold(III) Complexes

We have examined a class of gold(III) complexes using an integrated approach to the search for new metal-based anticancer drugs. This incorporates inorganic medicinal chemistry, *in vitro* screening, *in vivo* human tumour xenograft models and mechanistic studies.

Gold(III) is an interesting starting point as it is isoelectronic with platinum(II); the only clinically used metal anticancer drugs at present are the platinum(II) complexes cisplatin and carboplatin. Both gold(III) and platinum(II) adopt a square-planar configuration, so it is tempting to speculate that gold(III) complexes will have an antitumour activity similar to that of cisplatin. There are only a few reports of the testing of gold(III) compounds in the literature, possibly because they are generally very reactive compared with platinum(II) complexes[53,54] and, as mentioned earlier, usually toxic. We have approached this problem by synthesizing complexes with a single mononegative bidentate ligand dimethylbenzylamine, or damp (2-[(dimethylamino)methyl]phenyl), and two monodentate anionic ligands, e.g. Cl or acetate (6–10)[63]. The damp ligand forms part of a five-membered chelate ring in which the nitrogen of the amine group and the carbon of the aryl ring bond to the metal. The monodentate ligands are readily hydrolysed and are available for substitution.
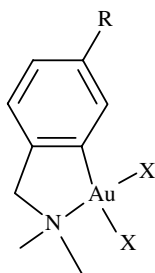
(6)	X = Cl	R = H
(7)	X = SCN	R = H
(8)	X = acetato	R = H
(9)	X_2 = oxalato	R = H
(10)	X_2 = malonato	R = H
(11)	X_2 = thiosalicylato	R = H
(12)	X_2 = thiosalicylato	R = OMe
(13)	X_2 = salicylato	R = OMe

We have also adopted a new approach to the biological evaluation of compounds. Historically compounds have been screened against rodent cancer models, the predominant models being the L1210 and P388 murine leukaemias[64,65]. These are grown as ascitic suspensions in the peritoneal cavity and test compounds are usually administered directly into the peritoneal cavity. These models have had some success in identifying drugs to treat leukaemias but have had only limited success in identifying drugs for the treatment of solid tumours. There are two possible explanations for this. One is that the cancer cells and test drug are in close proximity, whereas solid tumours are distant from the site of drug administration, so in the simple ascitic models there is no need to take into account the barriers a drug has to face both in terms of distribution and metabolism. The second is, being a mouse leukaemia, the cell type is not typical of a human solid tumour which will have different characteristics and susceptibilities to drugs.

The compounds were first tested against two panels of human tumour cell lines. The primary cell panel consisted of cells from tumours representative of different tissue types and with different chemosensitivities to cisplatin[66]. Differential cytotoxicity, as opposed to non-selective toxicity, was used as an indicator of potential antitumour activity of test compounds[65]. The second panel was disease-oriented and consisted of cell lines established from human ovarian tumours. This panel included two pairs of cisplatin-sensitive and cisplatin-resistant lines, with defined mechanisms of resistance (CH1/CH1-R, A2780/A2780-R), and also two inherently resistant cell lines (HX62 and SK-OV-3). This panel has been used to identify agents with the ability to circumvent cisplatin resistance[67].

Most of the cell lines used in this panel can also be grown as solid tumour xenografts in immune-deprived, nude mice, which means the compounds can be further evaluated in an *in vivo* setting. Initial *in vitro* studies indicated that the breast carcinoma cell line ZR-75-1 was sensitive to [AuCl$_2$(damp)][63]. This compound was then further tested *in vivo* against a xenograft of the same tumour cells where it demonstrated modest antitumour activity, seen as a reduction in tumour growth compared with controls, comparable to cisplatin. This prompted the synthesis of further analogues with enhanced solubility in order to improve upon the biological properties[68,69].

The activity of these analogues against the two cell line panels is shown in Tables 1 and 2. The compounds exhibited a cytotoxicity profile similar to cisplatin against the primary cell line panel with the HT1376 bladder carcinoma line being the most sensitive. Interestingly, in the ovarian cell line panel the compounds were equally active against the CH1/CH1-R sensitive/resistant pair[69].

TABLE 1.   Cytotoxicity (IC$_{50}$ μM) of Au(III) complexes towards the primary tumour cell line panel. Cisplatin is shown for comparison

Compound	SW620	SW1116	ZR-75-1	HT29/219	HT1376	SK-OV-3	Range
[AuCl$_2$(damp)]	124	119	27	55	30	45	4.6
[Au(SCN)$_2$(damp)]	51	47	34	25	6.7	20	7.6
[Au(OAc)$_2$(damp)]	281	238	45	67	13	13	21.6
[Au(ox)(damp)]^a	205	215	41	19	10	10	21.5
[Au(mal)(damp)]^a	67	80	36	36	11	11	7.3
Cisplatin	167	163	27	17	23	23	9.8

^{a}ox = oxalato; mal = malonato.

TABLE 2.   Cytotoxicity (IC$_{50}$ μM) of Au(III) complexes towards the ovarian tumour cell line panel. Cisplatin is shown for comparison. The numbers in parentheses represent resistance factors (IC$_{50}$ of resistant cell line: IC$_{50}$ sensitive cell line)

Compound	HX62	SK-OV-3	CH1	CH1-R	A2780	A2780-R	Range
[AuCl$_2$(damp)]	57	109	13	22 (1.7)	8.2	47 (5.7)	13.3
[Au(SCN)$_2$(damp)]	31	39	10	1 (1.1)	2.0	26 (13)	19.5
[Au(OAc)$_2$(damp)]	34	107	11	12 (1.1)	3.5	35 (10)	31
[Au(ox)(damp)]^a	30	42	11	13 (1.2)	3.7	35 (9.5)	11.4
[Au(mal)(damp)]^a	27	30	2.7	3.3 (1.2)	2.7	16 (5.9)	11.1
Cisplatin	18	5.2	0.12	0.56 (4.7)	1.2	10 (8.3)	150

^{a}ox = oxalato; mal = malonato.

The complexes (with the exception of [Au(SCN)$_2$(damp)] which had poor solubility) were evaluated against the HT1376 tumour *in vivo*[69]. Both the malonato and acetato complexes were active against the HT1376 tumour (see Figure 1). The chloro complex was less active, with the oxalato complex being inactive. This could be explained by the lower solubility in both water and octanol of the latter two compounds compared with the acetato and malonato complexes. This poor solubility of the chloro and oxalato complexes would reduce their absorption and limit their biodistribution. The acetato complex [Au(acetato)$_2$(damp)] was also tested against a xenograft of the CH1 ovarian cell line, PX/109/TC (Figure 2). This compound was also active against this xenograft, though the activity was significantly less than that reported for cisplatin against the same tumour[70].

The mechanistic studies focused on the interaction of the acetato complex [Au(OAc)$_2$(damp)] (**8**) with DNA, as cisplatin acts by forming both inter- and intra-strand cross-links with double-stranded DNA[71,72]. The initial studies examined the binding of the compound to a piece of closed circular DNA, the Col E1 plasmid. This was done by monitoring its mobility on an agarose gel[73]. Cisplatin, which binds to the plasmid, alters the plasmid mobility (cisplatin binding unwinds the plasmid, making it more bulky and less mobile). The gold(III) acetato complex only achieved this effect at very high concentrations (more than 1500 times the toxic concentration in cells)[69]. The cross-linking of DNA strands can be monitored in cells using a technique known as alkaline elution[74].
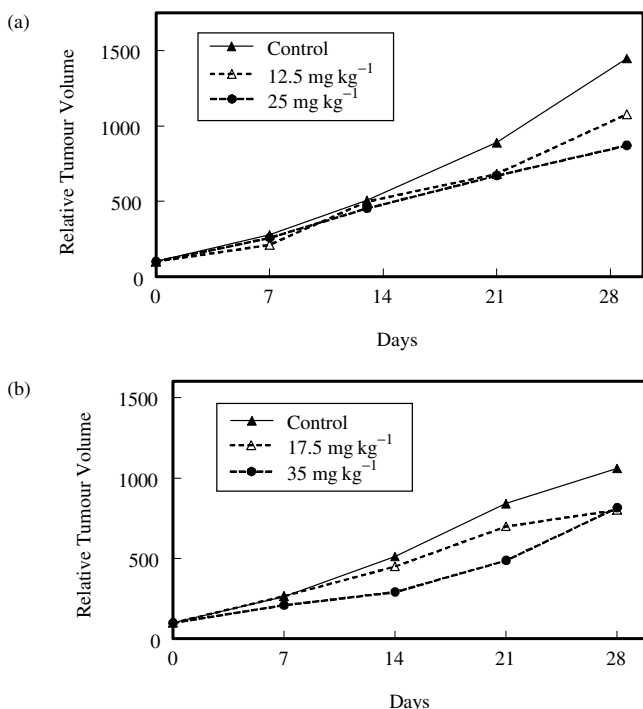
FIGURE 1. The activity of (a) [Au(OAc)$_2$(damp)] and (b) [Au(malonato)(damp)] against the HT1376 bladder carcinoma xenograft
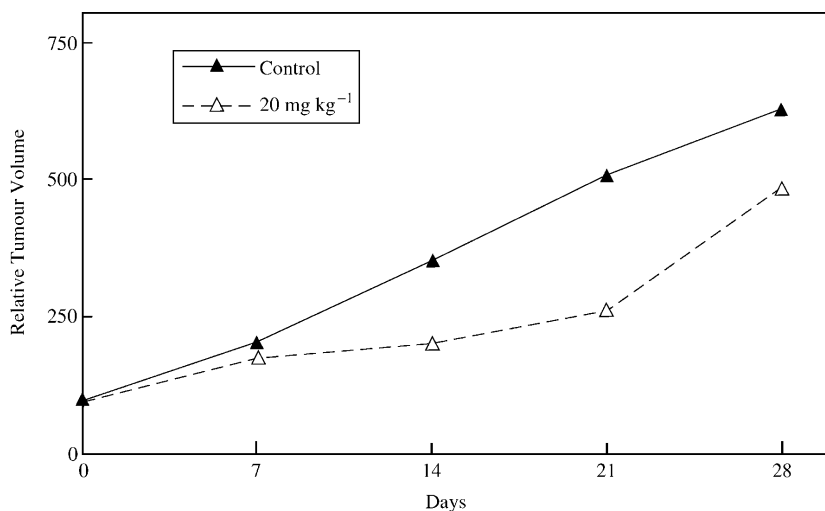
FIGURE 2. The activity of [Au(OAc)$_2$(damp)] against the CH1 (PX/109/TC) ovarian carcinoma xenograft

This is a filtration technique in which cross-linking impedes flow through a filter, whereas strand breakage enhances passage through the filter, compared with DNA from control cells. Cisplatin can be shown to produce cross-links by this technique. Unlike cisplatin, the Au(III) compound was unable to produce cross-links, but appeared to produce limited breaks in single strand DNA (Figure 3a); however, this was not evident in the subsequent experiment looking specifically for strand breakage (Figure 3b)[69]. Further evidence that DNA may not be the target for the gold(III) complexes comes from studies on the chemical interactions of these compounds with biological donor ligands. The results indicated that the gold(III) damp complexes had a preference for S-donor ligands such as glutathione and cysteine, with only limited reactivity against nucleosides and their bases[68].

At the cellular level cisplatin causes a block in the cell cycle at the point where DNA repair occurs, the S/G$_2$ interface. The stages of the cell cycle can be monitored using flow cytometry[75]. In this technique cells are fixed and stained with propidium iodide, a DNA fluorochrome, which binds quantitatively to DNA. The degree of fluorescence is therefore directly proportional to the DNA content of the cell, which in turn is an indicator of the position of the cells in the cell cycle. The ovarian cell line, SK-OV-3, was incubated with [Au(acetato)$_2$(damp)] for 4 hours at concentrations of either 30 μM or 100 μM and cell cycle analysis determined from DNA content. Using this technique it was apparent that the gold(III) complex [Au(OAc)$_2$(damp)], unlike cisplatin, did not exert a cell cycle specific effect[69].

These observations were further supported by the pharmacological studies. For example, in the ovarian cell line panel the acetate was equally active against a cisplatin-resistant cell line, CH1R, as against its cisplatin-sensitive counterpart, CH1. The mechanism of resistance to cisplatin in this cell line is repair of cisplatin-induced DNA damage. Also, [Au(OAc)$_2$(damp)] had little activity against the ADJ/PC6 murine tumour, which is known to be particularly sensitive to compounds which cross-link DNA, such as cisplatin[69].

| (a) DNA cross-link formation | (b) DNA strand breakage |

■ untreated control, ○ 100 μM cisplatin, ● 100 μM [Au(OAc)$_2$(damp)], ☆ irradiated control
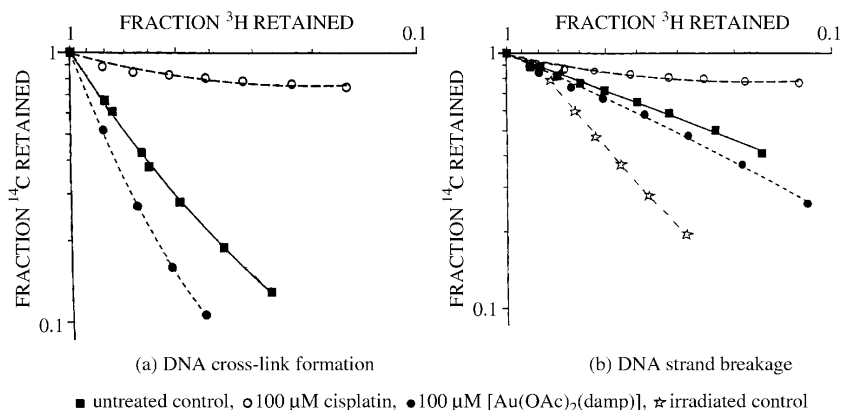
FIGURE 3. Alkaline elution studies in SK-OV-3 cells after exposure to 100 μM [Au(OAc)$_2$(damp)] or 100 μM cisplatin. DNA cross-link formation is indicated by reduced flow through the filter, as is the case with DNA from the cisplatin-treated cells (a). DNA strand breaks are indicated by enhanced flow through the filter, as demonstrated by DNA from irradiated cells (b). ■ untreated control, ○ 100 μM cisplatin, ● 100 μM [Au(OAc)$_2$(damp)], ☆ Irradiated control

TABLE 3. Cytotoxicity (IC$_{50}$ ng ml^{-1}) of thiosalicylato and salicylato complexes of N,N-dimethylbenzylamine and methoxy substituted N,N-dimethylbenzylamine against the P388 leukaemia cell line

Compound	IC$_{50}$ vs P388 cells
11	1937
12	301
13	5056

Dinger and Henderson have also demonstrated the potential pharmacological activity of this class of gold(III) compounds. They described the synthesis of cycloaurated N,N-dimethylbenzylamine complexes with either diphenylurea[76], or salicylate and thiosalicylate[77] as the dianionic ligands. Thiosalicylato complexes of N,N-dimethylbenzylamine and methoxy substituted N,N-dimethylbenzylamine, and the salicylato complex of Au(III) methoxy substituted N,N-dimethylbenzylamine, demonstrated antitumour activity *in vitro*, with the methoxy substituted N,N-dimethylbenzylamine cyclometallated gold(III) thiosalicylato complex being the most potent (Table 3). These compounds were, however, only evaluated against the P388 leukaemia cell line, therefore their potential activity against human tumours requires further investigation.

VI. ANTI-INFECTIVE

A. Antimicrobial Activity

The implication of microbial infection as an etiological agent in arthritis has been the main stimulus for the investigation of the antimicrobial properties of gold complexes. The

early work by Robert Koch demonstrated that gold compounds were active against the tubercle bacillus[6]. Subsequent extensive work in the 1930s and 1940s demonstrated that a variety of gold compounds were active against a broad spectrum of microorganisms[38]. However, there has been very little recent work on the antimicrobial activity of gold complexes. There are indications that the antiarthritic gold complexes may suppress *H. pylori* infections in the gastric mucosa, a causative agent for peptic ulcers[78], and that gold phosphine complexes *in vitro* are cytocidal towards *Pseudomonas putida*[79]. A gold chloroquine complex [(Au(PPh$_3$)(chloroquine)]PF$_6$ has been reported with activity against a chloroquine-resistant strain of the parasitic protozan *Plasmodium falciparum*, the causative agent of malaria[80].

There is a growing clinical need for new antimicrobial agents. The therapeutic efficacy of drugs currently available for the treatment of a class of bacteria known as the 'problem Gram-positive cocci' is limited by the emergence of multiply-resistant strains such as methicillin-resistant *Staphylococus aureus* (MRSA) and enterococci, e.g. *Enterococcus faecalis*[81]. Vancomycin is the drug of choice for these organisms, but it too has limitations as it must be administered by *i.v.* infusion, and has problems with resistance, particularly against the enterococci[82].

In our own laboratory we have tested a number of different metal complexes for potential antimicrobial activity[83]. The compounds were tested against a number of bacterial strains including clinical isolates of methicillin-resistant *S. aureus* (MRSA), methicillin-sensitive *S. aureus*, enteroccocci, coagulase-negative staphylococci and streptococci. A gold(I) thiocyanate complex [Au(SCN)(PMe$_3$)] demonstrated activity against Gram-positive bacteria including MRSA[84]. This led to the testing of further complexes and the identification of a series of gold(I) phosphonium dithiocarboxylato complexes with activity against Gram positive bacteria, including the 'problem Gram-positive cocci', with a MIC (minimum inhibitory concentration) of <1 µg ml^{-1} (Table 4). Preliminary *in vitro* cytotoxicity studies against a mammalian cell line demonstrated low toxicity at concentrations at least 10 times greater than the MIC (Table 5)[85]. The complex [Au(SCN)(PMe$_3$)] demonstrated good selectivity for bacteria over mammalian cells, and was also shown to be active in an *in vivo* model of topical infection[84].

The gold(III) salicylato and thiosalicylato complexes had moderate antimicrobial activity against a range of bacteria and fungi. It is, however, difficult to make a direct comparison of these data as quantitative MIC values were not determined for these compounds[77]. We have also examined the antimicrobial activity of the gold(III) compounds [AuCl$_2$(damp)] (**6**) and [Au(OAc)$_2$(damp)] (**8**)[63,68]. Both exhibit broad spectrum activity against a range of organisms, with a small degree of specificity against the Gram-positive organisms *S. aureus* and *E. faecalis* with the more water-soluble diacetato derivative being the most potent (Table 6). Both are similarly toxic against the

TABLE 4. Antibacterial activity of gold(I) complexes against the 'problem Gram-positive cocci', methicillin-resistant *Staphylococcus aureus* and *Enterococcus faecalis*

Compound	MIC$_{50}$	(µg ml^{-1})
	S. aureus	*E. faecalis*
[Au(SCN)(PMe$_3$)]	0.33	0.77
Au$_2$Cl$_2$(µ-S$_2$CPEt$_3$)]	1.1	2.5
[AuCl(S$_2$CPMe$_3$)]	1.0	4.8

TABLE 5. Comparative cytotoxicity of gold complexes against CHO mammalian cells. Results are expressed as % survival

Compound	Concentration ($\mu g\,ml^{-1}$)			
	0.1	1.0	10	100
[Au(SCN)(PMe$_3$)]	101.9	107.4	87.0	1.0
[Au$_2$Cl$_2$(μ-S$_2$CPEt$_3$)]	93.2	90.6	99.4	3.3
[AuCl(S$_2$CPMe$_3$)]	99.7	98.2	95.0	27.1
[AuCl$_2$(damp)]	91.3	84.3	69.6	2.2
[Au(OAc)$_2$(damp)]	99.5	97.9	96.1	0.4
Ciprofloxacin	96.7	99.9	101.2	90.0

TABLE 6. Antibacterial activity of gold(III) complexes against a range of bacteria. Ciprofloxacin is included for comparison

Compound	MIC ($\mu g\,ml^{-1}$)			
	S. aureus	E. faecalis	E. coli	P. aeruginosa
[AuCl$_2$(damp)]	1.0–2.5	1.0–2.5	10–25	10–25
[Au(OAc)$_2$(damp)]	0.25–1.0	0.25–1.0	2.5–10	50–100
Ciprofloxacin	<0.25	1.0–2.5	1.0–2.5	<0.25

mammalian CHO cells (Table 5), indicating that the diacetato complex is more selective towards bacteria over mammalian cells compared with the chloro derivative. There is still scope for improvement as both compounds are less potent than the control compound, the quinolone antibiotic ciprofloxacin.

B. Antiviral Activity

There is limited evidence to suggest that gold compounds may have antiviral activity. The gold(I) thiolates inhibit both cellular and herpes virus-induced DNA polymerases; however, there was no preferential inhibition of viral over cellular DNA polymerase[86]. Interestingly, the inhibition by gold(I) complexes was non-competitive whereas inhibition by the gold(III) complex was competitive. The gold(III) salt AuCl$_4$H has been shown to be an inhibitor of avian myeloblastosis virus reverse transcriptase at concentrations that were non-toxic to HeLa cells[87]. Reverse transcriptase (RT) is a drug target for HIV therapy, leading to the suggestion that gold compounds may have anti-HIV activity. As the enzyme inhibition was seen on cell-free enzyme, the lack of toxicity to HeLa cells may be due to poor cellular uptake. This would suggest that access to reverse transcriptase, as a drug target, could be limited.

Both gold(I) thiolates and AuCl$_4^-$ can inhibit the infectivity of HIV-1. It appears as if this effect is the result of inhibition of virus/cell fusion rather than by RT inhibition. The viral envelope protein gp120 is formed by the processing of a precursor protein gp160. The gp120 is retained on the cell surface by association with gp41. Site-directed mutagenesis studies have shown a requirement for a Cys-53 residue in gp41 and it has been proposed that modification of this essential cysteine by gold is the mechanism of inhibition of viral infectivity[88].

VII. CONCLUSION

Gold has been used by the medical profession since the earliest days of civilization. Chrysotherapy has become established in the twentieth century as an important component of the treatment regimen for rheumatic diseases, particularly rheumatoid arthritis. There have been no major changes in this area since the introduction of the orally available gold drug auranofin, and arthritis remains the predominant clinical use for gold drugs. There has been considerable research effort to find alternative therapeutic applications for gold drugs, particularly for the treatment of cancer, but after promising early indications the lead candidate [Au(dppe)$_2$]Cl failed to enter clinical trials due to cardiotoxicity. Despite this setback, research in this field has not abated. Recent work has indicated that gold(III) compounds have activity in disease models of human cancer and this may be the way forward in this area. Gold compounds also have potential as anti-infective agents, particularly against topical infections, and possibly HIV.

However, our understanding of the mechanism of these drugs continues to advance particularly with the recent findings of the effect of gold drugs on gene expression, and immunoreactivity. After sixty years of chrysotherapy it is still possible that an improved understanding of the molecular and biochemical mechanism of gold compounds will provide the impetus for new advances in the medical use of gold drugs.

VIII. ACKNOWLEDGEMENT

IX. REFERENCES

1. J. J. R. Frausto da Silva and R. J. P. Williams, *The Biological Chemistry of the Elements*, Clarendon Press, Oxford, 1991.
2. P. J. Sadler, *Adv. Inorg. Chem.*, **36**, 1 (1991).
3. C. F. J. Barnard, S. P. Fricker and O. J. Vaughan, in *Insights into Speciality Inorganic Chemicals* (Ed. D. Thompson), Chap. 3, Royal Society of Chemistry, Cambridge, 1995, pp. 35–61.
4. G. J. Higby, *Gold Bull.*, **15**, 130 (1982).
5. R. V. Parish, *Interdiscip Sci. Rev.*, **17**, 221 (1992).
6. R. Koch, *Dtsch. Med. Wochenschr.*, **16**, 756 (1890).
7. K. Landé, *Münch. Med. Wochenschr.*, **74**, 1132 (1927).
8. J. Forestier, *J. Lab. Clin. Med.*, **20**, 827 (1935).
9. T. G. Davis (Ed.), *Scand. J. Rheumatol., Supplement 63* (1986).
10. C. Moncur and H. J. Williams, *Phys. Ther.*, **75**, 511 (1995).
11. M. Stefanovic-Racic, J. Stadler and C. H. Evans, *Arthritis Rheum.*, **36**, 1036 (1993).
12. H. Ischiropoulos, L. Zhu and J. S. Beckman, *Arch. Biochem. Biophys.*, **298**, 446 (1992).
13. A. M. Badger and J. L. Adams, in *Annual Reports in Medicinal Chemistry* (Ed. J. A. Bristol), Chap. 20, Academic Press, San Diego, 1998, pp. 203–212.
14. R. V. Parish and S. M. Cottrill, *Gold Bull.*, **20**, 3 (1987).
15. R. C. Elder and M. K. Eidness, *Chem. Rev.*, **87**, 1027 (1987).
16. N. L. Gottlieb, *J. Rheumatol.*, **9 (Suppl. 8)**, 99 (1982).
17. D. T. Felson, J. J. Anderson and R. F. Meenan, *Arthritis Rheum.*, **33**, 1449 (1990).
18. M. Harth, *J. Rheumatol.*, **20**, 771 (1993).
19. M. H. Pioro and J. M. Cash, *Rheum. Dis. Clin. North Am.*, **21**, 129 (1995).
20. G. D. Champion, G. G. Graham and J. B. Ziegler, *Balliéré's Clin. Rheumatol.*, **4**, 491 (1990).
21. R. E. Thomas and R. A. Papandrea, *Med. J. Aust.*, **158**, 720 (1993).
22. B. A. Becker and A. A. Gaspari, *Dermatol. Clin.*, **11**, 429 (1991).
23. A. D. Ormerod, *Drugs*, **48**, 717 (1994).
24. P. J. Sadler, *Struct. Bonding*, **29**, 171 (1976).
25. C. F. Shaw III, *Inorg. Persp. Biol. Med.*, **2**, 278 (1979).

26. D. H. Brown and W. E. Smith, *Chem. Soc. Rev.*, **9**, 217 (1980).
27. P. J. Sadler and R. E. Sue, *Metal-Based Drugs*, **1**, 107 (1994).
28. C. F. Shaw III, *Comments Inorg. Chem.*, **8**, 233 (1989).
29. C. F. Shaw III and M. M. Savas, in *Metallothioneins: Synthesis, Structure, and Properties of Met-allothioneins, Phytochelatins, and Metal-Thiolate Complexes* (Eds. M. J. Stillman, C. F. Shaw III and K. T. Suzuki), Chap. 6, VCH, New York, 1992, pp. 144–163.
30. A. A. Isab and P. J. Sadler, *J. Chem. Soc., Dalton Trans.*, 135 (1982).
31. R. M. Snyder, C. K. Mirabelli and S. T. Crooke, *Semin. Arthritis Rheum.*, **17**, 71 (1987).
32. S. L. Best and P. J. Sadler, *Gold Bull.*, **29**, 87 (1996).
33. M. L. Handel, *Inflamm. Res.*, **46**, 282 (1997).
34. M. Grootveld, D. R. Blake, T. Sahinoglu, A. W. D. Claxson, P. Mapp, C. Stevens, R. E. Allen and A. Furst, *Free Rad. Res. Comms.*, **10**, 199 (1990).
35. P. E. Lipsky and M. Ziff, *Adv. Inflammation Res.*, **3**, 219 (1982).
36. M. Harth, K. Cousin and G. A. McCain, *Immumopharm. Immunotoxicol.*, **10**, 141 (1988).
37. P. Griem, K. Takahashi, H. Kalbacher and E. Gleichmann, *J. Immunol.*, **155**, 1575 (1995).
38. J. H. Liebarth and R. H. Persellin, *Agents Actions*, **11**, 458 (1981).
39. E. Choy and G. Kingsley, *Br. Med. Bull.*, **51**, 472 (1995).
40. D. T. Walz, M. J. Dimartino and D. E. Griswold, *J. Rheumatol.*, **9 (Suppl. 8)**, 54 (1982).
41. M. G. Peterson and V. R. Baichwal, *TIBTECH*, **11**, 11 (1993).
42. A. Travers, *DNA-Protein Interactions*, Chap. 3, Chapman and Hall, London, 1993, pp. 52–86.
43. D. P. Hollywood and H. C. Hurst, *Br. J. Cancer*, **71**, 753 (1995).
44. M. L. Handel, A. deFazio, C. K. W. Watts, R. O. Day and R. L. Sutherland, *Mol. Pharmacol.*, **40**, 613 (1991).
45. M. L. Handel, C. K. W. Watts, A. deFazio, R. O. Day and R. L. Sutherland, *Proc. Natl. Acad. Sci. USA*, **92**, 4497 (1995).
46. E. H. S. Choy, L. Gambling, S. L. Best, R. E. Jenkins, E. Kondeatis, R. Vaughan, M. M. Black, P. J. Sadler and G. S. Panayi, *Br. J. Rheumatol.*, **36**, 1054 (1997).
47. J. Verwilghen, G. H. Kingsley, L. Gambling and G. S. Panayi, *Arthritis Rheum.*, **35**, 1413 (1992).
48. D. Schumann, M. Kubicka-Muranyi, J. Mirtschewa, J. Gunther, P. Kind and E. Gleichmann, *J. Immunol.*, **145**, 2132 (1990).
49. F. Sinigaglia, *J. Invest. Dermatol.*, **102**, 398 (1994).
50. P. Griem, C. von Vultée, K. Panthel, S. L. Best, P. J. Sadler and C. F. Shaw III, *Eur. J. Immunol.*, **28**, 1941 (1998).
51. C. F. Shaw III, S. Schraa, E. Gleichmann, Y. P. Grover, L. Dunemann and A. Jagarlamudi, *Metal-Based Drugs*, **1**, 351 (1994).
52. S. L. Best, T. K. Chattopadhyay, M. I. Djuran, R. A. Palmer, P. J. Sadler, I. Sóvágó and K. Varngy, *J. Chem. Soc., Dalton Trans.*, 2587 (1997).
53. O. M. Ni Dhubhghaill and P. J. Sadler, in *Metal Complexes in Cancer Chemotherapy* (Ed. B. K. Keppler), VCH, Weinheim, 1993, pp. 221–248.
54. C. F. Shaw III, *Gold*, in *Metal Compounds in Cancer Therapy* (Ed. S. P. Fricker), Chap. 3, Chapman and Hall, London, 1994, pp. 46–64.
55. S. J. Berners-Price, C. K. Mirabelli, R. K. Johnson, M. R. Mattern, F. L. McCabe, L. F. Faucette, C. M. Sung, S. M. Mong, P. J. Sadler and S. T. Crooke, *Cancer Res.*, **46**, 5486 (1986).
56. S. J. Berners-Price, P. S. Jarrett and P. J. Sadler, *Inorg. Chem.*, **26**, 3074 (1987).
57. S. J. Berners Price and P. J. Sadler in *5th International Symposium on Platinum and Other Metal Coordination Compounds in Cancer Chemotherapy* (Ed. M. Nicolini), 1988, pp. 527–537.
58. G. D. Hoke, R. A. Macia, P. C. Meunier, P. J. Bugelski, C. K. Mirabelli, G. F. Rush and W. D. Matthews, *Toxicol. Appl. Pharmacol.*, **100**, 293 (1989).
59. Y. Dong, S. J. Berners-Price, D. R. Thorburn, T. Anatalis, J. Dickinson, T. Hurst, L. Qui, S. K. Khoo and P. G. Parsons, *Biochem. Pharmacol.*, **53**, 1673 (1997).
60. M. J. McKeage, P. Papathanasiou, G. Salem, A. Sjaarda, G. F. Sweigers, P. Waring and S. B. Wild, *Metal-Based Drugs*, **5**, 217 (1998).
61. S. J. Berners-Price, *Metal-Based Drugs*, in press.
62. M. Viotte, B. Gautheron, M. M. Kubicki, I. E. Nifant'ev and S. P. Fricker, *Metal-Based Drugs*, **2**, 311 (1995).
63. R. V. Parish, B. P. Howe, J. P. Wright, J. Mack, R. G. Pritchard, R. G. Buckley, A. M. Elsome and S. P. Fricker, *Inorg. Chem.*, **35**, 1659 (1996).
64. T. H. Corbett, F. A. Valeriote and L. H. Baker, *Invest. New Drugs*, **5**, 205 (1987).

65. S. P. Fricker, in *Metal Ions in Biology and Medicine* (Eds. Ph. Collery, L. A. Poirier, M. Manfait and J-C. Etienne), John Libby Eurotext, Paris, 1990, pp. 452–456.
66. S. P. Fricker and R. G. Buckley, *Anticancer Res.*, **16**, 3755 (1996).
67. L. R. Kelland, G. Abel, G. M. J. McKeage, M. Jones, P. M. Goddard, M. Valenti, A. Bryant, B. A. Murrer and K. R. Harrap, *Cancer Res.*, **53**, 2581 (1993).
68. R. V. Parish, J. Mack, L. Hargreaves, J. P. Wright, R. G. Buckley, A. M. Elsome, S. P. Fricker and B. R. C. Theobald, *J. Chem. Soc., Dalton Trans.*, 69 (1996).
69. R. G. Buckley, A. M. Elsome, S. P. Fricker, G. R. Henderson, B. R. C. Theobald, R. V. Parish, B. P. Howe and L. R. Kelland, *J. Med. Chem.*, **39**, 5208 (1996).
70. F. I. Raynaud, F. E. Boxall, P. M. Goddard, M. Valenti, M. Jones, B. A. Murrer, M. Abrams and L. R. Kelland, *Clin. Cancer Res.*, **3**, 2063 (1997).
71. S. L. Bruhn, J. H. Toney and S. J. Lippard, in *Progress in Inorganic Chemistry: Bioinorganic Chemistry*, *Vol 38*, (Ed. S. J. Lippard), Wiley, New York, 1990, pp. 477–516.
72. E. L. M. Lempers and J. Reedijk, *Adv. Inorg. Chem.*, **37**, 175 (1991).
73. C. K. Mirabelli, C.-M. Sung, J. P. Zimmerman, D. T. Hill, S. Mong and S. T. Crooke, *Biochem. Pharmacol.*, **35**, 1435 (1986).
74. K. W. Kohn, R. A. G. Ewig, L. C. Erickson and L. A. Zwelling, in *DNA Repair — A Laboratory Manual of Research Procedures, Vol. 1, Part B* (Eds. E. C. Friedberg and P. C. Hanawalt), Marcel Dekker, New York, 1981, pp. 379–401.
75. M. G. Ormerod, R. M. Orr and J. H. Peacock, *Br. J. Cancer*, **69**, 93 (1994).
76. M. B. Dinger and W. Henderson, *J. Organomet. Chem.*, **557**, 231 (1998).
77. M. B. Dinger and W. Henderson, *J. Organomet. Chem.*, **560**, 233 (1998).
78. L. Girgis, P. G. Conaghan and P. Brooks, *Curr. Opin. Rheumatol.*, **6**, 252 (1994).
79. M. D. Rhodes, P. J. Sadler, M. D. Scawen and S. Silver, *J. Inorg. Biochem.*, **46**, 129 (1992).
80. M. Navarro, H. Pérez and R. A. Sánchez-Delgado, *J. Med. Chem.*, **40**, 1937 (1997).
81. W. Brumfitt and J. M. T. Hamilton-Miller, *Drugs Exp. Clin. Res.*, **16**, 205 (1990).
82. A. P. Johnson, A. H. C. Uttley, N. Woodford and R. C. George, *Clin. Microbiol. Rev.*, **3**, 280 (1990).
83. A. M. Elsome, W. Brumfitt, J. M. T. Hamilton-Miller, P. D. Savage, R. O. King and S. P. Fricker, in *Program and Abstracts of the 31st Interscience Conference on Anti-Microbial Agents and Chemotherapy, Chicago*, American Society for Microbiology, Washington, DC, 1991, Abstract 387, p. 163.
84. A. M. Elsome, J. M. T. Hamilton-Miller, W. Brumfitt and W. C. Noble, *J. Antimicrob. Chemother.*, **37**, 911 (1996).
85. S. P. Fricker, *Toxicol. in Vitro*, **8**, 879 (1994).
86. H. S. Allaudeen, R. M. Snyder, M. H. Whitman, and S. T. Crooke, *Biochem. Pharmacol.*, **34**, 3243 (1985).
87. M. Semba, N. Tanaka, M. Yamada, F. Takeuchi, K. Matsuta, T. Miyamoto, F. Hanaoka, and M. Ui, *Jpn. J. Cancer Res.*, **81**, 1259 (1990).
88. T. Okada, B. K. Patterson, S. Ye and M. E. Gurney, *Virology*, **192**, 631 (1993).

CHAPTER **15**

Gold–thiol self-assembled monolayers

VICTOR CHECHIK and CHARLES J. M. STIRLING

Department of Chemistry, University of Sheffield, Sheffield S3 7HF, UK
Fax: 273-8673;   email: C.Stirling@Sheffield.ac.uk

The authors would like to dedicate this chapter to the memory of Saul Patai

I. ABBREVIATIONS

AFM	atomic force microscopy
μ CP	microcontact printing
DCM	dichloromethane
egg-pc	egg lecithicin/electron spectroscopy
ESCA	electron spectroscopy for chemical analysis
GIXD	grazing incidence X-ray diffraction
LEED	low energy electron diffraction
PDMS	polydimethylsiloxane
PIERS	polarized infrared external reflection spectroscopy
QCM	quartz crystal microbalance
RAIR	reflection-absorption infrared spectroscopy
SAM	self-assembled monolayer
SERS	surface-enhanced Raman spectroscopy
SIMS	secondary ion mass spectroscopy
SPR	surface plasmon resonance
STM	scanning tunnelling microscopy
XPS	X-ray photoelectron spectroscopy

II. INTRODUCTION

Systematic studies of films consisting of a single layer of molecules (monolayer films) date from ingenious work of Agnes Pockels who, at the end of the XIXth century, designed the first apparatus to study films at the air–water interface[1]. Irving Langmuir and Katherine Blodgett[2] developed methods for transfer of these layers onto the solid support, and this started a wave of research in surface science which has not subsided since.

The first systematic study of self-assembled monolayers was perhaps performed by Zisman and coworkers in 1940s. They noticed that a clean platinum object immersed and then carefully withdrawn from the solution of an amphiphile becomes hydrophobic and concluded that the amphiphile adsorbed on the surface to produce a monolayer[3]. Self-assembled films can be defined as 'molecular assemblies that are formed spontaneously by the immersion of an appropriate substrate into a solution of an active surfactant in an organic solvent'[4]. The driving force for self-assembly is usually the specific interactions between the head group of the surfactant and the surface of the substrate. Most surfactants used for monolayer studies consist of three distinctive parts: the surface active head group which binds strongly to the surface, the end (or tail) group which is located at the monolayer surface and normally determines the interfacial properties of the assembly, and the alkane chain which facilitates the packing of the molecules in the monolayer and

serves as a linker between the head and the end groups. Figure 1 illustrates formation of a self-assembled monolayer and shows some intermolecular interactions important for self-assembly.

Many examples of surface–surfactant interactions which promote self-assembly are known. Apart from gold–thiol monolayers which are formed because of the creation of the strong S−Au bond, other commonly studied monolayers include alkyltrichlorosilane layers on hydroxylated surfaces (such as SiO_2)[6], fatty acids on metal oxide surfaces[7,8] and alkyl phosphonate salts on zirconium[9].

So why did it happen that a 50-year-old phenomenon became, in the late 1990s, such a popular object of study? More than 660 papers were published on self-assembled monolayers in 1997 compared with a mere 100 in 1991. It seems that a number of favourable factors caused such a popularity of research in the area. Increasing demand for smaller and smaller electronic devices gave rise to researches to look for potential materials at the molecular level. Sensor technology became a major industrial target, and small, versatile and inexpensive sensors can only be produced via research in interfacial science. Recent advances in molecular biology made researchers look closer at the behaviour of biological molecules at interfaces. All of these achievements created a strong demand for studies of the solid–liquid and solid–gas interfaces at the molecular level. On the other hand, a growing number of commercially available analytical devices became sensitive enough to characterize single layers of molecules. Self-assembled monolayers (and especially gold–thiol films) were, however, quickly found to be much more versatile and easy to handle (*vide infra*) than such traditional objects of study as Langmuir–Blodgett (LB) films or monolayers at the air–water interface.

The ability of disulphides and thiols to self-assemble on gold surfaces was discovered by Nuzzo and Allara in 1983[10], and in the 1990s these films have probably become the most studied monolayers worldwide. There are several reasons for such popularity. Sulphur has a very strong affinity for gold, and self-assembly proceeds rapidly to give
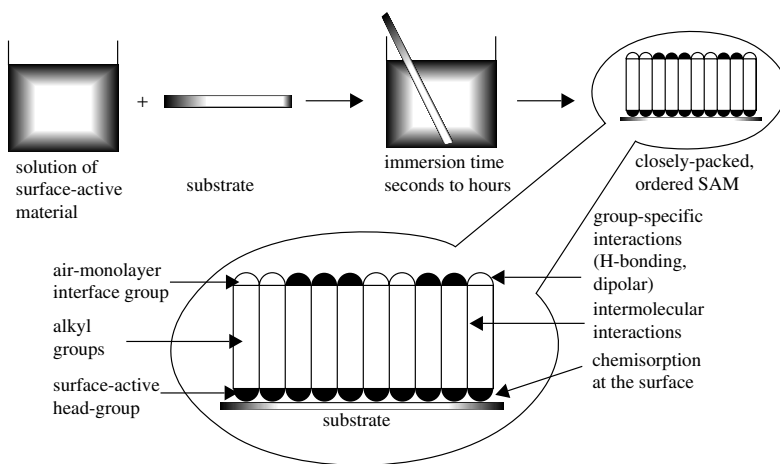
FIGURE 1. Formation of a self-assembled monolayer (SAM) by adsorption of a surface-active material on the surface of the substrate. Reprinted with permission from Reference 5. Copyright (1996) American Chemical Society

well-defined surfaces. Both thiols/disulphides and gold are stable under normal laboratory conditions, and no scrupulous precautions (such as exceptional purity of the reagents or clean room conditions) are required to produce monolayers. Thiols and disulphides are compatible with most organic functional groups and this makes it possible to incorporate a huge variety of terminal functionalities in gold–thiol monolayers. The synthetic chemistry of thiols and disulphides is well-established and in most cases very simple. Simple thiols and the starting reagents for more sophisticated adsorbates are commercially available and cheap. Gold surfaces, furthermore, can conveniently be prepared by thermal evaporation onto the surface of supports such as silicon or glass slides.

The above advantages of the gold–thiol system have resulted in the extensive use of gold–thiol monolayers by the whole scientific community. A brief research of the literature shows that more than 2000 papers have been published since 1983 studying self-assembled monolayers of thiols on gold. We have therefore made no attempts to make the present review comprehensive; however, we have endeavoured to include all recent seminal work in the area. The subject is highly interdisciplinary, and we put perhaps more emphasis on the chemical aspects of the monolayer science than the authors of some other reviews.

Literature up to 1992 has been summarized in two publications[4,11]. However, since 1992, despite the ever growing amount of research, there has been no general review of self-assembled monolayers, although some recent developments have been discussed[12]. A review by Finklea is probably the best recent account of gold–thiol monolayers, although it is primarily devoted to electrochemistry[13]. Individual issues in this interdisciplinary subject, have been reviewed in some cases, and where available the appropriate references are given in the beginning of the corresponding sections.

This review covers literature published up to mid-January 1998.

III. ANALYTICAL TOOLS FOR MONOLAYER CHARACTERIZATION

It will be going beyond the scope of the present review to give a detailed description of the techniques available, or to provide a comprehensive list of all methods used in surface analysis. Such information could be found in a number of monographs and review papers[4,14,15]. *Analytical Chemistry* publishes reviews every two years on the latest developments in surface characterization methods[16]. We will attempt to discuss briefly the most powerful and most readily available methods applicable to routine gold–thiol monolayer analysis with particular emphasis on the kind of information which can be obtained from these systems.

A. Thickness and Coverage Measurements

One of the most important characteristics of a surface layer is its thickness. Non-zero thickness is an important indicator that a layer is indeed formed. Comparison of the experimental thickness with the theoretical value shows whether a mono- or multilayer is formed and, in case of sub-monolayers, gives an estimate of surface coverage.

Traditionally the most common method of thickness analysis has been ellipsometry[17]. This is a non-destructive optical method based on the fact that the state of polarization of the light reflected from a coated surface depends on the thickness and refractive index of the coating. Experimentally, a plane-polarized laser beam is usually reflected from the surface coated with a monolayer and its polarization analysed with a compensator/detector couple (Figure 2a). Another related method is surface plasmon resonance (SPR)[18−20]. When p-polarized light is reflected from a metal surface, at a certain angle of incidence the part of the light is absorbed by the metal, due to the resonant excitation of the surface plasmons. In the common configuration of this method (so-called Kretschmann

configuration), a thin (*ca* 50 nm) layer of metal (gold or silver) is evaporated on the surface of a glass slide. The back of this slide is then optically connected to the back of a prism with a refractive index-matching liquid. p-Polarized laser light shines through the prism on the back of the slide and experiences total internal reflection from the metal surface (Figure 2b). The intensity of this reflected beam is analysed as a function of the angle of incidence. This angle depends on the thickness and refractive index of the metal support and organic film.
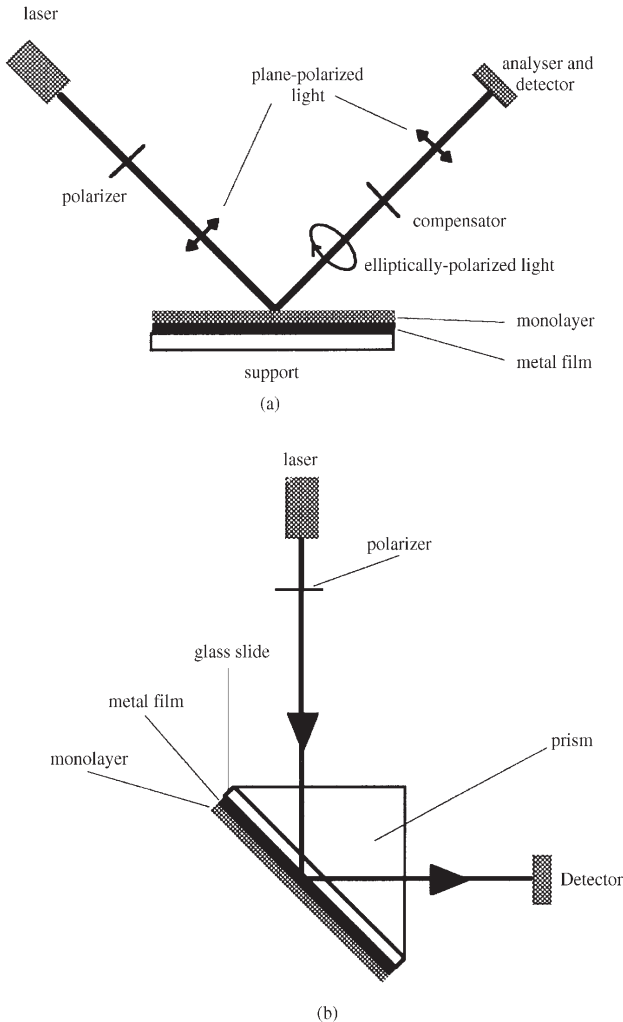
FIGURE 2. Typical experimental set-up for (a) ellipsometrical (adapted from Reference 4 by permission of Academic Press, Inc.) and (b) SPR measurements

In SPR and ellipsometry it is usually impossible to determine unambiguously both thickness and refractive index of monolayers. In most studies the latter parameter is therefore arbitrarily assumed to be $1.45-1.50$[20]. This, however, is only true for dense non-absorbing films. For incomplete monolayers, the response is usually assumed to be proportional to the coverage of monolayer, showing zero effective thickness for pure metal support and reaching the theoretical thickness at 100% coverage[18].

Importantly, an SPR device can easily be adjusted to monitor thickness *in situ*, both in the gas phase and in solution. This makes it one of the best methods for studying surface events associated with adsorption or desorption, and it is heavily and successfully used for this purpose.

The quartz crystal microbalance device (QCM)[21−24] allows one to measure the change of the mass of the films. This method is based on the ability of a piezoelectric quartz crystal to oscillate at a resonance frequency determined by the mass of the crystal. For these measurements, gold is evaporated directly onto the surface of such a quartz sensor which is then exposed to the vapour or solution of the adsorbate. What makes this method very valuable is that it can be used like SPR for monitoring molecular adsorption/desorption at the surfaces *in situ*.

B. Structure and Chemical Composition of the Film

Much informative data on the chemical composition of gold–thiol monolayers can be obtained from grazing angle FT-IR spectroscopy[15,25,26] (often abbreviated as RAIR or RAIS, reflection-absorption infrared (spectroscopy), or even PIERS (polarized infrared external reflection spectroscopy). The IR beam is reflected at a small (grazing) angle from the monolayer surface, and the intensity of the reflected beam recorded at the detector (Figure 3a). This method makes it possible to directly obtain the IR spectrum of a monolayer. Certain selection rules, however, apply to this type of spectroscopy. The intensity of the peaks is proportional to the cosine squared of the angle between the surface normal and the dipole moment of the corresponding vibrational mode. Figure 3b illustrates this effect for symmetrical stretching vibrations ν_s of methyl and methylene groups. If alkane chains are fully stretched and perpendicular to the surface, the transitional dipole moment of the $\nu_s(CH_2)$ vibration is parallel to the surface and the corresponding IR peak is invisible in the spectrum of the monolayer. Accurate measurements of the peak intensities therefore make it possible to calculate the orientation of functional groups in the monolayer. Application of FT-IR spectroscopy to the analysis of the arrangement of the alkane chains in gold–thiol monolayers is discussed in Section V.B.

Surface-enhanced Raman spectroscopy (SERS)[27−31] provides a means of obtaining the Raman spectrum of a monolayer. Although this method requires careful preparation of a roughened surface (necessary for intensity enhancement), and the absorbance may vary from sample to sample, it is very sensitive to the functionalities located close to the metal surface. The enhancement factor depends *inter alia* on the distance between the functional group and the metal surface on one hand and the surface coverage on the other. A typical distance at which the enhancement factor decreases to half of its initial value in a well-packed gold–thiol monolayer is about $3.5-7$ Å[32,33]. This technique provides useful information about the chemical structure of monolayers. Because normal (not enhanced) Raman absorption of the ambient medium is vanishingly low, this method can also be used for recording spectra of monolayers both in gas phase and in solutions.

X-ray photoelectron spectroscopy (XPS, or ESCA) measures the energy of the inner shell electrons ejected when the surface is irradiated with an X-ray beam in ultra-high

(a)

(b)
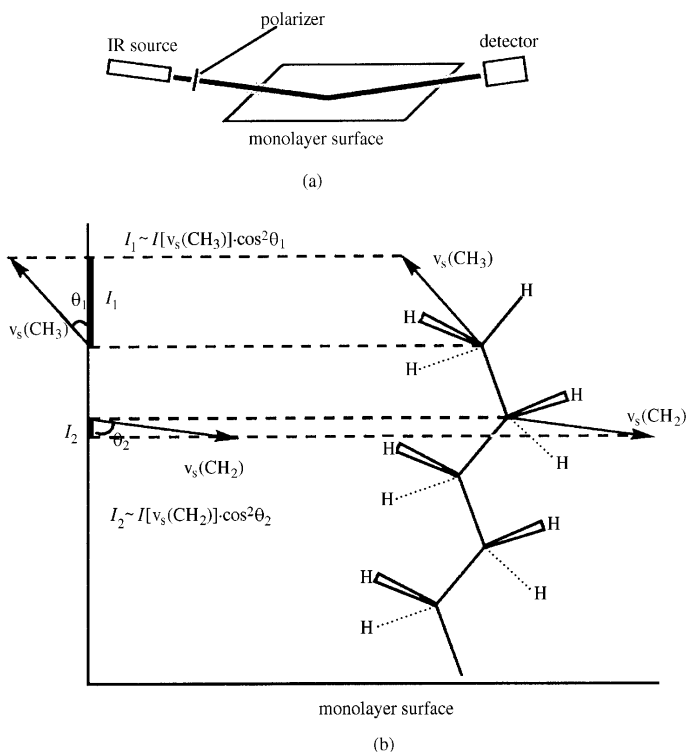
FIGURE 3. (a) A schematic diagram of a grazing angle FT-IR spectrometer. (b) The intensity of the peaks I depends on the angle θ between the dipole of the corresponding vibrational mode and the surface normal

vacuum (Figure 4a)[34,35]. This energy is specific for every chemical element, and effectively XPS provides an elemental analysis of the monolayer. The response from elements buried at different levels below the surface depends on the takeoff angle. The study of XPS response as a function of the takeoff angle allows one therefore to calculate how deeply certain elements are positioned with respect to the monolayer surface. Another important feature of the XPS spectra is that high resolution scans reveal differences between elements in different oxidation states. Thus, XPS studies can indicate if the thiolate head group in a monolayer has oxidized to a sulphonate group, $RSO_3{}^-$. XPS can also distinguish between amino and nitro groups.

Secondary ion mass spectroscopy (SIMS)[36,37] is another important technique which gives information about the chemical composition of monolayers. The samples are bombarded with so-called primary ions (usually Ar^+ or Xe^+) and the ejected secondary ions are detected (Figure 4b). The result is very similar to the conventional mass spectra of the bulk materials. Both molecular ions (often in clusters with one or several metal atoms) and fragment ions are detected.
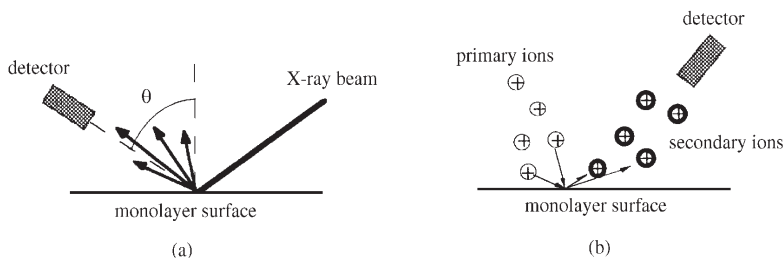
FIGURE 4. Schematic representations of XPS (a) and SIMS (b) experimental set-up

Unique information about the unit cell in quasi-crystalline monolayers can be obtained from X-ray[38−40], neutron[41,42], helium[43−45] or low energy electron diffraction (LEED)[46,47] data. In the grazing incidence X-ray diffraction (GIXD) experiment the beam is directed at the coated surface at a low angle and experiences total internal reflection from the metal support underneath the monolayer. The analysis of reflectivity and diffraction pattern of this reflected beam provides information about the molecular structure of the crystalline films, the thickness and refractive index of the layers and the roughness of the surface[48]. These experiments, however, require sophisticated and expensive equipment and are not therefore used routinely for monolayer characterization.

C. Interfacial Properties of the Film

Wettability measurements provide the simplest method for studying monolayers, yet give important information on the surface structure[49]. A drop of liquid (usually water) is placed with a syringe on the monolayer surface, and the contact angle between the drop and the monolayer surfaces is measured (Figure 5). The advancing contact angle is measured while the liquid is being added to the drop just before the boundary of the drop moves on the surface. Similarly, the receding angle is recorded when the liquid is slowly retracted, but before the boundary of the drop has moved. The sessile contact angle is the angle made by a resting drop. The value of the contact angle depends on the hydrophobicity of the outermost functions at the monolayer–air interface. Non-polar functional groups such as alkyl render the surface hydrophobic. Polar functional groups such as carboxyl, hydroxy and amino make the surface of a well-packed monolayer totally wetting, with contact angles close to zero. Some examples of the effect of terminal functionality on the wetting properties of the surface are given in Table 1. The hysteresis (difference between advancing and receding contact angles) is also sensitive to the degree of order in monolayers, increasing with increasing disorder in the film.
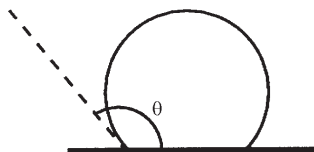
FIGURE 5. Contact angle θ of a drop of liquid on a surface

TABLE 1. Advancing contact angles of water on films prepared by adsorption of $HS(CH_2)_nX$ on gold[50]

X	n	Contact angle, (deg)
$(CF_2)_5CF_3$	2	119
CH_3	21	117
$CH=CH_2$	17	105
$OCOCF_3$	11	93
$CO_2CH_2CH_3$	10	89
Cl	11	89
OCH_3	11	85
CN	21	74
$CONHCH_3$	11	76
CO_2CH_3	10	74
OH	11	<15
$CONH_2$	10	<15
COOH	10	<15

A revolution in surface characterization came with the development of imaging techniques such as scanning tunneling (STM) and atomic force (AFM) microscopy[51−56]. Both can image surfaces with atomic resolution at low force loads. These methods are based on positioning an atomically sharp tip very close to the monolayer surface. The current (STM) or force (AFM) measurements and movement of a sample in a horizontal direction produce images in which individual atoms can be visualized. These experiments play a crucial role in determining the structure of the monolayer surfaces, and the results are discussed in Section V.A.

D. Electrochemical Methods

Electrochemical measurements with the thiol-coated gold surface acting as an electrode can provide very important information about the integrity and order of the monolayer[13,57,58]. Two main phenomena are usually used for monolayer characterization: capacitance measurements (with cyclic voltammetry or impedance spectroscopy) and heterogeneous electron transfer (cyclic voltammetry). The electrode in contact with solution acts as a capacitor whose capacitance strongly depends on the distance between the electrolyte and the metal surface, i.e. the thickness of the monolayer[59]. Therefore, for well-packed monolayers which are impermeable for electrolyte, the measured capacitance can be used to calculate the thickness of a monolayer. These data are usually in good agreement with the thickness measured by other methods.

In heterogeneous electron transfer experiments, the gold electrode with a monolayer film is placed in contact with the solution containing a redox couple [such as $Fe(CN)_6^{3-}/Fe(CN)_6^{4-}$ etc.][60−63]. The shape of the cyclic voltammogram depends on how effectively the monolayer blocks access for the redox probe to the electrode surface. This method is therefore invaluable for permeability studies. Absence of redox waves close to the formal potential of the probe indicates that the monolayer is completely impermeable for redox probe species. On the other hand, the presence of a redox wave shows either that the monolayer is loosely packed and easily penetrated by external molecules, or the presence of numerous defects and pin-holes in the monolayer.

Application of electrochemical methods to study other processes in gold–thiol mono-layers is discussed in Section VII.C.

In view of the limited stability of gold–thiol monolayers to laser light and X-ray, electron and metastable atom beams reported recently (see Section VI), one has to exercise caution to avoid damage of the monolayer in such experiments as SERS, XPS, GIXD, LEED etc.

IV. PREPARATION OF GOLD–THIOL MONOLAYERS

A. Experimental Procedures

It is partly because of the simplicity of their preparation that gold–thiol monolayers have been so extensively investigated. Gold is the only metal which does not react with oxygen even at high temperature[64] and gold substrates can be handled in ambient conditions in air. In addition, the affinity of thiols for gold is so strong that they replace most other adsorbates and form stable monolayers[65]. In principle, gold–thiol monolayers can be prepared by exposing virtually any gold surface to the vapours or solution of virtually any thiol in virtually any solvent. Clean gold surfaces, however, become readily contaminated in ambient atmospheres[66] and for the reproducible preparation of high quality monolayers certain precautions must be observed.

The lowest energy surface of gold is Au(111)[67] and in most studies gold–thiol mono-layers are prepared on these surfaces. Au(111) can be conveniently prepared by slow ($0.5-1.5 \, \mathrm{nm \, s^{-1}}$) thermal (resistive) evaporation of pure gold (usually 100 or 200 nm[68]) onto a freshly cleaned flat surface (such as a polished silicon or a glass wafer) in high vac-uum ($10^{-6}-10^{-7}$ Torr). A typical procedure for cleaning glass or silicon slides consists of their treatment with piranha solution (7 : 3 mixture of concentrated sulphuric acid and 30% hydrogen peroxide) at $80-90\,^{\circ}$C for 1 h followed by rinsing with copious amounts of water and ethanol and drying[68]. (Caution! Piranha solution reacts with most organic compounds with significant heat evolution and should be handled with extreme care[69,70]!)

Because of poor adhesion of gold to silicon and glass, slides prepared in this way suffer from low mechanical stability. They also cannot survive treatment with many chemical reagents such as strong acids, oxidizing reagents etc. To promote adhesion of the evaporated gold to the surface, a thin layer of Cr or Ti can be evaporated first onto the surface of a silicon wafer or glass[71,72]. This layer should be sufficiently thin to avoid contamination of the gold surface (usually $1-5$ nm). The evaporated surfaces have almost exclusively Au(111) orientation, although they may not be flat on an atomic level[73]. They are suitable for most monolayer studies including characterization with such methods as ellipsometry, QCM, grazing angle FT-IR, XPS and wettability measurements. Slides for SPR measurements are prepared similarly by evaporation of $1-3$ nm of Cr followed by $45-50$ nm of Au onto pre-cleaned glass slides[18,20].

For experiments requiring large atomically flat terraces of Au(111) (such as AFM or STM imaging), gold substrates are usually prepared by evaporation of gold onto the surface of freshly cleaved mica. Optimal evaporation conditions were found to be 0.3 nm/s and $360\,^{\circ}$C[74]. AFM studies of evaporated gold on mica showed that the most atomically flat gold is obtained by evaporation at higher temperatures ($450-500\,^{\circ}$C), but the formation of blocking monolayers on these surfaces was inhibited. The authors conclude that surface pretreatment immediately prior to monolayer deposition plays a more important role in preparing impermeable monolayers than evaporation conditions[75]. Effect of evaporation conditions on the growth mechanism of gold on mica was also studied by McKinley and coworkers[76]. Another method of making large atomically flat Au(111) terraces consists

of evaporation of a thin layer of gold on a silicon[77] wafer or on mica sheets[78]. A silicon or glass slide is then glued on top of the gold layer, and the original mica or silicon support is peeled off. Very slow Ar sputtering was also reported to produce atomically flat Au(111) and Ag(111) films on cleaved and heated mica[79].

Schlenoff and coworkers studied the effect of substrate preparation on the absolute coverage of monolayers and determined the roughness factor (r) for various substrates. The smoothest surface was evaporated gold on mica after annealing ($r = 1.15$). Polished gold foil showed $r = 1.44$ (1.2 after annealing)[80].

Surface-enhanced Raman spectroscopy (SERS) requires, on the contrary, rough surfaces on a 10–100 nm scale. The preparation of such roughened metal surfaces has been described in several review papers[81,82]. The surface of an ordinary gold-coated silicon slide can be roughened electrochemically by repetitive anodic–cathodic potential scans[83]. Another approach is to evaporate gold or silver on top of supports precoated with rough substrates (such as alumina, silica, polymers etc.)[84]. Evaporation of silver under certain conditions gives silver island layers which also provide high enhancement of the Raman signals. Alternatively, the gold surface could be treated with 2-mercaptoethylamine to generate an amino-terminated surface. Colloidal gold is then adsorbed on this film, and the resultant rough gold surface can be used for monolayer preparation[30]. A completely different approach to surface enhancement of Raman signals consists of evaporation of a thin layer of silver (*ca* 60 Å) on top of a self-assembled monolayer prepared on an ordinary gold-coated silicon slide[68]. The Raman spectra of the layers prepared in this manner show strongest signals from the functional groups closest to the monolayer–ambient interface.

For electrochemical studies, bulk gold electrodes are conveniently used. They are briefly etched in dilute aqua regia solutions ($HCl : HNO_3 : H_2O = 3 : 1 : 6$), or by cycling through potentials between $+0.17$ and $+1.87$ V before use. Monolayers prepared on this gold surface show very good insulating properties, superior to those adsorbed on evaporated gold[85].

Preparation of colloidal gold which can also be used for a monolayer assembly is described in Section IX.

Single crystals of Au, Ag or Pt can be polished in the appropriate direction to produce Au(111), Au(100), Au(110)[86] and Ag(111)[87] and Pt(111)[88]. The polished surfaces are then cleaned by Ar or Ne ion bombardment following by annealing in high vacuum at 500–700 °C[89].

Silver (111) slides can also be prepared by thermal evaporation of Ag onto cleaned Si or glass slides. However, as silver surfaces are readily oxidized in the ambient atmosphere, the slides must be transferred to the deposition solutions immediately, preferably in an inert atmosphere[71]. Auger electron spectroscopy showed that 2 h exposure of the freshly evaporated Ag slides to the ambient laboratory atmosphere doubles the oxygen content[90].

Underpotentially deposited ultra-thin layers of silver or copper on gold substrates are also suitable for monolayer assembly. Monolayers prepared on such surfaces are different from those that form on the parent bulk metal surfaces and show enhanced stability against thermal desorption or exchange with thiol-containing solutions[91,92].

Ideally, all gold substrates should be covered with adsorbates directly after preparation. However, this is not always practical, and evaporated gold slides can be stored in the laboratory environment for several days. As a gold surface has a high surface energy, it readily becomes contaminated on storage. This can be easily monitored by wettability, as originally hydrophilic gold becomes increasingly hydrophobic on contamination[65]. Ishida and coworkers studied the effect of gold contamination on the coverage of octadecanethiol monolayer. They found that contaminated surfaces prevent formation of fully

covered monolayers, whereas the slides cleaned by exposure to UV radiation followed by ethanol rinsing readily form complete monolayers. Interestingly, slides rinsed with pure chloroform for 1 h prior to immersion in the deposition solution gave the lowest coverage monolayers even after prolonged exposure to octadecanethiol[93].

Other methods of cleaning contaminated gold surfaces before deposition of a monolayer include treatment for short periods (5–10 min) with strong oxidizing reagents, such as piranha solution[94,95], ozone[96], chromic acid and HF[97], etching in aqua regia[98], hot conc. H_2SO_4[99] etc. following by rinsing with water and ethanol. Cleaning with oxygen plasma was reported to hinder formation of monolayers, probably due to formation of a metastable gold oxide[65].

Freshly evaporated or cleaned metal substrates are then exposed to the solution or vapours of sulphur-containing adsorbates. In a typical procedure, the slides are immersed in a 1 mM solution of the appropriate compound in high purity ethanol for 16–24 h at room temperature[65]. After this period, the slides are withdrawn, rinsed with ethanol and dried.

Sometimes, much shorter immersion times from several minutes to 1–2 h have been reported. Although the surface coverage is already very high after this period, the order and crystallinity of such monolayers is inferior to those prepared by longer immersion[100]. For some bulky adsorbates, elevated temperatures (up to 60 °C) are needed to achieve high coverage[101,102]. For most substrates, however, variation of deposition conditions (e.g. concentration or temperature) have surprisingly little effect on the properties of the monolayers obtained. More concentrated solutions or even neat thiols can be used for deposition. However, prolonged treatment of the substrate with thiols (>48 h) results in the increase of the number of defects in the resultant monolayer[100]. Prolonged treatment of silver substrates (>12 h) with thiol solutions was found to result in formation of a thin layer of Ag_2S beneath the alkanethiolate monolayer[71]. Recently, use of 5 μM solutions was reported to produce better quality monolayers as compared to the standard millimolar preparation; however, the purity of the solvent used for such high dilutions becomes a crucial issue[43].

The most popular solvent for monolayer deposition is ethanol. Other solvents, such as water, hexane, toluene, THF, dichloromethane, acetonitrile and DMF, can also be used without affecting the structure of the resultant monolayer. However, the monolayers prepared using long-chain alkanes as solvents (e.g. hexadecane) did not form high quality layers, probably because the monolayer is contaminated with the solvent molecules[65]. Hexadecanethiol was also reported to give monolayers with poorer conductivity blocking properties when deposited from DCM as compared to the standard deposition from the ethanol solution[103]. To ensure that the monolayer is not contaminated by coadsorption of adventitious impurities, only highest purity solvents should be used.

Monolayers can also be prepared by adsorption from the gas phase by passing an under-saturated vapour of the thiol mixed with nitrogen over the substrate[104]. Layers prepared in this way, however, show somewhat different electrochemical blocking properties compared to those prepared by solution deposition[95]. Alternatively, monolayers were prepared by exposing the gold substrates to the vapours of the pure thiol in ultra-high vacuum[89]. Exposure to 400–600 L (1 L = 10^{-6} Torr) of 6-hydroxyhexanethiol vapour results in the growth of a so-called striped phase of alkanethiol, with the molecules lying flat on the surface (see Section V.A). Above 2500 L, well-packed layers of alkanethiols are formed[105]. The dosages necessary for formation of a complete monolayer depend strongly on the nature of the thiol. 1-Octanethiol, for example, forms complete monolayers after exposure to a pressure of only *ca* 2 L[106].

B. Mechanism of Monolayer Formation

The mechanism of formation of gold–thiol monolayers has been intensively investigated over the last decade. A detailed record of these studies is given in a recent review[5]. Formation of monolayers from thiols is understood best, although some information on adsorption of disulphides and sulphides is also available. XPS analyses of the sulphur 2p peak in monolayers indicate that adsorption of thiols and disulphides on gold produces thiolate species, RS^{-}[71,89]. Raman spectra of monolayers of disulphides and thiols, respectively, adsorbed on gold[107] and silver[28] surfaces also show the absence of otherwise strong peaks of $S-S$[108] and $S-H$ vibrations. This suggests that thiols are oxidized on metal surfaces producing surface-bound thiolates (equation 1).

$$Au + RSH \longrightarrow Au-SR + \tfrac{1}{2}H_2 \tag{1}$$
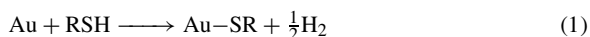
The fate of the hydrogen atom is not well understood, but the fact that the monolayers can be formed from the gas phase in the complete absence of oxygen[46,95], suggests the evolution of molecular hydrogen. However, the possibility associated oxidation giving water cannot be ruled out for solution preparations.

Adsorption of disulphides also produces thiolate species and it is believed to proceed via $S-S$ bond cleavage (equation 2).

$$2Au + RS-SR \longrightarrow 2Au-SR \tag{2}$$
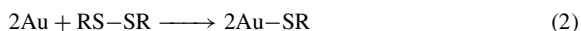
The evidence for the $S-S$ bond breakage, apart from XPS[73] and Raman data[108], comes from an elegant replacement experiment. Exposure of the monolayer prepared from the mixed disulphide $CF_3(CH_2)_{10}S-S(CH_2)_{10}OH$ to the solution of another thiol showed that the $CF_3(CH_2)_{10}S$ group in the mixed monolayer is replaced ca 10^3 times faster than the $HO(CH_2)_{10}S$ group[109] (monolayer replacement is discussed in Section IV.C). The fact that two different 'halves' of the mixed disulphide molecules behave independently in the monolayers proves the cleavage of the $S-S$ bond during deposition[110].

The similarity between XPS spectra and voltammetric curves of monolayers of thiols RSH and the corresponding dialkyl sulphides, RSR, led Porter and coworkers to conclude that adsorption of dialkyl sulphides proceeds via breakage of one of the $C-S$ bonds, and the adsorbed species are thiolate moieties, RS^{-}[111]. Detailed SIMS study of monolayers of asymmetrical sulphides RSR' showed, however, the presence of strong peaks of the intact disulphide [M+Au] and [M−H] (M = RSR'), which suggests that adsorption of sulphides occurs without breakage of any chemical bonds[112]. Coverage measurements also show that $C-S$ bond cleavage during deposition of sulphides is, if anything, minimal[80]. The nature of interactions between the gold surface and dialkyl sulphides and other sulphur-containing adsorbates (such as xanthates, thiophenes, thioureas etc.) is not yet clear. Formation of $\sigma-\pi$ delocalized coordinate bonding between sulphur and gold was suggested for thiourea monolayers on gold[113].

The energy of the adsorption process could be estimated on the basis of the literature data using bond energies for $RS-H$, H_2, $RS-SR$ and $RS-Au$ at 87, 104, 74 and 40 kcal mol^{-1}, respectively[72,114,115]. Values of −5 and −6 kcal mol^{-1} per gold thiolate unit are obtained for adsorption of thiols and disulphides, respectively. Schlenoff and coworkers estimated values of −5 and −12 kcal mol^{-1} for adsorption of thiols and disulphides, from his own and earlier published[116] data on the voltammetric curves corresponding to the thermodynamically controlled (equilibrium) electrodeposition of alkanethiolates on gold[80]. Recently, accurate thermodynamic parameters were obtained

from kinetic data on thiol adsorption/desorption[117], which are in agreement with earlier estimates[118]. For adsorption of 1-octadecanethiol from hexane onto gold, ΔG_{ads} is temperature dependent and, at room temperature, is ca -5.5 kcal mol^{-1}, $\Delta H_{ads} = -20 \pm 1$ kcal mol^{-1} and $\Delta S_{ads} = -48 \pm 1$ cal mol^{-1}K^{-1}. The total free energy of adsorption is therefore rather small. The relatively high energy of the Au−S bond compensates for the unfavourable entropic effect of immobilizing the molecules on the surface, as indicated by the large negative entropy of adsorption. It appears from the bond energy values that formation of monolayers from disulphides is more thermodynamically favourable than for the thiols. However, experimental data suggest the opposite: adsorption of thiols on gold appears to be a more favourable process than adsorption of disulphides and sulphides, at least kinetically. Competitive adsorption of these compounds showed preferential formation of monolayers from thiols[119]. If the presence of a bulky or charged functionality or another destabilizing group in the adsorbate makes formation of a monolayer less favourable, thiols give layers of better quality than disulphides, and sulphides produce the poorest layers. Higher coverage in monolayers of thiols as compared to corresponding disulphides was reported for sterically hindered secondary alkanethiols[120], derivatized norbornane[98] thiols and a heavily charged viologen derivative[121]. Simple dialkyl sulphides R−S−R give well-packed monolayers, comparable to those of the corresponding thiols, but the presence of a polar functional group (such as COOH) in the molecule of a sulphide makes the monolayers prepared from this sulphide disordered and incomplete[122,123]. Thiols were also shown to adsorb preferentially over amines, phosphines and other compounds[124].

Kinetics of monolayer formation have been intensively studied. SPR[18] and QCM[22] are the simple methods allowing monitoring of the adsorption *in situ*. It was shown that deposition usually proceeds through a two-step process (Figure 6). The first step is first order with respect to the concentration of adsorbate[18] and is well described by a Langmuir isotherm[125]. This is a fast reaction comprising adsorption and desorption processes in equilibrium. 60–80% of material adsorbs during this step[18]. It is usually accepted that this first step produces physi- or chemisorbed structures with alkane chains in a relatively disordered state[126].

The electrochemical deposition of ethanethiolate on the Ag(111) surface showed two energetically-distinct reaction steps. The second step is slower, and is accompanied by the ordering of the monolayer[127].

Effects of terminal functionality and the chain length on the rate of the first equilibrium step of adsorption have been studied. Apparently, intermolecular interactions between functionalized alkanethiols play only a minor role in the kinetics of monolayer adsorption. Alkane and ω-hydroxyalkanethiols form monolayers at almost the same rate[24,65]. Short-chain alkanethiols adsorb faster than their long-chain counterparts[18,128,129]. This probably reflects the fact that the first step of adsorption includes most of the entropy loss of the process, and this factor slows down the assembly of long-chain molecules.

Solvent was found to significantly affect the rate of monolayer formation. Alkanethiols form monolayers much faster from DMF than acetonitrile solutions[130]. Moreover, in acetonitrile, disordered multilayers form first, followed by slow desorption and reorganization, leading to a well-packed monolayer.

The second step of adsorption is much slower and is zeroth order with respect to the thiol concentration[20]. Saturation is usually reached after 16–24 h of exposure. During this step, the monolayer reorganizes, producing well-packed structure and freeing some more gold surface which is immediately occupied by additional thiol molecules. The alkane chains straighten and the order and orientation of the monolayer
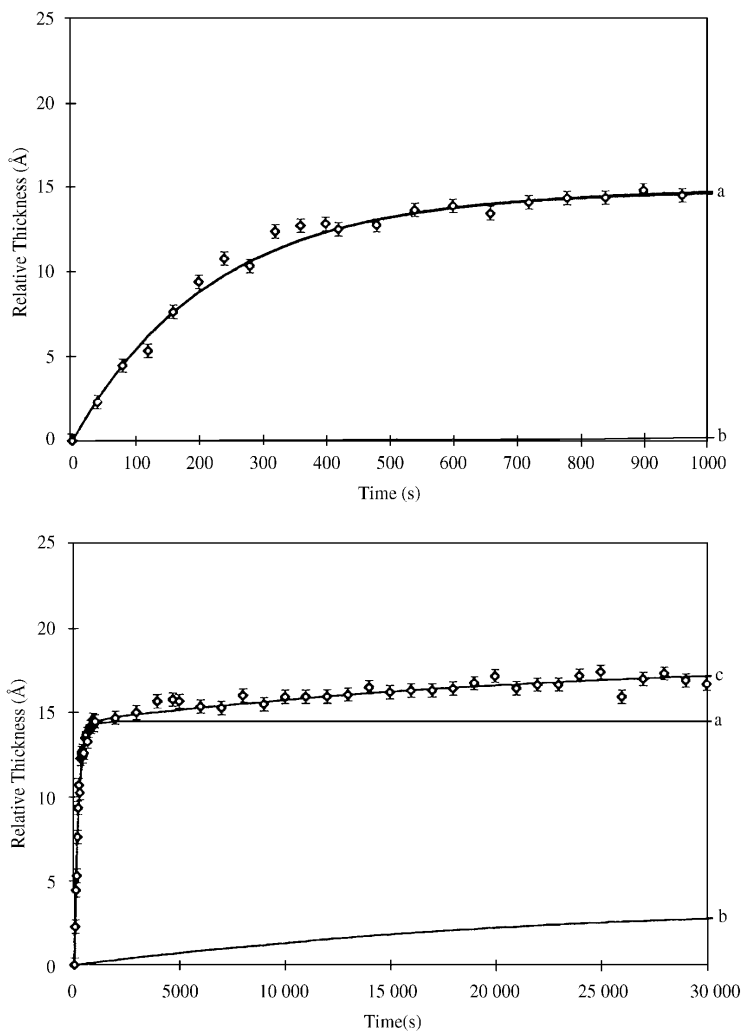
FIGURE 6. Two-step adsorption of dodecanethiol on the gold surface. (a) First step of adsorption, (b) second step of adsorption, (c) combined two-step model. Reproduced by permission of NRC Research Press from Reference 18

gradually improves. It is this reorganization which produces highly ordered quasi-crystalline structures[126,131] and makes the monolayers impermeable to ions, as shown by electrochemical measurements[132].

The very possibility of monolayer rearrangement and improvement of packing suggests that the thiolate moieties retain some lateral mobility on the gold surface. STM studies

indeed revealed the presence of the facile transport of gold atoms on the surface[133] and mobile defect sites on the gold surface[134]. Real-time motion of the domain boundaries in self-assembled monolayers of $CH_3O_2C(CH_2)_{15}SH$ on gold was directly observed by time-lapse imaging using STM[135]. Thus, the motion of the thiolate moieties RS–Au may play an important role in the adsorption process. Interestingly, migration of defects does not depend on the length of the alkane chain and is determined by the head group of the monolayer[136].

The above two-step process of thiol adsorption is a simplification, and formation of gold–thiol monolayers in fact involves a number of physical and chemical processes. Contrary to the earlier suggestion that monolayers grow uniformly on the surface[40], there appears to be an increasing amount of evidence (STM) that formation of monolayers starts with nucleation and growth of islands[137–139]. The islands consist of several tens of molecules each and locate at the turns of the herringbone Au(111) structure[140]. At very low coverage, a highly mobile lattice-gas phase is formed on the gold surface, which then forms a striped-phase surface, probably with the molecules lying flat on the gold. The structure of this striped phase is discussed in Section V.A. Above the critical coverage, nucleation of dense and well-packed islands occurs and these islands then grow until the surface reaches saturation[105]. This mechanism is shown schematically in Figure 7.

Voltammetric studies showed that the effective surface area of the gold electrodes irreversibly increases upon adsorption of thiols[141]. These morphological changes are probably due to the fact that some gold is etched away during deposition[142]. The average amount of gold in the deposition solution after 10 min of exposure to dodecanethiol corresponds to dissolution of *ca* 2% of a monolayer of Au(111), but this erosion of gold depends on the concentration of the thiol in the deposition solution and increases with more concentration solutions[143].
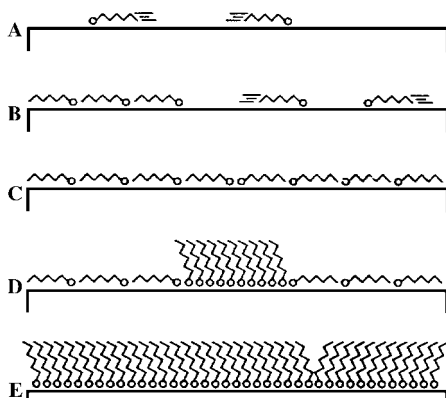
FIGURE 7. Schematic of self-assembly mechanism for alkanethiols on Au(111). **(A)** Thiols adopt the highly mobile lattice-gas phase at very low coverage. **(B)** Above a critical value of surface coverage, striped-phase islands nucleate and grow in equilibrium with lattice-gas phase. **(C)** Surface reaches saturation coverage of striped phase. **(D)** High-density islands nucleate at striped-phase domain boundaries. **(E)** High-density islands grow at the expense of the striped phase until the surface reaches saturation. Reproduced by permission of the American Association for the Advancement of Science from Reference 105

STM images showed that formation of gold–thiol monolayers is accompanied by the appearance of the pit-like defects in the surface. These pinholes were found to be 2.5 Å deep and were assigned to the defects in the Au surface layer, rather than to the defects in the monolayer[144]. Etching of gold during deposition was originally thought to be the reason for formation of these Au vacancy islands[142–144]. However, later studies found that formation of the vacancy islands occurs even in the case of vapour-phase deposition, and is due to the lateral displacement of Au atoms[145]. Poirier suggested a model in which the original compressed herringbone structure of a bare Au(111) surface relaxes during deposition, forcing excess gold atoms out of the surface and creating adatoms and vacancy islands[146]. Interestingly, these pit-like defects, which appear during monolayer formation, completely disappear when the monolayer is quantitatively removed by UV oxidation[147].

C. Preparation of Mixed Monolayers and Monolayer Exchange

Exposure of a gold slide to a mixture of two different thiols results in the formation of a mixed monolayer, in which both thiolate moieties are present[148]. The composition of such a monolayer (usually determined with XPS) is generally different from the composition of solution[149]. Coadsorption of different thiols provides an easy way to prepare mixed layers with variable controlled concentration of the components, and this method is routinely used to tailor the properties of monolayers. Mixed monolayers with the gradient of two thiols can be prepared using Sephadex gel to prevent diffusion[150,151].

The study of selectivity of this competitive adsorption revealed several interesting features. It was found that longer-chain alkanethiols adsorb preferentially over short-chain compounds[152]. Adsorption of $HS(CH_2)_{21}CH_3$ is preferred over adsorption of $HS(CH_2)_{11}CH_3$ in ethanol by a factor of $20–30$[152]. Electrostatic and steric interactions can also influence relative adsorptivity of alkanethiols. Incorporation of polar functional groups, such as carboxamide or especially charged groups such as quaternary ammonium, in one of the thiols leads to a smaller proportion of this adsorbate in the mixed monolayer[153]. Adsorption of compounds with bulky substituents is strongly disfavoured as compared to the adsorption of straight-chain alkanethiols. In an ethanol solution of octadecanethiol and t-butylthiol, adsorption of the former is preferred by a factor of $290–710$[154]. Selectivity of adsorption is similar for thiol–Ag(111) monolayers, but is less pronounced[155].

This selectivity is subject to a strong solvent effect, and is probably determined by the polarity and solubility of the substrates. The least soluble thiol usually adsorbs preferentially[124]. Thus, in a mixture of an alkanethiol and an ω-hydroxyalkanethiol, the adsorption of the former is strongly preferred if deposition is performed from ethanol solution. Adsorption from acetonitrile, on the other hand, does not show any preference, and adsorption from isooctane results in the preferential adsorption of a hydroxythiol[119,156]. The preference of long-chain thiols over the short-chain ones and compounds with bulky substituents also depends on the solvent, being much less pronounced in non-polar solvents[152]. Adsorption of octadecanethiol is preferred over adsorption of t-butylthiol in isooctane solution by a factor of only $40–100$ (the corresponding ratio in ethanol is $290–710$, *vide supra*), and by just a factor of $3–4$ over adsorption of straight-chain butanethiol (compared with a $20–30$ ratio for C_{22} *vs* C_{12} preference in ethanol, *vide supra*)[157].

The composition of the mixed monolayer may also depend on the deposition time[158] and temperature. Whitesides and coworkers found that at elevated temperatures ($60–70\,°C$) mixed monolayers tend not to form at all; the films obtained after co-deposition of

long- and short-chain thiols tend to exist as a single phase predominantly composed of either long-chain or short-chain thiolates, depending on the composition of the deposition solution[159].

Bain and Whitesides concluded that competitive adsorption is controlled thermodynamically rather than kinetically. They argue that it is difficult to imagine the adsorption mechanism which would kinetically favour preferential adsorption of longer-chain alkanethiols[152]. This is consistent with the recent observation that while thermodynamically controlled competitive adsorption leads to the preferential adsorption of long-chain thiols, short-chain alkanethiols actually adsorb faster[128,129,160].

Careful FT-IR analysis of mixed monolayers prepared by coadsorption of C_{12}-thiol/perdeuteriated C_{18}-thiol and C_{22}-thiol/perdeuteriated C_{12}-thiol mixtures showed that mixed monolayers consist of a well-packed inner region, and a disordered outer shell (Figure 8a)[161]. If a thiol with a terminal bulky group is coadsorbed with an alkanethiol terminating at or below the level of the bulky group, the monolayer obtained consists of a well-packed alkane layer with the bulky groups protruding above it (Figure 8b)[162,163]. This situation is often exploited for preparation of well-packed monolayers with bulky functional groups. A target thiol, which can have an electroactive group or even a

(a)

(b)
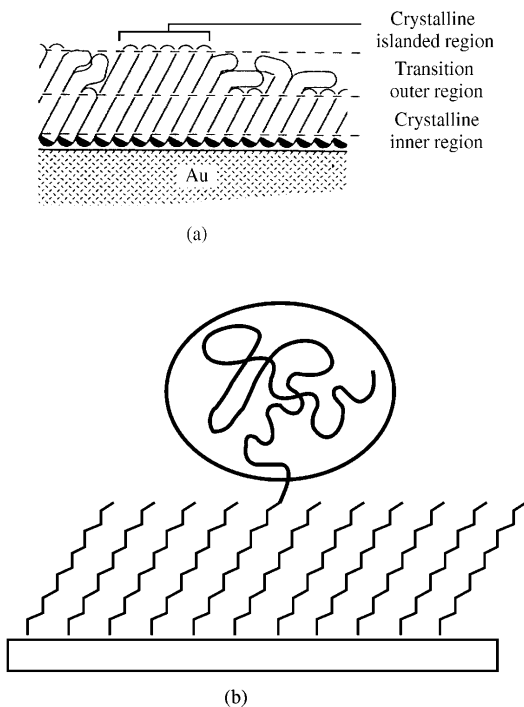
FIGURE 8. (a) Coadsorption of two alkane thiols with different chain length leads to the formation of a mixed monolayer. Reprinted with permission from Reference 161. Copyright (1992) American Chemical Society. (b) Schematic illustration of a mixed monolayer of a thiol with a bulky substituent and a shorter-chain alkanethiol. Reproduced by permission of Current Chemistry Ltd from Reference 164

biomolecule on its terminus, is coadsorbed with an alkanethiol of shorter length[164]. By manipulating the composition of the deposition solution, it is possible to vary the density of the functional groups protruding above the monolayer interface. The problem of phase separation in such mixed monolayers is discussed in Section V.D.

Mixed monolayers can also be prepared by coadsorption of thiols and disulphides. Hydroxyl and methyl-terminated alkanethiols adsorb preferentially to the parent disulphides by a factor of *ca* 75[119]. However, formation of identical monolayers was reported by coadsorption of ferrocenyl and methyl-terminated derivatives regardless of whether they were both in the form of a thiol, or whether one of them was a disulphide[165].

Adsorption of asymmetrical disulphides R^1S-SR^2 leads to formation of mixed monolayers, too. As the $S-S$ bond is broken during deposition, both thiolate moieties in the monolayers behave independently[109]. However, both groups R^1 and R^2 are present in the same concentration in these monolayers even if R^1 is a long-chain alkane and R^2 is a bulky *t*-butyl group[157].

An alternative approach to preparation of mixed monolayers is partial displacement of a monolayer by an adsorbate from solution. Exposure of a homogeneous monolayer to the solution of a different thiol results in an exchange process, during which the original surface-adsorbed thiolates are replaced with the thiolates from solution[65]. This is a complicated process and its rate and extent of replacement depend strongly on the nature of the thiols involved. Short-chain thiols are replaced quantitatively and relatively fast. Thus, propanethiol is completely displaced by octadecanethiol within 1.5 h[65]. Long-chain thiols are, however, displaced much more slowly, and replacement does not go to completion[109]. The exchange study with a ferrocene-terminated electroactive thiol showed similar behaviour: a small part of a monolayer is exchanged within 1 day, and virtually no further replacement was observed in a 10-day period[166]. The use of ^{35}S-labelled thiols showed that self-exchange is a partial first-order process, and remaining moieties can never be exchanged. Kinetic studies of desorption and exchange in a monolayer revealed close similarities. It was therefore suggested that there is a common mechanism for surface detachment, postulated to be a rate-limiting desorption step as a disulphide[80]. Formation of disulphides as a result of an exchange process was proved by Mohri and coworkers[167]. They found that self-exchange in solution of a thiol and gold powder coated with a monolayer results in accumulation of disulphide in solution.

Incomplete displacement of long-chain thiols is probably due to the domain structure of monolayers, and the different behaviour of molecules on the edges of domains and in the middle. Treatment of a mixed monolayer of hexadecanethiol and a ferrocenyl-terminated thiol with a solution of thiol **A** (Figure 9b) results in the loss of *ca* 30% of ferrocene groups in the monolayer. However, if this three-component mixed layer is immersed in the solution of thiol **B**, only thiol **A** can be replaced, but the remaining 70% of ferrocenethiolate groups resist replacement (Figure 9c)[168]. This is consistent with the exchange process proceeding mainly at the domain boundaries and defect sites of the monolayer. An STM study of the exchange process also showed that the domain boundaries act as important areas for exchange phenomena[169].

Incorporation of amide bonds into alkanethiols makes their monolayers surprisingly resistant to exchange. Thus, exposure of a monolayer of $CF_3CH_2NHCOCH_2SH$ to the solution of hexadecanethiol in ethanol showed that the replacement rate is *ca* 100–1000 times lower than that of butanethiol or 4,4,4-trifluorobutanethiol. The reason for such stability is probably the H-bonding between adjacent amide groups which cement the structure and make desorption a very unfavourable process. However, this stabilization only takes place with disordered short-chain thiols, and the monolayer of a long-chain
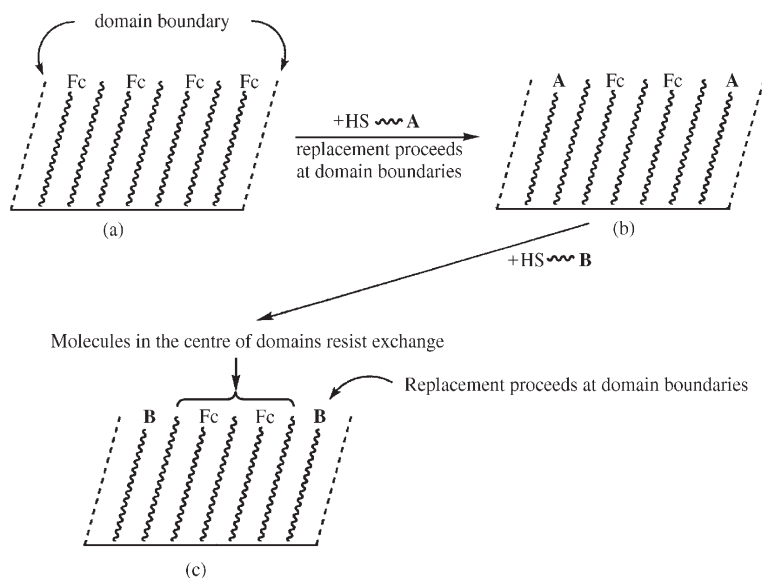
FIGURE 9. Exposure of a mixed monolayer (a) to the solution of thiol **A** leads to partial replacement of ferrocenethiol (b). Further exposure to thiol **B** leads to the replacement of thiol **A**, but remaining ferrocenethiol is not replaced (c) (F_c = ferrocenyl)

thiol, $CF_3(CH_2)_{11}NHCOCH_2SH$, is replaced at a rate similar to that of the monolayer of $CH_3(CH_2)_{15}SH$ (which is already an extremely slow process)[170].

Recently, the exchange phenomenon was suggested to be linked to the oxidation of the sulphur head group in the gold–thiol monolayers (see Section VI). Fritsch and coworkers found that the monolayers exposed to the ambient atmosphere for prolonged periods undergo exchange much more rapidly than the monolayers freshly prepared in the carefully controlled anaerobic conditions. They proposed a mechanism for exchange, starting with the oxidation of the thiolate moiety in the monolayer to a sulphinate or sulphonate derivative. Weakly bound sulphinate/sulphonate then dissolves in the exchange solution, and the resulting unoccupied gold surface is attacked by another thiol to effect replacement. Laser irradiation, however, may have catalysed the oxidation of thiolates in this study[171].

Knoll and coworkers found that octanethiol monolayers prepared by short (30 min) immersion in the deposition solution are more stable towards exchange than the monolayers prepared by a more prolonged (1 day) treatment[172].

Disulphides, unlike thiols, do not undergo appreciable exchange with monolayers[157].

V. STRUCTURE OF GOLD–THIOL MONOLAYERS

A. Structure of the Sulphur Adlayer

The arrangement of sulphur atoms in alkanethiolate monolayers on the Au(111) surface has been extensively studied by helium and electron diffraction and, more recently, by

AFM and STM microscopy. Results of these studies have been summarized in several recent reviews[4,5,11,54], and we give here only a brief description of the main results.

Alkanethiols form a hexagonal ($\sqrt{3} \times \sqrt{3}$) R 30° lattice commensurate with the underlying Au(111) surface. Sulphur atoms in this structure occupy the hollow sites between the gold atoms (Figure 10). The distance between adjacent S atoms in such a structure is 4.97 Å[4].

Despite the similarity between the structures of Au(111) and Ag(111) (the nearest-neighbour distances are 2.88 and 2.89 Å, respectively), the structure of the alkanethiolate overlayer on Ag(111) is completely different. Sulphur atoms occupy alternately hollow and on-top binding sites on the surface, forming a distorted ($\sqrt{7} \times \sqrt{7}$) R 10.9° lattice (Figure 11). The S···S distance in this structure is *ca* 4.6 Å.
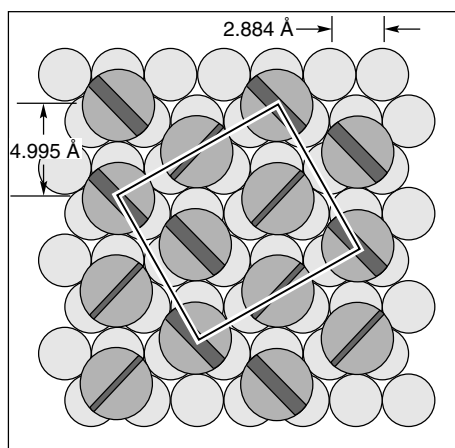
FIGURE 10. Alkanethiolate adlayer (large circles) on the Au(111) surface (small circles). The diagonal slash in the large circles represents the azimuthal orientation of the plane defined by the all-*trans* hydrocarbon chain. Reprinted with permission from Reference 54. Copyright (1997) American Chemical Society
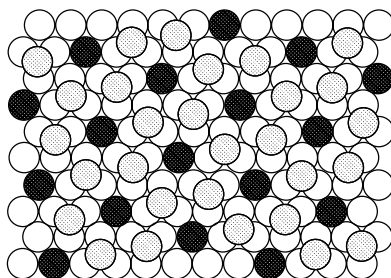
FIGURE 11. A possible arrangement of alkanethiolate on Ag(111) surface (open circles). Dark and light-shaded circles represent thiolates at the on-top and hollow sites, respectively. Reprinted with permission from Reference 5. Copyright (1996) American Chemical Society

Arrangements of alkanethiolates on other faces of the Au crystal are also different from those described for Au(111). Electron diffraction studies showed the square symmetry for alkanethiol monolayers on the Au(100) surface, with the distance between adjacent sulphur atoms being 4.54 Å. This arrangement may, however, be an oversimplification of a more complicated structure[5]. Possible overlayer structures of alkanethiolates on Au(110)[86] and Au(001)[173] surfaces are discussed by Scoles and coworkers. Gold–sulphur bonding was found to be stronger at the Au(110) than at the Au(111) surface[174].

There remains, however, some controversy about the structure of alkanethiolate on a Au(111) surface, described above. Fenter and coworkers suggested, on the basis of grazing incidence X-ray diffraction data, that there are two non-equivalent sulphur species on the surface of Au(111)[175]. According to his model, sulphur head groups dimerize on the surface, occupying one hollow and one bridge site and producing a structure with a S···S spacing of 2.2 Å. Later, several other reports were published in support of this model or suggesting co-existence of single and dimerized thiol species on Au(111)[169,176−181]. However, recent XPS study suggests that the 'second-type' S species might in fact belong to the unbound thiol[182] which was present in the monolayer, unless it had been thoroughly rinsed with appropriate solvent. The actual structure of the gold–sulphur interface therefore remains uncertain.

STM and AFM studies showed the presence of different types of defects in gold–thiol monolayers. Monolayers arrange in atomically flat domains of different size, which are clearly visualized in the AFM and STM images (Figure 12). Domains are separated by rotational barriers, tilt boundaries, stacking faults and antiphase boundaries. The size of domains varies from 5 to 15 nm[183]. Apart from domain boundaries, there are numerous pit-like defects. The depth of these defects was consistent with the Au(111) single atom steps, thus suggesting that the defects originate from the structure of the Au(111) surface, and not the imperfections of the alkanethiolate layer. These vacancy islands in the Au(111) surface are thought to be created during monolayer deposition (see Section IV.B)[142]. Similar images with domains and gold vacancy islands were observed in alkanethiolate monolayers on Ag(111)[184].

Whitesides and coworkers developed a procedure to estimate the density of defects in gold–thiol monolayers. The monolayer surface is exposed to the gold-etching solution, the pits obtained are transferred into pits on the Si surface through further chemical treatment and the number of pits per unit area counted. Long-chain alkanethiolate monolayers prepared by the standard technique show pit densities of *ca* 100 pits mm^{-2}. The number of pits sharply increase if the gold surface is stored for a long time in air prior to monolayer deposition[100].

Annealing of alkanethiol monolayers at 70–90 °C results in healing of some defects[136] and merging of small domains into larger ones[186]. The motion of vacancies and domain boundaries can be readily visualized[185]. The well-ordered molecular domains could extend in annealed monolayers over 100 Å[187]. Annealing at higher temperatures ($\geqslant$100 °C) results in partial desorption of the monolayer and formation of molecular vacancies. Further desorption results in the formation of striped pattern domains (so-called because of their stripy appearance in the STM images, Figure 13)[185].

Such 'striped' monolayers were first obtained by chemical vapour deposition in high vacuum and their structure was studied by Nuzzo and coworkers[46]. Later, these layers were shown to be different from the films prepared by standard solution deposition, and Poirier and Pylant suggested that the molecules in 'striped' layers lay flat on the surface[105]. This hypothesis was supported by the observation that the distance between adjacent 'stripes' equals the length of the fully stretched appropriate disulphide[45]. Further
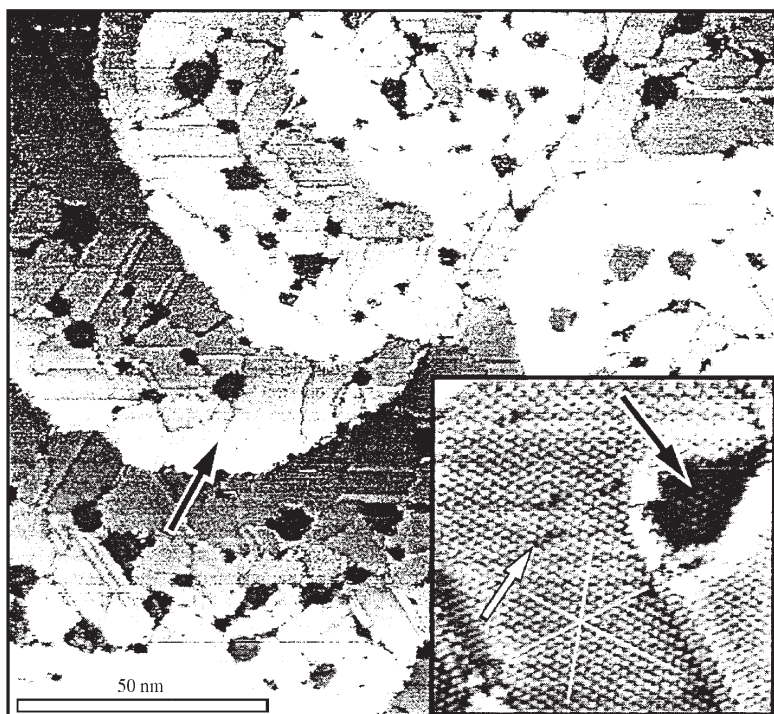
FIGURE 12. Large-area image of a dodecanethiol monolayer on Au(111) showing domains and pinhole defects. Reprinted with permission from Reference 185. Copyright (1995) American Chemical Society
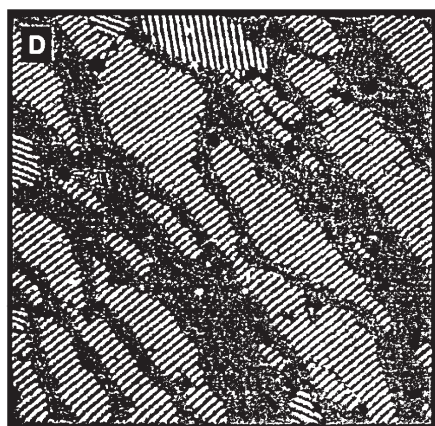
FIGURE 13. STM image of a 'striped' monolayer of 6-mercaptohexanol on Au(111) surface. Reproduced by permission of American Association for the Advancement of Science from Reference 105

studies of 'striped' monolayers by LEED and XPS also confirmed the flat orientation of the alkanethiol molecules in the monolayers (see Figure 7c)[188]. Interestingly, the striped layers obtained by partial thermal desorption of thiolate monolayers seem equivalent to those obtained by vapour deposition[185]. This points to the common mechanism of adsorption and desorption processes. Recently, very similar striped layers were observed *in situ* during formation of a gold–thiol monolayer from a very dilute (*ca* 0.3 μM) solution of decanethiol in heptane[139].

Most studies of the adlayer structure were performed on thiol monolayers deposited on either gold crystals or annealed Au/mica substrates known to possess large atomically flat terraces. However, recent AFM study of thiols adsorbed on the surface of sputtered gold, which has a granular structure, showed the same lattices as those observed for Au(111) terraces. This implies that even on sputtered gold, monolayers are formed with a high degree of local order[189].

B. Structure of the Alkane Overlayer

Arrangement of the alkane chains in the monolayers of alkanethiols on the gold surface was studied in detail by grazing angle FT-IR spectroscopy. A typical spectrum of an alkanethiol monolayer in the C−H stretching region is in Figure 14a. Analysis of such spectra considers the precise location of the $\nu(CH_2)$ peaks which is sensitive to the lateral interactions between the alkane chains and thus to the degree of order of the monolayer[190]. This relationship is illustrated in Table 2.

In crystalline materials, with the alkane chains tightly packed and in an all-*trans* conformation, the asymmetric stretch of the methylene groups $\nu_a(CH_2)$ shows at 2918 cm^{-1}, whereas in liquid state, with disordered orientation of alkane chains and high concentration of *gauche* interactions, the position of this peak is shifted towards higher frequencies (2921–2924 cm^{-1}).

Analysis of the data in Table 2 shows that alkanethiols with chain length $\geqslant 11$ form well-packed, crystalline-like monolayers on the gold surface [$\nu_a(CH_2) = 2918$ cm^{-1}]. Shorter-chain alkanethiols ($n < 11$) form more liquid-like, disordered structures [$\nu_a(CH_2) = 2920–2921$ cm^{-1}][191]. This chain-length dependence of the order in gold–thiol monolayers is readily confirmed by a variety of other methods, including thickness measurements[191], ion permeability measurements by heterogeneous electron transfer[191] and contact angle measurements[65]. More recent helium diffraction data also showed that long-chain alkanethiols form crystalline monolayers on Au(111). As the length of the carbon chain is shortened, an abrupt decrease in surface order at around ten carbon atoms per chain is observed[44].

Intensity of the peaks in the grazing angle FT-IR spectra of monolayers depends on the orientation of the functional groups (see Section III.B). In fully stretched crystalline-like monolayers of long-chain alkanethiols, the symmetrical stretch of the CH$_2$ groups is determined by the orientation of these groups with respect to the surface. In monolayers with alkane chains almost perpendicular to the surface (small tilt angle α, Figure 15), the dipole moments of the $\nu(CH_2)$ vibrations are almost parallel to the surface (Figure 3b), and the corresponding peaks become invisible in the IR spectrum. For significantly canted alkane chains (big tilt angle α), however, the $\nu(CH_2)$ peaks are intense in the spectra. Comparison of the FT-IR spectra of octadecanethiol monolayers on Au(111) and Ag(111) surfaces shows remarkable differences in the orientation of the alkane chains in these monolayers (Figure 14). Higher intensity of the $\nu_a(CH_2)$ peak of the gold–thiol monolayer compared to that of the silver–thiol film indicates a significantly increased tilt.

(a)

(b)
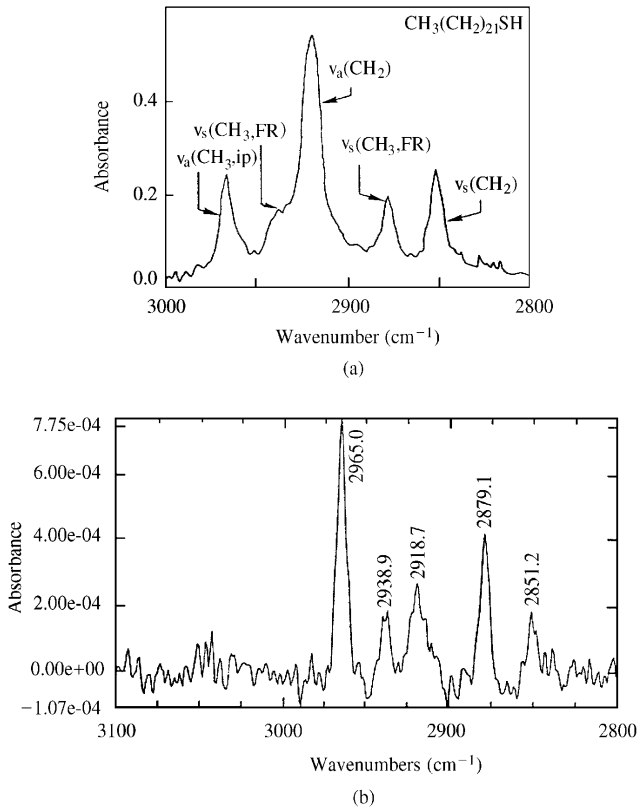
FIGURE 14. FT-IR spectra of docosanethiol monolayers on the Au(111) (a) and Ag(111) (b) surfaces in the C—H stretching region. Symbols ν_a and ν_s refer to the asymmetric and symmetric stretching vibrations, respectively. Symbol ip refers to the in-plane vibration, and FR stands for Fermi resonance, which causes the split of the $\nu_s(CH_3)$ band. Reproduced by permission of Academic Press, Inc. from Reference 4

TABLE 2. CH_2 stretching peak positions for $CH_3(CH_2)_n SH$ in crystalline and liquid states and adsorbed on gold[191]

CH_2 stretching mode	Peak positions in bulk phase (cm^{-1})		Peak positions in monolayer (cm^{-1})					
	crystalline	liquid	$n = 21$	$n = 15$	$n = 11$	$n = 9$	$n = 7$	$n = 5$
$\nu_a(CH_2)$	2918	2924	2918	2918	2919	2920	2921	2921
$\nu_s(CH_2)$	2851	2855	2850	2851	2851	2851	2852	2852
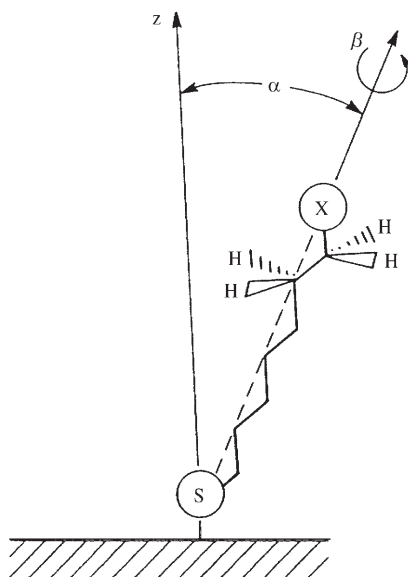
FIGURE 15. Tilt (α) and rotating (β) angles of an all-*trans* alkane chain in surface coordinates. Reprinted with permission from Reference 72. Copyright (1980) American Chemical Society

Comparison of the experimental spectra with those calculated for a hypothetical isotropic monolayer makes it possible to estimate quantitatively the value of the tilt angle (as the intensity of the peaks is proportional to the cosine squared of the tilt angle, Figure 3b)[8]. Calculations show a *ca* 30° tilt angle for alkanethiol monolayers on Au(111)[71,72] and 12° or less[5] for monolayers on Ag(111)[71]. The values of rotational angle (β, see Figure 15) are *ca* 53° and 45° for alkanethiol monolayers on Au(111) and Ag(111), respectively[71].

The difference in orientation of the alkane chains on Au(111) and Ag(111) is caused by the structure of the sulphur adlayer on surfaces of these metals (see Section V.A). The diameter of an alkane chain in all-*trans* conformation is *ca* 4.4 Å. The distance between adjacent S atoms in the monolayer on Ag(111) is *ca* 4.6 Å, which allows the chains to pack tightly without tilting away from the surface normal. On the other hand, the S$\cdots$S distance in the monolayers on Au(111) is *ca* 5.0 Å, substantially smaller than the distance between tightly packed alkane chains. Alkanethiol monolayers on Au(111) cannot therefore achieve close packing with the alkane chains perpendicular to the surface. The tight packing (resulting in maximizing the van der Waals interactions between the alkane chains) can, however, be achieved if the alkane chains tilt *ca* 30° away from the surface normal.

The validity of this approach was shown in experiments with gold–thiol monolayers having rod-like groups with the diameter bigger than that of an alkane chain. The distance between adjacent tightly packed perfluoro segments is *ca* 5.6 Å. As this is greater than the distance between adjacent S atoms on the Au(111) surface (5.0 Å), perfluoroalkanethiols can form tightly-packed monolayers with perfluoroalkane chains practically

perpendicular to the surface. Low tilt of these monolayers has indeed been observed experimentally[192−194]. Similarly, branched thiols, having two alkane chains attached to the same sulphur anchor, form monolayers with very small tilt[120], as do rigid rod-like aromatic thiols[195]. In these two latter cases the distance between the adjacent two molecules in a tightly packed structure is greater than the S···S distance, which leads to decrease of the tilt angle.

Near-edge X-ray absorption fine structure (NEXAFS)[196] and X-ray diffraction data[197] confirmed the existence of all-*trans*, well-packed crystalline-like alkane chains with tilt and rotational angles of *ca* 30° and 50°, respectively, in the long-chain ($n > 10$) alkanethiolate monolayers on the Au(111) surface. Helium diffraction data provided more details about their structure[198]. The alkanethiols were shown to form a $c(4 \times 2)$ superlattice at the surface of the monolayer, with the unit cell containing 4 molecules. This structure is consistent with the earlier FT-IR data[199], and it was confirmed by grazing incidence X-ray diffraction (GIXD)[200], low energy He diffraction data[43] and STM measurements[54]. The arrangement is shown in Figure 10. More recently, GIXD data showed that the tilt angle and its direction depend on the length of the alkane chain in the monolayer[201].

Calculations show that there are two binding modes for sulphur at the three-fold hollow sites of the Au(111) surface, one with Au−S−C angle 180°, sp-hybridization and tetrahedral sp^3 bonding with Au−S−C angle 104°[202]. The latter mode is more stable by *ca* 0.4 kcal mol^{-1}. The Au−S−C angle in most alkanethiolate monolayers is thought to be close to tetrahedral (104°)[5]. However, the very small tilt of the monolayers of some aromatic rigid-rod compounds (such as H−[−C$_6$H$_4$−C≡C−]$_n$−C$_6$H$_4$−SH)[195] implies that the Au−S−C angle is close to 180° and thus the sp-binding mode is also possible.

The effect of temperature on the interactions between the alkane chains in alkanethiolate monolayers have been studied. The helium diffraction study of the long-chain alkanethiols monolayers on Au(111) showed that at 35 K the terminal methyl groups of the monolayer have no conformational freedom. With increased temperature the thermal motion of the terminal groups gradually increases, and at 100 K no diffraction peaks could be observed[44]. The lower portion of the monolayer remains tightly packed, but with the further increase of temperature the *gauche* defects accumulate near the chain terminus, as shown by FT-IR spectroscopy[199,203]. These changes are reversible up to 350 K. Above this temperature, however, the *gauche* defects gradually spread across the alkane chains. This melting of the alkane chains at high temperatures is irreversible, and the transition from crystalline to liquid-like phase of the monolayer of C$_{22}$H$_{45}$SH occurs in the temperature range 350−400 K[204]. Fenter and coworkers observed a phase transition in the monolayer of dodecanethiol at 50 °C above which the crystalline form coexists with the liquid. Melting is complete at *ca* 70 °C. Tetradecanethiol also showed melting of alkane chains which is complete at *ca* 90 °C. However, tetradecanethiol undergoes another phase transition at the temperature above 60 °C which gives a non-hexagonal structure. These phase transitions are reversible[200]. Lennox and coworkers studied heterogeneous electron transfer on monolayers of long-chain alkanethiols and observed a maximum on the electrochemical thermogram at 55 °C. This behaviour is consistent with the coexistence at this temperature of melted and unmelted chains in the monolayer[205].

Computer simulations of monolayers also showed the presence of different phases at different temperatures[206,207]. A phase transition at 40 K in the monolayer of tridecanethiol refers to the change in the orientation of alkane chains from the nearest-neighbour direction to the next nearest neighbour. The melting of alkane chains was observed at *ca* 400 K[208].

More detailed discussion of thermally induced changes in self-assembled and Langmuir–Blodgett monolayers can be found in the review paper by Ulman[209]. Thermal
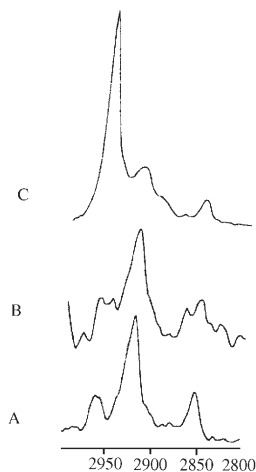
FIGURE 16. Polarization-modulation grazing angle FT-IR spectra of the monolayer of $CH_3(CH_2)_{17}-$ $S-(CH_2)_9CH_3$ on Au(111) in air (A), and in contact with D_2O (B) and acetonitrile (C) solutions. Reprinted with permission from Reference 210. Copyright (1996) American Chemical Society

behaviour of alkanethiolate monolayers on the surface of gold colloids, which show similar behaviour to the monolayers on planar gold, is discussed in Section IX.

Solvent effects on the arrangement of the alkane chains were analysed by Anderson and coworkers[210]. *In situ* polarization-modulation FT-IR data showed that well-packed octadecanethiol monolayers have a similar arrangement of the alkane chains in air and in contact with D_2O or acetonitrile solutions[211]. However, less well packed decanethiol films show spectral changes in acetonitrile. The changes are most prominent in the case of a completely disordered monolayer of dialkyl sulphide $CH_3(CH_2)_{17}-S-(CH_2)_9CH_3$ (Figure 16). While the FT-IR spectra in air and in D_2O are similar, the spectrum in acetonitrile shows a significant increase in the relative intensity of the asymmetric methyl vibration. These structural changes in the monolayer are explained by the solvation of the defective structure of the disordered monolayers. D_2O cannot solvate hydrophobic alkane chains, and the spectra in air and D_2O solutions are therefore similar. Tight packing of the alkane chains in the case of octadecanethiol monolayers also prevents solvation[210].

Similarly, monolayers of nonanethiol show preferential orientation of the alkane chains titled *ca* 30° with respect to the monolayer surface. However, upon immersion of the monolayer in an alkaline solution (0.1 M KOH), the *in situ* recorded FT-IR spectrum reveals a dramatic decrease in the order of the monolayer and complete loss of the preferential orientation for the alkane chains[212].

C. Functionalized Monolayers

The flexibility and ease of synthetic procedures has allowed a countless number of functional groups to be incorporated in gold–thiol monolayers. It is impossible to mention all examples; in this section we will discuss the structural issues of functionalized monolayers, and we will only refer to monolayers with well-investigated structures. Monolayers containing chemically reactive groups or groups capable of forming non-covalent interactions with the guest molecules are described in Sections VII and VIII, respectively.

Because of the geometric requirements of the tightly-packed monolayers, incorporation of virtually any functional group will affect their structure. The ultimate arrangement is determined by the size of the functionality and intermolecular interactions. Nuzzo and coworkers studied the monolayers of ω-functionalized alkanethiols on Au(111) with relatively small functional groups, $HS(CH_2)_{15}R$, R = CO_2CH_3, COOH, CONH$_2$, CH$_2$OH. He found that the structure of all these monolayers is very similar to the structure of unsubstituted alkanethiols, with the alkane chains tightly packed in all-*trans* conformation, tilted *ca* 30° with respect to the surface normal[72]. The small size of the functionalities studied apparently allowed their incorporation in the crystalline-like arrangement of the alkane chains without significant disruption of the order of the fims.

Incorporation of an aromatic group in the alkanethiol monolayers does not significantly perturb the order. Alkanethiols containing a *p*-substituted phenyl ring in the middle of the chain give well-packed layers, if the chain length above the aromatic moiety contains at least 8 methylene groups[68]. However, thiophenol, which has a mercapto group attached directly to the aromatic ring, forms an incomplete monolayer on the gold surface. Incorporation of a *p*-alkoxy substituent in the molecule of thiophenol leads to the increased coverage of the appropriate monolayer, probably due to the favourable van der Waals interactions between adjacent chains. Long-chain *p*-hexadecyloxythiophenol forms close-packed monolayers on gold[213].

Monolayers containing a polar sulphone group, SO$_2$, were studied by Ulman and coworkers[214,215]. They found that despite the significant volume of the sulphone group, it does not disrupt the order in the layers. FT-IR data suggest that the alkane chains in these layers are well-ordered, although the tilt angle is affected. The authors believe that the high order in these monolayers is a consequence of intermolecular SO$_2$···SO$_2$ interactions.

The presence of amido groups, capable of H-bonding with each other, was reported to strongly influence the stability of monolayers. Monolayers prepared from alkanethiols containing an amido group HSCH$_2$CONHR showed enhanced resistance towards replacement by other thiols. They were also shown to be very stable towards thermal desorption and UV damage[170]. This enhanced stability was attributed to the formation of H-bonds between adjacent amide moieties in the monolayers[170,193,216]. Alkane chains pack tightly in these monolayers and, compared to ordinary alkanethiol layers, have smaller tilt with respect to the surface normal.

Incorporation of more bulky functional groups was found to have a great effect on the structure of gold−thiol monolayers. Partially fluorinated alkanethiol, $CF_3CF_2(CH_2)_6SH$, forms monolayers on the Au(111) surface with alkane chains tilted 56−76° with respect to the surface normal. This large tilt is necessary to allow the large terminal CF$_3$CF$_2$ group (diameter 5.7 Å, compared to 4.2 Å for ordinary alkane chains) to pack closely in the monolayer[217]. Other studies of partially fluorinated alkanethiol derivatives $CF_3(CF_2)_nCH_2CH_2SH$, n = 5, 7, 11, showed that the structure of such monolayers is determined by the perfluoroalkane group, and not by the underlying alkane functions. Moreover, the hexagonal packing of perfluoroalkane chains was found to be incommensurate with the gold surface[192]. Similar results with an incommensurate structure were obtained with symmetrical and asymmetrical disulphides $CF_3(CF_2)_{10}O(CH_2)_2S-S(CH_2)_2OR$, R = $(CH_2)_{10}CH_3$, $(CF_2)_{10}CF_3$[218].

Perhaps the best known example of the end-group-dominated structure of gold−thiol monolayers is that of azobenzene derivatized alkanethiols. Planar azobenzene units in the monolayer of **1** arrange themselves in a herringbone structure, as shown by STM and UV spectroscopy[219]. This azobenzene layer is incommensurate with the underlying gold surface, and its orientation does not depend on the orientation of the gold lattice[218,220−222]. A schematic illustration of this azobenzene-dominated structure is shown in Figure 17.
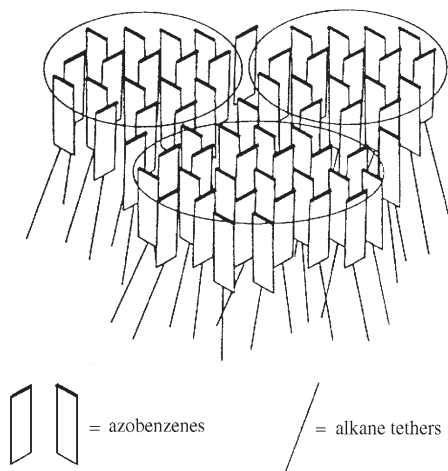
FIGURE 17. The structure of an azobenzene derivatized alkanethiol monolayer on Au(111). Reprinted with permission from Reference 220. Copyright (1995) American Chemical Society

(1)   (2)   (3)   (4)
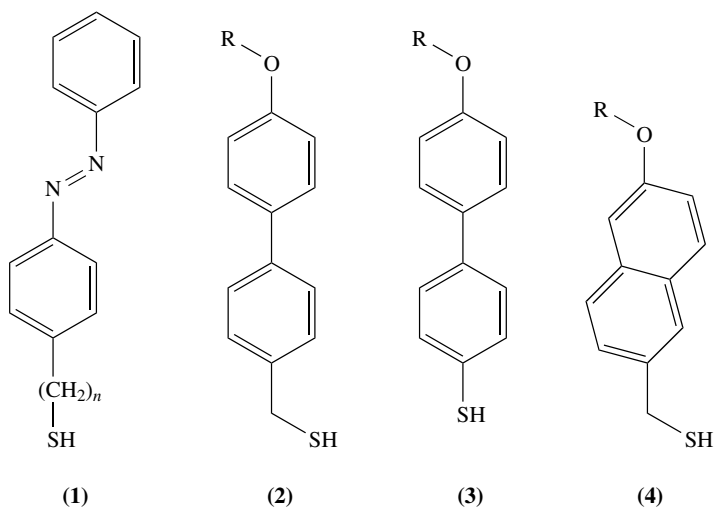
Similarly, thiols **2** and **3** give identical monolayers. Moreover, compounds **2–4** form indistinguishable monolayers on Ag(111) and Au(111), although the structure of unsubstituted alkanethiols on these two metals differs significantly (see Section V.B). The arrangement of alkane chains in these layers is dictated by the underlying herringbone structure of the aromatic lattice and not the metal surface[223]. In the monolayer of p-nitroanilino-terminated alkanethiol, p-$NO_2C_6H_4NH(CH_2)_{12}SH$, the nitroaniline units

form a well-packed layer which covers the disordered layer of alkane chains[224]. When the size of an aromatic moiety in monolayers matches the diameter of alkane chains, the resultant layers can be very well packed. Calixarenes having four thioether substituents (and therefore eight alkane chains per calixarene bowl) (Figure 18a) form dense monolayers. Alkane chains in these layers are well-packed and almost perpendicular to the surface[225].

The discotic molecule **5**, containing fused aromatic rings attached to a sulphur anchor via a long alkane chain, also shows ordered periodic structure determined by the arrangement of aromatic moieties. The same molecule containing six thioether substituents (**6**), however, has the aromatic group lying flat on the surface, covered with a disordered layer of the alkane chains[226]. Mercaptoalkylcyclodextrin derivatives show similar behaviour. Cyclodextrins having several mercaptoalkyl groups self-assemble on Au(111) to give monolayers in which the cyclodextrin cavity is orientated upwards, open to the solution interface. Monomercaptoalkyl derivatives with a long alkane chain give a structure with cyclodextrin cavities orientated parallel to the surface, and compounds with one thiol group directly attached to the cyclodextrin form disordered monolayers (Figure 18b)[227].

(5) **(6)**

$n = 6, 10, 11$; $R = C_{15}H_{31}, C_{16}H_{33}$; $R' = C_5H_{11}$
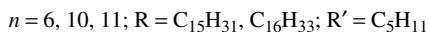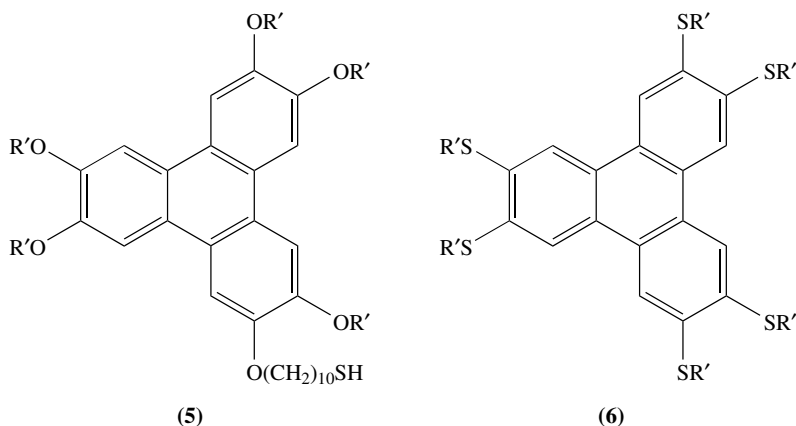
An interesting example of the structure-enforced arrangement in monolayers is the self-assembly of rigid molecules[228]. In the monolayers of thiol **7**, the molecules are well-packed (although electrochemical studies suggest the existence of a high density of defect sites)[103] and are almost perpendicular to the surface. The tilt angle is less than 20°. The structure is probably dictated by the phenyl rings which arrange themselves in a herringbone manner[195]. p-Mercaptophenylphthalimide (**8**) also forms monolayers with the molecules only slightly tilted away from the surface, but no preferred rotation angle for the imide ring was observed[229,230].

Notably, long rigid-rod molecules possessing two thiol groups on the rod termini are attached to the surface via only one thiol group, the other being at the monolayer–solution interface. By contrast, shorter molecules, such as 1,4-benzenedithiol, have both thiolate functions anchored to the Ag(111) surface, and therefore adopt an orientation parallel to the surface[31].
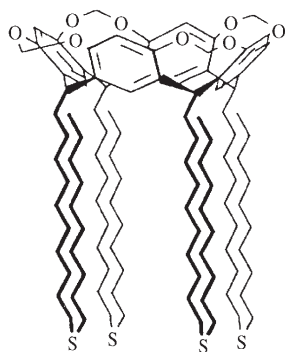
(a)
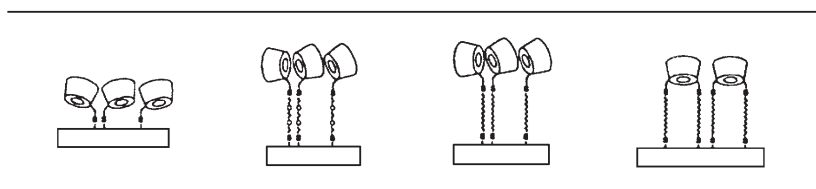
(b)

FIGURE 18. Structure of a calixarene thioether (a), and a model for the arrangement of substituted cyclodextrins in a monolayer (b). Reprinted respectively with permission from References 225 and 227 Copyright (1997, 1996) American Chemical Society
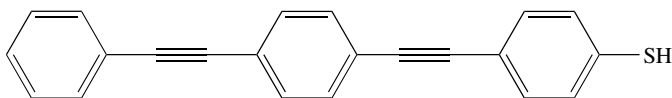
(7)
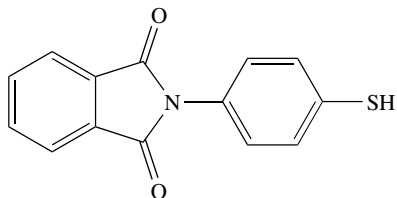
(8)

In 1,2-benzenedithiol **(9)** the sulphur–sulphur distance is *ca* 3.3 Å and the molecules chemisorb on Au(111) via formation of two sulphur–metal bonds. The benzene rings in these monolayers are significantly tilted with respect to the surface normal. Self-assembly on Ag(111), however, leads to formation of multilayers of the corresponding silver thiolate[231]. Interestingly, monolayers of rigid 1,8-naphthalenedisulphide **(10)** show a different structure. Although the S···S distance in the appropriate thiolate (*ca* 3.06 Å) is close to the Au–Au distance (2.88 Å), this disulphide was shown to associate with the Au(111) surface through only one thiolate group. The other thiolate is thought to be oxidized to a sulphonate group, $SO_3{}^{-}$[232].

(9)   **(10)**   **(11)**
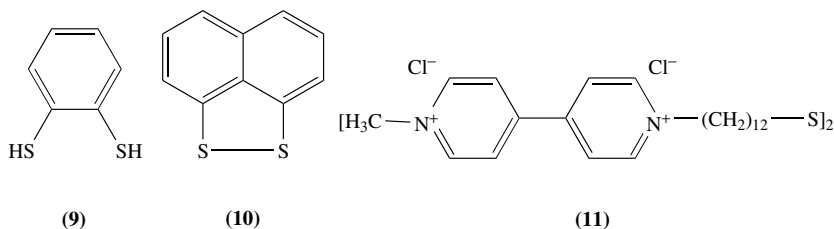
Incorporation of bulky functional groups in the alkanethiol monolayers results in the disruption of the molecular order in the layers. Charged groups, such as $^{+}N(CH_3)_3$[233] or viologen[121], affect the order most strongly. Viologen containing disulphide **11** forms layers which show liquid-like, rather than quasi-crystalline, behaviour as evident from the location of CH_2 stretching vibrations in their FT-IR spectra. The layers are easily permeable by external molecules, as shown by electrochemical methods. Reactive functional groups buried under the surface of such monolayers are readily accessible, as shown by their reaction with external reagents[121].

Wettability studies revealed some interesting structural features of ω-functionalized alkanethiol monolayers. Water contact angles of monolayers of $HS(CH_2)_{16}O(CH_2)_nCH_3$ ($n = 0-3$) were significantly lower than contact angles of longer-chain analogues ($n = 3-5$). Contact angles with less polar liquids did not show this behaviour. This seemed to be in contrast to an accepted assumption that contact angle depends only on the nature of atoms nearest to the interface[49]. A possible mechanism is the penetration of the water molecules through the terminal alkane group thereby allowing formation of H-bonds between water molecules and ether groups, even if the latter are buried 2–3 methylene units with respect to the monolayer surface[234]. However, it is more likely that this depth sensitivity is due to the disorder of the terminus of the monolayer by the polar wetting liquid, and not to the penetration. Contact angles of the same adsorbates on the Ag(111) surface were equivalent to those on Au(111), and as the alkane chains are known to be canted more on Au(111) than on Ag(111), the penetration should be easier with the monolayers on Au(111)[235].

Contact angles of ω-hydroxy-terminated monolayers, $HS(CH_2)_nOH$, were found to increase significantly during storage in the ambient atmosphere. Contact angles do not, however, change if the layers are stored in the atmosphere of water or acetic acid vapours. This is suggestive of a reorganization of the surface upon exposure to hydrophobic environment, with hydroxy groups curling down away from the monolayer surface. Suppressed chemical reactivity of the hydroxy groups in such layers indicates that the reorganization is irreversible[236].

Another interesting example of reorganization of the monolayer is the potential-dependent orientation of the nitrile groups in cyanoalkanethiols, $HS(CH_2)_nCN$ ($n = 2, 7$). The intensity of IR peaks of the nitrile and methylene groups changes with the potential applied, and the authors conclude that the nitrile groups become more nearly parallel to the surface as the potential becomes more positive[237]. Potential-dependent orientation was also observed for monolayers of 11-ferrocenyl-1-undecanethiol. With the oxidation of the ferrocene terminal group in the monolayer, the molecules become more closely perpendicular to the surface[238].

Experimental data and calculations show that monolayers of compounds capable of formation of intermolecular H-bonds (such as amino- or hydroxy-terminated layers) have a network of such bonds on the surface of dry monolayers, but exposure to water vapours results in adsorption of water and disruption of the intermolecular bonds[239,240].

D. Phase Segregation in Mixed Monolayers

Coadsorption of two different thiols results in the formation of a mixed monolayer (Section IV.C). This layer can either be a homogeneous mixture of two thiols, or it can consist of domains of the molecules of only one type (Figure 19). Similar phenomena in Langmuir films have been extensively studied; it was shown that in many cases the layers do phase-segregate[241−243]. Preparation of mixed gold–thiol monolayers is a convenient method of changing the properties of the interfaces in a continuous manner, for example to decrease the density of certain functional groups in the layer (dilute the monolayer) or, in the case of alkanethiols terminated with a bulky functionality, to fill in the empty space between this functionality and the gold surface (Figure 8b)[244]. Application of both these protocols implies homogeneity of the mixed layers, and the question of phase segregation in such systems is therefore very important.

It was clear from the outset that if there is any phase separation, the size of the domains is not macroscopic. The microscopic structure was, however, difficult to deduce. Whitesides and coworkers performed a detailed wettability study of mixed monolayers containing two alkanethiols of different lengths. They argue that if the monolayer separates into phases, and the domains contain only molecules of alkanethiols of the same length, the contact angle of the domains will be identical to that of a single-component monolayer of the alkanethiol, and if the domains are big enough, the contact angle of the mixed layer should be the same as the contact angle of pure single-component layers. In fact, however, the contact angle of the mixed layers is significantly smaller than that of single-component layers (Figure 20), showing that the domains in such a monolayer cannot be large. Whitesides and coworkers estimate the domain size (if any) to be under 20 Å across. Similar arguments were put forward for mixed monolayers of alkane and hydroxyalkanethiols[152,245].

Both systems were also studied by IR spectroscopy. It was found that the monolayers of hydroxy-terminated thiols show formation of intermolecular H-bonds in the IR spectra.

FIGURE 19. Possible arrangement in mixed monolayers: homogeneous mixture (a) or phase-separated domains (b)
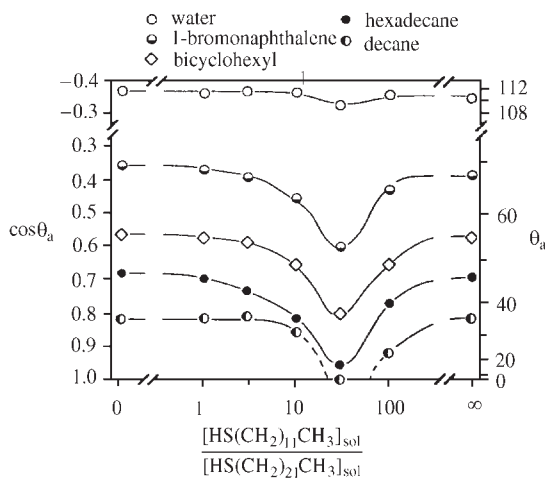
FIGURE 20. Contact angles θ_a of mixed monolayers of $HS(CH_2)_{11}CH_3$ and $HS(CH_2)_{21}CH_3$ as a function of the composition of the deposition solution. Reprinted with permission from Reference 152. Copyright (1989) American Chemical Society

In mixed monolayers with unsubstituted alkanethiols, containing up to 50% of the hydroxyalkanethiol, there is no indication of such H-bond formation. This is inconsistent with the phase-separation hypothesis, as hydroxy functions would surely form H-bonds with each other in domains, and Bertilsson and Liedberg concluded that the monolayers do not phase-segregate[246]. On the other hand, mixed layers of alkanethiols of different chain lengths showed, however, that these layers are at least partially crystalline, while disorder was expected for homogeneous monolayers. Existence of at least partial phase-separation was inferred[161].

The homogeneous model is also inconsistent with other data. Composition of a mixed monolayer could be modelled as a function of the composition of the deposition solution. This is based on the assumption that the binding sites on gold are independent (i.e. complete mixing of adsorbing species occurs) and that adsorption is governed by thermodynamic factors. The model shows systematic deviation from the experimental data, which suggests that the monolayers may phase-separate[247].

The break-through came when domains of phase-separated monolayers of $CH_3(CH_2)_{15}SH$ and $CH_3O_2C(CH_2)_{15}SH$ were directly observed with STM. The domains observed were *ca* 50–100 Å across, readily distinguishable by STM[248]. Slow motion of the domain boundaries with time was also observed. Several reports published since mostly give a similar picture. Lateral force microscopy and an adsorption isotherm study by Auger electron spectroscopy of mixed layers of *p*-aminothiophenol and octadecanethiol showed phase separation, although in some conditions homogeneous mixing of the components was observed[249]. Formation of monolayers from unsymmetrical alkane–perfluoroalkane disulphides and subsequent annealing of the obtained films did not show any single-component domains[250], but with a very similar system, phase segregation was reported after annealing[110]. The annealing procedure was similar in both cases, and the reason for the different behaviour is unclear.

Phase segregation was observed for mixed monolayers of n-alkanethiols[251]. A detailed STM study of mixed monolayers of butane and octadecanethiols showed that deposition from solutions containing more than 40- or less than 20-fold excesses of butanethiol exclusively produce single-component monolayers. Deposition from solutions containing 20- to 40-fold excess of butanethiol, however, showed clear formation of islands of phase-separated monolayers[129]. This picture seems consistent with that suggested in the earlier study by Whitesides and coworkers. They aimed to attain an equilibrium between the monolayer and deposition solution by studying adsorption for prolonged periods of time and at high temperatures ($60-70\,^\circ$C). It was found that under these conditions the monolayers tend not to phase-segregate but form single-component systems. The authors argue that thermodynamic formation of mixed thiol monolayers is unfavourable; depending upon intermolecular interactions, ideally mixed or single-component layers are formed instead. However, under normal deposition conditions the monolayers do not reach equilibrium, and these kinetically trapped systems are most likely to phase-segregate into nanoscopic domains[159].

E. Monolayers with Other than Thiol or Disulphide Head Groups

Although thiols appear to be in many respects the best adsorbates to prepare organic monolayers on the surface of silver and gold, compounds with other functional groups were also found to self-assemble on these metal surfaces. In this section sulphur-derived functionalities are considered first, followed by Se- and N-based groups.

The nature of interactions between organic sulphides $R-S-R^1$ and the gold surface remains unclear. Unlike thiols and disulphides, organic sulphides cannot form a chemical bond with the Au surface[112], and therefore the monolayers prepared from sulphides are less ordered and less stable. The layers are destroyed by treatment with a weak base (pH > 8). Although contact angles of long-chain dialkyl sulphide monolayers are almost as high as those of alkanethiols, and the ellipsometrically measured thickness is consistent with complete coverage, FT-IR data readily suggest a disordered state of the alkane chains in the monolayers. Incorporation of one or two carboxy groups in the adsorbates leads to significant decrease in thickness and increase in contact angles of the layers as compared to the films of the parent thiols[122,123]. Dialkyl sulphides containing a protonated amino group do not form self-assembled monolayers on the Au(111) surface at all[252]. However, polypodal compounds containing several thioether groups which could interact with the gold surface appear to form stable and well-packed monolayers. Examples include calix- and resorcinarene derivatives bearing four dialkyl sulphide groups[102,253,254], and discotic triphenylenes possessing six alkanethioether functionalities[226].

Other sulphur(II) compounds also form self-assembled layers on gold and silver surfaces. Alkyl xanthate ions $ROCS_2^-$ are coordinated to the surface through both S atoms and therefore have good stability. FT-IR analysis revealed that alkane chains in these monolayers are well-packed and ordered[255]. Alkyl xanthates and dithiocarbamates were also reported to form monolayers on the surface of Ag colloids[256]. Thioalkanoic acids RCOSH form well-packed monolayers on both Au(111) and Ag(111) surfaces. However, these monolayers exhibit only short-term stability due to hydrolysis of the thiocarboxyl group[257].

Substituted thioureas, isothiocyanates[258], thiophenes[259] and imidazole-2-thiones[260] also form stable self-assembled layers on the gold surface. Tetramethylurea layers can be imaged with STM[261]. Application of FT-IR spectroscopy to these layers shows that the

N−C(S)−N plane is parallel to the gold surface[262]. The driving force for formation of stable monolayers in such cases is thought to be formation of a $\sigma-\pi$ delocalized bond between sulphur and gold atoms[113].

The ability of compounds of sulphur in different oxidation states, such as sulphinates and sulphonates, to form self-assembled monolayers has been studied. The relative adsorptivities of aryl sulphur species were found to be $ArSO_3^- \ll ArSO_2^- < ArS^-$. While sulphonates can only adsorb electrochemically at positive potentials, sulphinates form self-assembled monolayers at normal conditions[263]. Sodium benzenesulphinate adsorbs from aqueous solution, but does not form monolayers from benzene. These monolayers of sulphinates are readily replaced by thiols[264].

The closest analogues of thiols, alkaneselenols R−SeH, were found to form well-packed monolayers on the Au(111) surface. The structure of these layers was studied by X-ray diffraction. An oblique unit cell was revealed, indicating a distorted hexagonal close-packed lattice of selenol molecules[265]. Benzeneselenol and diphenyl diselenide form identical monolayers on gold, as shown with STM microscopy. Monolayers of benzeneselenol do not have vacancy pits typical for thiolate monolayers, but show the presence of small islands of gold (20−200 Å) which were absent before deposition[266].

The affinity of Group V elements for gold is not as strong as that of sulphur. NPh_3, PPh_3, $AsPh_3$ and $SbPh_3$ nevertheless adsorb from solution on the surface of Au(111) to form monolayers. $BiPh_3$ is oxidized to give a polymeric structure. These monolayers are not very stable and desorb in vacuum (apart from $SbPh_3$) or upon prolonged treatment with solvents such as ethanol[267]. The long-chain phosphine $P[(CH_2)_{15}CH_3]_3$ and the isocyanide $^-C\equiv N^+(CH_2)_{22}CH_3$ form stable self-assembled monolayers on the gold surface. However, whereas the phosphine forms a well-packed film, the isocyanide produces a disordered layer, as evident from the contact angle values[124]. Long-chain aliphatic amines were also found to assemble on the Au(111) surface from the vapour phase producing well-packed monolayers[268]. These monolayers desorb in polar solvents. Gold colloids can, however, be successfully stabilized with long-chain amines and, unlike flat monolayers, these hydrophobic alkylamine-capped nanoparticles show remarkable stability. This stability appears to be largely a kinetic rather than thermodynamic factor[269]. Recently, amine-terminated dendrimers (hyperbranched polymers) were found to form stable monolayers on the surface of Au(111)[270]. The driving force for formation of stable layers here is formation of multiple amine−gold bonds.

Other nitrogen-containing compounds, such as pyridines, also adsorb on the Au(111) surface[271,272]. Electrodeposition at a positive potential (*ca* 0.4 V) leads to formation of complete layers. 2,2′-Bipyridine forms more stable monolayers as compared to those of 4,4′-bipyridine because both nitrogen atoms of the former compound could interact with the gold surface[273]. Aliphatic nitriles do not form well-packed monolayers on gold. The compounds with more than 10 methylene units form layers only 6−8 Å thick, and contact angles of these layers are *ca* 90−94°, significantly lower than those expected for a well-packed alkane layer (*ca* 114°)[274].

Organic compounds which do not contain sulphur or nitrogen do not generally self-assemble on the surface of gold. However, oligomeric or polymeric compounds capable of formation of multiple bonds with the substrate do form stable monolayers. Examples include adsorption of poly(ethyleneimine)[275], polyimides **12**[276] and polyphenylenes **13**[277], as well as polyketones and polybenzil from solution on the Au(111) surface to give relatively thick layers (*ca* 20 Å)[278]. Peptides[279] and oligonucleotides[280] also adsorb on the gold surface.

R=H, Ph; n=60–120

(12)

x=0,2; n=30–130

(13)
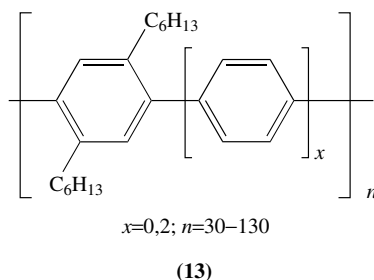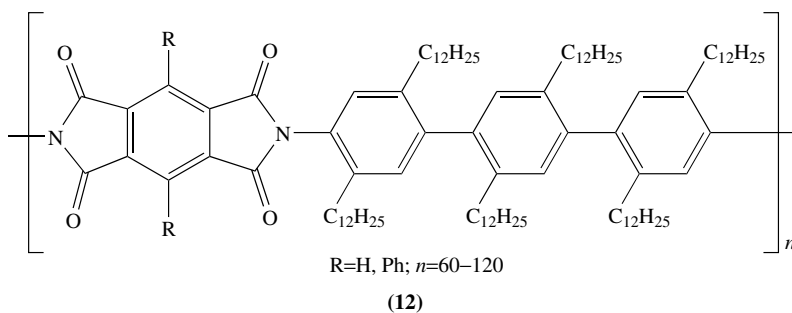
VI. STABILITY OF MONOLAYERS

Early studies of gold–thiol monolayers showed their remarkable stability. The layers can be stored in normal conditions (room temperature, laboratory environment) for weeks without any significant variations in the contact angle or thickness[65]. A detailed FT-IR study of the alkanethiolate monolayers as a function of storage time showed that after *ca* 20 days the relative intensities of the C−H peaks start to change. These intensity changes increase until *ca* 200 days. The changes are attributed to the increasing tilt of the alkane chains in the monolayers. The probable reason for tilting is the oxidation of the sulphur head group at the gold interface (*vide infra*)[281]. Alkanethiolate monolayers on the Ag surface are less stable and oxidize completely within *ca* one week of exposure to air[71].

Treatment of the monolayers with chemical reagents reveals their limited stability. Alkanethiolate monolayers on gold are destroyed by strong oxidizing reagents, such as piranha solution, halogens, ozone or peroxide, and compounds capable of attacking the gold surface, such as iodide ions, cyanide or aqua regia[65,80,282]. They are, however, stable in dilute (1 M) solutions of acids or bases[65].

Immersion of gold–thiol monolayers in neat solvents showed more rapid desorption as compared to storage in an ambient environment. Schlenoff and coworkers incorporated radioactive ^{35}S label in the alkanethiolate molecules and used these adsorbates to investigate stability of the monolayers in different solvents. The findings were surprising (Figure 21). Exposure of the ^{35}S-octadecanethiol monolayer on the Au(111) surface to all studied solvents for a period of several days resulted in a partial loss of monolayer. Desorption is slowest in water, and fastest in THF, with only *ca* 20% of the original monolayer remaining on the surface after 3 days of exposure. Experiments with the monolayers on the Ag(111) surface gave similar results[80].
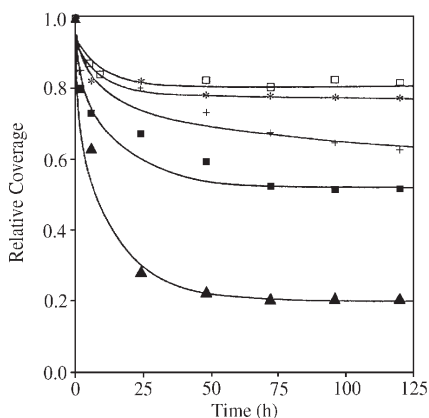
FIGURE 21. Desorption of ^{35}S-octadecanethiol monolayers on gold upon immersion in pure solvents at room temperature: water (*), hexane (+), ethanol (■), THF (▲), 0.1 M aqueous HClO$_4$ (□). Reprinted with permission from Reference 80, Copyright (1995) American Chemical Society

Similar behaviour was observed in the study of thermal desorption of the monolayers in solvents, monitored by thickness measurements. The desorption was fastest in hydrocarbon solvents, slower in water and the slowest in air[65]. Rapid thermal desorption of gold–thiol monolayers in air is usually observed at temperatures above 70–80 °C[65,283]. Annealing of gold–thiol monolayers in vacuum at ca 300 °C leads to complete desorption of the alkanethiolate layer and leaves a pure Au(111) surface[283]. Annealing in air, however, is accompanied by the oxidation and decomposition of the monolayer as shown by XPS, and results in the formation of a carbonaceous or sulphonate contamination layer[186]. Thermal desorption spectroscopy studies showed that alkanethiolate R−SH layers desorb at elevated temperatures to form a dimer, RS−SR[178]. A small amount of the thiol was also observed at lower temperatures[179].

The primary reason for the limited stability of the alkanethiolate monolayers in the ambient atmosphere is probably the oxidation of the sulphur head group. Laser-desorption mass spectrometry studies revealed not only the presence of thiolate ions, RS$^-$, but also sulphonate species RSO$_3{}^-$. The amount of the sulphonate peak increased dramatically if the monolayer was stored in the ambient atmosphere for several days prior to analysis. The rate of such oxidation of gold–thiol monolayers in a laboratory environment is a point of some controversy. XPS data show that the relative amount of sulphonate species in monolayers is still small even after prolonged storage[284], and it is likely that oxidation of the thiol head group occurs very slowly. On the other hand, Rieley and coworkers observed the sulphonate species in the NEXAFS spectra of even freshly prepared monolayers and suggested that the oxidation can occur much more rapidly than generally accepted[99,106]. Fritsch and coworkers also reported rapid oxidation of the thiolate head group to a sulphonate moiety (complete within 9 h of exposure to the ambient atmosphere), but this oxidation may have been triggered by the laser irradiation used in their study[171].

Monolayers of benzenethiol do not show any presence of sulphonate or sulphinate species after storage in the ambient atmosphere for 10 days. This was tentatively attributed to the higher stability of aromatic thiols against photo-oxidation[263].

Oxidation of monolayers is greatly increased under UV irradiation. Irradiation of alkanethiol monolayers with a mercury lamp at *ca* 0.16 W cm^{-2} for 25 min results in 60% oxidation of the thiolate group to the sulphonate[285]. Irradiation at 3 W cm^{-2} for 1 h leads to the complete oxidation of the monolayers[286]. The sulphonate monolayer obtained can be removed by rinsing with neat solvent or by exchange with solution of another thiol[287]. This method, along with electrochemical desorption (*vide infra*), is conveniently used to remove thiolate monolayers from the gold surface[286,288]. The application of these techniques to generate patterned monolayers is discussed in Section X.

Tarlov and coworkers studied the mechanism of photo-oxidation of the alkanethiol monolayers on the silver surface and found that UV irradiation leads first to the scission of the C−S bond and removal of the alkane portion of the monolayer. Remaining sulphur species are then oxidized to produce sulphite and sulphate ions[289]. As alkanesulphonate peaks were, however, observed in the aged alkanethiol monolayers on the Au(111) surface (*vide supra*), the generality of this mechanism is unclear.

Leggett and coworkers studied the effect of chain length on the rates of photo-oxidation of the alkanethiolate monolayers $HS(CH_2)_{n-1}CH_3$ on the Au(111) surface by XPS. The rate of photo-oxidation was found to vary strongly with alkyl chain length and was correlated with the amount of disorder within the monolayers. Monolayers of short-chain thiols ($n \leqslant 8$) have the highest disorder and oxidize the fastest, with the rate of oxidation increasing sharply with decreasing n, while close-packed monolayers of long-chain thiols ($n \geqslant 12$) oxidize much more slowly[290].

Electrochemical methods provide another way of removing the alkanethiolate monolayer from the gold and silver surfaces[291,292]. Thiolates are cleanly reductively desorbed at potentials of $ca > -1.5$ V in a process which is a reverse reaction of monolayer formation. This makes it possible to use electrochemical desorption for determination of surface coverage of alkanethiol monolayers (equation 3)[291].

$$RS{-}Au + e^- \longrightarrow RS^- + Au^0 \qquad\qquad (3)$$

Desorption of thiolates was also supported by *in situ* FT-IR measurements[212]. Shorter-chain thiols are desorbed at a lower potential than the longer ones[292]. This can be used to selectively remove shorter-chain thiols in the presence of their long-chain counterparts[293], and electrochemical desorption is successfully used in various applications (Section X).

These reductively desorbed long-chain thiols (thiolates), which are insoluble in the electrolyte, remain near the surface, probably forming micelles, and do not diffuse in the bulk solution[212]. They can be redeposited back on the surface of the electrode as a monolayer even if there was no thiol in the electrolyte prior to desorption[294,295]. The amount of material readsorbed depends directly on the solubility of the thiol. Shorter-chain (more soluble) thiols redeposit to give monolayers with smaller coverage. Redeposition also depends strongly on the pH of solution. Thiols become less soluble at lower pH, and therefore form monolayers with higher coverage under these conditions.

Thiolate monolayers can also be removed from the surface by anodic oxidation in 0.1 M KOH or in neutral electrolytes at 0.5−1.5 V. This process is much slower than the reductive desorption. It is not clear what products result from such oxidation. Formation of alkanesulphinic acids[292], sulphonic acids[237,296] and sulphate ions and CO_2 were reported[212].

The solvent effect on electrochemical oxidative and reductive desorption of alkanethiolate monolayers and rates of desorption at different potentials was studied by Everett and

coworkers[297,298]. They found that both processes occur much more rapidly in acetonitrile than in dichloromethane[298]. The potential window of greatest stability (-1.0 V to $+0.5$ V) is the same in both solvents and does not depend on the method of preparation of the underlying gold surface. Traces of water diminish stability of the monolayers, but the presence of oxygen, on the contrary, makes monolayers less susceptible to reduction/oxidation processes. The reason for these effects is not clear.

Irradiating the dodecanethiol monolayer with 355 nm laser pulses results in a partial desorption of the film (beam energy ca 1 mJ mm^{-2}; pulse duration 4–6 ns). Immersion of the layer obtained into solution of another thiol results in the formation of a mixed monolayer[299].

Other useful methods for the quantitative destruction of thiolate monolayers on the gold surface include metastable atom[300] or kiloelectronvolt ion bombardment[301] and electron beam damage techniques[302]. These methods are successfully used to prepare patterned monolayers. Quantitative removal of the thiol by an electron beam requires an e-beam dose of 10–100 mC cm^{-2}. Recently, X-rays were shown to damage gold–thiol monolayers[303,304].

The stability of a monolayer can be dramatically increased by 'cementing' the film with lateral chemical bonds. One example includes incorporation in the monolayers of the amide group, capable of intermolecular H-bonding with the adjacent molecules[170]. The monolayers of amide thiol RNHCOCH$_2$SH are 10 times more stable towards UV oxidation than the layers of the corresponding alkanethiol lacking an amide group. Enhanced electrochemical stability[305] and suppressed thermal desorption of these monolayers was also reported.

Another example of cross-linked monolayers is that of polymerized diacetylenic thiols. Well-packed monolayers of such thiols, HS(CH$_2$)$_{10}$C≡CC≡C(CH$_2$)$_{10}$COOH, can be polymerized in $situ$ by UV irradiation. The polymeric structures obtained are extremely robust and durable compared to similar monomeric layers. They can be repeatedly (more than 30 times) scanned between potentials -0.5 to -1.4 V in 0.5 M KOH without any appreciable signs of desorption. Heating of the films to 200 °C for 1 h showed only ca 15% decrease in the IR intensities of the CH$_2$ peaks, and exposure to 1 M KOH at 100 °C did not affect the integrity of the monolayer[306].

VII. CHEMICAL REACTIONS IN MONOLAYERS

A. Surface pK_a Values

The ability of the acidic and basic groups to exchange protons at the solid–liquid interface is different from the corresponding process in bulk media, and a significant number of studies was performed to establish the acidity and basicity of the functional groups on the surface of gold–thiol monolayers.

The deprotonation of the surface functional groups (such as COOH, PO$_3$H$_2$, NH$_3^+$ etc.) changes the wetting properties of the surface. In general, ionized surfaces are more hydrophilic than their neutral counterparts. The plot of the contact angle of an ionizable surface vs pH therefore resembles an ordinary titration curve. Such curves are usually significantly broader than the corresponding curves for bulk titrations, but nevertheless allow one to determine the pH value at which the functional groups at the interface are half-ionized (Figure 22). The value thus obtained is analogous to the pK_a value in the bulk medium and, in the present review, is referred to as surface pK_a for simplicity. The above procedure of measuring pH dependence of the surface wettability is known as 'contact angle titration'.
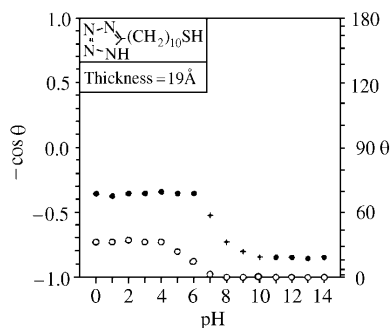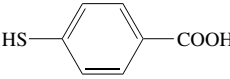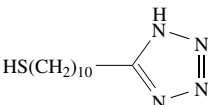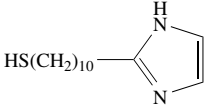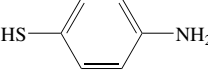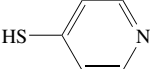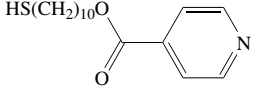
FIGURE 22. Contact angle titration of tetrazole-terminated alkanethiol. Advancing (●) and receding (o) angles with buffer solutions are shown as a function of pH values of the buffer. Crosses represent sessile rather than advancing angles because of the instability of the latter. Reprinted with permission from Reference 307. Copyright (1994) American Chemical Society

Table 3 lists some ionization properties of functionalized gold–thiol monolayers and relevant alkylsiloxane monolayers together with the appropriate bulk values. Monolayers with carboxylate terminal groups show abnormal wetting behaviour, which makes it difficult to determine accurately their surface pK_a values[308]. Apart from contact angle titration, other methods were also used to study proton transfer equilibria at the monolayer surfaces, such as quartz crystal microbalance (Table 3, line 1), measurements of the adhesion force between the monolayer deposited at the surface of an AFM tip and the same monolayer deposited on the substrate (chemical force microscopy, Table 3, lines 3, 4, 15), FT-IR spectroscopy (Table 3, line 7), adsorption of polyelectrolytes (Table 3, line 5) and differential capacitance measurements (Table 3, lines 12, 13).

It can be seen from Table 3 that the use of different methods to estimate ionization properties of the same monolayers gives somewhat different results. Some conclusions can, however, be reached. In general, acids and bases on the surface become less acidic and less basic, respectively. The difference between surface and bulk pK_a values is usually $2-5$ pK_a units. This conclusion is consistent with the data available for other solid–liquid interfaces. Three examples contradict the above trend (Table 3, lines 12, 13, 14). It can be argued, however, that in the former two cases the electrode potential used could significantly influence surface pK_a values. Interactions of nitrogen functionalities with the surface, which might have altered the surface pK_a values, also cannot be ruled out[307].

The simplest explanation for the observed differences in ionization behaviour of functional groups in the bulk and at interfaces is the difficulty of accumulating a charge at an interface (leading to unfavourable interactions between incipient ionized groups). Contact angle titration of mixed monolayers of ionizable compounds and appropriate alkanethiols showed, however, that the acid groups become *less acidic* with the *decreased* amount of acidic groups in the monolayer. Similarly, basic groups become less basic in the mixed monolayers with alkanethiols[307]. This is in contrast to the expectations that the smaller density of the charged groups in mixed monolayers would lead to weaker unfavourable interactions between them and therefore result in the increase of the strength of acid groups. Other reasons which may be responsible for the shift of surface pK_a values relative to their bulk counterparts include low interfacial dielectric constant[307,321,322], the presence of a low dielectric permittivity region surrounding the acidic/basic groups and changes in the number of degrees of freedom for the immobilized species[232]. Formation

TABLE 3. Bulk *vs* monolayer pK_a values

No.	Thiol	Surface pK_a	Bulk pK_a	Reference
Acids				
1	HS(CH$_2$)$_{15}$COOH	8.0	4.5	309
2	HS(CH$_2$)$_{10}$COOH	6.5	4.5	310
3	HS(CH$_2$)$_{10}$COOH	5.5	4.5	311
4	HS(CH$_2$)$_2$COOH	8.0	4.5	312
5	HS(CH$_2$)$_7$COOH	8.0	4.5	313
6	HS—(C$_6$H$_4$)—COOH	7	5.5	314
7	Cl$_3$Si(CH$_2$)$_{16}$COOH[a]	7.5	4.5	315
8	HS(CH$_2$)$_{10}$PO$_3$H$_2$	7.0	2.8	307
9	HS(CH$_2$)$_{11}$B(OH)$_2$	*ca* 12	10.7	316,317
10	HS(CH$_2$)$_{10}$—(tetrazole)	7.5	5.5	307
Bases				
11	HS(CH$_2$)$_{10}$—(imidazole)	3.0	8.0	307
12	HS—(C$_6$H$_4$)—NH$_2$	6.9	4.3	318
13	HS—(pyridine)	4.6	1.4	318
14	HS(CH$_2$)$_{10}$O—CO—(pyridine)	5.5	3.26	319
15	(RO)$_3$Si(CH$_2$)$_3$NH$_2$[a]	4.5	10.5	311
16	Cl$_3$Si(CH$_2$)$_4$NH$_2$[a]	6–8	10.5	320

[a] Alkylsiloxane monolayers on the surface of oxidized Si wafers.

of H-bonds between adjacent acid or base groups in the monolayers may also have some effect on their ionization properties[313], although this effect should decrease in mixed monolayers with alkanethiols.

B. Chemical Transformations in Monolayers

Chemical transformations in self-assembled monolayers were studied mainly with alkyl-siloxane films on oxidized silica, probably because these layers are more stable than

thiol–gold assemblies. It was shown that simple organic reactions, such as nucleophilic substitution[324,325], reduction and oxidation[326,327], can be performed on the terminus of these monolayers. Examples of reactions in gold–thiol films are less abundant, and there are only few detailed studies which clearly establish the nature of the reaction and show that a new functional group is indeed formed. In some cases researchers subject mono-layers to the conditions known to work in the bulk medium, and take for granted the fact that the reaction has proceeded. Eosin modified with an isothiocyanate group was reported to interact with the monolayers of cysteamine, and formation of the appropriate thiourea derivative was postulated (equation 4)[328].

$$AuISCH_2CH_2NH_2 + S{=}C{=}N{-}eosin \longrightarrow AuISCH_2CH_2NH{-}CS{-}NH{-}eosin \quad (4)$$
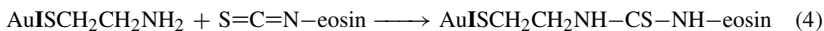
$$AuI = gold{-}thiol\ layer$$

It is known, however, that isothiocyanates on their own can form stable self-assembled monolayers on gold (Section V.E), and amine-terminated monolayers were reported to show unusually low reactivity towards electrophilic reagents[329,330]. It is therefore possible that the observed immobilization of eosin is due not to reaction with amino groups, but to either insertion of the eosin isothiocyanate into a disordered layer of cysteamine, or even replacement of cysteamine monolayer with the molecules of S=C=N–eosin. Because the experimental data on reactions in gold–thiol monolayers are scarce, chemical transformations described in this section should be interpreted with some caution.

Early studies showed that hydroxy- and amino-terminated monolayers react with silyl chlorides in the gas phase (equations 5 and 6). Increase in the monolayer thickness was monitored *in situ*, and FT-IR study of the former reaction product revealed the appearance of the strong Si–O peak[268,331].

(5)

(6)
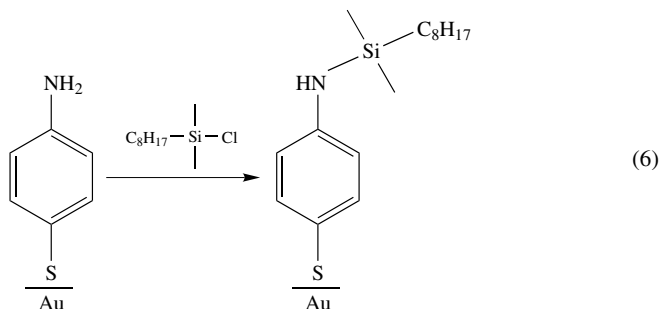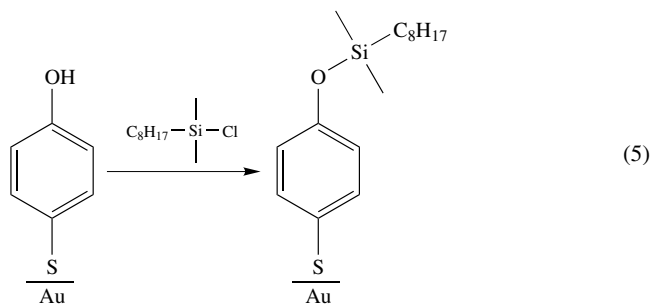
Acid terminal groups in monolayers can be converted to a reactive acid chloride functionality simply by exposure of the monolayer to the vapours of thionyl chloride for a few minutes[62,332]. The formation of COCl moieties was confirmed by IR spectroscopy. These functional groups can further react with amines or alcohols to produce amides and esters, which makes this method particularly useful for modification of alkanethiol monolayers. However, the acid chloride-terminated monolayers are destroyed by solvents such as methylene chloride, and the reaction has to be performed in the gas phase[332].

A recent study has further proven the applicability of gas-phase reactions to functional groups at the monolayer surface. Alcohol terminal groups were quantitatively converted to trifluoroacetates by exposure to the vapours of trifluoroacetic anhydride (equation 7). Reaction with perfluoropropionic and perfluorobutyric anhydrides proceeded similarly, but with *ca* 80% yield (XPS). Very high contact angles (>120°) of perfluoro-terminated layers proved the formation of esters[333].

(7)
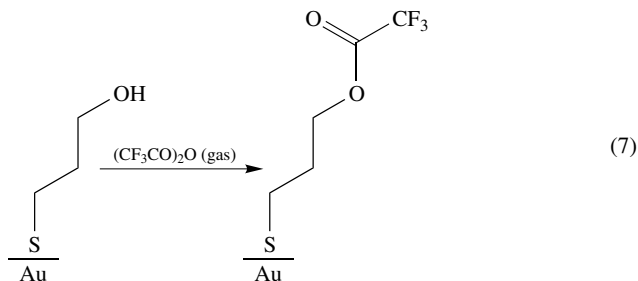
Exposure of hydroxy- and carboxy-terminated monolayers to the vapours of phenyl isocyanate in high vacuum (up to 60,000 L, $1 L = 10^{-6}$ Torr) did not result in any reaction. However, successive cooling of the monolayers to 130 K to condense multilayers of phenyl isocyanate and heating back to 290 K results in almost quantitative formation of appropriate mixed anhydride and urethane groups from the acid- and alcohol-terminated films, respectively[334].

Similar simple reactions can be carried out in solution. Terminal hydroxy groups can be esterified with trifluoroacetic anhydride[246] or glutaric anhydride[335], although the reaction in the latter case is probably incomplete. Amino groups in the monolayer of cysteamine were reported to react with active esters, such as *N*-hydroxysuccinimide (equation 8)[336]. No characterization of the resultant monolayer was, however, given. Cysteamine monolayers were also acylated with terephthaloyl chloride and an isocyanate derivative[337,338].

(8)
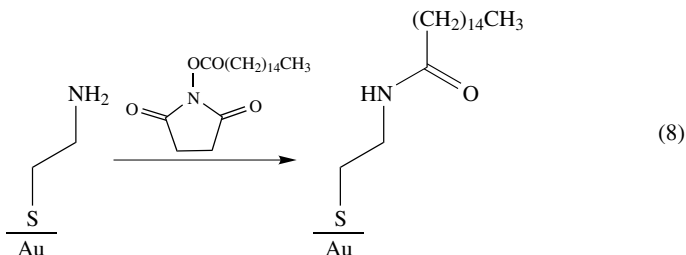
An elegant recent study described formation of an interchain anhydride from the monolayer of mercaptohexadecanoic acid. Reaction with trifluoroacetic anhydride in DMF in

the presence of triethylamine probably leads first to the formation of an intermediate mixed anhydride, which then reacts with the adjacent carboxylate group to produce the interchain product (equation 9).

$$\text{(9)}$$
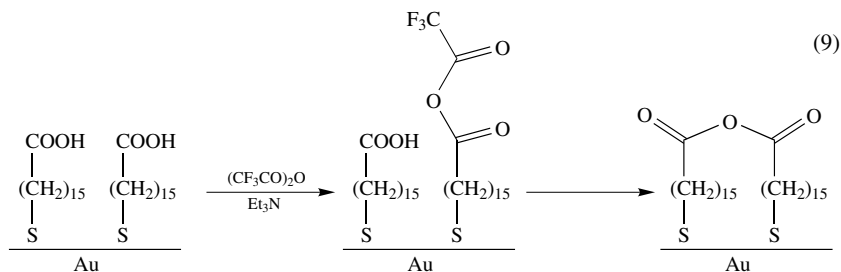
Formation of the anhydride was shown unambiguously with FT-IR spectroscopy. No fluorine was detected by XPS and FT-IR methods, which supports formation of the interchain product[339]. The monolayer anhydride is quite stable and can survive treatment with water for at least 1–2 min. It can further react with aliphatic amines producing mixed anhydride of amide and acid. The reaction is rapid and quantitative: the ratio of amide and acid in the resultant monolayer is *ca* 1 : 1.

A similar interchain reaction takes place during hydrolysis of the monolayers of (3-mercaptopropyl)trimethoxysilane, $HS(CH_2)_3Si(OMe)_3$. Although vibrational spectroscopy shows the existence of a small number of Si−OH groups on the surface after hydrolysis, the film is highly cross-linked via formation of Si−O−Si bonds with adjacent siloxane groups in the monolayer. The authors estimate that only *ca* 3–4% of the initial surface Si−O−CH₃ groups produced Si−OH bonds after hydrolysis[340].

Monolayers of anthracene modified with an ω-mercaptoalkane chain undergo photodimerization upon irradiation at 350 nm (equation 10). This process is confirmed by fluorescence and FT-IR measurements. The reaction can be reversed by irradiation at 254 nm, similar to the same process in the bulk medium. In the reverse reaction photodecomposition results in a partial loss of anthracene[341].

A similar reversible formation of a photodimer from an alkanethiol-substituted coumarin monolayer is described by Fox and coworkers[342]. Irradiation at 350 and 254 nm effects dimerization and dissociation of the dimer, respectively.

Formation of interchain chemical bonds can also be achieved by electro- or photochemical polymerization of the appropriate adsorbate. *N*-Pyrrolylalkanethiols can be adsorbed on the surface of a gold electrode. The films obtained have pyrrolyl groups at the monolayer surface. Scanning to +1.3 V in propylene carbonate results in the oxidation of the pyrrole groups to the corresponding radical cations, which then triggers polymerization, similar to bulk polymerization[343,344]. Oxidation rather than polymerization of the same monolayer was observed in acetonitrile[345].

Photopolymerization of (mercaptomethyl)styrene was monitored by Raman spectroscopy and mass spectrometry. The complex kinetics of the process cannot be described by 1st or 2nd order equations, but all monomer is consumed during polymerization[107].

In an elegant experiment, Niwa and coworkers prepared a mixed monolayer by co-depositing asymmetrical disulphides **14** and **15** in the ratio 200 : 1. The xanthate groups in disulphide **15** serves as a photo-initiator. Irradiation of the film results in the polymerization of the styrene moieties as seen by cyclic voltammetry. Virtually no polymerization occurs in the single-component monolayer of **14**, which proves the importance of having a photo-initiator in the film[346,347].

$$\text{(10)}$$

254 nm $\updownarrow$ 350 nm
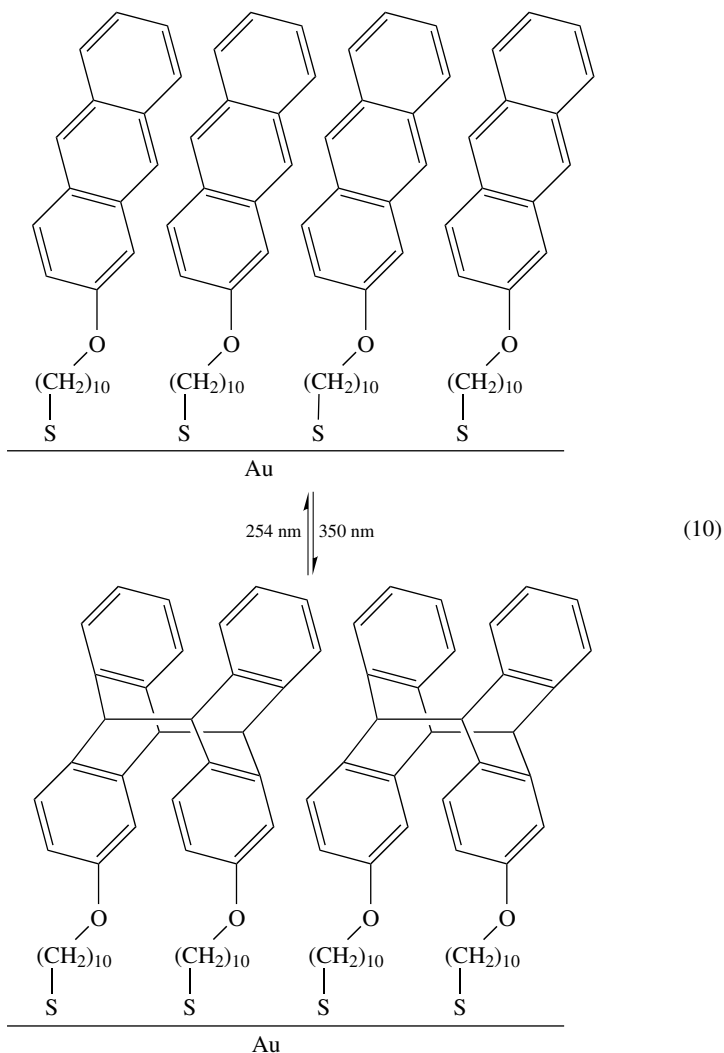
Diacetylenes containing a terminal mercapto group form monolayers on the gold surface. Irradiation of these monolayers with UV light causes polymerization (equation 11)[94,348]. Polymerization can also be induced by incident laser light at 647.1 nm. The structure of polymer layers was investigated in detail by SERS, FT-IR, UV spectroscopy and electrochemical measurements. Alkane chains undergo reorganization during polymerization necessary to form a rigid cross-linked structure. Irradiation was conducted in the absence of oxygen, to eliminate the possibility of air oxidation of the sulphur head group (see Section VI).

(14)

(15)

(11)

X = COOH, CH$_2$OH, CH$_3$
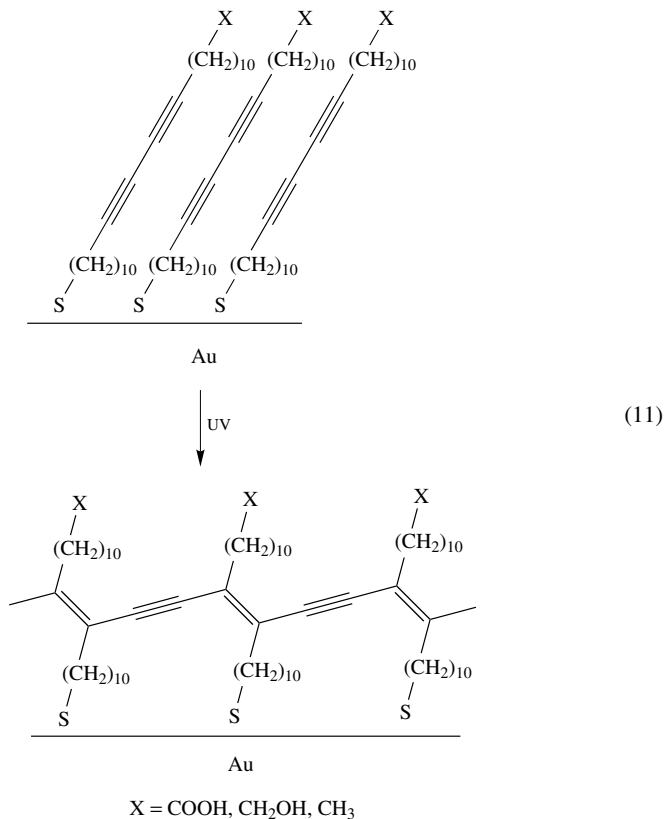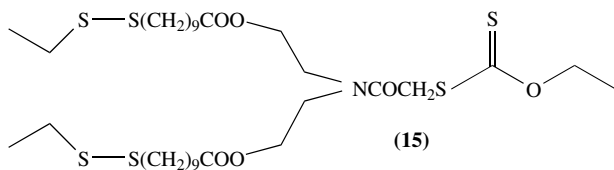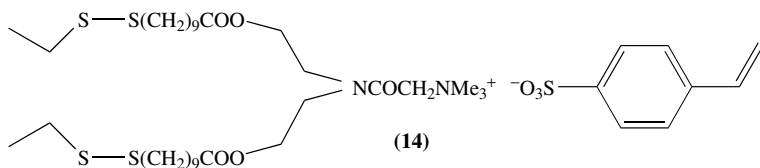
Polymerized diacetylenes show remarkably improved stability as compared to monomeric gold–thiol monolayers (see Section VI).

Monolayers of *cis*-and *trans*-stilbenes derivatized with a mercaptoalkane chain have different wetting properties. *cis*-Stilbene has a 60° bend between aromatic rings and the surface of its monolayer is probably dominated by the aromatic group; the contact angle with water is therefore relatively high (60°). The surface of the linear *trans*-monolayer is dominated by the hydrophilic nitrile group and has a lower contact angle (45°). Irradiation of the monolayer of the *cis*-isomer results in decrease of the contact angle to *ca* 45°, which implies photo-induced *cis*–*trans* isomerization (equation 12). Interestingly, condensation of water droplets on the surface of a partially irradiated monolayer makes the boundary between the pristine and irradiated parts visible to the naked eye[349].

$$\text{N} \equiv \text{C} - \text{(stilbene)} - \text{O} - (CH_2)_{10} - \text{S} - \text{Au} \quad \xrightarrow{\text{UV}} \quad \text{N} \equiv \text{C} - \text{(stilbene)} - \text{O} - (CH_2)_{10} - \text{S} - \text{Au}$$

(12)
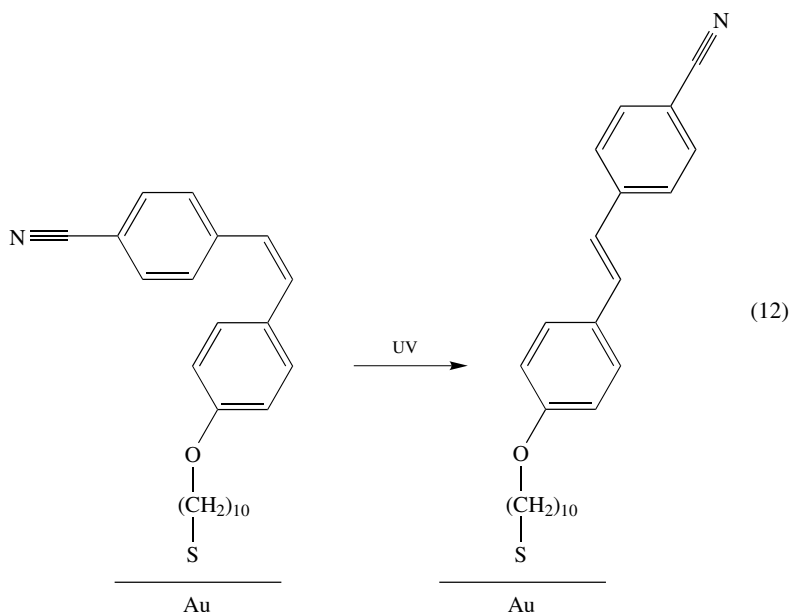
Other examples of photo-induced transformations in monolayers include reduction of *p*-nitrothiophenol assembled on a silver electrode to *p*-aminothiophenol initiated by laser radiation (monitored by SERS)[350]. UV irradiation of a monolayer terminated with aryl azide in the presence of amines results in incorporation of the amines in the monolayer as azepines and hydrazines. No surface attachment takes place without irradiation, and this makes it a convenient method to prepare photopatterned monolayers[351].

Some more complex reactions were also shown to be applicable to the monolayer assemblies. Peptide synthesis protocols are frequently used to attach biomolecules to the surface of the monolayer. However, such reactions are sometimes poorly characterized. *N*-Hydroxysuccinimide esters containing a mercapto group form well-behaved monolayers which are stable at neutral conditions and do not hydrolyse easily[352]. They react smoothly with amines in solution, giving rise to the appropriate amides[353]. This reaction can also be used to attach proteins to the surface of monolayers[352]. *N*-Hydroxysulphosuccinimide ester can be generated in the monolayer *in situ*, by treating the film of *ω*-mercaptoalkanoic

Victor Chechik and Charles J. M. Stirling

acid with *N*-hydroxysulphosuccinimide and a carbodiimide coupling reagent (EDC). After this procedure, only *ca* 50% of acid terminal groups are reacted. Higher yields of the target amide (up to *ca* 80%) can be achieved by repetitive (3–4 cycles) treatment of the half-converted amide, again with *N*-hydroxysuccinimide/carbodiimide mixture, followed by reaction with the amine (equation 13)[354].

$$(13)$$
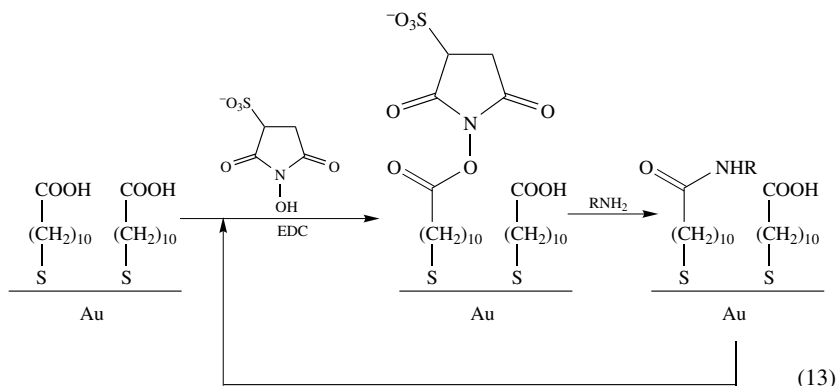
Dicyclohexylcarbodiimide-mediated coupling was also used for direct attachment of peptides to the acid-terminated monolayers[355,356].

Interestingly, carbodiimide coupling can be performed even in the gas phase, by direct exposure of the acid-terminated monolayer to the mixed vapour of a carbodiimide, an alcohol and a base (pyridine). The reaction does not go to completion; XPS estimated yield is *ca* 60% (equation 14)[333].

$$(14)$$
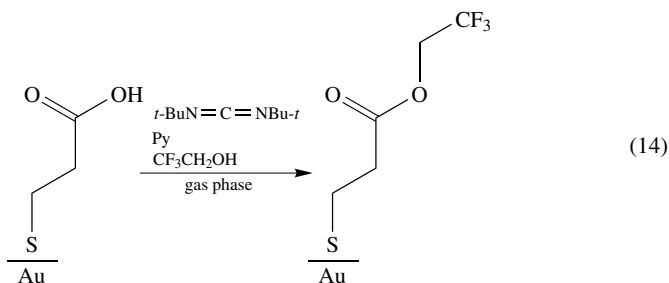
The mixed anhydride method was successfully employed to effect immobilization of an amino-terminated dendrimer to the surface. Treatment of the acid monolayer with the chloroformate ester gave rise to formation of a mixed anhydride on the monolayer terminus. Reaction of this surface with the dendrimer results in a multipodal attachment of the polymers to the surface[357].

Alternatively, hyperbranched polymers can be prepared *in situ* on the monolayer surface. Treatment of the acid-terminated layer with chloroformate and amine-terminated poly(*t*-butyl acrylate) produces ester groups on the surface. Hydrolysis of the ester functions with tosic acid gives carboxyl groups. The whole procedure is then repeated several times

to produce different generations of the hyperbranched polymer (equation 15)[358].

$$AuIS(CH_2)_{10}COOH \xrightarrow[\substack{\text{\textit{i}-BuOCOCl} \\ \text{H}_2\text{NR-[CH}_2\text{CH(COOBu-}t)]_n\text{-RNH}_2 \\ \text{\textit{N}-methylmorpholine}}]{} AuIS(CH_2)_{10}CONHR\text{-}(CHCH_2)_n\text{-RNH}_2$$

COOBu-t

TsOH

$$AuIS(CH_2)_{10}CONHR\text{-}(CHCH_2)_n\text{-RNH}_2 \qquad (15)$$

COOH

$$R = \begin{array}{c} CH_3 \quad O \\ | \qquad \| \\ -CCH_2CH_2CNHCH_2CH_2- \\ | \\ CN \end{array}$$

The reaction of thionyl chloride with acid-terminated monolayers was utilized to build up self-assembled multilayers on the gold surface. Monolayers of ω-mercaptoalkanoic acid containing a diacetylenic group in the middle of the chain (*vide supra*) were transformed into acid chlorides by treatment with $SOCl_2$ vapours. The resultant acid chloride layer was again immersed in the solution of ω-mercaptoalkanoic acid to form a second layer by formation of a thiolester group and the reaction sequence repeated (equation 16). At least 6 layers can be deposited in this way. The thickness of these films increases proportionally to the number of layers. Irradiation of the films effects polymerization of diacetylene units and creates rigid cross-linked polymer multilayers[359].

$$AuIS\sim COOH \xrightarrow{SOCl_2} AuIS\sim COCl \xrightarrow{HS\sim COOH} AuIS\sim COS\sim COOH \quad (16)$$

An alternative approach to formation of gold–thiol multilayers utilizes inorganic chemistry. Copper(II) carboxylate groups can be generated on the monolayer surface by treatment of the acid-terminated layer with the solution of a copper salt. The copper(II) ions have strong affinity for sulphur(II) compounds, and thiols self-assemble on top of this Cu-terminated film (equation 17)[360,361].

$$
\begin{array}{ccccc}
& & & & Cu^{2+} \\
& & COOH & COO^- \\
& & (CH_2)_{10} & (CH_2)_{10} \\
& & S^- & S^- \\
& Cu^{2+} & Cu^{2+} & Cu^{2+} \quad (17) \\
COOH & COO^- & COO^- & COO^- \\
(CH_2)_{10} \xrightarrow{Cu(OAc)_2} (CH_2)_{10} \xrightarrow{HS(CH_2)_{10}COOH} (CH_2)_{10} \xrightarrow{Cu(OAc)_2} (CH_2)_{10} \\
S & S & S & S \\
\overline{Au} & \overline{Au} & \overline{Au} & \overline{Au}
\end{array}
$$

In a similar approach, rigid linear dithiols (such as α, α'-xylyldithiol or 4,4'-biphenyldithiol) were shown to form monolayers with only one thiol group attached to gold and another 'sticky leg' (thiol functionality) is positioned on the monolayer

surface. These films can be used to covalently attach nanometer-sized gold clusters. Gold colloids also form monolayers on the surface of other self-assembled layers having pendant functional groups with high affinity for Au i.e. CN, NH_2)[362]. Rigid diisocyanides form monolayers on gold, and the films obtained were reported to covalently anchor nickel clusters[363,364]. Exposure of tetrathiafulvalene-terminated monolayers to tetracyanoquinodimethane (TCNQ) results in formation of charge-transfer complexes. FT-IR data suggest that the $TCNQ^-$ anion adopts an orientation parallel to the gold surface[365].

C. Electrochemistry at the Monolayer Surface

Electrochemical methods have an enormous potential for characterization and studying thin films on the metal surfaces. An excellent recent review describes in great detail the theory and applications of these methods to gold–thiol monolayers[13]. In this section we briefly discuss the main phenomena which can be addressed by electrochemical methods and describe the most popular surface-immobilized electroactive functional groups used for this purpose.

Deposition of a non-electroactive film on the surface of an electrode blocks the electron transfer from solution-based ions to the electrode. The efficiency of such blocking depends on the permeability of the film and the nature and density of defects, and heterogeneous electron transfer is routinely used to address these problems[366]. Capacitance measurements of the blocked electrodes also give valuable information about the thickness and integrity of the monolayer. These applications are described in Section II.D.

Electron transfer to the perfect blocked electrode is also possible due to electron tunneling, and gold–thiol monolayers provide a unique opportunity to study this phenomenon. Miller and coworkers showed that the level of defects in the monolayers of ω-hydroxyalkanethiols of medium chain length ($6 < n < 18$) has only a minor contribution to the electron transfer, and they performed detailed studies of the electron tunneling in this system[367–369].

Incorporation of the electroactive group in the gold–thiol monolayers significantly increases the scope of electrochemical experiments. Most electroactive groups, however, are significantly larger than the alkane chains, and monolayers of alkanethiol derivatized with these groups do not block the penetration of external ions to the electrode. Usually, these electroactive thiols are therefore coadsorbed with unsubstituted alkanethiols of shorter length, to prepare mixed monolayers with the well-packed inner alkane part, and redox groups protruding above this surface (Figure 23).
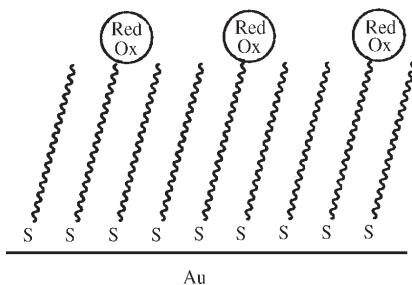
FIGURE 23. Incorporation of an electroactive group in the mixed gold–thiol monolayers

The most popular electroactive group is perhaps ferrocene. Use of ferrocene-terminated alkanethiols to study exchange phenomenona is described in Section IV.C. Incorporation of the ferrocenyl moiety in the monolayers results in the shift of its formal potential to more positive values. This phenomenon was studied in detail by several research groups. There are probably two causes of this shift: one is the change of the local dielectric constant in the vicinity of the ferrocene group embedded in the monolayer, and another is a double-layer effect[370,371]. Adsorption of long-chain alcohols on the surface of a ferrocene-containing monolayer has a similar effect on the formal potential[372]. The effect of different substituents in the five-membered ring of the ferrocene group on the redox potential was also addressed[153,373].

The rate of electron transfer in blocked ferrocene-terminated monolayers was studied by Murray and coworkers[374].

Ruthenium complexes $HS(CH_2)_nCONHCH_2pyRu(NH_3)_5{}^{2+}$ can be incorporated in the monolayers by using a derivatized pyridinium ligand (py) in the 4-position. Coadsorption of these thiols with carboxy-terminated alkanethiols of different chain lengths produced monolayers with exposed or buried Ru groups. The rate of electron transfer in these monolayers has been measured and interpreted in terms of electronic coupling between the redox centre and the diluent thiols dominating in the exposed cases[375]. An osmium complex was introduced in the monolayer using a similar substituted pyridine ligand[376].

Electrochemical studies with viologen (4,4′-bispyridinium ions) containing monolayers have been reviewed by Finklea and coworkers[377].

Thiol-derivatized cobalt porphyrins self-assemble on the surface of gold electrodes. The monolayers obtained catalyse reduction of oxygen to hydrogen peroxide. These layers retain their activity after as many as 10^5 turnovers[378,379].

Various approaches were probed to attach the molecule of cytochrome c to the surface of the monolayers. Covalent attachment could be achieved by carbodiimide coupling of the acid groups on the monolayer surface with the amine groups of the protein[356,380]. Electrostatic adsorption of the protein on the surface of acid-terminated monolayers[381,382] was achieved by Tarlov and coworkers. Cytochrome c also adsorbs on the surface of a pyridine-containing monolayer[383].

Electroactive monolayers of thiol-derivatized hydroquinones on the surface of platinum electrodes were prepared and studied by Hubbard and coworkers[384−386] even before Nuzzo and Allara reported formation of the first gold–thiol monolayers[10]. The redox potentials of quinone- or hydroquinone-containing monolayers vary with pH with a slope of 60 mV pH^{-1}, indicating a $2e^- + 2H^+$ reaction[387]. This observation was used in an elegant study by Hickman and coworkers. They codeposited hydroquinone and ferrocene-containing thiols on the surface of a gold electrode. The half-wave potential of the latter does not depend on the pH value of the solution, and therefore can be used as a reference. The whole assembly acts thus as a pH-sensitive sensor which does not require any separate reference electrodes[388].

A thiol which has a quinone moiety as an electron transport group and a porphyrin as a photoactive group was deposited on the surface of a gold electrode. Anodic and cathodic photocurrents were observed at potentials more positive and more negative, respectively, than the redox potential of the quinone moiety, indicating that the photo-induced electron transfer in the monolayer took place through the quinone group[389].

Azobenzenes buried at different levels with respect to the monolayer surface have been studied and the electrochemical behaviour of the films was clearly dominated by the length of the alkane chain above the level of the azobenzene group. This behaviour was attributed to the steric inhibition of the conformational change of the azobenzene moiety

during reduction[390,391]. In a similar approach, Mirkin and coworkers prepared an ω-ferrocenyl-substituted alkanethiol which has the azobenzene group between the thiol and ferrocene moieties. While the monolayer exhibits complete electrochemical accessibility for its outer layer of ferrocenyl groups, access to the azobenzene groups was blocked due to the densely-packed structure of the monolayer. Less densely packed monolayers prepared by coadsorption with ethanethiol showed greater accessibility to the azobenzene group[392].

Other electroactive groups incorporated in gold–thiol monolayers include tetrathiaful-valene[365] and fullerene[393]. Miller and coworkers prepared thiol-derivatized oligoimides with naphthalene diimide electroactive groups. Electron transfer to each electroactive function was observed[394,395].

Analytical applications of electrochemistry at thiol-modified gold electrodes are discussed in a recent review[396]. Some examples of these applications relevant to specific interactions between the monolayer and the analyte are discussed in Sections X and VIII.

D. Reactivity Issues

The fact that chemical reactions can be performed and monitored in monolayers prompts an intriguing question: what effect does placing a functional group in a monolayer environment have on its reactivity? Unfortunately, there are only few examples of such mechanistic studies in gold–thiol monolayers, and to give an integral picture we must bring into the discussion some results available for other monolayer assemblies, such as chlorosilane self-assembled films on oxidized silicon, Langmuir–Blodgett monolayers and monolayers at the air–water interface.

There are several reports in the literature on significant acceleration of reaction rates in monolayers. Such increase in reactivity is usually attributed either to enforced juxtaposition of the reactive functional groups in the ordered environment, or to the favourable orientation of the reactive group. Nakahara and coworkers found that long-chain alkane esters of aminoacids polycondense unexpectedly rapidly at the air–water interface, probably because of the close proximity of the amino and ester groups in the monolayer (equation 18)[397].

$$2n\ NH_2-CHR-COOR' \longrightarrow [-NH-CHR-CONH-CHR-CO-]_n \qquad (18)$$
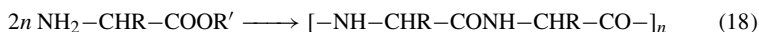
Long-chain barbiturates hydrolyse at the air–water interface in the presence of 2,4,6-triaminopyridine. The latter compound is thought to form a second layer at the interface through complementary H-bonds with the barbituric acid derivative and catalyse hydrolysis[398].

Recently, a significantly enhanced catalytic activity of a rhodium complex in hydrogenation of the C=O bond was reported in Langmuir–Blodgett films. The enforced favourable orientation of the complex within the film is thought to be responsible for the increased reactivity[399].

No such acceleration effects have so far been reported in gold–thiol monolayers. The existing studies are mainly concerned with the diminished reactivity of a functional group buried under the monolayer surface, due to partially blocked access of an external reagent to this group.

Reactivity of esters towards base-catalysed hydrolysis was studied by Stirling and coworkers. They have shown that well-packed monolayers of aliphatic esters with the carbonyl group buried deeply below the surface [$HS(CH_2)_{10}OCO(CH_2)_8CH_3$] are very resistant towards hydrolysis. At the same time, esters which have the carbonyl function close to the monolayer surface [$HS(CH_2)_{10}OCOCH_3$] hydrolyse more rapidly[400]. In such
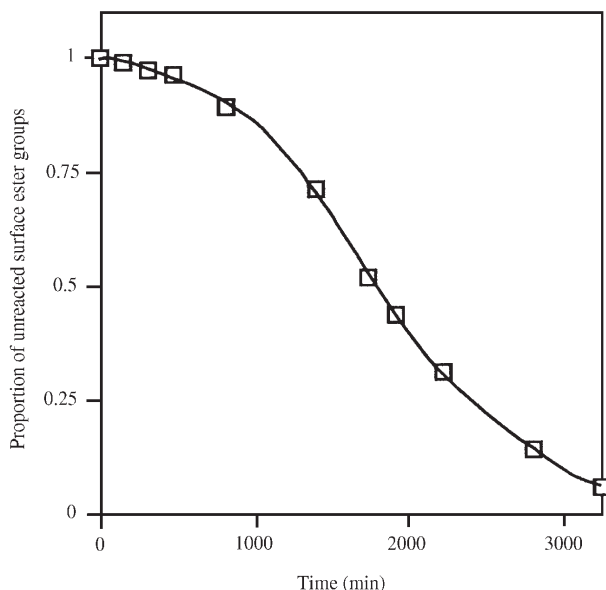
FIGURE 24. Rate plot for hydrolysis of the monolayer of $HS(CH_2)_{10}OCO(CH_2)_2CH_3$ in 1 M NaOH, 25 °C[401]

systems, where the access of an external reagent is blocked, the reaction is thought to start at defect sites and domain boundaries, which then grow and coalesce as the reaction proceeds. Rate plots of such reactions show an initial induction period (slow reaction at scarce defect sites) followed by a more rapid process, as the blocking groups are removed from the monolayer with increased conversion (Figure 24)[401].

The above results are consistent with those obtained by van Ryswyk and coworkers. They prepared mixed monolayers of isonicotinate esters and alkane thiols. By varying the relative amount of the alkanethiol and the ester in the deposition solution it is possible to control the surface density of the isonicotinate ester groups. Monolayers of pure ester hydrolyse extremely slowly, probably because of the blocked access to the carbonyl functional group[319].

Mixed monolayers of the isonicotinate ester and nonanethiol which have *ca* 25% of the surface isonicotinate groups are, however, susceptible to hydroxide-mediated hydrolysis (equation 19). The kinetic plots of this reaction showed clean first-order behaviour, implying that the access of hydroxide ion to the reaction centre in disordered layers is not hindered. Attachment of the Ru(II) complex to the pendant isonicotinate at the surface of the monolayer increases the rate of reaction, probably because of the high positive charge of the Ru(II) moiety.

Similar results were obtained by Chechik and Stirling in the study of aminolysis of surface-confined *p*-nitrophenyl esters. They found that disordered monolayers containing carbonyl group buried at different levels with respect to the surface react with amines with essentially the same rate; moreover, this reaction is actually faster than the corresponding process in the bulk medium. Apparently, a disordered monolayer can be easily penetrated by external reagents. Faster reaction in monolayers was tentatively assigned to the higher

concentration of the amine in the vicinity of the monolayer, as compared to the bulk solution[402].

(19)
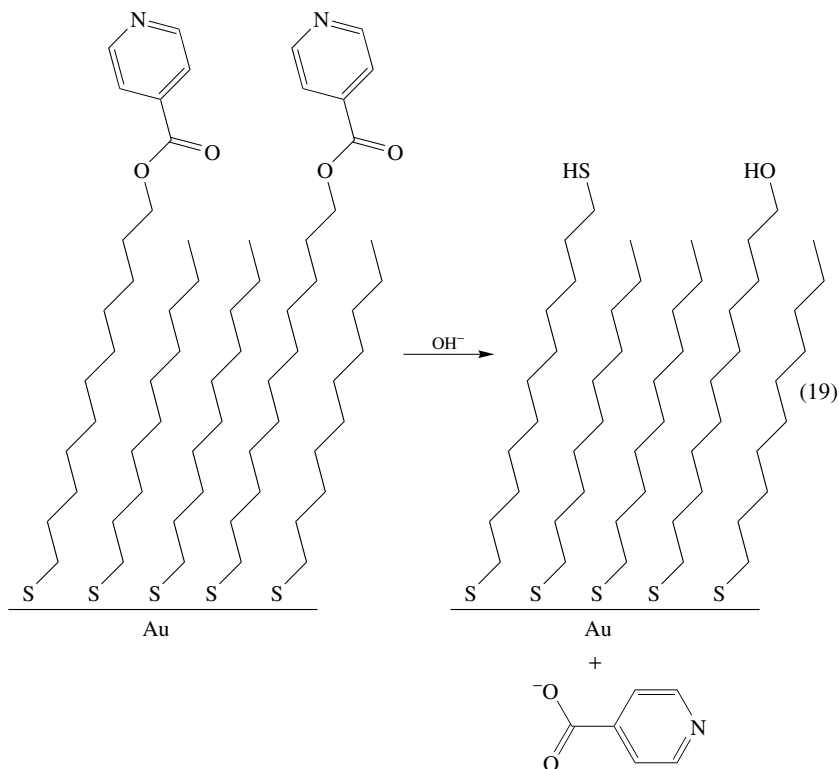
Nucleophilic reactivity of the amino group in gold–thiol monolayers was reported to be significantly suppressed as compared to the bulk reactions. This effect was observed in both inter- and intramolecular reactions in monolayers[330]. Failure of the amino-terminated monolayers on the surface of gold colloids to react with isothiocyanate compounds was reported by Buining and coworkers[329]. This unusually low reactivity of the amino group can be tentatively assigned to its interactions with the gold surface[330].

A detailed study of nucleophilic substitution reactions in silyl chloride monolayers on the Si/SiO$_2$ surface showed results similar to those observed on the Au surface. Well-packed monolayers with Br terminal groups undergo substitution readily with small nucleophiles (such as N$_3^-$ ion) but, with bulky nucleophiles, reaction does not go to completion. Sterically undemanding reaction with tin radicals proceeded rapidly and quantitatively. The possibility of condensation between two adjacent chains in the monolayer facilitated by their close proximity was also discussed[325].

To summarize, chemical reactivity in monolayers is often suppressed due either to blocked access of the reagents to the reaction centre, or to steric congestion during reaction. In rare cases where enforced orientation or juxtaposition of the functional groups in

the monolayer favours a reaction, enhanced reactivity is observed. In most other cases, chemical reactivity in monolayers seems to parallel that in the bulk solution[403].

VIII. NON-COVALENT INTERACTIONS OF MONOLAYERS WITH GUEST MOLECULES

A. Electrostatic, van der Waals and H-bond Driven Interactions

Interactions of surface-bound acids with gaseous bases was studied in detail by Crooks and coworkers. They established that amines adsorb to form a second layer on the surface of carboxylic and sulphonic acid-terminated monolayers. The strength of such binding depends on the acid–base properties of the acid and the amine. Strong bases, such as aliphatic amines, adsorb irreversibly and do not desorb upon prolonged storage in an inert atmosphere. Careful analysis of the FT-IR spectra of such acid–amine bilayers showed that the relatively disordered and flexible monolayers of short-chain carboxylic acid or mercaptobenzoic acid bind amines through a complete proton transfer. It is likely that in these structures there is some degree of intercalation of the charged parts of the acids and bases. In rigid, well-packed monolayers of long-chain mercaptoalkanoic acids, such intercalation is impossible, and FT-IR data suggest that the amines interact with the surface both through proton transfer and formation of H-bonds with the acid groups (Figure 25)[404,405].

Weaker bases, such as pyridine or pyrazine, do not deprotonate alkanoic acids and adsorption on the surface is exclusively through hydrogen bonding. Higher surface coverage is achieved with pyridine, which is a stronger base. Upon nitrogen purging, one-third of the pyridine layer and two-thirds of the pyrazine layer desorb, in accord with their
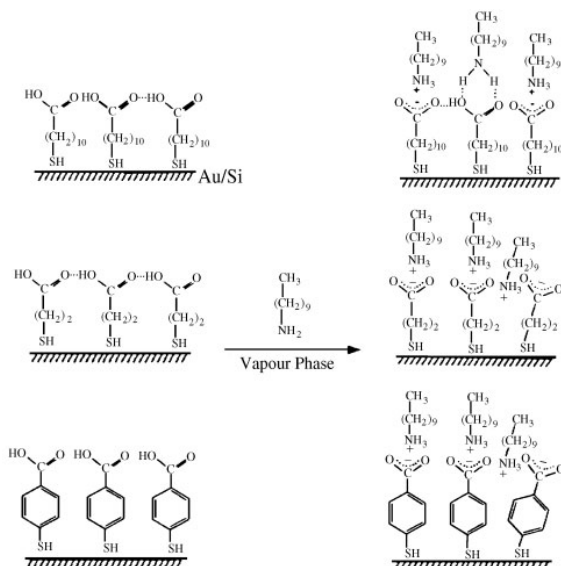
FIGURE 25. Schematic of decylamine binding to the surfaces of different acids. Reprinted with permission from Reference 405. Copyright (1996) American Chemical Society

608   Victor Chechik and Charles J. M. Stirling

relative basicity[405]. This experiment demonstrates the importance of the relative strengths of acid–base interactions for the strength of binding.

Steric effects on binding were investigated in monolayers of different isomers of mercaptobenzoic acid. Gaseous decylamine binds irreversibly to all monolayers, and analysis of FT-IR spectra suggests complete proton transfer between carboxylic and amino groups. However, the amount of bound amine is different for the three monolayers. Near-monolayer coverage was observed for adsorption on the *p*-isomer; *ca* 80 and 50% of the monolayer coverage was reported for the *m*- and *o*-isomer, respectively. This trend was linked with accessibility of the acid group buried under the surface (Figure 26)[406].

Long-chain alkanoic acids adsorb from the gas phase onto the surface of acid-terminated monolayers (e.g. a monolayer of 3-mercaptopropionic acid) through formation of complementary H-bonds. This binding is weak; only *ca* 25–35% of the monolayer adsorbs and no adsorption was observed for short-chain acids HS(CH$_2$)$_n$COOH, $n < 9$[407,408]. Binding of acetic acid to different monolayer surfaces, HS(CH$_2$)$_{10}$X; X = H, COOH, CONH$_2$, NH$_2$, was studied by Okahata and coworkers. They found that CH$_3$COOH binds most strongly
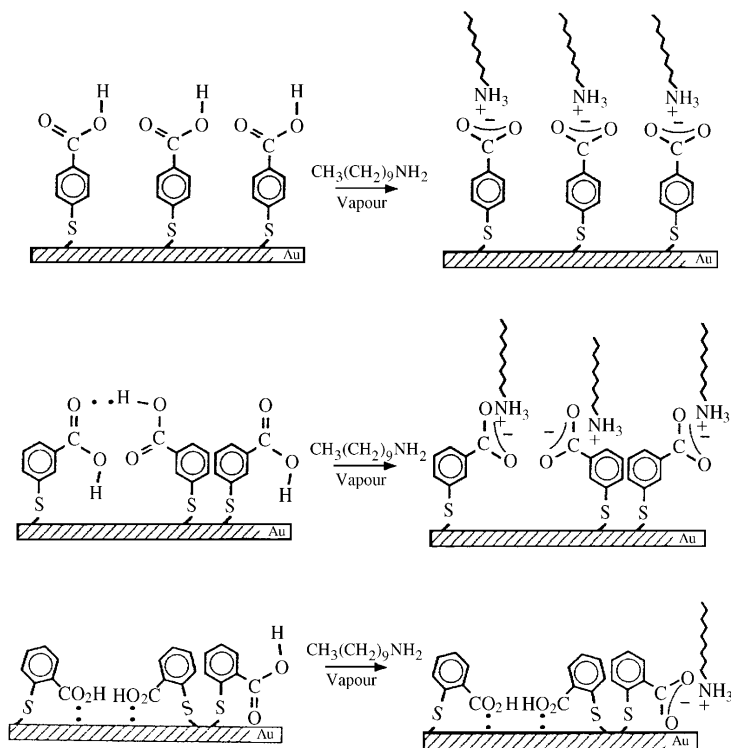
FIGURE 26. Binding of vapour-phase decylamine to the monolayers of 2-, 3- and 4-mercaptobenzoic acids. Reprinted with permission from Reference 406. Copyright (1996) American Chemical Society

to the amide-terminated surface with a binding constant of *ca* 5×10^4 M^{-1}. Multilayers form on both acid and amine-terminated surfaces[23].

Gas-phase adsorption of polar (methanol, acetonitrile, acetone) and non-polar adsorbates (hexane) on the surface of non-polar (hexadecanethiol) and polar (11-mercaptoundecanol) monolayers on gold was reported by Blanchard and Karpovich. The adsorption curves were fitted by a BET isotherm. The data suggest that an octadecanethiol surface is to some extent permeable for the adsorbates[409].

Solution-phase interactions between amino-terminated surfaces and phenols were studied by Anderson and coworkers. They found that phenols selectively adsorb from solution onto the surface of the monolayer of 4-aminothiophenol through H-bond interactions. Protonation of the amino groups on the monolayer terminus decreases the sensitivity towards the phenol solutes[410].

Strong polypodal H-bonding and van der Waals interactions between molecules can hold together several layers. Immersion of the monolayer of a thiol-terminated calix[4]resorcinarene in the hexane solution of a long-chain alkane-derivatized resorcinarene results in spontaneous formation of multilayers. Up to 40 layers are formed, which do not wash off with hexane. Individual layers are thought to be held together by H-bonds between hydroxy groups on the rims of the resorcinarene bowls, and van der Waals interactions between interdigitated hydrocarbon chains (Figure 27)[411].

Atomic force microscopy makes it possible to calculate the adhesion forces between different interfaces. In this type of experiment, both the sample and the tip of a force microscope are coated with a functionalized monolayer. The measurements of force *vs* distance between the two surfaces allows one to estimate the strength of attractive interactions (if any) between them. Crooks and coworkers obtained the following energy values for H-bond interactions: NH$_2$ *vs* NH$_2$ 1.3, COOH *vs* COOH 5 and COOH *vs* NH$_2$ 16 kcal mol^{-1}. Although adsorbed water molecules may have affected these data, they scale well with those expected for H-bond and acid–base interactions[412].

Investigation of adhesion forces between functionalized surfaces in solvents showed that they are mostly determined by the work required to exclude solvent between the two surfaces. Adhesion forces were found to be the strongest in water, and the weakest in non-polar solvents, such as hexadecane. The strongest interactions in water are those between two hydrophobic surfaces i.e. unsubstituted alkanethiol monolayers[413].

Adsorption of water in ultra-high vacuum and at low temperatures on the surface of a methyl 16-mercaptohexadecanoate monolayer which has a terminal COOCH$_3$ group showed that water molecules cause structural rearrangement of the film terminus and form H-bonds with the carbonyl oxygens[414]. Water does not penetrate alkane and ω-hydroxy-terminated monolayers; adsorption in this case is determined by strong H-bond interactions with the terminal hydroxy groups and very weak dipole–dipole interactions with the surface CH$_3$ groups[415,416]. A study of the water adsorption isotherm on the surface of the HS(CH$_2$)$_{15}$COOH monolayer showed strong interactions between water molecules and the terminal COOH group of the monolayer[417].

Crooks and coworkers studied electrostatic interactions between oppositely charged molecules and monolayer surfaces. They showed that anions of 2,6-anthraquinone disulphonic acid adsorb reversibly on the positively charged surfaces, such as those of protonated 4-mercaptopyridine or 4-mercaptoaniline monolayers at pH 2. Deprotonation of these surfaces at pH 7 effects desorption of the anions[418,419].

Inorganic ions capable of complexation with carboxylate groups, such as Cd^{2+}, Pb^{2+} and Ca^{2+}, adsorb on the surface of 4-carboxythiophenol and other acid-terminated monolayers. At high pH values, when all COOH groups are deprotonated, one metal ion adsorbs for every carboxylate, implying adsorption in the form of M(OH)$^+$. At low pH values,
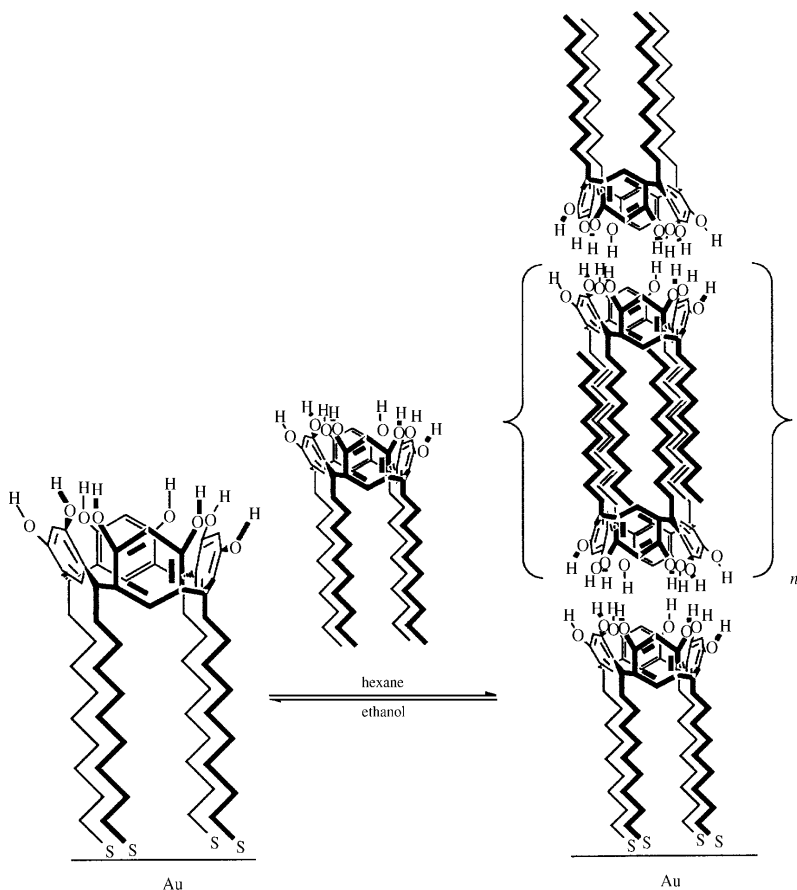
FIGURE 27. Spontaneous multilayering of alkane-derivatized calix[4]resorcinarene on the surface of a calixarene-terminated monolayer. Adapted with permission from Reference 411. Copyright (1995) American Chemical Society

adsorption proceeds to a much lesser extent[420]. Atoms only capable of ionic interactions (Cs^+, Ba^{2+}) do not adsorb[421]. Formation of polyion multilayers on the surface of gold–thiol monolayers is described by Finklea and coworkers[422]. Monolayers terminated with a nitrilotriacetic acid group, $-N(CH_2COOH)_3$, bind strongly Cu^{2+} and Ni^{2+} ions. Surface dissociation constants for these complexes are similar to the appropriate bulk solution values[423].

Rubinstein and coworkers prepared a monolayer containing an acetoacetate group (16). These films showed a remarkable sensitivity to the Cu^{2+} ions[424–426].

$$O^- \quad {}^-O$$
$$Cu$$
$$O \quad O$$
$$O \qquad\qquad O$$
$$S$$
$$Au$$

(16)
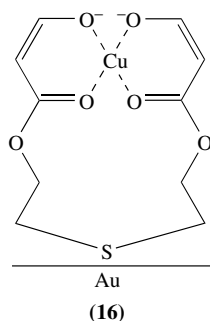
The fact that pyridinium derivatives form strong and stable complexes with $CrO_4{}^{2-}$ and $Cr_2O_7{}^{2-}$ was used to design a Cr(VI)-selective electrode. Monolayers of 4-(2-mercaptoethyl)pyridinium sulphate bind Cr(VI) from solution and the cathodic wave of Cr(VI)–Cr(III) reduction is recorded to determine the concentration of Cr(VI) in solution. The electrode can sense 0.001 ppb concentration of Cr(VI)[427].

Non-specific interactions between monolayer surfaces and solute molecules were studied by Whitesides and coworkers. They found that sodium dodecyl sulphate and other detergents reversibly adsorb from aqueous solutions on the surface of hexadecanethiolate monolayer on the gold surface. Adsorption is well described by the Langmuir isotherm. Formation of full monolayers was observed at concentrations close to the critical micelle concentration for the surfactant. Monolayers presenting ethylene glycol groups at the interface, $HS(CH_2)_{11}(OCH_2CH_2)_6OH$, resist adsorption of surfactants at these concentrations[428].

Adsorption of sodium dodecyl sulphate on the positively charged surface of the monolayer of $HSCH_2CH_2NH_3{}^+$ on Au results in the formation of a surfactant bilayer. At low surfactant concentration, electrostatic interactions between the negatively charged head group of the surfactant and the positively charged surface lead to the adsorption of dodecyl sulphate with its sulphate groups orientated towards the surface, and hydrophobic alkane facing solution. The total charge of the adsorbed surfactant counterbalances the surface charge at the bulk dodecyl sulphate concentration *ca* 1/1000 of the critical micelle concentration. At surfactant concentration close to the critical micelle concentration, a second layer is formed on the hydrophobic surface of the surfactant layer, this time with the sulphate groups facing the solution[429].

Exposure of octadecanethiol monolayer to the small phospholipid vesicles leads to their 'unrolling' and adsorption of a single lipid layer on top of the octadecanethiol film. Unrolling of vesicles on the surface of the hydrophilic monolayer, however, leads to the formation of the lipid bilayer on top of the original film. This principle was used by Evans and coworkers to create lipid bilayers supported by cholesterol moieties present in a mixed gold–thiol monolayer (Figure 28)[430].

Laval and coworkers similarly prepared a monolayer of a lipid on top of the octadecanethiol film on gold. The enzyme pyruvate oxidase was then incorporated in the lipid layer in a fashion similar to that of lipid vesicles, and the activity of the immobilized enzyme was measured[431].

A study of non-specific binding of proteins to the surface of functionalized gold–thiol monolayers showed that mixed monolayers containing hydrophobic and hydrophilic
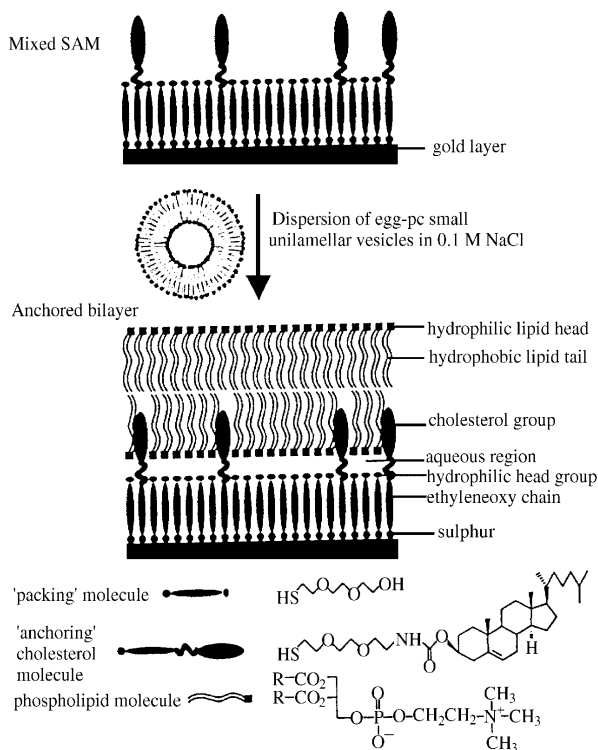
FIGURE 28. Formation of a lipid bilayer on the surface of a mixed gold–thiol monolayer. Reprinted with permission from Reference 430. Copyright (1997) American Chemical Society

alkanethiols can be tailored to select specific degrees of adsorption: the amount of protein adsorbed varies monotonically with the composition of the monolayer[432]. Binding of proteins to the surfaces of single-component monolayers decreased in the following order: $CH_3 \approx C_6H_5OH > COO^- > NH_2 > OH$. The poly(ethylene glycol)-terminated SAMs are the most effective in resisting protein adsorption; surface concentration of proteins on this surface was ca 10^3 lower than on the surface of a simple alkanethiolate monolayer[433]. Polyethylene glycol is not unique in its ability to resist protein adsorption: Whitesides and coworkers prepared a monolayer from propylene sulphoxide **17** and showed that it is only marginally less inert than the ethylene glycol films[434].
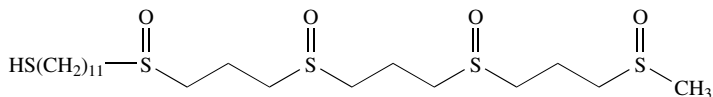
(17)

B. Molecular Recognition

Designing solid interfaces capable of selective host–guest interactions with molecules in gas mixtures or solutions has long been a tempting target for supramolecular chemists, and industrial potential implications of such surfaces are far reaching. Some examples of molecular recognition at the surface of gold–thiol monolayers are given in a recent publication[435]. We will discuss only briefly results covered by this review paper. Specific interactions of proteins and cells with the surfaces of gold–thiol monolayers have been reviewed by Mrksich and Whitesides[436].

Several groups designed various calix-[253] and resorcinarene[102] modified alkanethiols[411] and sulphides and used them for preparing self-assembled monolayers. A typical example **(18)** is shown below. These surfaces were reported to show selective response in gas phase to chlorinated hydrocarbons, especially C_2Cl_4[19,254,437,438]. Smaller response was observed for monolayers of unsubstituted alkanethiols (lacking a resorcinarene group), and this selectivity was attributed to the specific host–guest interactions between the resorcinarene moiety and tetrachloroethylene. Recently, however, this interpretation was questioned, as Grate and coworkers showed theoretically and experimentally that a very similar selectivity pattern arises from general dispersion interactions between the vapours and the surface. They concluded that the role of specific host–guest interactions in the binding of tetrachloroethylene is minimal[439].
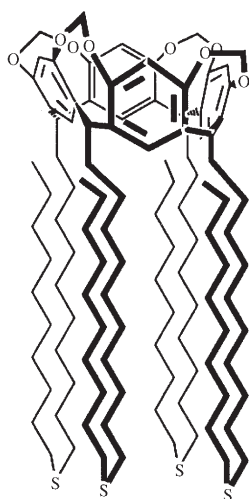
(18)

Surface-immobilized resorcinarenes were found to bind ascorbic acid specifically in solution phase. The binding is probably accompanied by a chemical reaction involving cleavage of the lactone ring of ascorbic acid[440].

A different approach to construction of calixarene-terminated surfaces was adopted by Crooks and coworkers who synthesized them by *in situ* conversion $CO_2H \rightarrow COCl$ of the acid-terminated monolayer by treatment with vapours of $SOCl_2$ followed by reaction

Victor Chechik and Charles J. M. Stirling

with hydroxy groups of a calixarene. Immobilized calixarene films also showed enhanced response to gas-phase tetrachloroethylene[441].

Specific interactions between calixarene and ferrocene groups were exploited by Kaifer and coworkers, who demonstrated that mixed monolayers containing ferrocenyl groups protruding above the surface of the film bind calix[6]arene host from aqueous solution at extremely low concentration (0.05–2 μM)[442].

A recent report describes preparation of the monolayers with a permanent inclusion guest. Carceplex molecules having a DMF molecule trapped in the cavity were self-assembled on a gold surface (Figure 29). While the orientation of the host is dictated by the monolayer environment, the guest can adopt different orientations inside the cavity and, in principle, these orientations can be made switchable[443].

Another popular host for molecular recognition studies in monolayers is thiol-derivatized cyclodextrin. Kaifer and coworkers have prepared monolayers from β-cyclodextrin **19** in which all primary hydroxyls are replaced by SH groups. This compound can form up to seven gold–sulphur chemical bonds on the surface. These monolayers are incomplete; to cover the gold surface completely, they were treated successively with ferrocene (to block the cyclodextrin cavities) and pentanethiol (to fill in the spaces between cavities). Cyclic voltammetry showed that the layers obtained bind ferrocene. Ferrocene trapped in the cyclodextrin cavities can be replaced by another known guest, electroinactive *m*-toluic acid[444].

Monolayers with much higher coverage were reported to form from the β-aminocyclodextrin derivative containing only one disulphide-terminated alkane chain attached to the amino group of the 6-deoxyaminoglucose unit. These layers were shown to bind naphthalenesulphonic acids[445]. A similar monolayer selectively binds a *trans*-azobenzene derivative[446]. β-Cyclodextrin modified layers also show selective transport of ferrocene carboxylic acid and hydroxyquinone. The selective transport can be controlled by blocking the β-cyclodextrin cavities with some guest molecules such as cyclohexanol, borneol and ursodeoxycholic acid[447,448].
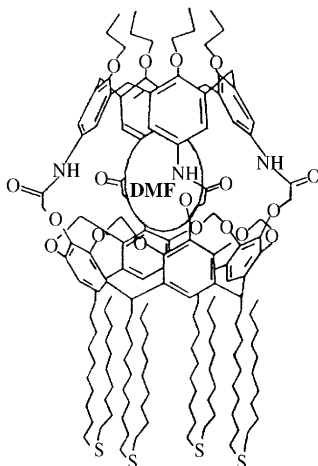
FIGURE 29. Carceplex adsorbate containing a trapped DMF molecule. Reprinted with permission from Reference 443. Copyright (1996) American Chemical Society
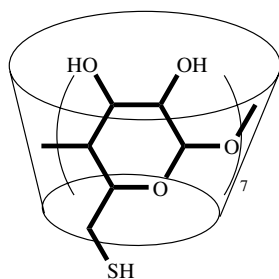
(19)

Yan and Dong found that β-cyclodextrin forms inclusion complexes with linear alka-nethiols in bulk medium and thereby effects solubilization of alkanethiols in the aqueous solution of β-cyclodextrin. Such complexes self-assemble on the gold surface to give stable monolayers[449]. 4,4′-Bipyridinium (viologen) containing thiols also form inclusion complexes with cyclodextrins in bulk solution which can be used to prepare self-assembled monolayers on gold[450,451]. *In situ* formation of a similar inclusion complex between the monolayer of mercaptopoly(ethylene glycol) and α-cyclodextrin was suggested by Nagashima and coworkers[452].

Phthalocyanines possessing ω-alkanethiol moieties **(20)** form monolayers on the gold surface. The fluorescent emission from the monolayers can be quenched by NO_2, which makes them potentially useful for sensing the environmentally important NO_2. Interactions with NO_2 can also be recorded by SPR measurements[453−455].
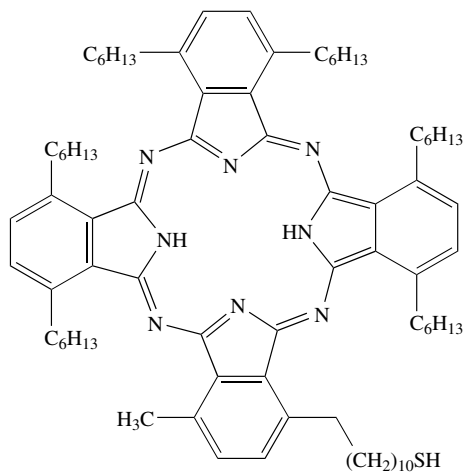
(20)

In an elegant recent study, a cyclic octapeptide was coadsorbed with the alkanethiols and sulphides on the gold surface (Figure 30). The peptide units form highly oriented
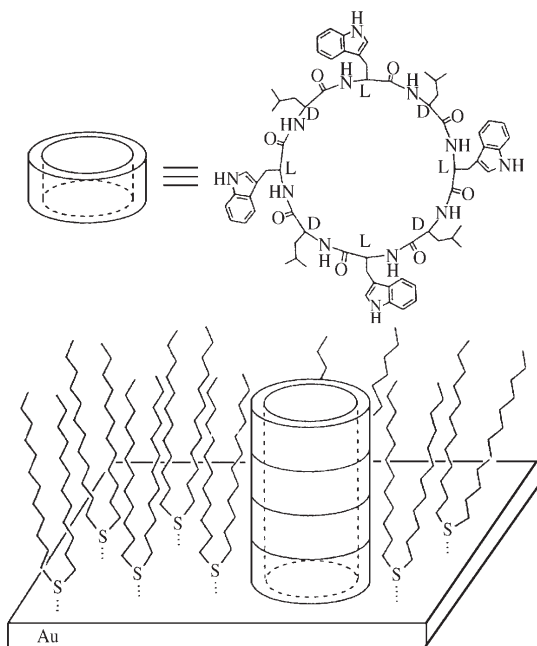
FIGURE 30. Incorporation of cyclic octapeptide nanotubes in gold–thiol monolayers. Reprinted with permission from Reference 279. Copyright (1997) American Chemical Society

tubular structures in the monolayer, creating nano-sized channels. Selective ion transport studies showed that while $[Fe(CN)_6]^{3-}$ and $[Ru(NH_3)_6]^{3+}$ can penetrate through these nanotubes, permeation by the bigger $[Mo(CN)_8]^{4-}$ ion is blocked[279].

The possibility of shape recognition was explored by Fuhrhop and coworkers. A steroid modified with a thiol group (21) forms incomplete monolayers on the gold surface. The gaps between the steroid molecules on the surface can be filled with octadecanethiol. The mixed monolayer obtained selectively and irreversibly binds *cis*-cyclohexanediol from aqueous solution. No binding was observed with the *trans*-diastereomer. The binding is tentatively assigned to penetration of the diol into hydrophobic gaps in the monolayer. Glucose, galactose and mannose are also bound by the steroid layer[456].

(21)
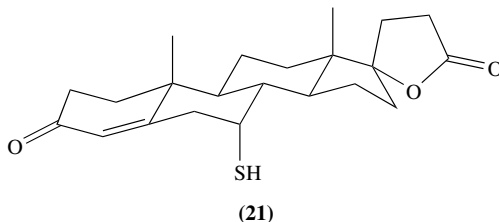
Crooks and coworkers noticed that monolayers of mercaptoundecanoic acid bind ben-zene vapours. The adsorbed molecules could not be removed by purging the monolayer with nitrogen. This behaviour is probably due to the intercalation of benzene into the monolayer lattice[405].

Eosin-modified electrodes showed specific interactions with a *cis*-azobenzene deriva-tive. As in the bulk medium chemistry, only weak interactions were registered with the *trans*-isomer[328].

Incorporation of two bipyridinium (viologen) ligands in monolayers was achieved via codeposition of the disulphide **22** and decanethiol onto the surface of a gold electrode[457]. The film obtained showed strong binding to a number of π-donor compounds, such as indole or catechol. The binding constants significantly exceed those observed for similar compounds in homogeneous solution.
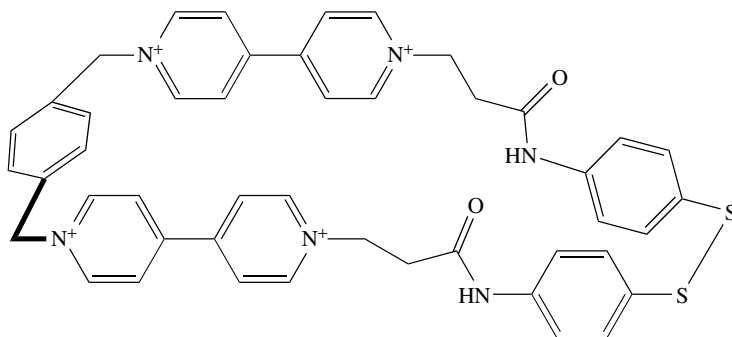
(22)

Crown ethers are known to form strong complexes with metal and ammonium ions in bulk solution. Exposure of the monolayer of the cysteamine layer, $HSCH_2CH_2NH_3^+$, to the solution of a crown ether derivative in dichloromethane results in fast and reversible binding[458].

Some traditional motifs based on the formation of several complementary H-bonds between the molecules of host and guest were applied to gold–thiol monolayers. In this type of experiment a recognition site usually protrudes above the surface of a mixed monolayer of the host adsorbate and a shorter alkanethiol (Figure 31). A mixed monolayer of a diaminopyridine derivative with an alkanethiol was shown to bind irreversibly a complementary barbiturate derivative from dichloromethane and acetonitrile solutions. Prolonged rinsing with ethanol disrupts hydrogen bonds and washes off the adsorbed barbiturate (Figure 31)[244].

Nucleic bases, adenine and thymine, have been modified with an ω-mercaptoalkyl group and self-assembled on gold. Binding of complementary guests (2-aminopyridine and γ-butyrolactone) from the gas phase was shown to be more favourable than inter-actions with non-complementary compounds. The ratios of the binding constants for complementary/non-complementary guests were comparable to the appropriate values in the bulk medium[459].

Selective binding of proteins to the surface of gold–thiol monolayers was the subject of several reports. To achieve selectivity, a thiol containing a specifically recognizable group is usually coadsorbed with poly(ethylene glycol)-terminated adsorbate, to reduce
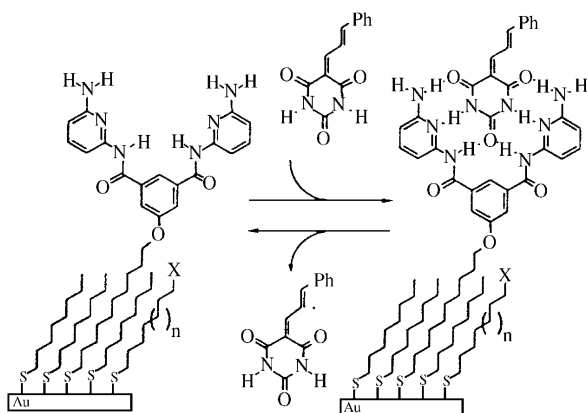
FIGURE 31. Binding of a barbiturate by an immobilized diaminopyridine derivative. Reprinted with permission from Reference 244. Copyright (1994) American Chemical Society

non-specific binding. *In situ* synthesis of a quaternary ammonium group on the surface of a monolayer makes the surface selective towards proteins containing choline-binding domains. The binding is reversible and can be inhibited by saturating the monolayer choline groups with the choline-binding fragment. Interestingly, the bound peptide retained its catalytic activity[460].

In a similar approach, Whitesides and coworkers prepared a mixed monolayer of poly(ethylene glycol)-terminated thiol and the adsorbate containing benzenesulphonamide groups, p-$C_6H_4SO_2NH_2$. This monolayer strongly binds bovine carbonic anhydrase, the dissociation constant of the bound protein (3×10^{-7} M) being slightly bigger than in the bulk solution (5×10^{-8} M)[461]. Mixed monolayers of poly(ethylene glycol)-terminated thiol and a thiol terminated with a nitrilotriacetic acid group $-N(CH_2CO_2H)_3$ form tetravalent chelate with Ni(II) ions. This surface-immobilized Ni(II) complex specifically binds proteins which are modified with a His-tag, a stretch of six consecutive histidine moieties. Control experiments showed that binding is specific for His-tagged proteins and required the presence of Ni(II) in the monolayer[462].

Several reports deal with incorporation of vitamin H, biotin, in self-assembled monolayers and probing interaction of this surface with the complementary protein streptavidin[463,464]. A detailed study of monolayers containing the biotin group in a different environment found the optimum conditions for binding. The biotin-containing adsorbate in the optimal monolayer is diluted by coadsorption with an alkanethiol. The biotin moiety not only protrudes above the surface of the monolayer, but is separated from it by a medium length spacer. The authors argue that better binding in such systems is due to reduced steric hindrance[464].

DNA can adsorb on the monolayers possessing a terminal quaternary ammonium function without impairing the native structure. Incorporation of a fullerene-substituted alkanethiol in the monolayer effects site-specific photocleavage of the DNA[465]. Single-stranded DNA can also adsorb on the surface of an ionizable gold–thiol monolayer through electrostatic interactions. Immobilized DNA does not, however, undergo hybridization[466]. Herne and Tarlov found that hybridization of such surface-bound DNA depends strongly on the surface coverage, and in mixed monolayers of the thiol-derivatized

DNA with a 'diluent' thiol the nucleotides are accessible for specific hybridization with complementary oligonucleotides and are able to discriminate between complementary and non-complementary target molecules[467].

Stirling and coworkers incorporated a chiral sulphoxide group in a gold–thiol mono-layer (23). Quick exposure of this chiral monolayer to the vapours of (±)-ethyl lactate shows non-selective adsorption of both enantiomers. However, prolonged exposure at 40 °C results in adsorption of exclusively one enantiomer[468]. The interactions can be followed by SPR[469].
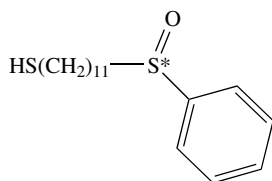
(23)

Recently, a stereoselective binding of R-1-phenylethylamine conjugate of methyl red by the β-cyclodextrin modified monolayer has been reported[470,471]. Electrocatalysed oxidation of glucose by glucose oxidase at the surface of chiral ferrocenyl-containing monolayers occurs enantioselectively[472]. Chiral recognition in the monolayers on the air–water interface is well-documented and has been summarized in a recent review[473].

IX. THIOL MONOLAYERS ON THE SURFACE OF GOLD COLLOIDS

Current research in the area of monolayer-protected colloids was summarized in a recent review[474] and the topics covered there will be discussed only briefly.

Ligands with strong affinity for gold have long been used to stabilize gold clusters[475,476]. However, thiol molecules have scarcely been used for this purpose, although polynuclear gold–thiolate clusters have been described[477,478]. With the increasingly detailed knowledge of thiol monolayers on planar gold, one could anticipate that thiols would self-assemble not only on the surface of flat substrates, but also on the surface of gold colloids. The first gold colloids stabilized by alkanethiolate were described by Giersig and coworkers in 1993[479]. Systematic studies of these systems started with the report by Brust and coworkers[480]. Their method was based on transfer of the $AuCl_4^-$ ions into toluene using a phase transfer catalyst, a tetralkylammonium salt, followed by reduction of the tetrachloroaurate ion by sodium borohydride in the presence of an alkanethiol (Figure 32). The incipient gold clusters were trapped by reaction with thiols, and produced small, 1–3 nm diameter, gold clusters coated with an alkanethiolate film. The average diameter of the gold clusters in the range 1.5–20 nm can, however, be manipulated by simply varying the gold-to-thiol ratio in the reaction mixture[481,482]. Surprisingly, these thiolate-protected colloids behave like ordinary organic compounds: they are soluble in organic solvents and can be repeatedly precipitated, dried and then redissolved without any appreciable coagulation[480].

Other methods for preparation of thiol-stabilized colloids have followed. Straightfor-ward reduction of tetrachloroaurate can be performed in ethanol in the presence of an ethanol-soluble thiol[329,483]. Gold colloids can be prepared first by any conventional method, and then the colloid dispersion in water is mixed with the ethanol solution
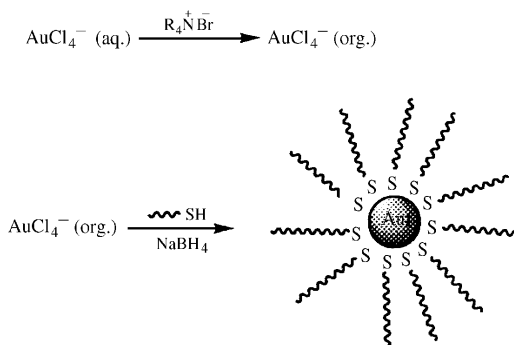
FIGURE 32. Formation of thiol-capped gold colloids

of the appropriate thiol[317]. Alternatively, shaking of the aqueous gold sol with a toluene solution of an appropriate thiol results in a very rapid formation of thiol monolayer on the surface of gold particles followed by the transfer of gold nanoparticles into organic phase[484]. Gold–thiolate clusters thus obtained show the same behaviour as thiol-protected colloids prepared by other methods. Platinum and silver sols can also be prepared in this way[484,485].

As for monolayers on planar gold, different functional groups can be introduced into monolayers on gold colloids, although the terminal groups may limit the solubility of the nanoparticles. The presence of an aromatic group with a large dipole moment surrounded by alkane chains in the adsorbate p-$C_{22}H_{45}SO_2C_6H_4OCH_2CH_2CH_2CH_2SH$ does not hamper formation of monolayers[486].

Whetten and coworkers separated the crude thiol-protected gold particles by fractional crystallization until monodisperse fractions were obtained. Electron microscopy of these nanocrystals showed that the major components of the thiol-capped colloid have the gold core as a truncated octahedron containing, in accord with the geometrical predictions, 140, 225, 314 and 459 gold atoms[487].

Thiolate monolayers on the surface of gold colloids have been studied by a variety of different methods. Both solution[488] and solid-state ^{13}C NMR[489] spectra show significant broadening of the signals close to the gold surface, which is explained by the interactions with the metal. The chemical shift of the two carbon atoms closest to the gold core (determined by ^{13}C-labelling) in the colloids coated with tetradecanethiol was very close to that of gold tetradecanethiolate, $[Au(C_{14}H_{29}S)]_n^{490}$. This strongly suggests a similarity of the nature of the Au−S chemical bond in these cases.

FT-IR[491] and NMR[489] spectra of the colloid particles showed that the alkane chains are mostly present in all-*trans* conformation, but also suggest a significant degree of conformational disorder. The high degree of order in monolayers on the surface of colloids is surprising given the high curvature of the surface. However, the distance between adjacent particles in the solid state equals approximately the length of one chain length, thus implying the possibility of the interdigitation of the alkane chains thereby creating crystalline regions[489].

Variable-temperature NMR and FT-IR studies coupled with differential scanning calorimetry revealed the presence of a phase transition which is attributed to the melting of the alkane chains in the monolayer[489,492,493], in agreement with recent molecular

dynamics simulations[494]. The phase transition temperature increases with the increase in chain length paralleling the melting of bulk alkanethiols. The measured enthalpies of melting are, however, significantly smaller than the corresponding values for the bulk thiols.

As well as thiols, long-chain amines (such as dodecyl- or octadecylamine) self-assemble on the surface of gold colloids. The materials obtained have properties similar to the corresponding thiol-protected colloids. This is somewhat surprising as amines do not self-assemble on the surface of planar gold substrates in the same conditions. The gold–amine bond in colloids was described as a charge-neutral weak covalent bond. The stability of the amine-protected colloids as compared to the planar amine–gold monolayers was attributed to kinetic factors[269].

Alkanethiolate coating of the gold particles protects them against action of chemical etchants. Protected colloids dissolve much more slowly in aqua regia than their unprotected counterparts. The level of protection observed from monolayers on the flat gold surface, however, is never achieved, probably because of the high curvature of the surface of gold colloids[317].

The rate of flocculation of thiolate-capped gold colloids in aqueous solutions depends on the nature of the terminal functional group. Colloids with acidic groups on the surface, such as carboxylic, phosphonic or boronic acid groups, flocculate more slowly at higher pH, as ionization of the surface results in repulsion between charged colloidal particles and thus stabilization of the colloid. Particles terminated with aliphatic carboxyl groups showed more complex behaviour[314,317]. Fan and Lopez studied adsorption of thiol-modified gold colloids on the surface of planar gold–thiol monolayers from aqueous solution. The fastest adsorption observed was for hydrophobic particles (i.e. unsubstituted alkanethiol-modified) and hydrophobic surfaces[495].

The properties of thiol-capped gold colloids resemble those of monolayers on planar gold substrates and both can undergo chemical reactions or exchange with other thiols. Addition of a functionalized thiol to the toluene solution of a thiol-protected gold colloid results in replacement of the latter thiolate by the former. The extent of such exchange is determined by the amount of thiol in solution and by the steric requirements of the adsorbing thiol. More than 50% of the original monolayer can be replaced by the unsubstituted alkanethiol[496]. Successive treatment of alkanethiolate-modified colloids with solutions of different thiols leads to the mixed monolayer-covered clusters which have up to 5 different terminal functional groups. Disulphides do not undergo exchange reaction with thiol-modified gold colloids[497]. Mixed monolayers on the surface of gold colloids can also be prepared by coadsorption of two different thiols[495].

Brust and coworkers studied chemical reactivity of thiol-capped gold colloids. A colloid modified with *p*-mercaptothiophenol is soluble in ethyl acetate. It can, however, be transferred into alkaline aqueous phase due to deprotonation of the phenolic groups. Acidification of the system effects protonation of phenolates and transfer of the colloid back to the aqueous phase[483]. Exposure of the above colloid to propionic anhydride leads to partial esterification. That phenolic groups, however, remain intact was attributed to steric hindrance.

Trimethoxysilane-terminated monolayers on gold colloids can be coupled with another substituted trialkoxysilane, creating a highly cross-linked functionalized bilayer (Figure 33). The terminal amino groups of these particles did not react with a model isothiocyanate. This probably suggests that the interactions between the former group and the gold surface or strong H-bonding between adjacent amino groups depresses their reactivity[329].
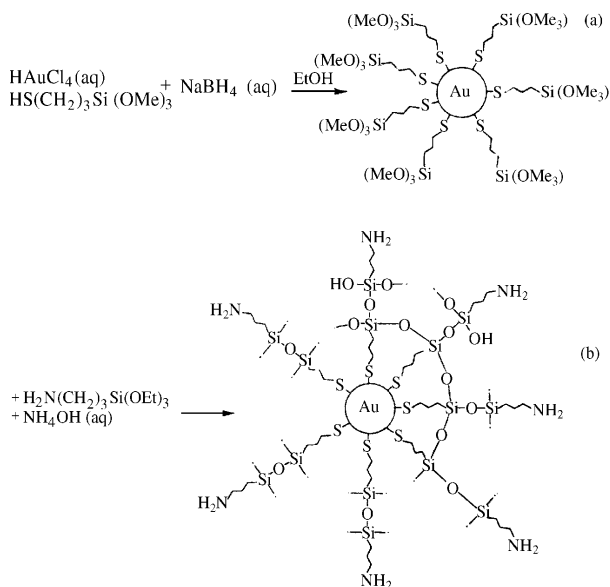
FIGURE 33. Formation of a cross-linked bilayer on the surface of the gold colloid. Reprinted with permission from Reference 329. Copyright (1997) American Chemical Society

Reduction of $AuCl_4{}^-$ ions in the presence of an α,ω-dithiol, such as 1,5-pentanedithiol or α,α'-xylyldithiol, leads to the formation of a cross-linked three-dimensional network of gold clusters separated by organic linkers[498]. These materials show interesting electrical properties[499].

Voltammetric experiments showed not only that faradaic current passes during inter-actions of functionalized gold nanoparticles with the electrode, but that double layer charging currents can be observed. This implies that each particle acts like a nano-sized electrode[500].

Takei and Shimizu evaporated gold on one side of temporarily immobilized latex spheres (Figure 34). Immersion of the spheres in a thiol solution results in the formation of a monolayer, and subsequent removal of the spheres from the substrate and dispersion in water gives particles as small as 100 nm in diameter functionalized from one side only. Such colloid suspensions might find a range of interesting applications[501].

An elegant approach to assembling nanoparticles was designed by Mirkin and cowork-ers. They attached to the surfaces of gold particles two different non-complementary DNA oligonucleotides capped with thiol groups. Addition of an oligonucleotide duplex with 'sticky ends' that are complementary to the two immobilized sequences results in the self-assembly of the nanoparticles into aggregates. The distance between clusters can be varied by changing the oligonucleotide linker. This assembly process can be reversed by thermal denaturation, while cooling restores the aggregates[502,503].

Similar mercaptoalkyloligonucleotide-modified gold nanoparticles showed a remarkable sensitivity to the single-stranded oligonucleotides. Introduction of the latter into solution
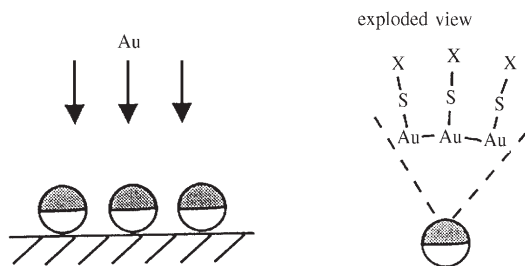
FIGURE 34. Formation of gold–thiol monolayers on the surface of latex spheres. Reprinted with permission from Reference 501. Copyright (1997) American Chemical Society

of the former results in the formation of a polymeric network of nanoparticles with a distinctive colour change. As little as 10 femtomoles of an oligonucleotide can be detected by this method[504].

X. APPLICATIONS

Gold–thiol monolayers find a very broad range of applications in various fields of research dealing with interfacial phenomena. The potential outlook in some areas has been reviewed, and the references are given in the next sentence. Applications include microelectronics[505], sensor devices[396,506,507], biochemical research[164,436], various uses of patterned films[508,509], adhesion and friction-related problems[510,511], anchoring of liquid crystals[512], corrosion inhibition and electrochemistry. General discussion of potential applications can be found in other references[12,513,514]. Electrochemical applications are discussed in Section VII.C. In this section we briefly describe some of the most common areas of applications.

A number of applications rely on preparing patterns on the surface. There are several methods for making patterned monolayers with high resolution. Perhaps the most popular and convenient method is microcontact printing (μCP)[508]. In this method, an elastomeric stamp is produced by casting a polydimethylsiloxane (PDMS) onto an appropriate master to make a negative image. The stamp is then inked with an ethanol solution of a long-chain alkanethiol and placed in contact with the gold surface for 20–30 s. Because alkanethiol layers are autophobic (on withdrawing the slide from solution the latter recedes from the surface and leaves it dry), no excess of alkanethiol remains on the surface, which is crucial for making patterns with sharp edges. Then the surface is exposed to the solution of another thiol which selectively modifies the untreated area (Figure 35). Features as small as 200 nm can be made by this method. Possible approaches to make smaller features were discussed by Whitesides and coworkers[515]. Similar methods can be used to prepare patterned monolayers on the silver surface[516]. Non-lithographic methods that generate patterned relief structures for casting the elastomeric stamps which are then used in fabrication of patterned monolayers, are described in a recent paper[517]. Automation of the microcontact printing process can also be envisaged[518].

The order and orientation in monolayers prepared by μCP was studied and compared with the ordinary gold–thiol films. The former layers differ from the latter mainly by the much shorter contact time used in their preparation, but they were shown to be, under certain conditions, indistinguishable from their planar counterparts[519,520].
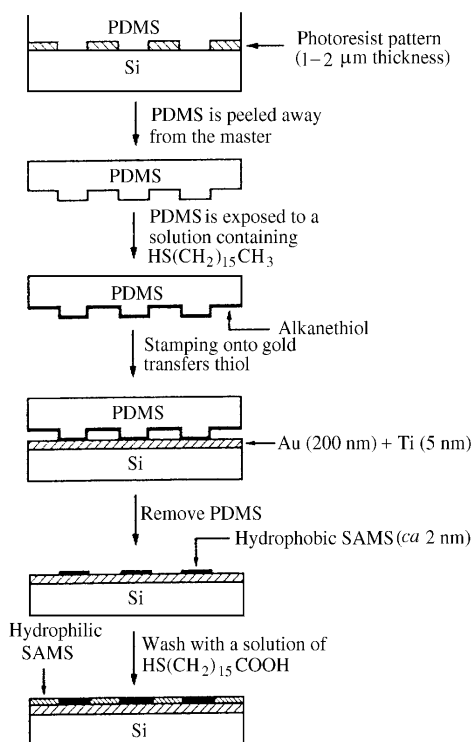
FIGURE 35. A schematic illustration of microcontact printing technique. Reprinted with permission from Reference 508. Copyright (1995) American Chemical Society

Microwriting is another simple technique to fabricate patterned layers. In this method a solution of alkanethiol is dispensed through the capillary on the surface, and this capillary is used to 'write' the patterns on the surface. Because of the autophobicity of alkanethiols, no excess of the deposition solution remains on the treated surface. Features down to 10 μm could be prepared[508].

Micromachining[521] refers to selective removal of the preformed monolayer on the surface by scratching the surface with a sharp object, such as a razor blade. Free binding sites on the scratched surface are filled by exposure with another thiol. Features as small as 100 nm could be made if a tip of carbon fibre is used as a scratching tool[508].

Photolithographic methods rely on irradiation of the monolayer through a mask[522]. The irradiated (or untreated) part of the monolayer is then selectively removed by the appropriate method and the free gold surface is exposed to the solution of another thiol. Irradiation of the monolayer by UV light in the presence of air results in the oxidation of the sulphur head group (Section VI). Rinsing the monolayer with the appropriate solvent achieves removal of the oxidized species in the irradiated area[286,288]. Another example of this method is described by Crooks and coworkers. A monolayer of a photopolymerizable monolayer containing a diacetylene unit is irradiated through a mask which causes

polymerization of the irradiated area. The monomeric layer is then removed from the untreated area by selective electrochemical desorption[523].

Patterned beams of neutral Ar or Cs atoms can also be used to selectively damage gold–thiol monolayers in the exposed areas[524,525]. Recently, use of AFM microscopy to selectively replace the monolayer of one alkanethiol with another with a resolution better than 2 nm was described[526].

Applications of patterned monolayers include fabrication of microelectrodes, patterned substrates for electron and scanning microscopies (an example of a patterned surface prepared by microcontact printing and analysed by STM is given in Figure 36), and preparation of microlenses by selective deposition of an organic prepolymer on the desired region of SAM. Directed adsorption of proteins and controlled attachment of cells[527], which can be achieved by using patterned monolayers[528–530], is needed for drug screening, tissue engineering and fundamental studies in cellular biology[508].

Another important area where gold–thiol monolayers might find promising applications is gas- and biosensing. Simple sensors sensitive to certain types of compounds, based on such detection methods as surface plasmon resonance or surface acoustic wave, have been described[454,455,531–533]. This type of device is usually made of a gold plate coated with a functionalized monolayer. The terminal functional group of such a monolayer is responsible for selective interactions with the analyte, and adsorption of the latter is then detected by the appropriate method.

Different permeability of the alkanethiol monolayers can also be used in fabrication of sensor devices. Selective transport[534] of hydrophobic compounds can be achieved by varying the chain length of the alkanethiol modifier[535]. Selective ion transport through mixed monolayers containing an electron transfer-blocking long-chain thiol and a shorter aromatic mercaptan which induces the molecular-sized defects in the monolayer[536,537] have been described. The molecular recognition principle is used to make biosensors. An appropriate protein or enzyme is immobilized in the monolayer and the interactions with the analyte are usually determined electrochemically[538–541]. Metal ions can also be selectively detected using specific interactions between metal ions and terminal functional groups of the monolayer. Electrodes very sensitive to such metals as Cr(VI), Cu(II), Pb(II) etc, have been described[425–427].

Blocking ability of well-packed alkanethiol monolayers made them potentially useful in protecting the surface of copper, iron, silver and gold against corrosion[542–544].

The fact that self-assembly of thiols on gold makes it possible to create well-defined surfaces with controlled properties was used extensively to understand the forces controlling orientation of liquid crystals adsorbed at surfaces[545–549].

The ability to control surface properties also made gold–thiol monolayers an attractive substrate for fabricating Langmuir–Blodgett (LB) films[550]. Direct correlation between LB film transfer properties and hydrophobicity of the gold–thiol monolayer was obtained[551,552].

Dynamic control of wettability of the surface was described by Whitesides and coworkers. They formed a hydrophobic monolayer of a short-chain alkanethiol in a small region surrounded by a longer-chain thiol. Application of an electric potential results in a selective desorption of the short-chain thiol which renders the surface hydrophilic. At neutral potentials, the thiol readsorbs on the surface, making it hydrophobic[293].

An interesting approach to control self-assembly of macroscopic objects coated with monolayers was described by Whitesides and coworkers. Millimeter-sized gold objects made hydrophobic by the thiol coating self-assemble in water in such a way as to minimize hydrophobic interactions with water. Objects of complimentary shapes 'recognize' each
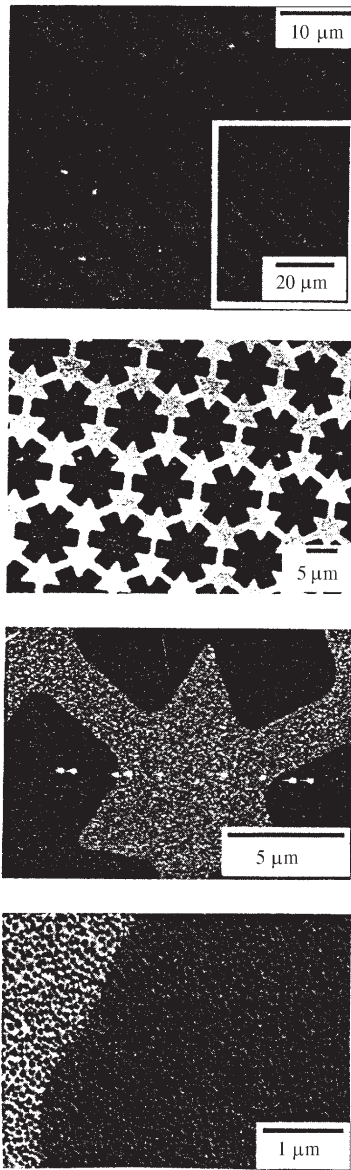
FIGURE 36. STM images of a patterned monolayer prepared by microcontact printing with increasing resolution. Reprinted with permission from Reference 508. Copyright (1995) American Chemical Society

other and aggregate as their contact results in the maximum water exclusion[553]. Similarly, gold disks coated with a thiol bearing a positively charged group adsorb on the gold surface coated with a thiol bearing a negatively-charged functionality, but not on the positively-charged surface (Figure 37)[554].
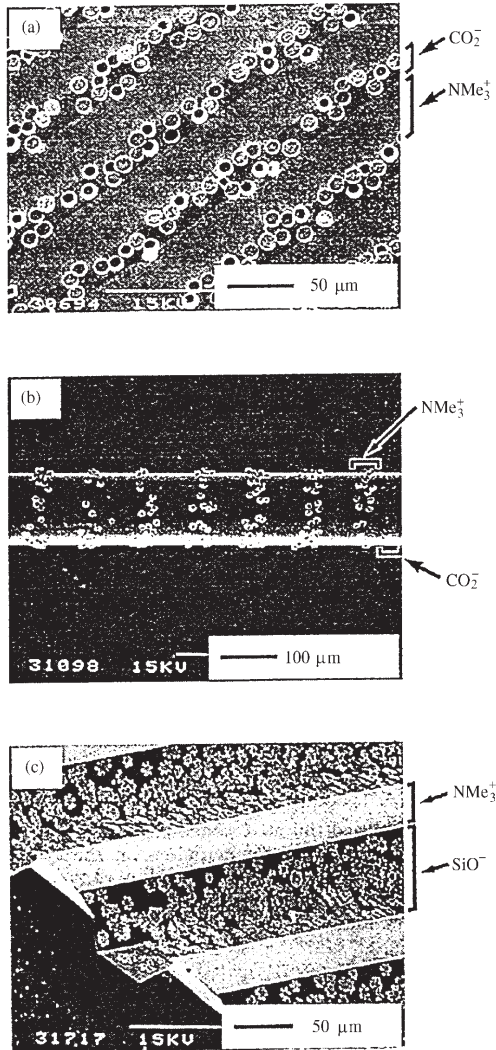
FIGURE 37. Scanning electron microscope images of patterns of gold disks (or stars) modified with a NMe_3^+ (a,c) and PO_3H^- (b) terminated thiol after electrostatic self-assembly in ethanol. Terminal functional groups of the gold surface are shown on the left. Reprinted with permission from Reference 554. Copyright (1997) American Chemical Society

XI. REFERENCES

1. A. Pockels, *Nature*, **43**, 437 (1891).
2. K. Blodgett, *J. Am. Chem. Soc.*, **56**, 495 (1934).
3. W. C. Bigelow, D. L. Pickett and W. A. Zisman, *J. Colloid Interface Sci.*, **1**, 513 (1946).
4. A. Ulman, *An Introduction to Ultrathin Organic Films: From Langmuir—Blodgett to Self-Assembly*, Academic Press, New York, 1991.
5. A. Ulman, *Chem. Rev.*, **96**, 1533 (1996). There are errors in the referencing system: References 156–161 should be 155–160, respectively.
6. R. Maoz, L. Netzer, J. Gun and J. Sagiv, *J. Chim. Phys. (Paris)*, **85**, 1059 (1988).
7. D. L. Allara and R. G. Nuzzo, *Langmuir*, **1**, 45 (1985).
8. D. L. Allara and R. G. Nuzzo, *Langmuir*, **1**, 52 (1985).
9. H. Lee, L. J. Kepley, H. G. Hong and T. E. Mallouk, *J. Am. Chem. Soc.*, **110**, 618 (1988).
10. R. G. Nuzzo and D. L. Allara, *J. Am. Chem. Soc.*, **105**, 4481 (1983).
11. L. H. Dubois and R. G. Nuzzo, *Annu. Rev. Phys. Chem.*, **43**, 437 (1992).
12. A. R. Bishop and R. G. Nuzzo, *Curr. Opin. Colloid Interface Sci.*, **1**, 127 (1996).
13. H. O. Finklea, *Electroanal. Chem.*, **19**, 109 (1996).
14. S. Mittlerneher, J. Spinke, M. Liley, G. Nelles, M. Weisser, R. Back, G. Wenz and W. Knoll, *Biosensors Bioelectronics*, **10**, 903 (1995).
15. M. K. Debe, *Prog. Surf. Sci.*, **24**, 1 (1987).
16. G. E. McGuire, P. S. Weiss, J. G. Kushmerick, J. A. Johnson, S. J. Simko, R. J. Nemanich, N. R. Parikh and D. R. Chopra, *Anal. Chem.*, **69**, R231 (1997). References to previous reviews in this series are given in the paper.
17. G. L. Gaines, Jr., *Insoluble Monolayers at Liquid–Gas Interfaces*, Interscience, New York, 1996.
18. R. F. Debono, G. D. Loucks, D. Dellamanna and U. J. Krull, *Can. J. Chem.*, **74**, 677 (1996).
19. B.-H. Huisman, R. P. H. Kooyman, F. C. J. M. van Veggel and D. N. Reinhoudt, *Adv. Mater.*, **8**, 561 (1996).
20. K. A. Peterlinz and R. Georgiadis, *Langmuir*, **12**, 4731 (1996).
21. M. D. Ward and D. A. Buttry, *Science*, **249**, 1000 (1990).
22. D. S. Karpovich and G. J. Blanchard, *J. Chem. Educ.*, **72**, 466 (1995).
23. Y. Okahata, K. Matsuura, K. Ito and Y. Ebara, *Langmuir*, **12**, 1023 (1996).
24. W. Pan, C. J. Durning and N. J. Turro, *Langmuir*, **12**, 4469 (1996).
25. H. Hoffmann, U. Mayer, H. Brunner and A. Krischanitz, *Vibrational Spectrosc.*, **8**, 151 (1995).
26. A. Ulman, *ACS Symp. Ser.*, **447**, 144 (1991).
27. Y. Maeda and H. Kitano, *Kobunshi Ronbunshu*, **52**, 737 (1995); *Chem. Abstr.*, **124**, 127574z (1996).
28. M. Futamata, *J. Phys. Chem.*, **99**, 11901 (1995).
29. J. Wang, T. Zhu, M. Tang, S. M. Cai and Z. F. Liu, *Japn. J. Appl. Phys. 2*, **35**, L1381 (1996).
30. T. Zhu, H. Z. Yu, J. Wang, Y. Q. Wang, S. M. Cai and Z. F. Liu, *Chem. Phys. Lett.*, **265**, 334 (1997).
31. S. H. Cho, H. S. Han, D. J. Jang, K. Kim and M. S. Kim, *J. Phys. Chem.*, **99**, 10594 (1995).
32. M. Tsen and L. Sun, *Anal. Chim. Acta*, **307**, 333 (1995).
33. Q. Ye, J. X. Fang and L. Sun, *J. Phys. Chem. B*, **101**, 8221 (1997).
34. For recent developments and historical background see references in: N. H. Turner and J. A. Schreifels, *Anal. Chem.*, **68**, R309 (1996).
35. T. L. Barr, *Crit. Rev. Anal. Chem.*, **22**, 115 (1991).
36. G. Gillen, J. Bennett, M. J. Tarlov and F. Burgess, *Anal. Chem.*, **66**, 2170 (1994).
37. B. Hagenhoff, A. Benninghoven, J. Spinke, M. Liley and W. Knoll, *Langmuir*, **9**, 1622 (1993).
38. D. Jacquemain, S. G. Wolf, F. Leveiller, M. Deutsch, K. Kjaer, J. Alsnielsen, M. Lahav and L. Leiserowitz, *Angew, Chem., Int. Ed. Engl.*, **31**, 130 (1992).
39. I. M. Tidswell, B. M. Ocko, P. S. Pershan, S. R. Wasserman, G. M. Whitesides and J. D. Axe, *Phys. Rev. B*, **41**, 1111 (1990).
40. S. R. Wasserman, G. M. Whitesides, I. M. Tidswell, B. M. Ocko, P. S. Pershan and J. D. Axe, *J. Am. Chem. Soc.*, **111**, 5852 (1989).
41. J. Penfold, R. M. Richardson, A. Zarbakhsh, J. R. P. Webster, D. G. Bucknall, A. R. Rennie, R. A. L. Jones, T. Cosgrove, R. K. Thomas, J. S. Higgins, P. D. I. Fletcher, E. Dickinson, S. J. Roser, I. A. McLure, A. R. Hillman, R. W. Richards, E. J. Staples, A. N. Burgess, E. A. Simister and J. W. White, *J. Chem. Soc., Faraday Trans.*, **93**, 3899 (1997).

42. G. Fragneto, J. R. Lu, D. C. McDermott, R. K. Thomas, A. R. Rennie, P. D. Gallagher and S. K. Satija, *Langmuir*, **12**, 477 (1996).
43. N. Camillone, T. Y. B. Leung and G. Scoles, *Surf. Sci.*, **373**, 333 (1997).
44. N. Camillone, C. E. D. Chidsey, G. Y. Liu, T. M. Putvinski and G. Scoles, *J. Chem. Phys.*, **94**, 8493 (1991).
45. N. Camillone, T. Y. B. Leung, P. Schwartz, P. Eisenberger and G. Scoles, *Langmuir*, **12**, 2737 (1996).
46. L. H. Dubois, B. R. Zegarski and R. G. Nuzzo, *J. Chem. Phys.*, **98**, 678 (1993).
47. F. Balzer, R. Gerlach, G. Polanski and H. G. Rubahn, *Chem. Phys. Lett.*, **274**, 145 (1997).
48. P. Dutta, *Curr. Opin. Solid State Mater. Sci.*, **2**, 557 (1997).
49. W. A. Zisman, in *Contact Angles, Wettability, and Adhesion* (Ed. F. M. Fowkes), Advances in Chemistry Series 43, American Chemical Society, Washington, DC, 1964, pp. 1−51.
50. P. E. Laibinis and G. M. Whitesides, *J. Am. Chem. Soc.*, **114**, 1990 (1992).
51. E. Delamarche, B. Michel, H. A. Biebuyck and C. Gerber, *Adv. Mater.*, **8**, 719 (1996).
52. A. Noy, C. D. Frisbie, L. F. Rozsnyai, M. S. Wrighton and C. M. Lieber, *J. Am. Chem. Soc.*, **117**, 7943 (1995).
53. G. U. Lee, L. A. Chrisey, C. E. Oferrall, D. E. Pilloff, N. H. Turner and R. J. Colton, *Isr. J. Chem.*, **36**, 81 (1996).
54. G. E. Poirier, *Chem. Rev.*, **97**, 1117 (1997).
55. O. Marti, H. O. Ribi, B. Drake, T. R. Albrecht, C. F. Quate and P. K. Hansma, *Science*, **239**, 50 (1988).
56. A. Noy, D. V. Vezenov and C. M. Lieber, *Annu. Rev. Mater. Sci.*, **27**, 381 (1997).
57. A. J. Bard, H. D. Abruna, C. E. D. Chidsey, L. R. Faulkner, S. W. Feldberg, K. Itaya, M. Majda, O. Melroy, R. W. Murray, M. D. Porter, M. P. Soriaga and H. S. White, *J. Phys. Chem.*, **97**, 7147 (1993).
58. C. Buessherman, *Prog. Surf. Sci.*, **46**, 335 (1994).
59. C. Miller, P. Cuendet and M. Gratzel, *J. Phys. Chem.*, **95**, 877 (1991).
60. K. Takehara, H. Takemura and Y. Ide, *Electrochim, Acta*, **39**, 817 (1994).
61. K. Takehara and H. Takemura, *Bull. Chem. Soc. Jpn.*, **68**, 1289 (1995).
62. M. V. Baker and J. Landau, *Aust. J. Chem.*, **48**, 1201 (1995).
63. J. Xu and H. L. Li, *J. Colloid Interface Sci.*, **176**, 138 (1995).
64. B. B. G. Johnson and R. Davis, in *The Chemistry of Copper, Silver and Gold* (Eds. J. C. Ballar, H. J. Emeleus, R. Nyholm and A. F. Trotman-Dickenson), Pergamon Press, Oxford, 1975, pp. 129−186.
65. C. D. Bain, E. B. Troughton, Y. T. Tao, J. Evall, G. M. Whitesides and R. G. Nuzzo, *J. Am. Chem. Soc.*, **111**, 321 (1989).
66. M. Forslund and C. Leygraf, *J. Electrochem. Soc.*, **144**, 105 (1997).
67. C. E. D. Chidsey, D. N. Loiacono, T. Sleator and S. Nakahara, *Surf. Sci.*, **200**, 45 (1988).
68. S. D. Evans, E. Urankar, A. Ulman and N. Ferris, *J. Am. Chem. Soc.*, **113**, 4121 (1991).
69. C. V. Erickson, *Chem. Eng. News*, **68**, *(33)*, 2 (1990).
70. D. A. Dobbs, R. G. Bergman and K. H. Theopold, *Chem. Eng. News*, **68**, *(17)*, 2 (1990).
71. P. E. Laibinis, G. M. Whitesides, D. L. Allara, Y. T. Tao, A. N. Parikh and R. G. Nuzzo, *J. Am. Chem. Soc.*, **113**, 7152 (1991).
72. R. G. Nuzzo, L. H. Dubois and D. L. Allara, *J. Am. Chem. Soc.*, **112**, 558 (1990).
73. R. G. Nuzzo, F. A. Fusco and D. L. Allara, *J. Am. Chem. Soc.*, **109**, 2358 (1987).
74. M. Levlin, A. Laakso, H. E. M. Niemi and P. Hautojarvi, *Appl. Surf. Sci.*, **115**, 31 (1997).
75. L. H. Guo, J. S. Facci, G. McLendon and R. Mosher, *Langmuir*, **10**, 4588 (1994).
76. Z. H. Liu, N. M. D. Brown and A. McKinley, *J. Phys. Condensed Matter*, **9**, 59 (1997).
77. D. Stamou, D. Gourdon, M. Liley, N. A. Burnham, A. Kulik, H. Vogel and C. Duschl, *Langmuir*, **13**, 2425 (1997).
78. M. Hegner, P. Wagner and G. Semenza, *Surf. Sci.*, **291**, 39 (1993).
79. M. Kawasaki and H. Uchiki, *Surf. Sci.*, **388**, L1121 (1997).
80. J. B. Schlenoff, M. Li and H. Ly, *J. Am. Chem. Soc.*, **117**, 12528 (1995).
81. I. Nabiev and M. Manfait, *Rev. Inst. Fr. Petr.*, **48**, 261 (1993); *Chem. Abstr.*, **120**, 182059c (1994).
82. P. Halevi (Ed.), *Photonic Probes of Surfaces*, Chap. 2, Elsevier Science, Amsterdam, 1995, pp. 65−92.
83. P. Gao, M. L. Patterson, M. A. Tadayyoni and M. J. Weaver, *Langmuir*, **1**, 173 (1985).

84. L. Maya, C. E. Vallet and Y. H. Lee, *J. Vac. Sci. Technol. A*, **15**, 238 (1997).
85. S. E. Creager, L. A. Hockett and G. K. Rowe, *Langmuir*, **8**, 854 (1992).
86. N. Camillone, C. E. D. Chidsey, G. Liu and G. Scoles, *J. Chem. Phys.*, **98**, 4234 (1993).
87. P. Fenter, P. Eisenberger, J. Li, N. Camillone, S. Bernasek, G. Scoles, T. A. Ramanarayanan and K. S. Liang, *Langmuir*, **7**, 2013 (1991).
88. J. Y. Gui, D. A. Stern, D. G. Frank, F. Lu, D. C. Zapien and A. T. Hubbard, *Langmuir*, **7**, 955 (1991).
89. R. G. Nuzzo, B. R. Zegarski and L. H. Dubois, *J. Am. Chem. Soc.*, **109**, 733 (1987).
90. M. M. Walczak, C. K. Chung, S. M. Stole, C. A. Widrig and M. D. Porter, *J. Am. Chem. Soc.*, **113**, 2370 (1991).
91. G. K. Jennings and P. E. Laibinis, *J. Am. Chem. Soc.*, **119**, 5208 (1997).
92. G. K. Jennings and P. E. Laibinis, *Langmuir*, **12**, 6173 (1996).
93. T. Ishida, S. Tsuneda, N. Nishida, M. Hara, H. Sasabe and W. Knoll, *Langmuir*, **13**, 4638 (1997).
94. D. N. Batchelder, S. D. Evans, T. L. Freeman, L. Häussling, H. Ringsdorf and H. Wolf, *J. Am. Chem. Soc.*, **116**, 1050 (1994).
95. O. Chailapakul, L. Sun, C. J. Xu and R. M. Crooks, *J. Am. Chem. Soc.*, **115**, 12459 (1993).
96. C. G. Worley, R. W. Linton and E. T. Samulski, *Langmuir*, **11**, 3805 (1995).
97. J. Cheng and C. J. Miller, *J. Phys. Chem. B*, **101**, 1058 (1997).
98. T. T. Wooster, P. R. Gamm, W. E. Geiger, A. M. Oliver, A. J. Black, D. C. Craig and M. N. Paddon-row, *Langmuir*, **12**, 6616 (1996).
99. H. Rieley, N. J. Price, T. L. Smith and S. Yang, *J. Chem. Soc., Faraday Trans.*, **92**, 3629 (1996).
100. X. M. Zhao, J. L. Wilbur and G. M. Whitesides, *Langmuir*, **12**, 3257 (1996).
101. E. U. T. van Velzen, J. F. J. Engbersen and D. N. Reinhoudt, *Synthesis*, 989 (1995).
102. E. U. T. van Velzen, J. F. J. Engbersen, P. J. Delange, J. W. G. Mahy and D. N. Reinhoudt, *J. Am. Chem. Soc.*, **117**, 6853 (1995).
103. R. W. Zehner and L. R. Sita, *Langmuir*, **13**, 2973 (1997).
104. R. C. Thomas, L. Sun, R. M. Crooks and A. J. Ricco, *Langmuir*, **7**, 620 (1991).
105. G. E. Poirier and E. D. Pylant, *Science*, **272**, 1145 (1996).
106. H. Rieley, N. J. Price, R. G. White, R. I. R. Blyth and A. W. Robinson, *Surf. Sci.*, **333**, 189 (1995).
107. J. F. Ford, T. J. Vickers, C. K. Mann and J. B. Schlenoff, *Langmuir*, **12**, 1944 (1996).
108. R. L. Garrell and J. E. Chadwick, *Coll. Surf. A*, **93**, 59 (1994).
109. H. A. Biebuyck and G. M. Whitesides, *Langmuir*, **9**, 1766 (1993).
110. T. Ishida, S. Yamamoto, W. Mizutani, M. Motomatsu, H. Tokumoto, H. Hokari, H. Azehara and M. Fujihira, *Langmuir*, **13**, 3261 (1997).
111. C.-J. Zhong and M. D. Porter, *J. Am. Chem. Soc.*, **116**, 11616 (1994).
112. M. W. J. Beulen, B.-H. Huisman, P. A. van der Heijden, F. C. J. M. van Veggel, M. G. Simons, E. M. E. F. Biemond, P. J. de Lange and D. N. Reinhoudt, *Langmuir*, **12**, 6170 (1996).
113. Y. G. Ning, H. Xie, H. T. Xing, W. L. Deng and D. B. Yang, *Surf. Interf. Anal.*, **24**, 667 (1996).
114. R. Shaw, in *The Chemistry of the Thiol Group* (Ed. S. Patai), Chap. 3, Wiley, London, 1974, p. 160.
115. S. W. Benson, *Chem. Rev.*, **78**, 23 (1978).
116. D. E. Weisshaar, B. D. Lamp and M. D. Porter, *J. Am. Chem. Soc.*, **114**, 5860 (1992).
117. H. M. Schessler, D. S. Karpovich and G. J. Blanchard, *J. Am. Chem. Soc.*, **118**, 9645 (1996).
118. D. S. Karpovich and G. J. Blanchard, *Langmuir*, **10**, 3315 (1994).
119. C. D. Bain, H. A. Biebuyck and G. M. Whitesides, *Langmuir*, **5**, 723 (1989).
120. V. Chechik, H. Schönherr, J. G. Vancso and C. J. M. Stirling, *Langmuir*, **14**, 3003 (1998).
121. X. Y. Tang, T. W. Schneider, J. W. Walker and D. A. Buttry, *Langmuir*, **12**, 5921 (1996).
122. E. B. Troughton, C. D. Bain, G. M. Whitesides, R. G. Nuzzo, D. L. Allara and M. D. Porter, *Langmuir*, **4**, 365 (1988).
123. M. H. Zhang and M. R. Anderson, *Langmuir*, **10**, 2807 (1994).
124. C. D. Bain, J. Evall and G. M. Whitesides, *J. Am. Chem. Soc.*, **111**, 7155 (1989).
125. P. W. Atkins, *Physical Chemistry*, 4th edn., Freeman, New York, 1990, pp. 885–887.
126. G. Hahner, C. Woll, M. Buck and M. Grunze, *Langmuir*, **9**, 1955 (1993).
127. D. W. Hatchett, K. J. Stevenson, W. B. Lacy, J. M. Harris and H. S. White, *J. Am. Chem. Soc.*, **119**, 6596 (1997).
128. T. Ishida, N. Nishida, S. Tsuneda, M. Hara, H. Sasabe and W. Knoll, *Jpn. J. Appl. Phys. 2*, **35**, L1710 (1996).

129. K. Tamada, M. Hara, H. Sasabe and W. Knoll, *Langmuir*, **13**, 1558 (1997).
130. T. W. Schneider and D. A. Buttry, *J. Am. Chem. Soc.*, **115**, 12391 (1993).
131. K. D. Truong and P. A. Rowntree, *Prog. Surf. Sci.*, **50**, 207 (1995).
132. K. Deweldige, M. Rohwerder, E. Vago, H. Viefhaus and M. Stratmann, *Fresenius J. Anal. Chem.*, **353**, 329 (1995).
133. G. E. Poirier, M. J. Tarlov and H. E. Rushmeier, *Langmuir*, **10**, 3383 (1994).
134. G. E. Porier and M. J. Tarlov, *J. Phys. Chem.*, **99**, 10966 (1995).
135. S. J. Stranick, A. N. Parikh, D. L. Allara and P. S. Weiss, *J. Phys. Chem.*, **98**, 11136 (1994).
136. R. L. McCarley, D. J. Dunnaway and R. J. Willicut, *Langmuir*, **9**, 2775 (1993).
137. J. T. Woodward and D. K. Schwartz, *J. Am. Chem. Soc.*, **118**, 7861 (1996).
138. K. D. Truong and P. A. Rowntree, *J. Phys. Chem.*, **100**, 19917 (1996).
139. R. Yamada and K. Uosaki, *Langmuir*, **13**, 5218 (1997).
140. M. Hara, H. Sasabe and W. Knoll, *Thin Solid Films*, **273**, 66 (1996).
141. J. J. Calvente, Z. Kovacova, M. D. Sanchez, R. Andreu and W. R. Fawcett, *Langmuir*, **12**, 5696 (1996).
142. E. Delamarche, B. Michel, C. Gerber, D. Anselmetti, H. J. Guntherodt, H. Wolf and H. Ringsdorf, *Langmuir*, **10**, 2869 (1994).
143. J. A. M. Sondag-Huethorst, C. Schönenberger and L. G. J. Fokkink, *J. Phys. Chem.*, **98**, 6826 (1994).
144. K. Edinger, A. Golzhauser, K. Demota, C. Woll and M. Grunze, *Langmuir*, **9**, 4 (1993).
145. M. H. Dishner, J. C. Hemminger and F. J. Feher, *Langmuir*, **13**, 2318 (1997).
146. G. E. Poirier, *Langmuir*, **13**, 2019 (1997).
147. M. H. Dishner, F. J. Feher and J. C. Hemminger, *Chem. Commun.*, 1971 (1996).
148. C. D. Bain and G. M. Whitesides, *J. Am. Chem. Soc.*, **110**, 6560 (1988).
149. C. D. Bain and G. M. Whitesides, *J. Am. Chem. Soc.*, **110**, 3665 (1988).
150. B. Liedberg and P. Tengvall, *Langmuir*, **11**, 3821 (1995).
151. B. Liedberg, M. Wirde, Y. T. Tao, P. Tengvall and U. Gelius, *Langmuir*, **13**, 5329 (1997).
152. C. D. Bain and G. M. Whitesides, *J. Am. Chem. Soc.*, **111**, 7164 (1989).
153. S. E. Creager and G. K. Rowe, *J. Electroanal. Chem.*, **370**, 203 (1994).
154. D. A. Offord, C. M. John, M. R. Linford and J. H. Griffin, *Langmuir*, **10**, 883 (1994).
155. P. E. Laibinis, M. A. Fox, J. P. Folkers and G. M. Whitesides, *Langmuir*, **7**, 3167 (1991).
156. C. D. Bain, J. Evall and G. M. Whitesides, *J. Am. Chem. Soc.*, **111**, 7155 (1989).
157. D. A. Offord, C. M. John and J. H. Griffin, *Langmuir*, **10**, 761 (1994).
158. G. K. Rowe and S. E. Creager, *Langmuir*, **10**, 1186 (1994).
159. J. P. Folkers, P. E. Laibinis, G. M. Whitesides and J. Deutch, *J. Phys. Chem.*, **98**, 563 (1994).
160. R. F. Debono, G. D. Loucks, D. Dellamanna and U. J. Krull, *Can. J. Chem.*, **74**, 677 (1996).
161. P. E. Laibinis, R. G. Nuzzo and G. M. Whitesides, *J. Phys. Chem.*, **96**, 5097 (1992).
162. H. O. Finklea and D. D. Hanshew, *J. Am. Chem. Soc.*, **114**, 3173 (1992).
163. H. O. Finklea and D. D. Hanshew, *J. Electroanal. Chem.*, **347**, 327 (1993).
164. M. Mrksich, *Curr. Opin. Colloid Interface Sci.*, **2**, 83 (1997).
165. Z. L. He, S. Bhattacharyya, W. E. Cleland and C. L. Hussey, *J. Electroanal. Chem.*, **397**, 305 (1995).
166. C. E. D. Chidsey, C. R. Bertozzi, T. M. Putvinski and A. M. Mujsce, *J. Am. Chem. Soc.*, **112**, 4301 (1990).
167. N. Mohri, M. Inoue, Y. Arai and K. Yoshikawa, *Langmuir*, **11**, 1612 (1995).
168. D. M. Collard and M. A. Fox, *Langmuir*, **7**, 1192 (1991).
169. N. Nishida, M. Hara, H. Sasabe and W. Knoll, *Jpn. J. Appl. Phys. 1*, **36**, 2379 (1997).
170. S. W. Tamchang, H. A. Biebuyck, G. M. Whitesides, N. Jeon and R. G. Nuzzo, *Langmuir*, **11**, 4371 (1995).
171. J. R. Scott, L. S. Baker, W. R. Everett, C. L. Wilkins and I. Fritsch, *Anal. Chem.*, **69**, 2636 (1997).
172. K. Kajikawa, M. Hara, H. Sasabe and W. Knoll, *Jpn. J. Appl. Phys. 2*, **36**, L1116 (1997).
173. J. Li, K. S. Liang, N. Camillone, T. Y. B. Leung and G. Scoles, *J. Chem. Phys.*, **102**, 5012 (1995).
174. C.-J. Zhong, J. Zak and M. D. Porter, *J. Electroanal. Chem.*, **421**, 9 (1997).
175. P. Fenter, A. Eberhardt and P. Eisenberger, *Science*, **266**, 1216 (1994).
176. C. Zubragel, C. Deuper, F. Schneider, M. Neumann, M. Grunze, A. Schertel and C. Woll, *Chem. Phys. Lett.*, **238**, 308 (1995).

177. M. S. Yeganeh, S. M. Dougal, R. S. Polizzotti and P. Rabinowitz, *Thin Solid Films*, **270**, 226 (1995).
178. N. Nishida, M. Hara, H. Sasabe and W. Knoll, *Jpn. J. Appl. Phys. 2*, **35**, L799 (1996).
179. N. Nishida, M. Hara, H. Sasabe and W. Knoll, *Jpn. J. Appl. Phys. 1*, **35**, 5866 (1996).
180. M. S. Yeganeh, S. M. Dougal, R. S. Polizzotti and P. Rabinowitz, *Phys. Rev. Lett.*, **74**, 1811 (1995).
181. J. J. Gerdy and W. A. Goodard, *J. Am. Chem. Soc.*, **118**, 3233 (1996).
182. D. G. Castner, K. Hinds and D. W. Grainger, *Langmuir*, **12**, 5083 (1996).
183. G. E. Poirier and M. J. Tarlov, *Langmuir*, **10**, 2853 (1994).
184. J. P. Bucher, L. Santesson and K. Kern, *Langmuir*, **10**, 979 (1994).
185. C. Schönenberger, J. Jorritsma, J. A. M. Sondag-Huethorst and L. G. J. Fokkink, *J. Phys. Chem.*, **99**, 3259 (1995).
186. E. Delamarche, B. Michel, H. Kang and C. Gerber, *Langmuir*, **10**, 4103 (1994).
187. O. Cavalleri, A. Hirstein, J. P. Bucher and K. Kern, *Thin Solid Films*, **285**, 392 (1996).
188. H. J. Himmel, C. Woll, R. Gerlach, G. Polanski and H. G. Rubahn, *Langmuir*, **13**, 602 (1997).
189. H. Schönherr and G. J. Vancso, *Langmuir*, **13**, 3769 (1997).
190. R. G. Snyder, H. L. Strauss and C. A. Elliger, *J. Phys. Chem.*, **86**, 5145 (1982).
191. M. D. Porter, T. B. Bright, D. L. Allara and C. E. D. Chidsey, *J. Am. Chem. Soc.*, **109**, 3559 (1987).
192. G. Y. Liu, P. Fenter, C. E. D. Chidsey, D. F. Ogletree, P. Eisenberger and M. Salmeron, *J. Chem. Phys.*, **101**, 4301 (1994).
193. T. J. Lenk, V. M. Hallmark, C. L. Hoffmann, J. F. Rabolt, D. G. Castner, C. Erdelen and H. Ringsdorf, *Langmuir*, **10**, 4610 (1994).
194. C. A. Alves and M. D. Porter, *Langmuir*, **9**, 3507 (1993).
195. A.-A. Dhirani, R. W. Zehner, R. P. Hsung, P. Guyot-Sionnest and L. R. Sita, *J. Am. Chem. Soc.*, **118**, 3319 (1996).
196. G. Hahner, M. Kinzler, C. Thummler, C. Woll and M. Grunze, *J. Vac. Sci. Technol. A*, **10**, 2758 (1992).
197. M. G. Samant, C. A. Brown and J. G. Gordon, *Langmuir*, **7**, 437 (1991).
198. N. Camillone, C. E. D. Chidsey, G. Y. Liu and G. Scoles, *J. Chem. Phys.*, **98**, 3503 (1993).
199. R. G. Nuzzo, E. M. Korenic and L. H. Dubois, *J. Chem. Phys.*, **93**, 767 (1990).
200. P. Fenter, P. Eisenberger and K. S. Liang, *Phys. Rev. Lett.*, **70**, 2447 (1993).
201. P. Fenter, A. Eberhardt, K. S. Liang and P. Eisenberger, *J. Chem. Phys.*, **106**, 1600 (1997).
202. H. Sellers, A. Ulman, Y. Shnidman and J. E. Eilers, *J. Am. Chem. Soc.*, **115**, 9389 (1993).
203. L. H. Dubois, B. R. Zegarski and R. G. Nuzzo, *J. Electron Spectrosc. Relat. Phenom.*, **54**, 1143 (1990).
204. F. Bensebaa, T. H. Ellis, A. Badia and R. B. Lennox, *J. Vac. Sci. Technol. A*, **13**, 1331 (1995).
205. A. Badia, R. Back and R. B. Lennox, *Angew. Chem., Int. Ed. Engl.*, **33**, 2332 (1994).
206. C. Taut, A. J. Pertsin and M. Grunze, *Langmuir*, **12**, 3481 (1996).
207. J. Hautman and M. L. Klein, *J. Chem. Phys.*, **93**, 7483 (1990).
208. R. Bhatia and B. J. Garrison, *Langmuir*, **13**, 765 (1997).
209. A. Ulman, *Adv. Mater.*, **3**, 298 (1991).
210. M. R. Anderson, M. N. Evaniak and M. H. Zhang, *Langmuir*, **12**, 2327 (1996).
211. M. R. Anderson and M. Gatin, *Langmuir*, **10**, 1638 (1994).
212. D. F. Yang, H. Almaznai and M. Morin, *J. Phys. Chem. B*, **101**, 1158 (1997).
213. Y. T. Tao, C. C. Wu, J. Y. Eu and W. L. Lin, *Langmuir*, **13**, 4018 (1997).
214. S. D. Evans, K. E. Goppert-Berarducci, E. Urankar, L. J. Gerenser and A. Ulman, *Langmuir*, **7**, 2700 (1991).
215. A. Ulman, S. D. Evans and R. G. Snyder, *Thin Solid Films*, **210**, 806 (1992).
216. R. S. Clegg and J. E. Hutchison, *Langmuir*, **12**, 5239 (1996).
217. M. Motomatsu, W. Mizutani, H. Y. Nie and H. Tokumoto, *Thin Solid Films*, **282**, 548 (1996).
218. M. Jaschke, H. Schönherr, H. Wolf, H. J. Butt, E. Bamberg, M. K. Besocke and H. Ringsdorf, *J. Phys. Chem.*, **100**, 2290 (1996).
219. R. Wang, T. Iyoda, L. Jiang, K. Hashimoto and A. Fujishima, *Chem. Lett.*, 1005 (1996).
220. W. B. Caldwell, D. J. Campbell, K. M. Chen, B. R. Herr, C. A. Mirkin, A. Malik, M. K. Durbin, P. Dutta and K. G. Huang, *J. Am. Chem. Soc.*, **117**, 6071 (1995).
221. H. Wolf, H. Ringsdorf, E. Delamarche, T. Takami, H. Kang, B. Michel, C. Gerber, M. Jaschke, H. J. Butt and E. Bamberg, *J. Phys. Chem.*, **99**, 7102 (1995).

222. E. Delamarche and B. Michel, *Thin Solid Films*, **273**, 54 (1996).
223. S. C. Chang, I. Chao and Y. T. Tao, *J. Am. Chem. Soc.*, **116**, 6792 (1994).
224. A. Wesch, O. Dannenberger, C. Woll, J. J. Wolff and M. Buck, *Langmuir*, **12**, 5330 (1996).
225. H. Schönherr, G. J. Vancso, B.-H. Huisman, F. C. J. M. van Veggel and D. N. Reinhoudt, *Langmuir*, **13**, 1567 (1997).
226. H. Schönherr, F. J. B. Kremer, S. Kumar, J. A. Rego, H. Wolf, H. Ringsdorf, M. Jaschke, H. J. Butt and E. Bamberg, *J. Am. Chem. Soc.*, **118**, 13051 (1996).
227. G. Nelles, M. Weisser, R. Back, P. Wohlfart, G. Wenz and S. Mittlerneher, *J. Am. Chem. Soc.*, **118**, 5039 (1996).
228. J. M. Tour, L. Jones, D. L. Pearson, J. J. S. Lamba, T. P. Burgin, G. M. Whitesides, D. L. Allara, A. N. Parikh and S. V. Atre, *J. Am. Chem. Soc.*, **117**, 9529 (1995).
229. Z. Zhang, T. L. Beck, J. T. Young and F. J. Boerio, *Langmuir*, **12**, 1227 (1996).
230. J. T. Young, F. J. Boerio, Z. Zhang and T. L. Beck, *Langmuir*, **12**, 1219 (1996).
231. Y. J. Lee, T. C. Jeon, W. K. Paik and K. Kim, *Langmuir*, **12**, 5830 (1996).
232. K. Bandyopadhyay, M. Sastry, V. Paul and K. Vijayamohanan, *Langmuir*, **13**, 866 (1997).
233. K. Doblhofer, J. Figura and J. H. Fuhrhop, *Langmuir*, **8**, 1811 (1992).
234. C. D. Bain and G. M. Whitesides, *J. Am. Chem. Soc.*, **110**, 5897 (1988).
235. P. E. Laibinis, C. D. Bain, R. G. Nuzzo and G. M. Whitesides, *J. Phys. Chem.*, **99**, 7663 (1995).
236. S. D. Evans, R. Sharma and A. Ulman, *Langmuir*, **7**, 156 (1991).
237. Y. Sato, S. Ye, T. Haba and K. Uosaki, *Langmuir*, **12**, 2726 (1996).
238. S. Ye, Y. Sato and K. Uosaki, *Langmuir*, **13**, 3157 (1997).
239. G. E. Poirier, E. D. Pylant and J. M. White, *J. Chem. Phys.*, **105**, 2089 (1996).
240. M. Sprik, E. Delamarche, B. Michel, U. Rothlisberger, M. L. Klein, H. Wolf and H. Ringsdorf, *Langmuir*, **10**, 4116 (1994).
241. T. Yuba, S. Yokoyama, M. Kakimoto and K. Y. Imai, *Adv. Mater.*, **6**, 888 (1994).
242. H. M. Wu, S. J. Xiao, Z. H. Tai and Y. Wei, *Phys. Lett. A*, **199**, 119 (1995).
243. A. Angelova, M. van der Auweraer, R. Ionov, D. Vollhardt and F. C. Deschryver, *Langmuir*, **11**, 3167 (1995).
244. K. Motesharei and D. C. Myles, *J. Am. Chem. Soc.*, **116**, 7413 (1994).
245. C. D. Bain and G. M. Whitesides, *Science*, **240**, 62 (1988).
246. L. Bertilsson and B. Liedberg, *Langmuir*, **9**, 141 (1993).
247. J. P. Folkers, P. E. Laibinis and G. M. Whitesides, *Langmuir*, **8**, 1330 (1992).
248. S. J. Stranick, A. N. Parikh, Y. T. Tao, D. L. Allara and P. S. Weiss, *J. Phys. Chem.*, **98**, 7636 (1994).
249. W. A. Hayes, H. Kim, X. H. Yue, S. S. Perry and C. Shannon, *Langmuir*, **13**, 2511 (1997).
250. H. Schönherr, H. Ringsdorf, M. Jaschke, H. J. Butt, E. Bamberg, H. Allinson and S. D. Evans, *Langmuir*, **12**, 3898 (1996).
251. S. J. Stranick, S. V. Atre, A. N. Parikh, M. C. Wood, D. L. Allara, N. Winograd and P. S. Weiss, *Nanotechnology*, **7**, 438 (1996).
252. V. Chechik and C. J. M. Stirling, unpublished results.
253. B.-H. Huisman, E. U. T. van Velzen, F. C. J. M. van Veggel, J. F. J. Engbersen and D. N. Reinhoudt, *Tetrahedron Lett.*, **36**, 3273 (1995).
254. K. D. Schierbaum, T. Weiss, E. U. T. van Velzen, J. F. J. Engbersen, D. N. Reinhoudt and W. Gopel, *Science*, **265**, 1413 (1994).
255. A. Ihs, K. Uvdal and B. Liedberg, *Langmuir*, **9**, 733 (1993).
256. T. Y. Koh, *Spectrochim. Acta A*, **51**, 2177 (1995).
257. Y. T. Tao, S. Pandiaraju, W. L. Lin and L. J. Chen, *Langmuir*, **14**, 145 (1998).
258. W. H. Han, S. M. Li, S. M. Lindsay, D. Gust, T. A. Moore and A. L. Moore, *Langmuir*, **12**, 5742 (1996).
259. M. H. Dishner, J. C. Hemminger and F. J. Feher, *Langmuir*, **12**, 6176 (1996).
260. A. J. Arduengo, J. R. Moran, J. Rodriguez-Parada and M. D. Ward, *J. Am. Chem. Soc.*, **112**, 6153 (1990).
261. E. Bunge, R. J. Nichols, B. Roelfs, H. Meyer and H. Baumgartel, *Langmuir*, **12**, 3060 (1996).
262. S. N. Port, S. L. Horswell, R. Raval and D. J. Schiffrin, *Langmuir*, **12**, 5934 (1996).
263. R. L. Garrell, J. E. Chadwick, D. L. Severance, N. A. McDonald and D. C. Myles, *J. Am. Chem. Soc.*, **117**, 11563 (1995).
264. J. E. Chadwick, D. C. Myles and R. L. Garrell, *J. Am. Chem. Soc.*, **115**, 10364 (1993).
265. M. G. Samant, C. A. Brown and J. G. Gordon, *Langmuir*, **8**, 1615 (1992).

266. M. H. Dishner, J. C. Hemminger and F. J. Feher, *Langmuir*, **13**, 4788 (1997).
267. U. B. Steiner, P. Neuenschwander, W. R. Caseri, U. W. Suter and F. Stucki, *Langmuir*, **8**, 90 (1992).
268. C. J. Xu, L. Sun, L. J. Kepley, R. M. Crooks and A. J. Ricco, *Anal. Chem.*, **65**, 2102 (1993).
269. D. V. Leff, L. Brandt and J. R. Heath, *Langmuir*, **12**, 4723 (1996).
270. H. Tokuhisa, M. Q. Zhao, L. A. Baker, V. T. Phan, D. L. Dermody, M. E. Garcia, R. F. Peez, R. M. Crooks and T. M. Mayer, *J. Am. Chem. Soc.*, **120**, 4492 (1998).
271. A. C. Chen, S. G. Sun, D. F. Yang, B. Pettinger and J. Lipkowski, *Can. J. Chem.* **74**, 2321 (1996).
272. D. F. Yang, D. Bizzotto, J. Lipkowski, B. Pettinger and S. Mirwald, *J. Phys. Chem.*, **98**, 7083 (1994).
273. F. Cunha, N. J. Tao, X. W. Wang, Q. Jin, B. Duong and J. Dagnese, *Langmuir*, **12**, 6410 (1996).
274. U. B. Steiner, W. R. Caseri and U. W. Suter, *Langmuir*, **8**, 2771 (1992).
275. J. J. Chance and W. C. Purdy, *Langmuir*, **13**, 4487 (1997).
276. U. B. Steiner, W. R. Caseri, U. W. Suter, M. Rehahn and L. Schmitz, *Langmuir*, **9**, 3245 (1993).
277. U. B. Steiner, W. R. Caseri, U. W. Suter, M. Rehahn and I. U. Rau, *Langmuir*, **10**, 1164 (1994).
278. U. B. Steiner, M. Rehahn, W. R. Caseri and U. W. Suter, *Langmuir*, **11**, 3013 (1995).
279. K. Motesharei and M. R. Ghadiri, *J. Am. Chem. Soc.*, **119**, 11306 (1997).
280. Y. J. Xiao and J. P. Markwell, *Langmuir*, **13**, 7068 (1997).
281. A. B. Horn, D. A. Russell, L. J. Shorthouse and T. R. E. Simpson, *J. Chem. Soc., Faraday Trans.*, **92**, 4759 (1996).
282. M. Ohtani, T. Sunagawa, S. Kuwabata and H. Yoneyama, *J. Electroanal. Chem.*, **429**, 75 (1997).
283. N. Camillone, P. Eisenberger, T. Y. B. Leung, P. Schwartz, G. Scoles, G. E. Poirier and M. J. Tarlov, *J. Chem. Phys.*, **101**, 11031 (1994).
284. Y. Z. Li, J. Y. Huang, R. T. McIver and J. C. Hemminger, *J. Am. Chem. Soc.*, **114**, 2428 (1992).
285. J. Y. Huang and J. C. Hemminger, *J. Am. Chem. Soc.*, **115**, 3342 (1993).
286. M. J. Tarlov, D. R. F. Burgess and G. Gillen, *J. Am. Chem. Soc.*, **115**, 5305 (1993).
287. M. J. Tarlov and J. G. Newman, *Langmuir*, **8**, 1398 (1992).
288. J. Y. Huang, D. A. Dahlgren and J. C. Hemminger, *Langmuir*, **10**, 626 (1994).
289. M. Lewis, M. Tarlov and K. Carron, *J. Am. Chem. Soc.*, **117**, 9574 (1995).
290. D. A. Hutt and G. J. Leggett, *J. Phys. Chem.*, **100**, 6657 (1996).
291. M. M. Walczak, D. D. Popenoe, R. S. Deinhammer, B. D. Lamp, C. K. Chung and M. D. Porter, *Langmuir*, **7**, 2687 (1991).
292. C. A. Widrig, C. Chung and M. D. Porter, *J. Electroanal. Chem.*, **310**, 335 (1991).
293. N. L. Abbott, C. B. Gorman and G. M. Whitesides, *Langmuir*, **11**, 16 (1995).
294. D. F. Yang, C. P. Wilde and M. Morin, *Langmuir*, **13**, 243 (1997).
295. D. F. Yang, C. P. Wilde and M. Morin, *Langmuir*, **12**, 6570 (1996).
296. S. Ye, A. Yashiro, Y. Sato and K. Uosaki, *J. Chem. Soc., Faraday Trans.*, **92**, 3813 (1996).
297. W. R. Everett, T. L. Welch, L. Reed and I. Fritschfaules, *Anal. Chem.*, **67**, 292 (1995).
298. W. R. Everett and I. Fritschfaules, *Anal. Chim. Acta*, **307**, 253 (1995).
299. K. Takehara, S. Yamada and Y. Ide, *J. Electroanal. Chem.*, **333**, 339 (1992).
300. A. Bard, K. K. Berggren, J. L. Wilbur, J. D. Gillaspy, S. L. Rolston, J. J. McClelland, W. D. Phillips, M. Prentiss and G. M. Whitesides, *J. Vac. Sci. Technol. B*. **15**, 1805 (1997).
301. D. E. Riederer, R. Chatterjee, S. W. Rosencrance, Z. Postawa, T. D. Dunbar, D. L. Allara and N. Winograd, *J. Am. Chem. Soc.*, **119**, 8089 (1997).
302. J. M. Sondag-Huethorst, H. R. J. van Helleputte and L. G. J. Fokkink, *Appl. Phys. Lett.*, **64**, 285 (1994).
303. M. Wirde, U. Gelius, T. Dunbar and D. L. Allara, *Nucl. Instrum. Methods Phys. Res. B*, **131**, 245 (1997).
304. B. Jager, H. Schurmann, H. U. Muller, H. J. Himmel, M. Neumann, M. Grunze and C. Woll, *Z. Phys. Chem.*, **202**, 263 (1997).
305. H. L. Zhang, H. Xia, H. L. Li and Z. F. Liu, *Chem. Lett.*, 721 (1997).
306. T. Kim, K. C. Chan and R. M. Crooks, *J. Am. Chem. Soc.*, **119**, 189 (1997).
307. T. R. Lee, R. I. Carey, H. A. Biebuyck and G. M. Whitesides, *Langmuir*, **10**, 741 (1994).
308. C. D. Bain and G. M. Whitesides, *Langmuir*, **5**, 1370 (1989).
309. J. Wang, L. M. Frostman and M. D. Ward, *J. Phys. Chem.*, **96**, 5224 (1992).
310. S. E. Creager and J. Clarke, *Langmuir*, **10**, 3675 (1994).
311. D. V. Vezenov, A. Noy, L. F. Rozsnyai and C. M. Lieber, *J. Am. Chem. Soc.*, **119**, 2006 (1997).

312. K. Hu and A. J. Bard, *Langmuir*, **13**, 5114 (1997).
313. L. A. Godinez, R. Castro and A. E. Kaifer, *Langmuir*, **12**, 5087 (1996).
314. K. S. Mayya, V. Patil and M. Sastry, *Langmuir*, **13**, 3944 (1997).
315. S. S. Cheng, D. A. Scherson and C. N. Sukenik, *Langmuir*, **11**, 1190 (1995).
316. R. I. Carey, J. P. Folkers and G. M. Whitesides, *Langmuir*, **10**, 2228 (1994).
317. C. S. Weisbecker, M. V. Merritt and G. M. Whitesides, *Langmuir*, **12**, 3763 (1996).
318. M. A. Bryant and R. M. Crooks, *Langmuir*, **9**, 385 (1993).
319. H. van Ryswyk, E. D. Turtle, R. Watson-Clark, T. A. Tanzer, T. K. Herman, P. Y. Chong, P. J. Waller, A. L. Taurog and C. E. Wagner, *Langmuir*, **12**, 6143 (1996).
320. B. Nitzan and S. Margel, *Polym. Sci. A*, **35**, 171 (1997).
321. W. R. Fawcett, M. Fedurco and Z. Kovacova, *Langmuir*, **10**, 2403 (1994).
322. G. M. Whitesides, H. A. Biebuyck, J. P. Folkers and K. L. Prime, *J. Adhes. Sci. Technol.*, **5**, 57 (1991).
323. B. V. Zhmud and A. A. Golub, *J. Colloid Interface Sci.*, **167**, 186 (1994).
324. Y. W. Lee, J. Reedmundell, C. N. Sukenik and J. E. Zull, *Langmuir*, **9**, 3009 (1993).
325. G. E. Fryxell, P. C. Rieke, L. L. Wood, M. H. Engelhard, R. E. Williford, G. L. Graff, A. A. Campbell, R. J. Wiacek, L. Lee and A. Halverson, *Langmuir*, **12**, 5064 (1996).
326. N. Balachander and C. N. Sukenik, *Langmuir*, **6**, 1621 (1990).
327. S. R. Wasserman, Y. T. Tao and G. M. Whitesides, *Langmuir*, **5**, 1074 (1989).
328. S. Marx-Tibbon, I. Bendov and I. Willner, *J. Am. Chem. Soc.*, **118**, 4717 (1996).
329. P. A. Buining, B. M. Humbel, A. P. Philipse and A. J. Verkleij, *Langmuir*, **13**, 3921 (1997).
330. V. Chechik and C. J. M. Stirling, *Langmuir*, **13**, 6354 (1997).
331. L. Sun, R. C. Thomas, R. M. Crooks and A. J. Ricco, *J. Am. Chem. Soc.*, **113**, 8550 (1991).
332. R. V. Duevel and R. M. Corn, *Anal. Chem.*, **64**, 337 (1992).
333. D. A. Hutt and G. J. Leggett, *Langmuir*, **13**, 2740 (1997).
334. H. J. Himmel, K. Weiss, B. Jager, O. Dannenberger, M. Grunze and C. Woll, *Langmuir*, **13**, 4943 (1997).
335. H. Keller, W. Schrepp and H. Fuchs, *Thin Solid Films*, **210**, 799 (1992).
336. P. Wagner, M. Hegner, H. J. Guntherodt and G. Semenza, *Langmuir*, **11**, 3867 (1995).
337. D. D. Schlereth and H. L. Schmidt, *J. Electroanal. Chem.*, **380**, 117 (1995).
338. D. D. Schlereth, E. Katz and H. L. Schmidt, *Electroanalysis*, **7**, 46 (1995).
339. L. Yan, C. Marzolin, A. Terfort and G. M. Whitesides, *Langmuir*, **13**, 6704 (1997).
340. W. R. Thompson, M. Cai, M. K. Ho and J. E. Pemberton, *Langmuir*, **13**, 2291 (1997).
341. M. A. Fox and M. D. Wooten, *Langmuir*, **13**, 7099 (1997).
342. W. J. Li, V. Lynch, H. Thompson and M. A. Fox, *J. Am. Chem. Soc.*, **119**, 7211 (1997).
343. R. J. Willicut and R. L. McCarley, *Adv. Mater.*, **7**, 759 (1995).
344. R. J. Willicut and R. L. McCarley, *J. Am. Chem. Soc.*, **116**, 10823 (1994).
345. R. J. Willicut and R. L. McCarley, *Langmuir*, **11**, 296 (1995).
346. N. Higashi, T. Mori and M. Niwa, *J. Chem. Soc., Chem. Commun.*, 225 (1990).
347. M. Niwa, T. Mori and N. Nigashi, *J. Mater. Chem.*, **2**, 245 (1992).
348. T. Kim, Q. Ye, L. Sun, K. C. Chan and R. M. Crooks, *Langmuir*, **12**, 6065 (1996).
349. M. O. Wolf and M. A. Fox, *J. Am. Chem. Soc.*, **117**, 1845 (1995).
350. N. Matsuda, T. Sawaguchi, M. Osawa and I. Uchida, *Chem. Lett.*, 145 (1995).
351. E. W. Wollman, C. D. Frisbie and M. S. Wrighton, *Langmuir*, **9**, 1517 (1993).
352. P. Wagner, M. Hegner, P. Kernen, F. Zaugg and G. Semenza, *Biophys. J.*, **70**, 2052 (1996).
353. E. Delamarche, G. Sundarababu, H. Biebuyck, B. Michel, C. Gerber, H. Sigrist, H. Wolf, H. Ringsdorf, N. Xanthopoulos and H. J. Mathieu, *Langmuir*, **12**, 1997 (1996).
354. B. L. Frey and R. M. Corn, *Anal. Chem.*, **68**, 3187 (1996).
355. C. M. Duan and M. E. Meyerhoff, *Mikrochim. Acta*, **117**, 195 (1995).
356. M. Collinson, E. F. Bowden and M. J. Tarlov, *Langmuir*, **8**, 1247 (1992).
357. M. Wells and R. M. Crooks, *J. Am. Chem. Soc.*, **118**, 3988 (1996).
358. Y. F. Zhou, M. L. Bruening, D. E. Bergbreiter, R. M. Crooks and M. Wells, *J. Am. Chem. Soc.*, **118**, 3773 (1996).
359. T. S. Kim, R. M. Crooks, M. Tsen and L. Sun, *J. Am. Chem. Soc.*, **117**, 3963 (1995).
360. S. D. Evans, A. Ulman, K. E. Goppert-Berarducci and L. J. Gerenser, *J. Am. Chem. Soc.*, **113**, 5866 (1991).
361. T. L. Freeman, S. D. Evans and A. Ulman, *Langmuir*, **11**, 4411 (1995).
362. K. C. Grabar, R. G. Freeman, M. B. Hommer and M. J. Natan, *Anal. Chem.*, **67**, 735 (1995).

363. R. P. Andres, T. Bein, M. Dorogi, S. Feng, J. I. Henderson, C. P. Kubiak, W. Mahoney, R. G. Osifchin and R. Reifenberger, *Science*, **272**, 1323 (1996).
364. J. I. Henderson, S. Feng, G. M. Ferrence, T. Bein and C. P. Kubiak, *Inorg. Chim. Acta*, **242**, 115 (1996).
365. C. M. Yip and M. D. Ward, *Langmuir*, **10**, 549 (1994).
366. P. Krysinski and M. Brzostowska-Smolska, *J. Electroanal. Chem.*, **424**, 61 (1997).
367. C. Miller and M. Gratzel, *J. Phys. Chem.*, **95**, 5225 (1991).
368. A. M. Becka and C. J. Miller, *J. Phys. Chem.*, **97**, 6233 (1993).
369. A. M. Becka and C. J. Miller, *J. Phys. Chem.*, **96**, 2657 (1992).
370. S. E. Creager and G. K. Rowe, *J. Electroanal. Chem.*, **420**, 291 (1997).
371. R. Andreu, J. J. Calvente, W. R. Fawcett and M. Molero, *J. Phys. Chem. B*, **101**, 2884 (1997).
372. S. E. Creager and G. K. Rowe, *Langmuir*, **9**, 2330 (1993).
373. T. Kondo, M. Takechi, Y. Sato and K. Uosaki, *J. Electroanal. Chem.*, **381**, 203 (1995).
374. M. T. Carter, G. K. Rowe, J. N. Richardson, L. M. Tender, R. H. Terrill and R. W. Murray, *J. Am. Chem. Soc.*, **117**, 2896 (1995).
375. H. O. Finklea, L. Liu, M. S. Ravenscroft and S. Punturi, *J. Phys. Chem.*, **100**, 18852 (1996).
376. R. L. Bretz and H. D. Abruna, *J. Electroanal. Chem.*, **408**, 199 (1996).
377. H. O. Finklea, J. Fedyk and J. Schwab, *ACS Symp. Ser.*, **378**, 431 (1988).
378. J. Zak, H. P. Yuan, M. Ho, L. K. Woo and M. D. Porter, *Langmuir*, **9**, 2772 (1993).
379. J. E. Hutchison, T. A. Postlethwaite and R. W. Murray, *Langmuir*, **9**, 3277 (1993).
380. J. M. Cooper, K. R. Greenough and C. J. McNeil, *J. Electroanal. Chem.*, **347**, 267 (1993).
381. M. J. Tarlov and E. F. Bowden, *J. Am. Chem. Soc.*, **113**, 1847 (1991).
382. S. Song, R. A. Clark, E. F. Bowden and M. J. Tarlov, *J. Phys. Chem.*, **97**, 6564 (1993).
383. A. Szucs, G. D. Hitchens and J. O. M. Bockris, *Electrochim. Acta*, **37**, 403 (1992).
384. M. P. Soriaga and A. T. Hubbard, *J. Am. Chem. Soc.*, **104**, 3937 (1982).
385. M. P. Soriaga and A. T. Hubbard, *J. Am. Chem. Soc.*, **104**, 2742 (1982).
386. M. P. Soriaga and A. T. Hubbard, *J. Electroanal. Chem. Interfacial Electrochem.*, **159**, 101 (1983).
387. Y. Sato, M. Fujita, F. Mizutani and K. Uosaki, *J. Electroanal. Chem.*, **409**, 145 (1996).
388. J. J. Hickman, D. Ofer, P. E. Laibinis, G. M. Whitesides and M. S. Wrighton, *Science*, **252**, 688 (1991).
389. T. Kondo, T. Ito, S. Nomura and K. Uosaki, *Thin Solid Films*, **285**, 652 (1996).
390. H. Z. Yu, Y. Q. Wang, S. M. Cai and Z. F. Liu, *Chem. Lett.*, 903 (1996).
391. Y. Q. Wang, H. Z. Yu, J. Z. Cheng, J. W. Zhao, S. M. Cai and Z. F. Liu, *Langmuir*, **12**, 5466 (1996).
392. D. J. Campbell, B. R. Herr, J. C. Hulteen, R. P. Vanduyne and C. A. Mirkin, *J. Am. Chem. Soc.*, **118**, 10211 (1996).
393. W. B. Caldwell, K. Chen, C. A. Mirkin and S. J. Babinec, *Langmuir*, **9**, 1945 (1993).
394. W. S. V. Kwan, L. Atanasoska and L. L. Miller, *Langmuir*, **7**, 1419 (1991).
395. V. W. S. Kwan, V. Cammarata, L. L. Miller, M. G. Hill and K. R. Mann, *Langmuir*, **8**, 3003 (1992).
396. D. Mandler and I. Turyan, *Electroanalysis*, **8**, 207 (1996).
397. M. H. Liu, H. Nakahara, Y. Shibasaki and K. Fukuda, *Chem. Lett.*, 967 (1993).
398. R. Ahuja, P. L. Caruso, D. Mobius, W. Paulus, H. Ringsdorf and G. Wildburg, *Angew. Chem., Int. Ed. Engl.*, **32**, 1033 (1993).
399. K. Töllner, R. Popovitz-Biro, M. Lahav and D. Milstein, *Science*, **278**, 2100 (1997).
400. P. Neogi, S. Neogi, and C. J. M. Stirling., *J. Chem. Soc., Chem. Commun.*, 1134 (1993).
401. V. Chechik and C. J. M. Stirling, in preparation.
402. V. Chechik and C. J. M. Stirling, *Langmuir*, **14**, 99 (1998).
403. J. Ahmad and K. B. Astin, *Langmuir*, **6**, 1797 (1990).
404. L. Sun, R. M. Crooks and A. J. Ricco, *Langmuir*, **9**, 1775 (1993).
405. H. C. Yang, D. L. Dermody, C. J. Xu, A. J. Ricco and R. M. Crooks, *Langmuir*, **12**, 726 (1996).
406. M. Wells, D. L. Dermody, H. C. Yang, T. Kim, R. M. Crooks and A. J. Ricco, *Langmuir*, **12**, 1989 (1996).
407. R. M. Crooks, O. Chailapakul, C. B. Ross, L. Sun and J. K. Schoer, *ACS Symp. Ser.*, **561**, 104 (1994).
408. L. Sun, L. J. Kepley and R. M. Crooks, *Langmuir*, **8**, 2101 (1992).
409. D. S. Karpovich and G. J. Blanchard, *Langmuir*, **13**, 4031 (1997).

410. J. A. Roush, D. L. Thacker and M. R. Anderson, *Langmuir*, **10**, 1642 (1994).
411. F. Davis and C. J. M. Stirling, *J. Am. Chem. Soc.*, **117**, 10385 (1995).
412. R. C. Thomas, J. E. Houston, R. M. Crooks, T. Kim and T. A. Michalske, *J. Am. Chem. Soc.*, **117**, 3830 (1995).
413. S. K. Sinniah, A. B. Steel, C. J. Miller and J. E. Reuttrobey, *J. Am. Chem. Soc.*, **118**, 8925 (1996).
414. I. Engquist, M. Lestelius and B. Liedberg, *J. Phys. Chem.*, **99**, 14198 (1995).
415. I. Engquist, I. Lundstrom, B. Liedberg, A. N. Parikh and D. L. Allara, *J. Chem. Phys.*, **106**, 3038 (1997).
416. I. Engquist and B. Liedberg, *J. Phys. Chem.*, **100**, 20089 (1996).
417. G. C. Herdt, A. W. Czanderna and D. E. King, *Surf. Sci.*, **355**, L371 (1996).
418. T. A. Jones, G. P. Perez, B. J. Johnson and R. M. Crooks, *Langmuir*, **11**, 1318 (1995).
419. L. Sun, B. Johnson, T. Wade and R. M. Crooks, *J. Phys. Chem.*, **94**, 8869 (1990).
420. M. Sastry, V. Patil and K. S. Mayya, *J. Phys. Chem. B*, **101**, 1167 (1997).
421. J. Li, K. S. Liang, G. Scoles and A. Ulman, *Langmuir*, **11**, 4418 (1995).
422. D. A. Lowy and H. O. Finklea, *Electrochim. Acta*, **42**, 1325 (1997).
423. T. Stora, R. Hovius, Z. Dienes, M. Pachoud and H. Vogel, *Langmuir*, **13**, 5211 (1997).
424. I. Rubinstein, S. Steinberg, Y. Tor, A. Shanzer and J. Sagiv, *Nature*, **332**, 426 (1988).
425. S. Steinberg and I. Rubinstein, *Langmuir*, **8**, 1183 (1992).
426. S. Steinberg, Y. Tor, E. Sabatani and I. Rubinstein, *J. Am. Chem. Soc.*, **113**, 5176 (1991).
427. I. Turyan and D. Mandler, *Anal. Chem.*, **69**, 894 (1997).
428. G. B. Sigal, M. Mrksich and G. M. Whitesides, *Langmuir*, **13**, 2749 (1997).
429. K. Hu and A. J. Bard, *Langmuir*, **13**, 5418 (1997).
430. L. M. Williams, S. D. Evans, T. M. Flynn, A. Marsh, P. F. Knowles, R. J. Bushby and N. Boden, *Langmuir*, **13**, 751 (1997).
431. O. Pierrat, N. Lechat, C. Bourdillon and J. M. Laval, *Langmuir*, **13**, 4112 (1997).
432. K. L. Prime and G. M. Whitesides, *Science*, **252**, 1164 (1991).
433. V. Silin, H. Weetall and D. J. Vanderah, *J. Colloid Interface Sci.*, **185**, 94 (1997).
434. L. Deng, M. Mrksich and G. M. Whitesides, *J. Am. Chem. Soc.*, **118**, 5136 (1996).
435. A. E. Kaifer, *Isr. J. Chem.*, **36**, 389 (1996).
436. M. Mrksich and G. M. Whitesides, *Annu. Rev. Biophys. Biomol. Struct.*, **25**, 55 (1996).
437. T. Weiss, K. D. Schierbaum, U. T. van Velzen, D. N. Reinhoudt and W. Gopel, *Sensors Actuators B*, **26**, 203 (1995).
438. J. Rickert, T. Weiss and W. Gopel, *Sensors Actuators B*, **31**, 45 (1996).
439. J. W. Grate, S. J. Patrash, M. H. Abraham and C. M. Du, *Anal. Chem.*, **68**, 913 (1996).
440. H. Adams, F. Davis and C. J. M. Stirling, *J. Chem. Soc., Chem. Commun.*, 2527 (1994).
441. D. L. Dermody, R. M. Crooks and T. Kim, *J. Am. Chem. Soc.*, **118**, 11912 (1996).
442. L. T. Zhang, L. A. Godinez, T. B. Lu, G. W. Gokel and A. E. Kaifer, *Angew. Chem., Int. Ed. Engl.*, **34**, 235 (1995).
443. B.-H. Huisman, D. M. Rudkevich, F. C. J. M. van Veggel and D. N. Reinhoudt, *J. Am. Chem. Soc.*, **118**, 3523 (1996).
444. M. T. Rojas, R. Koniger, J. F. Stoddart and A. E. Kaifer, *J. Am. Chem. Soc.*, **117**, 336 (1995).
445. C. Henke, C. Steinem, A. Janshoff, G. Steffan, H. Luftmann, M. Sieber and H. J. Galla, *Anal. Chem.*, **68**, 3158 (1996).
446. M. Lahav, K. T. Ranjit, E. Katz and I. Willner, *Chem. Commun.*, 259 (1997).
447. P. A. He, J. N. Ye, Y. H. Fang, I. Suzuki and T. Osa, *Anal. Chim. Acta*, **337**, 217 (1997).
448. P. G. He, Y. N. Ye, Y. Z. Fang, I. Suzuki and T. Osa, *Electroanalysis*, **9**, 68 (1997).
449. J. C. Yan and S. J. Dong, *Langmuir*, **13**, 3251 (1997).
450. J. C. Yan, S. J. Dong, J. H. Li and W. Q. Chen, *J. Electrochem. Soc.*, **144**, 3858 (1997).
451. J. C. Yan and S. J. Dong, *Electroanalysis*, **9**, 1219 (1997).
452. N. Nakashima, Y. Miyata and M. Tominaga, *Chem. Lett.*, 731 (1996).
453. T. R. E. Simpson, D. A. Russell, I. Chambrier, M. J. Cook, A. B. Horn and S. C. Thorpe, *Sensors Actuators B*, **29**, 353 (1995).
454. T. R. E. Simpson, M. J. Cook, M. C. Petty, S. C. Thorpe and D. A. Russell, *Analyst*, **121**, 1501 (1996).
455. T. R. E. Simpson, D. J. Revell, M. J. Cook and D. A. Russell, *Langmuir*, **13**, 460 (1997).
456. J. H. Fuhrhop, T. Bedurke, M. Gnade, J. Schneider and K. Doblhofer, *Langmuir*, **13**, 455 (1997).
457. M. T. Rojas and A. E. Kaifer, *J. Am. Chem. Soc.*, **117**, 5883 (1995).

458. F. Arias, L. A. Godinez, S. R. Wilson, A. E. Kaifer and L. Echegoyen, *J. Am. Chem, Soc.*, **118**, 6086 (1996).
459. K. Matsuura, Y. Ebara and Y. Okahata, *Langmuir*, **13**, 814 (1997).
460. J. Madoz, B. A. Kuznetzov, F. J. Medrano, J. L. Garcia and V. M. Fernandez, *J. Am. Chem. Soc.*, **119**, 1043 (1997).
461. M. Mrksich, J. R. Grunwell and G. M. Whitesides, *J. Am. Chem. Soc.*, **117**, 12009 (1995).
462. G. B. Sigal, C. Bamdad, A. Barberis, J. Strominger and G. M. Whitesides, *Anal. Chem.*, **68**, 490 (1996).
463. L. Häussling, H. Ringsdorf, F. J. Schmitt and W. Knoll, *Langmuir*, **7**, 1837 (1991).
464. J. Spinke, M. Liley, F. J. Schmitt, H. J. Guder, L. Angermaier and W. Knoll, *J. Chem. Phys.*, **99**, 7012 (1993).
465. N. Higashi, T. Inoue and M. Niwa, *Chem. Commun.*, 1507 (1997).
466. F. Caruso, E. Rodda, D. N. Furlong and V. Haring, *Sensors Actuators B*, **41**, 189 (1997).
467. T. M. Herne and M. J. Tarlov, *J. Am. Chem. Soc.*, **119**, 8916 (1997).
468. F. Davis, P. Neogi and C. J. M. Stirling, *J. Chem. Soc., Chem. Commun.*, 1199 (1994).
469. J. Laycock and C. J. M. Stirling, unpublished results.
470. Y. Maeda, T. Fukuda, H. Yamamoto and H. Kitano, *Langmuir*, **13**, 4187 (1997).
471. H. Yamamoto, Y. Maeda and H. Kitano, *J. Phys. Chem. B*, **101**, 6855 (1997).
472. G. L. Tao, E. Katz and I. Willner, *Chem. Commun.*, 2073 (1997).
473. P. L. Rose, N. G. Harvey and E. M. Arnett, *Adv. Phys. Org. Chem.*, **28**, 45 (1993).
474. M. J. Hostetler and R. W. Murray, *Curr. Opin. Colloid Interface Sci.*, **2**, 42 (1997).
475. G. Schon and U. Simon, *Colloid Polym. Sci.*, **273**, 202 (1995).
476. G. Schon and U. Simon, *Colloid Polym. Sci.*, **273**, 101 (1995).
477. E. Cerrada, E. J. Fernandez, P. G. Jones, A. Laguna, M. Laguna and R. Terroba, *Organometallics*, **14**, 5537 (1995).
478. D. B. Dell'Amico, F. Calderazzo, N. Pasqualetti, R. Hübener, C. Maichle-Mössmer and J. Strähle, *J. Chem. Soc., Dalton Trans.*, 3917 (1995).
479. M. Giersig and P. Mulvaney, *Langmuir*, **9**, 3408 (1993).
480. M. Brust, M. Walker, D. Bethell, D. J. Schiffrin and R. Whyman, *J. Chem. Soc., Chem. Commun.*, 801 (1994).
481. D. V. Leff, P. C. Ohara, J. R. Health and W. M. Gelbart, *J. Phys. Chem.*, **99**, 7036 (1995).
482. M. J. Hostetler, J. E. Wingate, C.-J. Zhong, J. E. Harris, R. W. Vachet, M. R. Clark, J. D. Londono, S. J. Green, J. J. Stokes, G. D. Wignall, G. L. Glish, M. D. Porter, N. D. Evans and R. W. Murray, *Langmuir*, **14**, 17 (1998).
483. M. Brust, J. Fink, D. Bethell, D. J. Schiffrin and C. Kiely, *J. Chem. Soc., Chem. Commun.*, 1655 (1995).
484. K. V. Sarathy, G. U. Kulkarni and C. N. R. Rao, *Chem. Commun.*, 537 (1997).
485. S. Y. Kang and K. Kim, *Langmuir*, **14**, 226 (1998).
486. S. R. Johnson, S. D. Evans, S. W. Mahon and A. Ulman, *Langmuir*, **13**, 51 (1997).
487. R. L. Whetten, J. T. Khoury, M. M. Alvarez, S. Murthy, I. Vezmar, Z. L. Wang, P. W. Stephens, C. L. Cleveland, W. D. Luedtke and U. Landman, *Adv. Mater.*, **8**, 428 (1996).
488. R. H. Terrill, T. A. Postlethwaite, C. H. Chen, C. D. Poon, A. Terzis, A. D. Chen, J. E. Hutchison, M. R. Clark, G. Wignall, J. D. Londono, R. Superfine, M. Falvo, C. S. Johnson, E. T. Samulski and R. W. Murray, *J. Am. Chem. Soc.*, **117**, 12537 (1995).
489. A. Badia, W. Gao, S. Singh, L. Demers, L. Cuccia and L. Reven, *Langmuir*, **12**, 1262 (1996).
490. A. Badia, L. Demers, L. Dickinson, F. G. Morin, R. B. Lennox and L. Reven, *J. Am. Chem. Soc.*, **119**, 11104 (1997).
491. M. J. Hostetler, J. J. Stokes and R. W. Murray, *Langmuir*, **12**, 3604 (1996).
492. A. Badia, S. Singh, L. Demers, L. Cuccia, G. R. Brown and R. B. Lennox, *Chem. Eur. J.*, **2**, 359 (1996).
493. A. Badia, L. Cuccia, L. Demers, F. Morin and R. B. Lennox, *J. Am. Chem. Soc.*, **119**, 2682 (1997).
494. W. D. Luedtke and U. Landman, *J. Phys. Chem.*, **100**, 13323 (1996).
495. H. Y. Fan and G. P. Lopez, *Langmuir*, **13**, 119 (1997).
496. M. J. Hostetler, S. J. Green, J. J. Stokes and R. W. Murray, *J. Am. Chem. Soc.*, **118**, 4212 (1996).
497. R. S. Ingram, M. J. Hostetler and R. W. Murray, *J. Am. Chem. Soc.*, **119**, 9175 (1997).
498. M. Brust, D. Bethell, D. J. Schiffrin and C. J. Kiely, *Adv. Mater.*, **7**, 795 (1995).
499. D. Bethell, M. Brust, D. J. Schiffrin and C. J. Kiely, *J. Electroanal. Chem.*, **409**, 137 (1996).

500. S. J. Green, J. J. Stokes, M. J. Hostetler, J. Pietron and R. W. Murray, *J. Phys. Chem. B*, **101**, 2663 (1997).
501. H. Takei and N. Shimizu, *Langmuir*, **13**, 1865 (1997).
502. C. A. Mirkin, R. L. Letsinger, R. C. Mucic and J. J. Storhoff, *Nature*, **382**, 607 (1996).
503. A. P. Alivisatos, K. P. Johnsson, X. G. Peng, T. E. Wilson, C. J. Loweth, M. P. Bruchez and P. G. Schultz, *Nature*, **382**, 609 (1996).
504. R. Elghanian, J. J. Storhoff, R. C. Mucic, R. L. Letsinger and C. A. Mirkin, *Science*, **277**, 1078 (1997).
505. C. A. Mirkin and M. A. Ratner, *Annu. Rev. Phys. Chem.*, **43**, 719 (1992).
506. T. Wink, S. J. van Zuilen, A. Bult and W. P. van Bennekom, *Analyst*, **122**, 43 (1997).
507. M. Mrksich and G. M. Whitesides, *Trends Biotechnol.*, **13**, 228 (1995).
508. A. Kumar, N. L. Abbott, E. Kim, H. A. Biebuyck and G. M. Whitesides, *Acc. Chem. Res.*, **28**, 219 (1995).
509. J. L. Wilbur, A. Kumar, H. A. Biebuyck, E. Kim and G. M. Whitesides, *Nanotechnology*, **7**, 452 (1996).
510. M. K. Chaudhury, *Curr. Opin. Colloid Interface Sci.*, **2**, 65 (1997).
511. R. W. Carpick and M. Salmeron, *Chem. Rev.*, **97**, 1163 (1997).
512. N. L. Abbott, *Curr. Opin. Colloid Interface Sci.*, **2**, 76 (1997).
513. D. L. Allara, *Biosensors Bioelectronics*, **10**, 771 (1995).
514. J. H. Fendler, *Chem. Mater.*, **8**, 1616 (1996).
515. Y. N. Xia and G. M. Whitesides, *Langmuir*, **13**, 2059 (1997).
516. Y. Xia, E. Kim and G. M. Whitesides, *J. Electrochem. Soc.*, **143**, 1070 (1996).
517. Y. N. Xia, J. Tien, D. Qin and G. M. Whitesides, *Langmuir*, **12**, 4033 (1996).
518. Y. N. Xia, D. Qin and G. M. Whitesides, *Adv. Mater.*, **8**, 1015 (1996).
519. N. B. Larsen, H. Biebuyck, E. Delamarche and B. Michel, *J. Am. Chem. Soc.*, **119**, 3017 (1997).
520. D. Fischer, A. Marti and G. Hahner, *J. Vac. Sci. Technol. A*, **15**, 2173 (1997).
521. N. L. Abbott, J. P. Folkers and G. M. Whitesides, *Science*, **257**, 1380 (1992).
522. J. M. Behm, K. R. Lykke, M. J. Pellin and J. C. Hemminger, *Langmuir*, **12**, 2121 (1996).
523. K. C. Chan, T. Kim, J. K. Schoer and R. M. Crooks, *J. Am. Chem. Soc.*, **117**, 5875 (1995).
524. K. K. Berggren, A. Bard, J. L. Wilbur, J. D. Gillaspy, A. G. Helg, J. J. McClelland, S. L. Rolston, W. D. Phillips, M. Prentiss and G. M. Whitesides, *Science*, **269**, 1255 (1995).
525. K. K. Berggren, R. Younkin, E. Cheung, M. Prentiss, A. J. Black, G. M. Whitesides, D. C. Ralph, C. T. Black and M. Tinkham, *Adv. Mater.*, **9**, 52 (1997).
526. S. Xu and G. Liu, *Langmuir*, **13**, 127 (1997).
527. C. D. Tidwell, S. I. Ertel, B. D. Ratner, B. J. Tarasevich, S. Atre and D. L. Allara, *Langmuir*, **13**, 3404 (1997).
528. M. Mrksich, C. S. Chen, Y. N. Xia, L. E. Dike, D. E. Ingber and G. M. Whitesides, *Proc. Natl. Acad. Sci. U.S.A.*, **93**, 10775 (1996).
529. D. A. Hutt, E. Cooper, L. Parker, G. J. Leggett and T. L. Parker, *Langmuir*, **12**, 5494 (1996).
530. M. Mrksich, L. E. Dike, J. Tien, D. E. Ingber and G. M. Whitesides, *Exp. Cell Res.*, **235**, 305 (1997).
531. M. L. Bruening, Y. F. Zhou, G. Aguilar, R. Agee, D. E. Bergbreiter and R. M. Crooks, *Langmuir*, **13**, 770 (1997).
532. X. C. Zhou, S. C. Ng, H. S. O. Chan and S. F. Y. Li, *Sensors Actuators B*, **42**, 137 (1997).
533. X. C. Zhou, L. Zhong, S. F. Y. Li, S. C. Ng and H. S. O. Chan, *Sensors Actuators B*, **42**, 59 (1997).
534. Y. Miyazaki, K. Hayashi, K. Toko, K. Yamafuji and N. Nakashima, *Jpn. J. Appl. Phys. 1*, **31**, 1555 (1992).
535. J. Wang, H. Wu and L. Angnes, *Anal. Chem.*, **65**, 1893 (1993).
536. O. Chailapakul and R. M. Crooks, *Langmuir*, **9**, 884 (1993).
537. O. Chailapakul and R. M. Crooks, *Langmuir*, **11**, 1329 (1995).
538. K. T. Kinnear and H. G. Monbouquette, *ACS Symp. Ser.*, **613**, 82 (1995).
539. J. Rickert, W. Gopel, W. Beck, G. Jung and P. Heiduschka, *Biosensors Bioelectronics*, **11**, 757 (1996).
540. S. Sampath and O. Lev, *Adv. Mater.*, **9**, 410 (1997).
541. P. G. He, J. N. Ye, Y. Z. Fang, J. Anzai and T. Osa, *Talanta*, **44**, 885 (1997).
542. M. Itoh, H. Nishihara and K. Aramaki, *J. Electrochem. Soc.*, **142**, 1839 (1995).
543. K. Nozawa, H. Nishihara and K. Aramaki, *Corros. Sci.*, **39**, 1625 (1997).

544. F. P. Zamborini and R. M. Crooks, *Langmuir*, **13**, 122 (1997).
545. R. A. Drawhorn and N. L. Abbott, *J. Phys. Chem.*, **99**, 16511 (1995).
546. V. K. Gupta and N. L. Abbott, *Langmuir*, **12**, 2587 (1996).
547. W. J. Miller, N. L. Abbott, J. D. Paul and M. G. Prentiss, *Appl. Phys. Lett.*, **69**, 1852 (1996).
548. V. K. Gupta and N. L. Abbott, *Phys. Rev. E*, **54**, R4540 (1996).
549. V. K. Gupta and N. L. Abbott, *Science*, **276**, 1533 (1997).
550. Z. F. Liu, C. X. Zhao, J. Zhang, M. Tang, T. Zhu and S. M. Cai, *Ber. Bunsenges. Phys. Chem. Phys.*, **101**, 1113 (1997).
551. P. Sanassy and S. D. Evans, *Langmuir*, **9**, 1024 (1993).
552. S. D. Evans, P. Sanassy and A. Ulman, *Thin Solid Films*, **243**, 325 (1994).
553. A. Terfort, N. Bowden and G. M. Whitesides, *Nature*, **386**, 162 (1997).
554. J. Tien, A. Terfort and G. M. Whitesides, *Langmuir*, **13**, 5349 (1997).

Author index

This author index is designed to enable the reader to locate an author's name and work with the aid of the reference numbers appearing in the text. The page numbers are printed in normal type in ascending numerical order, followed by the reference numbers in parentheses. The numbers in *italics* refer to the pages on which the references are actually listed.

Index compiled by K. Raven

Subject index

723

Index compiled by P. Raven